AD_____

Award Number: W81XWH–05–1-0035

TITLE: A Double Selection Approach to Achieve Specific Expression of Toxin Genes for Ovarian Cancer Gene Therapy

PRINCIPAL INVESTIGATOR: David T. Curiel, M.D., Ph.D.
Gene Siegal, M.D., Ph.D.
Minghui Wang, M.D

CONTRACTING ORGANIZATION: University of Alabama at Birmingham
Birmingham, AL 35294-0111

REPORT DATE: November 2007

TYPE OF REPORT: Final

PREPARED FOR: U.S. Army Medical Research and Materiel Command
Fort Detrick, Maryland 21702-5012

REPORT DOCUMENTATION PAGE

Form Approved
OMB No. 0704-0188

1. REPORT DATE *(DD-MM-YYYY)*	**2. REPORT TYPE**	**3. DATES COVERED** *(From - To)*
01-11-2007	Final	1 NOV 04 - 31 OCT 07

4. TITLE AND SUBTITLE

A Double Selection Approach to Achieve Specific Expression of Toxin Genes for Ovarian Cancer Gene Therapy

5a. CONTRACT NUMBER

5b. GRANT NUMBER
W81XWH–05–1-0035

5c. PROGRAM ELEMENT NUMBER

6. AUTHOR(S)
David T. Curiel, M.D., Ph.D.; Gene Siegal, M.D., Ph.D.; Minghui Wang, M.D.

E-Mail: curiel@uab.edu

5d. PROJECT NUMBER

5e. TASK NUMBER

5f. WORK UNIT NUMBER

7. PERFORMING ORGANIZATION NAME(S) AND ADDRESS(ES)

University of Alabama at Birmingham
Birmingham, AL 35294-0111

8. PERFORMING ORGANIZATION REPORT NUMBER

9. SPONSORING / MONITORING AGENCY NAME(S) AND ADDRESS(ES)
U.S. Army Medical Research and Materiel Command
Fort Detrick, Maryland 21702-5012

10. SPONSOR/MONITOR'S ACRONYM(S)

11. SPONSOR/MONITOR'S REPORT NUMBER(S)

12. DISTRIBUTION / AVAILABILITY STATEMENT
Approved for Public Release; Distribution Unlimited

13. SUPPLEMENTARY NOTES

14. ABSTRACT
Gene therapy is a novel treatment modality which offers great potential for the control of carcinoma of the ovary. The efficacy of such approaches, however, is currently limited due to the inability of available gene delivery vehicles (vectors) to achieve efficient and selective gene transfer to target tumor cells. Proposed herein is a strategy to modify one candidate vector, recombinant adenovirus, such that it embodies the requisite properties of efficacy and specificity. This approach is based on targeting the delivered anti-cancer gene to tumor via two complimentary approaches. This strategy is based upon restricting the expression of the anti-cancer gene exclusively to ovarian cancer tumor cells ("transcriptional targeting") plus directing the binding of the viral vector particle exclusively to tumor cells ("transductional targeting").This "double targeting" approach is highly novel. We have advanced this double targeting approach and shown its overall utility for improving ovarian cancer gene therapy. In the first regard, we have improved the infectivity of adenovirus (Ad) for ovarian cancer targets via a knob "switch" method exploiting fiber knobs of canine and ovine Ad fiber knobs. In the second instance, we have defined optimized tumor selective promoters for ovarian cancer (TSPs). Finally, we have shown that the combination of these targeting strategies can improve the overall therapeutic index of ovarian cancer gene therapy in a stringent murine model of human ovarian cancer. These studies have thus provided the framework for translation of targeting approaches to the context of human clinical trials.

15. SUBJECT TERMS
Ovarian cancer, targeting, gene therapy

16. SECURITY CLASSIFICATION OF:			**17. LIMITATION OF ABSTRACT**	**18. NUMBER OF PAGES**	**19a. NAME OF RESPONSIBLE PERSON**
a. REPORT	**b. ABSTRACT**	**c. THIS PAGE**			USAMRMC
U	U	U	UU	351	**19b. TELEPHONE NUMBER** *(include area code)*

Table of Contents

Page

INTRODUCTION

Ovarian cancer is one of the most common causes of cancer death in women. In large part this is due to the late presentation of the disease. On this basis, it is clear novel therapeutic approaches are warranted. In this regard, gene therapy represents one such novel approach which may be applied in the context of carcinoma of the ovary. For this technique to be successful clinically, highly efficient gene delivery vectors are necessary to deliver therapeutic genes specifically to tumor cells. Tropism-modified adenoviral vectors are the best agent for cell-specific gene delivery. Ovarian cancer-specific markers have been described which can be exploited as a means to achieve specific infection via "transductional targeting". The specificity of gene expression can be further improved by placing the gene under the control of an ovarian cancer-specific promoter via a "transcriptional targeting" approach. This "double-targeting" strategy achieves a synergistic improvement in specificity, thus enabling a therapeutic result to be obtained. This project sought to develop an optimized gene delivery system based on a combination of the best available transductional and transcriptional targeting approaches for ovarian cancer. This system resulted in highly efficient and specific expression of toxin encoding genes in tumor cells, enabling these cells to be selectivity eradicated and thus offering a novel technique for the achievement of ovarian cancer gene therapy.

BODY

We sought to derive adenoviral vectors (Ads) which embodied the capacity for double targeting – transcriptional targeting and transductional targeting functioning in operational synergy. In the first regard, we identified a series of tumor selective promoters (TSPs) relevant to targeting carcinoma of the ovary tumor cells. These TSPs were used to derive EIA/B-deleted replication incompetent Ads whereby the candidate TSP maintained control of expression of the reporter transgene (Luciferase). Viral genomes were constructed; viral plaques rescued; and derived recombined Ads upscaled for characterization. Genomic analysis confirmed the rescue of the designed Ad which were grown to high titer for subsequent functional analysis (Task 1) [1-2].

We next sought to validate the targeting physiology of the derived vector. Useful vector candidates would exhibit a "tumor on/liver off" phenotype. For this analysis, we employed immortalized human ovarian cancer cells and human primary tumor cells to validate inductivity of the TSP. In addition, we employed human liver explants maintained as "tissue slice" culture to validate the "liver off" profits of the candidate promoter. Analysis of the promoter containing Ads validated the identification of candidate promoters which embodied an inductivity profile useful for our ovarian targeting purposes (Task 2). This represents a major accomplishment as to this point there was a paucity of TSPs for ovarian cancer compared to other epithelial neoplasms. These characterized TSPs now represent a reagent set of field-wide utility. In Figure 1 we provide evidence of the relative inductivities of studied TSPs:

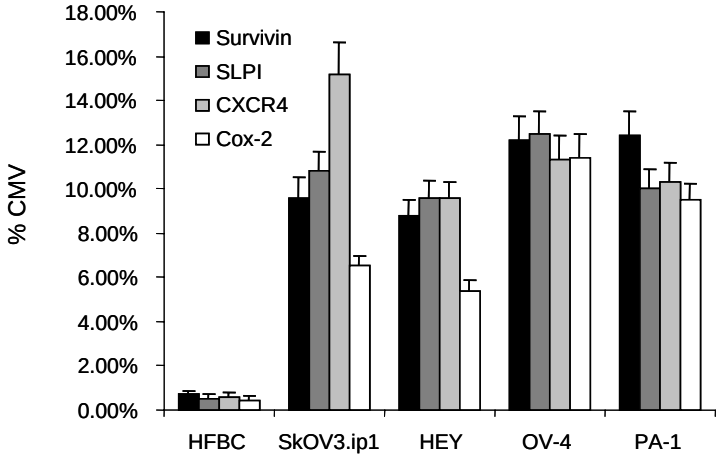

Figure 1: *Promoter activity in four ovarian cancer cell lines.* $5x10^4$ human ovarian cells (SKOV3.ip1, HEY, OV-4 and PA-1) and normal cells (HFBC) were plated on 24 well plates and infected at a MOI of 100 v.p./cell of Ad5-CMV.Luc, Ad5-Cox-2.Luc, Ad5-CXCR4.Luc, Ad5-SLPI.Luc or Ad5-Survivin.Luc, respectively. All the characteristics of the vectors are listed in Table 1. Luciferase activities were analyzed 48 hours later. Results are shown as relative light units (RLU) of luciferase activity. The % of luciferase activity = (RLU induced by TSP)/(RLU induced by the CMV promoter) x 100. The mean value ±SE of triplicate samples is shown.

Table 1. The characteristics of adenoviral vectors used in this study

Virus name	Promoter	Reporter	E1	E3	Fiber modification	Replication
Ad5-CMV.Luc	CMV (Cytomegalovirus)	Luciferase	No	No	No	No
Ad5-S.Luc	S (Survivin)	Luciferase	No	No	No	No
Ad5-SLPI.Luc	SLPI (Secretory leukoprotease inhibitor)	Luciferase	No	No	No	No
Ad5-C.Luc	C (CXCR4)	Luciferase	No	No	No	No
Ad5-Cox2.Luc	Cox-2 (Cyclooxygenase-2)	Luciferase	No	No	No	No
Ad-CMV.Luc.RGD	CMV	Luciferase	No	No	RGD peptide in HI loop	No
Ad-CMV.Luc.pk7	CMV	Luciferase	No	No	polylysine 7	No
Ad-CMV.Luc.pk7RGD	CMV	Luciferase	No	No	pk7/RGD	No
Ad-CMV.Luc.CK	CMV	Luciferase	No	No	Canine knob	No
Ad-CMV.Luc.CKpk7	CMV	Luciferase	No	No	Canine knob/pk7	No
Ad-CMV.Luc. F5/3	CMV	Luciferase	No	No	Chimeric fiber protiens possessing the Ad3 knob	No
Ad-CMV.Luc. F3/3	CMV	Luciferase	No	No	Chimeric fiber with Ad3 shaft and knob	No
Adwt.F5/3	Native	No	Yes	Yes	F5/3	Yes
Ad-Δ24.F5/3	Native	No	Δ24	Yes	F5/3	Yes
CRAd-C.F5/3	C (CXCR4)	No	Yes	Yes	F5/3	Yes
CRAd-M.F5/3	M (Mesothelin)	No	Yes	Yes	F5/3	Yes
CRAd-S.F5/3	S (Survivin)	No	Yes	Yes	F5/3	Yes

For transductional targeting, we had initially sought to employ retargeting adapters based upon the "sCAR-fusion" motif which our lab had developed. To this end, sCAR fusions were developed which allowed targeting to ovarian cancer markers CEA and CD40 [3-10]. In addition, we explored a strategy for infectivity enhancement based upon fiber knob serotype chimerism. We found that the fiber knob of the subgroup B type 3 allowed the highest levels of infectivity enhancement of otherwise Ad-refractory tumor cells (Task 3). This represented a major accomplishment as the ability to enhance gene delivery for tumor targets will improve the outcome of a wide range of interventions. We have identified a spectrum of infectivity enhancements which will have potentially field-wide utility. In Figure 2 we demonstrate the relative potency of these enhancements of human ovarian cancer targets:

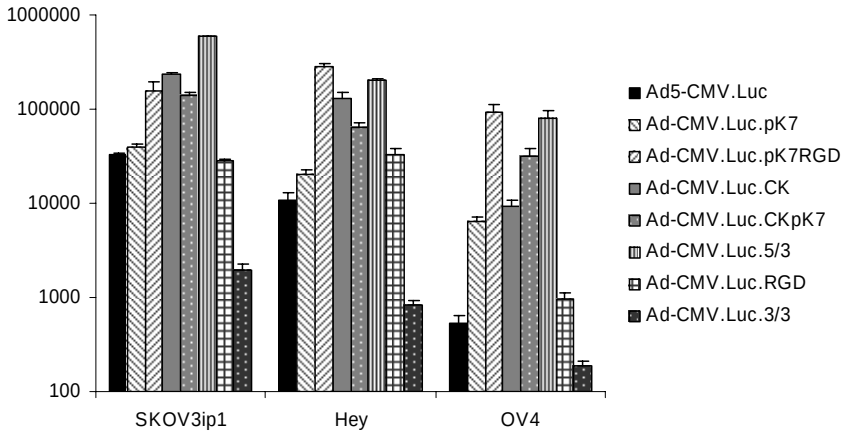

Figure 2: *Comparison of tranductional activity in ovarian cancer cell lines with different capsid modified adenovirus vectors.* Ovarian tumor cells ($5x10^4$ cells) were plated onto 24 well plates and infected at a MOI of 100 v.p./cell of Ad5-CMV.Luc and one of the fiber modified vectors, including Ad.RGD.Luc, Ad.pk7.Luc, Ad.F5/3.Luc Ad.F3/3, Ad.pk7.RGD.Luc, Ad.CK.Luc or Ad.CK.pk7.Luc (see Table 1), respectively. Luciferase activities were analyzed 48 hours later. Results are shown as relative light units (RLU) of luciferase activity. The % of luciferase activity = (RLU induced by TSP)/(RLU induced by the CMV promoter) x 100%. The mean value ± SE of triplicate samples is shown.

Based on successful identification of transcriptional and transductional targeting principles, we sought to combine these approaches towards our goal of double-targeting of ovarian cancer tumor cells. Our initial therapeutic payload was based upon the HSV-tk toxin gene approach. However, the rapid development of conditionally replicative adenoviral agents suggested a payload approach with higher amplification potential. To this end, we developed CRAds which embodied the double targeting principles we had characterized to this

point. Evaluation of these double targeted Ads allowed definition of those agents with the highest therapeutic index vis à vis ovarian cancer (Task 4) [11-12]. Of note, these studies (Figure 3) demonstrated that our double targeting maneuvers improved the potency of the derived agent while also improving its specificity.

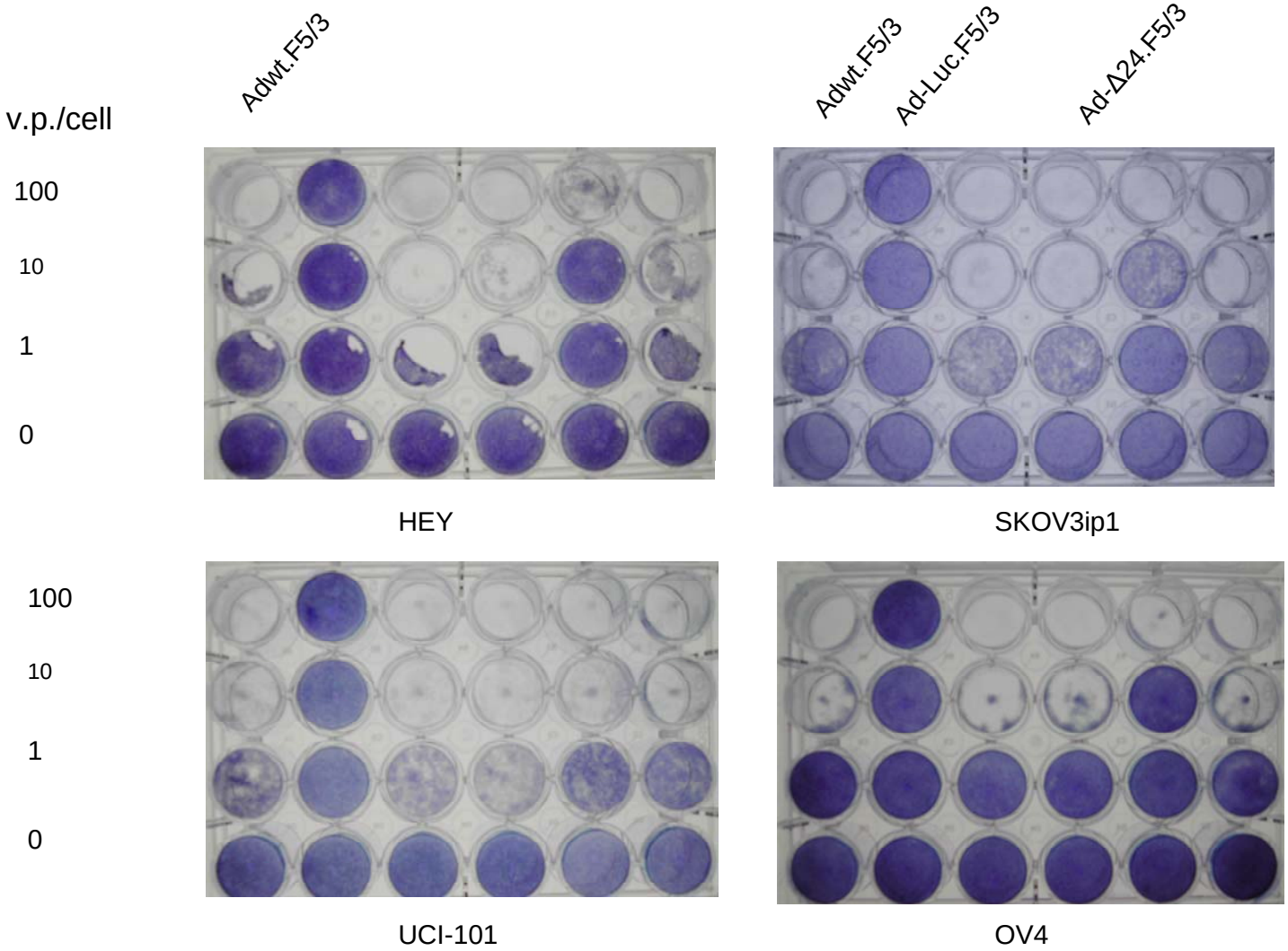

Figure 3: *Oncolytic effect of CRAds in ovarian cells.* 5 x 10^4 ovarian cells (HEY, SKOV3.ip1, UCI-101 and OV-4) cells were plated onto 24-well plates, and infected with one of the Ad vectors (Ad5-Δ24.F5/3, CRAd-C.F5/3, CRAd-M.F5/3, or CRAd-S.F5/3 and a positive control, Adwt.F5/3 [see Table 1]; a non-replicative negative control, Ad-Luc.F5/3) at the indicated MOIs (100, 10, 1v.p./cell) or mock-infected. After a 10 day incubation, cells were stained with crystal violet.

We ultimately sought to demonstrate the therapeutic gains which accrued our double targeting approach in human-like models. To this end, we exploited a hu/SCIP orthopic xenograft model which was operative in our laboratory. To enhance analysis of the therapeutic gains, we developed a method to accomplish dynamic/real time imaging analysis. Specifically, we derived a luciferase expressing variant of the human ovarian cancer cell line SkOV3ip.1. This line enabled light-based imaging analysis of tumor mass and provided a facile means to monitor the therapeutic effects of our viral agents. By means of this approach, we were able to identify an adenoviral agent with optimized double targeting as determined in a stringent human-like model of carcinoma of the ovary. On the basis of this analysis, we now have a lead agent for development in the context of human clinical trials (Task 5) [13-15]. We have confirmed the superior efficacy of our double targeted adenoviruses by imaging analysis in a stringent, human-like model of carcinoma of the ovary (Figure 4). These results establish clearly the gains which can accrue the targeting approach. Further, we have advanced for development a lead agent which embodies full translational potential.

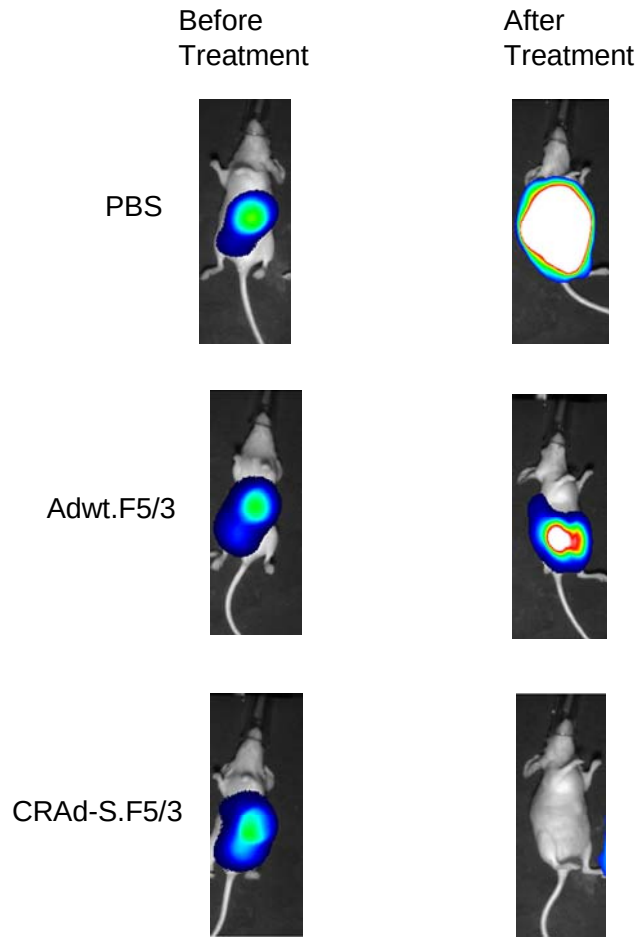

Figure 4: *Tumor growth inhibition:* $1x10^7$ of SKOV3Luc cells were inoculated i.p. and visible tumors were evident post 5 days post-injection. Ad vector and control ($1x10^9$ vp), including PBS, Adwt.F5/3 and CRAd-S.F5/3 (see Table 1), in 200ml volume was injected i.p. The injection continued once a week, 3 times. After inoculation and before treatment, the bioluminescent imaging was determined as described in the Materials and Methods. Comparison of the bioluminescence imaging signals before and after treatment by group and anti-tumor effect of CRAd agent.

KEY RESEARCH ACCOMPLISHMENTS

- Identified a series of novel tumor selective promoters useful for ovarian cancer targeting
- Identified adenoviral capsid modifications allowing enhanced infection of ovarian cancer tumor targeting
- Developed novel tissue slice assay to allow analysis of targeting principles in a stringent/human-like context
- Developed novel ovarian cancer mouse model which allows light-based imaging analysis of therapeutic intervention
- Defined a novel viral agent for ovarian cancer which embodies optimized transcriptional and transductional targeting

REPORTABLE OUTCOMES

Manuscripts

Copies may be found in the appendices

2005

1. Stoff-Khalili MA, Rivera AA, Glasgow JN, Le LP, Stoff A, Everts M, Tsuruta Y, Kawakami Y, Bauerschmitz GJ, Mathis JM, Pereboeva L, Seigal GP, Dall P, Curiel DT. A human adenoviral vector with a chimeric fiber from canine adenovirus type 1 results in novel expanded tropism for cancer gene therapy. Gene Ther. 2005 Dec;12(23):1696-706. PMID: 16034451
2. Tsuruta Y, Pereboeva L, Glasgow JN, Luongo CL, Komarova S, Kawakami Y, Curiel DT. Reovirus sigma1 fiber incorporated into adenovirus serotype 5 enhances infectivity via a CAR-independent pathway. Biochem Biophys Res Commun. 2005 Sep 16;335(1):205-14. PMID: 16061208

2006

3. Emdad L, Sarkar D, Lebedeva IV, Su ZZ, Gupta P, Mahasreshti PJ, Dent P, Curiel DT, Fisher PB. Ionizing radiation enhances adenoviral vector expressing mda-7/IL-24-mediated apoptosis in human ovarian cancer. J Cell Physiol. 2006 Aug;208(2):298-306. PMID: 16646087
4. Everts M, Saini V, Leddon JL, Kok RJ, Stoff-Khalili M, Preuss MA, Millican CL, Perkins G, Brown JM, Bagaria H, Nikles DE, Johnson DT, Zharov VP, Curiel DT. Covalently linked Au nanoparticles to a viral vector: potential for combined photothermal and gene cancer therapy. Nano Lett. 2006 Apr;6(4):587-91. PMID: 16608249
5. Glasgow JN, Everts M, Curiel DT. Transductional targeting of adenovirus vectors for gene therapy. Cancer Gene Ther. 2006 Sep;13(9):830-44. Review. PMID: 16439993
6. Gupta P, Su ZZ, Lebedeva IV, Sarkar D, Sauane M, Emdad L, Bachelor MA, Grant S, Curiel DT, Dent P, Fisher PB. mda-7/IL-24: multifunctional cancer-specific apoptosis-inducing cytokine. Pharmacol Ther. 2006 Sep;111(3):596-628. Review. PMID: 16464504
7. Hedley SJ, Auf der Maur A, Hohn S, Escher D, Barberis A, Glasgow JN, Douglas JT, Korokhov N, Curiel DT. An adenovirus vector with a chimeric fiber incorporating stabilized single chain antibody achieves targeted gene delivery. Gene Ther. 2006 Jan;13(1):88-94. PMID: 16107860
8. Hedley SJ, Chen J, Mountz JD, Li J, Curiel DT, Korokhov N, Kovesdi I. Targeted and shielded adenovectors for cancer therapy. Cancer Immunol Immunother. 2006 Nov;55(11):1412-9. Review. PMID: 16612598
9. Le LP, Le HN, Dmitriev IP, Davydova JG, Gavrikova T, Yamamoto S, Curiell DT, Yamamoto Y. Dynamic monitoring of oncolytic adenovirus in vivo by genetic capsid labeling. JNCI, 2006 Feb 1;98(3):203-14. PMID: 16449680
10. Nakayama M, Both GW, Banizs B, Tsuruta Y, Yamamoto S, Kawakami Y, Douglas JT, Tani K, Curiel DT, Glasgow JN. An adenovirus serotype 5 vector with fibers derived from ovine atadenovirus demonstrates CAR-independent tropism and unique biodistribution in mice. Virology. 2006 Jun 20;350(1):103-15. PMID: 16516257
11. Stoff A, Rivera AA, Banerjee NS, Mathis JM, Espinosa-de-los-Monteros A, Le LP, De la Torre JI, Vasconez LO, Broker TR, Richter DF, Stoff-Khalili MA, Curiel DT. Strategies to enhance transductional efficiency of adenoviral-based gene transfer to primary human fibroblasts and keratinocytes as a platform in dermal wounds. Wound Repair Regen. 2006 Sep-Oct;14(5):608-17. PMID: 17014674
12. Stoff-Khalili MA, Rivera AA, Stoff A, Michael Mathis J, Rocconi RP, Matthews QL, Numnum MT, Herrmann I, Dall P, Eckhoff DE, Douglas JT, Siegal GP, Zhu ZB, Curiel DT. Combining high selectivity of replication via CXCR4 promoter with fiber chimerism for effective adenoviral oncolysis in breast cancer. Int J Cancer. 2007 Feb 15;120(4):935-41. PMID: 17131341

2007

13. Huang D, Pereboev AV, Korokhov N, He R, Larocque L, Gravel C, Jaentschke B, Tocchi M, Casley WL, Lemieux M, Curiel DT, Chen W, Li X. Significant alterations of biodistribution and immune responses in Balb/c mice administered with adenovirus targeted to CD40(+) cells. Gene Ther. 2007 Nov 29:1-11. PMID: 18046426
14. Li HJ, Everts M, Pereboeva L, Komarova S, Idan A, Curiel DT, Herschman HR. Adenovirus tumor targeting and hepatic untargeting by a coxsackie/adenovirus receptor ectodomain anti-carcinoembryonic antigen bispecific adapter. Cancer Res. 2007 Jun 1;67(11):5354-61. PMID: 17545616
15. Miura Y, Yoshida K, Nishimoto T, Hatanaka K, Ohnami S, Asaka M, Douglas JT, Curiel DT, Yoshida T, Aoki K. Direct selection of targeted adenovirus vectors by random peptide display on the fiber knob. Gene Ther. 2007 Oct;14(20):1448-60. PMID: 17700705
16. Pereboeva L, Komarova S, Roth J, Ponnazhagan S, Curiel DT. Targeting EGFR with metabolically biotinylated fiber-mosaic adenovirus. Gene Ther. 2007 Apr;14(8):627-37. PMID: 17251987
17. Stoff-Khalili MA, Rivera AA, Mathis JM, Banerjee NS, Moon AS, Hess A, Rocconi RP, Numnum TM, Everts M, Chow LT, Douglas JT, Siegal GP, Zhu ZB, Bender HG, Dall P, Stoff A, Pereboeva L, Curiel

DT. Mesenchymal stem cells as a vehicle for targeted delivery of CRAds to lung metastases of breast carcinoma. Breast Cancer Res Treat. 2007 Oct;105(2):157-67. PMID: 17221158
18. Stoff-Khalili MA, Rivera AA, Nedeljkovic-Kurepa A, Debenedetti A, Li XL, Odaka Y, Podduturi J, Sibley DA, Siegal GP, Stoff A, Young S, Zhu ZB, Curiel DT, Mathis JM. Cancer-specific targeting of a conditionally replicative adenovirus using mRNA translational control. Breast Cancer Res Treat. 2007 May 17. PMID: 17508279
19. Tsuruta Y, Pereboeva L, Glasgow JN, Rein DT, Kawakami Y, Alvarez RD, Rocconi RP, Siegal GP, Dent P, Fisher PB, Curiel DT. A mosaic fiber adenovirus serotype 5 vector containing reovirus sigma 1 and adenovirus serotype 3 knob fibers increases transduction in an ovarian cancer ex vivo system via a coxsackie and adenovirus receptor-independent pathway. Clin Cancer Res. 2007 May 1;13(9):2777-83. PMID: 17473211
20. Waehler R, Russell SJ, Curiel DT. Engineering targeted viral vectors for gene therapy. Nat Rev Genet. 2007 Aug;8(8):573-87. Review. PMID: 17607305

In addition to the above reportable manuscripts, the following papers have been submitted:

- Glasgow JN, Hemminki A, Curiel DT. Modified adenoviruses for gene therapy. In *Gene and Cell Therapy: Therepeutic Mechanisms and Strategies*, 3rd edition. NS Templeton (ed). Taylor & Francis, CRC Press. In press.
- Li HJ, Everts M. Yamamoto Y, Curiel DT, Herschman HR. Combined transductional targeting and transcriptional restriction enhanced adenovirus gene delivery. Cancer Res. Submitted.
- Li HJ, Everts M, Curiel DT, Herschman HR. Trimerization of a bi-specific transductional adapter improves tumor targeting of adenoviral vectors, in culture and in vivo. Nat Biotech. Submitted.

Patents/Licenses

Not applicable

Cell Lines

SkOV3ip.1-Luc – An implantable human cell line which constitutionally expresses the luciferase allowing dynamic/real time imaging analysis of therapeutic interventions in murine model of ovarian cancer

Databases/animal models

See above

CONCLUSION

Targeting can improve the therapeutic index of adenoviral-based therapy for carcinoma of the ovary. The combination of transductional and transcriptional targeting can achieve an optimized therapeutic index. These strategies allowed the realization of a novel viral agent with direct translational potential.

REFERENCES

1. Waehler R, Russell SJ, Curiel DT. Engineering targeted viral vectors for gene therapy. Nat Rev Genet. 2007 Aug;8(8):573-87. Review. PMID: 17607305
2. Hedley SJ, Chen J, Mountz JD, Li J, Curiel DT, Korokhov N, Kovesdi I. Targeted and shielded adenovectors for cancer therapy. Cancer Immunol Immunother. 2006 Nov;55(11):1412-9. Review. PMID: 16612598
3. Pereboeva L, Komarova S, Roth J, Ponnazhagan S, Curiel DT. Targeting EGFR with metabolically biotinylated fiber-mosaic adenovirus. Gene Ther. 2007 Apr;14(8):627-37. PMID: 17251987
4. Glasgow JN, Everts M, Curiel DT. Transductional targeting of adenovirus vectors for gene therapy. Cancer Gene Ther. 2006 Sep;13(9):830-44. Review. PMID: 16439993
5. Tsuruta Y, Pereboeva L, Glasgow JN, Rein DT, Kawakami Y, Alvarez RD, Rocconi RP, Siegal GP, Dent P, Fisher PB, Curiel DT. A mosaic fiber adenovirus serotype 5 vector containing reovirus sigma 1 and adenovirus serotype 3 knob fibers increases transduction in an ovarian cancer ex vivo system via a coxsackie and adenovirus receptor-independent pathway. Clin Cancer Res. 2007 May 1;13(9):2777-83. PMID: 17473211
6. Nakayama M, Both GW, Banizs B, Tsuruta Y, Yamamoto S, Kawakami Y, Douglas JT, Tani K, Curiel DT, Glasgow JN. An adenovirus serotype 5 vector with fibers derived from ovine atadenovirus demonstrates CAR-independent tropism and unique biodistribution in mice. Virology. 2006 Jun 20;350(1):103-15. PMID: 16516257
7. Stoff A, Rivera AA, Banerjee NS, Mathis JM, Espinosa-de-los-Monteros A, Le LP, De la Torre JI, Vasconez LO, Broker TR, Richter DF, Stoff-Khalili MA, Curiel DT. Strategies to enhance transductional efficiency of adenoviral-based gene transfer to primary human fibroblasts and keratinocytes as a platform in dermal wounds. Wound Repair Regen. 2006 Sep-Oct;14(5):608-17. PMID: 17014674
8. Tsuruta Y, Pereboeva L, Glasgow JN, Luongo CL, Komarova S, Kawakami Y, Curiel DT. Reovirus sigma1 fiber incorporated into adenovirus serotype 5 enhances infectivity via a CAR-independent pathway. Biochem Biophys Res Commun. 2005 Sep 16;335(1):205-14. PMID: 16061208
9. Stoff-Khalili MA, Rivera AA, Glasgow JN, Le LP, Stoff A, Everts M, Tsuruta Y, Kawakami Y, Bauerschmitz GJ, Mathis JM, Pereboeva L, Seigal GP, Dall P, Curiel DT. A human adenoviral vector with a chimeric fiber from canine adenovirus type 1 results in novel expanded tropism for cancer gene therapy. Gene Ther. 2005 Dec;12(23):1696-706. PMID: 16034451
10. Hedley SJ, Auf der Maur A, Hohn S, Escher D, Barberis A, Glasgow JN, Douglas JT, Korokhov N, Curiel DT. An adenovirus vector with a chimeric fiber incorporating stabilized single chain antibody achieves targeted gene delivery. Gene Ther. 2006 Jan;13(1):88-94. PMID: 16107860
11. Li HJ, Everts M, Pereboeva L, Komarova S, Idan A, Curiel DT, Herschman HR. Adenovirus tumor targeting and hepatic untargeting by a coxsackie/adenovirus receptor ectodomain anti-carcinoembryonic antigen bispecific adapter. Cancer Res. 2007 Jun 1;67(11):5354-61. PMID: 17545616
12. Huang D, Pereboev AV, Korokhov N, He R, Larocque L, Gravel C, Jaentschke B, Tocchi M, Casley WL, Lemieux M, Curiel DT, Chen W, Li X. Significant alterations of biodistribution and immune responses in Balb/c mice administered with adenovirus targeted to CD40(+) cells. Gene Ther. 2007 Nov 29:1-11. PMID: 18046426
13. Stoff-Khalili MA, Rivera AA, Stoff A, Michael Mathis J, Rocconi RP, Matthews QL, Numnum MT, Herrmann I, Dall P, Eckhoff DE, Douglas JT, Siegal GP, Zhu ZB, Curiel DT. Combining high selectivity of replication via CXCR4 promoter with fiber chimerism for effective adenoviral oncolysis in breast cancer. Int J Cancer. 2007 Feb 15;120(4):935-41. PMID: 17131341
14. Le LP, Le HN, Dmitriev IP, Davydova JG, Gavrikova T, Yamamoto S, Curiell DT, Yamamoto Y. Dynamic monitoring of oncolytic adenovirus in vivo by genetic capsid labeling. JNCI, 2006 Feb 1;98(3):203-14. PMID: 16449680
15. Stoff-Khalili MA, Rivera AA, Nedeljkovic-Kurepa A, Debenedetti A, Li XL, Odaka Y, Podduturi J, Sibley DA, Siegal GP, Stoff A, Young S, Zhu ZB, Curiel DT, Mathis JM. Cancer-specific targeting of a conditionally replicative adenovirus using mRNA translational control. Breast Cancer Res Treat. 2007 May 17. PMID: 17508279

APPENDICES

I. Publications - 2005

1. Stoff-Khalili MA, Rivera AA, Glasgow JN, Le LP, Stoff A, Everts M, Tsuruta Y, Kawakami Y, Bauerschmitz GJ, Mathis JM, Pereboeva L, Seigal GP, Dall P, Curiel DT. A human adenoviral vector with a chimeric fiber from canine adenovirus type 1 results in novel expanded tropism for cancer gene therapy. Gene Ther. 2005 Dec;12(23):1696-706. PMID: 16034451
2. Tsuruta Y, Pereboeva L, Glasgow JN, Luongo CL, Komarova S, Kawakami Y, Curiel DT. Reovirus sigma1 fiber incorporated into adenovirus serotype 5 enhances infectivity via a CAR-independent pathway. Biochem Biophys Res Commun. 2005 Sep 16;335(1):205-14. PMID: 16061208

II. Publications - 2006

1. Emdad L, Sarkar D, Lebedeva IV, Su ZZ, Gupta P, Mahasreshti PJ, Dent P, Curiel DT, Fisher PB. Ionizing radiation enhances adenoviral vector expressing mda-7/IL-24-mediated apoptosis in human ovarian cancer. J Cell Physiol. 2006 Aug;208(2):298-306. PMID: 16646087
2. Everts M, Saini V, Leddon JL, Kok RJ, Stoff-Khalili M, Preuss MA, Millican CL, Perkins G, Brown JM, Bagaria H, Nikles DE, Johnson DT, Zharov VP, Curiel DT. Covalently linked Au nanoparticles to a viral vector: potential for combined photothermal and gene cancer therapy. Nano Lett. 2006 Apr;6(4):587-91. PMID: 16608249
3. Glasgow JN, Everts M, Curiel DT. Transductional targeting of adenovirus vectors for gene therapy. Cancer Gene Ther. 2006 Sep;13(9):830-44. Review. PMID: 16439993
4. Gupta P, Su ZZ, Lebedeva IV, Sarkar D, Sauane M, Emdad L, Bachelor MA, Grant S, Curiel DT, Dent P, Fisher PB. mda-7/IL-24: multifunctional cancer-specific apoptosis-inducing cytokine. Pharmacol Ther. 2006 Sep;111(3):596-628. Review. PMID: 16464504
5. Hedley SJ, Auf der Maur A, Hohn S, Escher D, Barberis A, Glasgow JN, Douglas JT, Korokhov N, Curiel DT. An adenovirus vector with a chimeric fiber incorporating stabilized single chain antibody achieves targeted gene delivery. Gene Ther. 2006 Jan;13(1):88-94. PMID: 16107860
6. Hedley SJ, Chen J, Mountz JD, Li J, Curiel DT, Korokhov N, Kovesdi I. Targeted and shielded adenovectors for cancer therapy. Cancer Immunol Immunother. 2006 Nov;55(11):1412-9. Review. PMID: 16612598
7. Le LP, Le HN, Dmitriev IP, Davydova JG, Gavrikova T, Yamamoto S, Curiell DT, Yamamoto Y. Dynamic monitoring of oncolytic adenovirus in vivo by genetic capsid labeling. JNCI, 2006 Feb 1;98(3):203-14. PMID: 16449680
8. Nakayama M, Both GW, Banizs B, Tsuruta Y, Yamamoto S, Kawakami Y, Douglas JT, Tani K, Curiel DT, Glasgow JN. An adenovirus serotype 5 vector with fibers derived from ovine atadenovirus demonstrates CAR-independent tropism and unique biodistribution in mice. Virology. 2006 Jun 20;350(1):103-15. PMID: 16516257
9. Stoff A, Rivera AA, Banerjee NS, Mathis JM, Espinosa-de-los-Monteros A, Le LP, De la Torre JI, Vasconez LO, Broker TR, Richter DF, Stoff-Khalili MA, Curiel DT. Strategies to enhance transductional efficiency of adenoviral-based gene transfer to primary human fibroblasts and keratinocytes as a platform in dermal wounds. Wound Repair Regen. 2006 Sep-Oct;14(5):608-17. PMID: 17014674
10. Stoff-Khalili MA, Rivera AA, Stoff A, Michael Mathis J, Rocconi RP, Matthews QL, Numnum MT, Herrmann I, Dall P, Eckhoff DE, Douglas JT, Siegal GP, Zhu ZB, Curiel DT. Combining high selectivity of replication via CXCR4 promoter with fiber chimerism for effective adenoviral oncolysis in breast cancer. Int J Cancer. 2007 Feb 15;120(4):935-41. PMID: 17131341

III. Publications - 2007

1. Huang D, Pereboev AV, Korokhov N, He R, Larocque L, Gravel C, Jaentschke B, Tocchi M, Casley WL, Lemieux M, Curiel DT, Chen W, Li X. Significant alterations of biodistribution and immune responses in Balb/c mice administered with adenovirus targeted to CD40(+) cells. Gene Ther. 2007 Nov 29:1-11. PMID: 18046426

2. Li HJ, Everts M, Pereboeva L, Komarova S, Idan A, Curiel DT, Herschman HR. Adenovirus tumor targeting and hepatic untargeting by a coxsackie/adenovirus receptor ectodomain anti-carcinoembryonic antigen bispecific adapter. Cancer Res. 2007 Jun 1;67(11):5354-61. PMID: 17545616
3. Miura Y, Yoshida K, Nishimoto T, Hatanaka K, Ohnami S, Asaka M, Douglas JT, Curiel DT, Yoshida T, Aoki K. Direct selection of targeted adenovirus vectors by random peptide display on the fiber knob. Gene Ther. 2007 Oct;14(20):1448-60. PMID: 17700705
4. Pereboeva L, Komarova S, Roth J, Ponnazhagan S, Curiel DT. Targeting EGFR with metabolically biotinylated fiber-mosaic adenovirus. Gene Ther. 2007 Apr;14(8):627-37. PMID: 17251987
5. Stoff-Khalili MA, Rivera AA, Mathis JM, Banerjee NS, Moon AS, Hess A, Rocconi RP, Numnum TM, Everts M, Chow LT, Douglas JT, Siegal GP, Zhu ZB, Bender HG, Dall P, Stoff A, Pereboeva L, Curiel DT. Mesenchymal stem cells as a vehicle for targeted delivery of CRAds to lung metastases of breast carcinoma. Breast Cancer Res Treat. 2007 Oct;105(2):157-67. PMID: 17221158
6. Stoff-Khalili MA, Rivera AA, Nedeljkovic-Kurepa A, Debenedetti A, Li XL, Odaka Y, Podduturi J, Sibley DA, Siegal GP, Stoff A, Young S, Zhu ZB, Curiel DT, Mathis JM. Cancer-specific targeting of a conditionally replicative adenovirus using mRNA translational control. Breast Cancer Res Treat. 2007 May 17. PMID: 17508279
7. Tsuruta Y, Pereboeva L, Glasgow JN, Rein DT, Kawakami Y, Alvarez RD, Rocconi RP, Siegal GP, Dent P, Fisher PB, Curiel DT. A mosaic fiber adenovirus serotype 5 vector containing reovirus sigma 1 and adenovirus serotype 3 knob fibers increases transduction in an ovarian cancer ex vivo system via a coxsackie and adenovirus receptor-independent pathway. Clin Cancer Res. 2007 May 1;13(9):2777-83. PMID: 17473211
8. Waehler R, Russell SJ, Curiel DT. Engineering targeted viral vectors for gene therapy. Nat Rev Genet. 2007 Aug;8(8):573-87. Review. PMID: 17607305

IV. Submitted & In-Press Manuscripts (as of Dec 18, 2007)

1. Glasgow JN, Hemminki A, Curiel DT. Modified adenoviruses for gene therapy. In *Gene and Cell Therapy: Therepeutic Mechanisms and Strategies*, 3rd edition. NS Templeton (ed). Taylor & Francis, CRC Press. In press.
2. Li HJ, Everts M. Yamamoto Y, Curiel DT, Herschman HR. Combined transductional targeting and transcriptional restriction enhanced adenovirus gene delivery. Cancer Res. Submitted.
3. Li HJ, Everts M, Curiel DT, Herschman HR. Trimerization of a bi-specific transductional adapter improves tumor targeting of adenoviral vectors, in culture and in vivo. Nat Biotech. Submitted.

I. Publications - 2005

3. Stoff-Khalili MA, Rivera AA, Glasgow JN, Le LP, Stoff A, Everts M, Tsuruta Y, Kawakami Y, Bauerschmitz GJ, Mathis JM, Pereboeva L, Seigal GP, Dall P, Curiel DT. A human adenoviral vector with a chimeric fiber from canine adenovirus type 1 results in novel expanded tropism for cancer gene therapy. Gene Ther. 2005 Dec;12(23):1696-706. PMID: 16034451
4. Tsuruta Y, Pereboeva L, Glasgow JN, Luongo CL, Komarova S, Kawakami Y, Curiel DT. Reovirus sigma1 fiber incorporated into adenovirus serotype 5 enhances infectivity via a CAR-independent pathway. Biochem Biophys Res Commun. 2005 Sep 16;335(1):205-14. PMID: 16061208

Gene Therapy (2005) 12, 1696–1706

www.nature.com/gt

RESEARCH ARTICLE

A human adenoviral vector with a chimeric fiber from canine adenovirus type 1 results in novel expanded tropism for cancer gene therapy

MA Stoff-Khalili[1,2], AA Rivera[1], JN Glasgow[1], LP Le[1], A Stoff[1,3], M Everts[1], Y Tsuruta[1], Y Kawakami[1], GJ Bauerschmitz[2], JM Mathis[4], L Pereboeva[1], GP Seigal[5], P Dall[2] and DT Curiel[1]

[1]Departments of Medicine, Surgery, Pathology and the Gene Therapy Center, Division of Human Gene Therapy, University of Alabama at Birmingham, Birmingham, AL, USA; [2]Department of Obstetrics and Gynecology, University of Duesseldorf, Medical Center, Duesseldorf, Germany; [3]Department of Plastic and Reconstructive Surgery, Dreifaltigkeits-Hospital, Wesseling, Germany; [4]Department of Cellular Biology and Anatomy, Louisiana State University Health Sciences Center, Shreveport, LA, USA; and [5]Department of Pathology, Cellular Biology and Surgery and the Gene Therapy Center, UAB, Birmingham, AL, USA

The development of novel therapeutic strategies is imperative for the treatment of advanced cancers like ovarian cancer and glioma, which are resistant to most traditional treatment modalities. In this regard, adenoviral (Ad) cancer gene therapy is a promising approach. However, the gene delivery efficiency of human serotype 5 recombinant adenoviruses (Ad5) in cancer gene therapy clinical trials to date has been limited, mainly due to the paucity of the primary Ad5 receptor, the coxsackie and adenovirus receptor (CAR), on human cancer cells. To circumvent CAR deficiency, Ad5 vectors have been retargeted by creating chimeric fibers possessing the knob domains of alternate human Ad serotypes. Recently, more radical modifications based on 'xenotype' knob switching with non-human adenovirus have been exploited. Herein, we present the characterization of a novel vector derived from a recombinant Ad5 vector containing the canine adenovirus serotype 1 (CAV-1) knob (Ad5Luc1-CK1), the tropism of which has not been previously described. We compared the function of this vector with our other chimeric viruses displaying the CAV-2 knob (Ad5Luc1-CK2) and Ad3 knob (Ad5/3Luc1). Our data demonstrate that the CAV-1 knob can alter Ad5 tropism through the use of a CAR-independent entry pathway distinct from that of both Ad5Luc1-CK2 and Ad5/3-Luc1. In fact, the gene transfer efficiency of this novel vector in ovarian cancer cell lines, and more importantly in patient ovarian cancer primary tissue slice samples, was superior relative to all other vectors applied in this study. Thus, CAV-1 knob xenotype gene transfer represents a viable means to achieve enhanced transduction of low-CAR tumors.
Gene Therapy (2005) **12,** 1696–1706. doi:10.1038/sj.gt.3302588; published online 21 July 2005

Keywords: *canine adenovirus; fiber chimerism; cancer; transductional targeting; gene therapy*

Introduction

Gene therapy is a novel approach for the treatment of malignancies resistant to traditional therapeutic modalities.[1–3] To achieve therapeutic gene delivery, adenoviral vectors (Ad) have been employed owing to their ability to achieve superior levels of *in vivo* gene transfer compared to alternative vector systems.[2] However, despite promising preclinical results obtained in model systems, the major limitation in clinical applications precluding positive outcomes has been inefficient transduction of target tissues by the routinely used human adenovirus serotype 5 vector (Ad5). This problem is mainly due to the insufficient levels of the primary adenoviral receptor, coxsackie-adenovirus receptor (CAR), on target cancer cells.[4,5] In particular, it has been demonstrated that ovarian and breast cancer cells exhibit relative resistance to adenoviral transduction as a result of CAR deficiency.[6,7] This observation predicates the need to develop strategies to alter adenovirus tropism for the goal of efficient gene delivery to cancer cells via 'CAR-independent' pathways.

A general approach to achieve tropism modification is based on genetic modification of certain adenoviral capsid proteins involved in viral binding and target cell entry. Such strategies have largely been directed towards modification of the adenoviral fiber capsid protein, which recognizes the primary receptor CAR. Methods to incorporate heterologeous-binding proteins have exploited locales at the fiber carboxy- terminus and the fiber–knob HI-loop.[8,9] In addition, the approach of fiber–knob serotype chimerism takes advantage of the fact that a subset of human adenovirus serotypes recognize non-CAR primary cellular receptors.[10,11] These various strategies have been successfully employed to achieve a CAR-independent infection capacity for Ad5 vectors. Of note, redirecting the binding of Ad5 to alternate receptors has allowed infectivity enhancement in CAR-deficient, Ad5-refractory tumor targets.[4,12,13]

Correspondence: Dr DT Curiel, Division of Human Gene Therapy, Gene Therapy Center, University of Alabama at Birmingham, 901, 19th Street South, BMR2 502, Birmingham, AL 35294, USA
Received 17 March 2005; accepted 21 June 2005; published online 21 July 2005

Not as rigorously explored, and perhaps more radical, is a recently described approach entailing the development of Ad 'xenotypes'.[14] In this scheme, the fiber–knob of a non-human adenovirus is incorporated into the capsid of a human Ad5 vector to confer novel tropism. Non-human adenoviruses, including those from avian, bovine, porcine, primate, feline, ovine, and canine hosts,[15–17] represent an underused resource in vector design which could offer alternate cellular entry pathways for adenovirus vectors. Although some of these viruses are being developed as gene delivery vectors themselves,[16] the substitution of the Ad5 fiber–knob with these various xenotype fiber–knobs provides an efficient means to analyze their tropism in the context of an Ad5 vector that has been rigourously studied and for which molecular methods have been well established.[2]

Previously, we exploited the unique tropism of canine adenovirus serotype 2 (CAV-2)[18] to generate an Ad5/CAV-2 chimeric vector, which exhibited profound infectivity enhancement of CAR-deficient human tumor cell targets.[14] Another canine adenovirus strain, serotype 1 (CAV-1), has also been partially characterized. Whereas, its cell entry biology has not been described to the extent that has been accomplished for CAV-2, the pathological, structural, biophysical, and serological dissimilarities of CAV1[19–24] in comparison to CAV-2 suggest that a distinct underlying tropism may be operational. In light of these considerations, we explored the potential utilization of an adenoviral xenotype possessing the fiber–knob of CAV-1.

Results

Generation of an Ad5 vector containing a chimeric fiber with the CAV-1 knob domain

Applying structural knowledge of the human Ad5 fiber protein[25] in the context of the CAV-1 fiber indicates that the CAV-1 fiber consists of an N-terminal tail of about 42 amino acids (aa), a shaft of 321 aa, and a remaining C-terminus of 179 aa forming the knob (Figure 1a).[26] A conserved threonine–leucine–tryptophan–threonine (TLWT) motif at the N-terminus of the fiber–knob domain is present in most mammalian Ads including CAV-1. A chimeric fiber was constructed by substitution of the Ad5 fiber–knob with the coding region of the CAV-1 knob domain while preserving the TLWT motif common to both Ad5 and CAV-1 fibers. This procedure was performed by using a two-plasmid rescue system essentially as described by Krasnykh *et al*.[11] We generated an E1-deleted recombinant Ad genome (Ad5Luc1-CK1) incorporating the chimeric Ad5 fiber shaft/CAV-1 knob gene along with a firefly luciferase reporter gene controlled by the CMV immediate early promoter/enhancer in the E1 region. Genomic clones of Ad5Luc1-CK1 were sequenced, and two correct clones

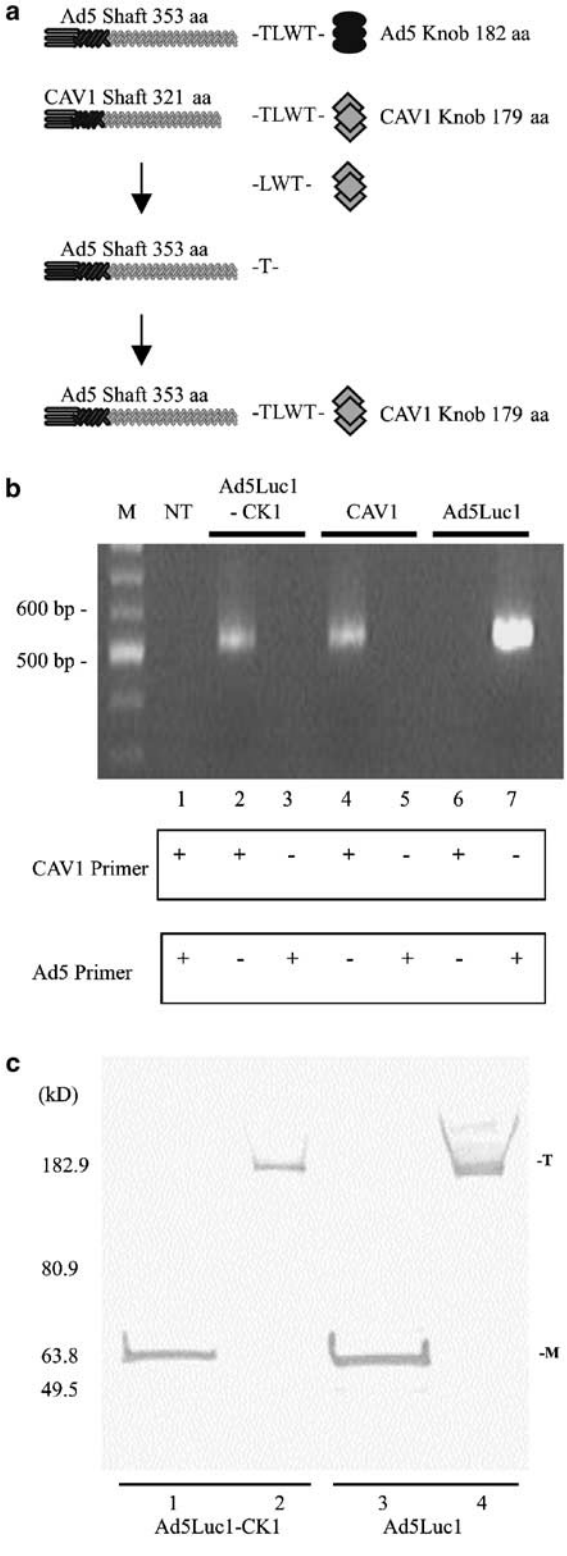

Figure 1 *Design and molecular validation of an Ad5 vector containing the CAV-1 fiber–knob domain. (a) Construction of the chimeric fiber of Ad5Luc1-CK1 by incorporating the CAV-1 knob into the Ad5 fiber-shaft protein. The T-L-W-T peptide sequence joining the shaft and knob regions of both fibers is shown in bold. (b) PCR analysis of the fiber genes using Ad genome templates from purified viral particles. CAV-1 virus was used as a positive control. Lanes containing DNA size standards (M) and no PCR template (NT) are designated. Primers used are specific for the CAV-1 or Ad5 fiber gene knob domain. (c) Western blot analysis of fiber protein trimerization. Purified virions (5×10^9 vp) of AdLuc1-CK1 with the chimeric fiber (lanes 1 and 2) and Ad5Luc1 with wild-type Ad5 fiber (lanes 3 and 4) were resuspended in Laemmli buffer before SDS-PAGE and Western analysis with an antitail fiber mAb. The samples in lanes 1 and 3 were heated to 95°C before electrophoresis. Fiber monomers (M) and trimers (T) are indicated. The markers represent molecular mass in kilodaltons.*

were chosen. Following transfection into HEK 293 cells, cytopathic effect was observed between 8 and 9 days post-transfection. Large-scale preparations of Ad5Luc1-CK1 and the Ad5Luc1 control vector were produced and purified by double cesium chloride gradient centrifugation. Of note, we applied isogenic vectors in this study based on the Ad5 genome, displaying either the Ad5 knob (Ad5Luc1), CAV1 knob (Ad5Luc1-CK1), or the CAV2 knob (previously named Ad5Luc1-CK but designated here as Ad5Luc1-CK2 for ease of distinction).[14] Using a common scheme would standardize vector-related properties including the reporter gene expression cassette and capsid structure while allowing analysis of gene transfer function as a result of modifying the knob.

The fiber–knob genes of Ad5Luc1 and Ad5Luc1-CK1 were confirmed by PCR using designed primer pairs to specifically amplify the respective knob domains from purified viral genome templates (Figure 1b). Trimerization of the chimeric fiber from viral particles was analyzed by SDS-PAGE followed by Western blot analysis. The monoclonal 4D2 primary antibody which recognizes the Ad5 fiber tail domain common to both wild type Ad5 and chimeric fiber molecules was used. Bands of approximately 200 kDa molecular weight corresponding to the nondenatured trimeric fiber molecule for both Ad5Luc1-CK1 and control virions were observed. On the other hand, bands from boiled samples of the same viruses resolved at an apparent molecular mass of approximately 70 kDa, indicative of the fiber monomer form (Figure 1c). Thus, both the correct sequence integrity and trimerization of Ad5Luc1-CK1 were confirmed.

Distinct binding and gene transfer properties of Ad5Luc1-CK1 and Ad5Luc1-CK2

The rationale for developing our novel Ad5Luc1-CK1 vector was founded on the hypothesis that the CAV-1 knob tropism is distinct from the CAV-2 knob tropism based on differences in the pathobiologies of the viruses during infection in their native canine hosts. To validate this concept, we first evaluated the receptor-binding properties of Ad5Luc1-CK1 (Figure 2a and b) and Ad5Luc1-CK2 (Figure 2c and d) on A549 human lung cancer cells in a recombinant knob competitive inhibition assay employing FACS-based detection of surface-bound virions. As a control, Ad5Luc1 cell binding was also analyzed with Ad5 knob protein blocking (Figure 2e). Interestingly, the data obtained in this competitive inhibition experiment show that the CAV-2 fiber–knob protein cannot effectively block the Ad5Luc1-CK1 cell binding (Figure 2b) whereas the CAV-1 fiber–knob protein can inhibit Ad5Luc1-CK2 cell binding (Figure 2d) to the same extent that each recombinant knob can prevent cell interaction of its respective vector.

To further confirm the distinction between Ad5Luc1-CK1 and Ad5Luc1-CK2-mediated tropism as indicated by the cell-binding assay, we sought to block Ad5Luc1-CK1 and Ad5Luc1-CK2-mediated gene transfer in DK dog kidney and SKOV3.ip1 ovarian cancer cells with the recombinant knob proteins. The data obtained in this competitive inhibition gene transfer experiment show that the CAV-2 knob protein can partially block Ad5-Luc1-CK1 gene transfer in only SKOV3.ip1 cells but not completely (Figure 3a). However, the CAV-1 knob can competitively block Ad5Luc1-CK1 gene transfer with increasing concentrations (Figure 3b). Conversely, the CAV-1 knob protein can totally inhibit Ad5Luc1-CK2 gene transfer in all tested cell lines (Figure 3c) in the same manner that the CAV-2 knob can mediate inhibition of Ad5Luc1-CK2 gene transfer (Figure 3d). These findings are consistent with the results of the cell-binding assay (Figure 2) and suggest the possibility of a common receptor between the CAV-1 and CAV-2 knobs although the Ad5Luc1-CK1 displayed a binding property distinct from the Ad5Luc1-CK2.

Since CAV-2 has been shown to bind to CAR,[14,27] we investigated whether CAR may be a common receptor for the CAV-1 and CAV-2 knobs. For this reason, we performed a blocking experiment of Ad5Luc1-mediated gene transfer in U118-hCAR-tailless cells (a CAR-positive U118 cell line variant that heterelogously expresses the extracellular domain of human CAR[28]) with CAV-1 and CAV-2 fiber–knob proteins. Ad5 fiber–knob protein was used as a control. Ad5Luc1 transduction in U118-hCAR-tailless cells was strongly blocked by all three CAV-1 (95%), CAV-2 (98%), and Ad5 fiber–knob proteins (98%) (data not shown), confirming that all three knobs can interact with the CAR receptor.

Infectivity enhancement of CAV-1 knob xenotype Ad in CAR-deficient cells

Our central goal was to investigate whether the CAV1 'xeno-knob' paradigm would mediate increased transduction in CAR-deficient target cancer cells. To evaluate the CAR-independent receptor-binding properties of our novel Ad5Luc1-CK1 vector in comparison with Ad5-Luc1, CAR-deficient U118MG glioma cell line and its CAR-positive variant U118-hCAR-tailless, which artificially expresses the extracellular domain of human CAR, were used in a cell-binding assay as described above. In CAR-deficient cells U118MG, only a modest level of cell surface-associated Ad5Luc1 (38%) was detected (Figure 4a). In contrast, 81% of the CAR-positive variant line U118-hCAR-tailless cells were positive for Ad5Luc1 binding (Figure 4b). Importantly, our novel vector Ad5Luc1-CK1 exhibited a remarkable 95% cell surface binding in U118 MG (glioma) cells (Figure 4a) and cell interaction comparable to that of Ad5Luc1 in U118-hCAR-tailless cells (Figure 4b).

Successful initial attachment on the cell surface via fiber–knob interaction does not necessarily result in increased gene transfer. To validate effective gene delivery conferred by the binding properties of the CAV-1 knob, we evaluated Ad5Luc1-CK1-mediated gene transfer in the U118MG and U118-hCAR-tailless cell lines (Figure 5). Ad5Luc1 (containing the wild-type Ad5 fiber), Ad5Luc1-CK2, and Ad5/3Luc1, (containing the Ad5 fiber shaft and the Ad3 knob) were used as controls. Ad5Luc1 exhibited clear CAR-dependent tropism as demonstrated by a 100-fold increase in transgene expression in U118-hCAR-tailless cells *versus* the CAR-deficient U118 MG cell line. Conversely, Ad5Luc1-CK1 gene delivery in U118 MG cells was about 100-fold higher than that of Ad5Luc1 while infection of the CAR-positive variant cell line yielded a comparable level of luciferase activity. Although the Ad5 fiber–knob competitively inhibited Ad5Luc1-mediated gene transfer in U118-hCAR-tailless (over 85% at 10 μg/ml), it had no

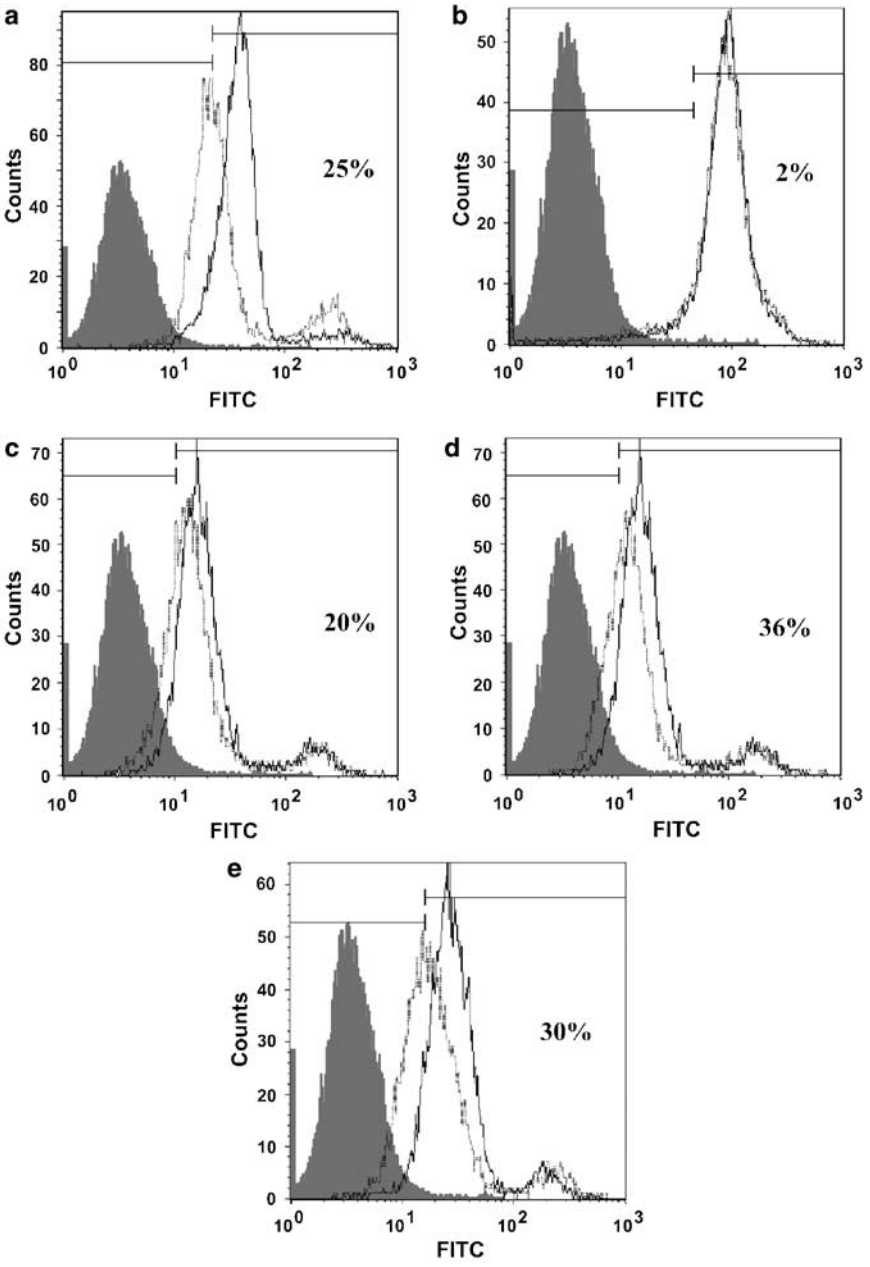

Figure 2 *Distinct binding of Ad5Luc1-CK1 and Ad5Luc1-CK2. Flow cytometry-binding assay of Ad5Luc1-CK1 and Ad5Luc1-CK2 on A549 cells in the presence of purified CAV-1 fiber–knob protein and CAV-2 fiber–knob protein (50 μg/ml) (a–d). (a) Ad5Luc1-CK1+CAV-1 knob, (b) Ad5Luc1-CK1+CAV-2 knob, (c) Ad5Luc1-CK2+CAV-2 knob, (d) Ad5Luc1-CK2+CAV-1 knob, (e) Ad5Luc1+Ad5 knob fiber protein. The histograms shown represent unstained cells (gray fill), cells preincubated with PBS and infected with virus (solid line), and cells preincubated with recombinant knob protein and incubated with virus (dashed line). The percent blocking of virus binding represents histogram gating to determine the number of stained cells preincubated in the absence of recombinant knob protein minus the number of stained cells preincubated in the presence of recombinant knob protein.*

appreciable effect on Ad5/3Luc1, Ad5Luc1-CK1, and Ad5Luc1-CK2 transduction (Figure 5). Thus, these data suggest that CAV1 knob-mediated gene delivery is CAR independent.

Ad3 receptor independence of CAV1 knob xenotype Ad

To further examine the distinct tropism of the CAV1 knob xenotype vector, interaction of the virus with the Ad3 receptor was indirectly studied with an Ad3 knob-blocking experiment. In this case, the SKOV3.ip1 human ovarian cancer cell line was used because it abundantly expresses the Ad3 receptor.[29] Transgene expression mediated by Ad5/3Luc1 decreased with increasing concentrations of the Ad3 knob protein. In contrast, the purified Ad3 knob exhibited no influence on transduction with Ad5Luc1-CK1 (Figure 6a). Thus, these data show that Ad5Luc1-CK1 also displays an Ad3 receptor-independent tropism.

Enhanced gene transfer of Ad5Luc1-CK1 in cancer cell lines and primary ovarian cancer cells

Finally, we evaluated Ad5Luc1-CK1 transduction in a variety of cancer cells, which are known to be deficient in CAR. In all cases, the Ad5Luc1-CK1 vector achieved

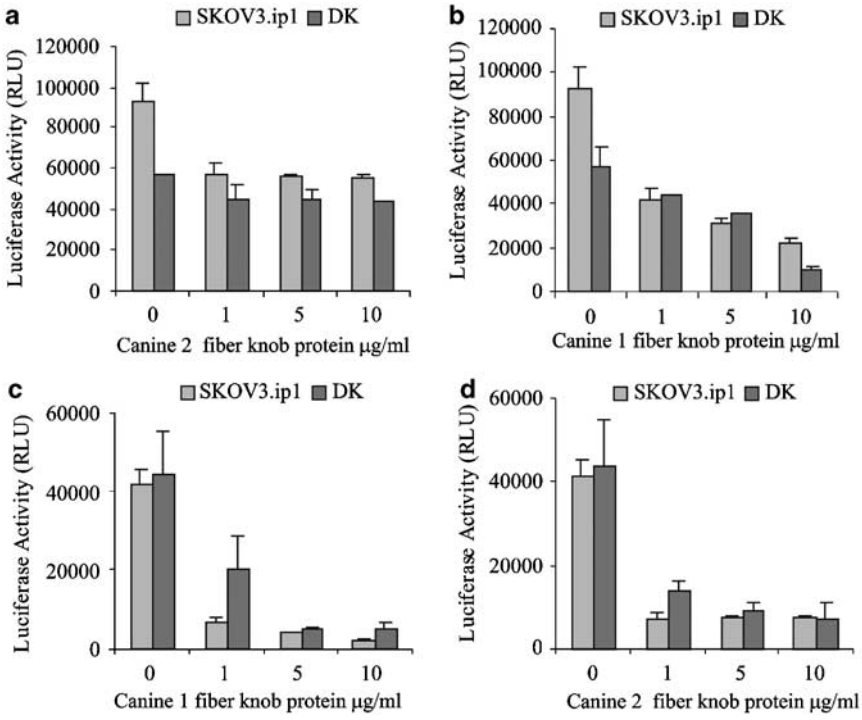

Figure 3 *Transduction efficiency of Ad5Luc1-CK1. Luciferase activities following infection of SKOV3.ip1 and DK cells with Ad5Luc1-CK1 (upper panels) and Ad5Luc1-CK2 (lower panels) in the presence of purified CAV-1 fiber–knob protein (b and c) and CAV-2 fiber–knob protein (a and d). Luciferase activity was determined 48 h postinfection and is presented as relative light units (RLU). Each column represents the average of six replicates using 100 vp/cell of each vector and the error bars indicate the s.d.*

enhanced transduction above the Ad5 vector, ranging from 11- and 32-fold in SKOV3.ip3 and HEY (ovarian cancer cell lines) to 65- and 100-fold in RD (rhabdomyosarcoma cell line) and U118MG (glioma cell line) (Figure 6b). This gene delivery level was also greatly improved relative to that of Ad5Luc1-CK2, further indicating the distinction between the tropism of the CAV-1 *versus* the CAV-2 knob. More importantly the excellent performance of Ad5Luc1-CK1 was also observed in primary ovarian cancer tissue samples, in which CAR levels are highly variable and often very low.[29] We utilized precision cut tissue slices of patient tumor samples, which represent a highly stringent *ex vivo* model system with three-dimensional characteristics for preclinical screening of adenoviral agents. Ad5Luc1-CK1 demonstrated increased gene transfer capability in ovarian cancer tissue slices (four patients) from 6.2- to 11.4-fold higher than Ad5Luc1 (Figure 6c). Notably, the transduction capacity of Ad5Luc1-CK1 was superior overall compared to our Ad5/3Luc1 and Ad5Luc1-CK2, two chimeric vectors, which themselves have already shown remarkable infectivity enhancements in the same disease context previously.[14,30] Of note, the Ad5Luc1-CK1 and Ad5Luc1-CK2-mediated gene transfer in fibroblasts and keratinocytes was poor.

Evaluation of Ad5Luc1-CK1 transduction in human liver tissue slices

To evaluate liver transduction of Ad5Luc1-CK1 in the most relevant context, the human liver, we infected precision-cut human liver tissue slices of three donors with Ad5Luc1 or Ad5Luc1-CK1. These precision-cut liver slices maintain the tissue architecture and contain the variety of cells normally found in liver.[31] As shown in Figure 7 the luciferase activity in human liver tissue slices infected with Ad5Luc1-CK1 was significantly less than luciferase activity in human liver tissue slices infected with Ad5Luc1 ($P<0.01$).

Discussion

For many target cancer cells it has been noted that low levels of the primary adenoviral receptor CAR may present a limiting factor that compromises the utility of Ad5 as a cancer gene therapy vector. To achieve the levels of efficiency required in the context of cancer gene therapy, it may be necessary to route conventional Ad via CAR-independent pathways. Therefore, achieving CAR-independent and expanded tropism is one of the central tasks in Ad5 vector development for cancer gene therapy. To this end, we endeavored such vector design by genetic capsid engineering to replace the Ad5 fiber–knob with the corresponding structure from a nonhuman 'xenotype' Ad, CAV-1. Interest has recently extended to animal adenoviruses due to the desire to expand the choice of novel gene delivery vectors and thus provide more options for therapeutic strategies and design. In this regard, there are two canine isolates, serotypes 1 and 2, which may offer novel adenovirus infection pathways.[32] CAV-2 is one of the few non-human adenoviruses that have been investigated as a gene transfer vector for human applications. Particularly, a replication-deficient CAV-2 vector has been constructed[14,16,33] and displayed a distinct tropism not exhibited by human

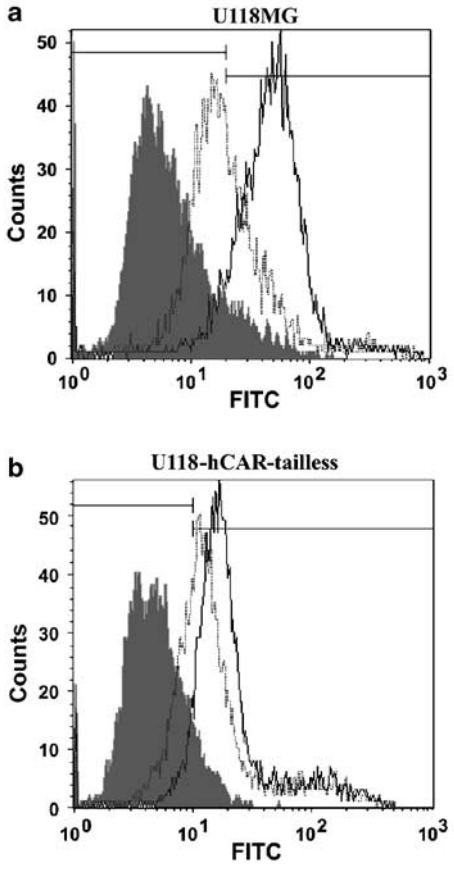

Figure 4 *Ad5Luc1-CK1 CAR-independent cell binding. Flow cytometry-binding assay of Ad5Luc1, Ad5Luc1-CK1 on CAR-deficient U118MG (glioma) cells (a) and the CAR-positive variant, U118-hCAR-tailless cells (b). Gray line = cells alone, solid line = cells+Ad5Luc1-CK1, dashed line = cells+Ad5Luc1.*

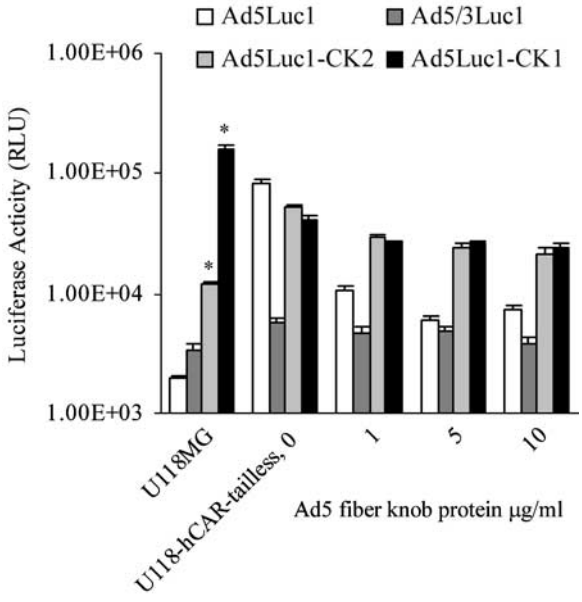

Figure 5 *Ad5Luc1-CK1CAR-independent gene transfer. Luciferase activities following infection of U118MG cells and U118-hCAR-tailless cells with Ad5Luc1, Ad5/3Luc1, and Ad5Luc1-CK1 are presented. The concentration of recombinant Ad5 fiber–knob protein used to block infection is indicated in μg/ml. Luciferase activity was determined 48 h postinfection and is presented as relative light units (RLU). Each column represents the average of three replicates using 100 vp/cell and the error bars indicate the s.d. *P < 0.05 versus Ad5.*

Ad5.[18] The tropism of CAV-2 fiber–knob has also been applied in the context of a chimeric Ad5 vector, which provided significant infectivity enhancement over an unmodified Ad5 virus.[14] CAV-1, however, has not been investigated for gene therapy purposes and represents a potential basis for achieving novel adenoviral tropism. In this regard, the data presented in this study represent the first attempt to explore the tropism of the CAV-1 knob.

The rationale of our study to generate a modified Ad5 vector containing the CAV-1 fiber–knob domain was established on the hypothesis that CAV-1 knob-mediated tropism is distinct from that of the CAV-2 knob. The reasons for this speculation include low DNA sequence homology[34,35] and the reported differences in disease manifestations between CAV-1 and CAV-2.[19,36,37] In addition to structural, biophysical, and serological dissimilarities, the two viruses differ greatly in their biological properties. CAV-1 is known to cause allergic uveitis, called the 'blue eye syndrome' and rarely hepatitis,[32] whereas CAV-2 is known to preferentially infect the upper respiratory tract in young dogs, resulting in a mild disease called kennel cough. Neither the CAV-1 nor the CAV-2 receptor(s) have been rigorously identified. Indeed, our blocking experiments employing recombinant fiber–knob proteins revealed that the CAV-1 and CAV-2 fiber–knobs may share a common receptor as evidenced by the ability of the CAV-1 knob to inhibit Ad5Luc1-CK2 function. CAV-2 has been shown to bind directly to soluble recombinant human CAR and can utilize human or murine CAR for cell entry *in vitro*.[27] This finding, combined with our observation that both CAV-1 and CAV-2 knobs can competitively decrease Ad5-mediated gene transfer, suggest that this common receptor may likely be CAR.

Despite the result that both CAV-2 knob-mediated cell binding and gene delivery was competitively inhibited by the CAV-1 knob, the reverse phenomenon of CAV-2 knob blocking CAV-1 knob-mediated gene delivery could not be demonstrated. This observation may be due to a stronger interaction of the CAV-1 knob to the common receptor relative to the CAV-2 knob. However, the data may also be interpreted to support the idea that the CAV-1 knob may possess the ability to bind to a second receptor that is distinct from CAR. Interestingly, the implication that CAV-2 binds to a second receptor has been previously proposed based on gene delivery results both in the context of a CAV-2 vector[27] as well as an Ad5 chimeric vector.[14] If both CAV-1 and CAV-2 knobs have the ability to interact with secondary receptors in addition to CAR, then the secondary receptors for these two knobs may in fact be distinct based on our competitive inhibition results. Certainly, further studies would have to be conducted to validate these hypotheses. In addition, the interplay between these chimeric vectors and other confirmed and putative adenovirus receptors, such as integrins and heparin sulfate, should also be investigated.

Our major goal was to evaluate whether the CAV-1 'xeno-knob' paradigm would mediate expanded CAR-independent tropism in CAR-negative target cancer cells.

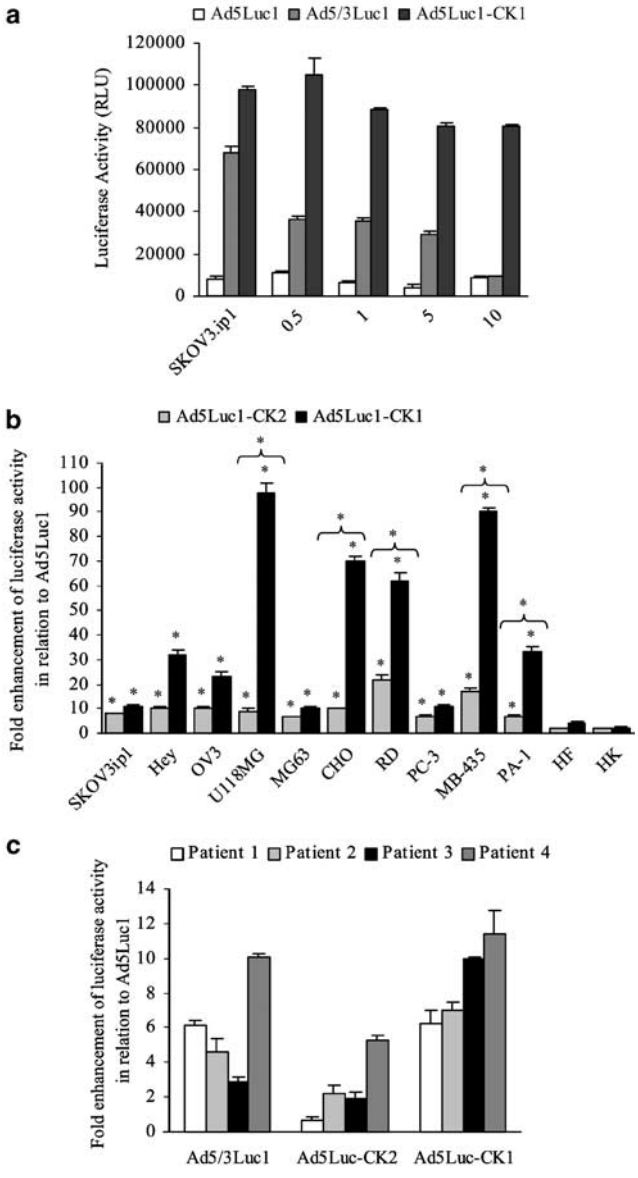

Figure 6 *Enhanced gene transfer by Ad5Luc1-CK1 in cancer cells. Luciferase activities following infection of ovarian cancer cell line SKOV3.ip1 (a), a panel of cancer cell lines (b), and primary ovarian tissue slices (four patients) (c) with the various vectors. Concentration of recombinant Ad3 fiber–knob protein used to block infection (a) is indicated in μg/ml. Luciferase activity was determined 48 h postinfection and is reported in relative units (RLU). Each column represents the average of six replicates using 100 vp/cell of the respective vector and the error bars indicate the s.d. (b) and (c) represent the fold enhancement of luciferase activity in cells infected with various vectors compared to Ad5Luc1. *P < 0.05 versus Ad5. Brackets represent *P < 0.05 Ad5Luc1-CK1 versus Ad5Luc1-CK2 (b).*

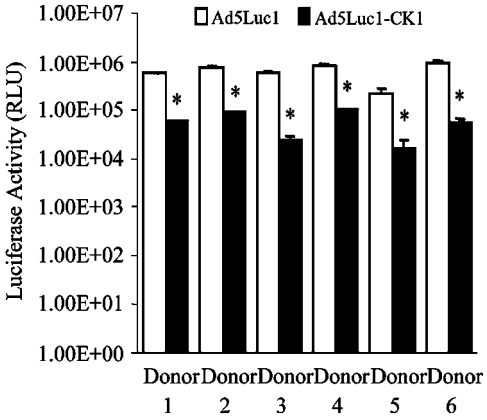

Figure 7 *Ad5Luc1-CK1 displays significant lower infectivity in human liver tissue slices compared to Ad5Luc1. Human liver tissue slices from liver samples of six donors were infected with Ad5Luc1 or Ad5Luc1-CK1 at 500 vp/cell and luciferase activity was measured after 24 h. Luciferase activity was normalized for total protein. Each point represents the mean of three experiments performed in triplicates (three liver tissue slices per donor). Error bars represent s.d. from the mean. *P < 0.05 versus Ad5.*

Even though our data show that the CAV-1 knob may interact with CAR, we were able to achieve enhanced gene transfer with Ad5Luc1-CK1 in a CAR-independent manner. Interestingly, with respect to the CAV-2 knob, this same phenomenon was also observed.[14] Previous studies have utilized other chimeric strategies to attain infectivity enhancement, including the use of the Ad3 knob in the context of an Ad5 vector. The Ad3 receptor appears to be expressed at higher levels than CAR on ovarian cancer cells, therefore allowing 5/3 serotype chimeras to achieve greatly improved gene delivery.[30] Our data revealed the inability of the Ad3 fiber–knob protein to block Ad5luc-CK1 gene transfer, suggesting that this CAV-1 knob chimera, in addition to being CAR independent and distinct from the CAV-2 chimera, does not enter cells via the Ad3 receptor, putatively identified to be CD80, CD86[38] and CD46.[39]

Variable expression of CAR has been documented in many cancer types, such as glioma, melanoma, breast cancer, prostate cancer, and rhabdomyosarcoma.[12,13,40,41] It is known that for entry, viruses often exploit cellular receptors important in conserved pathways. Interestingly, previous studies suggest that CAR may act as a tumor suppressor, which could be linked to its frequent downregulation seen in highly tumorigenic cells.[4] Overcoming this deficiency, both Ad5Luc1-CK1 and Ad5-Luc1-CK2[14] show the ability to bind to and transduce CAR-deficient human glioma cells. Importantly, the transduction by Ad5Luc1-CK1 was augmented by 100-fold *versus* Ad5Luc1 and 75-fold *versus* Ad5Luc1-CK2 in glioma cells and superior to Ad5Luc1 and Ad5Luc1-CK2 in human ovarian cancer, osteosarcoma, and rhabdomyosarcoma cell lines. The significant difference of transduction in the various cancer cell lines between Ad5Luc1-CK1 and Ad5Luc1-CK2 also strongly supports our finding that the CAV-1 knob has a distinct tropism from the CAV-2 knob.

Both Ad5/3Luc1[29,30] and Ad5Luc1-CK2[14] (Ad3 receptor independent) have been reported to exhibit increased infectivity enhancement in ovarian cancer cell lines and primary ovarian cancer cells.[29,30] We endeavored to compare the infectivity enhancement of our seemingly CAR, Ad3 receptor, and CAV2 receptor-independent novel chimeric vector with Ad5/3Luc1 and Ad5Luc1-CK2 in ovarian cancer targets. There is mounting evidence that primary ovarian cancer express highly variable and often low amounts of CAR.[42] Thus, for preclinical evaluation of therapeutic agents, it is crucial to analyze cancer cell substrates that most closely and stringently resemble the patient setting. Gene transfer experiments were performed using primary ovarian

cancer tissue slices obtained by precision cut slice technology, an in *vitro* model representing the architectural features of in *vivo* tissue.[43] In primary ovarian cancer tissue slices, the infectivity enhancement by Ad5Luc1-CK1 was greater than that of Ad5/3Luc1 and Ad5Luc1-CK2. Of note, the gene transfer by Ad5Luc1-CK2 *versus* Ad5Luc1 was only moderate in the primary ovarian cancer tissue slices, further supporting the distinction between the CAV-1 and CAV-2 knobs. The levels of transduction we were able to achieve with Ad5Luc1-CK1 in the primary ovarian cancer samples are one of the highest we have observed in our experience with genetically modified adenoviruses.

Finally, we wished to evaluate the hepatotropism of Ad5Luc1-CK1, since CAV-1 has been reported to rarely cause hepatitis in dogs.[32] Importantly, our data showed that liver transduction of Ad5Luc1-CK1 was significantly lower compared to Ad5Luc1.

Herein, we have constructed a novel Ad5 chimeric xenotype CAV-1 knob vector, which exhibited expanded tropism and displayed superior transduction efficiency in a panel of cancer cells. Importantly, primary tumor tissue slices were also more efficiently transduced with this CAV-1 knob chimeric vector compared to other vectors. The enhanced infectivity appears to be both CAR and Ad3 receptor independent and was also distinct from the transduction pathway of the CAV-2 knob. These results highlight the potential of applying the CAV-1 xeno knob for effective adenovirus cancer gene therapy.

Materials and methods

Cell culture

Human embryonic kidney 293 cells, human embryonic rhabdomyosarcoma RD cells, CAR-negative human glioma U118 MG cells, human osteosarcoma MG63 cells, human ovarian cancer OV3 cells, human lung adenocarcinoma A549 cells, prostate cancer PC-3 cells, breast cancer MB-435 cells, Chinese hamster ovary (CHO) and teratocarcinoma PA-1 cells were obtained from the American Type Culture Collection (ATCC, Manassas, VA, USA). Human ovarian adenocarcinoma cell lines, Hey and SKOV3.ip1, were kind gifts from Drs Judy Wolf and Janet Price (M.D. Anderson Cancer Center, Houston, TX, USA), and Dr Timothy J Eberlein (Harvard Medical School, Boston, MA, USA), respectively. Primary fibroblasts and primary keratinocytes were obtained from Dr NS Banerjee, Department of Biochemistry and Molecular Genetics, University of Alabama at Birmingham, Birnigham, AL, USA). All cells were maintained according to the suppliers' protocols. U118MG-hCAR-tailless cells, which express a truncated form of human CAR (comprising the extracellular domain, transmembrane, and the first two aa from the cytoplasmic domain) have been described previously.[28] These cells were propagated in a 50:50 mixture of Dulbecco's modified Eagle's medium and Ham's F-12 medium (DMEM/F-12) supplemented with 10% (v/v) fetal calf serum (FCS, Gibco-BRL, Grand Island, NY, USA), L-glutamine 2 mM, penicillin (100 U/ml), and streptomycin (100 μg/ml). Stably transfected U118MG-hCAR-tailless cells were maintained in 400 μg/ml G418. Media and supplements were purchased from Mediatech (Herndon, VA, USA).

Human primary ovarian cancer tissue samples

Approval was obtained from the Institutional Review Board prior to initiation of studies on human tissues. Human ovarian primary tumors were obtained from epithelial ovarian carcinoma patients who have undergone debulking as primary therapy and have not had prior chemotherapy (Department of Surgery, University of Alabama at Birmingham (UAB)). Omental samples with extensive tumor infiltration were used to obtain samples since these specimens were the most easily obtained and had large tumor volumes from which adequate slices could be acquired (Krumdieck Tissue Slicer). Time from harvest to slicing was kept to a minimum (<2 h).

Human primary liver tissue samples

Human liver samples were obtained (Department of Surgery, UAB) from six seronegative donor livers that were to be transplanted into waiting recipients. Approval was obtained from the Institutional Review Board prior to initiation of studies on human tissue. All liver samples were flushed with University of Wisconsin (UW) solution (ViaSpan, Barr Laboratories, Inc. Pomona, NY, USA) prior to harvesting and kept on ice in UW solution until slicing. Time from harvest to slicing was kept at an absolute minimum (<2 h).

Krumdieck tissue slicer

The Krumdieck tissue slicing system (Alabama Research & Development[44]) was used in accordance with the manufacturer's instructions and previously published techniques.[45] A coring device was used to create an 8 mm diameter core of ovarian cancer samples and human liver samples. This material was then placed in the slicer filled with ice-cold culture medium. Slice thickness was set at 250 μm using a tissue slice thickness gauge, and slices were cut using the reciprocating blade at 30 revolutions per minute (r.p.m.). Afterwards, the slices were stored in ice-cold culture media prior to culturing. The tissue slices were placed in six-well plates (one slice/well) containing 2 ml of complete media (RPMI with 1% antibiotics, 1% L-glutamine, and 10% FCS for ovarian cancer tissue slices and William's medium E with 1% antibiotics, 1% L-glutamine, and 10% FBS for liver tissue slices). The plates were then incubated at 37°C/5% CO_2 in a humified environment under normal oxygen concentrations for 2 h. A plate rocker set at 60 r.p.m. was used to agitate the slices and to ensure adequate oxygenation and viability.[45,46]

Flow cytometry virus-binding assay

Cells grown in T75 flasks were dislodged with EDTA (0.5 mmol) and resuspended in phosphate buffer solution (PBS) containing 1% bovine serum albumin (BSA). The cells (5×10^5 cells/ml) were incubated with 100 viral particles of the respective vector, or buffer alone, for 1 h at 4°C in 250 μl of PBS–BSA. After three washes with 4 ml of cold PBS–BSA, the cells were incubated with a 1:500 dilution of polyclonal rabbit anti-Ad5 hexon antiserum (Cocalico Biologicals, Reamstown, PA, USA) at 4°C in 250 μl of PBS–BSA. The cells were washed again three times in 4 ml of cold PBS–BSA and incubated with 250 μl of a 1:150 dilution of FITC-labeled goat anti-rabbit IgG secondary antibody (Jackson Immunoresearch Labs,

West Grove, PA, USA) for 1 h in PBS–BSA at 4°C. The cells were analyzed at the UAB FACS Core Facility using a FACScan flow cytometer (Beckton Dickenson, San Jose, CA, USA).

For the recombinant knob competitive inhibition binding assay, A549 cells (5×10^5 cells/ml in 100 μl) were incubated with 100 μl PBS–BSA alone or buffer containing 50 μg/ml recombinant fiber–knob at 4°C for 30 min prior to addition of the viruses, and then antibody staining was performed as described above. To determine the percent blocking of virus binding by the addition of recombinant fiber–knob, histograms representing the staining intensity of cells preincubated in the absence or presence of recombinant knob protein were analyzed. First, the number of cells in the histogram peak representing cells preincubated in the absence of recombinant knob protein was determined by gating the staining to include 99% of the events detected. Then, the percent change in staining intensity was determined by subtracting the number of gated cells in the histogram peak representing cells blocked in virus binding by preincubated in the presence of recombinant knob protein.

Plasmid construction

The CAV-1 fiber–knob (537 bp) domain was amplified from viral DNA isolated from wild-type CAV-1 virus, a kind present from MD Morrison.[32] The following primers were applied: (forward) 5′-TATGGACTGGAC CTGATCCAAACGTT-3′ and (reverse) 5′-TTTATCATTG ATTTTCCCCCACATAGGTGAAGG-3′ (the stop codon TGA and the poly-adenylation signal TAAA are underlined). The plasmid pSHAFT is a cloning vector, which contains the Ad5 fiber gene with the knob region deleted and replaced by a small linker containing *Sma*I and *Eco*ICRI restriction sites.[11] The plasmid was linearized by the enzymes *Sma*I and *Eco*ICRI digestion giving two blunt ends. After gel purification, the PCR product containing the CAV-1 knob was ligated into the linearized pSHAFT resulting in pSHAFT-CK1. This plasmid contains the chimeric fiber gene encoding the complete Ad5 fiber shaft with the CAV-1 knob domain followed by a stop codon and polyadenylation sequence at the 3′ end. The chimeric fiber gene in pSHAFT was digested with *Nco*I and *Mun*I to liberate a 0.75 kb DNA fragment containing the carboxy terminus of the shaft and the CAV-1 knob domain and then ligated into the *Nco*I–*Mun*I-digested shuttle vector PNEB.PK3.6[11] resulting in pNEB.PK.3.6-CK1.

Generation of recombinant adenovirus

Recombinant adenovirus genomes containing the chimeric CAV-1 fiber–knob gene were generated by homologous recombination in BJ5183 *Escherichia coli* with *Swa*I-linearized rescue plasmid PVK700 and the fiber containing *PacI-KpnI*-fragment of pNEB.PK.3.6-CK1. PVK700 was derived from pTG3602,[47] but contains an almost compete deletion of the fiber gene and a firefly luciferase reporter gene driven by the cytomegalovirus (CMV) immediate early promoter in place of the E1 region. Genomic clones were subjected to sequencing and PCR analysis prior to transfection into 293 cells. Ad5Luc1 is a replication-defective E1-deleted unmodified control Ad5 vector containing a firefly luciferase reporter gene also driven by the CMV promoter.[11] Ad5Luc1-CK2, previously named as Ad5Luc1-CK,[14] is a replication-defective E1-deleted Ad5-based vector containing the CAV-2 knob domain in a chimeric Ad5 fiber molecule. All vectors were propagated in 293 cells and purified by double cesium chloride (CsCl) ultracentrifugation and dialyzed against phoshate-buffered saline with Mg^{2+}, Ca^{2+}, and 10% glycerol. Final virus aliquots were analyzed for viral particle (vp) titer (absorbance at 260 nm) using a conversion factor of 1 OD = 10^{12} vp/ml. All vectors used in this study are essentially isogenic except for the fiber–knob modifications. Using a common vector structure would standardize all conditions including the reporter expression cassette while allowing analysis of gene transfer efficiency as a consequence of varying the knob.

PCR validation of viral genome

Viral DNA was extracted from 1×10^8 vp of Ad5Luc1, Ad5Luc1-CK1, and wild-type CAV-1[32] (Blood Mini Kit, Qiagen) and used as templates for PCR checking. To detect the presence of the Ad5 and CAV-1 fiber–knob genes, each viral genome was amplified in a PCR reaction mixture (Qiagen) containing 50 nM of primer pairs for 30 cycles of denaturation (94°C, 1 min), annealing (54°C, 1 min), and extension (72°C, 1 min). The sequences of the various fiber–knob primer sets are as follows: Ad5 (forward) 5′-AGTGCTCATCTTATTATA AGA-3′, Ad5 (reverse) 5′-CACCACCGCCCTATCCTG AT-3′; CAV-1 (forward) 5′-TATGGACTGGACCTGATC CAAACGTT-3′ and (reverse) 5′-TTTATCATTGATTTTCC CCCACATAGGTGAAGG-3′. PCR products were detected by 1% agarose gel electrophoresis with ethidium bromide staining.

Recombinant fiber–knob proteins

The Ad3, Ad5, and CAV-2 recombinant fiber proteins were produced and purified as described previously.[11,14] The recombinant knob domain of CAV-1 contains an N-terminus 6-histidine tag and was constructed in the pQE-81L expression plasmid (Qiagen, Hilden, Germany). The CAV-1 fiber–knob domain was amplified by PCR using the following primers: (forward) 5′-CAAACAC**GG** ATCCCCTCAAAACAAAA-3′ and (reverse) 5′-TTTAT CATTGATTTTCCCCCACATAGGTGAAGG-3′. The forward primer contains a two-basepair mutation (bold) to create a 5′- end *Bam*HI restriction site (underlined). The PCR product containing the canine 1 fiber–knob region was digested with *Bam*HI, gel purified, and ligated into *Bam*HI-*Sma*I-digested pQE-81L. The resulting plasmid pQE-81L-CAV-1 was analyzed by restriction analysis and sequenced. Expression plasmids were introduced into *E. coli*, and the 6-His-containing fiber–knob proteins from bacterial cultures were purified under native conditions in nickel-nitrilotriacetic acid (Ni-NTA) agarose columns (Qiagen). Concentrations of the final purified knob protein were determined by the Lowry method (Bio-Rad). The trimerization ability of the recombinant CAV-1 fiber–knob was confirmed by Western blot analysis of boiled and unboiled purified knob proteins using a mouse monoclonal Penta-His antibody (Qiagen) and a horseradish peroxidase-conjugated anti-mouse immunoglobulin antibody at a 1:3000 dilution (Dako Corporation, CA, USA), followed by incubation with 3-3′-diaminobenzene peroxidase substrate (DAB; Sigma Company, USA).

Western blot analysis

Aliquots of the Ad vectors equal to 5×10^9 viral particles were diluted into Laemmli buffer and incubated at room temperature or 95°C for 5 min and loaded onto a 4–20% gradient SDS-polyacrylamide gel (Bio-Rad, Hercules, CA, USA). Following electrophoresis protein separation, the protein samples were electroblotted onto a PVDF membrane. The primary 4D2 monoclonal antibody (recognizing the Ad5 fiber tail domain) was diluted 1:3000 (Lab Vision, Freemont, CA, USA) and used to probe the protein blot. Immunoblots were developed by addition of a secondary horseradish peroxidase-conjugated anti-mouse immuno-globulin antibody at a 1:3000 dilution (Dako Corporation, Carpentaria, CA, USA), followed by incubation with 3-3′-diaminobenzene peroxidase substrate for colorimetric development (DAB; Sigma Company, St Louis, MO, USA).

Ad-mediated gene transfer experiments

To determine gene transfer efficiency, 2×10^4 cells were seeded per well in a 24-well plate. The next day, the respective cells were infected for 1 h at 37°C with each vector at 100 vp/cell in 500 μl of infection medium containing 2% FCS. Luciferase activities of cell lysates were measured 48 h later using the Promega luciferase assay system (Madison, WI, USA). Experiments were performed in triplicates or six replicates (where indicated). Error bars represent standard deviations from the mean. For the gene transfer assays involving blocking conditions, recombinant fiber proteins at 0.5 and/or 1, 5, and 10 μg/ml final concentrations were incubated with the cells at 37°C in transduction media 30 min prior to the addition of the virus. Following infection for 1 h, the cells were washed with transduction media to remove unbound virus and the blocking agent. All cells were maintained at 37°C in an atmosphere of 5% CO_2. For gene transfer assays of patient tissue slices, all viral infections were performed with 500 vp/cell in 2% FCS complete culture media.[31] The cell number for the tissue slices was estimated at 1×10^6 cells/slice based on an approximate 10 cell slice thickness ($\sim$250 μm) and 8 mm slice diameter. Infections were allowed to proceed for 24 h. The medium was removed and replaced with 10% FCS-complete culture medium. The infected ovarian cancer tissue slices and human liver tissue slices were placed in cell culture lysis buffer (Promega) and homogenized with an ultra sonicator (Fisher Scientific Model 100) at a setting of 15 W for 10 s. The homogenate was centrifuged to pellet the debris, and the luciferase activities were measured using the Promega luciferase assay system (Madison, WI, USA). Experiments were performed in triplicate. Error bars represent s.d. from the mean. Protein concentration of the tissue homogenates was determined using a Bio-Rad DC protein assay kit (Bio-Rad, Hercules, CA, USA) to allow normalization of the gene expression data relative to the number of cells.

Statistics

Data are presented as mean values $\pm$ s.d. Statistical differences among groups were assessed with a two-tailed Student's *t*-test. $P(*) < 0.05$ was considered significant.

Acknowledgements

This work was supported by the following grants: Grant of the Deutsche Forschungsgemeinschaft Sto 647/1-1 (to MA Stoff-Khalili); Department of Defense W81XWH-05-1-0035, NIH Grant R01CA083821, R01CA94084 (to DT Curiel); R01CA93796 (to GP Siegal). We thank Lucretia Sumerel for invaluable technical assistance. DNA vectors pSHAFT, pNEB.PK.3.6, and pVK700 were generous gifts from Dr Victor Krasnykh.

References

1 Bauerschmitz GJ, Barker SD, Hemminki A. Adenoviral gene therapy for cancer: from vectors to targeted and replication competent agents (review). *Int J Oncol* 2002; **21**: 1161–1174.
2 Curiel DT, Douglas JT. *Adenoviral Vectors for Gene Therapy.* Academic Press: New York, 2002.
3 Yacoub A *et al*. MDA-7 regulates cell growth and radiosensitivity *in vitro* of primary (non-established) human glioma cells. *Cancer Biol Ther* 2004; **3**: 739–751.
4 Okegawa T *et al*. The dual impact of coxsackie and adenovirus receptor expression on human prostate cancer gene therapy. *Cancer Res* 2000; **60**: 5031–5036.
5 Qin M *et al*. Coxsackievirus adenovirus receptor expression predicts the efficiency of adenoviral gene transfer into non-small cell lung cancer xenografts. *Clin Cancer Res* 2003; **9**: 4992–4999.
6 Anders M *et al*. Inhibition of the Raf/MEK/ERK pathway up-regulates expression of the coxsackie and adenovirus receptor in cancer cells. *Cancer Res* 2003; **63**: 2088–2095.
7 Shayakhmetov DM, Li ZY, Ni S, Lieber A. Targeting of adenovirus vectors to tumor cells does not enable efficient transduction of breast cancer metastases. *Cancer Res* 2002; **62**: 1063–1068.
8 Wickham TJ, Carrion ME, Kovesdi I. Targeting of adenovirus penton base to new receptors through replacement of its RGD motif with other receptor-specific peptide motifs. *Gene Therapy* 1995; **2**: 750–756.
9 Dmitriev I *et al*. An adenovirus vector with genetically modified fibers demonstrates expanded tropism via utilization of a coxsackievirus and adenovirus receptor-independent cell entry mechanism. *J Virol* 1998; **72**: 9706–9713.
10 Shayakhmetov DM, Papayannopoulou T, Stamatoyannopoulos G, Lieber A. Efficient gene transfer into human CD34(+) cells by a retargeted adenovirus vector. *J Virol* 2000; **74**: 2567–2583.
11 Krasnykh VN, Mikheeva GV, Douglas JT, Curiel DT. Generation of recombinant adenovirus vectors with modified fibers for altering viral tropism. *J Virol* 1996; **70**: 6839–6846.
12 Hemmi S *et al*. The presence of human coxsackievirus and adenovirus receptor is associated with efficient adenovirus-mediated transgene expression in human melanoma cell cultures. *Hum Gene Ther* 1998; **9**: 2363–2373.
13 Miller CR *et al*. Differential susceptibility of primary and established human glioma cells to adenovirus infection: targeting via the epidermal growth factor receptor achieves fiber receptor-independent gene transfer. *Cancer Res* 1998; **58**: 5738–5748.
14 Glasgow JN *et al*. An adenovirus vector with a chimeric fiber derived from canine adenovirus type 2 displays novel tropism. *Virology* 2004; **324**: 103–116.
15 Zakhartchouk A, Connors W, van Kessel A, Tikoo SK. Bovine adenovirus type 3 containing heterologous protein in the C-terminus of minor capsid protein IX. *Virology* 2004; **320**: 291–300.
16 Kremer EJ, Boutin S, Chillon M, Danos O. Canine adenovirus vectors: an alternative for adenovirus-mediated gene transfer. *J Virol* 2000; **74**: 505–512.

17 Hess M *et al*. The avian adenovirus penton: two fibres and one base. *J Mol Biol* 1995; **252**: 379–385.
18 Soudais C *et al*. Canine adenovirus type 2 attachment and internalization: coxsackievirus-adenovirus receptor, alternative receptors, and an RGD-independent pathway. *J Virol* 2000; **74**: 10639–10649.
19 Curtis R, Barnett KC. The 'blue eye' phenomenon. *Vet Rec* 1983; **112**: 347–353.
20 Kremer EJ. CAR chasing: canine adenovirus vectors-all bite and no bark? *J Gene Med* 2004; (6 Suppl 1): S139–S151.
21 Marusyk RG, Norrby E, Lundqvist U. Biophysical comparison of two canine adenoviruses. *J Virol* 1970; **5**: 507–512.
22 Marusyk RG, Yamamoto T. Characterization of a canine adenovirus hemagglutinin. *Can J Microbiol* 1971; **17**: 151–155.
23 Marusyk RG. Comparison of the immunological properties of two canine adenoviruses. *Can J Microbiol* 1972; **18**: 817–823.
24 Marusyk RG, Hammarskjold ML. The genetic relationship of two canine adenoviruses as determined by nucleic acid hybridization. *Microbios* 1972; **5**: 259–264.
25 Green NM *et al*. Evidence for a repeating cross-beta sheet structure in the adenovirus fibre. *EMBO J* 1983; **2**: 1357–1365.
26 Rasmussen UB, Schlesinger Y, Pavirani A, Mehtali M. Sequence analysis of the canine adenovirus 2 fiber-encoding gene. *Gene* 1995; **159**: 279–280.
27 Soudais C *et al*. Canine adenovirus type 2 attachment and internalization: coxsackievirus-adenovirus receptor, alternative receptors, and an RGD-independent pathway. *J Virol* 2000; **74**: 10639–10649.
28 Kim M *et al*. The coxsackievirus and adenovirus receptor acts as a tumour suppressor in malignant glioma cells. *Br J Cancer* 2003; **88**: 1411–1416.
29 Kanerva A *et al*. Gene transfer to ovarian cancer *versus* normal tissues with fiber-modified adenoviruses. *Mol Ther* 2002; **5**: 695–704.
30 Kanerva A *et al*. Targeting adenovirus to the serotype 3 receptor increases gene transfer efficiency to ovarian cancer cells. *Clin Cancer Res* 2002; **8**: 275–280.
31 Kirby TO *et al*. A novel *ex vivo* model system for evaluation of conditionally replicative adenoviruses therapeutic efficacy and toxicity. *Clin Cancer Res* 2004; **10**: 8697–8703.
32 Morrison MD, Onions DE, Nicolson L. Complete DNA sequence of canine adenovirus type 1. *J Gen Virol* 1997; **78**: 873–878.
33 Hemminki A *et al*. A canine conditionally replicating adenovirus for evaluating oncolytic virotherapy in a syngeneic animal model. *Mol Ther* 2003; **7**: 163–173.
34 Hu RL *et al*. Detection and differentiation of CAV-1 and CAV-2 by polymerase chain reaction. *Vet Res Commun* 2001; **25**: 77–84.
35 Jouvenne P, Hamelin C. Comparative analysis of the canAV-1 and canAV-2 genomes. *Intervirology* 1986; **26**: 109–114.
36 Willis AM. Canine viral infections. *Vet Clin North Am Small Anim Pract* 2000; **30**: 1119–1133.
37 Erles K, Dubovi EJ, Brooks HW, Brownlie J. Longitudinal study of viruses associated with canine infectious respiratory disease. *J Clin Microbiol* 2004; **42**: 4524–4529.
38 Short JJ *et al*. Adenovirus serotype 3 utilizes CD80 (B7.1) and CD86 (B7.2) as cellular attachment receptors. *Virology* 2004; **322**: 349–359.
39 Sirena D *et al*. The human membrane cofactor CD46 is a receptor for species B adenovirus serotype 3. *J Virol* 2004; **78**: 4454–4462.
40 Li Y *et al*. Loss of adenoviral receptor expression in human bladder cancer cells: a potential impact on the efficacy of gene therapy. *Cancer Res* 1999; **59**: 325–330.
41 Cripe TP *et al*. Fiber knob modifications overcome low, heterogeneous expression of the coxsackievirus-adenovirus receptor that limits adenovirus gene transfer and oncolysis for human rhabdomyosarcoma cells. *Cancer Res* 2001; **61**: 2953–2960.
42 Vanderkwaak TJ *et al*. An advanced generation of adenoviral vectors selectively enhances gene transfer for ovarian cancer gene therapy approaches. *Gynecol Oncol* 1999; **74**: 227–234.
43 Vickers AE *et al*. Organ slice viability extended for pathway characterization: an *in vitro* model to investigate fibrosis. *Toxicol Sci* 2004; **82**: 534–544.
44 Krumdieck CL, dos Santos JE, Ho KJ. A new instrument for the rapid preparation of tissue slices. *Anal Biochem* 1980; **104**: 118–123.
45 Kirby To RA *et al*. A Novel *ex vivo* model system for evaluation of CRAds therapeitic efficacy and toxixity. *Clin Cancer Res* 2004; **10**: 8697–8703.
46 Olinga P *et al*. Comparison of five incubation systems for rat liver slices using functional and viability parameters. *J Pharmacol Toxicol Methods* 1997; **38**: 59–69.
47 Chartier C *et al*. Efficient generation of recombinant adenovirus vectors by homologous recombination in *Escherichia coli*. *J Virol* 1996; **70**: 4805–4810.

Available online at www.sciencedirect.com
SCIENCE DIRECT®
Biochemical and Biophysical Research Communications 335 (2005) 205–214
BBRC
www.elsevier.com/locate/ybbrc

Reovirus σ1 fiber incorporated into adenovirus serotype 5 enhances infectivity via a CAR-independent pathway

Yuko Tsuruta [a], Larisa Pereboeva [a], Joel N. Glasgow [a], Cindy L. Luongo [b], Svetlana Komarova [a], Yosuke Kawakami [a], David T. Curiel [a,*]

[a] *Division of Human Gene Therapy, Departments of Medicine, Pathology, and Surgery, and The Gene Therapy Center, The University of Alabama at Birmingham, Birmingham, AL 35294, USA*
[b] *Department of Microbiology, The University of Alabama at Birmingham, Birmingham, AL 35294, USA*

Received 23 June 2005
Available online 25 July 2005

Abstract

Adenovirus serotype 5 (Ad5) has been used for gene therapy with limited success because of insufficient infectivity in cells with low expression of the primary receptor, the coxsackie and adenovirus receptor (CAR). To enhance infectivity in tissues with low CAR expression, tropism expansion is required via non-CAR pathways. Serotype 3 Dearing reovirus utilizes a fiber-like σ1 protein to infect cells expressing sialic acid and junction adhesion molecule 1 (JAM1). We hypothesized that replacement of the Ad5 fiber with σ1 would result in an Ad5 vector with CAR-independent tropism. We therefore constructed a fiber mosaic Ad5 vector, designated as Ad5-σ1, encoding two fibers: the σ1 and the wild-type Ad5 fiber. Functionally, Ad5-σ1 utilized CAR, sialic acid, and JAM1 for cell transduction and achieved maximum infectivity enhancement in cells with or without CAR. Thus, we have developed a new type of Ad5 vector with expanded tropism, possessing fibers from Ad5 and reovirus, that exhibits enhanced infectivity via CAR-independent pathway(s).

Keywords: Gene therapy; Adenovirus; Reovirus; σ1 spike protein; Tropism expansion; Coxsackie and adenovirus receptor

Adenoviral vectors, in particular human serotype 5 (Ad5), have been widely employed for cancer gene therapy applications, owing to their unparalleled ability to accomplish in vivo gene transfer [1]. Despite this capacity, the limited efficacies noted in human gene therapy trials have suggested deficiencies of this vector vis-à-vis the achievement of efficient gene delivery. In this regard, it has been observed that human tumor cells frequently manifest a relative deficiency of the primary Ad receptor, coxsackie and adenovirus receptor (CAR) [2]. This CAR deficiency renders many tumor cells resistant to Ad infection, undermining cancer gene therapy strategies that require efficient tumor cell transduction. Thus, this unanticipated aspect of tumor biology potentially confounds direct exploitation of current generation of human Ad-based vectors.

To address this issue, strategies have been proposed to alter the tropism of Ad to accomplish CAR-independent infection of tumor cells [2]. Initial efforts to this end focused on the use of so-called retargeting adaptors that cross-link Ad to non-CAR receptors that are overexpressed on tumor cells [2,3].

Genetic capsid modification has also been endeavored to achieve these same functional ends. This approach has rationally focused on the fiber knob domain, the primary determinant of Ad tropism, to achieve CAR-independent cell entry. Ad fiber pseudotyping, the genetic substitution of either the entire fiber or the fiber knob domain with its structural counterpart from another human Ad serotype, has been realized. Fiber-pseudotyped vectors display CAR-independent

* Corresponding author. Fax: +1 205 975 7476.
E-mail address: curiel@uab.edu (D.T. Curiel).

0006-291X/$ - see front matter © 2005 Elsevier Inc. All rights reserved.
doi:10.1016/j.bbrc.2005.07.054

tropism by virtue of the natural diversity in receptor recognition found in species B and D Ad fibers. This approach has identified vectors with superior infectivity to Ad5 in several clinically relevant cell types [4–6]. These studies clearly established that genetic capsid modification can achieve the goal of enhanced transduction of tumor cells via CAR-independent cell entry.

On this basis, advanced strategies to achieve further infectivity enhancement have been proposed. We previously derived a fiber mosaic Ad5 vector that incorporates two distinct fibers: the Ad5 fiber and a chimeric fiber that incorporates the Ad3 fiber knob domain. This strategy provided viral entry via two different pathways with additive gains in infectivity [7]. We next explored a strategy to expand Ad tropism by means of exploiting the tropism of non-Ad viruses. Specifically, we endeavored the construction and characterization of fiber mosaic Ad5 vectors that contained fibers of Ad5 and reovirus. In particular, the receptor-binding molecule of serotype 3 Dearing (T3D) reovirus, called the σ1 protein, was incorporated into fiber mosaic Ad5 vectors together with the wild-type Ad5 fiber. This fiber-like σ1 attachment protein is known to bind sialic acid [8] and junction adhesion molecule 1 (JAM1) [9], which together determine T3D reovirus tropism. Since T3D reovirus tropism is clearly distinct from that of Ad, the σ1 protein is a promising candidate for incorporation into a fiber mosaic Ad vector, which could bind to neoplastic cells using the widely expressed cell receptors JAM1, sialic acid, and CAR. Our study establishes a novel strategy to achieve infectivity enhancement based on a fiber mosaic Ad5 vector, which contains fibers from different virus families.

Materials and methods

Cell lines. The 293 cells were purchased from Microbix (Toronto, Ontario, Canada). Human embryonic rhabdomyosarcoma RD cells, human glioma cell line U118MG, human head and neck tumor cell line FaDu, human ovarian cancer cell lines ES-2, OV-3, SK-OV-3, and OVCAR-3, Chinese hamster ovary (CHO) cells, and Lec2 cells were obtained from the American Type Culture Collection (ATCC, Manassas, VA). Human ovarian adenocarcinoma cell lines OV-4 and Hey were a kind gift from Dr. Timothy J. Eberlein (Harvard Medical School, Boston, MA) and Dr. Judy Wolf (M.D. Anderson Cancer Center, Houston, TX), respectively. L929 cells, U118MG-hCAR-tailless cells, and 211B cells were maintained as described previously [8,10,11]. Cell lines were cultured in media recommended by suppliers (Mediatech, Herndon, VA, and Irvine Scientific, Santa Ana, CA). FBS was purchased from Hyclone (Logan, UT). All cells were grown at 37 °C in a humidified atmosphere of 5% CO_2. Primary human ovarian carcinoma cells were established in culture from fresh malignant ascites fluid obtained from patients with pathologically confirmed ovarian adenocarcinoma during surgery at the University of Alabama at Birmingham (UAB) Hospital. Approval was obtained from the UAB Institutional Review Board before acquisition of samples. Cancer cells were purified from ascites fluid by a previously described immunomagnetic-based method [12].

Generation of the σ1 chimeric fiber construct. A schematic of the σ1 chimeric fiber structure is shown in Fig. 1A. To design the σ1 chimeric fiber, the fiber tail domain of Ad5 was amplified by PCR from plasmid pNEB.PK.3.6 [5]. The PCR product was cloned into pGEM4ZT3DS1 that encodes T3D reovirus σ1, resulting in pGEM4ZT3DS1delBamAd5tail. The Ad5tail and entire σ1 sequence was PCR-amplified from pGEM4ZT3DS1delBamAd5tail, using the primers 5′-GCCATG AAGCGCGCAAGACCGTCTGAA (sense), 5′-TTTACTAGATGA AATGCCCCAGTGCCGC (the first antisense for addition of stop codon and polyadenylation signal), and 5′-GAAATCAATTGTTTAC TAGATGAAATGCCC (the second antisense for addition of *Mun*I restriction site). The resultant PCR product of the σ1 chimeric fiber was cloned into pNEB.PK.3.6, resulting in pNEB.PK.3.6Ad5tail/σ1. The sequence of pNEB.PK.3.6Ad5tail/σ1 was confirmed by DNA sequencing. This σ1 chimeric fiber was designated as F5S1.

To design the expression vector for the σ1 chimeric fiber, we cloned the F5S1 sequence into plasmid pShuttle-CMV (Qbiogene, Carlsbad, CA). The resultant expression plasmid was designated as pShuttle-CMV-AdSig.

Generation of shuttle plasmids for fiber mosaic Ad5 genome. The construct was based on a fiber mosaic Ad genome that encodes two fiber genes (the wild-type Ad5 fiber and Fiber-Fibritin, designated as FF) in the L5 region, which has been described previously [13]. Our strategy was to replace the fibritin part in the chimeric fiber FF with the σ1 sequence and create the σ1 chimeric fiber (F5S1H). Coding sequence of σ1 was amplified from plasmid pNEB.PK.3.6Ad5tail/σ1 with the primers 5′-CAGAACGTTGGGGATCCTCGCCTACG TGAAGAAGTAGTAC and 5′-TCCTCTAGATCCGCCCGTGAAA CTACGCGGGTACGAAAC. The PCR product was cloned into *Acl*I/*Xba*I sites of FF in plasmid pZpTG 5FF3 [13]. We replaced the fibritin sequence with σ1 coding sequence in-frame with a carboxy-terminally encoded 6-histidine (6-His) stretch, resulting in F5S1H. The resulting plasmid was designated as pZpTG5F/S1.6H. An *Age*I/*Age*I fragment of this plasmid was cloned into the *Age*I site of pNEB.PK.FSP [5] to obtain a shuttle plasmid, designated as pNEB.PK.FSPF5S1/F5, which contains tandem fiber genes: the σ1 chimeric fiber, F5S1H, and the wild-type Ad5 fiber.

Generation of recombinant Ad. A schematic of the viruses used in this study is shown in Fig. 1B. Recombinant Ad5 genomes containing the tandem fiber genes were derived by homologous recombination in *Escherichia coli* BJ5183 with *Swa*I-linearized rescue plasmid pVK700 and the tandem fiber-containing *Pac*I and *Kpn*I-fragment of pNEB.PK.FSPF5S1/F5 essentially as described previously [14]. The recombinant region of the genomic clones was sequenced prior to transfection into 293 cells. All vectors were propagated in 293 cells and purified using a standard protocol [15]. The resultant fiber mosaic virus was Ad5-σ1. Viral particle (v.p.) concentration was determined by the method of Maizel et al. [16]. An infectious titer was determined according to the AdEasy Vector System (Qbiogene).

PCR amplification of viral genome fragments. Viral DNA was amplified using the Taq PCR Core Kit (Qiagen, Valencia, CA). The sequences of the primers were as follows: Ad5tail-sense 5′-ATGAAGC GCGCAAGACCGTCTGAAGAT; Ad5knob-antisense 5′-TTATTCT TGGGCAATGTATGAAAAAGT; and σ1head-antisense 5′-ATTCT TGCGTGAAACTACGCGG.

Protein electrophoresis and Western blotting. To detect the incorporation of fibers in virus particles, Ad vectors equal to 5.0×10^9 v.p. were resolved by SDS–PAGE and Western blotting as described previously [13].

To detect trimerization of the σ1 chimeric fiber, F5S1, the expression plasmid pShuttle-CMV-AdSig was transiently transfected into 293 cells using SuperFect Transfection Reagent (Qiagen). Cell lysates were used for SDS–PAGE and Western blotting. For JAM1 detection, a panel of cell lines was harvested for SDS–PAGE and analyzed by Western blotting using anti-JAM1 monoclonal antibody (BD Biosciences Clontech, Palo Alto, CA).

Recombinant proteins. Recombinant T3D σ1 was produced as described in Chandran et al. [17]. Ad5 fiber knob domain recombinant

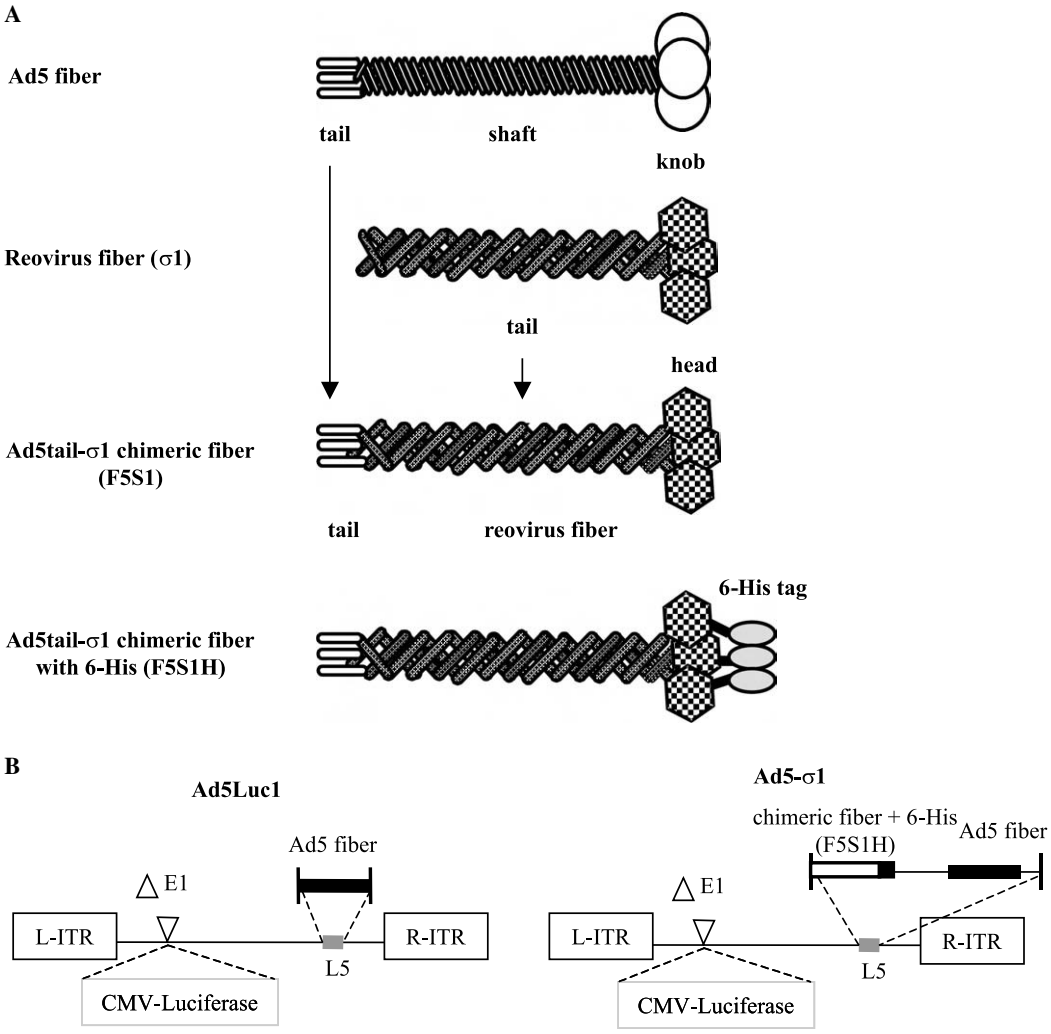

Fig. 1. Schema of fiber mosaic Ad5 genomes. (A) Key components of the σ1 chimeric fiber. In the σ1 chimeric fiber, the tail of Ad5 fiber is fused to the reovirus fiber protein σ1 (designated as F5S1). A six-histidine (6-His) tag is fused to the carboxy-terminus of the σ1 chimeric fiber through a linker (designated as F5S1H). (B) Map of Ad5 genomes with fiber modification. In both vectors, the E1 region is replaced by CMV promoter/luciferase transgene cassette. Ad5Luc1 is a control virus that carries the wild-type Ad5 fiber. Ad5-σ1 is a fiber mosaic vector that carries the σ1 chimeric fiber with a carboxy-terminal 6-His tag (F5S1H) as well as the wild-type Ad5 fiber.

protein was produced and purified as described previously [5]. Concentration of protein in all experiments was determined by the Bradford method (Bio-Rad Laboratories, Hercules, CA).

In vitro gene transfer assays. Cells were infected with virus at 37 °C for 1 h and unbound virus was washed away. After 24 h of incubation at 37 °C, a luciferase assay was performed (Promega, Madison, WI) according to the manufacturer's instructions. Data are presented as mean values ± SD.

Competitive inhibition assay. Recombinant Ad5 fiber knob proteins or anti-JAM1 polyclonal antibody (c-15, Santa Cruz Biotechnology, Santa Cruz, CA) was incubated with the cells at 37 °C for 15 min prior to infection. Alternatively, cells were treated with 333 milliunits/ml of *Clostridium perfringens* neuraminidase type X (Sigma–Aldrich, St. Louis, MO) at 37 °C for 30 min to remove cell-surface sialic acid, followed by two washes with PBS. Cells were then adsorbed with viruses at 37 °C for 1 h. Unbound virus and blocking agents were washed away. After 24 h of incubation at 37 °C, the cells were processed for luciferase assay, as described above. For σ1 blocking experiments, anti-T3D σ1 antibody (9BG5, a gift from Dr. Patrick W.K. Lee, University of Calgary, Calgary, Canada) [18] was incubated with virus at room temperature for 1 h prior to cell infection. Subsequent procedures were same as described above. Data are presented as mean values ± SD.

Flow cytometry. For CAR detection, the cells were incubated with 2 μg/ml of the anti-human CAR monoclonal antibody RmcB (hybridoma was purchased from ATCC) or normal mouse IgG1κ (Sigma–Aldrich) for 1 h on ice. Subsequently, the cells were washed and incubated with FITC-conjugated anti-mouse IgG (Sigma–Aldrich) for an additional 1 h. For sialic acid measurement, cells were incubated with 1 μg/ml FITC-labeled wheat germ agglutinin (WGA; Sigma–Aldrich) on ice for 1 h. After washing with 1% BSA/PBS, the cells were analyzed by flow cytometry at the UAB FACS Core Facility.

Results

Generation of a chimeric fiber (F5S1) containing reovirus σ1

To create a functional chimeric fiber structurally compatible with Ad5 capsid incorporation, we designed the

σ1 chimeric fiber to comprise the amino-terminal tail segment of the Ad5 fiber sequence genetically fused to the entire T3D σ1 protein, with (F5S1H) or without (F5S1) a carboxy-terminal 6-His tag as a detection marker (Fig. 1A).

Prior to Ad5 vector design, we evaluated the trimerization capacity of the σ1 chimeric fiber (F5S1), using pShuttle-CMV-AdSig, a fiber expression plasmid. Following transfection of 293 cells, cell lysates were subjected to SDS–PAGE and Western blot analysis using two primary antibodies, the 4D2 monoclonal antibody (Neomarkers, Fremont, CA) that recognizes the Ad5 fiber tail domain common to both the wild-type Ad5 and the σ1 chimeric fiber, and an anti-T3D σ1 polyclonal antibody (a gift from Dr. Max L. Nibert, Harvard Medical School, Boston, MA) that recognizes σ1. We detected a band for Ad5 fiber from 211B cell lysates [10] at approximately 180 kDa with the 4D2 antibody (Fig. 2, lane 1). This band corresponds to the trimeric fiber molecule, while an approximately 60 kDa band in boiled lysates represents fiber monomers (lane 2). The chimeric fiber was detected with both the 4D2 antibody (lane 3) and an anti-T3D σ1 antibody (data not shown) at an apparent molecular mass of 160–170 kDa. When heat denatured, the monomeric chimeric fiber was detected at an apparent molecular mass of 50 kDa (lane 4). This analysis demonstrates that the σ1 chimeric fiber F5S1 is capable of trimerization, which is required for Ad capsid incorporation.

Construction of fiber mosaic viruses

We sought to create a fiber mosaic Ad5 encoding both the Ad5 fiber and chimeric fibers in the L5 region of the Ad5 genome. We employed a tandem-fiber cassette wherein the F5S1H σ1 chimeric fiber was positioned upstream of the wild-type fiber gene. In this configuration, each fiber was positioned before the untranslated sequences of the wild-type fiber to provide equal transcription, splicing, polyadenylation, and regulation by the major late promoter. We constructed E1-deleted recombinant Ad genomes (Ad5-σ1) containing the wild-type Ad5 fiber, the σ1 chimeric fiber (F5S1H), and a firefly luciferase reporter gene controlled by the CMV immediate early promoter/enhancer. Following virus rescue and large-scale propagation in 293 cells, we obtained Ad5-σ1 vector at concentrations ranging from 1.1×10^{11} v.p./ml to 5.31×10^{12} v.p./ml, depending on the individual preparation. These concentrations compared favorably with that of Ad5Luc1 at 3.74×10^{12} v.p./ml. In addition, the v.p./plaque-forming unit (PFU) ratios determined for Ad5-σ1 and Ad5Luc1 were 22 and 13.3, respectively, indicating excellent virion integrity for both species. Of note, the control vector used throughout this study, Ad5Luc1, is isogenic to Ad5-σ1 in all respects except for the fiber locus.

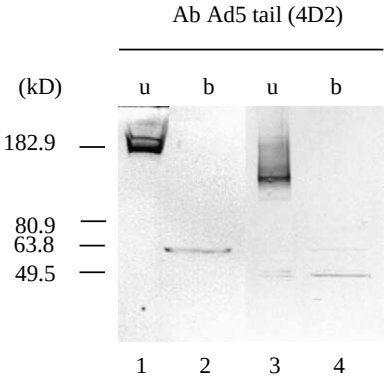

Fig. 2. Western blot analysis of F5S1 chimeric fiber protein in lysates of transiently transfected cells. Fiber proteins were detected by anti-Ad5 fiber tail antibody (4D2). Lanes 1 and 2, 211B cell lysate as a positive control for the wild-type Ad5 fiber; lanes 3 and 4, pShuttle-CMV-AdSig transfected 293 cell lysate for F5S1 chimeric fiber detection (without 6-His). We used cell lysates from 211B cells expressing the wild-type Ad5 fiber as a positive control for detection of Ad5 fiber. The samples in lanes 2 and 4 were heat denatured (b), which resulted in dissociation of trimeric proteins to monomers, while lanes 1 and 3 contain proteins in their native trimeric configuration (unboiled (u)).

Definition of fiber gene configurations for fiber mosaic Ad

We confirmed the fiber genotype of Ad5Luc1 and Ad5-σ1 via diagnostic PCR, using Ad5 fiber or the σ1 chimeric fiber primer pairs and genomes from purified virions as PCR templates (Fig. 3A). To confirm that Ad5-σ1 virions contained both trimerized fibers, we performed SDS–PAGE followed by Western blot analysis on viral particles. Using the 4D2 antibody we observed fiber bands at approximately 180 kDa for unboiled samples of Ad5Luc1 and Ad5-σ1 virions, corresponding to fiber trimers (Fig. 3B, lanes 1 and 3). In boiled samples, the 4D2 antibody detected bands of apparent molecular mass of approximately 60 kDa, indicative of fiber monomers (lanes 2 and 4). Due to the near-identical sizes of the σ1 chimeric and the wild-type Ad5 fiber proteins, it was difficult to visualize both fibers simultaneously via Western blot with 4D2.

To confirm the presence of the σ1 chimeric fiber protein in virions, we used the anti-Penta His monoclonal antibody (Qiagen) that recognizes 6-His tags (Fig. 3C) and the anti-T3D σ1 antibody (Fig. 3D). Using the anti-Penta His antibody, we observed the fiber bands corresponding to both trimeric and monomeric σ1 chimeric fiber proteins (Fig. 3C, lanes 2 and 3). The trimeric band of the σ1 chimeric fiber was also detected with the anti-T3D σ1 antibody (Fig. 3D, lane 3), however, the monomeric band of the σ1 chimeric fiber protein was faint because of relatively weak binding affinity of the anti-T3D σ1 antibody (Fig. 3D, lanes 2 and 4). These results confirm that the trimeric F5S1H σ1 chimeric fiber was incorporated into Ad5-σ1 virions.

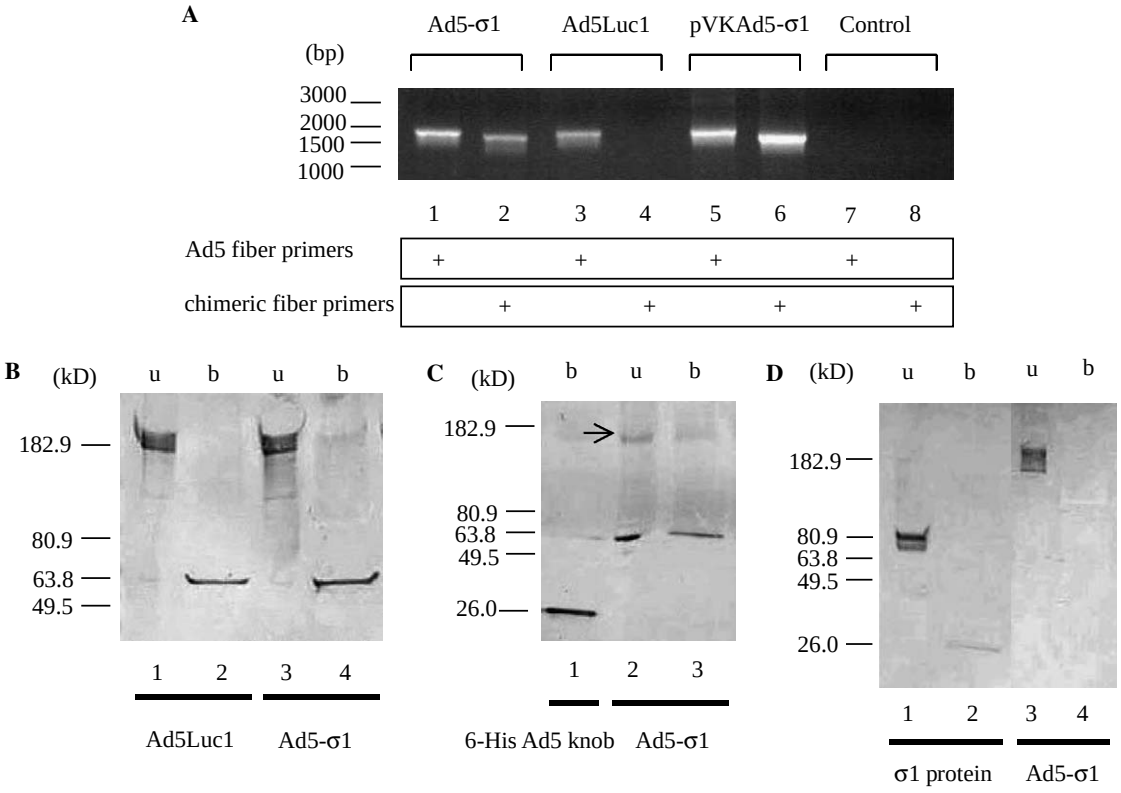

Fig. 3. Analysis of fibers in rescued viral particles. (A) Detection of fiber genes in Ad genome. Rescued viral particles were analyzed with PCR, using pairs of Ad5 fiber primers or σ1 chimeric fiber primers. pVKAd5-σ1 was used as a positive control for both fibers. No PCR template is designated as Control. (B–D) Western blot analysis of fiber proteins in purified virions. (B) A total of 5.0×10^9 v.p. per lane of Ad5Luc1 with the wild-type Ad5 fiber (lanes 1 and 2) or Ad5-σ1 with dual fibers (lanes 3 and 4) were resuspended in Laemmli buffer prior to SDS–PAGE and electrotransfer and detected with the 4D2 anti-Ad5 fiber tail antibody. The samples in lanes 2 and 4 were boiled (b), while lanes 1 and 3 (unboiled (u)) contain proteins in their native trimeric configuration. (C) A total of 5.0×10^9 v.p. per lane of Ad5-σ1 with dual fibers (lanes 2 and 3) was probed with an anti-6-His antibody. Lane 1, recombinant Ad5 knob with a 6-His tag as a positive antibody control; lane 2, unboiled Ad5-σ1 virions; and lane 3, boiled Ad5-σ1 virions. The arrow indicates the position of the trimeric σ1 chimeric fiber protein. (D) A total of 5.0×10^9 v.p. per lane of Ad5-σ1 with dual fibers (lanes 3 and 4) were probed with an anti-T3D σ1 antibody. Lanes 1 and 2, recombinant σ1 protein. The samples in lanes 2 and 4 were boiled, while lanes 1 and 3 contain proteins in their native trimeric configuration (unboiled).

Ad5-σ1 vector exhibits native Ad5 tropism

Our hypothesis was that the inclusion of the σ1 chimeric fiber, F5S1H, into an Ad5 vector would provide infectivity enhancement to Ad-refractory cell types via expanded vector tropism. To test whether this vector retained CAR-dependent tropism, we evaluated Ad5-σ1 infection in a pair of tumor cell lines that vary only in their CAR expression. The human U118MG glioma cell line is CAR-deficient [11]. The U118MG-hCAR-tailless cell is a CAR-positive variant line that artificially expresses the extracellular domain of human CAR [11]. Ad5Luc1 was used as a positive control for CAR binding. As shown in Fig. 4A, Ad5Luc1 exhibited CAR-dependent tropism, as shown by a 40-fold increase in luciferase transgene expression in U118MG-hCAR-tailless cells relative to the parental CAR-deficient U118MG cells. Similarly, Ad5-σ1 exhibited CAR-dependent tropism, as demonstrated by a 53-fold increase in transgene expression in U118MG-hCAR-tailless cells relative to the CAR-deficient U118MG cells (Fig. 4A). Incubation of U118MG-hCAR-tailless cells with recombinant Ad5 knob protein at 50 μg/ml prior to infection efficiently inhibited over 70% of Ad5Luc1 and Ad5-σ1 luciferase activity (Fig. 4B). These data indicate that Ad5-σ1 retains CAR-based tropism, confirming the functionality of the wild-type fiber in our fiber mosaic Ad5.

Ad5-σ1 vector exhibits sialic acid- and JAM1-dependent tropism

To confirm that Ad5-σ1 exploits the non-CAR receptor sialic acid and JAM1 by virtue of the chimeric fiber, we further characterized Ad5-σ1 tropism by performing competitive blocking experiments using 9BG5, a σ1-specific monoclonal antibody that recognizes the T3D σ1 head domain and blocks σ1/JAM1 interaction [18]. Pre-incubation of Ad5-σ1 with 9BG5 prior to infection blocks over 50% of Ad5-σ1 transgene expression in L929 cells, a sialic acid and JAM1-positive cell line commonly used for propagating reovirus (Fig. 4C).

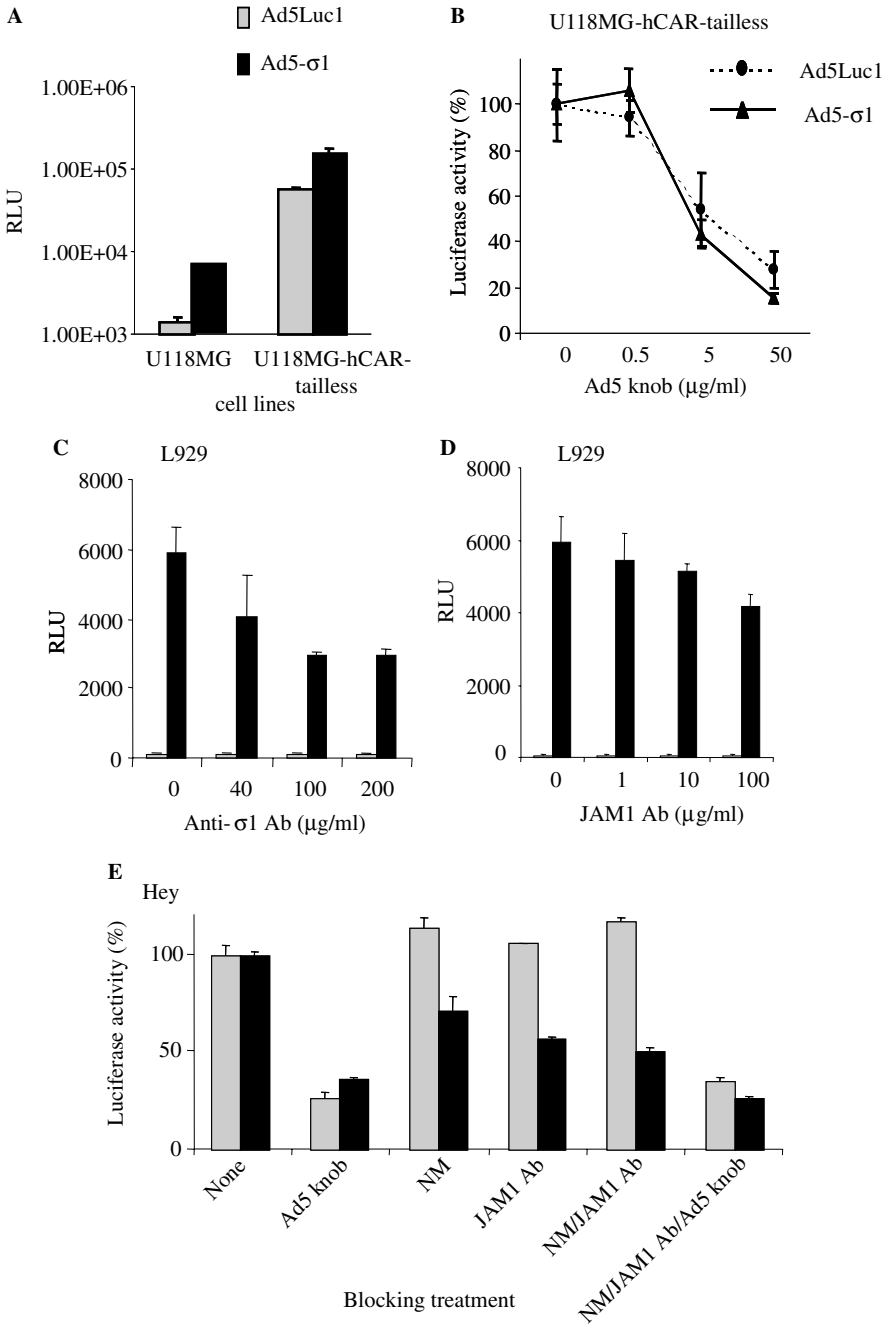

Fig. 4. Evaluation of the efficacy and receptor specificity of Ad5-σ1 mediated gene transfer. (A) Ad5-σ1 infection of a pair of tumor cell lines that vary only in their CAR expression. U118MG is a parental CAR-deficient human glioma cell line, whereas U118MG-hCAR-tailless stably expresses the extracellular domain of human CAR. Cells were infected with Ad5Luc1 (gray bar) and Ad5-σ1 (black bar) at 10 v.p./cell. Luciferase activity was measured 24 h post-infection and is expressed as relative light units (RLU). (B) Recombinant Ad5 fiber knob protein blocks Ad5-σ1 and Ad5Luc1 gene transfer. U118MG-hCAR-tailless cells were incubated with 100 v.p./cell of Ad5-σ1 or Ad5Luc1 with or without recombinant Ad5 fiber knob protein at the indicated concentrations. Luciferase activity was determined 24 h post-infection. All luciferase values were normalized against the activity of controls receiving no knob valued at 100%. (C) σ1 antibody blocks Ad5-σ1 gene transfer. σ1 antibody was incubated with Ad5-σ1 or Ad5Luc1 at 100 v.p./cell for 1 h prior to the infection to L929 cells. Luciferase activity was determined 24 h post-infection. (D) An anti-JAM1 antibody blocks Ad5-σ1 infection. L929 cells were incubated with 100 v.p./cell of Ad5-σ1 or Ad5Luc1 with or without anti-JAM1 antibody (JAM1 Ab) at the indicated concentrations. Luciferase activity was determined 24 h post-infection. (E) Analysis of Ad5-σ1 receptor usage in Hey cells. *C. perfringens* neuraminidase (NM), an anti-JAM1 antibody (JAM1 Ab), and recombinant Ad5 fiber knob protein (Ad5 knob) were employed to block Ad5-σ1 infection. Hey cells were either untreated or treated with 333 milliunits/ml neuraminidase, 100 μg/ml anti-JAM1 antibody, 50 μg/ml recombinant Ad5 fiber knob protein, both neuraminidase and an anti-JAM1 antibody or combined reagents with neuraminidase, anti-JAM1 antibody, and recombinant Ad5 fiber knob protein. Cells were incubated with Ad5-σ1 or Ad5Luc1 at 100 v.p./cell and harvested 24 h later for luciferase activity. All luciferase values were normalized against the activity of controls receiving no blocking treatment valued at 100%. Each data point is an average of four replicates. The error bars indicate standard deviation.

Table 1
Ad5-σ1 luciferase gene expression and co-receptor expression in various cell lines

Cell line	JAM1[a]	Sialic acid[b]	CAR[c]	CAR reference	Activity vs. Ad5Luc1[d]
Fold increase in luciferase					
L929	P	P	L/N	Flow cytometry data	45.3
OV-4	P	P	L/N	Flow cytometry data	5.8
Hey	P	P	L/N	Flow cytometry data	7.0
OV-3	P	P	L/N	Flow cytometry data	4.7
ES-2	P	P	L/N	Flow cytometry data	10.7
SK-OV-3	P	P	L/N	Kashentseva et al. [22]	4.4
OVCAR-3	P	P	M	Kelly et al. [21]	8.5
U118MG	L/N	P	L/N	Kim et al. [11]	6.1
U118MG-hCAR-tailless	L/N	P	P	Kim et al. [11]	5.5
RD	L/N	P	L/N	Cripe et al. [20]	6.4
FaDu	P	P	L/N	Kasono et al. [19]	3.9
CHO	L/N	P	L/N	Flow cytometry data	6.8
Lec2	L/N	N	L/N	Flow cytometry data	2.3

[a] P, highly JAM1-positive; L/N, little or none. As determined by Western blot analysis.
[b] P, highly sialic acid-positive; N, none. As determined by flow cytometric analysis.
[c] P, highly CAR-positive; M, moderate; L/N, little or none.
[d] Multiplicity of infection ranged from 10 to 1000 v.p./cell. Luciferase activity was measured at 24 h post-infection.

The σ1 protein has been reported to utilize the co-receptors JAM1 and sialic acid [8,9]. It has been shown that the σ1 knob-like head domain binds to JAM1 localized on the cell surface and that an anti-JAM1 antibody reduced reovirus replication 10- to 100-fold [9]. Similarly, in the presence of anti-σ1 or anti-JAM1 monoclonal antibodies, a 4-fold decrease in sialic acid-independent σ1 binding has been reported [9]. To further explore the role of JAM1 in Ad5-σ1 infection, we performed competitive blocking experiments using an anti-JAM1 antibody. We used the JAM1-positive L929 cell line for these studies. Exposure of L929 cells to 100 μg/ml anti-JAM1 antibody resulted in approximately 30% inhibition of Ad5-σ1 transgene expression (Fig. 4D). To further clarify Ad5-σ1 tropism, we performed neuraminidase treatment to remove cell-surface sialic acid and competitive blocking experiments using an anti-JAM1 antibody, and Ad5 knob protein. For this analysis, we used the low-CAR human ovarian cancer Hey cell line due to its high sialic acid and JAM1 expression. Transduction by Ad5-σ1 was inhibited 29% by neuraminidase, 42% by an anti-JAM1 antibody, and 50% by combined treatment with neuraminidase and an anti-JAM1 antibody (Fig. 4E). Combined treatment with neuraminidase, an anti-JAM1 antibody, and Ad5 knob protein reduced transduction 74% compared to controls receiving no blocking agent (Fig. 4E), with similar results in U118MG and OV-3 cells (data not shown). Together, these findings confirm that the Ad5-σ1 vector utilizes sialic acid and the JAM1-binding domain of the σ1 chimeric fiber (F5S1H) for cell transduction.

Ad5-σ1 vector exhibits increased transduction of CAR-deficient cells

To demonstrate the contribution of the σ1 chimeric fiber to Ad tropism expansion, we evaluated Ad5-σ1 infectivity in several cell lines. Table 1 shows the co-receptor expression profiles and infectivity of cell lines tested [19–22]. As expected, Ad5-σ1 provided the maximum increase in gene transfer (45-fold) relative to Ad5-Luc1 in L929 cells, which express σ1 receptors sialic acid and JAM1, but no detectable CAR (Table 1, Fig. 5A). In other sialic acid/JAM1-positive and low-CAR cancer cell lines, Ad5-σ1 also provided increased luciferase activity from 3.9-fold (FaDu) to 10.7-fold (ES-2) (Table 1, Fig. 5A). Furthermore, in cancer cells expressing only sialic acid that are JAM1/CAR-negative, Ad5-σ1 provided more than 6-fold higher luciferase activity relative to Ad5Luc1 in RD and U118MG cells (Table 1, Fig. 5A). Thus, we found that the presence of sialic acid and/or JAM1 co-receptors in cell lines contributed to the Ad5-σ1 infection via the usage of the σ1 chimeric fiber. To further demonstrate the σ1 chimeric fiber contribution to Ad5-σ1 infection, we selected a pair of cell lines, JAM1/CAR-negative CHO cells and its sialic acid-negative derivative Lec2 cells (Table 1, Fig. 5B). In CHO cells, Ad5-σ1 provided a 6.8-fold augmentation in luciferase activity versus Ad5Luc1, while infectivity enhancement of Ad5-σ1 on sialic acid-negative Lec2 cells was negligible, suggesting that Ad5-σ1 can exploit sialic acid as a co-receptor.

Many clinically relevant tissues are refractory to Ad infection, including ovarian cancer cells, due to negligible CAR levels [21]. To evaluate the Ad5-σ1 infectivity of patient tissue, we analyzed Ad5-σ1 transduction of primary human ovarian carcinoma cells. Importantly, Ad5-σ1 increased gene transfer to three unpassaged primary ovarian cancer patient samples from 3.9- to 13.5-fold versus Ad5Luc1 (Fig. 5C).

Herein, we have outlined the construction, rescue, purification, and initial tropism characterization of a novel vector containing a non-Ad fiber molecule. Our

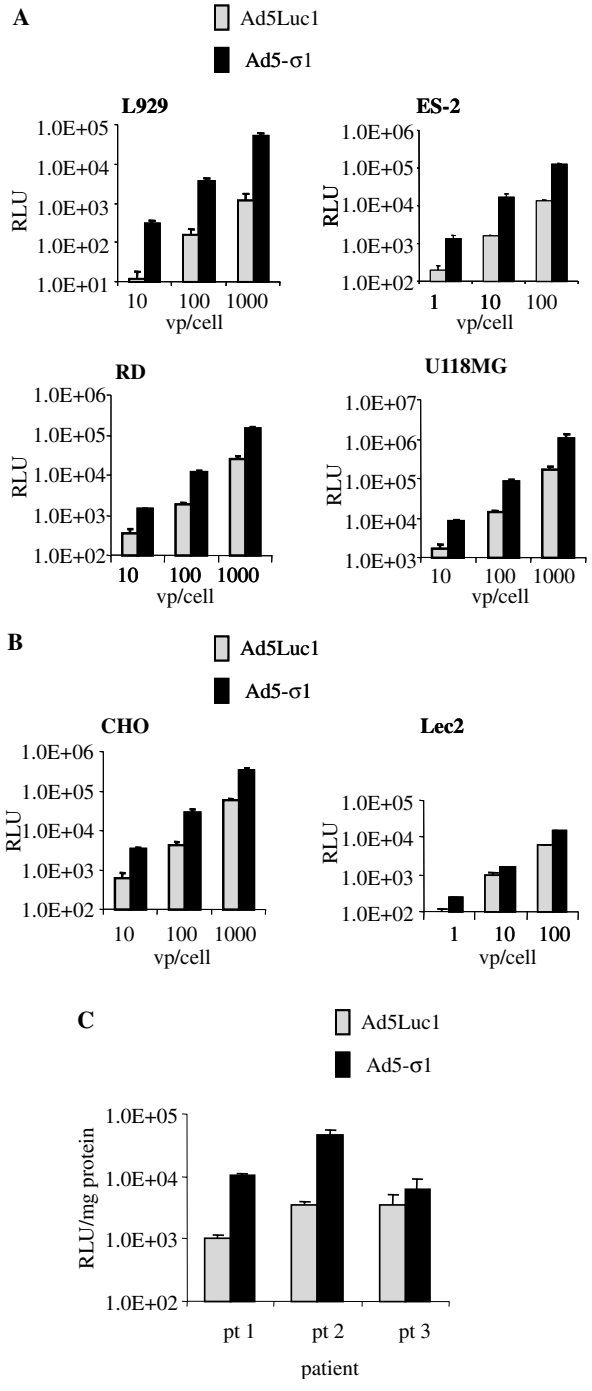

Fig. 5. Infectivity profiles of Ad5-σ1. (A,B) Representative cell lines. (A) Mouse fibroblast cells (L929), ovarian cancer cells (ES-2), human glioma cells (U118MG), and human embryonic rhabdomyosarcoma cells (RD), and (B) sialic acid-positive CHO and sialic acid-negative CHO derivative Lec2 cells were infected with Ad5Luc1 (gray bar) and Ad5-σ1 (black bar) at 1, 10, 100, and 1000 v.p./cell. Luciferase activity was measured 24 h post-infection and is expressed as relative light units (RLU). Each bar represents the mean of three experiments. The error bars indicate standard deviation. (C) Unpassaged primary ovarian cancer cells purified from patient ascites were infected with Ad5Luc1 (gray bar) and Ad5-σ1 (black bar) at 10 v.p./cell. Luciferase activity was measured 24 h post-infection and is expressed as RLU/mg protein. Each bar represents the mean of four experiments. The error bars indicate standard deviation.

results show that in low-CAR cells, Ad5-σ1 provides expanded tropism and increased gene transfer compared to wild-type Ad5 via an alternate infection pathway utilizing the reovirus co-receptors JAM1 and sialic acid. The expanded tropism of this vector represents a crucial attribute for Ad-based gene therapy vectors.

Discussion

A major obstacle to be overcome in Ad5-based cancer gene therapy is the paucity of the primary receptor, CAR, on human primary tumor cells. Variable, but usually low, expression of CAR has been documented in many cancer cell types including glioma, rhabdomyosarcoma, and ovarian cancer [4,11,20]. Thus, Ad gene therapy vectors with CAR-independent and/or expanded tropism may prove valuable for maximal transduction of low-CAR tumors at minimal vector doses.

To achieve expanded tropism by utilizing distinct receptors, we have established a new type of fiber mosaic Ad5 vectors, wherein two fibers derived from different virus families are incorporated in a single virion. This is a novel approach to genetically modify Ad5 vector tropism by means of adding the reovirus receptor-binding spike (σ1) protein to the Ad5 capsid. We selected the spike from reovirus T3D due to its ability to infect numerous tumor cell types that express either JAM1 or sialic acid [23,24].

The main technical feasibility for this new vector is the structural similarity between Ad fiber and the reovirus σ1 protein, which is a trimeric fiber-like molecule protruding from the 12 vertices of the icosahedral reovirus virion [25]. The crystal structure of the reovirus σ1 attachment protein reveals an elongated trimer with two domains: a compact head with a β-barrel fold and a fibrous tail containing a triple β-spiral [25]. The σ1 protein contains two receptor-binding domains: one within the fibrous tail that binds sialic acid [8] and the other in the globular head that binds to JAM1 [9].

In designing a σ1 chimeric fiber, we considered the Ad5 tail portion to be indispensable for incorporation of a σ1 chimeric fiber into the Ad5 penton base. We therefore designed our σ1 chimeric fiber to contain the Ad5 tail and reovirus σ1. The entire σ1 molecule was included since it contains receptor-binding domains in both the tail and head regions [26]. In addition, we engineered a 6-His tag into the C-terminus of σ1 for protein detection. We were initially concerned that the incorporation of the 6-His motif could alter JAM1 recognition, since the C-terminus is proximal to the predicted JAM1-binding motif in the D-E loop of the β-barrel structure [25]. To our knowledge, however, there are no reports suggesting that C-terminal additions are deleterious to normal σ1/JAM1 interaction(s). Indeed, it is unlikely that the 6-His tag interferes significantly with the σ1/JAM1 interaction

since the contribution of JAM1 to the tropism of our mosaic virus was sufficient to result in a 42% decrease in luciferase activity in the presence of an anti-JAM1 antibody (Fig. 5E). Further, we expect that the sialic acid-binding domain localized to the σ1 tail domain would remain unaffected by the C-terminal tag [8,27].

We confirmed the trimerization of the F5S1 σ1 chimeric fiber and constructed an Ad5 genome encoding a tandem fiber cassette, resulting in an Ad5 vector expressing both the Ad5 fiber and a σ1 chimeric fiber. We confirmed that the fiber mosaic Ad5 virions incorporated both fibers by Western blot analysis and by characterizing the functional ability of both fibers to utilize the appropriate receptor(s) for viral transduction.

Consistent with our hypothesis of enhanced infectivity, we observed augmented gene transfer with Ad5-σ1 in all cell lines tested, ranging from 2.3- to 45-fold. This augmentation was variable and often occurred in cell lines with supposedly similar receptor expression profiles. We believe this variation is due to variable receptor expression between cell lines. In this regard, we wish to highlight that the semi-quantitative methodology (Western blot analysis and FACS) used to determine receptor expression in these lines likely masks minor receptor variations between cell lines that accounts for the observed results. Importantly, the observed expanded tropism of Ad5-σ1 extended to a stringent clinical substrate, human primary ovarian tumor tissue, although the augmentation of gene transfer was also variable. While primary ovarian cancer cells are often low in CAR, the specific receptor profiles are unknown. On this basis, the variability in gene transfer very likely reflects natural variability of CAR, JAM1, and sialic acid expression between individual patient samples. These results serve to highlight the utility of Ad vectors that exhibit expanded tropism via utilization of multiple receptors. This vector capacity would be of importance in any future clinical application wherein tissue receptor expression is poorly defined.

During the course of this work, Mercier et al. [28] reported the construction and characterization of an Ad vector containing only the reovirus σ1 fiber. This vector demonstrated JAM1- and SA-dependent tropism that was CAR-independent, resulting in an Ad vector with reovirus tropism only. Mercier demonstrated a 3-fold infectivity enhancement in human dendritic cells relative to Ad5, but did not report any infectivity enhancement in human cancer cells or other substrates. In contrast, we have used the concept of ''fiber mosaicism,'' the use of two separate fibers with distinct receptor recognition, to provide maximum enhanced infectivity via use of multiple receptors. On this basis, we assert that our fiber mosaic Ad5-σ1 vector could offer distinct advantages over Ad vectors with single receptor recognition in the context of an infectivity-enhanced vector for cancer applications.

Our goal was to create a vector with expanded tropism to achieve maximum infectivity enhancement utilizing multiple receptors in CAR and non-CAR cell entry pathways. In this study, the fiber mosaic Ad5-σ1 vector provided enhanced infectivity in low-CAR cancer cell lines resulting from multi-receptor binding properties derived from different virus families. It is our ultimate intent to exploit mosaic adenovirus paradigms in various combinations in order to accomplish additivity or synergism of infectivity enhancements. On this basis, the infectivity gains we demonstrate in this study may contribute to a combinational approach of clinical relevance.

Acknowledgments

This work was supported by the following grants from the National Institute of Health: R01 CA83821, R01 CA94084, and R01 CA93796; Department of Defense W81XWH-05-1-0035; Ovarian Cancer SPORE P50 CA83591 and Breast Cancer SPORE P50 CA89019. We thank Dr. Victor Krasnykh for providing plasmids pVK700 and pNEB.PK.3.6. We also thank Dr. Joanne T. Douglas for providing cell line U118MG-hCAR-tailless, Dr. Dan J. Von Seggern for the cell line 211B, and Dr. Jerry L. Blackwell for the RmcB antibody. We also thank Dr. Maaike Everts for critical reading of the manuscript.

References

[1] J. Gomez-Navarro, D.T. Curiel, J.T. Douglas, Gene therapy for cancer, Eur. J. Cancer 35 (1999) 2039–2057.
[2] V. Krasnykh, I. Dmitriev, J.G. Navarro, N. Belousova, E. Kashentseva, J. Xiang, J.T. Douglas, D.T. Curiel, Advanced generation adenoviral vectors possess augmented gene transfer efficiency based upon coxsackie adenovirus receptor-independent cellular entry capacity, Cancer Res. 60 (2000) 6784–6787.
[3] J.N. Glasgow, G.J. Bauerschmitz, D.T. Curiel, A. Hemminki, Transductional and transcriptional targeting of adenovirus for clinical applications, Curr. Gene Ther. 4 (2004) 1–14.
[4] A. Kanerva, G.V. Mikheeva, V. Krasnykh, C.J. Coolidge, J.T. Lam, P.J. Mahasreshti, S.D. Barker, M. Straughn, M.N. Barnes, R.D. Alvarez, A. Hemminki, D.T. Curiel, Targeting adenovirus to the serotype 3 receptor increases gene transfer efficiency to ovarian cancer cells, Clin. Cancer Res. 8 (2002) 275–280.
[5] V.N. Krasnykh, G.V. Mikheeva, J.T. Douglas, D.T. Curiel, Generation of recombinant adenovirus vectors with modified fibers for altering viral tropism, J. Virol. 70 (1996) 6839–6846.
[6] D.J. Von Seggern, S. Huang, S.K. Fleck, S.C. Stevenson, G.R. Nemerow, Adenovirus vector pseudotyping in fiber-expressing cell lines: improved transduction of Epstein–Barr virus-transformed B cells, J. Virol. 74 (2000) 354–362.
[7] K. Takayama, P.N. Reynolds, J.J. Short, Y. Kawakami, Y. Adachi, J.N. Glasgow, M.G. Rots, V. Krasnykh, J.T. Douglas, D.T. Curiel, A mosaic adenovirus possessing serotype Ad5 and serotype Ad3 knobs exhibits expanded tropism, Virology 309 (2003) 282–293.
[8] J.D. Chappell, V.L. Gunn, J.D. Wetzel, G.S. Baer, T.S. Dermody, Mutations in type 3 reovirus that determine binding to sialic acid

are contained in the fibrous tail domain of viral attachment protein σ1, J. Virol. 71 (1997) 1834–1841.
[9] E.S. Barton, J.C. Forrest, J.L. Connolly, J.D. Chappell, Y. Liu, F.J. Schnell, A. Nusrat, C.A. Parkos, T.S. Dermody, Junction adhesion molecule is a receptor for reovirus, Cell 104 (2001) 441–451.
[10] D.J. Von Seggern, J. Kehler, R.I. Endo, G.R. Nemerow, Complementation of a fibre mutant adenovirus by packaging cell lines stably expressing the adenovirus type5 fibre protein, J. Gen. Virol. 79 (1998) 1461–1468.
[11] M. Kim, L.A. Sumerel, N. Belousova, G.R. Lyons, D.E. Carey, V. Krasnykh, J.T. Douglas, The coxsackievirus and adenovirus receptor acts as a tumour suppressor in malignant glioma cells, Br. J. Cancer 88 (2003) 1411–1416.
[12] S.D. Barker, E. Casado, J. Gomez-Navarro, J. Xiang, W. Arafat, P. Mahasreshti, T.B. Pustilnik, A. Hemminki, G.P. Siegal, R.D. Alvarez, D.T. Curiel, An immunomagnetic-based method for the purification of ovarian cancer cells from patient-derived ascites, Gynecol. Oncol. 82 (2001) 57–63.
[13] L. Pereboeva, S. Komarova, P.J. Mahasreshti, D.T. Curiel, Fiber-mosaic adenovirus as a novel approach to design genetically modified adenoviral vectors, Virus Res. 105 (2004) 35–46.
[14] N. Belousova, V. Krendelchtchikova, D.T. Curiel, V. Krasnykh, Modulation of adenovirus vector tropism via incorporation of polypeptide ligands into the fiber protein, J. Virol. 76 (2002) 8621–8631.
[15] F. Graham, L. Prevec, Manipulation of adenovirus vectors, in: E.J. Murray, J.M. Walker (Eds.), Methods in Molecular Biology, Humana Press, Clifton, NJ, 1991, pp. 109–128.
[16] J.V. Maizel Jr., D.O. White, M.D. Scharff, The polypeptides of adenovirus. I. Evidence for multiple protein components in the virion and a comparison of types 2, 7A, and 12, Virology 36 (1968) 115–125.
[17] K. Chandran, X. Zhang, N.H. Olson, S.B. Walker, J.D. Chappell, T.S. Dermody, T.S. Baker, M.L. Nibert, Complete in vitro assembly of the reovirus outer capsid produces highly infectious particles suitable for genetic studies of the receptor-binding protein, J. Virol. 75 (2001) 5335–5342.
[18] S.J. Burstin, D.R. Spriggs, B.N. Fields, Evidence for functional domains on the reovirus type 3 hemagglutinin, Virology 117 (1982) 146–155.
[19] K. Kasono, J.L. Blackwell, J.T. Douglas, I. Dmitriev, T.V. Strong, P. Reynolds, D.A. Kropf, W.R. Carroll, G.E. Peters, R.P. Bucy, D.T. Curiel, V. Krasnykh, Selective gene delivery to head and neck cancer cells via an integrin targeted adenoviral vector, Clin. Cancer Res. 5 (1999) 2571–2579.
[20] T.P. Cripe, E.J. Dunphy, A.D. Holub, A. Saini, N.H. Vasi, Y.Y. Mahller, M.H. Collins, J.D. Snyder, V. Krasnykh, D.T. Curiel, T.J. Wickham, J. DeGregori, J.M. Bergelson, M.A. Currier, Fiber knob modifications overcome low, heterogeneous expression of the coxsackievirus-adenovirus receptor that limits adenovirus gene transfer and oncolysis for human rhabdomyosarcoma cells, Cancer Res. 61 (2001) 2953–2960.
[21] F.J. Kelly, C.R. Miller, D.J. Buchsbaum, J. Gomez-Navarro, M.N. Barnes, R.D. Alvarez, D.T. Curiel, Selectivity of TAG-72-targeted adenovirus gene transfer to primary ovarian carcinoma cells versus autologous mesothelial cells in vitro, Clin. Cancer Res. 6 (2000) 4323–4333.
[22] E.A. Kashentseva, T. Seki, D.T. Curiel, I.P. Dmitriev, Adenovirus targeting to c-erbB-2 oncoprotein by single-chain antibody fused to trimeric form of adenovirus receptor ectodomain, Cancer Res. 62 (2002) 609–616.
[23] K. Hirasawa, S.G. Nishikawa, K.L. Norman, T. Alain, A. Kossakowska, P.W.K. Lee, Oncolytic reovirus against ovarian and colon cancer, Cancer Res. 62 (2002) 1696–1701.
[24] T. Alain, K. Hirasawa, K.J. Pon, S.G. Nishikawa, S.J. Urbanski, Y. Auer, J. Luider, A. Martin, R.N. Johnston, A. Janowska-Wieczorek, P.W.K. Lee, A.E. Kossakowska, Reovirus therapy of lymphoid malignancies, Blood 100 (2002) 4146–4153.
[25] J.D. Chappell, A.E. Prota, T.S. Dermody, T. Stehle, Crystal structure of reovirus attachment protein σ1 reveals evolutionary relationship to adenovirus fiber, EMBO J. 21 (2002) 1–11.
[26] J.C. Forrest, T.S. Dermody, Reovirus receptors and pathogenesis, J. Virol. 77 (2003) 9109–9115.
[27] E.S. Barton, J.L. Connolly, J.C. Forrest, J.D. Chappell, T.S. Dermody, Utilization of sialic acid as a coreceptor enhances reovirus attachment by multistep adhesion strengthening, J. Biol. Chem. 276 (2001) 2200–2211.
[28] G.T. Mercier, J.A. Campbell, J.D. Chappell, T. Stehle, T.S. Dermody, M.A. Barry, A chimeric adenovirus vector encoding reovirus attachment protein σ1 targets cells expressing junctional adhesion molecule 1, Proc. Natl. Acad. Sci. USA 101 (2004) 6188–6193.

II. Publications - 2006

11. Emdad L, Sarkar D, Lebedeva IV, Su ZZ, Gupta P, Mahasreshti PJ, Dent P, Curiel DT, Fisher PB. Ionizing radiation enhances adenoviral vector expressing mda-7/IL-24-mediated apoptosis in human ovarian cancer. J Cell Physiol. 2006 Aug;208(2):298-306. PMID: 16646087
12. Everts M, Saini V, Leddon JL, Kok RJ, Stoff-Khalili M, Preuss MA, Millican CL, Perkins G, Brown JM, Bagaria H, Nikles DE, Johnson DT, Zharov VP, Curiel DT. Covalently linked Au nanoparticles to a viral vector: potential for combined photothermal and gene cancer therapy. Nano Lett. 2006 Apr;6(4):587-91. PMID: 16608249
13. Glasgow JN, Everts M, Curiel DT. Transductional targeting of adenovirus vectors for gene therapy. Cancer Gene Ther. 2006 Sep;13(9):830-44. Review. PMID: 16439993
14. Gupta P, Su ZZ, Lebedeva IV, Sarkar D, Sauane M, Emdad L, Bachelor MA, Grant S, Curiel DT, Dent P, Fisher PB. mda-7/IL-24: multifunctional cancer-specific apoptosis-inducing cytokine. Pharmacol Ther. 2006 Sep;111(3):596-628. Review. PMID: 16464504
15. Hedley SJ, Auf der Maur A, Hohn S, Escher D, Barberis A, Glasgow JN, Douglas JT, Korokhov N, Curiel DT. An adenovirus vector with a chimeric fiber incorporating stabilized single chain antibody achieves targeted gene delivery. Gene Ther. 2006 Jan;13(1):88-94. PMID: 16107860
16. Hedley SJ, Chen J, Mountz JD, Li J, Curiel DT, Korokhov N, Kovesdi I. Targeted and shielded adenovectors for cancer therapy. Cancer Immunol Immunother. 2006 Nov;55(11):1412-9. Review. PMID: 16612598
17. Le LP, Le HN, Dmitriev IP, Davydova JG, Gavrikova T, Yamamoto S, Curiell DT, Yamamoto Y. Dynamic monitoring of oncolytic adenovirus in vivo by genetic capsid labeling. JNCI, 2006 Feb 1;98(3):203-14. PMID: 16449680
18. Nakayama M, Both GW, Banizs B, Tsuruta Y, Yamamoto S, Kawakami Y, Douglas JT, Tani K, Curiel DT, Glasgow JN. An adenovirus serotype 5 vector with fibers derived from ovine atadenovirus demonstrates CAR-independent tropism and unique biodistribution in mice. Virology. 2006 Jun 20;350(1):103-15. PMID: 16516257
19. Stoff A, Rivera AA, Banerjee NS, Mathis JM, Espinosa-de-los-Monteros A, Le LP, De la Torre JI, Vasconez LO, Broker TR, Richter DF, Stoff-Khalili MA, Curiel DT. Strategies to enhance transductional efficiency of adenoviral-based gene transfer to primary human fibroblasts and keratinocytes as a platform in dermal wounds. Wound Repair Regen. 2006 Sep-Oct;14(5):608-17. PMID: 17014674
20. Stoff-Khalili MA, Rivera AA, Stoff A, Michael Mathis J, Rocconi RP, Matthews QL, Numnum MT, Herrmann I, Dall P, Eckhoff DE, Douglas JT, Siegal GP, Zhu ZB, Curiel DT. Combining high selectivity of replication via CXCR4 promoter with fiber chimerism for effective adenoviral oncolysis in breast cancer. Int J Cancer. 2007 Feb 15;120(4):935-41. PMID: 17131341

JOURNAL OF CELLULAR PHYSIOLOGY 208:298–306 (2006)

Ionizing Radiation Enhances Adenoviral Vector Expressing *mda*-7/IL-24-mediated Apoptosis in Human Ovarian Cancer

LUNI EMDAD,[1] DEVANAND SARKAR,[1] IRINA V. LEBEDEVA,[1] ZAO-ZHONG SU,[1] PANKAJ GUPTA,[1] PARAMESHWAR J. MAHASRESHTI,[2,3] PAUL DENT,[4] DAVID T. CURIEL,[2,3] AND PAUL B. FISHER[1,5,6]*

[1]*Department of Urology, Herbert Irving Comprehensive Cancer Center, Columbia University Medical Center, College of Physicians and Surgeons, New York, New York*
[2]*Department of Medicine, Pathology, Surgery, Division of Human Gene Therapy and The Gene Therapy Center, University of Alabama at Birmingham, Birmingham, Alabama*
[3]*Department of Obstetrics and Gynecology, Division of Gynecologic Oncology, University of Alabama at Birmingham, Birmingham, Alabama*
[4]*Department of Biochemistry, Virginia Commonwealth University, Richmond, Virginia*
[5]*Department of Pathology, Herbert Irving Comprehensive Cancer Center, Columbia University Medical Center, College of Physicians and Surgeons, New York, New York*
[6]*Department of Neurosurgery, Herbert Irving Comprehensive Cancer Center, Columbia University Medical Center, College of Physicians and Surgeons, New York, New York*

Ovarian cancer is the fifth most common cause of cancer-related death in women. Current interventional approaches, including debulking surgery, chemotherapy, and/or radiation have proven minimally effective in preventing the recurrence and/or mortality associated with this malignancy. Subtraction hybridization applied to terminally differentiating human melanoma cells identified melanoma differentiation associated gene-7/interleukin-24 (*mda*-7/IL-24), whose unique properties include the ability to selectively induce growth suppression, apoptosis, and radiosensitization in diverse cancer cells, without causing any harmful effects in normal cells. Previously, it has been shown that adenovirus-mediated *mda*-7/IL-24 therapy (Ad.*mda*-7) induces apoptosis in ovarian cancer cells, however, the apoptosis induction was relatively low. We now document that apoptosis can be enhanced by treating ovarian cancer cells with ionizing radiation (IR) in combination with Ad.*mda*-7. Additionally, we demonstrate that *mda*-7/IL-24 gene delivery, under the control of a minimal promoter region of progression elevated gene-3 (*PEG*-3), which functions selectively in diverse cancer cells with minimal activity in normal cells, displays a selective radiosensitization effect in ovarian cancer cells. The present studies support the use of IR in combination with *mda*-7/IL-24 as a means of augmenting the therapeutic benefit of this gene in ovarian cancer, particularly in the context of tumors displaying resistance to radiation therapy. J. Cell. Physiol. 208: 298–306, 2006. © 2006 Wiley-Liss, Inc.

Ovarian cancer is the fifth leading cause of cancer deaths among US women and has the highest mortality rate of all gynecologic cancers (Jemal et al., 2004). The majority of patients initially present with stage III or IV disease and display poor prognosis. Unfortunately, despite advances in initial debulking surgery and chemotherapy, many patients will have recurrence in the abdomen or pelvis that frequently is not responsive to further chemotherapy and carries a negative prognosis (Christian and Thomas, 2001). Therefore, treatments that improve initial disease control in the abdomen and pelvis have the potential to extend the progression-free interval and possibly also survival. Additionally, mortality from epithelial ovarian carcinoma has remained high for the past few decades. These facts underscore the need for development of new effective therapies.

Since human ovarian carcinoma is considered to be the result of acquired genetic alterations, gene therapy offers a novel approach for treating this neoplastic disease (Gomez-Navarro et al., 1998; Wolf and Jenkins, 2002). However, to realize the promise of gene therapy, identifying a gene therapeutic that does not harm normal cells and can kill only tumor cells would represent an ideal weapon to combat this prevalent female disease and cancer in general. A number of diverse gene therapy approaches for ovarian cancer have been endeavored using adenoviral vectors (Ad), in both animal models (Barnes et al., 1997; Robertson et al., 1998; Alvarez et al., 2000; Casado et al., 2001) and human clinical trials (Alvarez and Curiel, 1997; Collinet

Contract grant sponsor: NIH; Contract grant numbers: R01 CA083821, R01 CA097318, R01 CA098712, P01 CA104177; Contract grant sponsor: Army DOD Idea Development Award; Contract grant number: W81XWH-05-1-0035; Contract grant sponsor: The Samuel Waxman Cancer Research Foundation; Contract grant sponsor: Chernow Endowment.

*Correspondence to: Paul B. Fisher, Department of Pathology and Urology, Columbia University Medical Center, College of Physicians and Surgeons, BB-1501, 630 West 168th Street, New York, NY 10032. E-mail: pbf1@columbia.edu

Received 15 February 2006; Accepted 8 March 2006

DOI: 10.1002/jcp.20663

et al., 2000). Some of these approaches have included Ad-mediated delivery of *p53*, a tumor suppressor gene, or *Bax*, a pro-apoptotic gene, or toxin encoding genes, such as *HSV-TK* and *cytosine deaminase*. Although many therapeutic approaches have been developed, most of them are limited in their application due to their low therapeutic potential and high toxicity to normal tissues. Of note, a recent Phase II/III trial of *p53* gene therapy failed due to low therapeutic benefit (Zeimet and Marth, 2003). Therefore, identification and development of novel genes with high therapeutic potential and minimal toxicity to normal tissues (high therapeutic index) are warranted. In principle, such genes would provide significant benefit in treating this prevalent cancer.

Melanoma differentiation associated gene-7 (*mda*-7) is a secreted cytokine belonging to the interleukin (IL)-10 family that has been designated IL-24. Multiple independent studies have confirmed that delivery of *mda*-7/IL-24 by a replication-incompetent adenovirus, Ad.*mda*-7, or as a GST-MDA-7 fusion protein selectively kills diverse cancer cells, without harming normal cells, and radiosensitizes various cancer cells, including non-small cell lung carcinoma, renal carcinoma, and malignant glioma (Kawabe et al., 2002; Su et al., 2003, 2005a; Yacoub et al., 2003a,b,c; Sauane et al., 2004; Lebedeva et al., 2005b). In addition, *mda*-7/IL-24 possesses potent anti-angiogenic, immunostimulatory, and bystander activities (Fisher, 2005). The sum of these attributes makes *mda*-7/IL-24 a significant candidate for cancer gene therapy (Fisher, 2005). Indeed, Ad.*mda*-7 has been successfully used for Phase I/II clinical trials for solid tumors and has shown promising results in tumor inhibition (Fisher et al., 2003; Cunningham et al., 2005; Fisher, 2005; Lebedeva et al., 2005a; Tong et al., 2005). Although the ultimate end-result of Ad.*mda*-7 infection is induction of apoptosis, it employs different signal transduction pathways, such as activation of p38 MAPK, PKR, TRAIL, in different tumor cell types to achieve this objective (Pataer et al., 2002; Saeki et al., 2002; Sarkar et al., 2002).

The therapeutic potential of *mda*-7/IL-24 gene therapy in the context of epithelial ovarian carcinoma has not been investigated extensively. We have previously demonstrated that Ad.*mda*-7 gene therapy induces apoptosis in ovarian cancer cells but not in normal mesothelial cells (Leath et al., 2004). However, the apoptosis induction efficiency was low. The purpose of the present study was: (1) to develop combinatorial approaches to improve apoptosis induction in ovarian carcinoma cells; and (2) to evaluate ovarian cancer cell targeted gene therapy by tumor-specific transgene expression using the novel promoter derived from progression elevated gene-3 (*PEG*-3) (Su et al., 1997, 1999). We now document that this resistance to Ad.*mda*-7 is reversible in ovarian cancer cells by employing ionizing radiation (IR). Additionally, we demonstrate that, *mda*-7/IL-24 gene delivery under the control of a minimal promoter region of *PEG*-3 (Su et al., 1997, 1999, 2000, 2001b) which functions selectively in diverse cancer cells with minimal activity in normal cells (Su et al., 2000, 2001b, 2005b; Sarkar et al., 2005a,b), displays a selective radiosensitization effect in ovarian cancer cells. The present study confirms that the therapeutic potential of *mda*-7/IL-24 can be augmented by IR with the added advantage of being able to sensitize both radiation- and *mda*-7/IL-24-resistant cells to programmed cell death.

MATERIALS AND METHODS

Cell lines, culture conditions, and radiation protocol

The SKOV3 (p53 null), human ovarian adenocarcinoma cells, and human mesothelial cells were purchased from the American Type Culture Collection (Manassas, VA). Human ovarian adenocarcinoma cell lines HEY (p53 wild-type), SKOV3.ip1 (p53 null), and OV-4 (p53 mutant) were kindly provided by Dr. Judy Wolf and Dr. Janet Price (M.D. Anderson Cancer Center, Houston, TX) and Dr. Timothy J. Eberlein (Harvard Medical School, Boston, MA), respectively. SKOV3, SKOV3.ip1, and OV-4 cells were cultured and maintained in complete medium composed of DMEM:F12 (Cellgro; Mediatech, Washington, DC) supplemented with 10% fetal bovine serum (FBS) (Hyclone Laboratories, Logan, UT), 5 mM glutamine (Cellgro; Mediatech), and 1% penicillin and streptomycin (Cellgro; Mediatech). HEY cells were cultured and maintained in complete medium composed of RPMI (Cellgro; Mediatech) supplemented with 10% FBS, 5 mM glutamine, and 1% penicillin and streptomycin. Human mesothelial cells were cultured and maintained in complete medium composed of a 1:1 mixture of Media 199 (Cellgro; Mediatech) and MCDB 105 Media (Sigma-Aldrich, St. Louis, MO) supplemented with 20% FBS, 5 mM glutamine, 1% penicillin and streptomycin, and 10 ng/ml human epidermal growth factor (Life Technologies, Grand Island, NY). All cells were grown in a humidified atmosphere of 5% CO_2 at 37°C. Infections of all cells utilized respective infection medium which contained 2% FBS. Cells were irradiated with 2 Gy of IR using a ^{137}Cs γ-irradiation source. SB203580 was purchased from Sigma Chemical Co.

Construction of adenovirus (Ad) and infection protocol

The recombinant replication-incompetent Ads, Ad.*CMV-GFP*, Ad.*PEG-GFP*, Ad.*CMV-Luc*, Ad.*PEG-Luc*, Ad.*CMV-mda*-7 (CMV promoter driving *mda*-7/IL-24 expression), and Ad.*PEG-mda*-7 (PEG-Prom driving *mda*-7/IL-24 expression) were created in two steps as described previously and plaque purified by standard procedures (Su et al., 2005a). As a control, a replication-incompetent Ad.*vec* without any transgene was used. Cells were infected with a multiplicity of infection (moi) of 100 plaque-forming units (pfu) per cell with different Ads.

Fluorescence microscopy for GFP evaluation

Cells (2×10^5/well) were plated in triplicate in 6-well plates. The next day, cells were infected with Ad.*CMV-GFP* and Ad.*PEG-GFP* at a moi of 100 pfu/cell for 2 h in 2% infection medium. Subsequently, 2 ml of complete media was added and incubated at 37°C. After 48 h, the cells were analyzed for green fluorescent protein (GFP) expression by observing under a fluorescent microscope.

Luciferase assay

Cells were plated in 12-well plates in 2 ml of complete medium. The next day, supernatant was aspirated and the cells were infected with *Ad.CMV.Luc* and *Ad.PEG.Luc* at a moi of 100 pfu/cell in 200 μl of 2% medium. Following incubation for 2 h, complete medium was added. Luciferase assays were performed using commercial kits (Promega, Madison, WI) 48 h after infection. Protein concentration was determined using BCA Protein Assay Kit from Pierce Biotechnology (Rockford, IL) as per manufacturer's recommendations. The luciferase activity was then determined by calculating relative luciferase activity (RLU)/mg of protein as previously described (Leath et al., 2004).

Cell viability assay

Cells were seeded in 96-well tissue culture plates (1.5×10^3 cells per well) and treated the next day as described in the figure legends. At the indicated time points, the medium was removed, and fresh medium containing 0.5 mg/ml MTT was added to each well. The cells were incubated at 37°C for 4 h and then an equal volume of solubilization solution (0.01 N HCl in 10% SDS) was added to each well and mixed thoroughly. The optical density from the plates was read on a Dynatech Laboratories MRX microplate reader at 540 nm.

Apoptosis and necrosis (Annexin-V binding assay)

Cells were trypsinized and washed with complete media and then twice with PBS. The aliquots of the cells (2×10^5) were resuspended in 1× binding buffer (0.5 ml) and stained with APC (allophycocyanin)-labeled Annexin-V (BD Biosciences, Palo Alto, CA) according to the manufacturer's instructions. DAPI was added to the samples after staining with Annexin-V to exclude late apoptotic and necrotic cells. The flow cytometry was performed immediately after staining.

Clonogenic survival assay

Cells were treated as described in the Figure legends. The following day, after trypsinization and counting, cells were replated in 60-mm dishes (500 cells per dish) in triplicates. After 2 or 3 weeks, cells were fixed with 4% formaldehyde and stained with 5% (w/w) solution of Giemsa stain in water. Colonies > 50 cells were scored and counted.

Western blot assay

Cell lines were grown on 10-cm plates and protein extracts were prepared with RIPA buffer containing a cocktail of protease inhibitors. A measure of 50 μg of protein was applied to 12% SDS–PAGE and transferred to nitrocellulose/PVDF membranes. The membranes were probed with polyclonal or monoclonal antibodies to *mda*-7/IL-24, anti-PEA-3, anti-c-JUN, phospho-P38 MAPK, total P38 MAPK, and EF-1α

RNA isolation and Northern blot analysis

Total RNA was extracted from cells using the Qiagen RNeasy mini kit according to the manufacturer's protocol and was used for Northern blotting as previously described (Su et al., 2001b). Briefly, 10 μg of RNA for each sample was denatured, electrophoresed in 1.2% agarose gels with 3% formaldehyde, and transferred onto nylon membranes. The blots were probed with an α-^{32}P[dCTP]-labeled, full-length human *mda*-7/IL-24 cDNA probe. Following hybridization, the filters were washed and exposed for autoradiography.

Statistical analysis

All of the experiments were performed at least three times. Results are expressed as mean ± SE. Statistical comparisons were made using an unpaired two-tailed student's *t*-test. A $P < 0.05$ was considered significant.

RESULTS

Ovarian cancer cell lines exhibits low levels of adenoviral-mediated gene expression

Previous studies document that ovarian cancer cell lines have low coxsackie adenovirus receptor (CAR) expression (Leath et al., 2004), which is a primary receptor for adenovirus infection. Two replication-incompetent adenoviruses expressing GFP, one under the control of the CMV promoter (Ad.*CMV*-GFP) and the other under the control of the PEG-Prom (Ad.*PEG*-GFP) were constructed (Su et al., 2005b). To determine the status of adenoviral infectivity we examined GFP expression by fluorescence microscopy following infection with Ad.*CMV-GFP* and Ad.*PEG-GFP* at a moi of 100 pfu/cell 2 days post-infection. Infection with Ad.*CMV-GFP* resulted in high GFP expression in normal human mesothelial cells and in SKOV3 cells and low level GFP expression in SKOV3.ip1, OV-4, and HEY cells. With Ad.*PEG-GFP* infection, none to barely detectable GFP could be observed in normal human mesothelial cells and in ovarian cancer cell lines the GFP expression level was comparable to that observed after Ad.*CMV-GFP* infection (Fig. 1A). These findings indicate that ovarian cancer cells have variable levels of CAR that preclude efficient adenoviral transduction and subsequent transgene expression.

PEG-Prom functions selectively in cancer cells

To quantify *PEG*-Prom activity in ovarian cancer and normal human mesothelial cells a luciferase-based reporter gene assay was employed. We constructed Ad.*PEG-Luc* in which the expression of the luciferase reporter gene was under the control of the *PEG*-Prom in a replication-incompetent adenoviral vector and infected normal mesothelial cells or the different ovarian cancer cell lines. Luciferase activity was measured 48 h after infection and expressed as RLU per mg protein. Normal human mesothelial cells demonstrated no activity supporting the limited GFP expression detected immunohistochemically following infection with Ad.*PEG-GFP* (Fig. 1B, upper part). When compared to normal human mesothelial cells, all of the ovarian cancer cells showed significantly increased *PEG*-Prom activity, although the activity in HEY cells was much lower than that in the other three ovarian cancer cell lines. The findings from GFP expression and luciferase reporter studies further confirm that the *PEG*-Prom functions selectively in cancer cells and is a useful tool to ensure cancer cell-targeted transgene expression.

PEA-3 and AP-1 controls *PEG*-Prom activity in ovarian cancer cells

PEA-3 and AP-1 are two transcription factors conferring cancer cell-selective function of the *PEG*-Prom in multiple cancer cell types, such as prostate, breast, central nervous system (malignant glioma), and pancreatic cancers (Sarkar et al., 2005a,b; Su et al., 2005b). To determine the involvement of these two factors in regulating *PEG*-Prom activity in ovarian cancer cells, the relative abundance of PEA-3 and Jun, a component of AP-1, proteins in ovarian cancer, and normal human mesothelial cells was analyzed by Western blot analysis (Fig. 1B, lower part). The expression of PEA-3 and Jun was significantly higher in all of the ovarian cancer cells when compared to that in normal human mesothelial cells, except for HEY cells, which showed comparable level of Jun expression to normal human mesothelial cells. These findings confirm that like other cell types previously examined, PEA-3 and AP-1 also control *PEG*-Prom activity in ovarian cancer cells.

Infection with Ad.CMV-*mda*-7 and Ad.PEG-*mda*-7 generates MDA-7/IL-24 protein

To extend our studies further we used two additional replication-incompetent adenoviruses expressing *mda*-7/IL-24, one under the control of CMV promoter (Ad.CMV-*mda*-7) and the other under the control of PEG-Prom (Ad.PEG-*mda*-7). The authenticity of these Ad were confirmed by Western blot analysis for MDA-7/IL-24 following infection of ovarian cancer cells and normal human mesothelial cells at a moi of 100 pfu/cell. Normal human mesothelial cells showed abundant MDA-7/IL-24 protein following Ad.CMV-*mda*-7 infection, but no MDA-7/IL-24 protein after Ad.PEG-*mda*-7 infection (Fig. 1C). In ovarian cancer cells, infection with Ad.CMV-*mda*-7 resulted in more intracellular MDA-7/IL-24 protein than infection with Ad.PEG-*mda*-7. The relative levels of MDA-7/IL-24 and GFP proteins correlated well in different ovarian cancer cell lines, with SKOV3 cells showing the highest level of transgenes and HEY cells showing the lowest. These findings further confirm that although the PEG-Prom is functionally less active than CMV promoter, it ensures cancer cell-specific expression of MDA-7/IL-24.

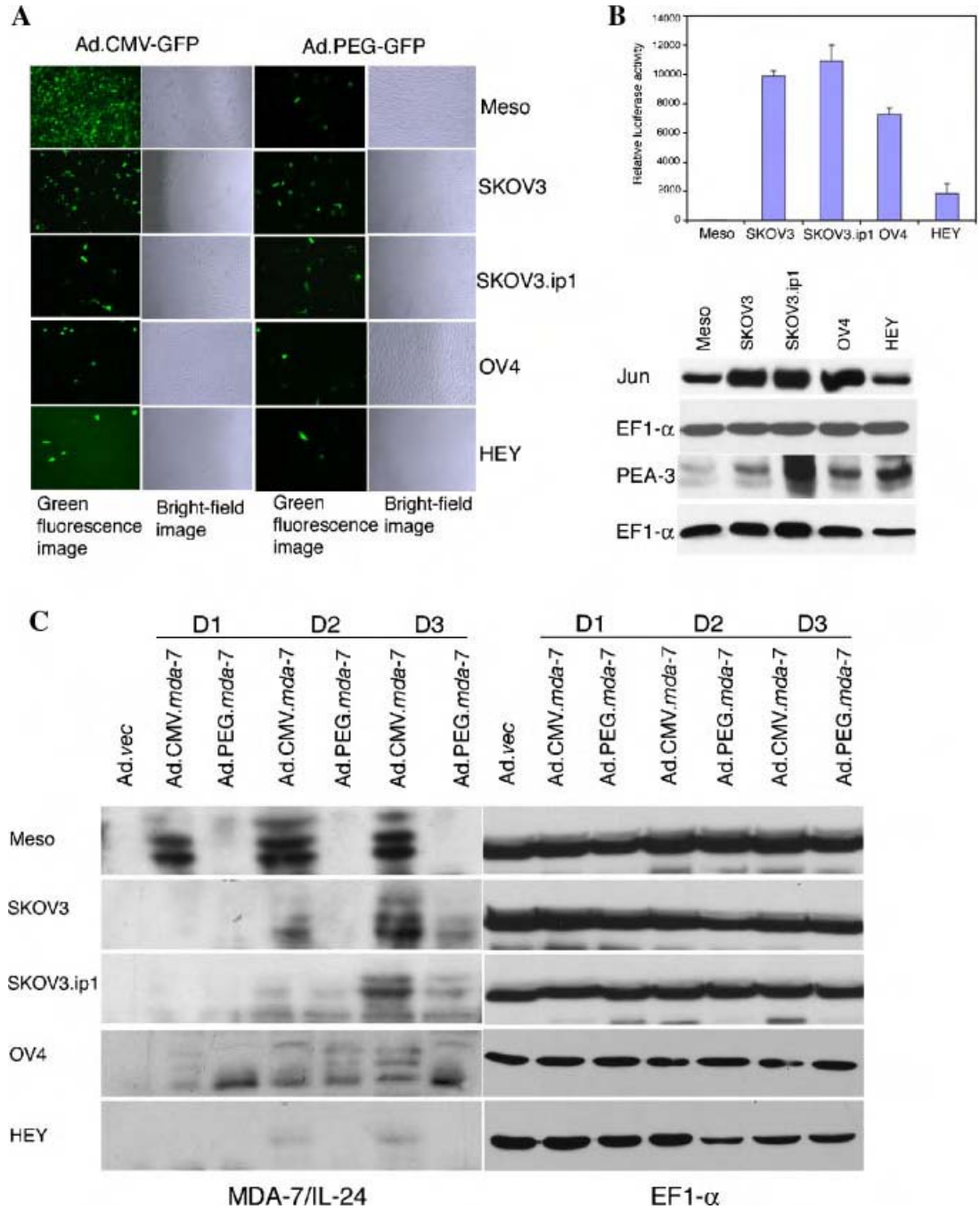

Fig. 1. GFP, Luc, and MDA-7/IL-24 expression following infection of normal mesothelial and ovarian carcinoma cells with various adenoviruses and de novo levels of Jun, PEA-3, and EF-1α protein in mesothelial and ovarian carcinoma cells. **A**: Variable infectivity of ovarian cancer cells by adenovirus as determined by GFP expression. The indicated cells were infected with either Ad.CMV-*GFP* or Ad.PEG-*GFP* at a moi of 100 pfu/cell, and GFP expression was analyzed by fluorescence microscopy at 2d post-infection. **B**: Upper part: PEG-promoter drives high luciferase expression in ovarian cancer cells, but not in normal human mesothelial cells. The indicated cells were infected with Ad.PEG-*luc* at a moi of 100 pfu/cell, and luciferase activity was measured at 48 h post-infection and expressed as RLU/mg protein. The data represent the mean ± SD of three independent experiments, each performed in triplicate. Lower part: The expressions of JUN, PEA-3, and EF-1α protein were analyzed by Western blot analysis in ovarian cancer cells and normal human mesothelial cells. **C**: Infection of ovarian cancer cells and normal human mesothelial cells with Ad.CMV-*mda*-7 or Ad.PEG-*mda*-7 results in variable amounts of intracellular MDA-7/IL-24 protein. Cells were infected with the indicated viruses at a moi of 100 pfu/cell and total cell lysates were prepared at d 1, d 2, and d 3 post-infection. The cell lysate used for Ad.*vec* was the lysate prepared at d 3 post-infection. The expression of MDA-7/IL-24 and EF-1α proteins were evaluated by Western blot analysis.

Ad.CMV-*mda*-7 and Ad.PEG-*mda*-7 induce apoptosis in ovarian cancer cells

Experiments were next performed to determine whether infection with Ad.CMV-*mda*-7 or Ad.PEG-*mda*-7 could induce growth suppression and apoptosis in ovarian cancer cells. Cell viability was assessed by standard MTT assay 3 and 6 days after Ad infection. As expected neither Ad.CMV-*mda*-7 nor Ad.PEG-*mda*-7 affected the viability of normal human mesothelial cells (Fig. 2A). Although both Ad.CMV-*mda*-7 and Ad.PEG-*mda*-7 decreased cell viability in all the ovarian cancer cells, the effect, although significant, was marginal, except for SKOV3 cells, which displayed a

more pronounced effect (Fig. 2A). Analysis of apoptosis by Annexin-V staining produced similar corroborating results as the MTT assays (Fig. 2B). No significant increase in apoptotic cells was observed in normal human mesothelial cells upon infection with Ad.CMV-*mda*-7 or Ad.PEG.*mda*-7. Both of these Ads induced marginal but significant increases in apoptotic cells in the ovarian cancer cells.

Ad.CMV-*mda*-7 and Ad.PEG-*mda*-7 induce apoptosis by activating p38 MAPK

Experiments were performed to determine whether Ad.CMV-*mda*-7 and Ad.PEG.*mda*-7 infection in ovarian cancer cells activates the p38 MAPK pathway that has been shown to mediate apoptosis induction by Ad.*mda*-7. In normal human mesothelial cells, infection with Ad.CMV-*mda*-7 or Ad.PEG.*mda*-7 did not increase phospho-p38 MAPK levels 2 days post-infection (Fig. 3A). In SKOV3, SKOV3.ip1, and OV-4 cells, which showed significant susceptibility to growth inhibition, Ad.CMV-*mda*-7 or Ad.PEG.*mda*-7 infection resulted in a significant increase in phospho-p38 MAPK levels. However, in HEY cells, which are relatively resistant to growth inhibition, the increase in phospho-p38 MAPK was marginal. Treatment with the specific p38 MAPK inhibitor SB203580 protected the cells from growth inhibition following infection with Ad.CMV-*mda*-7 or Ad.PEG.*mda*-7 (Fig. 3B). These findings indicate that activation of p38 MAPK also plays an important role in mediating growth inhibition by *mda*-7/IL-24 in ovarian cancer cells.

Combination of γ-irradiation and Ad.CMV-*mda*-7 or Ad.PEG.*mda*-7 infection overcomes resistance of ovarian cancer cells to both ionizing radiation and *mda*-7/IL-24

Since Ad.CMV-*mda*-7 or Ad.PEG.*mda*-7 alone showed relatively low apoptosis induction in ovarian cancer cells, we hypothesized that a combinatorial approach with other anti-cancer strategies might be useful in augmenting growth suppression and apoptosis. Previous studies confirm that *mda*-7/IL-24 is a potent radiosensitizer in multiple cancer subtypes, including non-small cell lung carcinoma, breast carcinoma, prostate carcinoma, and

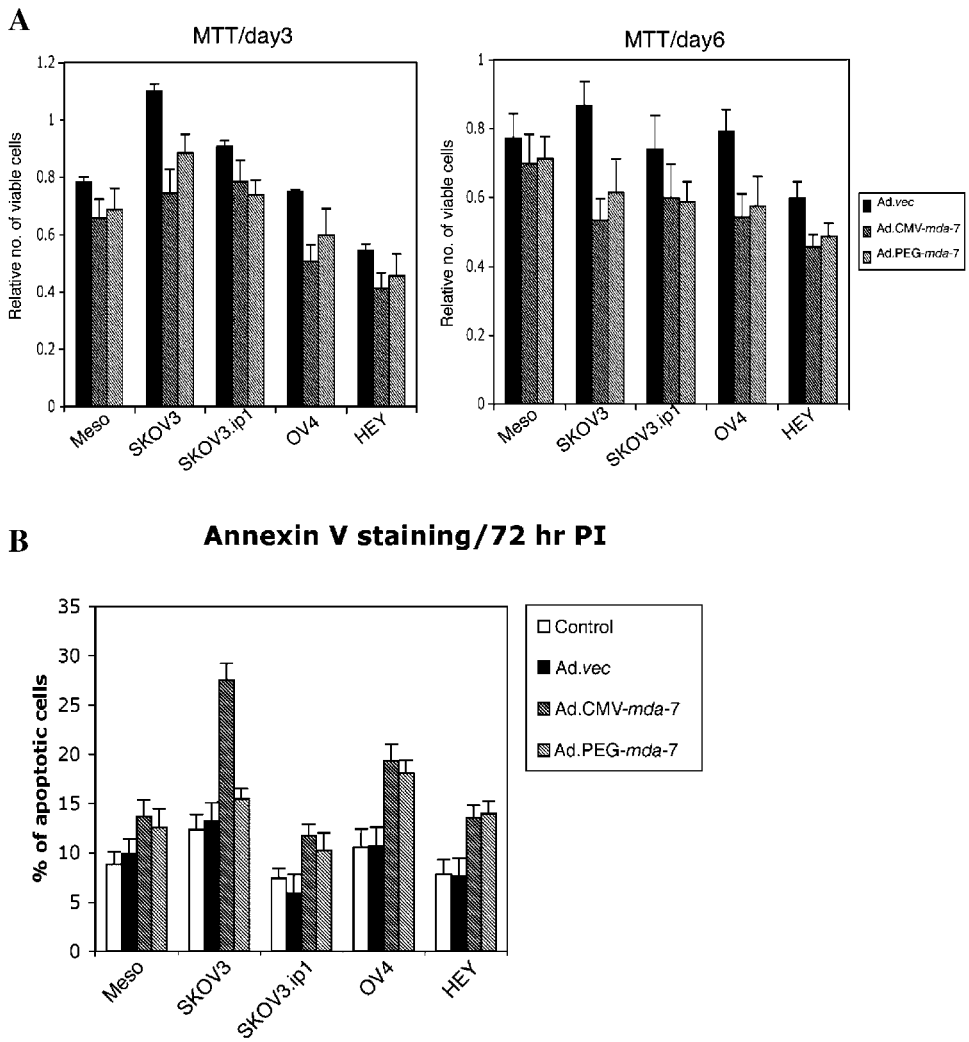

Fig. 2. Effect of infection of normal mesothelial and ovarian carcinoma cells with Ad.CMV-*mda*-7 or Ad.PEG-*mda*-7 on cell viability and apoptosis induction. **A**: Infection with Ad.CMV-*mda*-7 or Ad.PEG-*mda*-7 results in a decrease in cell viability in ovarian cancer cells. Cells were infected with the indicated viruses and cell viability was assessed by MTT assay at 3 d and 6 d post-infection. A significant loss in cell viability was evident in the SKOV3 and OV-4 cell lines. Results are the average from at least three experiments ±SD. **B**: Infection with Ad.CMV-*mda*-7 or Ad.PEG-*mda*-7 variably induces apoptosis in different ovarian cancer cells. The indicated cell type was infected with the designated viruses for 72 h, and Annexin-V binding assay was performed as described in Materials and Methods. Results are the average from at least three experiments ±SD.

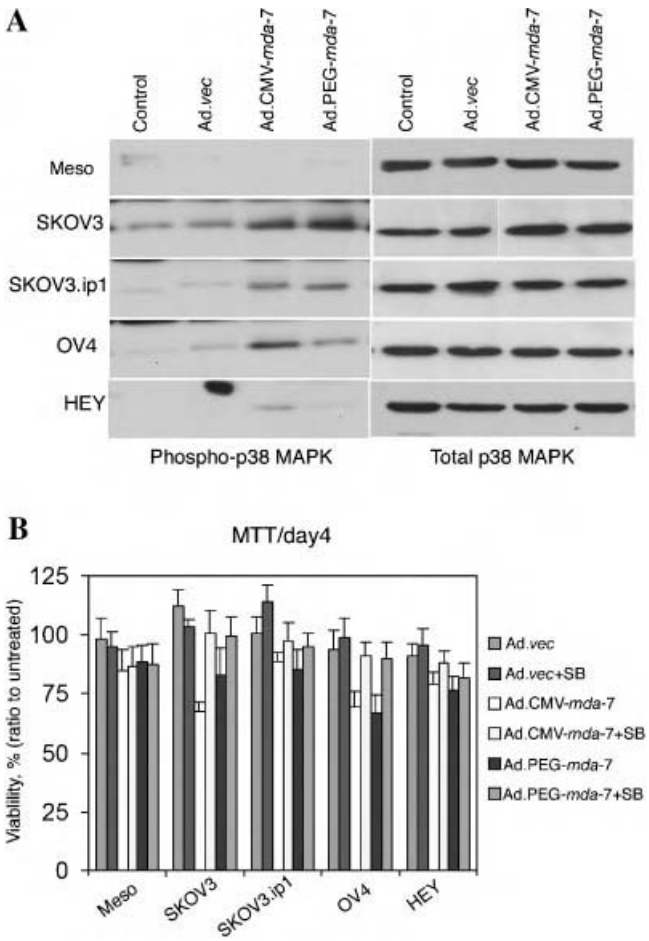

Fig. 3. Infection with Ad.CMV-*mda*-7 or Ad.PEG-*mda*-7 induces p38 MAPK phosphorylation and treatment with SB203580 protects ovarian cancer cells from *mda*-7-mediated apoptosis. **A**: Cells were infected with the indicated viruses as described in Figure 1C. Total cellular extracts were prepared at 48 h post-infection and the levels of phospho-p38 and total p38 MAPK were analyzed by Western blot analysis. **B**: Cells were infected with the indicated viruses and treated with 1 μM SB203580. Cell viability was assessed by MTT assay at 4 d post-infection. Results are the average from at least three experiments ±SD.

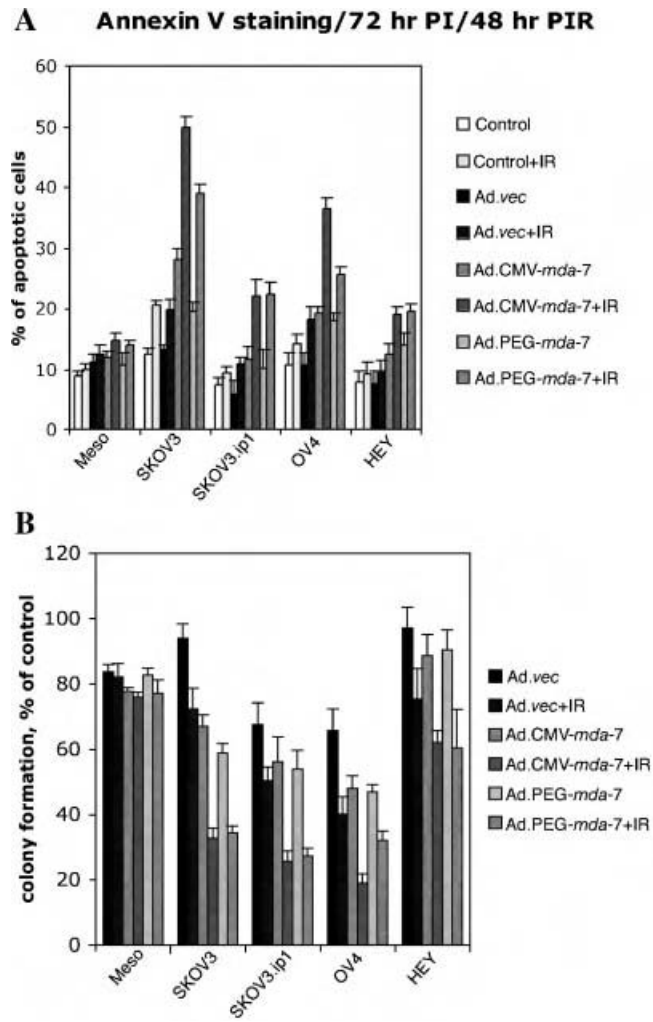

Fig. 4. Combination of Ad.CMV-*mda*-7 or Ad.PEG-*mda*-7 plus IR induces enhanced killing and apoptosis in ovarian cancer cells. **A**: Effect of single and combination treatment with Ad. CMV-*mda*-7 or Ad.PEG-*mda*-7 plus IR on apoptosis induction in ovarian cancer cells. The indicated cell type was either uninfected or infected with Ad.*vec*, Ad.CMV-*mda*-7, or Ad.PEG-*mda*-7 and the next day was exposed to 2 Gy of IR. An Annexin-V binding assay was performed at 48 h post-irradiation as described in Materials and Methods. Results are the average from at least three experiments ±SD. **B**: Effect of combination treatment with Ad.CMV-*mda*-7 or Ad.PEG-*mda*-7 plus IR on growth of ovarian cancer cells. Cells were either uninfected or infected and untreated or treated with IR as described in Figure 4A and colony forming assays were performed as described in the Materials and Methods section. Data are presented as a percentage of colony formation to that of the uninfected and untreated group. Results shown are averages ±SD of triplicate samples.

glioblastoma multiforme (Kawabe et al., 2002; Su et al., 2003; Yacoub et al., 2003a,b,c). These studies prompted us to test the effect of γ-radiation (IR) in combination with Ad.CMV-*mda*-7 or Ad.PEG.*mda*-7 in the context of ovarian cancer. In all four ovarian cancer cell lines, Ad.CMV-*mda*-7, Ad.PEG-*mda*-7, or 2 Gy of IR alone produced a marginal enhancement in the percentage of Annexin-V positive cells. However, a combination of 2 Gy of IR with Ad.CMV-*mda*-7 or Ad.PEG-*mda*-7 significantly enhanced Annexin-V staining in all four ovarian cancer cell lines (Fig. 4A). Similarly, in colony formation assays, infection with Ad.CMV-*mda*-7 or Ad.PEG-*mda*-7 alone significantly reduced colony formation only in the SKOV3 cell line; however, a combination treatment with 2 Gy IR further reduced the number of colonies not only in SKOV3 cell but also in the other three ovarian cancer cell lines (Fig. 4B). No significant induction of apoptosis or reduction in colony formation was apparent with this combinatorial treatment approach in normal human mesothelial cells. These results suggest that the combination of *mda*-7/IL-24 and IR might be a useful and efficacious approach for treating ovarian cancer patients.

MDA-7/IL-24 protein production in ovarian cancer cells directly correlates with a decrease in cell survival by combination treatment with Ad.CMV-*mda*-7 or Ad.PEG-*mda*-7 and IR

We next endeavored to define the possible mechanism of augmentation of *mda*-7/IL-24-induced cell killing by IR. Infection with Ad.CMV-*mda*-7 generated high levels of *mda*-7/IL-24 mRNA as early as 1 day after infection in SKOV3 and OV-4 cells (Fig. 5A). Although in SKOV3.ip1 and HEY cells *mda*-7/IL-24 mRNA level was not high 1 day after infection, which can be explained by low infectivity, it accumulated gradually and by 3 days post-infection all four ovarian cancer cells had high and comparable levels of *mda*-7/IL-24 mRNA. This finding

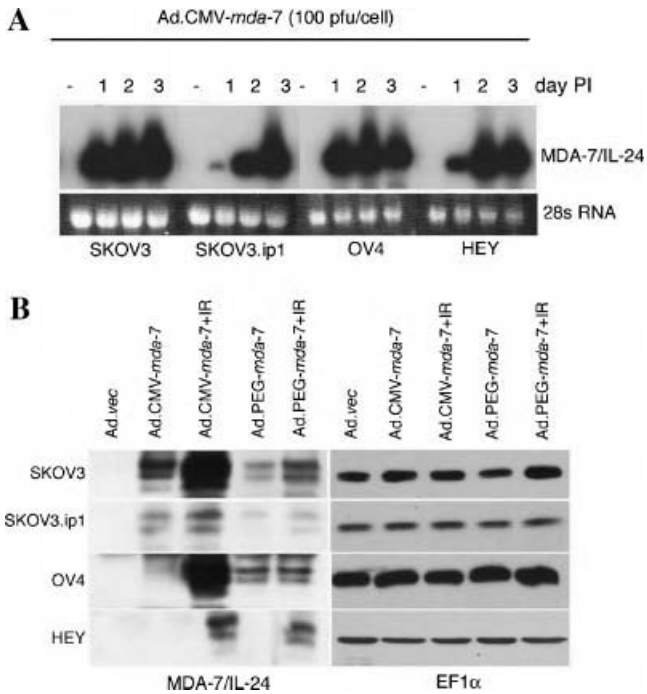

Fig. 5. Combination treatment with *mda*-7/IL-24 and IR reverses the translational block in ovarian cancer cells. **A**: Infection of Ad.CMV-*mda*-7 induces an abundant amount of MDA-7/IL-24 RNA. Total RNA was isolated at d 1, d 2, and d 3 after infection as described in Materials and Methods, and analyzed by Northern blotting. The blots were probed with a α-^{32}P[dCTP]-labeled, full-length human *mda*-7/IL-24 cDNA probe and exposed for autoradiography. **B**: Combination treatment of IR plus MDA-7/IL-24 enhances *mda*-7/IL-24 protein. Cells were infected with Ad.*vec*, Ad.CMV-*mda*-7, or Ad.PEG-*mda*-7 and untreated or treated with IR the next day. Protein lysates were prepared 24 h after IR and Western blotting was performed as described in Materials and Methods to determine the levels of MDA-7/IL-24 protein. Equal protein loading was confirmed by Western blotting with an EF-1α antibody.

contrasts with the observation that in HEY cells very little MDA-7/IL-24 protein levels were observed even at 2 days post-infection (Fig. 1C and 5B). An inherent block in *mda*-7/IL-24 mRNA translation into protein has been observed in pancreatic cancer cells that can be overcome by multiple combinatorial approaches such as inhibition of K-*ras* or induction of reactive oxygen species (Su et al., 2001a; Lebedeva et al., 2005b, 2006). When ovarian cancer cells were treated with γ-radiation elevated levels of MDA-7/IL-24 protein were detected upon infection with both Ad.CMV-*mda*-7 and Ad.PEG.*mda*-7 in all four ovarian cancer cells. These findings indicate that γ-radiation treatment helps overcome the translational block delimiting MDA-7/IL-24 protein production, thus facilitating augmentation of apoptosis induction.

DISCUSSION

We presently demonstrate a potentially clinically relevant phenomenon that a combination of *mda*-7/IL-24 with IR promotes apoptosis in ovarian cancer cells that are initially resistant to either agent used alone. In ovarian cancer cells, IR (at 2 Gy) or *mda*-7/IL-24 (either as Ad.CMV-*mda*-7 or as Ad.PEG-*mda*-7) alone did not significantly affect cell growth, except for SKOV3 cells, whereas a combination of both agents significantly reduced cell viability in all four ovarian cancer cell lines examined in the present study. Furthermore, we demonstrate that simultaneous treatment of IR plus *mda*-7/IL-24 could override the translational block of *mda*-7/IL-24 mRNA into protein in ovarian cancer cells, which could explain the enhanced efficacy of this combinatorial approach.

Several tumor-specific or ovarian cell carcinoma-specific promoters have been investigated in the preclinical settings. Robertson et al. (1998) found that a plasmid containing the HSV/TK gene, under the SLP1 (secretory leukoproteinase inhibitor gene, which is highly expressed in a variety of epithelial tumors, including ovarian cancer) promoter, could kill ovarian cancer cell. Another study (Tanyi et al., 2002) reported increased Luc production in several types of epithelial cancer cell lines, including ovarian cancer cell lines, with minimal activity in non-epithelial and immortalized normal cell lines when delivered under the control of SLP1 promoter. However, the same group found some non-specific Luc activity in many cell types, using OSP1, a retroviral promoter reported to be transcriptionally active only in rat ovaries. In our present study, besides the CMV promoter, we used the PEG-Prom to control *mda*-7/IL-24 gene expression (Su et al., 2000, 2001b, 2005b) selectively in cancer cells. We demonstrate that Ad.PEG-*mda*-7 induced apoptosis selectively in cancer cells without inducing harmful effects to normal human mesothelial cells. The advantage of using the PEG-Prom is that its cancer cell specificity is attributed to two transcription factors, PEA-3 and AP-1, which are overexpressed in >90% of cancers. Additionally, the PEG-Prom is functionally active in all cancer cells irrespective of their p53, Rb, or other tumor suppressor gene status. Thus, employing the PEG-Prom to drive transgene expression only in cancer cells has selective advantages over other tissue- or cancer-specific promoters.

Consistent with a previous report (Leath et al., 2004), this study demonstrates that *mda*-7/IL-24 induces a low and variable degree of apoptosis in ovarian cancer cells when delivered via a replication-incompetent adenovirus under the control of either the CMV or PEG promoters. One of the reasons for this finding is low expression of MDA-7/IL-24 protein due to low Ad-mediated *mda*-7/IL-24 gene delivery. However, defects (or blocks) in signaling mechanisms contributing to this low apoptosis induction require investigation. Currently, the signaling mechanisms involved in *mda*-7/IL-24-mediated apoptosis induction in specific ovarian cancer cells remain incompletely understood. Previous studies showed that activation of p38 MAPK plays an important role in mediating Ad.*mda*-7-induced apoptosis in melanoma, prostate carcinoma, and malignant glioma cells (Sarkar et al., 2002; Lebedeva et al., 2005a; Gupta et al., 2006). Using only one ovarian cancer cell line, a recent report showed that induction of the FAS-FASL pathway mediates Ad.*mda*-7-mediated cell killing (Gopalan et al., 2005). However, in this study we demonstrate that both Ad.CMV-*mda*-7 and Ad.PEG-*mda*-7 activated the p38 MAPK pathway in ovarian cancer cells and the level of phosphorylated p38 MAPK correlated with the killing effect of Ad.CMV-*mda*-7 and Ad.PEG-*mda*-7 in these cells. Additionally, SB203580, a selective p38 MAPK inhibitor significantly abolished the *mda*-7/IL-24-induced killing effect. Thus, activation of p38 MAPK might be a key element in *mda*-7/IL-24-induced apoptosis induction in multiple cell types, including ovarian carcinoma.

To circumvent the limitation of low transduction efficiency, we were interested in defining strategies that could be utilized to improve delivery of *mda*-7/IL-24,

especially to those cells that were most resistant (SKOV3.ip1, HEY). Treatment options for ovarian cancer patients frequently involve debulking surgery combined with various therapeutic approaches, including radiation, chemotherapy, immunotherapy, and recently anti-angiogenic therapy (Wolf and Jenkins, 2002; Jemal et al., 2004). In this context, methods enhancing the effectiveness of anti-cancer agents, without promoting toxicity, would be of immense value and could provide a means of significantly improving clinical responses. Studies in NSCLC (Kawabe et al., 2002) and malignant gliomas (Su et al., 2003; Yacoub et al., 2003b,c) formally showed that radiation enhances tumor cell sensitivity to *mda*-7/IL-24. In two recent studies (Su et al., 2005a, 2006), we have uncovered an important property of *mda*-7/IL-24: an ability to induce a potent radiation enhancement "bystander anti-tumor effect" not only in cancer cells inherently sensitive to this cytokine but also in tumor cells overexpressing the anti-apoptotic proteins BCL-2 or BCL-x_L and exhibiting resistance to the cytotoxic effects of both radiation and MDA-7/IL-24. These findings offer promise for dramatically expanding the use of *mda*-7/IL-24 for cancer therapy, especially in the context of radiation therapy. Additionally, recent reports indicate that Ad.*mda*-7 lethality in NSCLC cells can also be augmented by combination treatment with the non-steroidal anti-inflammatory drug sulindac (Oida et al., 2005) and that Ad.*mda*-7 amplifies the anti-tumor effects of Herceptin (trastuzumab), an anti-p185ErbB2 murine monoclonal antibody (mAb) that binds to the extracellular domain of ErbB2, in breast carcinoma cells overexpressing HER-2/neu (McKenzie et al., 2004). Overall, these studies employing radiation, a chemotherapeutic agent, and a mAb reinforce the possibility of augmenting the anti-cancer activity of *mda*-7/IL-24 and increasing its therapeutic index as a gene therapy for diverse cancers by using combinatorial therapy approaches (Fisher, 2005; Gupta et al., 2006). Our present studies reveal that radiation might be an effective component of the combinatorial treatment for ovarian cancer cells along with Ad.CMV-*mda*-7 or Ad.PEG-*mda*-7.

In summary, a combination of IR plus *mda*-7/IL-24 (administered as Ad.CMV-*mda*-7 or Ad.PEG-*mda*-7) enhances apoptosis induction in ovarian cancer cells, which initially demonstrated relative resistance to either of these agents alone. In contrast, similar experimental protocols applied to normal human mesothelial cells do not induce significant harmful effects. The unique synergy in ovarian cancer cells correlates with the ability of IR to relieve the translational block preventing conversion of *mda*-7/IL-24 mRNA into protein. These in vitro data suggest that combination treatment of Ad.*mda*-7 and IR has potential to increase tumor response to radiotherapy and/or gene therapy and warrants further investigation using in vivo tumor models.

ACKNOWLEDGMENTS

The present studies were supported in part by NIH grants R01 CA083821, R01 CA097318, R01 CA098712, P01 CA104177, UAB ovarian SPORE career development award NIH/NCIP50 CA83591, and Gynecology Foundation pilot Award; Army DOD Idea Development Award W81XWH-05-1-0035; the Samuel Waxman Cancer Research Foundation; and the Chernow Endowment. PBF is a Michael and Stella Chernow Urological Cancer Research Scientist and a SWCRF Investigator.

LITERATURE CITED

Alvarez RD, Curiel DT. 1997. A phase I study of recombinant adenovirus vector-mediated delivery of an anti-erbB-2 single-chain (sFv) antibody gene for previously treated ovarian and extraovarian cancer patients. Hum Gene Ther 8:229–242.

Alvarez RD, Gomez-Navarro J, Wang M, Barnes MN, Strong TV, Arani RB, Arafat W, Hughes JV, Siegal GP, Curiel DT. 2000. Adenoviral-mediated suicide gene therapy for ovarian cancer. Mol Ther 2:524–530.

Barnes MN, Deshane JS, Rosenfeld M, Siegal GP, Curiel DT, Alvarez RD. 1997. Gene therapy and ovarian cancer: A review. Obstet Gynecol 89:145–155.

Casado E, Gomez-Navarro J, Yamamoto M, Adachi Y, Coolidge CJ, Arafat WO, Barker SD, Wang MH, Mahasreshti PJ, Hemminki A, Gonzalez-Baron M, Barnes MN, Pustilnik TB, Siegal GP, Alvarez RD, Curiel DT. 2001. Strategies to accomplish targeted expression of transgenes in ovarian cancer for molecular therapeutic applications. Clin Cancer Res 7:2496–2504.

Christian J, Thomas H. 2001. Ovarian cancer chemotherapy. Cancer Treat Rev 27:99–109.

Collinet P, Lanvin D, Vereecque R, Quesnel B, Querleu D. 2000. (Gene therapy and ovarian cancer: Update of clinical trials). J Gynecol Obstet Biol Reprod (Paris) 29:532–537.

Cunningham CC, Chada S, Merritt JA, Tong A, Senzer N, Zhang Y, Mhashilkar A, Parker K, Vukelja S, Richards D, Hood J, Coffee K, Nemunaitis J. 2005. Clinical and local biological effects of an intratumoral injection of mda-7 (IL24; INGN 241) in patients with advanced carcinoma: A phase I study. Mol Ther 11: 149–159.

Fisher PB. 2005. Is mda-7/IL-24 a "magic bullet" for cancer? Cancer Res 65:10128–10138.

Fisher PB, Gopalkrishnan RV, Chada S, Ramesh R, Grimm EA, Rosenfeld MR, Curiel DT, Dent P. 2003. mda-7/IL-24, a novel cancer selective apoptosis inducing cytokine gene: From the laboratory into the clinic. Cancer Biol Ther 2: S23–S37.

Gomez-Navarro J, Siegal GP, Alvarez RD, Curiel DT. 1998. Gene therapy: Ovarian carcinoma as the paradigm. Am J Clin Pathol 109:444–467.

Gopalan B, Litvak A, Sharma S, Mhashilkar AM, Chada S, Ramesh R. 2005. Activation of the Fas-FasL signaling pathway by MDA-7/IL-24 kills human ovarian cancer cells. Cancer Res 65:3017–3024.

Gupta P, Su ZZ, Lebedeva IV, Sarkar D, Sauane M, Emdad L, Bachelor MA, Grant S, Curiel DT, Dent P, Fisher PB. 2006. mda-7/IL-24: Multifunctional cancer-specific apoptosis-inducing cytokine. Pharmacol Ther 2006 Feb 3, [Epub ahead of print].

Jemal A, Tiwari RC, Murray T, Ghafoor A, Samuels A, Ward E, Feuer EJ, Thun MJ. 2004. Cancer statistics, 2004. CA Cancer J Clin 54:8–29.

Kawabe S, Nishikawa T, Munshi A, Roth JA, Chada S, Meyn RE. 2002. Adenovirus-mediated *mda*-7 gene expression radiosensitizes non-small cell lung cancer cells via TP53-independent mechanisms. Mol Ther 6:637–644.

Leath CA III, Kataram M, Bhagavatula P, Gopalkrishnan RV, Dent P, Fisher PB, Pereboev A, Carey D, Lebedeva IV, Haisma HJ, Alvarez RD, Curiel DT, Mahasreshti PJ. 2004. Infectivity enhanced adenoviral-mediated *mda*-7/IL-24 gene therapy for ovarian carcinoma. Gynecol Oncol 94:352–362.

Lebedeva IV, Sauane M, Gopalkrishnan RV, Sarkar D, Su ZZ, Gupta P, Nemunaitis J, Cunningham C, Yacoub A, Dent P, Fisher PB. 2005a. mda-7/IL-24: Exploiting cancer's Achilles' heel. Mol Ther 11:4–18.

Lebedeva IV, Su ZZ, Sarkar D, Gopalkrishnan RV, Waxman S, Yacoub A, Dent P, Fisher PB. 2005b. Induction of reactive oxygen species renders mutant and wild-type K-*ras* pancreatic carcinoma cells susceptible to Ad.*mda*-7-induced apoptosis. Oncogene 24:585–596.

Lebedeva IV, Sarkar D, Su ZZ, Gopalkrishnan RV, Athar M, Randolph A, Valerie K, Dent P, Fisher PB. 2006. Molecular target-based therapy of pancreatic cancer. Cancer Res 66:2403–2413.

McKenzie T, Liu Y, Fanale M, Swisher SG, Chada S, Hunt KK. 2004. Combination therapy of Ad-*mda*7 and trastuzumab increases cell death in Her-2/neu-overexpressing breast cancer cells. Surgery 136:437–442.

Oida Y, Gopalan B, Miyahara R, Inoue S, Branch CD, Mhashilkar AM, Lin E, Bekele BN, Roth JA, Chada S, Ramesh R. 2005. Sulindac enhances adenoviral vector expressing *mda*-7/IL-24-mediated apoptosis in human lung cancer. Mol Cancer Ther 4:291–304.

Pataer A, Vorburger SA, Barber GN, Chada S, Mhashilkar AM, Zou-Yang H, Stewart AL, Balachandran S, Roth JA, Hunt KK, Swisher SG. 2002. Adenoviral transfer of the melanoma differentiation-associated gene 7 (*mda*7) induces apoptosis of lung cancer cells via up-regulation of the double-stranded RNA-dependent protein kinase (PKR). Cancer Res 62:2239–2243.

Robertson MW III, Barnes MN, Rancourt C, Wang M, Grim J, Alvarez RD, Siegal GP, Curiel DT. 1998. Gene therapy for ovarian carcinoma. Semin Oncol 25: 397–406.

Saeki T, Mhashilkar A, Swanson X, Zou-Yang XH, Sieger K, Kawabe S, Branch CD, Zumstein L, Meyn RE, Roth JA, Chada S, Ramesh R. 2002. Inhibition of human lung cancer growth following adenovirus-mediated *mda*-7 gene expression in vivo. Oncogene 21:4558–4566.

Sarkar D, Su ZZ, Lebedeva IV, Sauane M, Gopalkrishnan RV, Valerie K, Dent P, Fisher PB. 2002. *mda*-7 (IL-24) mediates selective apoptosis in human melanoma cells by inducing the coordinated overexpression of the GADD family of genes by means of p38 MAPK. Proc Natl Acad Sci USA 99:10054–10059.

Sarkar D, Su ZZ, Vozhilla N, Park ES, Gupta P, Fisher PB. 2005a. Dual cancer-specific targeting strategy cures primary and distant breast carcinomas in nude mice. Proc Natl Acad Sci USA 102:14034–14039.

Sarkar D, Su ZZ, Vozhilla N, Park ES, Randolph A, Valerie K, Fisher PB. 2005b. Targeted virus replication plus immunotherapy eradicates primary and distant pancreatic tumors in nude mice. Cancer Res 65:9056–9063.

Sauane M, Gopalkrishnan RV, Choo HT, Gupta P, Lebedeva IV, Yacoub A, Dent P, Fisher PB. 2004. Mechanistic aspects of *mda*-7/IL-24 cancer cell selectivity analysed via a bacterial fusion protein. Oncogene 23:7679–7690.

Su ZZ, Shi Y, Fisher PB. 1997. Subtraction hybridization identifies a transformation progression-associated gene *PEG*-3 with sequence homology to a growth arrest and DNA damage-inducible gene. Proc Natl Acad Sci USA 94:9125–9130.

Su ZZ, Goldstein NI, Jiang H, Wang MN, Duigou GJ, Young CS, Fisher PB. 1999. *PEG*-3, a nontransforming cancer progression gene, is a positive regulator of cancer aggressiveness and angiogenesis. Proc Natl Acad Sci USA 96:15115–15120.

Su ZZ, Shi Y, Fisher PB. 2000. Cooperation between AP1 and PEA3 sites within the progression elevated gene-3 (*PEG*-3) promoter regulate basal and differential expression of *PEG*-3 during progression of the oncogenic phenotype in transformed rat embryo cells. Oncogene 19:3411–3421.

Su ZZ, Lebedeva IV, Gopalkrishnan RV, Goldstein NI, Stein CA, Reed JC, Dent P, Fisher PB. 2001a. A combinatorial approach for selectively inducing programmed cell death in human pancreatic cancer cells. Proc Natl Acad Sci USA 98:10332–10337.

Su ZZ, Shi Y, Friedman R, Qiao L, McKinstry R, Hinman D, Dent P, Fisher PB. 2001b. PEA3 sites within the progression elevated gene-3 (*PEG*-3) promoter and mitogen-activated protein kinase contribute to differential *PEG*-3 expression in Ha-*ras* and v-*raf*oncogene transformed rat embryo cells. Nucleic Acids Res 29:1661–1671.

Su ZZ, Lebedeva IV, Sarkar D, Gopalkrishnan RV, Sauane M, Sigmon C, Yacoub A, Valerie K, Dent P, Fisher PB. 2003. Melanoma differentiation associated gene-7, *mda*-7/IL-24, selectively induces growth suppression, apoptosis and radiosensitization in malignant gliomas in a p53-independent manner. Oncogene 22:1164–1180.

Su ZZ, Emdad L, Sauane M, Lebedeva IV, Sarkar D, Gupta P, James CD, Randolph A, Valerie K, Walter MR, Dent P, Fisher PB. 2005a. Unique aspects of *mda*-7/IL-24 antitumor bystander activity: Establishing a role for secretion of MDA-7/IL-24 protein by normal cells. Oncogene 24:7552–7566.

Su ZZ, Sarkar D, Emdad L, Duigou GJ, Young CS, Ware J, Randolph A, Valerie K, Fisher PB. 2005b. Targeting gene expression selectively in cancer cells by using the progression-elevated gene-3 promoter. Proc Natl Acad Sci USA 102: 1059–1064.

Su ZZ, Lebedeva IV, Sarkar D, Emdad L, Gupta P, Kitada S, Dent P, Reed JC, Fisher PB. 2006. Ionizing radiation enhances therapeutic activity of *mda*-7/IL-24: Overcoming radiation- and mda-7/IL-24-resistance in prostate cancer cells overexpressing the antiapoptotic proteins bcl-xL or bcl-2. Oncogene 25:2339–2348.

Tanyi JL, Lapushin R, Eder A, Auersperg N, Tabassam FH, Roth JA, Gu J, Fang B, Mills GB, Wolf J. 2002. Identification of tissue- and cancer-selective promoters for the introduction of genes into human ovarian cancer cells. Gynecol Oncol 85:451–458.

Tong AW, Nemunaitis J, Su D, Zhang Y, Cunningham C, Senzer N, Netto G, Rich D, Mhashilkar A, Parker K, Coffee K, Ramesh R, Ekmekcioglu S, Grimm EA, van Wart Hood J, Merritt J, Chada S. 2005. Intratumoral injection of INGN 241, a nonreplicating adenovector expressing the melanoma-differentiation associated gene-7 (*mda*-7/IL24): Biologic outcome in advanced cancer patients. Mol Ther 11:160–172.

Wolf JK, Jenkins AD . 2002. Gene therapy for ovarian cancer (review). Int J Oncol 21:461–468.

Yacoub A, Mitchell C, Brannon J, Rosenberg E, Qiao L, McKinstry R, Linehan WM, Su ZS, Sarkar D, Lebedeva IV, Valerie K, Gopalkrishnan RV, Grant S, Fisher PB, Dent P. 2003a. MDA-7 (interleukin-24) inhibits the proliferation of renal carcinoma cells and interacts with free radicals to promote cell death and loss of reproductive capacity. Mol Cancer Ther 2:623–632.

Yacoub A, Mitchell C, Lebedeva IV, Sarkar D, Su ZZ, McKinstry R, Gopalkrishnan RV, Grant S, Fisher PB, Dent P. 2003b. *mda*-7 (IL-24) inhibits growth and enhances radiosensitivity of glioma cells in vitro via JNK signaling. Cancer Biol Ther 2:347–353.

Yacoub A, Mitchell C, Lister A, Lebedeva IV, Sarkar D, Su ZZ, Sigmon C, McKinstry R, Ramakrishnan V, Qiao L, Broaddus WC, Gopalkrishnan RV, Grant S, Fisher PB, Dent P. 2003c. Melanoma differentiation-associated 7 (interleukin 24) inhibits growth and enhances radiosensitivity of glioma cells in vitro and in vivo. Clin Cancer Res 9:3272–3281.

Zeimet AG, Marth C. 2003. Why did p53 gene therapy fail in ovarian cancer? Lancet Oncol 4:415–422.

NANO LETTERS

2006
Vol. 6, No. 4
587−591

Covalently Linked Au Nanoparticles to a Viral Vector: Potential for Combined Photothermal and Gene Cancer Therapy

Maaike Everts,[†] Vaibhav Saini,[†,‡] Jennifer L. Leddon,[†] Robbert J. Kok,[§] Mariam Stoff-Khalili,[†] Meredith A. Preuss,[†] C. Leigh Millican,[||] Guy Perkins,[⊥] Joshua M. Brown,[⊥] Hitesh Bagaria,[#] David E. Nikles,[#] Duane T. Johnson,[#] Vladimir P. Zharov,[+] and David T. Curiel*[,†]

Division of Human Gene Therapy, Departments of Medicine, Surgery, Pathology and the Gene Therapy Center, High-Resolution Imaging Facility, and Department of Physiology and Biophysics, University of Alabama at Birmingham, Birmingham, Alabama 35294, Department of Pharmacokinetics and Drug Delivery, University Center for Pharmacy, Groningen University Institute for Drug Exploration (GUIDE), 9713 AV Groningen, The Netherlands, National Center for Microscopy and Imaging Research, Center for Research on Biological Structure School of Medicine, University of California, San Diego, California 92093, Center for Materials for Information Technology (MINT), University of Alabama, Tuscaloosa, Alabama 35487, and Philips Classic Laser Laboratories, University of Arkansas for Medical Sciences, Little Rock, Arkansas 72205

Received January 11, 2005; Revised Manuscript Received February 11, 2006

ABSTRACT

Hyperthermia can be produced by near-infrared laser irradiation of gold nanoparticles present in tumors and thus induce tumor cell killing via a bystander effect. To be clinically relevant, however, several problems still need to be resolved. In particular, selective delivery and physical targeting of gold nanoparticles to tumor cells are necessary to improve therapeutic selectivity. Considerable progress has been made with respect to retargeting adenoviral vectors for cancer gene therapy. We therefore hypothesized that covalent coupling of gold nanoparticles to retargeted adenoviral vectors would allow selective delivery of the nanoparticles to tumor cells, thus feasibilizing hyperthermia and gene therapy as a combinatorial therapeutic approach. For this, sulfo-*N*-hydroxysuccinimide labeled gold nanoparticles were reacted to adenoviral vectors encoding a luciferase reporter gene driven by the cytomegalovirus promoter (AdCMVLuc). We herein demonstrate that covalent coupling could be achieved, while retaining virus infectivity and ability to retarget tumor-associated antigens. These results indicate the possibility of using adenoviral vectors as carriers for gold nanoparticles.

Cancer targeted therapies rely on exploiting susceptibility parameters of tumor versus normal cells. The increased susceptibility of tumors to heat makes hyperthermia a feasible treatment option.[1] A variety of heat sources have been explored, including laser light, focused ultrasound, as well as microwaves. More recently, the use of near-infrared-absorbing gold nanoparticles has successfully been applied to reduce tumor burden and increase survival in animal experiments.[2] Selectivity of heat induction is based on enhanced permeability of the tumor vasculature and subsequent retention of the intravenously administered nanoparticles, which can be heated using deep penetrating near-infrared (NIR) laser light.[3] However, enhanced permeability and retention pathophysiology do not occur in all tumors, mandating alternative methods of targeted nanoparticle tumor delivery before successful clinical application can be achieved.

We hypothesized that the recent improvements in targeted adenoviral vectorology might provide the platform for tumor selective delivery of these nanoparticles. We therefore sought

* Correspondence should be addressed to: David T. Curiel, Division of Human Gene Therapy, 901 19th Street South, BMRII-508, University of Alabama at Birmingham, Birmingham, AL 35294-2172; phone (205) 934 8627; fax (205) 975 7476; e-mail address curiel@uab.edu.

[†] Division of Human Gene Therapy, Departments of Medicine, Surgery, Pathology and the Gene Therapy Center, University of Alabama at Birmingham.

[‡] Department of Physiology and Biophysics, University of Alabama at Birmingham.

[§] Department of Pharmacokinetics and Drug Delivery, University Center for Pharmacy, Groningen University Institute for Drug Exploration (GUIDE).

[||] High-Resolution Imaging Facility, University of Alabama at Birmingham, Birmingham, Alabama.

[⊥] National Center for Microscopy and Imaging Research, Center for Research on Biological Structure School of Medicine, University of California.

[#] Center for Materials for Information Technology (MINT), University of Alabama.

[+] Philips Classic Laser Laboratories, University of Arkansas for Medical Sciences.

10.1021/nl0500555 CCC: $33.50
Published on Web 03/15/2006

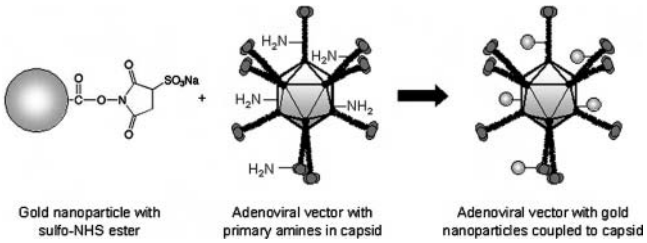

Figure 1. Gold nanoparticles can covalently be attached to primary amines present in capsid proteins. The sulfo-NHS ester attached on the 1.3-nm gold particle will react with primary amines of lysine residues present in the adenoviral capsid, resulting in an amide bond between the gold particle and the adenovirus. There are over 10 000 lysines in the proteins that make up the capsid, although not all of these will be accessible for chemical reaction.

to establish the feasibility of covalently coupling gold nanoparticles to adenoviral vectors, as a means to achieve the desired targeted localization. We anticipated that this linkage could be achieved without compromising key adenoviral infectivity properties that constitute the functional basis of its tumor-targeting capabilities. This combination of a targeted viral vector with an amplifying nanoparticle payload thus seeks to exploit favorable aspects of each component to realize an optimized anticancer effect. This type of combinatorial system represents a novel paradigm for the design of tumor-targeted nanoparticles.

Association of Gold Particles with Adenoviral Vectors. The sulfo-NHS-ester on the gold nanoparticles employed has reactivity toward primary amines that are abundantly present on the adenoviral capsid lysine residues (Figure 1).

For the initial characterization of the feasibility of coupling gold nanoparticles to adenoviral vectors, a ratio of 1000:1 gold:adenovirus (particle:particle) was employed in the synthesis procedure. After the reaction, the mixture was purified using CsCl gradient centrifugation—a standard method for adenoviral vector purification. Fractions collected from the bottom of the centrifugation tube were analyzed for the presence of virus using an anti-hexon antibody (Figure 2A) and for the presence of gold using silver staining (Figure 2B). Although staining for the presence of virus appears to be more sensitive than detection of gold, a comparison of the staining patterns of both slot blots demonstrated co-localization of virus with gold, indicating co-migration of both components through the CsCl gradient. These results suggested a covalent association between the gold nanoparticles and the adenoviral vectors.

During centrifugation of gold-labeled viral particles in a CsCl gradient, a shift in the height of the viral band in the centrifuge tube was observed, which was dependent on the amount of gold nanoparticles employed in the synthesis

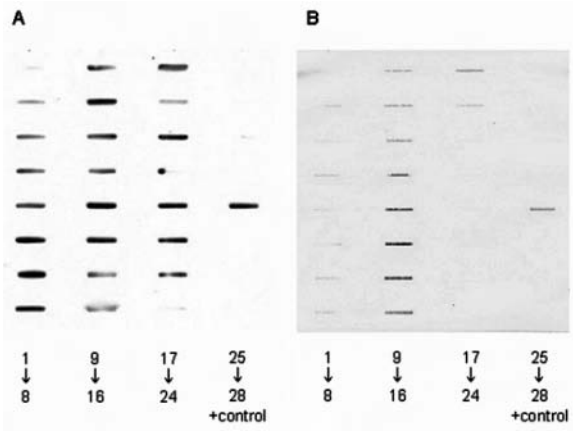

Figure 2. Slotblot analysis demonstrating the presence of adenovirus and gold in fractions collected after virus CsCl purification. Gold nanoparticles were first reacted with adenoviral vectors in a 1000:1 ratio. The reaction mixture was then purified using centrifugation over a CsCl gradient, a standard method of viral vector purification. After the bottom of the centrifugation tube was punctured, 28 fractions were collected and analyzed for the presence of adenovirus using staining for the hexon capsid protein (A) and the presence of gold nanoparticles using silver enhancement staining (B). The original reaction mixture prior to purification was used as a positive control (+control).

procedure, indicating an increased density of the viral particles upon gold labeling (Table 1, Figure 3). To exclude aspecific, noncovalent interaction of gold nanoparticles with the viral vectors, a synthesis procedure employing gold nanoparticles labeled with a nickel-nitrilotriacetic acid (Ni−NTA) instead of a sulfo-NHS reactive group was performed. In this reaction, the shift in vector band localization could not be observed (Table 1, Figure 3), confirming the covalent nature of interaction of the sulfo-NHS particles with the virions. It should be noted, however, that the surface charge of sulfo-NHS labeled particles is neutral, whereas the surface charge of Ni−NTA labeled particles is negative. Since adenoviruses have a net negative charge on their capsid surface as well,[4] nonspecific electrostatic absorption of Ni−NTA labeled particles to the virions could be less than electrostatic absorption of sulfo-NHS particles. Nonetheless, the absence of Ni−NTA labeled particles in CsCl purified virions indicates that association of nanoparticles with virions in the gradient is not based on the weight of the particles.

Electron Microscopy of Gold-Labeled Adenoviral Vectors. Electron microscopy was used to visualize gold nanoparticles reacted to the surface of adenoviral vectors that were purified by CsCl centrifugation as above. Vectors were deposited onto carbon-coated copper grids; no staining was used in order to avoid occlusion of the 1.4 nm nanoparticles on the surface of the virions. Gold nanoparticles could not

Table 1. Positions of Viral Bands in Centrifugation Tubes after CsCl Gradient Centrifugation

virus−gold combination	distance from bottom to lower band	distance from bottom to upper band (cm)	total distance gradient (cm)
virus alone, no gold nanoparticles	no lower band	4.3	6.6
virus + 10000 Ni−NTA gold nanoparticles	no lower band	4.2	6.6
virus + 10000 Sulfo-NHS gold nanoparticles	2.8 cm	4.2	6.6

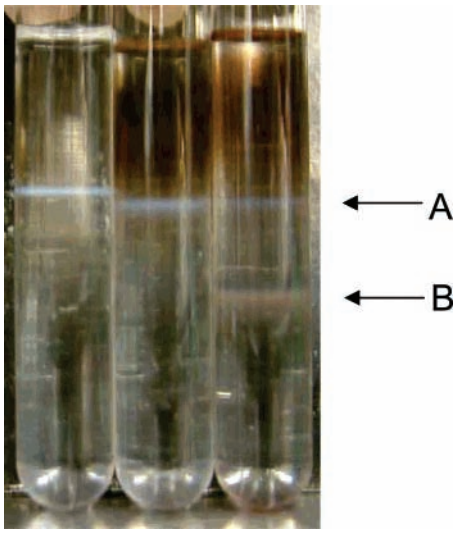

Figure 3. Photograph of gold-labeled adenoviral vectors in a CsCl gradient. 1×10^{12} viral particles were reacted with either no gold nanoparticles (left), 10 000 Ni−NTA gold particles per viral particle (middle) or 10 000 sulfo-NHS gold particles per viral particle. The gold nanoparticles not reacted to the virus in the middle and right tube remain in the upper portion of the gradient (brown color above arrow A). The white band in the area indicated by arrow A consists of remaining unlabeled virions, the light brown band indicated by arrow B indicates gold-labeled virions and can only be observed in the right centrifuge tube.

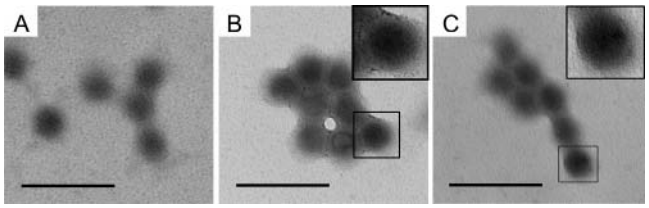

Figure 4. Electron microscopy identifies gold nanoparticles associated with adenoviral vectors. Vectors were either unlabeled (A), sulfo-NHS gold nanoparticles labeled (B), or Ni−NTA gold nanoparticles labeled (C). Adenoviral vectors were examined using electron microscopy using a JEOL JEM 1200FX operated at 80 kV. Original magnification 100000×, scale bar 100 nm.

be observed in virus preparations that were either unlabeled (Figure 4A) or labeled with Ni−NTA gold nanoparticles (Figure 4C). One does see some "texture", but this arises from the little bit of underfocus used to better see the virions and is not to be confused with gold particles. In contrast, gold nanoparticles could clearly be observed in the virus preparation labeled with sulfo-NHS gold nanoparticles (Figure 4B, small black dots on the edges of the virions, see magnified insert). The gold particles in Figure 4B have rather sharp boundaries and similar sizes, as opposed to the texture in Figure 4C. This further strengthened the observation of a covalent interaction between the two components.

Gold-Labeled Adenoviral Vectors Retain Infectivity in HeLa Cells. Modification of capsid proteins such as the here-described chemical modification with gold nanoparticles may result in a loss of infectivity of the adenoviral vectors. We therefore evaluated gene transfer of a luciferase encoding adenoviral vector AdCMVLuc, labeled with different amounts of gold in HeLa cells. These cells are previously reported to

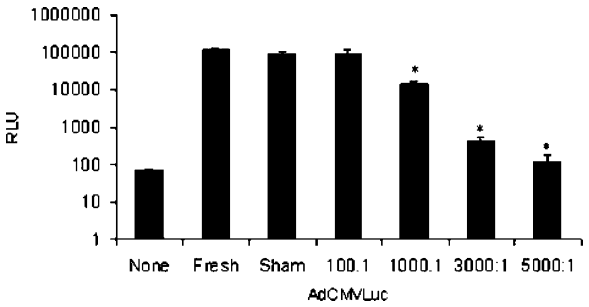

Figure 5. Infectivity of gold-labeled adenoviral vectors is retained at lower particle-to-vector ratios. Gold nanoparticles were reacted with AdCMVLuc at ratios of 100:1, 1000:1, 3000:1, and 5000:1. After reaction, HeLa cells were infected with 100 vp/cell and luciferase expression was determined after 24 h. Bars represent mean ± standard deviation. Asterisks indicate $p < 0.05$.

be readily infected with adenoviral vectors.[5] AdCMVLuc infectivity at a multiplicity of infection (MOI) of 25 was not affected by the synthesis procedure itself. This was demonstrated by the comparable levels of luciferase activity of sham-labeled versus fresh, unmodified AdCMVLuc (Figure 5). Further, a gold:adenovirus ratio of 100:1 (particle:particle) also did not affect infectivity. However, higher gold:adenovirus ratios did significantly decrease infectivity compared to unlabeled AdCMVLuc (Figure 5). Results were similar for both lower (5) and higher (125) MOIs (data not shown). This suggested a threshold of the number of gold nanoparticles that can be coupled to adenoviral vector without disrupting the natural infectivity mechanism of adenoviral gene transfer.

Gold-Labeled Adenoviral Vectors Can Be Retargeted to CEA Expressing Tumor Cells. A majority of human tumors are deficient in the primary receptor for adenoviral vectors, the Coxsackie adenovirus receptor (CAR), resulting in poor tumor cell transduction. To overcome this hurdle, approaches have been established whereby the adenoviral vector is physically retargeted to alternate receptors on the tumor cell surface. One example is retargeting of adenoviral vectors to the tumor-associated antigen carcino embryonic antigen (CEA), which is overexpressed on several neoplasias such as colon carcinoma. To establish whether gold-labeled adenoviral vectors could still be retargeted to CEA, AdCMVLuc was preincubated with the fusion protein sCAR-MFE, which on one side binds to the adenoviral capsid and on the other side binds to CEA. Gene transfer in MC38−CEA-2 cells, a CEA overexpressing cell line, was markedly increased upon preincubation of fresh, unmodified AdCMVLuc with the sCAR-MFE fusion protein (Figure 6, fresh AdCMVLuc, white versus black bar). Similar to results obtained in HeLa cells, a gold:adenovirus ratio of 100:1 (particle:particle) did not affect retargeting to and infectivity in CEA expressing cells. A gold:adenovirus ratio of 1000:1 significantly but moderately affected retargeting and infectivity, whereas ratios of 3000:1 and higher resulted in infectivity levels lower than untargeted, unmodified AdCMVLuc (Figure 6). This indicated that up to a ratio of 1000 gold nanoparticles per adenoviral vector in the reaction mixture, retargeting to tumor-associated antigens could still be achieved.

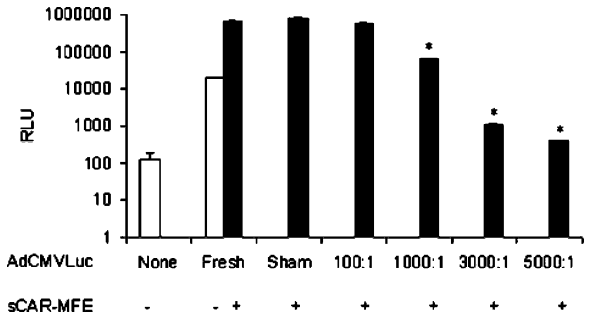

Figure 6. Retargeting of gold-labeled adenoviral vectors to CEA is retained at lower particle-to-vector ratios. Gold nanoparticles were reacted with AdCMVLuc at ratios of 100:1, 1000:1, 3000:1, and 5000:1. After reaction, MC38−CEA-2 cells were infected with 100 vp/cell of AdCMVLuc without (white bars) or with (black bars) sCAR-MFE fusion protein preincubation, to retarget the viral vector to the expressed CEA. Luciferase expression was determined after 24 h. Bars represent mean ± standard deviation. Asterisks indicate $p < 0.05$.

It has been recognized that exploitation of multiple treatment modalities will be needed to achieve success in cancer therapy. This has been pioneered using combinations of radiation, surgery, and chemotherapy, which are now standard therapeutic approaches. The addition of gene therapy to the arsenal of available treatment options will lead to a further increase in therapeutic combinatorial opportunities. This has already been demonstrated by synergistic effects between conditionally replicative adenoviruses (CRAds) together with radiation[6] or chemotherapy.[7] To extend this paradigm to a combination of gene therapy and hyperthermia, we herein investigated the possibility to covalently couple gold nanoparticles to adenoviral vectors, without affecting virus infectivity or retargetability. The herein established gold-labeled vectors can thus next be analyzed for hyperthermia-mediated tumor cell death induction.

It has been known that rapidly proliferating cells, such as tumor cells, are more sensitive to heat shock than slowly proliferating cells through a variety of mechanisms, including mitotic delay, cell cycle arrest, and plasma membrane damage.[8,9] The selectivity of hyperthermia for tumors is further conveyed by a tumor's usually limited blood supply, thus creating an environment with hypoxia and low pH, which is not found in healthy tissue.[1] One of the mechanisms by which hyperthermia has been induced is near-infrared absorption and subsequent heating of gold nanoparticles[10−12] or nanoshells.[3] So far, tumor selectivity of these particles has been achieved based on enhanced permeability and retention of particles due to "leaky" tumor architecture.[3] Although the tumor selectivity obtained by these mechanisms is promising, the specificity that would be obtained by covalent conjugation of the gold nanoparticles to tumor-targeted adenoviral vectors, as demonstrated in this paper, would be beneficial for an increased tumor to healthy tissue ratio and thus a better therapeutic index. This is particularly valid for smaller solid gold nanoparticles that are expected to interfere to a lesser extent with virus infectivity and retargeting compared to gold nanoshells, which have a size between 100 and 140 nm.

In the current work we have employed relatively small gold nanoparticles, for which effective heating will require extremely short (femto- or at least picosecond) laser pulses.[13] Alternatively, "nanoclusters" can be formed, where gold nanoparticles are clustered together, resulting in increased absorption efficiency.[13] Indeed, the proximity of the three-dimensional location of gold nanoparticles within one virus ("bio-nanoclusters") may provide the condition for plasmon−plasmon resonances that accompany increased absorption and a shift to the near-IR range. Nevertheless, we plan to explore the possibility of larger solid gold nanoparticles to be incorporated in the adenoviral platform.

Considerable advancements in tumor-specific targeting of adenoviral vectors for gene therapy have been achieved using both bispecific adapter molecules[14] as well as genetic capsid modification.[15] Furthermore, adenoviral vectors are compatible with chemical modification, as shown with fluorophores[16] or poly(ethylene glycol) derivatives.[17] This led us to explore the possibility of covalently coupling gold nanoparticles to targeted adenoviral vectors and thus retarget the nanoparticles to tumor-associated antigen expressing tumor cells, as demonstrated in this paper. The achieved targeting to tumor cells now creates the opportunity to test the therapeutic effects of near-infrared (NIR) laser-induced hyperthermia-mediated tumor cell death. These data further provide a rational basis to investigate the synergistic therapeutic gains accrued by a combination of hyperthermia with gene therapy. For example, hyperthermia-sensitive promoters such as hsp70 can drive the expression of cytokines such as interleukin-12 or tumor necrosis factor-alpha.[18] Furthermore, hyperthermia induced viral replication of CRAds might be a feasible strategy, thus combining multiple ways of cell death induction using a single vector.

Another important issue that still needs to be addressed is the optimal spatial location of the particles for most effective cancer cell killing. One option might be a location near the cell membrane (during initial vector binding and internalization) or even inside the membrane itself, since only a low laser energy is required for plasma membrane damage through thermal denaturation or bubble formation phenomena. This will lead to immediate cell death, mainly through necrosis.[19] Another option might be the nucleus (after complete penetration of the vector into the cells), where laser-induced nuclear damage may lead to cell damage through other mechanisms such as apoptosis, cell cycle arrest, etc.[8,9]

Along with adenoviral vectors, other methods of tumor-selective targeting have been exploited in the literature, such as direct conjugation of therapeutic modalities to antibodies[19] or inclusion of such modalities in liposomal formulations.[20] However, some potential limitations of directly conjugating gold nanoparticles to tumor-targeted antibodies include the limited number of modalities that can be attached without disrupting antibody specificity, whereas liposomes can be modified with particles to a higher extent, forming metallosomes.[21] These metallosomes may have a favorable body distribution and hence tumor specificity, as well as decreased immunogenicity compared to viral vectors. However, efficacy of adenoviral gene transfer is still unparalleled in in

vivo systems, favoring the use of adenoviral vectors for possible combinatorial approaches of hyperthermia with gene therapy, as described above.

In addition to gold, we are currently exploring the feasibility of coupling other metal nanoparticles to adenoviral vectors, such as iron−platinum (FePt) nanoparticles. These nanoparticles have magnetic properties that make them ideal for either imaging of particle localization (e.g., using MRI techniques), or magnetic-induced hyperthermia for cell killing, analogous to the gold NIR approach.[22,23]

Finally, to further improve on the herein established gold conjugated adenoviral vector paradigm, other methods of coupling nanoparticles to the adenoviral surface need to be investigated. The relatively nonspecific coupling via the sulfo-*N*-hydroxysuccinimide reactive group on the gold particle to primary amines of lysine-residues present in the capsid interferes with virus infectivity and retargetability at higher gold−virus ratios. Genetic manipulation of the nanoparticle binding locales will allow us to specifically conjugate particles to capsid proteins not involved in virus infectivity or interaction with targeting methods. Such modifications will allow for an increase in payload capacity of the virus, i.e., the number of nanoparticles that can be coupled without negatively affecting the virus, and thus create a wider therapeutic window. For example, nickel−nitrilotriacetic acid (Ni−NTA) modified gold particles,[24] used in the here-described experiments as a negative control, would be capable of binding six histidine residues that have carefully been inserted in certain capsid proteins, such as hexon[25] or pIX.[26] Ultimately, combination of multiple modalities within one viral particle, i.e., a targeting site in genetically modified virus capsid proteins allowing physical localization of the vector with the tumor cell, a nanoparticle binding site allowing induction of hyperthermia and imaging opportunities, combined with tumor-specific induction of therapeutic gene expression and viral replication may prove to be an optimal platform for cancer therapy.

Acknowledgment. The authors thank Dr. Kerry Chester for the kind gift of the scFv anti-CEA (MFE-23) encoding plasmid. This work was supported by the following grants: RO1 CA083821, RO1 CA94084, R01 EB000873, RR04050, W81XWH-04-1-0025, and W81XWH-05-1-0035. D. T. Johnson and D. E. Nikles would like to further acknowledge support from the Center for Information Technology and the Alabama NASA-EPSCoR (Grant SUB2002-036).

Supporting Information Available: Detailed description of the materials and methods. This material is available free of charge via the Internet at http://pubs.acs.org.

References

(1) van der Zee, J. *Ann. Oncol.* **2002**, *13* (8), 1173−1184.
(2) O'Neal, D. P.; Hirsch, L. R.; Halas, N. J.; Payne, J. D.; West, J. L. *Cancer Lett.* **2004**, *209* (2), 171−176.
(3) Hirsch, L. R.; Stafford, R. J.; Bankson, J. A.; Sershen, S. R.; Rivera, B.; Price, R. E.; Hazle, J. D.; Halas, N. J.; West, J. L. *Proc. Natl. Acad. Sci. U.S.A.* **2003**, *100* (23), 13549−13554.
(4) Konz, J. O.; Lee, A. L.; Lewis, J. A.; Sagar, S. L. *Biotechnol. Prog.* **2005**, *21* (2), 466−472.
(5) Wu, H.; Seki, T.; Dmitriev, I.; Uil, T.; Kashentseva, E.; Han, T.; Curiel, D. T. *Hum. Gene Ther.* **2002**, *13* (13), 1647−1653.
(6) Rogulski, K. R.; Freytag, S. O.; Zhang, K.; Gilbert, J. D.; Paielli, D. L.; Kim, J. H.; Heise, C. C.; Kirn, D. H. *Cancer Res.* **2000**, *60* (5), 1193−1196.
(7) Khuri, F. R.; Nemunaitis, J.; Ganly, I.; Arseneau, J.; Tannock, I. F.; Romel, L.; Gore, M.; Ironside, J.; MacDougall, R. H.; Heise, C.; Randlev, B.; Gillenwater, A. M.; Bruso, P.; Kaye, S. B.; Hong, W. K.; Kirn, D. H. *Nat. Med.* **2000**, *6* (8), 879−885.
(8) Maldonado-Codina, G.; Llamazares, S.; Glover, D. M. *J. Cell Sci.* **1993**, *105* (Pt 3), 711−720.
(9) Edwards, M. J.; Mulley, R.; Ring, S.; Wanner, R. A. *J. Embryol. Exp. Morphol.* **1974**, *32* (3), 593−602.
(10) Zharov, V. P.; Galitovsky, V. *Appl. Phys. Lett.* **2003**, *83*, 4897−4899.
(11) Zharov, V. P.; Letfullin, R. R.; Galitovskaya, E. *J. Phys. D*: *Appl. Phys.* **2005**, *38* (15), 2571−2581.
(12) El-Sayed, I. H.; Huang, X.; El-Sayed, M. A. *Cancer Lett.* **2005**.
(13) Zharov, V. P.; Kim, J. W.; Curiel, D. T.; Everts, M. *Nanomedicine* **2005**, *1* (4), 326−345.
(14) Kashentseva, E. A.; Seki, T.; Curiel, D. T.; Dmitriev, I. P. *Cancer Res.* **2002**, *62* (2), 609−616.
(15) Bauerschmitz, G. J.; Lam, J. T.; Kanerva, A.; Suzuki, K.; Nettelbeck, D. M.; Dmitriev, I.; Krasnykh, V.; Mikheeva, G. V.; Barnes, M. N.; Alvarez, R. D.; Dall, P.; Alemany, R.; Curiel, D. T.; Hemminki, A. *Cancer Res* **2002**, *62* (5), 1266−11270.
(16) Leopold, P. L.; Ferris, B.; Grinberg, I.; Worgall, S.; Hackett, N. R.; Crystal, R. G. *Hum. Gene Ther.* **1998**, *9*, (3), 367−378.
(17) Ogawara, K.; Rots, M. G.; Kok, R. J.; Moorlag, H. E.; Van Loenen, A. M.; Meijer, D. K.; Haisma, H. J.; Molema, G. *Hum. Gene Ther.* **2004**, *15* (5), 433−443.
(18) Huang, Q.; Hu, J. K.; Lohr, F.; Zhang, L.; Braun, R.; Lanzen, J.; Little, J. B.; Dewhirst, M. W.; Li, C. Y. *Cancer Res.* **2000**, *60* (13), 3435−3439.
(19) Zharov, V. P.; Galitovskaya, E. N.; Johnson, C.; Kelly, T. *Lasers Surg. Med.* **2005**, *37* (3), 219−226.
(20) Molema, G., Drug targeting: Basic concepts and novel advances. In *Drug Targeting. Organ-Specific Strategies*; Molema, G., Meijer, D. K. F., Eds.; Wiley-VCH Verlag GmbH: Weinheim, 2001; pp 1−22.
(21) Hainfeld, J. F.; Powell, R. D. *J. Histochem. Cytochem.* **2000**, *48* (4), 471−480.
(22) Moroz, P.; Jones, S. K.; Gray, B. N. *Int. J. Hyperthermia* **2002**, *18*, (4), 267−84.
(23) Bagaria, H. G.; Johnson, D. T. *Int. J. Hyperthermia* **2005**, *21* (1), 57−75.
(24) Hainfeld, J. F.; Liu, W.; Halsey, C. M.; Freimuth, P.; Powell, R. D. *J. Struct. Biol.* **1999**, *127* (2), 185−198.
(25) Wong, J. Y.; Chu, D. Z.; Williams, L. E.; Yamauchi, D. M.; Ikle, D. N.; Kwok, C. S.; Liu, A.; Wilczynski, S.; Colcher, D.; Yazaki, P. J.; Shively, J. E.; Wu, A. M.; Raubitschek, A. A. *Clin. Cancer Res.* **2004**, *10* (15), 5014−5021.
(26) Dmitriev, I. P.; Kashentseva, E. A.; Curiel, D. T. *J. Virol.* **2002**, *76* (14), 6893−6899.

NL0500555

Cancer Gene Therapy (2006) 13, 830–844
 0929-1903/06 $30.00
www.nature.com/cgt

REVIEW

Transductional targeting of adenovirus vectors for gene therapy

JN Glasgow[1], M Everts[1,2] and DT Curiel[1,2]

[1]*Division of Human Gene Therapy, Departments of Medicine, Pathology and Surgery, Birmingham, AL, USA and* [2]*Gene Therapy Center, University of Alabama at Birmingham, Birmingham, AL, USA*

Cancer gene therapy approaches will derive considerable benefit from adenovirus (Ad) vectors capable of self-directed localization to neoplastic disease or immunomodulatory targets *in vivo*. The ablation of native Ad tropism coupled with active targeting modalities has demonstrated that innate gene delivery efficiency may be retained while circumventing Ad dependence on its primary cellular receptor, the coxsackie and Ad receptor. Herein, we describe advances in Ad targeting that are predicated on a fundamental understanding of vector/cell interplay. Further, we propose strategies by which existing paradigms, such as nanotechnology, may be combined with Ad vectors to form advanced delivery vehicles with multiple functions.
Cancer Gene Therapy (2006) **13,** 830–844. doi:10.1038/sj.cgt.7700928; published online 27 January 2006

Keywords: review; vector targeting; adenovirus

Introduction

The understanding of the molecular basis of many pathologies, especially cancer, now demands rationally designed molecular interventions for therapeutic regimes. Over the last 15 years, the field of gene therapy has emerged as a potentially powerful therapeutic platform to serve this end.

The central dogma of gene therapy is employment of gene delivery as a therapeutic molecular intervention to selectively correct or eradicate defective tissues. Early gene therapy efforts, however, revealed that the clinical benefit of gene delivery modalities was irrevocably linked to specific localization of the therapeutic agent. For example, insufficient transduction of cancer cells and solid tumor masses may limit clinical efficacy of cancer gene therapy approaches.[1–5] Hence, a fundamental requirement for the achievement of cancer gene therapy is the employment of advanced molecular biology and disease-specific cellular physiology to design targetable gene delivery vectors.

Vectors based on human adenovirus (Ad) serotypes 2 and 5 continue to show increasing promise as gene therapy delivery vehicles, particularly in the context of cancer gene therapy, due to several key attributes: These replication-deficient Ad vectors display *in vivo* stability and superior gene transfer efficiency to numerous dividing and nondividing cell targets *in vivo*, and are rarely linked to any severe disease in humans. Further, production parameters for clinical grade Ad vectors are well established. In 2004, Ad vectors comprised one-fourth of all clinical trial gene therapy vectors (256 of 987), with almost two-thirds of gene therapy trials being for cancer (565 of 987).[6]

Nonetheless, clinical trial results of nontargeted Ad vectors have clearly exposed the need to advance Ad vector technology. The relatively poor clinical performance of Ad vectors can be attributed, in large part, to their broad native tropism, emphasizing the need for the derivation of Ad agents that have the capacity for intrinsic, self-directed, specific localization to the disease-affected target tissue. The following is a discussion of Ad biology, barriers to Ad targeting and a review of the strategies applied toward increasing the targeting capacity of this delivery vector. Lastly, we propose unique future applications for Ad-based vectors that derive from recently established targeting and molecular imaging feasibilities reported herein.

Adenovirus structure

The family *Adenoviridae* contains, among others, 51 human Ad serotypes that are divided into six species (A–F) based on genome homology and organization, oncogenicity and hemagglutination properties.[7–9] The human Ad is a nonenveloped icosahedral particle that encapsulates up to a 36-kilobase double-stranded DNA genome. The Ad capsid is comprised of several minor and three major capsid proteins: hexon is the most abundant structural component and constitutes the bulk of the protein shell; five subunits of penton form the penton base platform at each of the 12 capsid vertices to which the 12 fiber homotrimers attach (Figure 1). At the distal tip of each linear fiber is a globular knob domain, which serves as the major viral attachment site for cellular

Correspondence: Professor DT Curiel, Division of Human Gene Therapy, University of Alabama at Birmingham, 901 19th Street South, BMR2-502, Birmingham, AL 35294-2172, USA.
E-mail: curiel@uab.edu
Published online 27 January 2006

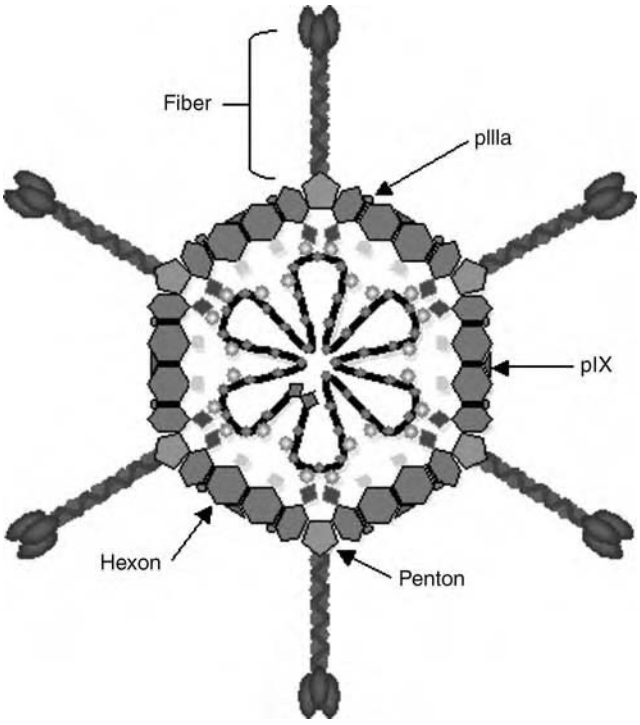

Figure 1 Generalized Ad structure depicting major structural components of a wild-type Ad capsid. Hexon, penton base, pIX, pIIIa and fiber structures are shown. Adenovirus capsids contain up to a 36-kilobase double-stranded DNA genome, shown as the dark line inside the capsid.

receptors. Hexon appears to play only a structural role as a coating protein, while the penton base and the fiber are responsible for virion–cell interactions that constitute Ad tropism. Detailed structures of hexon,[10–12] penton base[13] and fiber[14,15] have been determined by crystallography; the high-resolution structure of the entire virion has been determined by various methods.[16,17]

Adenovirus entry biology

Entry of Ad into cells involves two distinct steps: attachment to a primary receptor molecule at the cell surface, followed by interaction with molecules responsible for virion internalization. Initial high-affinity binding of the virion occurs via direct binding of the fiber knob domain to its cognate primary cellular receptor, which is the 46 kDa coxsackie and adenovirus receptor (CAR) for most serotypes, including Ad2 and Ad5, which are widely used in gene therapy approaches.[18,19] Other receptors have been described for Ad5, although the nature of their interaction(s) with the Ad5 virion is unclear and their roles appear limited. These receptors include heparin sulfate glycosaminoglycans,[20,21] class I major histocompatability complex[22] and vascular cell adhesion molecule-1.[23] Following receptor binding, receptor-mediated endocytosis of the virion is effected by interaction of penton base Arg–Gly–Asp (RGD) motifs with cellular integrins, including $\alpha v\beta 3$ and $\alpha v\beta 5$,[24] $\alpha v\beta 1$,[25] $\alpha_3\beta 1$ and $\alpha_5\beta 1$.[26] Virus enters the cell in clathrin-coated vesicles[27] and is transported to endosomes. Subsequent acidification of the endosome results in virion disassembly and release of the virus remains into the cytosol, then to the nucleus where viral replication takes place.

Transductional targeting of Ad

This mechanistic understanding of Ad cellular entry explains clinical findings by numerous groups that have demonstrated that cells expressing low levels of CAR are refractory to Ad infection and gene delivery. This CAR dependency results in a scenario wherein nontarget but high-CAR cells can be infected, whereas target tissues, if low in CAR, remain poorly infected. Of key relevance to cancer gene therapy, increased CAR expression appears to have a growth-inhibitory effect on some cancer cell lines, while loss of CAR expression correlates with tumor progression and advanced disease. In addition, CAR has been shown to play a role in cell adhesion, and its expression may be cell cycle dependent.[28,29] In short, while Ad delivery is uniquely efficient *in vivo*, CAR biodistribution is incompatible with many gene therapy interventions. We therefore hypothesized that if CAR expression could be induced in target tissues, resultant increases in Ad-mediated infection and gene expression would result in therapeutic gain. Indeed, a number of chemical agents predicted to affect cell cycle or cell adhesion were identified that increased CAR levels and Ad gene expression in ovarian cancer cells *in vitro* and *in vivo*.[30]

Adenovirus vector biodistribution *in vivo*, however, is not determined solely by receptor biodistribution.[31] Intravenous administration of Ad results in accumulation in the liver, spleen, heart, lung and kidneys of mice, although these tissues may not necessarily be the highest in CAR expression.[32,33] This is true with regard to the liver in particular, which sequesters the majority of systemically administered Ad particles via hepatic macrophage (Kupffer cell) uptake[34] and hepatocyte transduction,[35] leading to Ad-mediated inflammation and liver toxicity.[36–39] Thus, the nature of Ad–host interactions dictating the fate of systemically applied Ad has come under considerable scrutiny.

Initial attempts to 'de-target' the liver were based on the supposition that CAR- and integrin-based interactions were required for liver transduction *in vivo*. Strategies to inhibit hepatocyte and/or liver Kupffer cell uptake by ablating CAR- or integrin-binding motifs in the Ad capsid have been largely unsuccessful, however, indicating that native Ad tropism determinants contribute little to vector hepatotropism *in vivo*.[40–44] These data notwithstanding, work by several groups has implicated the fiber protein as a major structural determinant of liver tropism *in vivo* (reviewed by Nicklin *et al*.[45]). For example, shortening of the native fiber shaft domain of the Ad5 fiber[46] or replacement of the Ad5 shaft with the short Ad3 shaft domain[47] was shown to attenuate liver

uptake *in vivo* following intravenous delivery. In related work, Smith *et al*.[48] examined the role of a putative heparan sulfate proteoglycan (HSPG)-binding motif, KKTK, in the third repeat of the native fiber shaft. Replacement of this motif with an irrelevant peptide sequence reduced reporter gene expression in the liver by 90%. This was also the first indication of the importance of HSPG as an Ad receptor *in vivo*.

More recently, Shayakhmetov *et al*.[49] uncovered a major role for coagulation factor IX (FIX) and complement component C4-binding protein (C4BP) in hepatocyte and Kupffer cell uptake of intravenous Ad. Indeed, Ad5 vectors containing fibers genetically modified to ablate FIX and C4BP binding provided 50-fold lower liver transduction with reduced inflammation and hepatotoxicity. Further analysis demonstrated that these blood factors mediated *in vivo* tropism by crosslinking Ad to hepatocellular HSPG and the low-density lipoprotein (LDL)-receptor-related protein. Kupffer cell sequestration of Ad particles was likewise heavily dependent on Ad association with FIX and C4BP.

These efforts serve to highlight the complexity of vector/host interplay, and have identified important genetic modifications that have important practical implications for designing safer and more effective Ad-based vectors for clinical applications. In the absence of a clinically defined upper limit for ectopic liver transduction in humans, it is clear that the concepts of 'de-targeting' and 're-targeting' must be simultaneously employed to allow for maximum vector efficacy at the lowest possible dose. Therefore, engineering of targeted delivery with Ad requires the elimination of native tropism to be replaced by an alternative tropism based on targeting other receptor molecules, all while retaining innate Ad gene transfer efficiency. Two distinct approaches have been employed to transductionally target Ad-based therapeutic vectors: (1) adapter molecule-based targeting and (2) targeting achieved via structural manipulation of the Ad capsid via genetic means.

Adapter-based Ad targeting

The formation of a 'molecular bridge' between the Ad vector and a cell surface receptor constitutes the adapter-based concept of Ad targeting (Figure 2). Adapter function is performed by so-called 'bi-specific' molecules that crosslink the Ad vector to alternative cell surface receptors, bypassing the native CAR-based tropism. This approach is predicated by the aforementioned two-step entry mechanism of the Ad virion, wherein attachment is distinct from its ability to internalize into the targeted cell. In this way, alternative means of cellular attachment do not impede Ad cell entry. The majority of current adapter-based Ad targeting approaches incorporate the two mandates of delivery targeting, that of ablation of native CAR-dependent Ad tropism and formation of a novel tropism to previously identified cellular receptors. Bispecific adapter molecules include, but are not limited to: bi-specific antibodies, chemical conjugates between

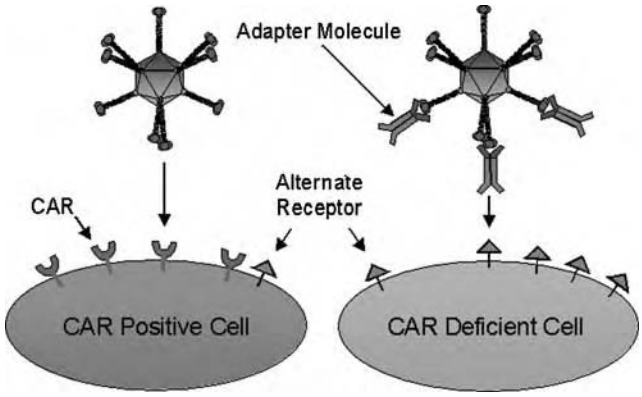

Figure 2 The Ad infection pathway. Shown are the basic steps of initial high-affinity binding of the virion fiber to its primary cellular receptor, CAR (left). Alternatively, a generalized adapter molecule ablates native CAR-based tropism and targets Ad to an alternate cellular receptor molecule (right). The dual specificity of the adapter molecule for both the Ad and the alternative receptor provides novel, CAR-independent cell binding.

antibody fragments (Fab) and cell-selective ligands such as folate, Fab-antibody conjugates using antibodies against target cell receptors, Fab-peptide ligand conjugates and recombinant fusion proteins that incorporate Fabs and peptide ligands (Figure 3a).

The first *in vitro* demonstration of Ad targeting via the adapter method resulted in CAR-independent, folate receptor-mediated cellular uptake of the virion by cancer cells overexpressing this receptor.[50] This was accomplished using a bispecific conjugate consisting of an anti-knob neutralizing Fab chemically linked to folate. A similar targeting adapter comprised of the same anti-knob Fab as above fused to a basic fibroblast growth factor (FGF2) was utilized to target Ad vectors to FGF receptor-positive Kaposi's sarcoma (KS) cells *in vitro*.[51] Importantly, this targeting system also reduced hepatic toxicity and resulted in increased survival in a melanoma xenograft mouse model.[52] Other Fab–ligand conjugates targeted against Ep-CAM, Tag-72, epidermal growth factor (EGF) receptor, CD-40 and other cell markers have been employed in a similar manner with promising results.[1,53–58]

Dmitriev *et al*.[60] developed an elegant alternative to the chemical conjugate approach by creating a single recombinant fusion molecule formed by a truncated, soluble form of CAR (sCAR) fused to either an anti-CD40 antibody[59] or epidermal growth factor (EGF). Using the latter, a nine-fold increase in reporter gene expression was achieved in several EGFR-overexpressing cancer cell lines compared to untargeted Ad or EGFR-negative cells *in vitro*. EGF-directed targeting to EGFR-positive cells was shown to be dependent on cell surface EGFR density, an additional confirmation of Ad targeting specificity. Addressed also was the issue of virion/adapter complex stability, a critical issue if targeting adapters are to be employed *in vivo*. In this regard, preformed Ad/sCAR–EGF complexes subjected to gel filtration purification showed the same targeting profile as those not purified,

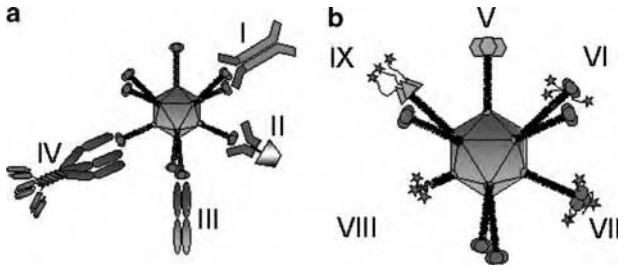

Figure 3 (**a**). Adenoviral particles can be re-targeted to TAAs, using bifunctional adapter molecules. Examples of such adapter molecules are chemical conjugates of a Fab fragment derived from an antiknob monoclonal antibody with a whole antibody directed against the target antigen (I), or naturally occurring ligands such as folate or basic fibroblast growth factor (II). The other class of adapter molecules consists of recombinant bispecific fusion proteins, examples of which include so-called diabodies, comprised of two single-chain antibodies (scFv), with one scFv recognizing the fiber knob and the other the TAA (III). Another example is the trimeric sCAR-fibritin-scFv, which uses the soluble ectodomain of the native Ad receptor CAR to bind to the Ad, thus ablating CAR recognition (IV). (**b**) Adenoviral particles can be re-targeted to TAAs using genetic targeting strategies in which the targeting ligands are incorporated into capsid proteins. The Ad5 knob protein can, for instance, be replaced with that of other serotypes (V), or it can be altered by incorporation of targeting ligands, such as RGD-containing peptide sequences or six histidine residues, at the C-terminus of the protein (VI). As an alternative to the C-terminus, peptide sequences can also be incorporated in the HI-loop of the Ad5 knob (VII). The entire fiber and knob domain can be replaced by an artificial fiber, for instance, consisting of the bacteriophage T4 fibritin trimerization domain and a targeting motif (VIII). Finally, multiple genetic modifications can be combined in a single particle, forming a so-called 'complex mosaic Ad'. An example is a particle containing Ad3 knob instead of Ad5 knob, in which a six-histidine targeting motif is incorporated at the C-terminus (IX).

indicating adequate Ad/adapter complex stability. To further increase Ad/sCAR–ligand complex stability, Kashentseva *et al*.[61] developed a trimeric sCAR-anti-c-*erb*B2 single-chain antibody adapter molecule. While untested as yet *in vivo*, the trimeric sCAR-c-*erb*B2 adapter displayed increased affinity for the Ad fiber knob, while augmenting gene transfer up to 17-fold in six c-*erb*B2-positive breast and ovarian cancer cell lines *in vitro*. In similar work, Itoh *et al*.[62] demonstrated improved efficiency of sCAR-based fusion molecule adapters. Kim *et al*.[63] showed that adapter trimerization yielded a 100-fold increase in infection of CAR-deficient human diploid fibroblasts compared to the monomeric sCAR adapter. Importantly, *in vivo* employment of a nontargeted trimeric sCAR adapter attenuated liver transduction in mice following intravenous administration, indicating the excellent *in vivo* stability of this Ad/trimeric adapter complex. These studies have supplied preliminary evidence of the systemic stability of adaptor–virus complexes, although it is likely that clinical trials will ultimately be needed to investigate this crucial aspect for individual agents.

The above proof-of-principle studies and others have rationalized the further testing of targeting adapters *in vivo*. In this regard, Reynolds *et al*.[56] employed a novel bispecific adapter composed of an anti-knob Fab chemically conjugated to a monoclonal antibody (9B9) raised against angiotensin-converting enzyme (ACE), a surface molecule expressed preferentially on pulmonary capillary endothelium and upregulated in various disease states of the lung. Following peripheral intravenous injection of the Ad/Fab–9B9 complex, reporter transgene expression and viral DNA in the lung were increased 20-fold over untargeted Ad. Importantly, reporter gene expression in the liver, a nontarget, high-CAR organ, was reduced by 83%. Further, in a unique adapter-based *in vivo* lung-targeting schema, Everts *et al*. used a bifunctional adapter molecule comprised of sCAR fused to a single-chain antibody (MFE-23) directed against carcinoembryonic antigen (CEA). Systemic administration of the Ad/sCAR–MFE-23 adapter complex increased gene expression in CEA-positive murine lung by 10-fold and reduced liver transduction, resulting in an improved lung-to-liver ratio of gene expression compared with untargeted Ad.

Overall, adapter-based Ad targeting studies provide compelling evidence that Ad tropism modification can be achieved by targeting alternate cellular receptors and that this modality augments gene delivery to CAR-deficient target cells *in vitro*. Adapter-targeted vectors have also performed well *in vivo*, although data so far are limited. While single-component systems have been favored for employment in human gene therapy trials, rigorous analysis of the pharmaco-dynamics and -kinetics, and systemic stability of vector/adapter complexes could potentially provide the rationale for clinical translation.

Adenovirus targeting via genetic modification: fiber

Genetic manipulation of capsid proteins has yielded increasingly promising data in terms of Ad targeting. Redirection of Ad tropism via genetic capsid modification is conceptually elegant, but genetic targeting efforts must work within narrow structural constraints. The success of this approach depends upon modulation of the complex protein structure/function relationships that result in Ad tropism modification, without disrupting the innate molecular interactions required for proper biological function. Based on a clear understanding of Ad infection biology, development of genetically targeted vectors has rationally focused on the fiber, the primary capsid determinant of Ad tropism. In general, there have been three basic strategies for genetic tropism modification via structural modification of the Ad fiber: (1) so-called 'fiber pseudotyping'; (2) ligand incorporation into the fiber knob and (3) 'de-knobbing' of the fiber coupled with ligand addition (Figure 3b).

As previously mentioned, many clinically relevant tissues are refractory to Ad5 infection, including several cancer cell types, due to negligible CAR levels. Adenovirus fiber pseudotyping, the genetic replacement of either the entire fiber or knob domain with its structural counterpart from another human Ad serotype that recognizes a

cellular receptor other than CAR, was first accomplished by Krasnykh *et al*.[64] These vectors display CAR-independent tropism by virtue of the natural diversity in receptor recognition found in human subgroup B and D fibers.[65] In this regard, primary receptors for subgroup B Ads have been recently identified, including the complement regulatory protein CD46,[66–69] CD80 and CD86,[70] although an additional unknown receptor is postulated.[67] Subgroup D Ad receptors include CD46 and α(2–3)-linked sialic acid, a common element of glycolipids.[71–73] This fiber pseudotyping approach has identified chimeric vectors with superior infectivity to Ad5 in several clinically relevant cell types, including primary ovarian carcinoma cells,[74–76] vascular endothelial cells,[77] dendritic cells,[78] B-cells,[79] CD34+ hematopoietic cells,[80] synovial tissue,[81] human cardiovascular tissue[82] and others.[83,84] Interestingly, this strategy has been extended to exploit fiber elements from non-human Ads[85,86] and the fiber-like σ1 reovirus attachment protein, which targets cells expressing junctional adhesion molecule.[87,88]

Direct ligand incorporation into the Ad knob domain without ablating native CAR-binding has resulted in Ad vectors with expanded, rather than restricted, cell recognition. These efforts are based on rigorous structural analysis of the knob domain and have exploited two separate locations within the knob that tolerate genetic manipulation without loss of fiber function, the C-terminus and the HI-loop. Since the C-terminus of the Ad knob is solvent exposed, extension of the knob peptide to include a targeting peptide moiety is conceptually simple. Ads with C-terminal integrin-binding RGD motifs and poly-lysine ligands have yielded some promising results *in vitro* and *in vivo*, but other peptide ligands were rendered ineffective in the C-terminus structural context,[89] presumably due to steric or other inhibition. Krasnykh *et al*.[90] inserted a FLAG peptide sequence into an exposed loop structure that connects β-sheets H and I (HI-loop) within the Ad5 knob, showing that this locale is structurally permissive to modification. Indeed, the Ad5 HI-loop tolerates peptide insertions up to 100 amino acids with minimal negative effects on virion integrity, thus suggesting considerable potential for ligand incorporation at this site.[91] Dmitriev *et al*.[4] introduced an integrin-binding RGD peptide sequence into the HI-loop. The resulting vector, Ad5lucRGD, used the RGD/cellular integrin interaction to enhance gene delivery to ovarian cancer cell lines and primary tumors versus unmodified Ad.[92,93] The expanded tropism of this vector has been useful in several other cancer contexts including carcinomas of the ovary, pancreas, colon cancer, and head and neck carcinomas, all of which frequently display highly variable CAR levels.[94] Wu *et al*.[95] demonstrated that Ad vectors with a double fiber modification consisting of a C-terminal poly-lysine stretch, which interacts with heparan sulfates, and the HI-loop RGD provided increased infectivity in several CAR-deficient cell lines, as well as human pancreatic islet cells,[96] ovarian carcinoma[97] and cervical cancer cells *in vivo*.[98] Other targeting peptides have functioned in the HI-loop locale, including a vascular endothelial cell-binding motif SIGYLPLP.[99] This fiber modification also provided cancer cell selective infection.[100]

Korokhov *et al*.,[101] Volpers *et al*.[102] and others[103] have developed similar targeting approaches that embody elements of both genetic fiber modification and adapter-based targeting by incorporating the immunoglobulin (Ig)-binding domain of *Staphylococcus aureus* protein A into the fiber C-terminus or HI-loop. As a result, these fiber-modified vectors form stable complexes with a wide variety of targeting molecules containing the Fc region of Ig. This provides the opportunity to screen numerous targeting molecules directed against a host of cell-surface elements. This approach was used to target and activate dendritic cells via an Fc-single-chain antibody directed against CD40.[104] This system was also used to target ovarian cancer cells via an antibody directed against mesothelin,[105] as well as the pulmonary endothelium in a rat model *in vitro*.[106]

The structural conflicts emerging from knob modifications and the observation that fiber-deleted Ad vectors could be produced[107,108] provided the conceptual basis for replacing the native fiber with knobless fibers. Virions containing a knobless fiber would be ablated for CAR binding, a hallmark of targeted Ad vectors. Simultaneous addition of a targeting ligand to the knobless fiber would result in a more specifically targeted Ad. The technical barrier to this approach is the innate trimerization function of the knob, required for proper fiber function and capsid incorporation. To overcome this structural conflict, addition of foreign trimerization motifs have been used to replace the native fiber and/or knob.[109] Krasnykh *et al*.[110] replaced the fiber and knob domains with bacteriophage T4 fibritin containing a C-terminal 6-His motif. This novel Ad variant lacks the ability to interact with CAR and demonstrated up to a 100-fold increase in reporter gene expression to cells presenting an artificial 6-His-binding receptor. A similar 'de-knobbing' strategy was employed by Magnussen *et al*.,[111] wherein an integrin-binding RGD motif was utilized, resulting in selective infection of integrin-expressing cell lines *in vitro*, as well as human glandular cells.[112] Based on the feasibility of fiber replacement with T4 fibritin, an elegant system was devised wherein the trimeric CD40 ligand was fused to the C-terminus of this artificial fiber.[113] Notably, this vector provided CD40-specific gene delivery *in vivo* following systemic delivery.[114] Further, this vector accomplished CD40-mediated infection of human monocyte-derived dendritic cells, suggesting a possible utility for cancer immunotherapy 'antigen-loading' approaches. In addition, Ad vectors simultaneously incorporating multiple fiber types with distinct receptor specificities have been proposed.[115,116]

Given the target specificity demonstrated by antibody-mediated targeting of Ad vectors using adapter molecules, the development of single-component Ad vectors with genetically incorporated antibodies, antibody-derived moieties or other multi-domain ligands has been a long-standing field milestone. Genetic capsid incorporation of any moiety requires that the heterologous peptide be compatible with the nonreducing environment within the

cytosol and nucleus, wherein Ad capsid proteins are translated and assembled. Indeed, capsid incorporation of several classes of complex-targeting ligands, including scFv and growth factors, has been severely hampered by the innate biosynthetic incompatibilities between the ligand and Ad capsid proteins, resulting in unstable or insoluble ligands and/or reduced Ad replication.[117] On this basis, rational development of complex ligands with cytoplasmic solubility and stability will be required for their application to Ad vectors. Exemplifying this concept, Hedley *et al.*[118] have developed a single-component antibody-targeted Ad vector by incorporating a novel, cytoplasmically stable scFv into a de-knobbed fiber. This vector demonstrated selective targeting to its cognate epitope expressed on the membrane surface of cells, and suggests that cytoplasmic stability of the targeting molecule, *per se*, allows retention of antigen recognition in the Ad capsid-incorporated context.

Adenovirus targeting via genetic modification: other capsid locales

The field-wide appreciation of the difficulty of incorporating complex ligands into the Ad fiber locale has prompted the identification of other capsid proteins amenable to ligand incorporation via genetic manipulation. These approaches have the potential, through increased capsid valency and unique capsid microenvironments, to incorporate an increased number of complex ligands per virion. To date, capsid protein hexon as well as minor capsid proteins polypeptide IX (pIX) and pIIIa have been used as platforms for incorporation of heterologous peptides.

Hexon is the largest and most abundant capsid protein, and as such is an attractive locale for peptide ligand incorporation due to both its surface exposure and high valency (240 hexon homotrimers per virion). The primary sequence of the hexon monomer is highly conserved among human serotypes, with the exception of nine nonconserved hypervariable regions (HVRs) of unknown function found mainly within solvent-exposed loops at the surface.[11,119,120] In this regard, Vigne *et al.*[121] exploited hexon hypervariable region 5 (HVR5), a loop structure in hexon, as a site for incorporation of an integrin-binding RGD motif. Notably, virion stability was unaffected by the addition of the foreign peptide, while providing enhanced, fiber-independent transduction to low-CAR vascular smooth muscle cells. Extending this work, Wu *et al.* identified HVRs 2, 3 and 5–7 as hexon sites tolerating 6-histidine (6-His) motifs without adverse affects to virion formation or stability. 6-His motifs in HVRs 2 and 5 mediated virion binding to anti-6-His antibodies; however, 6-His-mediated viral infection of cells was not observed, in contrast to Vigne *et al.* above, highlighting the importance of the nature and the length of the incorporated peptides.

Recently, pIX has emerged as a versatile capsid locale well suited for display of ligands with utility for both targeting and imaging modalities.[122] The 14.3 kDa pIX is the smallest of the minor capsid proteins, a subset of capsid proteins that generally function to stabilize the capsid shell. In the mature Ad virion, 80 pIX homotrimers[123] stabilize hexon–hexon interactions during capsid assembly, and it is therefore termed a 'cement' protein. Indeed, virions deleted for pIX have decreased thermostability and a DNA capacity that is approximately 2 kb less than the normal length.[124–126] Interest in employing pIX as a capsid site for incorporation of peptide ligands stemmed from the observation that the C-terminus of pIX is located at the capsid surface,[127,128] which prompted several groups to explore the fusion of several polypeptides to this terminus.

Dmitriev *et al.*[129] first reported the incorporation of functional targeting peptides at the pIX C-terminus by inserting poly-lysine or FLAG motifs, resulting in augmented, CAR-independent gene transfer via binding to cellular heparan sulfate moieties. In a similar approach, Vellinga *et al.*[130] fused an integrin-binding RGD peptide to pIX, and used α-helical spacers (up to 7.5 nm in length and 113 amino acids) to extend the RGD motif away from the virion surface. Increased gene transfer to CAR-deficient endothelioma cells was observed with increased spacer length, giving support to the notion that the pIX C-terminus may reside in a cavity formed by surrounding hexons. In order to evaluate the utility of multiple ligand types at the pIX capsid locale, Campos *et al.*[131] fused to the pIX-C-terminus a 71-amino-acid fragment of the *Propionibacterium shermanii* 1.3S transcarboxylase protein, which functions a biotin acceptor peptide (BAP). During virus propagation the BAP is metabolically biotinylated, rendering this virus compatible with a host of avidin-tagged ligands, including peptides, antibodies and carbohydrates. Importantly, it was noted in this study that coupling transferrin to virions via pIX-BAP resulted in specific transferrin receptor-mediated infection of C2C12 cells, but the use of an antibody directed against the transferrin receptor (CD71) did not. This dichotomy was not observed when these two ligands successfully redirected Ad tropism when incorporated into fiber. The authors speculate that the difference was not due to a lack of receptor recognition by the pIX–anti-CD71 complex, but rather a difference between the dissociation of targeted fiber and pIX from the Ad particle in endosomes, resulting in trapping of the pIX–anti-CD71 variant, but not the fiber–anti-CD71 in the endosome. If this notion is fully validated, it will represent a key finding showing that the nature of pIX-incorporated ligands may influence successful redirection of Ad infection.

Polypeptide IX has also been in use for the display of relatively large imaging molecules as C-terminal fusions. While Ad vector imaging is beyond the scope of this work, the successful incorporation of the 240-amino-acid enhanced green fluorescent protein (eGFP) into pIX bears mentioning due to the size and complexity of this fusion. Of note, the presence of the pIX–eGPF fusion in purified Ad virions did not appreciably decrease virus viability or capsid stability, and has allowed monitoring of Ad localization *in vitro* and *in vivo*.[132,133] Further, other Ad

vectors harboring complex ligands at the pIX locale have been reported.[134–136] As a whole, these studies have established pIX as a highly relevant capsid locale marked by the highest structural compatibility, with diverse targeting and imaging ligands observed to date.

Based on its surface capsid position, pIIIa has been proposed as a platform for ligand display for modification of Ad tropism.[137] High-resolution imaging techniques originally indicated that pIIIa is an elongated protein penetrating the capsid and is located along the icosahedral edges of the virion.[16] More recent structural studies performed at higher resolution place pIIIa only at the surface of the virion.[17] The minor capsid protein pIIIa is a 67-kDa monomer that is cleaved at the C-terminus during maturation of the virion, giving rise to the final 63.5 kDa form. To evaluate the utility of pIIIa for ligand display, Dmitriev *et al.*[138,139] have incorporated a 6-His motif singly into the N-terminus of pIIIa. The modified pIIIa proteins were well tolerated in mature virions, although whether pIIIa ligands can redirect Ad tropism remains to be conclusively demonstrated.

In the aggregate, these results highlight that genetic manipulation of a variety of Ad capsid proteins is currently feasible, and has brought to fruition several novel targeting and imaging paradigms. These successes confirm a level of capsid flexibility that was largely unexpected. There remains, however, an ongoing struggle to identify true targeting ligands that are structurally and/or biosynthetically compatible with Ad capsid formation and stability.

Identification of new tumor-associated antigens

Targeted gene delivery is ultimately predicated on the ability of the vector to discriminate between target cell or tissues types via interaction with unique cell- or disease-specific surface markers. On this basis, the discovery and characterization of novel cell-surface targets is of paramount importance. In the context of targeted gene delivery for cancer, considerable effort is being expended to identify new tumor-associated antigens (TAAs) for a variety of cancers, utilizing advanced technologies such as mRNA microarrays, proteomics and 'serological identification of antigens by recombinant expression cloning' (SEREX). The identification of more than 20 000 genes by the human genome project has provided a pool of possible new targets in cancer, and the screening for those has become significantly more facile in recent years due to commercialization and increased availability of mRNA microarray technology. Several new targets have been identified using this technology, such as the carcinoma-associated antigen GA733-2, and hepsin, a transmembrane serine protease found in prostate cancer.[140] Another example is the high expression of 'preferentially expressed antigen of melanoma' gene (PRAME), detected by microarray in ovarian cancer samples.[141]

Compared to the number of genes present in the human genome, the number of possible protein targets is increased several-fold due to the intermediate steps between mRNA and protein expression, and the protein variability potentially introduced with each of these steps. These variabilities include mRNA splicing, post-translational processing, glycosylation, as well as others. The Human Proteome Organization (HUPO), formed in 2001, aims to systematically characterize protein expression in health and disease, and its Plasma Proteome Project is a prime example in which several laboratories throughout the world participate to identify tumor markers that can be used for both screening as well as therapeutic targets.[142] The mRNA and protein array technologies can also be combined in order to discover new biomarkers, such as demonstrated by Nishizuka *et al.*,[143] who identified villin as a new marker for colon cancer using this combination.

Another method to identify new tumor targets is 'serological identification of antigens by recombinant expression cloning' (SEREX), which was first described by Sahin *et al.*[144] in 1995 and is based on the presence of TAA recognizing antibodies in the serum of cancer patients. In this approach, a cDNA library is constructed from tumor specimens and cloned into expression vectors. Clones are then screened for reactivity with the serum of the autologous patient, and the nucleotide sequence of the cDNA insert is determined.[144] In previous years, several antigens that can be classified into different groups have been identified, including cancer-testis antigens, differentiation antigens, overexpressed gene products, mutated gene products, splice variants and cancer-related autoantigens. Examples of antigens discovered using this technology are melanoma antigen gene-1 (MAGE-1) in melanoma and metastasis-associated protein-1 (MTA1) in prostate cancer.[145]

Identification of new ligands

In addition to the identification of new TAAs, new ligands that are able to target these antigens and are suitable for incorporation into adenoviral vectors need to be identified as well. One of such technologies is phage display, which was first pioneered by Smith[146] in 1985, that can identify high-affinity peptides for a target receptor of choice. As an example, Peletskaya *et al.*[147,148] screened a 15-mer library for peptides able to bind the Thomson–Friedenreich (TF) antigen, a glycoantigen present on several carcinomas, and identified peptides with an affinity around 1 μM. One of the most well-known examples of a peptide identified by phage display is the RGD amino-acid sequence, which has a high affinity for integrins that are expressed in tumor vasculature. This peptide, identified by the group of Ruoslathi[149] in 1993, has extensively been used in drug- or gene-targeting approaches, either a linear or cyclic format. For example, Schiffelers *et al.*[150] coupled this peptide to a liposome carrier, demonstrating selective localization of this drug-targeting construct in angiogenic vasculature in a dorsal skin chamber model, whereas genetic incorporation of RGD in both adenoviral and

adeno-associated viral vectors has led to a dramatic infectivity enhancement of these vectors in a variety of cancer cells.[4,151]

Since some promising targeting ligands lose their receptor specificity upon incorporation into adenoviral capsid proteins, it would be useful to screen these ligands in their appropriate context in a high-throughput manner. Pereboev *et al*.[152] have elegantly approached this problem by modifying the pJuFo phage system in such a way that the (modified) Ad5 knob is expressed on the surface of filamentous bacteriophage, allowing screening of incorporated ligands with traditional phage display techniques. This system may prove very useful in screening for candidate ligand fidelity and Ad structural compatibility, prior to genetic Ad modification.

Future applications

Despite the advances in tumor-targeted gene therapy as described in this article, several obstacles remain. The vascular endothelial wall is a significant physical barrier prohibiting access of systemically administered vectors to the tumor cell. To overcome this obstacle, strategies are currently being endeavored to route adenoviral vectors via transcytosis pathways through the endothelium. As an example, Zhu *et al*.[153] redirected Ad vectors to the transcytosing transferrin receptor pathway, using the bifunctional adapter molecule. The transcytosed Ad virions retained the ability to infect cells, establishing the feasibility of this approach. However, efficiency of Ad trafficking via this pathway is poor, and current efforts are directed towards exploring other transcytosing pathways such as the melanotransferrin pathway,[154] the poly-Ig A receptor pathway,[155] or caveolae-mediated transcytosis pathways.[156] One can envision the development of mosaic Ad vectors incorporating both targeting ligands directed to such transcytosis pathways as well as ligands mediating subsequent targeting and infection of tumor cells present beyond the vascular wall.

The often-limited therapeutic effects achieved by gene or virotherapy approaches mandate the development of alternative 'amplifying strategies', in which delivery of a vector to a single cell will result in the destruction of its neighboring cells as well. In this regard, the development of so-called multifunctional particles (MFPs) that incorporate targeting, imaging and amplifying capacities is an exciting possible new area of investigation (Figure 4). Adenovirus-based vectors are ideally positioned to represent such an MFP, by virtue of genetic capsid modifications, to incorporate functionalities as cited above. For example, incorporation of genetically modified fibers, combined with imaging motifs on the pIX protein, could be used to simultaneously target tumor cells while monitoring viral replication and spread. In this regard, in addition to optical imaging-based ligands that have been incorporated at pIX as mentioned above, recently Li *et al*.[136] have been successful in incorporating the enzyme Herpes Simplex Virus thymidine kinase (HSV-tk) at this capsid locale. This enzyme

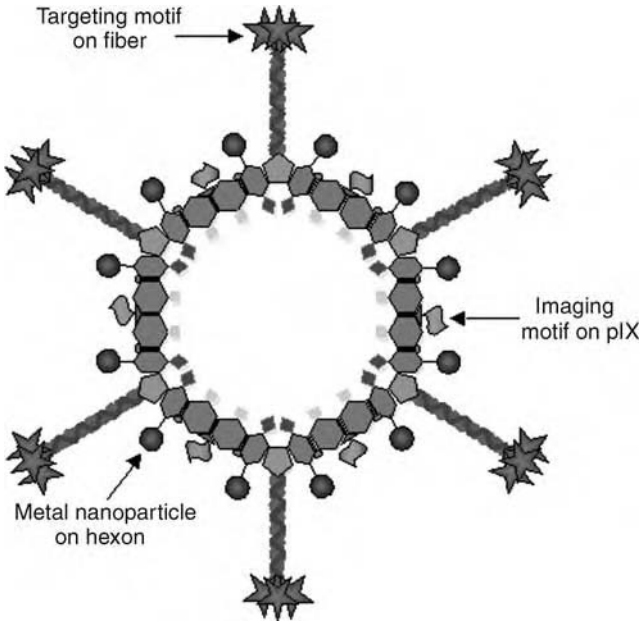

Figure 4 Schematic diagram showing an idealized MFP based on an empty Ad capsid. Adenoviral vectors can theoretically be used as a platform for the development of MFPs incorporating targeting, imaging and therapeutic motifs. For example, targeting motifs can be incorporated into the fiber protein, whereas simultaneous incorporation of imaging motifs such as thymidine kinase on the pIX protein will provide the ability to monitor particle and thus tumor localization, utilizing noninvasive technologies such as PET. Incorporation of metal nanoparticles with magnetic properties into such a platform will provide additional imaging opportunities via MRI, as well as therapeutic opportunities via hyperthermia induction.

is compatible with available PET imaging ligands such as ^{18}F-penciclovir, providing an imaging system for viral replication that can directly be translated for clinical applications. Interestingly, HSV-tk is an enzyme that has utility in so-called suicide gene therapy, in which the expressed enzyme converts a substrate such as ganciclovir to its toxic phosphorylated metabolite, resulting in cell death.[157] Also, tumor cells expressing this gene product induce the death of adjacent cells via the so-called 'bystander effect', thus representing an 'amplifying strategy' as mentioned above. Incorporation of this enzyme on the capsid surface of a targeted Ad could be exploited in an amplifying strategy for the induction of cell death, in addition to its use for imaging.

The concept of MFPs has also been introduced recently in the context of nanotechnology, often defined as the development of devices of 100 nm or smaller, having unique properties due to their scale. Applications in medicine are starting to emerge, with 'nanomedicine' recently being defined as the utilization of nanotechnology for treatment, diagnosis, monitoring and control of biological systems. The devices that are being developed generally incorporate inorganic or biological material. In this regard, the coupling of inorganic nanoscale materials to targeted Ad vectors would expand MFP functions,

capitalizing on the new treatment strategies being developed using nanotechnology. For example, magnetic nanoparticles have recently received much attention due to their potential application in clinical cancer treatment,[158–162] targeted drug delivery[163–165] and MRI contrast agents.[166,167] However, despite the useful functionalities that might derive from metal nanoparticle systems, the lack of targeting strategies has limited their application to locoregional disease. Thus, tumor-selective delivery is key to improve therapeutic applications of metal nanoparticle systems, rationalizing incorporation of such particles into targeted, multifunctional Ad vectors via conjugation to capsid proteins or other means.

For the development of targeted MFPs, it would be beneficial to minimize the adenoviral vector to empty capsid shells, based on the consideration that the so-called first-generation Ad vectors (i.e. Ad5- or Ad2-based nonreplicating viruses lacking E1, and sometimes E3 regions) still express low levels of the remaining viral genes. This low level of viral gene expression leads to direct toxicity and immunogenicity. Consequently, duration of transgene expression is shortened as the immune response clears the vector-transduced cells.[168,169] To overcome these problems, high-capacity Ad vectors have been developed. The only viral genomic elements retained in these vectors are the inverted terminal repeats (ITR) and packaging signal. This allows up to 36 kb of nonviral DNA to be inserted. Reduction in *in vivo* toxicity and immunogenicity are seen,[170–173] and in mice long-term transgene expression for more than a year has been observed.[173] The deletion of all the viral genes requires helper viruses to trans-complement all viral genes, including those for capsid proteins. Well-defined and efficient systems have been developed to allow production of high-capacity adenoviral vectors without contamination of helper virus, based on recombinase-mediated excision of the helper-virus packaging signal.[174–176] It is logical that the capsid proteins expressed by the helper virus would be genetically modified, allowing re-targeting of the resultant high-capacity adenoviral vector. This concept was recently demonstrated by using the RGD motif in the HI-loop of the fiber knob,[177] and this demonstration of combining re-targeting with high-capacity Ad illustrates the potential for utilization of gutless Ad as a nanoscale platform.

To extend the paradigm of limiting foreign gene expression, high-capacity adenoviral vectors have been further developed into empty Ad capsid shells.[178,179] The production of empty capsids has been based on a modification of the systems utilized in the construction of high-capacity Ad vectors, utilizing a Cre/lox recombination event. It has been demonstrated that, compared to recombinant Ad vectors, empty Ad capsid shells induce a significantly reduced number of genes after cellular interaction.[179] This suggests that these empty capsid shells could serve as an improved platform for the development of MFP systems, which would incorporate targeting, imaging and therapeutic elements, with minimal adverse effects after *in vivo* administration.

Summary

Adenovirus-based vectors are the most widely used platform for gene delivery. They are of particular utility for cancer gene therapy applications, where temporary gene expression is acceptable or even beneficial. The history of Ad-based gene therapy studies clearly illustrates and confirms the critical linkage between an improved delivery vector and increases in therapeutic potential. Very often, clinical breakthroughs have been dependent on advances in vector development. With regard to Ad-mediated cancer treatment, high-level tumor transduction remains a key developmental hurdle. To this end, Ad vectors possessing infectivity enhancement and targeting capabilities should be evaluated in the most stringent model systems possible. Advanced Ad-based vectors with imaging, targeting and therapeutic capabilities have yet to be fully realized; however, the feasibilities leading to this accomplishment are within close reach.

Acknowledgements

This work was supported by grants from the National Institutes of Health: R01 CA083821, R01 CA094084 and R01 CA111569-01A1, and grant W81XWH-05-1-0035 from the US Department of Defense. We wish to thank Dr Long P Le for assistance with graphic images.

References

1 Miller CR, Buchsbaum DJ, Reynolds PN, Douglas JT, Gillespie GY, Mayo MS *et al*. Differential susceptibility of primary and established human glioma cells to adenovirus infection: targeting via the epidermal growth factor receptor achieves fiber receptor-independent gene transfer. *Cancer Res* 1998; **58**: 5738–5748.
2 Li Y, Pong RC, Bergelson JM, Hall MC, Sagalowsky AI, Tseng CP *et al*. Loss of adenoviral receptor expression in human bladder cancer cells: a potential impact on the efficacy of gene therapy. *Cancer Res* 1999; **59**: 325–330.
3 Hemminki A, Alvarez RD. Adenoviruses in oncology: a viable option? *BioDrugs* 2002; **16**: 77–87.
4 Dmitriev I, Krasnykh V, Miller CR, Wang M, Kashentseva E, Mikheeva G *et al*. An adenovirus vector with genetically modified fibers demonstrates expanded tropism via utilization of a coxsackievirus and adenovirus receptor-independent cell entry mechanism. *J Virol* 1998; **72**: 9706–9713.
5 Cripe TP, Dunphy EJ, Holub AD, Saini A, Vasi NH, Mahller YY *et al*. Fiber knob modifications overcome low, heterogeneous expression of the coxsackievirus-adenovirus receptor that limits adenovirus gene transfer and oncolysis for human rhabdomyosarcoma cells. *Cancer Res* 2001; **61**: 2953–2960.
6 Clinicals Trials Database. *The Journal of Gene Medicine Clinical Trials Database* 2004, http://www.wiley.co.uk/genmed/clinical.
7 Davison AJ, Benko M, Harrach B. Genetic content and evolution of adenoviruses. *J Gen Virol* 2003; **84**(Part 11): 2895–2908.
8 Mei YF, Wadell G. Epitopes and hemagglutination binding domain on subgenus B:2 adenovirus fibers. *J Virol* 1996; **70**: 3688–3697.

9 Shenk T. Adenoviridae: and their replication. In: Fields B, Howley P, Knipe D (eds) (translator and editor). *Virology*. Raven Press: New York, 1996, pp 2111–2148.
10 Stewart PL, Burnett RM. Adenovirus structure by X-ray crystallography and electron microscopy. *Curr Top Microbiol Immunol* 1995; **199**(Part 1): 25–38.
11 Rux JJ, Kuser PR, Burnett RM. Structural and phylogenetic analysis of adenovirus hexons by use of high-resolution x-ray crystallographic, molecular modeling, and sequence-based methods. *J Virol* 2003; **77**: 9553–9566.
12 Roberts MM, White JL, Grutter MG, Burnett RM. Three-dimensional structure of the adenovirus major coat protein hexon. *Science* 1986; **232**: 1148–1151.
13 Zubieta C, Schoehn G, Chroboczek J, Cusack S. The structure of the human adenovirus 2 penton. *Mol Cell* 2005; **17**: 121–135.
14 van Raaij MJ, Louis N, Chroboczek J, Cusack S. Structure of the human adenovirus serotype 2 fiber head domain at 1.5 A resolution. *Virology* 1999; **262**: 333–343.
15 van Raaij MJ, Mitraki A, Lavigne G, Cusack S. A triple beta-spiral in the adenovirus fibre shaft reveals a new structural motif for a fibrous protein. *Nature* 1999; **401**: 935–938.
16 Stewart PL, Fuller SD, Burnett RM. Difference imaging of adenovirus: bridging the resolution gap between X-ray crystallography and electron microscopy. *EMBO J* 1993; **12**: 2589–2599.
17 Fabry CM, Rosa-Calatrava M, Conway JF, Zubieta C, Cusack S, Ruigrok RW *et al*. A quasi-atomic model of human adenovirus type 5 capsid. *EMBO J* 2005; **24**: 1645–1654.
18 Tomko RP, Xu R, Philipson L. HCAR and MCAR: the human and mouse cellular receptors for subgroup C adenoviruses and group B coxsackieviruses. *Proc Natl Acad Sci USA* 1997; **94**: 3352–3356.
19 Bergelson JM, Cunningham JA, Droguett G, Kurt-Jones EA, Krithivas A, Hong JS *et al*. Isolation of a common receptor for Coxsackie B viruses and adenoviruses 2 and 5. *Science* 1997; **275**: 1320–1323.
20 Dechecchi MC, Melotti P, Bonizzato A, Santacatterina M, Chilosi M, Cabrini G. Heparan sulfate glycosaminoglycans are receptors sufficient to mediate the initial binding of adenovirus types 2 and 5. *J Virol* 2001; **75**: 8772–8780.
21 Dechecchi MC, Tamanini A, Bonizzato A, Cabrini G. Heparan sulfate glycosaminoglycans are involved in adenovirus type 5 and 2-host cell interactions. *Virology* 2000; **268**: 382–390.
22 Hong SS, Karayan L, Tournier J, Curiel DT, Boulanger PA. Adenovirus type 5 fiber knob binds to MHC class I alpha2 domain at the surface of human epithelial and B lymphoblastoid cells. *EMBO J* 1997; **16**: 2294–2306.
23 Chu Y, Heistad D, Cybulsky MI, Davidson BL. Vascular cell adhesion molecule-1 augments adenovirus-mediated gene transfer. *Arterioscler Thromb Vasc Biol* 2001; **21**: 238–242.
24 Wickham TJ, Mathias P, Cheresh DA, Nemerow GR. Integrins alpha v beta 3 and alpha v beta 5 promote adenovirus internalization but not virus attachment. *Cell* 1993; **73**: 309–319.
25 Li E, Brown SL, Stupack DG, Puente XS, Cheresh DA, Nemerow GR. Integrin alpha(v)beta1 is an adenovirus coreceptor. *J Virol* 2001; **75**: 5405–5409.
26 Davison E, Diaz RM, Hart IR, Santis G, Marshall JF. Integrin alpha5beta1-mediated adenovirus infection is enhanced by the integrin-activating antibody TS2/16. *J Virol* 1997; **71**: 6204–6207.
27 Meier O, Boucke K, Hammer SV, Keller S, Stidwill RP, Hemmi S *et al*. Adenovirus triggers macropinocytosis and endosomal leakage together with its clathrin-mediated uptake. *J Cell Biol* 2002; **158**: 1119–1131.
28 Okegawa T, Pong RC, Li Y, Bergelson JM, Sagalowsky AI, Hsieh JT. The mechanism of the growth-inhibitory effect of coxsackie and adenovirus receptor (CAR) on human bladder cancer: a functional analysis of car protein structure. *Cancer Res* 2001; **61**: 6592–6600.
29 Seidman MA, Hogan SM, Wendland RL, Worgall S, Crystal RG, Leopold PL. Variation in adenovirus receptor expression and adenovirus vector-mediated transgene expression at defined stages of the cell cycle. *Mol Ther* 2001; **4**: 13–21.
30 Hemminki A, Kanerva A, Liu B, Wang M, Alvarez RD, Siegal GP *et al*. Modulation of coxsackie-adenovirus receptor expression for increased adenoviral transgene expression. *Cancer Res* 2003; **63**: 847–853.
31 Fechner H, Haack A, Wang H, Wang X, Eizema K, Pauschinger M *et al*. Expression of coxsackie adenovirus receptor and alphav-integrin does not correlate with adenovector targeting *in vivo* indicating anatomical vector barriers. *Gene Therapy* 1999; **6**: 1520–1535.
32 Wood M, Perrotte P, Onishi E, Harper ME, Dinney C, Pagliaro L *et al*. Biodistribution of an adenoviral vector carrying the luciferase reporter gene following intravesical or intravenous administration to a mouse. *Cancer Gene Ther* 1999; **6**: 367–372.
33 Reynolds P, Dmitriev I, Curiel D. Insertion of an RGD motif into the HI loop of adenovirus fiber protein alters the distribution of transgene expression of the systemically administered vector. *Gene Therapy* 1999; **6**: 1336–1339.
34 Tao N, Gao GP, Parr M, Johnston J, Baradet T, Wilson JM *et al*. Sequestration of adenoviral vector by Kupffer cells leads to a nonlinear dose response of transduction in liver. *Mol Ther* 2001; **3**: 28–35.
35 Connelly S. Adenoviral vectors for liver-directed gene therapy. *Curr Opin Mol Ther* 1999; **1**: 565–572.
36 Lieber A, He CY, Meuse L, Schowalter D, Kirillova I, Winther B *et al*. The role of Kupffer cell activation and viral gene expression in early liver toxicity after infusion of recombinant adenovirus vectors. *J Virol* 1997; **71**: 8798–8807.
37 Peeters MJ, Patijn GA, Lieber A, Meuse L, Kay MA. Adenovirus-mediated hepatic gene transfer in mice: comparison of intravascular and biliary administration. *Hum Gene Ther* 1996; **7**: 1693–1699.
38 Alemany R, Suzuki K, Curiel DT. Blood clearance rates of adenovirus type 5 in mice. *J Gen Virol* 2000; **81**(Part 11): 2605–2609.
39 Worgall S, Wolff G, Falck-Pedersen E, Crystal RG. Innate immune mechanisms dominate elimination of adenoviral vectors following *in vivo* administration. *Hum Gene Ther* 1997; **8**: 37–44.
40 Alemany R, Curiel DT. CAR-binding ablation does not change biodistribution and toxicity of adenoviral vectors. *Gene Therapy* 2001; **8**: 1347–1353.
41 Smith TA, Idamakanti N, Marshall-Neff J, Rollence ML, Wright P, Kaloss M *et al*. Receptor interactions involved in adenoviral-mediated gene delivery after systemic administration in non-human primates. *Hum Gene Ther* 2003; **14**: 1595–1604.
42 Smith T, Idamakanti N, Kylefjord H, Rollence M, King L, Kaloss M *et al*. *In vivo* hepatic adenoviral gene delivery occurs independently of the coxsackievirus-adenovirus receptor. *Mol Ther* 2002; **5**: 770–779.

43 Martin K, Brie A, Saulnier P, Perricaudet M, Yeh P, Vigne E. Simultaneous CAR- and alpha V integrin-binding ablation fails to reduce Ad5 liver tropism. *Mol Ther* 2003; **8**: 485–494.
44 Mizuguchi H, Koizumi N, Hosono T, Ishii-Watabe A, Uchida E, Utoguchi N *et al*. CAR- or alphav integrin-binding ablated adenovirus vectors, but not fiber-modified vectors containing RGD peptide, do not change the systemic gene transfer properties in mice. *Gene Therapy* 2002; **9**: 769–776.
45 Nicklin SA, Wu E, Nemerow GR, Baker AH. The influence of adenovirus fiber structure and function on vector development for gene therapy. *Mol Ther* 2005; **12**: 384–393.
46 Vigne E, Dedieu JF, Brie A, Gillardeaux A, Briot D, Benihoud K *et al*. Genetic manipulations of adenovirus type 5 fiber resulting in liver tropism attenuation. *Gene Therapy* 2003; **10**: 153–162.
47 Breidenbach M, Rein DT, Wang M, Nettelbeck DM, Hemminki A, Ulasov I *et al*. Genetic replacement of the adenovirus shaft fiber reduces liver tropism in ovarian cancer gene therapy. *Hum Gene Ther* 2004; **15**: 509–518.
48 Smith TA, Idamakanti N, Rollence ML, Marshall-Neff J, Kim J, Mulgrew K *et al*. Adenovirus serotype 5 fiber shaft influences *in vivo* gene transfer in mice. *Hum Gene Ther* 2003; **14**: 777–787.
49 Shayakhmetov DM, Li ZY, Ni S, Lieber A. Analysis of adenovirus sequestration in the liver, transduction of hepatic cells, and innate toxicity after injection of fiber-modified vectors. *J Virol* 2004; **78**: 5368–5381.
50 Douglas JT, Rogers BE, Rosenfeld ME, Michael SI, Feng M, Curiel DT. Targeted gene delivery by tropism-modified adenoviral vectors. *Nat Biotechnol* 1996; **14**: 1574–1578.
51 Goldman CK, Rogers BE, Douglas JT, Sosnowski BA, Ying W, Siegal GP *et al*. Targeted gene delivery to Kaposi's sarcoma cells via the fibroblast growth factor receptor. *Cancer Res* 1997; **57**: 1447–1451.
52 Gu DL, Gonzalez AM, Printz MA, Doukas J, Ying W, D'Andrea M *et al*. Fibroblast growth factor 2 retargeted adenovirus has redirected cellular tropism: evidence for reduced toxicity and enhanced antitumor activity in mice. *Cancer Res* 1999; **59**: 2608–2614.
53 Haisma HJ, Pinedo HM, Rijswijk A, der Meulen-Muileman I, Sosnowski BA, Ying W *et al*. Tumor-specific gene transfer via an adenoviral vector targeted to the pan-carcinoma antigen EpCAM. *Gene Therapy* 1999; **6**: 1469–1474.
54 Heideman DA, Snijders PJ, Craanen ME, Bloemena E, Meijer CJ, Meuwissen SG *et al*. Selective gene delivery toward gastric and esophageal adenocarcinoma cells via EpCAM-targeted adenoviral vectors. *Cancer Gene Ther* 2001; **8**: 342–351.
55 Kelly FJ, Miller CR, Buchsbaum DJ, Gomez-Navarro J, Barnes MN, Alvarez RD *et al*. Selectivity of TAG-72-targeted adenovirus gene transfer to primary ovarian carcinoma cells versus autologous mesothelial cells *in vitro*. *Clin Cancer Res* 2000; **6**: 4323–4333.
56 Reynolds PN, Zinn KR, Gavrilyuk VD, Balyasnikova IV, Rogers BE, Buchsbaum DJ *et al*. A targetable, injectable adenoviral vector for selective gene delivery to pulmonary endothelium *in vivo*. *Mol Ther* 2000; **2**: 562–578.
57 Tillman BW, de Gruijl TD, Luykx-de Bakker SA, Scheper RJ, Pinedo HM, Curiel TJ *et al*. Maturation of dendritic cells accompanies high-efficiency gene transfer by a CD40-targeted adenoviral vector. *J Immunol* 1999; **162**: 6378–6383.
58 Hakkarainen T, Hemminki A, Pereboev AV, Barker SD, Asiedu CK, Strong TV *et al*. CD40 is expressed on ovarian cancer cells and can be utilized for targeting adenoviruses. *Clin Cancer Res* 2003; **9**: 619–624.
59 Pereboev AV, Asiedu CK, Kawakami Y, Dong SS, Blackwell JL, Kashentseva EA *et al*. Coxsackievirus-adenovirus receptor genetically fused to anti-human CD40 scFv enhances adenoviral transduction of dendritic cells. *Gene Therapy* 2002; **9**: 1189–1193.
60 Dmitriev I, Kashentseva E, Rogers BE, Krasnykh V, Curiel DT. Ectodomain of coxsackievirus and adenovirus receptor genetically fused to epidermal growth factor mediates adenovirus targeting to epidermal growth factor receptor-positive cells. *J Virol* 2000; **74**: 6875–6884.
61 Kashentseva EA, Seki T, Curiel DT, Dmitriev IP. Adenovirus targeting to c-erbB-2 oncoprotein by single-chain antibody fused to trimeric form of adenovirus receptor ectodomain. *Cancer Res* 2002; **62**: 609–616.
62 Itoh A, Okada T, Mizuguchi H, Hayakawa T, Mizukami H, Kume A *et al*. A soluble CAR–SCF fusion protein improves adenoviral vector-mediated gene transfer to c-Kit-positive hematopoietic cells. *J Gene Med* 2003; **5**: 929–940.
63 Kim J, Smith T, Idamakanti N, Mulgrew K, Kaloss M, Kylefjord H *et al*. Targeting adenoviral vectors by using the extracellular domain of the coxsackie-adenovirus receptor: improved potency via trimerization. *J Virol* 2002; **76**: 1892–1903.
64 Krasnykh VN, Mikheeva GV, Douglas JT, Curiel DT. Generation of recombinant adenovirus vectors with modified fibers for altering viral tropism. *J Virol* 1996; **70**: 6839–6846.
65 Havenga MJ, Lemckert AA, Ophorst OJ, van Meijer M, Germeraad WT, Grimbergen J *et al*. Exploiting the natural diversity in adenovirus tropism for therapy and prevention of disease. *J Virol* 2002; **76**: 4612–4620.
66 Gaggar A, Shayakhmetov DM, Lieber A. CD46 is a cellular receptor for group B adenoviruses. *Nat Med* 2003; **9**: 1408–1412.
67 Segerman A, Arnberg N, Erikson A, Lindman K, Wadell G. There are two different species B adenovirus receptors: sBAR, common to species B1 and B2 adenoviruses, and sB2AR, exclusively used by species B2 adenoviruses. *J Virol* 2003; **77**: 1157–1162.
68 Segerman A, Atkinson JP, Marttila M, Dennerquist V, Wadell G, Arnberg N. Adenovirus type 11 uses CD46 as a cellular receptor. *J Virol* 2003; **77**: 9183–9191.
69 Sirena D, Lilienfeld B, Eisenhut M, Kalin S, Boucke K, Beerli RR *et al*. The human membrane cofactor CD46 is a receptor for species B adenovirus serotype 3. *J Virol* 2004; **78**: 4454–4462.
70 Short JJ, Pereboev AV, Kawakami Y, Vasu C, Holterman MJ, Curiel DT. Adenovirus serotype 3 utilizes CD80 (B7.1) and CD86 (B7.2) as cellular attachment receptors. *Virology* 2004; **322**: 349–359.
71 Arnberg N, Edlund K, Kidd AH, Wadell G. Adenovirus type 37 uses sialic acid as a cellular receptor. *J Virol* 2000; **74**: 42–48.
72 Arnberg N, Kidd AH, Edlund K, Nilsson J, Pring-Akerblom P, Wadell G. Adenovirus type 37 binds to cell surface sialic acid through a charge-dependent interaction. *Virology* 2002; **302**: 33–43.
73 Wu E, Trauger SA, Pache L, Mullen TM, von Seggern DJ, Siuzdak G *et al*. Membrane cofactor protein is a receptor for adenoviruses associated with epidemic keratoconjunctivitis. *J Virol* 2004; **78**: 3897–3905.

74 Kanerva A, Zinn KR, Chaudhuri TR, Suzuki K, Uil T, Hakkarainen T *et al*. Enhanced therapeutic efficacy for ovarian cancer with a serotype 3 receptor targeted oncolytic virus. *Mol Ther* 2003; **8**: 449–458.

75 Kanerva A, Wang M, Bauerschmitz GJ, Lam JT, Desmond RA, Bhoola SM *et al*. Gene transfer to ovarian cancer versus normal tissues with fiber-modified adenoviruses. *Mol Ther* 2002b; **5**: 695–704.

76 Kanerva A, Mikheeva GV, Krasnykh V, Coolidge CJ, Lam JT, Mahasreshti PJ *et al*. Targeting adenovirus to the serotype 3 receptor increases gene transfer efficiency to ovarian cancer cells. *Clin Cancer Res* 2002; **8**: 275–280.

77 Zabner J, Chillon M, Grunst T, Moninger TO, Davidson BL, Gregory R *et al*. A chimeric type 2 adenovirus vector with a type 17 fiber enhances gene transfer to human airway epithelia. *J Virol* 1999; **73**: 8689–8695.

78 Rea D, Havenga MJ, van Den Assem M, Sutmuller RP, Lemckert A, Hoeben RC *et al*. Highly efficient transduction of human monocyte-derived dendritic cells with subgroup B fiber-modified adenovirus vectors enhances transgene-encoded antigen presentation to cytotoxic T cells. *J Immunol* 2001; **166**: 5236–5244.

79 Von Seggern DJ, Huang S, Fleck SK, Stevenson SC, Nemerow GR. Adenovirus vector pseudotyping in fiber-expressing cell lines: improved transduction of Epstein–Barr virus-transformed B cells. *J Virol* 2000; **74**: 354–362.

80 Shayakhmetov DM, Papayannopoulou T, Stamatoyannopoulos G, Lieber A. Efficient gene transfer into human CD34(+) cells by a retargeted adenovirus vector. *J Virol* 2000; **74**: 2567–2583.

81 Goossens PH, Havenga MJ, Pieterman E, Lemckert AA, Breedveld FC, Bout A *et al*. Infection efficiency of type 5 adenoviral vectors in synovial tissue can be enhanced with a type 16 fiber. *Arthritis Rheum* 2001; **44**: 570–577.

82 Havenga MJ, Lemckert AA, Grimbergen JM, Vogels R, Huisman LG, Valerio D *et al*. Improved adenovirus vectors for infection of cardiovascular tissues. *J Virol* 2001; **75**: 3335–3342.

83 Gall J, Kass-Eisler A, Leinwand L, Falck-Pedersen E. Adenovirus type 5 and 7 capsid chimera: fiber replacement alters receptor tropism without affecting primary immune neutralization epitopes. *J Virol* 1996; **70**: 2116–2123.

84 Chillon M, Bosch A, Zabner J, Law L, Armentano D, Welsh MJ *et al*. Group D adenoviruses infect primary central nervous system cells more efficiently than those from group C. *J Virol* 1999; **73**: 2537–2540.

85 Stoff-Khalili MA, Rivera AA, Glasgow JN, Le LP, Stoff A, Everts M *et al*. A human adenoviral vector with a chimeric fiber from canine adenovirus type 1 results in novel expanded tropism for cancer gene therapy. *Gene Therapy* 2005; **12**: 1696–1706.

86 Glasgow JN, Kremer EJ, Hemminki A, Siegal GP, Douglas JT, Curiel DT. An adenovirus vector with a chimeric fiber derived from canine adenovirus type 2 displays novel tropism. *Virology* 2004; **324**: 103–116.

87 Tsuruta Y, Pereboeva L, Glasgow JN, Luongo CL, Komarova S, Kawakami Y *et al*. Reovirus sigma1 fiber incorporated into adenovirus serotype 5 enhances infectivity via a CAR-independent pathway. *Biochem Biophys Res Commun* 2005; **335**: 205–214.

88 Mercier GT, Campbell JA, Chappell JD, Stehle T, Dermody TS, Barry MA. A chimeric adenovirus vector encoding reovirus attachment protein sigma1 targets cells expressing junctional adhesion molecule 1. *Proc Natl Acad Sci USA* 2004; **101**: 6188–6193.

89 Wickham TJ, Tzeng E, Shears LL, Roelvink II PW, Li Y, Lee GM *et al*. Increased *in vitro* and *in vivo* gene transfer by adenovirus vectors containing chimeric fiber proteins. *J Virol* 1997; **71**: 8221–8229.

90 Krasnykh V, Dmitriev I, Mikheeva G, Miller CR, Belousova N, Curiel DT. Characterization of an adenovirus vector containing a heterologous peptide epitope in the HI loop of the fiber knob. *J Virol* 1998; **72**: 1844–1852.

91 Belousova N, Krendelchtchikova V, Curiel DT, Krasnykh V. Modulation of adenovirus vector tropism via incorporation of polypeptide ligands into the fiber protein. *J Virol* 2002; **76**: 8621–8631.

92 Hemminki A, Wang M, Desmond RA, Strong TV, Alvarez RD, Curiel DT. Serum and ascites neutralizing antibodies in ovarian cancer patients treated with intraperitoneal adenoviral gene therapy. *Hum Gene Ther* 2002; **13**: 1505–1514.

93 Hemminki A, Belousova N, Zinn KR, Liu B, Wang M, Chaudhuri TR *et al*. An adenovirus with enhanced infectivity mediates molecular chemotherapy of ovarian cancer cells and allows imaging of gene expression. *Mol Ther* 2001; **4**: 223–231.

94 Bauerschmitz GJ, Barker SD, Hemminki A. Adenoviral gene therapy for cancer: from vectors to targeted and replication competent agents (review). *Int J Oncol* 2002; **21**: 1161–1174.

95 Wu H, Seki T, Dmitriev I, Uil T, Kashentseva E, Han T *et al*. Double modification of adenovirus fiber with RGD and polylysine motifs improves coxsackievirus-adenovirus receptor-independent gene transfer efficiency. *Hum Gene Ther* 2002; **13**: 1647–1653.

96 Contreras JL, Wu H, Smyth CA, Eckstein CP, Young CJ, Seki T *et al*. Double genetic modification of adenovirus fiber with RGD polylysine motifs significantly enhances gene transfer to isolated human pancreatic islets. *Transplantation* 2003; **76**: 252–261.

97 Wu H, Han T, Lam JT, Leath CA, Dmitriev I, Kashentseva E *et al*. Preclinical evaluation of a class of infectivity-enhanced adenoviral vectors in ovarian cancer gene therapy. *Gene Therapy* 2004; **11**: 874–878.

98 Rein DT, Breidenbach M, Wu H, Han T, Haviv YS, Wang M *et al*. Gene transfer to cervical cancer with fiber-modified adenoviruses. *Int J Cancer* 2004; **111**: 698–704.

99 Nicklin SA, White SJ, Watkins SJ, Hawkins RE, Baker AH. Selective targeting of gene transfer to vascular endothelial cells by use of peptides isolated by phage display. *Circulation* 2000; **102**: 231–237.

100 Nicklin SA, Dishart KL, Buening H, Reynolds PN, Hallek M, Nemerow GR *et al*. Transductional and transcriptional targeting of cancer cells using genetically engineered viral vectors. *Cancer Lett* 2003; **201**: 165–173.

101 Korokhov N, Mikheeva G, Krendelshchikov A, Belousova N, Simonenko V, Krendelshchikova V *et al*. Targeting of adenovirus via genetic modification of the viral capsid combined with a protein bridge. *J Virol* 2003; **77**: 12931–12940.

102 Volpers C, Thirion C, Biermann V, Hussmann S, Kewes H, Dunant P *et al*. Antibody-mediated targeting of an adenovirus vector modified to contain a synthetic immunoglobulin g-binding domain in the capsid. *J Virol* 2003; **77**: 2093–2104.

103 Henning P, Andersson KM, Frykholm K, Ali A, Magnusson MK, Nygren PA *et al*. Tumor cell targeted gene delivery by adenovirus 5 vectors carrying knobless fibers with antibody-binding domains. *Gene Therapy* 2005; **12**: 211–224.

104 Korokhov N, de Gruijl TD, Aldrich WA, Triozzi PL, Banerjee PT, Gillies SD *et al*. High efficiency transduction of dendritic cells by adenoviral vectors targeted to DC-SIGN. *Cancer Biol Ther* 2005; **4**: 289–294.

105 Breidenbach M, Rein DT, Everts M, Glasgow JN, Wang M, Passineau MJ *et al*. Mesothelin-mediated targeting of adenoviral vectors for ovarian cancer gene therapy. *Gene Therapy* 2005; **12**: 187–193.

106 Balyasnikova IV, Metzger R, Visintine DJ, Dimasius V, Sun ZL, Berestetskaya YV *et al*. Selective rat lung endothelial targeting with a new set of monoclonal antibodies to angiotensin I-converting enzyme. *Pulm Pharmacol Ther* 2005; **18**: 251–267.

107 Von Seggern DJ, Chiu CY, Fleck SK, Stewart PL, Nemerow GR. A helper-independent adenovirus vector with E1, E3, and fiber deleted: structure and infectivity of fiberless particles. *J Virol* 1999; **73**: 1601–1608.

108 Falgout B, Ketner G. Characterization of adenovirus particles made by deletion mutants lacking the fiber gene. *J Virol* 1988; **62**: 622–625.

109 Papanikolopoulou K, Forge V, Goeltz P, Mitraki A. Formation of highly stable chimeric trimers by fusion of an adenovirus fiber shaft fragment with the foldon domain of bacteriophage T4 fibritin. *J Biol Chem* 2004; **279**: 8991–8998.

110 Krasnykh V, Belousova N, Korokhov N, Mikheeva G, Curiel DT. Genetic targeting of an adenovirus vector via replacement of the fiber protein with the phage T4 fibritin. *J Virol* 2001; **75**: 4176–4183.

111 Magnusson MK, Hong SS, Boulanger P, Lindholm L. Genetic retargeting of adenovirus: novel strategy employing 'deknobbing' of the fiber. *J Virol* 2001; **75**: 7280–7289.

112 Gaden F, Franqueville L, Magnusson MK, Hong SS, Merten MD, Lindholm L *et al*. Gene transduction and cell entry pathway of fiber-modified adenovirus type 5 vectors carrying novel endocytic peptide ligands selected on human tracheal glandular cells. *J Virol* 2004; **78**: 7227–7247.

113 Belousova N, Korokhov N, Krendelshchikova V, Simonenko V, Mikheeva G, Triozzi PL *et al*. Genetically targeted adenovirus vector directed to CD40-expressing cells. *J Virol* 2003; **77**: 11367–11377.

114 Izumi M, Kawakami Y, Glasgow JN, Belousova N, Everts M, Kim-Park S *et al*. *In vivo* analysis of a genetically modified adenoviral vector targeted to human CD40 using a novel transient transgenic model. *J Gene Med* 2005; **7**: 1517–1525.

115 Pereboeva L, Komarova S, Mahasreshti PJ, Curiel DT. Fiber-mosaic adenovirus as a novel approach to design genetically modified adenoviral vectors. *Virus Res* 2004; **105**: 35–46.

116 Takayama K, Reynolds PN, Short JJ, Kawakami Y, Adachi Y, Glasgow JN *et al*. A mosaic adenovirus possessing serotype Ad5 and serotype Ad3 knobs exhibits expanded tropism. *Virology* 2003; **309**: 282–293.

117 Magnusson MK, Hong SS, Henning P, Boulanger P, Lindholm L. Genetic retargeting of adenovirus vectors: functionality of targeting ligands and their influence on virus viability. *J Gene Med* 2002; **4**: 356–370.

118 Hedley SJ, Auf der Maur A, Hohn S, Escher D, Barberis A, Glasgow JN *et al*. An adenovirus vector with a chimeric fiber incorporating stabilized single chain antibody achieves targeted gene delivery. *Gene Therapy* 2006; **13**: 88–94.

119 Athappilly FK, Murali R, Rux JJ, Cai Z, Burnett RM. The refined crystal structure of hexon, the major coat protein of adenovirus type 2, at 2.9 A resolution. *J Mol Biol* 1994; **242**: 430–455.

120 Crawford-Miksza L, Schnurr DP. Analysis of 15 adenovirus hexon proteins reveals the location and structure of seven hypervariable regions containing serotype-specific residues. *J Virol* 1996; **70**: 1836–1844.

121 Vigne E, Mahfouz I, Dedieu JF, Brie A, Perricaudet M, Yeh P. RGD inclusion in the hexon monomer provides adenovirus type 5-based vectors with a fiber knob-independent pathway for infection. *J Virol* 1999; **73**: 5156–5161.

122 Parks RJ. Adenovirus protein IX: a new look at an old protein. *Mol Ther* 2005; **11**: 19–25.

123 Vellinga J, van den Wollenberg DJ, van der Heijdt S, Rabelink MJ, Hoeben RC. The coiled-coil domain of the adenovirus type 5 protein IX is dispensable for capsid incorporation and thermostability. *J Virol* 2005; **79**: 3206–3210.

124 Ghosh-Choudhury G, Haj-Ahmad Y, Graham FL. Protein IX, a minor component of the human adenovirus capsid, is essential for the packaging of full length genomes. *EMBO J* 1987; **6**: 1733–1739.

125 Colby WW, Shenk T. Adenovirus type 5 virions can be assembled *in vivo* in the absence of detectable polypeptide IX. *J Virol* 1981; **39**: 977–980.

126 Boulanger P, Lemay P, Blair GE, Russell WC. Characterization of adenovirus protein IX. *J Gen Virol* 1979; **44**: 783–800.

127 Akalu A, Liebermann H, Bauer U, Granzow H, Seidel W. The subgenus-specific C-terminal region of protein IX is located on the surface of the adenovirus capsid. *J Virol* 1999; **73**: 6182–6187.

128 Rosa-Calatrava M, Grave L, Puvion-Dutilleul F, Chatton B, Kedinger C. Functional analysis of adenovirus protein IX identifies domains involved in capsid stability, transcriptional activity, and nuclear reorganization. *J Virol* 2001; **75**: 7131–7141.

129 Dmitriev IP, Kashentseva EA, Curiel DT. Engineering of adenovirus vectors containing heterologous peptide sequences in the C terminus of capsid protein IX. *J Virol* 2002; **76**: 6893–6899.

130 Vellinga J, Rabelink MJ, Cramer SJ, van den Wollenberg DJ, Van der Meulen H, Leppard KN *et al*. Spacers increase the accessibility of peptide ligands linked to the carboxyl terminus of adenovirus minor capsid protein IX. *J Virol* 2004; **78**: 3470–3479.

131 Campos SK, Parrott MB, Barry MA. Avidin-based targeting and purification of a protein IX-modified, metabolically biotinylated adenoviral vector. *Mol Ther* 2004; **9**: 942–954.

132 Meulenbroek RA, Sargent KL, Lunde J, Jasmin BJ, Parks RJ. Use of adenovirus protein IX (pIX) to display large polypeptides on the virion-generation of fluorescent virus through the incorporation of pIX-GFP. *Mol Ther* 2004; **9**: 617–624.

133 Le LP, Everts M, Dmitriev IP, Davydova JG, Yamamoto M, Curiel DT. Fluorescently labeled adenovirus with pIX-EGFP for vector detection. *Mol Imaging* 2004; **3**: 105–116.

134 Le LP, Dmitriev I, Davydova J, Yamamoto M, Curiel D. Genetic labeling of adenovirus with red fluorescent proteins on PIX for vector detection. *Mol Ther* 2004; **9**(S1): S296.

135 Le LP, Dmitriev I, Davydova J, Yamamoto M, Curiel D. Genetic labeling of adenovirus with luciferase on pIX for vector detection. *Mol Ther* 2004; **9**(S1): 297–298.

136 Li J, Le LP, Sibley DA, Mathis JM, Curiel DT. Genetic incorporation of HSV-1 thymidine kinase into the adenovirus protein ix for functioal display on the virion. *Virology* 2005; **338**: 247–258.
137 Vellinga J, Van der Heijdt S, Hoeben RC. The adenovirus capsid: major progress in minor proteins. *J Gen Virol* 2005; **86**(Part 6): 1581–1588.
138 Dmitriev I, Kashentseva EA, Seki T, Curiel DT. Utilization of minor capsid polypeptides IX and IIIa for adenovirus targeting. *Mol Ther* 2001; **3**: S167.
139 Curiel D. Capsid-modified recombinant adenovirus vectors and methods of use. United States patent 6555368. 2003.
140 Welsh JB, Sapinoso LM, Su AI, Kern SG, Wang-Rodriguez J, Moskaluk CA *et al*. Analysis of gene expression identifies candidate markers and pharmacological targets in prostate cancer. *Cancer Res* 2001; **61**: 5974–5978.
141 Welsh JB, Zarrinkar PP, Sapinoso LM, Kern SG, Behling CA, Monk BJ *et al*. Analysis of gene expression profiles in normal and neoplastic ovarian tissue samples identifies candidate molecular markers of epithelial ovarian cancer. *Proc Natl Acad Sci USA* 2001; **98**: 1176–1181.
142 Omenn GS. The human proteome organization plasma proteome project pilot phase: reference specimens, technology platform comparisons, and standardized data submissions and analyses. *Proteomics* 2004; **4**: 1235–1240.
143 Nishizuka S, Chen ST, Gwadry FG, Alexander J, Major SM, Scherf U *et al*. Diagnostic markers that distinguish colon and ovarian adenocarcinomas: identification by genomic, proteomic, and tissue array profiling. *Cancer Res* 2003; **63**: 5243–5250.
144 Sahin U, Tureci O, Schmitt H, Cochlovius B, Johannes T, Schmits R *et al*. Human neoplasms elicit multiple specific immune responses in the autologous host. *Proc Natl Acad Sci USA* 1995; **92**: 11810–11813.
145 Li G, Miles A, Line A, Rees RC. Identification of tumour antigens by serological analysis of cDNA expression cloning. *Cancer Immunol Immunother* 2004; **53**: 139–143.
146 Smith GP. Filamentous fusion phage: novel expression vectors that display cloned antigens on the virion surface. *Science* 1985; **228**: 1315–1317.
147 Peletskaya EN, Glinsky VV, Glinsky GV, Deutscher SL, Quinn TP. Characterization of peptides that bind the tumor-associated Thomsen–Friedenreich antigen selected from bacteriophage display libraries. *J Mol Biol* 1997; **270**: 374–384.
148 Peletskaya EN, Glinsky G, Deutscher SL, Quinn TP. Identification of peptide sequences that bind the Thomsen–Friedenreich cancer-associated glycoantigen from bacteriophage peptide display libraries. *Mol Divers* 1996; **2**: 13–18.
149 Koivunen E, Gay DA, Ruoslahti E. Selection of peptides binding to the alpha 5 beta 1 integrin from phage display library. *J Biol Chem* 1993; **268**: 20205–20210.
150 Schiffelers RM, Koning GA, ten Hagen TL, Fens MH, Schraa AJ, Janssen AP *et al*. Anti-tumor efficacy of tumor vasculature-targeted liposomal doxorubicin. *J Control Release* 2003; **91**: 115–122.
151 Shi W, Bartlett JS. RGD inclusion in VP3 provides adeno-associated virus type 2 (AAV2)-based vectors with a heparan sulfate-independent cell entry mechanism. *Mol Ther* 2003; **7**: 515–525.
152 Pereboev A, Pereboeva L, Curiel DT. Phage display of adenovirus type 5 fiber knob as a tool for specific ligand selection and validation. *J Virol* 2001; **75**: 7107–7113.
153 Zhu ZB, Makhija SK, Lu B, Wang M, Rivera AA, Preuss M *et al*. Transport across a polarized monolayer of Caco-2 cells by transferrin receptor-mediated adenovirus transcytosis. *Virology* 2004; **325**: 116–128.
154 Moroo I, Ujiie M, Walker BL, Tiong JW, Vitalis TZ, Karkan D *et al*. Identification of a novel route of iron transcytosis across the mammalian blood–brain barrier. *Microcirculation* 2003; **10**: 457–462.
155 Mostov KE. Transepithelial transport of immunoglobulins. *Annu Rev Immunol* 1994; **12**: 63–84.
156 McIntosh DP, Tan XY, Oh P, Schnitzer JE. Targeting endothelium and its dynamic caveolae for tissue-specific transcytosis *in vivo*: a pathway to overcome cell barriers to drug and gene delivery. *Proc Natl Acad Sci USA* 2002; **99**: 1996–2001.
157 van Dillen IJ, Mulder NH, Vaalburg W, de Vries EF, Hospers GA. Influence of the bystander effect on HSV-tk/GCV gene therapy. A review. *Curr Gene Ther* 2002; **2**: 307–322.
158 Jordan A, Scholz R, Wust P, Fahling H, Krause J, Wlodarczyk W *et al*. Effects of magnetic fluid hyperthermia (MFH) on C3H mammary carcinoma *in vivo*. *Int J Hyperthermia* 1997; **13**: 587–605.
159 Brigger I, Dubernet C, Couvreur P. Nanoparticles in cancer therapy and diagnosis. *Adv Drug Deliv Rev* 2002; **54**: 631–651.
160 Ito A, Kuga Y, Honda H, Kikkawa H, Horiuchi A, Watanabe Y *et al*. Magnetite nanoparticle-loaded anti-HER2 immunoliposomes for combination of antibody therapy with hyperthermia. *Cancer Lett* 2004; **212**: 167–175.
161 Hergt R, Andra W, d'Ambly CG, Hilger I, Kaiser WA, Richter U *et al*. Physical limits of hyperthermia using magnetite fine particles. *IEEE Trans Mag* 1998; **34**: 3745–3754.
162 Hilger I, Hergt R, Kaiser WA. Towards breast cancer treatment by magnetic heating. *J Magn Magn Mater* 2005; **293**: 314–319.
163 Neuberger T, Schöpf B, Hofmann HMH, von Rechenberg B. Superparamagnetic nanoparticles for biomedical applications: possibilities and limitations of a new drug delivery system. *J Magn Magn E* 2005; **293**: 483–496.
164 Xu H, Song T, Bao X, Hu L. Site research of magnetic nanoparticles in magnetic drug targeting. *J Magn Magn E* 2005; **293**: 514–519.
165 Alexiou C, Jurgons R, Schmid R, Hilpert A, Bergemann C, Parak F *et al*. *In vitro* and *in vivo* investigations of targeted chemotherapy with magnetic nanoparticles. *J Magn Magn Mater* 2005; **293**: 389–393.
166 Pankhurst QA, Connolly J, Jones SK, Dobson J. Applications of magnetic nanoparticles in biomedicine. *J Phys D Appl Phys* 2003; **36**: R167–R181.
167 Choi H, Choi SR, Zhou R, Kung HF, Chen IW. Iron oxide nanoparticles as magnetic resonance contrast agent for tumor imaging via folate receptor-targeted delivery. *Acad Radiol* 2004; **11**: 996–1004.
168 Yang Y, Nunes FA, Berencsi K, Furth EE, Gonczol E, Wilson JM. Cellular immunity to viral antigens limits E1-deleted adenoviruses for gene therapy. *Proc Natl Acad Sci USA* 1994; **91**: 4407–4411.
169 Yang Y, Li Q, Ertl HC, Wilson JM. Cellular and humoral immune responses to viral antigens create barriers to lung-directed gene therapy with recombinant adenoviruses. *J Virol* 1995; **69**: 2004–2015.
170 Morral N, Parks RJ, Zhou H, Langston C, Schiedner G, Quinones J *et al*. High doses of a helper-dependent adenoviral vector yield supraphysiological levels of alpha1-antitrypsin with negligible toxicity. *Hum Gene Ther* 1998; **9**: 2709–2716.

171 Morsy MA, Gu M, Motzel S, Zhao J, Lin J, Su Q *et al*. An adenoviral vector deleted for all viral coding sequences results in enhanced safety and extended expression of a leptin transgene. *Proc Natl Acad Sci USA* 1998; **95**: 7866–7871.
172 Thomas CE, Schiedner G, Kochanek S, Castro MG, Lowenstein PR. Peripheral infection with adenovirus causes unexpected long-term brain inflammation in animals injected intracranially with first-generation, but not with high-capacity, adenovirus vectors: toward realistic long-term neurological gene therapy for chronic diseases. *Proc Natl Acad Sci USA* 2000; **97**: 7482–7487.
173 Schiedner G, Morral N, Parks RJ, Wu Y, Koopmans SC, Langston C *et al*. Genomic DNA transfer with a high-capacity adenovirus vector results in improved *in vivo* gene expression and decreased toxicity. *Nat Genet* 1998; **18**: 180–183.
174 Parks RJ, Graham FL. A helper-dependent system for adenovirus vector production helps define a lower limit for efficient DNA packaging. *J Virol* 1997; **71**: 3293–3298.
175 Hardy S, Kitamura M, Harris-Stansil T, Dai Y, Phipps ML. Construction of adenovirus vectors through Cre-lox recombination. *J Virol* 1997; **71**: 1842–1849.
176 Umana P, Gerdes CA, Stone D, Davis JR, Ward D, Castro MG *et al*. Efficient FLPe recombinase enables scalable production of helper-dependent adenoviral vectors with negligible helper-virus contamination. *Nat Biotechnol* 2001; **19**: 582–585.
177 Biermann V, Volpers C, Hussmann S, Stock A, Kewes H, Schiedner G *et al*. Targeting of high-capacity adenoviral vectors. *Hum Gene Ther* 2001; **12**: 1757–1769.
178 Stilwell JL, McCarty DM, Negishi A, Superfine R, Samulski RJ. Development and characterization of novel empty adenovirus capsids and their impact on cellular gene expression. *J Virol* 2003; **77**: 12881–12885.
179 Stilwell JL, Samulski RJ. Role of viral vectors and virion shells in cellular gene expression. *Mol Ther* 2004; **9**: 337–346.

Available online at www.sciencedirect.com
SCIENCE DIRECT®
Pharmacology & Therapeutics 111 (2006) 596 – 628
Pharmacology & Therapeutics
www.elsevier.com/locate/pharmthera

Associate editor: S. Pestka

mda-7/IL-24: Multifunctional cancer-specific apoptosis-inducing cytokine

Pankaj Gupta [a], Zao-zhong Su [a], Irina V. Lebedeva [a], Devanand Sarkar [a], Moira Sauane [a], Luni Emdad [a,b], Michael A. Bachelor [a], Steven Grant [c], David T. Curiel [d], Paul Dent [e], Paul B. Fisher [a,b,f,*]

[a] *Department of Pathology, Herbert Irving Comprehensive Cancer Center, Columbia University Medical Center, College of Physicians and Surgeons, 630 West 168th Street, New York, NY 10032, United States*
[b] *Department of Neurosurgery, Herbert Irving Comprehensive Cancer Center, Columbia University Medical Center, College of Physicians and Surgeons, 630 West 168th Street, New York, NY 10032, United States*
[c] *Department of Hematology and Onocology, Virginia Commonwealth University, Richmond, 401 College Street, Richmond, VA 23298, United States*
[d] *Division of Human Gene Therapy, Gene Therapy Center, University of Alabama in Birmingham, 901 19th Street South, Birmingham, AL 35294, United States*
[e] *Department of Biochemistry, Virginia Commonwealth University, Richmond, 401 College Street, Richmond, VA 23298, United States*
[f] *Department of Urology, Herbert Irving Comprehensive Cancer Center, Columbia University Medical Center, College of Physicians and Surgeons, 630 West 168th Street, New York, NY 10032, United States*

Abstract

"Differentiation therapy" provides a unique and potentially effective, less toxic treatment paradigm for cancer. Moreover, combining "differentiation therapy" with molecular approaches presents an unparalleled opportunity to identify and clone genes mediating cancer growth control, differentiation, senescence, and programmed cell death (apoptosis). Subtraction hybridization applied to human melanoma cells induced to terminally differentiate by treatment with fibroblast interferon (IFN-β) plus mezerein (MEZ) permitted cloning of melanoma differentiation associated (*mda*) genes. Founded on its novel properties, one particular *mda* gene, *mda-7*, now classified as a member of the interleukin (IL)-10 gene family (IL-24) because of conserved structure, chromosomal location, and cytokine-like properties has become the focus of attention of multiple laboratories. When administered by transfection or adenovirus-transduction into a spectrum of tumor cell types, melanoma differentiation associated gene-7/interleukin-24 (*mda-7*/IL-24) induces apoptosis, whereas no toxicity is apparent in normal cells. *mda-7*/IL-24 displays potent "bystander antitumor" activity and also has the capacity to enhance radiation lethality, to induce immune-regulatory activities, and to inhibit tumor angiogenesis. Based on these remarkable attributes and effective antitumor therapy in animal models, this cytokine has taken the important step of entering the clinic. In a Phase I clinical trial, intratumoral injections of adenovirus-administered *mda-7*/IL-24 (Ad.*mda-7*) was safe, elicited tumor-regulatory and immune-activating processes, and provided clinically significant activity. This review highlights our current understanding of the diverse activities and properties of this novel cytokine, with potential to become a prominent gene therapy for cancer.

Keywords: *mda-7*/IL-24; Differentiation therapy of cancer; Programmed cell death; Antitumor bystander activity; Radiosensitization; Angiogenesis; Cell signaling; Phase I clinical trial

Abbreviations: AKT, protein kinase B; APC, adenomatous polyposis coli gene; Bcl-2, B-cell CLL/lymphoma 2; bFGF, basic fibroblast growth factor; BiP, immunoglobulin binding protein; *DISH*, differentiation induction subtraction hybridization; ER, endoplasmic reticulum; Fak, focal adhesion kinase; GADD genes, growth arrest and DNA damage inducible genes; GSK-3β, glycogen synthase kinase 3 beta; IFN-β, fibroblast interferon; IL, interleukin; ILK-1, integrin-linked protein kinase 1; JNK, c-jun N-terminal MAP kinase; LPS, lipopolysaccharide; MAPK, mitogen-activated protein kinase; *mda*, melanoma differentiation associated genes; *mda-7*/IL-24, melanoma differentiation associated gene-7/interleukin-24; MEZ, mezerein; MPT, mitochondrial potential transition; NAC, *N*-acetyl-L-cysteine; NSCLC, non-small cell lung carcinoma; PBMC, peripheral blood leukocytes; PDGF, platelet-derived growth factor; PI3K, phosphoinositide 3-kinase; PLC-γ, phospholipase C gamma; PP2A, protein phosphatase 2A; PTEN, phosphatase and tensin homolog; PTP, permeability transition pore; RGP, radial growth

* Corresponding author. Department of Pathology, College of Physicians and Surgeons, Columbia University Medical Center, 630 West 168th Street, New York, NY 10032, USA. Tel.: 212 305 3642.
E-mail address: pbf1@columbia.edu (P.B. Fisher).

0163-7258/$ - see front matter © 2006 Elsevier Inc. All rights reserved.
doi:10.1016/j.pharmthera.2005.11.005

phase primary melanoma; ROS, reactive oxygen species; TCF/LEF, T-cell-specific transcription factor/lymphoid enhancer binding factor; Th1, Th2, helper T-lymphocytes, type 1 and type 2, respectively; TNF-α, tumor necrosis factor alpha; VEGF, vascular endothelial growth factor; VGP, vertical growth phase primary melanoma; XBP-1, X-box binding protein 1.

Contents

1. Introduction

Of the multitude of diseases afflicting mankind, cancer poses a major threat delimiting longevity and the quality of human life. Despite significant improvements in diagnosis and innovations in the therapy of specific cancers, effectively treating neoplastic diseases still present major challenges. The etiological factors mediating cancer development and progression are complex, involving genetic and epigenetic changes, and these processes are intimately associated with environmental factors, including diet, exposure to toxic, and carcinogenic chemicals and radiation (Fisher, 1984; Bishop, 1991; Knudson, 1993; Hartwell & Kastan, 1994; Leszczyniecka et al., 2001; Vogelstein & Kinzler, 2004). It is now accepted as

axiomatic that the vast majority of cancers do not result from a single genetic change but rather reflect the compilation of multiple genomic modifications, such as alterations in the expression of dominantly acting oncogenes, recessive tumor suppressor genes, and unique genetic elements directly affecting progression of the cancer phenotype (Fisher, 1984; Bishop, 1991; Knudson, 1993; Kang et al., 1998; Vogelstein & Kinzler, 2004; Emdad et al., 2005; Michor et al., 2005; Su et al., 2005a). In these contexts, it is the totality of the multitude of changes that ultimately result in a loss of proliferative control and changes in properties of the evolving tumor cells (Fisher, 1984; Bishop, 1991; Hartwell & Kastan, 1994; Jiang et al., 1994a, 1994b; Vogelstein & Kinzler, 2004; Emdad et al., 2005; Michor et al., 2005; Su et al., 2005a).

The most common modalities used to treat cancer are surgery, chemotherapy, and radiotherapy (Gregoire et al., 1999; Raman & Small, 1999; Akduman et al., 2005; Bucci et al., 2005; DeAngelis, 2005). Limitations of chemotherapy include development of drug resistance, non-specific toxicity, and additional side effects preventing optimization of this approach (Harris, 1985a, 1985b; Harris & Hochhauser, 1992; Sawicka et al., 2004; Liscovitch & Lavie, 2005). Radiotherapy is also associated with negative side effects, and when used at doses frequently necessary to achieve a clinically beneficial effect, it may itself promote cancer development (Gregoire et al., 1999; Ross, 1999; Gregoire et al., 2002). The limitations of current cancer therapies underscore the need to develop less toxic and potentially more specific and effective forms of treatment (Kobayashi et al., 2005; Lin et al., 2005; Tripathy, 2005; Vassal, 2005).

Hallmarks of the cancer cell include aberrant growth and abnormal differentiation (Sachs, 1987, 1989; Borden et al., 1993; Jiang et al., 1994a; Leszczyniecka et al., 2001; Zelent et al., 2005). In many contexts, these defects are reversible and tumor cells actually contain the appropriate genetic information for inducing restrained growth and terminal differentiation. However, appropriate genes are either not expressed or subthreshold levels of proteins are present that are necessary to maintain normal growth and differentiation. A potentially less toxic approach for treating cancer involves reprogramming tumor cells to undergo irreversible growth arrest and terminal differentiation, referred to as "differentiation therapy" (Sachs, 1978, 1987, 1989, 1990; Fisher et al., 1985; Borden et al., 1993; Jiang et al., 1993, 1994a; Leszczyniecka et al., 2001; Miller & Waxman, 2002; Zelent et al., 2005). In this scheme, neoplastic cells exhibiting aberrant patterns of differentiation upon treatment with an appropriate agent(s) lose proliferative capacity and terminally differentiate. The "differentiation therapy" stratagem was evaluated in HO-1 human melanoma cells, where treatment with recombinant human fibroblast interferon (IFN-β) and the protein kinase C activator mezerein (MEZ) resulted in irreversible cessation of growth, changes in cell morphology, modifications in gene expression, alterations in surface antigen expression, and terminal cell differentiation (Fisher et al., 1985; Guarini et al., 1989, 1992; Jiang & Fisher, 1993; Jiang et al., 1993, 1994a).

To characterize genes involved in terminal differentiation of HO-1 human melanoma cells, temporally spaced poly(A) RNAs from untreated and IFN-β+MEZ-treated HO-1 cells (Jiang & Fisher, 1993; Jiang et al., 1993) were collected and cDNA libraries were created (Fig. 1). These 2 cDNA libraries were subtracted resulting in construction of a temporally spaced substracted cDNA library, enriched for genes modified during HO-1 cell terminal differentiation (Jiang & Fisher, 1993). Improved versions of this scheme, such as reciprocal subtraction differential RNA display (RSDD) (Kang et al., 1998; Sarkar et al., in press) and rapid subtraction hybridization (RaSH) (Jiang et al., 2000; Kang et al., 2001, Boukerche et al., 2004, in press; Kang et al., in press), as well as cDNA microarrays (Huang et al., 1999a, 1999b), have revealed a broad spectrum of melanoma differentiation associated (*mda*) genes and differentiation induction subtraction hybridization (*DISH*) genes, which are either up-regulated or temporally down-regulated upon treatment of HO-1 cells with either IFN-β, MEZ, or IFN-β+MEZ. Originally, novel up-regulated genes identified by these techniques included $p21^{CIP1/WAF-1/mda-6}$ (Jiang & Fisher, 1993; Jiang et al., 1994b, 1995a), *mda*-2/the male germ cell-specific transcription repressor Tctex-1 (Jiang & Fisher, 1993), *mda*-5 (Jiang et al., 1994a; Kang et al., 2002, 2004), melanoma differentiation associated gene-7/interleukin-24 (*mda*-7/IL-24; Jiang & Fisher, 1993; Jiang et al., 1995c; Fisher et al., 2003; Sauane et al., 2003a, 2003b; Fisher, 2005; Lebedeva et al., 2005a), and *mda*-9/syntenin (Lin et al., 1996, 1998; Fernandez-Larrea et al., 1999; Koroll et al., 2001; Sarkar et al., 2004; Boukerche et al., 2005). Continuing studies indicate the functional importance and relevance of these genes to many significant physiological processes. *mda*-6, which is p21, is a universal cyclin-dependent kinase inhibitor that is intimately associated with cell cycle regulation and growth control (Jiang et al., 1994b, 1995a, 1995b, 1995c). *mda*-5 is a putative RNA-helicase with double-stranded RNA-dependent ATPase activity and a caspase recruiting domain involved in interferon response and viral infection (Kang et al., 2002; Andrejeva et al., 2004; Kang et al., 2004). *mda*-7/IL-24 is a novel cytokine that has a broad range of antitumor properties (Sarkar et al., 2002a; Fisher et al., 2003; Sauane et al., 2003b; Chada et al., 2004b; Gopalkrishnan et al., 2004; Cunningham et al., 2005; Fisher, 2005; Lebedeva et al., 2005a; Tong et al., 2005). *mda*-9/syntenin associates with syndecans involved in cell adhesion and early endosome formation and has recently been found to contribute to metastasis (Lin et al., 1996, 1998; Fernandez-Larrea et al., 1999; Koroll et al., 2001, 2002; Helmke et al., 2004; Sarkar et al., 2004; Boukerche et al., in press). Apart from these genes, several other growth-regulatory genes that are down-regulated during differentiation, such as c-myc, cyclin A, cyclin B, human ribosomal protein L23a, cdc2, and histone H1 and H4, have been identified that also contribute to the spectrum of molecular changes occurring during terminal differentiation in human melanoma cells (Jiang et al., 1995b, 1997). The present review focuses on *mda*-7/IL-24, its discovery and functional role in tumor suppression, as a cytokine, and the proposed signaling pathways responsible for inducing apoptosis in a cancer-specific manner, including a discussion of potential cell surface and intracellular targets

of activity. Additionally, an overview of its properties as an immune modulating agent, radiation-enhancing molecule, and anti-angiogenic agent is also provided. This review concludes with a discussion of the present status of clinical trials with *mda-7*/IL-24 administered intratumorally by means of a replication incompetent adenovirus (Ad.*mda-7*; INGN 241) (Fisher et al., 2003; Gopalkrishnan et al., 2004; Cunningham et al., 2005; Fisher, 2005; Lebedeva et al., 2005a; Tong et al., 2005).

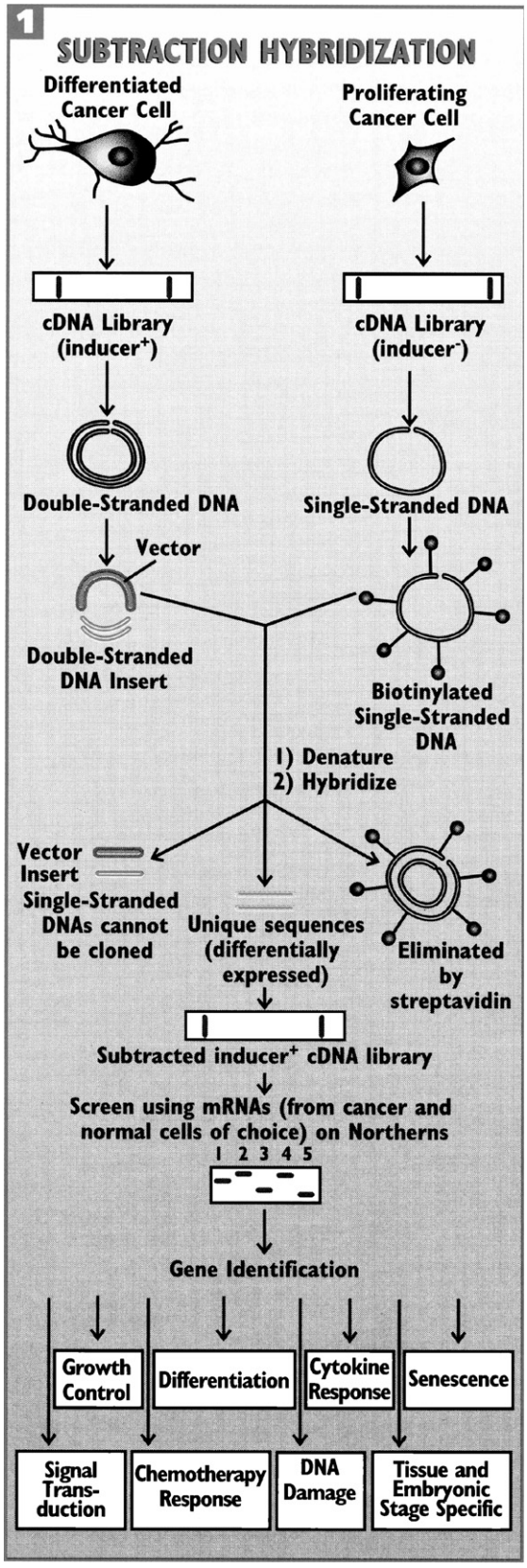

2. Identification and structural analysis of melanoma differentiation associated gene-7/interleukin-24

mda-7/IL-24 was first identified by subtraction hybridization from HO-1 human melanoma cells induced to irreversibly growth arrest and terminally differentiate by combined treatment with IFN-β+MEZ (Fig. 1) (Jiang et al., 1993, 1995c). RNA and immunohistochemical analyses confirmed expression of *mda-7*/IL-24 mRNA and protein in melanocytes with a progressive decline in expression during the process of melanoma progression from radial to vertical growth phase (VGP) primary melanoma to metastatic disease (Jiang et al., 1995c; Ekmekcioglu et al., 2001; Ellerhorst et al., 2002). These observations support a putative role of *mda-7*/IL-24 as a tumor suppressor gene, where loss of expression is a critical step in the process of melanoma progression from a non-invasive primary tumor to an invasive malignancy with metastatic potential (Ellerhorst et al., 2002). *mda-7*/IL-24 is localized on human chromosome 1q32–33, a genomic area spanning 195-kb and containing a family of genes associated with the interleukin (IL)-10 family of cytokines, including IL-10, IL-19, IL-20, and IL-24 (*mda-7*) (Huang et al., 2001; Pestka et al., 2004). The mRNA encoding *mda-7*/IL-24 is ~2-kb encoding a polypeptide of ~23.8-kDa (Jiang et al., 1995c). The open reading frame is flanked by 5′- and 3′-untranslated sequences of 274 and 823 bp, respectively. The 3′-UTR contains 3 consensus AU-rich elements and 3 polyadenylation signals (AAUAAA) playing a crucial role in the post-transcriptional stability of mRNA (Madireddi et al., 2000b; Huang et al., 2001). The *mda-7*/IL-24 gene is composed of 7 exons and 6 introns (Huang et al., 2001). Sequence analysis also reveals the presence of a 49-amino acid signal peptide that allows the molecule to be cleaved and secreted. Sequence analysis of *mda-7*/IL-24 reveals 3 putative glycosylation sites at amino acids 95, 109, and 126 resulting in different forms and molecular sizes of secreted *mda-7*/IL-24 (Fig. 2).

mda-7/IL-24 belongs to the 4-helix bundle family of cytokine molecules most closely related to the IL-10 subfamily

Fig. 1. Schematic of the differentiation induction subtraction hybridization (*DISH*) approach. This procedure has been used to identify and clone genes displaying differential expression as a function of induction of irreversible growth arrest, terminal differentiation, and loss of tumorigenic potential in HO-1 human melanoma cells. Temporally spaced libraries are constructed from actively growing HO-1 cells and from HO-1 cells treated with combination of IFN-β plus MEZ. The actively growing HO-1 cDNA library is then subtracted from the IFN-β plus MEZ-treated HO-1 library resulting in a subtracted cDNA library enriched for differentially expressed genes that associate with a multitude of processes, some of which are indicated in this figure. Further details of the subtraction approach and its application with reverse Northern blotting of cDNAs and high throughput cDNA microarrays can be found in Jiang and Fisher (1993) and Huang et al. (1999a, 1999b) (reproduced, by permission of the publisher, from Fisher et al., 2003).

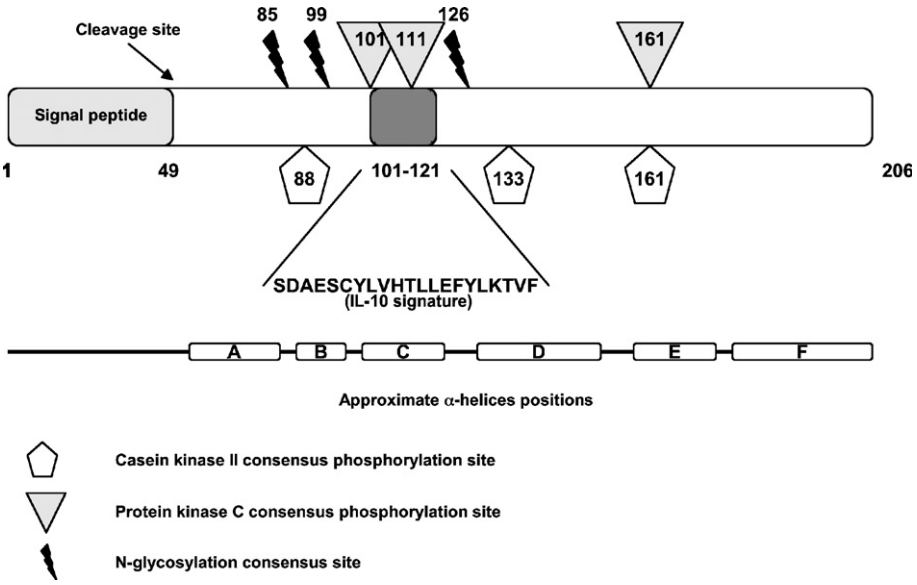

Fig. 2. Schematic representation of the MDA-7/IL-24 polypeptide showing various predicted and established protein motifs (reproduced in modified form, by permission of the publisher, from Sauane et al., 2003b).

(Kotenko, 2002; Pestka et al., 2004). Tertiary structure predictions, based on computer simulations, generate a compact globular structure consisting of 4 helical regions interspersed by loops of unpredicted structure (Kotenko, 2002; Pestka et al., 2004). The predicted organization of *mda-7*/IL-24 reveals greatest homology to the IL-10 subfamily, which includes IL-19, IL-20, IL-22, and IL-26/AK-155 (Chaiken & Williams, 1996; Gallagher et al., 2000; Xie et al., 2000; Huang et al., 2001; Kotenko, 2002; Pestka et al., 2004). Comparison of the amino acid sequence of IL-10 and *mda-7*/IL-24 indicates only 23% homology; however, the presence of an IL-10 signature sequence in *mda-7*/IL-24 supports its being a member of the IL-10 subfamily (Fig. 2) (Kotenko, 2002; Pestka et al., 2003, 2004). Expression analysis of *mda-7*/IL-24 demonstrates restricted expression to tissues associated with the immune system, such as thymus, spleen, and peripheral blood leukocytes (PBMC) (Fig. 3), further suggesting cytokine-like properties of this molecule (Huang et al., 2001). Based on its chromosomal location, structure, and expression profile, *mda-7* has been renamed IL-24 (*mda-7*/IL-24) by the Human Gene Organization (HUGO) (Caudell et al., 2002; Sarkar et al., 2002a, 2000b; Sauane et al., 2003b; Lebedeva et al., 2005a).

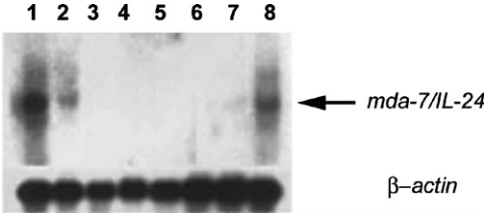

Fig. 3. Expression of *mda-7*/IL-24 message in the human immune system. Human multiple tissue Northern blot consisting of poly(A)+ mRNA from different tissues shows tissue-specific expression of *mda-7*/IL-24. The mRNAs immobilized on the blot are from spleen (1), thymus (2), prostate (3), testis (4), ovary (5), small intestine (6), colon (7), and peripheral blood leukocytes (8) (reproduced, by permission of the publisher, from Huang et al., 2001).

Southern blot analysis of DNA from different species using a cDNA probe identified homologous sequences in genomic DNA of yeast, monkey, cow, dog, and cat, suggesting that *mda-7*/IL-24 is an evolutionary conserved gene (Jiang et al., 1995c). Further studies by several groups have established the presence of *mda-7*/IL-24 orthologues in other species, *c49a*/*mob-5* in rat fibroblasts (Soo et al., 1999; Zhang et al., 2000; Wang et al., 2002; Wang & Liang, 2005) and FISP in Th2 cells in mouse (Schaefer et al., 2001) (Fig. 4). Of interest, the functions of the *mda-7*/IL-24 rat orthologue appear to be different than that of the human and potentially mouse version of this gene.

Using the differential display polymerase chain reaction (DD-PCR), new sets of genes up- or down-regulated during wound repair in rat fibroblasts were identified (Soo et al., 1999). A 260-nucleotide fragment of a gene designated *c49a* showed significant up-regulation 12 hr post-wounding in a rat cutaneous wound model. This fragment led to the cloning of the rat *c49a* cDNA, which is 1107-nucleotides in length and shares 82% homology with *mda-7*/IL-24 (Soo et al., 1999) (Fig. 4). Like *mda-7*/IL-24, the 3′-untranslated region of rat *c49a* also contains copies of the AUUUA sequence motif involved in mRNA destabilization. Alignment of the amino acid sequences of C49A and MDA-7/IL-24 protein reveals ~58.7% homology, suggesting that rat *c49a* and *mda-7*/IL-24 may be related molecules, rather than true homologues (Soo et al., 1999; Sauane et al., 2003b) (Fig. 4). Because *c49a* expression is seen in wounded rat dermal cells, it is believed to play a role in proliferation. An additional *mda-7*/IL-24-like molecule named *mob-5* was isolated by DD-PCR between rat embryo fibroblast cells Rat1 and Rat1:iras cells containing an inducible oncogenic Ha-*ras* gene (Zhang et al., 2000). MOB-5 protein is identical to the C49A protein, except for 2 amino acid mismatches. MOB-5 is a secreted protein and its

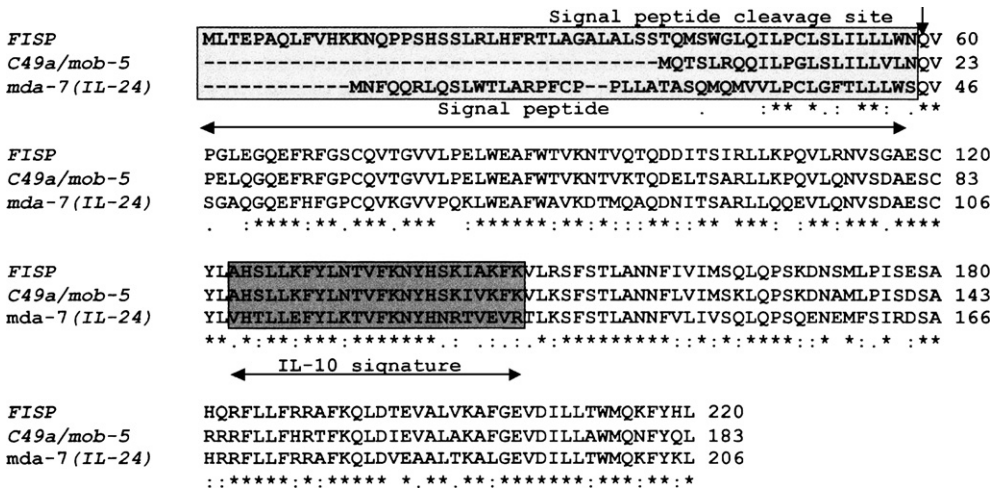

Fig. 4. MDA-7/IL-24-related molecules: alignment of mouse (FISP), rat (C49A/MOB-5), and human protein sequences showing identical (*) conserved (:) and similar (.) amino acid residues (reproduced, by permission of the publisher, from Sauane et al., 2003b).

expression is induced by oncogenic H-*ras* and K-*ras* and a role for this gene has been proposed in proliferation (Zhang et al., 2000; Wang et al., 2002; Wang & Liang, 2005). Thus, both C49A and MOB-5 resemble MDA-7/IL-24 protein but they may play a role in stimulating rather than inhibiting growth (Soo et al., 1999; Wang et al., 2002; Shinohara & Rothstein, 2004; Wang & Liang, 2005). These observations suggest that the function of *mda-7*/IL-24 in humans is distinct from that of its rat orthologue.

A mouse MDA-7/IL-24-like protein called FISP has also been identified using representational difference analysis between type 2 and type 1 helper T-lymphocyte (Th2 and Th1, respectively) cells as an IL-4-induced secreted protein in Th2 helper lymphocytes (Th2) (Schaefer et al., 2001). FISP is selectively expressed in lymphocytes under Th2 differentiation conditions and its expression is induced in CD4+ enriched Th2 cells, whereas no expression is observed in Th1 cells. FISP expression is regulated by the T-cell receptor and IL-4 and involves protein kinase C and STAT6 signaling pathways (Schaefer et al., 2001). FISP is a secreted protein of 220 amino acids with a predicted molecular mass of 25-kDa (Schaefer et al., 2001). It shares 93% homology with rat C49A/MOB-5 and 69% identity with MDA-7/IL-24 at the protein level (Fig. 4). Although MDA-7/IL-24 and FISP share several common properties, expression in the immune system, induced expression in response to differentiation and treatment with cytokine and protein kinase activators, the precise role of FISP in these processes remains to be established (Schaefer et al., 2001). Further work is clearly needed to address this question and to determine the precise function of FISP in Th1 and Th2 differentiation.

Direct support for similar functional attributes between human *mda*-7/IL-24 and mouse *mda*-7/IL-24 (mIL-24; FISP) in the context of antitumor activity has recently been provided in mice using mouse ML-1 hepatoma cells (Chen et al., 2005). Intramuscular electroporation of mIL-24 was shown to suppress mouse ML-1 hepatoma cell growth in vivo in female BALB/cJ mice. This effect was observed when ML-1 cells were administered by subcutaneous dorsal injection or when ML-1 cells were directly injected into the spleen, which resulted in tumor metastasis in the liver. These studies confirm the tumor growth-suppressive properties of mouse *mda*-7/IL-24 (mIL-24; FISP) in syngeneic mice and highlight potentially similar antitumor properties of both human MDA-7/IL-24 and murine mIL-24. These findings are intriguing and provide additional evidence that human MDA-7/IL-24 is more closely related functionally to murine mIL-24 than to the rat orthologue of this gene, *c49a/mob-5*, which appears to have growth stimulatory properties (Soo et al., 1999; Wang et al., 2002). Further experimentation is required to explain how the rat version of *mda*-7/IL-24 acquired its divergent function from that of the human and murine genes.

3. Expression analysis of melanoma differentiation associated gene-7/interleukin-24 and its regulation

Analysis of *mda*-7/IL-24 expression in normal and cancer cells indicated a lack of constitutive expression in most cellular contexts (Huang et al., 2001; Caudell et al., 2002; Garn et al., 2002; Wolk et al., 2002). However, expression was evident, using poly(A)+ RNA and Northern blotting in spleen, thymus, and peripheral blood leukocytes (PBMC), that is, cells of the immune system (Fig. 3) (Huang et al., 2001; Caudell et al., 2002; Wolk et al., 2002). Further experimentation with PBMC following treatment with various activators of the immune response revealed that lipopolysaccharide (LPS) or concanavalin A enhances transcription, translation, and secretion of *mda*-7/IL-24 in vitro (Wang et al., 2002). LPS treatment also induced expression of *mda*-7/IL-24 in monocytes from a healthy patient. Concanavalin A activation of T-cells promoted *mda*-7/IL-24 expression, suggesting a role of *mda*-7/IL-24 as a putative cytokine. Further studies are necessary to clarify a presumed role of *mda*-7/IL-24 as an immune-modulating cytokine (Garn et al., 2002).

Apart from tissues of the immune system, expression of *mda*-7/IL-24 mRNA can be transiently induced in certain cell

types under appropriate conditions that are not of melanocytic or hematopoietic origin (Huang et al., 2001). A 24-hr treatment of DU-145 (prostate carcinoma), HBL-100 (normal breast epithelium), MDA-MB-157 and MDA-MB-231 (breast carcinoma), HeLa (cervical carcinoma), NC (normal cerebellum astrocytes), GBM18 (glioblastoma multiforme), Saos-2 (osteosarcoma), and HONE-1 (nasopharyngeal carcinoma) cells with IFN-β+MEZ transiently induced *mda*-7/IL-24 mRNA expression (Huang et al., 2001). In contrast, constitutive expression or induction was not apparent in other normal/tumor-derived cell lines including HuPEC (normal prostate epithelial), PC-3 and LNCaP (prostate carcinoma), MCF-7, T47D, MDA-MB-453 (breast carcinoma), T98G (glioblastoma multiforme), and SW613 (colon carcinoma) (Huang et al., 2001). These results confirm that *mda*-7/IL-24 is not constitutively expressed in most normal or cancer cell types; however, by appropriate treatment (e.g., IFN-β+MEZ) this gene can be induced on an mRNA level confirming functional integrity of the *mda*-7/IL-24 locus in both normal and cancer cells of non-melanocytic and hematopoietic origins (Huang et al., 2001).

Gene expression programs are dramatically altered during growth suppression and terminal differentiation, including the modified expression of genes regulating cell cycle progression, transcriptional control, cytoskeletal architecture, and novel genetic elements with undefined functions (Huang et al., 1999a, 1999b; Leszczyniecka et al., 2001). Expression analysis of *mda*-7/IL-24 requires complete understanding of the regulatory mechanisms controlling transcription, translation, and other modifications in mRNA, including stability. The promoter region of *mda*-7/IL-24 was cloned and it was found that expression was regulated post-transcriptionally during melanoma differentiation (Madireddi et al., 2000b). In HO-1 and MeWo human melanoma cells, uninduced basal full-length promoter activity did not change upon treatment with IFN-β+MEZ (Madireddi et al., 2000b). This suggested that modulation of *mda*-7/IL-24 gene expression during differentiation in human melanoma cells might not be controlled on a transcriptional level. Terminal differentiation in human melanoma cells resulting from treatment with IFN-β+MEZ resulted in an elevation in the levels of *mda*-7/IL-24 mRNA and protein, but no or limited mRNA was detected in cells treated with IFN-β or MEZ alone. This led to the hypothesis that IFN-β +MEZ might function to stabilize *mda*-7/IL-24 mRNA and this stabilization may occur by post-transcriptional modifications (Madireddi et al., 2000b).

The cDNA of *mda*-7/IL-24 contains 3 AU-rich sequences in its 3′UTR (Madireddi et al., 2000b; Huang et al., 2001). Many transiently expressed genes, including lymphokines and other cytokine genes and proto-oncogene, such as c-*myc* and c-*fos*, contain AU-rich sequences in their 3′UTR. Another class 2 cytokine, IL-10, was found to be regulated in melanocytes and melanoma cells by AU-rich sequences in their 3′UTR (Brewer et al., 2003). The presence of AU-rich sequences in eukaryotic mRNA correlates with rapid mRNA turnover and post-translational control (Aharon & Schneider, 1993; Rajagopalan & Malter, 1997; McCormick & Ganem, 2005). To investigate the importance of the 3′UTR of *mda*-7/IL-24 in regulating mRNA stability, a luciferase gene construct was generated containing the 3′UTR of *mda*-7/IL-24 (Madireddi et al., 2000b). Expression of this construct was enhanced when transfected into terminally differentiated HO-1 cells (IFN-β +MEZ treated). This finding supports the conclusion that the steady-state level of *mda*-7/IL-24 mRNA is determined by post-translational degradation of this message, which decays in HO-1 cells that are uninduced or treated singly with IFN-β or MEZ, whereas in IFN-β+MEZ-treated HO-1 cells, *mda*-7/IL-24 mRNA does not undergo degradation at a comparable rate (Madireddi et al., 2000b).

Transcription regulation of *mda*-7/IL-24 occurs by binding 2 primary transcription factors at various sites in its promoter (Madireddi et al., 2000a). These transcription factors, identified by gel shift and super shift analyses, are AP-1 and C/EBP (Madireddi et al., 2000a). Increased binding of AP-1 and C/EBP was observed following IFN-β+MEZ treatment, whereas a dominant-negative form of c-*jun* (TAM67) (a member of the AP-1 family) abrogated *mda*-7/IL-24 basal activity. Overexpression of c-*jun* or C/EBP increased the activity of the *mda*-7/IL-24 promoter, suggesting that both of these factors play a central role in *mda*-7/IL-24 gene expression via transcriptional activation (Madireddi et al., 2000a).

4. Melanoma differentiation associated gene-7/interleukin-24, a novel cytokine belonging to the interleukin-10 gene family

Due to the existence of a large number of cytokines and their utilization of overlapping signal transduction pathways, addressing issues of functional specificity at a physiological level as well as key differences in signaling mechanisms presents a complex and difficult problem. The recent recognition of the expanded IL-10 subfamily of cytokines and the finding that individual members have the capacity to bind common receptor subunits has made the process even more daunting to decipher within this particular subset of genes (Burdin et al., 1993; Josephson et al., 2000, 2001; Dumoutier & Renauld, 2002; Langer et al., 2004; Pestka et al., 2004). As noted in previous sections, based on sequence homologies, structural analysis, and chromosomal location, the gene originally named *mda*-7 (Jiang et al., 1995c) has been redesignated IL-24 and recognized as a member of the increasing IL-10 subfamily (Caudell et al., 2002; Kotenko, 2002; Pestka et al., 2003, 2004; Sauane et al., 2003b). Further experimental evidence for this reclassification was provided by demonstrating secretion from PBMC and melanocytes (Caudell et al., 2002; Lebedeva et al., 2002), binding to cognate receptors (IL-20R1/IL-20R2 or IL-22R1/IL-20R2 heterodimers) (Dumoutier et al., 2001; Wang et al., 2002) and activation of the JAK/STAT (STAT 1 and 3) signaling pathway (Kotenko et al., 1997; Dumoutier et al., 2001; Wang et al., 2002). An examination of the various tissues and cell types expressing this cytokine has demonstrated restricted expression. Huang et al. (2001) reported expression in melanocyte, PBMC, and spleen-derived mRNAs from normal human tissues (Fig. 3). This study supported the initial report by

Jiang et al. (1995c) relating to the isolation of the gene from a growth arrested and in vitro differentiated human melanoma cell line as well as its loss of expression in human melanoma progression models (Jiang et al., 1995c; Ellerhorst et al., 2002).

The cytokine-related functions of *mda*-7/IL-24 through its secretion by melanocytes and loss of expression in a melanoma context are not fully understood. While no formal experimental demonstration has been made, it is possible that *mda*-7/IL-24 acts as a paracrine factor and contributes to short-range signaling and performs immune-related functions in skin. The related cytokines, IL-19 and IL-20, are expressed in skin and particularly in keratinocytes, either in normal or disease states, such as psoriatic lesions, and likely play a role in skin inflammation by inducing keratinocyte proliferation (Blumberg et al., 2001). The other members of this subfamily are not expressed in this tissue type. Presently, the responses mediated by *mda*-7/IL-24 appear to be primarily pro-inflammatory, when secreted by primary blood mononuclear cells (PBMC), as will be described later in this review. The melanocyte-derived protein is likely to function similarly (pro-inflammatory activity), barring the possibility that localized target cells in the skin microenvironment behave and respond differently to this cytokine. The putative role of *mda*-7/IL-24 as a tumor suppressor-like molecule, particularly in a human melanoma context, rests upon loss of expression associated with disease progression (Jiang et al., 1995c; Ellerhorst et al., 2002). The finding that iNOS and *mda*-7/IL-24 expressions are inversely correlated and that increased expression of iNOS is involved in melanoma progression provides a mechanistic link to tumor-suppressive properties, although at the present time the basis of this activity requires further investigation (Ekmekcioglu et al., 2003). In general, the intriguing suppressive property of *mda*-7/IL-24 expression in melanoma has not been definitively connected experimentally with its role as a secreted cytokine. Whether the recently discovered intracellularly localized activity of the molecule (Sauane et al., 2004a, 2004b; Sieger et al., 2004) plays some (or even a major) role in preventing melanocytes from undergoing malignant transformation compared to activity of the secreted cytokine form also remains to be determined.

As discussed previously, expression analysis of *mda*-7/IL-24 by Northern blotting using primary human tissues indicated restricted tissue-specific expression of *mda*-7/IL-24 in thymus, spleen, and PBMC (Fig. 3) (Huang et al., 2001; Caudell et al., 2002). A role for *mda*-7/IL-24 as a cytokine and its involvement in the immune system has been highlighted by independent studies from 3 different groups. By real-time PCR, Wolk et al. (2002) analyzed the expression of *mda*-7/IL-24 at an RNA level. Basal expression was confirmed in unstimulated monocytes, but not in other cell types such as T, NK, and B cells. Activation of monocytes by LPS treatment for 6 and 18 hr produced an ~10-fold and ~100-fold stimulation of expression of *mda*-7/IL-24 over unstimulated monocytes, which were also grown for the same time points, respectively. Induction of *mda*-7/IL-24 RNA in T-cell populations upon treatment with LPS was ~10-fold, although no increase occurred at 6 and 18 hr, but only at 66 hr. In contrast, no expression was apparent in NK or B cells either before or after stimulation (Wolk et al., 2002). Further analysis of expression in different subsets of T-helper cells (Type 1 or 2) revealed dual functionality, that is, activation in both lineages. In the initial phases of induction toward Th1, IL-22 is induced followed later by IL-26 at 42–66 hr post-stimulation. *mda*-7/IL-24 is initially down-regulated in a Th1 milieu (at 6 hr) and up-regulated in Th2 cells (Wolk et al., 2002); however, at later times (66 hr) up-regulation of *mda*-7/IL-24 is observed in a Th1 milieu. Expression of FISP, the mouse homologue of *mda*-7/IL-24, displayed highly specific Th2 expression, suggesting that the mouse and human genes might have distinct expression patterns (Schaefer et al., 2001).

Garn et al. (2002) confirmed expression of *mda*-7/IL-24 in response to stimulation by various members of the IL-10 family of cytokines in mouse and human macrophages. *mda*-7/IL-24 RNA and protein were present upon treatment of rat alveolar macrophages with LPS or IL-4, but not tumor necrosis factor alpha (TNF-α). Treating these cells with PMA, an activator of protein kinase C, promoted weak expression of *mda*-7/IL-24 over basal levels. The NR8383 mouse macrophage cell line produces steady-state levels of *mda*-7/IL-24, and following treatment with IL-4, gene transcription and mRNA levels were increased (Garn et al., 2002) but protein levels remained constant. These researchers further demonstrated that intracellular pools of MDA-7/IL-24 protein exist and the level of this pool did not change significantly post-induction. In human macrophages, the levels of *mda*-7/IL-24 mRNA increased significantly, peaking at 8 hr followed by a decline (Garn et al., 2002). The authors also found that addition of IL-10 inhibited *mda*-7/IL-24 gene transcription. Induction of *mda*-7/IL-24 mRNA correlated with expression of IL-1, IL-6, and TNF-α in cultured human monocytes infected with influenza virus indicating a proinflammatory role for this molecule (Garn et al., 2002).

Caudell et al. (2002) have investigated the effect of purified MDA-7/IL-24 protein on PBMC. Treatment of monocytes with pure MDA-7/IL-24 protein led to secretion of IL-6, TNF-α, and IFN-γ at robust levels while trace amounts of GM-CSF, IL-2, IL-4, and lL-10 were also observed. Production of IFN-γ and TNF-α was completely blocked by simultaneous treatment with IL-10, but IL-6 expression was reduced by approximately one third (Caudell et al., 2002). These observations highlight the different roles of *mda*-7/IL-24 and IL-10 on immune function, although both molecules belong to the same family of cytokines (Moore et al., 2001; Pestka et al., 2004). While IL-10 has anti-inflammatory and immune response suppressive roles, *mda*-7/IL-24 plays an immunomodulatory and pro-inflammatory role. It is hypothesized that cytokines induced by *mda*-7/IL-24 might activate antigen-presenting cells to present tumor antigens, thus triggering an antitumor immune response (Caudell et al., 2002). This possibility is supported by a recent Phase I clinical trial in patients with metastatic melanoma, in which injection of a tumor lesion resulted in a pronounced inflammatory response in the injected tumor and in distant metastases (Cunningham et al., 2005; Lebedeva et al., 2005a; Tong et al., 2005). However, despite these observations, the

immunomodulatory role of *mda*-7/IL-24 is not well established and further studies are required to clarify the role of *mda*-7/IL-24 in regulating immune responses.

5. Receptors for melanoma differentiation associated gene-7/interleukin-24

Ligand receptor crosstalk plays a crucial role in transmitting signals from ligands and other environmental cues to the cell nucleus. Cytokines are known to transmit signals from the site of release to the effector cells through specific receptors present at the cell surface. *mda*-7/IL-24 being a member of the IL-10 subfamily raises the obvious possibility of it having similar kinds of receptors as other members of the IL-10 subfamily of cytokines (Fickenscher et al., 2002; Pestka et al., 2004). Receptors of IL-10 belong to the class 2 cytokine receptor family, which comprises the various IFN receptor chains (Liu et al., 1994; Pestka et al., 2004). The IL-10 receptor was initially identified as a single R1 type of receptor with a long cytoplasmic domain, IL-10R1, which is the major signaling component (Liu et al., 1994; Pestka et al., 2004). Later it was found that the functional IL-10 receptor required a second chain of an R2 type of receptor, with a short membrane spanning cytoplasmic domain, IL-10R2 (Kotenko et al., 1997; Kotenko, 2002; Pestka et al., 2004). Subsequently, 3 R1 and 2 R2 types of receptor subunits of the IL-10 family were identified. The 3 R1 subunits are IL-10R1, IL-20R1, and IL-22R1 and the 2 R2 subunits are IL-10R2 and IL-20R2 (Josephson et al., 2000, 2001; Pestka et al., 2004). IL-20 receptors contain the long subunit IL-20R1 and IL-20R2, which join together on the surface of keratinocytes to form the functional IL-20 receptor (Josephson et al., 2000, 2001; Pestka et al., 2004). Recently, it was shown that IL-20 binds to 2 kinds of receptors, where the long chain can also be replaced by IL-22R1 (Blumberg et al., 2001; Pestka et al., 2004). In the case of the receptor for IL-22, the long chain IL-22R1 is complemented by IL-10R2 to form the functional receptor and thus play a role as a common chain in different cytokine receptors, in a manner similar to the common γ chain in the receptors for IL-2, IL-4 and others (Kotenko et al., 1997; Dumoutier & Renauld, 2002; Kotenko, 2002; Pestka et al., 2004). Receptors for IL-19 and *mda*-7/IL-24 resemble the receptors for IL-20 as the functional receptor for IL-19 contains IL-20R1 and IL-20R2, whereas the receptors for *mda*-7/IL-24 like the receptors of IL-20 signal through heterodimeric receptors IL-20R1/IL-20R2 and IL-22R1/IL-20R2 (Dumoutier et al., 2001; Wang et al., 2002; Pestka et al., 2004). Although many cytokines share receptors, receptor activation is ligand specific, and when activated by their ligands the receptors activate the JAK/STAT signaling pathway (Dumoutier et al., 2001; Pestka et al., 2004). Although alternative signaling pathways have not been investigated, Stat3 seems to be a major transcription factor mediating stimulatory effects. The tissue-specific structure and organization of the specific combination of receptor subunits are likely to play a crucial role in determining the function of different members of the IL-10 family (Kotenko, 2002; Langer et al., 2004; Pestka et al., 2004).

6. Melanoma differentiation associated gene-7/interleukin-24 and melanoma

Melanoma represents an aggressive cancer that most frequently metastasizes to regional lymph nodes and to distant sites as the disease progresses (Herlyn et al., 2000; Bevona & Sober, 2002; Bogenrieder & Herlyn, 2002). This propensity for metastasis combined with resistance of melanoma metastases to therapy represents limitations to current therapeutic regimens (Eigentler et al., 2003; Lens & Elsen, 2003; Chung et al., 2004). In the United States, the incidence of melanoma is increasing at a faster rate than any other cancer and it is believed that as many as 1 in 75 currently born children may eventually develop superficial spreading type melanoma (McGary et al., 2002; Bevona et al., 2003; Carlson et al., 2003; Eigentler et al., 2003). Presently, surgery is an option for treating metastases, as chemotherapy and radiotherapy do not achieve cures in the majority of patients and less than 5% of melanoma patients with systemic metastases survive 5 years or more (Baron et al., 2003; Lens & Elsen, 2003; Meric et al., 2003; Nguyen, 2004). However, a high level of IFN-α has shown significant increase in lifetime but is not curative (Kirkwood et al., 2004). Many other forms of therapy have been evaluated with unimpressive results and there is a need to define new molecules and methods for treating metastatic melanoma (Lens & Elsen, 2003; Nguyen, 2004). Gene therapy involving tumor suppressor gene replacement or supplementation represents a new approach for combating this disease (Volk et al., 2003; Liu et al., 2004; Wolkersdorfer et al., 2004). In these contexts, it is important to understand the potential regulatory molecules that are involved in melanoma development, progression, and invasion (Bogenrieder & Herlyn, 2002; Boukerche et al., 2004). Our research groups and others have established that *mda*-7/IL-24 mRNA and protein are expressed in melanocytes and they are the only skin cells expressing MDA-7/IL-24 protein constitutively (Jiang et al., 1995c; Ekmekcioglu et al., 2001; Huang et al., 2001; Ellerhorst et al., 2002).

Development of malignant melanoma in humans, with the exception of nodular-type melanoma, consists of a series of sequential alterations in the evolving tumor cells (Jiang et al., 1994a; Herlyn et al., 2000; Leszczyniecka et al., 2001; Baruch et al., 2005). These include conversion of a normal melanocyte to a nevus, followed by development of a dysplastic nevus, a radial growth phase (RGP) primary melanoma, a vertical growth phase (VGP) primary melanoma, and ultimately a metastatic melanoma. To evaluate the relationship between *mda*-7/IL-24 expression and melanoma progression, *mda*-7/IL-24 and GAPDH levels were determined by RT-PCR in actively growing melanocytes, RGP and VGP primary melanomas and metastatic melanoma cell lines, and in tissue samples (Jiang et al., 1995c). Normal melanocytes/nevi expressed more *mda*-7/IL-24 than the majority of RGP primary melanomas (Fig. 5). Lower expression of *mda*-7/IL-24 was evident in VGP primary and metastatic melanomas, with lowest levels expressed on average in metastatic melanomas (Fig. 5). The expression of *mda*-7/IL-24 during melanoma progression was analyzed using

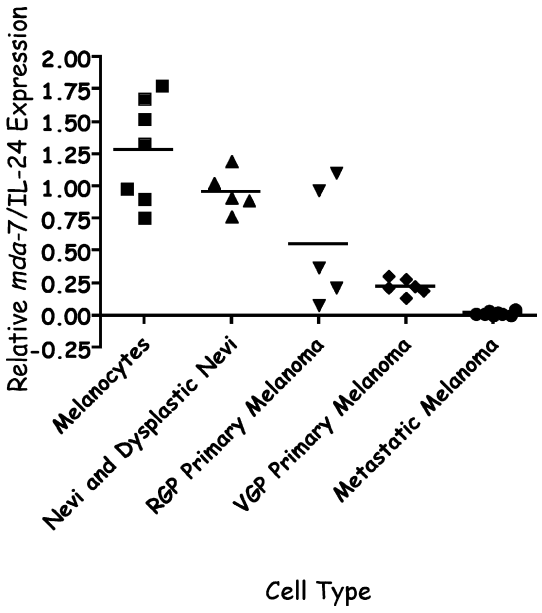

Fig. 5. Reduction in *mda*-7/IL-24 mRNA expression as a consequence of human melanoma progression. Quantitative RT-PCR-based analysis of *mda*-7/IL-24 mRNA expression versus GAPDH expression in independent normal melanocytes, primary melanoma, radial or early vertical growth phase (RGP and VGP, respectively), and metastatic melanoma cell cultures and patient-derived samples. Results are expressed as the ratio of *mda*-7/IL-24 mRNA to GAPDH mRNA. These data indicate progressive reduction or complete loss of *mda*-7/IL-24 expression in association with melanoma progression.

a melanoma Matrigel™ assisted tumorigenic growth model (Jiang et al., 1995c). This approach involved the coinjection of non-tumorigenic or weakly tumorigenic RGP or early VGP primary human melanomas with Matrigel™ into nude mice (Kobayashi et al., 1994). This process results in tumor progression that correlates with acquisition of tumorigenic potential in nude mice by previously non-tumorigenic RGP and VGP primary human melanoma cells (Kobayashi et al., 1994). No change was noticed in *mda*-7/IL-24 expression in a Matrigel™-progressed RGP primary melanoma cell line, whereas the amount of *mda*-7/IL-24 mRNA expressed in VGP primary human melanoma cell lines (WM793 and WM1341B) was less after Matrigel selection (Jiang et al., 1995c). These data correspond with the observation that ectopic transfer of *mda*-7/IL-24 by plasmid or by means of a replication-incompetent adenovirus leads to growth arrest and apoptosis in melanoma and other tumors suggesting that *mda*-7/IL-24 may function as a tumor suppressor gene and a decline in the levels of *mda*-7/IL-24 could play a crucial role in the progression of primary melanoma to invasive melanoma (Jiang et al., 1995c; Ekmekcioglu et al., 2001; Lebedeva et al., 2002). Confirmation of this possibility has come from studies by Ellerhorst et al. (2002), who studied the levels of MDA-7/IL-24 protein by immunohistochemistry during melanoma development and progression. Immunohistochemical analysis of MDA-7/IL-24 expression using tissue sections of melanomas indicated abundant expression of MDA-7/IL-24 protein in human nevi and in primary melanoma tumors. Additional data from this study indicated a decline in the levels of MDA-7/IL-24 protein as the melanoma progressed and invaded surrounding tissue (Ellerhorst et al., 2002). These results confirm that down-regulation of MDA-7/IL-24 protein occurs during progression of melanoma from primary non-invasive to advanced invasive stages of melanoma progression.

Based on the observation that expression of *mda*-7/IL-24 decreases as a function of melanoma development and progression (Fig. 5), it was hypothesized that this gene might exhibit growth-suppressive properties when reactivated (Jiang et al., 1995c). To test this possibility, the effect of *mda*-7/IL-24 gene replacement on tumor and normal cell growth was evaluated (Jiang et al., 1996). Transient transfection of *mda*-7/IL-24 into human melanoma cell lines, such as HO-1 and C8161, as well as in transformed rat cells and a spectrum of additional human cancer cells, including carcinomas from the breast, cervix, colon, and prostate, resulted in a reduction in colony formation (Jiang et al., 1996). In contrast, *mda*-7/IL-24 did not significantly alter the growth or colony formation of normal human and rat cells, respectively (Jiang et al., 1995c, 1996). These findings were confirmed and expanded using a replication incompetent adenovirus expressing *mda*-7/IL-24 (Ad.*mda*-7), which resulted in significant inhibition of growth in melanoma and other tumor cells, but not in normal fibroblasts, epithelial cells, astrocytes, or melanocytes (Su et al., 1998, 2001, 2003a, 2005c; Madireddi et al., 2000c; Saeki et al., 2000, 2002; Mhashilkar et al., 2001, 2003; Lebedeva et al., 2002, 2003a, 2003b, 2005a, 2005b; Sarkar et al., 2002a, 2002b; Pataer et al., 2002, 2005; Sauane et al., 2003a, 2003b, 2004a, 2004b; Yacoub et al., 2003a, 2003b, 2003c, 2004; Fisher et al., 2003; Chada et al., 2004b; Gopalkrishnan et al., 2004; Leath et al., 2004; Nishikawa et al., 2004; Dent et al., 2005; Fisher, 2005; Gopalan et al., 2005; Saito et al., 2005; Oida et al., 2005; Lebedeva et al., in press). Further analysis in melanoma cells and melanocytes indicated that growth suppression in melanoma cells was associated with selective induction of apoptosis (programmed cell death), without detrimental effects on normal early passage or immortal melanocytes (Lebedeva et al., 2002). Infection of human melanoma cells, but not normal melanocytes, with Ad.*mda*-7 resulted in a temporal change in cell cycle and induction of Annexin V staining and DNA fragmentation, markers of apoptosis (Lebedeva et al., 2002). In a comparative study, Ad.*mda*-7 was found to be as potent as Ad.*wtp53* or Ad.*p21*, a cyclin-dependent kinase inhibitor that is a downstream target of wild-type p53, in its growth inhibitory effects on melanoma cells (Lebedeva et al., 2002).

Recently, expression of inducible nitric oxide synthase (iNOS) was found to be increased in advanced stages of melanoma (Ekmekcioglu et al., 2000) and expression of *mda*-7/IL-24 negatively regulated iNOS expression in malignant melanoma cell lines (Ekmekcioglu et al., 2003). Infection of melanoma cells with Ad.*mda*-7 or recombinant MDA-7/IL-24 protein resulted in profound suppression of iNOS and this inverse expression of MDA-7/IL-24 and iNOS suggests a possible cause/effect relationship in melanoma (Ekmekcioglu

et al., 2003). Further studies are necessary to determine if one of these molecules might function to control the expression of the other. Understanding how *mda*-7/IL-24 regulates iNOS may provide insight into the apoptotic pathways regulated by this gene in melanoma.

7. Melanoma differentiation associated gene-7/interleukin-24 displays antitumor activity and cancer cell-specific apoptosis

As discussed above, *mda*-7/IL-24 may contribute to the physiology of human melanocytes and melanomas and this gene has potent growth inhibitory properties when over-expressed in human melanoma cells (Jiang et al., 1995c, 1996; Lebedeva et al., 2002). Our groups and others have shown that *mda*-7/IL-24 also has growth-suppressive properties in a wide variety of additional human cancer cell lines, without inducing harmful effects in normal cells (Table 1) (Jiang et al., 1996; Su et al., 1998, 2001, 2003a, 2005c; Madireddi et al., 2000c; Saeki et al., 2000; Mhashilkar et al., 2001, 2003; Lebedeva et al., 2002, 2003a, 2003b, 2005a, 2005b; Pataer et al., 2002; Sarkar et al., 2002a, 2002b; Chen et al., 2003; Fisher et al., 2003; Sauane et al., 2003a, 2003b, 2004a, 2004b; Yacoub et al., 2003a, 2003b, 2003c, 2004; Chada et al., 2004b; Gopalkrishnan et al., 2004; Leath et al., 2004; Nishikawa et al., 2004; Dent et al., 2005; Gopalan et al., 2005; Oida et al., 2005; Saito et al., 2005; Lebedeva et al., in press; Su et al., in press). The broad-spectrum antitumor activity of *mda*-7/IL-24 can be distinguished from other extensively scrutinized tumor suppressor genes and its growth inhibitory properties are independent of the status of p53, p*RB*, p21, and additional tumor suppressor genes in cancer cells (Jiang et al., 1996; Su et al., 1998; Madireddi et al., 2000c; Lebedeva et al., 2002; Su et al., 2003a). For example, Ad.*mda-7* produced similar growth suppression in T47D and MCF7 cells (T47D is a mutant p53 containing human breast carcinoma cell line and MCF7 has wild-type p53 status) as well as in MDA-MB-157 cells (which are null for p53) (Su et al., 1998). Moreover, growth suppression by *mda*-7/IL-24 can be dissociated from that observed with the p53, RB, and p16 suppressor genes and the mechanism is distinct from the mode of action of these tumor suppressor genes (Lebedeva et al., 2002; Fisher et al., 2003; Su et al., 2003a; Lebedeva et al., 2005a). In contrast, *mda*-7/IL-24 does not affect growth in normal cells, including HBL-100 and non-established early passage skin fibroblasts, breast epithelial cells, ovarian epithelial cells, prostate epithelial cells, endothelial cells, melanocytes, and astrocytes, thereby providing support for the hypothesis that *mda*-7/IL-24 has cancer-specific growth suppressing properties (Table 1) (Su et al., 1998, 2001, 2003a, 2005c; Madireddi et al., 2000c; Saeki et al., 2000, 2002; Mhashilkar et al., 2001, 2003; Lebedeva et al., 2002, 2003a, 2003b, 2005a; 2005b; Pataer et al., 2002; Sarkar et al., 2002a, 2002b; Fisher et al., 2003; Sauane et al., 2003a, 2003b, 2004a, 2004b; Yacoub et al., 2003a, 2003b, 2003c, 2004; Chada et al., 2004b; Gopalkrishnan et al., 2004; Leath et al., 2004; Nishikawa et al., 2004; Dent et al., 2005; Fisher, 2005; Gopalan et al., 2005; Oida et al., 2005; Saito et al., 2005; Lebedeva et al., in press; Su et al., in press).

To more efficiently administer *mda*-7/IL-24 and to study the mechanism by which this gene specifically suppresses growth of tumor cells, a replication incompetent adenovirus was constructed (Su et al., 1998). Supra-physiological levels of expression inhibited growth by inducing apoptosis in many cancer cell lines, including melanoma, malignant glioma, osteosarcoma and carcinomas of the breast, cervix, colon, lung, ovary, and prostate, whereas no suppression of growth was observed in various normal early passage and established human cell lines suggesting that this effect on growth was specific to cancer cells (Su et al., 1998, 2001, 2003a, 2005c; Madireddi et al., 2000c; Saeki et al., 2000, 2002; Mhashilkar et al., 2001, 2003; Lebedeva et al., 2002, 2003a, 2003b, 2005a, 2005b; Pataer et al., 2002; Sarkar et al., 2002a, 2002b; Fisher et al., 2003; Sauane et al., 2003a, 2003b, 2004a, 2004b; Yacoub et al., 2003a, 2003b, 2003c, 2004; Chada et al., 2004b; Gopalkrishnan et al., 2004; Leath et al., 2004; Nishikawa et al., 2004; Dent et al., 2005; Fisher, 2005; Oida et al., 2005; Saito et al., 2005; Lebedeva et al., in press; Su et al., in press). In-depth analyses into the mechanism of action of *mda*-7/IL-24 in eliciting cancer-specific killing by our laboratories and by other research groups have revealed the complexity of pathways that can be exploited by this gene in inducing programmed cell death (reviewed in Sarkar et al., 2002a; Fisher et al., 2003; Sauane et al., 2003b; Dent et al., 2005; Fisher, 2005; Lebedeva et al., 2005a). As recently highlighted, Ad.*mda-7* induces apoptosis in a wide spectrum of cancer cells by exploiting diverse signaling abnormalities ultimately culminating in cell death (Fisher et al., 2003; Lebedeva et al., 2005a, in press). Studies are currently focusing on enhancing these cancer-specific killing properties by employing this novel cytokine with additional agents or treatment protocols, including

Table 1
Ad.*mda-7* selectively inhibits growth in a wide spectrum of cancer cells, without affecting normal cells

Growth not affected	Growth inhibited
Mammary epithelial cells (HuMEC)	Breast carcinoma
Prostate epithelial cells (HuPEC)	Prostate carcinoma
Melanocytes (NHuMel)	Melanoma
Bronchial epithelial cells (HNBE)	Lung cancer
Fetal astrocytes (PHFA)	Glioblastoma multiforme
Skin fibroblasts (MJ90)	Osteosarcoma
Skin fibroblasts (HF)	Colon carcinoma
Lung fibroblasts (NHLF)	Nasopharyngeal carcinoma
Endothelial cells (HuVEC)	Pancreatic carcinoma*
Renal epithelial cells	Cervical carcinoma
Mesothelial cells	Ovarian carcinoma

*In pancreatic carcinoma cells containing a mutant K-*ras* gene, the combination of Ad.*mda-7* and inhibition of mutant K-*ras* induces growth inhibition. Ad.*mda-7* alone or in combination with inhibition of mutant K-*ras* fails to induce growth inhibition or apoptosis in BxPC-3 pancreatic carcinoma cells, which contain a wild-type K-*ras* gene.

chemotherapeutic agents, monoclonal antibodies, reactive oxygen species (ROS) inducers, and radiation (Kawabe et al., 2002; Lebedeva et al., 2003c, 2005b; Su et al., 2003a; Yacoub et al., 2003a, 2003b, 2003c, 2004; McKenzie et al., 2004; Nishikawa et al., 2004; Dent et al., 2005; Oida et al., 2005; Su et al., in press).

Initial therapy studies, in the context of MCF-7 human breast cancer and HeLa human cervical cancer cells, indicated that Ad.*mda-7* had antitumor activity in vivo in the context of nude mouse human tumor xenograft models (Su et al., 1998; Madireddi et al., 2000c). Breast cancer studies involved infection of MCF-7 human breast carcinoma cells in vitro with Ad.*mda-7* prior to injection into athymic nude mice, which resulted in an inhibition in tumor growth (Su et al., 1998). In the case of cervical cancer cells, HeLa cells were injected into nude mice and when tumors developed (100–150 mm^2) they received repeated injections with Ad.*mda-7* or Ad.null and tumor growth was monitored (Madireddi et al., 2000c). Using this experimental protocol, tumor growth and cancer progression were inhibited and this effect persisted after discontinuing administration of Ad.*mda-7*. These studies provided definitive evidence that *mda*-7/IL-24 had antitumor activity in vivo in animal models. Additional studies indicated that Ad.*mda-7* had antitumor activity in vivo in human non-small cell lung carcinoma (NSCLC) when applied as a single injected agent (Saeki et al., 2002) or in combination with radiation (Nishikawa et al., 2004) or sulindac (Oida et al., 2005), and in human pancreatic cancer cells containing a mutated K-*ras* gene when applied with a combination of antisense phosphorothioate oligonucleotides targeting K-*ras* (Su et al., 2001) or when administered in combination with arsenic trioxide (Lebedeva et al., 2005b).

Two recent studies suggest that employing a strategy embodying adenovirus replication to deliver *mda*-7/IL-24 can enhance the antitumor activity of this cytokine (Sarkar et al., 2005; Zhao et al., 2005). Sarkar et al. (2005) used the cancer-specific progression elevated gene-3 (PEG-3) promoter (Su et al., 2000, 2005b) to develop conditionally replication competent adenoviruses (CRCAs) that upon replication simultaneously express *mda*-7/IL-24 uniquely in the context of breast cancer cells. Infection of this CRCA (designated Ad.PEG-E1A-*mda*-7) in normal mammary epithelial cells and breast cancer cells confirmed cancer-cell-selective adenoviral replication, *mda*-7/IL-24 expression, growth inhibition, and apoptosis induction. Injecting Ad.PEG-E1A-*mda*-7 into human breast cancer xenografts established on both sides of athymic nude mice completely eradicated not only the primary injected tumor on one flank but also distant tumors (established on the opposite flank of the animal) thereby implementing a cure. In contrast, non-replicating viruses expressing *mda*-7/IL-24 or CRCAs not expressing *mda*-7/IL-24 displayed some antitumor activity, but this effect was greatly diminished in comparison with Ad.PEG-E1A-*mda*-7 (Sarkar et al., 2005). This dual cancer-specific targeting strategy provides an effective approach for treating breast and other human neoplasms with potential for eradicating both primary tumors and metastatic disease. Zhao et al. (2005) constructed a CRCA using the ZD55 vector, which contains a deletion of the adenoviral E1B 55-kDa gene, to regulate replication in cancer cells with p53 dysfunction, to deliver *mda*-7/IL-24 (ZD55-IL-24). Infection of normal cells did not induce a cytolytic effect, although MDA-7/IL-24 protein was detected, indicating potential leakiness of this vector relative to targeting genes only in cancer cells. However, even in the presence of MDA-7/IL-24, no toxicity was evident in normal lung fibroblast cells, further supporting the cancer-specific activity of this novel cytokine. Infection of human colorectal cancer cells with ZD55-IL-24 resulted in activation of caspases 3 and 9, induction of *bax*, and apoptosis. Moreover, infection of established SW620 colorectal tumors with ZD55-IL-24 showed a much stronger antitumor activity than observed with ONYX-015 (a virus preferentially replicating in cells with defective p53) or Ad-IL-24 (a non-replicating virus expressing *mda*-7/IL-24, similar to Ad.*mda-7*). These studies by Sarkar et al. (2005) and Zhao et al. (2005) demonstrate enhanced antitumor activity in vivo in nude mice when incorporating *mda*-7/IL-24 into a replicating oncolytic adenovirus as opposed to simply administering this cytokine in the context of a non-replicating adenovirus. These types of vectors hold significant promise for augmenting the therapeutic potential of *mda*-7/IL-24.

8. Role of PKR in Ad.*mda-7*-induced cancer-specific growth inhibition and apoptosis induction

Pataer et al. (2002) provided evidence linking the tumor suppressor activity of overexpressed Ad.*mda-7* to up-regulation of the interferon-induced serine/threonine protein kinase (PKR) in a p53-independent manner in the context of NSCLC cells. Double-stranded RNA-dependent protein kinase PKR appears to mediate anti-tumorigenic activity through activation of specific biochemical pathways resulting in growth inhibition and apoptosis. Activation occurs due to signals leading to autophosphorylation. Once activated, PKR phosphorylates various targets, which play a crucial role in growth control and apoptosis induction, such as eIF-2α, Stat1, Stat3, and p38 mitogen-activated protein kinase (MAPK) (Pataer et al., 2002). Inhibition of PKR with the inhibitor 2-aminopurine (2-AP) prevents Ad.*mda-7*-induced apoptosis, eIF-2α phosphorylation, and inhibition of protein synthesis. In this context, PKR activation appears to be crucial for Ad.*mda-7* induction of apoptosis in lung cancer cells. Additionally, induction of programmed cell death by Ad.*mda-7* in mouse embryo fibroblasts (MEF) was dependent on an active PKR locus because MEFs from $PKR^{-/-}$ animals were unable to undergo apoptosis, whereas wild-type $PKR^{+/+}$ MEFs were sensitive to *mda*-7/IL-24 (Pataer et al., 2002). This latter observation is puzzling because Ad.*mda-7* does not appear to induce apoptosis in normal rat cells, whereas it does induce this effect in transformed and tumor-derived rat cells. In their proposed model, *mda*-7/IL-24 and PKR act upstream of caspases and the pro-apoptotic Bak gene, where *mda*-7/IL-24 induces PKR up-regulation with subsequent activation of cellular pathways leading to caspase activation and apoptosis induction (Pataer et

al., 2002). It should be noted that activation of the PKR pathway may not be a general method of apoptosis induction by *mda*-7/IL-24 because a recent paper studying the bystander activity of secreted MDA-7/IL-24 indicated apoptosis induction in human melanoma cells by a PKR-independent death pathway (Chada et al., 2004a, 2004b).

In a recent report, Pataer et al. (2005) investigated potential interactions between MDA-7/IL-24 and PKR proteins in the context of human lung cancer cells. Infection of A549 and H1299 NSCLC cell lines with Ad.*mda-7* resulted in a dose- and time-dependent induction of PKR protein and apoptosis. RT-PCR failed to detect an increase in PKR mRNA following infection with Ad.*mda-7*, suggesting a post-transcriptional regulation of PKR by MDA-7/IL-24 protein. To determine if exogenously applied MDA-7/IL-24 could induce PKR or apoptosis, purified MDA-7 protein was administered extracellularly to the lung cancer cell lines. Under these experimental conditions, PKR was not induced and no apoptosis ensued. In contrast, treatment of A549 cells with a GST-MDA-7/IL-24 fusion protein (Sauane et al., 2004a), which internalizes in cells, induced growth suppression and apoptosis (Sauane & Fisher, unpublished data). These studies, combined with experiments using plasmid transfection approaches or an adenovirus to deliver *mda*-7/IL-24 lacking a signal peptide, thereby preventing secretion from cells, provide further support for a novel mode of killing by *mda*-7/IL-24 that involves intracellular action without the requirement for secretion from cancer cells (Sauane et al., 2004b; Sieger et al., 2004). Immunofluorescence and co-immunoprecipitation techniques suggest that MDA-7/IL-24 protein physically interacts with PKR (Pataer et al., 2005). Employing mouse embryo fibroblasts containing PKR ($PKR^{+/+}$) or lacking PKR ($PKR^{-/-}$) indicated phosphorylation of MDA-7/IL-24 and PKR proteins in the lysates of $PKR^{+/+}$ but not in $PKR^{-/-}$ cells. These studies suggest that in certain cellular contexts, such as lung cancer cells, Ad.*mda-7* can induce PKR and MDA-7/IL-24 (on threonine and serine residues) phosphorylation and MDA-7/IL-24 can physically interact with PKR (Pataer et al., 2005). Further studies are required to determine if this induction of PKR by Ad.*mda-7* is restricted to non-small cell lung carcinoma cells, or if it can also occur in additional cancer cell models.

9. Role of p38 MAP kinase and growth arrest and DNA damage-inducible genes in melanoma differentiation associated gene-7/interleukin-24-induced apoptosis in cancer cells

p38 MAPK, which is induced in response to stress and during growth signaling, is known to play a crucial role in apoptosis (Xia et al., 1995; Juo et al., 1997; Kummer et al., 1997; Schwenger et al., 1997; Dent et al., 2003). Sarkar et al. (2002a, 2000b) examined the role of the p38 MAPK pathway in response to Ad.*mda-7*-mediated growth suppression and apoptosis induction in melanoma cells. Ad.*mda-7* infection induced expression of the growth arrest and DNA damage (GADD)-inducible gene family. GADD genes are stress-induced genes that are up-regulated in response to agents/conditions such as UV radiation, chemical carcinogens, starvation, oxidative stress, and TNF-α. The GADD gene family comprises 5 gene members, GADD34, GADD45α, GADD45β, GADD45γ, and GADD153 (Zhan et al., 1994; Hollander et al., 1997, 2001; Connor et al., 2001). These GADD family members are believed to play a crucial role in transcriptional regulation and apoptosis. GADD153 acts by regulating the activity of the B-cell CLL/lymphoma 2 (Bcl-2) promoter (Ubeda et al., 1996, 1999). Overexpression of GADD genes promoted growth inhibition/apoptosis and combined expressions of GADD genes lead to synergistic or cooperative anti-proliferative effects. Activating the p38 MAPK pathway regulated induction of these GADD genes by Ad.*mda-7*. Blocking the p38 pathway using a specific inhibitor SB203580 suppressed the induction of the GADD genes and apoptosis (Fig. 6) (Sarkar et al., 2002b). Antisense inhibition of GADD genes also blocked induction of apoptosis and inhibition was greatest when the various antisense constructs were used in combination (Sarkar et al., 2002b). Apart from the GADD genes, p38 MAPK also acted on the downstream target heat shock protein (HSP27), which initiates apoptosis (Sarkar et al., 2002b).

Infection of lung cancer cells with Ad.*mda-7* results in phosphorylation of PKR and also its downstream targets, such as eIF-2α, Tyk2, Stat1, Stat3, and p38 MAPK (Pataer et al., 2002). Phosphorylation of eIF-2α activates the transcription factor ATF4, which activates GADD153 (Fawcett et al., 1999). In this context, there is a significant level of crosstalk between the PKR and the p38 MAPK pathway (Sarkar et al., 2002b). Further studies are needed to comprehend the relevance of this crosstalk and to identify upstream molecules regulating the PKR and the p38 MAPK pathway.

10. Role of β-catenin and the phosphoinositide 3-kinase signaling pathway in melanoma differentiation associated gene-7/interleukin-24-induced apoptosis in cancer cells

In breast and lung tumor cells, an inverse relationship between expression of β-catenin and the phosphoinositide 3-kinase (PI3K) signaling pathway was observed (Mhashilkar et al., 2003). β-Catenin and PI3K are involved in up-regulation of apoptotic and survival pathways as well as cell–cell adhesion and metastasis. β-Catenin is a downstream effector of the Wnt signaling pathway and binds to and activates the transcription factors in the T-cell-specific transcription factor/lymphoid enhancer binding factor (TCF/LEF) family leading to induction of TCF/LEF responsive genes (McCormick, 1999). Elevated levels of β-catenin have been observed in many tumors, such as colon and gastric carcinomas and adenocarcinoma of the breast. β-Catenin/TCF-responsive genes play a pivotal role in cell cycle progression and loss of cell differentiation properties and some of these gene products, for example, cyclin D1, matrilysin, and c-*myc*, are elevated in mammary tumors and cell lines expressing activated β-catenin (McCormick, 1999). PI3K plays a crucial role in the regulation of signal trans-

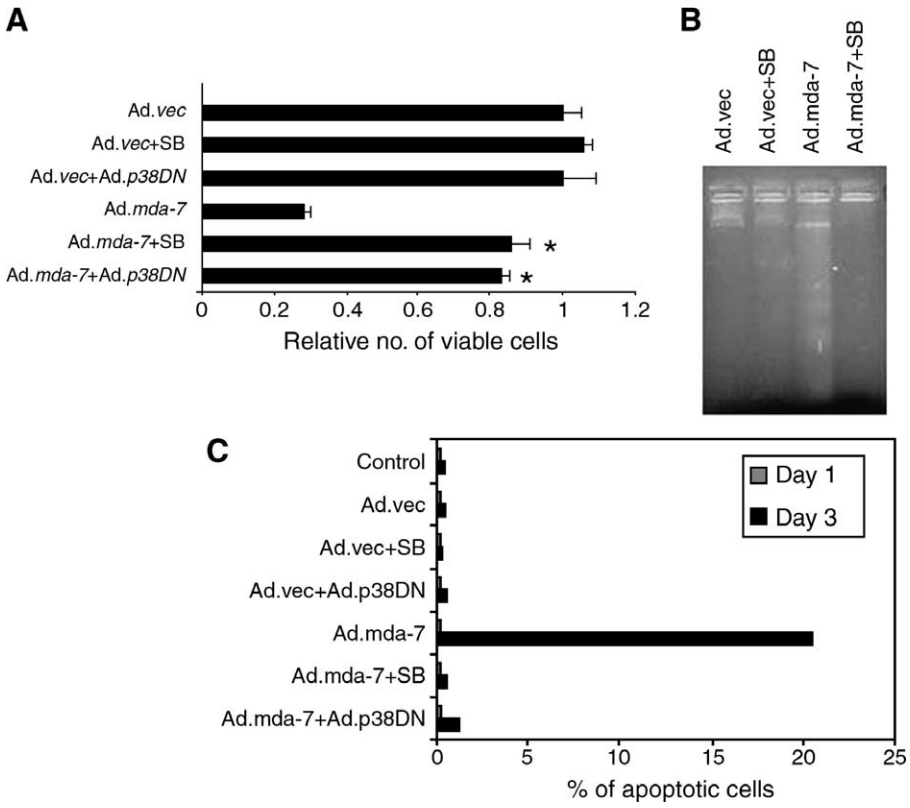

Fig. 6. Inhibition of the p38 MAPK pathway protects FO-1 melanoma cells from Ad.*mda-7*-mediated cell death. (**A**) FO-1 cells were infected with either Ad.vec or Ad.*mda-7* (100 pfu/cell) and treated with 1 μM SB203580 or infected with Ad.p38DN (an adenovirus expressing a dominant-negative p38 mutant gene) (100 pfu/cell). Cell viability was measured by MTT assay after 4 days. Cell viability of Ad.vec-treated cells was regarded as 1. *Significant differences from Ad.*mda-7* ($P<0.0001$). (**B**) FO-1 cells were infected with either Ad.vec or Ad.*mda-7* (100 pfu/cell) and treated with 1 μM SB203580 for 3 days. DNA was isolated from the cells and fragmentation was analyzed as described in Sarkar et al. (2002b). (**C**) FO-1 cells were infected with either Ad.vec or with Ad.*mda-7* (100 pfu/cell) and treated with 1 μM SB203580 or infected with Ad.p38DN (100 pfu/cell). Percentage of apoptotic cells at days 1 and 3 after infection in each group were plotted (reproduced, by permission of the publisher, from Sarkar et al., 2002b).

duction, cytoskeletal rearrangement, and membrane trafficking. The PI3K family members are known to play a role in development of human cancers, cell growth, differentiation, and survival (Berrie, 2001; Fry, 2001; Katso et al., 2001). Constitutive expression of the PI3K pathway is seen in many human tumors and it is believed to play a crucial role in increased tumor cell survival and resistance to chemotherapy and radiotherapy (Berrie, 2001; Fry, 2001; Katso et al., 2001). In these contexts, inhibition of the PI3K pathway by Ad.*mda-7* is proposed as a mechanism by which this gene could inhibit cancer cell proliferation.

Mhashilkar et al. (2003) investigated the effects of Ad.*mda-7* infection on β-catenin and PI3K signaling pathways in non-small cell lung carcinoma (NSCLC) cells and found that Ad.*mda-7* negatively regulates both the β-catenin and PI3K pathways by increasing steady-state levels of tumor-suppressive proteins, such as E-cadherin, adenomatous polyposis coli gene (APC), glycogen synthase kinase 3 beta (GSK-3β), phosphatase and tensin homolog (PTEN), and decreasing expression of oncogenic proteins, such as PI3K, focal adhesion kinase (FAK), integrin-linked protein kinase 1 (ILK-1), phospholipase C gamma (PLC-γ), and protein kinase B (AKT), in breast and lung cancer cells. Ad.*mda-7* is proposed to function upstream of PLCγ and blocks the PLC-γ →FAK→PI3K→AKT→GSK3 pathway, although it is unclear whether regulation of downstream molecules is a direct or indirect action of Ad.*mda-7*. Ad.*mda-7* causes redistribution of β-catenin from the nucleus to the plasma membrane, reducing TCF/LCF transcriptional activity and increasing cell–cell adhesion. No direct binding of *mda*-7/Il-24 to β-catenin was observed in the immunoprecipitation assays, suggesting that subcellular localization of *mda*-7/IL-24 is different than β-catenin. Ad.*mda-7* is contained within the secretory granules, whereas β-catenin staining reveals its presence in both nucleus and cytoplasmic compartments. Further studies are necessary to determine the mechanism by which *mda*-7/IL-24 modulates β-catenin/PI3K signaling pathways, how frequent these changes are in additional tumors, and what are the initiator signaling molecules that are activated. Moreover, it is essential to understand the role of protein–protein interactions to provide a better understanding of the molecules involved in regulating the β-catenin and PI3K signaling pathways.

11. Role of pro-apoptotic and anti-apoptotic proteins in Ad.*mda-7*-mediated killing of cancer cells: support for activation of the mitochondrial intrinsic pathway of apoptosis as a predominant mediator of apoptosis induction by melanoma differentiation associated gene-7/interleukin-24

The first observation that forced expression of *mda*-7/IL-24 by means of a replication incompetent adenovirus (Ad.*mda-7*) could alter the ratio of apoptotic proteins in cancer cells resulting in apoptosis was provided by Su et al. (1998). Ad.*mda-7* induced apoptosis in human breast cancer cells with different p53 genotypes, indicating p53 independence in its mode of action as an antitumor gene in breast cancer. Ad.*mda-7* reduced colony formation in MCF-7 (wt p53), MDA-MB-157 (null p53), MDA-MB-231, MDA-MB-453, and T47D (mut p53) cells (Su et al., 1998). Programmed cell death reflects a balance between signaling events and molecules that either promote or inhibit apoptosis (Reed, 1995, 1997; Danial & Korsmeyer, 2004; Reed, 2004). Proteins such as Bcl-2, Bcl-X_L, McL-1, Bcl-W, and Ad-E1B protect cells from apoptosis whereas proteins such as Bax, Bad, Bak, and Bcl-X_s stimulate apoptosis in specific target cells (Reed, 1995, 1997; Danial & Korsmeyer, 2004). In human breast carcinoma cells, Ad.*mda-7* altered the ratio of specific pro- and anti-apoptotic proteins tipping the balance from survival to death. Up-regulation of BAX protein after infection with Ad.*mda-7* was apparent in tumor cell lines containing wild-type or mutant p53 or that were devoid (null) of p53. Comparison of BAX to BCL-2 protein ratios revealed BAX/BCL-2 to be significantly higher in Ad.*mda-7*-infected breast cancer cells implicating BAX and a reduction in BCL-2 proteins as potential components in *mda*-7/IL-24-induced programmed cell death (Su et al., 1998). Ectopic overexpression of *bcl*-2 or Ad E1B by transfection with expression vector constructs expressing these different gene products, in combination with Ad.*mda-7* infection, protected T47D and MCF-7 cells from inhibition of colony formation that normally results following infection with Ad.*mda-7*. These results provided initial evidence that *mda*-7/IL-24-induced growth suppression and apoptosis could be modified by anti-apoptotic proteins (Su et al., 1998). This protection from apoptosis is consistent with the prominent role played by *mda*-7/IL-24-induced up-regulation of BAX protein in the apoptosis-inducing mechanism employed by this gene. Moreover, although *bax* is considered a p53-dependent downstream gene, the ability of *mda*-7/IL-24 to up-regulate BAX protein independent of p53 suggests that alternative pathways are involved in BAX up-regulation after ectopic expression of this cancer-specific apoptosis-inducing gene in specific cancer cells. Further studies have confirmed that infection with Ad.*mda-7* results in a significant reduction in the levels of specific anti-apoptotic proteins in a cancer cell-type-specific context. A 3- to 9-fold reduction in the levels of BCL-X_L protein was evident in HO-1, FO-1, MeWo, and WM35 cells, whereas a 3-fold reduction in the levels of BCL-2 protein was observed in MeWo and FO-1 cells, suggesting that decreases in the levels of single or multiple anti-apoptotic proteins may be major determinants of induction of apoptosis in human melanoma cells following infection with Ad.*mda-7* (Lebedeva et al., 2002).

In human prostate cancer cells, Ad.*mda-7* infection induces apoptosis in LNCaP, DU-145, and PC-3 cells, whereas in HuPEC normal early passage human prostate epithelial cells, growth and survival are not affected (Lebedeva et al., 2003a). A recent report by Saito et al. (2005) supports this differential effect of Ad.*mda-7* in the context of cancer versus normal prostate epithelial cells. In these cell types, Ad.*mda-7* infection elevates the levels of BAX and/or BAK proteins while significantly reducing the levels of anti-apoptotic proteins, BCL-2 and BCL-X_L, again supporting the hypothesis that it is the change in the ratio of pro-apoptotic to anti-apoptotic proteins that may directly participate in *mda*-7/IL-24-induced apoptosis in prostate cancer cells (Lebedeva et al., 2003a). Stable overexpression of *bcl*-2 and *bcl-X_L* differentially protect prostate cancer cells from Ad.*mda-7*-induced apoptosis (Lebedeva et al., 2003a). *bcl-X_L*, but not *bcl*-2, afforded protection from *mda*-7/IL-24-induced apoptosis in PC-3 and DU-145 cells, whereas in LNCaP cells *bcl*-2, but not *bcl-X_L*, protected these cells from *mda*-7/IL-24 (Lebedeva et al., 2003a). At present, it is not known why protection is not achieved in all the prostate carcinomas with a single functionally similar anti-apoptotic protein.

The complexity of potential mechanisms by which *mda*-7/IL-24 can selectively induce killing in specific cancer cell types is highlighted by a recent study by Gopalan et al. (2005). In a specific ovarian cancer cell line, MDAH 2774, but not in normal ovarian epithelial (NOE) cells, Ad.*mda-7* activated the Fas–Fas ligand (FasL) signaling pathway resulting in apoptosis. In this specific ovarian cancer cell line, Ad.*mda-7* induced activation of the transcription factors c-Jun and activating transcription factor 2 (ATF 2), which stimulated transcription of the death-inducer FasL and its cognate receptor Fas. This induction of FasL was associated with the activation of NF-κB and Fas-associated factor 1, Fas-associated death domain, and caspase 8. A potential cause and effect relationship between these changes was suggested by the ability of siRNA inhibiting Fas to significantly decrease Ad.*mda-7*-mediated death in MDAH2774 cells. Similarly, blocking FasL with NOK-1 Fas ligand antibody inhibited Ad.*mda-7*-mediated killing of this cell line. Collectively, these studies indicate that in specific tumor contexts, Ad.*mda-7* can exploit the Fas-FasL signaling pathway to kill cancer cells. In additional ovarian cancer cells, a mitochondrial-mediated killing effect elicited by *mda*-7/IL-24 has been demonstrated (Leath et al., 2004; I.V. Lebedeva, P. J. Mahasreshti, D.T. Curiel, & P.B. Fisher, unpublished data). Moreover, as reviewed recently by Lebedeva et al. (2005a), the studies by Gopalan et al. (2005) and Leath et al. (2004) provide additional examples of the ability of *mda*-7/IL-24 to selectively induce apoptosis in histologically similar cancer cell types using different pro-apoptotic signaling mechanisms; that is, this novel cytokine finds and exploits specific weaknesses in cancer cells promoting their death.

12. Mitochondrial dysfunction promoted by melanoma differentiation associated gene-7/interleukin-24 selectively promotes cell death in prostate cancer cells

Up-regulation of pro-apoptotic and down-regulation of anti-apoptotic proteins suggest a role of mitochondria in the induction of apoptosis in response to Ad.*mda-7* infection in specific cancer cell types. Studies by Lebedeva et al. (2003c) provide insights into the relationship between mitochondrial function and cellular redox status in response to Ad.*mda-7* infection. Reactive oxygen species (ROS), including singlet oxygen, superoxide ions, hydroxide, and hydroxyl radicals, are known to regulate apoptosis and proliferation in response to various stimuli, including TNF-α, UV, and γ-radiation (Jacobson, 1996). A relationship between ROS induction by Ad.*mda-7* and apoptosis induction has now been established in prostate cancer cells (Lebedeva et al., 2003c). Antioxidants such as *N*-acetyl-L-cysteine (NAC) and Tiron, at non-cytotoxic doses, inhibited the killing effect of Ad.*mda-7* in DU-145, PC-3, and LNCaP cells, whereas addition of compounds such as As_2O_3 and NSC656240 (a dithiophene) that promote ROS production in combination with Ad.*mda-7* infection potentiated cell death in all 3 carcinoma cell lines, but not in normal P69 cells, suggesting that free radicals are involved in the process of killing by Ad.*mda-7* in prostate carcinoma cells (Lebedeva et al., 2003c). FACS analysis revealed a 3- to 5-fold increase in the levels of ROS in prostate carcinoma cells, but not in P69 cells. Because ROS is a modulator of mitochondrial membrane potential (ψ_M) (Zamzami et al., 1995; Kroemer & Reed, 2000), time course evaluations of mitochondrial changes with membrane apoptotic changes after Ad.*mda-7* infection were determined. It was established that the initial decrease in $\Delta\Psi_m$ occurs before ROS production in Ad.*mda-7*-infected DU-145, LNCaP, and PC-3 carcinoma cells. The initial drop in $\Delta\Psi_m$ occurs 6–7 hr followed by increased ROS production (10–20 hr) and the decline in $\Delta\Psi_m$ continues up to 12 hr in LNCaP and up to 30 hr in DU-145 and PC-3 cells. At 45–50 hr, a secondary burst of ROS and concomitant final steep increase in $\Delta\Psi_m$ are observed, indicating complete mitochondrial dysfunction (Lebedeva et al., 2003c). The decline in ψ_M and the increase in annexin V binding occurred, concomitantly suggesting that Ad.*mda-7*-mediated apoptosis correlates with changes in mitochondrial function. Further studies focused on mitochondrial potential transition (MPT). MPT is characterized by opening of mitochondrial mega channels to allow solutes and water to enter mitochondria. MPT is triggered by ROS and other agents resulting in a decrease of $\Delta\Psi_m$ followed by depletion of ATP and activation of caspases/endonucleases (Jacobson, 1996). This process is controlled by a multiprotein complex found in the inner and outer membranes of mitochondria known as the permeability transition pore (PTP). Upon PTP opening, the mitochondria lose their $\Delta\Psi_m$ across the inner membrane resulting in apoptosis along with shutdown of mitochondrial biosynthesis. Inhibitors of the PTP,

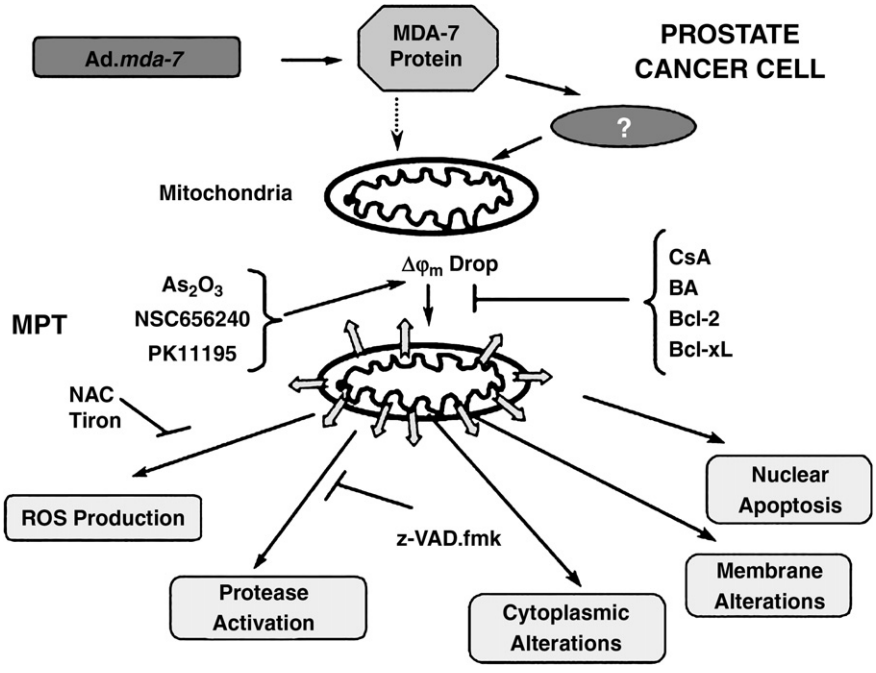

Fig. 7. Proposed model for Ad.*mda-7*-induced apoptosis in prostate cancer cell lines. Following Ad.*mda-7* infection, MDA-7 protein affects mitochondria directly or indirectly, causing alterations in mitochondrial function (decrease in $\Delta\Psi_m$ and MPT) and ROS production. The reductions in $\Delta\Psi_m$ and MPT are caspase-independent because they are not inhibited by the general caspase inhibitor z-VAD.fmk. Moreover, MPT can be blocked by inhibitors of MPT, such as CsA and BA, and can be promoted by activators of MPT, such as PK11195, a PBzR agonist. ROS inhibitors (NAC and Tiron) block Ad.*mda-7*-induced apoptosis, whereas ROS producers ($As_2 2O_3$ and NSC656240) enhance apoptosis only in the context of prostate cancer cells. Abbreviations: $\Delta\Psi_m$, mitochondrial transmembrane potential; MPT, mitochondrial permeability transition; ROS, reactive oxygen species; z-VAD.fmk, *N*-benzyloxycarbonyl-Val-Ala-Asp-fluoromethyl ketone; CsA, cyclosporin A; BA, bongkrekic acid; PK11195, 1-(2-chlorophenyl)-*N*-methyl-*N*-(1-methylpropyl)-3-isoquinolinecarboxamide; PBzR, peripheral benzodiazepine receptors; As_2O_3, arsenic trioxide; NSC656240, dithiophene (reproduced, by permission of the publisher, from Lebedeva et al., 2003c).

such as cyclosporin A and bongkrekic acid that bind to different components of the PTP, prevented cell death and the decline in $\Delta\Psi_m$, whereas pretreatment with the peripheral benzodiazepine receptor agonist (PK11195) potentiated the induction of MPT followed by apoptosis (Lebedeva et al., 2003c). These studies established the importance mitochondrial dysfunction and ROS production in Ad.*mda-7*-induced death in prostate carcinoma cells as overviewed in Fig. 7.

13. Secretion of melanoma differentiation associated gene-7/interleukin-24 is not mandatory for cancer-specific cell killing

The endoplasmic reticulum (ER) is a principal site for protein synthesis and folding, calcium signaling, and calcium storage (Berridge et al., 2000; Berridge, 2002). Alterations in calcium homeostasis and accumulation of misfolded protein in the ER cause "ER stress". This ER stress response triggers specific signaling pathways including the unfolded protein response (UPR), the ER-overload response (EOR), and the ER-associated degradation (ERAD) pathway to enable cells to survive pro-apoptotic ER stress (Herr & Debatin, 2001). Prolonged activation of these pathways leads ultimately to apoptosis. After Ad.*mda-7* infection, the expressed protein was shown to localize in the ER/Golgi compartments by 2 independent studies, one utilizing an adenovirus vector expressing a non-secreted version of MDA-7/IL-24 protein generated via deletion of its signal peptide (Sauane et al., 2004b) and the other utilizing plasmid-based analyses (Sieger et al., 2004). Earlier findings from our group indicated that Ad.*mda-7*-induced GADD genes, classically associated with the stress response including ER stress pathways in human melanoma cells, but not in immortalized melanocytes (Sarkar et al., 2002b). This induction of GADD genes and further upstream events such as activation of p38 MAPK as well as downstream pathways such as HSP-27 was reproducibly induced in a transformed cell-specific manner after Ad.*mda-7* infection (Sarkar et al., 2002b). In addition, studies with the virus producing the non-secreted as well as secreted versions of *mda*-7/IL-24, only in the context of transformed cells, specifically activated the p44/42 MAPK pathway (Sauane et al., 2004b). Furthermore, Ad.*mda-7* infection produced an up-regulation in inositol 1,4,5-trisphosphate receptor (IP3R) in H1299 cells (Mhashilkar et al., 2003). IP3R is an intracellular calcium release channel implicated in apoptosis and localized in the ER. Activation of a series of heat-shock-related chaperones as well as various stress proteins [GADDs, protein phosphatase 2A (PP2A), X-box binding protein 1 (XBP-1), immunoglobulin binding protein (BiP), etc.] indicates that adenovirus infection with *mda*-7/IL-24 induces ER stress and this might be the earliest contributor to the appearance of apoptosis in the different cancer cells lines after infection with Ad.*mda-7* (Sarkar et al., 2002b; Mhashilkar et al., 2003). Further investigation to determine the mechanism of specificity of MDA-7/IL-24-triggered ER stress is clearly needed to determine why cellular ER stress mechanisms are differentially activated in transformed cells by MDA-7/IL-24 and possibly other agents (Sauane et al., 2004b). From additional independent studies performed by our groups, we know that Ad.*mda-7* induces reactive oxygen species (ROS) in different cell lines (Lebedeva et al., 2003c, 2005b; Yacoub et al., 2003c). Nevertheless, it is not clear at the present time if the activation of mitochondrial-mediated events that trigger ROS and caspase-dependent and -independent pathways is temporally followed by ER stress, vice versa, or whether there is temporally coordinated co-stimulatory crosstalk between both pathways (Sauane et al., 2004a, 2004b).

Our observations are beginning to provide additional insights into the diverse pathways that are involved in selective *mda*-7/IL-24-induced apoptosis in tumor cells and identify ER- and mitochondrial-mediated events as important causative effectors of apoptosis by *mda*-7/IL-24. These experiments offer potential for developing ways of enhancing the clinical utility of this novel cancer-gene therapeutic for treating diverse human neoplasms.

14. Pancreatic cancer cells provide a unique model of melanoma differentiation associated gene-7/interleukin-24 action and highlight the potent "antitumor bystander" activity of this cytokine

Pancreatic cancer is an aggressive neoplastic disease where long-term survival of patients in which tumor spread has occurred outside the pancreas is only 4% (Perugini et al., 1998; Friess et al., 1999; Hilgers & Kern, 1999; Lorenz et al., 2000; Rosenberg, 2000). In pancreatic cancer, multiple subsets of genes undergo genetic changes in a temporal manner resulting in specific oncogene activation and tumor suppressor gene inactivation during tumor progression (Perugini et al., 1998; Friess et al., 1999; Hilgers & Kern, 1999; Bardeesy & DePinho, 2002). Genes such as the Kirsten-*ras* (K-*ras*) oncogene (85–95%) are activated whereas inactivation of genes such as *p16/RB1* (>90%), *p53* (75%), and *DPC* (55%) have been reported (Perugini et al., 1998; Friess et al., 1999; Hilgers & Kern, 1999; Bardeesy & DePinho, 2002), reinforcing the complexity of this disease and providing a potential genetic basis underlying its aggressiveness and resistance to conventional therapies. Antisense (AS) targeting of K-*ras* using a plasmid or mutation-specific phosphorothioate oligodeoxynucleotide (PSODN) inhibits the growth of pancreatic cancer cells containing K-*ras* mutations, but not those having a wild-type K-*ras* gene, suggesting that a single approach of inhibiting this oncogene is not sufficient to eradicate pancreatic carcinoma cells (Su et al., 2001). From these observations, it is believed that mutations in K-*ras* change the physiology of the pancreatic cancer cell and similar biochemical changes may not be evident in pancreatic cancers containing a wild-type K-*ras* genotype.

Unlike virtually all other cancers studied to date, pancreatic carcinoma cells are inherently resistant to ectopic expression of *mda*-7/IL-24 (Su et al., 2001; Lebedeva et al., 2005b, in press). Infection of human pancreatic tumor cells with 100 pfu/cell of Ad.*mda-7*, which promotes apoptosis and reduces colony formation in the vast majority of cancer cell types, does not significantly alter growth, inhibit colony formation, or induce

apoptosis in this tumor model (Su et al., 2001; Lebedeva et al., 2005b, in press). In contrast, higher doses of *mda*-7/IL-24 or vector modifications used to express *mda*-7/IL-24 result in growth inhibition, a reduction in colony forming ability and/or apoptosis in several K-*ras* mutant pancreatic carcinoma cell lines (Chada et al., 2005; Lebedeva et al., 2005b, in press). This failure to respond to standard concentrations of *mda*-7/IL-24 (effective in inducing apoptosis in virtually all other cancer cell types), combined with an understanding of potential changes induced by an activated K-*ras* gene, prompted us to propose that downstream signaling pathways may be altered in mutant K-*ras* pancreatic carcinoma cells rendering these cells resistant to *mda*-7/IL-24-induced growth suppression and apoptosis (Su et al., 2001). Studies were performed to directly test this hypothesis. Treatment of pancreatic tumor cells with AS K-*ras* PSODN or transfection with an AS K-*ras* expression plasmid and infection with Ad.*mda-7* had a profound synergistic growth inhibitory effect and decreased survival of MIA PaCa-2 cells, AsPc-1 and PANC-1 cells containing a mutant K-*ras* gene, but not in BxPC-3, which has a wild-type K-*ras* genotype (Fig. 8; data shown for MIA PaCa 2 cells) (Su et al., 2001). Suppression in tumor formation was also evident in athymic nude mice when MIA PaCa 2 cells were transfected with an AS K-*ras* plasmid and infected with Ad.*mda-7* prior to injection into animals (Su et al., 2001). This finding is worth commenting on because it provided the first definitive evidence for "antitumor bystander" activity of *mda*-7/IL-24. The combination of AS K-*ras* transfection plus infection with Ad.*mda-7* results in only ~8% of the cells receiving both agents; that is, ~3% to ~4% maximum delivery of the K-*ras* AS gene, ~100% delivery of *mda*-7/IL-24 (by Ad.*mda-7*), and potentiation of transfection efficiency following adenovirus infection (hence ~8% transfection efficiency), yet tumor formation was completely inhibited when these combination-treated cells were injected into nude mice (Su et al., 2001). These observations are very provocative, highlighting an interesting and relevant phenotypic property of *mda*-7/IL-24; that is, an ability of this cytokine to promote potent "antitumor bystander" activity. Moreover, this novel combinatorial approach of inhibiting a dominant-acting oncogene and administering a cancer-specific tumor suppressor gene (such as *mda*-7/IL-24) (Gazdar & Minna, 2001; Su et al., 2001; Lebedeva et al., 2005b, in press) provides a rationale for developing a potentially effective therapy for this aggressive and invariably fatal cancer.

Infection of pancreatic cancer cells, containing both mutated and wild-type K-*ras*, results in high levels of *mda*-7/IL-24 mRNA, but little if any of this mRNA is translated into protein (Su et al., 2001; Lebedeva et al., 2005b, in press). However, when expression of mutant K-*ras* is ablated, using an AS-based strategy (either AS PSODN or an AS K-*ras* expression vector) or by using a bipartite adenovirus (expressing *mda*-7/IL-24 and AS K-*ras*, Ad.m7/KAS), this "mRNA translational block" is reversed, large amounts of MDA-7/IL-24 protein are produced, and mutant pancreatic cancer cells undergo apoptosis. Although the mechanism involved in this altered translation is not currently known, it may result from inhibition of K-*ras* signaling through MAPK because studies by Rajasekhar et al. (2003) indicate that inhibiting this pathway facilitates the translation of specific mRNAs into protein. This occurs by enhancing the association of defined mRNAs with polysomes, thereby promoting their translation into protein. We have tested this hypothesis and shown that when mutant K-*ras* expression is extinguished in pancreatic carcinoma cells infected with Ad.*mda-7*, there is an increase in *mda*-7/IL-24 mRNA associated with polysomes (Lebedeva et al., in press). Additionally, we have now demonstrated that combining *mda*-7/IL-24 with inhibition of the K-*ras*-activated extracellular-regulated kinase 1/2 (ERK1/2) also results in reversal of the "translational block" culminating in MDA-7/IL-24 protein and apoptosis (Lebedeva et al., in press).

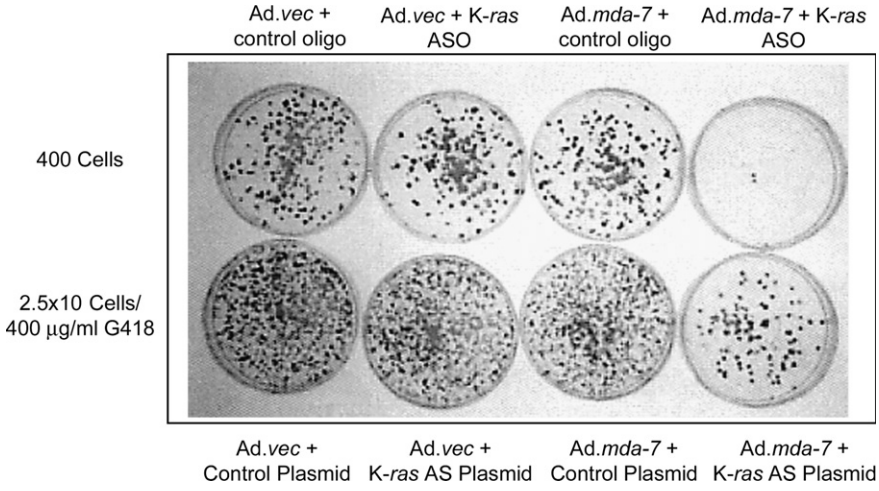

Fig. 8. The combination of Ad.*mda-7* plus AS K-*ras* PS ODN or AS K-*ras* plasmids synergistically inhibits colony formation in mutant K-*ras* MIA PaCa-2 pancreatic carcinoma cells. (Upper) Effect of Ad.*mda-7* plus AS K-*ras* PS ODN on MIA PaCa-2 colony formation. Cells were infected with 100 pfu/cell of Ad.vec or Ad.*mda-7*, treated with 0.5 µM AS K-*ras* PS ODN plus 10 µl of Lipofectamine, reseeded at a density of 400 cells per plate, and fixed and stained with Giemsa after 3 weeks. (Lower) Effect of Ad.*mda-7* plus AS K-*ras* plasmid transfection on MIA PaCa-2 G418-resistant colony formation. Cells were infected with 100 pfu/cell of Ad.vec or Ad.*mda-7*, transfected with 10 µg of plasmid (either control pcDNA3.1 lacking insert or the pcDNA3.1 vector containing a 346-nt AS K-*ras* fragment), reseeded at a density of 2.5×10^5 cells per plate, and selected in 400 µg/mL G418, and G418-resistant colonies were fixed and stained with Giemsa after 3 weeks (reproduced, by permission of the publisher, from Su et al., 2001).

Recent studies highlight an additional means of abrogating the *mda*-7/IL-24 "mRNA translational block" in pancreatic cancer cells (Lebedeva et al., 2005b). Treatment of both mutant and wild-type K-*ras* pancreatic carcinoma cells with compounds that induce reactive oxygen species (ROS), including arsenic trioxide, *N*-(4-hydroxyphenyl) retinamide, or dithiophene (NSC656240), results in the production of MDA-7/IL-24 protein and induction of apoptosis (Lebedeva et al., 2005b). Confirmation of a role for ROS induction in this process was provided by studies employing 2 ROS inhibitors, *N*-acetyl-L-cysteine and Tiron, which prevented a reversal of the "mRNA translational block," production of MDA-7/IL-24 protein, and induction of apoptosis when pancreatic carcinoma cells were subsequently treated with a ROS inducer and infected with Ad.*mda-7*. These effects were not associated with a reduction in the levels of K-*ras* protein in these cells, which supports a novel mode of action of this combinatorial approach. Because this dual treatment did not induce apoptosis in normal cells, these findings provide support for potentially using a ROS inducer with Ad.*mda-7* as a treatment modality for pancreatic cancer (Lebedeva et al., 2005b).

15. Further insights into the mechanism underlying the potent "antitumor bystander" activity of melanoma differentiation associated gene-7/interleukin-24

A limitation frequently encountered using tumor suppressor gene replacement therapy is an inability to transduce a significant portion of tumor cells with a bioactive suppressor gene (Lebedeva et al., 2003a; Su et al., 2005b). This impediment profoundly limits the effectiveness of this strategy of tumor suppressor gene replacement as a therapy for cancer. An approach for ameliorating this situation would be to exploit a tumor suppressor gene that not only affects cells that directly receive this genetic agent, but also exerts activity on tumor cells at a distance (Fisher et al., 2003; Fisher, 2005; Lebedeva et al., 2005a). As discussed above, the potential for *mda*-7/IL-24 to induce a potent "antitumor bystander" effect was first uncovered in the context of pancreatic cancer (Su et al., 2001). This effect has now been substantiated in a Phase I clinical trial involving intratumor injections into advanced carcinomas and melanomas (Fisher et al., 2003; Cunningham et al., 2005; Fisher, 2005; Lebedeva et al., 2005a) and the mechanism of this "antitumor bystander" activity in vitro has been investigated in 2 recent studies (Chada et al., 2004a; Su et al., 2005c). Chada et al. (2004a) determined the effect of secreted glycosylated, tumor-cell-produced MDA-7/IL-24 protein (released by a stable 293 cell clone expressing a transfected *mda*-7/IL-24 gene) on human melanoma cells. This form of MDA-7/IL-24 protein produced a dose-dependent induction of programmed cell death in human melanoma cells. Moreover, the apoptosis-inducing effect of secreted glycosylated tumor-derived MDA-7/IL-24 protein on melanoma cells was dependent on the presence of functional IL-20/IL-22 receptors in these cells. These studies also indicated that glycosylated MDA-7/IL-24 protein induced phosphorylation and nuclear translocation of STAT3 in melanoma cells and resulted in up-regulation of BAX protein and subsequent apoptosis. In contrast, additional IL-10 family members, including IL-10, -9, -20, and -22, which also activate STAT3, did not promote programmed cell death in melanoma cells. Additionally, in the context of normal cells, MDA-7/IL-24 was found to bind to its cognate (IL-20/IL-22) receptors and induce phosphorylation of STAT3 without initiating apoptosis. Experiments to define the role of PKR in this process indicated a lack of dependence on this signaling pathway in melanoma cells for MDA-7/IL-24 to induce apoptosis. These experiments provide further insight into MDA-7/IL-24 "antitumor bystander" activity and suggest that, at least in human melanoma cells, this process occurs by a receptor-mediated process and by pathways that are STAT3 and PKR independent.

In patients, *mda*-7/IL-24 is currently administered by intratumoral injections using a conventional type 5 adenovirus vector that is replication incompetent, Ad.*mda-7* (INGN 241) (Fisher et al., 2003; Cunningham et al., 2005; Fisher, 2005; Lebedeva et al., 2005a; Tong et al., 2005). In this adenovirus, the cytomegalovirus promoter controls *mda*-7/IL-24 gene expression. This will result after Ad.*mda-7* infection of both normal and tumor cells with secretion of MDA-7/IL-24 protein, which would be predicted to be self-limiting in cancer cells (because they will undergo apoptosis) but continuous in normal cells [as long as the Ad.*mda-7* (INGN 241) persists]. Su et al. (2005c) used several experimental protocols to investigate the role of MDA-7/IL-24 protein secreted by normal and cancer cells in the "antitumor bystander" activity of this novel cytokine. (1) Agar diffusion overlay assays were employed to define the effect of infecting normal cells with Ad.*mda-7* on the anchorage-independent growth of tumor cells. (2) Matrigel invasion assays were used to determine the ability of Ad.*mda-7* infection of normal cells to impact on the invasiveness of co-cultivated tumor cells. (3) The effect of co-cultivation of normal–cancer and cancer–cancer cells on cell survival following infection of one of the co-cultivating pair with Ad.*mda-7* was used to determine the role of normal versus tumor cell secreted MDA-7/IL-24 on tumor cell survival. Human cervical cancer (HeLa) cells, engineered to produce green fluorescence protein (GFP), facilitated these assays permitting the fate, that is, induction of apoptosis, of these tumor cells to be monitored by FACS analyses. (4) The effect of secreted MDA-7/IL-24 on agar (anchorage-independent) growth of *mda*-7/IL-24- and radiation-sensitive and -resistant prostate cancer cells in the presence or absence of radiation were evaluated using the agar diffusion overlay assay. These studies, in combination with assays designed to determine mRNA levels of the IL-20R1, IL-20R2, and IL-22R1 receptor subunits and STAT3 activation, confirm a role for functional IL-20/IL-22 receptor complexes in mediating the various "antitumor bystander" effects of MDA-7/IL-24 (Su et al., 2005c). Additionally, these experiments document and confirm several relevant aspects of the "antitumor bystander" effect of MDA-7/IL-24, including the following: (1) demonstrating a self-limiting role of MDA-7/IL-24 produced by cancer cells (which undergo apoptosis) and a more protracted

role of MDA-7/IL-24 produced by normal cells (which do not undergo apoptosis) in inducing apoptosis in co-cultivation experiments; (2) an ability of the combination of secreted MDA-7/IL-24 and radiation to promote antitumor activity not only in *mda*-7/IL-24- and radiation-sensitive cancer cells, but also in prostate tumor cells overexpressing the anti-apoptotic proteins, *bcl-2* or *bcl-X_L* (Lebedeva et al., 2003a), and displaying resistance to either agent alone; and (3) an ability to use a cell-type-specific promoter, in our studies the excitatory amino acid transporter 2 (EAAT2) promoter (Su et al., 2003b; Rothstein et al., 2005; Sitcheran et al., 2005), to target expression of *mda*-7/IL-24 in astrocytes resulting in the secretion of MDA-7/IL-24 that affects agar growth and sensitivity to radiation of malignant human glioma cells (Su et al., 2005c). These innovative studies support a novel approach for using *mda*-7/IL-24, by targeting expression in normal target cells, to produce a constant supply of MDA-7/IL-24 protein in a local organ environment, as well as systemically, to enhance the therapeutic applications of this novel cytokine not only in the context of organ-defined disease, but also for treating metastases.

16. Melanoma differentiation associated gene-7/interleukin-24 inhibits invasion and migration of cancer cells

Tumor development and metastasis are complex processes mediated by changes in cancer cell physiology and biochemistry that frequently occur in a temporal manner during the process of tumor progression (Fisher, 1984; Fidler, 2002; Fidler et al., 2002; Onn & Fidler, 2002). Key components of tumor progression that contribute to the metastatic phenotype are tumor cell invasion and migration (Fidler, 2002; Fidler et al., 2002; Onn & Fidler, 2002). The ability of *mda*-7/IL-24 to affect tumor cell invasion has been evaluated in the context of direct viral administration of this cytokine gene to tumor cells (Ramesh et al., 2004; Sauane et al., 2004b) and in experiments analyzing the putative "antitumor bystander" role of MDA-7/IL-24 secreted by normal cells (Su et al., 2005c). In the case of C8161 metastatic human melanoma cells, *mda*-7/IL-24 administered by adenovirus (Ad.*mda-7*) inhibited invasion through Matrigel without altering cell viability (Fig. 9) (Sauane et al., 2004b). This effect did not require secretion of *mda*-7/IL-24

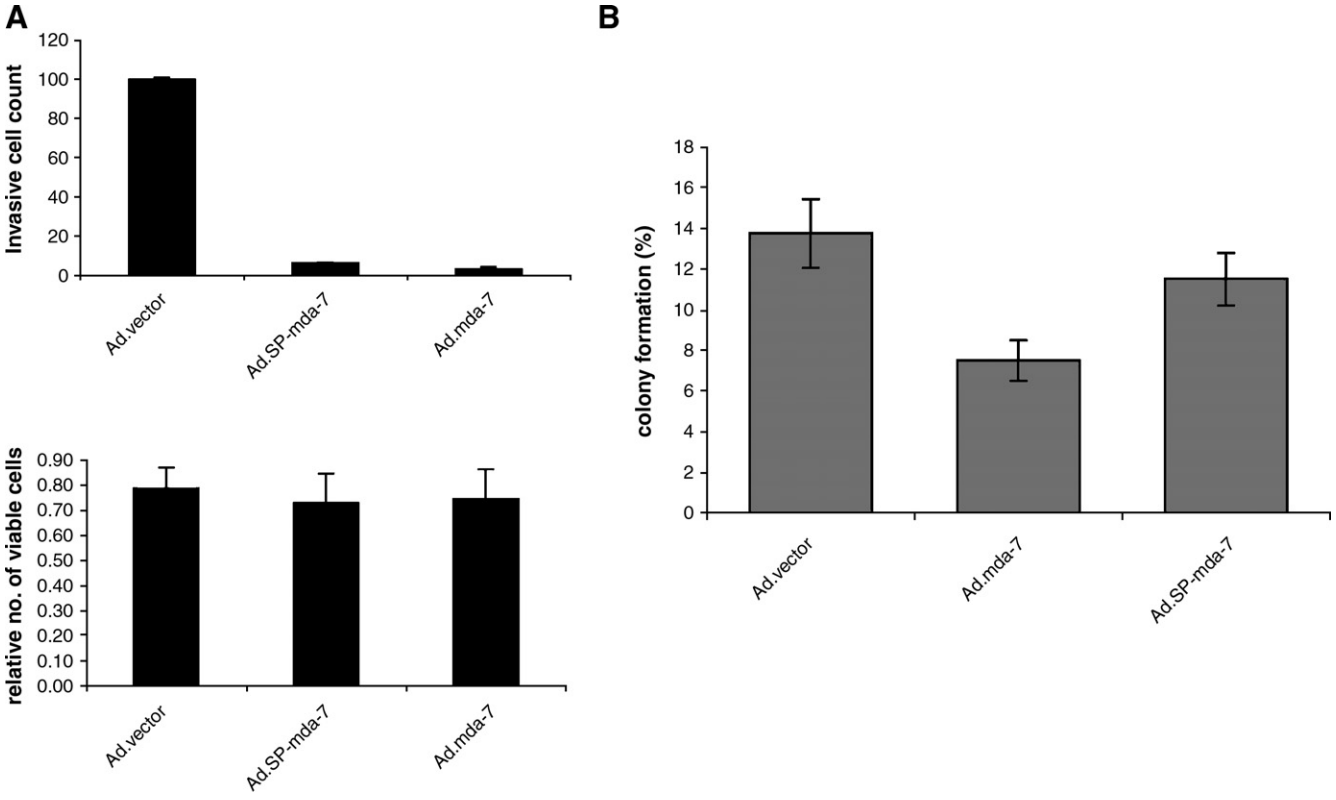

Fig. 9. Comparative mechanism of *mda-7*/IL-24 action after infection of various cell lines with Ad.vec, Ad.*mda-7*, and Ad.SP-*mda-7* (adenovirus expressing an *mda-7*/IL-24 cDNA lacking the signal peptide). (**A**) *mda-7*/IL-24 inhibits C8161 Matrigel invasiveness without altering C8161 viability. C8161 cells were infected with 100 pfu/cell of Ad.vec, Ad.*mda-7*, or Ad.SP-*mda-7*. After 24 hr, 1×10^6 cells were allowed to invade for 48 hr through transwell inserts (8-μm pores) coated with Matrigel. The cells that invaded through the Matrigel-coated inserts were stained, counted, and photographed under a light microscope at ×20 magnification. Cell viability was determined by the 3-(4,5-dimethylthiazol-2-yl)-2,5-diphenyltetrazolium bromide assay in parallel to ascertain whether the inhibition of invasion was associated with a decrease in growth or viability of infected C8161 cells, bars, ±SD. Direct cell counts were performed on all surviving, attached cells in the lower chamber to quantitate the relative efficiency of invasiveness. (**B**) "Bystander" suppression of anchorage-independent growth of DU-145 cells after adenovirus infection of P69 cells. P69 cells were seeded at 2×10^5/6-cm plate, infected 24 hr later with 25 pfu/cell of Ad.vec, Ad.*mda-7*, or Ad.SP-*mda-7* and overlaid with 1×10^5 DU-145 cells suspended in 0.4% agar. Fourteen days later, with agar medium feeding every 4 days, the number of anchorage-independent DU-145 colonies >2 mm was enumerated microscopically. Average number of colonies ± SD from triplicate plates. Qualitatively similar results were obtained in 2 additional studies. pfu, plaque-forming unit; IL, interleukin (reproduced, by permission of the publisher, from Sauane et al., 2004b).

because administering *mda*-7/IL-24 by means of an adenovirus expressing a signal peptide-deleted gene construct (Ad.SP-*mda-7*) was as effective as the native gene product in blocking invasion of C8161 cells (Fig. 10) (Sauane et al., 2004b). In the case of human A549 (non-small cell lung carcinoma) and H1299 (large cell lung carcinoma) cell lines, infection with Ad.*mda-7* inhibited invasion and migration prior to inducing cell death (Ramesh et al., 2004). This anti-invasion and anti-migration effect was comparable in these 2 cancer cell lines to that observed when these cells were treated with the phosphatidylinositol 3-kinase (PI3K) inhibitor LY294002 or with a matrix metalloproteinase II inhibitor. Analysis of gene expression changes indicated down-regulation of specific genes associated with invasion by Ad.*mda-7*, including PI3K/protein kinase B, focal adhesion kinase, and matrix metalloproteinase-2 (MMP-2) and metalloproteinase-9 (MMP-9). Decreased MMP-2 and MMP-9 expressions following Ad.*mda-7* infection of A549 and H1299 cells were confirmed by zymography and Western blot analyses and a decrease in metastasis was observed following injection of A549 cells infected with Ad.*mda-7* into nude mice (Ramesh et al., 2004).

Studies performed to evaluate the "antitumor bystander" effect of MDA-7/IL-24 secreted by normal cells indicated that functional IL-20/IL-22 receptors were necessary for this cytokine to inhibit tumor cell invasion (Su et al., 2005c). Co-cultivation of immortal normal P69 prostate epithelial cells infected with Ad.*mda-7* with DU-145 (prostate carcinoma cells) or BxPC-3 (pancreatic carcinoma cells), which have a full-repertoire of IL-20/IL-22 receptors on their surface, but not A549 cells, which lack complete receptors for MDA-7/IL-24, inhibited invasion through Matrigel. These results argue that the ability of *mda*-7/IL-24 to affect distant tumor cells, by means of its "antitumor bystander" effect, will be dependent on the presence of canonical receptors for MDA-7/IL-24 on secondary tumor cells. This raises the question as to whether the cytokine antitumor effects of MDA-7/IL-24 will be diminished when using this gene in the context of specific patient cancers, should their primary or secondary tumor cells lack appropriate receptors for MDA-7/IL-24. This will most likely not be the case because the vast majority of cancer cells, as well as normal cells, contain functional IL-22/IL-24 receptors (Sauane et al., 2003a; Chada et al., 2004a, 2004b; Su et al., 2005c). Moreover, the ability of *mda*-7/IL-24 when administered directly to cancer cells by virus and the use of a GST-MDA-7 fusion protein can still induce tumor-specific cell killing by an intracellular mechanism (Sauane et al., 2004a, 2004b).

17. Melanoma differentiation associated gene-7/interleukin-24 enhances the sensitivity of cancer cells to radiation, chemotherapy and monoclonal antibody therapies

Infection of human lung cancer cell lines, including A549 (wild-type p53 and wild-type RB1) and H1299 (deleted p53 and wild-type RB1), with Ad.*mda-7* increases their sensitivity

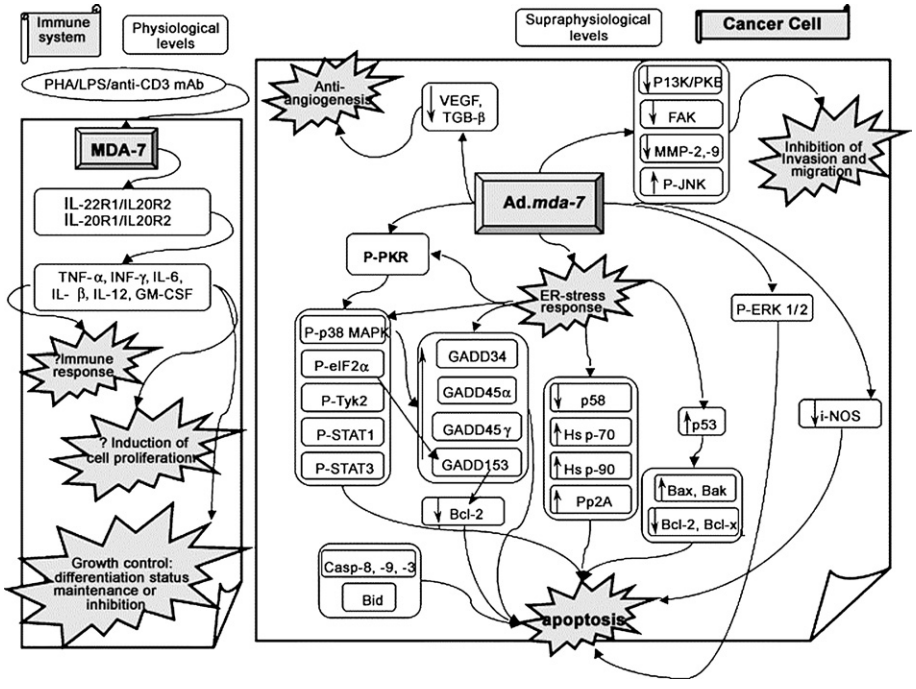

Fig. 10. Overview of the signaling pathways associated with Ad.*mda-7* and MDA-7/IL-24 activity in cancer cells and in the immune system. Abbreviations: P, phosphorylation; PHA, phytohemagglutinin; LPS, lipopolysaccharide; IL, interleukin; TNF-α, tumor necrosis factor alpha; IFN-γ, interferon-γ; GM-CSF, granulocyte macrophage-colony stimulating factor; VEGF; vascular endothelial growth factor; TGF-β, transforming growth factor-β; PI3K/PKB, phosphatidylinositol 3-kinase/protein kinase B; FAK, focal adhesion kinase; MMP, matrix metalloproteinase; PKR, double-stranded RNA-dependent protein kinase R; MAPK, mitogen-activated protein kinase; eIF2α, eukaryotic translation initiation factor-2α; Tyk2, tyrosine kinase-2; STAT, signal transducer and activator of transcription; GADD, growth-arrest and DNA-damage inducible; Hsp, heat shock protein; Pp2A, protein phosphatase-2A; iNOS, inducible nitric oxide synthase (reproduced, by permission of the publisher, from Lebedeva et al., 2005a).

to radiation (Kawabe et al., 2002). In contrast, a similar effect of radiation was not observed in normal lung fibroblast cell lines, CCD-16 and MRC-9 (Kawabe et al., 2002). The combination of Ad.*mda-7* and radiation resulted in ~38% TUNEL-positive cells, whereas radiation and Ad.*mda-7* infection alone resulted in ~10% and ~18% TUNEL-positive cells, respectively. These results confirm that Ad.*mda-7* increases the radiosensitivity of non-small cell lung and large cell lung carcinoma cells resulting in enhanced apoptosis (Kawabe et al., 2002). Radiation activates the c-jun N-terminal MAP kinase (JNK) pathway and the levels of c-jun and JNK proteins raising the possibility that Ad.*mda-7* mediates radiosensitivity and enhances apoptosis through activation of JNK kinase and subsequent activation of c-jun protein (Kawabe et al., 2002). This observation is seen predominantly in the context of radiosensitization studies because induction of JNK by *mda-7*/IL-24 is not readily observed in most cells in the absence of radiation. This enhancement of radiosensitization is independent of the p53, Fas, and BAX status in lung cancer cell lines (Kawabe et al., 2002).

Recent studies by our groups have revealed that treatment of malignant gliomas, both rat and human, with purified GST-MDA-7 fusion protein or infection with Ad.*mda-7* also sensitizes these tumor cells to radiation induced growth suppression and apoptosis (Su et al., 2003a; Yacoub et al., 2003b, 2003c, 2004; Sauane et al., 2004a; Dent et al., 2005). Ad.*mda-7* infection induced growth suppression and apoptosis in human malignant gliomas expressing both mutant and wild-type p53, and these effects correlated with enhanced expression of members of the GADD gene family (Su et al., 2003a). This effect differed from that observed using an adenovirus to deliver wild-type p53 (Ad.*wtp53*), in which biological (growth suppression and induction of apoptosis) and GADD gene family induction effects were restricted to malignant gliomas containing a mutant p53 gene. In the context of normal human primary fetal astrocytes, Ad.*mda-7* and Ad.*wtp53* were significantly less growth inhibitory than in malignant gliomas and no toxicity was apparent. When malignant gliomas (containing a wild-type or mutated p53 gene) were infected with Ad.*mda-7* or treated with a GST MDA-7/IL-24 fusion protein, GST-MDA-7, sensitivity to ionizing radiation's growth inhibitory and antisurvival effects correlated with increased expression of specific members of the GADD gene family. Based on the observation that heterogeneity of p53 expression is a common event in evolving gliomas, these findings suggest that in specific contexts *mda*-7/IL-24 may prove superior as a gene-based therapy for malignant gliomas, both with and without irradiation, than administration of wild-type p53.

Studies by Yacoub et al. (2003b, 2004) extended the findings of Su et al. (2003a), confirming that both Ad.*mda-7* and GST-MDA-7 reduce proliferation and decrease survival of human and rat malignant gliomas and these effects were increased in a greater than additive fashion. These cellular changes, which were not observed in cultures of non-transformed primary astrocytes, correlated with enhanced numbers of cells in the G_1/G_0 and G_2/M phases of the cell cycle, implying that Ad.*mda-7* radiosensitizes glioma cells in a cell-cycle-independent manner. Decreased growth correlated with increased necrosis and DNA degradation, suggesting that the combination of agents alters survival of malignant glioma cells by mechanisms involving both apoptosis and necrosis. A single infection with Ad.*mda-7* enhanced p38 and ERK 1/2 activity without altering JNK or Akt activity. When cells containing *mda*-7/IL-24 were irradiated, ERK 1/2 activity was suppressed while JNK 1/2 activity was enhanced, without altering either Akt or p38 activity. Moreover, abolishing JNK 1/2, but not p38, signaling extinguished the radiosensitizing properties of MDA-7/IL-24. In contrast, inhibition of neither ERK 1/2 nor PI3K signaling enhanced the anti-proliferative effects of Ad.*mda-7*, whereas combined inhibition of both pathways enhanced cell killing, suggesting that ERK and PI3K signaling can be protective against MDA-7/IL-24 lethality in specific cell contexts.

Ad.*mda-7* as well as GST-MDA-7 synergizes with radiation-induced free radicals, which further reduces the expression of the anti-apoptotic protein BCL-X_L and enhances expression of BAX protein leading to enhanced radiosensitivity in vitro (Yacoub et al., 2003b). This effect, induction of BAX protein following combination treatment with MDA-7/IL-24 and radiation in malignant rat and human glioma cells, was not evident in NSCLC cell lines (Kawabe et al., 2002). Forced expression of Bcl-X_L (administered by adenovirus transduction) protected RT2 (rat malignant glioma) cells from growth suppression and loss of viability induced by the combination of Ad.*mda-7* and ionizing radiation (Yacoub et al., 2003c). *N*-acetyl-L-cysteine (NAC), an antioxidant, inhibited the anti-proliferative interaction between *mda*-7/IL-24 and radiation in RT2 cells, suggesting that radiation-induced free radicals cooperates with changes induced by *mda*-7/IL-24 to enhance mitochondrial dysfunction thereby contributing to apoptosis (Yacoub et al., 2003b, 2003c). Infection of RT2 cells with Ad.*mda-7* prior to intracranial injection into the brains of Fischer 344 rats increased survival following 6 Gy of ionizing radiation in comparison with animals receiving only radiation or animals infected with Ad.*vec* (lacking the *mda-7*/IL-24 gene) or Ad.*mda-7* (which by itself enhanced survival, above Ad.*vec* or radiation treatment alone) (Yacoub et al., 2003c). Additional studies are required to understand the mechanism by which JNK and c-jun proteins are activated by Ad.*mda-7* or GST-MDA-7 and how this gene causes radiosensitization of malignant glioma cells thereby facilitating killing of these cancer cells both in vitro and in vivo.

To further evaluate the effects of GST-MDA-7 and ionizing radiation on malignant glioma cells, experiments were performed using primary (non-established) human glioblastoma multiforme (GBM) cells (Yacoub et al., 2004). For this study, a spectrum of primary GBM cells were chosen, including ones expressing mutated PTEN and p53 proteins, activated ERBB VIII, overexpressing wild-type ERBB1, or without receptor overexpression. GST-MDA-7 produced a dose-dependent decrease in proliferation of primary glioma cells, whereas viability was only decreased at high concentrations of this purified protein. Irradiation enhanced these effects in a greater

than additive manner, which was also dependent on JNK 1/2/3 activation. As observed in RT2 cells, the enhancement of killing by radiation and GST-MDA-7 was blocked by NAC (a ROS scavenger), a JNK 1/2/3 inhibitor (SP600125), a pan-caspase inhibitor (zVAD), and an inhibitor of caspase 9 (LEHD), but not by an inhibitor of caspase 8 (IETD). The combination of low concentrations of irradiation or GST-MDA-7 also decreased clonogenic survival of GBM cells, which was enhanced when both agents were employed together and blocked by inhibition of caspase 9 functions. In concordance with activation of the intrinsic caspase pathway, cell death correlated with reduced Bcl-X_L expression and with elevated levels of the pro-apoptotic proteins BAD and BAX. Inhibition of caspase 9 after combination treatment blunted neither JNK 1/2/3 activation nor the enhanced expression of BAD and BAX expression. These findings support an hypothesis that after combination treatment JNK 1/2/3 activation is a primary pro-apoptotic event and loss of BCL-X_L expression and ERK 1/2 activity are secondary caspase-dependent processes. These data also argue that GST-MDA-7 induces 2 overlapping pro-apoptotic pathways via ROS-dependent and -independent mechanisms. In total, these findings demonstrate that MDA-7/IL-24 reduces proliferation and enhances the radiosensitivity of non-established human GBM cell in vitro and that sensitization occurs independently of basal EGFR/ERK1/2/AKT activity or the functions of PTEN or p53.

Studies were performed to determine the effect of GST-MDA-7 alone and in combination with radiation on the growth and viability of human breast cancer cells (Sauane et al., 2004a). When applied to MDA-MB-231 (mutant p53) breast carcinoma cells, GST-MDA-7 induced a dose-dependent decrease in viability as determined by MTT assays. Additionally, growth suppression by GST-MDA-7 was enhanced in a greater than additive fashion when combined with radiation. These studies were extended to include additional breast cancer and normal immortal breast epithelial (HBL-100) cells. Whereas no significant change in viability or growth was apparent in HBL-100 cells treated with GST-MDA-7, decreased growth and viability was observed in breast carcinoma cells that were independent of their p53 status; that is, in MCF-7 (wild-type p53), T47D (mutant p53), and MDA-MB-157 (null for p53) cells.

In human prostate cancer cells, a role for mitochondrial dysfunction and induction of reactive oxygen species in the apoptotic process has been documented. Ectopic overexpression of *bcl-X_L* and *bcl-2* prevents these changes including apoptosis induction in prostate tumor cells by Ad.*mda-7* (Lebedeva et al., 2002, 2003a, 2003c). Recent studies document that resistance to apoptosis can be reversed by treating *bcl-2* family overexpressing prostate tumor cells with ionizing radiation in combination with Ad.*mda-7* or purified GST-MDA-7 protein (Su et al., in press). Additionally, radiation augments apoptosis induction by *mda-7*/IL-24 in parental neomycin-resistant prostate tumor cells. Radiosensitization to *mda-7*/IL-24 is dependent on JNK signaling because treatment with the JNK 1/2/3 inhibitor SP600125 abolishes this effect. Because elevated expression of *bcl-X_L* and *bcl-2* are frequent events in prostate cancer development and progression, these studies support the use of ionizing radiation in combination with *mda-7*/IL-24 as a means of augmenting the therapeutic benefit of this gene in prostate cancer, particularly in the context of tumors displaying resistance to radiation therapy due to *bcl*-2 family member overexpression.

The studies described briefly above indicate that MDA-7/IL-24 promotes radiation sensitivity in a wide spectrum of human cancers, including NSCLC, malignant gliomas, breast carcinomas, and prostate carcinomas. This diversity of targets suggests that employing MDA-7/IL-24 with ionizing radiation may provide a means of enhancing the therapeutic benefit of this multifunctional cytokine. It would be of immense clinical importance to better understand the mechanism of *mda-7*/IL-24-induced radiosensitization to treat cancers where radiotherapy may only provide minimum benefit, whereas the combination of *mda-7*/IL-24 and radiation may provoke a significant therapeutic response.

A recent study by Nishikawa et al. (2004) demonstrated that a combination of ionizing radiation and Ad.*mda-7* resulted in a substantial and long-lasting suppression of A549 NSCLC tumor growth in nude mice. This represents an interesting model because A549 cells to not contain a full complement of IL-20/IL-22 receptors (Chada et al., 2004a; Su et al., 2005c), making them resistant to “antitumor bystander” activity of secreted MDA-7/IL-24 (Chada et al., 2004a; Su et al., 2005c). Suppression of tumor growth by administering MDA-7/IL-24 by Ad.*mda-7* intratumorally into A549 xenograft tumors in animals in combination with ionizing radiation correlated with a reduction of angiogenic factors [basic fibroblast growth factor (bFGF), vascular endothelial growth factor (VEGF)] and microvessel density, which exceeded that observed with Ad.*mda-7* or radiation alone. Using soluble MDA-7/IL-24 (sMDA-7/IL-24) from 293 cells and in vitro assays, HUVECs were sensitized to radiation, whereas A549 cells and normal human lung fibroblasts were not affected. Similarly, infection of normal human cells with Ad.*mda-7* resulted in secretion of MDA-7/IL-24 that can inhibit tumor cell invasion and synergize with radiation in decreasing tumor cell growth in agar in cells that contain a complete set of functional IL-20/IL-22 receptors, but not in A549 tumor cells lacking appropriate receptors for MDA-7/IL-24 (Su et al., 2005c). These studies confirm that Ad.*mda-7* in combination with radiation can enhance apoptosis and sMDA-7/IL-24 can inhibit angiogenesis by sensitizing endothelial cells to ionizing radiation without affecting normal cells. These observations are interesting and provide further support for the use of a combination of MDA-7/IL-24 with radiation, which would in principle override resistance in tumor cells that lack complete IL-20/IL-22 receptors by targeting their tumor vasculature and inhibiting angiogenesis.

Recent studies document that the non-steroidal anti-inflammatory drug sulindac can augment the antitumor activity of Ad.*mda-7* in the context of human non-small cell lung carcinoma cells (Oida et al., 2005). The combination of

sulindac and Ad.*mda-7* promoted growth suppression and apoptosis in A549 and H1299 human lung cancer cells. This enhancement effect of Ad.*mda-7* was dose dependent for sulindac in the cancer cells, whereas no growth inhibitory or apoptotic effect was evident in normal human lung fibroblasts (CCD-16). The mechanism underlying this synergy was intriguing, in that sulindac increased expression of ectopic MDA-7/IL-24 protein in tumor cells, thereby elevating downstream targets of this cytokine in lung cells, including PKR, p38 MAPK, caspase-9, and caspase-3. Pulse-chase studies suggested that the increase in MDA-7/IL-24 protein in sulindac-treated cells was a consequence of elevated half-life of this protein. The combination of sulindac and Ad.*mda-7* also resulted in enhanced suppression in human lung tumor growth in nude mice as compared to a single treatment with either agent. This process also reflected an increased half-life of MDA-7/IL-24 protein. This study by Oida et al. (2005) supports the use of *mda-7*/IL-24 with other agents, in this case the drug sulindac, to enhance its therapeutic activity.

McKenzie et al. (2004) investigated the effect of Ad.*mda-7* in combination with Herceptin (Trastuzumab), an anti-$p185^{ErbB2}$ murine monoclonal antibody (4D5) that binds to the extracellular domain of ErbB2 and down-regulates expression of cell surface ErbB2 proteins, on Her-2/neu-overexpressing breast cancer cells. This combination treatment resulted in decreased levels of β-catenin, Akt, and phosphorylated Akt as compared with single treatment with Ad.*mda-7* or Herceptin. Additionally, in vivo studies in nude mice injected with MCF-7-Her-18 cells, in their thoracic mammary fat pads, indicated that the combination of Ad.*mda-7* plus Herceptin enhanced suppression in tumor growth of established Her-2/neu-overexpressing tumors to a greater extent than treatment with only Ad.*mda-7* or Herceptin. These studies suggest that a combination of Ad.*mda-7* plus Herceptin would be more efficacious for the therapy of Her-2/neu-overexpressing breast cancer than a single treatment modality. Although further studies are needed, this combinatorial effect could be a consequence of targeted inhibition of β-catenin and Akt pathways that are important in breast cancer cell growth.

18. Anti-angiogenic activity of melanoma differentiation associated gene-7/interleukin-24

A critical component of cancer development and tumor progression involves development of an adequate blood supply to insure survival of primary and secondary (metastatic) tumors (Folkman, 1996, 2002, 2003; Fidler et al., 2002). This process is dependent on the generation of new blood vessels, angiogenesis, which contributes to many pathological conditions (Folkman, 1996, 2001, 2002, 2003; Fidler et al., 2002). Key components of angiogenesis involve secreted factors, including primarily vascular endothelial growth factor (VEGF) as well as basic fibroblast growth factor (bFGF), platelet-derived growth factor (PDGF), and interleukin-8 (Fidler et al., 2002; Folkman, 2002, 2003). Defining ways of inhibiting this process, including approaches targeting the angiogenic factor itself or its receptors as well as the tumor vasculature, has now become a major focus for anticancer therapy, which has recently culminated in numerous clinical studies (Hegeman et al., 2004; Purow & Fine, 2004; Hoff, 2005). In this context, agents that can impact on the angiogenic process offer potential as significant therapeutic modalities for treating both primary and metastatic tumors.

Studies by Ramesh et al. (Saeki et al., 2002; Ramesh et al., 2003, 2004; Nishikawa et al., 2004) have demonstrated a unique aspect of *mda-7*/IL-24 action, an ability to inhibit angiogenesis. Initial studies in the context of human vascular endothelial cells (HUVECs) and A549 (NSCLC) and H1299 (large cell lung carcinoma) lung cancer cells demonstrated that Ad.*mda-7* had anti-angiogenic properties (Saeki et al., 2002). Infection of HUVEC cells, involved in new blood vessel formation, with Ad.*mda-7* inhibited endothelial tube formation, without affecting cell viability. When tested in in vivo animal models, containing injected A549 or H1299 cells, Ad.*mda-7* infection decreased tumor formation and this effect correlated with a decrease in CD31 expression, a marker of neoangiogenesis. These provocative studies supported the possibility that in addition to the ability of Ad.*mda-7* to induce apoptosis in tumor cells in animals, it also had the capacity to alter blood vessel formation, that is, it was an inhibitor of angiogenesis.

A more detailed follow-up study by Ramesh et al. (2003) confirmed that MDA-7/IL-24 secreted from a 293 cell clone transformed with a full-length *mda-7*/IL-24 cDNA, sMDA-7/IL-24, could regulate angiogenesis and this effect was dependent on the IL-22 receptor (Ramesh et al., 2003). Application of sMDA-7/IL-24 to endothelial cells in vitro inhibited their differentiation into tubes and their migration when exposed to VEGF or bFGF. This inhibitory effect surpassed that of endostatin, gamma interferon and IP-10 (interferon-inducible protein 10). Interferon alpha and beta that exhibit strong anti-angiogenic activity (Fidler et al., 2002; Folkman, 2002; Pestka, 2003) were not compared with MDA-7/IL-24. This activity of MDA-7/IL-24 was shown to involve the IL-22 receptor because blocking antibody to IL-22 receptor combined with sMDA-7/IL-24 inhibited VEGF-induced angiogenesis as shown by reduced vascularization and hemoglobin content in an in vivo Matrigel plug assay. When A549 cells were mixed with 293 cells producing sMDA-7/IL-24, tumor growth in vivo in nude mice was inhibited. Similarly, systemic administration of sMDA-7/IL-24 also inhibited lung tumor growth in a mouse xenograft model. This reduction in tumor growth correlated with a decrease in tumor microvessel density and hemoglobin content, supporting the concept of anti-angiogenic activity of MDA-7/IL-24. In this context, one would anticipate that *mda-7*/IL-24 may exert its antitumor properties in vivo by evoking multiple pathways, including direct cancer cell apoptosis, inhibition of angiogenesis, and as discussed previously modulation of immune responses (Fig. 10).

19. Phase I clinical studies with Ad.*mda-7* (INGN-241) indicate safety and clinical efficacy

mda-7/IL-24 has now reached a critical juncture relative to its evolution as a potential gene therapy for cancer. This novel

cytokine, administered by a replication incompetent adenovirus (Ad.*mda-7*; INGN 241), has been injected intratumorally in patients with advanced carcinomas and melanomas (Fisher et al., 2003; Cunningham et al., 2005; Lebedeva et al., 2005a; Tong et al., 2005). These studies, which will be expanded on below, indicate that *mda-7*/IL-24 is safe and provides evidence of clinically significant activity. Moreover, much of the responses observed in vitro and in animal tumor models have now been recapitulated in the context of patients. These early successes in patients suggest that *mda-7*/IL-24 has considerable potential as an effective gene therapy for multiple cancers.

Preclinical animal modeling studies confirmed that Ad.*mda-7* had potent growth inhibiting and apoptosis-inducing properties in various tumor models (Su et al., 1998; Madireddi et al., 2000c; Gopalkrishnan, 2002; Ramesh et al., 2003), supporting its potential as a gene therapeutic for cancer. In comparison with existing anticancer drugs, Ad.*mda-7* has distinct advantages, including the following: (1) robust activity toward a spectrum of genetically diverse cancers; (2) a defined dose–response pharmacologic relationship; (3) no apparent toxicity toward a wide array of normal human or rat cells; (4) novel mechanism of action that exploits multiple defects in cancer cell physiology resulting in induction of programmed cell death; and (5) ability to generate a profound "antitumor bystander" effect (reviewed in Fisher et al., 2003; Fisher, 2005; Lebedeva et al., 2005a). Additionally, *mda-7*/IL-24 is a potent inhibitor of angiogenesis, a profound stimulator of radiation sensitivity and an immune modulator, all of which may contribute further to its significant in vivo therapeutic properties.

To define safety and biologic activity of *mda-7*/IL-24, a Phase I clinical trial was conducted using intratumoral injections of Ad.*mda-7* (IL-24; INGN 241) in 28 patients with resectable solid tumors (Cunningham et al., 2005). In all cases, injected lesions demonstrated Ad.*mda-7* vector transduction, *mda-7*/IL-24 mRNA, MDA-7/IL-24 protein, and apoptosis induction, with greatest concentration and activity near the injection site (Fig. 11 and data not shown) (Cunningham et al., 2005; Lebedeva et al., 2005a). Ad.*mda-7* (INGN 241) vector DNA and mRNA were readily detected more than 1 cm from the injection site (Fig. 11), whereas MDA-7 protein and bioactivity were more widely disseminated. Minimal and mild self-limiting toxicity, attributable to the injections, were apparent in most patients. Of relevance, evidence of clinical activity was apparent in 44% of lesions receiving repeated injections, including complete and partial responses in 2 melanoma patients. Thus, intratumoral administration of Ad.*mda-7* (INGN 241) is apparently well tolerated, induces programmed cell death (apoptosis) in a predominant percentage

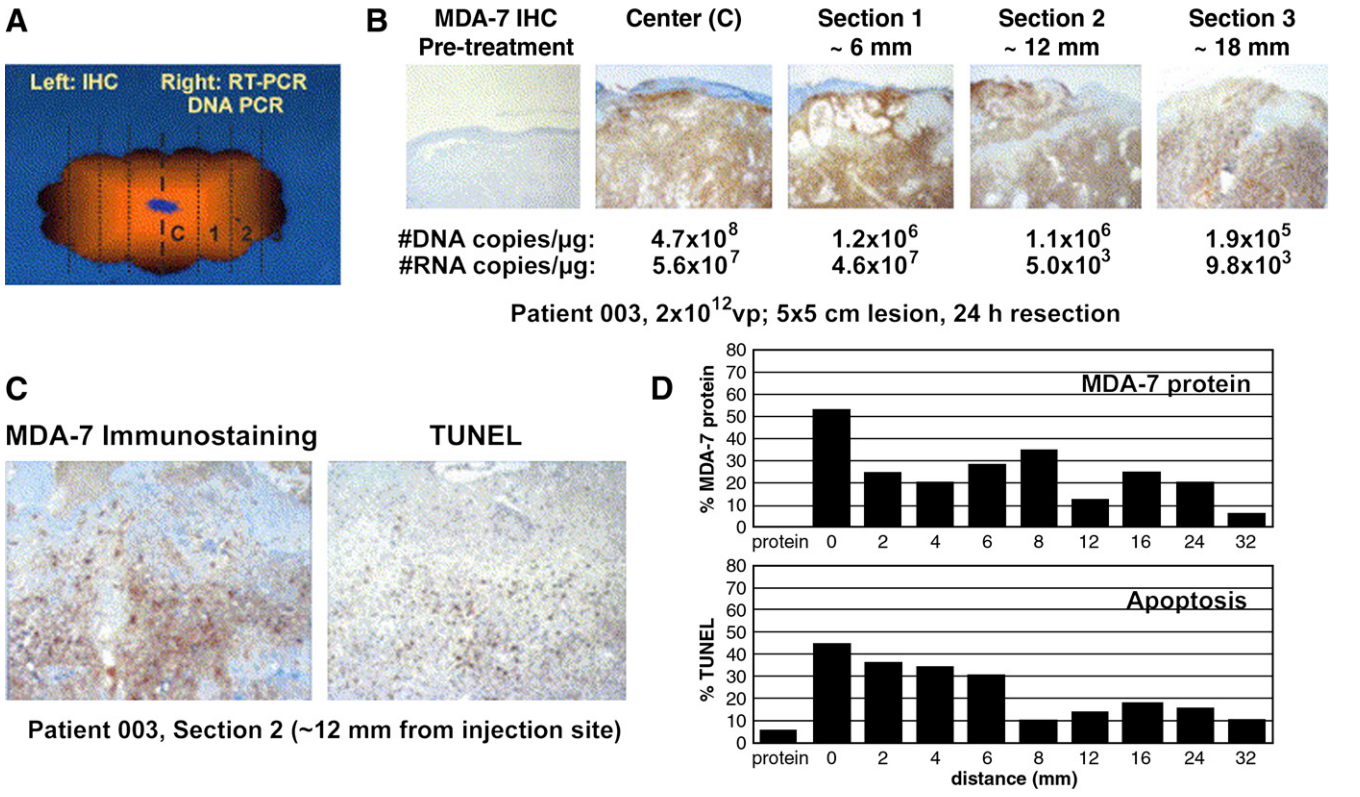

Fig. 11. Spread of *mda-7*/IL-24 RNA, DNA, and protein and biological effects (apoptosis) 24 hr after intratumoral injection. (**A**) Schematic representation of serial sections of tumor. (**B**) Decay of INGN 241 (Ad.*mda-7*) vector at the injection site. Immunohistochemical staining of different tumor sections and the median numbers of DNA and RNA copies determined by PCR and RT-PCR, respectively, are shown for each section. (**C**) Spread of MDA-7/IL-24 protein and biological effect (apoptosis) at the injection site. Protein expression correlates with apoptosis. Serial sections from each tumor were evaluated for MDA-7/IL-24 expression and TUNEL reactivity using immunohistochemistry. (**D**) Data from TUNEL assay and immunohistochemistry are plotted to indicate signals compared to distance from injection site (reproduced, by permission of the publisher, from Lebedeva et al., 2005a).

of tumor cells and provides clinically noteworthy activity (Fisher et al., 2003; Cunningham et al., 2005; Lebedeva et al., 2005a).

Additional results of a Phase I dose-escalation clinical trial using Ad.*mda-7* (INGN 241) in 22 patients with advanced cancer was presented by Tong et al. (2005). Tumors injected with Ad.*mda-7* (INGN 241) were excised and evaluated for vector-specific DNA and RNA, MDA-7/IL-24 expression and biologic effects. Effective gene transfer was demonstrated in 100% of patients evaluated using DNA- and RT-PCR. These studies confirmed a dose-dependent penetration of Ad.*mda-7* (INGN 241) with parallel dispersion of vector DNA and RNA, MDA-7/IL-24 protein, and apoptosis induction in all tumors, with signals diminishing from the initial injection site. Support for bioactivity of injected *mda-7*/IL-24 was provided by documentation of elevated expression of putative MDA-7/IL-24 target genes, including β-catenin, iNOS, and CD31. Moreover, transient increases (up to 20-fold) were also apparent in the serum levels of IL-6, IL-10, and TNF-α. In the context of IL-6 and TNF-α induction, a direct relationship between the levels of these cytokines and clinical response to *mda-7*/IL-24 was indicated. Patients injected with Ad.*mda-7* (INGN 241) also displayed significant increases in $CD3^+CD8^+$ T-cells, supporting the suggestion that this treatment increased systemic T_H1 cytokine production and activated $CD8^+$ T-cells. These observations are consistent with preclinical features of MDA-7/IL-24 and support the potential immune modulatory as well as direct antitumor apoptosis properties of this cytokine in patients.

Taken together, the initial clinical studies using Ad.*mda-7* are exciting and provide optimism of the clinical utility of MDA-7/IL-24 for cancer therapy. However, very few if any therapeutic agents have been found to elicit a complete cancer cure. Only further studies will indicate if *mda-7*/IL-24 is an exception to this rule. Of import, a number of studies have documented that combining *mda-7*/IL-24 with other therapeutic modalities or agents can further augment its antitumor properties. This includes radiation (Kawabe et al., 2002; Su et

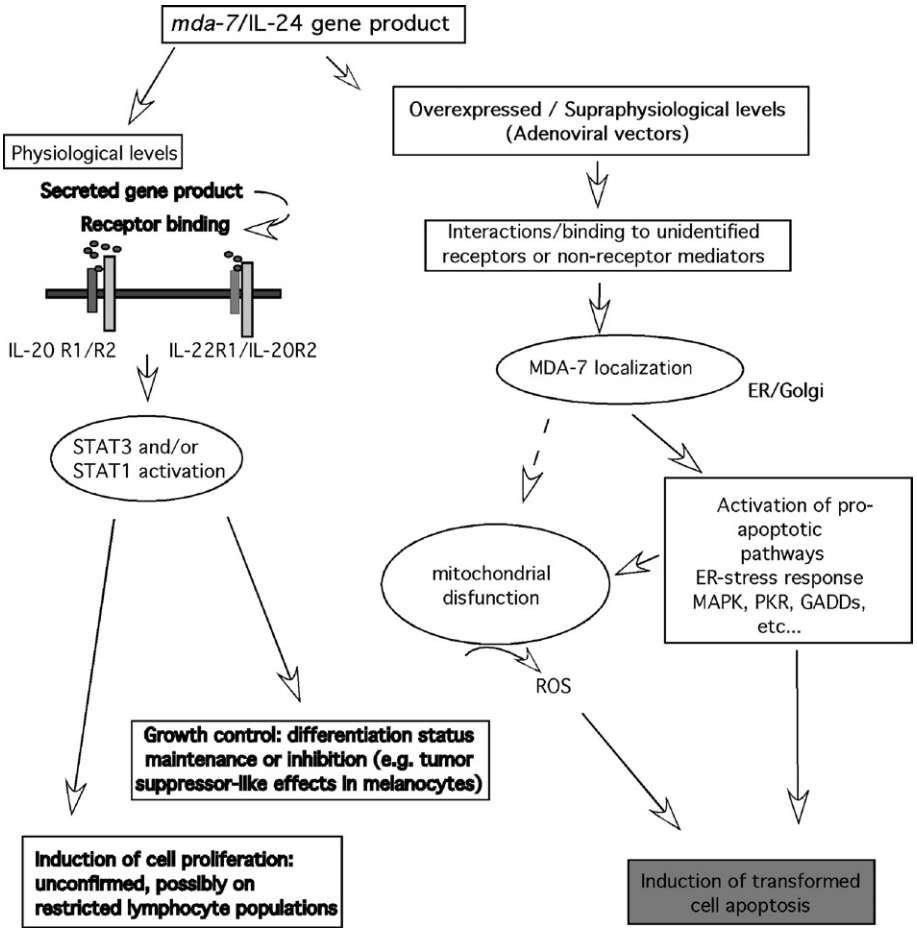

Fig. 12. Model illustrating the possible molecular basis of *mda-7*/IL-24 cancer cell-mediated apoptosis. The effects of known physiological and ectopic overexpression of *mda-7*/IL-24 are shown on left and right sides of the figure, respectively. Normally, *mda-7*/IL-24 binds to cognate receptors and activates STAT-1 and -3 transcription factors to mediate pathways affecting cell growth. Because *mda-7*/IL-24 mRNA and protein are normally seen in subpopulations of immune cells and melanocytes, effects are likely initiated in these cell types but might also affect neighboring non-producing cells because the protein is secreted. When normally or ectopically overexpressed, current findings indicate localization to the ER/Golgi compartments, whether or not the protein contains a secretory signal. Accumulation of MDA-7/IL-24 protein in this compartment triggers apoptosis that could apparently involve induction of pathways described currently as ER stress. However, MDA-7/IL-24 additionally acts indirectly on mitochondria to generate reactive oxygen species. A combination of pathways triggered by *mda-7*/IL-24 results in transformed cell-specific apoptosis. IL, interleukin; ER, endoplasmic reticulum; STAT, signal transducers and activators of transcription; ROS, reactive oxygen species (reproduced, by permission of the publisher, from Sauane et al., 2004b).

al., 2003a; Yacoub et al., 2003b, 2003c, 2004; Nishikawa et al., 2004) and recent reports indicating cooperativity between *mda-7*/IL-24 and monoclonal antibody therapy (McKenzie et al., 2004) and treatment with sulindac (Oida et al., 2005). Further studies are clearly necessary to determine if these and other agents will also result in enhanced therapeutic efficacy in patients, thereby improving the ability of *mda-7*/IL-24 to eradicate diverse cancers. Additionally, employing cancer-selective conditionally replicating adenoviruses to deliver *mda-7*/IL-24 has proven more active in vivo in animal models in inducing an antitumor response than using replication incompetent adenoviruses to deliver this cytokine (Sarkar et al., 2005; Zhao et al., 2005).

20. Concluding perspectives and future directions

In a short time frame, *mda-7*/IL-24 has progressed from a laboratory discovery to a potential therapy for cancer (Fisher, 2005). In this context, this distinctive molecule has become the focus of increasing scientific scrutiny. This intensive analysis has provided significant new insights into the multitude of properties of this molecule, confirming its selective antitumor apoptosis-inducing ability in vitro and in vivo in human tumor xenograft nude mouse tumor models, demonstrating anti-angiogenic properties, elucidating key signal transduction pathways and molecules mediating activity in specific cancers (including p38 MAPK, PKR, GADD gene induction, changes in the ratio of pro-apoptotic to anti-apoptotic proteins), demonstrating a unique ability to radiosensitize tumor cells and finally documenting safety and potential clinical efficacy in patients with advanced carcinomas and melanomas (specific aspects of *mda-7*/IL-24 have been reviewed in Sarkar et al., 2002a; Fisher et al., 2003; Sauane et al., 2003b; Chada et al., 2004b; Gopalkrishnan et al., 2004; Dent et al., 2005; Fisher, 2005; Lebedeva et al., 2005a). If anything, this rapid evolution in our knowledge has taught us to appreciate the complexity of action of *mda-7*/IL-24, culminating in the recent discovery that this gene can selectively kill cancer cells by a mechanism potentially independent of its cytokine properties, that is, by intracellular targeting and the stress response (Fig. 12). Although further studies are mandatory, it appears that *mda-7*/IL-24 is able to find kinks in the armor of most tumor cells and exploit inherent weaknesses to destroy these cancer cells (Fisher et al., 2003; Lebedeva et al., 2005a). Additionally, it can attack the fundamental lifeline of the cancer, blood vessel formation (angiogenesis) (Folkman, 1996, 2001, 2002, 2003; Fidler et al., 2002), providing an additional means of thwarting tumor growth and progression. Adding further to its potential clinical utility, *mda-7*/IL-24 is a potent sensitizer of cancer cells to radiation and chemotherapeutic agents (including specific drugs and monoclonal antibodies) (Kawabe et al., 2002; Lebedeva et al., 2003c, 2005b; Su et al., 2003a; Yacoub et al., 2003b, 2003c, 2004; McKenzie et al., 2004; Oida et al., 2005; Su et al., in press) and this secreted cytokine exerts potent "bystander" antitumor activity (increasing its range of action) (Su et al., 2001; Chada et al., 2004a; Su et al., 2005c). Finally, although not well understood, *mda-7*/IL-24 appears to embody potent immune modulating properties (Caudell et al., 2002; Fisher et al., 2003; Tong et al., 2005), providing still another method to quell tumor cell growth and spread. In these contexts, if one hoped to design the ideal anticancer gene therapy, a strong candidate would be *mda-7*/IL-24, which can obstruct cancer on many levels and by attacking it in so many ways may provide a means of developing a long-term effective therapy for this pervasive and debilitating malady of mankind. We are optimistic that the future will provide additional insights into the mechanism of action of this intriguing cytokine and with this knowledge will come ways of further enhancing the utility and efficacy of *mda-7*/IL-24 as a cancer gene therapeutic.

Acknowledgments

We are indebted to our numerous colleagues who have contributed to our understanding of *mda-7*/IL-24. The present studies were supported in part by National Institutes of Health grants CA35675, CA097318, CA098712, and P01 CA104177 to PBF; National Institutes of Health grants DK52825, CA88906, CA72955, CA108520, and P01 CA104177 to PD; National Institutes of Health Grant CA083821, CA094084, CA93796, CA111569, and P01 CA104177 to DTC; National Institutes of Health Grant CA63753, CA93738, and CA100866 to SG; Department of Defense grant DAMD17-03-1-0262 to PD; Department of Defense grant DAMD 17-03-1-0209 to SG; Department of Defense grant W81XWH-05-1-0035 to DTC; Department of Defense Army Postdoctoral Fellowships (DS and MS); the Leukemia and Lymphoma Society 6045-03 to SG; the Lustgarten Foundation for Pancreatic Cancer Research (PBF); the Samuel Waxman Cancer Research Foundation (PBF); and the Chernow Endowment (PBF). PBF is the Michael and Stella Chernow Urological Cancer Research Scientist and an SWCRF Investigator. PD is a Universal Leaf Professor in Cell Signaling.

References

Aharon, T., & Schneider, R. J. (1993). Selective destabilization of short-lived mRNAs with the granulocyte-macrophage colony-stimulating factor AU-rich 3′ noncoding region is mediated by a cotranslational mechanism. *Mol Cell Biol 13*, 1971–1980.

Akduman, B., Barquawi, A. B., & Crawford, E. D. (2005). Minimally invasive surgery in prostate cancer: current and future perspectives. *Cancer J 11*, 355–361.

Andrejeva, J., Childs, K. S., Young, D. F., Carlos, T. S., Stock, N., Goodbourn, S., et al. (2004). The V proteins of paramyxoviruses bind the IFN-inducible RNA helicase, mda-5, and inhibit its activation of the IFN-beta promoter. *Proc Natl Acad Sci U S A 101*, 17264–17269.

Bardeesy, N., & DePinho, R. A. (2002). Pancreatic cancer biology and genetics. *Nat Rev Cancer 2*, 897–909.

Baron, J. M., Heise, R., Merk, H. F., & Abuzahra, F. (2003). Current and future directions in the treatment of metastatic malignant melanoma. *Curr Med Chem Anti-Canc Agents 3*, 393–398.

Baruch, A. C., Shi, J., Feng, Y., & Nelson, M. A. (2005). New developments in staging of melanoma. *Cancer Investig 23*, 561–567.

Berridge, M. J. (2002). The endoplasmic reticulum: a multifunctional signaling organelle. *Cell Calcium 32*, 235–249.

Berridge, M. J., Lipp, P., & Bootman, M. D. (2000). The versatility and universality of calcium signaling. *Nat Rev Mol Cell Biol 1*, 11–21.

Berrie, C. P. (2001). Phosphoinositide 3-kinase inhibition in cancer treatment. *Expert Opin Investig Drugs 10*, 1085–1098.

Bevona, C., & Sober, A. J. (2002). Melanoma incidence trends. *Dermatol Clin 20*, 589–595.

Bevona, C., Goggins, W., Quinn, T., Fullerton, J., & Tsao, H. (2003). Cutaneous melanomas associated with nevi. *Arch Dermatol 139*, 1620–1624.

Bishop, J. M. (1991). Molecular themes in oncogenesis. *Cell 64*, 235–248.

Blumberg, H., Conklin, D., Xu, W. F., Grossmann, A., Brender, T., Carollo, S., et al. (2001). Interleukin 20: discovery, receptor identification, and role in epidermal function. *Cell 104*, 9–19.

Bogenrieder, T., & Herlyn, M. (2002). Cell-surface proteolysis, growth factor activation and intercellular communication in the progression of melanoma. *Crit Rev Oncol Hematol 44*, 1–15.

Borden, E. C., Lotan, R., Levens, D., Young, C. W., & Waxman, S. (1993). Differentiation therapy of cancer: laboratory and clinical investigations. *Cancer Res 53*, 4109–4115.

Boukerche, H., Su, Z. -z., Kang, D. -c., & Fisher, P. B. (2004). Identification and cloning of genes displaying elevated expression as a consequence of metastatic progression in human melanoma cells by rapid subtraction hybridization. *Gene 343*, 191–201.

Boukerche, H., Su, Z. -z., Emdad, L., Baril, P., Balme, B., Thomas, L., et al. (2005). Mda-9/syntenin: a positive regulator of melanoma metastasis. *Cancer Res 65*, 10901–10911.

Boukerche, H., Su, Z. -z., Kang, D. -c., & Fisher, P. B. (in press). Cloning differentially expressed genes using rapid subtraction hybridization (RASH). In Fisher, P. B. (Ed.), *Cancer Genomics and Proteomics, Methods in Molecular Biology*. Totowa, NJ: Humana Press Inc.

Brewer, G., Saccani, S., Sarkar, S., Lewis, A., & Pestka, S. (2003). Increased interleukin-10 mRNA stability in melanoma cells is associated with decreased levels of A-U-rich element binding factor AUF1. *J Interf Res 23*, 553–564.

Bucci, M. K., Bevan, A., & Roach, III M. (2005). Advances in radiation therapy: conventional to 3D, to IMRT, to 4D, and beyond. *CA Cancer J Clin 55*, 117–134.

Burdin, N., Peronne, C., Banchereau, J., & Rousset, F. (1993). Epstein–Barr virus transformation induces B lymphocytes to produce human interleukin 10. *J Exp Med 177*, 295–304.

Carlson, J. A., Slomisnki, A., Linette, G. P., Mysliborski, J., Hill, J., & Mihm, Jr. M. C., et al. (2003). Malignant melanoma 2003: predisposition, diagnosis, prognosis and staging. *Am J Clin Pathol 120*, S101–S127.

Caudell, E. G., Mumm, J. B., Poindexter, N., Ekmekcioglu, S., Mhashilkar, A. M., Yang, X. H., et al. (2002). The protein product of the tumor suppressor gene, melanoma differentiation-associated gene 7, exhibits immunostimulatory activity and is designated IL-24. *J Immunol 168*, 6041–6046.

Chada, S., Mhashilkar, A. M., Ramesh, R., Mumm, J. B., Sutton, R. B., Bocangel, D., et al. (2004a). Bystander activity of Ad-mda7: human MDA-7 protein kills melanoma cells via an IL-20 receptor-dependent but STAT3-independent mechanism. *Molec Ther 10*, 1085–1095.

Chada, S., Sutton, R. B., Ekmekcioglu, S., Ellerhorst, J., Mumm, J. B., Leitner, W. W., et al. (2004b). MDA-7/IL-24 is a unique cytokine-tumor suppressor in the IL-10 family. *Int Immunopharmacol 4*, 649–667.

Chada, S., Bocangel, D., Ramesh, R., Grimm, E. A., Mumm, J. B., Mhashilkar, A. M., et al. (2005). mda-7/IL-24 kills pancreatic cancer cells by inhibition of the Wnt/PI3K signaling pathways: identification of IL-20 receptor-mediated bystander activity against pancreatic cancer. *Molec Ther 11*, 724–733.

Chaiken, I. M., & Williams, W. V. (1996). Identifying structure–function relationships in four-helix bundle cytokines: towards de novo mimetics design. *Trends Biotechnol 14*, 369–375.

Chen, J., Chada, S., Mhashilkar, A., & Miano, J. M. (2003). Tumor suppressor MDA-7/IL-24 selectively inhibits vascular smooth muscle cell growth and migration. *Molec Ther 8*, 220–229.

Chen, W.-Y., Cheng, Y.-T., Lei, H.-Y., Chang, C.-P., Wang, C.-W., & Chang, M.-S. (2005). IL-24 inhibits the growth of hepatoma cells in vivo. *Genes Immun* 1–7.

Chung, E. S., Sabel, M. S., & Sondak, V. K. (2004). Current state of treatment for primary cutaneous melanoma. *Clin Exp Med 4*, 65–77.

Connor, J. H., Weiser, D. C., Li, S., Hallenbeck, J. M., & Shenolikar, S. (2001). Growth arrest and DNA damage-inducible protein GADD34 assembles a novel signaling complex containing protein phosphatase 1 and inhibitor 1. *Mol Cell Biol 21*, 6841–6850.

Cunningham, C. C., Chada, S., Merritt, J. A., Tong, A., Senzer, N., Zhang, Y., et al. (2005). Clinical and local biological effects of an intratumoral injection of mda-7 (IL24; INGN 241) in patients with advanced carcinoma: a phase I study. *Molec Ther 11*, 149–159.

Danial, N. N., & Korsmeyer, S. J. (2004). Cell death: critical control points. *Cell 116*, 205–219.

DeAngelis, L. M. (2005). Chemotherapy for brain tumors—a new beginning. *N Engl J Med 352*, 1036–1038.

Dent, P., Yacoub, A., Fisher, P. B., Hagan, M. P., & Grant, S. (2003). MAPK pathways in radiation responses. *Oncogene 22*, 5885–5896.

Dent, P., Yacoub, A., Grant, S., Curiel, D. T., & Fisher, P. B. (2005). Prospects: MDA-7/IL-24 regulates proliferation, invasion and radiosensitivity: a new cancer therapy? *J Cell Biochem 95*, 712–719.

Dumoutier, L., & Renauld, J. C. (2002). Viral and cellular interleukin-10 (IL-10)-related cytokines: from structures to functions. *Eur Cytokine Netw 13*, 5–15.

Dumoutier, L., Leemans, C., Lejeune, D., Kotenko, S. V., & Renauld, J. C. (2001). Cutting edge: STAT activation by IL-19, IL-20 and mda-7 through IL-20 receptor complexes of two types. *J Immunol 167*, 3545–3549.

Eigentler, T. K., Caroli, U. M., Radny, P., & Garbe, C. (2003). Palliative therapy of disseminated malignant melanoma: a systematic review of 41 randomised clinical trials. *Lancet Oncol 4*, 748–759.

Ekmekcioglu, S., Ellerhorst, J. A., Smid, C. M., Prieto, V. G., Munsell, M., Buzaid, A. C., et al. (2000). Inducible nitric oxide synthase (iNOS) and nitrotyrosine (NT) in human metastatic melanoma tumors correlate with poor survival. *Clin Cancer Research 6*, 4768–4775.

Ekmekcioglu, S., Ellerhorst, J., Mhashilkar, A. M., Sahin, A. A., Read, C. M., Prieto, V.G., et al. (2001). Down-regulated melanoma differentiation associated gene (mda-7) expression in human melanomas. *Int J Cancer 94*, 54–59.

Ekmekcioglu, S., Ellerhorst, J. A., Mumm, J. B., Zheng, M., Broemeling, L., Prieto, V. G., et al. (2003). Negative association of melanoma differentiation-associated gene (mda-7) and inducible nitric oxide synthase (iNOS) in human melanoma: MDA-7 regulates iNOS expression in melanoma cells. *Mol Cancer Ther 2*, 9–17.

Ellerhorst, J. A., Prieto, V. G., Ekmekcioglu, S., Broemeling, L., Yekell, S., Chada, S., et al. (2002). Loss of MDA-7 expression with progression of melanoma. *J Clin Oncol 20*, 1069–1074.

Emdad, L., Sarkar, D., Su, Z. -z., & Fisher, P. B. (2005). Emerging roles of centrosomal amplification and genomic instability in cancer. In S. E. Banerjee (Ed.), Growth Factors in Cancer. *Front Biosci, vol. 10*, (pp. 728–742).

Fawcett, T. W., Martindale, J. L., Guyton, K. Z., Hai, T., & Holbrook, N. J. (1999). Complexes containing activating transcription factor (ATF)/cAMP-responsive-element-binding protein (CREB) interact with the CCAAT/enhancer-binding protein (C/EBP)-ATF composite site to regulate Gadd153 expression during the stress response. *Biochem J 339*, 135–141.

Fernandez-Larrea, J., Merlos-Suarez, A., Urena, J. M., Baselga, J., & Arribas, J. (1999). A role for a PDZ protein in the early secretory pathway for the targeting of proTGF-alpha to the cell surface. *Mol Cell 3*, 423–433.

Fickenscher, H., Hor, S., Kupers, H., Knappe, A., Wittmann, S., & Sticht, H. (2002). The interleukin-10 family of cytokines. *Trends Immunol 23*, 89–96.

Fidler, I. J. (2002). Critical determinants of metastasis. *Semin Cancer Biol 12*, 89–96.

Fidler, I. J., Yano, S., Zhang, R. D., Fujimaki, T., & Bucana, C. D. (2002). The seed and soil hypothesis: vascularisation and brain metastases. *Lancet Oncol 3*, 53–57.

Fisher, P. B. (1984). Enhancement of viral transformation and expression of the transformed phenotype by tumor promoters. In T. J. Slaga (Ed.), *Tumor Promotion and Cocarcinogenesis In Vitro, Mechanisms of Tumor Promotion* (pp. 57–123). Boca Raton, FL: CRC Press.

Fisher, P.B. (2005). Is mda-7/IL-24 a "magic bullet" for cancer? *Cancer Res 65*, 10128–10138.

Fisher, P. B., Prignoli, D. R., Hermo, Jr. H., Weinstein, I. B., Pestka, S., (1985). Effects of combined treatment with interferon and mezerein on melanogenesis and growth in human melanoma cells. *J Interf Res 5*, 11–22.

Fisher, P. B., Gopalkrishnan, R. V., Chada, S., Ramesh, R., Grimm, E. A., Rosenfeld, M. R., et al. (2003). mda-7/IL-24, a novel cancer selective apoptosis inducing cytokine gene: from the laboratory into the clinic. *Cancer Biol Ther 2*, S23–S37.

Folkman, J. (1996). Fighting cancer by attacking its blood supply. *Sci Am 275*, 150–154.

Folkman, J. (2001). Angiogenesis-dependent diseases. *Semin Oncol 28*, 536–542.

Folkman, J. (2002). Role of angiogenesis in tumor growth and metastasis. *Semin Oncol 29*, 111–119.

Folkman, J. (2003). Fundamental concepts of the angiogenic process. *Curr Mol Med 3*, 643–651.

Friess, H., Kleeff, J., Korc, M., & Buchler, M. W. (1999). Molecular aspects of pancreatic cancer and future perspectives. *Dig Surg 16*, 281–290.

Fry, M. J. (2001). Phosphoinositide 3-kinase signaling in breast cancer: how big a role might it play? *Breast Cancer Res 3*, 304–312.

Gallagher, G., Dickensheets, H., Eskdale, J., Izotova, L. S., Mirochnitchenko, O. V., Peat, J. D., et al. (2000). Cloning, expression and initial characterization of interleukin-19 (IL-19), a novel homologue of human interleukin-10 (IL-10). *Genes Immun 1*, 442–450.

Garn, H., Schmidt, A., Grau, V., Stumpf, S., Kaufmann, A., & Becker, M., et al. (2002). IL-24 is expressed by rat and human macrophages. *Immunobiology 205*, 321–334.

Gazdar, A. F., & Minna, J. D. (2001). Targeted therapies for killing tumor cells. *Proc Natl Acad Sci U S A 98*(18), 10028–10030.

Gopalan, B., Litvak, A., Sharma, S., Mhashilkar, A. M., Chada, S., & Ramesh, R. (2005). Activation of the Fas-FasL signaling pathway by MDA-7/IL-24 kills human ovarian cells. *Cancer Res 65*, 3017–3024.

Gopalkrishnan, R. V. (2002). INGN-241. Introgen. *Curr Opin Investig Drugs 3*, 1773–1777.

Gopalkrishnan, R. V., Sauane, M., & Fisher, P. B. (2004). Cytokine and tumor cell apoptosis inducing activity of mda-7/IL-24. *Int Immunopharmacol 4*, 635–647.

Gregoire, V., Hittelman, W. N., Rosier, J. F., & Milas, L. (1999). Chemo-radiotherapy: radiosensitizing nucleoside analogues [Review]. *Oncol Rep 6*, 949–957.

Gregoire, V., Ang, K. K., Rosier, J. F., Beauduin, M., Garden, A. S., Hamoir, M., et al. (2002). A phase I study of fludarabine combined with radiotherapy in patients with intermediate to locally advanced head and neck squamous cell carcinoma. *Radiother Oncol 63*, 187–193.

Guarini, L., Temponi, M., Edwalds, G. M., Vita, J. R., Fisher, P. B., & Ferrone, S. (1989). In vitro differentiation and antigenic changes in human melanoma cell lines. *Cancer Immunol Immunother 30*, 177–181.

Guarini, L., Graham, G. M., Jiang, H., Ferrone, S., Zucker, S., & Fisher, P. B. (1992). Modulation of the antigenic phenotype of human melanoma cells by differentiation-inducing and growth-suppressing agents. *Pigment Cell Res 2*, 123–131.

Harris, A. L. (1985a). DNA repair and resistance to chemotherapy. *Cancer Surv 4*, 601–624.

Harris, A. L. (1985b). DNA repair: relationship to drug and radiation resistance, metastasis and growth factors. *Int J Radiat Biol Relat Stud Phys Chem 48*, 675–690.

Harris, A. L., & Hochhauser, D. (1992). Mechanisms of multidrug resistance in cancer treatment. *Acta Oncol 31*, 205–213.

Hartwell, L. H., & Kastan, M. B. (1994). Cell cycle control and cancer. *Science 266*, 1821–1828.

Hegeman, R. B., Liu, G., Wilding, G., & McNeel, D. G. (2004). Newer therapies in advanced prostate cancer. *Clin Prostate Cancer 3*, 150–156.

Helmke, B. M., Polychronidis, M., Benner, A., Thome, M., Arribas, J., Deichmann, M. (2004). Melanoma metastasis is associated with enhanced expression of the syntenin gene. *Oncol Rep 12*, 221–228.

Herlyn, M., Berking, C., Li, G., & Satyamoorthy, K. (2000). Lessons from melanocyte development for understanding the biological events in naevus and melanoma formation. *Melanoma Res 10*, 303–312.

Herr, I., & Debatin, K. M. (2001). Cellular stress response and apoptosis in cancer therapy. *Blood 98*, 2603–2614.

Hilgers, W., & Kern, S. E. (1999). Molecular genetic basis of pancreatic adenocarcinoma. *Genes Chromosomes Cancer 26*, 1–12.

Hoff, P. M. (2005). Future directions in the use of antiangiogenic agents in patients with colorectal cancer. *Semin Oncol 31*, 17–21.

Hollander, M. C., Zhan, Q., Bae, I., & Fornace, Jr. A. J. (1997). Mammalian GADD34, an apoptosis- and DNA damage-inducible gene. *J Biol Chem 272*, 13731–13737.

Hollander, M. C., Sheikh, M. S., Yu, K., Zhan, Q., Iglesias, M., Woodworth, C., et al. (2001). Activation of Gadd34 by diverse apoptotic signals and suppression of its growth inhibitory effects by apoptotic inhibitors. *Int J Cancer 96*, 22–31.

Huang, F., Adelman, J., Jiang, H., Goldstein, N. I., & Fisher, P. B. (1999a). Differentiation induction subtraction hybridization (DISH): a strategy for cloning genes displaying differential expression during growth arrest and terminal differentiation. *Gene 236*, 125–131.

Huang, F., Adelman, J., Jiang, H., Goldstein, N. I., & Fisher, P. B. (1999b). Identification and temporal expression pattern of genes modulated during irreversible growth arrest and terminal differentiation in human melanoma cells. *Oncogene 18*, 3546–3552.

Huang, E. Y., Madireddi, M. T., Gopalkrishnan, R. V., Leszczyniecka, M., Su, Z., Lebedeva, I. V., et al. (2001). Genomic structure, chromosomal localization and expression profile of a novel melanoma differentiation associated (mda-7) gene with cancer specific growth suppressing and apoptosis inducing properties. *Oncogene 20*, 7051–7063.

Jacobson, M. D. (1996). Reactive oxygen species and programmed cell death. *Trends Biochem Sci 21*, 83–86.

Jiang, H., & Fisher, P. B. (1993). Use of a sensitive and efficient subtraction hybridization protocol for the identification of genes differentially regulated during the induction of differentiation in human melanoma cells. *Mol Cell Differ 1*, 285–299.

Jiang, H., Su, Z.-Z., Boyd, J., & Fisher, P. B. (1993). Gene expression changes associated with reversible growth suppression and the induction of terminal differentiation in human melanoma cells. *Mol Cell Differ 1*, 41–66.

Jiang, H., Lin, J., & Fisher, P. B. (1994a). A molecular definition of terminal differentiation in human melanoma cells. *Mol Cell Differ 2*, 221–239.

Jiang, H., Lin, J., Su, Z. Z., Collart, F. R., Huberman, E., & Fisher, P. B. (1994b). Induction of differentiation in human promyelocytic HL-60 leukemia cells activates p21, WAF1/CIP1, expression in the absence of p53. *Oncogene 9*, 3397–3406.

Jiang, H., Lin, J., Su, Z. Z., Herlyn, M., Kerbel, R. S., Weissman, B. E., et al. (1995a). The melanoma differentiation-associated gene mda-6, which encodes the cyclin-dependent kinase inhibitor p21, is differentially expressed during growth, differentiation and progression in human melanoma cells. *Oncogene 10*, 1855–1864.

Jiang, H., Lin, J., Young, S. M., Goldstein, N. I., Waxman, S., Davila, V., et al. (1995b). Cell cycle gene expression and E2F transcription factor complexes in human melanoma cells induced to terminally differentiate. *Oncogene 11*, 1179–1189.

Jiang, H., Lin, J. J., Su, Z. Z., Goldstein, N. I., & Fisher, P. B. (1995c). Subtraction hybridization identifies a novel melanoma differentiation associated gene, mda-7, modulated during human melanoma differentiation, growth and progression. *Oncogene 11*, 2477–2486.

Jiang, H., Su, Z. Z., Lin, J. J., Goldstein, N. I., Young, C. S., & Fisher, P. B. (1996). The melanoma differentiation associated gene mda-7 suppresses cancer cell growth. *Proc Natl Acad Sci U S A 93*, 9160–9165.

Jiang, H., Lin, J. J., Tao, J., & Fisher, P. B. (1997). Suppression of human ribosomal protein L23A expression during cell growth inhibition by interferon-beta. *Oncogene 14*, 473–480.

Jiang, H., Kang, D. C., Alexandre, D., & Fisher, P. B. (2000). RaSH, a rapid subtraction hybridization approach for identifying and cloning differentially expressed genes. *Proc Natl Acad Sci U S A 97*, 12684–12689.

Josephson, K., DiGiacomo, R., Indelicato, S. R., Iyo, A. H., Nagabhushan, T. L., Parker, M. H., et al. (2000). Design and analysis of an engineered human interleukin-10 monomer. *J Biol Chem 275*, 13552–13557.

Josephson, K., Logsdon, N. J., & Walter, M. R. (2001). Crystal structure of the IL-10/IL-10R1 complex reveals a shared receptor binding site. *Immunity 15*, 35–46.

Juo, P., Kuo, C. J., Reynolds, S. E., Konz, R. F., Raingeaud, J., Davis, R. J., et al. (1997). Fas activation of the p38 mitogen-activated protein kinase signaling pathway requires ICE/CED-3 family proteases. *Mol Cell Biol 17*, 24–35.

Kang, D.-c., LaFrance, R., Su, Z. Z., & Fisher, P. B. (1998). Reciprocal subtraction differential RNA display: an efficient and rapid procedure for isolating differentially expressed gene sequences. *Proc Natl Acad Sci U S A 95*, 13788–13793.

Kang, D.-c., Jiang, H., Wu, Q., Pestka, S., & Fisher, P. B. (2001). Cloning and characterization of human ubiquitin-processing protease-43 from terminally differentiated human melanoma cells using a rapid subtraction hybridization protocol RaSH. *Gene* 233–242.

Kang, D.-c., Gopalkrishnan, R. V., Wu, Q., Jankowsky, E., Pyle, A. M., & Fisher, P. B. (2002). mda-5: an interferon-inducible putative RNA helicase with double-stranded RNA-dependent ATPase activity and melanoma growth-suppressive properties. *Proc Natl Acad Sci U S A 99*, 637–642.

Kang, D-c., Gopalkrishnan, R. V., Lin, L., Randolph, A., Valerie, K., & Pestka, S., et al. (2004). Expression analysis and genomic characterization of human melanoma differentiation associated gene-5, mda-5: a novel type I interferon-responsive apoptosis-inducing gene. *Oncogene 23*, 1789–1800.

Kang, D.-c., Su, Z.-z., Boukerche, H., & Fisher, P.B. (in press). Identification of differentially expressed genes using rapid subtraction hybridization (RaSH): detailed methodology for performing RaSH. In Hayat, M.A. (Ed.), *Immunohistochemistry and In Situ Hybridization of Human Carcinomas: Molecular Genetics, Liver Carcinoma, and Pancreatic Carcinoma*, vol. 3. San Diego, CA: Elsevier/Academic Press.

Katso, R., Okkenhaug, K., Ahmadi, K., White, S., Timms, J., & Waterfield, M. D. (2001). Cellular function of phosphoinositide 3-kinases: implications for development, homeostasis, and cancer. *Annu Rev Cell Dev Biol 17*, 615–675.

Kawabe, S., Nishikawa, T., Munshi, A., Roth, J. A., Chada, S., & Meyn, R. E. (2002). Adenovirus-mediated mda-7 gene expression radiosensitizes non-small cell lung cancer cells via TP53-independent mechanisms. *Molec Ther 6*, 637–644.

Kirkwood, J. M., Manola, J., Ibrahim, J., Sondak, V., Ernstoff, M. S., & Rao, U. (2004). A pooled analysis of eastern cooperative oncology group and intergroup trials of adjuvant high-dose interferon for melanoma. *Clin Cancer Res 10*, 1670–1677.

Knudson, A. G. (1993). Antioncogenes and human cancer. *Proc Natl Acad Sci U S A 90*, 10914–10921.

Kobayashi, H., Man, S., MacDougall, J. R., Graham, C. H., Lu, C., & Kerbel, R. S. (1994). Variant sublines of early-stage human melanomas selected for tumorigenicity in nude mice express a multicytokine-resistant phenotype. *Am J Pathol 144*, 776–786.

Kobayashi, S., Boggon, T. J., Dayaram, T., Janne, P. A., Kocher, O., Meyerson, M., et al. (2005). EGFR mutation and resistance of non-small-cell lung cancer to gefitinib. *N Engl J Med 352*, 786–792.

Koo, T. H., Lee, J. J., Kim, E. M., Kim, K. W., Kim, H. D., & Lee, J. H. (2002). Syntenin is overexpressed and promotes cell migration in metastatic human breast and gastric cancer cell lines. *Oncogene 21*, 4080–4088.

Koroll, M., Rathjen, F. G., & Volkmer, H. (2001). The neural cell recognition molecule neurofascin interacts with syntenin-1 but not with syntenin-2, both of which reveal self-associating activity. *J Biol Chem 276*, 10646–10654.

Kotenko, S. V. (2002). The family of IL-10-related cytokines and their receptors: related, but to what extent? *Cytokine Growth Factor Rev 13*, 223–240.

Kotenko, S. V., Krause, C. D., Izotova, L. S., Pollack, B. P., Wu, W., & Pestka, S. (1997). Identification and functional characterization of a second chain of the interleukin-10 receptor complex. *EMBO J 16*, 5894–5903.

Kroemer, G., & Reed, J. C. (2000). Mitochondrial control of cell death. *Nat Med 6*, 513–519.

Kummer, J. L., Rao, P. K., & Heidenreich, K. A. (1997). Apoptosis induced by withdrawal of trophic factors is mediated by p38 mitogen-activated protein kinase. *J Biol Chem 272*, 20490–20494.

Langer, J. A., Cutrone, E. C., & Kotenko, S. (2004). The class II cytokine receptor (CRF2) family: overview and patterns of receptor-ligand interactions. *Cytokine Growth Factor Rev 15*, 33–48.

Leath, III C. A., Kataram, M., Bhagavatula, P., Gopalkrishnan, R. V., Dent, P., Fisher, P. B., et al. (2004). Infectivity enhanced adenoviral-mediated mda-7/IL-24 gene therapy for ovarian carcinoma. *Gynecol Oncol 94*, 352–362.

Lebedeva, I. V., Su, Z. Z., Chang, Y., Kitada, S., Reed, J. C., & Fisher, P. B. (2002). The cancer growth suppressing gene mda-7 induces apoptosis selectively in human melanoma cells. *Oncogene 21*, 708–718.

Lebedeva, I. V., Sarkar, D., Su, Z. Z., Kitada, S., Dent, P., Stein, C. A., et al. (2003a). Bcl-2 and Bcl-xL differentially protect human prostate cancer cells from induction of apoptosis by melanoma differentiation associated gene-7, mda-7/IL-24. *Oncogene 22*, 8758–8773.

Lebedeva, I. V., Su, Z. Z., Sarkar, D., & Fisher, P. B. (2003b). Restoring apoptosis as a strategy for cancer gene therapy: focus on p53 and mda-7. *Semin Cancer Biol 13*, 169–178.

Lebedeva, I. V., Su, Z. Z., Sarkar, D., Kitada, S., Dent, P., Waxman, S., et al. (2003c). Melanoma differentiation associated gene-7, mda-7/interleukin-24, induces apoptosis in prostate cancer cells by promoting mitochondrial dysfunction and inducing reactive oxygen species. *Cancer Res 63*, 8138–8144.

Lebedeva, I. V., Sauane, M., Gopalkrishnan, R. V., Sarkar, D., Su, Z.-z., Gupta, P., et al. (2005a). mda-7:IL-24: exploiting cancer's Achilles' heel. *Molec Ther 11*, 4–18.

Lebedeva, I. V., Su, Z. Z., Sarkar, D., Gopalkrishnan, R. V., Waxman, S., Yacoub, A., et al. (2005b). Induction of reactive oxygen species renders mutant and wild-type K-*ras* pancreatic carcinoma cells susceptible to Ad.mda-7-induced apoptosis. *Oncogene 24*, 585–596.

Lebedeva, I.V., Sarkar, D., Su, Z.-z., Gopalkrishnan, R.V., Athar, M., Randolph, A., et al. (in press). Molecular target-based therapy of pancreatic cancer. *Cancer Res*.

Lens, M. B., & Elsen, T. G. (2003). Systemic chemotherapy in the treatment of malignant melanoma. *Expert Opin Pharmacother 4*, 2205–2211.

Leszczyniecka, M., Roberts, T., Dent, P., Grant, S., & Fisher, P. B. (2001). Differentiation therapy of human cancer: basic science and clinical applications. *Pharmacol Ther 90*, 105–156.

Lin, J., Jiang, H., & Fisher, P. B. (1996). Characterization of a novel melanoma differentiation associated gene, mda-9, that is down-regulated during terminal cell differentiation. *Mol Cell Differ 4*, 317–333.

Lin, J. J., Jiang, H., & Fisher, P. B. (1998). Melanoma differentiation associated gene-9, mda-9, is a human gamma interferon responsive gene. *Gene 207*, 105–110.

Lin, M. Z., Teitell, M. A., & Schiller, G. J. (2005). The evolution of antibodies into versatile tumor-targeting agents. *Clin Cancer Res 11*, 129–138.

Liscovitch, M., & Lavie, Y. (2005). Cancer multidrug resistance: a review of recent drug discovery research. *IDrugs 5*, 255–349.

Liu, Y., Wei, S. H., Ho, A. S., de Waal Malefyt, R., & Moore, K. W. (1994). Expression cloning and characterization of a human IL-10 receptor. *J Immunol 152*, 1821–1829.

Liu, Y., Ye, T., Sun, D., Maynard, J., & Deisseroth, A. (2004). Conditionally replication-competent adenoviral vectors with enhanced infectivity for use in gene therapy of melanoma. *Hum Gene Ther 15*, 637–647.

Lorenz, M., Heinrich, S., Staib-Sebler, E., Kohne, C. H., Wils, J., Nordlinger, B., et al. (2000). Regional chemotherapy in the treatment of advanced pancreatic cancer—is it relevant? *Eur J Cancer 36*, 957–965.

Madireddi, M. T., Dent, P., & Fisher, P. B. (2000a). AP-1 and C/EBP transcription factors contribute to mda-7 gene promoter activity during human melanoma differentiation. *J Cell Physiol 185*, 36–46.

Madireddi, M. T., Dent, P., & Fisher, P. B. (2000b). Regulation of mda-7 gene expression during human melanoma differentiation. *Oncogene 19*, 1362–1368.

Madireddi, M. T., Su, Z. Z., Young, C. S., Goldstein, N. I., & Fisher, P. B. (2000c). Mda-7, a novel melanoma differentiation associated

gene with promise for cancer gene therapy. *Adv Exp Med Biol 465*, 239–261.

McCormick, F. (1999). Signalling networks that cause cancer. *Trends Cell Biol 9*, M53–M56.

McCormick, C., & Ganem, D. (2005). The kaposin B protein of KSHV activates the p38/MK2 pathway and stabilizes cytokine mRNAs. *Science 307*, 739–741.

McGary, E. C., Lev, D. C., & Bar-Eli, M. (2002). Cellular adhesion pathways and metastatic potential of human melanoma. *Cancer Biol Ther 1*, 459–465.

McKenzie, T., Liu, Y., Fanale, M., Swisher, S.G., Chada, S., & Hunt, K.K. (2004). Combination therapy of Ad-mda7 and trastuzumab increases cell death in Her-2/neu-overexpressing breast cancer cells. *Surgery 136*, 437–442.

Meric, J. B., Rixe, O., & Khayat, D. (2003). Metastatic malignant melanoma. *Drugs Today 39*, 17–38.

Mhashilkar, A. M., Schrock, R. D., Hindi, M., Liao, J., Sieger, K., Kourouma, F., et al. (2001). Melanoma differentiation associated gene-7 (mda-7): a novel anti-tumor gene for cancer gene therapy. *Mol Med 7*, 271–282.

Mhashilkar, A. M., Stewart, A. L., Sieger, K., Yang, H. Y., Khimani, A. H., Ito, I., et al. (2003). MDA-7 negatively regulates the beta-catenin and PI3K signaling pathways in breast and lung tumor cells. *Molec Ther 8*, 207–219.

Michor, F., Iwasa, Y., Vogelstein, B., Lengauer, C., & Nowak, M. A. (2005). Can chromosomal instability initiate tumorigenesis? *Sem Cancer Biol 15*, 43–49.

Miller, Jr. W. H., & Waxman, S. (2002). Differentiation induction as a treatment for hematologic malignancies. *Oncogene 21*, 3496–3506.

Moore, K. W., de Waal Malefyt, R., Coffman, R. L., & O'Garra, A. (2001). Interleukin-10 and the interleukin-10 receptor. *Annu Rev Immunol 19*, 683–765.

Nguyen, T. H. (2004). Mechanisms of metastasis. *Clin Dermatol 22*, 209–216.

Nishikawa, T., Ramesh, R., Munshi, A., Chada, S., & Meyn, R. E. (2004). Adenovirus-mediated mda-7 (IL24) gene therapy suppresses angiogenesis and sensitizes NSCLC xenograft tumors to radiation. *Molec Ther 9*, 818–928.

Oida, Y., Gopalan, B., Miyahara, R., Inoue, S., Branch, C. D., Mhashilkar. A. M., et al. (2005). Sulindac enhances adenoviral vector expressing mda-7/IL-24-mediated apoptosis in human lung cancer. *Mol Cancer Ther 4*, 291–304.

Onn, A., & Fidler, I. J. (2002). Metastatic potential of human neoplasms. *In Vivo 16*, 423–429.

Pataer, A., Vorburger, S. A., Barber, G. N., Chada, S., Mhashilkar, A. M., Zou-Yang, H., et al. (2002). Adenoviral transfer of the melanoma differentiation-associated gene 7 (mda7) induces apoptosis of lung cancer cells via up-regulation of the double-stranded RNA-dependent protein kinase (PKR). *Cancer Res 62*, 2239–2243.

Pataer, A., Vorburgerm, S. A., Chada, S., Balachandran, S., Barber, G. N., Roth, J. A., et al. (2005). Melanoma differentiation-associated gene-7 protein physically associates with the double-stranded RNA-activated protein kinase PKR. *Molec Ther 11*, 717–723.

Perugini, R. A., McDade, T. P., Vittimberga, Jr. F. J., & Callery, M. P. (1998). The molecular and cellular biology of pancreatic cancer. *Crit Rev Eukaryot Gene Expr 8*, 377–393.

Pestka, S. (2003). A dance between interferon α/β and p53 demonstrates collaborations in tumor suppression and antiviral activities. *Cancer Cell 4*, 85–87.

Pestka, S., Kotenko, S. V., & Fisher, P. B. (2003). IL-24. In H. L. Henry, & A. W. Norman (Eds.), *Encyclopedia of Hormones* (pp. 507–513). San Diego, CA: Academic Press.

Pestka, S., Krause, C. D., Sarkar, D., Walter, M. R., Shi, Y., & Fisher, P. B. (2004). Interleukin-10 and related cytokines and receptors. *Annu Rev Immunol 22*, 929–979.

Purow, B., & Fine, H. A. (2004). Progress report on the potential of angiogenesis inhibitors for neuro-oncology. *Cancer Investig 22*, 577–587.

Rajagopalan, L. E., & Malter, J. S. (1997). Regulation of eukaryotic messenger RNA turnover. *Prog Nucleic Acid Res Mol Biol 56*, 257–286.

Raman, N. V., & Small, Jr. W. (1999). The role of radiation therapy in the management of esophageal cancer. *Cancer Control 6*, 53–62.

Ramesh, R., Mhashilkar, A. M., Tanaka, F., Saito, Y., Branch, C. D., Sieger, K., et al. (2003). Melanoma differentiation-associated gene 7/interleukin (IL)-24 is a novel ligand that regulates angiogenesis via the IL-22 receptor. *Cancer Res 63*, 5105–5113.

Ramesh, R., Ito, I., Gopalan, B., Saito, Y., Mhashilkar, A. M., & Chada, S. (2004). Ectopic production of MDA-7/IL-24 inhibits invasion and migration of human lung cancer cells. *Molec Ther 9*, 510–518.

Rajasekhar, V. K., Viale, A., Socci, N. D., Wiedmann, M., Hu, X., & Holland, E. C. (2003). Oncogenic Ras and Akt signaling contribute to glioblastoma formation by differential recruitment of existing mRNA to polysomes. *Mol Cell 12*, 889–901.

Reed, J. C. (1995). Bcl-2 family proteins: regulators of chemoresistance in cancer. *Toxicol Lett 82–83*, 155–158.

Reed, J. C. (1997). Double identity for proteins of the Bcl-2 family. *Nature 387*, 773–776.

Reed, J. C. (2004). Apoptosis mechanism: implications for cancer drug discovery. *Oncology 18*, 11–20.

Rosenberg, L. (2000). Pancreatic cancer: a review of emerging therapies. *Drugs 59*, 1071–1089.

Ross, G. M. (1999). Induction of cell death by radiotherapy. *Endocr-Relat Cancer 6*, 41–44.

Rothstein, J. D., Patel, S., Regan, M. R., Haenggeli, C., Huang, Y. H., Bergles, D. E., et al. (2005). Beta-lactam antibiotics offer neuroprotection by increasing glutamate transporter expression. *Nature 433*, 73–77.

Sachs, L. (1978). Control of normal cell differentiation and the phenotypic reversion of malignancy in myeloid leukaemia. *Nature 274*, 535–539.

Sachs, L. (1987). Cell differentiation and bypassing of genetic defects in the suppression of malignancy. *Cancer Res 47*, 1981–1986.

Sachs, L. (1989). Cell differentiation and tumour suppression, *Ciba Found Symp, 142*, 217–31 (discussion 231–233).

Sachs, L. (1990). The control of growth and differentiation in normal and leukemic blood cells. *Cancer 65*, 2196–2206.

Saeki, T., Mhashilkar, A., Chada, S., Branch, C., Roth, J. A., & Ramesh, R. (2000). Tumor-suppressive effects by adenovirus-mediated mda-7 gene transfer in non-small cell lung cancer cells in vitro. *Gene Ther 7*, 2051–2057.

Saeki, T., Mhashilkar, A., Swanson, X., Zou-Yang, X. H., Sieger, K., Kawabe, S., et al. (2002). Inhibition of human lung cancer growth following adenovirus-mediated mda-7 gene expression in vivo. *Oncogene 21*, 4558–4566.

Saito, Y., Miyahara, R., Gopalan, B., Litvak, A., Inoue, S., & Shanker, M., et al. (2005). Selective induction of cell cycle arrest and apoptosis in human prostate cancer cells through adenoviral transfer of the melanoma differentiation-associated-7 (*mda*-7)/interleukin-24 (IL-24) gene. *Cancer Gene Ther 12*, 238–247.

Sarkar, D., Su, Z. Z., Lebedeva, I. V., Sauane, M., Gopalkrishnan, R. V., Dent, P., et al. (2002). mda-7 (IL-24): signaling and functional roles. *BioTechniques* 30–39.

Sarkar, D., Su, Z. Z., Lebedeva, I. V., Sauane, M., Gopalkrishnan, R. V., Valerie, K., et al. (2002). mda-7 (IL-24) mediates selective apoptosis in human melanoma cells by inducing the coordinated overexpression of the GADD family of genes by means of p38 MAPK. *Proc Natl Acad Sci U S A 99*, 10054–10059.

Sarkar, D., Boukerche, H., Su, Z. Z., & Fisher, P. B. (2004). mda-9/syntenin: recent insights into a novel cell signaling and metastasis-associated gene. *Pharmacol Ther 104*, 101–115.

Sarkar, D., Su, Z. Z., Vozhilla, N., Park, E. S., Gupta, P., & Fisher, P. B. (2005). Dual cancer-specific targeting strategy cures primary and distant breast carcinomas in nude mice. *Proc Natl Acad Sci U S A 104*, 14034–14039.

Sarkar, D., Kang, D.-c. & Fisher, P.B. (in press). Reciprocal subtraction differential RNA display (RSDD): an efficient technology for cloning differentially expressed genes. Fisher, P.B. (Ed.). In *Cancer Genomics and Proteomics: Methods and Protocols*. Totowa, NJ: Humana Press Inc.

Sauane, M., Gopalkrishnan, R. V., Lebedeva, I., Mei, M. X., Sarkar, D., Su, Z. Z., et al. (2003a). Mda-7/IL-24 induces apoptosis of diverse cancer cell lines through JAK/STAT-independent pathways. *J Cell Physiol 196*, 334–345.

Sauane, M., Gopalkrishnan, R. V., Sarkar, D., Su, Z. Z., Lebedeva, I. V., Dent, P., et al. (2003b). MDA-7/IL-24: novel cancer growth suppressing and apoptosis inducing cytokine. *Cytokine Growth Factor Rev 14*, 35–51.

Sauane, M., Gopalkrishnan, R. V., Choo, H. T., Gupta, P., Lebedeva, I. V., Yacoub, A., et al. (2004a). Mechanistic aspects of mda-7/IL-24 cancer cell selectivity analysed via a bacterial fusion protein. *Oncogene 23*, 7679–7690.

Sauane, M., Lebedeva, I. V., Su, Z. Z., Choo, H. T., Randolph, A., Valerie, K., et al. (2004b). Melanoma differentiation associated gene-7/interleukin-24 promotes tumor cell-specific apoptosis through both secretory and nonsecretory pathways. *Cancer Res 64*, 2988–2993.

Sawicka, M., Kalinowska, M., Skierski, J., & Lewandowski, W. (2004). A review of selected anti-tumour therapeutic agents and reasons for multidrug resistance occurrence. *J Pharm Pharmacol 56*, 1067–1081.

Schaefer, G., Venkataraman, C., & Schindler, U. (2001). Cutting edge: FISP (IL-4-induced secreted protein), a novel cytokine-like molecule secreted by Th2 cells. *J Immunol 166*, 5859–5863.

Schwenger, P., Bellosta, P., Vietor, I., Basilico, C., Skolnik, E. Y., & Vilcek, J. (1997). Sodium salicylate induces apoptosis via p38 mitogen-activated protein kinase but inhibits tumor necrosis factor-induced c-Jun N-terminal kinase/stress-activated protein kinase activation. *Proc Natl Acad Sci U S A 94*, 2869–2873.

Shinohara, S., & Rothstein, J. (2004). Interleukin 24 is induced by the RET/PT3 oncoprotein and is an autocrine growth factor for epithelial cells. *Oncogene 23*, 7571–7579.

Sieger, K. A., Mhashilkar, A. M., Stewart, A., Sutton, R. B., Strube, R. W., Chen, S. Y., et al. (2004). The tumor suppressor activity of MDA-7/IL-24 is mediated by intracellular protein expression in NSCLC cells. *Molec Ther 9*, 355–967.

Sitcheran, R., Gupta, P., Fisher, P. B., & Baldwin, A. S. (2005). Positive and negative regulation of EAAT2 by NF-κB: a role for N-myc in TNFa-controlled repression. *EMBO J 24*, 510–520.

Soo, C., Shaw, W. W., Freymiller, E., Longaker, M. T., Bertolami, C. N., Chiu, R., et al. (1999). Cutaneous rat wounds express c49a, a novel gene with homology to the human melanoma differentiation associated gene, mda-7. *J Cell Biochem 74*, 1–10.

Su, Z. Z., Madireddi, M. T., Lin, J. J., Young, C. S., Kitada, S., Reed, J. C., et al. (1998). The cancer growth suppressor gene mda-7 selectively induces apoptosis in human breast cancer cells and inhibits tumor growth in nude mice. *Proc Natl Acad Sci U S A 95*, 14400–14405.

Su, Z. Z., Shi, Y., & Fisher, P. B. (2000). Cooperation between AP1 and PEA3 sites within the progression elevated gene-3 (PEG-3) promoter regulates basal and differential expression of PEG-3 during progression of the oncogenic phenotype in transformed rat embryo cells. *Oncogene 19*, 3411–3421.

Su, Z.-z., Lebedeva, I. V., Gopalkrishnan, R. V., Goldstein, N. I., Stein, C. A., Reed, J. C., et al. (2001). A combinatorial approach for selectively inducing programmed cell death in human pancreatic cancer cells. *Proc Natl Acad Sci U S A 98*, 10332–10337.

Su, Z. Z., Lebedeva, I. V., Sarkar, D., Gopalkrishnan, R. V., Sauane, M., Sigmon, C., et al. (2003a). Melanoma differentiation associated gene-7, mda-7/IL-24, selectively induces growth suppression, apoptosis and radiosensitization in malignant gliomas in a p53-independent manner. *Oncogene 22*, 1164–1180.

Su, Z. Z., Leszczyniecka, M., Kang, D. C., Sarkar, D., Chao, W., Volsky, D. J., et al. (2003b). Insights into glutamate transport regulation in human astrocytes: cloning of the promoter for excitatory amino acid transporter 2 (EAAT2). *Proc Natl Acad Sci U S A 100*, 1955–1960.

Su, Z.-z., Emdad, L., Sarkar, D., Randolph, A., Valerie, K., Yacoub, A., Dent, P., et al. (2005a). Potential molecular mechanism for rodent tumorigenesis: mutational generation of progression elevated gene-3 (PEG-3). *Oncogene 24*, 2247–2255.

Su, Z.-z., Sarkar, D., Emdad, L., Duigou, G. J., Young, C. S., Ware, H., et al. (2005b). Targeting gene expression selectively in cancer cells by using the progression-elevated gene-3 promoter. *Proc Natl Acad Sci U S A 102*, 1059–1064.

Su, Z.-z., Emdad, L., Sauane, M., Lebedeva, I.V., Sarkar, D., Gupta, P., et al. (2005). Unique aspects of mda-7/IL-24 antitumor bystander activity: establishing a role for secretion of MDA-7/IL-24 by normal cells. *Oncogene 24*, 7552–7566.

Su, Z.-z., Lebedeva, I. V., Sarkar, D., Emdad, L., Gupta, P., Kitada, S., et al. (in press). A combinatorial approach for enhancing therapeutic activity of mda-7/IL-24 in prostate cancer: reversal by ionizing radiation of resistance to mda-7/IL-24 in prostate cancer cells overexpressing the anti-apoptotic proteins bcl-xL or bcl-2. *Oncogene*.

Tong, A. W., Nemunaitis, J., Su, D., Zhang, Y., Cunningham, C., Senzer, N., et al. (2005). Intratumoral injection of INGN 241, a nonreplicating adenovector expressing the melanoma-differentiation associated gene-7 (mda-7/IL24): biologic outcome in advanced cancer patients. *Molec Ther 11*, 160–172.

Tripathy, D. (2005). Targeted therapies in breast cancer. *Breast J Suppl 1*, S30–S35.

Ubeda, M., Wang, X. Z., Zinszner, H., Wu, I., Habener, J. F., & Ron, D. (1996). Stress-induced binding of the transcriptional factor CHOP to a novel DNA control element. *Mol Cell Biol 16*, 1479–1489.

Ubeda, M., Vallejo, M., & Habener, J. F. (1999). CHOP enhancement of gene transcription by interactions with Jun/Fos AP-1 complex proteins. *Mol Cell Biol 19*, 7589–7599.

Vassal, G. (2005). Has chemotherapy reached its limits in pediatric cancer? *Eur J Cancer 41*, 564–575.

Vogelstein, B., & Kinzler, K. W. (2004). Cancer genes and the pathways they control. *Nat Med 10*, 789–799.

Volk, A. L., Rivera, A. A., Kanerva, A., Bauerschmitz, G., Dmitriev, I., Nettelbeck, D. M., et al. (2003). Enhanced adenovirus infection of melanoma cells by fiber-modification: incorporation of RGD peptide or Ad5/3 chimerism. *Cancer Biol Ther 2*, 511–515.

Wang, M., & Liang, P. (2005). Interleukin-24 and its receptors. *Immunology 114*, 166–170.

Wang, M., Tan, Z., Zhang, R., Kotenko, S. V., & Liang, P. (2002). Interleukin 24 (MDA-7/MOB-5) signals through two heterodimeric receptors, IL-22R1/IL-20R2 and IL-20R1/IL-20R2. *J Biol Chem 277*, 7341–7347.

Wolk, K., Kunz, S., Asadullah, K., & Sabat, R. (2002). Cutting edge: immune cells as sources and targets of the IL-10 family members? *J Immunol 168*, 5397–5402.

Wolkersdorfer, G. W., Morris, J. C., Ehninger, G., & Ramsey, W. J. (2004). Trans-complementing adenoviral vectors for oncolytic therapy of malignant melanoma. *J Gene Med 6*, 652–662.

Xia, Z., Dickens, M., Raingeaud, J., Davis, R. J., & Greenberg, M. E. (1995). Opposing effects of ERK and JNK-p38 MAP kinases on apoptosis. *Science 270*, 1326–1331.

Xie, M. H., Aggarwal, S., Ho, W. H., Foster, J., Zhang, Z., Stinson, J., et al. (2000). Interleukin (IL)-22, a novel human cytokine that signals through the interferon receptor-related proteins CRF2-4 and IL-22R. *J Biol Chem 275*, 31335–31339.

Yacoub, A., Mitchell, C., Brannon, J., Rosenberg, E., Qiao, L., McKinstry, R., et al. (2003). MDA-7 (interleukin-24) inhibits the proliferation of renal carcinoma cells and interacts with free radicals to promote cell death and loss of reproductive capacity. *Mol Cancer Ther 2*, 623–632.

Yacoub, A., Mitchell, C., Lebedeva, I. V., Sarkar, D., Su, Z. Z., McKinstry, R., et al. (2003a). mda-7 (IL-24) Inhibits growth and enhances radiosensitivity of glioma cells in vitro via JNK signaling. *Cancer Biol Ther 2*, 347–353.

Yacoub, A., Mitchell, C., Lister, A., Lebedeva, I. V., Sarkar, D., Su, Z. Z., et al. (2003b). Melanoma differentiation-associated 7 (interleukin 24) inhibits growth and enhances radiosensitivity of glioma cells in vitro and in vivo. *Clin Cancer Res 9*, 3272–3281.

Yacoub, A., Mitchell, C., Hong, Y., Gopalkrishnan, R. V., Su, Z. Z., Gupta, P., et al. (2004). MDA-7 regulates cell growth and radiosensitivity in vitro of primary (non-established) human glioma cells. *Cancer Biol Ther 3*, 739–751.

Zamzami, N., Marchetti, P., Castedo, M., Decaudin, D., Macho, A., Hirsch, T., et al. (1995). Sequential reduction of mitochondrial transmembrane potential and generation of reactive oxygen species in early programmed cell death. *J Exp Med 182*, 367–377.

Zelent, A., Petrie, K., Chen, Z., Lotan, R., Lubbbert, M., Tallman, M. S., et al. (2005). Molecular target-based treatment of human cancer: summary of the

10th international conference on differentiation therapy. *Cancer Res 65*, 1117–1123.

Zhan, Q., Lord, K. A., Alamo, Jr. I., Hollander, M. C., Carrier, F., Ron, D., et al. (1994). The gadd and MyD genes define a novel set of mammalian genes encoding acidic proteins that synergistically suppress cell growth. *Mol Cell Biol 14*, 2361–2371.

Zhang, R., Tan, Z., & Liang, P. (2000). Identification of a novel ligand-receptor pair constitutively activated by ras oncogenes. *J Biol Chem 275*, 24436–24443.

Zhao, L., Gu, J., Dong, A., Zhang, Y., Zhong, L., He, L., et al. (2005). Potent antitumor activity of oncolytic adenovirus expressing mda-7/IL-24 for colorectal cancer. *Hum Gene Ther 175*, 967–976.

Gene Therapy (2006) 13, 88–94

www.nature.com/gt

SHORT COMMUNICATION

An adenovirus vector with a chimeric fiber incorporating stabilized single chain antibody achieves targeted gene delivery

SJ Hedley[1], A Auf der Maur[2], S Hohn[2], D Escher[2], A Barberis[2], JN Glasgow[1], JT Douglas[3,4], N Korokhov[1] and DT Curiel[3,4]

[1]VectorLogics, Inc., Birmingham, AL, USA; [2]ESBATech AG, Zurich-Schlieren, Switzerland and [3]Division of Human Gene Therapy, Departments of Medicine, Pathology, and Surgery, and the Gene Therapy Center at the University of Alabama at Birmingham, Birmingham, AL, USA

Adenovirus (Ad) vectors are of utility for many therapeutic applications. Strategies have been developed to alter adenoviral tropism to achieve a cell-specific gene delivery capacity employing fiber modifications allowing genetic incorporation of targeting motifs. In this regard, single chain antibodies (scFv) represent potentially useful agents to achieve targeted gene transfer. However, the distinct biosynthetic pathways that scFv and Ad capsid proteins are normally routed through have thus far been problematic with respect to scFv incorporation into the Ad capsid. Utilization of stable scFv, which also maintain correct folding and thus functionality under intracellular reducing conditions, could overcome this restriction. We genetically incorporated a stable scFv into a de-knobbed, fibritin-foldon trimerized Ad fiber and demonstrated selective targeting to the cognate epitope expressed on the membrane surface of cells. We have shown that the scFv employed in this study retains functionality and that stabilizing the targeting molecule, per se, is critical to allow retention of antigen recognition in the adenovirus capsid-incorporated context.
Gene Therapy (2006) **13,** 88–94. doi:10.1038/sj.gt.3302603; published online 18 August 2005

Keywords: *adenovirus; targeting; stable scFv*

Adenovirus (Ad) vectors based on the human serotypes 2 and 5 are promising candidates as gene therapy delivery vehicles. In addition to attractive features such as low pathogenicity for humans, lack of integration in host cell genome and the ability to grow to high titers, adenoviruses have unique utility for *in vivo* applications due to their high efficacy compared with other approaches. In this regard, Ad vectors are currently involved in more than one-quarter of all human gene therapy trials and have a proven safe clinical profile. However, their efficacy within the clinic would clearly be improved by the development of Ad vectors with selective tissue targeting capabilities.

In this regard, motifs derived from antibody molecules represent potentially useful agents to achieve this desired goal of cell-specific targeting, as they embody unparalleled affinity and specificity for recognition and binding to target cell surface markers as well as encompassing a broad range of characterized targets. Thus, it is widely recognized that genetically incorporating antibody-derived targeting motifs into the adenoviral capsid represents the optimal means to achieve the field-wide goal of rendering Ad target cell specific. In particular, single chain antibodies (scFv), generally comprising a variable region of a heavy (V_H) domain fused to a light (V_L) domain of an immunoglobulin via a polypeptide linker, represent the antibody fragment of choice; tropism modification of several viral vectors has been attained via envelop incorporation of scFv.[1–10] However, attempts to directly incorporate scFv into the Ad capsid have been problematic to this point.[11] Consideration of the infectious life cycles and biological pathways of the different viral vectors is required to understand this phenomenon. Specifically viral envelop incorporation of scFv is directly achievable owing to the fact that glycoproteins of such viral vectors are routed in a manner similar to that of scFv, wherein synthesis of these proteins occurs with assembly and folding in the RER. On the other hand, Ad capsid proteins are synthesized in the host cell cytosol followed by cytosol-to-nuclear transport and full virion assembly in the nucleus. Relevant in this context is the fact that the redox state of the cytosol environment is potentially deleterious to scFv due to intra-chain disulfide bridges, found in each variable heavy and light chain. Thus, the nonnative routing imposed on scFv by Ad capsid incorporation methods likely confounds proper scFv folding, thus perturbing the structural configuration required for antigen recognition. This intranuclear assembly of adenovirus thus renders incorporation of scFv into Ad capsids an unprecedented challenge. As a

Correspondence: Dr DT Curiel, Division of Human Gene Therapy, 901 19th Street South, BMR2 502, Birmingham, AL 35294, USA.
E-mail: curiel@uab.edu
[4]Both these authors are equity holders in VectorLogics Inc.
Received 20 April 2005; revised 21 June 2005; accepted 7 July 2005; published online 18 August 2005

provisional alternative to genetic modification, targeting through two-component adaptor systems has demonstrated that the concept of re-targeting is attainable and defined key biologic aspects thereof.[12–18] Thus, with the advent of genetic development of cytosol stable scFv (known as 'intrabodies') (reviewed in Barberis *et al*.[19] and Stocks[20]), and the translation of technologies to scFvs that target cell surface markers of disease-related cells (e.g. CEA[21]), these potential pitfalls seen thus far with standard scFv may be overcome. It would therefore seem that these stabilized scFv provide a more relevant choice as targeting ligands to be utilized within the Ad capsid configuration.

We have recently reported on a novel intracellular screening system, the yeast genetic system named 'Quality control' that allows selection of scFvs, which are stable under reducing conditions.[22] These selected scFvs have shown high biochemical stability and solubility not only in the intracellular reducing environment, but also under normal extracellular conditions, and therefore these scFvs serve as acceptor backbones upon which to construct hypervariable loops that specifically recognize antigens. Through this library screening system soluble and stable scFv moieties for various antigens can be rapidly identified.[23] The antigen-specific scFv (referred to as Binder throughout) developed for this study is based on the FW4.4 scaffold.[24] It is able to specifically bind to an artificial receptor system composed of a transmembrane spanning part and a short extracellular peptide epitope.

Another key consideration in this context is the necessity to identify (or modify) capsid proteins that are compatible with the incorporation of heterologous ligands of comparable complexity to antibody-derived fragments. Underlying this general concept is the requirement to incorporate the antibody-related species into the adenoviral capsid via genetic capsid modifications. Whereas small peptides have been incorporable at the major capsid proteins penton,[25] hexon,[26,27] and in the so-called HI loop[28–33] and carboxy terminus of the Ad5 fiber protein,[34,35] these identified regions within the aforementioned capsid proteins have not been shown to be suitable for incorporation of molecules with the complexity represented by antibody-related molecules.[33,35] In addition, these resultant adenovirus vectors often have expanded, rather than restricted, cell recognition, as they do not address the question of ablation of CAR tropism. Realization of these limitations recently resulted in new strategies capitalizing on the modular structure of the native fiber protein, the natural determinant of Ad vector tropism. Hence, the development of the so-called 'knobless' fiber platforms have been endeavored, whereby modifications are based on the concept of replacing the native fiber with an alternative protein capable of providing the trimerization functions that the knob usually confers. The removal of the structural constraints imposed by the fiber knob would generate a theoretical universal ligand-presenting molecule, by which an expanded repertoire of incorporable and complex ligands can be utilized. Hence, several chimeric fibers based on this design have been constructed by utilizing various trimerizing motifs, including the trimerizing domain of Moloney murine leukemia virus envelope glycoprotein,[36] the neck region peptide of human lung surfactant protein D[37] and the σ1 attachment protein of the mammalian reovirus.[38] In this regard, our group has utilized the bacteriophage T4 fibritin protein for fiber replacement,[39] which permitted the incorporation of CD40L, a trimeric targeting ligand of comparable complexity, to scFv.[40] However, the structural integrity of these fibers is lessened[11,36,37,41] and in our own studies we have noted that targeting with these vectors, while CAR independent and target receptor specific, does not achieve the levels associated with an Ad5 fiber on a CAR expressing cell.[39,40] To address this point, we have further refined the fiber-fibritin platform, and developed a 566FF chimeric fiber containing the Ad5 tail and Ad5 shaft fused to the 12th coil of the fibritin molecule (as described[42]). This fiber demonstrating improved incorporation into the viral capsid provided us a new platform for the incorporation of the stabilized scFv (Figure 1).

To conduct preliminary analysis of these 566FF-scFv, the genes were assembled in the mammalian expression plasmid pVSII[43] and the resultant plasmids were then used to direct the expression of these proteins in 293T/17 cells. These expression experiments were intended to demonstrate that the designed fiber chimeras, when expressed in mammalian cells, possess structural and functional properties required both for the incorporation of these proteins into Ad virions and for binding to the cognate epitope (RA) present in a recombinant protein, GST-RA. As seen in Figure 2a, a Western blot of the lysates of pVS-transfected 293T/17 cells showed that the 566FF-scFv proteins, as well as the control 566FF-Cd (this control 566FF fiber instead of scFv as the ligand contains the Fc binding domain (termed Cd) from *Staphylococcus aureus* Protein A incorporated into the C terminus and this fiber is known to be structurally stable)[42] and wild-type Ad5 fiber expressed by the same plasmid system, were of the expected molecular weight without detectable signals indicating degradation. A comparison of the mobilities of the chimeras in denatured and non-denatured samples showed that all the newly designed proteins formed trimers upon self-association. We next examined the RA-binding capability of the Binder scFv in the context of the 566FF chimeras. This was accomplished by an ELISA which used the lysates of 566FF-scFv-expressing 293T/17 cells for a binding assay employing GST-RA as bait. This assay demonstrated that 566FF-Binder chimeras bound to GST-RA, while predictably 566FF-Scaffold did not bind to GST-RA even at the highest concentration used (Figure 2b). In the aggregate, these experiments clearly demonstrated that 566FF-Scaffold and 566FF-Binder proteins despite their size and complexity preserve the key properties essential for incorporation into virions and, with 566FF-Binder, targeting of Ad vectors.

The rescue and propagation of viruses with Binder and Scaffold scFv chimeric fibers were carried out according to the two-step procedure[40] with a final round of amplification on 293 cells. Analysis of fiber presence in virions indicated that similar levels of 566FF-Scaffold, 566FF-Binder and Ad5 fiber incorporation could be attained (Figure 3a). The lysate data demonstrate that for both 566FF-scFv fibers there was extensive expression of the fibers, and many of these fibers were degraded indicating the necessity of further optimization. However, it was evident that only full-length 566FF-Scaffold fibers were incorporated into the virions, whereas some

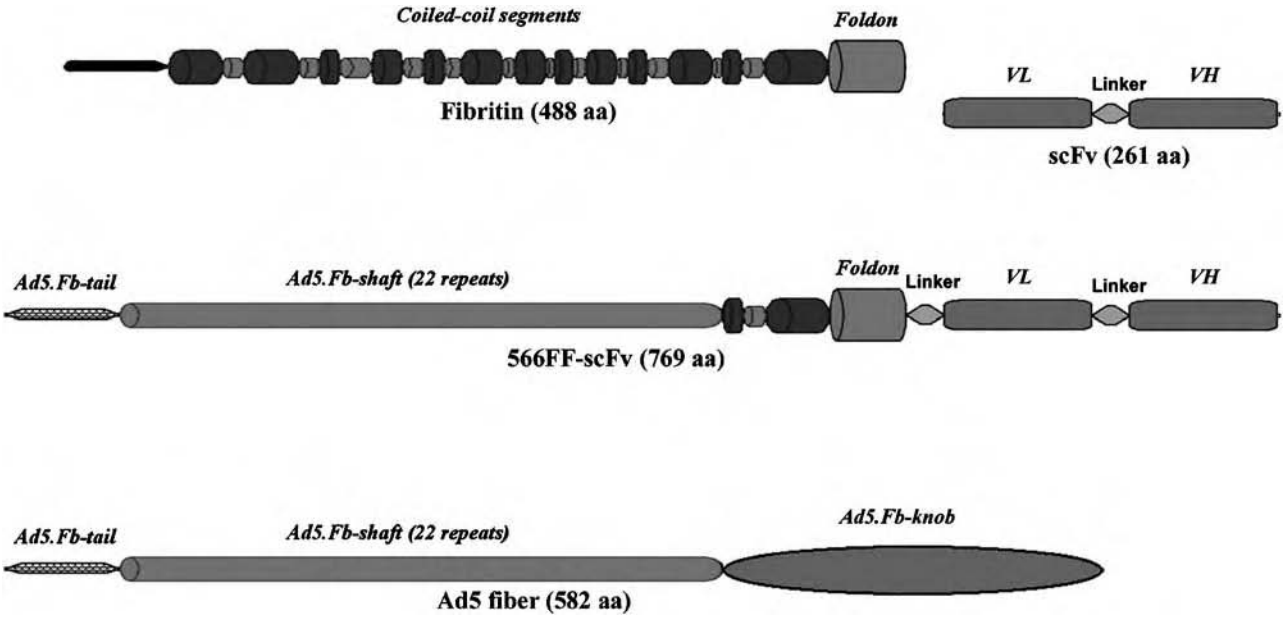

Figure 1 Schema of 566FF-scFv chimeric fiber. Single chain antibodies, either Scaffold scFv (non-Binder) or Binder scFv, were amplified from their respective plasmids using two reaction mixes with the following primer pairs:- (1) 5′-/Phos/GAT CCG ACT ACA AAG ACC AGT CTG-3′ (forward) and 5′-/Phos/GGC CCC CGA GGC CGA GGA G-3′ (reverse) and (2) 5′-/Phos/GAC TAC AAA GAC CAG TCT G-3′ (forward) and 5′-/Phos/TAT TAG GCC CCC GAG GCC GAG GAG-3′ (reverse). *Bae*I ends are underlined. For each scFv, following PCR, the fragments were gel purified, then mixed, denatured and re-annealed to create fragments with the *Bae*I sticky ends. This allowed for cloning into pKan-566FF-*Bae*I plasmid so that the scFv (Scaffold or Binder) was in the correct reading frame beside the 566FF chimeric fiber. The schematic composition of 566FF chimeric fiber, with the genetically fused scFv, is shown. The fiber itself is composed of the Ad5 tail and Ad5 shaft fused to the 12th coil of fibritin.[42]

fibers incorporated into the 566FF-Binder virions were partially degraded, with loss of either one or both domains of the scFv (products predominantly located around the 62 kDa region). We ruled out the possibility that these degraded products were contaminated with wild-type Ad5 fiber using an antibody that detects only trimeric Ad5 fiber in Western blots. Both nondenatured 566FF-Scaffold and 566FF-Binder virions were negative in this analysis, whereas nondenatured Ad.Luc1 (containing Ad5 fiber) was positive (data not shown). To establish functional properties of the chimeric fibers in the context of virion incorporation, consideration of the RA-binding capability of the 566FF-Binder virion was necessary. This was accomplished by an ELISA, which used purified virions for a binding assay employing GST-RA as bait. This assay demonstrated that Ad.Luc.566FF-Binder bound to GST-RA, despite there being the presence of sub-length fibers in this viral prep, while predictably the 566FF-Scaffold virions and Ad.Luc1 virions did not bind to GST-RA even at the highest concentration used (Figure 3b). In the aggregate, these experiments clearly demonstrated that 566FF-Scaffold and 566FF-Binder could incorporate into the virions at near wild-type levels. This confirmed our previous study that the 566FF chimeric fiber has utility as a fiber platform for targeting ligand incorporation.[42] Importantly, the Binder scFv within the context of fiber and virion retained functionality, a key property essential for the targeting of Ad vectors.

It was a requisite to develop an artificial receptor system to express the Binder epitope, termed eRA, and therefore we established CHO cells to express this receptor. Korokhov *et al.*,[43] have previously used this artificial receptor system to mimic the 'natural' situation and have demonstrated its utility in the context of a range of target antigen molecules. Analysis of the isolated clonal populations of cells indicated through Western blot analysis that high protein levels could be attained (data not shown), and via cell surface flow cytometry analysis, with the fusion fibers, we could identify clones with low, medium and high cell surface expression levels (Figure 4, for parental cells (a) and high receptor expressing clone, A16 (b)). In addition, this experiment, utilizing transiently expressed chimeric fibers as eRA-recognizing molecules, demonstrated that the Binder scFv could recognize the cell surface expression of the cognate epitope within the constraints of an Ad capsid protein. We therefore selected Clone A16 (Figure 4b) for further utility in gene delivery experiments. We found that Ad.Luc.566FF-Scaffold vector did not have increased transduction on A16 cells, compared to parental cells, whereas there was a 6–10-fold increase in transduction (dependent on experiment) for the Ad.Luc.566FF-Binder vector, when examined on A16 cells (Figure 4c, 10-fold increase in this representative example). This was specific as the increase was ablated by preincubation of virus with GST-RA and in addition, this ablation was dose dependent (Figure 4d). Further, CHO cells are CAR negative, and thus a direct comparison with an Ad5 virus containing Ad5 fiber could be achieved. We saw a 6.4-fold increase in transduction with Ad.Luc.566FF-Binder in comparison to Ad.Luc.1 on the A16 cells in this experiment (Figure 4c). These experiments clearly demonstrated that a combination of optimized fiber-replaced platform with stabilized scFv allows the feasibilization of Ad vector generation with

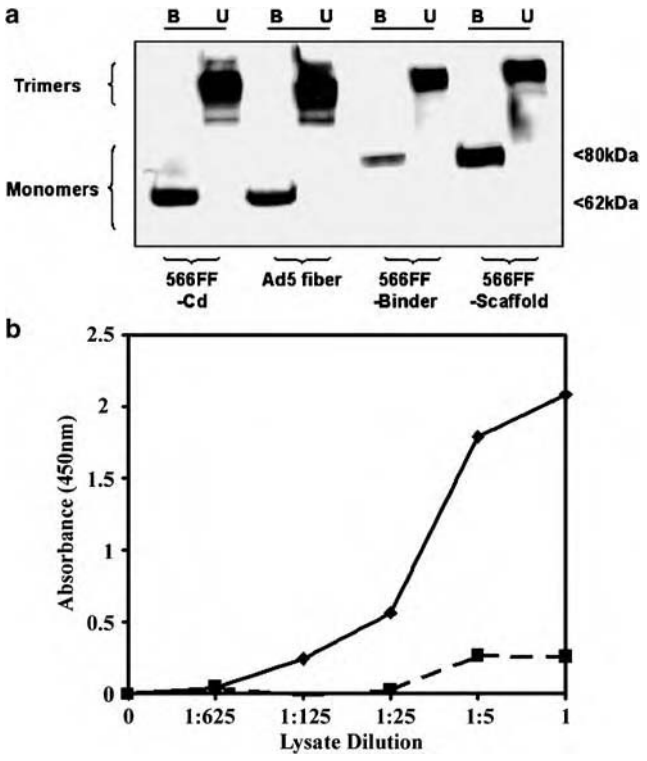

Figure 2 Monomeric and trimerization profiles (**a**) and binding (**b**) of transiently expressed 566FF-scFv fiber proteins to GST-RA. 566FF-Binder and 566FF-Scaffold were sub-cloned from the pKan shuttle vectors into the pVS expression plasmid,[43] to generate pVS-566FF-Binder and pVS-566FF-Scaffold. 293T/17 cells, grown to confluence in six-well dishes, were transfected with 5 μg plasmid DNA/well, of either pVSII (Ad5 fiber[43]), pVS-566FF-Cd (a control 566FF fiber),[42] pVS-566FF-Binder or pVS-566FF-Scaffold, using DOTAP liposomal transfection reagent (Roche) according to the manufacturer's protocol. Following 72 h of culture, cells were harvested into 200 μl serum-free media, freeze-thawed three times to release the fibers, and centrifuged supernatant collected. (**a**) Structural integrity and ability to form homotrimer chimeric fibers in the lysate of 293T/17 cells was assessed by Western blot analysis. Samples, nondenatured (U, unboiled) or denatured (B, boiled), were applied at 10 μl of lysate. The proteins were separated by 4–20% gradient polyacrylamide gel (Bio-Rad) and transferred to polyvinylidenedifluoride (PVDF) membrane where they were probed with 4D2 antibody (UAB), which detects the tail section of both monomeric and trimeric forms of Ad5 fiber. The blots were developed with the WesternBreeze immunodetection system (Invitrogen) according to the manufacturer's protocol. Samples are indicated in the figure, and as described, monomeric fibers migrate as follows: 566FF-Cd fiber and Ad5 fiber migrates at 62 kDa while 566FF-scFv migrate at 80 kDa. (**b**) Lysates of 293T cells transiently expressing 566FF-Binder (diamonds) or 566FF-Scaffold (squares) were tested for binding to GST-RA, a recombinant protein containing the scFv-binding epitope, RA, using ELISA methodology as follows. GST-RA was diluted in 50 mM $NaHCO_3$ [pH 9.6] to obtain 5 μg/ml and 100 μl added per well in Nunc-Maxisorp ELISA plates (Nunc). The plates were stored overnight at 4°C and then blocked with PBS containing 0.05% Tween 20 and 0.5% casein for 1 h at room temperature. Wells were washed with PBS containing 0.05% Tween 20. Lysates were diluted (dilutions indicated on *x*-axis) in binding buffer (TBS with 0.05% Tween 20 and 0.05% casein) and incubated at RT for 1 h in the wells following blocking and detection by the 4D2 antibody. Goat anti-mouse immunoglobulin antibody conjugated with horseradish peroxidase (HRP) (Dako) was used as a secondary Ab and the color was developed with the Sigma FAST *o*-phenylenediamine dihydrochloride tablet kit (Sigma) as recommended by the manufacturer. The color intensity was measured at 450 nm with an EL800 plate reader (Bio-Tek Instruments).

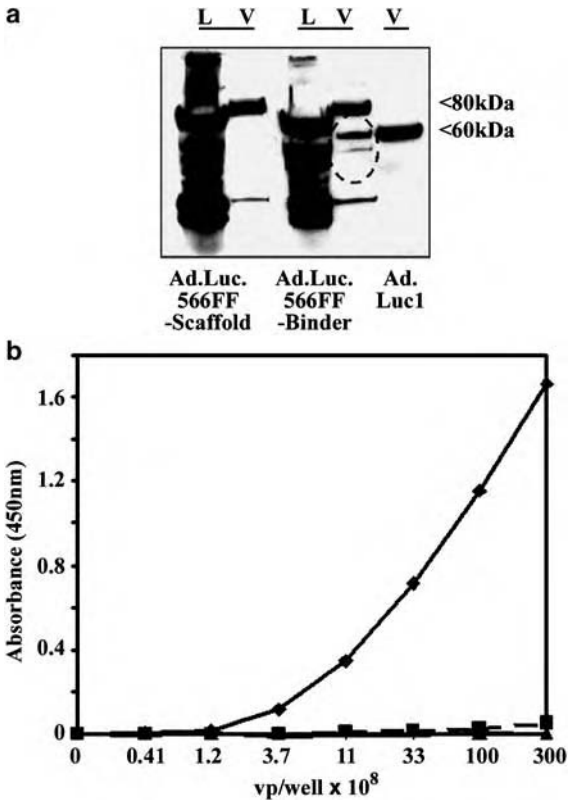

Figure 3 Structural (**a**) and functional (**b**) analysis of rescued viruses encoding variants of 566FF-scFv fiber proteins. The generated plasmids, pKan.566FF-Binder and pKan.566FF-Scaffold, were linearized with an *Eco*RI digest and recombined with *Swa*I digested pVK700 Ad5 modified genome[40] using standard bacterial methods. Resultant recombinant Ad vectors were digested with *Pac*I to release the viral genome and used to transduce 293-F28 cells,[44] a fiber complementing cell as the fibers are CAR ablated, to rescue viruses, Ad.Luc.566FF-Binder and Ad.Luc.566FF-Scaffold. These rescued viruses were in a mosaic format (i.e. the virion capsids contained modified fibers and Ad5 fibers in varying amounts). A large-scale amplification on 293 cells to retrieve non-mosiac viruses (i.e. those containing only the fiber encoded for in the genome) was performed. Standard methods for CsCl purification of mosiac and non-mosaic virions were undertaken. (**a**) Viruses were propagated on 293 cells and lysates (10 μl) and purified virions (5×10^9 vp) from these cells were analysed by Western blot using the 4D2 primary antibody to detect the presence of fibers as described previously. Lysate and virion samples are indicated as L and V, respectively, with viruses further indicated in the figure. Full-length 566FF-scFv chimeric fibers migrate at 80 kDa, while Ad5 fiber migrates at 62 kDa and degradation products of 566FF-scFv migrate at 62 kDa and lower (see circled region). (**b**) Abilities of Ad.566FF-Binder (diamond) and Ad.566FF-Scaffold (square) virions to bind to GST-RA were compared with Ad.Luc.1 virions (triangle) at the vp/well as indicated on the graphs. ELISA was performed as described in Figure 2 with these following modifications. Purified virions were detected by anti-Ad2 polyclonal antibody (NIAID), with the secondary HRP antibody being goat anti-rabbit immunoglobulin antibody (Dako).

novel tropism. Importantly, accrued gene transfer was precisely specific for the target cell receptor.

In summary, the modification of viral tropism is one of the major paradigms in generating clinically relevant gene delivery vectors. Highly attractive targeting moieties that provide utility for this concept are antibody-related molecules, in particular scFv. However, the biosynthetic incompatability of scFv and nuclear viral

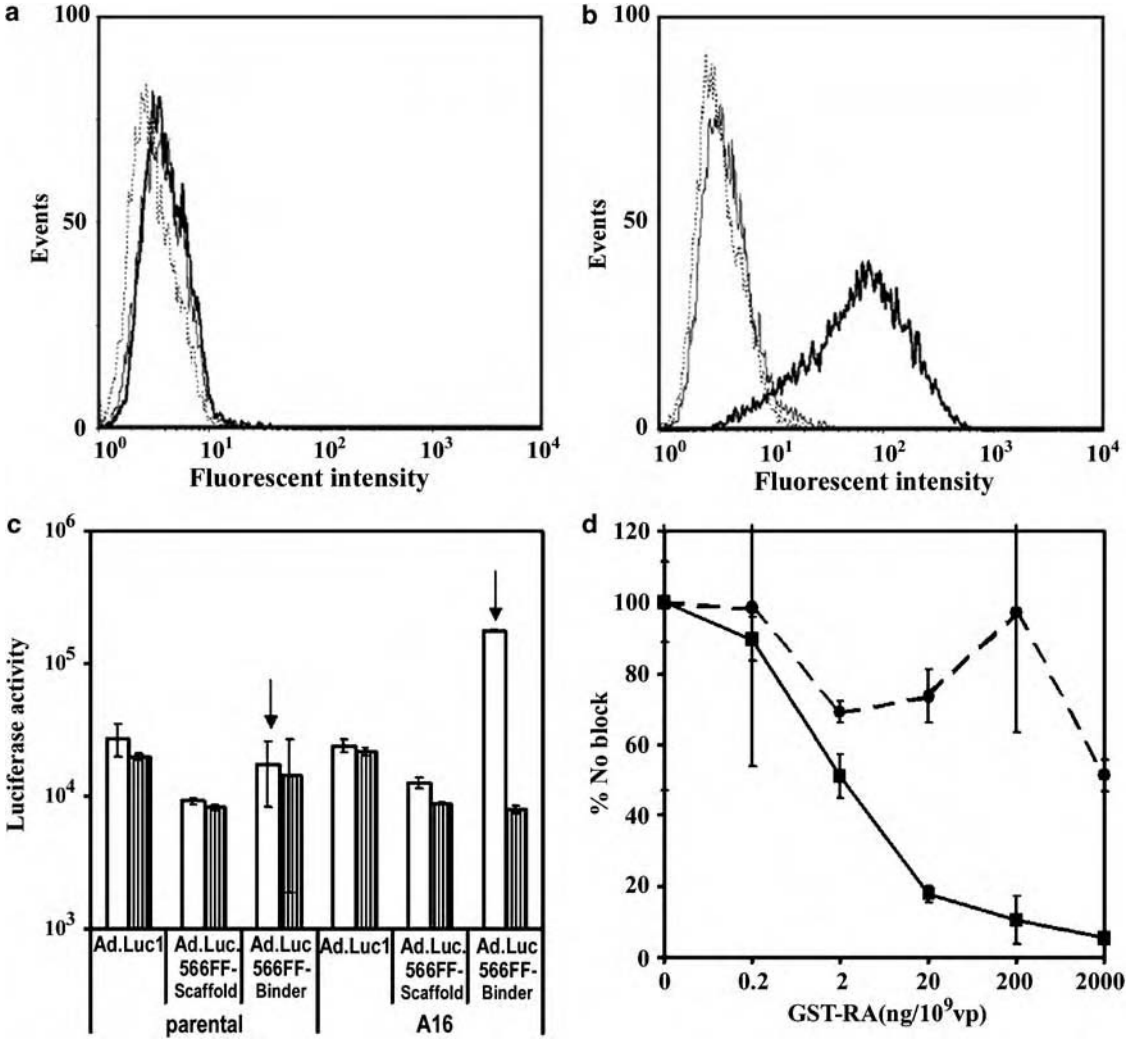

Figure 4 Evaluation of the efficiency and specificity of gene transfer by the rescued viruses. (**a**–**b**) Generation of a stable cell line to express the artificial receptor containing the scFv cognate epitope (eRA) was as follows. Complimentary ss oligos for the epitope (IDT) were annealed and inserted into *Sfi*I-*Sac*II digested pDisplay (Invitrogen), a plasmid that expresses artificial receptors, resulting in generation of pDisplay-eRA plasmid. Cells, which express eRA, were generated by transfection of CHO cells with pDisplay-eRA plasmid and subsequent selection with 1 mg/ml G418 (Mediatech Inc.). Clonal populations expressing eRA were identified by Western blotting of cell lysates with an antimyc antibody (Invitrogen), which recognizes one of the tags within the pDisplay receptor. The blots were developed with the WesternBreeze immunodetection system as before. Parental (**a**) and clonal CHO cells (**b**, clone A16) were analyzed for cell surface expression of eRA. Cells, 2×10^5 cells/sample, were treated either as controls (dotted line), or with the fusion proteins, 566FF-Scaffold (thin line) or 566FF-Binder (thick line) derived from pVS-transfected 293T/17 cells. All samples were probed with 4D2 antibody (final concentration of 0.5 μg/μl) for 1 h at 4°C and followed for a final 1 h at 4°C with a secondary Alexa-fluor conjugated goat anti-mouse antibody (Molecular Probes). Cells were fixed in 1% paraformaldehyde before analysis on a FACSCalibur machine (Becton Dickinson). (**c** and **d**) Evaluation of transduction ability of scFv-targeted Ad vector. Parental CHO and clonal CHO-eRA (A16) cells were grown to confluence in 24-well plates. Prior to transduction, viruses were either untreated or pretreated with GST-RA (2 μg per 1×10^9 vp (**c**)) or a range of GST-RA (0–2 μg (**d**)) for 15 min at RT. Cells were then incubated on ice for 1 h with unblocked or blocked Ad.Luc1, Ad.Luc.566FF-Scaffold or Ad.Luc.566FF-Binder at 1000 vp/cell, then washed twice with PBS, and returned to normal culture media and conditions. After 24 h, cells were lyzed with Luciferase Reporter Lysis Buffer (Promega) and assayed for luciferase activity, measured as relative light units according to the manufacturer's protocol (Promega Luciferase Kit). All the measurements were done in triplicate and are shown as means with error bars representing standard deviations. (**c**) This is a representative example of three individual experiments performed. Viruses are indicated as control (white bars) or pretreated with GST-RA (vertical lined bars). Further details of samples are indicated in the figure. Arrows indicate the 10-fold increase in transduction efficiency when Ad.Luc.566FF-Binder is incubated on A16 cells compared to parental cells. (**d**) This experiment was performed once. Viruses transduced on A16 cell lines are represented as follows; Ad.Luc.566FF-Scaffold (dashed line) or Ad.Luc.566FF-Binder (solid line).

capsid proteins as well as absence of identified locale in Ad capsid tolerant to incorporation of complex molecules have provided a challenge to generate an Ad vector that can target through capsid incorporated scFv. Thus, as a means to circumvent this hindrance in targeting Ad vectors with capsid-incorporated scFv we chose to utilize a stable scFv, which has been selected to be resistant to any cytosol-induced alterations, in combination with radical reconstructions of Ad fiber allowing restrictions on the size and complexity of incorporable targeting ligands to be reduced. We have thus shown that the scFv employed in this study retains functionality and, on this basis, it is clear that stabilizing the targeting molecule, *per se*, allows retention of antigen recognition in the

adenovirus capsid-incorporated context. Importantly, the concept of vector engineering exemplified in this research illustrates the necessity to understand the key cell biology aspects when considering targeting motifs for genetic incorporation into the Ad capsid. Our studies clearly validate the feasibility of achieving Ad-mediated targeted gene delivery via capsid incorporation of scFv. This study thus represents achievement of a universally recognized field milestone and provides the basis of advanced generation Ad vectors compatible with the goal of achieving targeted, cell-specific gene delivery.

Acknowledgements

We thank Wesam Noureddini for helpful discussion and support. This work was funded in part by the Muscular Dystrophy Association Inc., (MDA), Department of Defense, Contract W81XWH-05-1-0035 and NIH Grant 1P01HL076540. Dr Alcide Barberis and ESBATech AG were supported in part by the Commission of Technology and Innovation (CTI) of the Swiss Government.

References

1 Ager S, Nilson BH, Morling FJ, Peng KW, Cosset FL, Russell SJ. Retroviral display of antibody fragments; interdomain spacing strongly influences vector infectivity. *Hum Gene Ther* 1996; **7**: 2157–2164.
2 Konishi H, Ochiya T, Chester KA, Begent RH, Muto T, Sugimura T *et al*. Targeting strategy for gene delivery to carcinoembryonic antigen-producing cancer cells by retrovirus displaying a single-chain variable fragment antibody. *Hum Gene Ther* 1998; **9**: 235–248.
3 Martin F, Neil S, Kupsch J, Maurice M, Cosset F, Collins M. Retrovirus targeting by tropism restriction to melanoma cells. *J Virol* 1999; **73**: 6923–6929.
4 Hammond AL, Plemper RK, Zhang J, Schneider U, Russell SJ, Cattaneo R. Single-chain antibody displayed on a recombinant measles virus confers entry through the tumor-associated carcinoembryonic antigen. *J Virol* 2001; **75**: 2087–2096.
5 Karavanas G, Marin M, Bachrach E, Papavassiliou AG, Piechaczyk M. The insertion of an anti-MHC I ScFv into the N-terminus of an ecotropic MLV glycoprotein does not alter its fusiogenic potential on murine cells. *Virus Res* 2002; **83**: 57–69.
6 Bucheit AD, Kumar S, Grote DM, Lin Y, von Messling V, Cattaneo RB *et al*. An oncolytic measles virus engineered to enter cells through the CD20 antigen. *Mol Ther* 2003; **7**: 62–72.
7 Nguyen TH, Loux N, Dagher I, Vons C, Carey K, Briand P *et al*. Improved gene transfer selectivity to hepatocarcinoma cells by retrovirus vector displaying single-chain variable fragment antibody against c-Met. *Cancer Gene Ther* 2003; **10**: 840–849.
8 Peng KW, Donovan KA, Schneider U, Cattaneo R, Lust JA, Russell SJ. Oncolytic measles viruses displaying a single-chain antibody against CD38, a myeloma cell marker. *Blood* 2003; **101**: 2557–2562.
9 Chowdhury S, Chester KA, Bridgewater J, Collins MK, Martin F. Efficient retroviral vector targeting of carcinoembryonic antigen-positive tumors. *Mol Ther* 2004; **9**: 85–92.
10 Kuroki M. Gene therapy in cancer via use of a retrovector having a tumor specificity and expressing inducible nitric oxide synthase. *Methods Mol Biol* 2004; **279**: 201–211.
11 Magnusson MK, Hong SS, Henning P, Boulanger P, Lindholm L. Genetic retargeting of adenovirus vectors: functionality of targeting ligands and their influence on virus viability. *J Gene Med* 2002; **4**: 356–370.
12 Douglas JT, Rogers BE, Rosenfeld ME, Michael SI, Feng M, Curiel DT. Targeted gene delivery by tropism-modified adenoviral vectors. *Nat Biotechnol* 1996; **14**: 1574–1578.
13 Goldman CK, Rogers BE, Douglas JT, Sosnowski BA, Ying W, Siegal GP *et al*. Targeted gene delivery to Kaposi's sarcoma cells via the fibroblast growth factor receptor. *Cancer Res* 1997; **57**: 1447–1451.
14 Haisma HJ, Pinedo HM, Rijswijk A, der Meulen-Muileman I, Sosnowski BA, Ying W *et al*. Tumor-specific gene transfer via an adenoviral vector targeted to the pan-carcinoma antigen EpCAM. *Gene Therapy* 1999; **6**: 1469–1474.
15 Tillman BW, de Gruijl TD, Luykx-de Bakker SA, Scheper RJ, Pinedo HM, Curiel TJ *et al*. Maturation of dendritic cells accompanies high-efficiency gene transfer by a CD40-targeted adenoviral vector. *J Immunol* 1999; **162**: 6378–6383.
16 Dmitriev I, Kashentseva E, Rogers BE, Krasnykh V, Curiel DT. Ectodomain of coxsackievirus and adenovirus receptor genetically fused to epidermal growth factor mediates adenovirus targeting to epidermal growth factor receptor-positive cells. *J Virol* 2000; **74**: 6875–6884.
17 Reynolds PN, Zinn KR, Gavrilyuk VD, Balyasnikova IV, Rogers BE, Buchsbaum DJ *et al*. A targetable, injectable adenoviral vector for selective gene delivery to pulmonary endothelium *in vivo*. *Mol Ther* 2000; **2**: 562–578.
18 Kashentseva EA, Seki T, Curiel DT, Dmitriev IP. Adenovirus targeting to c-erbB-2 oncoprotein by single-chain antibody fused to trimeric form of adenovirus receptor ectodomain. *Cancer Res* 2002; **62**: 609–616.
19 Barberis A, Auf der Maur A, Tissot K, Lichtlen P. Intrabodies: development and application in functional genomics and therapy. In: Subramanian G (ed.), *Antibodies: Novel Technologies and Therapeutic Use*. London: Springer-Verlag, 2004.
20 Stocks MR. Intrabodies: production and promise. *Drug Discov Today* 2004; **9**: 960–966.
21 Graff CP, Chester K, Begent R, Wittrup KD. Directed evolution of an anti-carcinoembryonic antigen scFv with a 4-day monovalent dissociation half-time at 37 degrees C. *Protein Eng Des Sel* 2004; **17**: 293–304.
22 Auf der Maur A, Escher D, Barberis A. Antigen-independent selection of stable intracellular single-chain antibodies. *FEBS Lett* 2001; **508**: 407–412.
23 Auf der Maur A, Zahnd C, Fischer F, Spinelli S, Honegger A, Cambillau C *et al*. Direct *in vivo* screening of intrabody libraries constructed on a highly stable single-chain framework. *J Biol Chem* 2002; **277**: 45075–45085.
24 Auf der Maur A, Tissot K, Barberis A. Antigen-independent selection of intracellular stable antibody frameworks. *Methods* 2004; **34**: 215–224.
25 Einfeld DA, Brough DE, Roelvink PW, Kovesdi I, Wickham TJ. Construction of a pseudoreceptor that mediates transduction by adenoviruses expressing a ligand in fiber or penton base. *J Virol* 1999; **73**: 9130–9136.
26 Vigne E, Mahfouz I, Dedieu JF, Brie A, Perricaudet M, Yeh P. RGD inclusion in the hexon monomer provides adenovirus type 5-based vectors with a fiber knob-independent pathway for infection. *J Virol* 1999; **73**: 5156–5161.
27 Wu H, Han T, Belousova N, Krasnykh V, Kashentseva E, Dmitriev I *et al*. Identification of sites in adenovirus hexon for foreign peptide incorporation. *J Virol* 2005; **79**: 3382–3390.
28 Dmitriev I, Krasnykh V, Miller CR, Wang M, Kashentseva E, Mikheeva G *et al*. An adenovirus vector with genetically modified fibers demonstrates expanded tropism via utilization of a coxsackievirus and adenovirus receptor-independent cell entry mechanism. *J Virol* 1998; **72**: 9706–9713.
29 Krasnykh V, Dmitriev I, Mikheeva G, Miller CR, Belousova N, Curiel DT. Characterization of an adenovirus vector containing a heterologous peptide epitope in the HI loop of the fiber knob. *J Virol* 1998; **72**: 1844–1852.

30 Xia H, Anderson B, Mao Q, Davidson BL. Recombinant human adenovirus: targeting to the human transferrin receptor improves gene transfer to brain microcapillary endothelium. *J Virol* 2000; **74**: 11359–11366.
31 Mizuguchi H, Koizumi N, Hosono T, Utoguchi N, Watanabe Y, Kay MA *et al*. A simplified system for constructing recombinant adenoviral vectors containing heterologous peptides in the HI loop of their fiber knob. *Gene Therapy* 2001; **8**: 730–735.
32 Nicklin SA, Von Seggern DJ, Work LM, Pek DC, Dominiczak AF, Nemerow GR *et al*. Ablating adenovirus type 5 fiber-CAR binding and HI loop insertion of the SIGYPLP peptide generate an endothelial cell-selective adenovirus. *Mol Ther* 2001; **4**: 534–542.
33 Belousova N, Krendelchtchikova V, Curiel DT, Krasnykh V. Modulation of adenovirus vector tropism via incorporation of polypeptide ligands into the fiber protein. *J Virol* 2002; **76**: 8621–8631.
34 Wickham TJ, Roelvink PW, Brough DE, Kovesdi I. Adenovirus targeted to heparan-containing receptors increases its gene delivery efficiency to multiple cell types. *Nat Biotechnol* 1996; **14**: 1570–1573.
35 Wickham TJ, Tzeng E, Shears LL, Roelvink PW, Li Y, Lee GM *et al*. Increased *in vitro* and *in vivo* gene transfer by adenovirus vectors containing chimeric fiber proteins. *J Virol* 1997; **71**: 8221–8229.
36 van Beusechem VW, van Rijswijk AL, van Es HH, Haisma HJ, Pinedo HM, Gerritsen WR. Recombinant adenovirus vectors with knobless fibers for targeted gene transfer. *Gene Therapy* 2000; **7**: 1940–1946.
37 Magnusson MK, Hong SS, Boulanger P, Lindholm L. Genetic retargeting of adenovirus: novel strategy employing 'deknobbing' of the fiber. *J Virol* 2001; **75**: 7280–7289.
38 Mercier GT, Campbell JA, Chappell JD, Stehle T, Dermody TS, Barry MA. A chimeric adenovirus vector encoding reovirus attachment protein sigma 1 targets cells expressing junctional adhesion molecule 1. *Proc Natl Acad Sci USA* 2004; **101**: 6188–6193.
39 Krasnykh V, Belousova N, Korokhov N, Mikheeva G, Curiel DT. Genetic targeting of an adenovirus vector via replacement of the fiber protein with the phage T4 fibritin. *J Virol* 2001; **75**: 4176–4183.
40 Belousova N, Korokhov N, Krendelshchikova V, Simonenko V, Mikheeva G, Triozzi PL *et al*. Genetically targeted adenovirus vector directed to CD40-expressing cells. *J Virol* 2003; **77**: 11367–11377.
41 Henning P, Andersson KM, Frykholm K, Ali A, Magnussion MK, Nygren PA *et al*. Tumor cell targeted gene delivery by adenovirus 5 vectors carrying knobless fibers with antibody-binding domains. *Gene Therapy* 2005; **12**: 211–224.
42 Noureddini SC, Krendelshchikov A, Simonenko V, Hedley SJ, Douglas JT, Curiel DT *et al*. Generation and selection of targeted adenoviruses embodying optimized vector properties. *J Mol Biol* 2005, submitted.
43 Korokhov N, Mikheeva G, Krendelshchikov A, Belousova N, Simonenko V, Krendelshchikova A *et al*. Targeting of adenovirus via genetic modification of the viral capsid combined with a protein bridge. *J Virol* 2003; **77**: 12931–12940.
44 Von Seggern DJ, Kehler J, Endo RI, Nemerow GR. Complementation of a fibre mutant adenovirus by packaging cell lines stably expressing the adenovirus type 5 fibre protein. *J Gen Virol* 1998; **79** (Part 6): 1461–1468.

Cancer Immunol Immunother (2006) 55: 1412–1419
DOI 10.1007/s00262-006-0158-2

SYMPOSIUM PAPER

**Susan J. Hedley · Jian Chen · John D. Mountz
Jing Li · David T. Curiel · Nikolay Korokhov
Imre Kovesdi**

Targeted and shielded adenovectors for cancer therapy

Received: 27 January 2006 / Accepted: 8 March 2006 / Published online: 13 April 2006

Abstract Conditionally replicative adenovirus (CRAd) vectors are novel vectors with utility as virotherapy agents for alternative cancer therapies. These vectors have already established a broad safety record in humans and overcome some of the limitations of non-replicative adenovirus (Ad) vectors. In addition, one potential problem with these vectors, attainment of tumor or tissue selectivity has widely been addressed. However, two confounding problems limiting efficacy of these drug candidates remains. The paucity of the native Ad receptor on tumor tissues, and host humoral response due to pre-existing titers of neutralizing antibodies against the vector itself in humans have been highlighted in the clinical context. The well-characterized CRAd, AdΔ24-RGD, is infectivity enhanced, thus overcoming the lack of coxsackievirus and adenovirus receptor (CAR), and this agent is already rapidly progressing towards clinical translation. However, the perceived host humoral response potentially will limit gains seen from the infectivity enhancement and therefore a strategy to blunt immunity against the vector is required. On the basis of this caveat a novel strategy, termed shielding, has been developed in which the genetic modification of a virion capsid protein would provide uniformly shielded Ad vectors. The identification of the pIX capsid protein as an ideal locale for genetic incorporation of shielding ligands to conceal the Ad vector from pre-existing neutralizing antibodies is a major progression in the development of shielded CRAds. Preliminary data utilizing an Ad vector with HSV-TK fused to the pIX protein indicates that a shield against neutralizing antibodies can be achieved. The utility of various proteins as shielding molecules is currently being addressed. The creation of AdΔ24S-RGD, an infectivity enhanced and shielded Ad vector will provide the next step in the development of clinically and commercially feasible CRAds that can be dosed multiple times for maximum effectiveness in the fight against cancers in humans.

Keywords Adenovirus · Vector · Targeted · Shielded · Cancer

This article is a symposium paper from the Annual Meeting of the "International Society for Cell and Gene Therapy of Cancer", held in Shenzhen, China, on 9–11 December 2005.

S. J. Hedley · N. Korokhov · I. Kovesdi (✉)
VectorLogics, Inc., Birmingham,
AL 35294, USA
E-mail: ikovesdi@vectorlogics.com

J. Chen · J. D. Mountz
Division of Rheumatology, Department of Medicine,
University of Alabama at Birmingham, Birmingham,
AL 35294, USA

J. Li · D. T. Curiel
Division of Human Gene Therapy, Departments of Medicine,
Pathology, and Surgery, and the Gene Therapy Center,
University of Alabama at Birmingham, Birmingham,
AL 35294, USA

Conditionally replicative adenoviruses as virotherapy agents for cancer gene therapy

Virotherapy, the use of replicative viruses, is a highly attractive approach, and an alternate approach to standard cancer therapies, including gene therapies. Virotherapy exploits the lytic property of virus replication to kill tumor cells, and thus the self-amplification of the virus allows lateral spread in the tumor and greater tumor cell death from an initial infection of only a few cells (Fig. 1). While initial attempts at virotherapy were abandoned due to toxicity and inefficacy, decades ago [1], this approach has re-emerged in pursuit of the problem of limited tumor transduction experienced with alternate cancer gene therapy strategies [2, 3]. Virotherapy now has greater promise due to better understanding of virus biology and the ability to genetically modify viruses and hence, this knowledge allows researchers to design viruses to replicate in and kill tumor cells specifically.

Ad is a highly desirable vector for utilization in virotherapy approaches, as this virus has many attractive features such as low pathogenicity for humans, lack of

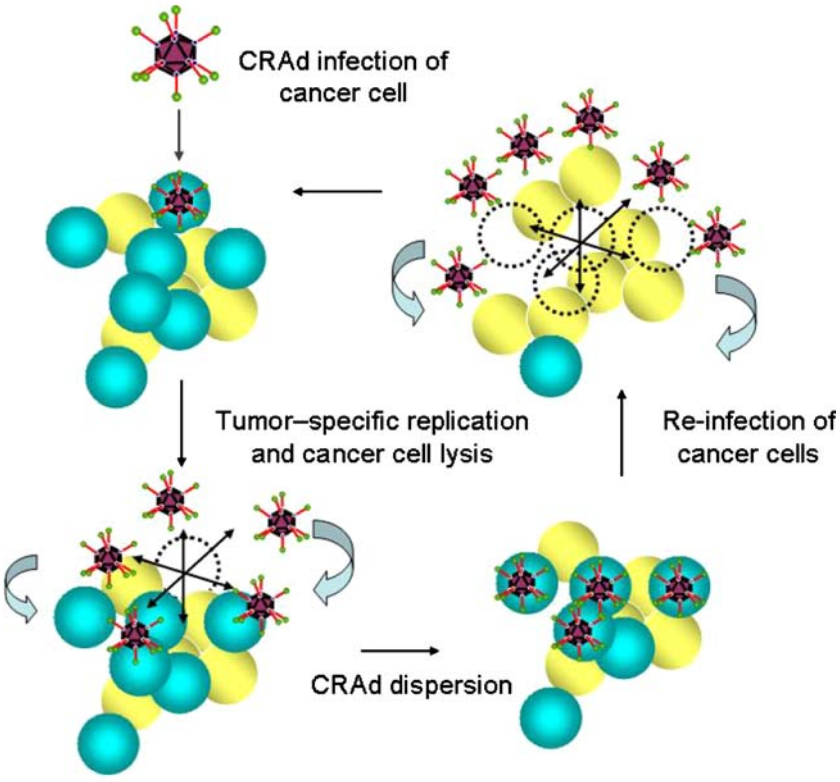

Fig. 1 Oncolytic viral spread

integration in host cell genome and these viruses can be grown to high titers. In addition, they have unique utility for in vivo application due to their high efficacy compared with other approaches [4, 5]. However, three potential limitations may affect the efficacy of the virotherapy approach with adenoviral vectors: (1) Ad does not have natural predilection to replicate in tumor cells, (2) Ad does not efficiently transduce some clinically relevant cancer cells, and (3) Ad cannot be efficiently multi-dosed because of the defense mechanisms of the human body against the vector. Solutions and technological advances to overcome these problems are described below.

Approaches to attain selectivity of replication in CRAd vectors

In the first instance, Ad vectors can be rendered specific for tumor replication through two divergent pathways, selective replication achieved by the regulation of viral genes with tumor-specific promoters (reviewed in depth [6]) and selective replication achieved in theory by the deletion of viral functions dispensable in tumor cells. This second approach to selective replication was pioneered through the use of a mutant Ad (*dl*1520, also known as ONYX-015) that is deleted in the Ad E1B-55 kD protein, which normally binds to and inactivates p53. While such a modification was hypothesized to make the virus (ONYX-015) replicate only in p53-defective cells [7] (the case in 50% of human tumors), this principle has been questioned [8–10]. Furthermore, the replication of this virus was severely hampered compared to wild type virus probably due to the late virus mRNA transcription function of the missing E1B-55 kD protein [10]. The progression of this approach, through second generation conditionally replicative adenoviruses (CRAds) with improved tumor selectivity, has continued despite or perhaps because of the drawbacks realized with ONYX-015 (reviewed [11]).

Of note is the Δ24 Ad with a 24 base pair deletion in the E1A gene domain interacting with the retinoblastoma (Rb) protein which was incorporated into a CRAd and developed independently by two groups [12, 13]. AdΔ24 was shown to be effective in gliomas [12], while its counterpart, dl922–947, was shown to be effective in a range of tumor types [13]. However, there is concern that the therapeutic index actually comes from reduced replication potential within non-dividing/slow growing cells (such as normal cells) versus normal replication within fast growing cells, and hence this mechanism is not fully tumor specific [14] and further modifications were included to improve tumor specificity. Therefore one should perhaps be guarded about using the term tumor specific replication with respect to these CRAds. Regardless of the terminology used many clinical trials have demonstrated safety but limited efficacy, in particular with ONYX-015 (reviewed [11] and [15]) and therefore highlighted the additional confounding limitations, the natural tropism of Ad vectors and the humoral response to Ad vectors.

Modification of natural tropism of adenoviral vectors

The paucity of the natural receptor for serotype Ad5 vectors, the coxsackievirus and adenovirus receptor (CAR), on many cancer tissues (e.g. [16–20]) hinders the efficacy of CRAd virotherapy and therefore the utility of Ad vectors would be further enhanced by re-directing their tropism to alternate receptors. The characterization of the adenovirus (Ad) entry pathway has provided an understanding of the means of modifying Ad tropism. Essentially, cellular recognition is mediated through the globular carboxy-terminal "knob" domain of the Ad fiber protein and CAR [21–23] with internalization of the virion by receptor-mediated endocytosis through the interaction of Arg–Gly–Asp (RGD) sequences in the penton base with secondary host cell receptors, integrins $\alpha_V\beta_3$ and $\alpha_V\beta_5$ [24]. Post-internalization, the virus is localized within the cellular vesicle system, initially in clathrin-coated pits and then in cell endosomes [25]. The virions escape and enter the cytosol due to acidification of the endosomes, which has been hypothesized to occur via a pH-induced conformational change. Essentially this causes an alteration in the hydrophobicity of the adenoviral capsid proteins, specifically penton base, to allow their interaction with the vesicle membrane. Upon capsid disassembly and cytoplasmic transport, the viral DNA localizes to the nuclear pore and is translocated to the nucleus of the host cell [26].

To develop a truly targeted Ad vector, it is necessary to ablate both native viral tropism and to introduce a novel specificity, which will allow infection of the cells of interest via alternative receptors. Adapter molecule-based, two component systems have demonstrated the feasibility of retargeting through various cell surface receptors (reviewed [27]). Ultimately genetic modification of the fiber protein and/or other capsid proteins provides a more rational approach for introducing a novel cell-specific tropism and permit ablation of CAR interaction. A variety of approaches have been undertaken to achieve novel adenoviral tropism (extensively reviewed [27]). Enhanced and expanded tropism, although not necessarily CAR-independent tropism can be achieved in several ways. One option is through the substitution of Ad5 fiber protein with fibers from other Ad serotypes recognizing alternative receptors. Alternatively this can be achieved through the introduction of relatively short peptide ligands into the so-called HI loop and/or the C terminus of the Ad5 fiber protein. In addition, to achieve selective and CAR-independent tropism an approach that has been described as de-knobbing of the fiber can be undertaken, whereby the fiber is re-trimerized by an alternate trimerization motif to knob that permits the inclusion of large, complex ligands into the chimeric fiber (reviewed [27]). The ablation of the native tropism is not relevant for a CRAd that is locally delivered to a solid tumor, which is its present use. However, the increased specificity achieved by targeting will ultimately allow lower and safer doses of Ad vectors to be provided when regional or systemic delivery is contemplated in the future. By administering the vector to the circulation, a vector with molecular targeting has the potential to reach disseminated cancer that neither be injected mechanically nor is too small to be detected. In this way, molecularly targeted vectors hold the promise to expand the types of diseases that can be treated and make the therapeutic applications of Ad vectors safer and more effective.

Development of infectivity enhanced CRAd, AdΔ24-RGD

In the case of the AdΔ24 CRAd vector, tumor cell specificity is achieved through control of the viral replication cycle. Therefore, instead of achieving specificity though targeting the infectivity enhancement approach was used to increase cancer cell transduction globally by the inclusion of a high affinity RGD motif into the HI loop to direct Ad binding to integrins. The RGD-4C motif was described as a 9 amino acid peptide which binds strongly to the Ad secondary receptors, integrins $\alpha_V\beta_3$ and $\alpha_V\beta_5$ [28, 29] and incorporation of this motif into the HI loop significantly increased Ad-mediated gene transfer to CAR deficient cell types relevant to various human diseases [30–33] and could restore infection efficiency of CAR-binding ablated Ad vector to the level of wild type Ad [34, 35]. Several cancer tissues are rich in the expression of appropriate integrins, e.g. [36, 37], whereas low in expression of CAR (as discussed previously and [38]). It was hypothesized that such targeting combined with replication control would improve selective killing or even enhance tumor killing [39], especially for cancers that are deficient in the primary adenoviral receptor [40]. The combination of viral gene mutation to control cell-specific replication and transductional targeting led to the development of the AdΔ24-RGD CRAd [39]. This vector has since been shown to enhance tumor killing in a variety of tumor models including gliomas, ovarian and cervical cancers [39, 41–45]. These studies thereby demonstrate great promise for the development of CRAds that can achieve safe, selective, and effective tumor eradication. However, it is still perceived that the host humoral response potentially will limit any gains seen from the infectivity enhancement of AdΔ24-RGD.

Alternate strategies to overcome the humoral response to adenovirus vectors

Within the human population, there are high titers of pre-existing neutralizing antibodies against Ad5 and Ad2 serotypes [46] due to the general exposure to Ads, an issue that has also been discussed in the context of CRAds [11]. Clinical trials utilizing ONYX-015 have confirmed a strong immune response in several patients that had a highly suggestive correlation with the ob-

served limited efficacy of the virus [47–49]. Mathematical modeling of oncolytic Ad spread throughout tumor mass has also predicted that the immune response will be limiting to viral clearance of the tumor [50]. In addition, the anticipated humoral response means effective repeat administration of Ad vectors to most tissues is hindered by a strong neutralizing antibody response to the vector. Thus far skeletal muscle was one of the few tissues where repeat Ad vector administration was successfully demonstrated [51]. However, the success of this procedure was highly dependent on the initial dose of Ad used in the experiment and therefore, it is still expected that repeat dosing in humans will be problematic. Therefore, there is a need to develop Ad vectors capable of evading the humoral response and hence improve clinical utility of these vectors.

In an attempt to circumvent this issue Ad vectors of different serotypes, in particular Ad11 and Ad35, to which the human population has a lower prevalence of neutralizing antibodies, are currently being investigated as alternative vectors to those of Ad5 [46, 52–54]. While these vectors have yet to be developed into CRAds, an oncolytic Ad based on the canine serotype 2 has been developed, although primarily for use in canine models [55, 56]. It is also important to note that different Ad serotype vectors have different intrinsic properties. For example, different serotype vectors use different cellular receptors [57] and it has been shown recently that Ad vectors based on serotype B (like Ad35 and Ad11) binding to their cognate receptor CD46 down regulate immune responses [58] which has yet to be fully determined as a desirable attribute. Other strategies to overcome the humoral response have included alternating serotypes of helper-dependent Ad vectors (in which the genome is completely removed) during repeat Ad vector administration [59] or using chimeric Ad vectors expressing capsid proteins from several different adenoviral serotypes [60, 61]. It is also likely that these approaches will not prevent the development of humoral and cellular immune responses when these vectors delivered multiple times. Therefore, the need for alternate means to develop an immune evasive Ad vector for clinical use still remains.

The process of biochemical modification of the capsid has highlighted a potentially useful strategy. In this way, the Ad vector is shielded from the immune response through molecules covering the capsid. Several studies have demonstrated that conjugation of functional PEG to free lysine groups on the adenoviral capsid enables Ad vectors to avoid neutralizing antibodies, in vitro or in vivo or limit the innate responses [62–66]. An alternate polymer methodology described by the group of L. Seymour performs equally well [67, 68]. In addition, slower clearance rates of Ad from the blood have been demonstrated [69, 70]. Transduction of cells can occur even in the presence of Ad-neutralizing antibodies [62, 65, 71, 72], although too much PEG causes the ablation of the Ad receptor (CAR) specificity resulting in low levels of transduction. Even though these shielded Ad vectors represent a major improvement in overcoming Ad vector limitations for clinical translation, problems such as the multi-component system and the randomness of PEGlyation, and thus heterogeneity of composition will confound potency in batch-to-batch production. These issues alone represent significant problems with respect to scale up and regulatory approval, but the most problematic limitation with this method is that the shielding molecule is lost, due to the replicative nature of CRAd, from the progeny vectors. The development of an alternative means to attach shielding proteins in order to create a uniform shielding method which carries through to the progeny, and in which the replication and lytic Ad function in vivo maintained is critical.

pIX as a novel site for genetic incorporation of shielding molecules

An alternative and potentially much simpler method to chemical shielding is genetic shielding. Essentially the shielding protein would be directly fused to a capsid protein and thus allowing direct incorporation into the viral capsid. This genetic fusion would provide a means to overcome the loss of the shield protein on the progeny of the CRAd. The identification of an optimal capsid locale to permit the genetic incorporation of such moieties is pivotal within the development of a genetic shield. The determination that the minor capsid protein, pIX, displays the carboxy terminus on the outside of the capsid [73, 74] has consequently suggested this capsid locale to be a novel candidate for genetic manipulation. Protein pIX functions as a "cement" stabilizing hexon–hexon interactions, although another function, transcriptional regulator, has been suggested (recent reviews on pIX [75, 76]). It is present at 80 locales, in 240 molecules per capsid, allowing for a defined number of shielding molecules to be included into the capsid, and is positioned to allow the shield proteins to potentially cover the immunodominant epitopes of hexons (Fig. 2).

Recent studies have demonstrated the employment of the carboxy terminus of pIX for genetic Ad capsid modification [77]. It is now known that small proteins such as polylysine, and large complex proteins such as green fluorescent protein (GFP), and herpes simplex virus thymidine kinase (HSV-TK) can be successfully incorporated into the C terminus of the pIX capsid protein with retention of their functionality [78–80], thus indicating a versatile range of proteins that can be incorporated.

To date HSV-TK, at 375 amino acids, is the largest protein to have been successfully fused to pIX, with retention of virion capsid incorporation [78]. Therefore, it was deemed rational to utilize this vector to perform preliminary experiments in the investigation of the shielding effect of a large protein fused to pIX. An ELISA methodology was employed to analyze the concept of shielding effects via HSV-TK fused to pIX capsid

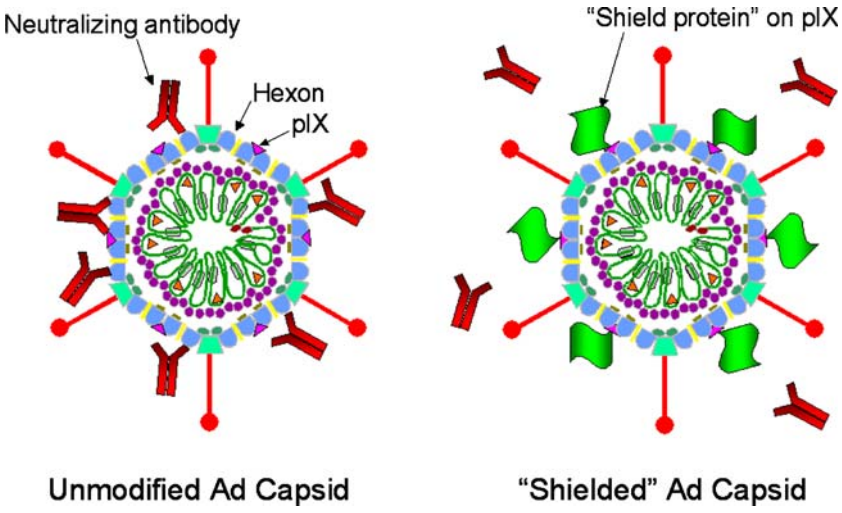

Fig. 2 The adenovirus shielding concept

protein. Serum from naïve mice (pre-immunization) and Ad5 immunized mice (post-immunization) was used as control serum and source of neutralizing antibodies, respectively, with the concept of shielding to be demonstrated through detection of immobilized virions by these antibodies. The preliminary data indicates that significantly fewer antibodies bound the pIX-TK virus from the post-immunized serum than the non-modified virus (approximately 60% less), indicating virion epitopes recognized by the antibodies were reduced due to the presence of TK on pIX. This experiment demonstrates that proteins fused to pIX provide a shielding effect.

However, the shielding protein of choice should embody several important characteristics, namely that it is a self-protein and has sufficient size to cover immunodominant Ad capsid epitopes. A very useful protein, which embodies these properties, is albumin, a large monomeric non-glycosylated polypeptide with wide in vivo distribution, long half-life and lack of substantial immunogenicity [81]. Several proteins have been fused to albumin to enhance circulating half-life and improve stability for therapeutic applications, including, human growth hormone-rHSA (Albutropin) [82], recombinant granulocyte colony stimulating factor-rHSA (Albugranin) [83], and serum albumin-CD4 genetic conjugate [84]. In addition, it has a safe record in clinical practice, e.g., as exemplified by Albuferon™ (albumin-interferon alpha) [85], which has completed phase II clinical trials by Human Genome Sciences [86].

Taken together our data clearly indicate that the ectodomain of pIX is a promising capsid locale for incorporation of heterologous proteins of augmented size and complexity to provide a shielding effect. Current research is underway to determine suitable shielding proteins that perhaps provide a less immunogenic format, i.e., the use of self-molecules, such as albumin rather than foreign molecules such as HSV-TK used in the preliminary study. HSV-TK, of commensurable size to many desired shielding proteins, retains full functionality within the context of the adenoviral capsid when genetically fused to pIX demonstrating structural integrity [78] and suggests large self-molecules may be incorporated into pIX. This body of work indicates the importance of this locale for utilization of an immunological shield for adenoviral vectors and allow for the design of a safe, infectivity-enhanced and shielded CRAd, AdΔ24S-RGD.

Conclusions

Oncolytic Ad provides a novel approach to cancer therapy, known as virotherapy. There are three recognized limitations with respect to CRAd efficacy: (1) tumor/tissue selectivity and hence safety, (2) limited transduction of tumor mass, and (3) the humoral response against the vector, preventing multiple dosing, and possibly spread of vector through the tumor mass. Many laboratories throughout the world are addressing these issues. Our lead product candidate is a well-characterized CRAd, AdΔ24-RGD, a novel infectivity enhanced vector that overcomes the first two limitations, and is the first ever proposed CRAd agent with enhanced infectivity to receive NIH RAC approval for a clinical trial for ovarian cancer and glioma, through the consortium of UAB, MD Anderson Cancer Center and Free University of Amsterdam. The third limitation, that of the humoral response still needs to be studied, and appropriate shielding proteins determined, with research ongoing. However, our data demonstrates that pIX capsid protein is ideal for the genetic incorporation of a shielding protein, due to the positioning of pIX itself within the capsid, and the versatility of ligand size and complexity that can be successfully fused to the C terminus of the pIX capsid protein. Thus, the development of shielded and infectivity-enhanced CRAds will provide an efficient, cost-effective and creative approach to combat not only local disease but also have further application for regional and systemic delivery that could

be potentially effective treatment for a large numbers of cancers including metastatic diseases. We envision the creation of AdΔ24S-RGD as a major progress in the development of clinically and commercially feasible shielded CRAds that can be dosed multiple times for maximum effectiveness against cancers in humans.

Acknowledgements Drs. David T. Curiel and Imre Kovesdi are equity holders in VectorLogics, Inc. The following work was supported in part by the Department of Defense grant #W81XWH-05-1-0035.

References

1. Sinkovics J, Horvath J (1993) New developments in the virus therapy of cancer: a historical review. Intervirology 36:193–214
2. Alemany R, Balague C, Curiel DT (2000) Replicative adenoviruses for cancer therapy. Nat Biotechnol 18:723–727
3. Kirn D, Martuza RL, Zwiebel J (2001) Replication-selective virotherapy for cancer: biological principles, risk management and future directions. Nat Med 7:781–787
4. Russell WC (2000) Update on adenovirus and its vectors. J Gen Virol 81:2573–2604
5. Glasgow JN, Bauerschmitz GJ, Curiel DT, Hemminki A (2004) Transductional and transcriptional targeting of adenovirus for clinical applications. Curr Gene Ther 4:1–14
6. Ko D, Hawkins L, Yu DC (2005) Development of transcriptionally regulated oncolytic adenoviruses. Oncogene 24:7763–7774
7. Bischoff JR, Kirn DH, Williams A, Heise C, Horn S, Muna M, Ng L, Nye JA, Sampson-Johannes A, Fattaey A, McCormick F (1996) An adenovirus mutant that replicates selectively in p53-deficient human tumor cells. Science 274:373–376
8. Harada JN, Berk AJ (1999) p53-Independent and dependent requirements for E1B-55 K in adenovirus type 5 replication. J Virol 73:5333–5344
9. Hay JG, Shapiro N, Sauthoff H, Heitner S, Phupakdi W, Rom WN (1999) Targeting the replication of adenoviral gene therapy vectors to lung cancer cells: the importance of the adenoviral E1b-55 kD gene. Hum Gene Ther 10:579–590
10. Vollmer CM, Ribas A, Butterfield LH, Dissette VB, Andrews KJ, Eilber FC, Montejo LD, Chen AY, Hu B, Glaspy JA, McBride WH, Economou JS (1999) p53 selective and nonselective replication of an E1B-deleted adenovirus in hepatocellular carcinoma. Cancer Res 59:4369–4374
11. Davis JJ, Fang B (2005) Oncolytic virotherapy for cancer treatment: challenges and solutions. J Gene Med 7:1380–1389
12. Fueyo J, Gomez-Manzano C, Alemany R, Lee PS, McDonnell TJ, Mitlianga P, Shi YX, Levin VA, Yung WK, Kyritsis AP (2000) A mutant oncolytic adenovirus targeting the Rb pathway produces anti-glioma effect in vivo. Oncogene 19:2–12
13. Heise C, Hermiston T, Johnson L, Brooks G, Sampson-Johannes A, Williams A, Hawkins L, Kirn D (2000) An adenovirus E1A mutant that demonstrates potent and selective systemic anti-tumoral efficacy. Nat Med 6:1134–1139
14. Johnson L, Shen A, Boyle L, Kunich J, Pandey K, Lemmon M, Hermiston T, Giedlin M, McCormick F, Fattaey A (2002) Selectively replicating adenoviruses targeting deregulated E2F activity are potent, systemic antitumor agents. Cancer Cell 1:325–337
15. Aghi M, Martuza RL (2005) Oncolytic viral therapies—the clinical experience. Oncogene 24:7802–7816
16. Kim M, Zinn KR, Barnett BG, Sumerel LA, Krasnykh V, Curiel DT, Douglas JT (2002) The therapeutic efficacy of adenoviral vectors for cancer gene therapy is limited by a low level of primary adenovirus receptors on tumour cells. Eur J Cancer 38:1917–1926
17. Miller CR, Buchsbaum DJ, Reynolds PN, Douglas JT, Gillespie GY, Mayo MS, Raben D, Curiel DT (1998) Differential susceptibility of primary and established human glioma cells to adenovirus infection: targeting via the epidermal growth factor receptor achieves fiber receptor-independent gene transfer. Cancer Res 58:5738–5748
18. Cripe TP, Dunphy EJ, Holub AD, Saini A, Vasi NH, Mahller YY, Collins MH, Snyder JD, Krasnykh V, Curiel DT, Wickham TJ, DeGregori J, Bergelson JM, Currier MA (2001) Fiber knob modifications overcome low, heterogeneous expression of the coxsackievirus-adenovirus receptor that limits adenovirus gene transfer and oncolysis for human rhabdomyosarcoma cells. Cancer Res 61:2953–2960
19. Li Y, Pong RC, Bergelson JM, Hall MC, Sagalowsky AI, Tseng CP, Wang Z, Hsieh JT (1999) Loss of adenoviral receptor expression in human bladder cancer cells: a potential impact on the efficacy of gene therapy. Cancer Res 59:325–330
20. Okegawa T, Li Y, Pong RC, Bergelson JM, Zhou J, Hsieh JT (2000) The dual impact of coxsackie and adenovirus receptor expression on human prostate cancer gene therapy. Cancer Res 60:5031–5036
21. Henry LJ, Xia D, Wilke ME, Deisenhofer J, Gerard RD (1994) Characterization of the knob domain of the adenovirus type 5 fiber protein expressed in Escherichia coli. J Virol 68:5239–5246
22. Krasnykh VN, Mikheeva GV, Douglas JT, Curiel DT (1996) Generation of recombinant adenovirus vectors with modified fibers for altering viral tropism. J Virol 70:6839–6846
23. Roelvink PW, Mi Lee G, Einfeld DA, Kovesdi I, Wickham TJ (1999) Identification of a conserved receptor-binding site on the fiber proteins of CAR-recognizing adenoviridae. Science 286:1568–1571
24. Wickham TJ, Mathias P, Cheresh DA, Nemerow GR (1993) Integrins alpha v beta 3 and alpha v beta 5 promote adenovirus internalization but not virus attachment. Cell 73:309–319
25. Wang K, Huang S, Kapoor-Munshi A, Nemerow G (1998) Adenovirus internalization and infection require dynamin. J Virol 72:3455–3458
26. Greber UF, Willetts M, Webster P, Helenius A (1993) Stepwise dismantling of adenovirus 2 during entry into cells. Cell 75:477–486
27. Mathis JM, Stoff-Khalili MA, Curiel DT (2005) Oncolytic adenoviruses - selective retargeting to tumor cells. Oncogene 24:7775–7791
28. Koivunen E, Wang B, Ruoslahti E (1995) Phage libraries displaying cyclic peptides with different ring sizes: ligand specificities of the RGD-directed integrins. Biotechnology (NY) 13:265–270
29. Pasqualini R, Koivunen E, Ruoslahti E (1997) Alpha v integrins as receptors for tumor targeting by circulating ligands. Nat Biotechnol 15:542–546
30. Kasono K, Blackwell JL, Douglas JT, Dmitriev I, Strong TV, Reynolds P, Kropf DA, Carroll WR, Peters GE, Bucy RP, Curiel DT, Krasnykh V (1999) Selective gene delivery to head and neck cancer cells via an integrin targeted adenoviral vector. Clin Cancer Res 5:2571–2579
31. Vanderkwaak TJ, Wang M, Gomez-Navarro J, Rancourt C, Dmitriev I, Krasnykh V, Barnes M, Siegal GP, Alvarez R, Curiel DT (1999) An advanced generation of adenoviral vectors selectively enhances gene transfer for ovarian cancer gene therapy approaches. Gynecol Oncol 74:227–234
32. Wesseling JG, Bosma PJ, Krasnykh V, Kashentseva EA, Blackwell JL, Reynolds PN, Li H, Parameshwar M, Vickers SM, Jaffee EM, Huibregtse K, Curiel DT, Dmitriev I (2001) Improved gene transfer efficiency to primary and established human pancreatic carcinoma target cells via epidermal growth factor receptor and integrin-targeted adenoviral vectors. Gene Ther 8:969–976
33. Hay CM, De Leon H, Jafari JD, Jakubczak JL, Mech CA, Hallenbeck PL, Powell SK, Liau G, Stevenson SC (2001) Enhanced gene transfer to rabbit jugular veins by an adenovirus containing a cyclic RGD motif in the HI loop of the fiber knob. J Vasc Res 38:315–323

34. Smith T, Idamakanti N, Kylefjord H, Rollence M, King L, Kaloss M, Kaleko M, Stevenson SC (2002) In vivo hepatic adenoviral gene delivery occurs independently of the coxsackievirus-adenovirus receptor. Mol Ther 5:770–779
35. Mizuguchi H, Koizumi N, Hosono T, Ishii-Watabe A, Uchida E, Utoguchi N, Watanabe Y, Hayakawa T (2002) CAR- or alphav integrin-binding ablated adenovirus vectors, but not fiber-modified vectors containing RGD peptide, do not change the systemic gene transfer properties in mice. Gene Ther 9:769–776
36. Albelda SM, Mette SA, Elder DE, Stewart R, Damjanovich L, Herlyn M, Buck CA (1990) Integrin distribution in malignant melanoma: association of the beta 3 subunit with tumor progression. Cancer Res 50:6757–6764
37. Gladson CL, Cheresh DA (1991) Glioblastoma expression of vitronectin and the alpha v beta 3 integrin. Adhesion mechanism for transformed glial cells. J Clin Invest 88:1924–1932
38. You Z, Fischer DC, Tong X, Hasenburg A, Aguilar-Cordova E, Kieback DG (2001) Coxsackievirus-adenovirus receptor expression in ovarian cancer cell lines is associated with increased adenovirus transduction efficiency and transgene expression. Cancer Gene Ther 8:168–175
39. Suzuki K, Fueyo J, Krasnykh V, Reynolds PN, Curiel DT, Alemany R (2001) A conditionally replicative adenovirus with enhanced infectivity shows improved oncolytic potency. Clin Cancer Res 7:120–126
40. Douglas JT, Kim M, Sumerel LA, Carey DE, Curiel DT (2001) Efficient oncolysis by a replicating adenovirus (ad) in vivo is critically dependent on tumor expression of primary ad receptors. Cancer Res 61:813–817
41. Lamfers ML, Grill J, Dirven CM, Van Beusechem VW, Geoerger B, Van Den Berg J, Alemany R, Fueyo J, Curiel DT, Vassal G, Pinedo HM, Vandertop WP, Gerritsen WR (2002) Potential of the conditionally replicative adenovirus Ad5-Delta24RGD in the treatment of malignant gliomas and its enhanced effect with radiotherapy. Cancer Res 62:5736–5742
42. Fueyo J, Alemany R, Gomez-Manzano C, Fuller GN, Khan A, Conrad CA, Liu TJ, Jiang H, Lemoine MG, Suzuki K, Sawaya R, Curiel DT, Yung WK, Lang FF (2003) Preclinical characterization of the antiglioma activity of a tropism-enhanced adenovirus targeted to the retinoblastoma pathway. J Natl Cancer Inst 95:652–660
43. Lam JT, Bauerschmitz GJ, Kanerva A, Barker SD, Straughn JM, Wang M, Barnes MN, Blackwell JL, Siegal GP, Alvarez RD, Curiel DT, Hemminki A (2003) Replication of an integrin targeted conditionally replicating adenovirus on primary ovarian cancer spheroids. Cancer Gene Ther 10:377–387
44. Bauerschmitz GJ, Kanerva A, Wang M, Herrmann I, Shaw DR, Strong TV, Desmond R, Rein DT, Dall P, Curiel DT, Hemminki A (2004) Evaluation of a selectively oncolytic adenovirus for local and systemic treatment of cervical cancer. Int J Cancer 111:303–309
45. Bauerschmitz GJ, Lam JT, Kanerva A, Suzuki K, Nettelbeck DM, Dmitriev I, Krasnykh V, Mikheeva GV, Barnes MN, Alvarez RD, Dall P, Alemany R, Curiel DT, Hemminki A (2002) Treatment of ovarian cancer with a tropism modified oncolytic adenovirus. Cancer Res 62:1266–1270
46. Vogels R, Zuijdgeest D, van Rijnsoever R, Hartkoorn E, Damen I, de Bethune MP, Kostense S, Penders G, Helmus N, Koudstaal W, Cecchini M, Wetterwald A, Sprangers M, Lemckert A, Ophorst O, Koel B, van Meerendonk M, Quax P, Panitti L, Grimbergen J, Bout A, Goudsmit J, Havenga M (2003) Replication-deficient human adenovirus type 35 vectors for gene transfer and vaccination: efficient human cell infection and bypass of preexisting adenovirus immunity. J Virol 77:8263–8271
47. Ganly I, Kirn D, Eckhardt G, Rodriguez GI, Soutar DS, Otto R, Robertson AG, Park O, Gulley ML, Heise C, Von Hoff DD, Kaye SB (2000) A phase I study of Onyx-015, an E1B attenuated adenovirus, administered intratumorally to patients with recurrent head and neck cancer. Clin Cancer Res 6:798–806
48. Nemunaitis J, Ganly I, Khuri F, Arseneau J, Kuhn J, McCarty T, Landers S, Maples P, Romel L, Randlev B, Reid T, Kaye S, Kirn D (2000) Selective replication and oncolysis in p53 mutant tumors with ONYX-015, an E1B-55 kD gene-deleted adenovirus, in patients with advanced head and neck cancer: a phase II trial. Cancer Res 60:6359–6366
49. Nemunaitis J, Cunningham C, Buchanan A, Blackburn A, Edelman G, Maples P, Netto G, Tong A, Randlev B, Olson S, Kirn D (2001) Intravenous infusion of a replication-selective adenovirus (ONYX-015) in cancer patients: safety, feasibility and biological activity. Gene Ther 8:746–759
50. Wu JT, Kirn DH, Wein LM (2004) Analysis of a three-way race between tumor growth, a replication-competent virus and an immune response. Bull Math Biol 66:605–625
51. Chen P, Kovesdi I, Bruder JT (2000) Effective repeat administration with adenovirus vectors to the muscle. Gene Ther 7:587–595
52. Seshidhar Reddy P, Ganesh S, Limbach MP, Brann T, Pinkstaff A, Kaloss M, Kaleko M, Connelly S (2003) Development of adenovirus serotype 35 as a gene transfer vector. Virology 311:384–393
53. Gao W, Robbins PD, Gambotto A (2003) Human adenovirus type 35: nucleotide sequence and vector development. Gene Ther 10:1941–1949
54. Holterman L, Vogels R, van der Vlugt R, Sieuwerts M, Grimbergen J, Kaspers J, Geelen E, van der Helm E, Lemckert A, Gillissen G, Verhaagh S, Custers J, Zuijdgeest D, Berkhout B, Bakker M, Quax P, Goudsmit J, Havenga M (2004) Novel replication-incompetent vector derived from adenovirus type 11 (Ad11) for vaccination and gene therapy: low seroprevalence and non-cross-reactivity with Ad5. J Virol 78:13207–13215
55. Hemminki A, Kanerva A, Kremer EJ, Bauerschmitz GJ, Smith BF, Liu B, Wang M, Desmond RA, Keriel A, Barnett B, Baker HJ, Siegal GP, Curiel DT (2003) A canine conditionally replicating adenovirus for evaluating oncolytic virotherapy in a syngeneic animal model. Mol Ther 7:163–173
56. Le LP, Li J, Ternovoi VV, Siegal GP, Curiel DT (2005) Fluorescently tagged canine adenovirus via modification with protein IX-enhanced green fluorescent protein. J Gen Virol 86:3201–3208
57. Zhang Y, Bergelson JM (2005) Adenovirus receptors. J Virol 79:12125–12131
58. Iacobelli-Martinez M, Nepomuceno RR, Connolly J, Nemerow GR (2005) CD46-utilizing adenoviruses inhibit C/EBPbeta-dependent expression of proinflammatory cytokines. J Virol 79:11259–11268
59. Parks R, Evelegh C, Graham F (1999) Use of helper-dependent adenoviral vectors of alternative serotypes permits repeat vector administration. Gene Ther 6:1565–1573
60. Roy S, Shirley PS, McClelland A, Kaleko M (1998) Circumvention of immunity to the adenovirus major coat protein hexon. J Virol 72:6875–6879
61. Wu H, Dmitriev I, Kashentseva E, Seki T, Wang M, Curiel DT (2002) Construction and characterization of adenovirus serotype 5 packaged by serotype 3 hexon. J Virol 76:12775–12782
62. O'Riordan CR, Lachapelle A, Delgado C, Parkes V, Wadsworth SC, Smith AE, Francis GE (1999) PEGylation of adenovirus with retention of infectivity and protection from neutralizing antibody in vitro and in vivo. Hum Gene Ther 10:1349–1358
63. Romanczuk H, Galer CE, Zabner J, Barsomian G, Wadsworth SC, O'Riordan CR (1999) Modification of an adenoviral vector with biologically selected peptides: a novel strategy for gene delivery to cells of choice. Hum Gene Ther 10:2615–2626
64. Croyle MA, Chirmule N, Zhang Y, Wilson JM (2001) "Stealth" adenoviruses blunt cell-mediated and humoral immune responses against the virus and allow for significant gene expression upon readministration in the lung. J Virol 75:4792–4801
65. Croyle MA, Chirmule N, Zhang Y, Wilson JM (2002) PEGylation of E1-deleted adenovirus vectors allows significant gene expression on readministration to liver. Hum Gene Ther 13:1887–1900

66. Mok H, Palmer DJ, Ng P, Barry MA (2005) Evaluation of polyethylene glycol modification of first-generation and helper-dependent adenoviral vectors to reduce innate immune responses. Mol Ther 11:66–79
67. Green NK, Herbert CW, Hale SJ, Hale AB, Mautner V, Harkins R, Hermiston T, Ulbrich K, Fisher KD, Seymour LW (2004) Extended plasma circulation time and decreased toxicity of polymer-coated adenovirus. Gene Ther 11:1256–1263
68. Seymour LW, Fisher KD, Green NK, Hale SJ, Lyons M, Mautner V, Nicum S, Onion D, Oupicky D, Stevenson M, Ulbrich K (2003) Adenovirus retargeting and systemic delivery. Ernst Schering Res Found Workshop:107–114
69. Alemany R, Suzuki K, Curiel DT (2000) Blood clearance rates of adenovirus type 5 in mice. J Gen Virol 81:2605–2609
70. Ogawara K, Rots MG, Kok RJ, Moorlag HE, Van Loenen AM, Meijer DK, Haisma HJ, Molema G (2004) A novel strategy to modify adenovirus tropism and enhance transgene delivery to activated vascular endothelial cells in vitro and in vivo. Hum Gene Ther 15:433–443
71. Chillon M, Lee JH, Fasbender A, Welsh MJ (1998) Adenovirus complexed with polyethylene glycol and cationic lipid is shielded from neutralizing antibodies in vitro. Gene Ther 5:995–1002
72. Eto Y, Gao JQ, Sekiguchi F, Kurachi S, Katayama K, Mizuguchi H, Hayakawa T, Tsutsumi Y, Mayumi T, Nakagawa S (2004) Neutralizing antibody evasion ability of adenovirus vector induced by the bioconjugation of methoxypolyethylene glycol succinimidyl propionate (MPEG-SPA). Biol Pharm Bull 27:936–938
73. Akalu A, Liebermann H, Bauer U, Granzow H, Seidel W (1999) The subgenus-specific C-terminal region of protein IX is located on the surface of the adenovirus capsid. J Virol 73:6182–6187
74. Rosa-Calatrava M, Grave L, Puvion-Dutilleul F, Chatton B, Kedinger C (2001) Functional analysis of adenovirus protein IX identifies domains involved in capsid stability, transcriptional activity, and nuclear reorganization. J Virol 75:7131–7141
75. Parks RJ (2005) Adenovirus protein IX: a new look at an old protein. Mol Ther 11:19–25
76. Vellinga J, Van der Heijdt S, Hoeben RC (2005) The adenovirus capsid: major progress in minor proteins. J Gen Virol 86:1581–1588
77. Dmitriev IP, Kashentseva EA, Curiel DT (2002) Engineering of adenovirus vectors containing heterologous peptide sequences in the C terminus of capsid protein IX. J Virol 76:6893–6899
78. Li J, Le L, Sibley DA, Mathis JM, Curiel DT (2005) Genetic incorporation of HSV-1 thymidine kinase into the adenovirus protein IX for functional display on the virion. Virology 338:247–258
79. Meulenbroek RA, Sargent KL, Lunde J, Jasmin BJ, Parks RJ (2004) Use of adenovirus protein IX (pIX) to display large polypeptides on the virion—generation of fluorescent virus through the incorporation of pIX-GFP. Mol Ther 9:617–624
80. Le LP, Everts M, Dmitriev IP, Davydova JG, Yamamoto M, Curiel DT (2004) Fluorescently labeled adenovirus with pIX-EGFP for vector detection. Mol Imaging 3:105–116
81. Peters T (1996) All about albumin: biochemistry, genetics, and medical applications. Academic, San Diego
82. Osborn BL, Sekut L, Corcoran M, Poortman C, Sturm B, Chen G, Mather D, Lin HL, Parry TJ (2002) Albutropin: a growth hormone-albumin fusion with improved pharmacokinetics and pharmacodynamics in rats and monkeys. Eur J Pharmacol 456:149–158
83. Halpern W, Riccobene TA, Agostini H, Baker K, Stolow D, Gu ML, Hirsch J, Mahoney A, Carrell J, Boyd E, Grzegorzewski KJ (2002) Albugranin, a recombinant human granulocyte colony stimulating factor (G-CSF) genetically fused to recombinant human albumin induces prolonged myelopoietic effects in mice and monkeys. Pharm Res 19:1720–1729
84. Yeh P, Landais D, Lemaitre M, Maury I, Crenne JY, Becquart J, Murry-Brelier A, Boucher F, Montay G, Fleer R, et al (1992) Design of yeast-secreted albumin derivatives for human therapy: biological and antiviral properties of a serum albumin-CD4 genetic conjugate. Proc Natl Acad Sci USA 89:1904–1908
85. Osborn BL, Olsen HS, Nardelli B, Murray JH, Zhou JX, Garcia A, Moody G, Zaritskaya LS, Sung C (2002) Pharmacokinetic and pharmacodynamic studies of a human serum albumin-interferon-alpha fusion protein in cynomolgus monkeys. J Pharmacol Exp Ther 303:540–548
86. hgsi, http://www.hgsi.com/products/albuferon.html

Dynamic Monitoring of Oncolytic Adenovirus In Vivo by Genetic Capsid Labeling

Long P. Le, Helen N. Le, Igor P. Dmitriev, Julia G. Davydova, Tatyana Gavrikova, Seiji Yamamoto, David T. Curiel, Masato Yamamoto

Background: **Conditionally replicative adenoviruses represent a promising strategy to address the limited efficacy and safety issues associated with conventional cancer treatment. Despite rapid translation into human clinical trials and demonstrated safety, the fundamental properties of oncolytic adenovirus replication and spread and host–vector interactions in vivo have not been completely evaluated.** ***Methods:*** **We developed a noninvasive dynamic monitoring system to detect adenovirus replication. We constructed capsid-labeled E1/E3-deleted and wild-type adenoviruses (Ad-wt) by fusing the minor capsid protein IX with red fluorescent proteins mRFP1 and tdimer2(12), resulting in Ad-IX-mRFP1, Ad-IX-tdimer2(12), and Ad-wt-IX-mRFP1. Virus DNA replication, encapsidation, cytopathic effect, thermostability, and binding to primary receptor (coxsackie adenovirus receptor) were analyzed using real-time quantitative polymerase chain reaction, cell viability (MTS) assay, and fluorescence microscopy. Athymic mice (*n* = 4) carrying xenograft tumors that were derived from A549 lung adenocarcinoma cells were intratumorally inoculated with Ad-wt-IX-mRFP1, and adenovirus replication was dynamically monitored with a fluorescence noninvasive imaging system. Correlations between fluorescence signal intensity and viral DNA synthesis and replication were calculated using Pearson's correlation coefficient (*r*).** ***Results:*** **The red fluorescence label had little effect on viral DNA replication, encapsidation, cytopathic effect, thermostability, and coxsackie adenovirus receptor binding. The fluorescent signal correlated with viral DNA synthesis and infectious progeny production both in vitro and in vivo (in A549 cells, *r* = .99 and *r* = .65; in tumors, *r* = .93 and *r* = .92, respectively). The replication efficiency of Ad-wt-IX-mRFP1 in vivo was variable, and replication and viral spreading and persistence were limited, consistent with clinical observations.** ***Conclusions:*** **Genetic capsid labeling provides a promising approach for the dynamic assessment of oncolytic adenovirus function in vivo. [J Natl Cancer Inst 2006;98:203–14]**

Cancer is the second leading cause of disease-related mortality in humans after heart disease despite technologic advances in clinical management *(1)*. Conventional tumor therapies, including surgery, radiotherapy, and chemotherapy, often have poor efficacy and may have undesirable side effects *(2–4)*. Oncolytic viral treatment (also known as virotherapy) has been proposed as a promising alternative to surgery, radiotherapy, and chemotherapy. Conditionally replicative adenoviruses represent a candidate agent in this endeavor and have the potential for transductional and transcriptional targeting *(5–8)*, and their rapid evaluation in clinical trials has demonstrated their safety. However, to date, conditionally replicative adenoviruses, when used as single agents, have not displayed the anticipated efficacy for cancer therapy *(9)*. Oncolytic adenovirus function in humans therefore needs to be carefully explored. Current clinical trial protocols and methods cannot provide the interval endpoint data necessary to fully study fundamental issues such as the extent of replication and spread, specificity, viral persistence, and host–vector interactions. The lack of tools to directly and dynamically observe the performance of conditionally replicative adenoviruses in vivo has been a major impediment in realizing the clinical utility of replicative adenoviral agents.

Current methods of vector detection include chemical labeling, DNA and RNA quantification or hybridization, immunohistochemistry, and reporter gene expression. Although these methods have been operative for certain in vitro and in situ studies of adenovirus biology and gene therapy, their limitations are evident when they are used in replicative vector systems. Most of these terminal assays only allow examination of a particular sample and of one moment in time. However, the adenovirus oncolytic mechanism revolves around the concept that the initial virus amplifies and spreads to eventually yield a tumorwide therapeutic effect *(9–11)*. Such dynamics cannot be captured and represented by static analysis. The shortcomings of current vector detection methods are further complicated by the need to acquire multiple biopsies using an invasive procedure that is prone to sampling error and is concomitantly impractical for repeated monitoring of the entire tumor *(12–15)*. Reporter genes can only provide indirect and relative information with respect to virus replication and localization based on transgene expression.

The ideal approach for evaluating the replication and dissemination of oncolytic adenoviral agents should directly measure the viral mass that accrues from the initial administration without compromising replication capacity and be capable of noninvasive detection. To this end, we hypothesized that the detection of viral capsid proteins genetically fused with an imaging reporter

Affiliations of authors: Division of Human Gene Therapy (LPL, HNL, IPD, JGD, TG, SY, DTC, MY), Departments of Medicine, Pathology, Surgery, and Obstetrics and Gynecology and the Gene Therapy Center (IPD, DTC, MY), University of Alabama at Birmingham, Birmingham, AL.

Correspondence to: David T. Curiel, MD, PhD, Division of Human Gene Therapy, 901 19th St. S., BMR2-502, Birmingham, AL 35294-2172 (e-mail: curiel@uab.edu) or Masato Yamamoto, MD, PhD, Division of Human Gene Therapy, 901 19th St. S., BMR2-410 Birmingham, AL 35294-2172 (e-mail: masatoy@uab.edu).

See "Notes" following "References."

DOI: 10.1093/jnci/djj022

would provide such an index of viral replication and localization. Previously, we established an adenovirus capsid labeling strategy by fusing the minor capsid protein IX with enhanced green fluorescent protein (EGFP) *(16)*. Herein, we expand the capsid labeling technology to develop red fluorescent protein (RFP)–labeled adenoviruses with conserved viral function to monitor adenoviral replication in vivo.

Methods

Cell Culture

Human embryonic kidney 293 (American Type Culture Collection [ATCC], Manassas, VA), human embryonic retinoblast 911 *(17)*, human lung adenocarcinoma A549 (ATCC), BALB/c mouse transformed liver BNL-1NG-A.2 (ATCC), and Chinese hamster ovary (CHO) (ATCC) cells were maintained according to the suppliers' protocols. The cells were incubated at 37 °C and 5% CO_2 under humidified conditions.

Recombinant Adenovirus Construction

All viruses were constructed by homologous recombination in *Escherichia coli (18)*. All parental plasmids have been previously described: pShuttle-cytomegalovirus (CMV) (AdEasy system; Qbiogene, Irvine, CA), pRSETB-mRFP1 and pRSETB-tdimer2 (12) *(19)*, pSh1pIXNheI *(20)*, and pShuttle-wt-IX-EGFP *(21)*. Shuttle plasmids for the E1/E3-deleted (replication-deficient) vectors were constructed using restriction cloning as follows: pShuttle-E1-CMV-mRFP1 → pShuttle-CMV/BglII/HindIII + pRSETB-mRFP1/BamHI/HindIII; pShuttle-E1-CMV-tdimer2 (12) → pShuttle-CMV/BglII/HindIII + pRSETB-tdimer2(12)/BamHI/HindIII; pShuttle-IX-mRFP1 → pShlpIXNhe/BmtI/blunt + pRSETB-mRFP1/BamHI/EcoRI/blunt; pShuttle-IX-tdimer2(12) → pSh1pIXNhe/BmtI/blunt + pRSETB-tdimer2(12)/BamHI/EcoRI. All blunted fragments were generated with large Klenow fragment (New England Biolabs, Beverly, MA). pShuttle-wt-IX-mRFP1 was made by ligating pShuttle-IX-mRFP1/BspHI/MfeI with the BspHI/MfeI fragment from pShuttle-wt-IX-EGFP containing the wild-type E1 region; pShuttle-wt-IX-tdimer2(12) was similarly constructed. All E1/E3-deleted final genomes were made by recombining the above shuttle plasmids (linearized with PmeI) with pAdEasyDS, a modified pAdEasy plasmid that allows double-selection recombination (unpublished data). The wild-type shuttle vector Ad-wt-IX-mRFP1, with the red fluorescent protein label IX-mRFP1, was recombined with pTG3602DS, a modified E1-deleted pTG3602 plasmid that also allows double-selection recombination. Clones were verified by digestion with restriction enzymes and 0.8% agarose gel electrophoresis. The viruses generated include E1/E3-deleted control vectors (with wild-type [wt] protein IX [pIX]) adenovirus (Ad)-E1-CMV-mRFP1 and Ad-E1-CMV-tdimer2(12), E1/E3-deleted Ad-IX-mRFP1 and Ad-IX-tdimer2(12) with pIX modifications, and wild-type E1/E3 Ad-wt-IX-mRFP1. We were unable to recover Ad-wt-IX-tdimer2(12). Therefore, Ad-wt-IX-mRFP1 served as a surrogate oncolytic replicative vector for our studies.

Virus Propagation and Purification

Replication-deficient viruses were propagated in E1-complementing 911 retinoblast cells, and Ad-wt-IX-mRFP1 was amplified in A549 lung cancer cells. Viruses were purified by double cesium chloride (CsCl) ultracentrifugation (AdEasy system; QBiogene) and were dialyzed against phosphate-buffered saline (PBS, 1 mM KH_2PO_4, 0.15 mM NaCL, 5.5 mM Na_2HPO_4) containing 0.5 mM Mg^{2+}, 0.9 mM Ca^{2+}, and 10% glycerol. Final aliquots of virus were analyzed for viral particle titer (absorbance at 260 nm), transducing unit titer, and cytopathic effect unit titer. Based on a previously described protocol *(22)*, the transducing unit was determined by infecting 911 cells in 96-well plates with 1:10 serial dilutions of the virus and counting the number of red fluorescent cells 2 days after infection ($n = 3$). The same plate was assayed with an MTS viability assay (3-[4,5-dimethylthiazol-2-yl]-5-[3-carboxymethoxyphenyl]-2-[4-sulfophenyl]-2H-tetrazolium; Promega, Madison, WI) to determine the viral dilution that is cytotoxic to 50% of the cells. The experiment was performed once in triplicate. Based on the number of cells seeded (15000/well), the cytopathic effect unit was calculated such that 1 unit is defined as the amount of virus that causes cytopathic effect in one 911 cell in 2 days *(23)*. All viruses were stored at –80 °C until use.

Characterization of Virus Gradient Fractions

For the fractionation studies, Ad-E1-CMV-mRFP1, Ad-E1-CMV-tdimer2(12), Ad-IX-mRFP1, and Ad-IX-tdimer2(12) were each propagated in 10 150-mm dishes of 911 cells. Cells were harvested by aspiration, and viruses were purified by double CsCl ultracentrifugation as described above, in which the top and bottom bands were retained in the same sample after two centrifugation steps, yielding one gradient from the 10 dishes. After the second centrifugation, fractions of 2 drops each (approximately 100 μL) were collected through a perforation at the bottom of the tube into a 96-well white opaque plate. Plates with the viral fractions were measured with a microplate fluorometer (Fluostar Optima; BMG Labtechnologies, Durham, NC) using a 560/10 nm excitation filter for all viruses, a 585/10 nm emission filter for Ad-IX-tdimer2(12), and a 605/10 nm emission filter Ad-IX-mRFP1. To determine viral DNA content, a sample (10 μL) of each fraction was diluted in 90 μL of 0.5% sodium dodecyl sulfate in PBS and incubated at room temperature for 10 minutes to release the viral genomes. Absorbance at 260 nm was then measured for each sample (MBA 2000; Perkin Elmer, Shelton, CT).

Tracking of Red Fluorescent Adenovirus Infection

A549 cells (2.5×10^5 cells/well) were seeded in phenol red–free growth medium (Dulbecco's modified Eagle [DME]–5% fetal calf serum [FCS]) in six-well plates containing glass coverslips (one per well). The next day, cells were incubated for 1 hour at 4 °C with (two wells) or without (four wells) recombinant adenovirus serotype 5 fiber knob *(24)* (1 μg/mL) in 500 μL of phenol red-free DME medium containing 25 mM HEPES buffer. Ad-IX-mRFP1 or Ad-IX-tdimer2(12) (10000 viral particles/cell) were added to the infection solution to a total volume of 1 mL. The viruses were allowed to bind to the cells at 4 °C for 1 hour (cell binding and Ad5 knob block). Two wells with the added viruses were further incubated at 37 °C for 1.5 hours (nuclear trafficking). Cells from binding and nuclear trafficking experiments were washed three times with PBS and then fixed to the coverslips with 3% formalin (Tousimis,

Rockville, MD) for 10 minutes. Cells were washed three times with PBS, stained with 1 μg/mL Hoescht 33342 (Molecular Probes, Eugene, OR) for 5 minutes at room temperature to visualize nuclear DNA, washed three times with PBS, mounted in mounting medium (Biomeda, Foster City, CA), and sealed to glass slides.

In Situ Detection of Ad-wt-IX-mRFP1 Biodistribution

All methods were approved by the Institutional Animal Care and Use Committee of the University of Alabama at Birmingham and performed according to their guidelines. Three C57/BL6 mice (8 weeks of age; Charles River Laboratories, Wilmington, MA) were anesthetized with 2% isoflurane at approximately 0.5 L/min, and 200 μL of PBS containing 10^{11} Ad-wt-IX-mRFP1 viral particles was injected into the tail vein of each mouse. The mice were killed by carbon dioxide gas euthanasia 20 minutes after virus injection, and their organs (lung, kidney, liver, and spleen) were surgically removed and frozen by flash freezing in liquid nitrogen. The samples were stored at –80 °C until sectioning (Minotome PLUS; Triangle Biomedical Sciences, Durham, NC). Sections (5-μm thick) of the frozen organs were fixed onto glass slides and stained with Hoechst 33342 as described above. Glass coverslips were mounted and sealed as above.

Fluorescence Microscopy

The slides from the cellular tracking and biodistribution experiments were observed under epifluorescence microscopy. This procedure was performed with an inverted IX-70 microscope (Olympus, Melville, NY) equipped with a Magnifire digital charge-coupled device camera (Optronics, Goleta, CA). Images were acquired with a 100× objective using oil immersion and digitally deconvolved with Iris version 4.15a *(25)* by applying the Richardson-Lucy algorithm with 15 iterations. An image of a single fluorescent virus particle with a high signal-to-noise ratio was used to estimate the point spread function, as suggested by the software documentation. Red fluorescent protein and Hoechst stain images were merged using Adobe Photoshop 7.0 (Adobe Systems, Inc., San Jose, CA).

DNA Packaging Analysis

DNA packaging was analyzed using a previously reported protocol *(26)*. Briefly, 911 cells (1×10^5/well) were infected with the control and pIX-modified vectors at 1 cytopathic effect unit/cell in 24-well plates. On days 1, 2, 3, and 4 after infection, the cells were collected by aspiration, and DNA was extracted using the QIAamp DNA Blood Mini Kit (QIAGEN, Valencia, CA) according to the manufacturer's instructions. Half of the cells were not pretreated before DNA extraction and were used to determine total intracellular viral DNA. The other half was used to measure intracellular encapsidated viral DNA. The cells were incubated in deoxycholate buffer (0.4% sodium deoxycholate, 0.1 M Tris-Cl, pH 9.0, and 20% ethanol) before DNA extraction to avoid disrupting the viral capsid and in 500 mM spermine to remove unencapsidated viral DNA. The viral genome copy number was determined by TaqMan quantitative real-time polymerase chain reaction (PCR) using E4-specific primers (LightCycler System; Roche Applied Science, Indianapolis, IN). The experiment was performed once in triplicate.

Cytopathic Effect Assay

911 cells ($n = 5000$) were infected with the control and pIX-modified E1/E3-deleted vectors (0.5, 0.05, and 0.005 cytopathic effect unit/cell) in 100 μL of phenol red–free DME–5% FCS (five replicates for each condition and five wells of noninfected cells as negative controls). Cytopathic effect was measured by an MTS assay (3-[4,5-dimethylthiazol-2-yl]-5-[3-carboxymethoxyphenyl]-2-[4-sulfophenyl]-2H-tetrazolium; Promega) on days 0, 2, 4, 6, 8, and 10 after infection. Results are presented as the percentage of noninfected cells after subtracting the blank values (medium only).

Thermostability Assay

Thermostability was analyzed using a modified version of a previously reported protocol *(20)*. Samples of E1/E3-deleted control and pIX modified vectors (10^6 transducing units in 80 μL of PBS) were incubated at 45 °C for 0, 5, 10, 20, and 40 minutes. Transducing unit infectious titers were then determined for the samples using the above-mentioned procedure.

TaqMan Real-Time Quantitative PCR Binding Assay

All steps were carried out with 1% bovine serum albumin (BSA)–PBS buffer. Suspended CHO and A549 cells (2×10^5 in 100 μL) in test tubes were incubated with 100 μL of buffer alone or buffer containing 2.5 μg/mL recombinant fiber knob (to examine blocking of the primary adenovirus receptor, CAR) at 4 °C with vigorous shaking for 1 hour. Ad-E1-CMV-mRFP1, Ad-E1-CMV-tdimer2(12), Ad-IX-mRFP1, or Ad-IX-tdimer2(12) were then added (5000 virus particles/cell) to the cells. The virus–cell mixtures were incubated with shaking for another hour at 4 °C. The cells were then washed three times and collected for total DNA preparation using the QIAamp DNA Blood Mini Kit, and the viral genome copy number was determined using TaqMan quantitative real-time PCR with E4 primers, as described above.

In Vitro Correlation of pIX-mRFP1 Signal With Replication

A549 (human lung adenocarcinoma, replication permissive, 5000 cells/well) and BNL-1NG-A.2 (BALB/c transformed liver, 5000 cells/well) cells were infected with 1, 0.1, 0.01, and 0.001 cytopathic effect unit/cell of Ad-wt-IX-mRFP1 and Ad-IX-mRFP1 (E1/E3-deleted) in five white opaque 96-well plates ($n = 6$ for each condition). Fluorescence was measured daily with a fluorometer (Fluostar Optima, BMG Labtechnologies, Durham, NC). On days 2, 4, 6, 8, and 10 after infection, the cells and medium (<100 μL) were collected from the wells, which were subsequently washed with 100 μL of PBS. The cells, medium, and washes were transferred to the corresponding sample microcentrifuge tubes to give a total volume <200 μL. All samples were subjected to three freeze-thaw cycles in a dry ice bath. The tubes were then centrifuged at 18 188 ×g and 4 °C for 10 minutes; 30 μL of the supernatant was reserved to determine the transducing unit titer, and the rest (170 μL) was processed for viral DNA using the QIAamp DNA Blood Mini Kit and quantified by TaqMan real-time quantitative PCR with E4 primers, as described above. The correlation coefficient (Pearson's r) was calculated with the CORREL function in Microsoft Excel, Office 2003 (Microsoft Corp., Redmond, WA).

Fluorescence-Based In Vivo Optical Imaging

pIX-mRFP1 fluorescence was detected noninvasively using a custom-built optical imaging system. Briefly, a cryogenically cooled, back-illuminated Princeton Instruments VersArray:1KB digital charge-coupled device camera (Roper Scientific, Trenton, NJ) with a liquid nitrogen autofill system was mounted on top of a light-tight enclosure. The camera was coupled with a 50-mm Nikkor *f*/1.2 lens (Nikon, Melville, NY) for image acquisition. Excitation light for fluorescence imaging was delivered by a Dolan-Jenner Fiber-Lite MH-100 metal halide light source equipped with a dual-fiberoptic gooseneck. Excitation and emission filter wheel assemblies were integrated with the light source and lens. Bandpass filters included 490/10 and 560/10 nm for excitation and 535/30 and 605/55 nm for emission (Chroma Technology, Rockingham, VT).

A549 cells (7.5×10^6) were inoculated in the left and right flanks of athymic nude mice ($n = 6$) (National Cancer Institute-Frederick Animal Production Area, Frederick, MD) to establish tumors. When the tumors reached 5–10 mm in diameter (in approximately 3 weeks), a single intratumoral injection of Ad-wt-IX-mRFP1 (10^{10} viral particles in 10 μL total volume of PBS) was performed for each tumor without deliberate spreading of the virus with the needle. Mice (up to three) were placed in the imaging chamber and maintained with 2% isoflurane gas anesthesia at a flow rate of approximately 0.5–1 L/min per mouse (Highland Medical Equipment, Temecula, CA). Images were acquired with WinView/32 software (Roper Scientific). To detect red fluorescence, images were captured at *f*/4 and *f*/2 with 2- and 5-second exposure times using two filter combinations: 560/605 and 490/605 (excitation/emission). The former filter setting applies to a red fluorescence signal and the latter configuration pertains to background autofluorescence. A bright-field image was also taken at *f*/16 for 1 second and at the lowest light level. Background subtraction was performed in WinView/32 after scaling the background image with a factor determined from areas surrounding tumors of individual mice *(27)*. The positive signal from background subtracted images was segmented and analyzed in ImageTool 3.0 (The University of Texas Health Science Center in San Antonio, TX) for integrated density (the product of mean intensity and signal area). Index color image overlays were created in Photoshop 7.0 (Adobe) using the segmentation or thresholding parameters determined in ImageTool.

In Vivo Correlation of pIX-mRFP1 Signal With Replication and Dynamic Monitoring

All mice ($n = 6$) were imaged daily and analyzed using the above procedure. On day 6 after injection, the day after the maximal signal intensity was observed, four mice were killed. Dissected tumors were imaged in their anatomic position ex vivo and then frozen at –80 °C until use. The tumors were homogenized with the Mini-Beadbeater (BioSpect Products, Bartlesville, OK) and incubated with liver digest medium (4 μL/mg of tumor; Invitrogen, Carlsbad, CA) for 1 hour at 37 °C to further disrupt the tissue. Samples of the tumor homogenate (40 μL [or roughly 10 mg] for large tumors and 10 μL [or approximately 2.5 mg] for small tumors) were used for total DNA determination and viral DNA copy number as described above. The transducing unit titer and cytopathic effect unit titers were determined in the homogenate using the same methods described for purified virus. However, in this case, the cytopathic effect unit was determined 10 days after infection and would give higher values than the same assay read 2 days after infection. All results are presented as total values scaled for the entire tumor mass. The correlation coefficient (Pearson's *r*) was calculated with the CORREL function in Microsoft Excel. Two of the six original mice were maintained and imaged over the 30-day experiment. Images were processed and analyzed accordingly.

Comparison of In Situ Detection of pIX-mRFP1 Signal With Hexon Staining

Established A549 tumors injected with Ad-wt-IX-mRFP1 were excised on day 7 after injection and frozen in a dry ice–ethanol bath. Frozen tumor sections (5 μm) were fixed onto glass slides with 3% formalin, blocked with 1% BSA–PBS, and probed with a polyclonal goat anti-hexon antibody at approximately 20 μg/mL (1 : 200 dilution; Chemicon, Temecula, CA) for 1 hour at room temperature. The slides were then washed with 1% BSA–PBS and incubated with an Alexa Fluor 488–labeled secondary donkey anti-goat antibody (1:200 dilution; Molecular Probes, Eugene, OR). The slides were washed again with 1% BSA–PBS, and the cells were counterstained with Hoechst 33342 (Molecular Probes) and prepared for fluorescence microscopy as described above.

Statistical Analysis

All statistical analyses were performed with a two-sided single-factor analysis of variance test. P values <.05 were considered statistically significant.

Results

Incorporation of pIX-mRFP1 and pIX-tdimer2(12) Into Viral Particles

We initially constructed E1/E3-deleted viruses with carboxyl-terminal fusions of pIX with monomeric and tandem dimer red fluorescent proteins [mRFP1 and tdimer2(12), respectively] *(19)*. After standard CsCl double ultracentrifugation of the two vectors, we observed that the colors of the empty (top) and mature (bottom) viral bands were different from those obtained from purified conventional unlabeled vectors: Ad-IX-mRFP1 was purple and Ad-IX-tdimer2(12) was pink (Fig. 1, A, data not shown). The difference in color between these two vectors is probably due to the excitation and emission properties of the fluorescent proteins *(19)*. Applying our previously established approach *(21)*, we collected fractions of each viral gradient and analyzed each sample for red fluorescence and viral DNA content. Fluorescent peaks were detected for both the bottom and top bands of the two viruses, which coincided with the optical absorbance peaks of viral DNA (Fig. 1, B). Red fluorescent purified viral particles could be easily visualized using fluorescence microscopy for both vectors (Fig. 1, C).

Tracking of Ad-IX-mRFP1

To examine the use of the red fluorescent adenoviruses for virus tracking, we incubated A549 cells with Ad-IX-mRFP1 at 4 °C for 1 hour to allow virus binding but not internalization.

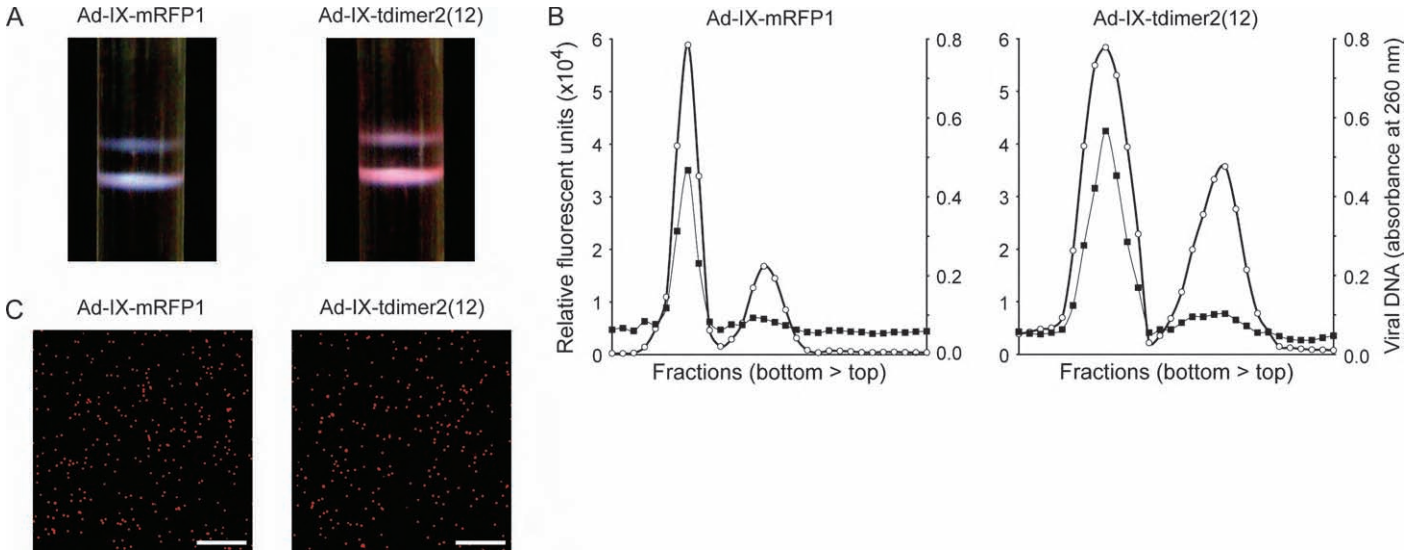

Fig. 1. Characterization of red fluorescent protein IX (pIX)–labeled adenovirus gradients. **A**) Images of Ad-IX-mRFP1 and Ad-IX-tdimer2(12) top and bottom virus bands after cesium chloride (CsCl) ultracentrifugation that were captured under normal ambient lighting. **B**) Fractions from Ad-IX-mRFP1 and Ad-IX-tdimer2(12) CsCl virus gradients were measured for red fluorescence (**open circles**) and viral DNA content (absorbance at 260 nm, **closed squares**). **C**) Also shown are the purified red fluorescent adenoviral particles visualized under fluorescence microscopy. **Bar** = 10 μm.

Fluorescence microscopy revealed distinct binding of Ad-IX-mRFP1 particles to the plasma membrane (Fig. 2, A, cell binding). In another experiment, we allowed the viruses to bind to the cells at 4 °C for one hour and then at 37 °C for 1.5 hours. After the incubation at 37 °C, numerous viruses were detected at the nuclear membrane or inside the nucleus (Fig. 2, A, nuclear trafficking). We also examined whether preincubation with recombinant Ad5 knob would mitigate virus binding. Indeed, few particles remained bound to the A549 cells after washing when knob blocking was implemented (Fig. 2, A, Ad5 knob block), suggesting that the pIX-mRFP1 fusion did not negatively affect the virus's interaction with its primary coxsackie adenovirus receptor. Similar results were also obtained for Ad-IX-tdimer2(12) (data not shown).

Detection of Ad-wt-IX-mRFP1 in Tissue

To test the ability to detect red fluorescent virus in situ, we injected Ad-wt-IX-mRFP1 (10^{11} virus particles) into the tail veins of C57/BL6 mice. Twenty minutes after injection, the lungs, kidneys, liver, and spleen were surgically removed, frozen, and sectioned for microscopy. In the lungs, red particles were occasionally visualized around blood vessels and endothelial cells. Likewise, very few particles were detected in the kidneys. Numerous viral particles were seen in the liver, with accumulation being especially prominent in the sinusoids, where the Kupffer cells reside. Single particles (orange arrows, Fig. 2, B) were observed in the hepatocytes. This localization pattern in the liver closely resembles what we observed with Ad-wt-IX-EGFP *(16)*. A substantial amount of virus was also detected in the spleen, mostly in the marginal zones between the white and red pulp (Fig. 2, B).

DNA Encapsidation Efficiency of Red Fluorescent Viruses

Our goal was to establish genetic labeling of adenovirus with minimal perturbation of normal viral function to retain efficient oncolytic activity. One important function for viral replication is the DNA encapsidation efficiency of the red fluorescent adenoviruses. To analyze this function, we assayed lysates from 911 cells infected with the two red fluorescent adenoviruses and their respective E1-CMV expression vector controls for both total and encapsidated viral DNA copy number using TaqMan quantitative real-time PCR (Fig. 3, A, left and middle panels). The data revealed no differences in the total viral DNA replication of the two labeled vectors relative to their controls during 4 days of infection, except for total viral DNA comparison between the tdimer2(12) vectors on day 4 [Ad-E1-CMV-tdimer2(12) versus Ad-IX-tdimer2(12) at day 4, means = 5.50×10^6 versus 9.84×10^6, difference = 4.33×10^6, 95% confidence interval = 2.98×10^6 to 5.69×10^6]. Similarly, there were no differences in encapsidated viral DNA between the two labeled vectors and their controls during the first 3 days of infection. When the data were expressed as encapsidated viral DNA fraction, no differences were noted between the two labeled vectors and their controls (Fig. 3, A, right panel).

Cytopathic Effect of Red Fluorescent Adenoviruses

The red fluorescent adenoviruses were also evaluated with respect to their ability to induce a cytopathic effect in infected cells. This assay gauges viral function on a more comprehensive level than the previous assays because the cytopathic effect is dependent not only on efficient transduction and virus replication but also on spread to neighboring cells. Any defect in the infection process would result in decreased cytotoxicity. 911 cells were infected with 0.5, 0.05, or 0.005 cytopathic effect units/cell of Ad-E1-CMV-mRFP1, Ad-IX-mRFP1, Ad-E1-CMV-tdimer2(12), and Ad-IX-tdimer2(12). Cell viability was measured every 2 days after infection for a total of 10 days. Under the various conditions examined, there were statistically significant differences noted at some time points and similarities at other time points between the labeled vectors and their controls (Fig. 3). Overall, however, the differences were minor. Moreover, all four viruses

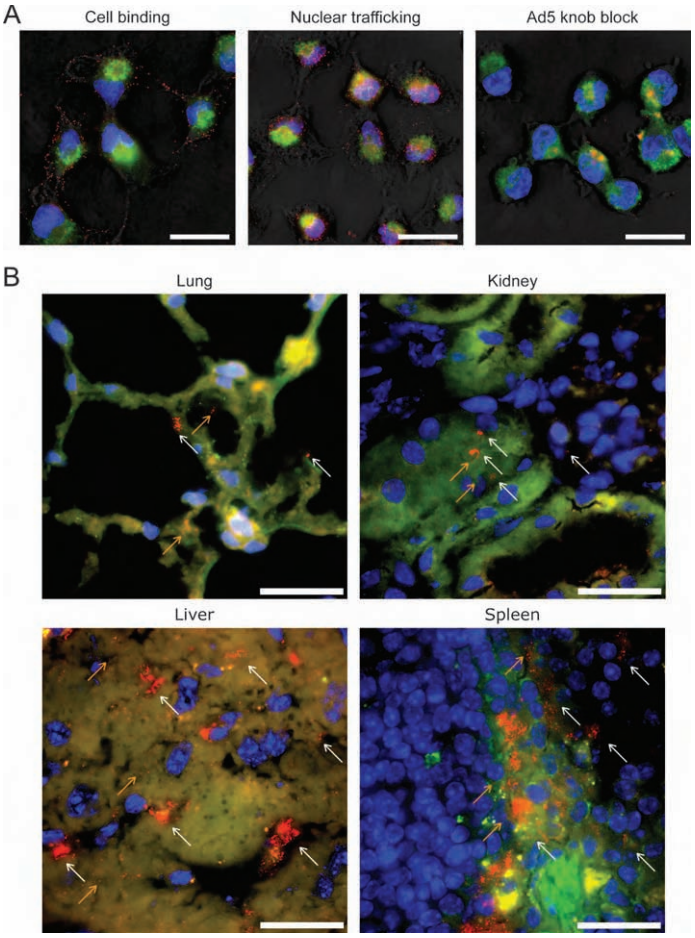

Fig. 2. Detection of Ad-IX-mRFP1 particles in vitro. **A**) Tracking of adenovirus infection in cultured cancer cells. A549 lung adenocarcinoma cells incubated with the respective red fluorescent adenoviruses were imaged using fluorescence microscopy to visualize virus binding (**left panel**) and nuclear trafficking (**middle panel**). In the **right panel**, A549 cells were blocked with recombinant Ad5 knob before the viruses were added. **Red**, Ad-IX-mRFP1; **blue**, Hoechst stain for nuclear DNA; **green**, cytoplasmic and nuclear autofluorescence; and **black/white**, phase-contrast image of the cells. **Bar** = 20 μm. **B**) Detection of Ad-wt-IX-mRFP1 in tissues. Ad-wt-IX-mRFP1 particles were detected in the lung, kidney, liver, and spleen of a C57/BL6 mouse after intravenous injection with 10^{10} virus particles. **White arrows** designate clusters of fluorescent viral particles and **orange arrows** show single particles. **Bar** = 20 μm.

achieved total oncolysis with similar kinetics in a dose-dependent manner (Fig. 3, B).

Thermostability of Red Fluorescent Adenoviruses

Adenovirus protein IX functions as a minor protein in capsid stabilization *(28,29)*. To test whether the fusion of red fluorescent proteins to pIX destabilizes the adenovirus capsid structure, we incubated the labeled viruses and their controls at 45 °C. After exposing the viruses to 45 °C for various time intervals, we determined the transducing unit to assess the presence of the remaining infectious virions that survived the temperature stress treatment. No statistically significant decrease in thermostability was detected for Ad-IX-mRFP1 and Ad-IX-tdimer2(12) compared with their controls Ad-E1-CMV-mRFP1 and Ad-E1-CMV-tdimer2(12) after 5 or 10 minutes at 45 °C (Fig. 4, A). After 20 minutes of heat treatment, no infectious viruses remained for any of the four vectors (Fig. 4, A).

Coxsackie Adenovirus Receptor–Dependent Binding of Red Fluorescent Adenoviruses

We next evaluated the extent of the red fluorescent adenovirus interaction with the Ad5 primary coxsackie adenovirus receptor. Coxsackie adenovirus receptor–deficient CHO cells were chosen as the negative control and high coxsackie adenovirus receptor–expressing A549 cells as the positive control. The viruses were incubated with A549 and CHO cells at 4 °C using vigorous agitation for 1 hour and were then washed to remove unbound viruses. TaqMan real-time quantitative PCR was used to quantify the number of bound virions. As expected, CHO cells showed minimal binding of all four vectors, similar to cell samples with no virus addition (Fig. 4, B). A549 cells, however, demonstrated abundant binding of Ad-IX-mRFP1 and Ad-IX-tdimer2(12) that was equal to that of the control viruses Ad-E1-CMV-mRFP1 and Ad-E1-CMV-tdimer2(12). Similar to the tracking assay, binding was greatly attenuated when the A549 cells were initially incubated with recombinant Ad5 knob (Fig. 4, B).

Correlation of pIX-mRFP1 Signal With DNA Replication and Progeny Production In Vitro

To determine whether the fluorescence intensity of the label itself corresponds to the level of virus mass and replication, we constructed a pIX-mRFP1–labeled virus with intact E1 and E3 regions to serve as a surrogate oncolytic agent. In contrast, a wild-type pIX-tdimer2(12) virus could not be recovered, probably owing to compromise of the pIX function required in packaging full-length genomes *(30)*. As a result, we used Ad-wt-IX-mRFP1 to further investigate the genetic labeling system. We infected A549 and BNL-1NG-A.2 cells in vitro with various amounts of Ad-wt-IX-mRFP1. A549 cells are human lung adenocarcinoma cells that are frequently used to efficiently propagate replication-competent Ad vectors (possessing E1). BNL-1NG-A.2 cells are transformed BALB/c liver cells. Because human adenoviruses in general do not replicate productively in murine cells *(31)*, these two cell lines represent distinct substrates, the former being replication permissive and the latter being replication nonpermissive for human Ad5.

Cell infection was monitored daily over 10 days by measuring the kinetics of red fluorescence resulting from Ad-wt-IX-mRFP1 replication. In BNL-1NG-A.2 cells, no increase in pIX-mRFP1 red fluorescence was detected relative to baseline levels under any of the conditions tested (Fig. 5, A, left panel). By contrast, strong, dose-dependent augmentation of red fluorescence signal with time was observed in A549 cells (Fig. 5, A, middle panel). These data support the concept that the pIX-mRFP1 signal can serve as an index of virus replication. Fluorescence microscopy of BNL-1NG-A.2 and A549 cells infected with Ad-wt-IX-mRFP1 corresponded to the quantitative fluorescence observations (data not shown). A red fluorescence signal was correlated with two parameters of virus replication over the 10-day infection depicted for 0.1 cytopathic effect unit/cell of Ad-wt-IX-mRFP1: viral DNA synthesis (r = .99) and transducing unit titer (r = .65). The poor correlation between fluorescence and transducing unit titer was much improved during the first 8 days, when cellular and medium conditions were suitable for active replication and progeny stability (r = .92) (Fig. 5, A, right panel).

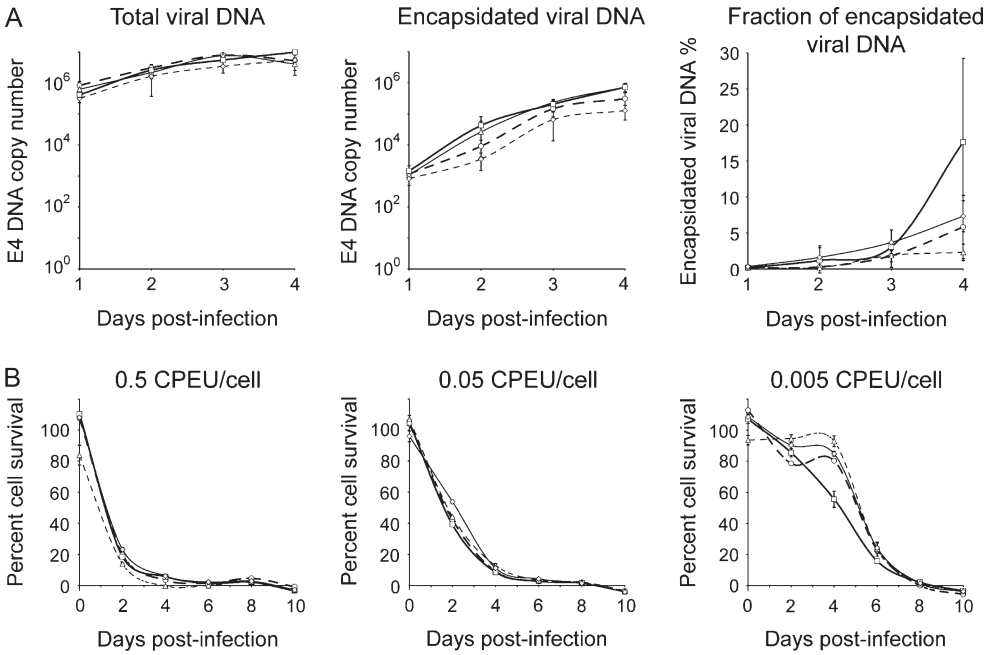

Fig. 3. DNA packaging efficiency of Ad-IX-mRFP1 and Ad-IX-tdimer2(12). **A**) Viral DNA copy number for Ad-E1-CMV-mRFP1 (**open circles**), Ad-IX-mRFP1 (**open squares**), Ad-E1-CMV-tdimer2(12) (**open triangles**), and Ad-IX-tdimer2(12) (**open diamonds**) were quantified during infection of 911 cells over 4 days. Three replicates were performed. **Error bars** represent 95% confidence intervals. Comparison of total viral DNA over 4 days: Ad-E1-CMV-mRFP1 versus Ad-IX-mRFP1 (P = .23, P = .40, P = .58, and P = .56, for days 1, 2, 3, and 4, respectively) and Ad-E1-CMV-tdimer2(12) versus Ad-IX-tdimer2(12) (P = .20, P = .11, P = .07, and P<.001 for days 1, 2, 3, and 4, respectively). Comparison of encapsidated viral DNA over 4 days: Ad-E1-CMV-mRFP1 versus Ad-IX-mRFP1 (P = .76, P = .35, P = .08, and P = .05 for days 1, 2, 3, and 4, respectively), and Ad-E1-CMV-tdimer2(12) versus Ad-IX-tdimer2(12) (P = .17, P = .12, P = .06, and P = .005 for days 1, 2, 3, and 4, respectively). The results are also expressed as fraction of encapsidated viral DNA (encapsidated divided by total viral DNA). Comparison of encapsidated viral DNA fraction over 4 days: Ad-E1-CMV-mRFP1 versus Ad-IX-mRFP1 (P = .36, P = .37, P = .08, and P = .14 for days 1, 2, 3, and 4, respectively) and Ad-E1-CMV-tdimer2(12) versus Ad-IX-tdimer2(12) (P = .29, P = .33, P = .27, and P = .06 for days 1, 2, 3, and 4, respectively). **B**) Cytopathic effect of Ad-E1-CMV-mRFP1 (**open circles**), Ad-IX-mRFP1 (**open squares**), Ad-E1-CMV-tdimer2(12) (**open triangles**), and Ad-IX-tdimer2(12) (**open diamonds**) was determined in 911 cells every 2 days over 10 days after infection (n = 5). Cell viability was measured by an MTS (3-[4,5-dimethylthiazol-2-yl]-5-[3-carboxymethoxyphenyl]-2-[4-sulfophenyl]-2H-tetrazolium) assay and displayed as the percentage of noninfected cells. Comparison of Ad-E1-CMV-mRFP1 versus Ad-IX-mRFP1 over the respective days: 0.5 cytopathic effect unit (CPEU)/cell (P = .05, P = .13, P<.001, P = .72, P<.001, and P<.001); 0.05 CPEU/cell (P = .51, P = .003, P = .33, P = .59, P = .11, and P = .11); and 0.005 CPEU/cell (P = .01, P = .004, P = .01, P = .03, P = .001, and P = .002). P values for comparison of Ad-E1-CMV-tdimer2(12) versus Ad-IX-tdimer2(12) over the respective days: 0.5 CPEU /cell (P<.001, P<.001, P<.001, P = .51, and P = .51); 0.05 CPEU/cell (P<.001, P<.001, P = .07, P = .06, P = .05, and P = .05); and 0.005 CPEU/cell (P<.001, P = .08, P = .003, P = .83, P = .78, and P = .71). All P values are two-sided and were calculated by single-factor analysis of variance.

Correlation of pIX-mRFP1 Signal With DNA Replication and Progeny Production In Vivo

The ultimate utility of our genetic capsid labeling system requires a correlation between fluorescence and viral mass in vivo. To establish such a correlation, we used a fluorescence based noninvasive optical imaging system to detect the replication of Ad-wt-IX-mRFP1 in vivo. Six athymic nude mice with established A549 tumors in the left and right flanks were injected intratumorally with a single dose of Ad-wt-IX-mRFP1 and imaged daily for red fluorescence. After 6 days, tumors from four of the mice were excised, imaged ex vivo, and homogenized. A portion of each tumor homogenate was used to measure viral DNA content, and the clarified supernatant of the remaining homogenate was used to quantify transducing unit titer and cytopathic effect unit titer.

An array of replication patterns in the different tumors were observed, despite the initial similarity in tumor sizes and viral treatment (Fig. 5, B). The variation in fluorescence intensity among the eight tumors allowed us to perform a correlative analysis of the underlying level of viral replication for a wide range of signals. Based on our hypothesis, we expected lower levels of adenovirus in tumors with weaker fluorescence and vice versa. The fluorescence-integrated densities (product of the mean intensity and segmented signal area) were strongly correlated with total viral genome copy number, transducing unit titer, and cytopathic effect unit titer in the tumors (Fig. 5, C, r = .93, r = .92, and r = .97, respectively). Likewise, associating the integrated densities observed in the ex vivo images with these same parameters of adenovirus detectionresulted in even stronger correlation (Fig. 6, A and B, r = .96, r = .97, and r = .97, respectively). We also conducted the same experiment with BNL-1NG-A.2 xenograft tumors (human Ad5 replication nonpermissive) as a negative control, which did not produce any red fluorescence signal (data not shown). In addition to strong correlation between fluorescence signal and viral replication, pIX-mRFP1 localization corresponded with the localization of hexon immunostaining (Fig. 7), a technique that is often used to detect adenovirus in participants of clinical trials *(32,33)*.

Dynamic Monitoring of Red Fluorescent Ad-wt-IX-mRFP1 Replication In Vivo

We used the genetic adenovirus labeling system to dynamically monitor the replication and oncolysis of Ad-wt-IX-mRFP1 in vivo in two of the six mice with established A549 tumors on the left and right flanks for 30 days. The images

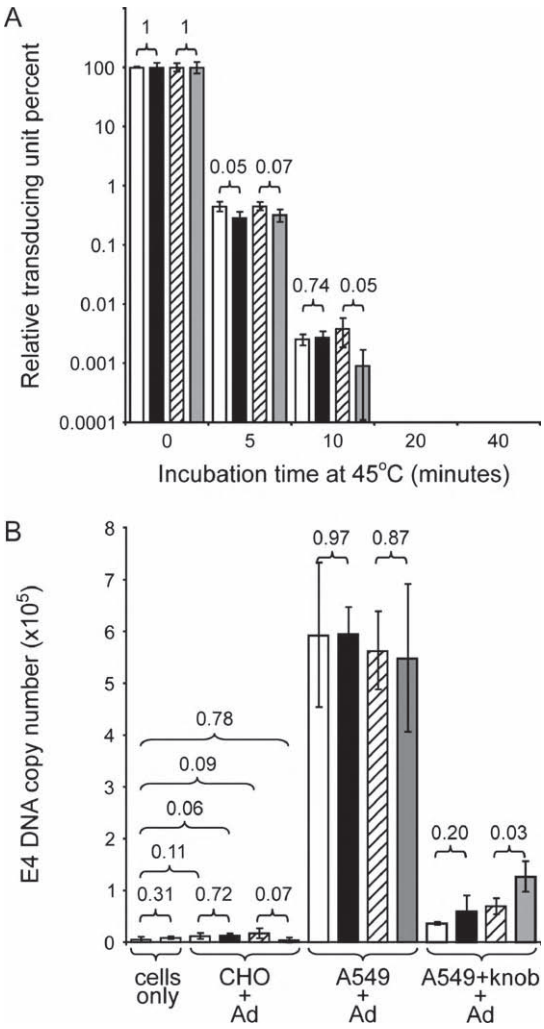

Fig. 4. Thermostability and coxsackie adenovirus receptor–dependent binding of red fluorescent adenoviruses. **A**) Thermostabilities of Ad-E1-CMV-mRFP1 (**open bar**), Ad-IX-mRFP1 (**filled bar**), Ad-E1-CMV-tdimer2(12) (**hatched bar**), and Ad-IX-tdimer2(12) (**gray bar**) were determined at 45 °C for various times. Results are presented as the percentage of nontreated virus based on transducing unit titer. Three replicates were performed. **Error bars** represent 95% confidence intervals. *P* values (two-sided) calculated by analysis of variance are shown for comparison of the two groups indicated by the **brackets**. **B**) The coxsackie adenovirus receptor binding ability of red fluorescent adenoviruses was assessed in A549 (coxsackie adenovirus receptor positive) and Chinese hamster ovary (CHO) (coxsackie adenovirus receptor negative) cells. A549 cells were also blocked with recombinant Ad5 knob before incubation with the viruses. The **labels** below each set of bars indicate the various conditions tested. The extent of binding is represented as the number of bound genome copy number quantified by TaqMan real-time polymerase chain reaction. Three replicates were performed. No virus was added to the "cells only" group. The vectors analyzed include Ad-E1-CMV-mRFP1 (**open bar**), Ad-IX-mRFP1 (**filled bar**), Ad-E1-CMV-tdimer2(12) (**hatched bar**), and Ad-IX-tdimer2(12) (**gray bar**). *P* values (two-sided) calculated by analysis of variance are shown for comparison of the two groups indicated by the **brackets**.

shown are for one representative mouse with a strong response to the virus over 30 days (Fig. 6). Initially, different virus behavior between the left and right tumors could be discerned, similar to that observed in the in vivo correlation experiment and other studies (data not shown). Similar to other mice, a peak in pIX-mRFP1 signal intensity was always detected several days following injection, after which the fluorescence appeared to decay over time. For example, the signal peaked at day 2 in the left tumor, whereas the same event occurred at day 4 in the right tumor (Fig. 8, A). We typically observed maximal signal between 2 and 6 days after injection (data not shown). After the signal peaked, it eventually disappeared completely (day 9 for the left tumor and day 20 for the right tumor; Fig. 8, A). Note that the occurrence of a second strong signal in the right tumor starting on day 6 appears to be close to the injection site where granulation tissue eventually formed. Interestingly, the right tumor with the most intense pIX-mRFP1 signal regressed almost completely (day 20); however, it eventually relapsed after the pIX-mRFP1 signal abated, indicating little or no residual viral replication activity after 2 weeks to produce an ongoing antitumor effect. Quantification of the fluorescence signal intensity in the tumors of this mouse further highlights the transient behavior of Ad-wt-IX-mRFP1 replication in vivo (Fig. 8, B). These data show the feasibility of using this genetic capsid labeling system to dynamically monitor adenovirus replication in vivo and to capture the kinetic changes in this process.

Discussion

We have created a genetic capsid adenovirus labeling system by fusing the minor capsid protein IX with mRFP1 and tdimer2(12). The capsid fusion protein label was incorporated into virions to allow vector detection in tracking assays and in various tissues with high resolution. Modification of the pIX capsid protein with the red fluorescent proteins had a minimal effect on virus DNA replication, encapsidation, cytopathic effect, thermostability, and binding to its primary receptor coxsackie adenovirus receptor. pIX-mRFP1 signal represented the underlying level of adenovirus replication both in vitro and in vivo and correlated well with viral DNA synthesis and infectious progeny production. Furthermore, the localization of pIX-mRFP1 matched results obtained with the conventional hexon staining method used to detect the presence of adenovirus. We also successfully applied the genetic capsid labeling system to dynamically follow the kinetics of adenovirus replication in vivo.

The data we obtained in vivo demonstrate that this new imaging method to detect adenovirus replication greatly differs from conventional vector detection methods. With our method, the kinetics of viral mass and localization could be visualized in real time with a noninvasive procedure. Although our study was designed primarily to validate the basic utility of our system, we observed a number of important findings pertaining to adenovirus oncolytic function. In particular, we found that adenovirus replication was highly variable from tumor to tumor, even in the same mouse. If this differential response is an inherent aspect of intratumoral injection techniques, then studies relying on methods such as tumor size measurements to gauge oncolysis function should be carefully revisited. The natural heterogeneity of tumor microarchitecture and host response to vectors can substantially impact the function of replicative vectors in vivo *(34)*. Therefore, a well-designed conditionally replicative adenovirus evaluation should embody tools that not only gauge tumor response to vectors but also simultaneously delineate vector function. Robust tumor regression should be attributed to oncolytic effect as a consequence of strong viral replication and spread. Indeed, our detection system showed that strong virus replication does lead to regression of the affected tumor

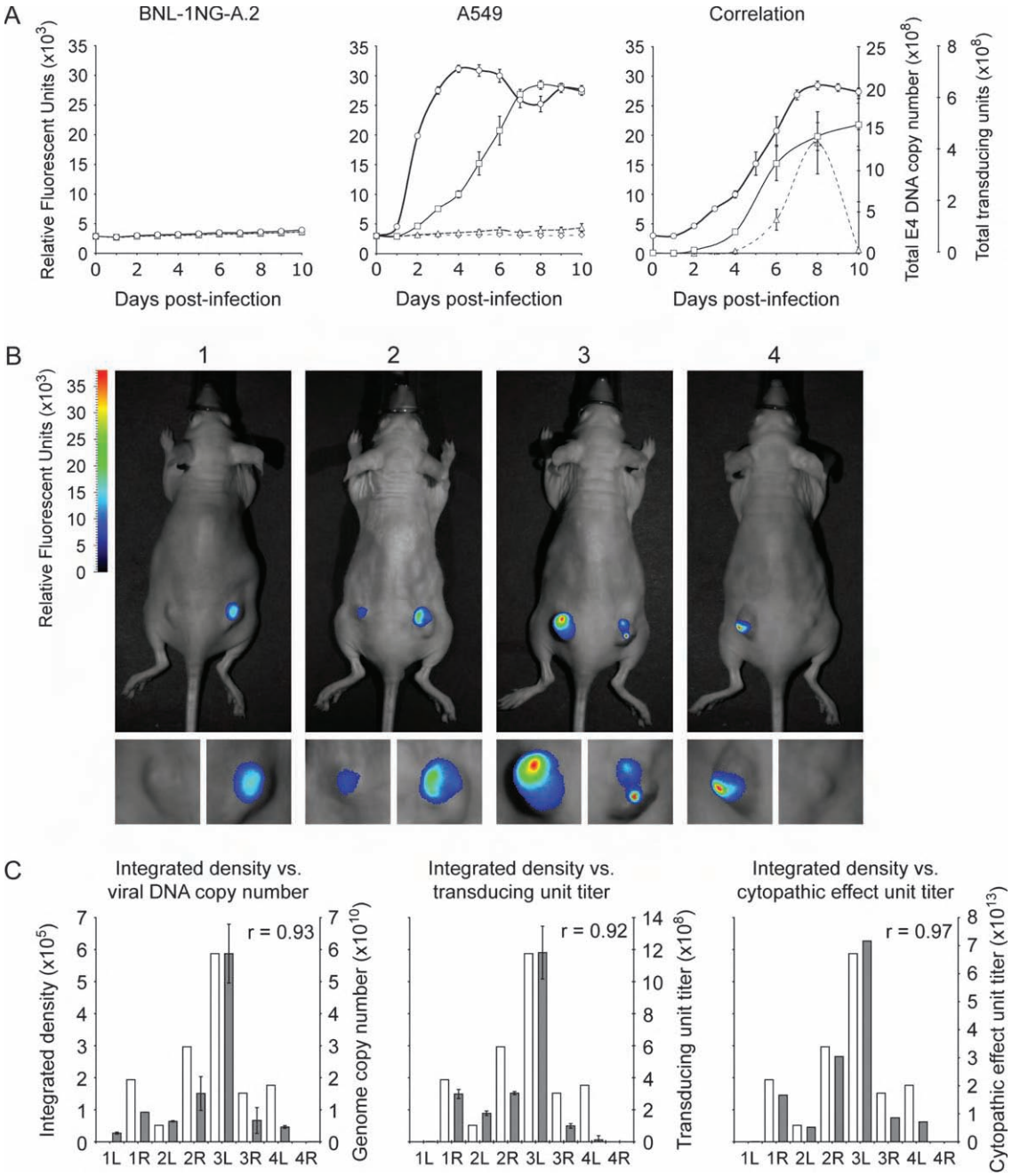

Fig. 5. In vitro and in vivo correlation of protein IX (pIX)-mRFP1 signal with replication. **A**) Ad-wt-IX-mRFP1 red fluorescent signal (relative fluorescent unit) was monitored in BNL-1NG-A.2 (replication nonpermissive) and A549 (replication permissive) cells over 10 days: 1 (**open circles**), 0.1 (**open squares**), 0.01 (**open triangles**), and 0.001 (**open diamonds**) cytopathic effect units. On days 1, 2, 4, 6, 8, and 10 after infection, samples were infected with 0.1 cytopathic effect unit/cell, and E4 viral DNA copy number (**open squares**) and transducing unit titer (**open triangles**) were determined. Also shown in the correlation panel is the red fluorescence curve of A549 cells infected with 0.1 cytopathic effect unit/cell (**open circles**). Pearson's correlation coefficient between red fluorescence and E4 viral DNA copy number, $r = .99$. Correlation coefficient between red fluorescence and transducing unit titer (days 1, 2, 4, 6, 8, and 10), $r = .65$. Correlation coefficient between red fluorescence and transducing unit titer (days 1, 2, 4, 6, and 8), $r = .92$. **Error bars** represent 95% confidence intervals. **B**) Noninvasive detection of pIX-mRFP1 signal. A549 tumors from four mice, 6 days after intratumoral injection with Ad-wt-IX-mRFP1, were imaged in vivo. Images shown are pseudocolored with the indicated index scale. Above the images are the mouse numbers. Below the whole body images are enlarged pictures of the left and right tumors of the respective mouse. **C**) Correlation of the in vivo pIX-mRFP1 signal with replication. E4 viral DNA copy number, transducing unit titer, and cytopathic effect unit titer were determined in tumor homogenates, as described in "Materials and Methods." In each graph, signal quantification from in vivo images (**open bars**: total integrated density) is displayed with the various virus detection measurements (**gray bars**: viral DNA copy number, transducing unit titer, and cytopathic effect unit infectious titer) and the correlation coefficients. The order in the charts corresponds to the tumors depicted in the in vivo images with the mouse number and left or right tumor indicated below each set of bars. The **left axis** in each chart represents the in vivo integrated density. **Error bars** represent 95% confidence intervals.

(Fig. 8). Furthermore, we noted that weak replication or subsequent attenuation of replication allows the tumor to actively progress (Fig. 8). Without a noninvasive detection method, one that allows repeated monitoring of virus replication, failure or success in achieving a therapeutic effect would be difficult to determine.

What was not clearly ascertained with our adenovirus monitoring system was true spread of virus replication in the tumor,

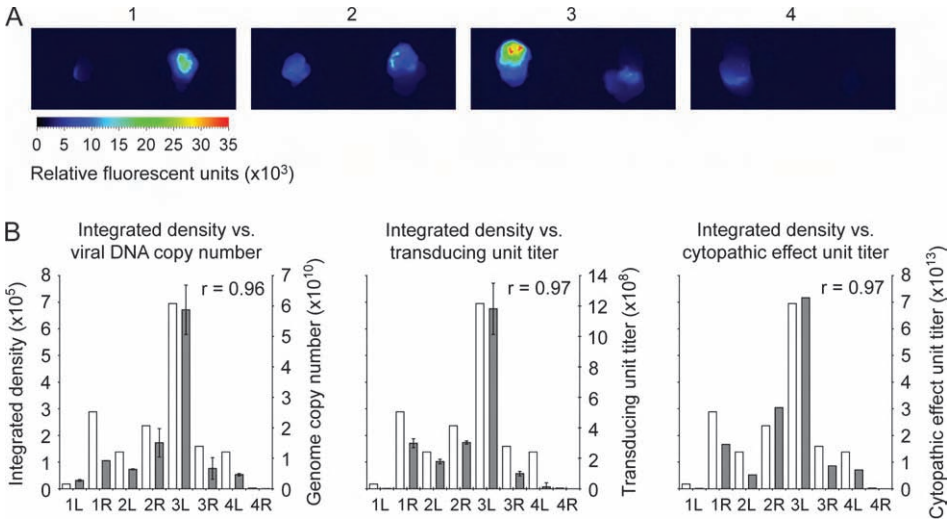

Fig. 6. Correlation of ex vivo protein IX (pIX)-mRFP1 signal with replication. **A**) Excised tumors from the same mice shown in Fig. 5, B, were imaged for red fluorescence in their respective anatomic positions. **B**) E4 viral DNA copy number, transducing unit titer, and cytopathic effect unit titer were determined in tumor homogenates. In each chart, signal quantification of ex vivo images (**open bars**: total integrated density) is displayed with the various virus detection measurements (**gray bars**: viral DNA copy number, transducing unit titer, and cytopathic effect unit titer) and the correlation coefficients. The order in the charts corresponds to the tumors depicted in the ex vivo images with the mouse number and left or right tumor indicated below each set of bars. The numbers above the ex vivo images correspond to the respective mouse shown in the in vivo correlation study (Fig. 5, B). **Error bars** represent 95% confidence intervals.

even though we attempted to use a minimal volume (10 μL) of injected virus and deliberately avoided moving the needle to distribute the virus in effect to create an initial small locus of infection from which virus spread could be properly visualized. We have injected a similar amount and volume of virus (10^{10} virus particles, 10 μL) in mice with larger tumors (greater than 10 mm in diameter), and imaging also did not reveal the degree of spread expected from a replicative adenovirus (data not shown). A positive pIX-mRFP1 signal was not detected in the margins of the tumors, and the intense signal in the center of the tumor never spread far beyond the initial injection site. Our results are consistent with preclinical studies demonstrating the limited ability of oncolytic adenoviruses to spread intratumorally *(35)*, probably owing to confinement by surrounding necrotic and connective tissues *(36)*. The poor lateralization capability of adenovirus in tumors is also suggested by in situ viral DNA hybridization data from clinical trials that show a few focal patches of positive cells rather than gross, widespread presence of viral DNA *(12,13,15)*. For this very reason, most preclinical conditionally replicative adenovirus studies rely on much larger volumes for virus injection (50 or even 100 μL), apply multiple viral administrations, and practice intentional distribution of the virus to achieve widespread infection for an effective antitumor response *(37,38)*. Future studies should be devised to address this issue of virus lateralization and perhaps incorporate strategies to enhance dissemination of progeny virions. Our genetic capsid labeling system would provide the means to evaluate spreading of oncolytic adenoviruses in this respect.

The transient nature of virus replication detected in vivo in this study also raises questions regarding the persistence of adenovirus replication in subcutaneous tumors of athymic nude mice. We have routinely noticed this trend; i.e., a number of mice besides the ones used in this study showed attenuation of pIX-mRFP1 signal in a matter of weeks (data not shown). The short-lived intratumoral replication of adenovirus observed in our experiments corresponds with persistence data obtained in clinical trials. In patients, a peak in circulating viral DNA was typically detected several days after virus administration, indicative of active replication. Yet, over the course of a few weeks, a substantial decrease to baseline followed, indicating clearance of the oncolytic agent *(14,39,40)*. Replicative adenovirus persistence in the tumor requires efficient infection of viable cells for replication as well as effective release and spread to neighboring cells for subsequent infection. Moreover, the virus has to elude the challenge mounted by the host immune system. Our adenovirus monitoring system offers the potential to study these host–vector interactions that are consequential for replicative adenovirus function. It is conceivable that in vivo clearance of the vector may have been due to immunogenicity of not only the native viral capsid proteins but also the red fluorescent protein used to label the exterior of the capsid. Further investigation is needed to determine the extent to which the exposed fluorescent label on the viral capsid contributes to the immune response directed against the vector.

Certain limitations are associated with the use of fluorescence imaging in our genetic capsid labeling system. The detection

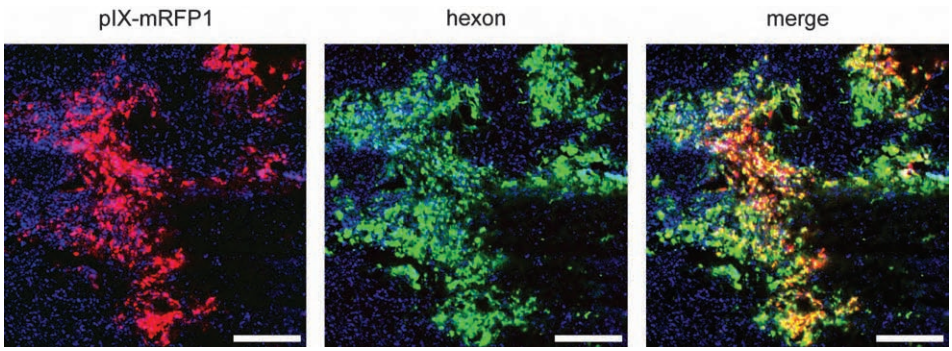

Fig. 7. Comparison of protein IX (pIX)-mRFP1 in situ localization with hexon staining. A frozen tissue section from an A549 tumor injected with Ad-wt-IX-mRFP1 (7 days after injection) was immunostained for adenovirus hexon protein, as described in "Materials and Methods." pIX-mRFP1 (**red**), hexon (**green**), and nuclear DNA (**blue**) signals were detected under fluorescence microscopy. In the overlay (**merge**), areas of **yellow** indicate overlap of red and green fluorescence. **Bar** = 100 μm.

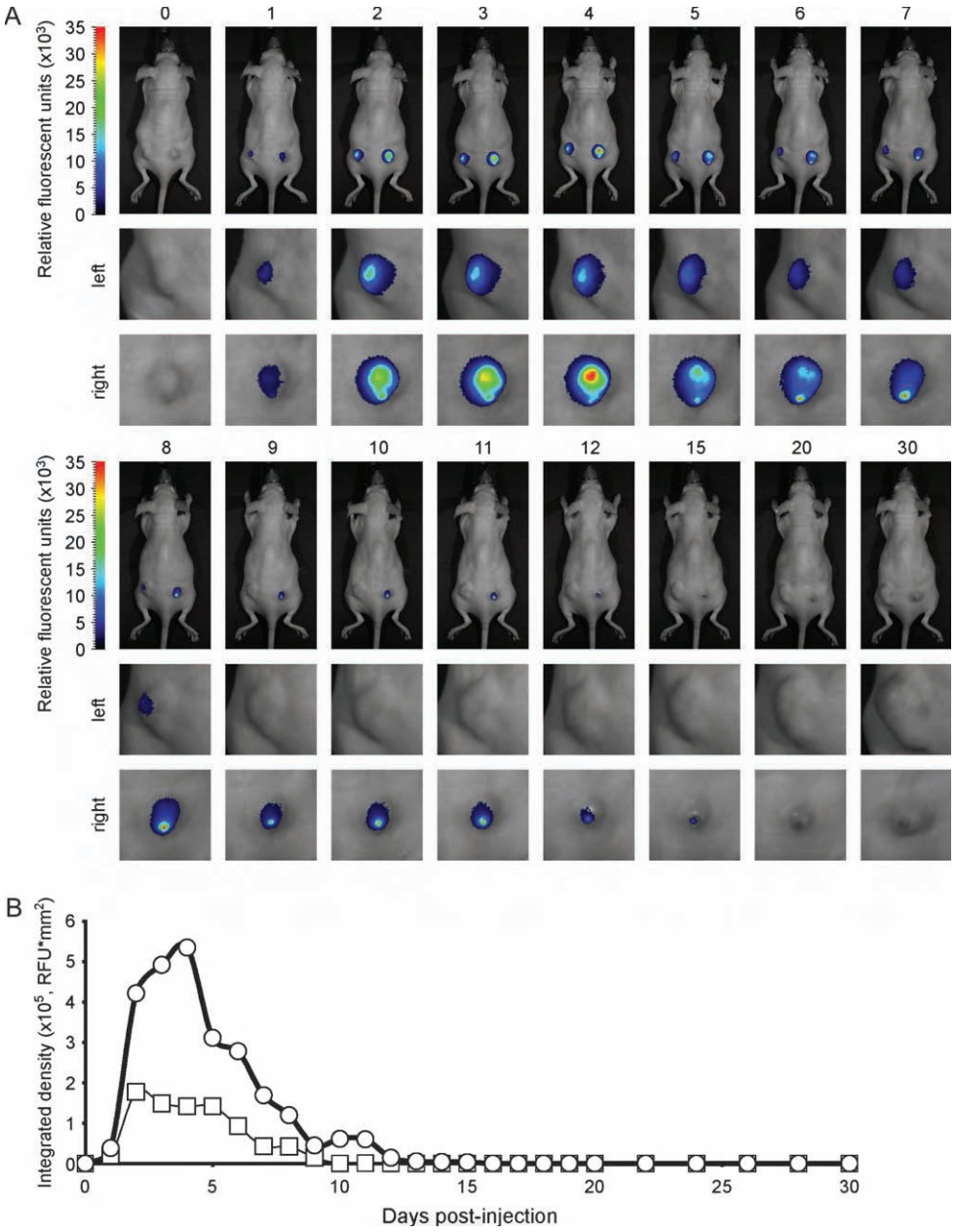

Fig. 8. Dynamic monitoring of Ad-wt-IX-mRFP1 replication in vivo. **A**) Established A549 flank tumors in nude mice (n = 2) were injected intratumorally with Ad-wt-IX-mRFP1 (10^{10} virus particles in 10 μL). With a noninvasive fluorescence-based optical imaging system, viral replication and oncolysis were dynamically monitored in vivo over 30 days. The results are shown for one representative mouse as pseudocolored images with the indicated index scale. The number above each set of images corresponds to the day number after injection. The two images below the whole body image are enlarged pictures of the left and right tumors from each day. **B**) Time course dynamics of in vivo monitoring. Quantified Ad-wt-IX-mRFP1 signal (integrated density) from the left (**squares**) and right (**circles**) tumors of the mouse depicted in **A**. RFU = relative fluorescence units.

depth associated with current fluorescence-based optical imaging technology remains limited *(41)*. Additionally, the possibility of achieving tomographic data from fluorescence imaging for volumetric quantification is still under development and not widely available *(42)*. As a result, conventional fluorescence imaging is presently limited to application for superficial or accessible tumors and would not be adequate for accurate quantification of volumetric fluorescence signals. Other imaging ligands that may be more practical for deeper detection within tissue, such as luciferases *(43,44)* and herpes simplex virus thymidine kinase *(45,46)*, should be considered for genetic capsid labeling of adenovirus.

In summary, we have devised a genetic capsid labeling strategy that allows dynamic monitoring of oncolytic adenoviruses. This in vivo imaging system provides the means to study adenovirus replication, spread, persistence, and antitumor function for the purpose of addressing key issues that are fundamental to the design of replicative adenoviral agents for cancer therapy. Furthermore, capsid-labeled viruses will also have utility for vector targeting and adenovirus biology studies.

References

(1) Jemal A, Clegg LX, Ward E, Ries LA, Wu X, Jamison PM, et al. Annual report to the nation on the status of cancer, 1975–2001, with a special feature regarding survival. Cancer 2004;101:3–27.

(2) Chatelut E, Delord JP, Canal P. Toxicity patterns of cytotoxic drugs. Invest New Drugs 2003;21:141–8.

(3) Maduro JH, Pras E, Willemse PH, de Vries EG. Acute and long-term toxicity following radiotherapy alone or in combination with chemotherapy for locally advanced cervical cancer. Cancer Treat Rev 2003;29:471–88.

(4) Donnelly JG. Pharmacogenetics in cancer chemotherapy: balancing toxicity and response. Ther Drug Monit 2004;26:231–5.

(5) Krasnykh VN, Douglas JT, van Beusechem VW. Genetic targeting of adenoviral vectors. Mol Ther 2000;1(5 Pt 1):391–405.

(6) Wickham TJ. Ligand-directed targeting of genes to the site of disease. Nat Med 2003;9:135–9.

(7) Nettelbeck DM, Jerome V, Muller R. Gene therapy: designer promoters for tumour targeting. Trends Genet 2000;16:174–81.
(8) Glasgow JN, Bauerschmitz GJ, Curiel DT, Hemminki A. Transductional and transcriptional targeting of adenovirus for clinical applications. Curr Gene Ther 2004;4:1–14.
(9) Kirn D, Martuza RL, Zwiebel J. Replication-selective virotherapy for cancer: Biological principles, risk management and future directions. Nat Med 2001;7:781–7.
(10) Chiocca EA. Oncolytic viruses. Nat Rev Cancer 2002;2:938–50.
(11) Everts B, van der Poel HG. Replication-selective oncolytic viruses in the treatment of cancer. Cancer Gene Ther 2005;12:141–61.
(12) Nemunaitis J, Ganly I, Khuri F, Arseneau J, Kuhn J, McCarty T, et al. Selective replication and oncolysis in p53 mutant tumors with ONYX-015, an E1B-55kD gene-deleted adenovirus, in patients with advanced head and neck cancer: a phase II trial. Cancer Res 2000;60:6359–66.
(13) Khuri FR, Nemunaitis J, Ganly I, Arseneau J, Tannock IF, Romel L, et al. A controlled trial of intratumoral ONYX-015, a selectively-replicating adenovirus, in combination with cisplatin and 5-fluorouracil in patients with recurrent head and neck cancer. Nat Med 2000;6:879–85.
(14) Nemunaitis J, Khuri F, Ganly I, Arseneau J, Posner M, Vokes E, et al. Phase II trial of intratumoral administration of ONYX-015, a replication-selective adenovirus, in patients with refractory head and neck cancer. J Clin Oncol 2001;19:289–98.
(15) Galanis E, Okuno SH, Nascimento AG, Lewis BD, Lee RA, Oliveira AM, et al. Phase I-II trial of ONYX-015 in combination with MAP chemotherapy in patients with advanced sarcomas. Gene Ther 2005;12:437–45.
(16) Le LP, Everts M, Dmitriev IP, Davydova JG, Yamamoto M, Curiel DT. Fluorescently labeled adenovirus with pIX-EGFP for vector detection. Mol Imaging 2004;3:105–16.
(17) Fallaux FJ, Kranenburg O, Cramer SJ, Houweling A, Van Ormondt H, Hoeben RC, et al. Characterization of 911: a new helper cell line for the titration and propagation of early region 1-deleted adenoviral vectors. Hum Gene Ther 1996;7:215–22.
(18) He TC, Zhou S, da Costa LT, Yu J, Kinzler KW, Vogelstein B. A simplified system for generating recombinant adenoviruses. Proc Natl Acad Sci U S A 1998;95:2509–14.
(19) Campbell RE, Tour O, Palmer AE, Steinbach PA, Baird GS, Zacharias DA, et al. A monomeric red fluorescent protein. Proc Natl Acad Sci U S A 2002; 99:7877–82.
(20) Dmitriev IP, Kashentseva EA, Curiel DT. Engineering of adenovirus vectors containing heterologous peptide sequences in the C terminus of capsid protein IX. J Virol 2002;76:6893–9.
(21) Le LP, Dmitriev IP, Davydova JG, Yamamoto M, Curiel DT. Fluorescently labeled adenovirus with pIX-EGFP for vector detection. Mol Imaging 2004;3:105–16.
(22) Alemany R, Suzuki K, Curiel DT. Blood clearance rates of adenovirus type 5 in mice. J Gen Virol 2000;81(Pt 11):2605–9.
(23) O'Carroll SJ, Hall AR, Myers CJ, Braithwaite AW, Dix BR. Quantifying adenoviral titers by spectrophotometry. Biotechniques 2000;28:408–10, 412.
(24) Short JJ, Pereboev AV, Kawakami Y, Vasu C, Holterman MJ, Curiel DT. Adenovirus serotype 3 utilizes CD80 (B7.1) and CD86 (B7.2) as cellular attachment receptors. Virology 2004;322:349–59.
(25) Buil C. IRIS: An astronomical images processing software version 5.10. Available at: http://www.astrosurf.org/buil/us/iris/iris.htm. [Last accessed May 8, 2004.]
(26) Yamamoto M, Davydova J, Wang M, Siegal GP, Krasnykh V, Vickers SM, et al. Infectivity enhanced, cyclooxygenase-2 promoter-based conditionally replicative adenovirus for pancreatic cancer. Gastroenterology 2003;125:1203–18.
(27) Troy T, Jekic-McMullen D, Sambucetti L, Rice B. Quantitative comparison of the sensitivity of detection of fluorescent and bioluminescent reporters in animal models. Mol Imaging 2004;3:9–23.
(28) Colby WW, Shenk T. Adenovirus type 5 virions can be assembled in vivo in the absence of detectable polypeptide IX. J Virol 1981;39:977–80.
(29) Rosa-Calatrava M, Grave L, Puvion-Dutilleul F, Chatton B, Kedinger C. Functional analysis of adenovirus protein IX identifies domains involved in capsid stability, transcriptional activity, and nuclear reorganization. J Virol 2001;75:7131–41.
(30) Ghosh-Choudhury G, Haj-Ahmad Y, Graham FL. Protein IX, a minor component of the human adenovirus capsid, is essential for the packaging of full length genomes. EMBO J 1987;6:1733–9.
(31) Eggerding FA, Pierce WC. Molecular biology of adenovirus type 2 semipermissive infections. I. Viral growth and expression of viral replicative functions during restricted adenovirus infection. Virology 1986;148:97–113.
(32) DeWeese TL, van der Poel H, Li S, Mikhak B, Drew R, Goemann M, et al. A phase I trial of CV706, a replication-competent, PSA selective oncolytic adenovirus, for the treatment of locally recurrent prostate cancer following radiation therapy. Cancer Res 2001;61:7464–72.
(33) Wadler S, Yu B, Tan JY, Kaleya R, Rozenblit A, Makower D, et al. Persistent replication of the modified chimeric adenovirus ONYX-015 in both tumor and stromal cells from a patient with gall bladder carcinoma implants. Clin Cancer Res 2003;9:33–43.
(34) Wang Y, Hallden G, Hill R, Anand A, Liu TC, Francis J, et al. E3 gene manipulations affect oncolytic adenovirus activity in immunocompetent tumor models. Nat Biotechnol 2003;21:1328–35.
(35) Ganly I, Kirn D, Eckhardt G, Rodriguez GI, Soutar DS, Otto R, et al. A phase I study of Onyx-015, an E1B attenuated adenovirus, administered intratumorally to patients with recurrent head and neck cancer. Clin Cancer Res 2000;6:798–806.
(36) Sauthoff H, Hu J, Maca C, Goldman M, Heitner S, Yee H, et al. Intratumoral spread of wild-type adenovirus is limited after local injection of human xenograft tumors: virus persists and spreads systemically at late time points. Hum Gene Ther 2003;14:425–33.
(37) Heise C, Hermiston T, Johnson L, Brooks G, Sampson-Johannes A, Williams A, et al. An adenovirus E1A mutant that demonstrates potent and selective systemic anti-tumoral efficacy. Nat Med 2000;6:1134–9.
(38) Wirth T, Zender L, Schulte B, Mundt B, Plentz R, Rudolph PL, et al. A telomerase-dependent conditionally replicating adenovirus for selective treatment of cancer. Cancer Res 2003;63:3181–8.
(39) Freytag SO, Khil M, Stricker H, Peabody J, Menon M, DePeralta-Venturina M, et al. Phase I study of replication-competent adenovirus-mediated double suicide gene therapy for the treatment of locally recurrent prostate cancer. Cancer Res 2002;62:4968–76.
(40) Reid T, Warren R, Kirn D. Intravascular adenoviral agents in cancer patients: Lessons from clinical trials. Cancer Gene Ther 2002;9:979–86.
(41) Weissleder R, Ntziachristos V. Shedding light onto live molecular targets. Nat Med 2003;9:123–8.
(42) Ntziachristos V, Schellenberger EA, Ripoll J, Yessayan D, Graves E, Bogdanov A Jr, et al. Visualization of antitumor treatment by means of fluorescence molecular tomography with an annexin V-Cy5.5 conjugate. Proc Natl Acad Sci U S A 2004;101:12294–9.
(43) Wu JC, Sundaresan G, Iyer M, Gambhir SS. Noninvasive optical imaging of firefly luciferase reporter gene expression in skeletal muscles of living mice. Mol Ther 2001;4:297–306.
(44) Bhaumik S, Gambhir SS. Optical imaging of Renilla luciferase reporter gene expression in living mice. Proc Natl Acad Sci U S A 2002;99:377–82.
(45) Tjuvajev JG, Avril N, Oku T, Sasajima T, Miyagawa T, Joshi R, et al. Imaging herpes virus thymidine kinase gene transfer and expression by positron emission tomography. Cancer Res 1998;58:4333–41.
(46) Gambhir SS, Bauer E, Black ME, Liang Q, Kokoris MS, Barrio JR, et al. A mutant herpes simplex virus type 1 thymidine kinase reporter gene shows improved sensitivity for imaging reporter gene expression with positron emission tomography. Proc Natl Acad Sci U S A 2000;97:2785–90.

NOTES

We thank Dr. Roger Y. Tsien (University of California at San Diego) for providing the mRFP1 and tdimer2(12) constructs. This work was supported with grants from the National Institutes of Health (R01CA083821, R01CA94084, R01DK063615, and R01CA111569), Department of Defense (W81XWH-04-1-0025, W81XWH-05-1-0035, and DAMD17-03-1-0104), and the Medical Scientist Training Program of the University of Alabama at Birmingham.

Funding to pay the Open Access publication charges for this article was provided by the above grant resources.

Manuscript received May 25, 2005; revised December 2, 2005; accepted December 15, 2005.

Available online at www.sciencedirect.com
SCIENCE DIRECT
Virology 350 (2006) 103–115
VIROLOGY
www.elsevier.com/locate/yviro

An adenovirus serotype 5 vector with fibers derived from ovine atadenovirus demonstrates CAR-independent tropism and unique biodistribution in mice

Masaharu Nakayama [a], Gerald W. Both [c], Boglarka Banizs [a,1], Yuko Tsuruta [a], Seiji Yamamoto [a], Yosuke Kawakami [a], Joanne T. Douglas [a,b], Kenzaburo Tani [d], David T. Curiel [a,b], Joel N. Glasgow [a,*]

[a] *Division of Human Gene Therapy, Departments of Medicine, Obstetrics and Gynecology, Pathology, Surgery, University of Alabama at Birmingham, 901 19th Street South BMR2-572, Birmingham, AL 35294-2180, USA*
[b] *Gene Therapy Center, University of Alabama at Birmingham, Birmingham, AL 35294, USA*
[c] *CSIRO Molecular and Health Technologies, North Ryde, NSW 2113, Australia*
[d] *Division of Molecular and Clinical Genetics, Medical Institution of Bioregulation, Kyushu University, Fukuoka 812-8582, Japan*

Received 30 November 2005; returned to author for revision 23 December 2005; accepted 26 January 2006
Available online 3 March 2006

Abstract

Many clinically important tissues are refractory to adenovirus (Ad) infection due to negligible levels of the primary Ad5 receptor the coxsackie and adenovirus receptor CAR. Thus, development of novel CAR-independent Ad vectors should lead to therapeutic gain. Ovine atadenovirus type 7, the prototype member of genus *Atadenovirus*, efficiently transduces CAR-deficient human cells in vitro, and systemic administration of OAdV is not associated with liver sequestration in mice. The penton base of OAdV7 does not contain an RGD motif, implicating the long-shafted fiber molecule as a major structural dictate of OAdV tropism. We hypothesized that replacement of the Ad5 fiber with the OAdV7 fiber would result in an Ad5 vector with CAR-independent tropism in vitro and liver "detargeting" in vivo. An Ad5 vector displaying the OAdV7 fiber was constructed (Ad5Luc1-OvF) and displayed CAR-independent, enhanced transduction of CAR-deficient human cells. When administered systemically to C57BL/6 mice, Ad5Luc1-OvF reporter gene expression was reduced by 80% in the liver compared to Ad5 and exhibited 50-fold higher gene expression in the kidney than the control vector. To our knowledge, this is the first report of a fiber-pseudotyped Ad vector that simultaneously displays decreased liver uptake and a distinct organ tropism in vivo. This vector may have future utility in murine models of renal disease.

Keywords: Gene therapy; Adenovirus; Targeting; Tropism modification; Coxsackie and adenovirus receptor (CAR); Liver tropism; Kidney tropism

Introduction

Vectors based on human adenovirus (Ad) serotypes 2 and 5 continue to show increasing promise as gene therapy delivery vehicles, especially for cancer gene therapy, due to several key attributes: Ad vectors display in vivo stability and excellent gene transfer efficiency to numerous dividing and non-dividing cell targets. In addition, Ad vectors are rarely linked to any severe disease in immunocompetent humans, providing rationale for further development of these vehicles.

The first step in Ad5 infection occurs via high-affinity binding of the virion fiber knob domain to its cognate cellular receptor known as the coxsackie and adenovirus receptor (CAR) (Henry et al., 1994; Xia et al., 1994; Bergelson et al., 1997; Tomko et al., 1997). Following knob-CAR binding, receptor-mediated endocytosis of the virion is dramatically increased by interaction of the penton base Arg–Gly–Asp (RGD) motif with cellular integrins αvβ3, αvβ5, αvβ1, α3β1 or other integrins (Bai et al., 1993; Wickham et al., 1993; Louis

* Corresponding author. Fax: +1 205 975 7949.
E-mail addresses: mnakayam@uab.edu (M. Nakayama), gerry.both@csiro.au (G.W. Both), bbanizs@uab.edu (B. Banizs), yuko.tsuruta@uab.edu (Y. Tsuruta), yamasei@uab.edu (S. Yamamoto), ykawaka@zj9.so-net.ne.jp (Y. Kawakami), jdouglas@uab.edu (J.T. Douglas), taniken@bioreg.kyushu-u.ac.jp (K. Tani), curiel@uab.edu (D.T. Curiel), jng@uab.edu (J.N. Glasgow).
[1] Current address: Department of Cell Biology, University of Alabama at Birmingham, Birmingham, AL 35294, USA.

0042-6822/$ - see front matter © 2006 Elsevier Inc. All rights reserved.
doi:10.1016/j.virol.2006.01.037

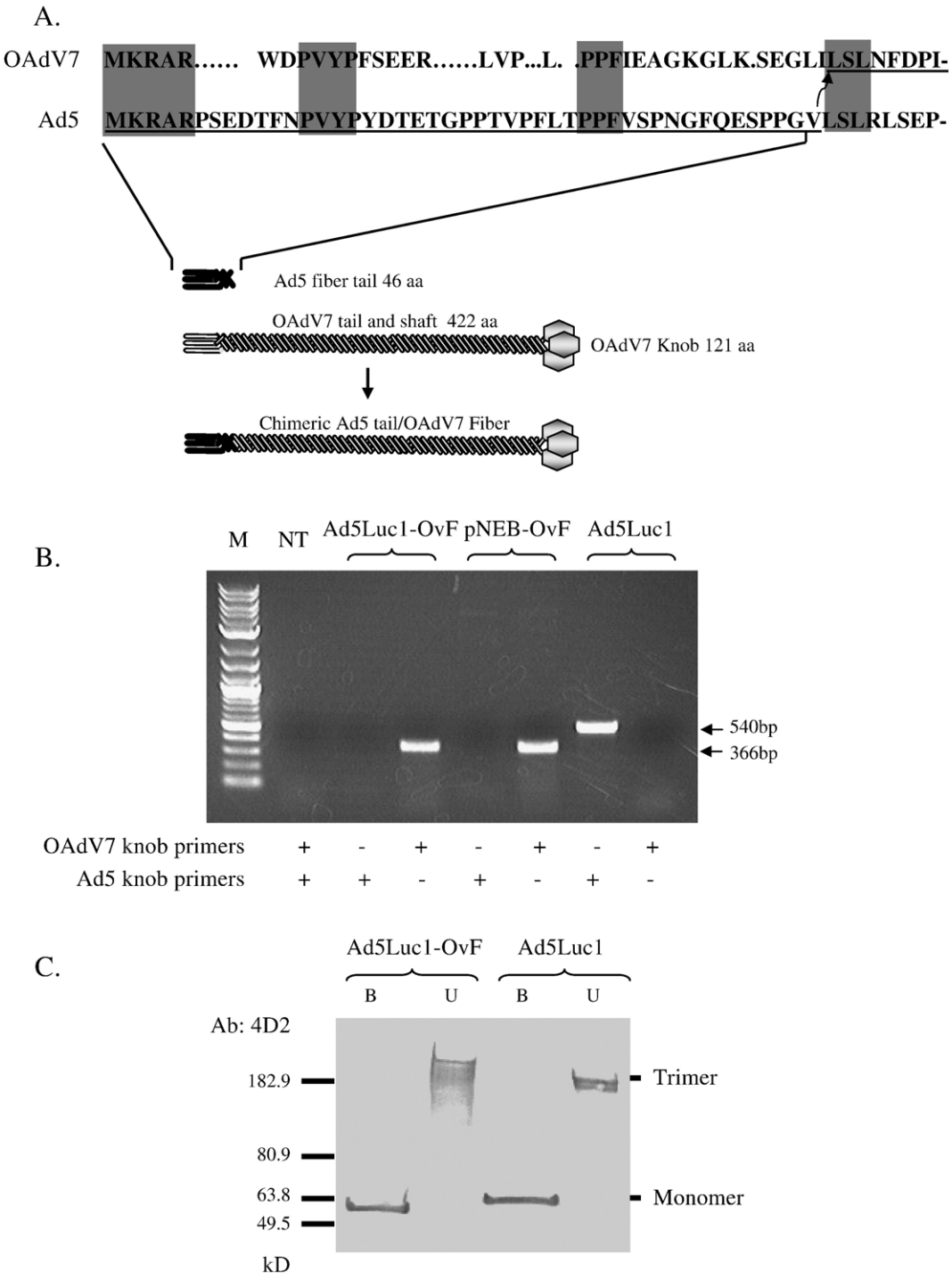

Fig. 1. Diagram depicting the design of the chimeric fiber and molecular validation of Ad5Luc1-OvF. (A) Construction of the 553-amino-acid chimeric fiber of Ad5Luc1-OvF, including the N-terminal amino acid sequences of the OAdV7 and human Ad5 fiber proteins. The LSL sequence common to both fibers that served as the junction for the replacement of the OAdV7 tail domain, as well as other common sequences, is highlighted. The final Ad5Luc1-OvF fiber sequence is underlined, and the arrow highlights that Val^{46} of the Ad5 tail domain is followed by Leu^{37} in the OAdV7 fiber. (B) PCR analysis of fiber genes using Ad genomes from rescued viral particles as the PCR templates. Ad5Luc1 virions and fiber shuttle plasmid pNEB.PK3.6-OvF (designated as pNEB-OvF in the figure) were used as controls. Lanes containing DNA size standards (M) and no PCR template (NT) are designated. Primers used are specific for the OAdV7 or Ad5 fiber gene knob domain. PCR products indicating the presence of the Ad5 or OAdV7 fiber knob domains are 540 and 366 bp, respectively. (C) Western blot analysis of fiber proteins from purified virions. 1×10^{10} vp of Ad5Luc1 with wild-type Ad5 fiber (lanes 3,4) or Ad5Luc1-OvF with chimeric OAdV7 fiber (lanes 1, 2) were resuspended in Laemmli buffer prior to SDS-PAGE and Western analysis with an anti-tail Ad5 fiber mAb. Samples in lanes 1 and 3 were heated to 99 °C prior to electrophoresis. Fiber monomers (M) and trimers (T) are indicated. Molecular mass markers indicate kilodaltons.

et al., 1994; Davison et al., 1997; Li et al., 2001; Salone et al., 2003).

Understanding of this two-step Ad entry pathway explains clinical findings by several groups that have demonstrated that cells expressing low levels of CAR are refractory to Ad infection and gene delivery. Native CAR-dependent tropism results in a scenario wherein non-target but high-CAR cells can be infected while target tissues, if low in CAR, are resistant to Ad infection. Essentially, while Ad delivery is uniquely efficient in vivo, the biodistribution of CAR is incompatible with many gene therapy interventions and in vivo co-localization of applied Ad vectors and the receptor is poor (Dmitriev et al., 1998; Miller et al., 1998; Fechner et al., 1999; Li et al., 1999; Cripe et al., 2001).

Based on a clear understanding of native Ad cell recognition, the development of CAR-independent Ad vectors has rationally focused on the fiber protein, the primary determinant of Ad tropism. Ad fiber pseudotyping, the genetic replacement of the knob domain or entire fiber with its structural counterpart from another human Ad serotype, has been employed as a means to derive Ad5-based vectors with CAR-independent tropism by virtue of the natural diversity in receptor recognition found in species B and D Ad fibers (Büchen-Osmond, 2002) and has identified chimeric vectors with superior infectivity to Ad5 in a variety of clinically relevant cell types (Gall et al., 1996; Shayakhmetov et al., 2000; Von Seggern et al., 2000; Chiu et al., 2001; Goossens et al., 2001; Havenga et al., 2001; Jakubczak et al., 2001; Havenga et al., 2002; Kanerva et al., 2002).

The development of non-human adenoviruses as gene therapy vehicles has been proposed (Khatri et al., 1997; Rasmussen et al., 1999; Reddy et al., 1999a, 1999b; Kremer et al., 2000; Loser et al., 2002; Hemminki et al., 2003). The rationale for these efforts has been three-fold: (1) no pre-existing humoral or cellular immunity will exist against "xeno" Ads in the majority of humans (Hofmann et al., 1999; Kremer et al., 2000), (2) several non-human Ads have been demonstrated to efficiently infect human cells without subsequent replication, including canine, bovine and murine mastadenoviruses (Gelhe and Smith, 1969; Nguyen et al., 1999; Rasmussen et al., 1999; Soudais et al., 2000) and ovine atadenovirus (Loser et al., 2000; Kumin et al., 2002) and (3) novel entry biologies of xeno Ads may circumvent CAR deficiency in clinically relevant human target tissues refractory to Ad5-based vectors.

Consistent with these considerations, the 287 isolate of the ovine adenovirus type 7 (OAdV7) has been evaluated as a potential human gene therapy vector (Voeks et al., 2002; Loser et al., 2003; Martiniello-Wilks et al., 2004; Wang et al., 2004). OAdV7 is the prototype isolate of a novel genus of viruses referred to as atadenovirus (Benko and Harrach, 1998). OAdV7 causes only mild symptoms in sheep and infects numerous human cell types efficiently, although replication in human cells is abortive due to the lack of viral promoter function (Boyle et al., 1994; Khatri et al., 1997; Rothel et al., 1997). OAdV7 displays CAR-independent tropism that is distinct from that of serotype 2 and 5 Ads, utilizing an unknown primary receptor(s) (Xu and Both, 1998). In addition, systemically applied OAdV7 exhibits a distinctive tissue distribution in vivo that is less hepatotropic in mice compared to Ad5-based vectors (Hofmann et al., 1999).

OAdV7 tropism is mediated via a 543-residue fiber molecule comprised of a 35 residue N-terminal tail region, a long shaft domain predicted to consist of 25 pseudorepeats and a relatively small 121-amino-acid C-terminal region comprising the knob domain (Vrati et al., 1995). In contrast to Ad5, the OAdV7 fiber does not contain the lysine-rich KKTK sequence found in the third repeat of the Ad5 fiber, a motif suggested to mediate hepatotropism of Ad5 vectors in rodents and primates in vivo (Smith et al., 2003a, 2003b). In addition, neither the penton nor fiber of OAdV7 contains an RGD sequence or other identifiable integrin-binding domain, suggesting that interaction with cell-surface integrins may not be required for infection (Vrati et al., 1996; Xu and Both, 1998). Thus, the fiber protein is the only structural determinant of OAdV7 tropism identified to date.

Based on the unique tropism of OAdV7 that combines CAR independence with a non-hepatotropic biodistribution profile, we hypothesized that an Ad5 vector, containing the OAdV7 fiber as well as its native penton base RGD, would achieve enhanced infectivity of Ad-refractory cell types in vitro and liver detargeted tropism in vivo.

Results

Generation of modified Ad5 containing the OAdV7 fiber

The OAdV7 fiber molecule is composed of homotrimers of a 543-amino-acid polypeptide. Predicted functional domains within the fiber are the tail domain spanning residues 1 to 35, the shaft domain from 36 to 422 containing approximately 25 pseudorepeats motifs and the 121-amino-acid fiber knob domain from 423 to 543 (Vrati et al., 1995). Most mammalian Ads contain a conserved threonine–leucine–tryptophan–threonine (TLWT) motif at the N-terminus of the fiber knob domain, and in human Ad2 and Ad5, a flexible region separating the shaft and the knob domains precedes this motif (van Raaij et al., 1999). The OAdV7 fiber does not contain this motif, thus the start of the knob domain is poorly defined.

Following examination of Ad5 and OAdV7 fiber polypeptide sequences, we identified a common leucine–serine–leucine (LSL) sequence common to both fibers immediately downstream of each tail domain (Fig. 1A). The LSL region was considered a common element in both fibers; therefore, we substituted the 44-amino-acid Ad5 tail domain for the native OAdV7 tail domain upstream of the LSL sequence to provide the correct penton base insertion domain for incorporation into the Ad5 capsid. This was accomplished using a two-plasmid rescue system essentially as described (Krasnykh et al., 1996; Glasgow et al., 2004). We constructed an E1-deleted recombinant Ad genome (Ad5Luc1-OvF) containing the chimeric Ad5 tail/OAdV7 fiber gene and a firefly luciferase reporter gene controlled by the CMV immediate early promoter/enhancer in the E1 region. Genomic clones of Ad5Luc1-OvF were sequenced, and two correct clones were chosen. Ad5Luc1-

Table 1
Ad5Luc1-OvF luciferase gene expression in various cancer cell lines

Cell line	Origin	CAR [a]	Fold increase in luciferase activity vs. Ad5 [b]	Reference
CHO	Hamster ovary	L/N	22	Soudais et al., 2000
RD	Rhabdomyosarcoma	L/N	1.5	Dmitriev et al., 1998; Cripe et al., 2001
PC-3	Prostate cancer	L/N	7.8	Okegawa et al., 2000
LNCaP	Prostate cancer	M	5% of Ad5	Okegawa et al., 2000
T24	Bladder cancer	L/N	9.8	Li et al., 1999
MCF7	Breast cancer	L/N	9.2	Y. Kawakami, unpublished data
HeLa	Cervical cancer	H	13% of Ad5	Bergelson et al., 1997
LoVo	Colon cancer	ND	60% of Ad5	
oLE	Ovine normal stroma	ND	2.7	
JS8JSRV	Ovine lung cancer	ND	5% of Ad5	
U118MG	Glioma	L/N	2.2	Kim et al., 2003
U118 CAR-tailless	Glioma	H	1% of Ad5	Kim et al., 2003
OV-3	Ovarian cancer	ND	23	
OV-4	Ovarian cancer	L/N	3.0	Hemminki et al., 2003
HEY	Ovarian cancer	L/N	6.5	Hemminki et al., 2003
SKOV	Ovarian cancer	ND	1	
SKOV3.ip1	Ovarian cancer	L/N	5.0	Hemminki et al., 2003
FaDu	Pharynx cancer	L/N	21% of Ad5	Blackwell et al., 1999
SCC-4	Tongue cancer	L/N	9.7	Blackwell et al., 1999
SCC-25	Tongue cancer	M	9% of Ad5	Blackwell et al., 1999
THLE-3	Normal liver epithelial	ND	10% of Ad5	
Primary Cells				
Patient 1	Ovarian cancer	ND	4	

[a] H, high levels of CAR; M, moderate; L/N, little or no CAR; ND, not determined. As determined by FACS analysis.
[b] 100 vp/cell, luciferase activity measured at 24 h post-infection.

OvF was rescued in 911 cells, and large-scale preparations of Ad5Luc1-OvF were purified by double CsCl gradient centrifugation. The concentration of Ad5Luc1-OvF was 2.7×10^{12} viral particles (vp)/ml, while the control vector Ad5Luc1 was 3.74×10^{12} vp/ml. Ad5Luc1 contains the wild-type Ad5 fiber and is isogenic to Ad5Luc1-OvF in all respects except for the fiber shaft and knob domains.

We confirmed the fiber knob genotype of Ad5Luc1-OvF via diagnostic PCR, using knob-domain-specific primer pairs and genomes from purified virions as PCR templates. Plasmids containing the fiber sequence of the wild-type OAdV7 fiber (data not shown) or the chimeric fiber gene were used as positive controls (Fig. 1B). To further confirm that Ad5Luc1-OvF virions contained trimeric fibers, we performed SDS-PAGE followed by Western blot analysis of vector particles. We used the monoclonal 4D2 primary antibody that recognizes the Ad5 fiber tail domain common to both the Ad5 and chimeric OAdV7 fiber molecules. We observed bands at approximately 185 kDa for Ad5Luc1-OvF and control Ad5Luc1 virions, corresponding to trimeric fiber molecules. Bands of boiled samples resolved at an apparent molecular mass of approximately 60–65 kDa, indicative of fiber monomers (Fig. 1C).

Ad5Luc1-OvF vector exhibits expanded tropism and enhanced gene transfer

We hypothesized that the incorporation of the OAdV7 fiber into the Ad5 capsid would provide augmented

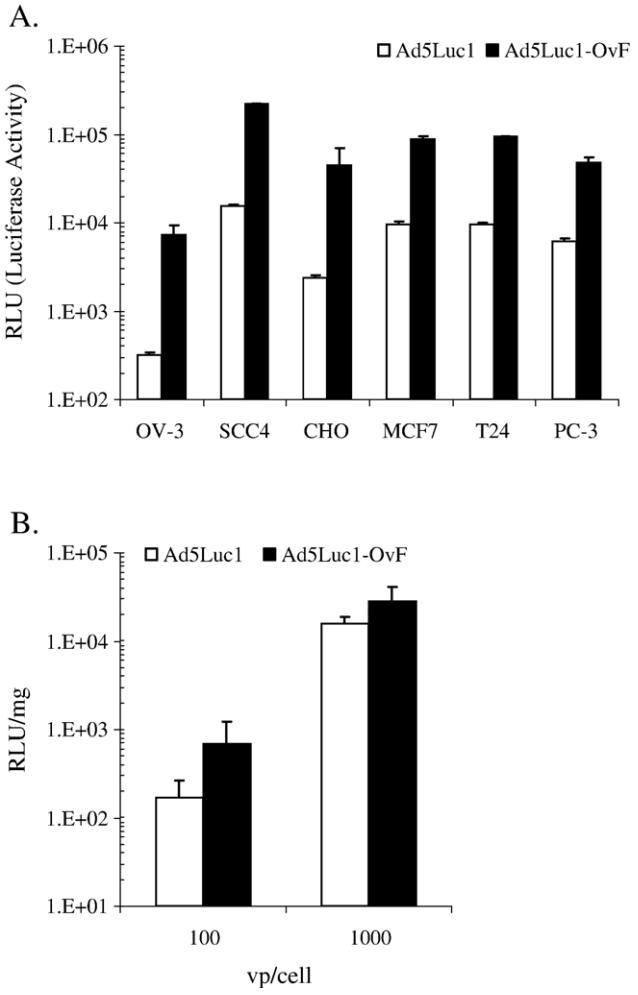

Fig. 2. Ad5Luc1-OvF-mediated gene transfer. Luciferase activities following transduction of a panel of CAR-deficient cell lines (A) and precision-cut human ovarian cancer tissue slices (B). Luciferase activity was determined 24 h post-transduction and is reported in relative light units (RLU) in panel A and RLU/mg cellular protein in panel B. Each column is average of 4 replicates using 100 vp/cell, and the error bar indicates the standard deviation.

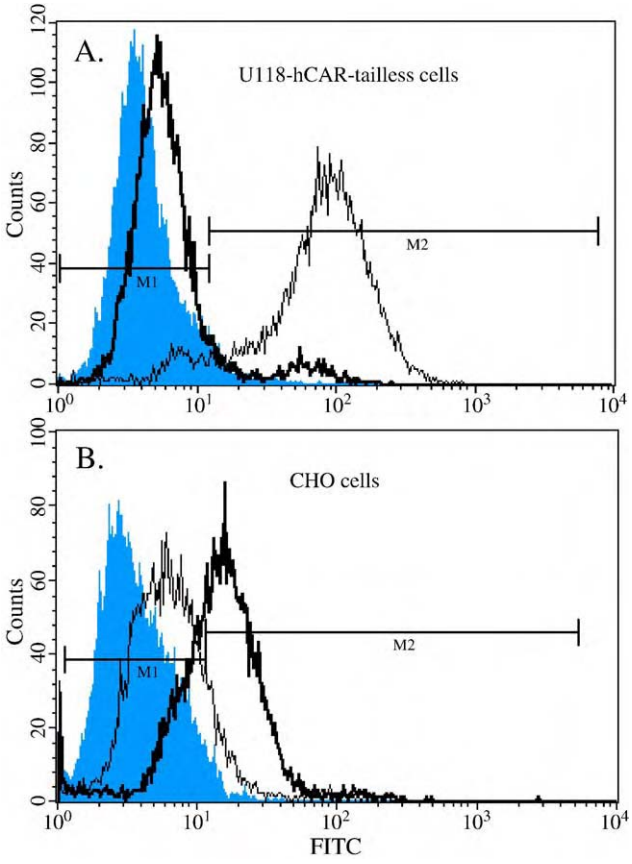

Fig. 3. FACS analysis of Ad5Luc1 and Ad5Luc1-OvF binding to U118-hCAR-tailless (upper panel) or CHO cells (lower panel). Aliquots of 2×10^5 cells were incubated with polyclonal rabbit anti-Ad5 antiserum following binding of virus to the cells at 4 °C (to block internalization). Cells were incubated in the presence of anti-rabbit FITC-labeled secondary antibody and subjected to flow cytometry analysis. The gray peaks in the histograms represent negative control cells incubated with primary and secondary antibodies only. The thin line indicates Ad5 cellular attachment, and the heavy line indicates Ad5Luc1-OvF attachment. In U118-hCAR-tailless cells, approximately 94% of cells were positive for Ad5Luc1 surface attachment (thin line), while only 8% of cells were positive for Ad5Luc1-OvF (heavy line) versus control cells receiving primary and secondary antibodies (gray peak). In CHO cells, 10% of cells were positive for Ad5Luc1 attachment compared to 60% of positive cells for Ad5Luc1-OvF.

transduction through expanded Ad vector tropism, including CAR-independent tropism. We therefore evaluated Ad5Luc1-OvF transduction of a panel of cell lines expressing variable levels of CAR (Table 1). As shown in Fig. 2A, Ad5Luc1-OvF provided augmented reporter gene delivery to several CAR-deficient cell lines, with augmentation up to 23-fold compared to Ad5Luc1. Furthermore, Ad5Luc1-OvF increased gene transfer to an unpassaged primary ovarian cancer patient sample as much as 5-fold versus Ad5Luc1 (Fig. 2B). Of interest, Ad5Luc1-OvF gene delivery augmentation to CAR-deficient RD cells (human rhabdomyosarcoma, 1.5-fold) was markedly lower than that of OV-3 cells (human ovarian cancer, 23-fold) and CAR-deficient CHO cells (Chinese hamster ovary, 22-fold), suggesting that RD cells do not express the requisite cell-surface molecule(s) for OAdV7 fiber recognition. We also evaluated Ad5Luc1-OvF transduction on a normal human liver epithelial cell line (THLE-3) and observed a 10-fold reduction in gene transfer compared to Ad5Luc1.

Ad5Luc1-OvF exhibits increased cell-surface binding in the absence of CAR

To investigate whether Ad5Luc1-OvF mediates increased gene transfer via enhanced cell-surface interaction and not altered intracellular trafficking, we performed cell-binding

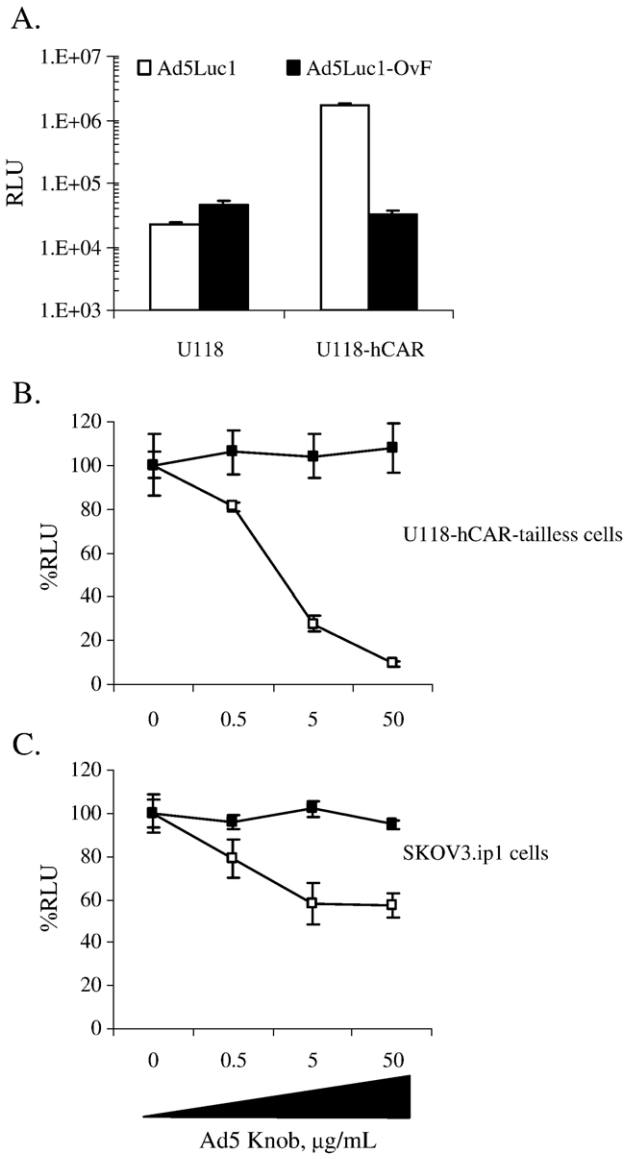

Fig. 4. Ad5Luc1 and Ad5Luc1-OvF-mediated gene transfer with Ad5 knob blocking. Luciferase activities following transduction of low-CAR U118MG cells and CAR-expressing U118-hCAR-tailless cells (A), transduction of U118-hCAR-tailless with Ad5Luc1 (white squares) or Ad5Luc1-OvF (black squares) with Ad5 knob block (B) and low-CAR SKOV3.ip1 cells with Ad5 knob block (C). Concentration of recombinant Ad5 fiber knob protein used to block transduction is indicated in µg/ml. Luciferase activity was determined 24 h post-transduction and is reported in relative light units (RLU) (A) or in percent total of unblocked luciferase activity for ease of comparison (B,C). Each column is average of 4 replicates using 100 vp/cell, and error bar indicates standard deviation.

assays employing FACS-based detection of surface-bound virions. We hypothesized that Ad5Luc1-OvF would display increased attachment to CAR-deficient cells, and possibly even CAR-positive cells, compared to Ad5 by virtue of novel virion/cell interaction. For these studies, we selected cell lines that exhibited maximally different gene transfer profiles between Ad5Luc1 and Ad5Luc1-OvF: CAR-deficient CHO cells and the CAR-positive U118-hCAR-tailless cell line that artificially expresses the extracellular domain of human CAR (Kim et al., 2002). Cells were incubated with Ad vectors at 4 °C to allow virion attachment, but not internalization, followed by labeling of bound virions with an anti-Ad primary antibody and an FITC-conjugated secondary antibody, with subsequent FACS analysis (see Materials and methods). As shown in Fig. 3A, surface-bound Ad5Luc1 was detected on 94% of U118-hCAR-tailless cells, while only 8% of these cells were positive for Ad5Luc1-OvF. This observation is consistent with the 100-fold disparity in gene transfer observed for these vectors in the same cell line (Table 1, Fig. 4A). In contrast, only 10% of CAR-negative CHO cells bound Ad5Luc1, while over 60% of CHO cells were positive for Ad5Luc1-OvF (Fig. 3B). These data indicate that a direct positive correlation exists between increased Ad5Luc1-OvF cell-surface interaction and enhanced gene delivery in CAR-deficient cells.

The OAdV7 fiber in Ad5Luc1-OvF dictates CAR-independent tropism

As shown in Table 1 and Fig. 3, Ad5Luc1-OvF gene transfer and cell binding were not dependent on the presence of CAR. To confirm this aspect of Ad5Luc1-OvF tropism, we performed knob-blocking assays using recombinant Ad5 fiber knob protein, a well-established method for demonstrating or ruling out CAR-mediated infection (Krasnykh et al., 1998; Einfeld et al., 2001; Glasgow et al., 2004). As shown in Fig. 4A, Ad5Luc1 exhibited clear CAR-dependent tropism as demonstrated by a 100-fold increase in transgene expression in U118-hCAR-tailless cells versus the CAR-deficient U118MG cell line. Furthermore, preincubation of cells with recombinant Ad5 knob protein at 50 μg/ml inhibited 90% and 50% of Ad5 Luc1 gene transfer to U118-hCAR-tailless cells and low-CAR SKOV3.ip1 cells, respectively (Figs. 4B, C). Conversely, Ad5Luc1-OvF gene delivery to U118MG cells was 2-fold higher than that of Ad5Luc1, and transduction of the highly CAR-positive variant line yielded no increase in luciferase values. Furthermore, competitive inhibition with Ad5 knob did not appreciably block Ad5Luc1-OvF-mediated gene transfer in either cell line, confirming the CAR-independent tropism of this vector.

Biodistribution of Ad5Luc1-OvF gene expression in mice

Following confirmation of our first hypothesis that the Ad5Luc1-OvF vector would exhibit enhanced infectivity in low CAR substrates via a novel, non-CAR based tropism, we next addressed the biodistribution profile of Ad5Luc1-OvF. Based on the biodistribution of intravenously applied OAdV7 in mice (Hofmann et al., 1999) and the lack of the putative heparin sulfate binding motif KKTK in the OAdV7 fiber shaft, we hypothesized that an Ad5 vector containing this fiber would demonstrate decreased hepatotropism in vivo. To this end, we evaluated the biodistribution of transgene expression of a panel of Ad vectors including Ad5Luc1-OvF, Ad5Luc1 and our Ad5Luc1-ΔKKTK vector (with the native KKTK sequence deleted from the fiber shaft) as a liver detargeted control vector,

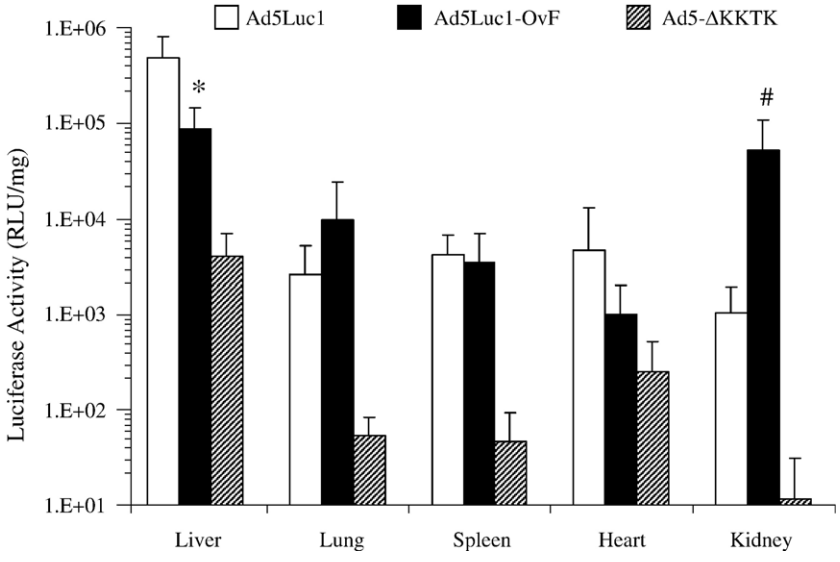

Fig. 5. In vivo biodistribution of Ad5-based vectors after intravenous injection into female C57BL/6 mice. Mice 6–8 weeks of age were injected with 1×10^{11} vp of Ad5Luc1 (open bars), Ad5Luc1-OvF (black bars) or Ad5-ΔdKKTK (cross-hatched bars). Luciferase activity was determined 48 h post-injection. Results from two individual experiments using different preparations of Ad5Luc1-OvF were combined and are presented as relative light units (RLU) normalized for total protein concentration for each individual organ. Each data point is an average of 8–10 mice (Ad5Luc1, $n = 10$; Ad5Luc1-OvF, $n = 8$; Ad5-ΔKKTK, $n = 10$), and error bars indicate standard deviation. *$P < 0.0028$ versus Ad5Luc1 in liver, #$P < 0.042$ versus Ad5Luc1 in kidney. For all tissues except heart, Ad5ΔKKTK luciferase values were significantly lower than Ad5Luc1, $P < 0.017$. In all cases, a two-tailed t test assuming unequal variance between groups was used for increased stringency.

similar to that described (Smith et al., 2003b). Mice were injected via the tail vein with 1×10^{11} viral particles. Forty-eight hours post-injection, the liver, spleen, lung, heart and kidney were harvested and homogenized, and luciferase activity and protein concentrations of cleared homogenates were measured. As expected, Ad5Luc1 produced the highest transgene expression in the liver, while Ad5-ΔKKTK vector gene expression in liver was reduced to 1% of control (Fig. 5). In all other organs examined, Ad5-ΔKKTK gene expression was markedly reduced to less than 7% of Ad5Luc1 control levels. Ad5Luc1-OvF gene expression was more evenly distributed among the major organs and was significantly decreased in the liver to approximately 18% of Ad5Luc1 levels ($P < 0.0028$). Ad5Luc1-OvF gene expression in the heart, spleen and lung was not significantly different from Ad5Luc1. Ad5Luc1-OvF gene expression in the kidney was increased 50-fold versus the Ad5Luc1 control vector ($P < 0.042$), resulting in a liver-to-kidney gene expression ratio of 0.59 for Ad5Luc1-OvF and 0.002 for Ad5Luc1, a difference of 280-fold. Of note, we observed a vector-specific difference in animal survival during the biodistribution studies. In this regard, all animals receiving control Ad survived the duration of the experiment; however, 3 of 11 mice receiving Ad5Luc1-OvF expired before the 48 h time point. Further analysis of this phenomenon is under investigation. In the aggregate, Ad5Luc1-OvF, a vector containing fibers from OAdV7 that are unable to bind CAR, demonstrates enhanced gene delivery to CAR-deficient human cells in vitro and displays a unique biodistribution characterized by attenuated liver transduction with significant kidney tropism.

Discussion

Despite a variety of avenues explored to improve human adenovirus serotype 5 as a therapeutic agent, this vector exhibits innate drawbacks of CAR dependency and hepatotropism. Of particular concern is that many clinically important tissues, including several cancer types, are refractory to Ad5 infection due to low CAR expression. Indeed, down-regulation of CAR has been reported for several tumor types, including glioma, ovarian, lung, breast and others (Miller et al., 1998; Hemminki and Alvarez, 2002; Bauerschmitz et al., 2002). As a consequence of limiting CAR levels in many clinically relevant target cells, high Ad vector dosage is often required for in vivo efficacy. Given that over 95% of systemically administered Ad particles are sequestered in the liver via hepatic macrophage (Kupffer cell) uptake (Tao et al., 2001) and hepatocyte transduction (Connelly, 1999) of both rodents and primates, therapeutically relevant Ad doses often result in vector-related liver toxicity (Peeters et al., 1996; Lieber et al., 1997; Sullivan et al., 1997; Worgall et al., 1997; Alemany et al., 2000; Shayakhmetov et al., 2004). Thus, Ad vectors exhibiting CAR-independent and/or expanded tropism coupled with low hepatotropism should prove valuable for maximal transduction of low-CAR targets at the lowest possible vector dose.

We sought to achieve this vector design mandate by replacing the Ad5 fiber with the corresponding structure from ovine atadenovirus serotype 7. The fiber of OAdV7 is the only identified structural determinant of native OAdV7 tropism, which is CAR-independent in vitro and non-hepatotropic when applied systemically. Genetic incorporation of the OAdV7 fiber molecule into the Ad5 virion ablated its CAR dependence as evidenced by competitive Ad5 knob blocking assays as well as increased cellular attachment to CAR-deficient CHO cells. Our results are consistent with previous findings showing that Ad5 and OAdV7 do not compete with each other for cell entry in cells that both viruses can infect (Xu and Both, 1998). Ad5Luc1-OvF exhibited enhanced infectivity in vitro, providing 3- to 23-fold increased gene transfer to several CAR-deficient cell lines and primary ovarian cancer tissue versus Ad5. However, Ad5Luc1-OvF gene transfer to other CAR-deficient human cancer cell lines such as SCC-25, FaDu and LNCaP, as well as the human THLE-3 normal liver cell line, was markedly reduced compared to the Ad5Luc1 control vector. These findings suggest that the receptor(s) for the OAdV7 fiber is not ubiquitously expressed, a biological phenomenon that may provide the basis of a level of cell- or tissue-type selectivity of potential utility.

Intravenous administration of Ad results in accumulation in the liver, spleen, heart, lung and kidneys of mice, although these tissues may not necessarily be the highest in CAR expression (Fechner et al., 1999; Reynolds et al., 1999; Wood et al., 1999). Instead, anatomic barriers, the structure of the vasculature and the degree of blood flow and in each organ probably contribute to the biodistribution, in addition to non-specific viral particle uptake by macrophages. This is true with regard to the liver in particular, which sequesters the majority of systemically administered Ad particles via hepatic macrophage (Kupffer cell) uptake (Tao et al., 2001) and hepatocyte transduction (Connelly, 1999), leading to cytokine release, inflammation and liver toxicity (Peeters et al., 1996; Lieber et al., 1997; Worgall et al., 1997; Shayakhmetov et al., 2004, 2005b). Thus, the nature of adenovirus–host interactions dictating the fate of systemically applied Ad has come under considerable scrutiny.

To this end, attempts to design Ad5 vectors that "detarget" the liver have been based on the assumption that CAR- and integrin-based interactions are required for liver uptake in vivo. The majority of attempts to inhibit hepatocyte and/or liver Kupffer cell uptake using Ad5 vectors with ablated CAR- or integrin-binding motifs in the Ad capsid have failed (Alemany and Curiel, 2001; Mizuguchi et al., 2002; Smith et al., 2002; Martin et al., 2003; Smith et al., 2003a), although some mutations of the Ad5 fiber knob have attenuated liver tropism of vectors following systemic administration (Einfeld et al., 2001; Koizumi et al., 2003; Yun et al., 2005). Indeed, recent studies focused on Ad vector biodistribution have demonstrated that Kupffer cell and hepatocyte uptake in vivo are largely CAR-independent (Liu et al., 2003; Shayakhmetov et al., 2004), confirming that native Ad5 tropism determinants at work in vitro contribute little to vector biodistribution in vivo.

The Ad fiber is a major structural determinant of liver tropism in vivo, even in the absence of knob/Ad receptor interaction (Nicklin et al., 2005). In this regard, Smith and co-

workers have examined the role of a putative heparan sulfate proteoglycan (HSPG)-binding motif, KKTK, in the third repeat of the native fiber shaft. Replacement of this motif with an irrelevant GAGA peptide sequence reduced reporter gene expression and Ad DNA in the liver by 90% in mice and non-human primates (Smith et al., 2003a). The authors postulated that removal of the KKTK inhibited Ad5 interaction with heparin sulfate proteoglycans (HSPG) in the liver; however, direct binding of this motif to HSPG has not been demonstrated.

Pseudotyping Ad5 with short-shafted fibers from Ad3, Ad35 or Ad40 that contain no native KKTK results in significant reduction of liver uptake (Table 2) (Nakamura et al., 2003; Sakurai et al., 2003; Vigne et al., 2003). Furthermore, the use of a shortened Ad5 fiber shaft that retains the native KKTK motif (Vigne et al., 2003) or replacement of the Ad5 shaft with the short Ad3 shaft domain (Breidenbach et al., 2004) was shown to attenuate liver uptake in vivo following intravenous delivery. Indeed, Shayakhmetov and co-workers have recently shown that short-shafted Ad vectors with either CAR- or non-CAR-interacting knob domains do not efficiently interact with hepatocytes in vivo and are not taken up by Kupffer cells (Shayakhmetov et al., 2004).

The Ad5Luc1-OvF fiber contains 25 pseudorepeats, no KKTK motif and likely forms a fiber at least as long as the native Ad5 fiber. Long-shafted Ads have been shown to accumulate within liver sinusoids and subsequently infect hepatocytes in a CAR-independent manner (Shayakhmetov et al., 2004). Thus, our result demonstrating marked reduction of in vivo liver gene expression appears to be unique for a long-shafted Ad vector and is comparable to results obtained with some short-shafted Ads (Table 2).

Recent evidence has highlighted the importance of serum factors in the hepatic uptake of systemically applied Ad vectors. Shayakhmetov and colleagues demonstrated that coagulation factor IX (FIX) and complement component C4-binding protein (C4BP) can direct Ad biodistribution in vivo by cross-linking Ad to hepatocellular HSGP and the LDL-receptor-related protein. Kupffer cell sequestration of Ad particles was likewise dependent on Ad association with FIX and C4BP (Shayakhmetov et al., 2005a). This work also demonstrated a key vector design approach whereby genetic modification of solvent-exposed loop structures in the Ad5 fiber knob attenuated serum factor binding resulting in reduced liver uptake in vivo. In addition to the Ad5Luc1-OvF vector, this serum-factor-ablated Ad vector is the only other long-shafted liver-detargeted Ad

Table 2
Fiber composition of Ad vectors displaying decreased liver localization in vivo

Ad Vector	Tail	Shaft	Knob	Liver detargeting	New in vivo tropism	Dose (vp)/Strain	Reference
Ad5Luc1	Ad5	Ad5 (22 repeats w/KKTK)	Ad5	No	–	1×10^{11}/C57BL/6	This report
Ad5Luc1-OvF	Ad5	OAdV7 (25 repeats, no KKTK)	OAdV7	20% of Ad5	Kidney, equal to liver	1×10^{11}/C57BL/6	This report
Ad5.Ad3.SH	Ad5	Ad3 (6 repeats, no KKTK)	Ad5	10% of Ad5	None reported	5×10^{10}/C57BL/6	Breidenbach et al., 2004
Ad5.Ad3.SH/knob3	Ad5	Ad3 (6 repeats, no KKTK)	Ad3	No	None reported	5×10^{10}/C57BL/6	Breidenbach et al., 2004
Ad5 DB6	Ad5	Ad3 (6 repeats, no KKTK)	Ad3	10% of Ad5	None reported	1×10^{11}/C57BL/6	Vigne et al., 2003
Ad5 BS1	Ad5	Ad5 (9 repeats, w/KKTK)	Ad5	10% of Ad5	None reported	1×10^{11}/C57BL/6	Vigne et al., 2003
Ad5.35F	Ad35	Ad35 (6 repeats, no KKTK)	Ad35	4% of Ad5	None reported	2×10^{11}/C57BL/6	Smith et al., 2003a,b
Ad5.5S35H	Ad5	Ad5	Ad35	No	None reported	2×10^{11}/C57BL/6	Smith et al., 2003a,b
Ad5.35S5H	Ad35	Ad35 (6 repeats, no KKTK)	Ad5	25% of Ad5	None reported	2×10^{11}/C57BL/6	Smith et al., 2003a,b
Ad5/35	Ad5	Ad35 (6 repeats, no KKTK)	Ad35	No	Kidney, 1% of liver	1×10^{10}/C57BL/6	Mizuguchi et al., 2002
Ad5.KO1	Ad5	Ad5	CAR-ablated Ad5	No	None reported	2×10^{11}/C57BL/6	Smith et al., 2003a,b
Ad5.S	Ad5	Ad5 (KKTK to GAGA)	Ad5	6% of Ad5	None reported	2×10^{11}/C57BL/6	Smith et al., 2003a,b
Ad5.K01.S	Ad5	Ad5 (KKTK to GAGA)	CAR-ablated Ad5	0.001% of Ad5	None reported	2×10^{11}/C57BL/6	Smith et al., 2003a,b
Ad5F35L	Ad5	Ad35 (6 repeats, no KKTK)	Ad35	0.001% of Ad5	None reported	1.5×10^{10}/C57BL/6	Sakurai et al., 2003
Ad5F/40S	Ad40	Ad40 (7 repeats, no KKTK)	Ad40	1% of Ad5	None reported	2×10^{10}/C57BL/6	Nakamura et al., 2003
Ad5/35L	Ad5	Ad5 (22 repeats, w/KKTK)	Ad35	No	None reported	1×10^{11}/C57BL/6	Shayakhmetov et al., 2004
Ad5/35S	Ad5	Ad35 (6 repeats, no KKTK)	Ad35	<10% of Ad5/35L	None reported	1×10^{11}/C57BL/6	Shayakhmetov et al., 2004
Ad5/9L	Ad5	Ad5 (22 repeats)	Ad9	No	None reported	1×10^{11}/C57BL/6	Shayakhmetov et al., 2004
Ad5/9S	Ad5	Ad9 (7 repeats, no KKTK)	Ad9	<10% of Ad5/9L	None reported	1×10^{11}/C57BL/6	Shayakhmetov et al., 2004

reported to date. Therefore, it is reasonable to posit that reduced liver uptake observed with Ad5Luc1-OvF is the result of the unique structure of the ovine fiber resulting in reduced and/or altered interaction with blood factors that mediate native Ad5 liver uptake.

Gene transfer to the kidney could have significant utility for the treatment of renal disease and in transplantation paradigms (Imai et al., 2004). While Ad, adeno-associated virus (AAV) and retroviral vectors transduce renal cells in vitro, systemic delivery of viral vectors has resulted in insufficient gene delivery to the kidney (Moullier et al., 1994; Takeda et al., 2004; Fujishiro et al., 2005). To increase in vivo gene transfer to the kidney, perfusion (Heikkila et al., 1996), catheter infusion (Takeda et al., 2004; Fujishiro et al., 2005) and direct interstitial injection (Ortiz et al., 2003) have been employed. Considering the established difficulty of generating Ad-mediated renal gene transfer via systemic injection, our result demonstrating abundant kidney gene expression by Ad5Luc1-OvF is notable. While the mechanism of enhanced kidney gene expression remains under investigation, we interpret this result as a consequence of unique, direct interaction(s) of Ad5Luc1-OvF with kidney and/or renal vasculature, and not solely as a result of decreased liver sequestration, since other Ad vectors exhibiting decreased hepatotropism have not demonstrated appreciable novel tissue tropism (Table 2).

The kidney is a complex organ with numerous specialized compartments including the glomeruli, tubules, interstitium and vasculature. The glomerular capillary endothelium is fenestrated, resulting in the "leaky" vasculature that would allow intravenous Ad vectors to contact the underlying filtration membrane and access to the epithelium of the renal tubule system. Indeed, injection of an Ad vector directly into the renal artery can result in gene transfer to cells of the proximal tubule (Moullier et al., 1994). Given the unique renal localization observed, we are currently extending our studies to determine the precise localization of Ad5Luc1-OvF gene expression within kidney substructures. An important issue related to the renal localization is the toxicity we observed while carrying out these studies. Given that only animals receiving Ad5Luc1-OvF vector expired before tissue harvest at 48 h post-injection and that liver gene expression was decreased in surviving animals, it is reasonable to suspect that the increased levels of Ad5Luc1-OvF in the kidney resulted in the toxicity. In this regard, further examination of renal tissue inflammation, apoptosis or other patho-physiology should provide the basis for understanding this effect observed in some animals.

To our knowledge, this is the first report of a fiber-pseudotyped Ad vector that simultaneously displays decreased hepatotropism and a distinct organ tropism in vivo. Furthermore, this novel redirection of vector biodistribution is directly attributable to fiber replacement with a non-CAR binding long-shafted fiber, an outcome seemingly at odds with recent fiber pseudotyping reports employing short-shafted vectors. In vitro, Ad5Luc1-OvF displays CAR-independent tropism with a positive correlation between increased Ad5Luc1-OvF cell-surface interaction and enhanced gene delivery in CAR-deficient cells, suggesting the use of as-yet unidentified receptor molecule(s). In addition, this vector may prove useful in murine models of renal disease.

Materials and methods

Cell lines

The Ad5 DNA-transformed 293 human embryonic cell line was purchased from Microbix (Toronto, ON, Canada). Human embryonic rhabdomyosarcoma RD cells, CAR-negative human U118MG glioma cells, PC-3 and LNCaP human prostate cancer cells, MCF7 human breast cancer cells, T24 human bladder cancer cells, Chinese hamster ovary cells (CHO), human squamous cell carcinoma SCC-4 and SCC-25 cells, FaDu human pharynx cancer cells, HeLa and SKOV ovarian cancer cells, LoVo colon cancer cells and OV-3 ovarian cancer cells were obtained from the American Type Culture Collection (ATCC) (Manassas, VA). The human ovarian adenocarcinoma cell lines Hey, SKOV3.ip1 and OV-4 were obtained from Drs. Judy Wolf, Janet Price (both of M.D. Anderson Cancer Center, Houston, TX) and Timothy J. Eberlein, (Harvard Medical School, Boston, MA), respectively. These cell lines were propagated in 50:50 mixture of Dulbecco's modified Eagle's medium and Ham's F-12 medium (DMEM/F-12) supplemented with 10% (v/v) fetal calf serum (FCS), L-glutamine (2 mM), penicillin (100 units/ml) and streptomycin (100 μg/ml). U118-hCAR-tailless cells, which express a truncated form of human CAR comprising the extracellular domain, transmembrane domain and the first two amino acids from the cytoplasmic domain (Wang and Bergelson, 1999), have been described previously (Kim et al., 2003) and were grown in DMEM/F12 as above except for the addition of 400 μg/ml G418. The ovine OLE stroma cell line and ovine lung cancer cell line JS8JSRV were generous gifts from Dr. Massimo Palmarini, University of Glasgow, UK. All cell lines were cultured at 37 °C in 5% CO_2 using culture media recommended by each respective supplier. FCS was purchased from Gibco-BRL (Grand Island, NY) and media, and supplements were from Mediatech (Herndon, VA).

Precision-cut human ovarian cancer slices

Human ovarian cancer tissue was obtained taken from ovarian cancer patients following institutional review board approval, essentially as described previously (Kirby et al., 2004). Briefly, excess material was received from the Department of Obstetrics and Gynecology, the University of Alabama at Birmingham Hospital. Precision-cut ovarian cancer slices were prepared using a Krumdiek Tissue Slicer (Alabama Research and Development, Munford, AL) fitted with a 4 mm coring device to produce a core biopsy of 4 mm diameter. The cores were then sliced to 150 μm thickness. Each slice was transferred into a well of a 24-well plate containing 1 ml William's Medium E and placed on a rocker. Tumor slices were maintained at 37 °C in a 5% CO_2 environment on a rocker and allowed to preincubate for 2 h before treatment. Ovarian cancer slices were infected with 100 and 1000 vp/cell with Ad5Luc1, Ad5/OAdV7 or no virus. Ovarian cancer slices were harvested

and frozen at 24 h after infection. Gene transfer was determined using a luciferase activity assay system (Promega, Madison, WI) according to the manufacturer's instructions.

Flow cytometry

Cells grown in T75 flasks were removed by addition of EDTA in PBS and resuspended in PBS containing 1% bovine serum albumin (BSA). Cells (2×10^5) were incubated with 3.5×10^9 viral particles of adenovirus, or buffer only, for 1 h at 4 °C in 250 μl PBS–BSA. Cells were then washed twice in 4 ml cold PBS–BSA and incubated with a 1:500 dilution of polyclonal rabbit anti-Ad5 antiserum (Cocalico Biologicals, Reamstown, PA) at 4 °C in 250 μl PBS–BSA. Cells were washed twice in 4 ml cold PBS–BSA and incubated in 250 μl of a 1:150 dilution of FITC-labeled goat anti-rabbit IgG secondary antibody (Jackson Immunoresearch Labs, West Grove, PA) for 1 h in PBS–BSA at 4 °C. Flow cytometry analysis was performed at the UAB FACS Core Facility using FACScan (Beckton Dickenson, San Jose, CA).

Plasmid construction

To create the chimeric fiber used in this study, we fused the Ad5 tail domain to the OAdV7 fiber shaft and knob domains. A 1553-bp PCR product containing a 5′ *Sca*I site, the OAdV7 fiber shaft and knob domains and a 3′ *Mun*I site was amplified from plasmid pAK containing the right hand *Bam*HI fragment of the OAdV7 genome cloned into Bluescribe M13+ *Bam*HI/*Hin*cII sites. The forward primer designated OAdS*Sca*IF was 5′-AGC GAA GGG TTA GTA CTA TCT TTA AAC-3′, and the reverse primer was designated OAd*Mun*I-R2 5′-TCA TAC AAT TGT TTA **TTA** TTG TCT GAA TTG-3′. The underlined bases indicate insertion of restriction sites, and the stop codon is shown in bold. Next, a PCR product containing a 5′ *Pac*I site, the Ad5 tail domain and a 3′ *Sca*I site was amplified from plasmid pNEB.PK.3.6, a pNEB193-based shuttle vector containing the Ad5 fiber (Krasnykh et al., 1996). The forward primer is designated NEB36*Pac*IF 5′-ATT ACG CCA AGC TTG CAT GCC TGC-3′ and reverse primer NEB36*Sca*IR 5′-GCA AAG AGA GTA CTC CAG GGG GAC-3′. This PCR product was then digested with *Pac*I and *Sca*I and gel-purified. Shuttle vector pNEB.PK.3.6-OvF was created by a 3-piece ligation of *Pac*I/*Mun*I-digested pNEB.PK.3.6 and the two digested PCR fragments containing the Ad5 tail region and the OAdV7 shaft and knob domains. Direct sequencing confirmed that the coding region for the chimeric fiber was correct.

Generation of recombinant adenovirus

Recombinant Ad5 genomes containing the chimeric OAdV7 fiber gene were derived by homologous recombination in *E. coli* BJ5183 with *Swa*I-linearized rescue plasmid pVK700 (Belousova et al., 2002) and the fiber-containing *Pac*I–*Kpn*I fragment of the shuttle vector pNEB.PK.3.6-OvF (described above) essentially as described (Krasnykh et al., 1998). pVK700 is derived from pTG3602 (Chartier et al., 1996) but contains an almost complete deletion of the fiber gene and contains a firefly luciferase reporter gene driven by the cytomegalovirus immediate early promoter in place of the E1 region. Genomic clones were sequenced and analyzed by PCR prior to transfection of 911 cells. Ad5Luc1 is a replication-defective E1-deleted Ad vector containing a firefly luciferase reporter gene in the E1 region driven by the cytomegalovirus immediate early promoter/enhancer (Krasnykh et al., 2001). All vectors were propagated on 911 cells and purified by equilibrium centrifugation in CsCl gradients by a standard protocol. Viral particle (vp) concentration was determined at 260 nm by the method of Maizel et al. (1968) by using a conversion factor of 1.1×10^{12} vp/absorbance unit.

Western blot analysis

Aliquots of Ad vectors containing 2.0×10^{10} viral particles were diluted into Laemmli buffer and incubated at room temperature or 99 °C for 15 min and loaded onto a 4–20% gradient SDS-polyacrylamide gel (Bio-Rad, Hercules, CA). Following electrophoretic protein separation, proteins were electroblotted onto a PVDF membrane. The primary antibody (monoclonal 4D2 recognizing the Ad5 fiber tail domain) was diluted 1:3000 (Lab Vision, Freemont, CA). Immunoblots were developed by addition of a secondary horseradish-peroxidase-conjugated anti-mouse immunoglobulin antibody at a 1:3000 dilution (Dako Corporation, Carpentaria, CA) followed by incubation with 3-3′-diaminobenzene peroxidase substrate (DAB; Sigma Company, St. Louis, MO).

Recombinant fiber knob proteins

The knob domain of Ad5 was expressed in *E. coli* with an N-terminus 6-histidine tag using the pQE81 expression plasmid (Qiagen, Hilden, Germany). The Ad5 fiber knob domain was PCR-amplified using primers that amplified the entire fiber knob domain and the three carboxy-terminal fiber shaft repeats using the following primers: Ad5 (fwd) 5′-CAAACAC***GG***ATCCCCT-TTTATTATTCTTGGGCAATGTATGA-3′ using plasmid pNEB.PK.3.6 as the template. The forward primer contains a 2-bp mutation (in bold) that creates a 5′-end *Bam*HI restriction site (underlined). The stop codon (TAA) and polyadenylation signal (AATAAA) are underlined in the reverse primer. The PCR products containing the Ad5 fiber knob region were digested with *Bam*HI, gel-purified and ligated into *Bam*HI–*Sma*I-digested pQE81. The resulting plasmid pQE81-Ad5 was sequenced to identify correct clones. The expression plasmid was introduced into *E. coli*, and 6-His-containing fiber knob proteins from bacterial cultures were purified on nickel-nitrilotriacetic acid (Ni-NTA) agarose columns (Qiagen). The ability to form trimers was confirmed by Western blot analysis of boiled and unboiled purified knob proteins using a mouse penta-His monoclonal antibody (Qiagen) and a horseradish-peroxidase-conjugated anti-mouse immunoglobulin antibody at a 1:3000 dilution (DAKO Corporation) followed by incubation with 3-3′-diaminobenzene peroxidase substrate (DAB; Sigma Company). Concentration of purified knob proteins was determined by the method of Lowry (Bio-Rad).

In vitro Ad-mediated gene transfer experiments

For virus gene transfer experiments using adherent cell lines, cells were grown in wells of 24-well plates and were incubated for 1 h at 37 °C with each Ad vector diluted to 100 vp/cell in 500 μl of transduction media containing 2% FCS. Following the incubation, cells were rinsed in transduction media and were maintained at 37 °C in an atmosphere of 5% CO_2. Cells were harvested 24 h post-transduction, and gene transfer was determined using a luciferase activity assay system (Promega, Madison, WI) according to the manufacturer's instructions.

For experiments containing blocking agents, recombinant fiber knob proteins at 0.5, 5.0 and 50 μg/ml final concentration were incubated with the cells at 37 °C in transduction media 15 min before the addition of the virus. Following the transduction, cells were rinsed with transduction media to remove unbound virus and blocking agent and were maintained at 37 °C in an atmosphere of 5% CO_2.

Animals

Mice were obtained at 4 to 6 weeks of age and quarantined at least 1 week before the study. Mice were kept under pathogen-free conditions according to the American Association for Accreditation of Laboratory Animal Care guidelines. Animal protocols were reviewed and approved by the Institutional Animal Care and Use Committee of UAB.

Biodistribution

Female C57BL/6 mice (Charles River Laboratories, Wilmington, MA), aged 6–8 weeks, were injected intravenously through the lateral tail vein with 1×10^{11} vp of Ad5Luc1, Ad5Luc1-OvF or Ad5-ΔKKTK in 100 μl of PBS. After 48 h, mice were sacrificed and livers, lungs, spleens, hearts and kidneys were harvested and representative sections were frozen in the liquid nitrogen immediately. The frozen organ samples were homogenized with a Mini Beadbeater (BioSpec Products, Inc., Bartlesville, OK) in 2 ml micro-tubes (Research Product International Corp., Mt. Prospect, IL) with 100 μl of 1.0 mm zirconia/silica beads (BioSpec Products, Inc.) and 1 ml of Cell Culture Lysis Buffer (Promega) then centrifuged at 14,000 rpm for 2 min. Luciferase activity was measured as before. Mean background luciferase activity was subtracted. All luciferase activities were normalized by protein concentration in the tissue lysates. Protein concentrations were determined using a Bio-Rad DC protein assay kit (Bio-Rad, Hercules, CA).

Statistics

Data were presented as mean values ± deviation. Statistical differences among groups were assessed by a two-tailed *t* test assuming unequal variance between groups for increased stringency; $P < 0.05$ was considered significant.

Acknowledgments

This work was supported by grants from the National Institutes of Health: 2R01CA083821 and 1P01HL076540, and from the US Department of Defense: DOD W81XWH-05-1-0035.

References

Alemany, R., Curiel, D.T., 2001. CAR-binding ablation does not change biodistribution and toxicity of adenoviral vectors. Gene Ther. 8 (17), 1347–1353.

Alemany, R., Suzuki, K., Curiel, D.T., 2000. Blood clearance rates of adenovirus type 5 in mice. J. Gen. Virol. 81 (Pt. 11), 2605–2609.

Bai, M., Harfe, B., Freimuth, P., 1993. Mutations that alter an Arg–Gly–Asp (RGD) sequence in the adenovirus type 2 penton base protein abolish its cell-rounding activity and delay virus reproduction in flat cells. J. Virol. 67 (9), 5198–5205.

Bauerschmitz, G.J., Barker, S.D., Hemminki, A., 2002. Adenoviral gene therapy for cancer: from vectors to targeted and replication competent agents (Review). Int. J. Oncol. 21 (6), 1161–1174.

Belousova, N., Krendelchtchikova, V., Curiel, D.T., Krasnykh, V., 2002. Modulation of adenovirus vector tropism via incorporation of polypeptide ligands into the fiber protein. J. Virol. 76 (17), 8621–8631.

Benko, M., Harrach, B., 1998. A proposal for a new (third) genus within the family Adenoviridae. Arch. Virol. 143 (4), 829–837.

Bergelson, J.M., Cunningham, J.A., Droguett, G., Kurt-Jones, E.A., Krithivas, A., Hong, J.S., et al., 1997. Isolation of a common receptor for Coxsackie B viruses and adenoviruses 2 and 5. Science 275 (5304), 1320–1323.

Blackwell, J.L., Miller, C.R., Douglas, J.T., Li, H., Reynolds, P.N., Carroll, W.R., et al., 1999. Retargeting to EGFR enhances adenovirus infection efficiency of squamous cell carcinoma. Arch. Otolaryngol. Head Neck Surg. 125 (8), 856–863.

Boyle, D.B., Pye, A.D., Kocherhans, R., Adair, B.M., Vrati, S., Both, G.W., 1994. Characterisation of Australian ovine adenovirus isolates. Vet. Microbiol. 41 (3), 281–291.

Breidenbach, M., Rein, D.T., Wang, M., Nettelbeck, D.M., Hemminki, A., Ulasov, I., et al., 2004. Genetic replacement of the adenovirus shaft fiber reduces liver tropism in ovarian cancer gene therapy. Hum. Gene Ther. 15 (5), 509–518.

Büchen-Osmond, C. 2002. The Universal Virus Database of the International Committee on Taxonomy of Viruses. http://www.ncbi.nlm.nih.gov/ICTVdb/index.htm.

Chartier, C., Degryse, E., Gantzer, M., Dieterle, A., Pavirani, A., Mehtali, M., 1996. Efficient generation of recombinant adenovirus vectors by homologous recombination in *Escherichia coli*. J. Virol. 70 (7), 4805–4810.

Chiu, C.Y., Wu, E., Brown, S.L., Von Seggern, D.J., Nemerow, G.R., Stewart, P.L., 2001. Structural analysis of a fiber-pseudotyped adenovirus with ocular tropism suggests differential modes of cell receptor interactions. J. Virol. 75 (11), 5375–5380.

Connelly, S., 1999. Adenoviral vectors for liver-directed gene therapy. Curr. Opin. Mol. Ther. 1 (5), 565–572.

Cripe, T.P., Dunphy, E.J., Holub, A.D., Saini, A., Vasi, N.H., Mahller, Y.Y., et al., 2001. Fiber knob modifications overcome low, heterogeneous expression of the coxsackievirus–adenovirus receptor that limits adenovirus gene transfer and oncolysis for human rhabdomyosarcoma cells. Cancer Res. 61 (7), 2953–2960.

Davison, E., Diaz, R.M., Hart, I.R., Santis, G., Marshall, J.F., 1997. Integrin alpha5beta1-mediated adenovirus infection is enhanced by the integrin-activating antibody TS2/16. J. Virol. 71 (8), 6204–6207.

Dmitriev, I., Krasnykh, V., Miller, C.R., Wang, M., Kashentseva, E., Mikheeva, G., et al., 1998. An adenovirus vector with genetically modified fibers demonstrates expanded tropism via utilization of a coxsackievirus and adenovirus receptor-independent cell entry mechanism. J. Virol. 72 (12), 9706–9713.

Einfeld, D.A., Schroeder, R., Roelvink, P.W., Lizonova, A., King, C.R., Kovesdi, I., et al., 2001. Reducing the native tropism of adenovirus vectors

requires removal of both CAR and integrin interactions. J. Virol. 75 (23), 11284–11291.
Fechner, H., Haack, A., Wang, H., Wang, X., Eizema, K., Pauschinger, M., et al., 1999. Expression of coxsackie adenovirus receptor and alphav-integrin does not correlate with adenovector targeting in vivo indicating anatomical vector barriers. Gene Ther. 6 (9), 1520–1535.
Fujishiro, J., Takeda, S., Takeno, Y., Takeuchi, K., Ogata, Y., Takahashi, M., et al., 2005. Gene transfer to the rat kidney in vivo and ex vivo using an adenovirus vector: factors influencing transgene expression. Nephrol. Dial. Transplant. 20 (7), 1385–1391.
Gall, J., Kass-Eisler, A., Leinwand, L., Falck-Pedersen, E., 1996. Adenovirus type 5 and 7 capsid chimera: fiber replacement alters receptor tropism without affecting primary immune neutralization epitopes. J. Virol. 70 (4), 2116–2123.
Gelhe, W.D., Smith, K.O., 1969. Abortive infection of human cell cultures by a canine adenovirus. Proc. Soc. Exp. Biol. Med. 131, 87–93.
Glasgow, J.N., Kremer, E.J., Hemminki, A., Siegal, G.P., Douglas, J.T., Curiel, D.T., 2004. An adenovirus vector with a chimeric fiber derived from canine adenovirus type 2 displays novel tropism. Virology 324 (1), 103–116.
Goossens, P.H., Havenga, M.J., Pieterman, E., Lemckert, A.A., Breedveld, F.C., Bout, A., et al., 2001. Infection efficiency of type 5 adenoviral vectors in synovial tissue can be enhanced with a type 16 fiber. Arthritis Rheum. 44 (3), 570–577.
Havenga, M.J., Lemckert, A.A., Grimbergen, J.M., Vogels, R., Huisman, L.G., Valerio, D., et al., 2001. Improved adenovirus vectors for infection of cardiovascular tissues. J. Virol. 75 (7), 3335–3342.
Havenga, M.J., Lemckert, A.A., Ophorst, O.J., van Meijer, M., Germeraad, W.T., Grimbergen, J., et al., 2002. Exploiting the natural diversity in adenovirus tropism for therapy and prevention of disease. J. Virol. 76 (9), 4612–4620.
Heikkila, P., Parpala, T., Lukkarinen, O., Weber, M., Tryggvason, K., 1996. Adenovirus-mediated gene transfer into kidney glomeruli using an ex vivo and in vivo kidney perfusion system—First steps towards gene therapy of Alport syndrome. Gene Ther. 3 (1), 21–27.
Hemminki, A., Alvarez, R.D., 2002. Adenoviruses in oncology: a viable option? BioDrugs 16 (2), 77–87.
Hemminki, A., Kanerva, A., Kremer, E.J., Bauerschmitz, G.J., Smith, B.F., Conductier, G., et al., 2003. A canine conditionally replicating adenovirus for evaluating oncolytic virotherapy in a syngeneic animal model. Mol. Ther. 7 (2), 163–173.
Henry, L.J., Xia, D., Wilke, M.E., Deisenhofer, J., Gerard, R.D., 1994. Characterization of the knob domain of the adenovirus type 5 fiber protein expressed in *Escherichia coli*. J. Virol. 68 (8), 5239–5246.
Hofmann, C., Loser, P., Cichon, G., Arnold, W., Both, G.W., Strauss, M., 1999. Ovine adenovirus vectors overcome preexisting humoral immunity against human adenoviruses in vivo. J. Virol. 73 (8), 6930–6936.
Imai, E., Takabatake, Y., Mizui, M., Isaka, Y., 2004. Gene therapy in renal diseases. Kidney Int. 65 (5), 1551–1555.
Jakubczak, J.L., Rollence, M.L., Stewart, D.A., Jafari, J.D., Von Seggern, D.J., Nemerow, G.R., et al., 2001. Adenovirus type 5 viral particles pseudotyped with mutagenized fiber proteins show diminished infectivity of coxsackie B-adenovirus receptor-bearing cells. J. Virol. 75 (6), 2972–2981.
Kanerva, A., Mikheeva, G.V., Krasnykh, V., Coolidge, C.J., Lam, J.T., Mahasreshti, P.J., et al., 2002. Targeting adenovirus to the serotype 3 receptor increases gene transfer efficiency to ovarian cancer cells. Clin. Cancer Res. 8 (1), 275–280.
Khatri, A., Xu, Z.Z., Both, G.W., 1997. Gene expression by atypical recombinant ovine adenovirus vectors during abortive infection of human and animal cells in vitro. Virology 239 (1), 226–237.
Kim, M., Zinn, K.R., Barnett, B.G., Sumerel, L.A., Krasnykh, V., Curiel, D.T., et al., 2002. The therapeutic efficacy of adenoviral vectors for cancer gene therapy is limited by a low level of primary adenovirus receptors on tumour cells. Eur. J. Cancer 38 (14), 1917–1926.
Kim, M., Sumerel, L.A., Belousova, N., Lyons, G.R., Carcy, D.E., Krasuykh, V., et al., 2003. The coxsackievirus and adenovirus receptor acts as a tumour suppressor in malignant glioma cells. Br. J. Cancer 88 (9), 1411–1416.
Kirby, T.O., Rivera, A., Rein, D., Wang, M., Ulasov, I., Breidenbach, M., et al., 2004. A novel ex vivo model system for evaluation of conditionally replicative adenoviruses therapeutic efficacy and toxicity. Clin. Cancer Res. 10 (24), 8697–8703.
Koizumi, N., Mizuguchi, H., Sakurai, F., Yamaguchi, T., Watanabe, Y., Hayakawa, T., 2003. Reduction of natural adenovirus tropism to mouse liver by fiber-shaft exchange in combination with both CAR- and alphav integrin-binding ablation. J. Virol. 77 (24), 13062–13072.
Krasnykh, V.N., Mikheeva, G.V., Douglas, J.T., Curiel, D.T., 1996. Generation of recombinant adenovirus vectors with modified fibers for altering viral tropism. J. Virol. 70 (10), 6839–6846.
Krasnykh, V., Dmitriev, I., Mikheeva, G., Miller, C.R., Belousova, N., Curiel, D.T., 1998. Characterization of an adenovirus vector containing a heterologous peptide epitope in the HI loop of the fiber knob. J. Virol. 72 (3), 1844–1852.
Krasnykh, V., Belousova, N., Korokhov, N., Mikheeva, G., Curiel, D.T., 2001. Genetic targeting of an adenovirus vector via replacement of the fiber protein with the phage T4 fibritin. J. Virol. 75 (9), 4176–4183.
Kremer, E.J., Boutin, S., Chillon, M., Danos, O., 2000. Canine adenovirus vectors: an alternative for adenovirus-mediated gene transfer. J. Virol. 74 (1), 505–512.
Kumin, D., Hofmann, C., Rudolph, M., Both, G.W., Loser, P., 2002. Biology of ovine adenovirus infection of nonpermissive cells. J. Virol. 76 (21), 10882–10893.
Li, Y., Pong, R.C., Bergelson, J.M., Hall, M.C., Sagalowsky, A.I., Tseng, C.P., et al., 1999. Loss of adenoviral receptor expression in human bladder cancer cells: a potential impact on the efficacy of gene therapy. Cancer Res. 59 (2), 325–330.
Li, E., Brown, S.L., Stupack, D.G., Puente, X.S., Cheresh, D.A., Nemerow, G.R., 2001. Integrin alpha(v)beta1 is an adenovirus coreceptor. J. Virol. 75 (11), 5405–5409.
Lieber, A., He, C.Y., Meuse, L., Schowalter, D., Kirillova, I., Winther, B., et al., 1997. The role of Kupffer cell activation and viral gene expression in early liver toxicity after infusion of recombinant adenovirus vectors. J. Virol. 71 (11), 8798–8807.
Liu, Q., Zaiss, A.K., Colarusso, P., Patel, K., Haljan, G., Wickham, T.J., et al., 2003. The role of capsid–endothelial interactions in the innate immune response to adenovirus vectors. Hum Gene Ther. 14 (7), 627–643.
Loser, P., Hillgenberg, M., Arnold, W., Both, G.W., Hofmann, C., 2000. Ovine adenovirus vectors mediate efficient gene transfer to skeletal muscle. Gene Ther. 7 (17), 1491–1498.
Loser, P., Huser, A., Hillgenberg, M., Kumin, D., Both, G.W., Hofmann, C., 2002. Advances in the development of non-human viral DNA-vectors for gene delivery. Curr. Gene Ther. 2 (2), 161–171.
Loser, P., Hofmann, C., Both, G.W., Uckert, W., Hillgenberg, M., 2003. Construction, rescue, and characterization of vectors derived from ovine atadenovirus. J. Virol. 77 (22), 11941–11951.
Louis, N., Fender, P., Barge, A., Kitts, P., Chroboczek, J., 1994. Cell-binding domain of adenovirus serotype 2 fiber. J. Virol. 68 (6), 4104–4106.
Maizel Jr., J.V., White, D.O., Scharff, M.D., 1968. The polypeptides of adenovirus: I. Evidence for multiple protein components in the virion and a comparison of types 2, 7A, and 12. Virology 36 (1), 115–125.
Martin, K., Brie, A., Saulnier, P., Perricaudet, M., Yeh, P., Vigne, E., 2003. Simultaneous CAR- and alpha V integrin-binding ablation fails to reduce Ad5 liver tropism. Mol. Ther. 8 (3), 485–494.
Martiniello-Wilks, R., Wang, X.Y., Voeks, D.J., Dane, A., Shaw, J.M., Mortensen, E., 2004. Purine nucleoside phosphorylase and fludarabine phosphate gene-directed enzyme prodrug therapy suppresses primary tumour growth and pseudo-metastases in a mouse model of prostate cancer. J. Gene Med. 6 (12), 1343–1357.
Miller, C.R., Buchsbaum, D.J., Reynolds, P.N., Douglas, J.T., Gillespie, G.Y., Mayo, M.S., et al., 1998. Differential susceptibility of primary and established human glioma cells to adenovirus infection: targeting via the epidermal growth factor receptor achieves fiber receptor-independent gene transfer. Cancer Res. 58 (24), 5738–5748.
Mizuguchi, H., Koizumi, N., Hosono, T., Ishii-Watabe, A., Uchida, E., Utoguchi, N., et al., 2002. CAR- or alphav integrin-binding ablated adenovirus vectors, but not fiber-modified vectors containing RGD peptide, do not change the systemic gene transfer properties in mice. Gene Ther. 9 (12), 769–776.
Moullier, P., Friedlander, G., Calise, D., Ronco, P., Perricaudet, M., Ferry, N.,

1994. Adenoviral-mediated gene transfer to renal tubular cells in vivo. Kidney Int. 45 (4), 1220–1225.

Nakamura, T., Sato, K., Hamada, H., 2003. Reduction of natural adenovirus tropism to the liver by both ablation of fiber-coxsackievirus and adenovirus receptor interaction and use of replaceable short fiber. J. Virol. 77 (4), 2512–2521.

Nguyen, T., Nery, J., Joseph, S., Rocha, C., Carney, G., Spindler, K., et al., 1999. Mouse adenovirus (MAV-1) expression in primary human endothelial cells and generation of a full-length infectious plasmid. Gene Ther. 6 (7), 1291–1297.

Nicklin, S.A., Wu, E., Nemerow, G.R., Baker, A.H., 2005. The influence of adenovirus fiber structure and function on vector development for gene therapy. Mol. Ther. 12 (3), 384–393.

Okegawa, T., Li, Y., Pong, R.C., Bergelson, J.M., Zhou, J., Hsieh, J.T., 2000. The dual impact of coxsackie and adenovirus receptor expression on human prostate cancer gene therapy. Cancer Res. 60 (18), 5031–5036.

Ortiz, P.A., Hong, N.J., Plato, C.F., Varela, M., Garvin, J.L., 2003. An in vivo method for adenovirus-mediated transduction of thick ascending limbs. Kidney Int. 63 (3), 1141–1149.

Peeters, M.J., Patijn, G.A., Lieber, A., Meuse, L., Kay, M.A., 1996. Adenovirus-mediated hepatic gene transfer in mice: comparison of intravascular and biliary administration. Hum. Gene Ther. 7 (14), 1693–1699.

Rasmussen, U.B., Benchaibi, M., Meyer, V., Schlesinger, Y., Schughart, K., 1999. Novel human gene transfer vectors: evaluation of wild-type and recombinant animal adenoviruses in human-derived cells. Hum. Gene Ther. 10 (16), 2587–2599.

Reddy, P.S., Idamakanti, N., Chen, Y., Whale, T., Babiuk, L.A., Mehtali, M., et al., 1999a. Replication-defective bovine adenovirus type 3 as an expression vector. J. Virol. 73 (11), 9137–9144.

Reddy, P.S., Idamakanti, N., Hyun, B.H., Tikoo, S.K., Babiuk, L.A., 1999b. Development of porcine adenovirus-3 as an expression vector. J. Gen. Virol. 80 (Pt. 3), 563–570.

Reynolds, P., Dmitriev, I., Curiel, D., 1999. Insertion of an RGD motif into the HI loop of adenovirus fiber protein alters the distribution of transgene expression of the systemically administered vector. Gene Ther. 6 (7), 1336–1339.

Rothel, J.S., Boyle, D.B., Both, G.W., Pye, A.D., Waterkeyn, J.G., Wood, P.R., et al., 1997. Sequential nucleic acid and recombinant adenovirus vaccination induces host-protective immune responses against *Taenia ovis* infection in sheep. Parasite Immunol. 19 (5), 221–227.

Sakurai, F., Mizuguchi, H., Yamaguchi, T., Hayakawa, T., 2003. Characterization of in vitro and in vivo gene transfer properties of adenovirus serotype 35 vector. Mol. Ther. 8 (5), 813–821.

Salone, B., Martina, Y., Piersanti, S., Cundari, E., Cherubini, G., Franqueville, L., et al., 2003. Integrin alpha3beta1 is an alternative cellular receptor for adenovirus serotype 5. J. Virol. 77 (24), 13448–13454.

Shayakhmetov, D.M., Papayannopoulou, T., Stamatoyannopoulos, G., Lieber, A., 2000. Efficient gene transfer into human CD34(+) cells by a retargeted adenovirus vector. J. Virol. 74 (6), 2567–2583.

Shayakhmetov, D.M., Li, Z.Y., Ni, S., Lieber, A., 2004. Analysis of adenovirus sequestration in the liver, transduction of hepatic cells, and innate toxicity after injection of fiber-modified vectors. J. Virol. 78 (10), 5368–5381.

Shayakhmetov, D.M., Gaggar, A., Ni, S., Li, Z.Y., Lieber, A., 2005a. Adenovirus binding to blood factors results in liver cell infection and hepatotoxicity. J. Virol. 79 (12), 7478–7491.

Shayakhmetov, D.M., Li, Z.Y., Ni, S., Lieber, A., 2005b. Interference with the IL-1-signaling pathway improves the toxicity profile of systemically applied adenovirus vectors. J. Immunol. 174 (11), 7310–7319.

Smith, T., Idamakanti, N., Kylefjord, H., Rollence, M., King, L., Kaloss, M., et al., 2002. In vivo hepatic adenoviral gene delivery occurs independently of the coxsackievirus–adenovirus receptor. Mol. Ther. 5 (6), 770–779.

Smith, T.A., Idamakanti, N., Marshall-Neff, J., Rollence, M.L., Wright, P., Kaloss, M., et al., 2003a. Receptor interactions involved in adenoviral-mediated gene delivery after systemic administration in non-human primates. Hum. Gene Ther. 14 (17), 1595–1604.

Smith, T.A., Idamakanti, N., Rollence, M.L., Marshall-Neff, J., Kim, J., Mulgrew, K., et al., 2003b. Adenovirus serotype 5 fiber shaft influences in vivo gene transfer in mice. Hum. Gene Ther. 14 (8), 777–787.

Soudais, C., Boutin, S., Hong, S.S., Chillon, M., Danos, O., Bergelson, J.M., et al., 2000. Canine adenovirus type 2 attachment and internalization: coxsackievirus–adenovirus receptor, alternative receptors, and an RGD-independent pathway. J. Virol. 74 (22), 10639–10649.

Sullivan, D.E., Dash, S., Du, H., Hiramatsu, N., Aydin, F., Kolls, J., et al., 1997. Liver-directed gene transfer in non-human primates. Hum. Gene Ther. 8 (10), 1195–1206.

Takeda, S., Takahashi, M., Mizukami, H., Kobayashi, E., Takeuchi, K., Hakamata, Y., et al., 2004. Successful gene transfer using adeno-associated virus vectors into the kidney: comparison among adeno-associated virus serotype 1–5 vectors in vitro and in vivo. Nephron. Exp. Nephrol. 96 (4), e119–e126.

Tao, N., Gao, G.P., Parr, M., Johnston, J., Baradet, T., Wilson, J.M., et al., 2001. Sequestration of adenoviral vector by Kupffer cells leads to a nonlinear dose response of transduction in liver. Mol. Ther. 3 (1), 28–35.

Tomko, R.P., Xu, R., Philipson, L., 1997. HCAR and MCAR: the human and mouse cellular receptors for subgroup C adenoviruses and group B coxsackieviruses. Proc. Natl. Acad. Sci. U.S.A. 94 (7), 3352–3356.

van Raaij, M.J., Mitraki, A., Lavigne, G., Cusack, S., 1999. A triple beta-spiral in the adenovirus fibre shaft reveals a new structural motif for a fibrous protein. Nature 401 (6756), 935–938.

Vigne, E., Dedieu, J.F., Brie, A., Gillardeaux, A., Briot, D., Benihoud, K., et al., 2003. Genetic manipulations of adenovirus type 5 fiber resulting in liver tropism attenuation. Gene Ther. 10 (2), 153–162.

Voeks, D., Martiniello-Wilks, R., Madden, V., Smith, K., Bennetts, E., Both, G.W., et al., 2002. Gene therapy for prostate cancer delivered by ovine adenovirus and mediated by purine nucleoside phosphorylase and fludarabine in mouse models. Gene Ther. 9 (12), 759–768.

Von Seggern, D.J., Huang, S., Fleck, S.K., Stevenson, S.C., Nemerow, G.R., 2000. Adenovirus vector pseudotyping in fiber-expressing cell lines: improved transduction of Epstein–Barr virus-transformed B cells. J. Virol. 74 (1), 354–362.

Vrati, S., Boyle, D., Kocherhans, R., Both, G.W., 1995. Sequence of ovine adenovirus homologs for 100K hexon assembly, 33K, pVIII, and fiber genes: early region E3 is not in the expected location. Virology 209 (2), 400–408.

Vrati, S., Brookes, D.E., Strike, P., Khatri, A., Boyle, D.B., Both, G.W., 1996. Unique genome arrangement of an ovine adenovirus: identification of new proteins and proteinase cleavage sites. Virology 220 (1), 186–199.

Wang, X., Bergelson, J.M., 1999. Coxsackievirus and adenovirus receptor cytoplasmic and transmembrane domains are not essential for coxsackievirus and adenovirus infection. J. Virol. 73 (3), 2559–2562.

Wang, X.Y., Martiniello-Wilks, R., Shaw, J.M., Ho, T., Coulston, N., Cooke-Yarborough, C., et al., 2004. Preclinical evaluation of a prostate-targeted gene-directed enzyme prodrug therapy delivered by ovine atadenovirus. Gene Ther. 11 (21), 1559–1567.

Wickham, T.J., Mathias, P., Cheresh, D.A., Nemerow, G.R., 1993. Integrins alpha v beta 3 and alpha v beta 5 promote adenovirus internalization but not virus attachment. Cell 73 (2), 309–319.

Wood, M., Perrotte, P., Onishi, E., Harper, M.E., Dinney, C., Pagliaro, L., et al., 1999. Biodistribution of an adenoviral vector carrying the luciferase reporter gene following intravesical or intravenous administration to a mouse. Cancer Gene Ther. 6 (4), 367–372.

Worgall, S., Wolff, G., Falck-Pedersen, E., Crystal, R.G., 1997. Innate immune mechanisms dominate elimination of adenoviral vectors following in vivo administration. Hum. Gene Ther. 8 (1), 37–44.

Xia, D., Henry, L.J., Gerard, R.D., Deisenhofer, J., 1994. Crystal structure of the receptor-binding domain of adenovirus type 5 fiber protein at 1.7 A resolution. Structure 2 (12), 1259–1270.

Xu, Z.Z., Both, G.W., 1998. Altered tropism of an ovine adenovirus carrying the fiber protein cell binding domain of human adenovirus type 5. Virology 248 (1), 156–163.

Yun, C.O., Yoon, A.R., Yoo, J.Y., Kim, H., Kim, M., Ha, T., et al., 2005. Coxsackie and adenovirus receptor binding ablation reduces adenovirus liver tropism and toxicity. Hum. Gene Ther. 16 (2), 248–261.

Strategies to enhance transductional efficiency of adenoviral-based gene transfer to primary human fibroblasts and keratinocytes as a platform in dermal wounds

Alexander Stoff, MD[1,2,3]; Angel A. Rivera, PhD[1]; N. S. Banerjee, PhD[4]; J. Michael Mathis, PhD[5]; Antonio Espinosa-de-los-Monteros, MD[3]; Long P. Le, PhD[1]; Jorge I. De la Torre, MD[3]; Luis O. Vasconez, MD[3]; Thomas R. Broker, PhD[4]; Dirk F. Richter, MD[2]; Mariam A. Stoff-Khalili, MD[1,6]; David T. Curiel, MD, PhD[1]

1. Division of Human Gene Therapy, Departments of Medicine, Obstetrics and Gynecology, Pathology, Surgery, and the Gene Therapy Center, University of Alabama at Birmingham, Birmingham, Alabama,
2. Department of Plastic and Reconstructive Surgery, Dreifaltigkeits-Hospital, Wesseling, Germany,
3. Department of Plastic and Reconstructive Surgery, University of Alabama at Birmingham, Birmingham, Alabama,
4. Department of Biochemistry and Molecular Genetics, University of Alabama at Birmingham, Birmingham, Alabama,
5. Department of Cellular Biology and Anatomy, Louisiana State University Health Sciences Center, Shreveport, Louisiana, and
6. Department of Gynecology and Obstetrics, University of Duesseldorf, Medical Center, Duesseldorf, Germany

Reprint requests:
Mariam A. Stoff-Khalili, MD, Division of Human Gene Therapy, Gene Therapy Center, University of Alabama at Birmingham, 901 19th Street South, BMR2 502, Birmingham, AL 35294.
Fax: +(205) 975-7476;
Email: stoff-khalili@t-online.de

Manuscript received: January 28, 2006
Accepted in final form: March 28, 2006

DOI:10.1111/j.1743-6109.2006.00168.x

ABSTRACT

Genetically modified keratinocytes and fibroblasts are suitable for delivery of therapeutic genes capable of modifying the wound healing process. However, efficient gene delivery is a prerequisite for successful gene therapy of wounds. Whereas adenoviral vectors (Ads) exhibit superior levels of in vivo gene transfer, their transductional efficiency to cells resident within wounds may nonetheless be suboptimal, due to deficiency of the primary adenovirus receptor, coxsackie-adenovirus receptor (CAR). We explored CAR-independent transduction to fibroblasts and keratinocytes using a panel of CAR-independent fiber-modified Ads to determine enhancement of infectivity. These fiber-modified adenoviral vectors included Ad 3 knob (Ad5/3), canine Ad serotype 2 knob (Ad5CAV-2), RGD (Ad5.RGD), polylysine (Ad5.pK7), or both RGD and polylysine (Ad5.RGD.pK7). To evaluate whether transduction efficiencies of the fiber-modified adenoviral vectors correlated with the expression of their putative receptors on keratinocytes and fibroblasts, we analyzed the mRNA levels of CAR, α_v integrin, syndecan-1, and glypican-1 using quantitative polymerase chain reaction. Analysis of luciferase and green fluorescent protein transgene expression showed superior transduction efficiency of Ad5.pK7 in keratinocytes and Ad5.RGD.pK7 in fibroblasts. mRNA expression of α_v integrin, syndecan-1 and glypican-1 was significantly higher in primary fibroblasts than CAR. In keratinocytes, syndecan-1 expression was significantly higher than all the other receptors tested. Significant infectivity enhancement was achieved in keratinocytes and fibroblasts using fiber-modified adenoviral vectors. These strategies to enhance infectivity may help to achieve higher clinical efficacy of wound gene therapy.

Characterization of the key cellular and molecular components of the processes of wound healing has led to the development of targeted interventions designed to foster the repair process. In this regard, direct delivery of genes in situ represents a desirable approach to achieve wound healing gene therapy. Indeed, a number of described approaches have exploited this delivery paradigm to achieve the high local levels of cytokines and growth factors critical for realizing effective gene-based wound repair.[1–3] These genetic approaches to augment the wound healing process have included in vitro-mediated gene transfer to cells with autologous transplantation, and in vivo-mediated gene transfer to cells resident within a wound to allow these cells to produce therapeutic proteins that will modify the wound healing process.[4–6] These diverse approaches have validated the basic concept that gene-based methods may be adjunctive to the achievement of effective wound healing.

Ads	Adenoviral vectors
CAR	Coxsackie-adenovirus receptor
CMV	Cytomegalovirus
DAPI	4′,6′-diamidino-2-phenylindole
GAPDH	Glyceraldehyde 3-phosphate dehydrogenase
GFP	Green fluorescent protein
GM	Growth medium
MOI	Multiplicity of infection
NHEK	Normal human epithelial keratinocytes
PBS	Phosphate buffered saline solution
PCR	Polymerase chain reaction
pK7	Polylysine
RGD	Arginine–glycine–aspartate
VP	Viral particle

A unifying aspect of these interventions is the requirement to achieve effective expression of therapeutic genes (such as vascular endothelial growth factor, transforming growth factor-β, platelet-derived growth factor, fibroblast growth factor, and keratinocyte growth factor) in the context of cells involved in the wound healing process.[7,8] One candidate vector for this application is the adenovirus, which embodies unparalleled gene delivery efficacy in selected contexts. The advantage of the adenovirus as a gene transfer vector lies in its ability to transduce dividing and nondividing target cells, to induce high transgene expression in vivo, its well characterized biology, and ability to incorporate large DNA inserts. However, cells resident in wounds such as human fibroblasts and keratinocytes, which are targets of wound healing strategies, may not be efficiently infected by adenoviruses.[9–11] In these instances, deficiency of the primary adenovirus receptor, coxsackie-adenovirus receptor (CAR) on keratinocytes and fibroblasts has been understood to be the biological basis of this phenomenon.[9–11] Hence, to achieve the levels of efficiency required in the context of wound gene therapy, it may be necessary to route the adenovirus via CAR-independent pathways. In this regard, several capsid modification strategies have been endeavored to circumvent CAR deficiency. These include the incorporation of short heterologous peptide motifs like RGD (Arg-Gly-Asp) or polylysine (pK7)[12,13] into the fiber knob domain, as well as knob switching strategies.[14] In addition, more radical modifications based on xenotype knob switching have been exploited to achieve enhanced infectivity.[15,16] These modified vectors have been shown to transduce a variety of cells with greatly enhanced infectivity.[15–18] Heretofore, these different targeting strategies have not been explored nor compared in the context of targeting strategies relevant with wound healing gene therapy.

In this study, we systematically evaluated a panel of fiber-modified adenoviral vectors (Ads) to enhance transduction of immortalized cell lines as well as primary fibroblasts and primary keratinocytes. Our results indicate that polylysine incorporation onto the C-terminus of the adenoviral fiber knob provides the best infectivity enhancement for the transduction of keratinocytes, whereas the Ads containing a double modification with an RGD motif in the HI loop and a polylysine motif at the C-terminus of the fiber results in the highest infectivity enhancement for the transduction of fibroblasts. Our study thus provides valuable information for adenoviral-based gene therapy in wounds of the skin with respect to the most efficient targeting strategies and a rational basis for further development of Ads for their clinical application in gene therapy of dermal wound healing.

MATERIALS AND METHODS

Human fibroblast cell lines CRL-1474, CCL-148, Detroit 5510, and CRL-2106 were obtained from the ATCC (Manassas, VA). The 293 human-transformed embryonal kidney cell line was purchased from Microbix (Toronto, Canada). All cell lines were maintained in a humidified 37 °C atmosphere containing 5% CO_2 and cultured with the recommended media. Infections were performed in medium with 2% fetal calf serum (Hyclone, Logan, UT). Normal adult primary human epidermal keratinocytes (NHEK and NHEK-neo Cambrex, Walkersville, MD) were propagated in complete keratinocyte growth medium (GM; Cambrex).

Primary fibroblasts and keratinocytes and cell culture

Approval was obtained from the Institutional Review Board for all studies on human tissue. Human dermal fibroblasts were derived from adult skin by trypsinization as described.[19,20] Human dermal fibroblasts obtained from outgrowth of explant cultures, were grown in Dulbecco's modified Eagle's medium (BioWhittaker, Walkersville, MD) supplemented with 10% fetal calf serum, 2 mM glutamine, 100 U/mL penicillin, and 100 μg/mL streptomycin and grown as monolayers on plastic Petri dishes in a humidified atmosphere of a CO_2 incubator at 37 °C. Primary keratinocytes were isolated from skin as described previously.[21]

RNA preparation and polymerase chain reaction (PCR) analysis

Total cellular RNA of primary fibroblasts and keratinocytes was extracted from 2×10^5 cells using the RNeasy mini-prep kit (Qiagen, Santa Clarita, CA) and treated with DNase I (Life Technologies, Rockville, MD) for 30 minutes. The GeneAmp RNA PCR core kit (Applied Biosystems, Foster City, CA) was used for cDNA synthesis and PCR amplification of cDNA products. TaqMan primers and probes were designed by Primer Express 1.0 software (Applied Biosystems) and synthesized by Applied Biosystems.

Oligonucleotide sequences for amplification of the CAR gene were as follows: forward primer, 5′-GGA CTT GGC CAC GTT CAT G-3′, and reverse primer, 5′-ACC TCA GCC ACA GTC AAC GG-3′ and probe 6FAM-AGC ACC GCA TCC GTC CGC AG-TAMRA. The sequences to amplify CD80 were: forward primer 5′-AAG TGG CAA CGC TGT CCT G-3′, reverse primer 5′-CCT TTT GCC AGT AGA TGC GAG-3′ and probe 6FAM-TTG TGC CAG CTC TTC AAC AGA AAC ATT GTG-TAMRA; the sequences to amplify CD86 were: forward primer 5′-CAG ACC TGC CAT GCC AAT T-3′, reverse primer 5′-TTT CCT GGT CCT GCC AAA AT-3′ and 6FAM-CAA ACT CTC AAA ACC AAA GCC TGA GTG AGC-TAMRA; and the sequences to amplify CD46 were: forward primer 5′-CTT TCC TTC CTG GCG CTT TC-3′, reverse primer 5′-CGG AGA AGG AGT ACA GCA GCA-3′ and 6FAM-CAC CAT GGC CGC CAG AAG CAA-TAMRA. Oligonucleotide sequences for amplification of the subunit β_3 of the $\alpha_v\beta_3$ integrin were as follows: forward primer 5′-CGG ACA CAG GAG AAG TCG-3′, reverse primer 5′-CCA CAG CAG TGA CTT TGG CA-3′ and probe 6FAM-CAC ACT CGC AGT ACT TGC CCG TGA TC-TAMRA,[22] the sequences to amplify the subunit β_5 of the $\alpha_v\beta_5$ integrin were as follows forward primer 5′-GGA AGT TCG GAA ACA GAG GGT-3′, reverse primer 5′-TGG AGT ACT GCA TCA AAG CCC-3′ and probe 6FAM-CCG GAA CCG AGA TGC CCC TGA-TAMRA, the sequences to amplify α_v integrin subunit were as follows: forward primer 5′-GCG GGA CCA TCT CAT CAC TAA-3′, reverse primer 5′-GAG CAA CTC CAC AAC CCA AAG-3′ and probe

6FAM-CCG GAA CCG AGA TGC CCC TGA-TAMRA[22].

Oligonucleotide sequences to amplify syndecan-1 were as follows forward primer 5′-AGG ACG AAG GCA GCT ACT CCT-3′, reverse primer 5′-TTT GGT GGG CTT CTG GTA GG-3′ and probe 6FAM-AGG AGC CGA AAC AAG CCA ACG GC-TAMRA, glypican-1 were as follows forward primer 5′-GTC TCT GAA GCC AGG CCC-3′, reverse primer 5′-GCG GTC ATC ACT GGC AGT G-3′ and probe 6FAM-CCG CGA CGT CCA GGA CTT CTG G-TAMRA.

The human housekeeping gene glyceraldehyde-3-phosphate dehydrogenase (GAPDH) was used as an internal control. The sequences to amplify the GAPDH gene were: forward primer 5′-GGT TTA CAT GTT CCA ATA TGA TTC CA-3′, reverse primer 5′-ATG GGA TTT CCA TTG ATG ACA AG-3′ and probe 6FAM-CGT TCT CGC CTT GAC GGT GCC AT-TAMRA.

With optimized concentration of primers and probe, the components of real-time PCR mixtures were designed to result in a master mix with a final volume of 9 μL per reaction containing 1X TaqMan® EZ RT-PCT kit (Applied Biosystems), 100 nM forward primer, 100 nM reverse primer, 100 nM probe, and 0.025% bovine serum albumin. One microliter of total RNA sample was added to 9 μL of PCR mixture in each reaction capillary. A no template control received 1 μL of water. All capillaries were then sealed and centrifuged using an LC Carousel centrifuge (Roche Molecular Biochemicals, Indianapolis, IN) to facilitate mixing. All PCR reactions were carried out using a LightCycler™ system (Roche Molecular Biochemicals). Thermal cycling conditions were subjected to 2 minutes at 50 °C, 30 minutes at 60 °C, 5 minutes at 95 °C and 40 cycles of 20 seconds at 94 °C, and 1 minute at 60 °C. Data were analyzed with LightCycler software.

Viral preparations

Ad5, Ad5/3, Ad5CK-1, Ad5CK-2 (Figure 1) are replication-defective Ads containing a luciferase reporter gene driven by the cytomegalovirus (CMV) promoter in the E1 region and have been described previously.[16,23,24] Ad5.RGD, Ad5.pK7, and Ad5.RGD.pK7 are replication-defective Ads containing a luciferase reporter gene and a green fluorescent protein (GFP) and driven by the CMV promoter in the E1 region as described previously[12,13,17,25] and were compared with their isogenic control Ad5. The viruses are all isogenic and were propagated on 293 cells and purified by double CsCl density centrifugation. Of note, the firefly luciferase gene incorporated into Ad5CK-1, Ad5CK-2, and Ad5/3 contains the wild-type sequence. The firefly luciferase gene incorporated into Ad5.RGD, Ad5.pK7, and Ad5.RGD.pK7 contains a modified coding region for firefly luciferase (pGL3; Promega, Madison, WI) that has been optimized for monitoring transcriptional activity in transfected eukaryotic cells.

Physical viral particle (VP) concentration (VP/mL) was determined by OD_{260} reading. All experiments were based on VP numbers, although plaque assays were performed to ensure sufficient quality of each virus preparation. We performed crystal violet viability assays[26] on fibroblasts and keratinocytes using our adenoviral constructs before performing the lysis and luciferase assays. However, no cell toxicity was observed at the multiplicity of infection (MOI) used in these experiments at 10 and 100 VP/cell, and was only detected at concentrations greater than 1,000 VP/cell (data not shown).

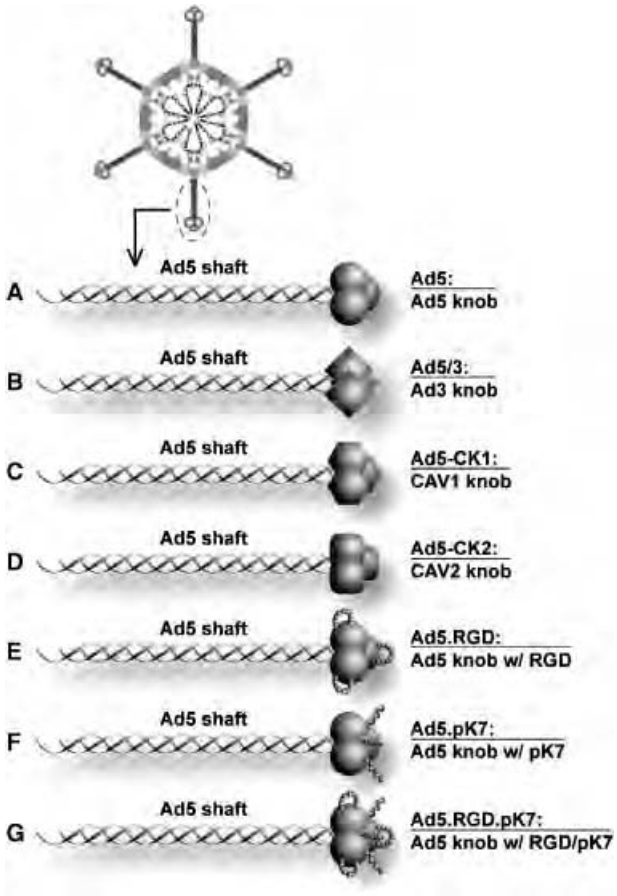

Figure 1. Diagram of the fiber structure of Ad5 vectors used in this study. (A) The knob of Ad5 was substituted (B) by that of Ad3 (Ad5/3), (C) by that of canine adenovirus serotype 1 (Ad5-CK1), or (D) that of canine adenovirus serotype 2 (Ad5-CK1). (E) The RGD motif (CDCRGDCFC) was incorporated into the HI loop (Ad5.RGD), or (F) the pK7 motif (GSGSGSGSGSKKKKKK) was incorporated at the C-terminus of the fiber (AD5.pK7). (G) The mosaic Ad incorporates both the RGD motif and the pK7 motif (Ad5.RGD.pK7).

To facilitate comparison of the different vectors, we normalized luciferase activity to relative fold induction compared with the Ad5 counterpart. Thus, to directly compare each of the infectivity-enhanced vectors, luciferase activity of cells infected with Ad5CK-1, Ad5CK-2, and Ad5/3 were normalized to fold activity of cells infected with the isogenic control Ad5Luc1. The ratios of VP:infectious particles were very close, at 4.8, 5.0, 4.2, and 3.9, respectively, for Ad5Luc1, Ad5CK-1, Ad5CK-2, and Ad5/3Luc1.

Likewise, to directly compare each of the infectivity enhanced vectors, luciferase activity of cells infected with

Ad5.RGD, Ad5.pK7, and Ad5.RGD.pK7 were normalized to fold activity of cells infected with the isogenic control Ad5.GL3. The ratios of VP:infectious particles were very close at 40, 52.2, 45.8, and 51.5, respectively, for Ad5.GL, Ad5.RGD, Ad5.pK7, and Ad5.RGD.pK7.

In vitro gene-transfer assays of cells

Cell lines were plated on day 1 at 30,000 cells/well on 24-well plates in 1 mL of 10% GM. On day 2, cells were infected with recombinant Ads at MOI of 10 and 100 for 2 hours in 200 μL of 2% GM on a rocker. Afterward, cells were washed once with 1 mL of phosphate buffered saline solution (PBS), and 1 mL of 10% GM was added per well. After 24 hours, the GM was removed; cells were washed once with PBS, lysed with 200 μL of lysis buffer (Reporter Lysis Buffer; Promega) and freeze-thawed three times. Twenty microliters of these samples were mixed with 100 μL of luciferase assay reagent (Promega) and measured with a Berthold (Wildbad, Germany) Lumat LB 9501. Standardization was accomplished by setting values obtained with Ad5 as 100% for each cell line and primary cells of the skin of each patient.

Visualization of gene transfer via fluorescent microscopy

Cells infected with Ad5.RGD, Ad5.pK7, and Ad5.RGD.pK7 were cultured submerged in two- or four-well Lab-Tek® glass chamber slides (Nunc International, Naperville, IL) for 24 hours, washed in PBS and fixed in 4% paraformaldehyde in PBS as per the standard protocol. Fixed slides were mounted with Vectashield® mounting medium containing DAPI (4′,6′-diamidino-2-phenylindole; Vector Laboratories Inc, Burlingame, CA). GFP expression and DAPI staining was analyzed at ×20 objective magnification using an Olympus Provis AX70 fluorescence microscope (Tokyo, Japan) using fluorescein isothiocyanate and DAPI filters. Images were digitally recorded with Axiocam charge-coupled device digital camera (Carl Zeiss, Oberkochen, Germany) using Axiovision image capture software. Images were processed using Photoshop 6.0 software (Adobe Systems, San Jose, CA). The fraction of GFP-positive cells was determined by counting DAPI-positive nuclear signals and GFP-positive cells in five randomly selected high-powered fields (0.031 mm^2 each) microscopic fields.

Statistics

Data are presented as mean values ± standard deviation. Statistical differences among groups were assessed with a two-tailed Student's *t*-test. $p(*)<0.05$ was considered significant.

RESULTS

Gene delivery efficiency of the fiber-modified nonreplicative adenoviruses (Figure 1) was evaluated in two established human keratinocyte cell lines, one adult and one neonatal (NHEK, NHEK neo). Cells were infected with Ad5/3, Ad5CK-1, Ad5-CK2, Ad5.RGD, Ad5.pK7, and Ad5.RGD.pK7 at MOI=10 and 100 (Figure 2). These vectors include serotype knob switching of the Ad5 knob with that of Ad3, "xeno" knob switching of the Ad5 knob with that of canine adenovirus serotype 1 and 2, RGD peptide incorporation into the HI loop of the fiber knob domain, and incorporation of the pK7 motif at the C-terminus of the fiber. The mosaic Ad5.RGD.pK7 incorporates both the RGD motif and the pK7 motif. Infectivity enhancement was assessed by measuring the fold induction of transgene expression compared to an unmodified isogenic Ad5-based vector. Ad5-CK1 and Ad5-CK2 did

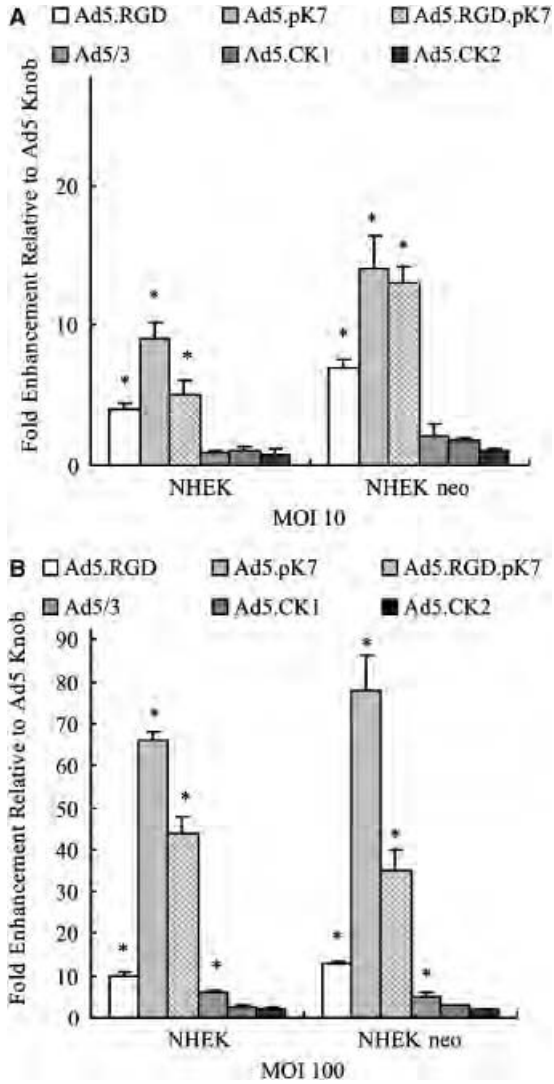

Figure 2. Evaluation of fiber modified vectors for targeting keratinocyte cell lines. Established keratinocyte cell lines (normal human epithelial keratinocytes [NHEK], normal human epithelial keratinocytes-neonatal NHEK-neo) were infected with Ad5, Ad5/3, Ad5CK-1, Ad5CK-2, Ad5.RGD, Ad5.pK7, or Ad5.RGD.pK7 at MOI=10 or 100. Luciferase activity was measured after 24 hours and is expressed as relative light units (RLU) normalized for total protein concentration. Each bar represents the mean of six experiments ± SD. *$p<0.05$ vs. Ad5.

not significantly increase gene transfer rates compared to Ad5 ($p > 0.05$). Although Ad5/3 did not show a significant increase of infectivity at MOI of 10 (Figure 2A), significant infectivity enhancement could be shown at a MOI of 100 (Figure 2B). In contrast, Ad5.RGD, Ad5.pK7 and Ad5.RGD.pK7 displayed a statistically significant increased gene transfer compared with Ad5 at both MOIs ($p < 0.05$). In the aggregate, of all vectors tested Ad5.pK7 showed the highest enhancement in infectivity in both keratinocyte cell lines (66- to 78-fold higher compared with Ad5 at MOI 100; $p < 0.05$).

Transduction efficiency of primary human keratinocytes by Ads in vitro

Cell lines passaged in vitro for years may not reflect the biology of cells in vivo, making the applicability of preclinical results to the clinical situation unclear. To more closely model the condition of human keratinocytes found in vivo, gene transfer experiments were performed using human primary keratinocytes that were obtained from five patients (Figure 3). Infection with Ad5-CK1 and Ad5-CK2 resulted in similar transgene expression compared with unmodified Ad5. Ad5/3, Ad5.RGD, Ad5.pK7, and Ad5.RGD.pK7 significantly enhanced transduction of primary keratinocytes ($p < 0.05$ at MOI 10 and 100). Thus, in concordance with the results obtained in keratinocyte cell lines above, Ad5.pK7 showed the highest increase in transgene expression of primary keratinocytes (67- to 134-fold higher in comparison with Ad5 at MOI=100).

Transduction efficiency of human fibroblast cell lines by Ads in vitro

Fibroblasts are a second major target for gene therapy in wounds. Therefore, four established human fibroblast cell lines were infected to evaluate the gene-delivery efficiency of the fiber-modified vectors (Ad5/3, Ad5CK-1, Ad5CK-2, Ad5.RGD, Ad5.pK7, and Ad5.RGD.pK7). As shown in Figure 4, cells were infected with viruses at MOI=10 and 100, and infectivity enhancement was assessed by measuring the fold induction of transgene expression compared with unmodified Ad5-based vector. In the aggregate, among all the vectors tested Ad5.RGD, Ad5.pK7, and Ad5.RGD.pK7 significantly increased ($p<0.05$) gene transfer levels compared with the Ad5 vector. In the aggregate, among all the vectors tested, Ad5.RGD.pK7 showed the highest infectivity rates of all the viruses tested, with 71- to 123-fold higher luciferase activity compared with Ad5 at MOI=100.

Transduction efficiency of primary human fibroblasts by Ads vectors

To more closely model the condition of human fibroblasts in vivo, gene transfer experiments were performed using human primary fibroblasts obtained from human skin and infected with our panel of fiber-modified vectors (Figure 5). In primary human fibroblasts, all fiber-modified vectors displayed a significant increase in infectivity in comparison with the unmodified vector Ad5. However, the

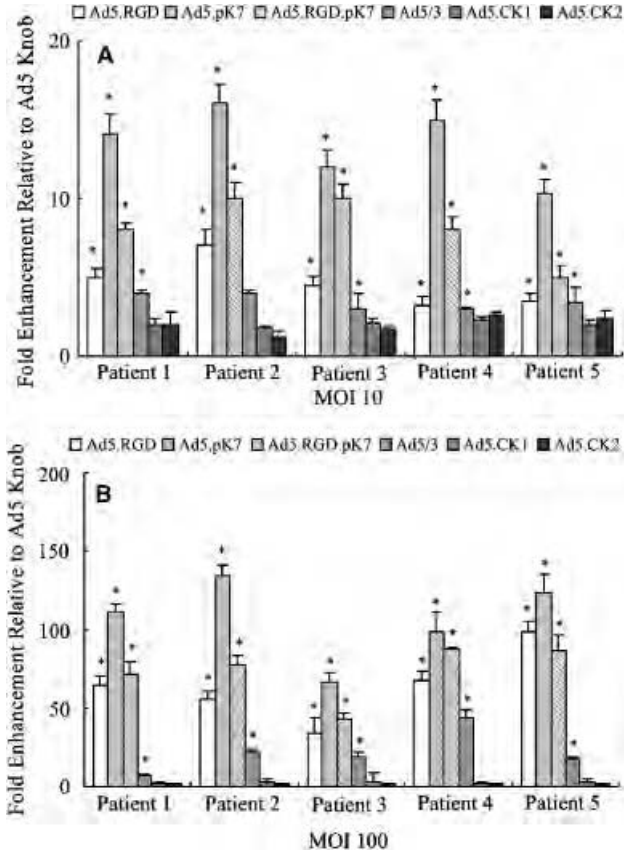

Figure 3. Targeted transduction of primary human keratinocytes. Unpassaged human primary keratinocytes cells obtained from skin explants from five patients were infected with Ad5, Ad5/3, Ad5CK-1, Ad5CK-2, Ad5.RGD, Ad5.pK7, or Ad5.RGD.pK7 at MOI=10 or 100. Luciferase activity was measured after 24 hours and is expressed as relative light units (RLU) normalized for total protein concentration. Each bar represents the mean of six experiments ± SD. *$p<0.05$ vs. Ad5.

transduction efficiency among the vectors tested was highest with Ad5RGD.pK7 in all fibroblast samples with 199- to 537-fold higher luciferase expression compared with the unmodified Ad5 vector at MOI=100.

Expression of CAR, CD80, CD86, CD46, integrin subunit α_v, β3, β5, glypican-1, and syndecan-1 in primary keratinocytes and fibroblasts

Quantitative real-time PCR was performed to evaluate the correlation between the transductional efficiency of the fiber-modified adenoviral vectors and the expression levels of their putative receptors[27,28] in primary keratinocytes (Figure 6A). All receptor mRNA levels were normalized for expression using expression of the housekeeping gene GAPDH. The mRNA expression levels of the integrin subunits (receptor-ligands of Ad5.RGD, Ad5.RGD.pK7), glypican-1 and syndecan-1 (members of heparin sulfate proteoglycans, receptors for Ad5.pK7 and Ad5.RGD.pK7) were significantly higher than the expression

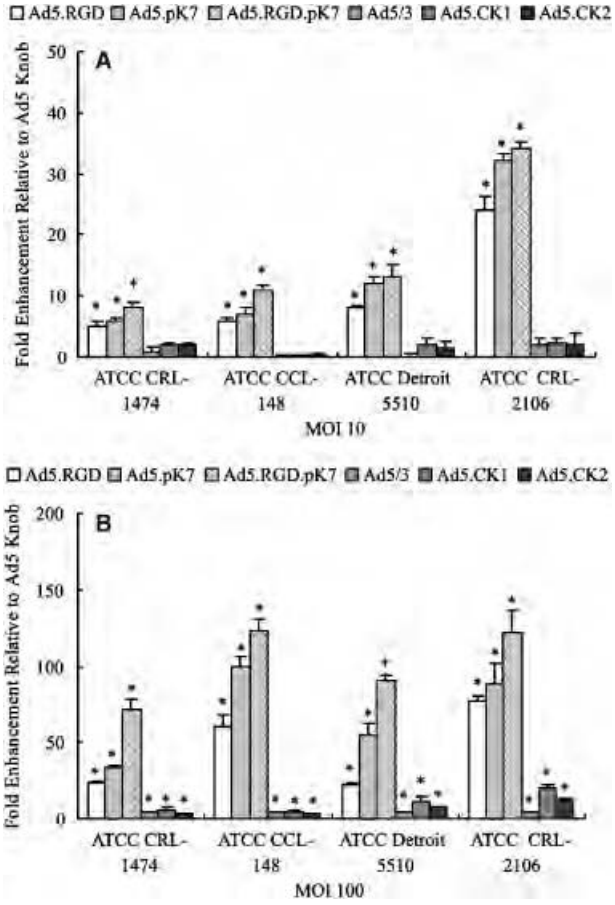

Figure 4. Evaluation of fiber-modified vectors for targeting fibroblast cell lines. Established fibroblast cell lines (CRL-1474, CCL-148, Detroit 5510 and CRL-2106) were infected with Ad5, Ad5/3, Ad5CK-1, Ad5CK-2, Ad5.RGD, Ad5.pK7, or Ad5.RGD.pK7 at MOI=10 or 100. Luciferase activity was measured after 24 hours and is expressed as relative light units (RLU) normalized for total protein concentration. Each bar represents the mean of six experiments ± SD. *$p<0.05$ vs. Ad5.

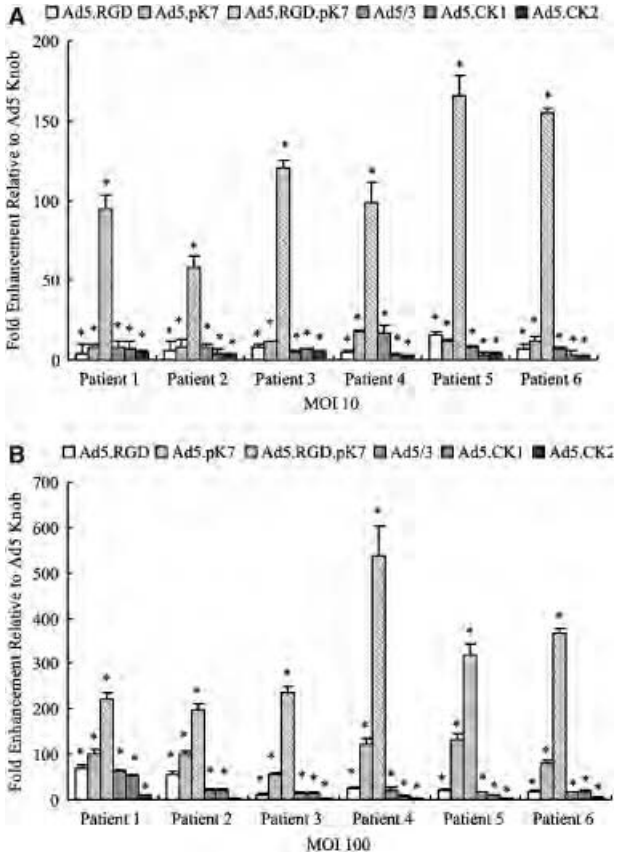

Figure 5. Targeted transduction of primary human fibroblasts. Unpassaged human primary fibroblasts cells obtained from skin explants from six patients were infected with Ad5, Ad5/3, Ad5-CK-1, Ad5CK-2, Ad5.RGD, Ad5.pK7, or Ad5.RGD.pK7 at multiplicity of infection=10 or 100. Luciferase activity was measured after 24 hours and is expressed as relative light units (RLU) normalized for total protein concentration. Each bar represents the mean of six experiments ± SD. *$p<0.05$ vs. Ad5.

level of CAR (receptor for the unmodified Ad5 vector). Of note, among the putative receptors for Ad5/3 (CD80, CD86, and CD46) only the expression level for CD46 was significantly higher in comparison with CAR. However, syndecan-1 showed the highest expression level in comparison with all other receptors evaluated. These results in receptor expression levels are in concordance with the increased transduction of keratinocytes by Ad5.pK7 compared with the unmodified Ad5.

Next, we evaluated the expression levels of the putative receptors of the fiber-modified vectors in primary fibroblasts (Figure 6B). The mRNA expression levels of the integrin subunits (receptors for Ad5.RGD, Ad5.RGD.pK7), glypican-1 and syndecan-1 (members of the two major gene families of membrane bound heparin sulfate proteoglycans, receptors for Ad5.pK7 and Ad5.RGD.pK7) were significantly higher than the expression level of CAR. Of the putative receptors for Ad5/3 only CD46 was significantly increased. However, among all receptors tested the integrin subunit α_v and syndecan-1 displayed the highest expression levels.

Visualization of enhanced gene transfer of GFP by Ad5.RGD, Ad5.pK7, and Ad5.RGD.pK7 in primary keratinocytes and fibroblasts

Finally, we examined transductional efficiency by visualizing and quantifying the gene transfer of the GFP using the fiber-modified Ad5.RGD, Ad5.pK7, and Ad5.RGD.pK7 in keratinocytes (Figure 7A) and in fibroblasts (Figure 7B) vs. the unmodified Ad5 vector by fluorescent microscopy in chamber slides. In this analysis, the fraction (%) of GFP^+ keratinocytes was 10, 55, and 20 after infection with Ad5.RGD, Ad5.pK7, and Ad5.RGD.pK7, respectively. Likewise, the fraction (%) of GFP^+ fibroblasts was 5, 15, and 45 after infection with Ad5.RGD, Ad5.pK7, and Ad5.RGD.pK7. Thus, the superior transduction efficiency of Ad5.pK7 in keratinocytes and Ad5.RGD.pK7 in

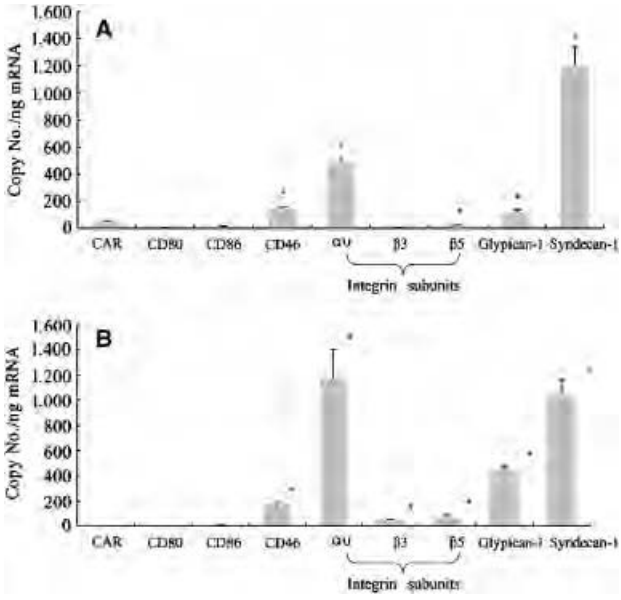

Figure 6. Determination of CAR, CD80, CD86, CD46, integrin subunits α_v, β3, β5, glypican-1 and syndecan-1 in primary keratinocyte and fibroblast mRNA levels. Real-time PCR analysis was performed to quantify the expression of the putative receptors of Ad5 (CAR), Ad5/3 (CD80, CD86, CD46), Ad5.RGD (integrin subunits α_v, β3, β5), Ad5.pK7 (glypican-1 and syndecan-1) in (A) primary keratinocytes from five patients (same patients as in Figure 3) and (B) primary fibroblasts from six patients (same patients as in Figure 5). For each patient, real-time PCR analysis was performed in triplicates. Gene copy numbers are normalized by the GAPDH copy number. Each bar represents the mean copy number per nanogram mRNA of (A) five patients and (B) six patients ± SD. $*p < 0.05$ vs. CAR.

fibroblasts was further confirmed by the higher number of cells being infected by these vectors in comparison with Ad5.

DISCUSSION

Dermal wounds are attractive targets for gene transfer because of their accessibility for manipulation and inspection, as well as the self-renewing capacity of the epidermis.[29–31] Gene transfer vectors based on recombinant adenoviruses have gained increasing attention for use in addressing wounds as a potential target site.[32–34] However, overall efficacy of adenoviral based gene therapy in cells resident within wounds, such as keratinocytes and fibroblasts, may remain limited by suboptimal vector efficiency. Indeed, the limitation in adenoviral gene transfer has been recently understood to result from a deficiency of the primary adenoviral cellular receptor CAR in fibroblasts[35] and keratinocytes.[36] Thus, it is clear that augmenting the gene transfer efficiency of Ads of fibroblasts and keratinocytes is of fundamental importance with respect to deriving their full benefit in the context of adenoviral-based wound gene therapy. To circumvent disadvantageous CAR-dependence of Ad5 based vectors for gene therapy, our group previously developed genetically modified Ads with CAR-independent tropism.[13,16,17,23,25]

In the present study, we explored the possibility of achieving higher transduction in primary fibroblasts and keratinocytes using this repertoire of fiber-modified vectors. These strategies include incorporation of an RGD4C peptide into the HI loop of the fiber knob domain[13] (Ad5.RGD), to redirect Ad binding to cellular integrins $\alpha_v\beta_3$ and $\alpha_v\beta_5$,[13] incorporation of a positively charged polylysine pK7 motif at the C-terminus of the fiber (Ad5.pK7) to redirect binding to heparan sulfate proteoglycans,[12] a double modification of the fiber with both RGD and pK7 motifs (Ad5.RGD.pK7), serotype knob switching of the Ad5knob with that of Ad3 (Ad5/3)[14] to redirect binding to the putative Ad3 receptors CD80, CD86, or CD46[37,38] and "xeno" knob switching of the A5knob with that of canine adenovirus serotype 1 (Ad5-CK1)[23] and 2 (Ad5-CK2),[16] for which the receptors have not been identified yet, but is thought to be different from CAR. These transductionally modified vectors have been shown to increase gene-transfer efficiency in various selected contexts.[16,26,28]

To evaluate the use of these transductional targeting strategies, we first analyzed gene transfer efficiency in established fibroblast and keratinocyte cell lines. Of all the tested modified vectors, Ad5.pK7 exhibited the highest transductional enhancement in keratinocyte cell lines and Ad5.RGD.pK7 in fibroblast cell lines. These types of cell lines are often used as the standard test system for adenoviral based gene therapy, but often lose essential cell surface proteins and gain gene mutations when grown in culture. In this regard, the adenoviral receptor proteins such as CAR and heparin sulfate glycosamininoglycan expression were previously shown to differ upon culturing the same cell line under various conditions.[39–41] Therefore, we next used primary cultures of keratinocytes and fibroblasts. This approach represents a more stringent model for reliable clinical evaluation of efficacy and could help avoid confounding variability, due to genotypic and phenotypic changes involved in the clonal selection process.

In primary keratinocytes, Ad5.pK7, Ad5.RGD, and Ad5.pK7.RGD showed significantly increased transductional efficiency of all fiber-modified vectors tested, with the highest values for Ad5.pK7, corresponding to the results obtained using the keratinocyte cell lines. Ad5.pK7 targets to heparan sulfate proteoglycans via positively charged pK7 motifs.[12] In this regard, cell surface heparan sulfate proteoglycans are mostly members of two major gene families of membrane-bound proteoglycans, the syndecans and glypicans.[42,43] Syndecans and glypicans bind proteins of the extracellular environment via their heparin sulfate chains, regulating a wide spectrum of biological activities, including cell proliferation and differentiation, morphogenesis, wound repair and host defense. To evaluate whether the observed significantly increased transduction efficiencies of Ad5.RGD, Ad5.RGD.pK7 and, importantly, Ad5.pk7 correlated with the expression of their putative receptors on keratinocytes, we analyzed the mRNA expression levels of CAR, α_v integrins, syndecan-1, and glypican-1 on primary keratinocytes using quantitative PCR. Indeed, mRNA expression of heparan sulfate proteoglycans and α_v integrins was significantly higher than CAR, correlating with the results of the gene transfer. In

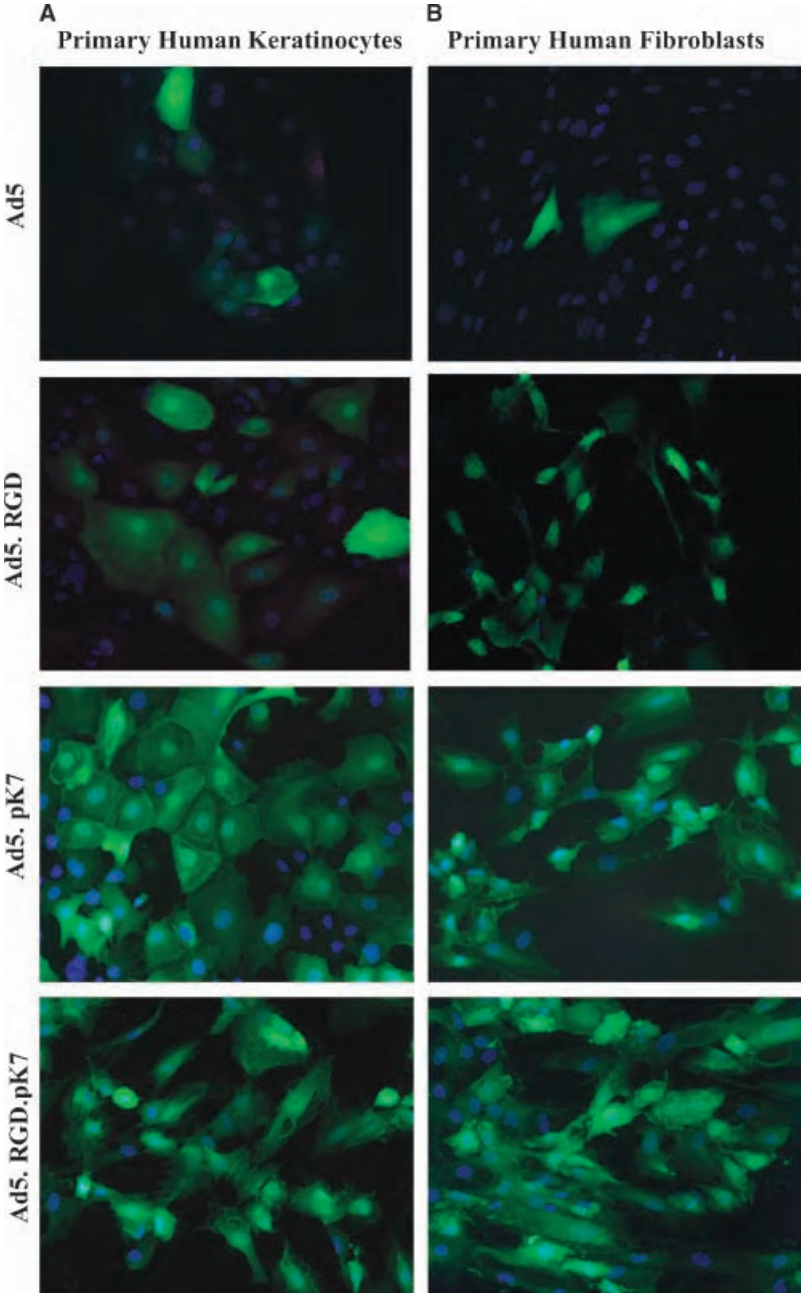

Figure 7. Visualization of enhanced gene transfer by fiber-modified adenoviral vectors via fluorescent microscopy. (A) Primary keratinocytes and (B) fibroblasts were infected with the unmodified vector Ad5 and the fiber-modified vectors Ad5.RGD, Ad5.pK7, and Ad5.RGD.pK7 containing GFP driven by the CMV promoter in the E1 region. Infected cells were cultured submerged in 2 or 4 well Lab-Tek® glass chamber slides for 24 hours, washed in PBS and fixed in 4% paraformaldehyde in PBS. GFP expression (green, indicating the reporter gene) and DAPI staining (blue, indicating the nuclei) was analyzed at ×20 objective magnification.

addition, these results suggest that the high levels of heparan sulfate expression by keratinocytes are rather due to syndecan-1 than to glypican-1.[42,44] Importantly, syndecan-1 expression was significantly higher than CAR and all the other putative receptors tested on keratinocytes, and thus correlated with the high transduction efficiency of Ad5.pK7. Of note, syndecan-1 expression is increased during epithelial differentiation and wound healing, underlining the utility of Ad5.pK7 for targeting in gene therapy of wounds.[42,45]

In primary fibroblasts, Ad5.RGD, Ad5pK7 and Ad5.RGD.pK7 displayed significantly enhanced infectivity among the various vectors evaluated in this study, with Ad5.RGD.pK7, the double modified adenovirus containing an RGD motif in the HI loop and a pK7 motif at the C-terminus of the fiber, revealing the highest efficacy. This suggests that the RGD and pK7 motif may act additively to mediate Ad5.RGD.pK7 infection in fibroblasts. The additive effect of the double-modified Ad5.RGD.pK7 vector has been described in selected contexts.[25,28,46] When we compared the two single-modified vectors, Ad5.pK7 resulted in comparable high gene transfer efficacy than Ad5.RGD.[35] To evaluate whether observed transduction efficiencies of the vectors achieving the highest infectivity enhancement in

fibroblasts (Ad5.RGD, Ad5.pK7, and Ad5.RGD.pK7) correlated with the expression of their putative receptors, we analyzed the mRNA expression levels of CAR, α_v integrins, syndecan-1 and glypican-1 on primary fibroblasts using quantitative PCR. Importantly, mRNA expression of α_v integrins, syndecan-1, and glypican-1 was significantly higher than CAR correlating the results of the gene transfer by the fiber-modified vectors to fibroblasts.[10,11,47]

At this point, it is clear that the complete characterization of the putative receptors for fiber-modified adenoviruses is still under investigation. For example, receptor identity for Ad serotype 3 remains disputed. Short et al.[37] showed that Ad3 utilizes CD80 (B7.1) and CD86 (B7.2) as cellular attachment receptors; however, Sirena et al. [38] demonstrated that Ad3 can use CD46 as a receptor. We have demonstrated differences in receptor expression compared to CAR, based on quantitative real-time PCR analysis. Whether or not these differences in RNA levels correlate to receptor levels depends on efficiency of translation, receptor stability, and cell surface exposure. Future studies are in progress to further characterize the putative receptors for fiber-modified adenoviruses.

Finally, the superior transduction efficiency of Ad5.pK7 in keratinocytes and Ad5.RGD.pK7 in fibroblasts assessed by luciferase assay was confirmed by gene transfer of GFP and visualization via fluorescent microscopy. This result underlines that the enhanced transduction of these fiber-modified vectors is due to increased number of cells being infected and not due to the increased luciferase expression per cell.

In conclusion, significant infectivity enhancement could be achieved in primary keratinocytes by the Ad5.pK7 vector and in primary fibroblasts by the Ad5.RGD.pK7. Future studies will be necessary to determine if the enhanced transduction of fibroblasts by Ad5.RGD.pK7 is additive or synergistic compared with Ad5.RGD or Ad5.pK7. This study is the first to provide a systemic evaluation and comparison of CAR-independent Ad transduction strategies in keratinocytes and fibroblasts. These data establish the foundation for rational development of infectivity enhanced Ad-based wound gene therapy and may help to achieve higher clinical efficacy of wound gene therapy in the future.

ACKNOWLEDGMENTS

We thank Minghui Wang for his kind technical support. This work was supported by a Grant of the Deutsche Forschungsgemeinschaft Sto 647/1-1 (M. A. Stoff-Khalili); Department of Defense W81XWH-05-1-0035 and National Institutes of Health RO1CA083821 (D. T. Curiel).

REFERENCES

1. Tepper OM, Mehrara BJ. Gene therapy in plastic surgery. *Plast Reconstr Surg* 2002; 109: 716–34.
2. Hoeller D, Petrie N, Yao F, Eriksson E. Gene therapy in soft tissue reconstruction. *Cells Tissues Organs* 2002; 172: 118–25.
3. Roman S, Lindeman R, O'Toole G, Poole MD. Gene therapy in plastic and reconstructive surgery. *Curr Gene Ther* 2005; 5: 81–99.
4. Liu W, Chua C, Wu X, Wang D, Ying D, Cui L, Cao Y. Inhibiting scar formation in rat wounds by adenovirus-mediated overexpression of truncated TGF-beta receptor II. *Plast Reconstr Surg* 2005; 115: 860–7.
5. Sumiyoshi K, Nakao A, Setoguchi Y, Okumura K, Ogawa H. Exogenous Smad3 accelerates wound healing in a rabbit dermal ulcer model. *J Invest Dermatol* 2004; 123: 229–36.
6. Romano Di Peppe S, Mangoni A, Zambruno G, Spinetti G, Melillo G, Napolitano M, Capogrossi MC. Adenovirus-mediated VEGF(165) gene transfer enhances wound healing by promoting angiogenesis in CD1 diabetic mice. *Gene Ther* 2002; 9: 1271–7.
7. Vranckx JJ, Yao F, Petrie N, Augustinova H, Hoeller D, Visovatti S, Slama J, Eriksson E. In vivo gene delivery of Ad-VEGF121 to full-thickness wounds in aged pigs results in high levels of VEGF expression but not in accelerated healing. *Wound Rep Reg* 2005; 13: 51–60.
8. Chandler LA, Doukas J, Gonzalez AM, Hoganson DK, Gu DL, Ma C, Nesbit M, Crombleholme TM, Herlyn M, Sosnowski BA, Pierce GF. FGF2-Targeted adenovirus encoding platelet-derived growth factor-B enhances de novo tissue formation. *Mol Ther* 2000; 2: 153–60.
9. Panetti TS, Wilcox SA, Horzempa C, McKeown-Longo PJ. Alpha v beta 5 integrin receptor-mediated endocytosis of vitronectin is protein kinase C-dependent. *J Biol Chem* 1995; 270: 18593–7.
10. Gailit J, Clark RA. Studies in vitro on the role of alpha v and beta 1 integrins in the adhesion of human dermal fibroblasts to provisional matrix proteins fibronectin, vitronectin, and fibrinogen. *J Invest Dermatol* 1996; 106: 102–8.
11. Gailit J, Clarke C, Newman D, Tonnesen MG, Mosesson MW, Clark RA. Human fibroblasts bind directly to fibrinogen at RGD sites through integrin alpha(v)beta3. *Exp Cell Res* 1997; 232: 118–26.
12. Wickham TJ, Roelvink PW, Brough DE, Kovesdi I. Adenovirus targeted to heparan-containing receptors increases its gene delivery efficiency to multiple cell types. *Nat Biotechnol* 1996; 14: 1570–3.
13. Dmitriev I, Krasnykh V, Miller CR, Wang M, Kashentseva E, Mikheeva G, Belousova N, Curiel DT. An adenovirus vector with genetically modified fibers demonstrates expanded tropism via utilization of a coxsackievirus and adenovirus receptor-independent cell entry mechanism. *J Virol* 1998; 72: 9706–13.
14. Krasnykh VN, Mikheeva GV, Douglas JT, Curiel DT. Generation of recombinant adenovirus vectors with modified fibers for altering viral tropism. *J Virol* 1996; 70: 6839–46.
15. Stoff-Khalili MA, Rivera AA, Glasgow JN, Le PL, Stoff A, Everts M, Tsuruta Y, Kawakami Y, Bauerschmitz GJ, Siegal GP, Mathis M, Pereboeva L, Dall P, Curiel DT. A human adenoviral vector with a chimeric fiber from canine adenovirus type 1 results in novel expanded tropism for cancer gene therapy. *Gene Ther* 2005; 12: 1696–706.
16. Glasgow JN, Kremer EJ, Hemminki A, Siegal GP, Douglas JT, Curiel DT. An adenovirus vector with a chimeric fiber derived from canine adenovirus type 2 displays novel tropism. *Virology* 2004; 324: 103–16.
17. Kanerva A, Wang M, Bauerschmitz GJ, Lam JT, Desmond RA, Bhoola SM, Barnes MN, Alvarez RD, Siegal GP, Curiel DT, Hemminki A. Gene transfer to ovarian cancer versus normal tissues with fiber-modified adenoviruses. *Mol Ther* 2002; 5: 695–704.

18. Wu H, Han T, Lam JT, Leath CA, Dmitriev I, Kashentseva E, Barnes MN, Alvarez RD, Curiel DT. Preclinical evaluation of a class of infectivity-enhanced adenoviral vectors in ovarian cancer gene therapy. *Gene Ther* 2004; 11: 874–8.
19. Stark HJ, Baur M, Breitkreutz D, Mirancea N, Fusenig NE. Organotypic keratinocyte cocultures in defined medium with regular epidermal morphogenesis and differentiation. *J Invest Dermatol* 1999; 112: 681–9.
20. Satish L, Babu M, Tran KT, Hebda PA, Wells A. Keloid fibroblast responsiveness to epidermal growth factor and activation of downstream intracellular signaling pathways. *Wound Rep Reg* 2004; 12: 183–92.
21. Banerjee NS, Rivera AA, Wang M, Chow LT, Broker TR, Curiel DT, Nettelbeck DM. Analyses of melanoma-targeted oncolytic adenoviruses with tyrosinase enhancer/promoter-driven E1A, E4, or both in submerged cells and organotypic cultures. *Mol Cancer Ther* 2004; 3: 437–49.
22. Zhou X, Murphy FR, Gehdu N, Zhang J, Iredale JP, Benyon RC. Engagement of alphavbeta3 integrin regulates proliferation and apoptosis of hepatic stellate cells. *J Biol Chem* 2004; 279: 23996–400.
23. Stoff-Khalili MA, Rivera AA, Glasgow JN, Le LP, Stoff A, Everts M, Tsuruta Y, Kawakami Y, Bauerschmitz GJ, Mathis JM, Pereboeva L, Seigal GP, Dall P, Curiel DT. A human adenoviral vector with a chimeric fiber from canine adenovirus type 1 results in novel expanded tropism for cancer gene therapy. *Gene Ther* 2005; 12: 1696–706.
24. Kanerva A, Mikheeva GV, Krasnykh V, Coolidge CJ, Lam JT, Mahasreshti PJ, Barker SD, Straughn M, Barnes MN, Alvarez RD, Hemminki A, Curiel DT. Targeting adenovirus to the serotype 3 receptor increases gene transfer efficiency to ovarian cancer cells. *Clin Cancer Res* 2002; 8: 275–80.
25. Wu H, Seki T, Dmitriev I, Uil T, Kashentseva E, Han T, Curiel DT. Double modification of adenovirus fiber with RGD and polylysine motifs improves coxsackievirus-adenovirus receptor-independent gene transfer efficiency. *Hum Gene Ther* 2002; 13: 1647–53.
26. Kanerva A, Zinn KR, Chaudhuri TR, Lam JT, Suzuki K, Uil TG, Hakkarainen T, Bauerschmitz GJ, Wang M, Liu B, Cao Z, Alvarez RD, Curiel DT, Hemminki A. Enhanced therapeutic efficacy for ovarian cancer with a serotype 3 receptor-targeted oncolytic adenovirus. *Mol Ther* 2003; 8: 449–58.
27. Stoff-Khalili MA, Stoff A, Rivera AA, Mathis JM, Everts M, Wang M, Kawakami Y, Waehler R, Mathews QL, Yamamoto M, Rocconi RP, Siegal GP, Richter DF, Dall P, Zhu ZB, Curiel DT. Gene transfer to carcinoma of the breast with fiber-modified adenoviral vectors in a tissue slice model system. *Cancer Biol Ther* 2005; 4: 1203–10.
28. Rein DT, Breidenbach M, Wu H, Han T, Haviv YS, Wang M, Kirby TO, Kawakami Y, Dall P, Alvarez RD, Curiel DT. Gene transfer to cervical cancer with fiber-modified adenoviruses. *Int J Cancer* 2004; 111: 698–704.
29. Eriksson E, Velander P. Gene transfer in wound healing. *Br J Surg* 2004; 91: 1093–4.
30. Petrie NC, Yao F, Eriksson E. Gene therapy in wound healing. *Surg Clin North Am* 2003; 83: 597–616, vii.
31. Andree C, Voigt M, Wenger A, Erichsen T, Bittner K, Schaefer D, Walgenbach KJ, Borges J, Horch RE, Eriksson E, Stark GB. Plasmid gene delivery to human keratinocytes through a fibrin-mediated transfection system. *Tissue Eng* 2001; 7: 757–66.
32. Keswani SG, Katz AB, Lim FY, Zoltick P, Radu A, Alaee D, Herlyn M, Crombleholme TM. Adenoviral mediated gene transfer of PDGF-B enhances wound healing in type I and type II diabetic wounds. *Wound Rep Reg* 2004; 12: 497–504.
33. Crombleholme TM. Adenoviral-mediated gene transfer in wound healing. *Wound Rep Reg* 2000; 8: 460–72.
34. Sylvester KG, Nesbit M, Radu A, Herlyn M, Adzick NS, Crombleholme TM. Adenoviral-mediated gene transfer in wound healing: acute inflammatory response in human skin in the SCID mouse model. *Wound Rep Reg* 2000; 8: 36–44.
35. Hidaka C, Milano E, Leopold PL, Bergelson JM, Hackett NR, Finberg RW, Wickham TJ, Kovesdi I, Roelvink P, Crystal RG. CAR-dependent and CAR-independent pathways of adenovirus vector-mediated gene transfer and expression in human fibroblasts. *J Clin Invest* 1999; 103: 579–87.
36. Huber M, Limat A, Wagner E, Hohl D. Efficient in vitro transfection of human keratinocytes with an adenovirus-enhanced receptor-mediated system. *J Invest Dermatol* 2000; 114: 661–6.
37. Short JJ, Pereboev AV, Kawakami Y, Vasu C, Holterman MJ, Curiel DT. Adenovirus serotype 3 utilizes CD80 (B7.1) and CD86 (B7.2) as cellular attachment receptors. *Virology* 2004; 322: 349–5.
38. Sirena D, Lilienfeld B, Eisenhut M, Kalin S, Boucke K, Beerli RR, Vogt L, Ruedl C, Bachmann MF, Greber UF, Hemmi S. The human membrane cofactor CD46 is a receptor for species B adenovirus serotype 3. *J Virol* 2004; 78: 4454–62.
39. Carson SD, Hobbs JT, Tracy SM, Chapman NM. Expression of the coxsackievirus and adenovirus receptor in cultured human umbilical vein endothelial cells: regulation in response to cell density. *J Virol* 1999; 73: 7077–9.
40. Spruck CH III, Gonzalez-Zulueta M, Shibata A, Simoneau AR, Lin MF, Gonzales F, Tsai YC, Jones PA. p16 gene in uncultured tumours. *Nature* 1994; 370: 183–4.
41. Dechecchi MC, Melotti P, Bonizzato A, Santacatterina M, Chilosi M, Cabrini G. Heparan sulfate glycosaminoglycans are receptors sufficient to mediate the initial binding of adenovirus types 2 and 5. *J Virol* 2001; 75: 8772–80.
42. Shafti-Keramat S, Handisurya A, Kriehuber E, Meneguzzi G, Slupetzky K, Kirnbauer R. Different heparan sulfate proteoglycans serve as cellular receptors for human papillomaviruses. *J Virol* 2003; 77: 13125–3.
43. Bernfield M, Gotte M, Park PW, Reizes O, Fitzgerald ML, Lincecum J, Zako M. Functions of cell surface heparan sulfate proteoglycans. *Annu Rev Biochem* 1999; 68: 729–77.
44. Oksala O, Salo T, Tammi R, Hakkinen L, Jalkanen M, Inki P, Larjava H. Expression of proteoglycans and hyaluronan during wound healing. *J Histochem Cytochem* 1995; 43: 125–3.
45. Marchisio PC, Trusolino L, De Luca M. Topography and biological role of integrins in human skin. *Microsc Res Tech* 1997; 38: 353–60.
46. Contreras JL, Wu H, Smyth CA, Eckstein CP, Young CJ, Seki T, Bilbao G, Curiel DT, Eckhoff DE. Double genetic modification of adenovirus fiber with RGD polylysine motifs significantly enhances gene transfer to isolated human pancreatic islets. *Transplantation* 2003; 76: 252–61.
47. Elenius K, Jalkanen M. Function of the syndecans – a family of cell surface proteoglycans. *J Cell Sci* 1994; 107 (Part 11): 2975–82.

Int. J. Cancer: **120,** 935–941 (2006)

Combining high selectivity of replication *via* CXCR4 promoter with fiber chimerism for effective adenoviral oncolysis in breast cancer

Mariam A. Stoff-Khalili[1,2], Angel A. Rivera[1], Alexander Stoff[1,3]*, J. Michael Mathis[4], Rodney P. Rocconi[1], Qiana L. Matthews[1], Michael T. Numnum[1], Isabell Herrmann[2], Peter Dall[2], Devin E. Eckhoff[5], Joanne T. Douglas[1], Gene P. Siegal[1], Zeng B. Zhu[1] and David T. Curiel[1]

[1]*Division of Human Gene Therapy, Departments of Medicine, Surgery, Pathology and the Gene Therapy Center, University of Alabama at Birmingham, Birmingham, AL*
[2]*Department of Obstetrics and Gynecology, University of Duesseldorf Medical Center, 40225 Duesseldorf, Germany*
[3]*Department of Plastic and Reconstructive Surgery, Dreifaltigkeits-Hospital, 50389 Wesseling, Germany*
[4]*Gene Therapy Program, Department of Cellular Biology and Anatomy, Louisiana State University Health Sciences Center, Shreveport, LA*
[5]*Division of Transplantation, University of Alabama at Birmingham, Birmingham, AL*

Conditionally replicative adenoviruses (CRAds) represent novel therapeutic agents that have been recently applied in the context of breast cancer therapy. However, deficiencies in the ability of the adenovirus to infect target tumor cells and to specifically replicate within the tumor target represent key deficiencies preventing the realization of the full potential of this therapeutic approach. Minimal expression of the adenovirus serotype 5 (Ad5) receptor CAR (coxsackie and adenovirus receptor) on breast cancer cells represents a major limitation for Ad5-based virotherapy. Genetic fiber chimerism is a method to alter the tropism of Ad5-based CRAds to achieve CAR-independent infectivity of tumor cells. Here, we describe the use of a CRAd with cancer specific transcriptional control of the essential Ad5 E1A gene using the human CXCR4 gene promoter. We further modified the fiber protein of this agent by switching the knob domain with that of the adenovirus serotype 3. The oncolytic activity of this 5/3 fiber-modified CRAd was studied in breast cancer cell lines, primary breast cancer and human liver tissue slices from patients, and in a xenograft breast cancer mouse model. This infectivity enhanced CRAd agent showed improved replication and killing in breast cancer cells *in vitro* and *in vivo* with a remarkable specificity profile that was strongly attenuated in nonbreast cancer cells, as well as in normal human breast and liver tissues. In conclusion, utilization of a CRAd that combined infectivity enhancement strategies and transcriptional targeting improved the CRAd-based antineoplastic effects for breast cancer therapy.

Key words: conditionally replicative adenovirus; breast cancer; virotherapy; CXCR4; adenovirus serotype 3; fiber chimerism

Breast cancer is the most commonly diagnosed cancer in women worldwide. Despite advances in early detection methods and conventional treatment paradigms, 20% of all women with breast cancer will die from this disease. Clearly, new therapies are required. One such novel therapy is virotherapy, an exciting therapeutic approach for the treatment of cancer in which the replicating virus itself is the anticancer agent. Among various attenuated viruses, the adenovirus-based vector has emerged as a leading candidate for *in vivo* cancer virotherapy. In this regard, conditionally replicative adenovirus-based agents (CRAds) have been designed to replicate in tumor cells, whereby the viral replication results in oncolysis and subsequent release of the virus progeny. An amplification effect is achieved *via* replication of the viral vector postinfection and spread in the tumor from an initial infection of only a few cells.

Heretofore, highly effective clinical use of CRAd agents has been hindered by low tumor transduction and suboptimal replicative specificity.[1] Thus, a high level of tumor transduction is critical to derive the full therapeutic benefits from this treatment modality. In breast cancers, transduction efficacy by adenovirus serotype 5 (Ad5) is often suboptimal due to the highly variable and often low expression pattern of the primary adenovirus receptor, coxsackie and adenovirus receptor (CAR).[2,3] To circumvent this, genetic alterations of the virus fiber protein that utilizes CAR-independent entry pathways have been identified, thus bypassing CAR deficiency on cancer cells. In this regard, a genetically modified nonreplicating adenoviral vector with CAR-independent tropism, achieved by incorporating the knob domain from the human adenovirus serotype 3 (Ad5/3), was recently shown to have superior enhancement in breast cancer cell infection.[4]

With respect to replication specificity, the strategy of transcriptional targeting exploits heterogeneous gene promoters that are active preferentially in tumor cells, but not in normal host cells, to control key adenoviral genes. In this regard, we evaluated the potential utility of the transcriptional control region of the human CXCR4 gene as a tumor selective promoter (TSP) for breast cancer virotherapy. Recent evidence indicates that the CXCR4/SDF-1α axis plays a role in the progression to metastasis in a number of cancer types.[5–7] In particular, CXCR4 has recently been shown to be highly expressed in breast cancer and metastases with minimal expression in mammary epithelial, ductal or stromal cells.[8]

For these reasons, we hypothesized that the utilization of a CRAd combining infectivity enhancement strategies and transcriptional targeting would improve the CRAd-based antineoplastic effects for breast cancer therapy. Heretofore, this approach of combining infectivity enhancement and transcriptional targeting strategies has not been exploited for virotherapy of breast cancer. Thus, it was the purpose of this study to develop a novel 5/3 fiber-modified CXCR4-based CRAd for breast cancer. In the present study, we evaluated for the first time a 5/3 fiber-modified CXCR4-based CRAd (Ad5/3.CXCR4) by determining the oncolytic activity in breast cancer cell lines, in primary breast cancer tissue slices from patients and in a xenograft breast cancer mouse model.

Material and methods

Cell lines and cell culture

The MDA-MB361, MDA-MB231 and ZR-751 breast cancer cell lines were obtained from the American Type Culture Collection and cultured as described. In brief, the cells were maintained in DME/F-12 medium (Life Technologies, Grand Island, NY),

Grant sponsor: Deutsche Forschungsgemeinschaft Sto; Grant number: 647/1-1; Grant sponsor: National Institutes of Health; Grant number: 5T32CA075930; Grant sponsor: Department of Defense; Grant number: W81Xwh-05-1-035; Grant number: R01CA108585.
***Correspondence to:** Division of Human Gene Therapy, Gene Therapy Center, University of Alabama at Birmingham, 901 19th Street South, BMR2 502, Birmingham, AL 35294, USA. Fax: 205-975-7476.
E-mail: alexander.stoff@t-online.de
Received 27 February 2006; Accepted 9 August 2006
DOI 10.1002/ijc.22338
Published online 27 November 2006 in Wiley InterScience (www.interscience.wiley.com).

containing 10% fetal bovine serum (Gemini Bio-Products, Woodland, CA) and 1% antibiotic–antimycotic solution (penicillin–streptomycin–fungizone; Sigma Chemicals, St. Louis, MO). The cells were maintained in T-150 flasks at 37°C and 5% humidified CO_2, and were subcultured using 1% trypsin–EDTA (Gibco BRL; Life Technologies). Human mammary epithelial cells (HMEC) were obtained from Clonetics (Walkersville, MD), and were maintained in serum-free mammary epithelial growth media or human stromal cell growth media (Clonetics) and passaged as recommended by the vendor.

Primary human cells

Human dermal fibroblasts were derived from adult skin by trypsinization, as previously described.[9–11] Human dermal fibroblasts obtained from outgrowth of explant cultures were grown in Dulbecco's modified Eagle's medium (Bio Whittaker, Walkersville, MD, USA) supplemented with 10% fetal calf serum, 2 mM glutamine, 100 U/ml penicillin and 100 μg/ml streptomycin and grown as monolayers on plastic petri dishes in a humidified atmosphere of a CO_2 incubator at 37°C.

Tissue slices and culture

Approval was obtained from the Institutional Review Board for all studies on human tissue. Human breast cancer samples and normal breast tissue samples were obtained (Department of Pathology, University of Alabama at Birmingham [UAB]) from 3 patients. Human liver samples were obtained (Department of Surgery, UAB) from 3 seronegative donor livers prior to transplantation into recipients. All liver samples were flushed with University of Wisconsin (UW) solution (ViaSpan; Barr Laboratories, Pomona, NY) before harvesting and kept on ice in UW solution until slicing. The precision tissue cut technique was performed *via* the Krumdieck tissue slicer, as previously described.[12] Time from harvest to slicing was kept at an absolute minimum (<2 hr). All samples were flushed with UW solution (ViaSpan; Barr Laboratories, Pomona, NY) before harvesting and kept on ice in UW solution until slicing. Tissue slices were placed into 6-well plates (1 slice per well) containing 2 ml of complete culture media (liver; William's Medium E with 1% antibiotics, 1% L-glutamine and 10% FCS; normal breast and breast tumor tissue; RPMI with 1% antibiotics, 1% L-glutamine and 10% FCS). The plates were then incubated at 37°C/5% CO_2 in a humidified environment under normal oxygen concentrations for up to 48 hr. A plate rocker set at 60 rpm was used to agitate slices and ensure adequate oxygenation and viability.[13]

Construction and production of adenoviruses

The plasmid pBSKCAT/CXCR4, which contains a 279 bp sequence from the human CXCR4 promoter (−191 to +88), was a kind gift of Dr. Nelson L. Michael.[14] The CXCR4 promoter sequence (NCBI Accession No. AY728138, from 1780 to 2059 bp) containing the 279 bp CXCR4 promoter and the simian virus 40 (SV40) polyadenylation (poly A) signal was cloned by PCR into the *NotI*/*XhoI* site of pScsE1 plasmid[15,16] (the pSCsE1 plasmid was a kind gift from Dr. Dirk Nettelbeck, Department of Dermatology, University Medical Center-Erlangen, Erlangen, Germany), resulting in pScsE1CXCR4 that contained the E1A gene downstream the CXCR4 gene promoter. The Ad vector, pAdback 5/3, was a kind gift from Dirk Nettelbeck and contains both the E3 gene and a capsid-modified F5/3.[15,16] After cleavage with *PmeI*, the shuttle vector, pScsE1CXCR4, was recombined with pAdback5/3 to generate a CRAd, where the human Ad knob serotype 5 is replaced by human Ad knob serotype 3. The recombinant plasmids were linearized with *PacI* and transfected into 293 cells using superfect reagent (Qiagen, Valencia, CA) to generate the Ad5/3CXCR4 adenoviruses. The adenoviruses were propagated in the A549 cells (a lung cell line in which the CXCR4 gene is overexpressed), and purified by double CsCl density gradient centrifugation, followed by dialysis against phosphate buffered saline (PBS) containing 10% glycerol. The concentration of total viral particle numbers (PN) was determined by measuring absorption at 260 nm. Infectious PNs were determined by measuring the concentration of viral hexon protein-positive 293 cells after a 48-hr infection period, using an Adeno-X Rapid Titer Kit (Clontech, Mountain View, CA). Wild type Ad5wt, Ad5/3wt[15,16] and AdCXCR4Luc[17] were used for replication positive and negative control, respectively, in the CRAd agent analysis.

Quantitating virus replication

Purification of the DNA and quantitative real-time PCR for E4 were performed as previously described.[18] 1.5×10^5 cells were seeded per well in a 6-well plate. The next day, cells were infected with the indicated viruses at 100 vp/cell or mock infected and growth medium was collected at the indicated time points. Viral infection of the tissue slices was performed as previously described[12]; 200 μl of the supernatant was collected at the indicated time points. Negative controls without templates were performed for each reaction series, and an internal control (human GAPDH) was used to normalize the copy number for the E4 genes. Comparison of replication rates of different treatment groups were performed with a Student's *t* test.

In vitro *cytotoxicity assay*

For determination of virus-mediated cytotoxicity, 1.5×10^4 cells were seeded and infected with adenoviruses at indicated titers or were mock-infected.[16] To visualize cell killing, cells were fixed and stained with 1% crystal violet in 70% ethanol for 20 min followed by washing with tap water to remove excess dye. The plates were dried and images were captured with a Kodak DC260 digital camera (Eastman Kodak, Rochester, NY).

In vitro *oncolysis*

All experimental protocols are approved by the Institutional Animal Care and Use Committee of UAB. To establish subcutaneous tumors, 4–5-week-old BALB/c nude mice were inoculated in both flanks with 5×10^6 MDA-MB361 cells (n = 5/group; 10 tumors/group). The tumor cells were verified to have 95% viability by trypan blue exclusion. When the tumor reached 5 mm in widest diameter, 5×10^6 pfu of Ad5Luc (as a nonreplicating control), Ad5/3.CXCR4, Ad5/3wt or Ad5wt were injected intratumorally in a 100 μl volume (5 mice per group). Control tumors were injected with an equal volume of PBS only. Animals were examined every other day and killed if tumor size reached 1.0×1.0 cm^2 or if there was any evidence of pain or distress. The tumor volume was calculated by the formula: $1/2xy^2$, where x is the longest distance of the tumor. The statistical differences among groups were assessed with Student's *t* test.

Results

Evidence of Ad5/3.CXCR4 replication in breast cancer cell lines

To assay CRAd replication,[18] the presence of the adenoviral E4 gene was determined in MDA-MB361 human breast cancer cells (Fig. 1*a*) and in HMEC normal human mammary epithelial (Fig. 1*b*) cells at days 1, 3 and 6 after infection with Ad5/3wt, Ad5/3.CXCR4, AdCXCR4Luc and Ad5wt. The replication levels of Ad5/3.CXCR4 and Ad5/3wt were significantly higher ($p < 0.05$) than those of Ad5wt in the MDA-MB361 cancer cell line. Importantly, in MDA-MB361 cells, Ad5/3.CXCR4 displayed replication levels comparable to Ad5/3wt, whereas in HMEC cells, the replication levels of Ad5/3 were significantly lower ($p < 0.05$) compared with Ad5/3wt and Ad5wt. Thus, Ad5/3.CXCR4 demonstrated breast cancer selective replication.

Evidence of CRAd cytolysis (Ad5/3CXCR4) in breast cancer cell lines in vitro

After finding specific replication of Ad5/3.CXCR4 in breast cancer cells, we evaluated the tumor specific cytolysis of Ad5/3.CXCR4. In all cancer cell lines examined, the crystal violet

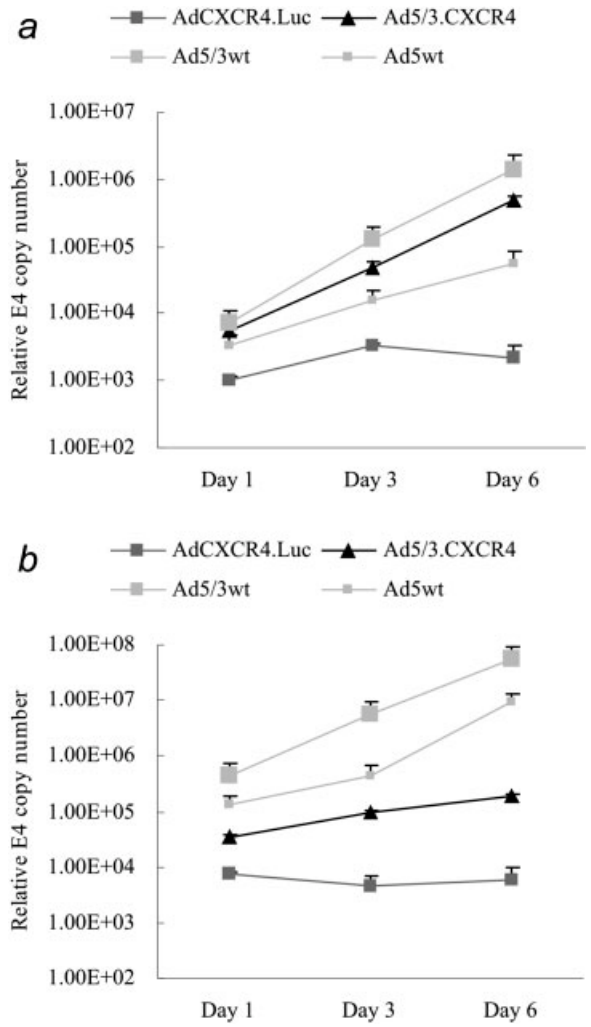

FIGURE 1 – Ad5/3 displays breast cancer specific replication *in vitro*. To assay CRAd replication, (*a*) MDA-MB361 (breast cancer cells) and (*b*) HMEC cells (normal mammary epithelial cells) were plated in a 24-well plate and infected with Ad5/3wt, Ad5/3.CXCR4, Ad5/3Luc and Ad5wt. After a 3-hr infection of MOI = 10, the cells were washed with PBS to remove free noninternalized viruses and provided with fresh medium. The presence of the E4 gene was determined using quantitative real-time PCR of DNA samples at days 1, 3 and 6 postinfection. Each point represents the mean of triplicate experiments ± SD.

staining-based cell killing assay showed superior oncolytic activity by Ad5/3.CXCR4 comparable to Ad5/3 wt (Fig. 2*a*). Of note, in comparison with Ad5wt, Ad5/3.CXCR4 and Ad5/3wt displayed a comparable oncolytic activity in MDA-MB231 cells, a 10-fold higher oncolytic activity in MDA-MB361 cells and a 100-fold higher oncolytic activity in ZR-751 cells. Most importantly, in HMEC cells and in normal human fibroblasts (Fig. 2*b*), Ad5/3.CXCR4 showed little cytolytic activity, at least 100-fold less compared with Ad5wt and 1,000-fold less compared to Ad5/3wt. These results demonstrate increased oncolytic potency of the infectivity enhanced CRAd Ad5/3.CXCR4 compared with Ad5wt, and more importantly, enhanced tumor specificity compared with Ad5wt and Ad5/3wt.

The infectivity enhanced CRAd Ad5/3.CXCR4 show tumor specificity in a human tissue slice model of breast cancer in vitro

To more closely model the clinical situation, we examined breast cancer selective replication of the infectivity enhanced CRAd Ad5/3.CXCR4 in the most stringent available preclinical model, using precision cut tissue slices of normal breast and breast cancer clinical samples. To measure viral copy number, the presence of the E4 gene was determined using quantitative real-time PCR of DNA samples extracted from medium at days 1 and 3 postinfection.[12] Ad5/3.CXCR4 and Ad5/3wt generated DNA copy numbers in breast cancer tissue slices that were significantly higher ($p < 0.05$) compared with Ad5wt (Fig. 3*a*). In contrast, in normal breast tissue slices, Ad5/3.CXCR4 showed a significantly ($p < 0.05$) lower viral copy number compared with both Ad5wt and Ad5/3wt (Fig. 3*b*). In summary, Ad5/3.CXCR4 demonstrated breast cancer selective enhanced replication in a human tissue slice model, which corresponded to the results obtained in breast cancer and normal breast cell lines.

In vitro *antitumor effect of the infectivity enhanced CRAd Ad5/3.CXCR4*

The ultimate goal of this study was to demonstrate the oncolytic superiority of the infectivity enhanced CRAd over that of unmodified adenoviruses *in vivo* in a breast cancer model. Because low dose of virus allow several cycles of replication along with destruction of tumor cells, even a single dose would produce an exponential rise in the number of killed cells, which would extend to the entire tumor. To demonstrate this hypothesis, we treated MDA-MB361 xenografts in nude mice with a single intratumoral injection of one of the 4 viruses or with PBS alone. No side effects related to virus administration were observed. Variation in the tumor volume of treated and control mice are shown in Figure 4. A statistically significant reduction in tumor growth ($p < 0.05$) was achieved for treatments with Ad5/3.CXCR4 or Ad5/3wt compared with Ad5wt. However, residual tumor lesions could be persistently detected in most of the treated animals. At day 36 after viral injection, tumor growth was inhibited by 63 and 61%, respectively, in the CRAd Ad5/3.CXCR4 and Ad5/3wt groups, compared with baseline. In contrast, relative tumor volumes increased to 205 and 140%, respectively, in groups treated with PBS and AdCXCR4.-Luc (serving as a nonreplicative Ad control) compared with baseline. Thus, these results using the infectivity enhanced CRAd Ad5/3.CXCR4 in a breast cancer xenograft model show promising *in vivo* tumor growth inhibition.

Replication profile of Ad5/3.CXCR4

Finally, we wished to investigate the replication profile of Ad5/3.CXCR4 in liver. To evaluate the liver toxicity of human CRAds preclinically is a challenge. It is known that human adenoviruses replicate only poorly in mice. Therefore, we measured adenoviral replication as a surrogate marker of liver toxicity in the most relevant preclinically available model, the human liver tissue slice model.[12] To measure viral copy number, the presence of the E4 gene was determined by using real-time PCR from DNA samples extracted from medium after 2 and 4 days postinfection.[19,20] As shown in Figure 5, the transcriptional targeted enhanced CRAd Ad5/3.CXCR4 revealed a significant lower copy number ($p < 0.05$) compared with the Ad5/3wt in human liver tissue slices. Thus, exploiting transcriptional targeting in the context of an infectivity enhanced CRAd significantly reduced replication in human liver tissue.

Discussion

In the present study, we have shown that infectivity enhancement based upon capsid modification/fiber modification allows improved antitumor potency of replicative CRAds in virotherapy of breast cancer. We have addressed the key point of breast cancer cell specific adenoviral replication by incorporation of a breast cancer relevant TSP element in these infectivity enhanced class of capsid/fiber-modified CRAd agents. In this regard, we have shown that Ad5/3.CXCR4 achieves augmented oncolysis by virtue of enhanced infectivity of established breast cancer cells *in vitro*. Additionally, we have demonstrated the capacity of Ad5/3.CXCR4 to

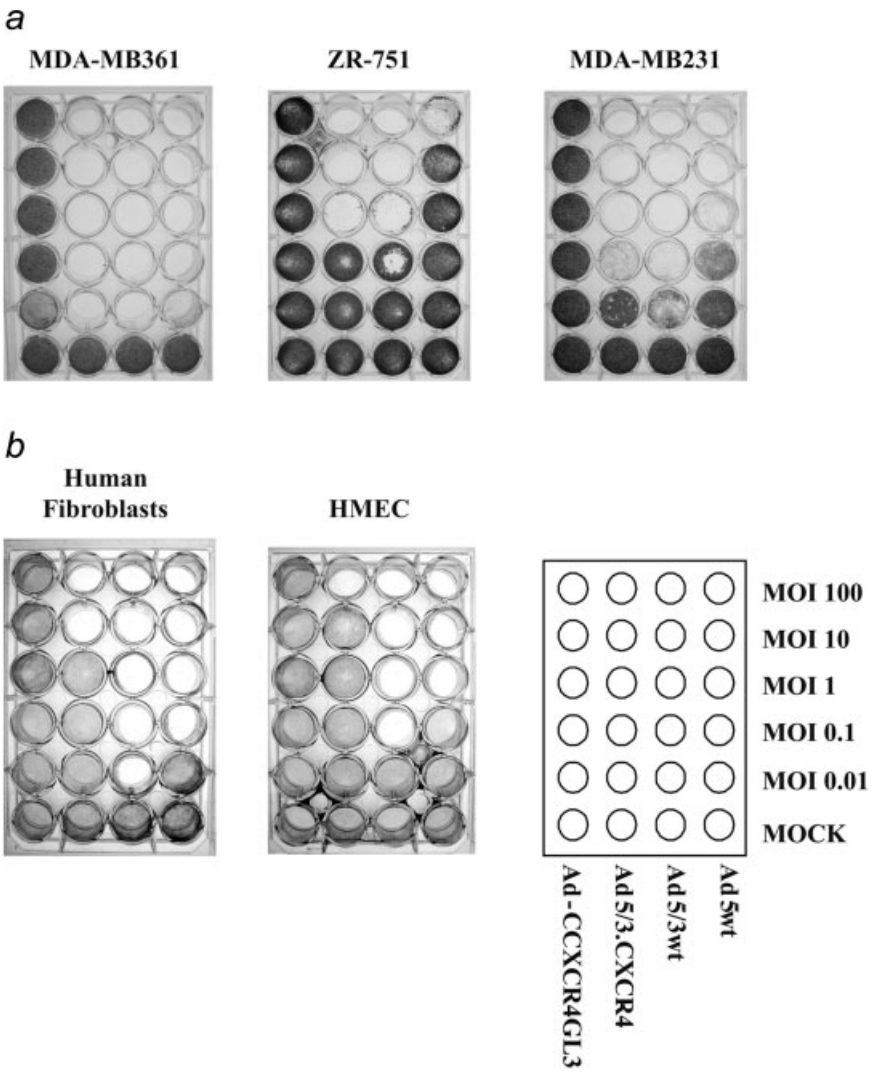

FIGURE 2 – Oncolytic potency and specificity of the infectivity enhanced CRAd in breast cancer cells *in vitro*. (*a*) MDA-MB361, ZR-751, MD-MB231 and (*b*) human fibroblasts and mammary epithelial cells (HMEC) were infected with Ad5/3Luc (as a nonreplicating control), Ad5/3.CXCR4, Ad5/3wt and Ad5wt. Oncolytic activity was evaluated by crystal violet staining.

accomplish a decrease in breast cancer tumors and to achieve survival advantage *in vivo* in a murine model of breast cancer. Since Ad replication is generally species specific and human Ads replicate poorly in cells from other species, our murine model of breast cancer might not accurately reflect how oncolytic Ad vectors behave in humans. For this reason, we have confirmed cancer specificity in the most stringent preclinical available human breast cancer model system, human breast cancer and normal breast precision cut tissue slices. Of note, the Ad5/3.CXCR4 displayed a ''liver-off'' replication profile in human liver tissue slices. Thus, these efforts have achieved the two key mandates of our CRAd agent, namely, enhanced tumor infectivity and specificity *in vitro* as well as antitumor potency *in vivo*.

In this study, we evaluated the efficacy of an infectivity enhanced capsid/fiber-modified CRAd using the CXCR4 promoter. Our results suggest that the CXCR4 promoter exhibits a ''tumor on/liver off'' phenotype in a CRAd context. This is a central objective in cancer Ad virotherapy since ectopic liver replication as at best one possible surrogate marker of hepatotoxicity is the major predicate of Ad vector-induced toxicity. We had previously demonstrated that the CXCR4 exhibits unparalleled differential with respect to tumor on/liver off profile among a panel of breast cancer specific promoters in a nonreplicating Ad context.[21] In addition, tumor cell migration and metastasis have recently been shown to be regulated by chemokines and their respective receptors (*e.g.*, SDF-1α/CXCR4). The CXCR4/SDF-1α axis appears to be involved in migration, invasiveness, metastasis and proliferation of breast cancer cells.[8,22,23] Thus, our CRAd construct was designed to exploit these findings that CXCR4 overexpression is a key phenotypic attribute of breast cancer.

In our study, we achieved enhanced infectivity by replacing the Ad5 fiber knob domain with the knob domain from human adenovirus serotype 3 (Ad5/3). In this regard, several other capsid modification strategies have been performed to augment the infectivity of adenoviruses in tumor cells by circumventing CAR, which include the incorporation of short heterologous peptides like RGD[24] or polylysine[25] into the fiber knob domain, as well as knob switching strategies.[26] In addition, more radical modifications based on xenotype knob switching have recently been exploited to achieve enhanced infectivity.[27,28] Based on these observations that, among capsid modifications examined, the Ad5/3 has revealed the highest infectivity enhancement in breast cancer cell lines and breast cancer tissue slices obtained from breast cancer patients in nonreplicating Ad systems, we chose this capsid modification for the design of our CRAd. Indeed, the Ad5/3 capsid modification maintained its superior infectivity enhancement in CRAd agents for breast cancer. Earlier studies have shown the increased expression of Ad3 receptors compared with Ad5 receptors in breast cancer cell lines and primary breast cancer cells isolated from patients. It is conceivable that the Ad3 receptor, as opposed to CAR, may not be involved in the carcinogenic process and thus not down regulated in advanced tumors. Interestingly, it

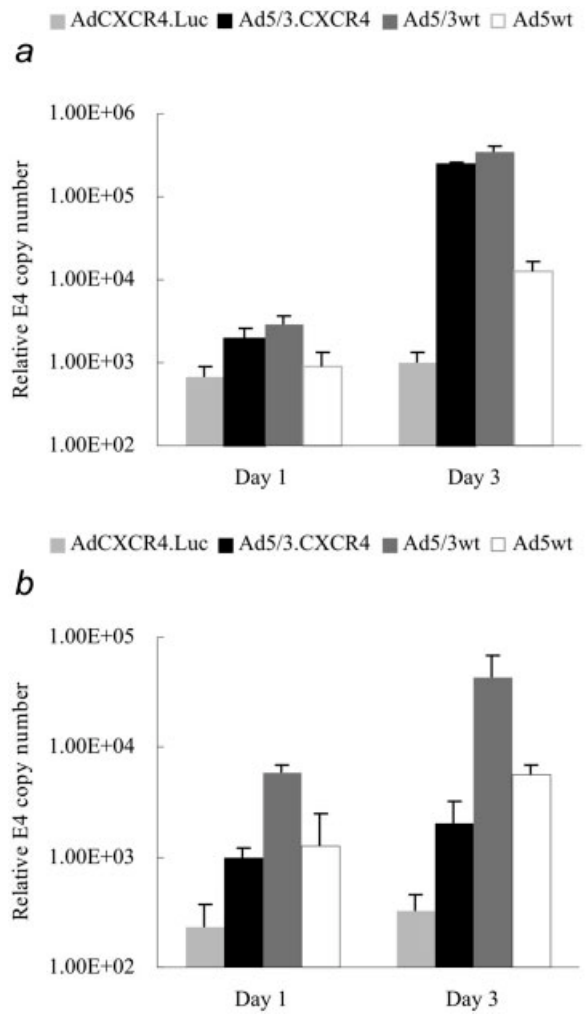

FIGURE 3 – Ad5/3.CXCR4 reveals cancer specificity in a human tissue slice model of breast cancer *in vitro*. Tissue slices of 3 primary human breast cancer (*a*) and normal breast samples (*b*) were infected with Ad5Luc (as a nonreplicating control), Ad5/3.CXCR4, Ad5/3wt and Ad5wt. All experiments were performed in triplicates for each patient. Each bar represents the mean of 3 patient samples ± SD.

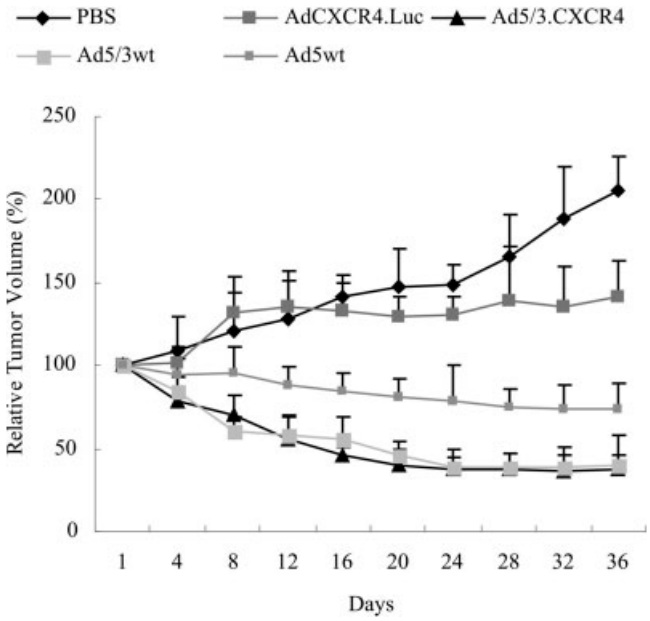

FIGURE 4 – Antitumor effect of Ad5/3.CXCR4 *in vivo*. Human breast cancer xenografts were established in BALB/c nude mice by injection of MDA-MB-361 into the flanks. When the tumor reached 5 mm in widest diameter, 5×10^6 pfu of Ad5Luc (as a nonreplicating control), Ad5/3.CXCR4, Ad5/3wt or Ad5wt were injected intratumorally in a 100 µl volume (5 mice per group). Control tumors were injected with an equal volume of PBS only. The tumor volume was calculated by the formula: $1/2xy^2$, where x is the longest distance of the tumor. The relative tumor volume = (tumor volume/tumor volume at day 1) × 100%.

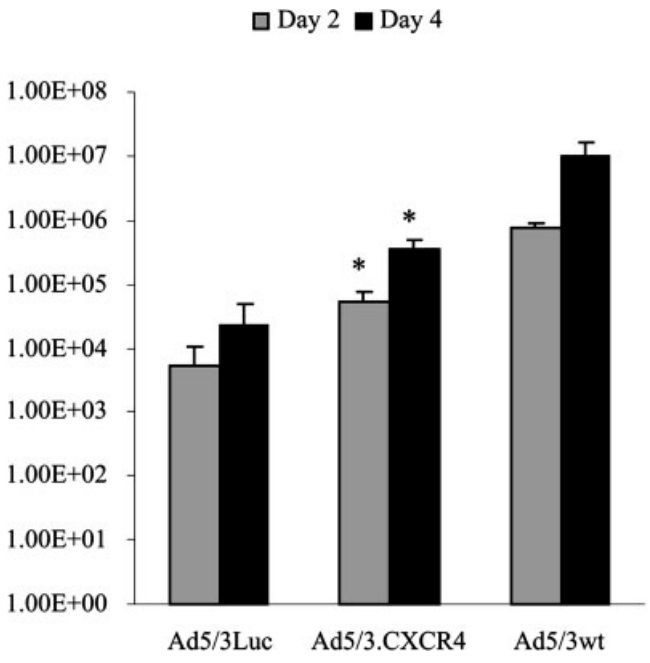

FIGURE 5 – Evaluation of replication of the CRAd Ad5/3.CXCR4 in a human liver tissue slice model. Adenoviral replication (viral copy number) was measured as a surrogate marker of liver toxicity in precision cut tissue slices of normal human liver obtained from 3 donors. Growth medium was collected at days 2 and 4 after infection with Ad5/3Luc (as a nonreplicating control), Ad5/3.CXCR4 and Ad5/3wt. Each bar presents the mean of 3 experiments ± SD. *$p < 0.05$ Ad5/3.CXCR4 versus Ad5/3wt.

has been reported that CAR expression may correlate inversely with the aggressiveness of a tumor.[29,30]

In these studies, we presently describe a CRAd addressing two key points, infectivity enhancement and specific replication with subsequent cell killing, as a novel approach for virotherapy of breast cancer. To our knowledge, this strategy exploiting infectivity enhancement *via* fiber-chimerism and transcriptional targeting has not been described and exploited for virotherapeutical strategies for breast cancer heretofore. Ad5/3.CXCR4 is promising as an agent for achieving enhanced but selective replication, which could reduce adverse effects in clinical trial. However, further optimization of virus administration may be required to obtain full therapeutic results.

While important preclinical *in vivo* therapeutic studies using CRAds have been derived from human tumor xenograft models in immunodeficient mice, it is critical to develop immunocompetent tumor model systems. In this regard, mouse tumor cell lines have been identified that are permissive for viral replication and show therapeutic effects in syngeneic immunocompetent mouse models.[31] Using the cotton rat, a rodent species that is semipermissive

for human Ads, the utility of this *in vivo* model was demonstrated for testing the selectivity, immunogenicity and efficacy of oncolytic Ad vectors.[32] In addition, cross-species replication of Ad5 was demonstrated in canine cells.[33] Since the biological behavior and clinical presentation of certain dog tumors closely resemble those of their human counterparts, these results raise the possibility of exploiting canine models for preclinical analysis of candidate CRAd agents designed for human virotherapy. A report was recently published suggesting the Syrian hamster model as a permissive immunocompetent animal model for the study of oncolytic adenoviral vectors.[34] The exploitation of the Syrian hamster model with regard to breast cancer for the analysis of our novel introduced CRAd will be an item of future investigations.

It is clear that gene therapy of breast cancer is a very difficult undertaking. The results of breast cancer gene therapy clinical trials to date have demonstrated little toxicity. However, the rate of clinical response has been low to date and efficient transgene expression remains to be a challenge. We believe that Ad5/3.CXCR4 could be an effective and safe Ad therapeutic agent for the treatment of breast cancer or other neoplastic diseases featuring high expression of CXCR4 and low expression of CAR. We have demonstrated that genetic capsid modifications using knob switching strategies can achieve infectivity enhancement in order to overcome CAR deficiency in breast cancer cells. Most importantly, we have demonstrated cancer specificity of our novel CRAd in the most stringent preclinical available human breast cancer model system, human breast cancer and normal breast precision cut tissue slices. In the normal breast tissue slices, while Ad5/3.CXCR4 showed a significantly lower viral copy number compared with both Ad5wt and Ad5/3wt, replication was not completely eliminated. This low level of viral replication may have some therapeutic benefit, such as in the destruction of supporting tumor vasculature. We recognize that additional genetic capsid modifications may also serve to enhance tumor selective targeting. For example, it has recently been demonstrated that single chain antibodies (scFv), which represent useful agents for cell specific targeting, can be genetically incorporated into the Ad capsid to foster targeted transduction.[35] Thus, our future goal for the design of a targeted CRAd for breast cancer may include the combination of tumor specific transcriptional targeting and specific transductional targeting *via* a genetically incorporated motif such as a single chain antibody.

The immediate future of breast cancer gene therapy is likely to involve the use of adjunct therapeutic regimens for locoregional control. Thus, we envisage future studies involving a multimodality approach, integrating curative or debulking resections, followed by adjuvant therapies including concurrent or sequential CRAd virotherapy, chemotherapy and radiotherapy.

References

1. Mathis JM, Stoff-Khalili MA, Curiel DT. Oncolytic adenoviruses—selective retargeting to tumor cells. Oncogene 2005;24:7775–91.
2. Liu Y, Ye T, Maynard J, Akbulut H, Deisseroth A. Engineering conditionally replication-competent adenoviral vectors carrying the cytosine deaminase gene increases the infectivity and therapeutic effect for breast cancer gene therapy. Cancer Gene Ther 2005.
3. Hemminki A, Kanerva A, Liu B, Wang M, Alvarez RD, Siegal GP, Curiel DT. Modulation of coxsackie-adenovirus receptor expression for increased adenoviral transgene expression. Cancer Res 2003; 63(4):847–53.
4. Stoff-Khalili MA, Stoff A, Rivera AA, Mathis JM, Everts M, Wang M, Kawakami Y, Waehler R, Mathews QL, Yamamoto M, Rocconi RP, Siegal GP, et al. Gene transfer to carcinoma of the breast with fiber-modified adenoviral vectors in a tissue slice model system. Cancer Biol Ther 2005;4:1203–10.
5. Moore M. The role of chemoattraction in cancer metastases. Bioessays 2001;23:674–76.
6. Murakami T, Maki W, Cardones AR, Fang H, Tun Kyi A, Nestle FO, Hwang ST. Expression of CXC chemokine receptor-4 enhances the pulmonary metastatic potential of murine B16 melanoma cells. Cancer Res 2002;62:7328–34.
7. Taichman RS, Cooper C, Keller ET, Pienta KJ, Taichman NS, McCauley LK. Use of the stromal cell-derived factor-1/CXCR4 pathway in prostate cancer metastasis to bone. Cancer Res 2002;62: 1832–7.
8. Muller A, Homey B, Soto H, Ge N, Catron D, Buchanan ME, McClanahan T, Murphy E, Yuan W, Wagner SN, Barrera JL, Mohar A, et al. Involvement of chemokine receptors in breast cancer metastasis. Nature 2001;410:50–6.
9. Smola H, Thiekotter G, Fusenig NE. Mutual induction of growth factor gene expression by epidermal–dermal cell interaction. J Cell Biol 1993;122:417–29.
10. Stark HJ, Baur M, Breitkreutz D, Mirancea N, Fusenig NE. Organotypic keratinocyte cocultures in defined medium with regular epidermal morphogenesis and differentiation. J Invest Dermatol 1999; 112: 681–91.
11. Satish L, Babu M, Tran KT, Hebda PA, Wells A. Keloid fibroblast responsiveness to epidermal growth factor and activation of downstream intracellular signaling pathways. Wound Repair Regen 2004; 12:183–92.
12. Kirby TO, Rivera A, Rein D, Wang M, Ulasov I, Breidenbach M, Kataram M, Contreras JL, Krumdieck C, Yamamoto M, Rots MG, Haisma HJ, et al. A novel ex vivo model system for evaluation of conditionally replicative adenoviruses therapeutic efficacy and toxicity. Clin Cancer Res 2004;10:8697–703.
13. Olinga P, Groen K, Hof IH, De Kanter R, Koster HJ, Leeman WR, Rutten AA, Van Twillert K, Groothuis GM. Comparison of five incubation systems for rat liver slices using functional and viability parameters. J Pharmacol Toxicol Methods 1997;38:59–69.
14. Wegner SA, Ehrenberg PK, Chang G, Dayhoff DE, Sleeker AL, Michael NL. Genomic organization and functional characterization of the chemokine receptor CXCR4, a major entry co-receptor for human immunodeficiency virus type 1. J Biol Chem 1998;273:4754–60.
15. Nettelbeck DM, Rivera AA, Balague C, Alemany R, Curiel DT. Novel oncolytic adenoviruses targeted to melanoma: specific viral replication and cytolysis by expression of E1A mutants from the tyrosinase enhancer/promoter. Cancer Res 2002;62:4663–70.
16. Rivera AA, Davydova J, Schierer S, Wang M, Krasnykh V, Yamamoto M, Curiel DT, Nettelbeck DM. Combining high selectivity of replication with fiber chimerism for effective adenoviral oncolysis of CAR-negative melanoma cells. Gene Ther 2004;11:1694–702.
17. Zhu ZB, Makhija SK, Lu B, Wang M, Kaliberova L, Liu B, Rivera AA, Nettelbeck DM, Mahasreshti PJ, Leath CA, III, Yamaoto M, Alvarez RD, et al. Transcriptional targeting of adenoviral vector through the CXCR4 tumor-specific promoter. Gene Ther 2004;11: 645–8.
18. Kanerva A, Zinn KR, Chaudhuri TR, Lam JT, Suzuki K, Uil TG, Hakkarainen T, Bauerschmitz GJ, Wang M, Liu B, Cao Z, Alvarez RD, et al. Enhanced therapeutic efficacy for ovarian cancer with a serotype 3 receptor-targeted oncolytic adenovirus. Mol Ther 2003;8: 449–58.
19. Zhu ZB, Makhija SK, Lu B, Wang M, Rivera AA, Kim-Park S, Ulasov IV, Zhou F, Alvarez RD, Siegal GP, Curiel DT. Incorporating the survivin promoter in an infectivity enhanced CRAd-analysis of oncolysis and anti-tumor effects in vitro and in vivo. Int J Oncol 2005; 27:237–46.
20. Yamamoto M, Davydova J, Wang M, Siegal GP, Krasnykh V, Vickers SM, Curiel DT. Infectivity enhanced, cyclooxygenase-2 promoter-based conditionally replicative adenovirus for pancreatic cancer. Gastroenterology 2003;125:1203–18.
21. Stoff-Khalili MA, Stoff A, Rivera AA, Banerjee NS, Everts M, Young S, Siegal GP, Richter DF, Wang M, Dall P, Mathis JM, Zhu ZB et al. Preclinical evaluation of transcriptional targeting strategies for carcinoma of the breast in a tissue slice model system. Breast Cancer Res 2005;7:R1141–52.
22. Salvucci O, Bouchard A, Baccarelli A, Deschenes J, Sauter G, Simon R, Bianchi R, Basik M. The role of CXCR4 receptor expression in breast cancer: a large tissue microarray study. Breast Cancer Res Treat 2005:1–9.
23. Lee BC, Lee TH, Avraham S, Avraham HK. Involvement of the chemokine receptor CXCR4 and its ligand stromal cell-derived factor 1α in breast cancer cell migration through human brain microvascular endothelial cells. Mol Cancer Res 2004;2(6):327–38.
24. Dmitriev I, Krasnykh V, Miller CR, Wang M, Kashentseva E, Mikheeva G, Belousova N, Curiel DT. An adenovirus vector with genetically modified fibers demonstrates expanded tropism via utilization of a coxsackievirus and adenovirus receptor-independent cell entry mechanism. J Virol 1998;72:9706–13.

25. Wickham TJ, Roelvink PW, Brough DE, Kovesdi I. Adenovirus targeted to heparan-containing receptors increases its gene delivery efficiency to multiple cell types. Nat Biotechnol 1996;14: 1570–3.
26. Krasnykh V, Dmitriev I, Navarro JG, Belousova N, Kashentseva E, Xiang J, Douglas JT, Curiel DT. Advanced generation adenoviral vectors possess augmented gene transfer efficiency based upon coxsackie adenovirus receptor-independent cellular entry capacity. Cancer Res 2000;60:6784–7.
27. Glasgow JN, Kremer EJ, Hemminki A, Siegal GP, Douglas JT, Curiel DT. An adenovirus vector with a chimeric fiber derived from canine adenovirus type 2 displays novel tropism. Virology 2004; 324:103–16.
28. Stoff-Khalili MA, Rivera AA, Glasgow JN, Le LP, Stoff A, Everts M, Tsuruta Y, Kawakami Y, Bauerschmitz GJ, Mathis JM, Pereboeva L, Seigal GP, et al. A human adenoviral vector with a chimeric fiber from canine adenovirus type 1 results in novel expanded tropism for cancer gene therapy. Gene Ther 2005;12:1696–706.
29. Seidman MA, Hogan SM, Wendland RL, Worgall S, Crystal RG, Leopold PL. Variation in adenovirus receptor expression and adenovirus vector-mediated transgene expression at defined stages of the cell cycle. Mol Ther 2001;4:13–21.
30. Okegawa T, Li Y, Pong RC, Bergelson JM, Zhou J, Hsieh JT. The dual impact of coxsackie and adenovirus receptor expression on human prostate cancer gene therapy. Cancer Res 2000;60:5031–6.
31. Hallden G, Hill R, Wang Y, Anand A, Liu TC, Lemoine NR, Francis J, Hawkins L, Kirn D. Novel immunocompetent murine tumor models for the assessment of replication-competent oncolytic adenovirus efficacy. Mol Ther 2003;8:412–24.
32. Toth K, Spencer JF, Tollefson AE, Kuppuswamy M, Doronin K, Lichtenstein DL, La Regina MC, Prince GA, Wold WS. Cotton rat tumor model for the evaluation of oncolytic adenoviruses. Hum Gene Ther 2005;16:139–46.
33. Ternovoi VV, Le LP, Belousova N, Smith BF, Siegal GP, Curiel DT. Productive replication of human adenovirus type 5 in canine cells. J Virol 2005;79:1308–11.
34. Thomas MA, Spencer JF, La Regina MC, Dhar D, Tollefson AE, Toth K, Wold WS. Syrian hamster as a permissive immunocompetent animal model for the study of oncolytic adenovirus vectors. Cancer Res 2006;66:1270–6.
35. Hedley SJ, Auf der Maur A, Hohn S, Escher D, Barberis A, Glasgow JN, Douglas JT, Korokhov N, Curiel DT. An adenovirus vector with a chimeric fiber incorporating stabilized single chain antibody achieves targeted gene delivery. Gene Ther 2006;13:88–94.

III. Publications - 2007

9. Huang D, Pereboev AV, Korokhov N, He R, Larocque L, Gravel C, Jaentschke B, Tocchi M, Casley WL, Lemieux M, Curiel DT, Chen W, Li X. Significant alterations of biodistribution and immune responses in Balb/c mice administered with adenovirus targeted to CD40(+) cells. Gene Ther. 2007 Nov 29:1-11. PMID: 18046426
10. Li HJ, Everts M, Pereboeva L, Komarova S, Idan A, Curiel DT, Herschman HR. Adenovirus tumor targeting and hepatic untargeting by a coxsackie/adenovirus receptor ectodomain anti-carcinoembryonic antigen bispecific adapter. Cancer Res. 2007 Jun 1;67(11):5354-61. PMID: 17545616
11. Miura Y, Yoshida K, Nishimoto T, Hatanaka K, Ohnami S, Asaka M, Douglas JT, Curiel DT, Yoshida T, Aoki K. Direct selection of targeted adenovirus vectors by random peptide display on the fiber knob. Gene Ther. 2007 Oct;14(20):1448-60. PMID: 17700705
12. Pereboeva L, Komarova S, Roth J, Ponnazhagan S, Curiel DT. Targeting EGFR with metabolically biotinylated fiber-mosaic adenovirus. Gene Ther. 2007 Apr;14(8):627-37. PMID: 17251987
13. Stoff-Khalili MA, Rivera AA, Mathis JM, Banerjee NS, Moon AS, Hess A, Rocconi RP, Numnum TM, Everts M, Chow LT, Douglas JT, Siegal GP, Zhu ZB, Bender HG, Dall P, Stoff A, Pereboeva L, Curiel DT. Mesenchymal stem cells as a vehicle for targeted delivery of CRAds to lung metastases of breast carcinoma. Breast Cancer Res Treat. 2007 Oct;105(2):157-67. PMID: 17221158
14. Stoff-Khalili MA, Rivera AA, Nedeljkovic-Kurepa A, Debenedetti A, Li XL, Odaka Y, Podduturi J, Sibley DA, Siegal GP, Stoff A, Young S, Zhu ZB, Curiel DT, Mathis JM. Cancer-specific targeting of a conditionally replicative adenovirus using mRNA translational control. Breast Cancer Res Treat. 2007 May 17. PMID: 17508279
15. Tsuruta Y, Pereboeva L, Glasgow JN, Rein DT, Kawakami Y, Alvarez RD, Rocconi RP, Siegal GP, Dent P, Fisher PB, Curiel DT. A mosaic fiber adenovirus serotype 5 vector containing reovirus sigma 1 and adenovirus serotype 3 knob fibers increases transduction in an ovarian cancer ex vivo system via a coxsackie and adenovirus receptor-independent pathway. Clin Cancer Res. 2007 May 1;13(9):2777-83. PMID: 17473211
16. Waehler R, Russell SJ, Curiel DT. Engineering targeted viral vectors for gene therapy. Nat Rev Genet. 2007 Aug;8(8):573-87. Review. PMID: 17607305

Gene Therapy (2007), 1–11

www.nature.com/gt

ORIGINAL ARTICLE

Significant alterations of biodistribution and immune responses in Balb/c mice administered with adenovirus targeted to CD40(+) cells

D Huang[1], AV Pereboev[2], N Korokhov[2], R He[3], L Larocque[1], C Gravel[1], B Jaentschke[1], M Tocchi[1], WL Casley[1], M Lemieux[1], DT Curiel[2], W Chen[4] and X Li[1,5]

[1]Centre for Biologics Research, Biologics and Genetic Therapies Directorate, HPFB, Health Canada, Ottawa, Ontario, Canada; [2]Departments of Medicine, Obstetrics and Gynecology, Pathology and Surgery, Division of Human Gene Therapy, Gene Therapy Center, University of Alabama at Birmingham, Birmingham, AL, USA; [3]National Microbiology Laboratory, Public Health Agency of Canada, Winnipeg, Manitoba, Canada; [4]Institute of Biological Sciences, National Research Council, Ottawa, Ontario, Canada and [5]Department of Biochemistry, Microbiology and Immunology, University of Ottawa, Ottawa, Ontario, Canada

CD40 ligation has been shown to promote antigen-presenting functions of dendritic cells, which express CD40 receptor. Here we reported significantly altered biodistribution and immune responses with the use of CD40-targeted adenovirus. Compared with unmodified adenovirus 5, the CD40-targeted adenovirus following intravenous administration (i.v.) resulted in increased transgene expressions in the lung and thymus, which normally do not take up significant amounts of adenovirus. Intradermal injection saw modified adenovirus being mainly processed in local draining lymph nodes and skin. Following intranasal administration (i.n.), neither unmodified nor targeted viruses were found to be in the liver or spleen, which predominantly took up the virus following i.v. administration. However, inadvertent infection of the brain was found with unmodified adenoviruses, with the second highest gene expression among 14 tissues examined. Importantly, such undesirable effects were largely ablated with the use of targeted vector. Moreover, the targeted adenovirus elicited more sustained antigen-specific cellular immune responses (up to 17-fold) at later time points (30 days post boosting), but also significantly hampered humoral responses irrespective of administration routes. Additional data suggest the skewed immune responses induced by the targeted adenoviruses were not due to the identity of the transgene but more likely a combination of overall transgene load and CD40 stimulation.

Gene Therapy advance online publication, 29 November 2007; doi:10.1038/sj.gt.3303085

Keywords: *recombinant adenovirus; CD40; dendritic cells; biodistribution; immunogenicity; re-targeting*

Introduction

A variety of viruses, such as adenovirus (Ad) and poxvirus, have been explored as vaccine and gene delivery vectors for the prevention and/or treatment of various human diseases.[1,2] Among the viral vectors, recombinant Ad is a preferred and promising delivery system[1] since the virus exhibits relatively low cytotoxicity, large cloning capacity, replication to high titres and ability to infect both dividing and undividing cells. Recently, adenoviral vectors were found to be very effective for mucosal vaccination due to their natural tropism for the mucosal surfaces.[2] It is noted, however, that the main cellular receptor for Ad, coxsackievirus and adenovirus receptor (CAR), has been readily detected in a wide range of human tissues, which may potentially have undesirable consequences.[3–5] These findings prompted several groups to conduct various genetic modifications of the Ads to improve the delivery efficiency and/or minimize the relatively random distribution of the injected Ads by re-targeting the Ads to dendritic cells (DCs).

DCs are antigen-presenting cells playing crucial roles in establishing antigen-specific adaptive immune response and therefore stimulate potent immune responses. The possibilities of DC-based strategies for immunotherapy and immunoprotection of cancer, infectious disease and transplantation have been vigorously investigated during the past several years.[1] However, DCs are deficient in expression of the CAR receptor, presenting a challenge for effective transduction of these cells by Ads.[1] In addition, there is also a concern that the cytopathic effect of high-dose Ad on DCs could compromise clinical value of recombinant Ads.[3] To overcome these limitations, re-targeting delivery strategies via modification of the tropism of the virus have been developed for better transduction into DCs. One approach involves genetic modification of the fiber/knob proteins of Ad to target the surface intergrins of DCs.[6,7] Another approach is to target the CD40 surface receptor of DCs[8,9] since the CD40 receptor may play essential

Correspondence: Dr X Li, Centre for Biologics Research, Biologics and Genetic Therapies Directorate, HPFB, Health Canada, Tunney's Pasture, AL 2201C, Ottawa, Ontario, Canada K1A 0K9.
E-mail: Sean_Li@hc-sc.gc.ca
Received 18 June 2007; revised 6 November 2007; accepted 6 November 2007

roles in promoting both DC activation and antigen presentation.[10–14] To this end, the viruses were usually complexed with bi-specific adaptor molecules comprised of either anti-Ad single-chain antibody or the extracellular domain of CAR with the targeting CD40 ligand (CD40L).[8,9] While marked improvement of transduction efficiency and enhanced immune responses against the transgenes delivered by various targeted Ad vectors have been reported by others and us, systematic analyses of biodistribution, toxicity and immune responses following various administration routes remains poorly documented. Uncertainties also remain with respect to other forms of delivery (DNA- and protein-based system). For instance, even though CD40L has been consistently shown to enhance Th1 (cellular) immune response, its role in Th2 (humoral) response remains unclear, with some reports suggesting an increased antibody response and others reporting no adjuvant effect of CD40L.[15–19] Lack of knowledge in these areas could substantially hinder the transition from laboratory investigations to clinical application of CD40-targeted gene delivery and genetic vaccination.

This study focused on the *in vivo* analyses of the biodistribution and immunogenicity of a modified Ad complexed with an adaptor protein (CFm40L), a fusion protein comprised of human Ad receptor CAR fused to mouse CD40L via a trimerization motif.[9] We reported previously that CFm40L can significantly enhance *in vitro* gene transfer to DCs expressing CD40.[9] Here we demonstrate that the modified Ad, denoted as tAd in this report, irrespective of the route of administration, can profoundly alter the patterns of biodistribution and immune responses against the transgene. The potential mechanisms underlying these differences between the unmodified and targeted vectors are discussed.

Results

CFm40L facilitates Ad transduction of CD40(+) DCs in the presence of Ad-neutralizing antibodies

We showed previously that CFm40L could direct Ad into CD40(+) DCs.[9] In addition, we have also found that the mouse bone marrow-derived DCs stimulated by Ad–CFm40L complex resulted in elevated levels of maturation markers (CD11c, CD11c, CD54, CD40, CD80, CD86 and I-A^d).[9] Prior to the initiation of the biodistribution study in Balb/c mice, we first tested whether anti-CD40 mAb could prevent *in vitro* gene transfer by tAd-Luc (Ad5 expressing luciferase gene and conjugated with CFm40L). To this end, Ad-Luc conjugated with CFm40L as described previously[9] was used to transduce human CD40(+) DCs in the presence or absence of anti-CD40L. As compared with the unmodified Ad, the relative luciferase activity for the CFm40L-complexed Ads is 1307-fold higher with the addition of 80 ng CFm40L, 1491-fold with 120 ng and 1799-fold with 200 ng (Figure 1a), respectively. Each reaction had four replicates. The experiments were repeated three times with similar findings. Importantly, the addition of 0.5 and 2.0 μg of anti-CD40L mAb into the pre-complexed Ads largely prevented the enhanced luciferase activities, while premixing with 2.0 μg of normal mouse immunoglobulin (Ig) G did not show any inhibition of luciferase activity. Also as a control, Ads pre-complexed with 120 ng of bovine serum albumin (BSA) did not result in enhancement of luciferase activity in the transduced cells. These results further confirmed that the enhanced gene transduction into both human and murine DCs by Ads complexed with CFm40L is mediated by the CD40 receptor. We next determined whether tAd could still transduce DCs in the presence of Ad-neutralizing antibodies. Towards this end, we infected human peripheral blood-derived DCs with Ad–CFm40L complexes in the presence of Ad-negative and Ad-positive ascites fluids collected from ovarian cancer patients from a phase I gene therapy clinical trial. The ascites M56 (patient 'M', day 56 after Ad administration) has been shown to have high (>1:16 000) Ad-neutralizing antibody titres, and the ascites B0 (patient 'B', day 0 of Ad administration) to have none.[20] Furthermore, the ability of the ascites M56 to neutralize Ad infectivity and the lack of neutralizing capability by the ascites B0 was previously documented in the same studies.[20] We again

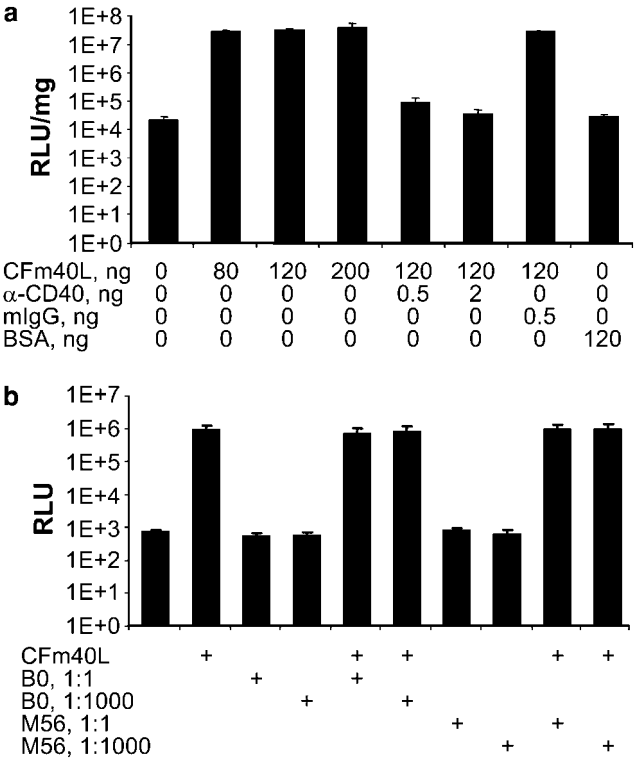

Figure 1 Enhanced entry of tAd into DCs in the presence of Ad-neutralizing antibodies. (**a**) Determination of tAd entry into CD40(+) DCs *in vitro*. Ad-Luc denotes Ad-5-expressing luciferase, tAd-Luc–Ad-Luc conjugated with CFm40L. CD40(+) DCs were cultured in 24-well plates (1×10^5 cells per well) for 4 days in RPMI-1640 medium containing rh-IL-4 and rhGM-CSF. tAd-Luc (2.5×10^6 PFU or 2.5×10^7 VP) was prepared by incubating Ad-Luc with various amount of CFm40L at 80, 120 and 200 ng, respectively and used to infect cultured DCs at MOI of 50. After 2 days of infection, luciferase activities were determined. The experiments were repeated three times, with results being presented as relative light units (RLU) normalized for protein concentration. Bars represent mean (four replicates) ± s.d. (same below). (**b**) The effects of Ad-neutralizing antibodies on CFm40L mediated DCs transduction. Human DCs were infected with CD40-targeted Ad-encoding luciferase reporter in the presence of human ascites fluids 'B0' (Ad Ab negative) and 'M56' (Ad Ab positive) at 1:1 and 1:1000 dilutions. Luciferase activity in cell lysates was assessed 36 h post transduction.

confirmed the absence of anti-Ad antibodies in ascites B0 and their presence in ascites M56 with the titre of 1:65 610 in Ad enzyme-linked immunosorbent assay (ELISA; Supplementary Figure S1). Then Ad vector-encoding luciferase was pre-complexed with CFm40L (50 ng per 1.25×10^6 PFU per 2.5×10^4 cells) mixed with the ascites at 1:1 and 1:1000 dilutions and applied to DCs. Luciferase activity was measured in cell lysates 36 h post transduction. The results (Figure 1b) indicate that neutralizing antibodies had no inhibitory effects on CFm40L mediated Ad-Luc transduction of human DCs.

CFm40L directs more rapid capturing of the vector by the liver, thymus and lung following i.v. administration

The tAds encoding firefly luciferase reporter gene (tAd-Luc) were then injected into Balb/c mice intravenous (i.v.) for the analysis of tissue distribution. A total of 1×10^{10} VP (viral particle) of Ad was chosen for Ad and tAd since excess amount of Ad (>1–2×10^{10}) could saturate tissue macrophages in mice following systemic administration, resulting in non-receptor-mediated process.[21] For tAd preparation, 1×10^9 PFU ($\sim 1 \times 10^{10}$ VP) of Ads were complexed with 16 μg of CFm40L, equivalent to 80 ng of CFm40L for 5×10^6 PFU of Ad. We chose this ratio between Ad and CFm40L since 80 ng of CFm40L is sufficient to complex 2.5×10^6 Ad for enhanced transduction *in vitro* (Figure 1a). In agreement with other reports with i.v. administration,[14,22–25] the Ad was detected after 3 and 7 days in a wide range of tissues, with the liver and spleen expressing the highest luciferase activities on day 3, followed by mesenteric lymph nodes (a visible cluster of lymph nodes inside the peritoneal cavity), heart, colon and others (Figure 2a). Yet, a noticeably altered biodistribution was observed with tAd-Luc (Figure 2b), that is in addition to the predominant disposition to the liver and spleen, the viruses were also effectively captured by thymus and the lung on day 3 (Figure 2b).

Localized expression of transgenes following i.d. administration

Following intradermal (i.d.) administration, high levels of luciferase expression were detected in the skin surrounding the injection site and in the local draining lymph nodes (inguinal) for both Ad-Luc and tAd-Luc and, as expected, the luciferase activity with tAd-Luc administration was significantly lower than that with Ad-Luc (~ 300 times lower) since tAd-Luc could only get into CD40(+) cells and express the luciferase gene (Figures 3a and b), consistent with results shown in Figure 1a. Clearly, no virus was detected in other organs and tissues, suggesting the viruses were processed near the injection site sites and local draining lymph nodes, with little spillover of the virus into the circulation.

CF40mL prevented inadvertent infection of the brain and attenuated local inflammatory reaction in the lung following i.n. administration

Following intranasal (i.n.) delivery of Ad-Luc, there was gene transfer with the Ad in various organs/tissues with the i.n. injection (Figure 4a). It is of note that the expression level of luciferase in the brain is high following Ad-Luc administration (Figure 4a), only second to the one detected in the lung. Clearly, the

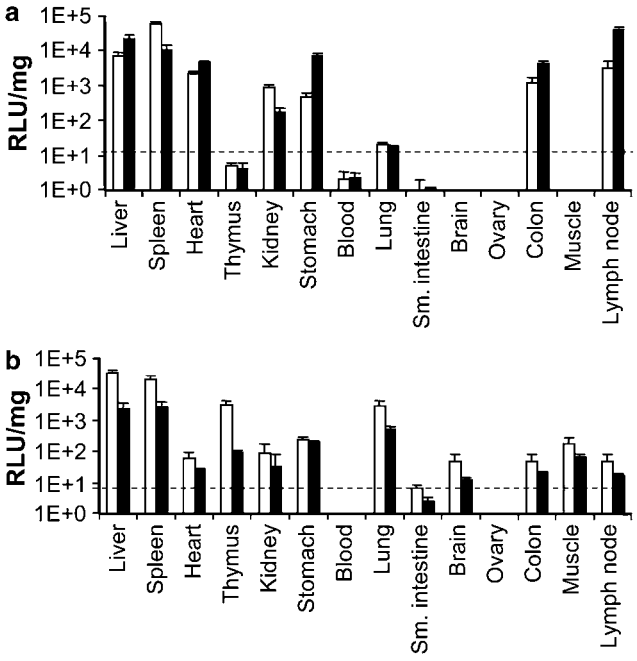

Figure 2 Biodistribution of Ad-Luc and tAd-Luc (Ad-Luc pre-complexed with CFm40L) following i.v. administration (tail vein). Five mice were injected with 1×10^{10} VP of either Ad-Luc (**a**) or tAd-Luc (**b**). Three and seven days post-injection the indicated tissues were isolated, homogenized and measured for luciferase activity. Values below 10 RLU (relative light units) per mg, as indicated by the dashed lines in the figures, are background readings (same below). Open bars and filled bars represent 3 and 7 days after injection, respectively.

infection of the brain was largely ablated with the use of tAd-Luc, but not the infection of other tissues such as lung, heart, thymus, colon, muscle and mesenteric lymph nodes (Figures 4a and b), suggesting CAR-mediated inadvertent infection of the brain by non-modified Ad. This interpretation is further supported by the observation that pre-complex of Ad-Luc with BSA did not prevent brain infection (Figure 4c). Interestingly, no significant difference of virus deposition between tAd-Luc and Ad-Luc in the heart was observed following i.n. administration (Figures 4a and b), an observation that differs from that following i.v. injection, which shows the heart took up more Ad-Luc than tAd-Luc following i.v. administration (Figure 2). We have no definite explanation for these findings. It is plausible, however, that since the heart is in close proximity of the lung, tAd-Luc could gain access more easily to the heart following i.n. delivery than with the i.v. route (tail vein).

The high level of luciferase activity in the lung following i.n. administration prompted us to conduct histological examination of the lung. As compared to the control mice injected with buffers only (Figure 5, panel a), i.n. delivery of Ad-Luc resulted in moderate accumulations of mononuclear leukocytes in many peribronchial and perivascular areas, typical of inflammatory reactions (Figure 5, panel b). Following the i.n. administration of Ad-NP expressing the nucleocapsid protein (NP) of SARS-CoV (SARS-CoV NP was used here as a model antigen), however, there are much more significant accumulations of mononuclear leukocytes in the peribronchial and perivascular areas throughout the entire histological section and infiltration of mononuclear cells

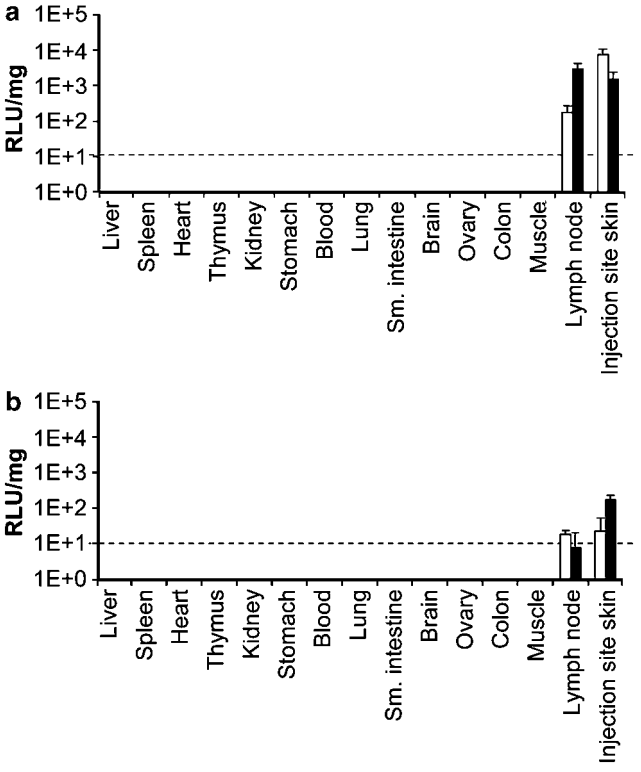

Figure 3 Biodistribution of Ad-Luc and tAd-Luc administrated i.d. (inguinal). (**a**) Mice that were injected with 1×10^{10} VP of Ad-Luc in 50 µl PBS. (**b**) Mice that were injected with 1×10^{10} VP of tAd-Luc. Three (open bar) and seven days (filled bar) post injection the indicated tissues were isolated, homogenized and measured for luciferase activity.

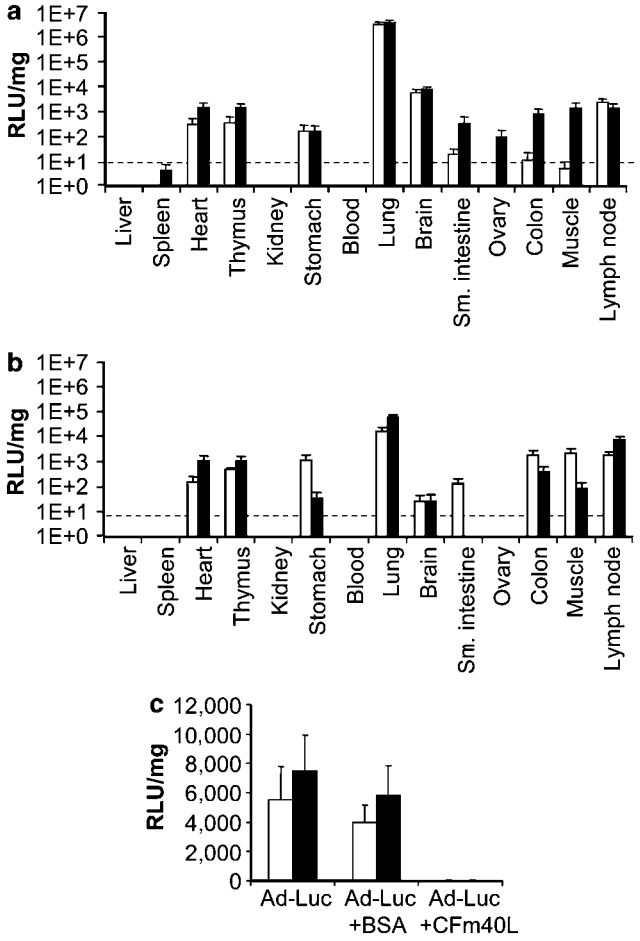

Figure 4 Biodistribution of Ad-Luc and tAd-Luc administrated i.n.. (**a** and **b**) Results from studies with mice administrated i.n. with Ad-Luc and tAd-Luc, respectively. The mice were injected with 1×10^{10} VP of virus in 100 µl PBS. Three (open bar) and seven days (filled bar) post injection the indicated tissues were isolated, homogenized and analysed for luciferase activities. (**c**) CFm40L abolishes inadvertent infection of the brain by the virus: Ad-Luc was conjugated with either CFm40L or bovine serum albumin (BSA) and injected (i.n.) into the mice. RLU were determined from the brain tissues of mice injected with 1×10^{10} VP of Ad-Luc pre-complexed either with CFm40L or BSA. Open bar depicts 3 days post administration, while filled bar designates 7 days post administration.

in the alveolar spaces (Figure 5, panel c). In the severely affected area, the airway epithelial cells demonstrate mild-to-moderate damage and sloughing, revealing an 'exaggerated' inflammatory reaction in the lung (Figure 5, panels c and e). The reason for the visible damage to the airway epithelial cell layers by Ad-NP but not by Ad-Luc could be due to the intrinsic property of NP, a strong immunogen in severe acute respiratory syndrome (SARS) patients, as was suggested (see below for discussion). It is of note that with the addition of CFm40L (denoted as tAd-NP), the excessive infiltration of inflammatory cells and the damage of epithelial cells were abolished (Figure 5, panel d). Taken together, a significantly altered pattern of biodistribution of Ad complexed with CFm40L was observed following i.v. and i.n. administrations. Attenuation of inadvertent infection of the brain and aggravated local inflammation has been demonstrated in the airway of the lung following i.n. administration. Finally, none of the Ad preparations (unconjugated or conjugated, irrespective of administration route) resulted in detectable signs of systematic toxicity following analyses of various blood biomarkers (blood chemistry) pertinent to vital organs such as kidney, heart and liver (data not shown), even though visible damages to the airway epithelial cells were found following i.n. administration of Ad-NP. We also conducted immunohistological examinations of available lung tissues using antibodies against both luciferase and CD11c, one of the surface markers for DCs. Preliminary results suggest that the tAd-Luc was mainly found in CD11c(+) cells, while Ad-Luc were not restricted to CD11c(+) cells (Supplementary Figure S2). Clearly, more vigorous investigations will be needed to identify all cell types that also express CD40.

CFm40L elicited a more sustained Ag-specific cellular immune response

To determine the adjuvant and targeting effects of CFm40L, Ad expressing the SARS-CoV NP protein (Ad-NP) was compared with the same virus complexed with CFm40L (tAd-NP) following either i.d. or i.n. administration, with tAd-Luc serving as the baseline control. We chose the same amount of virus used in the above biodistribution experiments. Thirty days post-prime, the mice were boosted once. The splenocytes were isolated on days 0, 15 and 30 post boosting for the determination of interferon-γ (IFN-γ) and interleukin-2

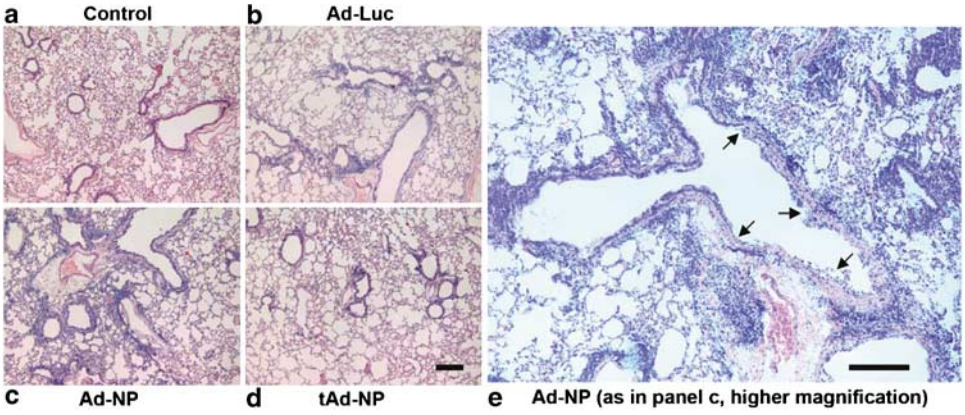

Figure 5 Histological examination of the lungs in mice administrated i.n. with various preparations of Ads. The lung tissues from mice were collected and snap frozen in liquid nitrogen and then storied at −80 °C. The tissue sections were prepared and stained by hematoxylin and eosin. (**a**) Normal lung from a mouse which received PBS only; (**b**) Lung from mouse which received Ad-Luc; (**c**) Lung from a mouse which received Ad-NP (Ad-5 expressing the NP of SARS-CoV); (**d**) Lung from a mouse which received tAd-NP (Ad-N complexed with CFm40L). Panel e represents panel c at high magnification. Significant accumulations of mononuclear leukocytes in the peribronchial and perivascular areas throughout the entire section and infiltration of mononuclear cells in the alveolar spaces were observed as shown in (**b**) and (**c**), with (**c**) demonstrating signs suggestive of a much stronger local inflammatory reaction. In the severely affected area of lungs from mice, which received Ad-NP, layers of airway epithelial cells display sloughing (indicated by arrows in (**e**)). These data are representative photos among at least five vision fields from >three mice. Scale bar: 100 μM.

(IL-2). As shown in Figures 6a and b, following i.d. administration, both IFN-γ and IL-2 specific for SARS-CoV NP, have been increased in mice immunized with either Ad-NP or tAd-NP compared with the control (mice receiving Ad-Luc). However, it is of note that on day 30 after boosting, the levels of IFN-γ and IL-2 in mice receiving tAd-NP were substantially higher than those immunized with Ad-NP, suggesting a more sustained Th1 response with the use of CFm40L (Figures 6a and b). Furthermore, such an enhancement of Ag-specific host immune response by CFm40L has also been observed with the i.n. injection route (Figures 6c and d). Collectively, these data revealed that CFm40L elicited a more sustained Ag-specific cellular immune response ($P<0.01$).

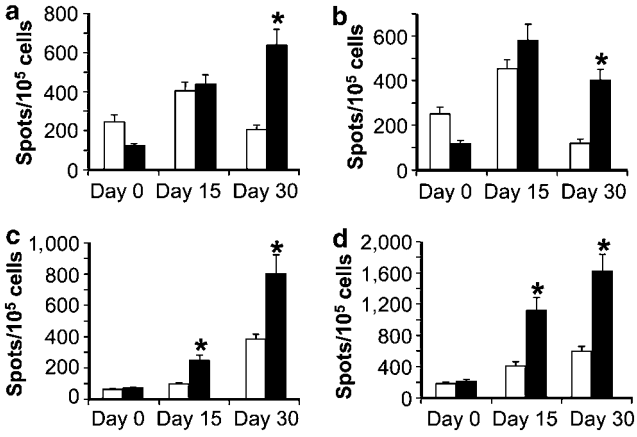

Figure 6 Determination of interferon-γ (IFN-γ) and interleukin-2 (IL-2) in mice receiving either Ad-NP or tAd-NP. The mice were administrated with either Ad-NP (open bar) or tAd-N (filled bar) and boosted 4 weeks later. The splenocytes were then harvested on days 0, 15 and 30 for the analyses of Ag-specific IFN-γ or IL-2 using ELISPOT as described in the 'Materials and methods' section. Data represent spots per 10^5 splenocytes stimulated by 10 μg ml^{-1} of NP. (**a**) IFN-γ levels in mice injected with either Ad-NP or tAd-NP (i.d. route); (**b**) IL-2 levels in mice injected with either Ad-NP or tAd-NP (i.d. route); (**c**) IFN-γ levels in mice injected with either Ad-NP or tAd-NP through the i.n. route); (**d**) IL-2 levels in mice injected with either Ad-NP or tAd-NP (i.n. route). All data represent the means ± s.d. from four mice. Asterisks (*) indicate significant difference between Ad-NP and tAd-NP (same below). Statistical comparisons were conducted with the use of a two-tailed *t*-test, with $P<0.05$ being considered significant. Open bar depicts Ad-NP, while filled bar designates tAd-NP.

CFm40L delayed Ag-specific humoral responses and reduced IgG 1/IgG 2a ratio

Specific IgG and IgA antibodies against the NP protein were determined by ELISA to measure the antibodies present in the sera or the trachea and lung (mucosal antibodies). Surprisingly, the levels of IgG and IgA in the sera following tAd-NP administration (i.d.) was significantly lower than that with Ad-NP immunization via the i.d. administration route ($P<0.01$) (Figures 7a and b).

Next we determined the titres of IgG and IgA present in the sera and trachea/lung lavage following i.n. administration and found that the humoral responses were similar to that with the i.d. route. As shown in Figure 8, both the IgG and IgA titres in mice immunized with tAd-NP were significantly lower than those with Ad-NP, especially on Days 0 and 15 post-boosting ($P<0.01$). It is of note, however, that the antibody titres did reach similar levels 30 days post-boosting following i.n. administration (Figure 8). In addition, similar findings in terms of Ag-specific antibody responses against a different transgene (luciferase) were also obtained with the use of tAd-Luc (Supplementary Figure S3). These data collectively suggest that the reduction of Ag-specific humoral responses is not linked to the identity of the transgene but to the use of CFm40L in conjunction with adenoviral vectors.

We then determined the relative ratio of IgG1 and IgG2a delivered by either unmodified or CD40-targeted vectors. To this end, horseradish peroxidase (HRP)-conjugated anti-mouse IgG1 and IgG2a were used in place of HRP-conjugated anti-mouse IgG in ELISA.[26]

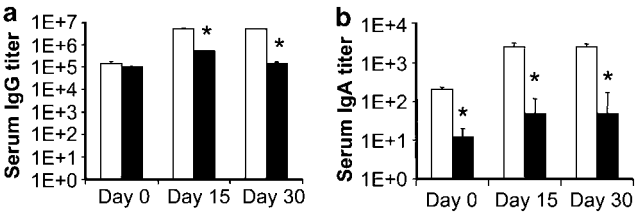

Figure 7 Ag-specific antibody responses in mice following i.d. administration of either Ad-NP or tAd-NP. Mice immunized (i.d. route) with either Ad-NP (open bar) or tAd-NP (filled bar) were analysed for Ag-specific antibody levels using ELISA. (**a**) Serum immunoglobulin G (Ig) G levels in mice following i.d. administration; (**b**) serum IgA levels in mice following i.d. administration. $^*P<0.05$.

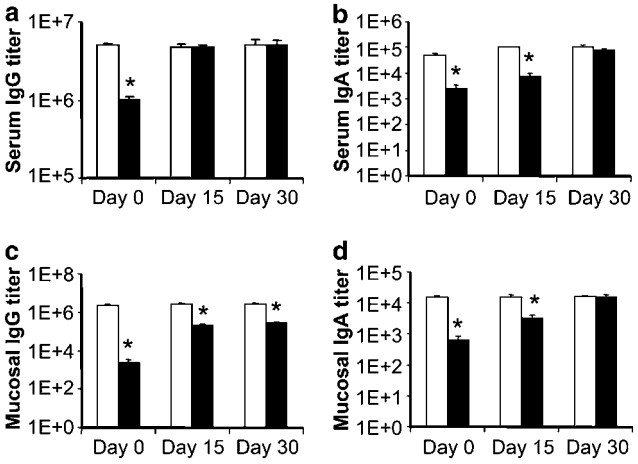

Figure 8 Ag-specific antibody responses in mice following i.n. administration of either Ad-NP or tAd-NP. Mice immunized (i.n. route) with either Ad-NP (open bar) or tAd-NP (filled bar) were analysed for Ag-specific antibody levels using ELISA assays. (**a**) Serum immunoglobulin (Ig) G levels in mice (**b**) serum IgA levels in mice; (**c**) mucosal IgG levels (antibodies present in the trachea and lung); (**d**) mucosal IgA levels (antibodies present in the trachea and lung). $^*P<0.05$.

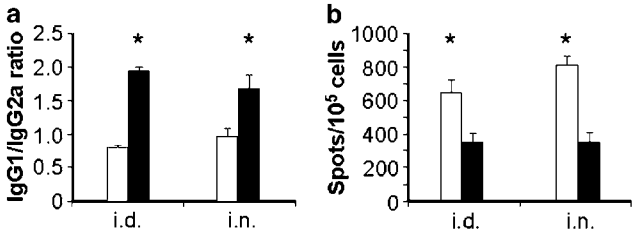

Figure 9 Determination of transgene-specific immunoglobulin (Ig) G1/IgG2a ratio and IL-4 level. Panel **a** represents IgG1/IgG2a ratio while panel **b** depicts IL-4 level. HRP-conjugated anti-mouse IgG1 and IgG2a were used to substitute the HRP-conjugated anti-mouse IgG in ELISA as described.[26] The serum samples were derived from mice 30 days post boosting. Similar results were obtained from 15 days after the boosting (data not shown). $^*P<0.05$.

As shown in Figure 9a, a reduced ratio of IgG1 and IgG2a was observed with the use of the targeted vector. We also observed lower levels of IL-4 (Figure 9b). These data, in addition to the increased levels of Th1 cytokines (IL-2 and IFN; Figure 6), suggest that the CD40-targeted immunization might have elicited a Th1-skewed immune response.

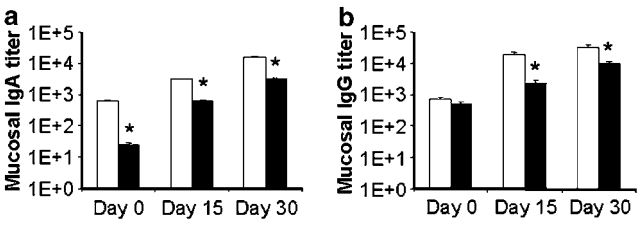

Figure 10 Detection of antibodies against Ad proteins in lung lavage in mice receiving i.n. administration of tAd-NP. The lung lavage was collected from the same group of mice as in Figure 7 and analysed for the level of antibodies against adenoviral proteins by ELISA. The antigens used in the ELISA are adenoviral lysate from Ad-E (an irrelevant Ad virus expressing a different transgene), which were purified by sucrose gradient. **(a)** Immunoglobulin (Ig) A titres, while **(b)** describes IgG levels from mice which received either Ad-NP or tAd-NP. Open bar depicts Ad-NP, while filled bar designates tAd-NP. $^*P<0.05$.

CFm40L attenuates anti-Ad vector antibody responses

We then determined whether conjugation of Ad with CFm40L could affect generation of anti-Ad antibody responses. To this end, we analysed Ad-specific IgA in lung lavage collected from the same mice immunized with tAd-NP (i.n. administration) by ELISA. We used sucrose gradient-purified Ad viral lysate derived from Ad-E (Ads expressing a different exogenous gene) as antigens in place of the NP protein in the ELISA. As shown in Figure 10, the antibody responses against the other Ad proteins were markedly suppressed in mice immunized with tAd-NP compared with that following immunization with Ad-NP. Furthermore, these data also provided additional evidence that the decreased Ag-specific antibody responses were linked to the use of CFm40L/adenoviral vectors not to the identity of the transgene, in agreement with Figures 7, 8 and Supplementary Figure S3.

Discussion

A variety of macromolecules with immunostimulatory or immunomodulatory properties have been explored in recent years as molecular adjuvants to enhance the efficiency of genetic vaccination and/or gene therapy in pre-clinical and clinical settings.[1,27] CD40L, a member of the tumor necrosis factor superfamily, is a very attractive candidate since it can potently activate DCs, which express CD40 and are well known to be professional antigen-presenting cells.[27–32] Numerous studies reported in the literatures revealed that administration of the model antigens together with CD40L or DNA constructs expressing fusion proteins comprised of the antigen and CD40L resulted in substantial enhancement of cellular (type I) and humoral (type II) immune responses.[15–17,33–36] Three lines of evidences prompted us to conduct the current studies. First, it was noted that data are lacking from systematic analyses of CD40L/viral vector in terms of biodistribution, toxicity and immunogenicity. Second, although enhanced immune responses were observed, knowledge remains poor regarding the outcome following an alternative route, that is i.n. administration. It is noteworthy that Ad has been found to be effective for mucosal delivery due to the natural tropism of Ads for mucosal surfaces.[2] Third, although cellular immune responses appeared to be markedly improved with the

use of CD40L as adjuvant, conflicting results have been observed for humoral responses with the use of protein- and DNA-based administrations. In this report, a head-to-head comparison between the unmodified Ad5 (Ad) and CD40-targeted Ad5 (tAd) was conducted in terms of biodistribution and immune responses.

Biodistribution of tAd following intravascular administration

As expected from *in vitro* transduction assay, the adaptor protein CFm40L, comprised of human Ad receptor CAR fused to mouse CD40L, noticeably altered the pattern of tissue distribution of the viruses *in vivo*, with predominant deposition of the viruses detected in the liver, spleen, thymus and lung (Figure 2). Such an altered biodistribution pattern is unlikely due to detargeting of CAR since modified adenoviral vectors ablated for CAR have been shown to have an overall reduced efficiency of gene expression in tissues but not a change of biodistribution pattern.[36,37] In contrast, we found the expression levels of transgenes delivered by the two vectors were comparable in certain tissues such as liver and spleen (i.v. administration). Furthermore, we observed the thymus and lung took up more tAd than Ad, a fact that also differs from the detargeting of CAR following i.v. administration.[36,38] These data suggest that the altered biodistribution pattern is due to CD40 targeting rather than detargeting of CAR.

The higher expression of tAd in lung may suggest the likely presence of abundant CD40(+) cells in these organs. It has been shown that epithelial/endothelial cells and antigen-presenting cells (DCs, activated monocytes and B cells) are CD40(+).[39] The presence of these CD40(+) cells in the lung may suggest that the innate host defences are well in place to fend off invading pathogens from the air. It is interesting that under normal circumstances the lung is not the major tissue/organ that takes up unmodified Ad following intravascular administration (Figure 2a). The pulmonary intravascular macrophages, however, can take up unexpectedly high amounts of the Ad5 virus in animals with hepatic disorders, such as cirrhosis, resulting in severe pulmonary pathology.[5] Clearly, better understanding of the biodistribution of both unmodified and modified Ad vector is of importance, given that such knowledge helps understand the clearance of virus vector as well as identify the tissues/organs, which could be predisposed to adverse events during the course of gene therapy.[5,40]

Biodistribution of tAd following i.n. administration

As a result of comparison between Ad and tAd following i.n. administration, it appears that the inadvertent infection of central nervous system (CNS) is mediated by the CAR receptor but not other receptors, such as $\alpha_v\beta$ integrin, and heparin sulphate glycosaminoglycans, which were shown to mediate the entry of Ads.[36,41,42] As discussed above, inadvertent infection of the CNS by live viral vectors could be a safety concern if the vectors are given i.n.[43,44] Moreover, we observed visible lesions of the lungs, especially the airway epithelial cells, in mice receiving unmodified Ad-NP. Such deleterious effects of Ad-NP were apparently caused by strong local inflammatory reactions as suggested by a massive infiltration of lymphocytes and macrophages. Yet, no such exaggerated local inflammatory reactions were observed in mice receiving tAd-NP. At this time, we have no definite explanation for the marked differences of local inflammatory reactions between Ad-NP and tAd-NP. Yet, it is interesting to note that we and others reported that the SARS-CoV NP protein itself, used in this study as model antigen, could alter cellular signal transduction pathways, stimulate pro-inflammatory cytokine production and/or even cell death.[45,46] Therefore, the excessive inflammatory reactions or toxicity induced by Ad-NP are likely due to the combined immunostimulatory or immunopathologic effects of Ad infection and NP protein. This notion is also supported by the observation that Ad-Luc failed to induce the same magnitude of local inflammatory reactions (Figure 5b).

Ag-specific immune responses

The substantially increased production of Ag-specific IL-2 and IFN-γ with the use of tAd-NP at later time points was largely expected since ligation of CD40 has been suggested to promote the activation and antigen-presenting functions of DCs, which express CD40 and are well known to initiate immune response.[39] Interestingly, at early time points the levels of Ag-specific IL-2 and IFN-γ were rather comparable between the unmodified and targeted vector groups. At later time points, however, the levels of these two cytokines remain elevated with the use of targeted vectors, accompanied by the lower level of IL-4 and the reduced ratio of IgG1/IgG2a. Whether the more sustained IL-2 and IFN-γ responses with the use of targeted vectors were due to a better development of memory T-cell compartment would require further investigation. It is of note, however, that CD40 stimulation has been shown to facilitate the development of memory T-cell compartment[39,47–49] under other experimental conditions.

The markedly delayed Ag-specific mucosal and systemic antibody responses with the use of CFm40L adaptor proteins were somewhat surprising, given the fact that most reports in the literature suggest that CD40L activates both cellular and humoral immune responses against antigens delivered in the form of proteins or DNA constructs.[15–19] However, our findings are in partial agreement with two studies demonstrating CD40L lacks stimulatory effects on the production of Ag-specific antibodies.[17,50] It is unlikely that the biased immune responses reported here were linked to the identity of the transgene as similar observations (more sustained IL-2 and IFN-γ but reduced antibody titres at later time points) were observed with both tAd-NP and tAd-Luc (Supplementary Figure S3). In addition, the use of tAd resulted in decreased antibody levels against other adenoviral proteins (Figure 10). However, since both transgenes in this current study (SARS-CoV NP and firefly luciferase) were intracellular proteins, it remains to be determined whether tAd encoding a secreted transgene would result in a similar pattern of immune responses. It is noted, however, others recently reported in a different system (soluble proteins) that CD40-targeted secreted proteins failed to generate a stronger antibody response compared with the untargeted secreted proteins.[17] At this time, we think a variety of factors could be ascribed to the differences of results with respect to the patterns of immune responses among

various groups. One of them might be due to the differences in the vector systems. It is understood that ours is the only study employing live viral vector in conjunction with CD40L, while other systems were designed to deliver the antigens in the form of DNA plasmid, soluble proteins or virus-like particles.[15–19] Second, the biased immune response might be due to a much lower level of transgene expression with the use of tAd vector at the site of the body receiving the viral vectors. For instance, as compared with Ad, ~300-fold less transgene expression in the injection site skin (Figures 3a and b) was observed following i.d. injection of tAd, while about 180-fold less in the lungs 3 days after i.n. administration (Figures 4a and b). In general, Ag-specific humoral responses are not preferentially elicited in response to smaller amounts of antigens as compared with cellular immune responses. Third, the tAd-induced biased immune responses could be tAd interacting with B cells. There are previous reports documenting that CD40 ligation could lead to largely positive growth outcomes for resting B cells, but inhibited the growth and Ig production of activated B cells which are also known to be CD40(+).[39,51–53] Given these findings, caution appears to be warranted when considering CD40L as targeting moiety for adenoviral vectors in genetic immunization when induction of humoral immune response is crucial, that is, neutralizing antibodies against pathogens. Nevertheless, therapeutic manipulation to facilitate biased or skewed immune responses could be beneficial in clinical applications. For instance, type 2-biased immune responses (predominant antibody reactions) may be associated with certain immunopathologic complications, such as allergy, asthma and autoimmune diseases. Thereby, redirection of the immune response or therapeutic manipulation towards a biased immune response, that is suppression of antibody responses, could help reverse medical conditions related to certain immunopathologic complications.[38,54] Furthermore, enhanced cellular immune responses are well known to play critical roles eliminating or containing certain intracellular pathogens and cancers.[10–12,28,41] Finally, as preliminary data presented in this report, the efficient *in vitro* gene transduction by tAd even in the presence of anti-Ad neutralizing antibodies and lower levels of antibodies against Ad viral proteins *in vivo* might also help allay one of the major concerns associated with pre-existing immunity against Ad. We are currently conducting more in-depth *in vivo* studies to address these issues.

Materials and methods

Reagents

Anti-CD40 mAb, rh-IL-4, recombinant human granulocyte-macrophage colony-stimulating factor (rhGM-CSF), the ELISPOT kits with various controls, including IFN-γ (EL485) and IL-2 (EL402), were purchased from R&D systems, Minneapolis, MN, USA. Bright-Glo luciferase assay system was obtained from Promega, Madison, WI, USA. Unless specified, other antibodies and peroxidase-conjugated secondary antibodies were purchased from Cedarlane Labs (Burlington, Ontario, Canada).

Production, purification and characterization of CFm40L adaptor protein

The adaptor protein, CFm40L, is a fusion protein that consists of human Ad receptor CAR fused to mouse CD40L via a trimerization motif. CFm40L was constructed and used to target Ad vectors to mouse DCs expressing CD40.[9] CFm40L was purified from the supernatants in stable HEK293 cells transfected with the expression vector. The production and purification of CFm40L was described previously.[9] Briefly, the stable cell line producing CFm40L as a secreted protein was cultured in DMEM:F12 (1:1) medium supplemented with 10% fetal calf serum, 2 mM L-glutamine, 100 $\mu g\ ml^{-1}$ G_{418} and 40 $\mu g\ ml^{-1}$ gentamicin sulphate. The medium from the CFm40L-expressing 293 cell cultures were collected and the proteins were precipitated by addition of an equal volume of cold-saturated ammonium sulphate. The precipitates were then collected by centrifugation and dissolved in 1/20 of the original medium volume in phosphate-buffered saline (PBS), followed by dialysis against PBS. The recombinant CFm40L protein was purified from the dialysed protein solution by immobilized metal affinity chromatography using cobalt-immobilized TALON affinity resin (Clontech, Mountain View, CA, USA). The purity of the adaptor protein was confirmed by Coomassie blue staining and western blotting.[9]

Construction and production of recombinant Ads

All transgenes were cloned into adenoviral transfer vector, Ad5.[9] The vector expressing SARS-CoV NP[45] was used here as a model antigen. The isogenic control vector expressing the luciferase gene was constructed similarly. Replication defective recombinant Ads were generated from the constructed transfer vectors as described.[9] Transgene expression by recombinant Ads was confirmed by luciferase activity assay or by western blot analysis with anti-SARS N-protein antibody. Ad particles were purified by CsCl gradient centrifugation and titrated as plaque-forming units (PFU) per ml using Adeno-X Rapid Titer kit according to the manufacturer's instructions (BD Biosciences, San Jose, CA, USA).

DC culture, Ad infection and luciferase activity assay

Myeloid DCs were obtained from AllCELLS, Emeryville, CA, USA. Over 80% of these monocyte-derived cells are CD40(+) in addition to other surface markers including CD1a, CD11c, CD86 and HL-DR. We previously reported elevated levels of maturation markers (CD11c, CD54, CD40, CD80, CD86) in DCs treated with CFm40L-targeted Ad,[9] consistent with other studies which show that CD40 stimulation could facilitate DC maturation.[1,39] The DCs were cultured in RPMI-1640 medium containing rh-IL-4 and rhGM-CSF (1×10^5 cells per well in 24-well plates) for 4 days prior to being subjected to treatments with Ads. The preparation of the tAd-Luc (Ad-5 encoding luciferase gene and conjugated with CFm40L) and infection of DCs *in vitro* were described previously.[9] In brief, Ad expressing luciferase genes (Ad-Luc) was pre-mixed with the CFm40L adaptor protein and incubated at 37 °C for 30 min and then used to infect DCs at 50 PFU per cell. After 2 days of infection, the cells were harvested to measure luciferase activity using Bright-Glo luciferase assay system.

Biodistribution and pathological examination

Female Balb/c mice were purchased from Charles River Lab, Montreal, Quebec, Canada. All animal experiments were conducted in accordance with the guidelines and protocols for animal experiments at Health Canada. The mice were maintained in a laminar airflow cabinet under pathogen-free conditions and used at 6–7 weeks of age. A total of 1×10^9 PFU ($\sim 1 \times 10^{10}$ viral particles) of Ads suspended in 100 μl of PBS per mouse was administrated using a syringe with a 29-gauge needle by i.v. (tail veil), intradermal (i.d.) (inguinal) or i.n. routes. Control mice were injected with 100 μl of PBS. The preparation of Ads complexed with CFm40L was described previously.[9] In brief, the same amounts of Ads was mixed with 16 μg CFm40L (that is 80 ng CFm40L/5×10^6 PFU Ads) in 100 μl of PBS and incubated at 37 °C for 30 min. The mice were killed on days 3 and 7 after administration of Ads, with tissues collected for subsequent analyses of biodistribution. The levels of luciferase activity, normalized by protein concentration, were determined. Five mice were used in each group. Pathological examination of tissues using hematoxylin and eosin staining method was conducted using a standard procedure.

Isolation of splenocyte and ELISPOT assay for the measurement of cytokines

To determine the adjuvant effects of CFm40L, non-modified Ad expressing the SARS-CoV NP protein (Ad-NP) was compared with the same virus complexed with CFm40L (tAd-NP) following either i.d. or i.n. administration, with tAd-Luc serving as the baseline control. We chose the same amount of virus as in the above biodistribution experiments. For immunization, five mice were primed with 1×10^{10} VP of Ad-NP, tAd-NP or tAd-Luc (negative control). Thirty days post administration, the mice were boosted once. The splenocytes were isolated on days 0, 15 and 30 post boosting for the determination of IFN-γ and IL-2. Splenocytes were isolated from mouse spleens by grinding them between the frosted ends of two microscope slides. The slides were rinsed with 5 ml of RPMI 1640 medium to collect the cells. Afterwards, the cell suspension was passed through a fine nylon mesh to obtain a single cell suspension. The spleen pieces were then gently mashed with the rubber end of a syringe plunger. A second filtration was then performed by pipetting the 5 ml suspensions of dispersed cells through a fresh 70-μm nylon mesh cell strainer into a 50-ml conical tube (on ice). This procedure was repeated with additional washes of 5 ml medium until the splenic capsules turned white (3–4 more times). The total volume of cell suspension was brought up to 20 ml with medium. Cell pellets were then obtained by centrifugation at 400 g for 5 min at 4 °C. About 1 ml of 0.84% NH_4Cl solution was used to lyse the red blood cells. The tubes were gently rolled by hand for 2 min at room temperature, followed by the addition of 30 ml of chilled RPMI medium After passing the cells through another layer of 70-μm nylon mesh, cells were collected by centrifugation at 400 g for 5 min at 4 °C. The pellet was then gently resuspended to 2×10^6 cells per 100 μl (2×10^7 cells per ml) in RPMI 1640 containing 10% heat-inactivated fetal bovine serum in the presence of 10 purified SARS-CoV NPs (10 μg ml^{-1}) to stimulate Ag-specific cytokine.[43] As stimulation with NP of splenocytes derived from the control animals receiving Ad-Luc did not result in any detectable production of cytokines (background), all subsequent experiments were conducted in the presence of 10 μg ml^{-1} of NP. These cells were then used at 100 μl per well for ELISPOT assays using procedures as provided by the supplier, R&D system.

Determination of Ag-specific antibody responses and IgG 1/IgG 2a ratio

ELISA was conducted to determine the titre of antibodies against the SARS-CoV NP protein. To this end, the Nunc 96-well plates were coated with the 100 μl of NP protein at 5 μg ml^{-1} in 50 mM carbonate buffer (pH 8.6) and incubated at 4 °C overnight. The wells were then washed five times with PBS, 0.05% Tween-20, followed by the addition of blocking buffer comprised of PBS, 0.05% Tween-20 and 5% BSA. After incubation at 37 °C for 1 h, the blocking buffer was removed, followed by the addition of samples of serum or washing fluids of the lung from the mice. The plates were incubated again at 37 °C for 1 h. Afterwards, secondary antibodies (peroxidase-conjugated goat anti-mouse IgG, IgM or IgA) were added at concentrations recommended by the supplier (Cedarlane Labs). Following an additional incubation at 37 °C for 1 h, the plates were washed five times before *o*-phenylenediamine dihydrochloride (OPD) was added for colorimetric development. The positive controls (mouse anti-SARS monoclonal antibodies) were purchased from BD Pharmingen, San Diego, CA, USA). The cut-off was defined as mean of five negative samples (from un-immunized control) plus two s.d. For the determination of relative levels of transgene (NP)-specific IgG subclasses, anti-mouse IgG1 and IgG2a conjugated with HRP (Cedarlane Labs) were substituted for anti-mouse IgG-HRP prior to the addition of OPD for colorimetric development.[26]

Statistical analysis

Results are presented with the means ± s.d. Statistical comparisons were conducted with the use of a two-tailed Student's *t*-test, with $P < 0.05$ being considered to be significant.

Acknowledgements

Mary Hefford, Remy Aubin, and Terry Cyr (Health Canada) are acknowledged for discussions and technical consultations. Anthony Ridgway and Habiba Chakir (Health Canada) are thanked for comments. Matt LeBrun (Health Canada), Todd Cutts (Public Health Agency of Canada) and Rhonda Kuolee (National Research Council of Canada) are acknowledged for technical assistance. We thank Frank Yin for statistical analyses.

Disclosure/conflicts of interest

The authors declare no conflict of financial interests. This research was funded by Canadian Regulatory Strategy for Biotechnology. AVP and DTC are supported in part by DOD—W81XWH-05-0035, NIH/NCI—5P01CA104177, and NIH/NIAID—5 U54 AIO57157-04.

References

1 Noureddini SC, Curiel DT. Genetic targeting strategies for adenovirus. *Mol Pharm* 2005; **2**: 341–347.
2 Santosuosso M, McCormick S, Xing Z. Adenoviral vectors for mucosal vaccination against infectious diseases. *Viral Immunol* 2005; **18**: 283–291.
3 Okada N, Masunaga Y, Okada Y, Mizuguchi H, Iiyama S, Mori N *et al*. Dendritic cells transduced with gp100 gene by RGD fiber-mutant adenovirus vectors are highly efficacious in generating anti-B16BL6 melanoma immunity in mice. *Gene Therapy* 2003; **10**: 1891–1902.
4 Cichon G, Schmidt HH, Benhidjeb T, Loser P, Ziemer S, Haas R *et al*. Intravenous administration of recombinant adenoviruses causes thrombocytopenia, anemia and erythroblastosis in rabbits. *J Gene Med* 1999; **1**: 360–371.
5 Smith JS, Tian J, Muller J, Byrnes AP. Unexpected pulmonary uptake of adenovirus vectors in animals with chronic liver disease. *Gene Therapy* 2004; **11**: 431–438.
6 Rea D, Havenga MJ, van Den Assem M, Sutmuller RP, Lemckert A. Highly efficient transduction of human monocyte-derived dendritic cells with subgroup B fiber-modified adenovirus vectors enhances transgene-encoded antigen presentation to cytotoxic T cells. *J Immunol* 2001; **166**: 5236–5244.
7 Worgall S, Busch A, Rivara M, Bonnyay D, Leopold PL, Merritt R *et al*. Modification to the capsid of the adenovirus vector that enhances dendritic cell infection and transgene-specific cellular immune responses. *J Virol* 2004; **78**: 2572–2580.
8 Brandao JG, Scheper RJ, Lougheed SM, Curiel DT, Tillman BW, Gerritsen WR *et al*. CD40-targeted adenoviral gene transfer to dendritic cells through the use of a novel bispecific single-chain Fv antibody enhances cytotoxic T cell activation. *Vaccine* 2003; **21**: 2268–2272.
9 Pereboev AV, Nagle JM, Shakhmatov MA, Triozzi PL, Matthews QL, Kawakami Y *et al*. Enhanced gene transfer to mouse dendritic cells using adenoviral vectors coated with a novel adapter molecule. *Mol Ther* 2004; **9**: 712–720.
10 Mackey MF, Gunn JR, Maliszewsky C, Kikutani H, Noelle RJ, Barth Jr RJ. Dendritic cells require maturation via CD40 to generate protective antitumor immunity. *J Immunol* 1998; **161**: 2094–2098.
11 Schoenberger SP, Toes RE, van der Voort EI, Offringa R, Melief CJ. T-cell help for cytotoxic T lymphocytes is mediated by CD40-CD40L interactions. *Nature* 1998; **393**: 480–483.
12 Bennett SR, Carbone FR, Karamalis F, Flavell RA, Miller JF, Heath WR. Help for cytotoxic-T-cell responses is mediated by CD40 signalling. *Nature* 1998; **393**: 478–480.
13 Shayakhmetov DM, Eberly AM, Li ZY, Lieber A. Deletion of penton RGD motifs affects the efficiency of both the internalization and the endosome escape of viral particles containing adenovirus serotype 5 or 35 fiber knobs. *J Virol* 2005; **79**: 1053–1061.
14 Nakamura T, Sato K, Hamada H. Reduction of natural adenovirus tropism to the liver by both ablation of fiber-coxsackievirus and adenovirus receptor interaction and use of replaceable short fiber. *J Virol* 2003; **77**: 2512–2521.
15 Tripp RA, Jones L, Anderson LJ, Brown MP. CD40 ligand (CD154) enhances the Th1 and antibody responses to respiratory syncytial virus in the BALB/c mouse. *J Immunol* 2000; **164**: 5913–5921.
16 Ninomiya A, Ogasawara K, Kajino K, Takada A, Kida H. Intranasal administration of a synthetic peptide vaccine encapsulated in liposome together with an anti-CD40 antibody induces protective immunity against influenza A virus in mice. *Vaccine* 2002; **20**: 3123–3129.
17 Stone GW, Barzee S, Snarsky V, Kee K, Spina CA, Yu XF *et al*. Multimeric soluble CD40 ligand and GITR ligand as adjuvants for human immunodeficiency virus DNA vaccines. *J Virol* 2006; **80**: 1762–1772.
18 Ito D, Ogasawara K, Iwabuchi K, Inuyama Y, Onoe K. Induction of CTL responses by simultaneous administration of liposomal peptide vaccine with anti-CD40 and anti-CTLA-4 mAb. *J Immunol* 2000; **164**: 1230–1235.
19 Lu Z, Yuan L, Zhou X, Sotomayor E, Levitsky HI, Pardoll DM. CD40-independent pathways of T cell help for priming of CD8(+) cytotoxic T lymphocytes. *J Exp Med* 2000; **191**: 541–550.
20 Hemminki A, Wang M, Desmond RA, Strong TV, Alvarez RD, Curiel DT. Serum and ascites neutralizing antibodies in ovarian cancer patients treated with intraperitoneal adenoviral gene therapy. *Hum Gene Ther* 2002; **13**: 1505–1514.
21 Tao N, Gao GP, Parr M, Johnston J, Baradet T, Wilson JM *et al*. Sequestration of adenoviral vector by Kupffer cells leads to a nonlinear dose response of transduction in liver. *Mol Ther* 2001; **3**: 28–35.
22 Zinn KR, Douglas JT, Smyth CA, Liu HG, Wu Q, Krasnykh VN *et al*. Imaging and tissue biodistribution of 99mTc-labeled adenovirus knob (serotype 5). *Gene Therapy* 1998; **5**: 798–808.
23 Wood M, Perrotte P, Onishi E, Harper ME, Dinney C, Pagliaro L *et al*. Biodistribution of an adenoviral vector carrying the luciferase reporter gene following intravesical or intravenous administration to a mouse. *Cancer Gene Ther* 1999; **6**: 367–372.
24 Groot-Wassink T, Aboagye EO, Wang Y, Lemoine NR, Reader AJ, Vassaux G. Quantitative imaging of Na/I symporter transgene expression using positron emission tomography in the living animal. *Mol Ther* 2004; **9**: 436–442.
25 Rock KL, Shen L. Cross-presentation: underlying mechanisms and role in immune surveillance. *Immunol Rev* 2005; **207**: 166–183.
26 Kim JJ, Nottingham LK, Sin JI, Tsai A, Morrison L, Oh J *et al*. CD8 positive T cells influence antigen-specific immune responses through the expression of chemokines. *J Clin Invest* 1998; **102**: 1112–1124.
27 Calarota SA, Weiner DB. Enhancement of human immunodeficiency virus type 1-DNA vaccine potency through incorporation of T-helper 1 molecular adjuvants. *Immunol Rev* 2004; **199**: 84–99.
28 Ridge JP, Di Rosa F, Matzinger P. A conditioned dendritic cell can be a temporal bridge between a CD4+ T-helper and a T-killer cell. *Nature* 1998; **393**: 474–478.
29 Dubois B, Vanbervliet B, Fayette J, Massacrier C, Van Kooten C, Briere F *et al*. Dendritic cells enhance growth and differentiation of CD40-activated B lymphocytes. *J Exp Med* 1997; **185**: 941–951.
30 Clark EA. Regulation of B lymphocytes by dendritic cells. *J Exp Med* 1997; **185**: 801–803.
31 Fayette J, Dubois B, Vandenabeele S, Bridon JM, Vanbervliet B, Durand I *et al*. Human dendritic cells skew isotype switching of CD40-activated naive B cells towards IgA1 and IgA2. *J Exp Med* 1997; **185**: 1909–1918.
32 Cella M, Scheidegger D, Palmer-Lehmann K, Lane P, Lanzavecchia A, Alber G. Ligation of CD40 on dendritic cells triggers production of high levels of interleukin-12 and enhances T cell stimulatory capacity: T-T help via APC activation. *J Exp Med* 1996; **184**: 747–752.
33 Mendoza RB, Cantwell MJ, Kipps TJ. Immunostimulatory effects of a plasmid expressing CD40 ligand (CD154) on gene immunization. *J Immunol* 1997; **159**: 5777–5781.
34 Gurunathan S, Irvine KR, Wu CY, Cohen JI, Thomas E, Prussin C *et al*. CD40 ligand/trimer DNA enhances both humoral and cellular immune responses and induces protective immunity to infectious and tumor challenge. *J Immunol* 1998; **161**: 4563–4571.
35 Staveley-O'Carroll K, Schell TD, Jimenez M, Mylin LM, Tevethia MJ, Schoenberger SP *et al*. *In vivo* ligation of CD40 enhances priming against the endogenous tumor antigen and promotes CD8+ T cell effector function in SV40 T antigen transgenic mice. *J Immunol* 2003; **171**: 697–707.

36 Koizumi N, Kawabata K, Sakurai F, Watanabe Y, Hayakawa T, Mizuguchi H. Modified adenoviral vectors ablated for coxsackievirus-adenovirus receptor, alpha V integrin, and heparan sulfate binding reduce *in vivo* tissue transduction and toxicity. *Hum Gene Ther* 2006; **17**: 264–279.
37 Leissner P, Legrand V, Schlesinger Y, Hadji DA, Van Raaij M, Cusack S *et al*. Influence of adenoviral fiber mutations on viral encapsidation, infectivity and *in vivo* tropism. *Gene Therapy* 2001; **8**: 49–57.
38 Sherer Y, Gorstein A, Fritzler MJ, Shoenfeld Y. Autoantibody explosion in systemic lupus erythematosus: more than 100 different antibodies found in SLE patients. *Semin Arthritis Rheum* 2004; **34**: 501–537.
39 van Kooten C, Banchereau J. CD40-CD40 ligand. *J Leukoc Biol* 2000; **67**: 2–17.
40 Manickan E, Smith JS, Tian J, Eggerman TL, Lozier JN, Muller J *et al*. Rapid Kupffer cell death after intravenous injection of adenovirus vectors. *Mol Ther* 2006; **13**: 108–117.
41 Hong SS, Karayan L, Tournier J, Curiel DT, Boulanger PA. Adenovirus type 5 fiber knob binds to MHC class I alpha2 domain at the surface of human epithelial and B lymphoblastoid cells. *EMBO J* 1997; **16**: 2294–2306.
42 Dechecchi MC, Melotti P, Bonizzato A, Santacatterina M, Chilosi M, Cabrini G. Heparan sulfate glycosaminoglycans are receptors sufficient to mediate the initial binding of adenovirus types 2 and 5. *J Virol* 2001; **75**: 8772–8780.
43 Lemiale F, Kong WP, Akyurek LM, Ling X, Huang Y, Chakrabarti BK *et al*. Enhanced mucosal immunoglobulin A response of intranasal adenoviral vector human immunodeficiency virus vaccine and localization in the central nervous system. *J Virol* 2003; **77**: 10078–10087.
44 Franklin R, Quick M, Haase G. Adenoviral vectors for *in vivo* gene delivery to oligodendrocytes: transgene expression and cytopathic consequences. *Gene Therapy* 1999; **6**: 1360–1367.
45 He R, Leeson A, Andonov A, Li Y, Bastien N, Cao J *et al*. Activation of AP-1 signal transduction pathway by SARS coronavirus nucleocapsid protein. *Biochem Biophys Res Commun* 2003; **311**: 870–876.
46 Nicholls JM, Butany J, Poon LL, Chan KH, Beh SL, Poutanen S *et al*. Time course and cellular localization of SARS-CoV nucleoprotein and RNA in lungs from fatal cases of SARS. *PLoS Med* 2006; **3**: e27.
47 Hawiger D, Inaba K, Dorsett Y, Guo M, Mahnke K, Rivera M *et al*. Dendritic cells induce peripheral T cell unresponsiveness under steady state conditions *in vivo*. *J Exp Med* 2001; **194**: 769–779.
48 Bonifaz LC, Bonnyay DP, Charalambous A, Darguste DI, Fujii S, Soares H *et al*. *In vivo* targeting of antigens to maturing dendritic cells via the DEC-205 receptor improves T cell vaccination. *J Exp Med* 2004; **199**: 815–824.
49 Schjetne KW, Fredriksen AB, Bogen B. Delivery of antigen to CD40 induces protective immune responses against tumors. *J Immunol* 2007; **178**: 4169–4176.
50 Skountzou I, Quan FS, Gangadhara S, Ye L, Vzorov A, Selvaraj P *et al*. Incorporation of glycosylphosphatidylinositol-anchored granulocyte-macrophage colony-stimulating factor or CD40 ligand enhances immunogenicity of chimeric simian immunodeficiency virus-like particles. *J Virol* 2007; **81**: 1083–1094.
51 Rothstein TL, Wang JK, Panka DJ, Foote LC, Wang Z, Stanger B *et al*. Protection against Fas-dependent Th1-mediated apoptosis by antigen receptor engagement in B cells. *Nature* 1995; **374**: 163–165.
52 Majlessi L, Bordenave G. Role of CD40 in a T cell-mediated negative regulation of Ig production. *J Immunol* 2001; **166**: 841–847.
53 Erickson LD, Durell BG, Vogel LA, O'Connor BP, Cascalho M, Yasui T *et al*. Short-circuiting long-lived humoral immunity by the heightened engagement of CD40. *J Clin Invest* 2002; **109**: 613–620.
54 Schilizzi BM, Boonstra R, The TH, de Leij LF. Effect of B-cell receptor engagement on CD40-stimulated B cells. *Immunology* 1997; **92**: 346–353.

Supplementary Information accompanies the paper on Gene Therapy website (http://www.nature.com/gt)

Adenovirus Tumor Targeting and Hepatic Untargeting by a Coxsackie/Adenovirus Receptor Ectodomain Anti–Carcinoembryonic Antigen Bispecific Adapter

Hua-Jung Li,[1] Maaike Everts,[2] Larisa Pereboeva,[2] Svetlana Komarova,[2] Anat Idan,[2] David T. Curiel,[2] and Harvey R. Herschman[1]

[1]Departments of Biological Chemistry and Molecular and Medical Pharmacology, David Geffen School of Medicine at University of California at Los Angeles, Los Angeles, California and [2]Division of Human Gene Therapy, Departments of Medicine, Obstetrics and Gynecology, Pathology, Surgery, and the Gene Therapy Center, University of Alabama at Birmingham, Birmingham, Alabama

Abstract

Adenovirus vectors have a number of advantages for gene therapy. However, because of their lack of tumor tropism and their preference for liver infection following systemic administration, they cannot be used for systemic attack on metastatic disease. Many epithelial tumors (e.g., colon, lung, and breast) express carcinoembryonic antigen (CEA). To block the natural hepatic tropism of adenovirus and to "retarget" the virus to CEA-expressing tumors, we used a bispecific adapter protein (sCAR-MFE), which fuses the ectodomain of the coxsackie/adenovirus receptor (sCAR) with a single-chain anti-CEA antibody (MFE-23). sCAR-MFE untargets adenovirus-directed luciferase transgene expression in the liver by >90% following systemic vector administration. Moreover, sCAR-MFE can "retarget" adenovirus to CEA-positive epithelial tumor cells in cell culture, in s.c. tumor grafts, and in hepatic tumor grafts. The sCAR-MFE bispecific adapter should, therefore, be a powerful agent to retarget adenovirus vectors to epithelial tumor metastases. [Cancer Res 2007;67(11):5354–61]

Introduction

Gene therapy presents a novel therapeutic approach for the treatment of cancer, in which corrective or toxin genes are delivered to neoplastic cells. Many gene therapy strategies, however, are limited due to the lack of "effective gene delivery" (efficient and specific delivery of genes to the target cell). Both non-viral and viral vectors for gene therapy have been proposed. Several viral species have been adapted for gene delivery purposes (e.g., retrovirus, herpes simplex virus, and adenovirus). Adenovirus vectors have several characteristics that make them attractive gene delivery vehicles: high levels of transgene expression, large DNA insertion capacity, high stability *in vivo*, and low pathogenicity in humans. However, therapeutic application of adenovirus vectors is currently limited to i.t. delivery for local/regional neoplastic disease; current generation adenovirus gene delivery vectors cannot achieve selective transgene delivery to tumor cells *in vivo*.

Adenovirus binding to target cell surfaces is mediated by interaction between virus fiber protein "knob" domains and cellular coxsackie/adenovirus receptors (CAR; refs. 1–3). Hepatocytes express high CAR levels; consequently, i.v. adenovirus vector administration results in extensive liver infection, which can lead to liver toxicity (4–6). In contrast, most human tumor cells produce relatively low CAR levels. Moreover, tumor cells with low CAR levels are often more invasive and have greater propensity to metastasize (7, 8). The differential expression of CAR between cancer cells and normal cells makes it difficult to target tumors with adenovirus vectors. Thus, both hepatic CAR-dependent binding resulting in liver infection and reduced tumor cell infection by adenovirus are serious limitations to systemic use of adenovirus vectors for therapy of metastatic disease. Application of cancer gene therapy approaches for disseminated disease will require adenovirus modifications to allow selective transgene delivery, based upon tumor targeting, in combination with virus untargeting for liver.

One method to selectively target adenovirus vector transgene expression to tumors is "transductional untargeting and retargeting," in which the virus particle is physically prevented from binding to CAR on normal cells and simultaneously redirected to receptors expressed preferentially or exclusively on tumor cells. To achieve transductional targeting, bispecific adapter molecules have been developed. Bispecific adapters bind with one domain to the virus, usually the "knob" of the viral fiber protein, thereby blocking native tropism, and bind with their other domain to target receptors, thus bridging the adenovirus vector with the target cell. Bispecific adapters also mediate infectivity via CAR-independent cellular pathways. Both sCAR, the soluble CAR ectodomain, and antibodies to the adenovirus fiber knob have been used as "untargeting" components of bispecific adapters (9–13). Ligands for cell surface receptors [e.g., fibroblast growth factor-2, epidermal growth factor (EGF), folate] and antibodies to cell surface antigens are used as "retargeting" components of bispecific adapters (9–11, 14). Transductional targeting of adenovirus vectors to cell receptors/antigens with bispecific adapters facilitates increased adenovirus infectivity, both *in vitro* (9, 11, 14–17) and, most importantly, *in vivo* (15, 18, 19).

Carcinoembryonic antigen (CEA), a cell surface antigen, is expressed in nearly all colorectal cancer tumors, in 70% of non–small-cell lung cancers, and in 50% of breast cancers. In contrast, CEA expression is substantially restricted in normal adult tissues; there is little or no detectable CEA expression in the liver. Bispecific adapters with a CEA-binding domain should untarget adenovirus vectors from normal tissues and retarget them to CEA-positive tumors. MFE-23, a single-chain antibody with high affinity for CEA, is currently in phase I studies both as an imaging agent for radioimmunoguided surgery and as a tumor-targeting agent for antibody-directed enzyme prodrug therapy (20–22). To retarget CEA-positive cells, MFE-23 has been fused to sCAR to form sCAR-MFE, a bispecific transductional reagent. sCAR-MFE successfully

Requests for reprints: Harvey R. Herschman, Molecular Biology Institute, University of California at Los Angeles, 341 Boyer Hall, 611 Charles E. Young Drive East, Los Angeles, CA 90095. Phone: 310-825-8735; Fax: 310-825-1447; E-mail: hherschman@mednet.ucla.edu.

doi:10.1158/0008-5472.CAN-06-4679

targets adenovirus to cells that express CEA (19). sCAR-MFE should therefore be useful in retargeting adenovirus vectors to CEA-positive hepatic metastases. In this report, we show that sCAR-MFE can dramatically reduce hepatic infection following systemic administration and can redirect adenoviral gene therapy vectors to CEA-positive epithelial tumor cells in cell culture, in s.c. tumor grafts, and in hepatic tumor grafts.

Materials and Methods

Cell culture. AML12 cells were from the American Type Culture Collection. MC38 and MC38-cea-2 cells (23) were provided by Dr. Jeffrey Schlom (NIH). A427 and H2122 cells were provided by Dr. Steven Dubinett (University of California at Los Angeles). LS174T cells were provided by Dr. Anna Wu (University of California at Los Angeles). AML12, LS174T, MC38, and MC38-cea-2 were grown in DMEM (Life Technologies) containing 10% fetal bovine serum (FBS; Cellegro) with penicillin-streptomycin (Life Technologies), 0.1 mmol/L nonessential amino acids (Life Technologies), and 1.0 mmol/L sodium pyruvate (Life Technologies). A427 and H2122 were grown in RPMI 1640 (Life Technologies) containing 10% FBS with penicillin-streptomycin.

Virus construction and production. The adenovirus vector encoding firefly luciferase (fLuc) under transcriptional control of the constitutively active cytomegalovirus (CMV) promoter Ad.CMVfLuc was constructed as described by Liang et al. (24). Ad.CMVgfp, an adenovirus in which the green fluorescent protein (GFP) is expressed from the CMV promoter, was a gift from Dr. Sanjiv Gambhir (Stanford University). Virus was prepared in 293 cells by double cesium chloride (CsCl) gradient centrifugation. Cells were infected in medium containing 2% FBS. After overnight incubation, cells were shifted to medium containing 10% serum and incubated until a total cytopathic effect was observed. Cells were harvested, frozen, and thawed thrice, and virus was purified using standard CsCl purification methods. Viral particle number was determined by measuring absorbance at 260 nm, using a conversion factor of 1.1×10^{12} viral particles (vp) per absorbance unit. Viral titers were determined with the Adeno-X Rapid Titer kit (BD Clontech). "vp" is used to indicate virus particles when considering virus mass interactions with bispecific adapter; "pfu" (for plaque forming units) is used when viral infectivity is described.

Stable transfection. To establish stable cell lines that over express *Renilla* luciferase (rLuc) or red fluorescence protein (RFP), LS174T cells were transfected with pcDNA3 expression vectors encoding rLuc or RFP and a neomycin selectable marker, using LipofectAMINE 2000 (Invitrogen). Neomycin-resistant cells were selected using medium containing G418 (1 mg/mL). G418-resistant cells were screened for rLuc expression with the Luciferase assay system (Promega) or for RFP by fluorescence microscopy.

Immunoblot analysis. Cells were washed twice with PBS and incubated on ice for 10 min in lysis buffer containing 50 mmol/L Tris-HCl (pH 7.4), 1% NP40, 1% Triton X-100, 1% sodium deoxycholate, 150 mmol/L NaCl, 1 mmol/L EDTA, and protease inhibitors (Complete Tablet; Roche). After 10,000 × *g* centrifugation for 10 min, supernatant protein concentrations were measured with the Bio-Rad Protein Assay (Bio-Rad). To examine CEA protein expression, protein extracts were denatured in loading buffer. To examine the expression of CAR protein, the protein extracts were heated at 37°C for 10 min in non-reducing conditions before loading. Equal amounts of protein (30 μg) were loaded on SDS-polyacrylamide gels (8% for CEA and 12% for CAR) for electrophoresis. Proteins were subsequently transferred to nitrocellulose membranes. The membranes were probed with anti-CEA antibody, cT84.66 (1:10,000 dilution; ref. 25), anti-CAR antibody (RmcB; 1:2,000 dilution; Upstate Biologicals), or anti-14-3-3θ antibody (1:3,000 dilution; Santa Cruz Biotechnology) overnight at 4°C followed by incubation at room temperature for 60 min with horseradish peroxidase–conjugated secondary antibody. Immunoreactivity was determined by enhanced chemiluminescence (Amersham).

Immunofluorescence staining. Cells were seeded in four-well chamber slides (1×10^5 per chamber) and cultured overnight. Anti-CEA primary antibody cT84.66 (1:1,000) was added for 60 min at room temperature. Antibody was aspirated, and cells were fixed (37% formaldehyde diluted 1:10 with PBS) for 20 min. After aspirating, cells were washed thrice with washing buffer [1 mmol/L $CaCl_2$, 140 mmol/L NaCl, 3 mmol/L KCl, and 25 mmol/L Tris-Cl (pH 7.4)] for 10 min. Cells were incubated for 20 min with blocking buffer [3% dry milk, 0.1% Triton X-100, 1 mmol/L $CaCl_2$, and 50 mmol/L Tris-Cl (pH 7.5)]. After aspirating, cells were incubated with FITC-conjugated goat anti-human IgG secondary antibody (1:500 dilution in blocking buffer; Jackson ImmunoResearch) for 30 min in the dark. After incubation, cells were washed thrice for 10 min with washing buffer. Fluorescence was observed with a Zeiss AIOSKOP fluorescence microscope.

Adenovirus untargeting and retargeting on cultured cell lines. sCAR-MFE was constructed and produced as described by Everts et al. (19). Ad.CMVfLuc or Ad.CMVgfp (3×10^8 vp) were mixed with sCAR-MFE (1.3 mg/mL) in concentrations ranging from 0 to 500 ng in 0.5 μL and incubated for 60 min at room temperature. The sCAR-MFE:Ad complexes were diluted to 150 μL with medium containing 2% FBS and then added to cell monolayers in 24-well plates (2×10^5 per well). Virus-treated cells were incubated at 37°C for 90 min. Medium was aspirated, and cells were washed with PBS. After a 40-h incubation at 37°C in medium containing 10% FBS, cells were lysed, and luciferase activity was measured. Ad.CMVgfp-infected cells were observed using fluorescence microscopy. For competition experiments, recombinant CEA (rCEA) protein (Protein Sciences Corp.) and albumin (Sigma) were added to the cultures immediately before addition of [Ad.CMVfLuc][sCAR-MFE].

Adenovirus untargeting and retargeting on mixed cell cultures. Ad.CMVfLuc (1.2×10^9 vp) was mixed with sCAR-MFE (500 ng) or PBS (control) and incubated for 60 min at room temperature. To mimic hepatic tumor metastasis, plates containing LS174T(RFP) cell colonies were seeded with mouse hepatocyte–derived AML12 cells in six-well plates. Mixtures containing Ad.CMVfLuc and [Ad.CMVfLuc][sCAR-MFE] were diluted to 600 μL with medium supplemented with 2% FBS and added to the mixed cell cultures. After incubation at 37°C for 90 min, virus-containing media were aspirated, and the cells were washed with PBS. After a 40-h incubation in medium, fLuc-mediated bioluminescence and RFP fluorescence were observed with an IVIS Optical Imaging System (Xenogen). Before imaging, culture medium was replaced with PBS. Cells were first scanned for 10 s to obtain an RFP fluorescence image. D-Luciferin (150 μg/mL; Xenogen) was then added to the wells, and repeated 1-min bioluminescence scans were acquired until maximum photon accumulation in a 1-min period was obtained.

Systemic adenovirus administration to measure hepatic untargeting. For *in vivo* transductional hepatic untargeting studies, 5×10^8 pfu per mouse Ad.CMVfLuc or [Ad.CMVfLuc][sCAR-MFE] were administered by tail vein injection. Before the injection, viruses were incubated for 1 h either with sCAR-MFE or with PBS. Injection volumes were 100 μL in all cases. On the 3rd day after virus administration, the mice were injected i.p. with D-luciferin (250 μL; ~125 mg/kg body weight) and scanned to image adenovirus-directed fLuc activity. Immediately after imaging, mice were sacrificed, and the livers were removed and imaged for fLuc (adenovirus dependent) bioluminescence. After optical imaging, liver extracts were prepared and assayed for fLuc activity.

Adenovirus untargeting and retargeting following i.t. injection in s.c. tumor grafts. MC38 and MC38-cea-2 s.c. tumors were prepared in nude mice (*nu/nu*; Charles River Laboratories) by mixing 2×10^6 cells in 50 μL of PBS with Matrigel (50 μL; BD Biosciences) and injecting the mixtures s.c. into the flanks. Each mouse received MC38 cells on one flank and MC38cea-2 cells on the opposite flank. When tumors reached ~0.5 cm in diameter (in 11–14 days), Ad.CMVfLuc (1×10^8 pfu; about 5×10^9 vp) or [Ad.CMVfluc][sCAR-MFE] (3 μg) in 20 μL was injected into the centers of tumors. Three days after i.t. virus injection, the mice were anesthetized with ketamine/xylazine (80/4 mg/kg; Phoenix Pharmaceutical), injected i.p. with D-luciferin (250 μL; ~125 mg/kg body weight), and imaged with the Xenogen Optical Imaging System. Sequential 1-min scans were collected until maximum photon accumulation in a 1-min period was obtained. After optical imaging, mice were sacrificed. Luciferase activity in tumor extracts was measured, and protein concentrations were determined with the Bio-Rad Protein Assay (Bio-Rad).

Adenovirus untargeting and retargeting following i.v. injection of mice carrying hepatic tumor grafts. Eight-week-old (*nu/nu*) nude mice were anesthetized with ketamine/xylazine (100/10 mg/kg). A transverse incision was made across the xyphoid process and extended ~2 cm. MC38 and MC38-cea-2 cells (1×10^6 per mouse) in 15 μL were injected into the front of the left upper liver lobe, using a 27-gauge needle. The lobe was returned to the abdomen, and the incision was closed with sutures and wound clips. Buprenorphine was administered every 12 h for 48 h. Wound clips were removed after 5 days. Experiments were done 5 days after surgery. For transductional untargeting and retargeting, 5×10^8 pfu per mouse of AdCMVfLuc or [Ad.CMVfLuc][sCAR-MFE] in 100 μL were administered by tail vein injection. Before injection, viruses were incubated for 1 h either with 10 μg sCAR-MFE per mouse or with PBS. Mice were sacrificed on the 4th day after virus injection. Tumor and liver extracts were prepared and assayed for luciferase activity.

Bioluminescence quantitation. Bioluminescence images were analyzed with Living Image software version 2.20 (Xenogen). Regions of interest (ROI) were drawn over the tumor or liver area, and total photons of the ROI were calculated. ROI in all images of an experiment were kept with a consistent area (24).

Statistical analysis. All experiments were done at least in triplicate. Data are presented as means ± SE and compared by Student's *t* test.

Results

sCAR-MFE increases adenovirus infection of CEA-positive cells. To evaluate the retargeting efficacy of sCAR-MFE to CEA-positive, CAR-expressing tumor cells, we used cell lines with differing levels of CEA and CAR expression. Levels of CEA and CAR protein in various cell lines were determined by immunoblotting (Fig. 1*A*). CEA protein is not detectable in MC38, AML12, and A427 cells. LS174T and H2122 express a 180-kDa full-length CEA protein; MC38-cea-2 expresses a 70-kDa truncated CEA isoform (23). CAR is detectable by Western blotting in A427 and LS174T cells but not in H2122 cells. Thus, human A427 cells have relatively high hCAR levels but low CEA protein; LS174T and H2122 cells have intermediate and low CAR expression and express CEA protein.

To retarget cells with recombinant bispecific adapters, the retargeting protein must be expressed on the cell surface. The cell surface location of CEA was confirmed by immunofluorescence on unfixed cells. Cell surface staining with anti-CEA antibody is observed for MC38-cea-2, LS174T, and H2122 cells; no CEA is detectable on MC38, AML12, or A427 cells (Fig. 1*B*).

To initially evaluate sCAR-MFE targeting efficacy, cells were infected with Ad.CMVfLuc, an adenovirus carrying a *fLuc* reporter gene driven by the CMV promoter, and pre-incubated either with incubation buffer or with a single concentration of sCAR-MFE. fLuc activity of the cell extracts reflects the degree of virus infection. Prior incubation with sCAR-MFE increased Ad.CMVfLuc infectivity between 5- and 55-fold for CEA-positive MC38-cea-2 ($P < 0.01$), H2122 ($P < 0.01$), and LS174T ($P < 0.05$) cells but did not increase infection of CEA-negative MC38 and A427 cells (Fig. 1*C*).

To determine an optimal sCAR-MFE:Ad ratio for retargeting efficacy, AdCMVfLuc virus was incubated with various amounts of

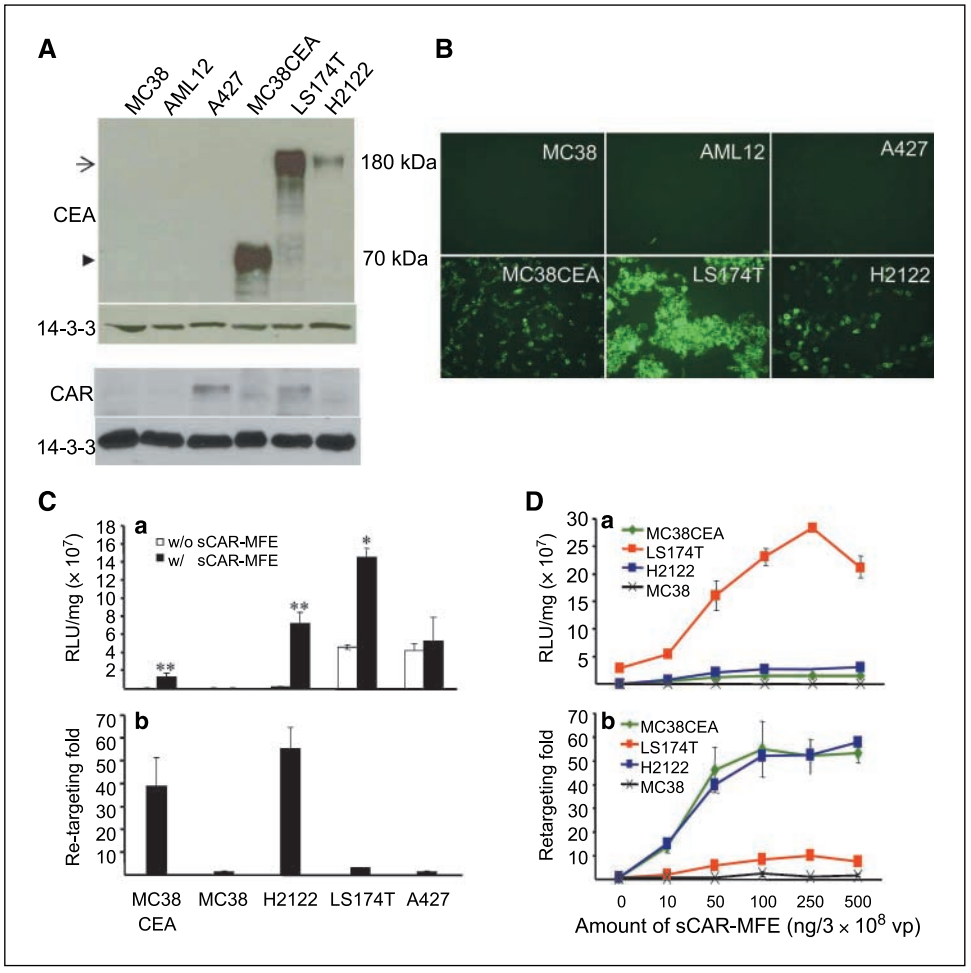

Figure 1. sCAR-MFE increases adenovirus infection of CEA-positive cells. *A,* CEA and CAR protein levels expressed in cell lines, analyzed by Western blotting. 14-3-3 was used as a loading control. *Arrow,* full-length CEA; *arrowhead,* truncated CEA. *B,* cell surface CEA expression. Unfixed cells were incubated with anti-CEA antibody to detect CEA on the cell surface. *C,* adenovirus targeting with sCAR-MFE in CEA-positive and CEA-negative cell lines. The cell lines were infected with Ad.CMVfLuc (3×10^8 vp per well) or with [Ad.CMVfLuc][sCAR-MFE] (50 ng) as described in Materials and Methods. Cell extracts were assayed for fLuc activity and protein concentration. Luciferase activities (*a*); fold increases in luciferase activity by sCAR-MFE targeting (*b*). *Columns,* averages for four cultures; *bars,* SE. *, $P < 0.05$; **, $P < 0.01$, for cells infected with [Ad.CMVfLuc][sCAR-MFE] versus cells infected with Ad.CMVfLuc. *D,* titration of sCAR-MFE retargeting activity on cell lines expressing varying CEA levels. Ad.CMVfLuc (3×10^8 vp per well) was pre-incubated with increasing amounts of sCAR-MFE (0–500 ng). Cells were then infected with the viral preparations. Cell extracts were assayed for luciferase activity and protein concentration. *Points,* averages of four cultures; *bars,* SE. Luciferase activity (*a*); fold increase in luciferase activity by sCAR-MFE retargeting (*b*).

sCAR-MFE before addition to cultured cells. sCAR-MFE:Ad retargeting is optimal at ~100 ng sCAR-MFE per 3×10^8 vp. At this ratio, sCAR-MFE can increase the Ad.CMVfLuc infectivity ~50-fold on MC38-cea-2 and H2122 cells and 10-fold on LS174T cells (Fig. 1*D*).

To show the specificity of sCAR-MFE retargeting to CEA-positive cells, the ability of rCEA protein to block retargeting was examined. Increasing concentrations of rCEA protein, but not albumin, can block sCAR-MFE–mediated retargeting of Ad.CMVfLuc infection to MC38-cea-2 (CEA positive) and LS174T (CEA positive) cells (Fig. 2). In contrast, rCEA protein has no effect on Ad.CMVfLuc infection of MC38 (CEA negative) cells.

sCAR-MFE untargets adenovirus from CAR-positive, CEA-negative cells and retargets adenovirus to CEA-positive cells. To visualize sCAR-MFE untargeting and retargeting in cultured cells, we used Ad.CMVgfp, an adenovirus in which the CMV promoter drives GFP. A427, LS174T, and H2122 cells were infected with Ad.CMVgfp or Ad.CMVgfp pre-incubated with sCAR-MFE. For A427 cells, which express high hCAR levels and low CEA levels (Fig. 1*A*), sCAR-MFE *reduces* Ad.CMVgfp infection (Fig. 3*A, a* and *b*). In contrast, for LS174T and H2122 cells, which express CEA, sCAR-MFE pre-incubation substantially *increases* infection by Ad.CMVgfp (Fig. 3*A, c–f*). Thus, sCAR-MFE can untarget adenovirus from CAR-mediated infection and can retarget adenovirus to CEA-positive cells.

To show the ability of sCAR-MFE to specifically target CEA-positive cells in the presence of CAR-positive cells, Ad.CMVgfp retargeting was done with a mixture of CEA-positive and CEA-negative cells. Mixtures of CAR-positive, CEA-negative A427 cells and CEA-positive LS174T cells expressing RFP, LS174T(RFP), were infected with Ad.CMVgfp (Fig. 3, *a–c*) or [Ad.CMVgfp][sCAR-MFE] (Fig. 3, *d–f*). Red fluorescence identifies LS174T(RFP) cells in the cell mixture (Fig. 3*B*, *a* and *d*); green fluorescence identifies Ad.CMVgfp-infected cells (Fig. 3*B*, *b* and *e*). The RFP and GFP images are merged in Fig. 3*c* and *f*. Ad.CMVgfp preferentially infects A427 cells, which express a high level of CAR and a low level of CEA protein, and does not infect LS174T(RFP) cells, which have low CAR levels and high CEA levels, very well (Fig. 3*B*, *a–c*). In contrast, [Ad.CMVgfp][sCAR-MFE] preferentially infects LS174T(RFP) cells in the A427/LS174T(RFP) mixtures (Fig. 3*B*, *d–f*). Thus, in cell mixtures, sCAR-MFE can both untarget adenovirus from CAR-positive cells and retarget the virus to CEA-positive cells.

To more closely model hepatic metastases in cell culture, we created colonies of LS174T(RFP) cells in a lawn of transformed mouse hepatocyte AML12 cells. LS174T(RFP) colonies were grown on culture dishes. The remaining space was filled with CEA-negative AML12 cells to mimic surrounding liver tissue (Fig. 3*C*, *a* and *d*). The cell cultures were infected either with Ad.CMVfLuc or [Ad.CMVfLuc][sCAR-MFE]. Location of LS174T(RFP) colonies was observed by RFP optical imaging (Fig. 3*C*, *b* and *e*). Following luciferin addition to the cultures, bioluminescence indicates the degree of Ad.CMVfLuc infection (Fig. 3*C*, *c* and *f*). Comparing ROI bioluminescence and fluorescence measurements of the LS174T(RFP) colonies infected with Ad.CMVfLuc and [Ad.CMVfluc][sCAR-MFE] shows that sCAR-MFE transductional retargeting increases Ad.CMVfLuc infectivity 6-fold for CEA-positive LS174T(RFP) colonies cultured in the presence of AML12 cells (Fig. 3*D*).

sCAR-MFE retargets adenovirus to CEA-positive s.c. tumor grafts. CEA-negative MC38 cells were injected s.c. in the left flanks of nude mice, and CEA-positive MC38-cea-2 cells were injected in the right flanks. Because adenovirus injected systemically does not reach s.c. tumors effectively (data not shown), Ad.CMVfLuc or [Ad.CMVfLuc][sCAR-MFE] (20 μL) were injected i.t. when the tumors reached ~0.5 cm in diameter. Three days later, the mice were anesthetized, injected with D-luciferin, and imaged to monitor bioluminescence.

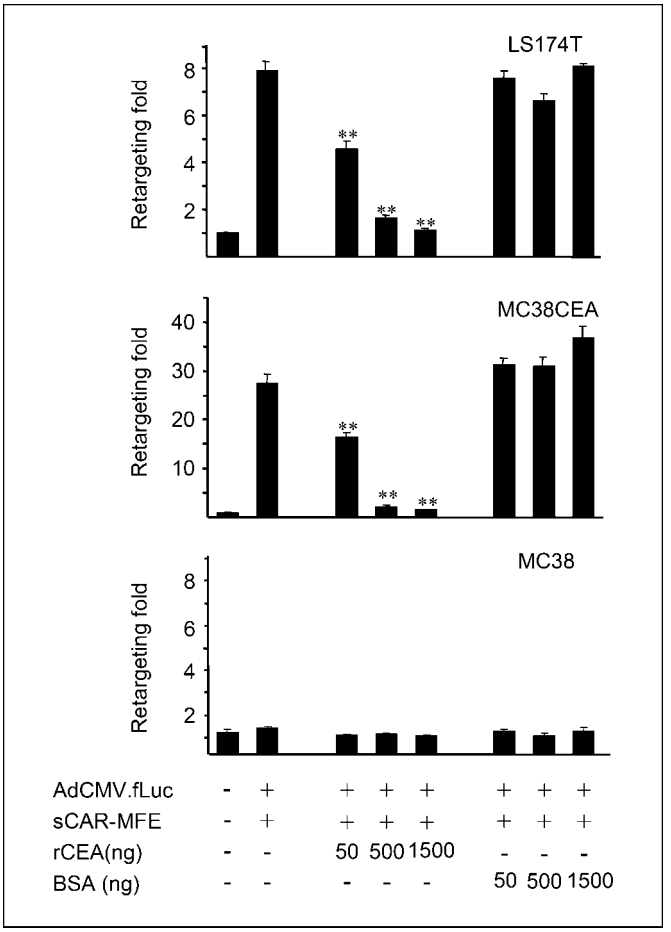

Figure 2. CEA blocks sCAR-MFE–directed retargeting of adenovirus infection to CEA-positive cells. LS174T (CEA^+), MC38-cea-2 (CEA^+), and MC38 (CEA^-) cells were infected with AdCMVfLuc (3×10^8 vp per well) or with [Ad.CMVfLuc][sCAR-MFE] (100 ng) in the presence of increasing amounts of recombinant CEA or bovine serum albumin (*BSA*). Cell extracts were assayed for fLuc activity and protein concentration. Fold retargeting is the ratio of luciferase activity in the presence of sCAR-MFE relative to activity in cells infected with Ad.CMVfLuc. *Columns,* averages ($n = 4$); *bars,* SE. **, $P < 0.01$, comparing the fold retargeting in the cells infected by [Ad.CMVfLuc][sCAR-MFE] in the absence versus the presence of rCEA.

CEA-negative MC38 tumors and CEA-positive MC38-cea-2 tumors injected with Ad.CMVfLuc show essentially equivalent virus infection (Fig. 4*A, top*). CEA-negative MC38 tumors injected with [Ad.CMVfLuc][sCAR-MFE] show substantially reduced (untargeted) bioluminescence when compared with MC38 tumors injected with Ad.CMVfLuc (compare tumors on the left flank in Fig. 4*A, bottom* with tumors on the left flank in Fig. 4*A, top*). In contrast, CEA-positive MC38-cea-2 tumors expressed substantially more bioluminescence following [Ad.CMVfluc][SCAR-MFE] injection than following Ad.CMVfLuc injection (compare tumors on the right flank in Fig. 4*A, bottom* with tumors on the right flank in Fig. 4*A, top*).

The tumor untargeting and retargeting results from quantitative ROI analyses of bioluminescence data obtained from the living

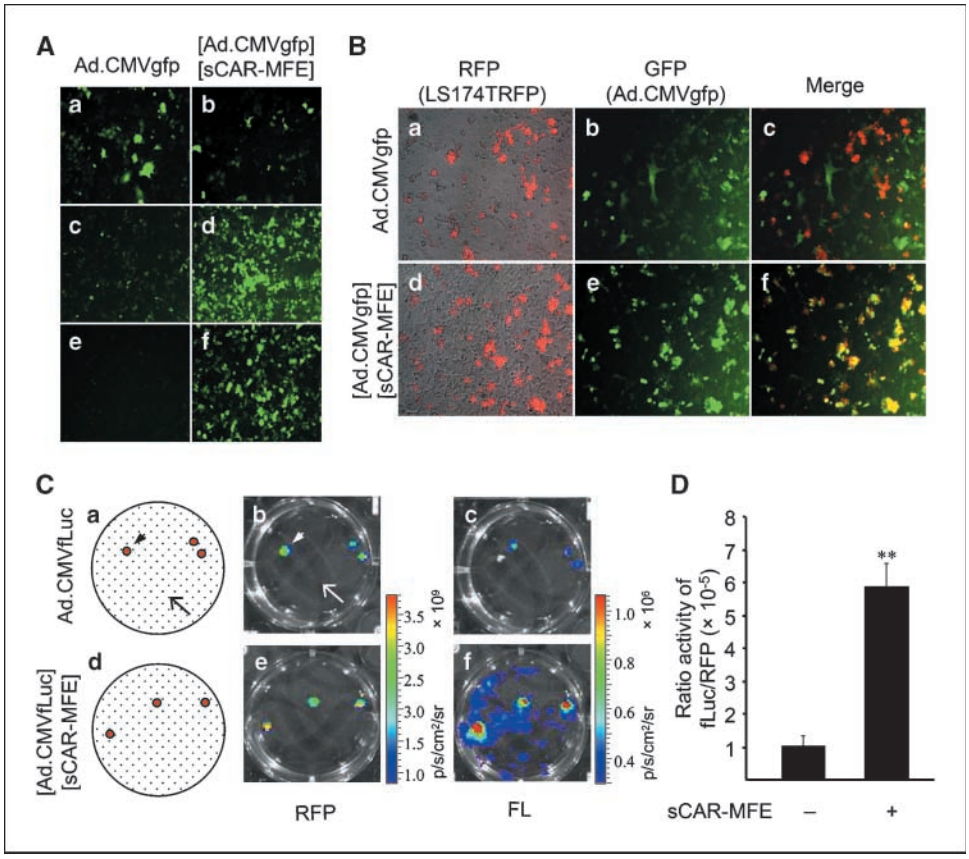

Figure 3. sCAR-MFE untargets adenovirus from CAR-positive cells and retargets adenovirus to CEA-positive cells. *A,* sCAR-MFE untargets CAR-dependent adenovirus infection and retargets infection to CEA-positive cells. Tumor cells were infected with Ad.CMVgfp or with [Ad.CMVgfp][sCAR-MFE]. GFP fluorescence reflects viral infection. *B,* adenovirus is untargeted by sCAR-MFE from CAR-positive, CEA-negative cells and retargeted to CEA-positive cells in cell mixtures. LS174T(RFP) CEA^+ cell and A427 CEA^- cell mixtures were infected with Ad.CMVgfp or [Ad.CMVgfp][sCAR-MFE]. Red fluorescence reflects RFP expression in the LS174T(RFP) cells; green fluorescence reflects Ad.CMVgfp infection. *Yellow signal,* colocalization of GFP and RFP fluorescence (*c* and *f*). *C,* adenovirus is targeted to CEA-positive colonies by sCAR-MFE. Colonies of LS174T(RFP) CEA^+ cells (*arrowheads*) in a monolayer of AML12 CEA^- cells (*arrows*) were infected with Ad.CMVfLuc or [Ad.CMVfLuc][sCAR-MFE]. RFP fluorescence and luciferin-dependent bioluminescence were monitored with a CCD camera. RFP fluorescence shows LS174T(RFP) colonies; fLuc (FL) bioluminescence reflects Ad.CMVfLuc infection. *D,* Quantitation of RFP fluorescence and luciferase activity for colonies (*C*). ROIs for each colony were kept constant for fluorescent and bioluminescent analyses. Luciferase activity, measured by bioluminescence, was normalized by the RFP fluorescent ROI data for each colony. *Columns,* averages; *bars,* SE. **, $P < 0.01$.

mice are displayed in Fig. 4*B* (*top*). Following optical imaging, the mice were sacrificed. Tumors were excised, and extracts were assayed for fLuc activity, using a conventional *in vitro* assay. The "untargeting" effect of sCAR-MFE on CEA-negative MC38 cells and the "retargeting" effect on CEA-positive MC38-cea-2 cells, using data from the conventional luciferase assay, are shown in Fig. 4*B* (*c* and *d*). sCAR-MFE significantly reduces Ad.CMVfLuc infection of CEA-negative MC38 tumors. In contrast, SCAR-MFE increases Ad.CMVfLuc infection of CEA-positive MC38-cea-2 tumors ~12-fold. sCAR-MFE thus untargets adenovirus infection of CEA-negative s.c. tumors and retargets adenovirus infection of CEA-positive tumors following i.t. injection.

sCAR-MFE untargets adenovirus from liver. To examine the efficacy of sCAR-MFE hepatic untargeting, Ad.CMVfLuc and [Ad.CMVfLuc][sCAR-MFE] were injected systemically via the tail vein into groups of three mice. Three days after viral injection, the mice were anesthetized, injected i.p. with D-luciferin, and imaged. Immediately following imaging, mice were sacrificed, and the livers were removed and imaged (Fig. 5*A*). The livers were then homogenized, and extracts were assayed by conventional luciferase assays. Adenovirus-mediated, luciferin-dependent bioluminescence was quantitated from the hepatic CCD images (Fig. 5*B, a*) and from the conventional luciferase assays (Fig. 5*B, b*). Hepatic Ad.CMVfLuc infection following i.v. administration is decreased ~80% to 90%

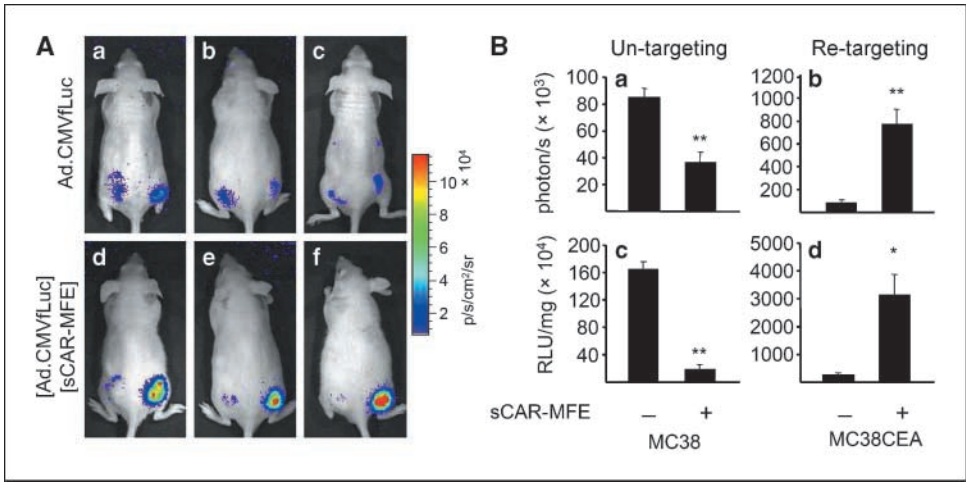

Figure 4. Adenovirus infection is decreased in CEA-negative MC38 s.c. tumors and increased in CEA-positive MC38-cea-2 s.c. tumors by sCAR-MFE, following i.t. injection. *A,* MC38 (left flank) and MC38-cea-2 (right flank) s.c. tumors were injected with Ad.CMVfLuc (1×10^8 pfu per tumor; *top*) or [Ad.CMVfLuc][sCAR-MFE] (3 μg per tumor; *bottom*). Luciferin-dependent bioluminescence was imaged 3 days after virus administration. *B,* quantitation of luciferase activity from the tumors of (*A*). Luciferase activity was quantitated from ROIs of the tumors (*a* and *b*). After bioluminescent imaging, the mice were sacrificed; tumor extracts were prepared; and luciferase activity was assayed by conventional assays (*c* and *d*). *Columns,* averages ($n = 3$); *bars,* SE. *, $P < 0.05$; **, $P < 0.01$, comparing tumors injected with Ad.CMFfLuc versus [Ad.CMVfLuc][sCAR-MFE].

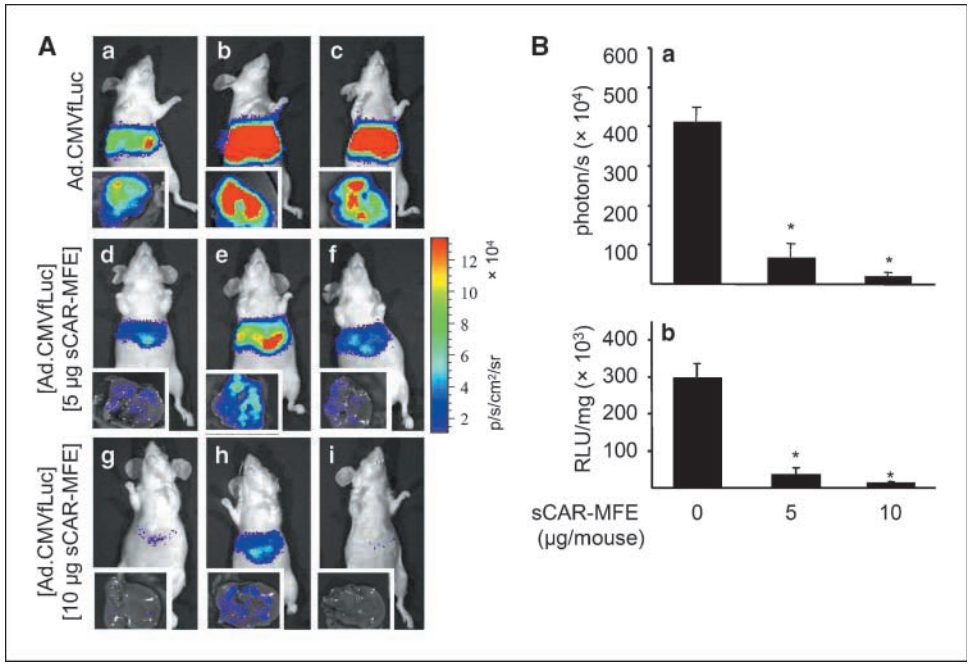

Figure 5. sCAR-MFE hepatic untargeting of adenovirus injected i.v. *A,* Ad.CMVfLuc (5×10^8 pfu per mouse; *a–c*), [Ad.CMVfLuc][sCAR-MFE] (5 μg per mouse; *d–f*), and [Ad.CMVfLuc][sCAR-MFE] (10 μg per mouse; *g–i*) were injected by tail vein into groups of three mice. The living mice and their isolated livers were imaged by bioluminescence 3 d after virus injection. *B,* quantitation of luciferase activity from the livers of (*A*). After imaging, liver extracts were prepared. Luciferase activity was quantitated by ROI analysis of luciferin-dependent bioluminescent activity in (*a*) and by conventional luciferase assays of liver extracts (*b*). *Columns,* averages ($n = 3$); *bars,* SE. *, $P < 0.05$, comparing mice injected with Ad.CMFfLuc versus [Ad.CMVfLuc][sCAR-MFE].

by 5 μg per mouse of sCAR-MFE and ~95% to 97% by 10 μg per mouse of sCAR-MFE.

sCAR-MFE retargets systemically administered adenovirus to CEA-positive hepatic tumor grafts. To show effective Ad.CMVfLuc retargeting to CEA-positive tumors following systemic virus administration, we used mice bearing hepatic grafts of MC38 and MC38-cea-2 tumors. Five days after tumor cell injection into the liver, mice were injected i.v. with Ad.CMVfLuc or [Ad.CMVfLuc][sCAR-MFE] (10 μg). Four days later, mice were sacrificed, and tumor and liver extracts were assayed for luciferase activity. Liver infectivity is reduced ~80% by sCAR-MFE untargeting for mice carrying both MC38-cea-2 and MC38 tumors (Fig. 6, *a* and *b*). A nearly 2-fold increase in Ad.CMVfLuc infection of MC38-cea-2 tumors occurs if sCAR-MFE is used for virus retargeting (Fig. 6, *a*). In contrast, sCAR-MFE reduces Ad.CMVfLuc infection of hepatic MC38 hepatic tumors (Fig. 6, *b*), presumably as a result of sCAR-MFE untargeting of CAR-dependent infection of the tumor cells.

The combined effect of CAR-dependent hepatic untargeting and CEA-dependent MC38-cea-2 tumor retargeting by sCAR-MFE, as determined by the tumor/liver luciferase activity ratio, is ~10-fold (Fig. 6, *c*). sCAR-MFE–mediated untargeting of both liver and MC38 tumor is essentially equivalent; consequently, the tumor/liver infectivity ratio is not altered by sCAR-MFE (Fig. 6, *d*).

Discussion

In this report, we show effective tumor cell gene delivery using an adapter retargeted adenovirus, both in cell culture and in tumor graft models. Specifically, we have employed an sCAR-based fusion adapter system to achieve vector retargeting. In addition to tumor cell–selective enhanced targeting, this recombinant adapter also accomplished liver untargeting of the adenovirus gene delivery vector. Given the overwhelming natural hepatotropism of adenovirus, liver untargeting is particularly noteworthy. Indeed, liver untargeting provides the major practical basis for improved "target cell specificity" *in vivo* for adenoviral vectors, ablating the major site of vector sequestration. Consequently, tumor retargeting with sCAR-based fusion adapters should be simultaneously coupled with reduction of potentially limiting liver-associated vector toxicities. The combination of tumor retargeting and liver

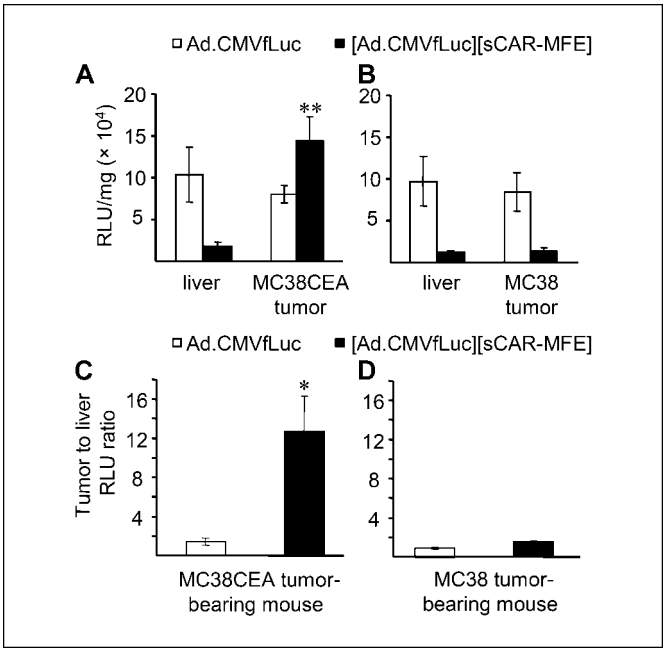

Figure 6. Adenovirus infection is untargeted in liver and MC38 hepatic tumors but increased in MC38-cea-2 hepatic tumors, following i.v. injection with sCAR-MFE. Mice bearing MC38-cea-2 (*A*) and MC38 (*B*) hepatic tumors were injected i.v. with Ad.CMVfLuc (5×10^8 pfu per mouse) or [Ad.CMVfLuc][sCAR-MFE] (10 μg per mouse). Four days later, mice were sacrificed, and luciferase activity and protein concentration were determined in tumor and liver extracts. *C* and *D,* tumor/liver luciferase ratios following injection with Ad.CMVfLuc (*open columns*) and [Ad.CMVfLuc][sCAR-MFE] (*closed columns*). *Columns,* averages ($n = 4$); *bars,* SE. *, $P < 0.05$, comparing tumor/liver luciferase ratios for infection by [Ad.CMVfLuc][sCAR-MFE] versus infection by AdCMVfLuc; **, $P < 0.01$, for luciferase activity in MC38-cea-2 tumors versus liver following systemic infection with [Ad.CMVfLuc][sCAR-MFE].

untargeting allows a dramatic enhancement of the targeting index achievable *in vivo* via adenovirus vectors.

The key accomplishment of our study is the achievement of tumor-selective targeting in combination with liver untargeting. In the first instance, the sCAR adapter molecule provides a functional cross-link between the adenovirus particle and a target "receptor" on the tumor cell. In particular, the sCAR-MFE adapter places the anti-CEA scFv tumor-targeting moiety at the natural locus of cellular recognition within the adenovirus capsid. The adapter thus allowed viral-target cell interaction to occur primarily on the basis of the association of MFE with CEA. We have previously shown successful targeting of adenovirus vectors to CEA artificially expressed in murine pulmonary vasculature, using sCAR-MFE as an adapter molecule (19). The data presented herein show successful targeting to CEA expressing tumors, both *in vitro* and *in vivo*. Our previous studies with sCAR-EGF retargeting of adenovirus to EGF-expressing tumor cells, both in culture and in tumor xenografts (15), suggest that sCAR-ligand fusions are likely to be a generalizable class of reagents for properly presenting adenoviral vectors to tumor cell "receptors" *in vivo*.

Liver is the most common site of metastasis for a number of epithelial cancers. Dramatic reduction in adenovirus liver infection, >90%, is observed for sCAR-MFE adapter–treated virus following systemic i.v. infection. An 80% to 90% reduction in adenovirus liver infection, following i.v. injection of virus pre-incubated with an sCAR-EGF adapter (15), suggests that sCAR-ligand fusions are also likely to be a generalizable class of reagents for achieving substantial hepatic untargeting of systemically administered therapeutic adenovirus vectors. These results provide a strong rational for further study of sCAR adapter–based targeting methods for adenovirus vectors, particularly in the context of hepatic metastatic disease, using systemic injection as the route of administration.

The precise basis of adenovirus liver untargeting observed with the use of the adapter systems remains obscure. In this regard, it has been shown in recent years that liver uptake of adenovirus vectors is not, as first postulated, solely mediated by fiber interaction with CAR or penton interaction with integrins on hepatocytes. This was illustrated by the observation that genetic mutations that abolish both CAR and penton interactions do not eliminate liver transduction (26, 27). These results exemplify that, *in vivo*, adenovirus hepatic transduction is a complex process. For example, a major effect on adenovirus liver tropism was achieved via ablation of binding to heparan sulfate proteoglycans (27, 28). Moreover, recent observations show that systemically administered adenovirus particles can interact with serum factors that foster their uptake and sequestration by the liver. This process may be based upon the presence of serum factor binding motifs in the fiber knob (29, 30). We can speculate that the sCAR adapter molecules mask the fiber domains that otherwise interact with either heparan sulfate proteoglycans or serum factors involved in hepatic sequestration. Irrespective of the mechanism, our data with both sCAR-MFE and sCAR-EGF (15) clearly show that the adapter-based approach can effectively untarget the liver from adenovirus transduction while simultaneously promoting tumor targeting.

The demonstrations of tumor antigen selective targeting (shown here) and tumor cell receptor overexpression targeting (15) provide a clear basis to advance adenovirus-based gene therapy/virotherapy approaches for disseminated neoplastic disease. In this regard, a synergy of effect has been observed with the combination of tumor transductional targeting and tumor-enhanced transcriptional targeting. The latter modality is based upon tumor-selective promoter control methods in which gene expression is enhanced in tumors and restricted in normal tissues. Indeed, in our groups, we have improved the targeting index several orders of magnitude with this combination, in the context of pulmonary vascular endothelial–selective gene delivery (31) and ovarian cancer therapy (32). Clearly, it would thus be logical to apply next such a double targeting approach in metastatic cancer models to further build upon the gains described herein. Additionally, cancer-selective gene expression that exploits cancer-specific patterns of translation (33) has recently been reported. In this schema, the employment of selective mRNA 5′ untranslated regions can provide expression differentials between tumor and non-tumor targets. These alternate targeting technologies provide a practical basis for combinational approaches to tumor targeting of adenoviruses, to build upon the targeting gains we have shown in the current report.

Acknowledgments

Received 12/21/2006; revised 3/9/2007; accepted 3/16/2007.

Grant support: National Cancer Institute grants R01 CA84572 and P50 CA86306 (H.R. Herschman) and NIH and Department of Defense grants R01CA111569 and W81HWH-05-0035 (D.T. Curiel).

The costs of publication of this article were defrayed in part by the payment of page charges. This article must therefore be hereby marked *advertisement* in accordance with 18 U.S.C. Section 1734 solely to indicate this fact.

We thank the members of the Herschman and Curiel laboratories for helpful discussions and David Stout and the members of the University of California at Los Angeles Small Animal Imaging Shared Resource for technical advice and experimental assistance.

References

1. Louis N, Fender P, Barge A, Kitts P, Chroboczek J. Cell-binding domain of adenovirus serotype 2 fiber. J Virol 1994;68:4104–6.
2. Bergelson JM, Cunningham JA, Droguett G, et al. Isolation of a common receptor for Coxsackie B viruses and adenoviruses 2 and 5. Science 1997;275:1320–3.
3. Bergelson JM, Krithivas A, Celi L, et al. The murine CAR homolog is a receptor for coxsackie B viruses and adenoviruses. J Virol 1998;72:415–9.
4. Kass-Eisler A, Falck-Pedersen E, Elfenbein DH, Alvira M, Buttrick PM, Leinwand LA. The impact of developmental stage, route of administration and the immune system on adenovirus-mediated gene transfer. Gene Ther 1994;1:395–402.
5. Yee D, McGuire SE, Brunner N, et al. Adenovirus-mediated gene transfer of herpes simplex virus thymidine kinase in an ascites model of human breast cancer. Hum Gene Ther 1996;7:1251–7.
6. Terazaki Y, Yano S, Yuge K, et al. An optimal therapeutic expression level is crucial for suicide gene therapy for hepatic metastatic cancer in mice. Hepatology 2003;37:155–63.
7. Okegawa T, Li Y, Pong RC, Bergelson JM, Zhou J, Hsieh JT. The dual impact of coxsackie and adenovirus receptor expression on human prostate cancer gene therapy. Cancer Res 2000;60:5031–6.
8. Okegawa T, Pong RC, Li Y, Bergelson JM, Sagalowsky AI, Hsieh JT. The mechanism of the growth-inhibitory effect of coxsackie and adenovirus receptor (CAR) on human bladder cancer: a functional analysis of car protein structure. Cancer Res 2001;61:6592–600.
9. Dmitriev I, Kashentseva E, Rogers BE, Krasnykh V, Curiel DT. Ectodomain of coxsackievirus and adenovirus receptor genetically fused to epidermal growth factor mediates adenovirus targeting to epidermal growth factor receptor-positive cells. J Virol 2000;74:6875–84.
10. Pereboev AV, Asiedu CK, Kawakami Y, et al. Coxsackievirus-adenovirus receptor genetically fused to anti-human CD40 scFv enhances adenoviral transduction of dendritic cells. Gene Ther 2002;9:1189–93.
11. Douglas JT, Rogers BE, Rosenfeld ME, Michael SI, Feng M, Curiel DT. Targeted gene delivery by tropism-modified adenoviral vectors. Nat Biotechnol 1996;14:1574–8.
12. Goldman CK, Rogers BE, Douglas JT, et al. Targeted gene delivery to Kaposi's sarcoma cells via the fibroblast growth factor receptor. Cancer Res 1997;57:1447–51.
13. Gu DL, Gonzalez AM, Printz MA, et al. Fibroblast growth factor 2 retargeted adenovirus has redirected cellular tropism: evidence for reduced toxicity and enhanced antitumor activity in mice. Cancer Res 1999;59:2608–14.

14. Kashentseva EA, Seki T, Curiel DT, Dmitriev IP. Adenovirus targeting to c-erbB-2 oncoprotein by single-chain antibody fused to trimeric form of adenovirus receptor ectodomain. Cancer Res 2002;62:609–16.
15. Liang Q, Dmitriev I, Kashentseva E, Curiel DT, Herschman HR. Noninvasive of adenovirus tumor retargeting in living subjects by a soluble adenovirus receptor-epidermal growth factor (sCAR-EGF) fusion protein. Mol Imaging Biol 2004;6:385–94.
16. Haisma HJ, Pinedo HM, Rijswijk A, et al. Tumor-specific gene transfer via an adenoviral vector targeted to the pan-carcinoma antigen EpCAM. Gene Ther 1999; 6:1469–74.
17. Kelly FJ, Miller CR, Buchsbaum DJ, et al. Selectivity of TAG-72-targeted adenovirus gene transfer to primary ovarian carcinoma cells versus autologous mesothelial cells *in vitro*. Clin Cancer Res 2000;6:4323–33.
18. Reynolds PN, Zinn KR, Gavrilyuk VD, et al. A targetable, injectable adenoviral vector for selective gene delivery to pulmonary endothelium *in vivo*. Mol Ther 2000;2:562–78.
19. Everts M, Kim-Park SA, Preuss MA, et al. Selective induction of tumor-associated antigens in murine pulmonary vasculature using double-targeted adenoviral vectors. Gene Ther 2005;12:1042–8.
20. Mayer A, Tsiompanou E, O'Malley D, et al. Radioimmunoguided surgery in colorectal cancer using a genetically engineered anti-CEA single-chain Fv antibody. Clin Cancer Res 2000;6:1711–9.
21. Chester KA, Mayer A, Bhatia J, et al. Recombinant anti-carcinoembryonic antigen antibodies for targeting cancer. Cancer Chemother Pharmacol 2000;46 Suppl:S8–12.
22. Chester K, Pedley B, Tolner B, et al. Engineering antibodies for clinical applications in cancer. Tumour Biol 2004;25:91–8.
23. Robbins PF, Kantor JA, Salgaller M, Hand PH, Fernsten PD, Schlom J. Transduction and expression of the human carcinoembryonic antigen gene in a murine colon carcinoma cell line. Cancer Res 1991;51: 3657–62.
24. Liang Q, Yamamoto M, Curiel DT, Herschman HR. Noninvasive imaging of transcriptionally restricted transgene expression following intratumoral injection of an adenovirus in which the COX-2 promoter drives a reporter gene. Mol Imaging Biol 2004;6:395–404.
25. Neumaier M, Shively L, Chen FS, et al. Cloning of the genes for T84.66, an antibody that has a high specificity and affinity for carcinoembryonic antigen, and expression of chimeric human/mouse T84.66 genes in myeloma and Chinese hamster ovary cells. Cancer Res 1990;50:2128–34.
26. Martin F, Chowdhury S, Neil SJ, Chester KA, Cosset FL, Collins MK. Targeted retroviral infection of tumor cells by receptor cooperation. J Virol 2003;77:2753–6.
27. Smith TA, Idamakanti N, Rollence ML, et al. Adenovirus serotype 5 fiber shaft influences *in vivo* gene transfer in mice. Hum Gene Ther 2003;14:777–87.
28. Nicol CG, Graham D, Miller WH, et al. Effect of adenovirus serotype 5 fiber and penton modifications on *in vivo* tropism in rats. Mol Ther 2004;10:344–54.
29. Shayakhmetov DM. Binding of Adenovirus Fiber Knob to Blood Coaglation Factors Mediates CAR-independent Liver Tropism. Mol Ther 2003;7:S164–1.
30. Shayakhmetov DM, Gaggar A, Ni S, Li ZY, Lieber A. Adenovirus binding to blood factors results in liver cell infection and hepatotoxicity. J Virol 2005;79:7478–91.
31. Reynolds PN, Nicklin SA, Kaliberova L, et al. Combined transductional and transcriptional targeting improves the specificity of transgene expression *in vivo*. Nat Biotechnol 2001;19:838–42.
32. Barker SD, Dmitriev IP, Nettelbeck DM, et al. Combined transcriptional and transductional targeting improves the specificity and efficacy of adenoviral gene delivery to ovarian carcinoma. Gene Ther 2003;10:1198–204.
33. Mathis JM, Williams BJ, Sibley DA, et al. Cancer-specific targeting of an adenovirus-delivered herpes simplex virus thymidine kinase suicide gene using translational control. J Gene Med 2006;8:1105–20.

Gene Therapy (2007) 14, 1448–1460

www.nature.com/gt

ORIGINAL ARTICLE

Direct selection of targeted adenovirus vectors by random peptide display on the fiber knob

Y Miura[1], K Yoshida[1], T Nishimoto[2], K Hatanaka[1], S Ohnami[1], M Asaka[3], JT Douglas[4], DT Curiel[4], T Yoshida[1] and K Aoki[2]

[1]*Genetics Division, National Cancer Center Research Institute, Tokyo, Japan;* [2]*Section for Studies on Host-Immune Response, National Cancer Center Research Institute, Tokyo, Japan;* [3]*Department of Gastroenterology and Hematology, Graduate School of Medicine, Hokkaido University, Sapporo, Japan and* [4]*Division of Human Gene Therapy, Departments of Medicine, Obstetrics and Gynecology, Pathology and Surgery, and the Gene Therapy Center, The University of Alabama at Birmingham, Birmingham, AL, USA*

Targeting of gene transfer at the level of cell entry is one of the most attractive challenges in vector development. However, attempts to redirect adenovirus vectors to alternative receptors by engineering the capsid-coding region have shown limited success because proper targeting ligand–receptor systems on the cells of interest are generally unknown. Systematic approaches to generate adenovirus vectors targeting any given cell type need to be developed to achieve this goal. Here, we constructed an adenovirus library that was generated by a Cre-lox-mediated in vitro *recombination between an adenoviral fiber-modified plasmid library and genomic DNA to display random peptides on a fiber knob. As proof of concept, we screened the adenovirus display library on a glioma cell line and observed selection of several particular peptide sequences. The targeted vector carrying the most frequently isolated peptide significantly enhanced gene transduction in the glioma cell line but not in many other cell lines. Because the insertion of a pre-selected peptide into a fiber knob often fails to generate an adenovirus vector, the selection of targeting peptides is highly useful in the context of the adenoviral capsid. This vector-screening system can facilitate the development of a targeted adenovirus vector for a variety of applications in medicine.*

Gene Therapy (2007) **14,** 1448–1460; doi:10.1038/sj.gt.3303007; published online 16 August 2007

Keywords: *adenovirus; random peptide display; library; fiber; glioma*

Introduction

Recombinant adenovirus vectors have been widely used for gene delivery to a range of cell types and employed in a number of gene therapy approaches.[1,2] However, a selective delivery of a therapeutic gene to target cells by adenovirus vectors is precluded by the widespread distribution of the primary cellular receptors for adenoviruses.[3,4] Therefore, strategies are being developed to redirect the tropism of the adenovirus vector to permit efficient target gene delivery to specific cell types.[2]

Most of the presently used adenovirus vectors are based on the serotype 5 (Ad5). The entry of Ad5 into susceptible cells requires two distinct and sequential steps. The initial step is facilitated by an interaction of the fiber protein with its cellular receptor coxsackievirus and adenovirus receptor (CAR).[3,4] Following attachment to CAR, internalization of the virus is promoted by the interaction of the penton base with αv integrins on the cell surface.[5,6] Recently, several promising approaches have been examined for cell-specific gene delivery by adenovirus vectors. One approach is to link a ligand for cell surface receptors with capsid proteins of adenovirus vectors via bispecific conjugates.[7–9] However, this approach may be hampered by the instability of the adaptor–vector complex *in vivo*. In another approach, chimeric adenoviruses are created usually based on Ad5 with the fiber or its knob domain replaced by that of another serotype. Ad5 with Ad3 or Ad7 fibers showed CAR-independent infectivity, while vectors constructed with the Ad17 fiber have improved transduction of airway epithelial tissue, Ad35 for hematopoietic cells and Ad16 for cardiovascular tissue.[10–12] However, the tropisms of chimeric viruses are restricted to those of the replaced serotypes. Thus, retargeting adenovirus vectors by incorporating ligands directly into their viral capsid may be preferable. Such targeting has been achieved by direct genetic modifications of the capsid proteins: targeting ligands can be incorporated into the C terminus and HI-loop of fiber proteins ablated for native tropism through loss of binding with CAR and αv integrins, and these vectors provide an important platform for evaluating the targeting potential of selected peptide ligands.[13–16] However, cell type-specific ligands for targeted adenovirus vectors are generally unknown, which impedes the wider application of fiber-modified adenovirus vectors for targeted therapies. Although a phage display library has been used to identify targeting peptide motifs,[17–19] the incorporation of the peptides selected by phage

Correspondence: Dr K Aoki, Section for Studies on Host-Immune Response, National Cancer Center Research Institute, 5-1-1 Tsukiji, Chuo-ku, Tokyo 104-0045, Japan.
E-mail: kaoki@gan2.res.ncc.go.jp
Received 12 March 2007; revised 11 July 2007; accepted 12 July 2007; published online 16 August 2007

display into the adenoviral capsid has not been successful in developing the targeted vectors except for a few cases:[20–22] the possible reasons may include the conformation of the peptide is altered in the virus capsid, the specificity and affinity of ligand–receptor binding is decreased or lost, or the respective receptors do not internalize it in a manner supporting gene transduction.[23] Moreover, the insertion of a specific peptide into an adenovirus fiber knob often causes a significant suppression of the adenovirus production as shown in this study, indicating that selection of targeting peptides should be accomplished directly on the adenovirus library displaying random peptides within the context of a viral capsid protein.

We previously reported a simple and efficient method for constructing an adenovirus cDNA expression library by *in vitro* Cre-loxP recombination.[24,25] Based on that technology, we have developed a novel system for producing adenoviral libraries displaying a variety of peptides on the HI-loop of the fiber knob (Figure 1a), and used the libraries to select an adenoviral vector with the high infectivity in target cells (Figure 1b). Our system may allow the selection of targeted vectors to any cell type of interest, and may have broad implications for the development of targeted therapies.

Results

Development of basic constructs for making fiber-modified adenovirus vector

To establish a basic construct for making fiber-modified adenovirus vectors, we first examined whether the vectors could be produced by an *in vitro* Cre–lox recombination system[24] between a fiber-modified shuttle plasmid and the left hand of adenovirus genome DNA. The pBHI(Csp) (Figure 2a) was recombined with the adenoviral cosmid cAd-GFP (green fluorescent protein) by Cre and transfected into 293 cells. Adenoviral foci expressing GFP were detected 8 days after transfection (Figure 2b, upper left) and the infectivity of the 293 cells with the crude viral lysate (CVL) was more than 95% 2 days later (Figure 2b, upper right). We next confirmed whether the insertion of mutations into the AB-loop of a fiber knob could ablate the native tropism of an adenovirus.[26] In using pBHIΔCAR(Csp), only a tiny adenovirus focus was detected 12 days after the transfection of recombined DNA into 293-38 cells (Figure 2b, middle left) and a few GPF-positive cells were recognized 2 days after the infection of the 293-38.HissFv.rec cells with the CVL (Figure 2b, middle right). We then examined whether the artificial ligand (6-histidine incorporated in C terminus of the fiber knob) and receptor (293 cells expressing anti-His sFV) system could propagate a CAR binding-ablated adenovirus vector.[16] In using pBHIΔCAR-fs(−), an adenovirus was successfully generated after the transfection of recombinant DNA into 293.HissFv.rec cells (Figure 2b, lower panel).

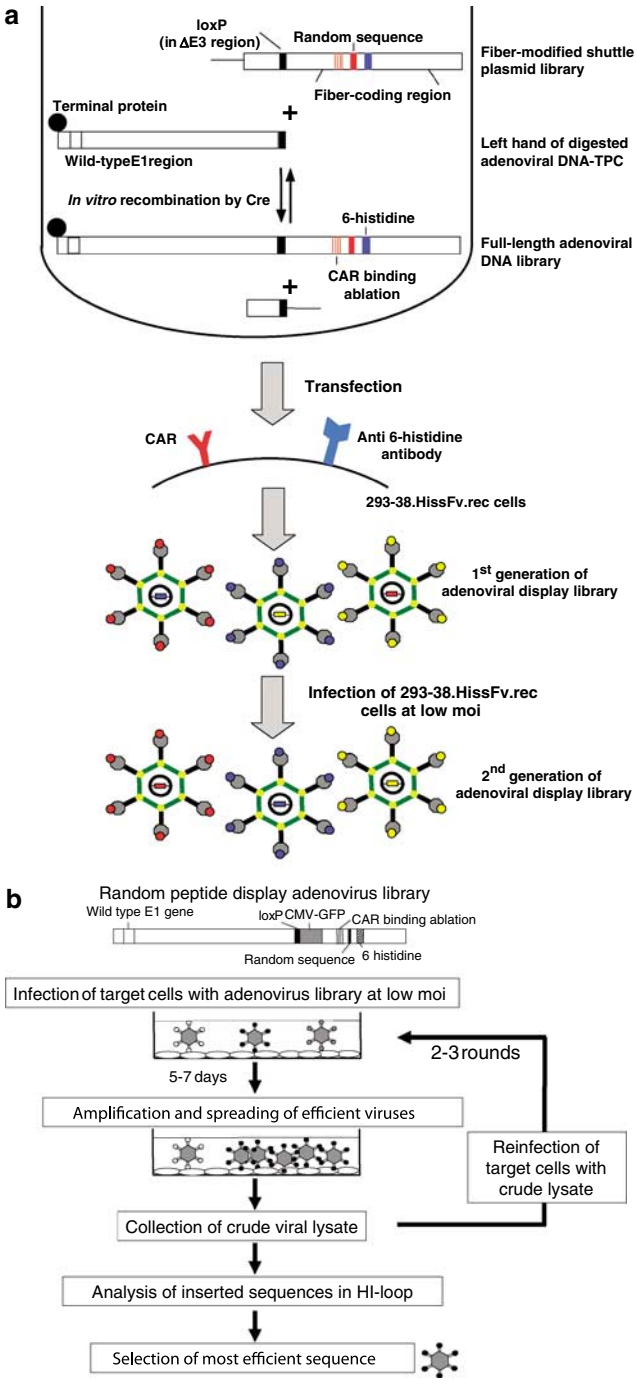

Figure 1 Construction and screening of a random peptide display adenovirus library. (**a**) Construction of an adenovirus library. The linearized shuttle plasmid library is mixed with left hand of digested adenoviral DNA-TPC by Cre recombinase to produce a full-length recombinant adenoviral DNA library *in vitro*. The first generation of an adenovirus display library was produced by transfection of the DNA library into adenovirus producer cells (293-38.HissFv.rec). This might lead to the uptake of more than one library DNA per cell and produce a chimeric fiber knob with packaged adenoviral genes. Therefore, the 293-38.HissFv.rec cells were next infected with the first generated libraries at a low MOI to ensure that the modified fiber-knob genome encodes for the displayed fiber-modification. (**b**) Screening of an adenovirus library. First, a given cell type of interest is infected with the adenovirus display library. Next, the expanded adenoviruses are recovered from the cells and subjected to two or three more rounds of selection. The DNA region containing the oligonucleotide insert of the selected adenoviruses is then analyzed. It takes less than 6 weeks to perform 3–4 rounds of selection and determine the targeted sequences. CAR, coxsackievirus and adenovirus receptor.

The library backbone plasmids (pBHIΔCAR-fs(+) and pBHIΔCAR-GFP-fs(+)) were designed so that an oligonucleotide insertion is required to shift the reading frame back to the original as in the wild-type fiber coding region (Figures 2a and c). The plasmid libraries, pBHIΔCAR-lib, pBHIΔCAR-GFP-lib and pBHI-lib, were generated from pBHIΔCAR-fs(+), pBHIΔCAR-GFP-fs(+) and pBHI(Csp), respectively, to display a random seven amino-residues peptide on the HI-loop of the fiber knob domain. Both pBHIΔCAR-lib and pBHIΔCAR-GFP-lib contained 4×10^6 clones, excluding insertless and other unsuitable clones such as those showing abnormal size. To test how the insertions of peptides into the HI-loop of the fiber knob affect the efficiency of adenovirus production, we randomly picked up a number of clones from the fiber-modified shuttle plasmid library both with CAR binding (pBHI-lib) and ablated for CAR binding (pBHIΔCAR-lib). After the recombination with cAd-GFP, each clone was transfected into 293 or 293.HissFv.rec cells. The generation of adenoviral GFP-expressing foci was detected in only 6 of 60 and 4 of 42 clones in each library, showing that approximately only 10% of the clones in the shuttle plasmid libraries appeared to be converted successfully into adenovirus virions, whereas 90% of the peptide insertions into the HI-loop may disturb virus production. The fiber trimerization is essential for the assembly and maturation of adenovirus virion,[27,28] and although the virus particle formation could occur in the absence of fiber, the infectivity of such fiberless viruses is severely impaired.[29] The insertion of an exogenous peptide sequence into the fiber knob may result in a conformational change of the fiber and disturbance of the fiber trimerization.

Production of a random peptide display adenovirus library

The fiber-modified shuttle plasmid library pBHIΔCAR-GFP-lib was recombined with the left hand of digested DNA-TPC, transfected into 293-38.HissFv.rec cells; and 12–14 days after the transfection, the first generation of the adenovirus display library was produced (Figure 1a). Since direct transfer of the full-length adenoviral DNA into 293-38.HissFv.rec cells might lead to an uptake of more than one library DNA per cell, the packaged adenovirus genome may not encode the peptide displayed on the fiber knob, impeding the selection process and subsequent identification of the displayed peptide. To avoid this problem, the first-generated library was used to infect the 293-38.HissFv.rec cells again at an MOI of 1, thus estimating an uptake and propagation of approximately 1 adenovirus genome per cell. The second generation of the library was efficiently produced 4 days after the infection. The DNA sequences of 100 randomly selected clones of PCR products from the library DNA verified that each clone contained a different peptide sequence and that the frequencies of amino acids in the adenovirus library were comparable to those in the plasmid library (Figure 2d).

The virus production efficiency was highly improved by optimizing several factors such as utilization of the adenoviral terminal protein in this library construction method,[25] and in fact, GFP-expressing foci in a 60-mm dish were too numerous to count (more than 1000) following the transfection of recombined DNA. Therefore, to estimate how many different peptides were displayed on these adenoviruses, we set up dilution experiments with two shuttle plasmid libraries as described:[25] the pBHIΔCAR-GFP-lib were mixed with pBHIΔCAR-lib at various ratios (1:300, $1:3 \times 10^3$, $1:1 \times 10^4$, $1:3 \times 10^4$, $1:3 \times 10^5$), recombined with left hand of digested DNA-TPC and transfected into 293-38.HissFv.rec cells. After 10–14 days, 5% of the CVL was used to infect the 293-38.HissFv.rec cells again to detect any GFP-expressing adenovirus, which is produced only from pBHIΔCAR-GFP-lib. GFP-expressing adenoviruses were detected at up to 1×10^4 dilution (Table 1), and the GFP-expressing adenoviruses were confirmed to have GFP gene by DNA sequencing following large-scale preparation of viruses. Together with the fact that 100 randomly isolated clones from the unselected adenovirus display library showed different peptide sequences, the dilution experiment suggested that the library displays more than 1×10^4 peptides on the fiber knob per 60-mm dish. The conversion rate of transfected plasmid library DNA into a virus in the process of library generation was considered to be around 10%, based on the results of shuttle plasmid clones described in the previous section.

Selection of library clones targeting cells poorly susceptive to adenovirus

To demonstrate that *in vitro* screening could select peptides displayed on the fiber knob that produces higher transduction efficiency to target cells, the

Figure 2 Design of random peptide display adenovirus library constructs. (**a**) Schematic presentation of adenoviral cosmids and fiber-modified shuttle plasmids. A single copy of a loxP sequence substitutes for the E3 gene (76.1–84.8 m.u.). The cAd-WT has a wild-type E1 gene, and in the cAd-GFP and cAd-LuciGFP, the E1 gene is replaced with the CMV promoter-driven GFP or luciferase-GFP fusion gene (LuciGFP). In the pBHIΔCAR-AQG and pBHI-AQG plasmids, the AQGQWAL sequence is inserted into the HI-loop of the fiber knob. (**b**) Establishment of a basic system to construct a fiber-modified adenovirus vector. Original magnification $\times 100$. Upper panel: the production of adenovirus vector by *in vitro* Cre-lox recombination between the fiber-modified shuttle plasmid and left hand of adenoviral genome DNA. Linearized pBHI(Csp) and cAd-GFP were recombined with Cre *in vitro* and transfected into 293 cells. Upper left: GFP-expressing adenoviral foci 8 days after the transfection. Upper right: 2 days after the infection of the crude viral lysate (CVL). Middle panel: ablation of naïve CAR tropism by insertion of point mutations into CAR binding portions in fiber knob. Linearized pBHIΔCAR(Csp) and cAd-GFP were recombined, and transfected into 293-38 cells. Middle left: a tiny adenovirus focus 12 days after the transfection. Middle right: Two days after the infection with the CVL. Lower panel: Propagation of adenovirus vector ablated for CAR binding by using the 6-histidine in the C terminus of the fiber and 293 cells expressing an artificial receptor for 6-histidine. Linearized pBHIΔCAR-fs(−) and cAd-GFP were recombined, and transfected into 293.HissFv.res cells. Lower left: GFP-expressing adenoviral foci 12 days after the transfection. Lower right: Two days after the infection of the CVL. (**c**) Modified HI-loop sequence in shuttle plasmids. In the pBHIΔCAR-fs(+) and pBHIΔCAR-GFP-fs(+), one nucleotide (A) was inserted between *Csp*45I and *Spe*I sites, and an oligonucleotide insertion is required to shift the reading frame back to the original as in the wild-type fiber coding region. (**d**) Frequencies of amino acids of shuttle plasmid library and adenovirus library. Randomly picked 100 clones of both libraries were sequenced. 'Theoretical' means amino acid frequencies deduced from random 7 codon sequences.

U138MG cell line was infected with the adenovirus display library at an MOI of 1 (Figure 1b). Since the CAR expression on the U138MG cells was very low (Figure 3a) as described,[30] the cells were poorly susceptible to wild-type adenovirus infection compared with CAR-expressing cells (AsPC-1) (Figure 3b). Since the library used in the screening was collected from twenty 60-mm dishes, the complexity of the peptide sequences displayed in the library was estimated to be approximately at a 2×10^5 level, and the final concentration of the virus library was

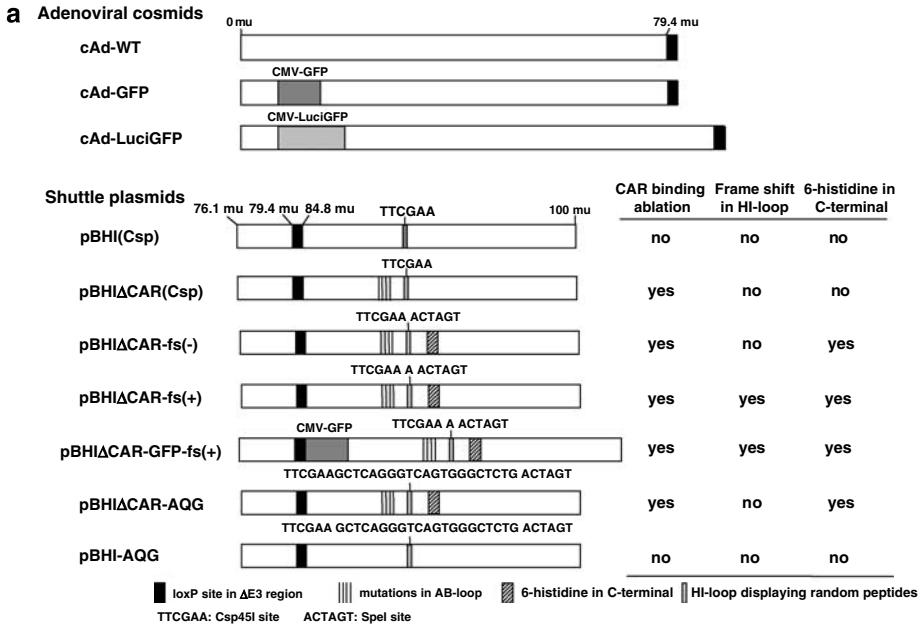

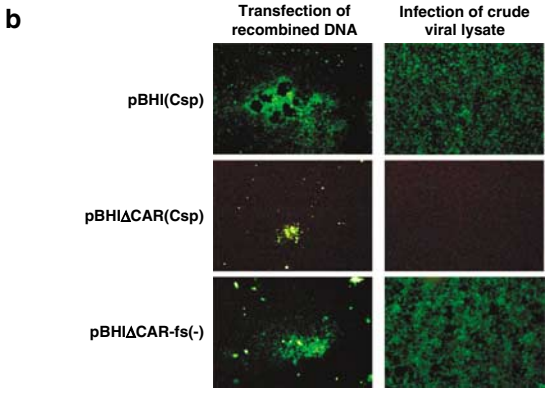

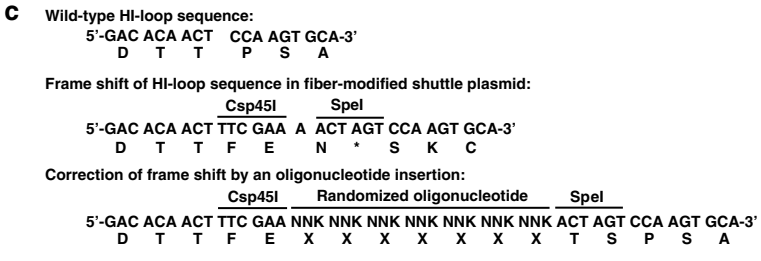

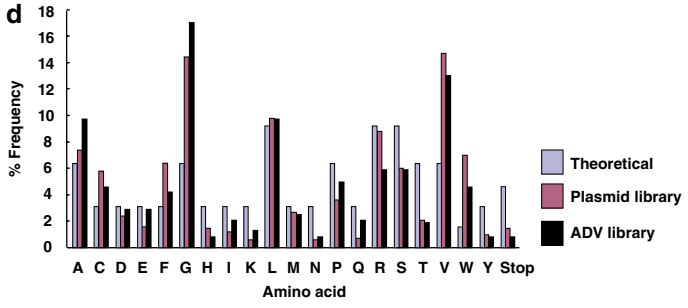

prepared as 1×10^9 pfu/ml. The infection of U138MG cells at low MOI allowed a chance of adenovirus exposure at less than 1 virus genome per cell, preventing a mismatch between the peptide displayed on the adenovirus and the sequence coding in the adenovirus genome. In the initial phase of the screening, many low-affinity or nonspecific viruses might bind and internalize into the U138MG cells; however, the use of a replication-competent type of adenovirus could allow for the rapid spreading of the most efficient viruses present in the library, leading to an effective enrichment of such viruses. Amplified and expanded adenoviruses on U138MG cells were recovered and subjected to three more rounds of selection. The DNA region containing the oligonucleotide insert of adenoviruses recovered from 2–4 rounds of selection was then amplified by PCR.

DNA sequencing of the PCR products revealed enrichment of several peptides, and the most abundant consensus sequence was AQGQWAL (71% in the 1st screening) after four rounds of selection. The screening was repeated to confirm the reproducibility of the results, and the 2nd screening also enriched the same AQGQWAL motif (43%) on U138MG cells from the same library (Table 2). None of the selected sequences was found in the 100 randomly isolated clones from the unselected adenovirus library. The fact that the identical sequence was repeatedly enriched in the two-independent screenings potentially indicates the feasibility and reliability of a screening procedure to select targeted vectors to a given cell type of interest. Some sequences are composed of only six amino acids. In fact, the sequence analysis of shuttle plasmid clones showed that several clones contained nucleotide inserts longer or shorter than 21 bp in the HI-loop portion; the sequence variations might occur in the process of PCR amplification with degenerate oligonucleotides and ligation into the shuttle plasmids. To prove that the selected peptides are a result of binding-mediated selection and not due to a low complexity bias in the library, AsPC-1 cells were also screened using the same library. We were able to isolate several enriched sequences for the AsPC-1 cells after 3–4 rounds of selection, and all peptide sequences selected from the library during AsPC-1 screening were different from those selected from U138MG cells (data not shown).

Characterization of adenovirus displaying a selected peptide

To test the targeting effect of the selected peptide, U138MG cells were infected with a luciferase expressing targeted vector ablated for CAR binding (AdΔCAR-LuciGFP-AQG). Although several peptide sequences were repeatedly selected in two-independent screenings, the only peptide whose frequency increased along with the succeeding rounds of selections in both screenings was AQGQWAL. Therefore, we focused on the AQGQWAL sequence in this study. The assay of luciferase activity showed that gene transduction efficiency of a targeted vector was 4- to 5-fold higher ($P < 0.01$) than that of an untargeted adenovirus (AdΔCAR-LuciGFP) in a U138MG cell line but not in other cell lines (AsPC-1, A549 and hepatocytes) (Figure 4a).

Then, to examine whether the insertion of a targeting peptide sequence into the HI-loop of a wild-type fiber knob could maintain cell-type specificity and affect the adenoviral native tropism, a targeted vector that also retains the CAR binding capacity (Ad-LuciGFP-AQG) was used to infect various cells. Transduction efficiency was significantly enhanced in PC3 as well as in U138MG cells ($P < 0.01$), whereas transduction of other cell lines resulted in a 78.1–99.9% decrease compared to the vector carrying a wild-type fiber knob (Ad-LuciGFP; Figure 4b), suggesting that the insertion of a targeting peptide into the HI-loop might inhibit native tropism, contributing to the targeting nature of the virus. However, it seems that the insertion of a targeting peptide into the HI-loop does not always decrease the infectivity of a targeted vector on other cells, because the several peptides selected from AsPC-1 did not show this inhibitory effect on infection of other cells (data not shown). GFP expression 48 h after infection with the targeted vectors corresponded with the results of luciferase activity in U138MG and AsPC-1 cells (Figure 4c).

To validate that the targeting is mediated by the selected peptide, the transduction efficiency of Ad-LuciGFP-AQG in U138MG cells and PC3 cells was determined in the presence or absence of the cognate peptide. A substantial competitive inhibition by the cognate peptide, but not by a control unrelated peptide, was observed at various MOI in a dose-dependent manner (Figure 4d), whereas these peptides did not interfere the infection of control vector Ad-LuciGFP (data not shown), confirming that the enhanced transduction of the targeted vector in the cells is mediated by the insertion of the selected peptide.

Since U138MG could not form any subcutaneous nor brain tumor in immune incompetent mice, the *in vivo* infectivity of the targeted virus was examined by intratumoral injection of the target vector (Ad-LuciGFP-AQG) into PC3 subcutaneous tumors. The luciferase assay showed that the targeted vector had a significantly higher infectivity in the PC3 tumor compared with the control virus (Ad-LuciGFP) ($P < 0.05$; Figure 4e).

To examine whether the high infectivity of the targeted vector enhances the oncolytic activity of an adenovirus vector ablated for CAR binding, U138MG and PC3 cells were infected with a replication-competent adenovirus displaying the selected peptide (AdΔCAR-WT-AQG) at various MOI. The growth of cells infected with AdΔCAR-WT-AQG was significantly ($P < 0.01$) inhibited compared with those of the control replication-competent adenovirus (Figure 4f), demonstrating that the targeted

Table 1 Efficiency of GFP-expressing adenovirus production

	pBHIΔCAR-GFP-lib/pBHIΔCAR-lib[a]				
Cells	*1/300*	*1/3000*	*1/10 000*	*1/30 000*	*1/300 000*
293-38.HissFv.rec	Yes[b]	Yes	Yes	No[c]	No

Abbreviation: GFP, green fluorescent protein.
An independent replica experiment showed the similar results.
[a]Various ratios of pBHIΔCAR-GFP-lib and pBHIΔCAR-lib were mixed and recombined with DNA-TPC by Cre. GFP-expressing adenovirus was only produced from pBHIΔCAR-GFP-lib.
[b]GFP-expressing cells were detected.
[c]GFP-expressing cells were not detected.

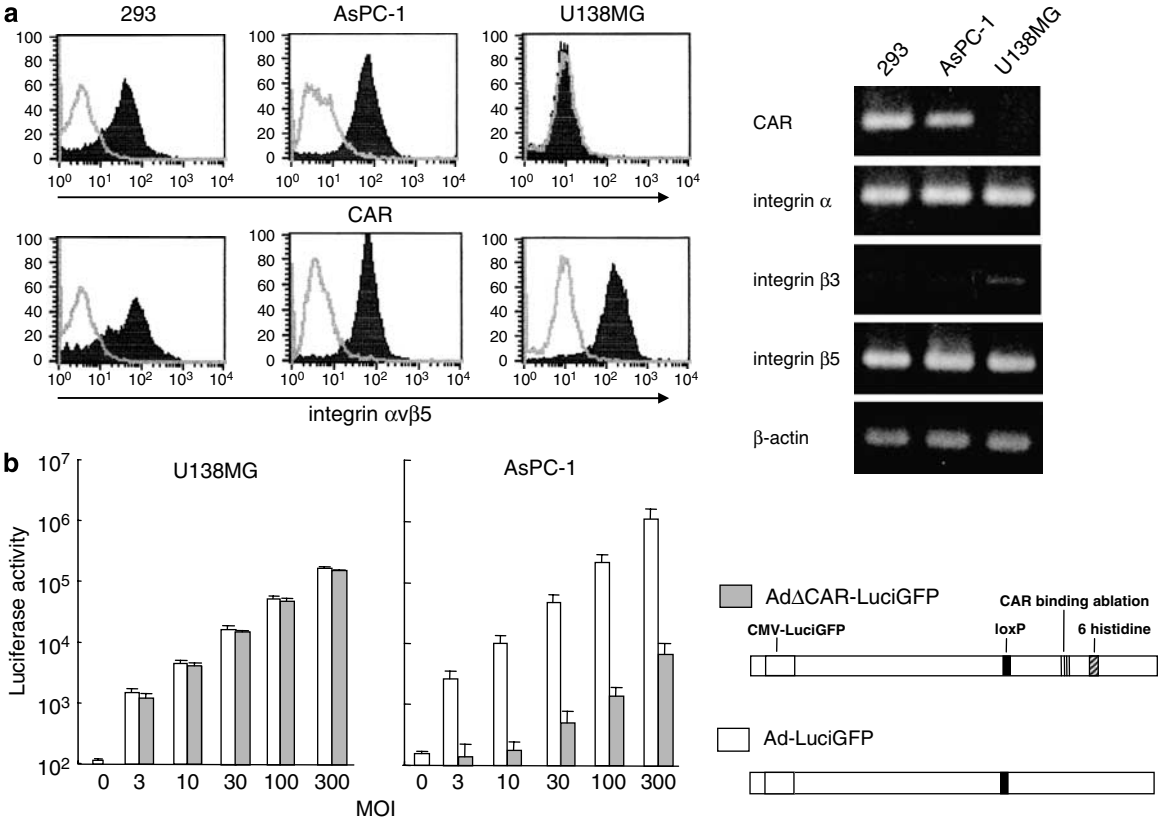

Figure 3 Poor susceptibility of U138MG cells to wild-type adenovirus vector. (**a**) Expression of CAR and integrins. Left panel: flow cytometic analyses of CAR and integrin $\alpha v\beta 5$. Cells were incubated with anti-CAR antibody (RmcB; ATCC) (filled curve, upper portion) or anti-integrin $\alpha v\beta 5$ antibody (P1F6; Chemicon International Inc., Temecula, CA, USA) (filled curve, lower portion) or isotype control antibody (open curve), and flow cytometry was carried out using an FACScan system (Becton Dickinson, Franklin Lakes, NJ, USA). Right panel: Reverse transcriptase-PCR analyses of CAR and integrins. Total RNA was extracted from cell lines, and after reverse transcription the mRNA of CAR, integrin αv, integrin $\beta 3$ and integrin $\beta 5$ was detected by PCR as described.[30] (**b**) Luciferase activities following infection of adenovirus vector *in vitro*. The cells were infected with luciferase-expressing adenovirus vectors, and 24 h later the luciferase activities were measured.

sequence might be useful to improve the efficacy of oncolytic vectors.

Discussion

The redirection of virus tropism is one of the most rational approaches to targeted vector development. We show here that the screening of a random peptide display adenovirus library on a cell type of interest allows the selection of targeted vectors. Although random peptide display libraries have been developed in retrovirus[31–33] and adeno-associated virus vectors,[23] this is the first report to generate targeted adenovirus vectors by a library-based approach.

The construction of an adenovirus display library was based on our original method for adenovirus cDNA expression libraries, in which we optimized several factors such as isolation of high-efficiency virus-producing 293 clones and utilization of the adenoviral terminal protein to develop high-complexity libraries.[24,25] Although it is impossible to determine directly the complexity of a final adenovirus display library product, a plasmid-based library containing a GFP clone at an abundance of 0.01% was readily converted to the adenovirus library in a convenient 60-mm dish scale (Table 1), suggesting that the complexity of the virus library could be more than 1×10^4 by the present method. In the previously reported adenovirus cDNA libraries, we estimated that a 3×10^4–3×10^5 complexity of adenoviruses could be produced in the same 60-mm dish.[25] The difference of complexity between the two virus libraries is possibly due to the significant disturbance of adenovirus generation by the insertion of a peptide into the HI-loop and to the lower infection efficiency of an artificial 6-histidine and anti-6His sFv system compared with the native CAR-fiber knob binding.

We were able to select a peptide that provided a gene transduction five-fold higher than an insertless vector from the 2×10^5 complexity level of the library. Although the selected peptide may be the most efficient sequence among this complexity level, the theoretical peptide complexity of seven amino acids is over 10^9. Therefore, the library used in this screening represents only a very small fraction of the possible vector clones, even after considering the fact that the majority of the peptides may not be compatible with the adenovirus fiber knob

Table 2 Peptide sequences selected from adenovirus display library on U138MG cells

Preparation	*1st screening*			*2nd screening*		
Selection round	*2*	*3*	*4*	*2*	*3*	*4*
Sequence	AQGQWAL	AQGQWAL	AQGQWAL	AQGQWAL	AQGQWAL	AQGQWAL
	AQGQWAL	AQGQWAL	AQGQWAL	AQGQWAL	AQGQWAL	AQGQWAL
	AQGQWAL	AQGQWAL	AQGQWAL	AQGQWAL	AQGQWAL	AQGQWAL
	AQGQWAL	AQGQWAL	AQGQWAL	AQGQWAL	AQGQWAL	AQGQWAL
	AQGQWAL	AQGQWAL	AQGQWAL	AQGQWAL	AQGQWAL	AQGQWAL
	AQGQWAL	FGGCIG	AQGQWAL	ATRRG*	AQGQWAL	AQGQWAL
	AQGQWAL	FGGCIG	AQGQWAL	ASGLLG	AQGQWAL	AQGQWAL
	AQGQWAL	FGGCIRF	AQGQWAL	FGGCIG	AQGQWAL	AQGQWAL
	CGRV*V	LFRPFAI	AQGQWAL	FGGCIG	ASIGFL	AQGQWAL
	FGGCIRF	MGGMRV	AQGQWAL	GAAGLAV	DAGGILN	AQGQWAL
	FGGCIRF	MGGMRV	FGGCIRF	GAAGLAV	FGGCIG	AQGQWAL
	G*CELAS	MGGMRV	LFRPFAI	GACSWCF	FGGCIG	AQGQWAL
	GCCGVWGG	VAGLSLC	LFRPFAI	GAGGILN	FGGCIG	AQGQWAL
	GFMVWGS	VAGLSLC	MGGMRV	GAGGILN	FGGCIG	FGGCIG
	GFMVWGS			GAMFLAR	GAGGILNC	FGGCIG
	GGGSLQA			GVGSLQA	GAGGILNC	FGGCIG
	GVGSLQA			IGRLLV	GAGGILNC	GCGVWGG
	QRVSGCP			IGRLLV	GCGVWGG	GFMVWGP
	RVGSVLVV			LFRPFAI	GFMVWGS	GRAGVMG
	RWSWVSV			MGGMRV	GLVEGR	GRAGVMG
	RWSWVSV			MGGMRV	IGRLLV	MGGMRV
				RVGSVLVV	IGRLLV	MGGMRV
				RWSWVSV	MGGMRV	MGGMRV
				RWSWVSV	MGGMRV	MGGMRV
				RWSWVSV	MGGMRV	MGGMRV
				VAGLSLC	MGGMRV	MGGMRV
				VAGLSLC	MGGMRV	MGGMRV
				VAGLSLC	MGGMRV	MGGMRV
				VRW*GVV	MGGMRV	VAGLSLC
				WVVCVC	MGGMRV	VAGLSLC
AQGQWAL	7/21 (33%)	5/14 (36%)	10/14 (71%)	5/30 (17%)	8/30 (27%)	13/30 (43%)

integrity. Therefore, more efficient peptide motifs could be isolated by a scaling up of the library size. Since the complexity of an adenovirus library depends on the number of helper cell transfected with recombined DNA, the simple scaling up of the number and the size of plates could increase the complexity of the library. Furthermore, we incorporated seven amino acids into the HI-loop of the fiber to construct the adenovirus library, since phage peptide libraries displaying seven amino acids have been effective for isolating tissue-specific sequences.[17,18] However, it is possible that more efficient motifs can be identified from libraries with different lengths of peptide inserts. It should be also noted that the insertion of peptides longer than seven amino acids into a HI-loop may cause excessive conformational change of a fiber knob and strongly disturb the virus assembly and maturation, leading to an overall decrease of library complexity, and the binding affinity may be determined by the overall conformation of a modified fiber and not by inserted peptides alone.

Since any cell should express a large number of different receptors on its surface, a wide variety of sequences might have been isolated in screening. However, our screening identified a limited number of specific sequences, which were already apparent in the second round of screening (Table 2). Possible reasons for this efficient enrichment include the following: many seven amino acids in the conformation of fiber may not be able to bind effectively enough with the receptors to mediate the infection; many receptors may not be internalized into the cell in a manner supporting gene transduction following virus binding; and the use of replication-competent viruses in the system may result in the rapid enrichment of the most efficient viruses among the many clones of viruses that can bind receptors.

The selected sequences did not contain any RGD sequences. Theoretically, the 2×10^5 complexity of seven amino acids should contain more than 20 RGD triples in the inserted peptides. However, the RGD sequences successfully inserted into the HI-loop of a fiber knob to bind with integrins in the previous studies were the RGD-4C peptides such as CDCRGDCFC.[14,34] We think that the seven amino acid peptide library in our vector system does not contain this type of RGD-4C sequences, and other RGD sequences present in the HI-loop of the adenovirus library could not effectively enough bind with the integrins to mediate the infection in the context of fiber conformation.

Although there was a possibility to isolate peptide sequences that can generally enhance gene transduction in many cells, a selected peptide showed cell type-directed infection (Figures 4a and b), suggesting that the corresponding target receptor is a specific cell surface molecule or its expression is significantly higher on the

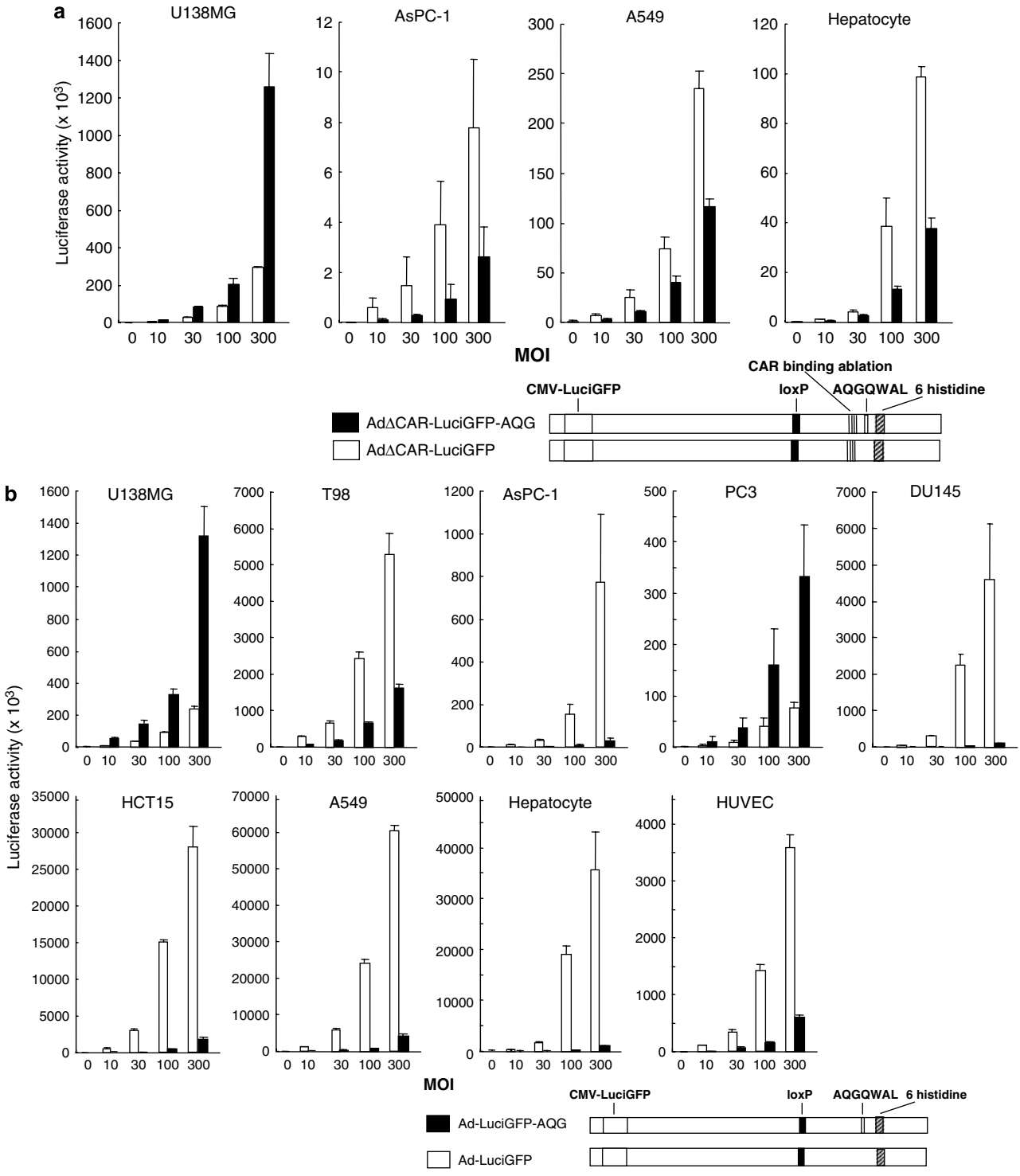

Figure 4 High transduction efficiency of adenovirus vectors displaying a selected peptide on the target cells. (**a**) Luciferase activities after infection with adenovirus vectors ablated for CAR binding. The cells were infected with AdΔCAR-LuciGFP-AQG or AdΔCAR-LuciGFP at various MOI, and 24 h later the luciferase activities were measured. (**b**) Luciferase activities after infection of adenovirus vector with CAR binding. The cells were infected with Ad-LuciGFP-AQG or Ad-LuciGFP at various MOI, and 24 h later the luciferase activities were measured. (**c**) GFP expression after infection with adenovirus vector displaying a selected peptide. AsPC-1 and U138MG cells were infected with AdΔCAR-LuciGFP, AdΔCAR-LuciGFP-AQG, Ad-LuciGFP or Ad-LuciGFP-AQG and 24 h later GFP expression was examined by fluorescence microscopy (original magnification $\times 100$). AsPC-1, MOI = 100. U138MG, MOI = 300. The cells were almost confluent in the wells. (**d**) Competitive inhibition of transduction of the adenovirus vector with selected peptide. Transduction efficiencies of adenovirus vectors into U138MG cells and PC3 cells were evaluated at various MOI in the presence of the cognate or a control-unrelated peptide at 0.2–1.5 mmol/l. The data are expressed as the relative luciferase activity (luciferase activity in the presence of peptide/that in the absence of peptide). (**e**) *In vivo* infectivity of the adenovirus vector with selected peptide. The Ad-LuciGFP-AQG and Ad-LuciGFP were injected into the PC3 subcutaneous tumors, and 48 h later the luciferase activities were measured ($n = 4$–6). The luciferase activity was expressed as light unit per milligram of protein. (**f**) Growth suppression of cells infected with replication-competent adenovirus vectors displaying a selected peptide. U138MG cells and PC3 were infected with AdΔCAR-WT-AQG or control adenovirus at various MOI. Cell growth was determined by cell proliferation assay 7 days after the infection.

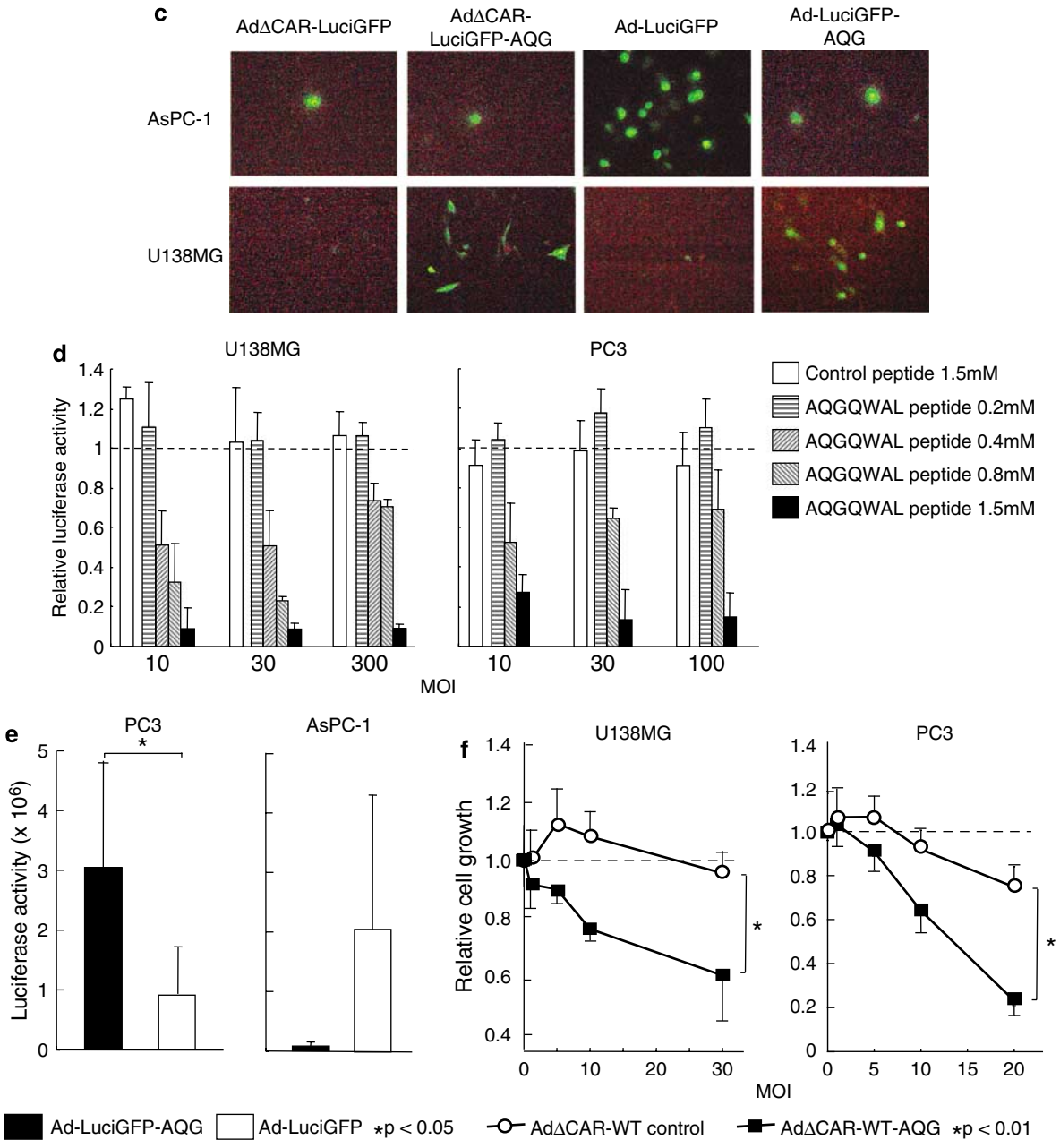

Figure 4 Continued

target cells. Unexpectedly, the targeted peptide display vector selected on the U138MG glioma cells showed a similarly high-efficiency gene transduction on the PC3 prostate cancer cells. The receptor may be shared by the U138MG and PC3 cells, or the selected peptide motif binds to different receptors, which are specifically expressed in each U138MG and PC3 cell line. The identification of the receptors may be useful to understand the molecular characteristics of the target cells and can be applied for diagnosis, such as the detection of a relapse, and therapy of the disease. On the other hand, the target receptors do not seem to be commonly expressed in all gliomas and prostate cancers, since the enhancement of gene transduction by a selected adenovirus was not observed in the T98G glioma cells and DU145 prostate cancer cells (Figure 4b). Database searches (BLAST) revealed sequence homology of the selected peptide with known human proteins such as *ELTD1* (AQGQWSL)[35] and major histocompatibility complex class I-related protein A/B (*MICA/B*) (PQGQWAE).[36] However, whether the receptors for *ELTD1* and *MICA/B* are responsible for the AQGQWAL-mediated infection is unknown. Additional work is necessary to identify the corresponding receptors.

The findings presented here open new perspectives in the field of gene therapy. Recently, promising preclinical and clinical data on the treatment of cancer have been reported using a conditionally replication-competent adenovirus (CRAd).[37,38] Although the infection and spreading of such replication-competent adenovirus are

restricted to tumor tissue in theory, several levels of safety devices are definitely required in the clinical setting. Therefore, the combination of CRAds with target specificity is a highly encouraging strategy for gene therapy.

Although the virus with the selected peptide showed the high infectivity in PC3 subcutaneous tumors, the expression levels and kinds of cell surface receptors may be substantially different between *in vitro* culture and *in vivo* tumor tissue. Screening of our peptide display adenovirus library should be performed *in vivo*, which may allow development of vectors to specifically transduce certain tumors and tissues even through systemic administration. Another line of future development will be a screening on the biopsy and surgical materials of the tumor, thereby leading to a generation of individualized-targeted viruses. Similarly, the library selection on immobilized proteins might be useful to isolate a vector targeted to any kind of molecule, although these cases may require an addition of an efficient screening step, which does not depend on viral replication to select a targeted virus. This technology of a specific adenovirus vector selection on any cell type or tissue of interest may have broad implications for the development of targeted gene therapy.

Materials and methods

Cell lines

Used in this study were a human embryonic kidney cell line (293), glioma cell lines (U138MG and T98G), a pancreatic cancer cell line (AsPC-1), a non-small cell lung cancer cell line (A549), prostate cancer cell lines (PC3 and DU145), a colon cancer cell line (HCT15) and primary cultures of human normal cell lines (hepatocytes and human umbilical vascular endothelial cells: HUVEC). All the cancer cell lines were obtained from American Tissue Culture Collection (ATCC; Rockville, MD, USA). 293 cells were cultured in Dulbecco's modified Eagle's medium (Sigma, St Louis, MO, USA) with 10% fetal bovine serum (FBS), U138MG cells were in Eagle's minimum essential medium (Sigma) with 10% FBS, and A549 cells were in an RPMI-1640 medium (Nissui Pharmaceutical, Tokyo, Japan) with 10% FBS. Hepatocytes were purchased from Dainippon Pharmaceutical Co. (Osaka, Japan). 293.HissFv.rec cells express an artificial receptor against six histidine (His) residues, containing an anti-His single chain antibody (sFv).[16] The 293-38 is a high-efficiency virus-producing clone of 293 cells,[25] and the 293-38 cells expressing an anti-His sFv stably (293-38.HissFv.rec) were generated by retrovirus-mediated transduction.

Shuttle plasmids and recombinant adenovirus DNA

The fiber-modified adenoviral shuttle plasmids include a 76.1–100 map unit (m.u.) of the adenoviral genome with a single loxP site at the E3 region deleted (79.4–84.8 m.u.).[24] The pBHI(Csp) plasmid has a *Csp*45I site in the HI-loop of the fiber knob[34] and pBHIΔCAR(Csp) includes 4-point mutations in the AB-loop of the fiber knob that abolishes CAR binding (Figure 2a).[26] The pBHIΔCAR-fs(−) and -fs(+) plasmids have the 4-point mutations as well, and six histidine residues were incorporated into the carboxy terminus of the fiber knob, so that the vector can be propagated in the 293 cells expressing an anti-His sFv as described.[16] The pBHIΔCAR-fs(−) and -fs(+) contain two incompatible *Csp*45I and *Spe*I restriction sites in the HI-loop to display random peptides, but in the pBHIΔCAR-fs(+) one nucleotide was inserted between *Csp*45I and *Spe*I sites to shift the reading frame of the fiber knob (Figure 2c). The pBHIΔCAR-GFP-fs(+) was constructed by inserting a cytomegalovirus immediate early enhancer/promoter (CMV promoter), the green fluorescent protein (GFP) gene and a SV40 poly(A) signal into the downstream of a loxP site of pBHIΔCAR-fs(+). The pBHI-AQG and pBHIΔCAR-AQG plasmids have a GCTCAGGGTCAG TGGGCTCTG (AQGQWAL) sequence in the HI-loop of pBHI(Csp) and pBHIΔCAR-fs(−) plasmids, respectively. The adenoviral cosmid cAd-WT includes the 0–79.4 m.u. of the adenovirus genome containing a wild-type E1 region and a single loxP site at 79.4 m.u. In the cAd-GFP and cAd-LuciGFP, the E1 gene is replaced with the CMV promoter-driven GFP or luciferase-GFP fusion gene (LuciGFP). The cAd-WT was recombined with pBHIΔ CAR(Csp) to generate adenovirus vectors AdΔCAR-WT for preparation of adenoviral DNA tagged with a terminal protein, and was recombined with pBHIΔ CAR-AQG to generate replication-competent adenovirus vectors displaying the AQGQWAL peptide (AdΔCAR-WT-AQG). The cAd-LuciGFP was recombined with pBHI(Csp), pBHIΔCAR-fs(−), pBHI-AQG and pBHIΔ CAR-AQG plasmids to generate adenovirus vectors Ad-LuciGFP, AdΔCAR-LuciGFP, Ad-LuciGFP-AQG and AdΔCAR-LuciGFP-AQG, respectively.

Construction of a fiber-modified shuttle plasmid library

Adenovirus libraries were based on the library backbone plasmids (pBHIΔCAR-fs(+) and pBHIΔCAR-GFP-fs(+)) to display a random seven amino acid residues peptide on the HI-loop of the fiber knob domain. To generate fiber-modified shuttle plasmid libraries, the degenerate oligonucleotide 5′-AACGGTACACAGGAAACAGGAG ACACAACTTTCGAA(NNK)$_7$ACTAGTCCAAGTGCAT ACTCTATGTCATTTTCATGG-3′ (N = A, T, G or C, K = G or T) served as a template for PCR with the primers 5′-GAAACAGGAGACACAACTTTCGAA-3′ and 5′-ACTA GTCCAAGTGCATACTCTATG-3′. The PCR product was digested with *Csp*45I and *Spe*I (restriction sites underlined) and ligated into the same sites of pBHIΔCAR-fs(+) and pBHIΔCAR-GFP-fs(+) and transfected into Max Efficiency electrocompetent cells (Invitrogen, Carlsbad, CA, USA) by electroporation. The plasmid libraries constructed from pBHIΔCAR-fs(+) and pBHIΔCAR-GFP-fs(+) were designated as pBHIΔCAR-lib and pBHIΔCAR-GFP-lib, respectively. The pBHI(Csp) was also employed to generate the shuttle plasmid library pBHI-lib: the degenerate oligonucleotide 5′-AACGGTACACAGGAAA CAGGAGACACAACTTTCGAA(NNK)$_7$TTCGAACCA AGTGCATACTCTATGTCATTTTCATGG-3′ served as a template for PCR, and the PCR product was digested with *Csp*45I (underlined) and ligated into the same site of pBHI(Csp). Both pBHIΔCAR-lib and pBHIΔCAR-GFP-lib contained 4×10^6 clones, excluding insertless and unsuitable clones. The complexity of plasmid libraries was estimated by the number of clones growing from a representative aliquot of the transformed bacteria on agar plates containing ampicillin. DNA sequencing of

100 clones verified that different random sequences are encoded in each clone (data not shown).

Construction of a random peptide display adenovirus library

First, the adenoviral DNA tagged with terminal protein (DNA-TPC) from AdΔCAR-WT was prepared through a buoyant CsCl density gradient with 4 M guanidine hydrochloride.[39] DNA-TPC was then digested with *Cla*I and *Csp*45I to remove the right hand of the adenoviral DNA containing the 3′ ITR and fiber-coding region, and was filtered through a centrifugal filter device (Centricon YM-100; Amicon, Beverly, MA, USA). Namely, the left hand of the digested DNA-TPC included 0–79.4 m.u. of the adenoviral genome and a single loxP site at 79.4 m.u. Fiber-modified shuttle plasmid libraries were linearized at the right end by *Pac*I and recombined with equal moles of the left hand of the digested DNA-TPC by Cre recombinase (Clontech, Madison, WI, USA) *in vitro* to produce a full-length adenovirus genomic DNA library. For example, 5 μg of shuttle plasmid and 15 μg of DNA-TPC were mixed with 500 ng of Cre recombinase (25 ng per 1 μg of DNA) in 600 μl of reaction mixture at 37°C for 3 h. Removal of the unrecombined DNA is not necessary, because only the recombined adenoviral DNA among the four molecules in the reaction mixture can give rise to an adenovirus. Then, to generate adenovirus display libraries, 7.5 μg of recombined adenoviral DNA was transfected by the lipofection method (Lipofectamine Reagent; Invitrogen) into 2×10^6 293-38.HissFv.rec cells in a 60-mm dish. After 12–14 days, when the cells showed an expansion of cytopathic effect, the first generation of the adenovirus display library was harvested. The CVLs were titrated as GFP expression forming units on 293-38.HissFv.rec cells, and then 293-38.HissFv.rec cells were infected with the CVL again at an MOI of 1. The second generation of the library was harvested 3–4 days after the infection (Figure 1a).

Biopanning of a random peptide display adenovirus library

The 2×10^6 of U138MG cells were seeded in 60-mm dishes. One day later the cells were infected with an adenovirus display library at an MOI of 1, and 2 h later the cells were washed with phosphate-buffered saline. After 5–7 days following the infection, the replicated adenoviruses were harvested from the cells, and CVLs were titrated by GFP expression on 293-38.HissFv.rec cells. For each subsequent selection round on U138MG cells, the CVL from a preselected adenovirus library was reapplied to the target cells at an MOI of less than 1 and the process was repeated 3–4 times (Figure 1b).

PCR and sequencing of adenovirus display library clones

DNA was extracted from the CVL of each selection round and then served as a template for a PCR with the primers containing upstream and downstream sequences of the HI-loop: 5′-GAAACAGGAGACACAA CTTTCGAA-3′ and 5′-ACTAGTCCAAGTGCATACTCT ATG-3′. PCR products were cloned into the *Csp*45I and *Spe*I sites of the pBHIΔCAR-fs(+) plasmid. Randomly assigned clones were sequenced using the primer 5′- GGAGATCTTACTGAAGGCACAGCC-3′.

Assay for luciferase activity in vitro

The cells were seeded at 1×10^4 per well in 96-well plates (Optilux multiplate; BD Biosciences, Franklin Lakes, NJ, USA) and infected with adenoviruses at various MOI. Twenty-four hours after the infection, the cells were lysed with 100 μl of luciferase assay buffer (Bright-Glo luciferase assay system; Promega, Madison, WI, USA) and then 100 μl of assay substrate (Promega) was added. The light units of luciferase activity were measured using a luminometer (EnVision multilabel plate reader; PerkinElmer, Shelton, CT, USA). The assays (carried out in eight wells) were repeated for a minimum of two times and the mean $\pm$ s.d. was plotted. Comparative analysis of luciferase activity was performed by the Student's *t*-test, and differences were considered statistically significant when $P < 0.05$.

To validate that the targeting is mediated by the selected peptide, transduction efficiency of Ad-LuciGFP-AQG was determined in the presence of the cognate peptide at a high concentration, because it is usually difficult to inhibit an adenovirus infection by peptide competitive inhibitors.[40] The control peptide is SYENFSA, which is an unrelated sequence to the peptides isolated from the U138MG screening.

Assay for luciferase activity in vivo

Five-week-old female BALB/c nude mice were obtained from Charles River Japan (Kanagawa, Japan). To examine the *in vivo* infectivity of the targeted virus, PC3 (50 μl of 1×10^7 cells) and AsPC-1 cell suspensions (50 μl of 5×10^6 cells) were injected subcutaneously into the legs. When the tumor mass was established ($\sim$0.8 cm in diameter), 50 μl of a viral solution (1×10^{10} pfu/ml) of Ad-LuciGFP-AQG and Ad-LuciGFP was injected into the tumor with a 29-gauge hypodermic needle. The luciferase assay was performed as described previously.[41]

In vitro *cell growth assay*

The U138MG and PC3 were seeded at 2×10^3 per well in 96-well plates and infected with AdΔCAR-WT-AQG or control replication-competent adenovirus ablated for CAR binding at MOI 1, 5, 10, 20 and 30. The cell numbers were assessed by a colorimetric cell viability assay using a water-soluble tetrazolium salt (Tetracolor One; Seikagaku Corp, Tokyo, Japan) 7 days after the infection. The absorbance was determined by spectrophotometry using a wavelength of 450 nm with 595 nm as a reference. The data were expressed as the relative cell growth (OD_{450} of virus-infected cells/that of parental cells) and the mean $\pm$ s.d. was plotted.

Acknowledgements

This work was supported in part by a grant-in-aid for the 3rd Term Comprehensive 10-Year Strategy for Cancer Control from the Ministry of Health, Labour and Welfare of Japan, grants-in-aid for Cancer Research from the Ministry of Health, Labour and Welfare of Japan, and a grant-in-aid (#W81XWH-05-1-0035) from the Department of Defense of the United States. We thank Gary Quinn for useful discussion and Miwa Kushida and Atushi Kondo for technical help. Y Miura, K Hatanaka and T Nishimoto are awardees of a Research Resident

Fellowship from the Foundation (Japan) for the Promotion of Science.

References

1 Zhang WW. Development and application of adenoviral vectors for gene therapy of cancer. *Cancer Gene Ther* 1999; **6**: 113–138.
2 Volpers C, Kochanek S. Adenoviral vectors for gene transfer and therapy. *J Gene Med* 2004; **6** (Suppl 1): S164–S171.
3 Bergelson JM, Cunningham JA, Droguett G, Kurt-Jones EA, Krithivas A, Hong JS *et al*. Isolation of a common receptor for Coxsackie B viruses and adenoviruses 2 and 5. *Science* 1997; **275**: 1320–1323.
4 Tomko RP, Xu R, Philipson L. HCAR and MCAR: the human and mouse cellular receptors for subgroup C adenoviruses and group B coxsackieviruses. *Proc Natl Acad Sci USA* 1997; **94**: 3352–3356.
5 Bai M, Harfe B, Freimuth P. Mutations that alter an Arg-Gly-Asp (RGD) sequence in the adenovirus type 2 penton base protein abolish its cell-rounding activity and delay virus reproduction in flat cells. *J Virol* 1993; **67**: 5198–5205.
6 Wickham TJ, Mathias P, Cheresh DA, Nemerow GR. Integrins alpha v beta 3 and alpha v beta 5 promote adenovirus internalization but not virus attachment. *Cell* 1993; **73**: 309–319.
7 Douglas JT, Rogers BE, Rosenfeld ME, Michael SI, Feng M, Curiel DT. Targeted gene delivery by tropism-modified adenoviral vectors. *Nat Biotechnol* 1996; **14**: 1574–1578.
8 Wickham TJ, Segal DM, Roelvink PW, Carrion ME, Lizonova A, Lee GM *et al*. Targeted adenovirus gene transfer to endothelial and smooth muscle cells by using bispecific antibodies. *J Virol* 1996; **70**: 6831–6838.
9 Miller CR, Buchsbaum DJ, Reynolds PN, Douglas JT, Gillespie GY, Mayo MS *et al*. Differential susceptibility of primary and established human glioma cells to adenovirus infection: targeting via the epidermal growth factor receptor achieves fiber receptor-independent gene transfer. *Cancer Res* 1998; **58**: 5738–5748.
10 Havenga MJ, Lemckert AA, Grimbergen JM, Vogels R, Huisman LG, Valerio D *et al*. Improved adenovirus vectors for infection of cardiovascular tissues. *J Virol* 2001; **75**: 3335–3342.
11 Zabner J, Chillon M, Grunst T, Moninger TO, Davidson BL, Gregory R *et al*. A chimeric type 2 adenovirus vector with a type 17 fiber enhances gene transfer to human airway epithelia. *J Virol* 1999; **73**: 8689–8695.
12 Shayakhmetov DM, Papayannopoulou T, Stamatoyannopoulos G, Lieber A. Efficient gene transfer into human CD34(+) cells by a retargeted adenovirus vector. *J Virol* 2000; **74**: 2567–2583.
13 Krasnykh V, Dmitriev I, Mikheeva G, Miller CR, Belousova N, Curiel DT. Characterization of an adenovirus vector containing a heterologous peptide epitope in the HI loop of the fiber knob. *J Virol* 1998; **72**: 1844–1852.
14 Dmitriev I, Krasnykh V, Miller CR, Wang M, Kashentseva E, Mikheeva G *et al*. An adenovirus vector with genetically modified fibers demonstrates expanded tropism via utilization of a coxsackievirus and adenovirus receptor-independent cell entry mechanism. *J Virol* 1998; **72**: 9706–9713.
15 Yoshida Y, Sadata A, Zhang W, Saito K, Shinoura N, Hamada H. Generation of fiber-mutant recombinant adenoviruses for gene therapy of malignant glioma. *Hum Gene Ther* 1998; **9**: 2503–2515.
16 Douglas JT, Miller CR, Kim M, Dmitriev I, Mikheeva G, Krasnykh V *et al*. A system for the propagation of adenoviral vectors with genetically modified receptor specificities. *Nat Biotechnol* 1999; **17**: 470–475.
17 Arap W, Haedicke W, Bernasconi M, Kain R, Rajotte D, Krajewski S *et al*. Targeting the prostate for destruction through a vascular address. *Proc Natl Acad Sci USA* 2002; **99**: 1527–1531.
18 Arap W, Kolonin MG, Trepel M, Lahdenranta J, Cardo-Vila M, Giordano RJ *et al*. Steps toward mapping the human vasculature by phage display. *Nat Med* 2002; **8**: 121–127.
19 Laakkonen P, Porkka K, Hoffman JA, Ruoslahti E. A tumor-homing peptide with a targeting specificity related to lymphatic vessels. *Nat Med* 2002; **8**: 751–755.
20 Nicklin SA, Von Seggern DJ, Work LM, Pek DC, Dominiczak AF, Nemerow GR *et al*. Ablating adenovirus type 5 fiber-CAR binding and HI loop insertion of the SIGYPLP peptide generate an endothelial cell-selective adenovirus. *Mol Ther* 2001; **4**: 534–542.
21 Joung I, Harber G, Gerecke KM, Carroll SL, Collawn JF, Engler JA. Improved gene delivery into neuroglial cells using a fiber-modified adenovirus vector. *Biochem Biophys Res Commun* 2005; **328**: 1182–1187.
22 Nicklin SA, White SJ, Nicol CG, Von Seggern DJ, Baker AH. *In vitro* and *in vivo* characterisation of endothelial cell selective adenoviral vectors. *J Gene Med* 2004; **6**: 300–308.
23 Muller OJ, Kaul F, Weitzman MD, Pasqualini R, Arap W, Kelinshmidt JA *et al*. Random peptide libraries displayed on adeno-associated virus to select for targeted gene therapy vectors. *Nat Biotechnol* 2003; **21**: 1040–1046.
24 Aoki K, Barker C, Danthinne X, Imperiale MJ, Nabel GJ. Efficient generation of recombinant adenoviral vectors by Cre-lox recombination *in vitro*. *Mol Med* 1999; **5**: 224–231.
25 Hatanaka K, Ohnami S, Yoshida K, Miura Y, Aoyagi K, Sasaki H *et al*. A simple and efficient method for constructing an adenoviral cDNA expression library. *Mol Ther* 2003; **8**: 158–166.
26 Einfeld DA, Schroeder R, Roelvink PW, Lizonova A, King CR, Kovesdi I *et al*. Reducing the native tropism of adenovirus vectors requires removal of both CAR and integrin interactions. *J Virol* 2001; **75**: 11284–11291.
27 D'Halluin JC, Milleville M, Martin GR, Boulanger P. Morphogenesis of human adenovirus type 2 studied with fiber- and fiber and penton base-defective temperature-sensitive mutants. *J Virol* 1980; **33**: 88–99.
28 Hong JS, Engler JA. Domains required for assembly of adenovirus type 2 fiber trimers. *J Virol* 1996; **70**: 7071–7078.
29 Legrand V, Spehner D, Schlesinger Y, Settelen N, Pavirani A, Mehtali M. Fiberless recombinant adenoviruses: virus maturation and infectivity in the absence of fiber. *J Virol* 1999; **73**: 907–919.
30 Mori T, Arakawa H, Tokino T, Mineura K, Nakamura Y. Significant increase of adenovirus infectivity in glioma cell lines by extracellular domain of hCAR. *Oncol Res* 1999; **11**: 513–521.
31 Bupp K, Roth MJ. Altering retroviral tropism using a random-display envelope library. *Mol Ther* 2002; **5**: 329–335.
32 Khare PD, Rosales AG, Bailey KR, Russell SJ, Federspiel MJ. Epitope selection from an uncensored peptide library displayed on avian leukosis virus. *Virology* 2003; **315**: 313–321.
33 Hartl I, Schneider RM, Sun Y, Medvedovska J, Chadwick MP, Russell SJ *et al*. Library-based selection of retroviruses selectively spreading through matrix metalloprotease-positive cells. *Gene Ther* 2005; **12**: 918–926.
34 Mizuguchi H, Koizumi N, Hosono T, Utoguchi N, Watanabe Y, Kay MA *et al*. A simplified system for constructing recombinant adenoviral vectors containing heterologous peptides in the HI loop of their fiber knob. *Gene Ther* 2001; **8**: 730–735.
35 Nechiporuk T, Urness LD, Keating MT. ETL, a novel seven-transmembrane receptor that is developmentally regulated in the heart. ETL is a member of the secretin family and belongs to the epidermal growth factor-seven-transmembrane subfamily. *J Biol Chem* 2001; **276**: 4150–4157.
36 Groh V, Rhinehart R, Secrist H, Bauer S, Grabstein KH, Spies T. Broad tumor-associated expression and recognition by tumor-derived gamma delta T cells of MICA and MICB. *Proc Natl Acad Sci USA* 1999; **96**: 6879–6884.

37 Everts B, van der Poel HG. Replication-selective oncolytic viruses in the treatment of cancer. *Cancer Gene Ther* 2005; **12**: 141–161.
38 Wildner O. Comparison of replication-selective, oncolytic viruses for the treatment of human cancers. *Curr Opin Mol Ther* 2003; **5**: 351–361.
39 Miyake S, Makimura M, Kanegae Y, Harada S, Sato Y, Takamori K *et al*. Efficient generation of recombinant adenoviruses using adenovirus DNA-terminal protein complex and a cosmid bearing the full-length virus genome. *Proc Natl Acad Sci USA* 1996; **93**: 1320–1324.
40 Communal C, Huq F, Lebeche D, Mestel C, Gwathmey JK, Hajjar RJ. Decreased efficiency of adenovirus-mediated gene transfer in aging cardiomyocytes. *Circulation* 2003; **107**: 1170–1175.
41 Aoki K, Furuhata S, Hatanaka K, Maeda M, Remy JS, Behr J-P *et al*. Polyethylenimine-mediated gene transfer into pancreatic tumor dissemination in the murine peritoneal cavity. *Gene Ther* 2001; **8**: 508–514.

Gene Therapy (2007) 14, 627–637

www.nature.com/gt

ORIGINAL ARTICLE

Targeting EGFR with metabolically biotinylated fiber-mosaic adenovirus

L Pereboeva[1], S Komarova[1], J Roth[1], S Ponnazhagan[2] and DT Curiel[1]
[1]Division of Human Gene Therapy, Departments of Medicine, Obstetric and Gynecology, Pathology and Surgery, Gene Therapy Center, University of Alabama at Birmingham, Birmingham, AL, USA and [2]Department of Pathology, Gene Therapy Center, University of Alabama at Birmingham, Birmingham, AL, USA

Adenovirus (Ad)-based vectors are useful gene delivery vehicles for a variety of applications. Despite their attractive properties, many in vivo *applications require modulation of the viral tropism. Targeting approaches applied to adenoviral vectors included genetic modification of the viral capsid, controlled expression of the transgene and combinatorial approaches that combine two or more targeting elements in single vectors. Most of these studies confirmed successful retargeting in cell cultures, however,* in vivo *gains of targeted adenoviral vectors have not been widely demonstrated. We have developed a combinatorial retargeting approach utilizing metabolically biotinylated Ad, where the biotin acceptor peptide was incorporated in one of the fibers in a dual fiber viral particle resulting in metabolically biotinylated fiber-mosaic Ad (mBfMAd). We have utilized this vector in complex with epidermal growth factor (EGF)-Streptavidin to retarget fiber-mosaic virus to EGF receptor (EGFR) expressing cells* in vitro *and confirmed an increased infectivity of the retargeting complex. Most importantly, the utility of this strategy was demonstrated* in vivo *in two distinct animal models. In both models tested, retargeted mBfMAd demonstrated an increased ratio of gene expression in target tissues compared to the liver expression profile. Thus, metabolically biotinylated fiber-mosaic virus in combination with appropriate adapters can be successfully exploited for adenoviral retargeting strategies.*
Gene Therapy (2007) **14,** 627–637. doi:10.1038/sj.gt.3302916; published online 25 January 2007

Keywords: *targeted delivery; EGFR; adenoviral vector; fiber-mosaic; metabolic biotinylation*

Introduction

Adenovirus (Ad)-based vectors remain one of the most useful gene delivery vehicles for a variety of clinical contexts and a preferable vector for cancer gene therapy. However, several limitations preclude safe and efficient Ad-based gene transfer, specifically for *in vivo* settings. One limitation is the broad tropism of Ad, due to the ubiquitous expression pattern of the primary cell receptor CAR and secondary integrin receptors, which leads to undesired virus uptake and gene expression in non-target tissues. Furthermore, low and inconsistent expression of CAR on tumor cells raises concerns about the efficacy of Ad-mediated gene therapy in cancer applications. Thus, for efficient and versatile use of Ad as an *in vivo* gene therapy vector, modulation of the viral tropism is highly desirable.

Various targeting approaches have been designed to change viral tropism. One approach includes genetic modification of the viral capsid proteins via addition of foreign targeting ligands such as short peptides or polypeptide binding domains or the substitution of the fiber with other types of Ad fiber. In adapter-mediated approaches, the tropism of the virus is modified by a targeting moiety utilizing a ligand, which associates with the Ad virion. Adapter molecules successfully used for Ad targeting include bispecific antibody (Ab) conjugates,[1] genetic fusions of single-chain Ab (scFv) with soluble CAR,[2] or scFv–scFv diabodies.[3]

The combined use of two or more targeting components in single vector has also been reported to significantly enhance the utility of individual targeting approaches. The immunoglobulin (Ig)-binding domain of the *Staphylococcus aureus* protein A has been genetically-incorporated into Ad fiber, allowing antigen-specific Ig to serve as bifunctional adapter molecules. Another complex targeting system designed by Barry, Campos and co-workers utilizes the high affinity biotin-avidin interaction.[4,5] This system exploits the incorporation of a biotin acceptor peptide (BAP) into the structural proteins of Ad, which allowed metabolic biotinylation of these vectors during propagation in 293 cells. All of these studies have demonstrated successful retargeting of Ads *in vitro* through alternative receptors. However, several limitations could be envisioned for the translation of these targeting approaches for *in vivo* applications. For instance, viruses with incorporated IgG-binding domains may face a competition with IgGs abundantly present in serum and other biological fluids. On the other hand, drastic modifications of adenoviral structural proteins usually hamper infection and subsequent steps in the viral life cycle, limiting the ability to scale up viral

Correspondence: Dr DT Curiel, Division of Human Gene Therapy, Departments of Medicine, Pathology and Surgery, Gene Therapy Center, University of Alabama at Birmingham, Birmingham, AL 35294, USA.
E-mail: david.curiel@ccc.uab.edu
Received 14 August 2006; revised 25 October 2006; accepted 26 November 2006; published online 25 January 2007

preparations. This could explain why no targeting gains have been reported to date using this strategy *in vivo*.

In this study, we developed a variation of the combined retargeting approach utilizing metabolically biotinylated fibers in the context of a fiber-mosaic viral capsid. The fiber mosaic construct allows expression of two fibers: fiber-fibritin (FF) and the wild-type (wt) fiber, both of which are incorporated into viral particles (vp). We have previously demonstrated that inclusion of a second fiber with distinct binding properties can provide virus binding and infection.[6] In contrast to studies by Barry *et al*., the BAP was incorporated into one of the fibers resulting in metabolically biotinylated fiber-mosaic Ad (mBfMAd). The wt fiber facilitates the viral life cycle and allows the fiber-mosaic virus to be propagated to levels near that of the wt Ad. In our study, we have exploited biotinylated FF in complex with adapter epidermal growth factor (EGF)-Streptavidin to retarget the fiber-mosaic virus to EGF receptor (EGFR) expressing cells both *in vitro* and *in vivo*.

Results

Design and characterization of mBfMAd

The genome design of the mBfMAd Ad5FF.PSTCD.F5luc (mBfMAd) was similar to that previously described for AdFF6H.F5luc.[6] A minimal domain of the 1.3S subunit of *Propionibacterium shermanii* transcarboxylase (PSTCD) was added to the C-terminus of chimeric protein FF. This domain is naturally biotinylated at lysine 89, when expressed in *Escherichia coli* (*E. coli*) and *Saccharomyces cerevisiae* by each organism's cellular biotin ligase enzyme[7] and is also metabolically biotinylated in mammalian cells.[8] Thus, the mBfMAd genome encodes two fibers in the L5 region: a chimeric FF containing a C-terminal 6His tag and the PSTCD domain (FF.PSTCD.6H) and the Ad5 wt fiber (Figure 1a). Both fibers contain the tail portion of Ad5 fiber, which anchors them to the penton of the virion and also allows both fibers to be detected with anti-fiber tail AB. The coding sequences of both fibers were spanned by untranslated 5′ and 3′ sequences of the wt fiber thereby providing equal transcription conditions (splicing, polyadenylation as well as regulation by the Major Late Promoter) for both fibers. The fiber-mosaic vector carries the firefly luciferase gene under the control of the cytomegalovirus (CMV) promoter in the E1 region of the Ad5 genome (Figure 1a). The mBfMAd was rescued in 293 cells expressing the complementary E1 region for Ad5 growth. The titer of fiber-mosaic virus used for this study was 4.83×10^{12} vp/ml. 293 cell culture infected by these viruses at the same multiplicity of infection (MOI) exhibited similar rates of CPE development, indicating a comparable time course

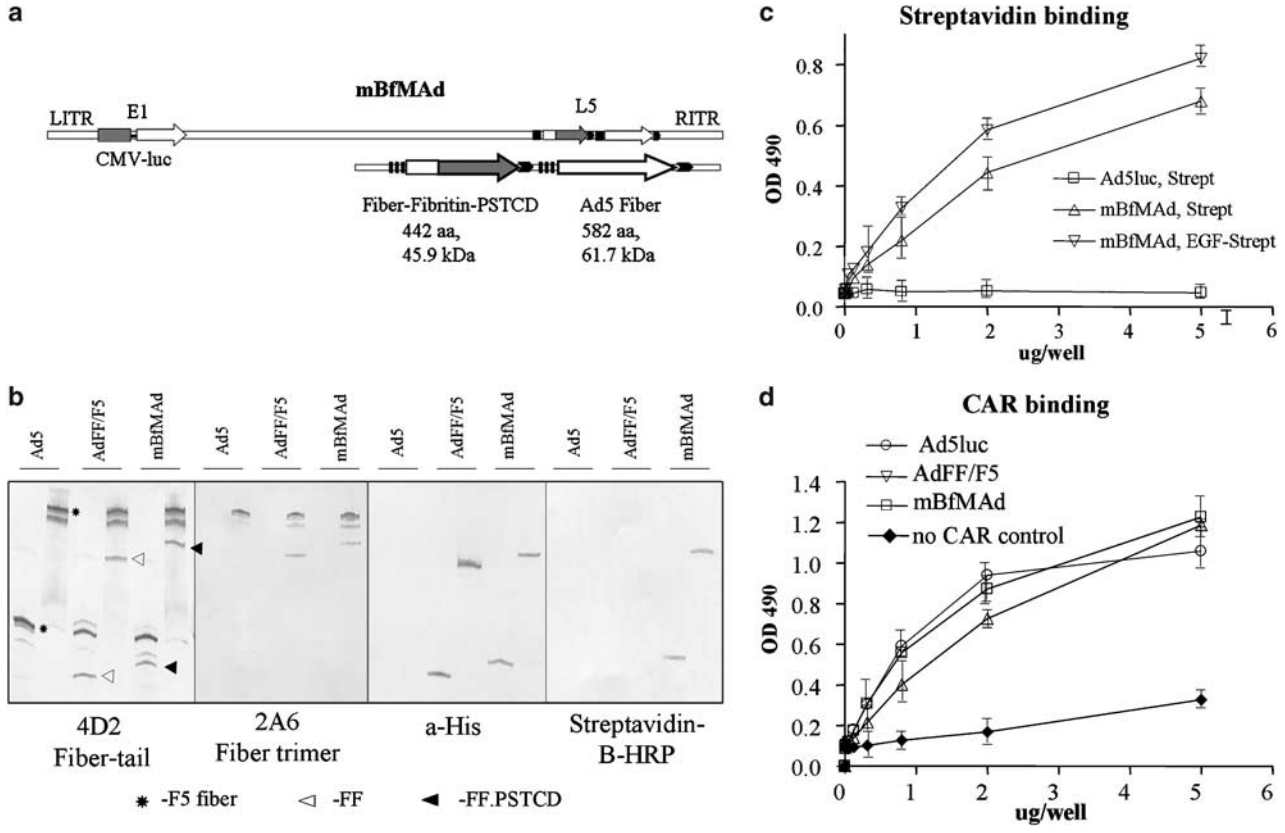

Figure 1 Design and characterization of mBfMAd (**a**) Diagram of the fiber-mosaic adenovirus Ad.FF.PSTCD.6H.F5luc (mBfMAd) genome. Modification of L5 region of Ad genome includes tandem of fiber genes: FF with BAP PSTCD and 6His tag and wt Ad5 fiber. (**b**) Fiber content in fiber-mosaic AdFF6H.F5luc virions. Equal amounts of Ad5luc AdFF6 H.F5luc and Ad.FF.PSTCD.6H.F5luc (5×10^9 vp) in SDS sample buffer were loaded on gradient (4–20%) SDS gel either boiled or unboiled. Electrophoretically separated viral proteins were transferred to PVDF membrane and developed with monoclonal antibodies specific to fiber tail (4D2), fiber trimer (2A6), 6His-Tag and Streptavidin-HRP. (**c**, **d**) Binding characteristics of mBfMAd. Binding of mBfMAd to streptavidin (**c**) and recombinant CAR (**d**) was tested in ELISA. The number of virus particles used for binding experiments was within the range of 1×10^7–2×10^{10}, which corresponded to 0.01–5 μg of viral protein per well. Control lane shown represents nonspecific binding of mBfMAd to the plastic surface in the absence of CAR.

of infection. Furthermore, the total yield of mBfMad and physical titers calculated in vp were comparable to the preps of wt virus, indicating that viral yield was not affected. Several lots of the virus have been obtained in the standard lab preparations with the titers ranged from 1.5×10^{12} to 1.3×10^{13} vp/ml. Thus, the yield of mBfMAd was similar to the yield routinely observed for the recombinant Ad5 preparations with unmodified capsid, suggesting that the additional fiber did not hamper virus propagation and packaging and allowed efficient production of the fiber-mosaic virus.

Fiber content in fiber-mosaic virions

To examine fiber incorporation into mosaic virions, we performed a series of Western blots where an equal number of vp (2×10^9) of Ad5luc, Ad5.FF6H. F5luc and Ad5FF.PSTCD.F5luc were loaded on sodium dodecyl sulfate-polyacrylamide gel electrophoresis (SDS-PAGE) (Figure 1b). Incorporation of FF.PSTCD.6H into vp was confirmed by the interaction with antibodies specific to fiber tail (4D2), trimeric fiber (2A6) and 6His. Western blots with the 4D2 and 2A6 antibodies revealed fiber monomers and timers of the correct size. The anti-His Ab only reacted with chimeric fibers from mosaic virions: FF.6H and FF.PSTCD.6H. Attachment of biotin on FF.PSTCD.6H fiber was confirmed by interaction with streptavidin both in Western blot (Figure 1b) and enzyme-linked immunosorbent assays (ELISA), where mBfMAd was captured either by streptavidin or EGF-Streptavidin coated on plates (Figure 1c). In addition, the mBfMAd retained CAR binding through wt fiber as demonstrated in Figure 1d. Thus, the presence of the FF.PSTCD.6H in the capsid of the mosaic virus was detected by antibodies directed to all of the functional domains of the protein – fiber tail, fiber trimer and 6His, thereby demonstrating that the additional fiber was incorporated into the virion and correctly displays all of its functional motifs. The presence of the biotin on this fiber has also been confirmed, thus, enabling utilization of our vector in combination with bioltinylated adapters for Ad retargeting strategies.

The fiber content in the mosaic virions was semi-quantitatively estimated by the protein band intensity after staining with 4D2 AB employing Image Tool software. This analysis showed that the average ratio of FF.PSTCD.6H to wt fiber in mBFmAd was similar to the average ratio of FF.6H to wt fiber in AdFF.6H and has been estimated as 1:5 (ranging from 1:3 to 1:6, where higher ratios were obtained analyzing fiber monomers and lower ratios were obtained based on fiber trimers). Therefore, it could be expected that fiber-mosaic has 1–3 vertices of the viral capsid that contained biotinylated fiber, which can be utilized in retargeting strategy.

Targeting metabolically biotinylated fiber-mosaic vectors to EGFR using the bi-functional adapter EGF-Streptavidin in vitro

Theoretically, any molecule equipped with bispecific binding affinities, one to biotin and another to a target cell-specific receptor, can function as an adapter to redirect biotinylated virus to specific cell types. The bispecific adapter contained human EGF fused to the core-streptavidin[9] has been previously expressed in the bacterial system and its design and production was described in detail by Ponnazhagan *et al*.[10] This adapter has been thoroughly characterized and used to retarget AAV to EGFR expressing cell lines. Thus, the availability of this adapter enabled us to test the utility of our vector in an EGFR retargeting strategy. We first wanted to determine the infectivity of our vector when applied with the EGF-Streptavidin adapter *in vitro*.

To analyze EGFR targeting *in vitro*, we evaluated adapter-mediated infection by mBfMAd of several cell lines with different EGFR expression status. Cancer cell lines with low (MDA-MB-453) and high EGFR expression (A431, SKOV3ip1, A549) were transduced with Ad5luc or mBfMAd at 100 vp/cell. Viruses were preincubated with EGF-Streptavidin at concentration of 10 μg/ml and purified from excess of adapter using Microcon filter tubes. The results are shown in Figure 2. On the cell line with low EGFR expression (MDA-MB-453), both viruses showed comparable infectivity as measured by luciferase transgene activity. However, EGF-Streptavidin targeted transduction of mBfMAd resulted in significantly enhanced luciferase activity on EGFR-positive cells compared to that obtained with Ad5luc. The increase in transduction varied from more than 10-fold in A431 to more than 30-fold in SKOV3ip1 cells (Figure 2a). Additional evidence of efficient *in vitro* retargeting with the bispecific adapter was also obtained using stable cell lines that express the extracelular domain of human EGFR.[11] Murine fibroblasts NR6 (EGFR-deficient) or NR6wt (EGFR-expressing) were preincubated with either phosphate-buffered saline (PBS) (no adapter) or with increasing concentration of EGF-Streptavidin 1–25 μg/ml, washed, and then transduced with Ad5luc or mBfMAd. Addition of the adapter enhanced the transduction of EGFR-positive cells in a dose-dependent manner, but had no effect on cells lacking EGFR receptor expression. The highest concentration of adapter used for retargeting mBfMAd to EGFR-positive NR6wt cells resulted in an eightfold increase in transgene expression, whereas it only increased transduction of wt Ad by 3.2-folds at the same experimental conditions (Figure 2b). Thus, mBfMAd can achieve enhanced transduction via bispecific adapter in cell lines expressing target receptor.

Targeting metabolically biotinylated fiber-mosaic vectors to EGFR in vitro *after blocking fiber-CAR interaction*

Our EGFR retargeting strategy relies upon the incorporation of modified FF, which is one of the two fibers present in the capsid of the fiber-mosaic virus. Retaining the wt fiber gene in the viral genome (i.e. the wt fiber protein in the vp) gives the potential advantage of facilitation of viral life cycle and virus propagation. A possible disadvantage for retargeting is the presence of the wt fiber, which can direct the infection of fiber-mosaic via the CAR-mediated pathway on CAR-positive cell lines. To confirm that biotinylated fibers, which represent only a fraction in the context of viral capsid, are able to mediate virus infectivity and to confirm the dependence of transgene expression on EGF–EGFR interaction, we performed retargeting gene transfer experiments in the presence of the Ad5knob. Virus infectivity in conditions when the binding ability of the wt fiber is blocked would indicate the relative contribution of the second fiber to the overall virus infectivity.

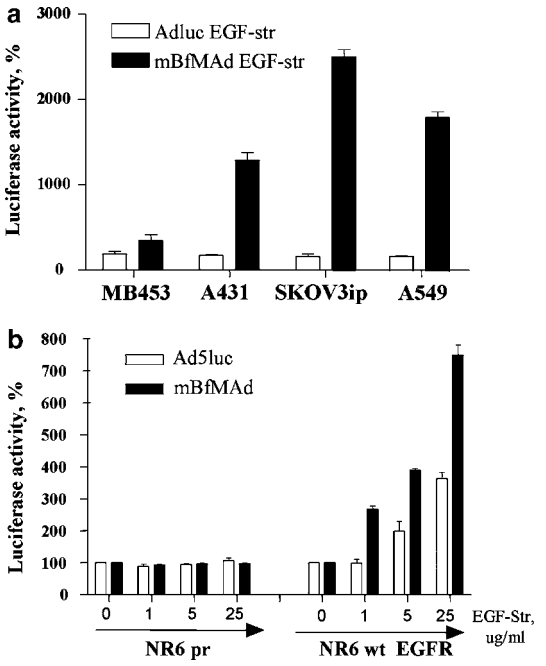

Figure 2 Increased gene transfer to EGFR-expressing cell lines. (**a**) Cancer cell lines with low (MDA-MB-453) and high (A431, SKOV3ip1, A549) EGFR expression were transduced with Ad5luc or mBfMAd at 100 vp/cell. Viruses were preincubated with EGF-Streptavidin at concentration of 10 μg/ml, purified from excess of adapter using centricon tubes and applied on cells. Results are presented as % of increase of luciferase expression with adapter. Mean luciferase expression of the same virus without adapter was designated as 100%. (**b**) Murine fibroblasts NR6 or NR6wt EGFR, expressing extracellular domain of human EGFR, were preincubated with either PBS (no adapter) or with increasing concentration of EGF-Streptavidin 1–25 μg/ml. Cells has been were transduced with Ad5luc or mBfMAd at 50 PFU/cell. Results are presented as increase of luciferase expression with adapter. Mean luciferase expression of the same virus without adapter was designated as 100%.

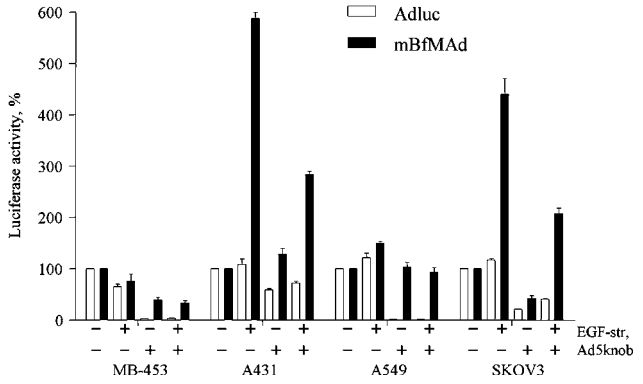

Figure 3 Infectivity of mBfMAd Ad after blocking fiber-CAR interaction. Cell lines with low EGFR expression (MDA-MB-453) and cell lines overexpressing EGFR (A431, A549, SKOV3) were transduced with Ad5luc or mBfMAd at 50 PFU/cell preincubated either with PBS (no adapter) or with EGF-Streptavidin at concentration of 10 μg/ml. To block infection via wt fiber cells were preincubated with Ad5 knob recombinant protein at 50 μg/ml. Twenty-four hours later the cells were processed for luciferase assay. Results are presented as % of luciferase expression compared to infection of this virus without adapter or knob blocking. Data presented are mean average of triplicates plus sample standard deviation.

The low EGFR-expressing cell line, MDA-MB-453, and cell lines overexpressing EGFR (A431, A549, SKOV3) were transduced with Ad5luc or mBfMAd at 50 PFU/cell preincubated either with PBS (no adapter) or with EGF-Streptavidin at concentration of 10 μg/ml. To block the infection via wt fiber, cells were preincubated with 50 μg/ml of recombinant Ad5 knob protein. We have previously shown that this concentration of Ad5knob blocked infectivity of wt virus more than 95% on high CAR-expressing cell lines. The results are shown in Figure 3. In line with previous experiments, an addition of the EGF-Streptavidin retargeting adapter augmented infectivity of the fiber-mosaic virus only, whereas it did not influence the infectivity of Ad5luc in any cell line tested. In general, mBfMAd demonstrated similar patterns of EGFR-dependent transduction as in the previous *in vitro* experiment with significant gene transfer increase in EGFR-overexpressing cells (A431, SKOV3) and no effect in cells with low EGFR expression (MDA-MB-453). In the presence of Ad5 knob, Ad5luc had predicted pattern of infection block for all cell lines tested. The results of CAR blocking was particularly clear in the highly CAR-positive cell line A549, where gene transfer was blocked by 99% in the presence of Ad5knob. Wt Ad infectivity remained at 20–50% of normal levels in other cell lines that express lower levels of CAR, presumably via infection through cellular integrins (A451, SKOV3). Ad5 knob-mediated blocking of mBfMAd infection in the absence of adapter did not reduce infectivity as significantly as that for the Ad5luc, and was either similar to the infectivity levels without blocking or only decreased to 37–45% of the initial infectivity levels. Most importantly, the fiber-mosaic virus demonstrated efficient adapter-based retargeting in EGFR-positive cells in Ad5 knob blocking conditions. Infectivity was increased by approximately 300% in A431 cells and 200% in SKOV3 cells in blocking conditions, where wt fiber presumably did not participate in infection. The level of EGFR-based infectivity was higher on cell lines with high EGFR expression and moderate CAR expression, indicating that in the situation where CAR-mediated infection is negligible, transduction via a second fiber dominates and is sufficient to mediate infection. Thus, biotinylated fiber can mediate adapter-driven transduction in the context of mosaic virions.

Analysis of EGFR retargeting with mBfMAd in vivo *using a murine model of ovarian carcinoma*

Next, we wanted to test whether our retargeting strategy gives any benefits when applied *in vivo*. The SKOV3ip1 cell line has been previously shown to have high expression of EGFR.[12] This cell line also demonstrated high levels of EGFR-mediated retargeting in our *in vitro* experiments. Thus, we utilized an intraperitoneal (i.p.) xenograft model of human ovarian cancer based on i.p. injection of SKOV3ip1 cells into CB17 severely combined-immunodeficient (SCID) mice for analysis of *in vivo* targeting by mBFmAd. After tumors have been developed, the animals were injected i.p. with Ad5luc or mBfMAd viruses with or without preincubation with the EGF-Streptavidin adapter. Expression of luciferase was measured 48 h later in tumor and liver tissue lysates. As shown in Figure 4a, EGFR-mediated infection with

mBFmAd resulted in a statistically significant increase in luciferase expression in tumors. Addition of the adapter augmented mBfMAd-mediated gene transfer in EGFR-expressing tumors by over sevenfold, with average of relative light units (RLU)/mg protein values of 1668 000 ± 530 100 and 223 900 ± 38 910 for groups with and without adapter, respectively. Liver gene transfer was not influenced by addition of the adapter in animals receiving mBfMAd with or without the adapter. Ad5luc showed higher levels of the gene transfer both in tumors and in livers (Figure 4b) compared to mBfMAd. However, the pattern of retargeting with adapter for Ad5luc was different from mBfMAd. Preincubation of Ad5luc with EGF-Streptavidin resulted in only a slight increase of gene transfer noted for both tumors and livers in all groups, but this enhancement was not statistically significant. Despite of potential of adenoviral vectors for cancer gene therapy, a major impediment of Ad-based delivery is liver tropism of the vector. Vector modifications that could minimize liver uptake and maximize tumor transduction would enhance vector applicability. In this context, we were also interested how our retargeting efforts were reflected in changing the tumor-to-liver gene transfer ratio. The tumor-to-liver ratio was calculated for each individual animal and presented as individual dots on a graph in Figure 4c. The mean values of these ratios for the two groups receiving Ad5luc with or without adapter were similar and corresponded to 9.4 and 8.9. The mean ratio calculated for the group receiving mBfMAd increased from 39 for the group receiving virus without adapter to 69 for the group receiving EGFR-retargeted virus. Large variations between the values calculated for individual animals within each group were noted, and rendered the differences between these two groups statistically insignificant. However, the EGF-mediated targeting capacities of mBfMAd and Ad5luc as measured by the tumor-to-liver luciferase activity ratio, were statistically significant ($P = 0.01$). Thus, these data demonstrate the gains of adapter-based retargeting to EGFR-expressing tumor xenografts in the model of localized tumor.

In vivo *retargeting of mBfMAd to EGFR-expressing lung endothelium in EGFR transient transgenic human CAR (hCAR) mice*

We also explored the feasibility of targeting mBFmAd to hEGFR expressed in the pulmonary vasculature of mice. For these experiments we have utilized the model recently developed in our group that is based on transient induction of the target molecule in the pulmonary endothelium. This is accomplished using a combination of hCAR transgenic mice and Ad-based vectors that allowed endothelial cell-specific antigen expression via placing the transgene under control of the endothelial specific flt-1 promoter.

The hCAR transgenic mice express a truncated hCAR under control of the ubiquitin promoter, resulting in hCAR protein expression in all organs including the lungs and therefore sensitizing the animal to adenoviral infection.[13] The major benefit of this model for testing vector targeting gains is the accessibility of the antigen to systemically introduced targeted vectors. To transiently induce human EGFR in the pulmonary endothelium of hCAR transgenic mice, we used the AdfltEGFR adenovirus. We have previously confirmed the functionality of this virus *in vitro*. Further, we confirmed the expression of hEGFR in the pulmonary vasculature of hCAR mice upon tail vein injection of AdflthEGFR (1×10^{11} vp) by

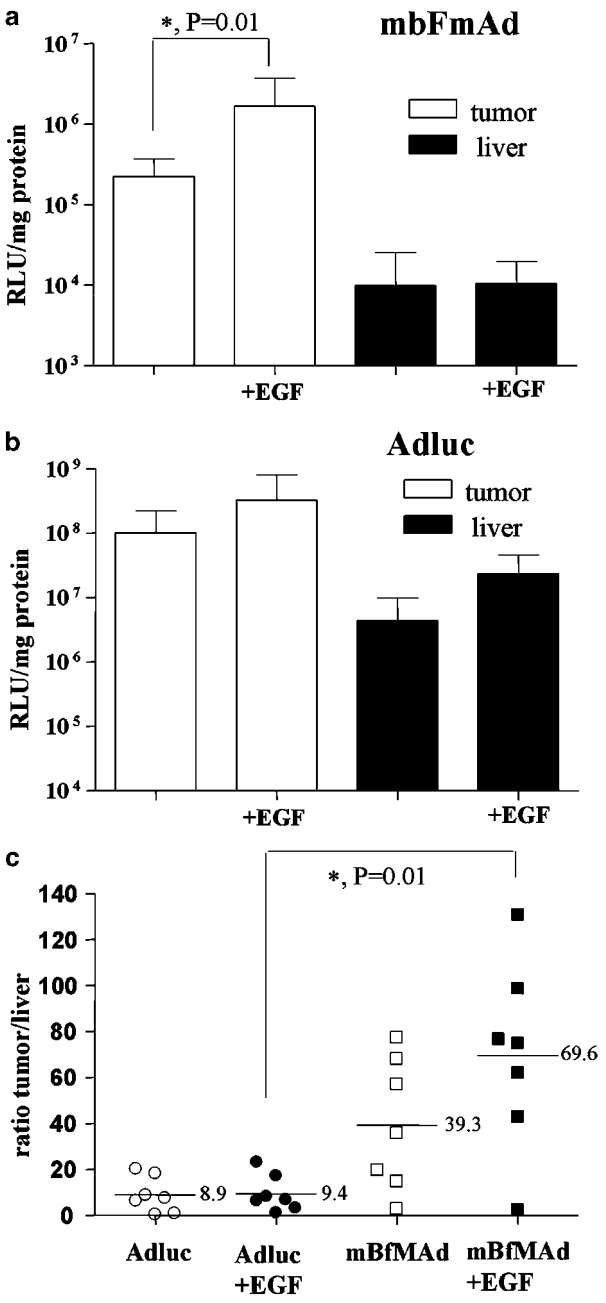

Figure 4 *In vivo* retargeting of mBfMAd to EGFR using animal model of ovarian carcinoma. CB17 SCID mice were injected i.p. with 10×10^6 SKOV3ip1 cells to establish i.p. ovarian tumors. At day 21 after SKOV3ip injection, four groups of mice ($n = 7$) were injected with Ad5luc or mBfMAd viruses either without adapter or preincubated with EGF-streptavidin. Viruses were injected i.p. at 1×10^{10} vp/animal. Mice were killed 48 h later, tumors and livers were excised and luciferase assay was performed in tissue lysates. Results are presented as luciferase expression (RLU) normalized for protein content (mg protein) for mBfMAd (**a**) and Ad5luc (**b**), and as tumor-to-liver ratio of luciferase expression (**c**). Tumor-to-liver ratio was calculated for individual animals, each represented as one dot on the graph. Bars represent averages of values in each group ($n = 7$), $P = 0.01$.

staining for EGFR in lung sections (data not shown). To validate EGFR targeting *in vivo*, hCAR mice preconditioned with AdfIthEGFR injection were reinjected 48 h later with 5.0×10^{10} vp of mBfMAd preincubated with either PBS or EGF-Streptavidin. The animals were killed 48 h subsequent to the second injection, and luciferase activities in the lungs and livers were quantified. As shown in Figure 5a, EGF-mediated luciferase activity of mBfMAd in the lungs of pre-treated animals was increased by almost fivefold compared to that in animals receiving mBfMAd without the adapter (341 587 vs 70 625 mean RLU/mg protein, respectively). This indicates that mBfBAd complexed with molecular adapter was able to efficiently target cells expressing antigen in the lung of mice following intravenous administration. Furthermore, liver transduction by the targeted virus did not increase. This outcome provided a significantly higher lung-to-liver ratio for the EGFR-retargeted group vs the control virus infected group (6.5 vs 1.3 mean ratios, respectively; $P = 0.01$) (Figure 5b). Therefore, the accessibility of EGFR expressed in the lung vasculature enables to augment EGFR-based transduction of targeted cells by systemically introduced mBfBAd. In aggregate, these results demonstrate the targeting capacities of our strategy *in vivo*.

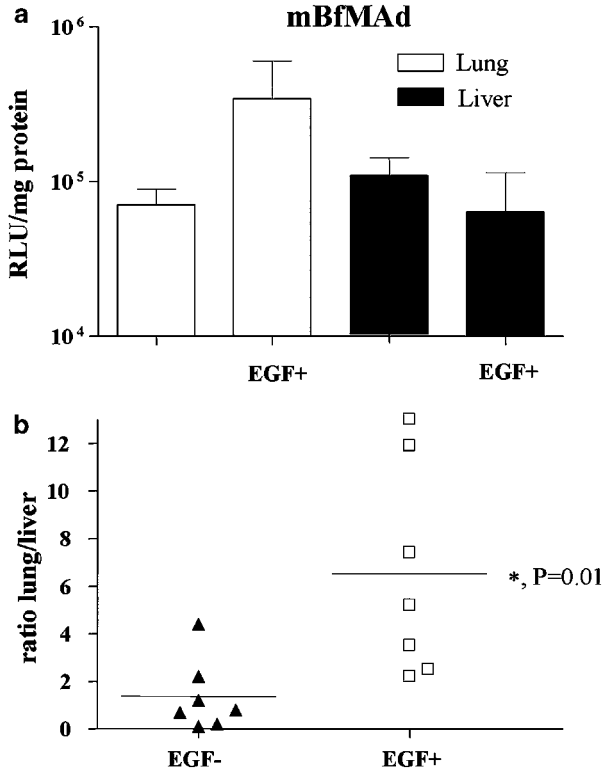

Figure 5 *In vivo* retargeting of mBfMAd to EGFR-expressing lung endothelium in EGFR transient transgenic hCAR mice. hCAR transgenic mice were injected with AdfltEGFR at 10^{11} vp/mice via tail vein for expression of EGFR in lung endothelium followed by a second injection of mBfMAd with or without adapter at 5×10^{10} vp/animal via tail vein 48 h later. Forty-eight hours after mBfMAd all animals were killed. (**a**) Lung and liver luciferase activities 48 h after intravenous administration of mBfMAd with or without the EGF-Streptavidin adapter. Results are presented as lung and liver luciferase expression (RLU) normalized for protein content (mg protein). (**b**) Lung-to-liver ratios of luciferase activities in individual animals ($n = 7$). Bars represent averages of values in each group ($P = 0.01$).

Discussion

In this study, we evaluated a targeting approach, utilizing a genetically modified Ad fiber and adapter-mediated retargeting, both combined in the context of a fiber-mosaic viral capsid. We applied this approach for EGFR targeting, to demonstrate the functionality of our strategy *in vitro* and to establish the potential of this system for *in vivo* targeting applications.

Bifunctional adapter molecules have been engineered with specificity for both the Ad capsid protein (mainly Ad fiber) and to alternative cellular receptors distinct from CAR. The main advantage of this system is in its flexibility for using high affinity binders, regardless of their nature and size. However, the necessity for producing complex adapter molecules, such as whole antibodies, Ab fragments or recombinant fusion proteins, has always been regarded as an inherent drawback of this approach. Nevertheless, efficient adenovirus targeting *in vivo* has only been reported using adapter-based approaches.[14–16]

Genetically modified vectors have a theoretical advantage in that they do not require additional soluble components for infectivity. A number of viruses with fibers constructed in this manner have been reported ranging from minor modifications, including single amino-acid substitutions[17] and addition of small peptides[18,19] to more substantial alterations, such as switching entire protein functional domains (knob, shaft)[20–22] and generation of artificial fiber-like scaffolds that retain the essential functional properties of the whole Ad fiber.[23,24] These vectors generally fulfill the basic targeting requirements on cells *in vitro*, but the expected targeting efficacy has not yet been translated to *in vivo* experiments. In fact, the genetically modified single component vectors most often require careful optimization of vector design by trial and error. In view of these obstacles, we hypothesized that the fiber mosaic platform, where two fibers are included in the viral genome, presents a more flexible mode for Ad vector modification and may simplify optimization of targeting efforts.

Here, we engineered a novel fiber-mosaic Ad vector, which comprises two fiber types: the wt fiber and FF chimera fused to the BAP. This strategy has previously been used to metabolically conjugate biotin to viral proteins in mammalian cells, which allows them to be coupled to retargeting adapter molecules that contain streptavidin.[4,5,25] However, the utility of biotin incorporation for virus retargeting has thus far only been demonstrated *in vitro* and, among all of the structural proteins tested, only fiber-incorporated biotin was capable of efficient retargeting.[5] These studies established that biotin attachment is determined by the locale for BAP incorporation and provided the rationale for our fiber-based retargeting strategy.

Although our fiber-mosaic vector does provide an alternative tropism, the native tropism is not completely ablated due to the retention of the wt fiber in the viral capsid. The targeting function is delegated to a recombinant fiber, while keeping the structural and functional integrity of the wt fiber during all stages of the viral life

cycle. The presence of wt fiber served to amplify the fiber-mosaic Ad to titers as high as 10^{12}–10^{13} vp/ml in regular laboratory-scale preparations. The presence of wt fiber may undermine the efficiency of retargeting, as just a fraction of fibers present on the viral capsid will serve for retargeting purposes. However, efficient redirection of our vector towards cells expressing EGFR was validated *in vitro*. The adapter-driven mBfMAd increased transduction of EGFR-positive cell lines 10- to 23-fold, compared to transduction without adapter. This level of enhancement is comparable with previously reported values obtained utilizing a complex of the wt virus with different bispecific molecular adapters.[12,26] Similarly, adenovirus retargeted through an 'adenobody' strategy demonstrated a 10-fold enhancement of infectivity on A431 cell line.[27] Efficient utilization of the retargeting fiber was demonstrated using blocking experiments. The mBfMAd vector complexed with EGF-Streptavidin maintained a high level of gene transfer in the presence of Ad5 fiber knob concentrations that blocked infectivity of the Ad5luc control virus in the presence or absence of the adapter. These data additionally support the ability of mBfMAd to redirect infection through the EGFR pathway. Thus, we believe that the proposed mosaic virus can efficiently utilize one of the mosaic fibers to redirect virus to alternative receptor *in vitro*.

Retargeting of different viruses through cell growth factor receptors, such as EGFR, which is highly expressed on tumors of different origin, has been validated in several adapter-based studies.[12,26–29] All reported adapter constructs were effective at coupling Ad to EGFR and resulted in increased gene transfer to EGFR expressing cell lines. This proved that EGFR pathway is compatible with the adenoviral infection cycle. EGF exhibits high affinity binding to EGFR, which leads to rapid internalization via the receptor-mediated endocytic pathway but no recycling of the receptor-ligand complex.[30] Thus, the EGFR pathway is one of the best studied and proven pathways for adenoviral retargeting *in vitro*. However, *in vivo* studies involving such experiments are scarce and primarily utilize intratumoral administration of retargeted viruses.[28,31] There is often a disconnect between the virus targeting efficacy *in vitro* and that *in vivo*, whereby the retargeting results obtained in cell culture does not translated into *in vivo* gains. Thus, we next wanted to test if our retargeting strategy using fiber-mosaic virus can be effective *in vivo* and retarget mBFmAd to EGFR expressing cells.

Initial *in vivo* studies for retargeting adenoviral vectors were carried out using adapter-mediated approaches in i.p. models of human cancer in mice.[32,33] This approach allows evaluation of targeting without the major hurdle of systemic virus administration, sequestration of the injected virus by the liver. The SKOV3ip ovarian cancer cell line expresses a very high level of EGFR and thus presents a good model to test EGFR targeting. Depending on the experimental conditions, mBfmAd demonstrated a 5-to 20–fold increase in gene transfer on these cells *in vitro*. Thus, it seemed logical to test whether the targeting gains would be paralleled *in vivo*. When injected in mice with pre-established i.p. SKOV3ip xenografts, EGFR-retargeted mBfmAd increased tumor luciferase expression sevenfold, whereas gene expression in the liver was not affected. Gene transfer efficiency with the Ad5luc vector was also slightly enhanced by the presence of the adapter. We have noted the similar effect of adapter on Ad5luc infectivity *in vitro*, but the adapter-based gene transfer enhancement of Ad5luc was lower than that of the mBFmAd. Moreover, the addition of the adapter to Ad5luc increased gene transfer in both tumor and liver to the same extent, which finally resulted in similar tumor-to-liver ratios for Ad5luc with or without adapter (9.4 vs 8.9), whereas the mean tumor-to-liver ratio calculated for the group receiving mBfMAd increased from 39 to 69 for virus without adapter and EGFR-retargeted virus, respectively. Of note, previous publications on adapter-mediated Ad retargeting, under similar experimental conditions, report only qualitative data on targeting gains[32,34] or targeting gains of at most two- to fivefold. Thus, the retargeting strategy applied to mBFmAd allowed to achieve comparable increase in tumor gene transfer in the context of ovarian cancer xenografts.

Another approach to test retargeting properties of adenoviral vectors in an efficient manner was recently developed in our group.[2] As systemically introduced vectors retargeted to tumors are to overcome multiple physiological barriers before reaching their targets, it has been proposed that the display of targeting molecules at accessible sites would facilitate testing of targeting gains of systemically administered adenoviral vectors. An hCAR-transgenic mouse model that is sensitized to Ad infection and is used to transiently express tumor antigens in the lung vasculature was recently reported to be efficient for evaluating vectors targeted to CD40 and carcinoembryonic antigen (CEA).[2,35] Thus, the hCAR mice were used to confirm whether our targeting strategy using the combination of two targeting modes in a single vector could efficiently target hEGFR expressed in the lungs. Expression of hEGFR was transiently induced in the mice pulmonary endothelium by systemic injection of recombinant adenovirus Ad-fltEGFR. In this model, mBFmAd retargeted to EGFR expressed in mouse lungs showed a fivefold enhancement in the lung gene transfer, which resulted in increased the lung-to-liver retargeting ratio from 1.3 for the virus without adapter to 6.3 for the retargeted virus. The lung-to-liver ratios calculated in our experiment for the retargeted fiber-mosaic vector correlated well with the values obtained in a previous study utilizing this model for CD40 retargeting (lung-to-liver ratio of 5.2 for CD40-retargeted virus and 1.2 for irrelevant virus),[35] thus providing a good estimate of the level of transductional retargeting gains achievable in this *in vivo* model. Overall, this transient transgenic model system allowed our targeting strategy to be evaluated.

Despite the fact that statistically significant differences in gene transfer was obtained by targeted vs untargeted virus in both models tested, a considerable variation of gene transfer values were obtained for individual animals, particularly for the calculated tumor-to-liver or lung-to-liver ratios. Specifically, this was observed in the groups receiving mBFmAd with adapter. These variations could be associated with the individual *in vivo* conditions, experimental errors or factors related to the retargeting system itself in its current design, such as uniformity of virus prep and virus-adapter formulation.

All experimental work included in this study was carried out using single mBFmAd and Ad5luc preps, which were characterized for vp and PFU content, as

well as the degree of fiber incorporation and biotinylation. However, we would like to stress that the uniformity of viral preparation in terms of the fiber content of each individual vp remains unknown. It is likely that the preparation of fiber-mosaic virus could contain (i) truly fiber-mosaic particles having both fibers in one viral capsid, (ii) a mixture of viral capsids displaying just one of the fibers and (iii) a combination of both variants. This factor may affect the overall performance of the fiber-mosaic virus. Of note, native fiber-mosaic viruses of serotype 40 and 41 have equal presentation of both fibers and apparently display both fibers in a single vp.

Another possible cause for inconsistence of viral preps is potential recombination. Although we were trying to minimize homologous sequences in mosaic genome, the rearrangement at low level still exists. DNA isolated from several viral preps of mBFmAd was tested for rearrangement and reversion to the single fiber genome by PCR. A low level of PCR product with that size corresponded to the recombination event was detected in viral preps, and in plasmid preps of mBFmAd Shuttle vector and Ad genome, which are the standard steps of designing adenoviral vector. We believe that recombination at some low level occurred in the plasmid DNA, whereas it is being propagated in bacteria, thus mBFmAd viral prep also may carry the low level of contamination with viruses with one fiber. To minimize recombination in improved generations of fiber-mosaics, silent point mutations can be introduced into fiber tail sequences. In addition, we also cannot exclude possible batch to batch variation of mBFmAd preps in terms of biotinylated fiber incorporation. For this experiment virus was pre-incubated with the adapter without any additional purification. However, further optimization for obtaining the virus-adapter complex can be considered. The crude viral prep obtained after the first virus CsCl banding can be further purified on avidin columns to eliminate virions lacking the recombinant fibers fibers. We are currently testing the consistency of fiber-mosaic virus preparations. Several lots of virus preparation did show a similar ratio of wt fiber to biotinylated fiber incorporation as described previously. However, different experimental and viral amplification conditions may bias or favor incorporation of the retargeting fiber and influence the overall efficiency of the retargeting strategy.

In this study, we have demonstrated enhanced gene transfer based on transductional retargeting of our vector. It would be of a considerable interest to investigate the extent to which it will translate to therapeutic end points. Several publications indicated the feasibility of conversion of the vector targeting gains to the treatment benefits in experimental animal models.[28,33] Thus, our future goal will include the introduction of an anticancer therapeutic gene in the context of the proposed fiber-mosaic platform to test therapeutic efficacy of our retargeting strategy.

In summary, we have confirmed that mBfMAd complexed with EGF-Streptavidin could successfully retarget virus to EGFR-expressing cancer cell lines. Most importantly, the evidence of utility of this strategy was demonstrated *in vivo*. The targeting potential of mBfMAd complexed with EGF-Streptavidin was tested on two *in vivo* models that overexpress EGFR in different tissues. First, we utilized a mouse model of locoregional EGFR-positive ovarian xenografts. Secondly, the retargeting capacity of mBfMAd/EGF was tested on a 'transient transgenic' mouse model with transient expression of hEGFR in the mouse lung vasculature. mBfMAd/EGF achieved a higher transduction level in the lung compared to mBfMAd without adapter. Moreover, tumor-to-liver or lung-to-liver gene expression ratios for retargeted mBfMAd increased in both models tested. Thus, we demonstrated that an additional fiber in fiber-mosaic virions could be used for biotinylation and this modification, in combination with appropriate adapters, can be successfully exploited for adenoviral retargeting strategies. Importantly, our study demonstrated the proof of preclinical utility of our targeting strategy in animal models.

Materials and methods

Cells

The 293 human kidney cell line was purchased from Microbix (Toronto, Ontario, Canada). The human ovarian carcinoma cell line SKOV3.ip1 was obtained from Janet Price (MD Anderson Cancer Center, Houston, TX, USA). The human epidermoid carcinoma (A-431), human ovarian carcinoma (SKOV3), lung carcinoma (A549) and human breast cancer (MDA-MB-453) cell lines were from the American Type Culture Collection (Manassas, VA, USA). NR6 and NR6wt cell lines were obtained from Dr Alan Wells (University of Pittsburgh, Pittsburgh, PA, USA). These cell lines represent 3T3-derived fibroblasts lacking endogenous EGFRs (NR6) or the same cell line retrovirally transduced with the complete human EGFR (NR6wt).[11]

Antibodies

Monoclonal antibodies against the Ad5 fiber tail (4D2) and the fiber trimer (2A6) were purchased from Lab Vision (Fremont, CA, USA). Anti-His Ab was obtained from Qiagen (Valencia, CA, USA). Secondary goat anti-mouse IgG horseradish peroxidase (HRP)-conjugated Ab was obtained from DAKO (Carpinteria, CA, USA). Streptavidin and biotinylated HRP for Western blot were from Vector Labs (components of Vectastain ABC kit). Streptavidin for ELISA was from Southern Biotechnology Association (Birmingham, AL, USA).

Recombinant proteins

Recombinant soluble CAR protein was provided by Dr Igor Dmitriev, The Gene Therapy Center, University of Alabama at Birmingham.[12] The fiber-knob domain of Ad5 fibers was produced in *E. coli* with N-terminal tags of six consecutive histidine residues (6His), using the pQE30 expression vector (Qiagen, Valencia, CA, USA). Recombinant EGF-Streptavidin was obtained as described by Ponnazhagan *et al*.[10] Briefly, this adapter was obtained by cloning the coding sequences of EGF in frame with core-streptavidin in the vector pSTE2-215 Yol. For large-scale production of the fusion protein, 1 l of bacterial culture was induced with 20 μM IPTG (isopropyl-β-D-thiogalactopyranoside) for 5 h at 30°C. Protein was purified from both soluble periplastic extract and remaining inclusion bodies. To obtain soluble periplasmic extract of recombinant protein the cell pellet was resuspended in 1/100 of the original culture volume

in a buffer containing 50 mM Tris-HCl and 20% sucrose (pH 8.0). To purify protein from inclusion bodies, the pellet remaining after previous step was resuspended in 1/50 volume (to that of the original culture) of a buffer containing 6 M guanidine-HCl and 100 mM Tris (pH 7.0) and left rotating overnight. Following centrifugation at 13 000 r.p.m. for 30 min, the supernatant containing the fusion protein was affinity purified with a Ni-nitrilotriacetic acid (Ni-NTA) column (Qiagen) according the manufacturers instruction. The eluted fusion protein was dialyzed against a buffer containing 100 mM Tris and 400 mM L-arginine and stored as frozen in aliquots at −20°C.

Viruses

Adenoviral vector having wt fiber (Ad5luc) was used as a control for infectivity assessment of fiber-mosaic virus. Fiber mosaic virus AdFF/F5[6] genetically encoding two fibers: FF containing 6His at C-teminus[23] and wt fiber was used in virus binding experiments. Both viral genomes are isogenic to mBfMAd except the fiber region and contain the firefly luciferase gene under CMV promoter in E1 region. AdfltEGFR was used for transient expression of human EGFR in mouse lung vasculature in experiments testing systemic targeting of mBfMAd. The design of this virus is similar to the virus AdfltCEA described by Everts *et al*.,[2] where EGFR cDNA replaced CEA. EGFR cDNA was amplified from plasmid pcDNA3-EGFR.[36] All viruses were CsCl purified and vp titer was determined according to standard procedure.

Generation of mBfmAd

The design of the genome of mBfMAd Ad5-FF.PSTCD.F5luc (mBfMAd) was similar to that described previously for AdFF6H.F5luc,[6] where the virus genome encodes two fibers in the L5 region: chimeric FF containing C-terminal 6His (FF6H)[37] and Ad5 wt fiber. The coding sequences of both fibers are spanned by untranslated 5′ and 3′ sequences of wt fiber, with intent to provide equal transcription conditions for both fibers (splicing, polyadenylation and regulation by the Major Late Promoter). To create Ad5FF.PSTCD.F5luc we added a minimal domain of the 1.3S subunit of PSTCD to the chimeric protein FF. This domain is naturally biotinylated at lysine 89, when expressed in *E. coli* and *Saccharomyces cerevisiae* by each organism's cellular biotin ligase enzyme[7] and also can be metabolically biotinylated in mammalian cells.[8] DNA of PSTCD domain was amplified by PCR from the PinPoint-Xa2 plasmid (Promega, Madison, WI, USA) using primers 5′-GGCT CTAGAGCCGGTAAGGCCGGAGAG and 5′-CCGTCTA GAGAGATCCCCGATCTTGATG. The amplified fragment was then inserted into the *Xba*I site of plasmid pZeroFF6H, to obtain FF.PSTCD.6H. The cDNA of the resulting fiber FF.PSTCD.6H was amplified and cloned into a fiber mosaic shuttle vector pTGbx using *Cla*I and *Swa*I sites, therefore the shuttle plasmid finally has tandem fibers: FF.PSTCD.6H and Ad5 wt fiber flanked by Ad sequences. The Ad5 fiber-mosaic genome was obtained by homologous recombination of the mosaic shuttle vector (pTGbx FF.PSTCD.6H) with SwaI-linearized Ad5 genome backbone plasmid pVK700[38] in *E. coli* BJ5183. The pVK700 plasmid contains CMV promoter-driven firefly luciferase gene in the E1 region as a reporter gene. The plasmid obtained was designated as pAdFF.PSTCD.6 H.F5luc. The fiber-mosaic virus AdFF.PSTCD.6H.F5luc was rescued in 293 cells and purified by a standard CsCl gradient protocol. Titers of viral preps were determined in physical (vp) units, and infectious (PFU) units by TCID50 method according to the AdEasy protocol (Strategene, La Jolla, CA, USA). Single virus preps of both Ad5luc and mBfMAd were used throughout the entire study. The physical titers obtained were 4.15×10^{12} and 4.83×10^{12} vp/ml for Ad5luc and the mBfMAd vector, whereas the infectious titers were 4.50×10^{11} and 8.97×10^{9} PFU/ml, respectively. Ratio of vp/PFU for Ad5luc and mBfMAd was 1:9 and 1:530, respectively.

Western blot analysis

Western blot to detect virus fibers and confirm fiber biotinylation was performed as described.[6] Briefly, aliquots of Ad vectors equal to 5×10^{9} vp were loaded on sodium dodecyl sulfate 4–20% gradient PAGE (BioRad, Hercules, CA, USA) either boiled or unboiled. After separation, viral proteins were electroblotted onto a polyvinylidene difluoride (PVDF) membrane and detected with 4D2, 2A6, anti-His monoclonal AB followed by secondary Ab conjugated with HRP or strepavidin/biotinylated HRP for detection of fiber biotinylation. The blots were developed with 3,3′-diaminobenzidine.

Enzyme-linked immunosorbent assay

To test the binding properties of fiber-mosaic Ad, solid-phase binding ELISA was performed. Binding attributed to wt Ad fiber was confirmed by interaction with CAR as described.[6] Binding properties of the mosaic virus attributed to the biotinylated fiber were tested in interaction with streptavidin and EGF-streptavidin, which were coated on plastic at 50 and 5 μg/ml correspondingly in 100 μl of 100 mM carbonate buffer (pH 9.5) during overnight incubation at 4°C. After washing and blocking, the wells were incubated with the virus followed the secondary antibodies.

Ad-mediated gene transfer assay

Infectivity of the mBfMAd in tumor cell lines was determined by gene transfer assay. The amount of mBfMAd or Ad5luc was calculated for each gene transfer experiment, depending on cell numbers in the experimental protocol, to correspond to the desired MOI. Viruses were preincubated with EGF-Streptavidin at the concentration of 10 μg/ml in 300 μl of PBS for 1 h at room temperature (RT) and purified from excess of adapter using Microcon Centrifugal Filter Devices YM-100 (molecular weight cutoff 100 kDa) (Amicon Bioseparation, Millipore, Bedford, MA, USA). Viruses used as no adapter control underwent the same procedure as above except PBS was added instead of the adapter. Aliquots of the prepared viruses in DMEM-F12 containing 2% fetal bovine serum (FBS) were added to the cells and infection was carried out for 2 h at 37°C. The cells were incubated in complete media with 10% FBS at 37°C to allow expression of the luciferase gene for 24 h. Luciferase activity in the cell lysates was analyzed by using the Promega (Madison, WI, USA) luciferase assay system and a Berthold (Gaithersburg, MD, USA) luminometer.

In the system with artificial expression of human EGFR, mouse fibroblast cells NR6 or NR6wt stably

transduced with human EGFR were first preincubated for 10 min at RT with either PBS (no adapter) or with increasing concentration of EGF-Streptavidin (1–25 μg/ml). After washing with PBS cells were transduced with Ad5luc or mBfMAd at 50 PFU/cell. Luciferase assay was performed as described above.

Competitive inhibition assay

Cell lines with low (MDA-MB-453) or high EGFR expression (A431, A549, SKOV3) were plated in 24-well plates at a density of 1×10^6 cells/well. On the following day the cells were preincubated with recombinant Ad5 knob at 50 μg/ml for 10 min at RT to block infection via the wt fiber. Viruses were prepared as described in previous section and applied to cells, after the blocking step was completed, at MOI 50 PFU/cell for 2 h at 37°C. Unbound virus was washed away with PBS, and medium with 10% FBS was added to each well. Forty hours later, the cells were processed for luciferase assay as described above.

In vivo *retargeting of mBfMAd to EGFR using animal model of ovarian carcinoma*

CB17 SCID female mice 6–8 weeks of age (Charles River) were injected i.p. with 10×10^6 SKOV3ip1 cells to establish i.p. ovarian tumors. At day 21 after SKOV3ip injection, mice ($n = 7$ per group) were followed with i.p. injection of Ad5luc or mBfMAd viruses at 1×10^{10} vp/animal preincubated either with adapter EGF-Streptavidin (10 μg) or PBS. Mice were killed 48 h later, all visible tumor nodules (combined and treated as one tumor sample from each animal) and livers were excised and luciferase assay was performed in tissue lysates. Same lysates were used to determine protein concentration by Bio-Rad assay.

In vivo *retargeting of mBfMAd to EGFR-expressing lung endothelium in EGFR transient transgenic hCAR mice*

The transgenic hCAR mice were a generous gift from Dr Sven Pettersson (Karolinska Institute, Sweden). These mice express truncated hCAR under the control of the human ubiquitin-C promoter, thus allowing hCAR expression in a variety of tissues, including the lungs, kidneys, liver, heart, brain and muscle.[13] In this study, 8-to 12-week-old hCAR mice screened for presence of hCAR using PCR and flow cytometry were used. First, hCAR transgenic mice were preconditioned to achieve transient EGFR expression in lung endothelium. For that mice were injected via tail vein with 1×10^{11} vp of AdfltEGFR per animal. Transient expression of Ad transgene in lung endothelium under these conditions has been first demonstrated by Everts *et al*.[2] Forty-eight hours after the first injection, each mouse was injected iv with 5×10^{10} vp of mBfMAd preincubated either with EGF-Streptavidin (100 ng) or PBS. All animals were killed 48 h after the last viral injection. Lung and liver luciferase activities were measured and normalized for protein content determined by Bio-Rad assay.

Animal experiments and protocols were reviewed and approved by the Institutional Animal Care and Use Committee of University of Alabama at Birmingham.

Statistics

Student's *t*-test was employed for statistical analysis where $P < 0.05$ was considered to be statistically significant.

Acknowledgements

We thank Joel Glasgow and Alex Pereboev for proofing the manuscript and helpful critique. This study was supported, in part, by NIH grants RO1CA083821-06, 1P01HL076540, 1P01CA104177-01A2, CA075930-07 and DOD grant W81XWH-05-1-0035 and Muscular Dystrophy Association.

References

1 Reynolds PN, Zinn KR, Gavrilyuk VD, Balyasnikova IV, Rogers BE, Buchsbaum DJ *et al*. A targetable, injectable adenoviral vector for selective gene delivery to pulmonary endothelium *in vivo*. *Mol Ther* 2000; **2**: 562–578.
2 Everts M, Kim-Park SA, Preuss MA, Passineau MJ, Glasgow JN, Pereboev AV *et al*. Selective induction of tumor-associated antigens in murine pulmonary vasculature using double-targeted adenoviral vectors. *Gene Therapy* 2005; **12**: 1042–1048.
3 Nettelbeck DM, Miller DW, Jerome V, Zuzarte M, Watkins SJ, Hawkins RE *et al*. Targeting of adenovirus to endothelial cells by a bispecific single-chain diabody directed against the adenovirus fiber knob domain and human endoglin (CD105). *Mol Ther* 2001; **3**: 882–891.
4 Campos SK, Parrott MB, Barry MA. Avidin-based targeting and purification of a protein IX-modified, metabolically biotinylated adenoviral vector. *Mol Ther* 2004; **9**: 942–954.
5 Campos SK, Barry MA. Comparison of adenovirus fiber, protein IX, and hexon capsomeres as scaffolds for vector purification and cell targeting. *Virology* 2006; **349**: 453–462.
6 Pereboeva L, Komarova S, Mahasreshti PJ, Curiel DT. Fiber-mosaic adenovirus as a novel approach to design genetically modified adenoviral vectors. *Virus Res* 2004; **105**: 35–46.
7 Cronan Jr JE. Biotination of proteins *in vivo*. A post-translational modification to label, purify, and study proteins. *J Biol Chem* 1990; **265**: 10327–10333.
8 Parrott MB, Barry MA. Metabolic biotinylation of recombinant proteins in mammalian cells and in mice. *Mol Ther* 2000; **1**: 96–104.
9 Sano T, Pandori MW, Chen X, Smith CL, Cantor CR. Recombinant core streptavidins. A minimum-sized core streptavidin has enhanced structural stability and higher accessibility to biotinylated macromolecules. *J Biol Chem* 1995; **270**: 28204–28209.
10 Ponnazhagan S, Mahendra G, Kumar S, Thompson JA, Castillas Jr M. Conjugate-based targeting of recombinant adeno-associated virus type 2 vectors by using avidin-linked ligands. *J Virol* 2002; **76**: 12900–12907.
11 Chen P, Murphy-Ullrich JE, Wells A. A role for gelsolin in actuating epidermal growth factor receptor-mediated cell motility. *J Cell Biol* 1996; **134**: 689–698.
12 Dmitriev I, Kashentseva E, Rogers BE, Krasnykh V, Curiel DT. Ectodomain of coxsackievirus and adenovirus receptor genetically fused to epidermal growth factor mediates adenovirus targeting to epidermal growth factor receptor-positive cells. *J Virol* 2000; **74**: 6875–6884.
13 Tallone T, Malin S, Samuelsson A, Wilbertz J, Miyahara M, Okamoto K *et al*. A mouse model for adenovirus gene delivery. *Proc Natl Acad Sci USA* 2001; **98**: 7910–7915.
14 Gu DL, Gonzalez AM, Printz MA, Doukas J, Ying W, D'Andrea M *et al*. Fibroblast growth factor 2 retargeted adenovirus has

redirected cellular tropism: evidence for reduced toxicity and enhanced antitumor activity in mice. *Cancer Res* 1999; **59**: 2608–2614.
15 Fisher KD, Stallwood Y, Green NK, Ulbrich K, Mautner V, Seymour LW. Polymer-coated adenovirus permits efficient retargeting and evades neutralising antibodies. *Gene Therapy* 2001; **8**: 341–348.
16 Lanciotti J, Song A, Doukas J, Sosnowski B, Pierce G, Gregory R *et al*. Targeting adenoviral vectors using heterofunctional polyethylene glycol FGF2 conjugates. *Mol Ther* 2003; **8**: 99–107.
17 Roelvink PW, Mi Lee G, Einfeld DA, Kovesdi I, Wickham TJ. Identification of a conserved receptor-binding site on the fiber proteins of CAR-recognizing adenoviridae. *Science* 1999; **286**: 1568–1571.
18 Dmitriev I, Krasnykh V, Miller CR, Wang M, Kashentseva E, Mikheeva G *et al*. An adenovirus vector with genetically modified fibers demonstrates expanded tropism via utilization of a coxsackievirus and adenovirus receptor-independent cell entry mechanism. *J Virol* 1998; **72**: 9706–9713.
19 Wickham TJ, Tzeng E, Shears II LL, Roelvink PW, Li Y, Lee GM *et al*. Increased *in vitro* and *in vivo* gene transfer by adenovirus vectors containing chimeric fiber proteins. *J Virol* 1997; **71**: 8221–8229.
20 van Beusechem VW, van Rijswijk AL, van Es HH, Haisma HJ, Pinedo HM, Gerritsen WR. Recombinant adenovirus vectors with knobless fibers for targeted gene transfer. *Gene Therapy* 2000; **7**: 1940–1946.
21 Magnusson MK, Hong SS, Boulanger P, Lindholm L. Genetic retargeting of adenovirus: novel strategy employing 'deknobbing' of the fiber. *J Virol* 2001; **75**: 7280–7289.
22 Mercier GT, Campbell JA, Chappell JD, Stehle T, Dermody TS, Barry MA. A chimeric adenovirus vector encoding reovirus attachment protein sigma1 targets cells expressing junctional adhesion molecule 1. *Proc Natl Acad Sci USA* 2004; **101**: 6188–6193.
23 Krasnykh V, Belousova N, Korokhov N, Mikheeva G, Curiel DT. Genetic targeting of an adenovirus vector via replacement of the fiber protein with the phage T4 fibritin. *J Virol* 2001; **75**: 4176–4183.
24 Belousova N, Korokhov N, Krendelshchikova V, Simonenko V, Mikheeva G, Triozzi PL *et al*. Genetically targeted adenovirus vector directed to CD40-expressing cells. *J Virol* 2003; **77**: 11367–11377.
25 Parrott MB, Adams KE, Mercier GT, Mok H, Campos SK, Barry MA. Metabolically biotinylated adenovirus for cell targeting, ligand screening, and vector purification. *Mol Ther* 2003; **8**: 688–700.
26 Haisma HJ, Grill J, Curiel DT, Hoogeland S, van Beusechem VW, Pinedo HM *et al*. Targeting of adenoviral vectors through a bispecific single-chain antibody. *Cancer Gene Ther* 2000; **7**: 901–904.
27 Watkins SJ, Mesyanzhinov VV, Kurochkina LP, Hawkins RE. The 'adenobody' approach to viral targeting: specific and enhanced adenoviral gene delivery. *Gene Therapy* 1997; **4**: 1004–1012.
28 Hemminki A, Dmitriev I, Liu B, Desmond RA, Alemany R, Curiel DT. Targeting oncolytic adenoviral agents to the epidermal growth factor pathway with a secretory fusion molecule. *Cancer Res* 2001; **61**: 6377–6381.
29 van Beusechem VW, Grill J, Mastenbroek DC, Wickham TJ, Roelvink PW, Haisma HJ *et al*. Efficient and selective gene transfer into primary human brain tumors by using single-chain antibody-targeted adenoviral vectors with native tropism abolished. *J Virol* 2002; **76**: 2753–2762.
30 Kolibaba KS, Druker BJ. Protein tyrosine kinases and cancer. *Biochim Biophys Acta* 1997; **1333**: F217–F248.
31 Liang Q, Dmitriev I, Kashentseva E, Curiel DT, Herschman HR. Noninvasive of adenovirus tumor retargeting in living subjects by a soluble adenovirus receptor-epidermal growth factor (sCAR-EGF) fusion protein. *Mol Imag Biol* 2004; **6**: 385–394.
32 Printz MA, Gonzalez AM, Cunningham M, Gu DL, Ong M, Pierce GF *et al*. Fibroblast growth factor 2-retargeted adenoviral vectors exhibit a modified biolocalization pattern and display reduced toxicity relative to native adenoviral vectors. *Hum Gene Ther* 2000; **11**: 191–204.
33 Rancourt C, Rogers BE, Sosnowski BA, Wang M, Piche A, Pierce GF *et al*. Basic fibroblast growth factor enhancement of adenovirus-mediated delivery of the herpes simplex virus thymidine kinase gene results in augmented therapeutic benefit in a murine model of ovarian cancer. *Clin Cancer Res* 1998; **4**: 2455–2461.
34 Tanaka T, Huang J, Hirai S, Kuroki M, Watanabe N, Tomihara K *et al*. Carcinoembryonic antigen-targeted selective gene therapy for gastric cancer through FZ33 fiber-modified adenovirus vectors. *Clin Cancer Res* 2006; **12**: 3803–3813.
35 Izumi M, Kawakami Y, Glasgow JN, Belousova N, Everts M, Kim-Park S *et al*. *In vivo* analysis of a genetically modified adenoviral vector targeted to human CD40 using a novel transient transgenic model. *J Gene Med* 2005; **7**: 1517–1525.
36 Bonner JA, Buchsbaum DJ, Russo SM, Fiveash JB, Trummell HQ, Curiel DT *et al*. Anti-EGFR-mediated radiosensitization as a result of augmented EGFR expression. *Int J Radiat Oncol Biol Phys* 2004; **59**: 2–10.
37 Krasnykh V, Belousova N, Korokhov N, Mikheeva G, Curiel DT. Genetic targeting of an adenovirus vector via replacement of the fiber protein with the phage T4 fibritin. *J Virol* 2001; **75**: 4176–4183.
38 Belousova N, Krendelchtchikova V, Curiel DT, Krasnykh V. Modulation of adenovirus vector tropism via incorporation of polypeptide ligands into the fiber protein. *J Virol* 2002; **76**: 8621–8631.

Breast Cancer Res Treat
DOI 10.1007/s10549-006-9449-8

PRECLINICAL STUDY

Mesenchymal stem cells as a vehicle for targeted delivery of CRAds to lung metastases of breast carcinoma

Mariam A. Stoff-Khalili · Angel A. Rivera · J. Michael Mathis · N. Sanjib Banerjee · Amanda S. Moon · A. Hess · Rodney P. Rocconi · T. Michael Numnum · M. Everts · Louise T. Chow · Joanne T. Douglas · Gene P. Siegal · Zeng B. Zhu · Hans Georg Bender · Peter Dall · Alexander Stoff · Larissa Pereboeva · David T. Curiel

Received: 29 October 2006 / Accepted: 31 October 2006

Abstract
Purpose Alternative and complementary therapeutic strategies need to be developed for metastatic breast cancer. Virotherapy is a novel therapeutic approach for the treatment of cancer in which the replicating virus itself is the anticancer agent. However, the success of virotherapy has been limited due to inefficient virus delivery to the tumor site. The present study addresses the utility of human mesenchymal stem cells (hMSCs) as intermediate carriers for conditionally replicating adenoviruses (CRAds) to target metastatic breast cancer in vivo.
Experimental design HMSC were transduced with CRAds. We used a SCID mouse xenograft model to examine the effects of systemically injected CRAd loaded hMSC or CRAd alone on the growth of MDA-MB-231 derived pulmonary metastases (experimental metastases model) in vivo and on overall survival.
Results Intravenous injection of CRAd loaded hMSCs into mice with established MDA-MB-231 pulmonary metastatic disease homed to the tumor site and led to extended mouse survival compared to mice treated with CRAd alone.
Conclusion Injected hMSCs transduced with CRAds suppressed the growth of pulmonary metastases, presumably through viral amplification in the hMSCs. Thus, hMSCs may be an effective platform for the targeted delivery of CRAds to distant cancer sites such as metastatic breast cancer.

Keywords Breast cancer · Cell vehicle · CRAds · Metastases · Stem cells · Virotherapy

M. A. Stoff-Khalili · A. A. Rivera · R. P. Rocconi · T. M. Numnum · M. Everts · J. T. Douglas · G. P. Siegal · Z. B. Zhu · A. Stoff · L. Pereboeva · D. T. Curiel (✉)
Division of Human Gene Therapy, Departments of Medicine, Surgery, Pathology and the Gene Therapy Center, University of Alabama at Birmingham, 901 19th Street South, BMR2 502, Birmingham, AL 35294-2172, USA
e-mail: curiel@uab.edu

M. A. Stoff-Khalili · A. Hess · H. G. Bender · P. Dall
Department of Obstetrics and Gynecology, Medical Center, University of Duesseldorf, 40225 Duesseldorf, Germany

J. M. Mathis
Gene Therapy Program, Department of Cellular Biology and Anatomy, Louisiana State University Health Sciences Center, Shreveport, LA 71130, USA

N. S. Banerjee · L. T. Chow
Department of Biochemistry and Molecular Genetics, University of Alabama at Birmingham, Birmingham, AL 35294-2172, USA

A. Stoff
Department of Plastic and Reconstructive Surgery, Dreifaltigkeits-Hospital, 50389 Wesseling, Germany

A. S. Moon
Animal Resources Program, University of Alabama at Birmingham, Birmingham, AL 35294-2172, USA

Introduction

In the United States, breast cancer remains the most common malignancy in women. In some women, breast cancer is a local disease without spread. Such early breast cancers are usually diagnosed by screening mammography and are highly curable with local or regional treatment alone. However, most women with primary cancer have subclinical metastases, and in a high percentage of those treated with apparently curative surgery, distant metastases ultimately develop. The clinical course of metastatic breast cancer is variable. Chemotherapy, hormonal therapy, radiotherapy, and limited surgery are all used in the treatment of women with metastatic breast cancer, although the overwhelming majority of these women will die of their disease. In view, of the limited success of available treatment modalities for metastatic breast cancer, alternative and complementary strategies need to be developed.

In this regard, virotherapy is an exciting therapeutic approach for the treatment of cancer in which the replicating virus itself is the anticancer agent. Among various viruses, the adenovirus-based vector has emerged as a leading candidate for in vivo cancer virotherapy. Conditionally replicative adenovirus based agents (CRAds) have been designed to replicate in tumor cells whereby the virus can self-amplify and spread in the tumor from an initial infection of only a few cells. However, highly effective use of CRAd agents in tumors clinically has been heretofore hindered by three main factors: (1) low viral infectivity, (2) suboptimal replicative specificity and (3) inefficient viral agent delivery to the tumor site [10]. With respect to breast cancer, transduction efficacy by adenovirus serotype 5 (Ad5) is often suboptimal due to the highly variable and often low expression pattern of the primary adenovirus receptor, coxsackie adenovirus receptor (CAR) [4, 9]. To circumvent this, genetic alterations of the virus fiber protein that utilizes CAR-independent entry pathways have been identified, thus bypassing CAR deficiency on cancer cells and enhancing tumor transduction. In parallel, strategies have been developed to enhance the transcription selectivity of current vector systems toward tumor cells by using tumor specific promoter (TSP) that limit ectopic expression in non-tumor cells and decrease treatment-associated toxicities. However, efficient virus delivery to the tumor site is a central mandate of virotherapy.

In this regard, cell carriers exhibiting endogenous tumor homing activity have been recently exploited to chaperone virus delivery to the tumor site. Although the utility of cells as vehicles for toxic genes, anti-angiogenic molecules, and immunostimulatory genes has been suggested in several studies, there have been only limited studies whereby cells have been exploited as carriers for virotherapeutic agents. In this regard, we have proposed human mesenchymal stromal cells (hMSCs) as carriers of oncolytic viruses in vitro [15]. MSCs are bone marrow-derived non-hematopoietic precursor cells that when systemically administered, home to the tumor, preferentially survive and proliferate in the presence of malignant cells and become incorporated into the tumor architecture as stromal fibroblasts [20]. In this regard, it has been recently shown that systemically administered hMSCs home to breast cancer metastasis of the lung [21].

Based upon these findings, we hypothesized that hMSCs could be used as a targeting strategy for CRAds in the treatment of breast cancer metastasis of the lung. Our results, demonstrating that systemic administration of hMSC carriers can target CRAds to metastatic disease, constitute a novel therapeutic paradigm for breast cancer that couples cell therapy with virotherapy.

Materials and methods

Adenoviral vectors

The CRAd Ad5/3.CXCR4 was constructed as follows: the plasmid pBSKCAT/CXCR4, which contains a 279 bp sequence from the human CXCR4 promoter (–191 to +88), was a kind gift of Dr. Nelson L. Michael [25]. The CXCR4 promoter sequence (NCBI Accession Number AY728138, from 1780 to 2059 bp) containing the 279 bp CXCR4 promoter and the simian virus 40 (SV40) polyadenylation (poly A) signal was cloned by PCR into the *NotI/XhoI* site of pScsE1 plasmid [12, 17] (a kind gift from Dr. Dirk Nettelbeck, Department of Dermatology, University Medical Center-Erlangen, Erlangen, Germany), resulting in pScsE1CXCR4 that contained the E1A gene downstream of the CXCR4 gene promoter. The Ad vector, pAdback 5/3 was a kind gift from Dirk Nettenbeck and contains both the E3 gene and a capsid modified F5/3 [12, 17]. After cleavage with *PmeI*, the shuttle vector, pScsE1CXCR4, was recombined with pAdback5/3 to generate the CRAd Ad5/3.CXCR4, where the human Ad knob serotype 5 is replaced by human Ad knob serotype 3. The Ad vector, pVK503c, was a kind gift from Dr. V. Krasnykh (M.D. Anderson, Houston, TX), and contains both the E3 gene and a capsid modified RGD4C [23]. After cleavage with *PmeI*, the shuttle

vector, pScsE1CXCR4, was recombined with *Cla I* linearized pVK503c to generate the CRAd Ad5RGD.CXCR4 with a fiber protein incorporating an RGD-motif in the HI-loop of Ad5 fiber. The recombinant plasmids were linearized with *PacI* and transfected into 293 cells using superfect reagent (Qiagen; Valencia, CA) to generate the Ad5/3.CXCR4 and Ad5R6D.CXCR4 adenoviruses. The other replication competent adenoviruses used in this study were: wild type Ad5wt with unmodified fiber [22], Ad5/3wt with a chimeric fiber having the knob of Ad5 fiber replaced by knob of Ad3 fiber [12, 17], Ad5.RGDwt with a fiber protein incorporating an RGD-motif in the HI-loop of Ad5 fiber. Ad.CXCR4Luc [26] was used for replication negative control. The adenoviruses were propagated in the A549 cells (a lung cancer cell line in which the CXCR4 gene is overexpressed), and purified by double CsCl density gradient centrifugation, followed by dialysis against phosphate buffered saline (PBS) containing 10% glycerol. The concentration of total viral particle numbers (PN) was determined by measuring absorption at 260 nm. Infectious PNs were determined by measuring the concentration of viral hexon protein-positive 293 cells after a 48-h infection period, using an Adeno-X Rapid Titer Kit (Clontech; Mountain View, CA).

Cell line and cell culture

MDA-MB-231 breast cancer cell lines were obtained from the American Type Culture Collection (ATCC) and cultured as described. In brief, the cells were maintained in DME/F-12 medium (Life Technologies, Inc., Grand Island, NY), containing 10% fetal bovine serum (FBS: Gemini Bio-Products, Woodland, Ca), and 1% antibiotic–antimycotic solution (penicillin–streptomycin–fungizone, Sigma Chemicals Co., St. Louis, MO). The cells were maintained in T-175 flasks at 37°C and 5% humidified CO_2, and were sub-cultured using 1% trypsin–EDTA (Gibco BRL, Life Technologies).

Human mesenchymal stem cells and labeling

Human mesenchymal stem cells were obtained from the Tulane Center for Gene Therapy (Tulane University Health Sciences Center, New Orleans, LA, USA) and cultured according to the protocol provided. Carbocyanine dye (CellTracker CM-Dil; Molecular Probes Inc, Eugene, Ore) was used to label the human mesenchymal stem cells according to the manufacturer's standard protocol as previously described [3].

In vitro cytotoxicity assay of CRAds

For determination of virus-mediated cytotoxicity, 1×10^4 MDA-MB-231 cells were seeded in 48-well plates and infected with adenoviruses at MOI of 1–1000 or were mock-infected [17]. To visualize cell killing, cells were fixed and stained with 1% crystal violet in 70% ethanol for 20 min followed by washing with tap water to remove excess dye at day 3, 5, 7 and 9. The plates were dried and images were captured with a Kodak DC260 digital camera (Eastman Kodak, Rochester, NY, USA).

In vitro cytotoxicity assay of human mesenchymal stem cells loaded with CRAd

About 3×10^5 hMSCs were plated in 6 well plates and infected with Ad5/3.CXCR4 at MOI of 1–1000 in 2% media. After 18 h the Ad5/3.CXCR4 infected hMSCs, now called hMSC-Ad5/3.CXCR4, were washed three times with PBS and trypsinized. Next, 5×10^4 MDA-MB-231 breast cancer cells plated in 48 well plates were co-cultured with 5×10^4 hMSCs carrying Ad5/3.CXCR4 at different MOIs. To visualize cell killing, cells were fixed and stained with 1% crystal violet in 70% ethanol for 20 min followed by washing with tap water to remove excess dye at day 3, 5, 7, and 9. The plates were dried and images were captured with a Kodak DC260 digital camera (Eastman Kodak, Rochester, NY, USA).

Quantitating virus replication

Purification of the DNA and quantitative real-time PCR for E4 was performed as previously described [6]. About 1.5×10^5 cells were seeded per well in a six-well plate. The next day cells were infected with the indicated viruses at different MOIs or mock infected and growth medium was collected at the indicated time points. Negative controls without templates were performed for each reaction series, and an internal control (human GAPDH) was used to normalize the copy number for the E4 genes. Comparison of replication rates of different treatment groups were performed with a Student's *t*-test.

Mouse xenograft model for experimental metastatic breast cancer to the lung

Female C.B-17 SCID mice (6-weeks old) were obtained from Charles River Laboratories, Inc (Wilmington, MA, USA). Mice were used according

to approved institutional protocols. The mouse xenograft model for metastatic breast cancer to the lung and the route of hMSC injection was performed as described [21]. Mice were injected intravenously in the lateral tail vein with 2×10^6 MB-MDA-231 suspended in 200 µl of PBS [21]. In preliminary experiments, we determined that all mice injected with 2×10^6 MB-MDA-231 developed macroscopic tumor nodules in their lungs at 14 days after tumor cell injection (data not shown). Fourteen days later, treatment was started. The following preparations were made prior intravenous injection: 10^6 hMSCs were infected with Ad5/3.CXCR4 at MOI of 1000 in 2% media. After 18 h the Ad5/3.CXCR4 infected hMSCs, now called hMSC-Ad5/3.CXCR4, were washed three times with PBS and trypsinized. Then hMSC-Ad5/3.CXCR4 and hMSCs alone were labeled with dye (CellTracker CM-Dil; Molecular Probes Inc., Eugene, Ore) at 37°C in complete media for 30 min followed by three washes with PBS and resuspended in 100 ul of PBS. Then, at day 14, mice were we injected intravenously in the lateral tail vein with either 10^6 hMSCs which had been infected with Ad5/3.CXCR4 of MOI 1000 ($n = 8$), hHMSC alone ($n = 8$) or Ad5/3.CXCR4 of MOI of 1000 alone ($n = 8$) suspended in 100 μL PBS. Non-treated MDA-MB-231 tumor bearing mice ($n = 8$) and healthy mice ($n = 8$) served as a control.

Determination of effect of CRAd loaded hMSCs on MB-MDA-231 tumor weight in mouse lung

Fourteen days after MB-MDA-231 tumor cell injection (as described above), the mice obtained treatment intravenously in the lateral tail vein with either 10^6 hMSCs which had been infected with Ad5/3.CXCR4 of MOI 1000 ($n = 4$), MSC alone ($n = 4$) or Ad5/3.CXCR4 of MOI of 1000 alone ($n = 4$) suspended in 100 µl PBS. Mice injected with MB-MDA-231 tumor cells alone ($n = 4$) and healthy mice with no tumor cell injection ($n = 4$) served as controls. Mice were sacrificed by asphyxiation with CO_2 30 days after tumor cell injection. We measured the weight of whole lungs in all groups of mice and used whole lung weight as a surrogate endpoint of MD-MBA-231 tumor burden in the lung and to assess the effect of hMSCs, Ad5/3.CXCR4 on tumor growth [21]. All mice were followed daily until euthanasia. None of the mice had to be sacrificed because of excessive bleeding, open wound infection, moribund status, or prostration with weight loss of more than 25% of initial body weight.

Determination of effect of CRAd loaded hMSCs on survival in mice bearing metastatic breast cancer

Fourteen days after MD-MBA-231 tumor cell injection (as described above), the mice obtained treatment intravenously in the lateral tail vein either 10^6 hMSCs which had been infected with Ad5/3.CXCR4 of MOI 1000 ($n = 10$), hMSC alone ($n = 10$) or Ad5/3.CXCR4 of MOI of 1000 alone ($n = 10$) suspended in 100 µl PBS. Mice injected with MB-MDA-231 tumor cells alone ($n = 10$) and healthy mice with no tumor cell injection ($n = 10$) served as controls. All mice were followed daily until day 150. None of the mice had to be sacrificed because of excessive bleeding, open wound infection, moribund status, or cachexia.

MDA-MB-231 lung metastases

To assess the effect of transient transfection of hMSC-Ad5/3.CXCR4 on MDA-MB-231 lung metastasis, lungs were harvested 30 days later, fixed in 10% neutral-buffered Formalin, longitudinally trisected, paraffin embedded, and three 5–7 µm thickness sections were cut at 200 µm intervals from each embedded block. Tissue sections were stained with hematoxylin and eosin, examined for the presence of tumor nodules by a pathologist unaware of the treatments.

Tissue processing and imaging studies

Lungs from each group of mice were harvested 30 days after treatment, fixed in 10% neutral-buffered formalin, longitudinally trisected, paraffin embedded, and three 5–7 µm thickness sections were cut at 200 µm intervals from each embedded block. Tissue sections were stained with hematoxylin and eosin, examined for the presence of tumor nodules by a pathologist. In addition, lungs for each group of mice were embedded in Tissue TEK OTC compound (Miles, Elkhart, IN), snap-frozen in liquid nitrogen, and stored at –80°C.

Immunofluorescence

GFP labeled hMSCs were identified in the lung as following: Frozen tissue sections were air dried, fixed in 4% paraformaldehyde for 1 h, permeabilized in PBS with 0.2% Triton X-100, washed 5 min in PBS and blocked in 25% goat serum for 30 min. The sections were washed in PBS three times for 5 min, mounted with VectaShield mounting medium with 4′,6-diamidino-2-phenylindole (H-1200; Vector Laboratories) and then analyzed by fluorescence microcopy. Aden-

oviral hexon was identified in the lung as following: Frozen tissue sections were air dried, fixed in 4% paraformaldehyde for 1 h, permeabilized in PBS with 0.2% Triton X-100, washed 5 min in PBS and blocked in 25% goat serum for 30 min. Then the tissue sections were treated overnight with goat anti-hexon antibody (Chemicon) at 4°C. The sections were washed in PBS three times for 5 min. The tissue sections were treated with Alexa 534 labeled anti-goat secondary antibody (Alexa 534, Molecular Probes, Invitrogen) for 1 h, washed three times in PBS. All sections were mounted with VectaShield mounting medium with 4′,6-diamidino-2-phenylindole (H-1200; Vector Laboratories). The images were captured with either a Texas Red or a FITC filter in an Olympus AX70 fluorescence microscope equipped with a Zeiss Axiocam camera (Carl Zeiss, Oberkochem, Germany). Individual images were processed and merged using Adobe Photoshop 5.5 application software.

Statistical methods

We used the Wilcoxon rank sum test to perform pairwise comparisons of treatment effect on lung weight between all groups. Survival was measured from the day of MDA-MB-231 cell injection until the day of 130. For the survival data, the log-rank test was used to assess differences in survival among the four treatment groups. Because this overall test showed that the difference between MSC-Ad5/3.CXCR4–treated and control mice was statistically significant ($P < 0.001$), pairwise log-rank tests were performed. All statistical tests were two-sided; a P value of less than 0.05 was considered statistically significant. Statistical analyses were performed by using GraphPad Prism software (GraphPad Software, San Diego, CA).

Results

Identification of a CRAd allowing efficient loading of hMSCs and maximal oncolysis of breast cancer cells

One prerequisite of exploiting hMSCs as cell carriers for CRAds in vivo was to identify a CRAd agent, which combined efficient loading of the hMSCs with maximal killing potency of tumor cells. Therefore, our goal was to identify a CRAd possessing a limited oncolytic activity in the carrier cells in vitro while exhibiting efficient cytotoxicity in breast cancer cells. In this regard, previous studies have demonstrated that efficient transduction of hMSCs as well as breast cancer cells were hampered due to the paucity of the primary adenoviral receptor CAR. Thus, we determined the transduction efficiency of a panel of replication competent Ads, which utilize CAR-independent viral entry pathways. As shown in Fig. 1, we tested the cytotoxicity in hMSCs and in the metastatic breast cancer cell line MDA-MB-231. The hMSCs and MDA-MB-231 cells were infected with replication competent Ads that have: wild-type Ad5 fiber (Ad5wt), an RGD peptide incorporated into the HI loop of the Ad5 fiber knob domain (Ad5RGDwt and Ad5RGD.CXCR4) or a serotype switching of the Ad5 knob with that of Ad3 (Ad5/3wt and Ad5/3.CXCR4). In these experiments, Ad.CXCR4Luc served as a non-replicating control. While the crystal violet staining-based cell-killing assay showed that hMSCs were most sensitive to RGD peptide-containing Ads (Ad5RGDwt and Ad5RGD.CXCR4), the Ad5wt, Ad5/3wt, and Ad5/3.CXCR4 viruses had an attenuated cytopathic effect on hMSCs. In MDA-MB-231 cells, the most

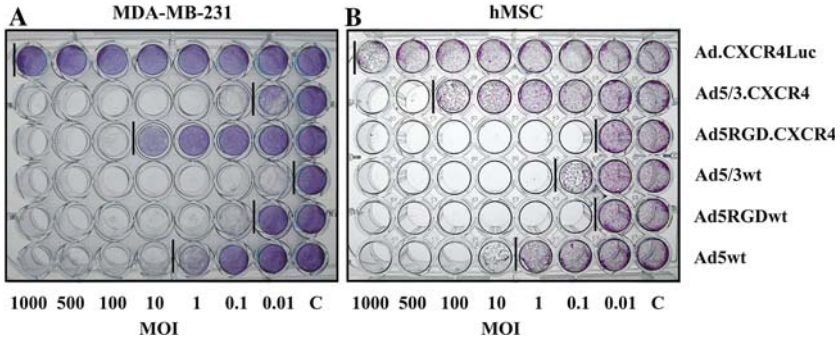

Fig. 1 Cytopathic effect of infectivity enhanced CRAds in breast cancer cells and human mesenchymal stem cells as carrier cells in vitro. (**A**) MDA-MB-231 cells and (**B**) human mesenchymal stem cells (hMSCs) were infected with Ad.CXCR4Luc (as a non-replicating control), the CRAd Ad5/3.CXCR4, the CRAd Ad5RGD.CXCR and the replication competent vectors Ad5RGDwt and Ad5wt at different MOIs. Cytotoxic activity was evaluated by crystal violet staining. Control without any viral infection is indicated as C

prominent oncolysis was attributed to Ad5/3 viruses (Ad5/3wt and CRAd Ad5/3.CXCR4). Thus, the Ad5/3.CXCR4 exhibited sufficient hMSC infectivity with limited cytotoxic effect, while it was substantially more cytopathic in MDA-MB-231 cells. Based on these data, we selected the CRAd Ad5/3.CXCR4 for our subsequent in vitro and in vivo experiments. Cells carrying this CRAd were designated as hMSC-Ad5/3.CXCR4.

Ad5/3.CXCR4 loaded human mesenchymal stem cells display oncolysis of breast cancer cells in vitro

Next, we tested the proof-of-principle that Ad5/3.CXCR4 loaded hMSCs (hMSC-Ad5/3.CXCR4 cells) could affect oncolysis of MDA-MB-231 breast cancer cells in vitro. In addition, we evaluated the time course by which hMSC-Ad5/3.CXCR4 could produce oncolysis of MDA-MB-231 cells in vitro. As shown in Fig. 2, MDA-MB-231 cells were co-cultured with hMSCs loaded with Ad5/3.CXCR4 at MOI ranging from 0 to 1000 oncolysis, and oncolysis was assessed by crystal violet staining on days 3, 5, 7, 9 and 11. To exclude any toxic effects of the adenovirus infection itself that may also contribute to cell lysis, tumor cells were also mixed with HMSC carrier cells infected with non-replicative virus. In addition, any oncolytic effect from adenovirus infection alone was assessed by direct infection with non-replicative virus. These control experiments demonstrated that non-replicative Ad does not cause cell lysis of breast cancer tumor cells when applied directly or carried in hMSCs.

At day 3 of the co-culture experiment, hMSC-Ad5/3.CXCR4 cells showed evidence of initial oncolysis in MDA-MB-231 cells at MOI of 1000, which was completed at day 7. Interestingly, between days 7 and 9 of co-culture, an increase of oncolysis of MDA-MB231 of more than 3 orders of magnitude was achieved, resulting in complete oncolysis at MOI of 1. These results were correlated with PCR assays of Ad DNA in the culture media, which showed a significant increase in viral copy number between days 7 and 9 corresponding to enhanced viral oncolysis (data not shown). In the aggregate, co-culturing of MDA-MB-231 cells with hMSC-Ad5/3.CXCR4 resulted in increased oncolysis of MDA-MB-231 cells with time, suggesting viral amplification in hMSCs. The killing of MDA-MB-231 was protracted, thus indicating a sufficient time window to manipulate hMSCs with CRAds.

MSC-Ad5/3.CXCR4 homes to breast cancer metastases in the lung in vivo

We investigated the homing capacity of hMSCs loaded with CRAds to breast cancer metastases in the lung in vivo. In this experiment, we injected MDA-MB-231 cells intravenously into the tail veins of SCID mice to establish pulmonary metastases as previously described [21]. Fourteen days later, the mice were injected intravenously with Ad5/3.CXCR4 loaded hMSCs and labeled with fluorescent dye, with Ad5/3.CXCR4, or with fluorescent dye labeled hMSCs alone. At day 3 after treatment the mice were sacrificed and lung samples were assessed for the presence of hMSCs loaded with CRAds. Fluorescence microcopy was performed to identify cell populations in lung sections. Dye labeled hMSCs were identified by green fluorescence and cells immunostained against Ad hexon (as an indicator of viral replication [1]) were identified by red fluorescence. HMSCs carrying CRAd would appear as orange overlay. As shown in Fig. 3A, fluorescent microscopy demonstrated orange fluorescent cells

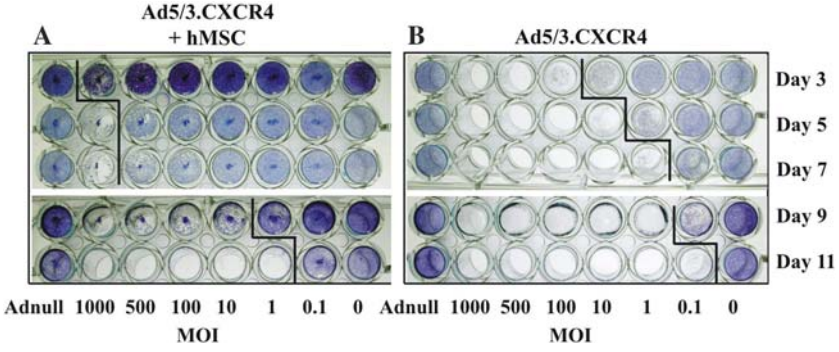

Fig. 2 Ad5/3.CXCR4 loaded human mesenchymal stem cell display oncolysis in breast cancer cells in vitro. (**A**) Co-culture of Ad5/3.CXCR4 loaded human mesenchymal stem cells (hMSC-Ad5/3.CXCR4) and MDA-MB-231 breast cancer tumor cells at days 3, 5, 7, 9 and 11. Oncolytic activity was evaluated by crystal violet staining. (**B**) Direct oncolytic effect of Ad5/3.CXCR4 on MDA-MB-231 cells by infection with Ad5/3.CXCR4 at same MOIs at day 3, 5, 7, 9 and 11. Both experiments (**A**) and (**B**) were started in parallel at the same time point. Oncolytic activity was evaluated by crystal violet staining

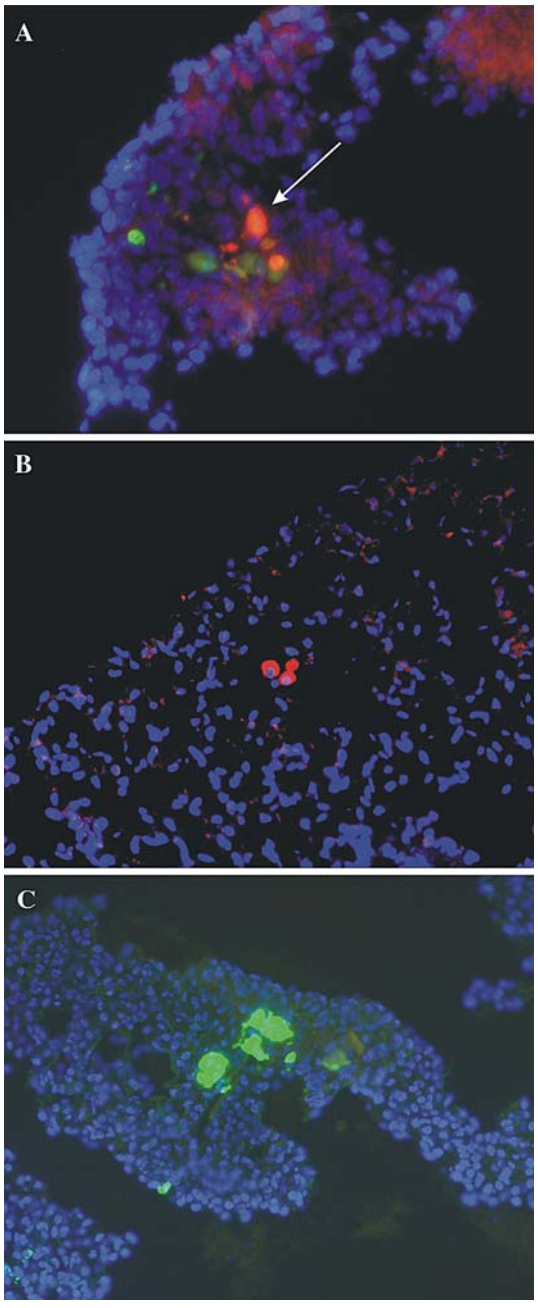

Fig. 3 Evaluation of homing capacity of systemically administered CRAd loaded human mesenchymal stem cells to metastatic breast cancer to the lungs by fluorescence microscopy. Established pulmonary metastases of MDA-MB231 carcinoma intravenously injected with hMSC-Ad5/3.CXCR4 (**A**), Ad5/3.CXCR4 (**B**) or hMSC (**C**). Fluorescence microscopy was performed to detect hexon of Ad5/3.CXCR4 (red, see **B**), GFP label of hMSCs (green, see **A** and **C**) and hMSC carrying hexon (orange, see **A** →) in established pulmonary metastatses of MDA-MB231 carcinoma at day 3 after treatment

indicative of hMSCs positive for Ad hexon localized to tumor nodules in lung tissue from tumor bearing mice injected with Ad5/3.CXCR4 loaded hMSCs. In lung tissue from tumor bearing mice injected with Ad5/3.CXCR4, only red fluorescent cells positive for Ad hexon immunostaining were observed (Fig. 3B). In tumor bearing mice injected with HMSCs alone, these cells were detected in the tumor nodules as indicated by green fluorescence (Fig. 3C). Interestingly, no evidence of hMSCs could be found in non-MDA-MB-231 bearing lungs (data not shown). Thus, these results suggest that hMSCs loaded with Ad5/3.CXCR4 are capable to home to breast cancer metastases in the lung after systemic injection.

Systemically administered MSC-Ad5/3.CXCR4 reduces the growth of MDA-MB-231 cell derived lung metastases in vivo

Next, we investigated the in vivo anti-tumor activity of hMSC-Ad5/3.CXCR4. We injected MDA-MB-231 cells intravenously into the tail veins of SCID mice to establish pulmonary metastases (Fig. 4A). Fourteen days later, we injected 1×10^6 hMSCs loaded with Ad5/3.CXCR4 (Fig. 4B) or Ad5/3.CXCR4 alone (Fig. 4C) intravenous. Control mice received either no treatment (Fig. 4A) or intravenous injection of 1×10^6 hMSCs (Fig. 4D). Thirty days after tumor cell injection, the mice were sacrificed, and the weights of whole lungs were measured. A group of healthy mice that received no cell injection served as a reference for measurement of normal lung weight. As shown in Fig. 5, the mean lung weight of mice injected with MDA-MB-231 tumor cells was statistically significantly greater than the mean lung weight of healthy mice. Much of this weight difference was due to the tumor tissue occupying substantial portions of the lungs of the mice injected with the tumor cells. Therefore, we used whole lung weight as a surrogate endpoint of tumor burden in lungs and as an assessment of treatment, as previously described [21]. Mice injected with tumor cells and intravenously with hMSC-Ad5/3.CXCR4 had smaller mean lung weight than Ad5/3.CXCR4 treated mice or control untreated mice injected with tumor cells only ($P < 0.05$). Thus, the tumor burden of breast cancer metastases in the lungs was significantly less in animals treated with CRAd loaded hMSCs than with the CRAd alone.

Treatment with hMSC-Ad5/3.CXCR4 improved survival of mice bearing breast cancer metastases in the lungs

Finally, we examined whether hMSCs loaded with Ad5/3.CXCR4 improved the survival of mice with pre-established pulmonary metastases derived from

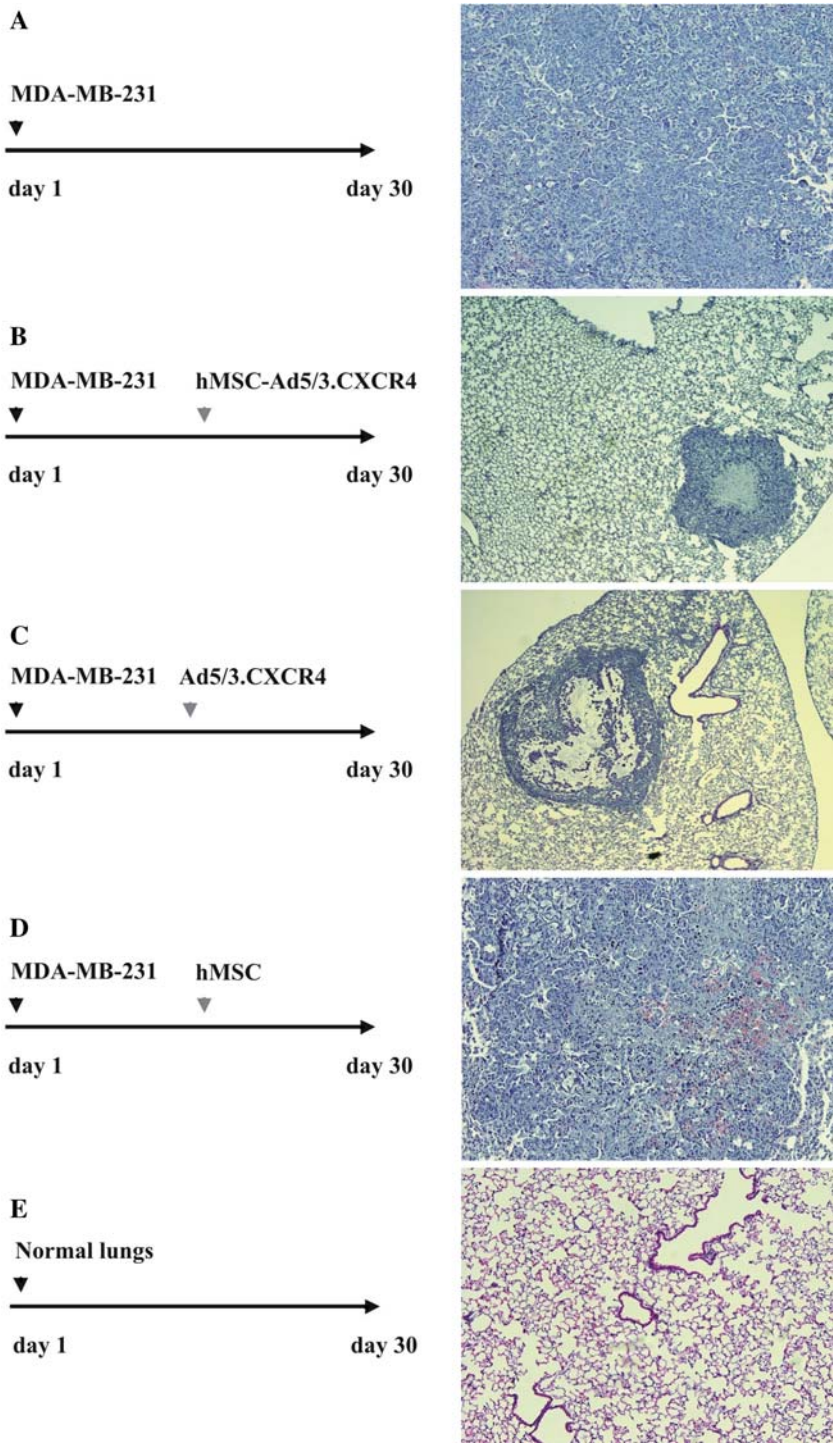

Fig. 4 Treatment schedules of MDA-MB-231 cell derived lung metastases in vivo. Pulmonary breast cancer metastases were established in mice (**A**). Mice were treated on day 14 after intravenous injection with MDA-MB231 with one dose of intravenous injection of hMSC-Ad5/3.CXCR4 (**B**), Ad5/3.CXCR4 alone (**C**), hMSC alone (**D**), or no treatment (**E**). Representative lung sections are shown, lungs were analyzed by histology and H&E staining

MDA-MB-231 cells. Mice were treated either with hMSC-Ad5/3.CXCR4, Ad5/3.CXCR4, or with hMSCs alone. Untreated mice served as a control group. Among mice bearing pulmonary metastases derived from MDA-MB-231 cells, the group treated with hMSC-Ad5/3.CXCR4 survived significantly longer ($P < 0.05$) than Ad5/3.CXCR4 treated, hMSC treated or untreated mice (Fig. 6). Thus, these results indicate that the delivery of CRAds with hMSCs resulted in a greater survival benefit compared to CRAd injection alone.

Discussion

In the present study, we have exploited the utility of hMSCs as cellular carriers of CRAds for the therapy of

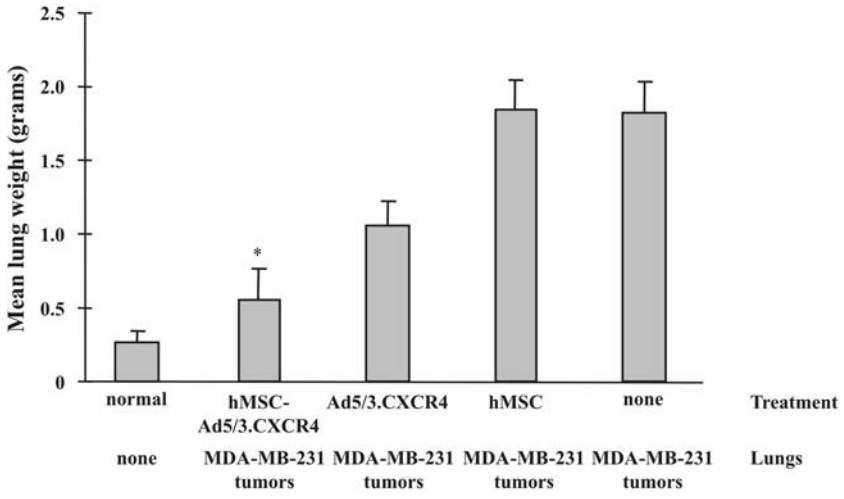

Fig. 5 Effect of systemically administered hMSC-Ad5/3.CXCR4 on the weight-growth of MDA-MB-231 cell derived lung metastases in vivo. Lung weights after treatment with hMSC-Ad5/3.CXCR4, Ad5/3.CXCR4 or hMSC compared with those of untreated mice with MDA-MB231 metastasis at day 30 after tumor cell injection. Lung weights of healthy animals with no tumors are included for comparison. Each bar presents the mean of four experiments ± SD. *, $P < 0.05$, hMSC-Ad5/3.CXCR4 versus Ad5/3.CXCR4

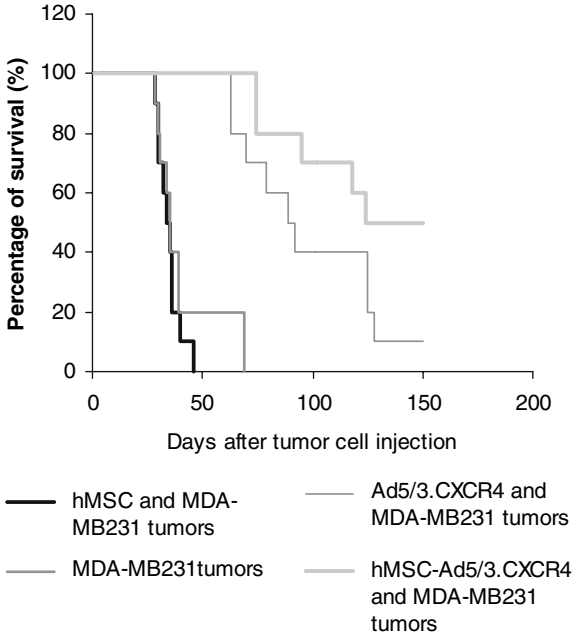

Fig. 6 Survival analysis. Survival of mice with established pulmonary metastases of MDA-MB231 breast carcinoma intravenously injected with hMSC-Ad5/3.CXCR4, Ad5/3.CXCR4 or hMSC compared with those of untreated mice

metastatic breast cancer to the lung. We have demonstrated both in vitro and in vivo the capability of hMSCs as intermediate carriers for CRAds. Importantly, we have shown the ability of systematically administered CRAd loaded hMSCs to home to and to kill breast cancer pulmonary metastases. The exploitation of mammalian cells represents a novel approach of coupling virotherapy with cell therapy. In this regard, delivery of conditional replication HSV type 1 viruses by neural precursor cells has been endeavored for the treatment of glioma [5]. Tumor cells have also been used as cellular carriers of replication competent parvoviruses for the treatment of hepatic cancer [16]. Recently, the ability of mesenchymal stem cells to deliver replication competent adenoviruses to ovarian and cervical cancer cells in vitro was investigated [15]. Herein, our present study extends this paradigm to an in vivo approach to distant metastatic cancer.

In the design of our study we investigated a combined cell vehicle therapy and virotherapy approach by exploiting a CRAd agent designed with enhanced tumor infectivity and specificity in vitro as well as antitumor potency in vivo. With respect to virotherapy, our CRAd was designed to address the biological requirements of breast cancer. Tumor infectivity enhancement of this CRAd was achieved by incorporation of the knob domain from the human adenovirus serotype 3 (Ad5/3) to provide CAR-independent tropism [19]. Enhanced specificity was achieved by placing the CRAd E1A gene under the transcriptional control of the tumor selective promoter CXCR4. In this regard, the CXCR4 gene promoter revealed a superior ''breast cancer—on/liver-off'' profile in a preclinical evaluation of transcriptional targeting strategies for carcinoma of the breast in a tissue slice model system [18]. Furthermore, recent evidence

points to the SDF-1α-CXCR4 complex as having an important role in progression to metastasis in several tumor contexts [13, 24]. This CRAd combining transductional and transcriptional targeting strategies has been recently shown to exhibit superior infectivity and tumor selective replication in breast cancer (Stoff-Khalili et al., unpublished observations).

The present study addresses the utility of hMSCs as intermediate carriers for CRAds to target metastatic breast cancer in vivo. The choice of hMSCs as cellular vehicles was based on their described tumor homing capacity and the observation that intravenously administered hMSCs do not engraft in healthy organs (i.e. lung, liver, spleen, kidney and muscle) [7, 14, 21]. Indeed, fluorescence microscopy of lung tissue sections showed homing of labeled hMSCs to the breast cancer metastases, while no hMSCs could be identified in healthy regions of the lung. It has been suggested that signals mediating increased turnover and proliferation of connective stromal cells in tumors may induce the homing of MSCs to this site [20, 21]. In this regard, it has been recently suggested that this process may be related to high local concentrations of paracrine growth factors such as fibroblast growth factor, platelet-derived growth factor, epidermal growth factor, transforming growth factor-β, or other mediators within the tumor microenvironment [2].

In order to exploit hMSCs as cellular carriers for CRAds, it was important to consider how to limit viral activity in the carrier cells until the hMSCs would reach the metastatic breast cancer cells in the lung. We selected the Ad5/3.CXCR4 CRAd as optimal for our strategy because this agent exhibited limited cytotoxicity in hMSCs and maximal cytotoxicity in breast cancer cells. Indeed, the identification of labeled hMSCs loaded with the CRAd at metastatic tumor sites in the lungs after systemic injection suggested a sufficient time window for the hMSCs to carry this agent to the disease. The prevention of cytotoxicity of viruses on cell carriers is an important practical issue relevant to our strategy [8, 11]. In this regard, several approaches have been designed to attenuate the cytotoxicity of viruses on cell carriers, such as mimosine treatment to avoid premature destruction of neural precursors serving as cellular carriers for conditionally replicative herpes simplex virus type 1 vectors [5]

We demonstrated here that hMSC based viral delivery enhanced the oncolytic effect of virotherapeutic treatment and increased the survival of tumor-bearing animals. This result validates the feasibility of using hMSCs as cellular carriers for replication competent adenoviruses. The amount of virus loaded into hMSCs was measured at the time of in vivo delivery and corresponded to the titer of CRAd injected alone. Therefore, the superior therapeutic response of metastatic breast cancer in the lung from treatment with CRAd loaded hMSCs cannot be attributed to a higher dose of the CRAd initially introduced. This response may result from the amplification of viral load in the hMSC carriers or from targeted virus delivery and release of the virus in the vicinity of tumor cells at multiple foci. Further studies are in progress to investigate our hypothesis that hMSCs may function as local factories of CRAds to explain the superior oncolysis of CRAd loaded hMSCs compared to CRAd alone in vivo. In our study, we used an immune-compromised animal model. In future studies, we will investigate if hMSCs could also serve as a ''Trojan horse'' for CRAd delivery by evading an antiviral immune response. As a result of the transport of CRAds inside hMSCs, CRAds may be protected not only from untargeted trapping but also from inactivation through hemaglutination and neutralization through preexisting antiviral immunity.

In conclusion, this study represents to the best of our knowledge, the first attempt to demonstrate the proof of principle that hMSCs can serve as cellular carriers to deliver CRAds to distant tumors such as breast cancer metastases in the lungs and mediate oncolysis in vivo after systemic administration. This work provides the first evidence to suggest that hMSCs as carrier cells represent a promising mode of administration of CRAds for the treatment of distant neoplastic metastatic disease.

Acknowledgements This work was supported by Grant of the Deutsche Forschungsgemeinschaft Sto 647/1-1 (to M. A. Stoff-Khalili), by grants from the National Institutes of Health 5T32CA075930 (NIH Training Grant) and Department of Defense: W81Xwh-05-1-035 (to D. T. Curiel). R01CA93796, R01CA98543 and AR46031 (to G. P. Siegal) and from the Louisiana Gene Therapy Research Consortium, Inc. (to J. M. Mathis) and R01CA108585 (to J. T. Douglas).

References

1. Banerjee NS, Rivera AA, Wang M, Chow LT, Broker TR, Curiel DT, Nettelbeck DM (2004) Analyses of melanoma-targeted oncolytic adenoviruses with tyrosinase enhancer/promoter-driven E1A, E4, or both in submerged cells and organotypic cultures. Mol Cancer Ther 3:437–449
2. Hanahan D, Weinberg RA (2000) The hallmarks of cancer. Cell 100:57–70
3. Hebda PA, Dohar JE (1999) Transplanted fetal fibroblasts: survival and distribution over time in normal adult dermis compared with autogenic, allogenic, and xenogenic adult fibroblasts. Otolaryngol Head Neck Surg 121:245–251
4. Hemminki A, Kanerva A, Liu B, Wang M, Alvarez RD, Siegal GP, Curiel DT (2003) Modulation of coxsackie-adenovirus receptor expression for increased adenoviral transgene expression. Cancer Res 63:847–853

5. Herrlinger U, Woiciechowski C, Sena-Esteves M, Aboody KS, Jacobs AH, Rainov NG, Snyder EY, Breakefield XO (2000) Neural precursor cells for delivery of replication-conditional HSV-1 vectors to intracerebral gliomas. Mol Ther 1:347–357
6. Kanerva A, Zinn KR, Chaudhuri TR, Lam JT, Suzuki K, Uil TG, Hakkarainen T, Bauerschmitz GJ, Wang M, Liu B et al (2003) Enhanced therapeutic efficacy for ovarian cancer with a serotype 3 receptor-targeted oncolytic adenovirus. Mol Ther 8:449–458
7. Koc ON, Peters C, Aubourg P, Raghavan S, Dyhouse S, DeGasperi R, Kolodny EH, Yoseph YB, Gerson SL, Lazarus HM et al (1999) Bone marrow-derived mesenchymal stem cells remain host-derived despite successful hematopoietic engraftment after allogeneic transplantation in patients with lysosomal and peroxisomal storage diseases. Exp Hematol 27:1675–1681
8. Li S, Tokuyama T, Yamamoto J, Koide M, Yokota N, Namba H (2005) Bystander effect-mediated gene therapy of gliomas using genetically engineered neural stem cells. Cancer Gene Ther 12:600–607
9. Liu Y, Ye T, Maynard J, Akbulut H, Deisseroth A (2005) Engineering conditionally replication-competent adenoviral vectors carrying the cytosine deaminase gene increases the infectivity and therapeutic effect for breast cancer gene therapy. Cancer Gene Ther 13:346–356
10. Mathis JM, Stoff-Khalili MA, Curiel DT (2005) Oncolytic adenoviruses—selective retargeting to tumor cells. Oncogene 24:7775–7791
11. Namba H, Tagawa M, Miyagawa T, Iwadate Y, Sakiyama S (2000) Treatment of rat experimental brain tumors by herpes simplex virus thymidine kinase gene-transduced allogeneic tumor cells and ganciclovir. Cancer Gene Ther 7:947–953
12. Nettelbeck DM, Rivera AA, Balague C, Alemany R, Curiel DT (2002). Novel oncolytic adenoviruses targeted to melanoma: specific viral replication and cytolysis by expression of E1A mutants from the tyrosinase enhancer/promoter. Cancer Res 62:4663–4670
13. Payne AS, Cornelius LA (2002) The role of chemokines in melanoma tumor growth and metastasis. J Invest Dermatol 118:915–922
14. Pereboeva L, Curiel DT (2004) Cellular vehicles for cancer gene therapy: current status and future potential. BioDrugs 18:361–385
15. Pereboeva L, Komarova S, Mikheeva G, Krasnykh V, Curiel DT (2003) Approaches to utilize mesenchymal progenitor cells as cellular vehicles. Stem Cells 21:389–404
16. Raykov Z, Balboni G, Aprahamian M, Rommelaere J (2004) Carrier cell-mediated delivery of oncolytic parvoviruses for targeting metastases. Int J Cancer 109:742–749
17. Rivera AA, Davydova J, Schierer S, Wang M, Krasnykh V, Yamamoto M, Curiel DT, Nettelbeck DM (2004) Combining high selectivity of replication with fiber chimerism for effective adenoviral oncolysis of CAR-negative melanoma cells. Gene Ther 11:1694–1702
18. Stoff-Khalili MA, Stoff A, Rivera AA, Banerjee NS, Everts M, Young S, Siegal GP, Richter DF, Wang M, Dall P et al (2005) Preclinical evaluation of transcriptional targeting strategies for carcinoma of the breast in a tissue slice model system. Breast Cancer Res 7:R1141–R1152
19. Stoff-Khalili MA, Stoff A, Rivera AA, Mathis JM, Everts M, Wang M, Kawakami Y, Waehler R, Mathews QL, Yamamoto M et al (2005) Gene transfer to carcinoma of the breast with fiber-modified adenoviral vectors in a tissue slice model system. Cancer Biol Ther 4:1203–1210
20. Studeny M, Marini FC, Champlin RE, Zompetta C, Fidler IJ, Andreeff M (2002). Bone marrow-derived mesenchymal stem cells as vehicles for interferon-beta delivery into tumors. Cancer Res 62:3603–3608
21. Studeny M, Marini FC, Dembinski JL, Zompetta C, Cabreira-Hansen M, Bekele BN, Champlin RE, Andreeff M (2004) Mesenchymal stem cells: potential precursors for tumor stroma and targeted-delivery vehicles for anticancer agents. J Natl Cancer Inst 96:1593–1603
22. Suzuki K, Alemany R, Yamamoto M, Curiel DT (2002) The presence of the adenovirus E3 region improves the oncolytic potency of conditionally replicative adenoviruses. Clin Cancer Res 8:3348–3359
23. Suzuki K, Fueyo J, Krasnykh V, Reynolds PN, Curiel DT, Alemany R (2001). A conditionally replicative adenovirus with enhanced infectivity shows improved oncolytic potency. Clin Cancer Res 7:120–126
24. Taichman RS, Cooper C, Keller ET, Pienta KJ, Taichman NS, McCauley LK (2002) Use of the stromal cell-derived factor-1/CXCR4 pathway in prostate cancer metastasis to bone. Cancer Res 62:1832–1837
25. Wegner SA, Ehrenberg PK, Chang G, Dayhoff DE, Sleeker AL, Michael NL (1998). Genomic organization and functional characterization of the chemokine receptor CXCR4, a major entry co-receptor for human immunodeficiency virus type 1. J Biol Chem 273:4754–4760
26. Zhu ZB, Makhija SK, Lu B, Wang M, Kaliberova L, Liu B, Rivera AA, Nettelbeck DM, Mahasreshti PJ, Leath CA 3rd et al (2004) Transcriptional targeting of adenoviral vector through the CXCR4 tumor-specific promoter. Gene Ther 11:645–648

Breast Cancer Res Treat
DOI 10.1007/s10549-007-9587-7

PRECLINICAL STUDY

Cancer-specific targeting of a conditionally replicative adenovirus using mRNA translational control

Mariam A. Stoff-Khalili · Angel A. Rivera · Ana Nedeljkovic-Kurepa · Arrigo DeBenedetti · Xiao-Lin Li · Yoshinobu Odaka · Jagat Podduturi · Don A. Sibley · Gene P. Siegal · Alexander Stoff · Scott Young · Zheng B. Zhu · David T. Curiel · J. Michael Mathis

Received: 24 March 2007 / Accepted: 26 March 2007

Abstract
Background In view of the limited success of available treatment modalities for a wide array of cancer, alternative and complementary therapeutic strategies need to be developed. Virotherapy employing conditionally replicative adenoviruses (CRAds) represents a promising targeted intervention relevant to a wide array of neoplastic diseases. Critical to the realization of an acceptable therapeutic index using virotherapy in clinical trials is the achievement of oncolytic replication in tumor cells, while avoiding non-specific replication in normal tissues. In this report, we exploited cancer-specific control of mRNA translation initiation in order to achieve enhanced replicative specificity of CRAd virotherapy agents. Heretofore, the achievement of replicative specificity of CRAd agents has been accomplished either by viral genome deletions or incorporation of tumor selective promoters. In contrast, control of mRNA translation has not been exploited for the design of tumor specific replicating viruses to date. We show herein, the utility of a novel approach that combines both transcriptional and translational regulation strategies for the key goal of replicative specificity.
Methods We describe the construction of a CRAd with cancer specific gene transcriptional control using the CXCR4 gene promoter (TSP) and cancer specific mRNA translational control using a 5′-untranslated region (5′-UTR) element from the FGF-2 (Fibroblast Growth Factor-2) mRNA.
Results Both in vitro and in vivo studies demonstrated that our CRAd agent retains anti-tumor potency. Importantly, assessment of replicative specificity using stringent tumor and non-tumor tissue slice systems demonstrated significant improvement in tumor selectivity.
Conclusions Our study addresses a conceptually new paradigm: dual targeting of transgene expression to cancer cells using both transcriptional and mRNA translational control. Our novel approach addresses the key issue of replicative specificity and can potentially be generalized to a wide array of tumor types, whereby tumor selective patterns of gene expression and mRNA translational control can be exploited.

Keywords Virotherapy · Adenovirus · Conditionally replicative · CRAd · E1A · Tumor selective promoter · TSP · Transcription · Transcriptional control · CXCR4 · mRNA translation · mRNA translational control ·

Mariam A. Stoff-Khalili and Angel A. Rivera contributed equally to this work.

M. A. Stoff-Khalili · A. A. Rivera · G. P. Siegal · A. Stoff · S. Young · Z. B. Zhu · D. T. Curiel
Division of Human Gene Therapy, Departments of Medicine, Surgery, Pathology and the Gene Therapy Center, University of Alabama at Birmingham, Birmingham, AL 35294-2172, USA

M. A. Stoff-Khalili
Department of Obstetrics and Gynecology, University of Duesseldorf, Medical Center, Duesseldorf 40225, Germany

A. Nedeljkovic-Kurepa · A. DeBenedetti · X.-L. Li · Y. Odaka · J. Podduturi · D. A. Sibley · J. M. Mathis (✉)
Gene Therapy Program, Departments of Cellular Biology and Anatomy and Biochemistry and Molecular Biology, Louisiana State University Health Sciences Center, 1501 Kings Hwy, Shreveport, LA 71130, USA
e-mail: jmathi@lsuhsc.edu

A. Stoff
Department of Plastic and Reconstructive Surgery, Dreifaltigkeits-Hospital, Wesseling 50389, Germany

5'-untranslated region · 5'-UTR · Fibroblast growth factor · FGF-2 · Eukaryotic initiation factor 4E · eIF4E · Breast cancer · Breast tumor

Introduction

In view of the limited success of available treatment modalities for breast cancer, alternative and complementary strategies need to be developed. Virotherapy marks an innovative approach in the development of new treatment regimes, in which a replicating virus itself is the anticancer agent. In this regard, virotherapy employing conditionally replicative adenoviruses (CRAds) represents a promising targeted intervention relevant to a wide array of neoplastic diseases. Critical to the realization of an acceptable therapeutic index in clinical trials using virotherapy is the achievement of oncolytic replication in tumor cells, while avoiding nonspecific replication in normal tissues [1–4]. In this regard, the elucidation of the critical pathways involved in the adenoviral infectious cycle has provided the basis of multiple levels of potential control to achieve the goal of selective replication. For example, modification of viral tropism via altered cell surface binding provides the practical basis of transductional targeting [5, 6]. Alternatively, controlling expression of critical adenoviral regulatory genes via tumor selective promoters (TSPs) is the basis of transcriptional targeting [7]. These multiple targeting strategies thus provide the potential for a combinatorial approach to achieve an optimized level of selective CRAd replication.

Thus far, transcriptional targeting has been the most frequently applied strategy in the design of CRAd agents. Due to the native adenoviral hepatotropism [4, 8], the ideal TSP should exhibit the widest differential between ''tumor on'' and ''liver off'' expression profiles [1]. Whereas candidate promoters have been identified that embody this profile, direct TSP employment in the CRAd context may not necessarily provide the level of cancer specificity required. In this regard, heterologous promoters incorporated into the adenovirus (Ad) genome may exhibit altered induction patterns due to endogenous *cis* and *trans* regulatory elements derived from the Ad genome. To address this issue, the addition of insulator elements has been proposed. Such strategies however, may not be generally applicable to all TSPs [9]. These observations demonstrate that additional regulatory strategies may be necessary to achieve an optimized cancer selective replication of CRAds.

To this end, control of gene expression at the level of mRNA translation offers an additional approach relevant to targeting cancer cells. Recently, the control of mRNA stability via tumor-associated proteins has been explored for tumor-specific replicating viruses. This approach utilized sequences from the 3′ untranslated region (3′-UTR) of the PTGS2 (prostaglandin-endoperoxide synthase 2) mRNA to control selective mRNA stability and degradation of the adenovirus E1A gene transcript [10]. In contrast, control of mRNA translation has not been exploited for the design of tumor specific replicating viruses to date. Of note, dysregulation of mRNA translation in cancer is a well-recognized mechanism, which may contribute to neoplastic conversion and progression. In particular, overexpression of the translation eukaryotic initiation factor eIF4E has been documented in cellular transformation and tumorigenesis [11]. The eIF4E factor specifically binds to the cap structure of mRNAs during the first step of mRNA recruitment for translation [12, 13]. It is also a subunit of a pre-initiation complex, which contains a helicase activity that unwinds the secondary structure at the 5′-UTR of mRNA. This latter function is critical during scanning for the translation start site of mRNAs with long 5′-UTRs capable of forming complex stable secondary structures [14, 15].

Recognizing the nearly ubiquitous eIF4E over-expression in solid tumors, we hypothesized that mRNA translation could be exploited as an additional regulatory strategy to control replication of adenoviral vectors for cancer virotherapy. We hypothesized that the addition of a long and highly structured 5′-UTR preceding the adenoviral E1A coding sequence would limit efficient translation exclusively to cells that express high levels of the translation initiation factor eIF4E. We describe herein, the construction of a CRAd with cancer specific gene transcriptional control using the CXCR4 gene promoter as a TSP and cancer specific mRNA translational control utilizing a 5′-UTR element from the FGF-2 (Fibroblast Growth Factor-2) mRNA. Our study thus addresses a conceptually new paradigm: dual targeting of transgene expression to cancer cells using both transcriptional and mRNA translational control. Our novel approach addresses the key issue of replicative specificity and may be very valuable both scientifically and clinically. It can potentially be applied to a wide array of tumor types, whereby tumor selective patterns of gene expression and mRNA translational control can be exploited, resulting in a new class of virotherapeutic agents.

Materials and methods

Cell lines and cell culture

The MDA-MB-231, MDA-MB-361, and MDA-MB-435 breast cancer cell lines were obtained from the American Type Culture Collection (ATCC) and cultured as

described. In brief, the cells were maintained in DMEM/F-12 medium (Life Technologies, Inc., Grand Island, NY), containing 10% fetal bovine serum (FBS; Gemini Bio-Products, Woodland, Ca), and 1% antibiotic-antimycotic solution (penicillin-streptomycin-fungizone; Sigma Chemicals Co., St. Louis, MO). The cells were maintained in T150 flasks at 37°C and 5% humidified CO_2, and were subcultured using 1% trypsin-EDTA (Gibco BRL, Life Technologies). Human mammary epithelial cells (HMEC) were obtained from Clonetics (Walkersville, MD), and were maintained in serum-free mammary epithelial growth media (Clonetics) and passaged as recommended by the vendor.

Primary human cells

Human dermal fibroblasts were derived from neonatal skin by trypsinization as described [16–18]. Human dermal fibroblasts obtained from outgrowth of explant cultures, were grown in DMEM (Dulbecco's modified Eagle's medium; Bio Whittaker) supplemented with 10% fetal calf serum, 2 mM glutamine, 100 U/ml penicillin, and 100 μg/mL streptomycin and grown as monolayers on plastic tissue culture dishes in a humidified atmosphere of a CO_2 incubator at 37°C.

Tissue slices and culture

Approval was obtained from the Institutional Review Board for all studies on human tissue. Human breast cancer samples were obtained (Department of Pathology, University of Alabama at Birmingham) from three patients undergoing mastectomy for primary invasive ductal carcinoma; normal breast tissue samples were obtained from three patients undergoing reduction mammoplasty. Human liver samples were obtained (Department of Surgery, University of Alabama at Birmingham) from three HIV seronegative donor livers prior to transplantation into recipients. All tissue samples were flushed with University of Wisconsin (UW) solution (ViaSpan, Barr Laboratories, Inc. Pomona, NY) before harvesting and kept on ice in UW solution until slicing. Time from harvest to slicing was kept at an absolute minimum (<2 h).

The precision tissue cut technique was performed using the Krumdieck Tissue Slicer as previously described [19]. Tissue slices (250 micron) were placed into six-well plates (1 slice per well) containing 2 mL of complete culture media (liver, William's Medium E with 1% antibiotics, 1% L-glutamine, and 10% FCS; normal breast and breast tumor tissue, RPMI with 1% antibiotics, 1% L-glutamine, and 10% FCS). The plates were then incubated at 37°C and 5% CO_2 in a humidified environment under normal oxygen concentrations for up to 48 h. A plate rocker set at 60 rpm was used to agitate slices and ensure adequate oxygenation and viability [20]

Construction and production of adenoviruses

The plasmid pBSKCAT/CXCR4, which contains a 279 bp sequence from the human CXCR4 promoter (–191 to +88), was a kind gift of Dr. Nelson L. Michael [21]. The CXCR4 promoter sequence (NCBI Accession Number AY728138, from 1780 to 2059 bp) was cloned by PCR into the SpeI/PmeI site of pAdenoVator-CMV5 (Qbiogene; Irvine, CA) replacing the CMV promoter to generate pAdenoVator-CXCR4. This construct contained the 279 bp CXCR4 promoter and the simian virus 40 (SV40) polyadenylation (poly A) signal. The adenoviral type 5 E1A gene (NCBI Accession Number AY728138, from 560 to 1545 bp) was then cloned by PCR into the PmeI/BamHI site of pAdenoVator-CXCR4 to generate the pAdenoVator-CXCR4-E1A plasmid. The 5′ upstream-untranslated region sequence of the rat FGF-2 cDNA (NCBI Accession Number NM_019305, from 1 to 532 bp) was inserted in the PmeI site immediately upstream of the E1A sequence to produce the pAdenoVator-CXCR4-UTR-E1A plasmid. After cleavage with FseI, the pAdenoVator-CXCR4-E1A and the pAdenoVator-CXCR4-UTR-E1A plasmids were used for homologous recombination in BJ5183 bacteria with the pAdEasy-1 genome (Stratagene; La Jolla, CA). The resulting pAdEasy-CXCR4-E1A and pAdEasy-CXCR4-UTR-E1A recombinant plasmids were identified by PCR screening.

The recombinant plasmids were linearized with Pac I and transfected into 293 cells using Superfect reagent (Qiagen; Valencia, CA) to generate the Ad5-CXCR4-E1A and Ad5-CXCR4-UTR-E1A adenoviruses. The adenoviruses were propagated in the FaDu cell line (a human head and neck cancer cell line in which CXCR4 is over expressed), and purified by double CsCl density gradient centrifugation, followed by dialysis against phosphate buffered saline (PBS) containing 10% glycerol. The concentration of total viral particle numbers (PN) were determined by measuring absorption at 260 nm. Infectious PN (IFN) were determined by measuring the concentration of viral hexon protein-positive 293 cells after a 48 h infection period, using an Adeno-X Rapid Titer Kit (Clontech; Mountain View, CA). Wild type Ad5 (Ad-wt-dE3) and Ad-CXCR4-GL3 [22] were used for replication positive and negative control, respectively, in the CRAd agent analysis.

Western blot analysis

Levels of endogenous human eIF4E, CXCR4, and β-actin expressed in uninfected cells, were determined by Western immunoblot analysis, from 20 μg of total cellular protein.

Cells were solubilized in lysis buffer (150 mM NaCl, 1.0% NP-40, 0.5% deoxycholate, 0.1% sodium dodecyl sulfate (SDS), 50 mM Tris pH 8.0) and the protein concentration was determined using the Bradford protein assay (Bio-Rad Laboratories, Richmond, CA, USA). For eIF4E expression, cells were harvested and solubilized in lysis buffer. Samples were electrophoresed on a 10% SDS/polyacrylamide gel and subsequently transferred to nitrocellulose in a semidry electrophoretic blotting system (NovaBlot; Pharmacia, Piscataway, NJ, USA). The nitrocellulose membranes were incubated for 1 h in a blocking buffer of 5% bovine serum albumin (BSA) in TTBS buffer (500 mM NaCl, 100 mM Tris, 0.1% Tween 20), followed by incubation with buffer containing 1% BSA and either (a) a mouse anti-human eIF4E monoclonal antibody (BD Transduction Labs), (b) a mouse anti-human CXCR4 monoclonal antibody (BD Transduction Labs), or (c) a mouse anti-human β-actin monoclonal antibody (Pharmingen). Subsequently, membranes were washed in TTBS buffer and incubated with a horseradish peroxidase (HRP) conjugated secondary anti-mouse or anti-rabbit antibody (Santa Cruz Biotechnology; Santa Cruz, CA). Specific protein bands were detected using the ECL Western blotting system (Amersham Biosciences; Piscataway, NJ). Finally, the membranes were washed and incubated with ECL reagent and analyzed by autoradiography. Densitometry analysis was performed using a VersaDoc 3000 imaging system (Bio-Rad).

Levels of adenoviral E1A protein were determined by Western immunoblot analysis. Cells infected Ad-CXCR4-E1A, Ad-CXCR4-UTR-E1A, Ad-CXCR4-GL3, or Ad-wt-dE3 at a multiplicity of infection (MOI) of 100:1 were harvested at 48 h. Cells were harvested and solubilized in lysis buffer. Samples were subjected to electrophoresis on a 10% SDS/polyacrylamide gel and subsequently transferred to nitrocellulose. The nitrocellulose membranes were incubated for 1 h in a blocking buffer of 5% BSA in TTBS buffer, followed by incubation with TTBS buffer containing 1% BSA and a mouse anti-Adenovirus type 5 E1A monoclonal antibody (Lab Vision; Fremont, CA). Subsequently, the membranes were washed in TTBS buffer and incubated with a HRP conjugated goat anti-mouse IgG secondary antibody (Santa Cruz Biotechnology). Specific protein bands were detected using the ECL reagent and analyzed by autoradiography.

Quantifying viral transcription

For quantification of E1A mRNA expression 1.5×10^5 cells were seeded per well in a six-well plate. The next day, cells were infected with the indicated viruses at 100 MOI, or mock infected. After 48 h, purification of total RNA and quantitative real-time PCR for E1A were performed as previously described [23]. Viral infection of the tissue slices was performed as previously described [19]. After infection and frozen storage, tissue slices were thawed and placed in RLT buffer (RNEasy RNA extraction kit, Qiagen, Valencia, CA) with ß-mercaptoethanol (Sigma, St. Louis, MO). Slices were homogenized immediately with an ultrasonic sonicator (Fisher Scientific Model 100) at a setting of 15 watts for 10 sec. The homogenate was centrifuged, and the supernatant was removed to separate Eppendorf tubes for subsequent RNA purification with the RNEasy RNA purification kit according to the manufacturer's directions. Comparison of transcription rates of different treatment groups were performed with a Student's *t*-test.

Quantifying virus replication

Purification of the DNA and quantitative real-time PCR for E4 was performed as previously described [24]. 1.5×10^5 cells were seeded per well in a six-well plate. The next day cells were infected with the indicated viruses at 100:1 MOI or mock infected. Growth medium was collected at the indicated time points, and assessment of viral copy number in 200 µL aliquots was performed as previously described [19]. Negative controls without template were performed for each reaction series, and an internal control (human GAPDH) was used to normalize the copy number for the E4 genes. Comparison of replication rates of different treatment groups were performed with a Student's *t*-test.

In vitro cytotoxicity assay

For determination of virus-mediated cytotoxicity, 1.5×10^4 cells were seeded in 24 well tissue culture plates and were infected with adenoviruses at indicated titers or were mock-infected [25]. To visualize cell killing, cells were fixed and stained with 1% crystal violet in 70% ethanol for 20 min, followed by washing with tap water to remove excess dye. The plates were dried and images were captured with a Kodak DC260 digital camera (Eastman Kodak, Rochester, NY, USA).

In vivo oncolysis

All experimental protocols were approved by the Institutional Animal Care and Use Committees of LSU Health Sciences Center and University of Alabama at Birmingham. To establish subcutaneous tumors, 4–5 week old BALB/c nude mice were inoculated in both flanks with 5×10^6 MDA-MB-361 cells ($n = 5$ animals/group; 2 tumors/animal). Before injection, the tumor cells were verified to have >95% viability by trypan blue exclusion. When

the tumor reached 5 mm in widest diameter, 1×10^8 IFN of Ad-CXCR4-E1A, Ad-CXCR4-UTR-E1A, Ad-CXCR4-GL3 or Ad-wt-dE3 was injected intratumorally, in a 0.05 mL volume. Control tumors were injected with an equal volume of PBS only. Animals were examined every other day and killed if tumor size reached 1.0×1.0 cm. The tumor volume was calculated by the formula: $1/2\ xy^2$, where x is the longest distance of the tumor and y is the distance perpendicular to x.

Results

A model for using differential expression of eIF4E

We constructed a dual-level targeted CRAd with the Ad E1A gene that is essential for viral replication, with transcriptional control using the CXCR4 gene promoter and mRNA translational control using the FGF-2 5′-UTR sequence placed upstream of the coding sequence (Fig. 1). This CRAd construct (Ad-CXCR4-UTR-E1A) was compared to a single-level targeted CRAd (Ad-CXCR4-E1A) with transcriptional control using the CXCR4 gene promoter alone. Experiments were performed to compare regulation of E1A expression in cells in infected with Ad-CXCR4-E1A (using gene transcriptional control alone) with regulation of E1A expression in cells infected with Ad-CXCR4-UTR-E1A (using mRNA translational and gene transcriptional control). E1A expression was compared in infected breast cancer cell lines (MDA-MB-231, MDA-MB-361, and MDA-MB-435) and in infected normal breast epithelial cells (HMEC) and normal human fibroblasts.

First, to correlate the differential expression of endogenous expression of eIF4E and CXCR4 between normal and cancer cell lines, Western blot analysis was performed, and the amounts of each protein were quantified by densitometry and normalized using the relative expression of β-actin. As shown in Fig. 2, normal HMEC and fibroblasts showed low levels of eIF4E expression. However, the breast cancer cell lines MDA-MB-231, MDA-MB-361, and MDA-MB-435 showed between 37- and 41-fold higher levels of eIF4E compared to normal HMEC, and between 23- and 25-fold higher levels compared to normal fibroblasts. In contrast, to the differential expression of eIF4E between normal and breast cancer cell lines, CXCR4 showed high levels of expression in normal HMEC and fibroblasts as well as in breast cancer cell lines. These results suggest that using gene transcriptional control alone may be insufficient to target cancer cells, and that the addition of mRNA translational control may be necessary to achieve tumor specificity.

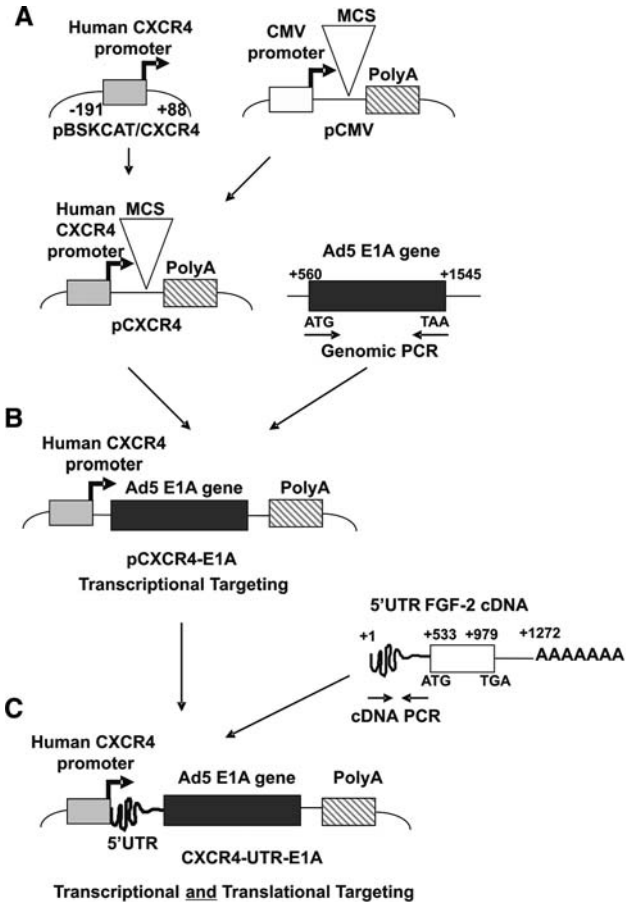

Fig. 1 Strategy to exploit translational targeting as an adjunct to transcriptional targeting. (**A**) Construction of pAdenoVator-CXCR4. This construct contains the 279 bp CXCR4 promoter and the simian virus 40 (SV40) polyadenylation (poly A) signal. (**B**) The adenoviral type 5 E1AcDNA was cloned by PCR into pAdenoVator-CXCR4 to generate the pAdenoVator-CXCR4-E1A plasmid. (**C**) The 5′ upstream-untranslated region sequence of the rat FGF-2 cDNA was inserted immediately upstream of the E1A sequence to produce the pAdenoVator-CXCR4-UTR-E1A plasmid

Transcription of the dual-level targeted CRAd is Independent of eIF4E protein level

A real-time RT-PCR was used to quantify transcription levels of E1A in breast epithelial and stromal cell lines expressing low levels of eIF4E (HMEC and fibroblasts) and in breast cancer cell lines having high levels of eIF4E (MDA-MB-231, MDA-MB-361, and MDA-MB-435), at 48 h after infection with either Ad-CXCR4-E1A or with Ad-CXCR4-UTR-E1A. Transcription levels of E1A were also quantified in cells infected with an untargeted replicative Ad-wt-dE3 as a positive control and in cells infected with a non-replicative Ad-CXCR4-GL3 as a negative control. As shown in Fig. 3, there were no statistically significant differences in the levels of E1A mRNA observed for any of the cell lines, whether the cells were

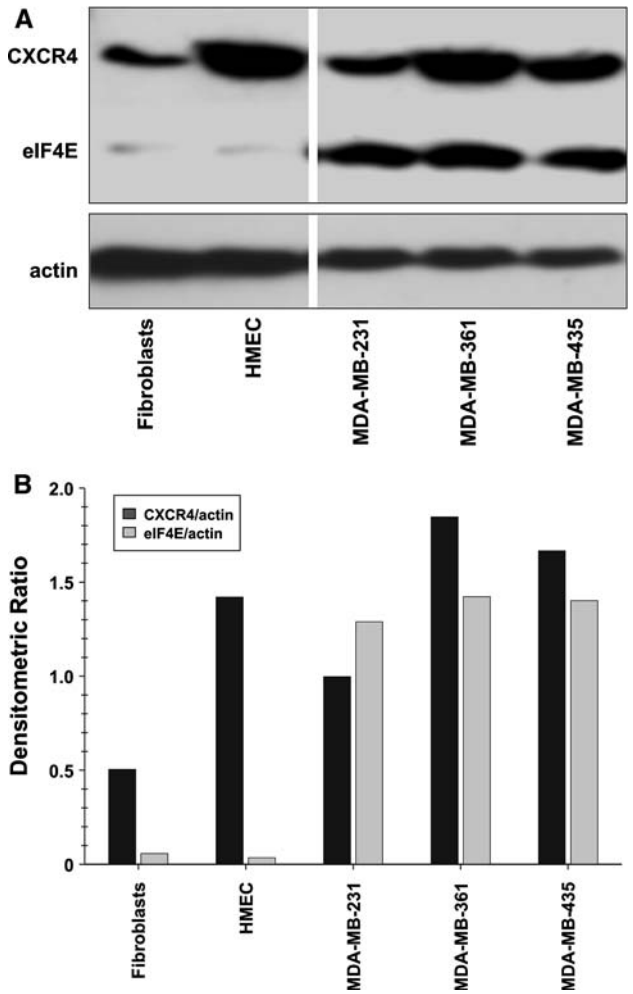

Fig. 2 Western blot analysis of eIF4E protein levels in normal breast epithelial and stromal cells and breast cancer cell lines. An analysis was performed for each cell line used (fibroblasts, HMEC, MDA-MB-231, MDA-MB-361, and MDA-MB-435) for expression of CXCR4, eIF4E and β-actin. (**A**) A representative of three independent Western blot experiments. (**B**) Densitometric ratios of CXCR4 and eIF4E levels normalized to β-actin

infected with Ad-CXCR4-E1A or with Ad-CXCR4-UTR-E1A. Importantly, these levels were similar to levels of E1A in cells infected with Ad-wt-dE3. These results serve to confirm our hypothesis that the transcription of E1A in these systems is independent of eIF4E protein levels and is unaffected by the FGF-2 5′UTR sequence.

Dual-Level targeting allows specific 5′UTR-E1A mRNA translation during CRAd infection

In the following experiments we tested the feasibility of translational regulation in the context of CRAd, based on eIF4E dependent translational control. The breast cancer cell lines (MDA-MB-231, MDA-MB-361, and MDA-MB-435) and normal cell lines (HMEC and fibroblasts) were infected with either Ad-CXCR4-E1A or Ad-CXCR4-UTR-E1A, and Western blot analysis of E1A protein levels was performed (Fig. 4). Western blot analysis was also performed on cells infected with an untargeted replicative Ad-wt-dE3 as a positive control and on cells infected with a non-replicative Ad-CXCR4-GL3 as a negative control. In breast cell lines that express relatively high levels of eIF4E, the E1A protein expression levels in cells infected with Ad-CXCR4-UTR-E1A were similar to cells infected with Ad-CXCR4-E1A or with Ad-wt-dE3. Importantly, in breast epithelial and stromal cell lines that express relatively low levels of eIF4E, the E1A expression level was significantly lower (in fact, lower than the detection limit) after infection with Ad-CXCR4-UTR-E1A compared to infection with Ad-CXCR4-E1A or Ad-wt-dE3. Thus, these results confirm our hypothesis that the translation of the 5′-UTR-E1A mRNA in the dual-level targeted CRAd is strongly dependent on the presence of elevated levels of eIF4E.

eIF4E selective replication of dual-level targeted cRAds

To assay and compare eIF4E selective replication of the single-level targeted CRAd (Ad-CXCR4-E1A) and the dual-level targeted CRAd (Ad-CXCR4-UTR-E1A) after infection of cells with different levels of eIF4E, viral replication was determined by viral copy number. In this assay, the presence of the E4 gene was determined using real-time PCR from DNA samples extracted from medium after 1, 3, and 9 days post-infection [26, 27]. Viral replication was also determined in cells infected with an untargeted replicative Ad-wt-dE3 as a positive control and in cells infected with a non-replicative Ad-CXCR4-GL3 as a negative control. Infection of breast cancer cell lines (MDA-MB-231, MDA-MB-361, and MDA-MB-435) expressing relatively high levels of eIF4E with either the single-level targeted CRAd or the dual-level targeted CRAd generated comparably high DNA copy numbers, which were similar to the untargeted replicative Ad-wt-dE3 control (Fig. 5). In contrast, in normal cells (HMEC and fibroblasts) expressing low levels of eIF4E the dual-level targeted CRAd displayed significantly ($P < 0.05$) lower viral copy number in comparison to the single-level targeted CRAd. Thus, the dual-level targeted CRAd demonstrated specific eIF4E selective replication.

Dual-Level targeting exploiting both gene transcriptional and mRNA translational control displays oncolytic specificity in cells over expressing eIF4E

We next compared the oncolytic profile of the single-level targeted and the dual-level targeted CRAd in cells expressing different levels of eIF4E (Fig. 6). Cell sur-

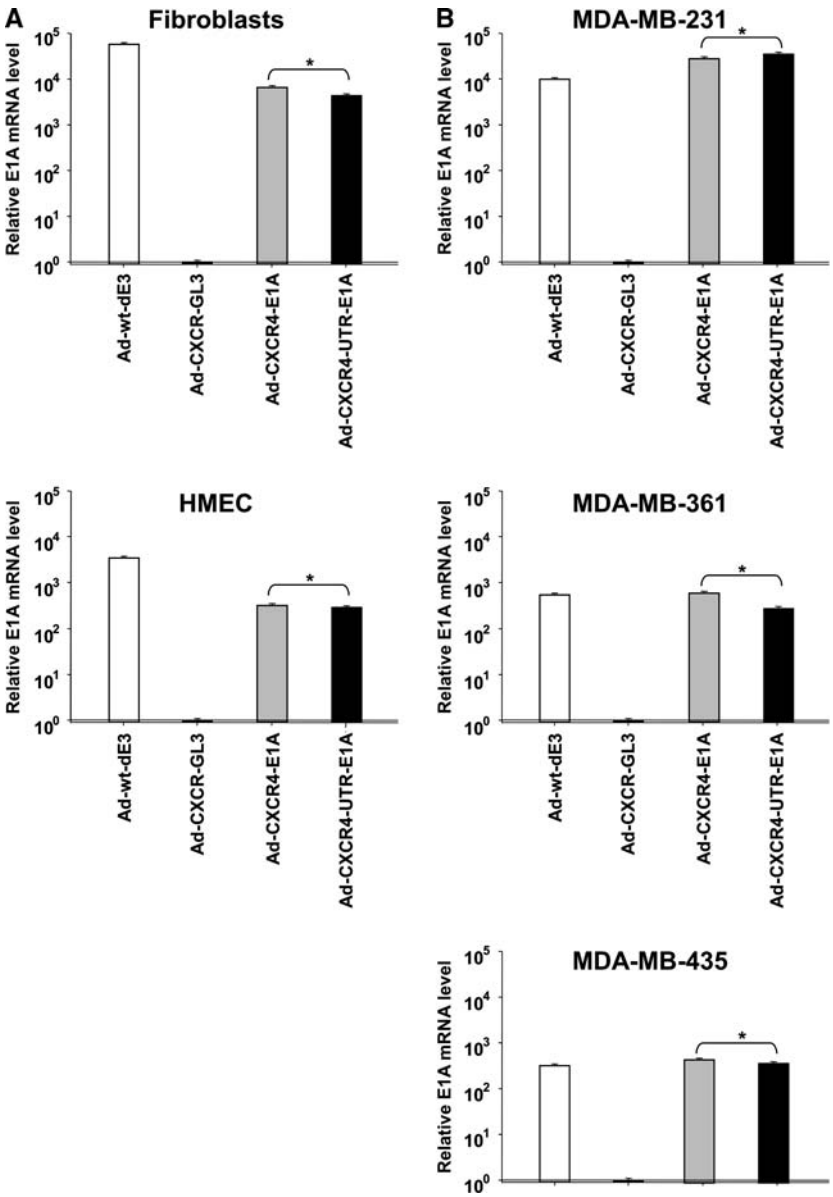

Fig. 3 Evaluation of transcription of the E1A gene of the single and dual-level targeted CRAd by quantitative Real-time PCR. (**A**) Quantification of E1A mRNA expression after infection with Ad-CXCR4-E1A, Ad-CXCR4-UTR-E1A, Ad-CXCR4-GL3 (negative control) or Ad-wt-dE3 (positive control) in normal cells expressing relatively low levels of eIF4E. (**B**) Quantification of E1A mRNA expression after infection with AdCXCR4-GL3, Ad-CXCR4-E1A, Ad-CXCR4-UTR-E1A and Ad-wt-dE3 in breast cancer cell lines expressing relatively high levels of eIF4E. The mRNA copy numbers are normalized by the GAPDH copy number. Each bar represents the mean of three experiments ± SD. *P = ns

vival was determined by crystal violet staining. In all the breast cancer cell lines tested, the single and dual-level targeted CRAds displayed oncolytic potency comparable to Ad-wt-dE3. In contrast, in the normal HMEC and fibroblasts expressing low levels of eIF4E, the dual-level targeted CRAd (Ad-CXCR4-UTR-E1A) showed a cytotoxicity that was severely attenuated relative to the wild type adenovirus control (Adwt-dE3). Importantly, Ad-CXCR4-UTR-E1A displayed an oncolytic activity that was one order of magnitude lower compared to Ad-CXCR4-E1A in fibroblasts and HMEC. In the aggregate, these data clearly demonstrate that differential E1A protein expression and replication by the dual-level targeted CRAd Ad-CXCR4-UTR-E1A in cells expressing low and high levels of eIF4E results in eIF4E specific oncolytic activity.

Dual-Level targeted CRAd maintains its cancer specificity in a human tissue slice model

To more closely mimic the clinical situation, we aimed to determine eIF4E selective replication of the dual-level targeted CRAd in the most stringent available preclinical model, precision cut tissue slices of normal breast and breast cancer samples. To measure viral copy number, the presence of the E4 gene was determined using real-time PCR from DNA samples extracted from medium at 1, 3, and 9 days post-infection [26, 27]. Infection of

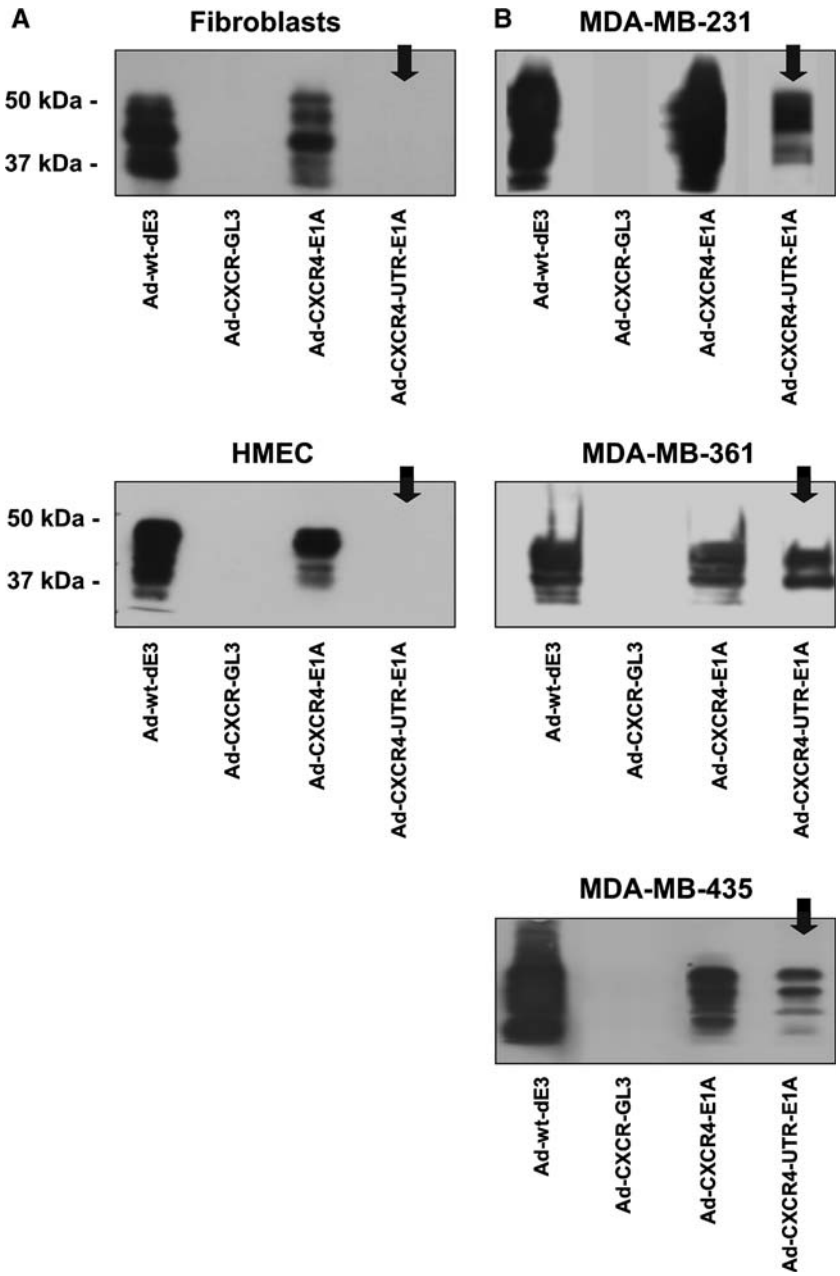

Fig. 4 Dual-level targeting allows specific 5′UTR-E1A mRNA translation during CRAd infection. Western blot analysis was performed using lysates from normal cells expressing relatively low levels of eIF4E (**A**) and breast cancer cell lines expressing relatively high levels of eIF4E (**B**) after infection with after infection with Ad-CXCR4-E1A, Ad-CXCR4-UTR-E1A, Ad-CXCR4-GL3 (negative control) or Ad-wt-dE3 (positive control)

breast cancer tissue samples expressing relatively high levels of eIF4E with either the single-level targeted CRAd or the dual-level targeted CRAd generated comparably high DNA copy numbers, (Fig. 7), which were similar to the untargeted replicative Ad-wt-dE3 control. However, in normal breast tissue samples expressing low levels of eIF4E the dual-level targeted CRAd (Ad-CXCR4-UTR-E1A) showed a significantly lower ($P < 0.05$) viral copy number in comparison to the single-level targeted CRAd (Ad-CXCR4-E1A). Importantly, the results determined in normal human breast tissues and primary human breast cancer samples correspond to the results obtained in cell lines expressing low and high levels of eIF4E. Thus, exploiting translational targeting as an adjunct to transcriptional targeting in a CRAd allows distinctive cancer-selective replication.

Dual-Level targeted CRAd is oncolytic in vivo in a murine model of breast cancer

Next, the anti-tumor effects of the single-level targeted CRAd (Ad-CXCR4-E1A) and the dual-level targeted CRAd (Ad-CXCR4-UTR-E1A) were analyzed in vivo using MDA-MB-361 breast cancer cells injected subcu-

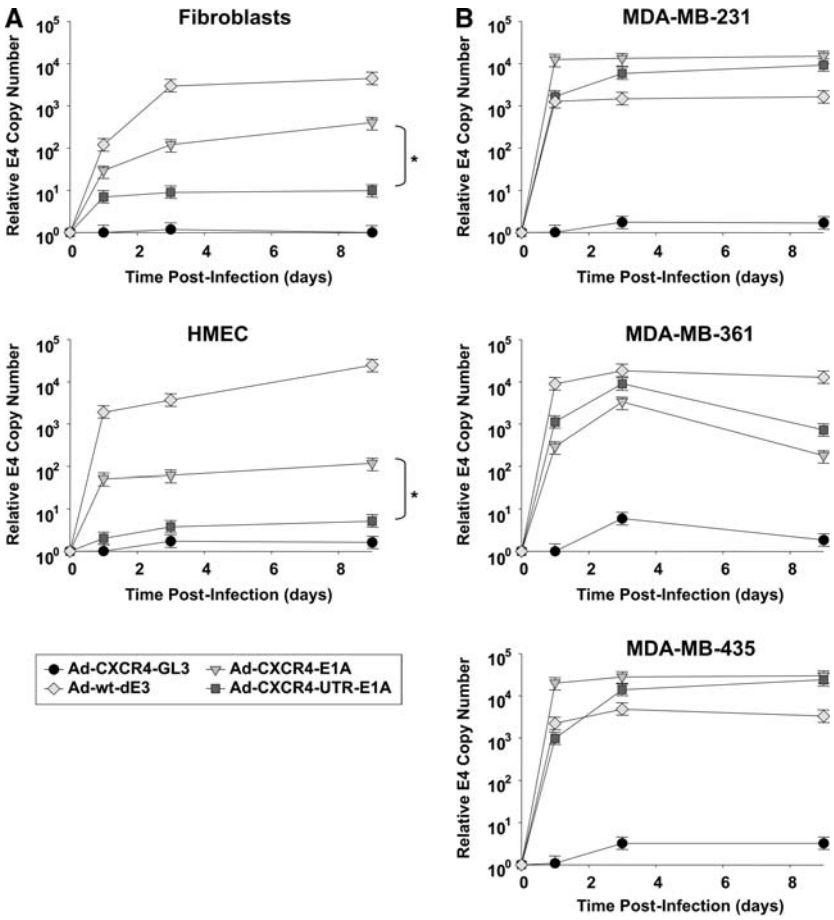

Fig. 5 eIF4E selective replication of dual-level targeted CRAds. Viral copy number as an indicator of viral replication in normal cells expressing relatively low levels of eIF4E (**A**) and breast cancer cell lines expressing relatively high levels of eIF4E (**B**). Growth medium was collected at day 1, 3 and 9 after infection with Ad-CXCR4-E1A, Ad-CXCR4-UTR-E1A, Ad-CXCR4-GL3 (negative control) or Ad-wt-dE3 (positive control). Each bar represents the mean of three experiments ±SD. *$P < 0.05$ Ad-CXCR4-E1A versus Ad-CXCR4-UTR-E1A

taneously in an athymic mouse xenograft model. As shown in Fig. 8, the decrease of the relative tumor volume in Ad-CXCR4-UTR-E1A treated mice was comparable to the Ad-CXCR4-E1A injected mice and the untargeted replicative Ad-wt-dE3 control. Taken together, these in vivo results are consistent with the in vitro data demonstrating a comparable oncolytic effect between the dual-level targeted CRAd (Ad-CXCR4-UTR-E1A) and the single-level targeted CRAd (Ad-CXCR4-E1A). Interestingly, treatment with a negative control (non-replicative) Ad-CXCR4-GL3 virus resulted in a partial therapeutic effect. The effect of transient tumor inhibition by a non-therapeutic adenovirus has previously been observed [28–31], and has been attributed to the recruitment and activation of the innate immune system (e.g., natural killer cells and macrophages) [32–35]. These findings may explain the non-specific tumor inhibition we observed.

Dual-Level targeted CRAd displays reduced replication in a human liver tissue slice model

To preclinically evaluate the liver toxicity of human CRAds is a challenge. It is known that human adenoviruses replicate only poorly in mice. Therefore, we evaluated adenoviral replication in the most relevant preclinically available model, the human liver tissue slice model. To measure viral copy number, the presence of the E4 gene was determined using real-time PCR from DNA samples extracted from medium 2 and 4 days post-infection [26, 27]. As shown in Fig. 9, the dual-level targeted CRAd (Ad-CXCR4-UTR-E1A) showed the lowest copy number among the replication competent viruses tested, which was significantly lower compared to the single-level targeted CRAd (Ad-CXCR4-E1A) or Ad-wt-dE3. Thus, exploiting translational targeting as an adjunct to transcriptional targeting in a CRAd allows a significant reduction of replication in human liver tissue.

Discussion

In this report, we exploited cancer-specific control of mRNA translation initiation in order to achieve enhanced replicative specificity of CRAd virotherapy agents. Both in vitro and in vivo studies demonstrated that the CRAd agent, which utilized a heterologous mRNA translational control element, retained anti-tumor potency. Importantly,

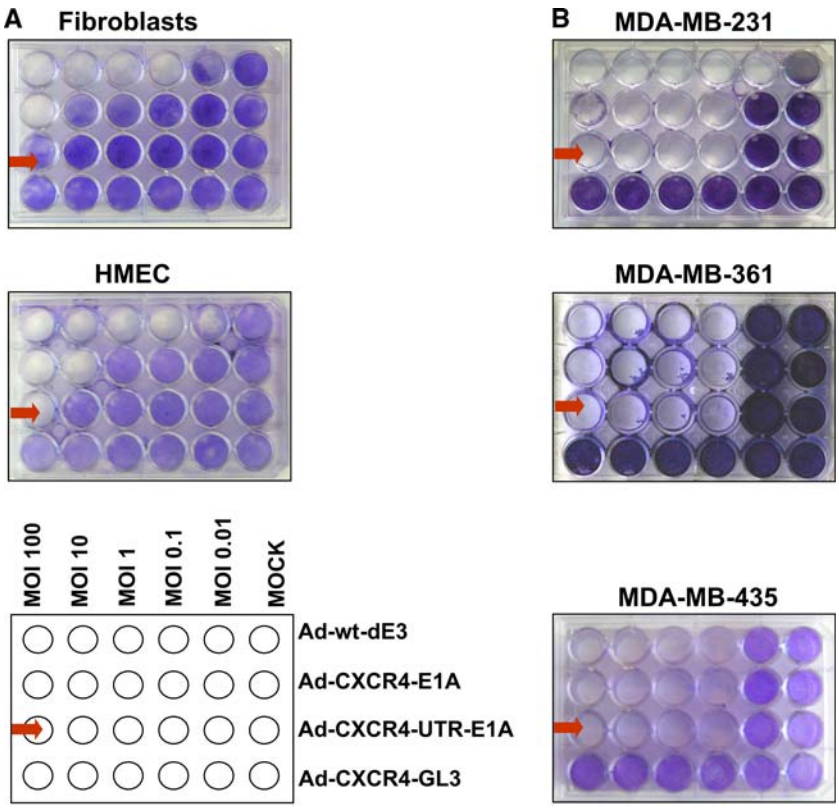

Fig. 6 Dual-level targeting exploiting both gene transcriptional and mRNA translational control displays cytotoxic specificity in cells over expressing eIF4E. Oncolysis was evaluated by crystal violet staining in normal cells expressing relatively low levels of eIF4E (**A**) and breast cancer cell lines expressing relatively high levels of eIF4E (**B**) after infection with Ad-CXCR4-E1A, Ad-CXCR4-UTR-E1A, Ad-CXCR4-GL3 (negative control) or Ad-wt-dE3 (positive control) as described in Material and methods

assessment of replicative specificity using stringent tumor and non-tumor tissue slice systems demonstrated significant improvement in tumor selectivity. Heretofore, the achievement of replicative specificity of CRAd agents has been accomplished solely with gene transcriptional control elements based upon incorporation of tumor selective promoters. Our report herein demonstrates the utility of a novel approach that combines both transcriptional and translational regulation strategies for the key goal of replicative specificity.

In cancer cells, translational regulation has become a well-recognized mechanism contributing to the neoplastic phenotype. Processes linked to aberrant translation regulation include cell cycle alterations, motility and invasiveness, angiogenesis, metastasis, and resistance to apoptosis. Therefore, translational regulation represents a very attractive point of attack to for therapy of cancer, because of the multitude of downstream effectors that can be modulated at one time. Clearly, eIF4E is a central player in translational regulation and is critical to the genesis and/or progression of cancer cells as indicated by the fact that it is over-expressed in the majority of solid tumors studied to date [11, 36, 37]. In addition to the importance of eIF4E in early changes in the primary tumor, eIF4E has been identified as one of eight genes that when elevated constitutes a molecular signature of metastasis potential [38]. In this regard, elevated eIF4E expression results in drastically increased synthesis of basic fibroblast growth factor (FGF-2) [39] and vascular endothelial growth factor (VEGF) [40], both of which are encoded by mRNAs with a long and complex 5′-UTR. Both of them powerful mitogens for vascular endothelia and are essential for tumor vascularization [41].

In this study, use of an mRNA translational control element in combination with the use of a gene transcriptional control element maintained oncolytic CRAd activity, both in vitro in tumor cells and in vivo in a xenograft breast cancer mouse model. Importantly, our CRAd agent demonstrated selective cytotoxicity in vitro, which was dependent upon eIF4E activity. Murine models are not an appropriate in vivo model to test non-specific adenoviral replication and spread, because normal murine tissues are poorly permissive for Ad replication [42, 43]. Thus we utilized the human tissue slice model, the most stringent preclinical substrate system currently available [44, 45]. In this model, we showed using normal human liver and

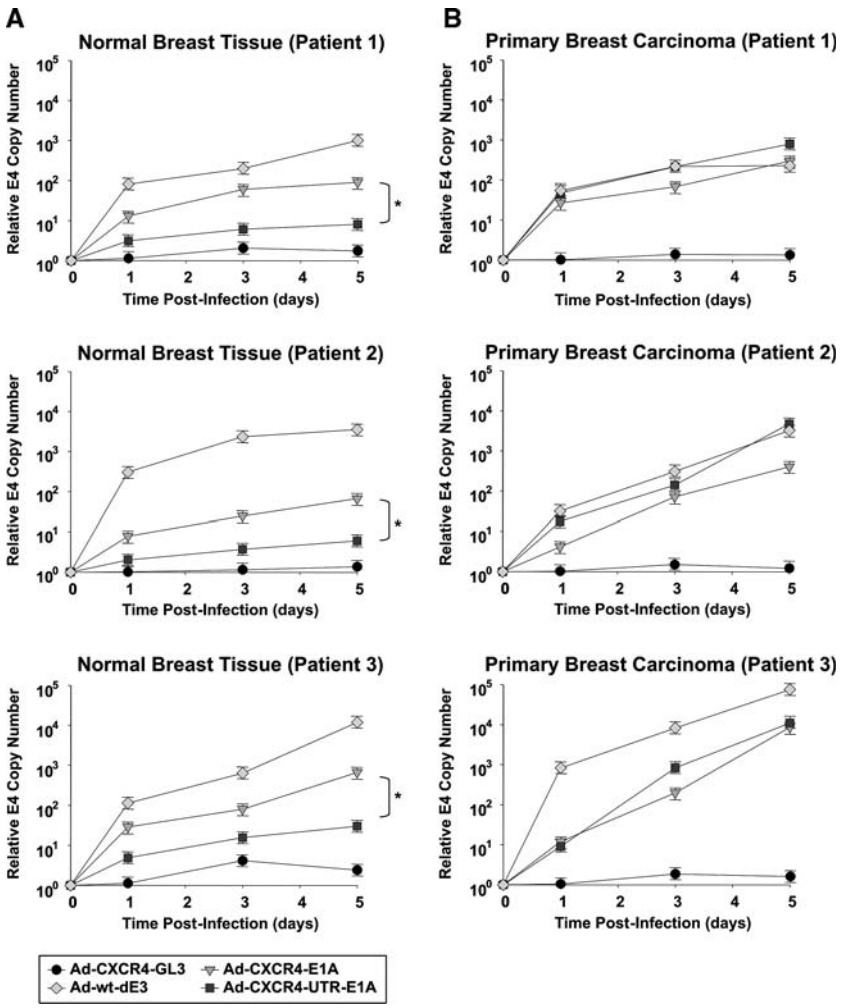

Fig. 7 Evaluation of dual-level targeted CRAds in primary normal breast and breast cancer cells (4 patients). Viral copy number as an indicator of viral replication in precision cut tissue slices of normal breast (**A**) and breast cancer samples (**B**) obtained from three patients. Growth medium was collected at day 1, 3, 5 after infection with Ad-CXCR4-E1A, Ad-CXCR4-UTR-E1A, Ad-CXCR4-GL3 (negative control) or Ad-wt-dE3 (positive control). Each bar represents the mean of three experiments ±SD. *$P < 0.05$ Ad-CXCR4-E1A versus Ad-CXCR4- UTR -E1A

breast tissue that the dual-level targeted CRAd significantly reduced non-specific adenoviral replication compared to a transcriptional targeted CRAd.

Our study exploited the 5′-UTR sequence from the FGF-2 mRNA as an mRNA translational control element. In our construct, protein expression of the modified Ad5 E1A transcript, which is essential for CRAd replication function, was restricted to cancer cells expressing high levels of elF-4E. Recently, another study exploited mRNA stabilization in the context of virotherapy for tumor specific replication [10]. In this design, the 3′-UTR sequence from the PTGS2 (prostaglandin-endoperoxide synthase 2) mRNA was exploited as a targeting element that allowed activated RAS/P-MAPK dependant mRNA stability of a modified Ad5 E1A transcript in cancer cells. Importantly, however, this design only tested a single targeting approach, with the use of a non-specific CMV promoter for E1A expression. In our approach, we extended CRAd targeting using mRNA translational control by placing the E1A gene under a second targeting element, using gene transcriptional control from a candidate TSP, the CXCR4 gene promoter [22].

To our knowledge, the conditionality of adenoviral replication and oncolysis through a post-transcriptional level of control of E1A expression using an mRNA translational control element has not been previously demonstrated. At this point, it is clear that reliance on a single targeting control of adenovirus replication could allow toxicity in non-target tissues. Thus, the combination of CRAd replication control at the level of both transcription and translation should provide greater cancer selectivity in vivo than either control element alone.

Our study has highlighted specificity gains that accrue from the employment of methods combining transcriptional and translational targeting. In this regard, the parent vector of our CRAd construct is based on adenovirus serotype 5. Genetic capsid modifications have recently been shown to allow for cell-specific targeted infection. This transductional targeting represents an additional strategy for the achievement of specificity, which can be

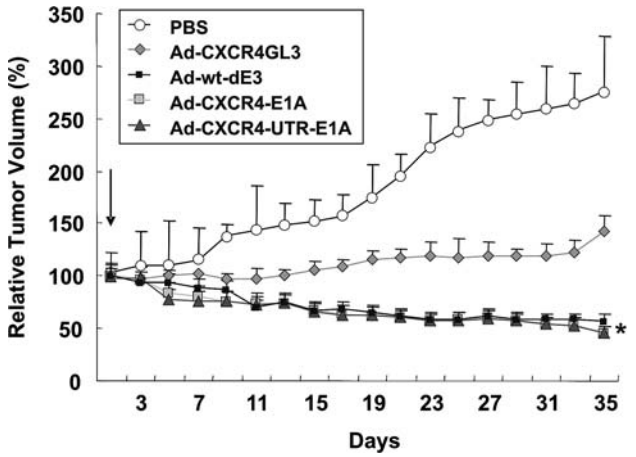

Fig. 8 Oncolytic activity of dual-level targeted controlled CRAds is maintained in an orthotopic murine model of breast cancer. Anti-tumor effect of CRAd agents were determined using MDA-MB-361 mouse xenograft model. When the tumor reached 5 mm in widest diameter, 1×10^8 IFN of Ad-CXCR4-E1A, Ad-CXCR4-UTR-E1A, Ad-CXCR4-GL3 (negative control) or Ad-wt-dE3 (positive control) were injected intratumorally in a 0.05 ml volume. Control tumors were injected with an equal volume of PBS only. The tumor volume was calculated by the formula: $1/2\ xy^2$, where x is the longest distance of the tumor. The relative tumor volume = tumor volume/tumor volume at day 1 × 100%. Each bar represents the mean of 10 tumors ±SD

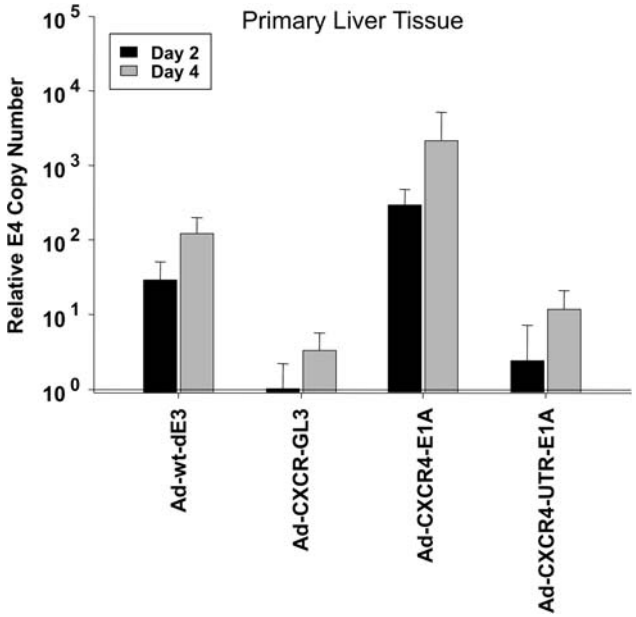

Fig. 9 Evaluation of liver toxicity of the single-level and dual-level controlled CRAd in a human liver tissue slice model. Viral copy number as an indicator of viral replication in precision cut tissue slices of normal human liver obtained from three individual donors. Growth medium was collected at day 2 and 4 after infection with Ad-CXCR4-E1A, Ad-CXCR4-UTR-E1A, Ad-CXCR4-GL3 (negative control) or Ad-wt-dE3 (positive control). Each bar represents the mean of three experiments ±SD. *$P < 0.05$ Ad-CXCR4-UTR-E1A versus Ad-CXCR4-E1A and Ad-wt-dE3

employed with the methods we describe in this study. In conclusion, our future efforts are aimed toward the development of multiple-component targeted CRAds that will be the most effective at generating truly tumor selective vectors. Based on our studies, we propose that mRNA translation may be considered as one of the targeting component of such multiple targeted CRAds.

Augmentation of the specificity of adenoviruses for cancer targets is urgently required for deriving their full benefit and safety profile with regard to clinical trials. We presently describe an innovative dual cancer-specific targeting approach resulting in a new class of CRAds. We envisage/believe that the mRNA translational control element will play an important role in the vector design of virotherapeutic CRAds in future virotherapeutic clinical trials.

Acknowledgements This work was supported by Grant of the Deutsche Forschungsgemeinschaft Sto 647/1-1 (to M. A. Stoff-Khalili), by grants from the NIH P01CA104177, R01CA083821, and R01CA113454 (to D. T. Curiel), R01CA93796, R01CA98543 and AR46031 (to G. Siegal) and Department of Defense W81XWH-05-1-035 (to D. T. Curiel) and grants from the Department of Defense W81XWH-05-1-5500, NIH R41CA114921, and the Louisiana Gene Therapy Research Consortium, Inc. (to J. M. Mathis).

References

1. Mathis JM, Stoff-Khalili MA, Curiel DT (2005) Oncolytic adenoviruses - selective retargeting to tumor cells. Oncogene 24(52):7775–7791
2. Biederer C et al (2002) Replication-selective viruses for cancer therapy. J Mol Med 80(3):163–175
3. Vile RG, Russell SJ, Lemoine NR (2000) Cancer gene therapy: hard lessons and new courses. Gene Ther 7(1):2–8
4. Alemany R, Suzuki K, Curiel DT (2000) Blood clearance rates of adenovirus type 5 in mice. J Gen Virol 81(Pt 11):2605–2609
5. Krasnykh V et al (2001) Genetic targeting of an adenovirus vector via replacement of the fiber protein with the phage T4 fibritin. J Virol 75(9):4176–4183
6. Alemany R, Balague C, Curiel DT (2000) Replicative adenoviruses for cancer therapy. Nat Biotechnol 18(7):723–727
7. Siders WM, Halloran PJ, Fenton RG (1996) Transcriptional targeting of recombinant adenoviruses to human and murine melanoma cells. Cancer Res 56(24):5638–5646
8. Bernt KM et al (2003) The effect of sequestration by nontarget tissues on anti-tumor efficacy of systemically applied, conditionally replicating adenovirus vectors. Mol Ther 8(5):746–755
9. Ring CJ et al (1996) Suicide gene expression induced in tumour cells transduced with recombinant adenoviral, retroviral and plasmid vectors containing the ERBB2 promoter. Gene Ther 3(12):1094–1103
10. Ahmed A et al (2003) A conditionally replicating adenovirus targeted to tumor cells through activated RAS/P-MAPK-selective mRNA stabilization. Nat Biotechnol 21(7):771–777
11. DeFatta RJ et al (1999) Elevated expression of eIF4E in confined early breast cancer lesions: possible role of hypoxia. Int J Cancer 80(4):516–522
12. De Benedetti A et al (1991) Expression of antisense RNA against initiation factor eIF-4E mRNA in HeLa cells results in length-

ened cell division times, diminished translation rates, and reduced levels of both eIF-4E and the p220 component of eIF-4F. Mol Cell Biol 11(11):5435–5445
13. Rhoads RE (1988) Cap recognition and the entry of mRNA into the protein synthesis initiation cycle. Trends Biochem Sci 13(2):52–56
14. Kozak M (1991) An analysis of vertebrate mRNA sequences: intimations of translational control. J Cell Biol 115(4):887–903
15. Pelletier J, Sonenberg N (1987) The involvement of mRNA secondary structure in protein synthesis. Biochem Cell Biol 65(6):576–581
16. Smola H, Thiekotter G, Fusenig NE (1993) Mutual induction of growth factor gene expression by epidermal-dermal cell interaction. J Cell Biol 122(2):417–429
17. Stark HJ et al (1999) Organotypic keratinocyte cocultures in defined medium with regular epidermal morphogenesis and differentiation. J Invest Dermatol 112(5):681–691
18. Satish L et al (2004) Keloid fibroblast responsiveness to epidermal growth factor and activation of downstream intracellular signaling pathways. Wound Repair Regen 12(2):183–192
19. Kirby TO et al (2004) A novel ex vivo model system for evaluation of conditionally replicative adenoviruses therapeutic efficacy and toxicity. Clin Cancer Res 10(24):8697–8703
20. Olinga P et al (1997) Comparison of five incubation systems for rat liver slices using functional and viability parameters. J Pharmacol Toxicol Methods 38(2):59–69
21. Wegner SA et al (1998) Genomic organization and functional characterization of the chemokine receptor CXCR4, a major entry co-receptor for human immunodeficiency virus type 1. J Biol Chem 273(8):4754–4760
22. Zhu ZB et al (2004) Transcriptional targeting of adenoviral vector through the CXCR4 tumor-specific promoter. Gene Ther 11(7):645–648
23. Zhu ZB et al (2004) Transcriptional targeting of tumors with a novel tumor-specific survivin promoter. Cancer Gene Ther 11(4):256–262
24. Kanerva A et al (2003) Enhanced therapeutic efficacy for ovarian cancer with a serotype 3 receptor-targeted oncolytic adenovirus. Mol Ther 8(3):449–458
25. Rivera AA et al (2004) Combining high selectivity of replication with fiber chimerism for effective adenoviral oncolysis of CAR-negative melanoma cells. Gene Ther 11(23): 1694–1702
26. Zhu ZB et al (2005) Incorporating the surviving promoter in an infectivity enhanced CRAd-analysis of oncolysis and anti-tumor effects in vitro and in vivo. Int J Oncol 27(1):237–246
27. Yamamoto M et al (2003) Infectivity enhanced, cyclooxygenase-2 promoter-based conditionally replicative adenovirus for pancreatic cancer. Gastroenterology 125(4):1203–1218
28. Carroll JL et al (2001) The role of natural killer cells in adenovirus-mediated p53 gene therapy. Mol Cancer Ther 1(1):49–60
29. Kianmanesh A et al (2001) Intratumoral administration of low doses of an adenovirus vector encoding tumor necrosis factor alpha together with naive dendritic cells elicits significant suppression of tumor growth without toxicity. Hum Gene Ther 12(17):2035–2049
30. Hall SJ et al (2002) A novel bystander effect involving tumor cell-derived Fas and FasL interactions following Ad.HSV-tk and Ad.mIL-12 gene therapies in experimental prostate cancer. Gene Ther 9(8):511–517
31. Ruzek MC et al (2002) Adenoviral vectors stimulate murine natural killer cell responses and demonstrate antitumor activities in the absence of transgene expression. Mol Ther 5(2):115–124
32. Bessis N, GarciaCozar FJ, Boissier MC (2004) Immune responses to gene therapy vectors: influence on vector function and effector mechanisms. Gene Ther 11(Suppl 1):S10–S17
33. Muruve DA (2004) The innate immune response to adenovirus vectors. Hum Gene Ther 15(12):1157–1166
34. Liu Q, Muruve DA (2003) Molecular basis of the inflammatory response to adenovirus vectors. Gene Ther 10(11):935–940
35. Perricone MA et al (2004) Enhanced efficacy of melanoma vaccines in the absence of B lymphocytes. J Immunother 27(4):273–281
36. Rosenwald IB et al (1999) Upregulation of protein synthesis initiation factor eIF-4E is an early event during colon carcinogenesis. Oncogene 18(15):2507–2517
37. Miyagi Y et al (1995) Elevated levels of eukaryotic translation initiation factor eIF-4E, mRNA in a broad spectrum of transformed cell lines. Cancer Lett 91(2):247–252
38. Ramaswamy S et al (2003) A molecular signature of metastasis in primary solid tumors. Nat Genet 33(1):49–54
39. Kevil C et al (1995) Translational enhancement of FGF-2 by eIF-4 factors, and alternate utilization of CUG and AUG codons for translation initiation. Oncogene 11(11):2339–2348
40. Kevil CG et al (1996) Translational regulation of vascular permeability factor by eukaryotic initiation factor 4E: implications for tumor angiogenesis. Int J Cancer 65(6):785–790
41. Goto F et al (1993) Synergistic effects of vascular endothelial growth factor and basic fibroblast growth factor on the proliferation and cord formation of bovine capillary endothelial cells within collagen gels. Lab Invest 69(5):508–517
42. Ginsberg HS et al (1991) A mouse model for investigating the molecular pathogenesis of adenovirus pneumonia. Proc Natl Acad Sci USA 88(5):1651–1655
43. Hjorth RN et al (1988) A new hamster model for adenoviral vaccination. Arch Virol 100(3–4):279–283
44. Stoff-Khalili MA et al (2006) Employment of liver tissue slice analysis to assay hepatotoxicity linked to replicative and nonreplicative adenoviral agents. Cancer Gene Ther 13(6):606–618
45. Stoff-Khalili MA et al (2005) Preclinical evaluation of transcriptional targeting strategies for carcinoma of the breast in a tissue slice model system. Breast Cancer Res 7(6):R1141–R1152

A Mosaic Fiber Adenovirus Serotype 5 Vector Containing Reovirus σ1 and Adenovirus Serotype 3 Knob Fibers Increases Transduction in an Ovarian Cancer *Ex vivo* System via a Coxsackie and Adenovirus Receptor–Independent Pathway

Yuko Tsuruta,[1] Larisa Pereboeva,[1,2] Joel N. Glasgow,[1,2,3] Daniel T. Rein,[1,6] Yosuke Kawakami,[1] Ronald D. Alvarez,[2,4] Rodney P. Rocconi,[4] Gene P. Siegal,[2,5] Paul Dent,[7] Paul B. Fisher,[8] and David T. Curiel[1,2]

Abstract

Purpose: Adenovirus serotype 5 (Ad5) has been used for gene therapy with limited success due to insufficient infectivity in cells with low expression of the primary receptor, the coxsackie and adenovirus receptor (CAR). Evidence that adenovirus serotype receptors other than CAR may be of use was presented in previous studies that showed that the Ad3 receptor is expressed at high levels in ovarian cancer cells. We hypothesized that combined use of unique chimeric fibers in the context of novel mosaic adenovirus vectors would enhance infectivity via non-CAR pathways in ovarian cancer cells.

Experimental Design: We constructed and characterized Ad5 vectors that use Ad3 knob and reovirus fibers to generate a mosaic fiber virion. Serotype 3 Dearing reovirus uses a fiber-like σ1 protein to infect cells expressing sialic acid and junction adhesion molecule 1. We therefore constructed a mosaic fiber Ad5 vector, designated Ad5/3-σ1, encoding two fibers: a σ1 chimeric fiber and the chimeric Ad5/3 fiber composed of an Ad3 knob.

Results: Functionally, Ad5/3-σ1 used sialic acid, junction adhesion molecule 1, and Ad3 receptor for cell transduction and achieved maximum infectivity enhancement in ovarian cancer cells with low CAR expression. Furthermore, Ad5/3-σ1 achieved infectivity enhancement in primary tissue slices of human ovarian tumor.

Conclusions: We have developed a new type of Ad5 vector with the novel tropism, possessing fibers from Ad3 and reovirus, which exhibits enhanced infectivity via CAR-independent pathway(s). In addition, the flexible genetic platform of vector allows different combination of fiber variants that can be incorporated within the same particle.

Authors' Affiliations: [1]Division of Human Gene Therapy, Departments of Medicine, Obstetrics and Gynecology, Pathology, and Surgery, [2]University of Alabama at Birmingham Gene Therapy Center, [3]Division of Cardiovascular Disease, [4]Department of Obstetrics and Gynecology, and [5]Departments of Pathology, Cell Biology, and Surgery, The University of Alabama at Birmingham, Birmingham, Alabama; [6]Department of Obstetrics and Gynecology, University of Düsseldorf Medical Center, Düsseldorf, Germany; [7]Department of Biochemistry, Massey Cancer Center, Virginia Commonwealth University, Richmond, Virginia; and [8]Departments of Pathology, Neurosurgery, and Urology, Herbert Irving Comprehensive Cancer Center, Columbia University Medical Center, College of Physicians and Surgeons, New York, New York

Received 11/13/06; revised 1/20/07; accepted 2/13/07.

Grant support: NIH grants CA35675, CA97318, CA104177, CA083821, and P01HL076540; Department of Defense grant W81XWH-05-1-0035; and Waxman Foundation for Cancer Research.

The costs of publication of this article were defrayed in part by the payment of page charges. This article must therefore be hereby marked *advertisement* in accordance with 18 U.S.C. Section 1734 solely to indicate this fact.

Requests for reprints: David T. Curiel, Division of Human Gene Therapy, Departments of Medicine, Obstetrics and Gynecology, Pathology, and Surgery, and The Gene Therapy Center, The University of Alabama at Birmingham, 901 19th Street South, BMR2-508, Birmingham, AL 35294-2172. Phone: 205-934-8627; Fax: 205-975-7476; E-mail: curiel@uab.edu.

doi:10.1158/1078-0432.CCR-06-2706

Cancer gene therapy has been widely investigated in the last decade as one of the new approaches for ovarian cancer. Adenoviral vectors, particularly vectors based on human serotype 5 (Ad5), have shown a great applicability in preclinical evaluations (1). Despite exciting preclinical data, adenoviral gene therapy approaches have yet to display significant clinical benefit. In general, poor therapeutic results have been attributed in large part to insufficient transduction of tumor cells. Human tumor cells frequently express little to none of the primary adenovirus receptor coxsackie and adenovirus receptor (CAR; refs. 2, 3). This CAR deficiency renders many tumor cells resistant to adenovirus infection, undermining cancer gene therapy strategies that require efficient tumor cell transduction. To address this issue, strategies are being developed that aim at modifying the adenovirus vector tropism to achieve CAR-independent transduction.

Genetic capsid modification has rationally focused on the fiber knob domain, which is the primary determinant of adenovirus tropism, to achieve CAR-independent cell entry. We previously showed that a mosaic fiber Ad5 vector provided viral entry via two different pathways, resulting in an additive gain in

infectivity in a variety of transformed cells, including ovarian cancer cells (4). We derived a mosaic fiber Ad5 vector that incorporates two distinct fibers: the Ad5 fiber and a reovirus chimeric fiber (4). The reovirus chimeric fiber includes the fiber-like σ1 protein, which is a receptor-binding molecule of serotype 3 Dearing reovirus. The σ1 protein has been reported to use the coreceptors junction adhesion molecule 1 (JAM1) and sialic acid for cellular binding (5, 6). These receptors are clearly distinct from the Ad5 receptor and together determine serotype 3 Dearing reovirus tropism. Of note, this mosaic fiber modification greatly enhanced vector infectivity in cancer cells compared with the wild-type Ad5 fiber. To further increase infectivity of the mosaic fiber Ad5 vector, and to gain more specific infectivity for ovarian cancer, we replaced the Ad5 wild-type fiber gene in a tandem fiber cassette with the gene for a chimeric Ad5/3 fiber. The Ad5/3 fiber contains the tail and shaft domains of Ad5 and the knob domain of serotype 3. It has been suggested that the Ad3 receptor is expressed at high levels in ovarian cancer cells. Ad5 vectors that express a chimeric fiber consisting of the adenovirus serotype 3 knob domain (Ad5/3) have been shown to significantly increase infectivity in ovarian cancer cells. Thus, we engaged in the construction and characterization of Ad5 vectors that were mosaics of Ad3 knob and reovirus fibers. The goal is to develop mosaic fiber adenovirus vector, which could bind to ovarian cancer cells using the Ad3 receptor JAM1 and sialic acid cell receptors, thus establishing a novel strategy to achieve infectivity enhancement based on a CAR-independent tropism.

A noteworthy aspect of our mosaic fiber strategy is the flexibility whereby different combinations of fiber variants can be incorporated within the same particle. On this basis, mosaic fiber virions can be proposed, which embody ever greater potential for enhancement of vector infectivity.

To evaluate the efficacy of the newly established adenovirus vector, we introduced a thin-slice tumor model technique that has been evaluated in our group. In this regard, Kirby et al. (7) has clarified that the thin-slice tumor model system represents a stringent method of *ex vivo* evaluation of novel adenoviral vectors. For this technique, the Krumdieck tissue slicer is a novel instrument, which was introduced in 1980s to cut precise tissue slices from an organ of interest (8). Tissue slices thus obtained, including those of human derivation, are capable of maintaining their original *in vivo* structure and composition. This study provides a means for rigorous preclinical analysis of adenovirus-based transduction of patient tumors. We explored the infectivity efficacy of our newly developed mosaic fiber adenovirus vector using this established technique for preclinical evaluation, thus providing a powerful tool to determine the therapeutic index for clinical translation.

Materials and Methods

Cell lines. The 293 cells were purchased from Microbix. Human ovarian cancer cell lines ES-2 and OV-3 were obtained from the American Type Culture Collection. Human ovarian adenocarcinoma cell lines OV-4 and Hey were a kind gift from Dr. Timothy J. Eberlein (Harvard Medical School, Boston, MA) and Dr. Judy Wolf (M. D. Anderson Cancer Center, Houston, TX), respectively. L929 cells were maintained as described previously (6). All other cell lines were cultured in medium recommended by suppliers (Mediatech and Irvine Scientific). Fetal bovine serum was purchased from Hyclone. All cells were grown at 37°C in a humidified atmosphere of 5% CO_2.

Generation of the σ1 chimeric fiber construct. A schematic of the σ1 chimeric fiber structure is shown in Fig. 1A. To design the σ1 chimeric fiber, the fiber tail domain of Ad5 was fused in its whole length to the entire σ1 coding region in frame with a C-terminally encoded 6-histidine (6-His) sequence, resulting in F5S1H as described previously (4).

Generation of shuttle plasmids for the mosaic fiber Ad5 genome. We previously created a shuttle vector, pNEB.PK.FSPF5S1/F5, which contained tandem fiber genes for the σ1 chimeric fiber F5S1H and the wild-type Ad5 fiber (4). The current shuttle vector was based on pNEB.PK.FSPF5S1/F5. We replaced the Ad5 knob sequence of the wild-type Ad5 fiber with the Ad3 knob coding sequence in frame, resulting in pNEBσ5/3. Technically, a fiber shuttle vector, pNEB.PK.F5/3 (9), containing an Ad5 tail, Ad5 shaft, and an Ad3 knob was used to extract the coding sequence of the Ad3 knob with *Nhe*I-*Mun*I digestion. Another shuttle vector, pNEB.PK.FSPF5S1/F5, was digested with *Nhe*I and *Mun*I for removal of the Ad5 knob sequence. A *Nhe*I/*Mun*I fragment containing the coding sequence of the Ad3 knob from pNEB.PK.F5/3 was cloned into the *Nhe*I-*Mun*I–digested pNEB.PK.FSPF5S1/F5, resulting in pNEBσ5/3, containing the σ1 chimeric fiber F5S1H and the chimeric Ad5/3 fiber genes in tandem.

Generation of recombinant adenovirus. A schematic of the viruses used in this study is shown in Fig. 1B. Recombinant Ad5 genomes containing the tandem fiber genes were derived by homologous recombination in *Escherichia coli* BJ5183 with *Swa*I-linearized rescue plasmid pVK700 and the *Pac*I and *Kpn*I fragment of pNEBσ5/3 containing tandem fibers essentially as described previously (10). The recombinant region of the genomic clones was sequenced before transfection into 293 cells. All vectors were propagated in 293 cells and purified using a standard protocol (11). The resultant mosaic fiber virus was Ad5/3-σ1. Viral particle (vp) concentration was determined by the A_{260} method as described by Maizel et al. (12). The infectious titer was determined according to the AdEasy Vector System (Qbiogene, Inc.).

PCR amplification of viral genome fragments. Viral DNA was amplified using the Taq PCR Core kit (Qiagen, Inc.). The sequences of the primers were as follows: Ad5tail-sense, 5′-ATGAAGCGCGCAAGACCGTCTGAAGAT; Ad3knob-antisense, 5′-GTCATCTTCTCTAATATAGGAAAAGGTAAATGGGG; and σ1head-antisense, 5′-ATTCTTGCGTGAAACTACGCGG.

Protein electrophoresis and Western blotting. To detect the incorporation and the trimerization of fibers in vp, adenovirus vectors equal to 1.0×10^{10} to 1.0×10^{11} vp were resolved by SDS-PAGE and Western blotting as described previously (13).

Recombinant proteins. The fiber knob domains of Ad5 and Ad3 fibers were produced and purified as described previously (9). The protein concentrations in all experiments were determined by the Bradford method (Bio-Rad Laboratories).

Gene transfer assays. Cells were infected with viruses at 37°C for 1 h and unbound virus was washed away. A luciferase assay was done 24 h after infection (Promega) according to the manufacturer's instructions. Tumor slices were cut, infected, and processed for luciferase assay after 24 h of incubation at 37°C as described previously (7, 14).

Competitive inhibition assay. Recombinant Ad3 fiber knob protein or anti-JAM1 polyclonal antibody (c-15; Santa Cruz Biotechnology, Inc.) was incubated with the cells at 37°C for 15 min before infection. Alternatively, cells were treated with 333 milliunits/mL of *Clostridium perfringens* neuraminidase type X (Sigma-Aldrich Co.) at 37°C for 30 min to remove cell surface sialic acid followed by two washes with PBS. Cells were then exposed to viruses at 37°C for 1 h. Unbound virus and blocking agents were washed away. After 24 h of incubation at 37°C, the cells were processed for luciferase assay as described previously. Subsequent procedures were the same as described previously.

Precision-cut human ovarian tumor slices. Following institutional review board approval, primary human ovarian tumors were obtained from newly diagnosed ovarian cancer patients who underwent debulking surgery as primary treatment. Precision-cut ovarian tumor slices were prepared using a Krumdieck tissue slicer (Alabama Research

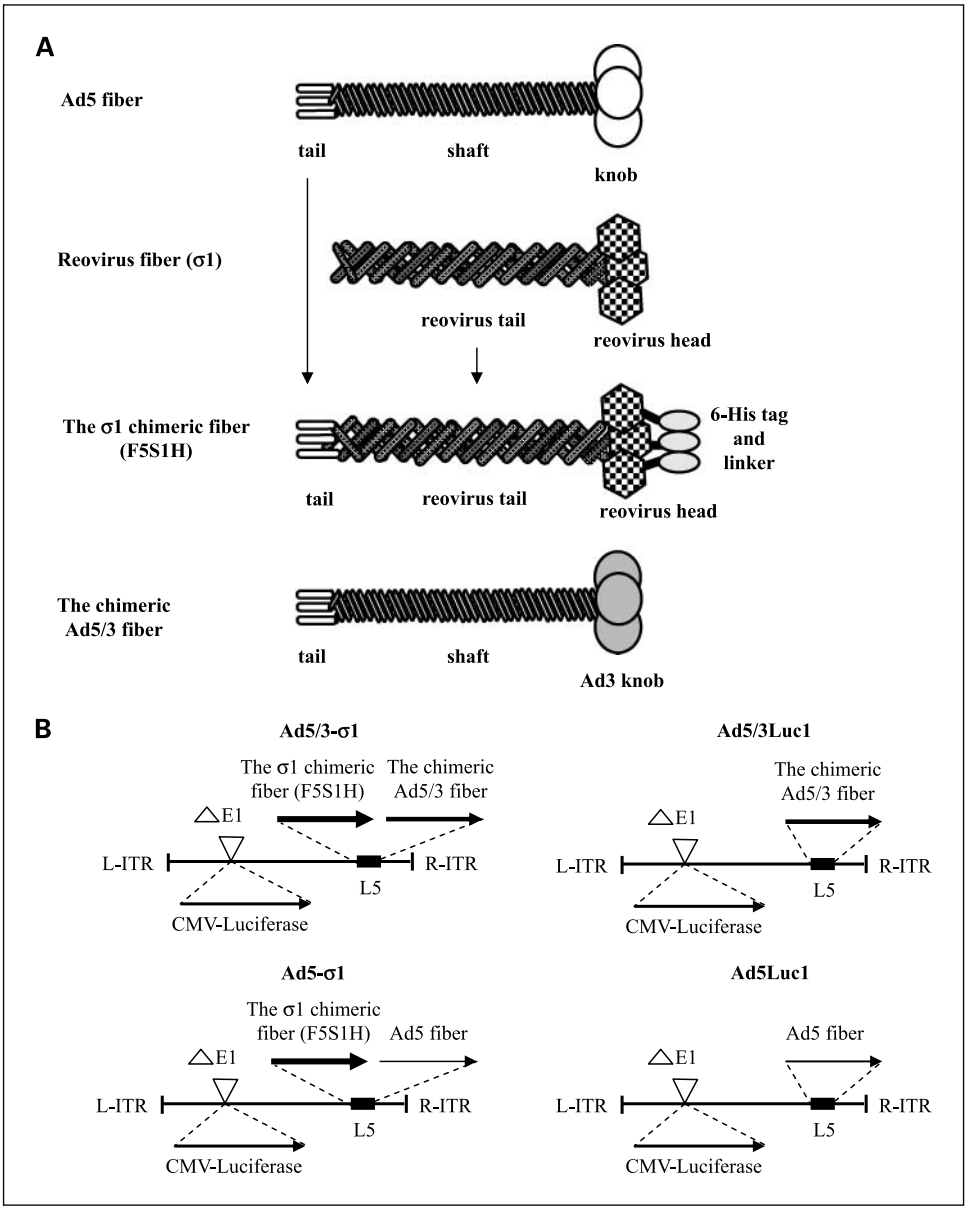

Fig. 1. Schema of mosaic fiber Ad5 genomes. *A,* key components of the σ1 chimeric fiber. In the σ1 chimeric fiber, the tail of Ad5 fiber is fused to the reovirus fiber protein σ1 and a 6-His tag is fused to the C-terminus of the σ1 chimeric fiber through a linker (designated *F5S1H*). *B,* map of Ad5 genomes with fiber modification. In all vectors, the E1 region is replaced by cytomegalovirus (*CMV*) promoter/luciferase transgene cassette. Ad5/3-σ1 is a mosaic fiber vector that carries the σ1 chimeric fiber with a C-terminal 6-His tag (F5S1H) as well as the chimeric Ad5/3 fiber. Ad5/3Luc1 is a control virus that carries the chimeric Ad5/3 fiber. Ad5-σ1 is a mosaic fiber vector that carries the σ1 chimeric fiber with a C-terminal 6-His tag (F5S1H) as well as the wild-type Ad5 fiber. Ad5Luc1 is a control virus that carries the wild-type Ad5 fiber.

and Development; ref. 7). The number of cells contained within each tissue slice was determined using the method of Kirby et al. using an estimation of 1×10^6 cells per slice based on a 10-cell thick slice (~ 250 μm) and 8-mm slice diameter (7).

Statistics. Data are presented as mean values ± SD. Student's *t* test was used for pairwise comparison. The difference is deemed statistically significant if $P < 0.05$.

Results

Construction of mosaic fiber viruses. To create a chimeric fiber structurally compatible with Ad5 capsid incorporation, the σ1 chimeric fiber (F5S1H) was designed to comprise the N-terminal tail segment of the Ad5 fiber sequence genetically fused to the entire serotype 3 Dearing σ1 protein, and a C-terminal 6-His tag was included as a detection marker (Fig. 1A; ref. 4). Our previous mosaic fiber virus (Ad5-σ1) contained tandem fiber genes, wherein the F5S1H σ1 chimeric fiber was positioned in front of the Ad5 wild-type fiber gene. We replaced the Ad5 wild-type fiber gene of the tandem fiber cassette with the genome of the chimeric Ad5/3 fiber containing the tail and shaft domains of adenovirus serotype5 and the knob domain of serotype 3 (9). Our current tandem fiber cassette contained tandem fiber genes, wherein the F5S1H σ1 chimeric fiber was positioned in front of the chimeric Ad5/3 fiber gene in the L5 region of the Ad5 genome (Fig. 1B). In this configuration, each fiber was positioned before the untranslated sequences of the wild-type fiber to provide equal transcription, splicing, polyadenylation, and regulation by the major late promoter. We constructed E1-deleted recombinant adenovirus genomes (Ad5/3-σ1) containing the σ1 chimeric fiber (F5S1H), the chimeric Ad5/3 fiber, and a firefly luciferase reporter gene controlled by the cytomegalovirus immediate early promoter/enhancer. Following virus rescue and large-scale propagation in 293 cells, we obtained Ad5/3-σ1 vector at concentrations of 6.48×10^{12} vp/mL. These concentrations compared favorably with that of Ad5Luc1 at

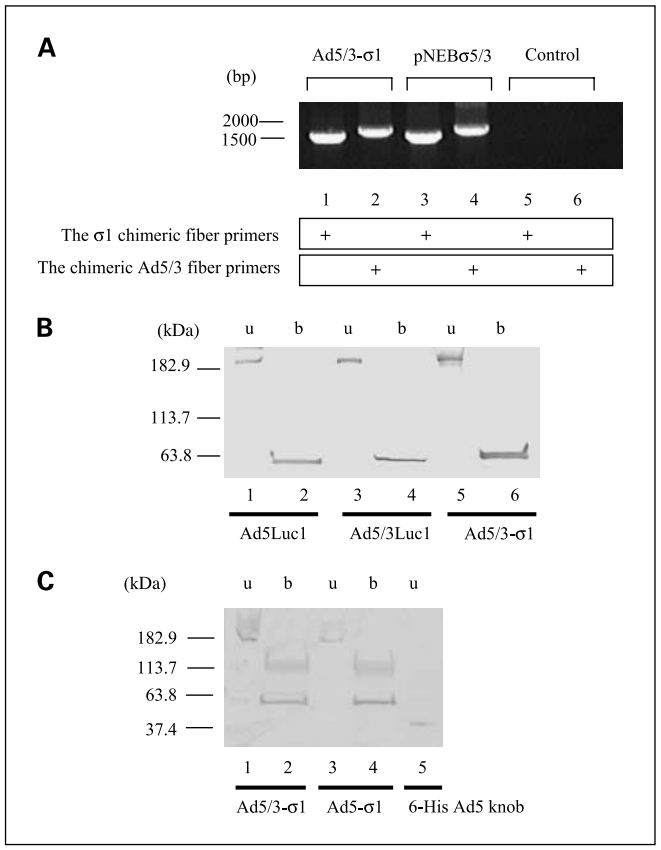

Fig. 2. Analysis of fibers in rescued vp. *A,* detection of fiber genes in the adenovirus genome. Rescued vp were analyzed with PCR using pairs of the σ1 chimeric fiber primers or the chimeric Ad5/3 fiber primers. pNEBσ5/3 was used as a positive control for both fibers. Absence of a PCR template was designated as the "Control." *B* and *C,* Western blot analysis of fiber proteins in purified virions. *B,* a total of 1.0×10^{10} vp per lane of Ad5Luc1 with the wild-type Ad5 fiber (*lanes 1* and *2*), Ad5/3Luc1 with the chimeric Ad5/3 fiber (*lanes 3* and *4*), or Ad5/3-σ1 with dual fibers (*lanes 5* and *6*) was resuspended in Laemmli buffer before SDS-PAGE, electrotransferred, and detected with the 4D2 anti-Ad5 fiber tail antibody. The samples in lanes 2, 4, and 6 were boiled (*b*), whereas lanes 1, 3, and 5 [unboiled (*u*)] contain proteins in their native trimeric configuration. *C,* a total of 1.0×10^{11} vp per lane of Ad5/3-σ1 (*lanes 1* and *2*) and Ad5-σ1 (*lanes 3* and *4*) with dual fibers was probed with an anti-6-His antibody. Lane 1, unboiled Ad5/3-σ1 virions; lane 2, boiled Ad5/3-σ1 virions; lane 3, unboiled Ad5-σ1 virions; lane 4, boiled Ad5-σ1 virions; lane 5, recombinant Ad5 knob with a 6-His tag as a positive antibody control. We consider the protein band appearing at ~113 kDa to be the dimeric form of the σ1 chimeric fiber.

3.74×10^{12} vp/mL, Ad5/3Luc1 at 8.7×10^{11} vp/mL, and Ad5-σ1 vector at 5.31×10^{12} vp/mL. In addition, the vp per plaque-forming unit ratios determined for Ad5/3-σ1, Ad5Luc1, Ad5/3Luc1, and Ad5-σ1 were 13.8, 13.3, 2.76, and 22, respectively, indicating excellent virion integrity for both species. Of note, the control vectors used throughout this study, Ad5Luc1 and Ad5/3Luc1 each contained one fiber and are isogenic to Ad5/3-σ1 in all respects, except for the fiber locus.

Definition of fiber gene configurations for mosaic fiber adenovirus. We confirmed the fiber genotype of Ad5/3-σ1 via diagnostic PCR using the σ1 chimeric fiber or the chimeric Ad5/3 fiber primer pairs and genomes from purified virions as PCR templates (Fig. 2A). To confirm that Ad5/3-σ1 virions contained both trimerized fibers, we did SDS-PAGE followed by Western blot analysis on vp. The 4D2 anti-Ad5 fiber tail monoclonal antibody (NeoMarkers) was used and fiber bands were observed at ~180 kDa for unboiled samples of Ad5Luc1, Ad5/3Luc1, and Ad5/3-σ1 virions, corresponding to fiber trimers (Fig. 2B, *lanes 1*, *3*, and *5*). In boiled samples, the 4D2 antibody detected bands of apparent molecular mass of ~60 kDa, indicative of fiber monomers (Fig. 2B, *lanes 2*, *4*, and *6*). The mosaic fiber viruses were difficult to resolve by Western blotting due to the near-identical sizes of the σ1 chimeric and the chimeric Ad5/3 fiber proteins.

To confirm the presence of the σ1 chimeric fiber protein in virions, we used the anti-Penta His monoclonal antibody (Qiagen, Inc.), which recognizes 6-His tags (Fig. 3C). Fiber bands corresponding to both trimeric and monomeric σ1 chimeric fiber protein were observed using the anti-Penta His antibody (Fig. 3C, *lanes 1* and *2*). These results confirm that the trimeric F5S1H σ1 chimeric fiber was incorporated into Ad5/3-σ1 virions.

The Ad5/3-σ1 vector exhibits sialic acid–dependent, JAM1-dependent, and Ad3 receptor–dependent tropism. Our hypothesis was that inclusion of both the σ1 chimeric fiber (F5S1H)

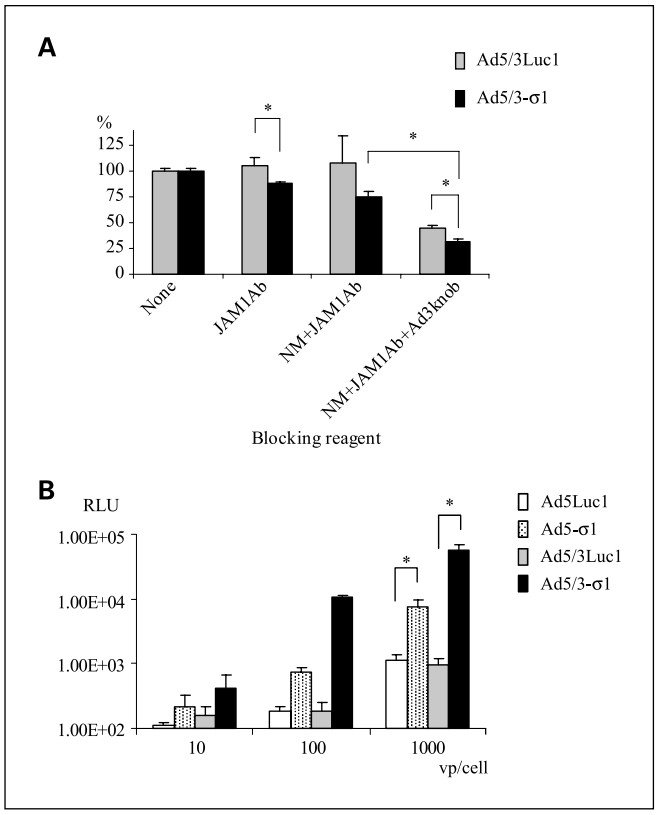

Fig. 3. Evaluation of the efficacy and receptor specificity of Ad5/3-σ1 – mediated gene transfer. *A,* analysis of Ad5/3-σ1 receptor usage in Hey cells. *C. perfringens* neuraminidase (*NM*), an anti-JAM1 antibody (*JAM1Ab*), and recombinant Ad3 fiber knob protein (*Ad3knob*) were used to block Ad5/3-σ1 infection. Hey cells were either untreated or treated with 100 μg/mL anti-JAM1 antibody, both an anti-JAM1 antibody and 333 milliunits/mL neuraminidase, or combined reagents with neuraminidase, anti-JAM1 antibody, and 50 μg/mL recombinant Ad3 fiber knob protein. Cells were incubated with 100 vp/cell of Ad5/3Luc1 (*gray column*) or Ad5/3-σ1 (*black column*) and harvested 24 h later for luciferase activity. All luciferase values were normalized against the activity of controls receiving no blocking treatment valued at 100%. Similar results were obtained in three independent experiments. Columns, average of four replicates; error bars, SD. *, $P < 0.05$, Student's *t* test. *B,* mouse fibroblast cells (L929) were incubated with Ad5Luc1 (*white column*), Ad5-σ1 (*dotted column*), Ad5/3Luc1 (*gray column*), or Ad5/3-σ1 (*black column*) at 10, 100, and 1,000 vp/cell. Luciferase activity was determined 24 h after infection and is expressed as relative light units (*RLU*). Columns, average of three replicates; error bars, SD. *, $P < 0.005$, Student's *t* test.

and the chimeric Ad5/3 fiber into an Ad5 vector would enhance infectivity of adenovirus-refractory cell types via expanding the vector tropism. To test the Ad5/3-σ1 tropism, we did neuraminidase treatment to remove cell surface sialic acid and competitive blocking experiments using an anti-JAM1 antibody or recombinant Ad3 knob protein. Ad5/3Luc1 was used as a positive control for the chimeric Ad5/3 fiber function. For this analysis, we used the low CAR-expressing human ovarian cancer cell line Hey due to its high sialic acid, JAM1, and Ad3 receptor expression (4). Transduction with Ad5/3-σ1 was inhibited by 12% using the anti-JAM1 antibody, which increased to 25% when combined with neuraminidase (Fig. 3A). Combined treatment with neuraminidase, anti-JAM1 antibody, and the Ad3 knob protein reduced transduction by 78% compared with controls receiving no blocking agent (Fig. 3A). Together, these data confirm that the Ad5/3-σ1 vector uses the sialic acid and JAM1-binding domains of the σ1 chimeric fiber (F5S1H), and the Ad3 receptor–binding domain of the chimeric Ad5/3 fiber for cell transduction. These findings indicate that Ad5/3-σ1 created sialic acid–dependent, JAM1-dependent, and Ad3 receptor–dependent tropism, confirming the functionality of the σ1 chimeric fiber (F5S1H) and the chimeric Ad5/3 fiber in our mosaic fiber Ad5.

Ad5/3-σ1 vector exhibits increased transduction of CAR-deficient cells. To determine the contribution of the σ1 chimeric fiber to the expanded adenovirus tropism, we evaluated Ad5/3-σ1 infectivity in L929 murine fibroblast cells that are commonly used for propagating reovirus. L929 cells express both the sialic acid and JAM1 σ1 receptors but no detectable CAR. As expected, Ad5/3-σ1 resulted in the maximum increase level of gene transfer (57-fold) relative to both Ad5Luc1 and Ad5/3Luc1 in L929 cells (Fig. 3B).

Ad5/3-σ1 vector exhibits increased transduction of low CAR ovarian cancer cells. In our previous study, we confirmed that the Hey, OV-4, ES-2, and OV-3 ovarian cancer cell lines were sialic acid/JAM1 positive but low CAR (4). Ad5/3-σ1 results in a 33-fold (OV-3) to 62-fold (Hey) increase in luciferase activity compared with Ad5Luc1. Luciferase activities were also enhanced in OV-4 (1.74-fold) and OV-3 (3.43-fold) cells using Ad5/3-σ1 compared with Ad5/3Luc1 (Fig. 4A). Many clinically relevant tissues are refractory to adenovirus infection, including ovarian cancer cells, due to negligible CAR levels (15). To more closely model the clinical situation with the most stringent substrate, we analyzed Ad5/3-σ1 transduction of primary human ovarian carcinoma cells. Importantly, Ad5/3-σ1 increased gene transfer to precision-cut ovarian cancer tissue slices from 1.7- to 59-fold versus Ad5Luc1 (Fig. 4B). Herein, we have outlined the construction, rescue, purification, and initial tropism characterization of a novel vector containing a nonadenovirus fiber molecule. Our results show that, in low CAR cells, Ad5/3-σ1 provides novel tropism and results in increased gene transfer rates compared with wild-type Ad5. This is accomplished using the reovirus coreceptors JAM1 and sialic acid in combination with the Ad3 receptor. The novel tropism of this vector represents a crucial attribute for adenovirus-based gene therapy vectors.

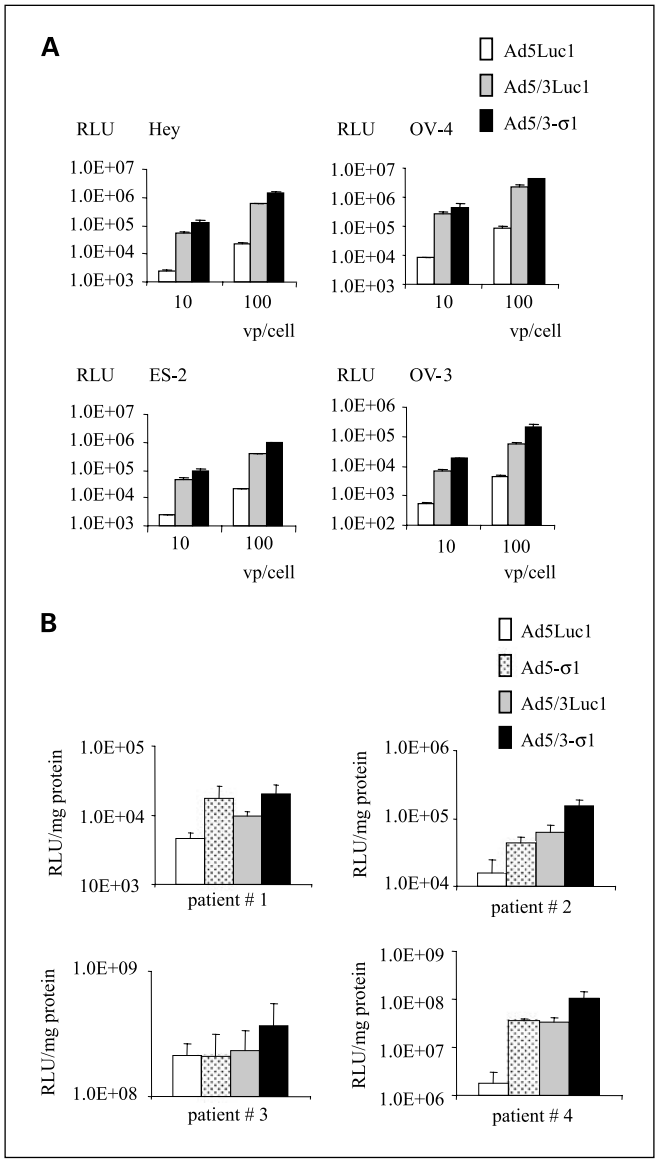

Fig. 4. Infectivity profiles of Ad5/3-σ1. *A,* representative ovarian cancer cell lines Hey, OV-4, ES-2, and OV-3 were infected with Ad5/3Luc1 (*gray column*) and Ad5/3-σ1 (*black column*) at 10 and 100 vp/cell. Luciferase activity was measured 24 h after infection and is expressed as relative light units. Columns, mean of three experiments; error bars, SD. *B,* human tumor slices of ovarian cancer patient were infected with Ad5Luc1 (*white column*), Ad5-σ1 (*dotted column*), Ad5/3Luc1 (*gray column*), or Ad5/3-σ1 (*black column*) at 100 vp/cell. Luciferase activity was measured 24 h after infection and is expressed as relative light units/mg protein. Columns, mean of four experiments; error bars, SD.

Discussion

One strategy to enhance the therapeutic potential of Ad5-based vectors has been to alter the native tropism toward non-CAR receptors that are abundant on the surface of primary tumor cells. Variable and/or low expression of CAR has been documented in many cancer cell types, including glioma, rhabdomyosarcoma, and ovarian cancer (16–18). We have reported that a mosaic fiber Ad5 vector provided viral entry via two different pathways with additive gains in infectivity in a variety of cell types (4). In this study, we evaluated the use of a mosaic fiber Ad5 vector that uses both the Ad3 and serotype 3 Dearing reovirus receptors, which are independent of native Ad5 tropism. This vector was based on our previously reported mosaic fiber Ad5 vector that incorporates two distinct fibers: the Ad5 fiber and a reovirus chimeric fiber. The current mosaic fiber Ad5 vector was generated by substituting the Ad3 knob in

place of the Ad5 knob domain. We constructed an Ad5 genome using a tandem fiber cassette, which resulted in an Ad5 vector that expressed both the Ad5/3 and σ1 chimeric fibers. We confirmed that these virions incorporated both fibers by Western blot analysis and by the functional ability of both fibers to use the appropriate receptor(s) for viral transduction. This is the first vector that contains non–CAR-binding fibers from two different virus families to replace Ad5 tropism.

We further confirmed that the addition of the σ1 chimeric fiber contributed to augmentation of gene transfer compared with adenovirus vectors with single fiber in cells lacking the Ad5 and Ad3 receptors. Ad5/3-σ1 provided a 57-fold increase in gene transfer relative to the wild-type fiber control virus, the Ad5Luc1, and the single Ad5/3 fiber control virus, Ad5/3Luc1, in L929 cells that lack Ad5 and Ad3 receptor expression.

Consistent with our hypothesis of enhanced infectivity, we observed augmented gene transfer with Ad5/3-σ1 in all ovarian cancer cell lines tested, ranging from 33-fold to 62-fold, when compared with the wild-type fiber control virus. However, compared with Ad5/3Luc1, augmented gene transfer on the same cell lines was modest, ranging from 1.74-fold to 3.43-fold.

Our thin-slice tissue culture is an ideal method for preclinical *ex vivo* infectivity analysis because it allows evaluation of adenovirus in primary tumors derived from cancer patients (7). Importantly, the enhanced infectivity of the Ad5/3-σ1 virus was observed on more stringent clinical substrates, human primary ovarian tumor tissue slices, although the augmentation of gene transfer was variable, ranging from 1.7-fold to 59-fold. This variability in augmentation was likely due to differential receptor expression between tumors from different patients. Clearly, it would be of interest to directly correlate receptor expression with the degree of infectivity in clinical specimens. Unfortunately, this was not possible with the samples studied here because the whole tumor specimen was necessary for analysis of infectivity enhancement. However, we have shown a positive correlation between primary receptor density, infectivity, and oncolysis in our previous studies (16, 19–23).

There are two possible explanations for the modest level of Ad5/3-σ1 gene transfer compared with the single Ad5/3 fiber control virus Ad5/3Luc1. At first, it may be due to reduced levels of the σ1 chimeric fiber incorporation compared with the chimeric Ad5/3 fiber in mosaic fiber Ad5 particles. We previously confirmed that both 4D2 anti-Ad5 tail antibody and 6-His antibody detect fibers with similar band intensity in Western blot when equal numbers of vp are loaded. Figure 2B and C shows the presence of both fibers in Ad5/3-σ1 virions. However, to detect the σ1 chimeric fiber in our mosaic fiber Ad5 vector with the 6-His antibody, we had to load 10 times the number of vp compared with the chimeric Ad5/3 fiber as detected by using 4D2 anti-Ad5 tail antibody. This result suggests that incorporation of the σ1 chimeric fiber is decreased compared with the chimeric Ad5/3 fiber on Ad5/3-σ1. This could explain the limited additivity of transductional efficiency by the σ1 chimeric fiber in ovarian cancer cells even when JAM1 or sialic acid is expressed. We have previously investigated a series of mosaic fiber adenoviruses that possess two genetically distinct fibers from different origins (13). Although the ratio of virion-incorporated fibers varies, both fiber properties have been functionally confirmed in each mosaic fiber adenovirus. A second explanation is that the Ad3 receptor is widely expressed on ovarian cancer cell surfaces of epithelial origin, and the chimeric Ad5/3 fiber in the Ad5/3-σ1 vector was used preferentially, minimizing the role of the σ1 chimeric fiber in these cells (16).

In a clinical setting of ovarian cancer, adenovirus-based vectors might be administered i.p. It would therefore be critical that vector used in this manner has decreased tropism for normal mesothelial cells or liver. We have not yet evaluated the Ad5/3-σ1 vector in an *in vivo* model of peritoneal administration. In this regard, however, our group has previously investigated the infectious properties *in vivo* of an adenovirus expressing a single Ad5/3 fiber (21). We showed that Ad5/3Luc1 had higher transgene expression but fewer virus copies in the liver and less transgene expression in peritoneum in comparison with Ad5Luc1 via i.p. administration into tumor-bearing mice. Additionally, histologic studies revealed that serotype 3 Dearing reovirus infection *in vivo* was restricted to tumor cells, whereas the surrounding normal tissue remained uninfected (24). Considering these facts, we fully expect that the Ad5/3-σ1 vector will not have increased tissue tropism for liver or other normal tissues.

Thus, we have used the "fiber mosaicism" concept, the use of two separate fibers with distinct receptor recognition, to combine the use of multiple receptors to enhance viral infectivity (4). In this study, the mosaic fiber Ad5/3-σ1 vector provided enhanced infectivity in low CAR-expressing ovarian cancer cell lines. This was the result of multiple non-CAR receptor-binding properties provided by the fiber elements of different virus families. Adenovirus gene therapy vectors with CAR-independent tropism may prove valuable for maximal transduction of low CAR-expressing tumors using minimal vector doses. Furthermore, this study used a preclinical assay that involved primary human ovarian tumor tissue to evaluate the mosaic fiber adenovirus vectors and proved further evidence of a preclinical screening strategy for examining improved gene therapy agents.

Acknowledgments

We thank Dr. Victor Krasnykh for providing plasmids pVK700, pNEB.PK.F5/3, and pNEB.PK.3.6 and Dr. Justin C. Roth for his critical reading of the manuscript.

References

1. Gomez-Navarro J, Curiel DT, Douglas JT. Gene therapy for cancer. Eur J Cancer 1999;35:867–85.
2. Krasnykh V, Dmitriev I, Navarro JG, et al. Advanced generation adenoviral vectors possess augmented gene transfer efficiency based upon coxsackie adenovirus receptor-independent cellular entry capacity. Cancer Res 2000;60:6784–7.
3. Glasgow JN, Bauerschmitz GJ, Curiel DT, Hemminski A. Transductional and transcriptional targeting of adenovirus for clinical applications. Curr Gene Ther 2004; 4:1–14.
4. Tsuruta Y, Pereboeva L, Glasgow JN, et al. Reovirus σ1 fiber incorporated into adenovirus serotype 5 enhances infectivity via a CAR-independent pathway. Biochem Biophys Res Commun 2005;335:205–14.
5. Barton ES, Forrest JC, Connolly JL, et al. Junction adhesion molecule is a receptor for reovirus. Cell 2001;104:441–51.
6. Chappell JD, Gunn VL, Wetzel JD, Baer GS, Dermody TS. Mutations in type 3 reovirus that determine binding to sialic acid are contained in the fibrous tail domain of viral attachment protein σ1. J Virol 1997;71: 1834–41.
7. Kirby TO, Rivera A, Rein D, et al. A novel *ex vivo* model system for evaluation of conditionally replicative adenoviruses therapeutic efficacy and toxicity. Clin Cancer Res 2004;10:8697–703.

8. Krumdieck CL, dos Santos JE, Ho KJ. A new instrument for the rapid preparation of tissue slices. Anal Biochem 1980;104:118–23.
9. Krasnykh VN, Mikheeva GV, Douglas JT, Curiel DT. Generation of recombinant adenovirus vectors with modified fibers for altering viral tropism. J Virol 1996; 70:6839–46.
10. Belousova N, Krendelchtchikova V, Curiel DT, Krasnykh V. Modulation of adenovirus vector tropism via incorporation of polypeptide ligands into the fiber protein. J Virol 2002;76:8621–31.
11. Graham F, Prevec L. Manipulation of adenovirus vectors. In: Murray EJ, Walker JM, editors. Methods in molecular biology. Clifton (NJ): Humana Press; 1991. p. 109–28.
12. Maizel JV, Jr., White DO, Scharff MD. The polypeptides of adenovirus. I. Evidence for multiple protein components in the virion and a comparison of types 2, 7A, and 12. Virology 1968;36:115–25.
13. Pereboeva L, Komarova S, Mahasreshti PJ, Curiel DT. Fiber-mosaic adenovirus as a novel approach to design genetically modified adenoviral vectors. Virus Res 2004;105:35–46.
14. Breidenbach M, Rein DT, Schondorf T, et al. A new targeting approach for breast cancer gene therapy using the heparanase promoter. Cancer Lett 2006; 240:114–22.
15. Kelly FJ, Miller CR, Buchsbaum DJ, et al. Selectivity of TAG-72-targeted adenovirus gene transfer to primary ovarian carcinoma cells versus autologous mesothelial cells *in vitro*. Clin Cancer Res 2000;6: 4323–33.
16. Kanerva A, Mikheeva GV, Krasnykh V, et al. Targeting adenovirus to the serotype 3 receptor increases gene transfer efficiency to ovarian cancer cells. Clin Cancer Res 2002;8:275–80.
17. Kim M, Sumerel LA, Belousova N, et al. The coxsackievirus and adenovirus receptor acts as a tumour suppressor in malignant glioma cells. Br J Cancer 2003;88:1411–6.
18. Cripe TP, Dunphy EJ, Holub AD, et al. Fiber knob modifications overcome low, heterogeneous expression of the coxsackievirus-adenovirus receptor that limits adenovirus gene transfer and oncolysis for human rhabdomyosarcoma cells. Cancer Res 2001;61: 2953–60.
19. Yamamoto M, Davydova J, Wang M, et al. Infectivity enhanced, cyclooxygenase-2 promoter-based conditionally replicative adenovirus for pancreatic cancer. Gastroenterology 2003;125:1203–18.
20. Kanerva A, Zinn KR, Chaudhuri TR, et al. Enhanced therapeutic efficacy for ovarian cancer with a serotype 3 receptor-targeted oncolytic adenovirus. Mol Ther 2003;8:449–58.
21. Kanerva A, Wang M, Bauerschmitz GJ, et al. Gene transfer to ovarian cancer versus normal tissues with fiber-modified adenoviruses. Mol Ther 2002;5:695–704.
22. Douglas JT, Kim M, Sumerel LA, Carey DE, Curiel DT. Efficient oncolysis by a replicating adenovirus (ad) *in vivo* is critically dependent on tumor expression of primary ad receptors. Cancer Res 2001;61: 813–7.
23. Hemminki A, Dmitriev I, Liu B, Desmond RA, Alemany R, Curiel DT. Targeting oncolytic adenoviral agents to the epidermal growth factor pathway with a secretory fusion molecule. Cancer Res 2001;61: 6377–81.
24. Hirasawa K, Nishikawa SG, Norman KL, Alain T, Kossakowska A, Lee PW. Oncolytic reovirus against ovarian and colon cancer. Cancer Res 2002;62: 1696–701.

Nature Reviews Genetics | AOP, published online 3 July 2007; doi:10.1038/nrg2141

Engineering targeted viral vectors for gene therapy

Reinhard Waehler, Stephen J. Russell and David T. Curiel

Abstract | To achieve therapeutic success, transfer vehicles for gene therapy must be capable of transducing target cells while avoiding impact on non-target cells. Despite the high transduction efficiency of viral vectors, their tropism frequently does not match the therapeutic need. In the past, this lack of appropriate targeting allowed only partial exploitation of the great potential of gene therapy. Substantial progress in modifying viral vectors using diverse techniques now allows targeting to many cell types *in vitro*. Although important challenges remain for *in vivo* applications, the first clinical trials with targeted vectors have already begun to take place.

Tropism
Affinity of a virus or vector for a particular tissue and cell type.

Despite the remarkable preclinical success of gene therapy, its clinical applications remain limited[1–3]. Clinical trials have been crucial for highlighting the main challenges, one of which is the high cost of vector production. Another challenge relates to vector targeting: to achieve successful gene therapy, the appropriate genes must be delivered to and expressed in target cells, without harming non-target cells. One approach is to use promoters that are active only in the target cell (transcriptional targeting; for a review, see REF. 4). Although this strategy can reduce or even eliminate potential toxic side effects of the transgene, it does not address the need to avoid those that result from the mislocalization of vector particles. Furthermore, transcriptional targeting alone is not sufficient to ensure gene expression in the target cell, which also requires efficient introduction of the therapeutic nucleic acid into the correct cells.

The development of technologies that allow targeting of specific cells has progressed substantially in recent years for several types of vectors, particularly viral vectors, which have been used in 70% of gene therapy clinical trials as of January 2007 (REF. 5). Non-viral gene therapy, although promising, presents greater challenges with regard to gene-transfer efficiency (these approaches are discussed in REFS 6,7). This reflects the vast time that viruses have had to evolve naturally into efficient gene-transfer vehicles (FIG. 1). Building on this advantage, many groups are currently working towards improving the features of viral vectors for gene therapy purposes.

One major technical challenge in facilitating the efficient infection of the correct cells by viral vectors — known as transductional targeting — is that the native tropism of the virus often does not meet the therapeutic need. To avoid toxic side effects, the natural tropism of the vector must often be ablated or diminished. The vector might also need to be engineered to infect target cells that it does not infect naturally. If target cells are easily isolated from the patient (for example, from the blood or bone marrow) and re-transferred, *ex vivo* gene transfer might be ideal, and broadening of the vector tropism might be advantageous. Alternatively, a local application might be sufficient (for example, for a locally restricted tumour or a small organ such as the eye) and, depending on the possible side effects of gene transfer to local non-target cells, broadening or narrowing the tropism might be required. Finally, systemic treatment might be necessary, for example, to reach disseminated metastases or a large number of somatic cells to correct a genetic defect. In this situation, the tropism must be narrowed down to the target cells only.

Here we discuss new approaches aimed at improving viral vector targeting, focusing mainly on systemic targeting, which promises ease of application and great therapeutic returns. There are several obstacles that need to be overcome in order for a systematically applied vector to reach its target cells (BOX 1). The challenge that has been most widely studied, and on which we focus here, is the final step of infecting the target cell. To accomplish this, the vector must display a suitable ligand to bind a target-cell receptor. The natural tropism of some viruses matches their vector utility, as is the case for the herpes virus, which can be used for neuronal gene delivery[8], but in many cases the vector must be engineered to have a new tropism. This final obstacle to targeting has received

Division of Human Gene Therapy, 502 Biomedical Research Building II, 901 19th Street, South Birmingham, Alabama 35294-2172, USA.
Correspondence to D.T.C.
e-mail: curiel@uab.edu
doi:10.1038/nrg2141
Published online 3 July 2007

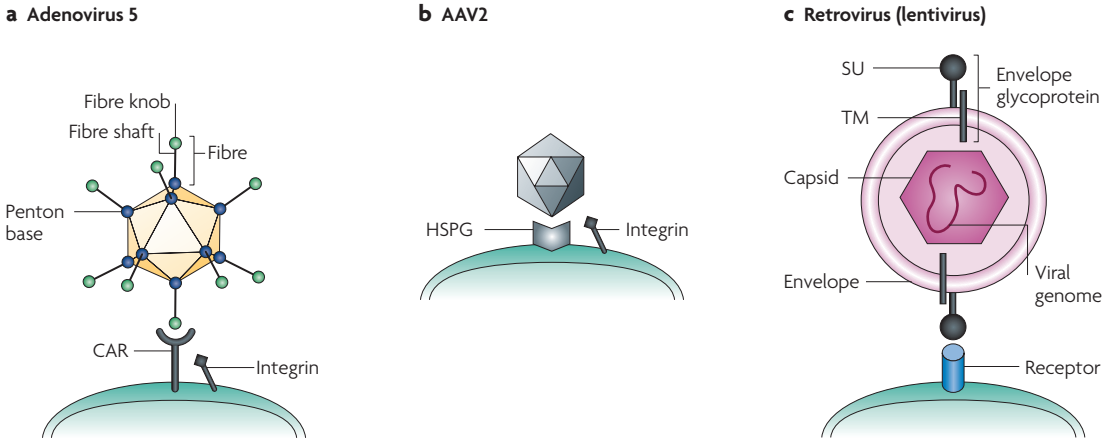

Figure 1 | **Native entry mechanisms of unmodified viral vectors. a** | Adenovirus (Ad). Ad serotype 5 binds to its receptor CAR (coxsackie and adenovirus receptor) through its fibre knob. Subsequently, integrins interact with the RGD peptide motif in the penton base (the capsid protein at the base of the fibre) and facilitate cell entry by endocytosis[138]. **b** | Adeno-associated virus (AAV). Several basic residues of the AAV2 (adeno-associated virus serotype 2) capsid protein VP3 (especially positions R585 and R588) are involved in heparin binding. AAV2 first binds to heparan-sulphate proteoglycan (HSPG)[139] and then to the co-receptor, which can be either an integrin (shown here), human fibroblast growth factor receptor or hepatocyte growth factor receptor. The virus is internalized by endocytosis. Other AAV serotypes either resemble AAV2 in its heparin binding (such as AAV3 and AAV6), or use different primary receptors (for example, sialic acid for AAV4 and AAV5)[140]. **c** | Retrovirus (lentivirus): Membrane fusion is the main mechanism whereby enveloped viruses deliver their genomes into target cells[141]. After initial nonspecific adhesion of the virus to the cell surface[142], viral attachment glycoproteins bind specifically to their cognate receptors, whereupon binding becomes irreversible. The host range of retroviral vectors is determined by the interaction of the viral envelope protein (Env) and the cellular receptor[143]. Subsequent steps in the viral entry process vary between different viruses but always result in fusion between the lipid membranes of the virus and the host cell, following which the viral nucleocapsid is released into the cytoplasm[144]. In some cases, receptor binding triggers conformational changes in the viral proteins that mediate membrane fusion. In others, the cell-bound virus is transported by its receptor into an endosomal compartment where a reduction in pH triggers a conformational rearrangement of the viral fusion machinery. SU, surface subunit; TM, transmembrane subunit.

the most attention from researchers, mainly owing to the fact that its study has been easier because of the availablity of *in vitro* models (BOX 2), unlike the other obstacles that are discussed in BOX 1.

Most progress in vector development has been achieved using adenovirus (Ad), adeno-associated virus (AAV) and vectors that are derived from retroviruses, particularly lentiviruses (TABLE 1). The technical hurdles that must be overcome in developing effective therapeutic systems are similar for most viral vector systems; so, methods to enhance one vector system often have general relevance. Here we discuss the main approaches that have been applied to vector targeting, and outline the important challenges that need to be addressed in order for gene therapy using viral vectors to reach widespread clinical application.

Vector targeting by pseudotyping

Pseudotyping, which was the first method used to alter viral vector tropism, involves transferring viral attachment proteins either between strains within a family of viruses or between virus families (FIG. 2; TABLE 2). Pseudotyping can be achieved by co-transfection of plasmids, with one encoding the attachment protein to be pseudotyped and separate plasmids encoding all other vector components. This approach is used routinely to pseudotype AAV and retroviral or lentiviral vectors. Alternatively, the viral attachment protein can be expressed in *trans* from the production cell line, or genetically incorporated into the viral genome, an approach that is particularly well suited to the generation of adenovirus pseudotypes.

Pseudotyping of enveloped vectors. Pseudotyping has been used most extensively to modulate the host-cell tropisms of retroviral (including lentiviral) vectors because they are highly permissive for incorporation of heterologous attachment glycoproteins[9,10]. The most widely used retroviral vector pseudotypes are those that incorporate the attachment glycoprotein of the vesicular stomatitis virus (VSV-G)[11], which both allows the production of high-titre vector stocks and confers a broad host range. The list of other foreign envelope glycoproteins that have been incorporated into lentiviral vectors is long, including representatives from several virus families. These pseudotypes show large differences in their relative transduction efficiencies for different tissues. Notable *in vivo* findings include the high efficiencies of neural tissue transduction by lyssavirus pseudotypes (the rabies and Mokola viruses)[9] and efficient transduction of airway epithelium by filovirus (Ebola Zaire)[9] or paramyxovirus (Sendai) pseudotypes[12]. If lentiviral gene transfer gains broader acceptance as a clinically viable vector system, these vectors could be used to explore gene therapies for Parkinson disease and cystic fibrosis, respectively.

Pseudotyping
Changing the tropism of a virus by replacing the viral attachment protein with that of a related virus.

Viral attachment protein
A protein that is part of the virus or vector and can bind the cellular receptor.

Box 1 | **Obstacles to systemic targeting**

Many of the obstacles to systemic delivery have been studied most thoroughly for adenovirus (Ad), and still need to be addressed in other systems in terms of their impact and how they might be overcome. However, the areas discussed below are likely to be relevant to all vectors.

The first potential hurdles for a vector are found in the form of the immune system and other factors in the blood circulatory system. Reactions with the complement system[99,100] and pre-existing antibodies[101,102] (either naturally occurring or from previous vector applications) can impede the vector in reaching its target. Coating Ad vectors with polyethylene glycol (PEG) can help to escape both the antibody-mediated and innate immune responses, but should be combined with targeting as this modification can otherwise reduce the efficiency of gene transfer[29,103]. Blood factors (for example, coagulation factor IX and complement protein C4BP) can bind the adenoviral fibre and redirect the virus from the bloodstream into the liver via uptake through heparan-sulphate proteoglycans and LDL-receptor-related protein[104,105]. Furthermore, Ad can interact with human blood cells (erythrocytes, neutrophils and monocytes), which can prevent the vector from reaching its target[106]. Serotype switching and modifications of capsid proteins may circumvent such interactions.

The next hurdle is the endothelial cell layer: the vector must exit the bloodstream at the right tissue, move beyond the endothelial cell lining, and transduce the target cells. Some vascular beds are accessible for vector exit (for example, Ad can exit into the liver)[107], and some vectors naturally possess mechanisms to allow transcytosis beyond the endothelium (for example, some AAV subtypes[90] and HIV[108] can cross certain monolayers). However, in most cases the vascular bed presents a barrier and the vector is unable to cross the endothelium[109], necessitating vector modification. Engineering the ability to undergo transcytosis is one potential mechanism to achieve this transition; another method involves the use of cellular vehicles (such as stem cells) to carry the vector and home in to the target tissue[110,111]. Cellular vehicles might be especially helpful if one needs to overcome an extracellular matrix that separates the target cells (for example, tumour cells) from the endothelium[112]. After entering the correct target tissue, the final step for the vector is to infect the target cell (FIG. 1), as discussed in detail in the main text.

Additional obstacles can exist when tumours are targeted. Despite the fact that lesions are accessible on systemic treatment in some experimental models[23], such models do not fully recapitulate a clinical scenario. Frequently, tumour-cell islets can be surrounded by a basal-membrane-like structure within stromal cells. In one animal model, blood vessels were observed to be in direct contact with only the stromal cells[113]. The vector would need to cross the stroma and the basal-membrane-like structure to reach the tumour. It might be possible to overcome these obstacles using stem cells carrying the vector or by first targeting the surrounding area of the tumour to weaken stroma- and basal-membrane-like structures (for example, with matrix metalloproteinases) and then targeting the tumour. However, targeting of the tumour environment might be sufficient for a therapeutic effect, at least in some cases[114].

Unfortunately, the specificities of naturally occurring viral attachment proteins frequently do not coincide with those that are required for targeted gene delivery. In response to this, several encouraging studies have demonstrated the feasibility of pseudotyping retroviral vectors with chimeric envelope glycoproteins from Sindbis viruses and gammaretroviruses that have been genetically engineered to incorporate polypeptide ligands that direct targeting to specific cell types[9,13,14] (see later for a detailed discussion of the genetic incorporation of targeting ligands into viruses). As for many retroviral targeting approaches, however, accuracy often comes at the price of low gene-transfer efficiency via the targeted receptors, and optimizing the efficiency of targeted gene transfer will be needed to justify clinical testing.

The concept of pseudotyping has recently been extended to the incorporation of host-cell viral receptors (CD4 and CXCR4 or CCR5) into viral envelopes for targeted entry into HIV-infected cells. Feasibility was demonstrated using a replication-competent rhabdovirus (VSV) and non-replicating lentiviral or murine leukaemia virus (MLV) vectors to mediate the targeted destruction of HIV-infected cells by redirecting them to use the HIV-derived glycoprotein HIVgp120 as a receptor[15–17]. However, the efficiency of targeted entry into HIV-infected cells was low, for reasons that are not understood.

Pseudotyping of non-enveloped vectors. Pseudotyping has also been used for non-enveloped vectors, including AAV and adenovirus. An important challenge here is that the viral attachment protein must be incorporated into a protein capsid instead of a lipid bilayer. This has mainly been achieved by substituting coat proteins with homologous proteins of other related serotypes, giving rise to a new tropism without changing the rest of the genome and thus enabling the use of established cloning systems that have been developed for the previous serotype. It is also possible to incorporate the coat proteins of unrelated viruses, although structural incompatibility can preclude this. For example, on the basis of the structural similarities of the trimeric Ad fibre and the trimeric reovirus attachment protein σ1, a chimeric fibre–σ1 protein was introduced into the Ad capsid by modifying the Ad genome, enabling efficient infection of primary dendritic cells and intestinal epithelial cells[18]. In cases in which structural incompatibilities hinder incorporation of the desired part of the foreign viral attachment protein, artificial fibre molecules can be used. For example, these have been exploited for fusing single-chain variable fragment (scFv) antibodies to the Ad vector[19].

Combining prokaryotic and eukaryotic vectors. Current eukaryotic viral vectors can infect cells with high efficiency, but they have the disadvantage that their native tropism must be ablated to achieve ligand-directed targeting upon systemic administration. Prokaryotic viruses infect mammalian cells with a low efficiency at best, but can be adapted to bind mammalian receptors by genetically engineering a eukaryotic ligand into their capsid. For example, one study reported the construction of a hybrid vector that comprises an AAV cassette inserted in the phage genome and that targets α_v integrins through an Arg-Gly-Asp (RGD-4C) peptide motif that is displayed on the phage capsid[20]. Following systemic application in nude mice, this vector showed specific targeting to tumours derived from injection of human prostate cancer cells, and tumour shrinkage was achieved when a therapeutic transgene was introduced into the vector. Monitoring the biodistribution of the vectors in this study was facilitated using *in vivo* vector imaging (BOX 3). Remarkably, the chimeric vector was also highly effective for anti-tumour therapy in the context of immunocompetent mice, even following prior phage vaccination and high anti-phage antibody titres. A similar strategy could be used for other vectors with double-stranded genomes, such as adenoviruses.

Vascular bed
An intricate network of minute blood vessels that extends through the tissues of the body or one of its parts.

Gammaretroviruses
Simple viruses that are characterized by a C-type morphology; this genus has the most members in the retroviruses family, including murine leukaemia viruses, feline leukaemia viruses and the gibbon ape leukaemia virus.

Serotypes
Antigenically distinct forms of microorganisms, including viruses, that elicit different antibody responses by the immune system.

Adenoviral fibre
The attachment protein of an adenoviral vector.

Primary-tumour spheroids
A three-dimensional aggregate of purified and unpassaged cancer cells.

Oncolytic
An agent that induces lysis of tumour cells.

Vector targeting using adaptors

Pseudotyping is limited by the number of viral attachment proteins for which receptors are expressed exclusively and abundantly on target cells of interest. Genetic modifications that can overcome this limitation require structural knowledge to guide modification of the viral attachment protein — knowledge that is only just becoming available. The use of adaptor proteins, which can be applied even with a limited knowledge of the viral structure, has been explored as an alternative. Adaptors are molecules with dual specificities: one end binds the viral attachment protein and the other binds the receptor on the target cell. The advantages of this approach are its great flexibility, as different adaptors can readily be coupled to the same vector, and the fact that it does not require changes in vector structure that could be detrimental to vector production or gene transfer. Most adaptors can achieve the two main goals of targeted delivery: ablating native tropism and conferring a novel tropism towards the desired target. Adaptor systems have proved particularly useful for proof-of-principle preclinical studies, allowing easy testing of several target receptors[21].

Receptor–ligand complexes. Receptor–ligand complexes are an important class of adaptors that exploit native viral tropisms and are widely used for retargeting vectors. The viral receptor is genetically fused to the ligand of a receptor that is expressed on the target cell. For example, fusing the ectodomain of the adenovirus receptor (coxsackie and adenovirus receptor; CAR) with CD40L (the ligand for the CD40 receptor on dendritic cells) through a trimerization motif successfully targeted Ad vectors to dendritic cells with more than four orders of magnitude higher efficiency than untargeted Ad vectors[22] (FIG. 2Ba). Fusing the ectodomain of CAR to a single-chain antibody against human carcinoembryonic antigen (CEA) allowed vector targeting to subcutaneous tumours as well as hepatic metastases of colon cancer in nude mice, while simultaneously ablating liver tropism[23].

The same principle has been applied for retroviral vectors. A fusion of the extracellular domain of the avian sarcoma and leukaemia virus (ASLV) retroviral receptor (tumour virus subgroup A receptor; TVA) to heregulin-β1 successfully targeted the vector to cells expressing heregulin receptors[24], providing a potential therapeutic strategy for the treatment of various malignancies. Adaptors that incorporate the ASLV receptor as the virus-binding moiety have been explored in particular, as they can trigger conformational changes in the ASLV envelope glycoprotein that are required for membrane fusion and virus entry.

In another important example, this type of targeting has been achieved for one of the coronaviruses (a class of enveloped RNA viruses), which are potential oncolytic agents. The tropism of a replication-competent coronavirus, mouse hepatitis virus (MHV), was recently retargeted by engineering the viral genome to express an adaptor protein that consisted of part of the natural cellular receptor of MHV and a targeting peptide, allowing multiround infection and killing of target cells[25].

Altogether, the receptor–ligand approach shows promise for use in a range of preclinical studies. However, for clinical applications, other targeting methods (such as genetic targeting, discussed below) might be preferable because of the potential risk that the adaptor could dissociate from the vector.

Chemical conjugation. Chemical conjugation is a method for coupling adaptors to vectors in which the targeting ligand is covalently linked to the vector. Polyethylene glycol (PEG) and PEG-derived polymers have been used to couple Ad vectors to ligands such as fibroblast growth factor 2, which was used to target ovarian cancer cells[26]. Endothelial cells have also been targeted using this approach, by coupling the Ad vector to PEG and then

Box 2 | Model systems for evaluating vector targeting

Cell-culture systems. The first step in evaluating the targeting capabilities of a vector is usually testing in cell lines. However, this has limited predictive value for *in vivo* scenarios (for example, cell lines can overexpress viral receptors relative to more clinically relevant primary cells[115]). Two-dimensional cell-culture systems are also limited in their predictive value as they usually represent only one or two cell types, and are grown on an artificial surface in an artificial two-dimensional context. As a first step towards three-dimensional culture, primary-tumour spheroids have been used to evaluate targeted Ad vectors. The vectors that were tested were replication competent in tumour cells and showed gradual penetration of the spheroids[116]. However, these spheroids were almost exclusively composed of tumour cells whereas, within a naturally occurring tumour, therapeutic effects can be modified by the presence of stromal cells and the extracellular matrix.

Another drawback of two-dimensional culture systems for assessing anti-cancer gene therapy mediated by viral vectors is that possible toxic effects on stromal cells cannot be evaluated. Three-dimensional cell-culture models can include endothelial cells, fibroblasts, immunocompetent cells and extracellular matrix. Although they are currently expensive, three-dimensional scaffolds provide a promising system to emulate the native structure of living tissue[117] and could become a valuable tool for vector testing.

Tissue explants. The next step up in sophistication for model systems is the use of tissue explants. For example, tissue-slice systems can be used to evaluate targeting to any tissue. Although such systems do not directly resemble systemic administration, valuable data concerning the transduction of target and non-target tissues can be easily obtained. These systems have been available for different applications for some time, but their implementation in targeting studies is recent. In one example, this approach was used to analyse targeted Ad vector transduction of breast tumour and liver cells[71]. Another tissue explant model is represented by the human skin substrate system. Plastic surgery frequently yields skin that can be used *ex vivo* to evaluate vector targeting. This model has recently proved its potential usefulness for gene therapy assessment in the context of an Ad vector targeted to dendritic cells[118].

Animal models. Although their circulatory system is comparable to humans, animal models have limitations with respect to evaluating transductional targeting. For example, they do not express human receptors and, in the case of xenotransplantation models in cancer research, they lack a complete immune system. New immunocompetent transgenic mouse models that express human receptors are being developed for the evaluation of vector targeting. For example, transgenic mice have been generated that express human CD46 in an expression pattern that is similar to that in humans[119]; CD46 is the receptor for several viruses, and this mouse model has been used to evaluate a pseudotyped Ad5 vector[120].

In some cases, ectopic transgenic expression of the human receptor in a mouse model will suffice, and relevant mouse models promise to reduce the effort and costs compared with those needed to generate a transgenic model for each target. Such a system was recently developed and used for the evaluation of targeted adenoviral vectors[121–123].

Table 1 | **Key features of viral vectors**

Feature	Adenoviral vector	Helper-dependent adenoviral vector	AAV vector	Retroviral vector	Lentiviral vector
Particle size (nm)	70–100	70–100	20–25	100	100
Cloning capacity (kb)	8–10	~30	4.9 (10 after heterodimerization of two AAV virions)	8	9
Chromosomal integration	No	No	No (yes if *rep* gene is included)	Yes	Yes
Vector yield (transducing units/ml)	High (10^{12})	High (10^{12})	High (10^{12})	Moderate (10^{10})	Moderate (10^{10})
Entry mechanism	Receptor (CAR)-mediated endocytosis, endosomal escape and microtubule transport to the nucleus		Receptor-mediated endocytosis, endosomal escape and transport to the nucleus	Receptor binding, conformational change of Env, membrane fusion, internalization, uncoating, nuclear entry of reverse-transcribed DNA	
Transgene expression and practical application	Weeks to months; highly efficient short-term expression (e.g. for cancer or in acute cardiovascular diseases)	>1 year; highly efficient medium- to long-term expression	>1 year; medium- to long-term gene expression for non-acute diseases (onset of transgene expression after ~3 weeks)	Long-term correction of genetic defects	
Oncolytic potential?	Yes	No	No	No (but has potential to spread through the tumour without lysis, thereby spreading a suicide gene that encodes a pro-drug-converting enzyme)	
Emergence of replication-competent vector *in vivo*?	Possible but not a major concern	Negligible, low risk	Possible but not a major concern	Risk is a concern	Risk is a concern
Infects quiescent cells?	Yes	Yes	Yes	No	Yes
Transcriptional targeting affected by chromosomal integration site?	No	No	No	Yes	Yes
Risk of oncogene activation by the vector?	No	No	No	Yes	Yes

AAV, adeno-associated virus; CAR, coxsackie and adenovirus receptor; Env, viral envelope protein.

coupling the Ad–PEG complex to an RGD peptide or E-selectin-antibody[27]. Importantly, PEGylation has the potential to shield the vector from the innate immune system *in vivo*[28], and it allows infection in the presence of Ad antibodies[29], which might enable repeated vector application. Whereas PEGylation can impede cell transduction *in vitro*, this effect does not seem to occur *in vivo*, possibly owing to different hydrodynamic conditions[28]. So far, targeting by PEGylation has been used for AAV and Ad vectors, but could potentially be extended to enveloped vectors, for which a PEGylation strategy has been recently developed[30].

A promising extension of the chemical conjugation approach was recently introduced in a study that combined the flexibility of adaptor systems with the advantage of the stable covalent bonds that are provided by genetic targeting (see below)[31]. Highly reactive thiol groups were introduced into the Ad capsid by genetically inserting cysteines at solvent-exposed positions. The thiol groups were then coupled to transferrin, which mediated the successful targeting of the vector to cells expressing the receptor for this protein. Because the thiol groups are at the tip of the fibre, and thus distant from the surface amino groups that are used for PEGylation, both systems can be used simultaneously. This novel thiol-group coupling system allows not only the convenient introduction of full-length proteins such as transferrin, but also receptor ligands that cannot be introduced by genetic methods, such as sugars, fatty acids and small molecules. This approach has the potential to be extended to other vector systems, possibly with the exception of enveloped vectors: these vectors lack the necessary capsid sites for modification and, in addition, coupling to the Env protein (retroviral or lentiviral viral envelope protein) might be deleterious to its function and the chemical steps involved might disrupt the viral envelope.

Adaptor systems using avidin and biotin. The high-affinity binding between avidin and biotin has been used in many biotechnological applications[32,33], and gene therapists have taken advantage of this to provide an adaptor strategy that has been exploited for several viral vectors and forms a valuable basis for targeting studies.

One of the first studies to demonstrate the feasibility of this approach for an enveloped virus was reported as long ago as 1989 (REF. 34). An ecotropic retrovirus was crosslinked to human major histocompatibility complex class I (MHCI) in an adaptor strategy in which the virus was coated with a biotinylated anti-envelope antibody, then with streptavidin, and finally with a biotinylated anti-MHC antibody to redirect its attachment. Although entry via class I MHC was convincingly demonstrated *in vitro*, the efficiency of this approach was low, for reasons that were not fully determined[35].

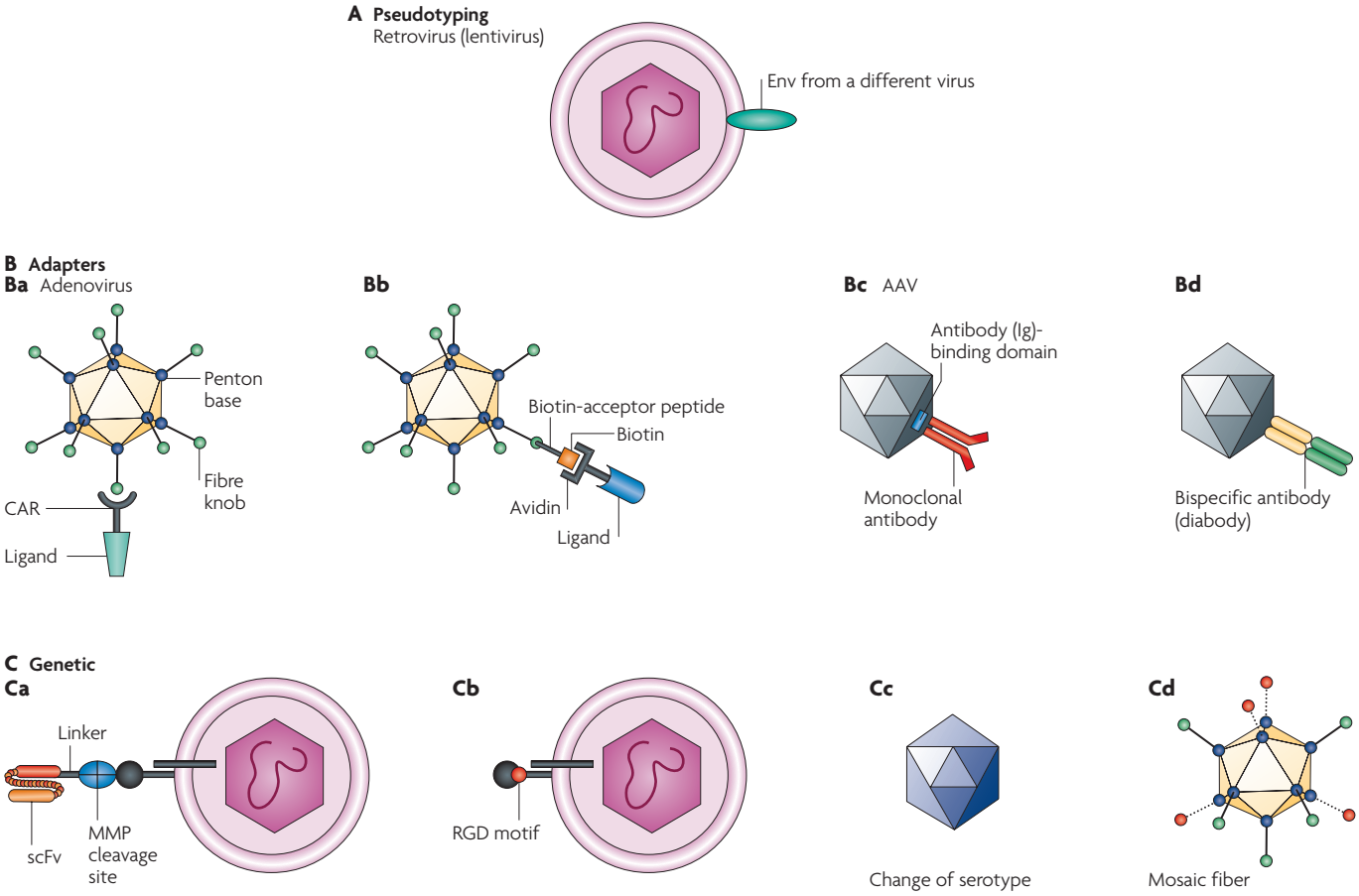

Figure 2 | **Targeting options for viral vectors.** Many targeting modalities have been implemented for all three vector types discussed in this Review. The targeting techniques are illustrated for only one viral attachment protein in most of the panels. **A** | Pseudotyping. A retroviral (lentiviral) vector is pseudotyped with an envelope protein (Env) from a different virus[9]. **B** | Adaptors. In part **Ba**, an adenoviral vector is coupled with a receptor–ligand fusion; in this example, the ectodomain of the adenoviral receptor is fused to a ligand that is expressed on a target cell type (for example, CD40L, the ligand for the CD40 receptor on dendritic cells)[22]. In part **Bb**, a biotin-acceptor peptide is integrated into the fibre knob, biotinylated and coupled to an avidin-containing ligand[21]. In part **Bc**, an antibody-binding domain is genetically incorporated into the adeno-associated virus (AAV) capsid to couple a monoclonal antibody to the vector[43]. In part **Bd**, a bispecific antibody is attached to the AAV capsid[145]. **C** | Genetic incorporation of a targeting ligand. In part **Ca**, a single-chain antibody (single-chain variable fragment (scFv) against human carcinoembryonic antigen (CEA)) and a matrix metalloprotease (MMP) cleavage site are coupled to the viral envelope protein (Env). This allows binding to tumour cells that express CEA, followed by cleavage of the MMP cleavage site by tumour-secreted MMP[48]. The vector can also be targeted to tumour cells by incorporating a tumour-specific scFv directly into Env. However, these insertions can perturb infection if the targeted receptor does not support the required post-binding steps towards viral entry. The MMP cleavage site allows release of the scFv before fusion with the target cell. In part **Cb**, incorporation of a small targeting ligand (for example, an RGD peptide) can be used to target a vector to integrin receptors[73]. In part **Cc**, the serotype is changed to achieve desired targeting[140]. In part **Cd**, the use of different fibres in the same vector allows multifunctionality in a mosaic fibre virus[93]. CAR, coxsackie and adenovirus receptor.

Biotinylation strategies have also been developed for Ad vectors. A biotin-acceptor peptide (BAP) has been cloned into the fibre capsid protein to produce the Ad–BAP fusion. The BAP is biotinylated during vector production in mammalian cells and can therefore be coupled to a biotinylated targeting ligand via tetrameric avidin (FIG. 2Bb). Compared with coating the vector with biotinylated antibody, this strategy makes use of a more robust covalent attachment of biotin to the vector. This approach has been used to screen for potential targeting ligands[21], to purify adenoviral vectors[36] and to evaluate Ad capsid proteins for targeting[37]. In terms of potential clinical applications, the avidin–biotin system has been used to target Ad vectors to dendritic cells *in vitro* using monoclonal antibodies or high-affinity binding peptides as ligands for the targeted cell receptor[38]. The high-affinity binding of avidin to biotin (10^{-15}) qualifies this system for *in vivo* applications, including therapeutic ones. Possible toxicity from high levels of avidin — which can complex biotin in the circulation — could be a concern; however, we consider this risk to be low, because only vector-bound avidin is expected to be introduced into the patient.

Table 2 | **Targeting systems**

Approach	Principle	Advantages	Disadvantages	Examples
Pseudotyping				
Approach overview	Use of a viral attachment protein from a different virus strain or family	Technically easy when the biology is supportive or compatible	Limited availability of pseudotypes that fit the desired target cell; possible reduction of transfection efficiency (retrovirus)	Ad (*in vitro*)[18] (*in vivo*)[120]; AAV (*in vivo*)[138]; Lentivirus (*in vivo*)[30]
Adaptor systems				
Approach overview	Use of a molecule that binds both the vector and target-cell receptor to facilitate transduction	Limited knowledge of capsid structure is sufficient; flexibility; no/minimal change in vector structure; easy preclinical testing of different targeting ligands	Two-component system; stoichiometry of adaptor to vector might vary between batches; two molecules must be produced separately; issues with regulatory agencies; adaptor might dissociate *in vivo*; clinical applicability can be limited	
Receptor–ligand	A native viral receptor is fused to the targeting ligand	Easy preclinical testing	Correct folding of each new receptor–ligand pair must be determined	Ad (*in vivo*)[22]; retrovirus (*in vitro*)[24]
Bispecific antibody	Two antibodies are coupled, with the resulting molecule having specificity for the vector and the target	Using existing reagents, the antibody is easy to make; screening for different targets is readily possible	Binding affinity of the targeting complex to the vector can vary	Ad (*in vivo*)[139]; AAV (*in vitro*)[145]; coronavirus (*in vitro*)[148]
Chemical linkage	Targeting moiety is bound to the vector by chemical means	A covalent bond is formed with the targeting complex, thus no adaptor dissociation from the vector	Technically more demanding than other adaptor systems (but nevertheless scaleable for clinical applications)	Ad (*in vitro*)[29,31]
Avidin–biotin	Biotin is coupled to the vector and then bound to the avidin–ligand complex	High-affinity binding of the targeting complex to the vector; allows easy vector purification	Some risk for toxicity in clinical applications (biotin from the circulation could be complexed)	Ad (*in vitro*)[38]; AAV (*in vitro*)[39]; retrovirus (*in vitro*)[34,35]
Antibody	Antibody binds to a genetically incorporated Ig-binding domain of the vector	Vast pool of available antibodies for targeting; easy coupling	Antibodies from the circulation could interfere with targeting	Ad (*in vitro*)[44]; AAV (*in vitro*)[43]; retrovirus (*in vitro*)[45]
Genetic systems				
Approach overview	A polypeptide is incorporated into the vector by genetic means to facilitate transduction	Single-component system; favoured for clinical application; ease of high-titre vector production	Technically more challenging than adaptor approaches; can be detrimental to vector or ligand structure	
Serotype switching	Use of a different serotype from within the same virus family	Biological compatibility makes it feasible	Limited availability of serotypes; the precise cellular receptor is frequently unknown	AAV (*in vivo*)[140]; Ad (*in vivo*)[149]
Small targeting motifs	Small peptides are inserted into the capsid or viral attachment protein	Minimal disturbance of vector structure	Broadens tropism without ablating native tropism; limited number of available motifs, thus not applicable for all cell types	Ad (*in vivo*)[76]; AAV (*in vitro*)[70]; retrovirus (*in vitro*)[73]; phage–AAV (*in vivo*)[20]
Single-chain antibody	A single-chain antibody is incorporated into the viral attachment protein	Vast pool of tested antibodies available for targeting	Antibody might need adaptation to a biosynthetic pathway of virus protein production (Ad)	Ad (*in vivo*)[19]; AAV (*in vitro*)[47]; retrovirus (*in vivo*)[48]
Mosaic viral attachment proteins	Two viral attachment proteins with different properties are combined, allowing targeting, production or imaging in parallel	True multifunctionality in a virion can be achieved	Desired stoichiometry can be difficult to achieve	Ad (*in vitro*)[93]; AAV (*in vitro*)[70]
Ablation of native tropism	Mutation of the amino acids responsible for native tropism	Can be combined with other techniques	Can confound production in packaging cell line	Ad (*in vivo*)[88]; AAV (*in vivo*)[87]; Lentivirus (*in vivo*)[13]

AAV, adeno-associated virus; Ad, adenovirus.

AAV vectors can be biotinylated in a similar way to Ad vectors, and this system is now being used as a platform for purification and targeting of this vector type[39]. A different biotinylation approach has recently been taken with vaccinia viral vectors and has proved successful for *in vitro* targeting. The virus was chemically biotinylated, followed by the addition of avidin and subsequent incubation with a biotinylated antibody, which allowed targeting to MHCI- and B7.2-transfected tumour cells[40]. The avidin–biotin system seems to be suitable for any

Box 3 | **Imaging technologies for evaluating vector targeting**

Until recently, testing the biodistribution of targeted vectors required sacrificing animals to evaluate transgene expression or viral particle concentration in various organs[124,125]. Several clinical trials have shown a lack of useful end points that would allow evaluation of vector targeting[126,127]. Approaches that allow imaging of viral vector distribution *in vivo* have the advantage that animals do not need to be sacrificed for analysis, enabling multiple real-time measurements of vector distribution. Vectors with novel modalities that allow *in vivo* imaging are now being developed. Imaging moieties are generally either expressed in the form of a reporter transgene from the viral genome or attached to the vector by genetic fusion to a capsid protein.

Gene-based imaging can make use of radioactive systems, such as the vector-mediated gene transfer of herpes simplex thymidine kinase, which can phosphorylate radiolabelled nucleoside analogues. Quantification is carried out using positron emission tomography (PET) imaging[128], which is applicable in clinical settings. Alternatively, light-emitting systems can be used, including those using luciferase and green or red fluorescent proteins[129,130].

A recent example illustrates how imaging can greatly facilitate the evaluation of targeting approaches. A lentiviral vector that was pseudotyped with the envelope protein (Env) of the Sindbis virus was successfully retargeted to metastatic melanoma *in vivo*[13]. To achieve this, the Sindbis Env was mutated to ablate liver or spleen tropism, and the ZZ domain (Ig-binding domain) of protein A was genetically fused to this protein. This allowed coupling to a monoclonal antibody that targeted P-glycoprotein-expressing melanoma cells (see part **a** in the figure). Biodistribution was monitored through imaging, which was facilitated by vector-mediated luciferase expression. Part **b** in the figure shows ablation of the native tropism of the vector. SCID (severe combined immunodeficiency) mice were injected systemically with a lentivirus that was pseudotyped with a Sindbis Env protein that contained an antibody-binding domain. The upper panel shows strong liver and spleen tropism owing to domains within the Sindbis Env protein that target the vector to these tissues. Mutating these domains largely ablated this natural tropism (shown in the lower panel). Light emission is measured in photons (p) s^{-1} cm^{-2} steridian $(sr)^{-1}$. In part **c**, mice were injected first with tumour cells that form lung metastases, and 12 days later with the vector. Use of a nonspecific control antibody did not lead to tumour-cell transduction (shown in the upper panel), whereas use of a tumour-cell-specific antibody leads to transduction of tumour cells in the lung (lower panel). This study shows how combining several targeting techniques (pseudotyping, ablation of native tropism and adaptor coupling) can lead to truly targeted gene transfer after systemic application, and how imaging is essential for the analysis.

For Ad vectors, it has recently become possible to incorporate imaging ligands into the capsid. Green and red fluorescent proteins[131–133], herpes simplex virus thymidine kinase (HSVtk)[134] and an HSVtk–luciferase fusion protein[135] have been fused to the capsid protein pIX, allowing multi-modality imaging. In all cases, the imaging ligands retained their activity. Because of the localization of the imaging signal, capsid labelling seems to be especially promising in the context of tracking the intracellular fate of vectors, which would not be possible otherwise, and for observing the spread of targeted oncolytic vectors.

Another approach exploits magnetic resonance imaging (MRI), which has been used in a gene therapy context[136] but only recently became applicable for direct vector imaging. Räty *et al.* used MRI-based imaging of an avidin-coated baculovirus that was conjugated with biotinylated superparamagnetic iron oxide particles[137]. This technique should be easily applicable to other capsid-coated viruses. The spatial resolution of MRI is in the millimetre (typical for medical MRI) to micrometre (typical for research MRI) range, which is much greater than for the other imaging methods (which generally have a resolution of several millimetres) and which will allow assignment of vector location to individual cells. However, MRI is considerably less sensitive than radioactive or light-based imaging systems.

Parts **b** and **c** reproduced with permission from *Nature Medicine* REF. 13 © (2005) Macmillan Publishers Ltd.

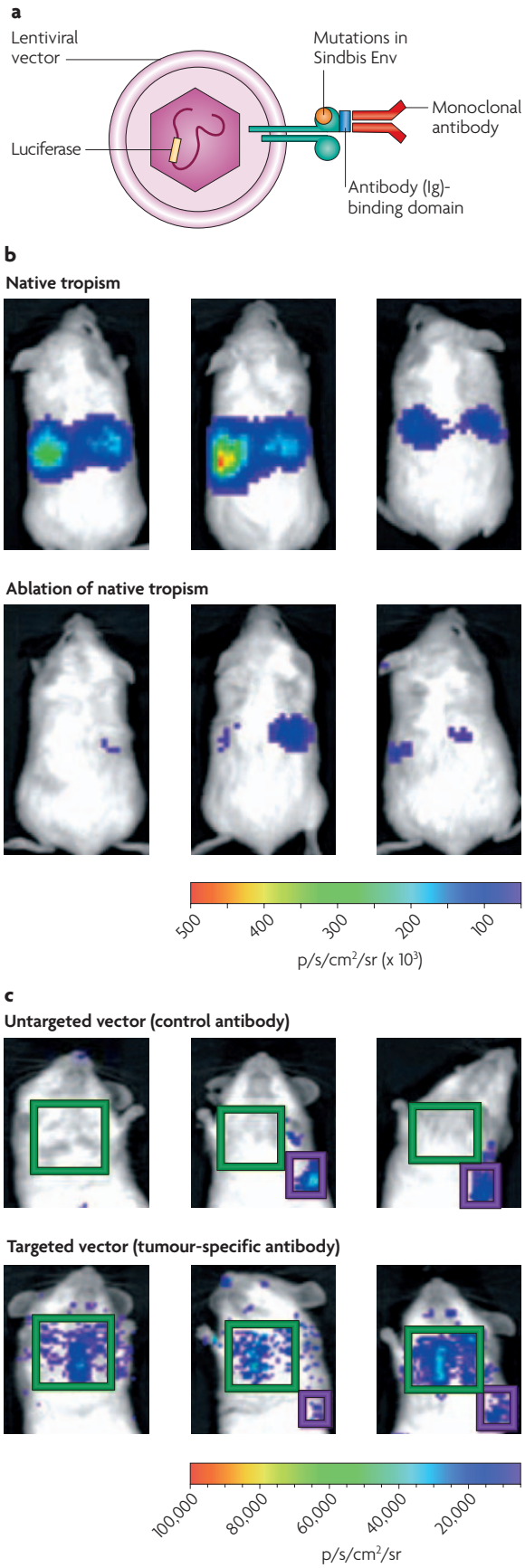

vector type that allows incorporation of a BAP, or that can be chemically biotinylated — techniques that should be universally applicable — and is expected to be utilized in many more applications in the future.

Monoclonal antibodies as adaptors. Antibodies have been used as targeting tools in various applications[41,42], and many researchers are working on ways to capitalize on the diversity and wide availability of these reagents. Vectors have been genetically modified to allow coupling of monoclonal antibodies; for example, a region of a bacterial immunoglobulin (Ig)-binding protein (usually the Z-domain of the staphylococcus protein A) can be inserted into the viral attachment proteins of various vector systems[14,43–45]. In this way, the unmodified antibody can work like an adaptor, bridging the Ig-binding domain that is incorporated in the vector to the target receptor through its antibody specificity (FIG. 2Bc). This approach has been successfully used *in vitro* and in SCID (severe combined immunodeficiency) mice[13]. However, a significant limitation of this approach is that polyclonal Igs in the bloodstream might compete to displace the monoclonal antibody from the virally displayed Ig-binding protein before it reaches its target site. The approach has not yet been advanced to clinical testing and might be better suited to *ex vivo* gene therapy applications that require transduction of specific target cells in a mixed cell population (for example, stem cells in bone marrow).

Challenges facing adaptor systems. Most of the adaptor systems described above have disadvantages that detract from their potential use for gene therapy. One disadvantage relates to the potentially suboptimal stability of the vector–adaptor complex, especially *in vivo*, which might result from unforeseen interactions with factors that perturb the non-covalent binding. Systems that rely on either the BAP, with their strong binding of the targeting complex, or on chemical conjugation are the least likely to be affected by this. In addition, difficulties can arise in terms of scaling up adaptor protein production, and the coupling efficiency might vary between different batches. Finally, regulatory agencies favour single-component systems and consider the adaptor and the virus to be separate drugs. One perceived problem is that the crosslinker might elute from the surface of the virus *in vivo*; the adaptor approach is also considered more cumbersome for clinical applications.

None of the adaptor approaches has been tested extensively *in vivo*, which has limited our understanding of their potential utility. Systems based on the BAP have great flexibility and are expected to be widely applied, including potentially in patients. The other systems are likely to have their greatest potential in preclinical proof-of-principle studies.

Genetic incorporation of targeting ligands

To avoid the potential complexities of adaptor systems, researchers have investigated methods for the genetic incorporation of targeting ligands into viral vectors. Genetic fusion of these ligands into the capsid or the envelope protein yields a single virion molecule that recognizes the target cell. Despite being more technically challenging than the use of adaptors, such single-component systems provide homogenous retargeted vector particles, unlike adaptor-based approaches. As well as overcoming the regulatory issues of two-component systems, this approach facilitates high-titre production by eliminating the need to create a separate adaptor molecule.

Systems involving polypeptide ligands. Several promising single-component systems involve the genetic incorporation of polypeptide ligands into viral surface proteins, giving vectors new and highly specific tropisms for cells expressing the target antigen. This approach was pioneered in 1993 with the display of a single-chain antibody on the surface of an enveloped virus[46]. In this case, an anti-hapten antibody was genetically fused near the N-terminus of the MLV surface (SU) component of the envelope glycoprotein, and retroviral vectors incorporating the chimeric protein were shown to bind to hapten via the displayed antibody.

The single-chain antibody approach has been applied to several vectors — AAV[47], adenovirus[19], retrovirus[48] (FIG. 2Ca), measles virus[49] and herpes simplex virus[50] — underlining the versatility of this approach. Many other complex polypeptide ligands, including growth factors and cytokines, have since been displayed on various gammaretroviral envelope glycoproteins, as either N-terminal fusions, insertions into the proline-rich hinge region or substitutions for the N-terminal protein domains[51]. Similar engineering has been attempted for other enveloped viruses: ligands have been fused proximal to the N-termini of herpesvirus proteins gC and gD[52], influenza haemagglutinin[53,54] and the VSV-G protein[55], and a ligand has been inserted within the N-terminal receptor-binding domain of the E2 attachment protein of Sindbis virus[14].

Despite the great potential of this approach in terms of specificity, one limitation to applying it more generally is that the introduction of large proteins can be deleterious to the structure of the viral protein into which they are inserted, or can impede the correct folding of the incorporated polypeptide. Incorporation of a single-chain antibody fusion into an Ad vector was initially impeded because of the different biosynthetic pathways that are used to produce the scFv (which is synthesized in the rough endoplasmic reticulum (ER), facilitating formation of disulphide bridges) and the Ad capsid proteins (which are synthesized in the cytosol, interfering with the formation of these bridges)[56]. In addition, incorporation of such large proteins into the Ad fibre can impede proper folding (trimerization) of the fibre and hence viral rescue. The use of cytosolically stabilized scFvs (intrabodies) and the generation of an artificial fibre allowed genetic coupling of the fibre and scFv in the Ad system[19]. The artificial fibre has the added advantage of ablating the native tropism of Ad. One challenge in using this system relates to identifying scFvs that will fold correctly in the cytosol, requiring expertise in scFv technology and complex fibre

B7.2
B7.2 (CD86) is a co-stimulatory transmembrane protein in the B7 family. It is found on antigen presenting cells (APCs) and interacts with receptors on T cells.

modifications. By contrast, the glycoproteins of enveloped vectors are routed through the ER, which supports the folding and post-translational modification of complex proteins fused to the envelope[57,58]. Thus, polypeptide ligands with multiple disulphide bonds, stringent glycosylation requirements or oligomeric structures can be more readily displayed on enveloped viruses than on non-enveloped viruses.

Targeted virus attachment does not necessarily lead to targeted entry. In the case of retroviral envelope glycoproteins, displayed targeting ligands usually impede infectivity because the normal functions of the viral attachment protein are altered. This can lead to direction of the virus into a non-functional entry pathway, steric blocking of its natural receptor interactions or prevention of conformational changes that are required for effective fusion triggering[51]. These problems led to the concept of inverse targeting, whereby the viral envelope glycoprotein is modified to selectively destroy its infectivity for cells expressing a targeted receptor[59]. Thus, amphotropic retroviral vectors that display epidermal growth factor (EGF), stem-cell factor (SCF) or insulin-like growth factor 1 (IGF1) are selectively non-infectious for cells that express the cognate receptors (EGFR, KIT or IGFR), but remain fully infectious for other (receptor-negative) human cells[59–61]. This inverse targeting provides a useful way to detarget the liver (EGFR positive) or marrow stem cells (KIT positive), and can be used to ameliorate specific vector toxicities against these targets, although the number of potential applications is limited.

Protease targeting is another concept that has emerged from early unsuccessful efforts to reprogramme retrovirus entry. Here virus infectivity is engineered to depend on the proteolytic maturation of a viral surface protein. This can be achieved through cleavage of a protease-susceptible linker that tethers an infectivity-blocking polypeptide to the viral surface. Another approach is cleavage of an engineered junctional sequence between the SU and transmembrane (TM) components of a retroviral envelope glycoprotein, or between the F1 and F2 components of a measles attachment glycoprotein[62]. In this way, the vector is targeted to cells that are bathed in the appropriate protease. Examples include the targeting of protease-rich tumours[63] by vectors with an infectivity that is selectively activated by matrix metalloproteinases (MMPs) (FIG. 2) or by plasmin. Other potential protease-rich targets include the sites of new blood vessel formation in diabetic retinopathy and in the pannus tissue of joints affected by rheumatoid arthritis, as well as sites of acute and chronic inflammation.

Several animal studies have demonstrated the feasibility of *in vivo* transductional targeting using retroviral and lentiviral vectors with genetically incorporated polypeptide ligands. In one study, a retroviral vector that was activated by MMP and displayed a melanoma-targeting single-chain antibody was shown to target gene delivery to MMP-rich melanoma xenografts[64]. In another study, the liver was successfully detargeted by pseudotyping lentiviral vectors with an amphotropic MLV envelope glycoprotein that displayed EGF as an N-terminal fusion[65]. The reduced hepatic transduction in this case resulted from inverse targeting, which was possible because EGF receptors are expressed abundantly on hepatocytes.

A third example is represented by the first and so far only targeted vector that has been tested in the clinic: the retroviral vector Rexin-G, which expresses a cytocidal dominant-negative form of cyclin G1. This vector displays the collagen-binding portion of von Willebrand factor (vWF), which is required for the adhesion of platelets to sites of injured endothelium[66], incorporated in its Env protein. Exploiting this targeting mechanism allows preferential vector delivery to the tumour site where angiogenesis and collagen matrix exposure occur (tumour neovessels)[67]. Rexin-G is targeted to the extracellular matrix of tumour tissue[68] and has been tested for its anti-tumour activities in three clinical studies[69]. Several cases of partial responses and stable disease demonstrated the effectiveness of the vector.

The limitations that are encountered during retroviral or lentiviral vector targeting using engineered polypeptide ligands do not necessarily apply for other enveloped viruses. In contrast to retroviruses, the attachment and fusion functions of the measles virus are encoded on separate proteins, making it easier to manipulate binding specificity without negatively impacting the efficiency of fusion triggering (see below). However, measles is still the only virus that can be efficiently retargeted through a wide range of cellular receptors using a variety of cell-targeting polypeptides without significant reductions in its entry efficiency.

Small-peptide motifs. Small-peptide motifs are less likely to perturb the structure of the viral attachment protein, which permits their insertion at various regions of the protein. Despite their small size (generally 3–20 amino acids), they can change the targeting characteristics of a vector dramatically.

Small peptides containing an RGD motif, which targets vectors to integrins, have most often been used for this purpose, facilitating diverse applications that include targeting of the vasculature and of tumour cells. Such targeting has been achieved for AAV (*in vitro*)[70], adenovirus (*ex vivo* in tissue-slice assays[71], and *in vivo*)[72], retroviral vectors (*in vitro*)[73] (FIG. 2Cb), and for a phage–AAV hybrid vector (*in vivo*)[20]. Another useful small-peptide targeting moiety is the poly-lysine (pK7) peptide that targets vectors to heparan sulphates, which are overexpressed in a number of malignancies[74] and other pathologies. Adenoviral vectors carrying pK7 in their fibre knob showed an increased transduction of various CAR-deficient targets, such as skeletal muscle *in vivo*[75]. In addition, RGD and pK7 have recently been used together in the Ad capsid to improve the efficiency of vector delivery (and hence survival) in a murine model of cancer[76]. Generally, both of these modifications broaden the vector tropism, which makes them especially useful for local administrations. An RGD-modified conditionally replicating Ad[77] is soon to be used clinically for local applications in ovarian carcinoma at the University of Alabama at Birmingham, USA, following the recent completion of animal safety tests[78].

Amphotropic
Describes a pathogen such as a virus or a bacteria that has a wide host range and can infect more than one species or cell-culture line.

Although small-peptide motifs are versatile and can be used to target viral vectors to several cell types, other cell types cannot be targeted in this way and require different targeting approaches.

Library-selection approaches. As described above, genetic targeting approaches are limited by the size, and sometimes the structure, of the ligand that can be incorporated without compromising assembly, stability or infectivity of the vector. It is also crucial that the displayed ligand maintains its bridging ability towards the target after fusion to the viral attachment protein. These considerations have driven library-selection approaches, which display the ligand in the context of the viral attachment protein and then select for the desired increase in infectivity by binding to a column that displays the targeting receptor[79], by repeated cycles of binding to target cells[80,81], or by serial passage through the target cells[82].

In one example, the H and I sheets of the Ad fibre knob were inserted into the pIII protein of a bacteriophage. A random peptide library was introduced between the Ad knob sheets and selected against the target cells. This resulted in identification of a peptide that improved Ad transduction of mouse muscle cells 14-fold compared with unmodified Ad[81]. A different approach was used for library screening with AAV[79]. First, the AAV capsid protein CAP was subjected to PCR-based mutagenesis and recombination, followed by insertion into an AAV packaging plasmid and creation of an AAV library. This library was then screened for desired properties, for example, using heparin affinity chromatography to select for low or high heparin affinity, or incubation with neutralizing serum to select for mutants that evaded antibody responses. Library selection for changes in retroviral vector tropism has also been carried out. For example, in one study[82], feline leukemia virus (FeLV) envelope glycoproteins were randomized in the cell-targeting region by oligonucleotide insertions[83,84] and subjected to transduction-based selection strategies in cancer cells. The resulting FeLV vector was able to transduce prostate cancer cell lines, but required the presence of a murine retrovirus (4070A) helper envelope glycoprotein to facilitate virus entry. Although this example demonstrates the feasibility of selecting vectors with new tropisms from retroviral libraries, the selection strategy cannot be focused on a specific known receptor; it can only be focused on a particular cell type. However, in cases in which no targeting ligands are known, such library-selection approaches can provide one way forward, and proof of principle for this approach has been established for targeting all the major vector classes[79,81,85,86].

Ablation of native vector tropism. For systemic applications, the native vector tropism of gene therapy vectors might need to be ablated to avoid the transduction of non-target tissue. In some instances, the addition of the targeting ligand reduces the native tropism sufficiently. For example, the incorporation of peptides that target human venous endothelial cells into AAV capsids resulted in significantly lower hepatocyte transduction, but greatly increased venous-cell transduction[87]. However, there are other cases in which additional steps must be taken to ablate the native tropism of the vector.

For example, for the Ad serotype 5 vector, which is the most commonly used Ad vector, detargeting is of central importance to enable successful systemic treatments that avoid effects on the liver; the addition of a targeting moiety alone is frequently insufficient. Many fibre mutants have been generated in attempts to achieve liver detargeting. The most dramatic effect has been seen for Ad fibres with deletions in a putative heparan-sulphate proteoglycan-binding motif that resulted in a 15-fold decrease in liver transduction and a 1,000-fold decrease when combined with a CAR-ablating mutation. However, the effects of detargeting mutations seem to be highly dependent on the strain and species of rodent[88], highlighting the importance of using multiple and complementary preclinical model systems.

Examples for tropism ablation regarding retroviral vectors are discussed above in the context of inverse targeting, and an example for a lentiviral vector is discussed in BOX 3. Generally, each vector requires specific changes in the viral attachment protein to ablate its native tropism. These modifications can then be used in a wide range of applications, with the exception of reverse targeting used for enveloped vectors, which is specific for a particular cell type.

An alternative to the above approaches is the use of a vector with no tropism in the target organism. When using a prokaryotic vector that normally does not infect eukaryotic cells, but can be modified with an RGD motif, systemic application becomes feasible and can lead to tumour-specific transduction, as shown for an AAV–phage hybrid[20].

Outlook and future directions

Cell-type-specific targeting *in vivo* by gene therapy vectors is a milestone that has only recently been realized. For some applications, direct translation of that achievement to the clinic might be possible; for example, local application of genetically modified vectors with a broadened tropism or systemic administration of vectors with specific targeting and ablated native tropism could see application in a few years. Other therapeutic interventions will require further research to achieve the desired targeting specificity, which should be facilitated by several recent developments. For example, single-component systems (such as Ad with an artificial fibre that is genetically fused to a scFv) are easy to prepare in high titres and are not expected to face problems for clinical approval. By contrast, a lentiviral vector coupled to an adaptor might face more problems during large-scale preparation and in regard to the general safety issues of lentiviral vectors. As we have seen, in many cases the challenges to developing a successful targeting vector relate to the biology of the individual vector type.

Despite the vast range of experimental studies that have been carried out with targeted vectors, transition to a clinical setting has been slow. This delay is related to general problems in the field of gene therapy that

Complement system
A protein system in the blood that forms a defense against pathogens.

Transcytosis
Transport of macromolecules (including pathogens) across a cell, which consists of the endocytosis of a macromolecule at one side of a monolayer and its exocytosis at the other side.

concern high costs of vector production for clinical use and acquisition of financial support for this production. Several rounds of clinical trials will be needed to optimize a particular gene therapy approach, as is the case for other therapies (for example, monoclonal antibodies), which needed several trials to find their way into clinical practice. The important aspect of the clinical studies that have begun, and are beginning now, is that targeted vectors can gain regulatory (Food and Drug Administration (FDA)) approval in the USA[69]. With most western nations being geared to FDA procedures, this approval represents an encouraging sign for targeted gene therapy protocols worldwide.

Although this Review has focused largely on the final step of targeting — transduction of the target cell — other aspects are equally important, especially for systemic vector administration. We have briefly discussed other potential obstacles, such as the immune system (antibodies, complement system) or other blood factors that impact the vector in the blood stream, and ways to escape these problems that are currently being investigated (BOX 1). The exit of vectors from the blood stream into the target tissue will also be an important step to address. Ensuring that vectors move beyond the vascular endothelial layer after systemic application, for example, by transcytosis, will be of crucial importance to achieve clinical success in many instances (such as disseminated metastases).

Strategies to enable transcytosis have recently moved to the forefront of vector targeting research. Whereas transcytosis for a lentivirus, HIV, has been described[89], this area is only just beginning to be explored for viruses that form the basis of the other types of gene therapy vectors. In the context of AAV, three serotypes out of five that were tested showed transcytosis; this ability was both serotype and cell-type specific[90]. Serotype switching, which can be achieved by transfection of plasmids with different capsid backbones, can therefore be a valuable tool when transcytosis of AAV is required. Coupling the Ad vector with an adaptor that targets the transferrin-receptor pathway has enabled transcytosis, albeit at low efficiency[91]. Exploitation of other transcytosis pathways[92] and elucidation of the natural transcytosis pathways of some viruses might allow for rational design of transcytosing vectors. Furthermore, the generation of vectors that are mosaic for their viral attachment protein (having two genetically distinct versions)[93] could prove valuable (FIG. 2Cd). One attachment protein could carry a ligand for transcytosis, whereas the other could carry the ligand for transduction of the target cell. Alternatively, the transcytosis ligand could be placed onto other capsid proteins (for example, pIX in the case of Ad), while having the transduction ligand on all viral attachment proteins.

Besides improving established vector systems, new viruses are also being developed for targeted gene therapy. One promising example is the measles virus, an enveloped virus that has recently been retargeted to tumour cells to exploit its oncolytic potential. In contrast to retroviruses, because the attachment and fusion functions of the measles virus are encoded on separate proteins, it is easier to manipulate binding specificity without negatively impacting the efficiency of cell entry. Several large polypeptide ligands have been displayed on the surface of the measles virus as extensions of the viral attachment glycoprotein[94]. In most cases, the ligand-displaying measles viruses have been able to enter cells efficiently via the targeted receptor[95,96]. Mutations that are known to ablate the natural measles tropisms for CD46 and SLAM (signalling lymphocytic activation molecule) were subsequently incorporated into the chimeric viral attachment proteins, thereby generating fully retargeted measles viruses with entirely new receptor specificities[49]. Several fully retargeted measles viruses have been shown to mediate targeted *in vivo* destruction of receptor-positive tumours[97,98]. In this way, new gene-transfer vehicles can be created, combining established targeting principles (such as ablation of native tropism and targeting through single-chain antibodies) with the natural abilities of different vectors, thus continuously expanding the gene therapist's toolbox.

The concepts of vector targeting that are described in this Review are now recognized throughout the gene therapy field. In regard to non-viral vectors, the efficiencies of gene transfer after systemic delivery are low unless vectors are administered under high pressure (for example, hydrodynamic delivery in mice, which selectively transduces the liver). Non-viral vectors, which are essentially DNA-containing nanoparticles, can be retargeted by incorporating ligands into their lipid or protein shells, but to date there are no convincing studies to demonstrate the *in vivo* utility of retargeted non-viral vectors. However, once their efficiencies approach those of viral vectors, the targeting principles that are outlined in this Review are also likely to be applicable to non-viral vectors.

1. Aghi, M. & Martuza, R. L. Oncolytic viral therapies — the clinical experience. *Oncogene* **24**, 7802–7816 (2005).
2. Rocconi, R. P. *et al.* Targeted gene therapy for ovarian cancer. *Curr. Gene Ther.* **5**, 643–653 (2005).
3. Zeimet, A. G. & Marth, C. Why did p53 gene therapy fail in ovarian cancer? *Lancet Oncol.* **4**, 415–422 (2003).
4. Sadeghi, H. & Hitt, M. M. Transcriptionally targeted adenovirus vectors. *Curr. Gene Ther.* **5**, 411–427 (2005).
5. Edelstein, M. L., Abedi, M. R., Wixon, J. & Edelstein, R. M. Gene therapy clinical trials worldwide 1989–2004 — an overview. *J. Gene Med.* **6**, 597–602 (2004).
6. Boulaiz, H., Marchal, J. A., Prados, J., Melguizo, C. & Aranega, A. Non-viral and viral vectors for gene therapy. *Cell Mol. Biol. (Noisy-le-grand)* **51**, 3–22 (2005).
7. Rolland, A. Nuclear gene delivery: the Trojan horse approach. *Expert Opin. Drug Deliv.* **3**, 1–10 (2006).
8. Burton, E. A., Fink, D. J. & Glorioso, J. C. Replication-defective genomic HSV gene therapy vectors: design, production and CNS applications. *Curr. Opin. Mol. Ther.* **7**, 326–336 (2005).
9. Cronin, J., Zhang, X. Y. & Reiser, J. Altering the tropism of lentiviral vectors through pseudotyping. *Curr. Gene Ther.* **5**, 387–398 (2005).
An excellent review on pseudotyped lentiviral vectors. Targeting of particular organs or cell types (for example, neurons, airway epithelia, tumours and others) is emphasized.
10. Schnierle, B. S. *et al.* Pseudotyping of murine leukemia virus with the envelope glycoproteins of HIV generates a retroviral vector with specificity of infection for CD4-expressing cells. *Proc. Natl Acad. Sci. USA* **94**, 8640–8465 (1997).
11. Zavada, J. VSV pseudotype particles with the coat of avian myeloblastosis virus. *Nature New Biol.* **240**, 122–124 (1972).
12. Kobayashi, M., Iida, A., Ueda, Y. & Hasegawa, M. Pseudotyped lentivirus vectors derived from simian immunodeficiency virus SIVagm with envelope glycoproteins from paramyxovirus. *J. Virol.* **77**, 2607–2614 (2003).
13. Morizono, K. *et al.* Lentiviral vector retargeting to P-glycoprotein on metastatic melanoma through intravenous injection. *Nature Med.* **11**, 346–352 (2005).

Describes tumour targeting after systemic vector application by combining several targeting principles: pseudotyping, ablation of native tropism and antibody coupling. Imaging powerfully illustrates how these techniques contribute to successful targeting.
14. Ohno, K., Sawai, K., Iijima, Y., Levin, B. & Meruelo, D. Cell-specific targeting of Sindbis virus vectors displaying IgG-binding domains of protein A. *Nature Biotechnol.* **15**, 763–767 (1997).
15. Schnell, M. J., Johnson, J. E., Buonocore, L. & Rose, J. K. Construction of a novel virus that targets HIV-1-infected cells and controls HIV-1 infection. *Cell* **90**, 849–857 (1997).
16. Endres, M. J. *et al.* Targeting of HIV- and SIV-infected cells by CD4-chemokine receptor pseudotypes. *Science* **278**, 1462–1464 (1997).
17. Somia, N. V., Miyoshi, H., Schmitt, M. J. & Verma, I. M. Retroviral vector targeting to human immunodeficiency virus type 1-infected cells by receptor pseudotyping. *J. Virol.* **74**, 4420–4424 (2000).
18. Mercier, G. T. *et al.* A chimeric adenovirus vector encoding reovirus attachment protein σ1 targets cells expressing junctional adhesion molecule 1. *Proc. Natl Acad. Sci. USA* **101**, 6188–6193 (2004).
19. Hedley, S. J. *et al.* An adenovirus vector with a chimeric fiber incorporating stabilized single chain antibody achieves targeted gene delivery. *Gene Ther.* **13**, 88–94 (2006).
20. Hajitou, A. *et al.* A hybrid vector for ligand-directed tumor targeting and molecular imaging. *Cell* **125**, 385–398 (2006).
A groundbreaking study on the use of a prokaryotic phage vector containing an AAV genome. *In vivo* tumour transduction is achieved through integrin targeting by display of a small-peptide motif (RGD-4C) on the phage capsid, and imaging was accomplished by positron emission tomography.
21. Parrott, M. B. *et al.* Metabolically biotinylated adenovirus for cell targeting, ligand screening, and vector purification. *Mol. Ther.* **8**, 688–700 (2003).
A novel system for coupling ligands to adenoviral vectors is established, exploiting the high affinity of biotin to avidin. This system has wide-ranging applications, not only in targeting but also in ligand screening and vector purification.
22. Pereboev, A. V. *et al.* Enhanced gene transfer to mouse dendritic cells using adenoviral vectors coated with a novel adapter molecule. *Mol. Ther.* **9**, 712–720 (2004).
23. Li, H.-J. *et al.* Adenovirus tumor targeting and hepatic untargeting by a CAR ectodomain-antiCEA bi-specific adapter. *Cancer Res.* **67**, 5354–5361.
24. Snitkovsky, S. & Young, J. A. Targeting retroviral vector infection to cells that express heregulin receptors using a TVA-heregulin bridge protein. *Virology* **292**, 150–155 (2002).
25. Verheije, M. H. *et al.* Redirecting coronavirus to a nonnative receptor through a virus-encoded targeting adapter. *J. Virol.* **80**, 1250–1260 (2006).
26. Lanciotti, J. *et al.* Targeting adenoviral vectors using heterofunctional polyethylene glycol FGF2 conjugates. *Mol. Ther.* **8**, 99–107 (2003).
27. Ogawara, K. *et al.* A novel strategy to modify adenovirus tropism and enhance transgene delivery to activated vascular endothelial cells *in vitro* and *in vivo*. *Hum. Gene Ther.* **15**, 433–443 (2004).
28. Mok, H., Palmer, D. J., Ng, P. & Barry, M. A. Evaluation of polyethylene glycol modification of first-generation and helper-dependent adenoviral vectors to reduce innate immune responses. *Mol. Ther.* **11**, 66–79 (2005).
29. Eto, Y. *et al.* PEGylated adenovirus vectors containing RGD peptides on the tip of PEG show high transduction efficiency and antibody evasion ability. *J. Gene Med.* **7**, 604–612 (2005).
30. Croyle, M. A. *et al.* PEGylation of a vesicular stomatitis virus G pseudotyped lentivirus vector prevents inactivation in serum. *J. Virol.* **78**, 912–921 (2004).
31. Kreppel, F., Gackowski, J., Schmidt, E. & Kochanek, S. Combined genetic and chemical capsid modifications enable flexible and efficient de- and retargeting of adenovirus vectors. *Mol. Ther.* **12**, 107–117 (2005).
32. Diamandis, E. P. & Christopoulos, T. K. The biotin-(strept)avidin system: principles and applications in biotechnology. *Clin. Chem.* **37**, 625–636 (1991).
33. Laitinen, O. H., Nordlund, H. R., Hytonen, V. P. & Kulomaa, M. S. Brave new (strept)avidins in biotechnology. *Trends Biotechnol.* **25**, 269–277 (2007).
34. Roux, P., Jeanteur, P. & Piechaczyk, M. A versatile and potentially general approach to the targeting of specific cell types by retroviruses: application to the infection of human cells by means of major histocompatibility complex class I and class II antigens by mouse ecotropic murine leukemia virus-derived viruses. *Proc. Natl Acad. Sci. USA* **86**, 9079–9083 (1989).
35. Etienne-Julan, M., Roux, P., Carillo, S., Jeanteur, P. & Piechaczyk, M. The efficiency of cell targeting by recombinant retroviruses depends on the nature of the receptor and the composition of the artificial cell-virus linker. *J. Gen. Virol.* **73**, 3251–3255 (1992).
36. Campos, S. K., Parrott, M. B. & Barry, M. A. Avidin-based targeting and purification of a protein IX-modified, metabolically biotinylated adenoviral vector. *Mol. Ther.* **9**, 942–954 (2004).
37. Campos, S. K. & Barry, M. A. Comparison of adenovirus fiber, protein IX, and hexon capsomeres as scaffolds for vector purification and cell targeting. *Virology* **349**, 453–462 (2006).
38. Maguire, C. A. *et al.* Recombinant adenovirus type 5 vectors that target DC-SIGN, ChemR23 and $\alpha_v\beta_5$ integrin efficiently transduce human dendritic cells and enhance presentation of vectored antigens. *Vaccine* **24**, 671–682 (2006).
39. Arnold, G. S., Sasser, A. K., Stachler, M. D. & Bartlett, J. S. Metabolic biotinylation provides a unique platform for the purification and targeting of multiple AAV vector serotypes. *Mol. Ther.* **14**, 97–106 (2006).
40. Purow, B. & Staveley-O'Carroll, K. Targeting of vaccinia virus using biotin–avidin viral coating and biotinylated antibodies. *J. Surg. Res.* **123**, 49–54 (2005).
41. Hohlfeld, R. & Wekerle, H. Drug Insight: using monoclonal antibodies to treat multiple sclerosis. *Nature Clin. Pract. Neurol.* **1**, 34–44 (2005).
42. Imai, K. & Takaoka, A. Comparing antibody and small-molecule therapies for cancer. *Nature Rev. Cancer* **6**, 714–727 (2006).
43. Gigout, L. *et al.* Altering AAV tropism with mosaic viral capsids. *Mol. Ther.* **11**, 856–865 (2005).
44. Korokhov, N. *et al.* Targeting of adenovirus via genetic modification of the viral capsid combined with a protein bridge. *J. Virol.* **77**, 12931–12940 (2003).
45. Tai, C. K. *et al.* Antibody-mediated targeting of replication-competent retroviral vectors. *Hum. Gene Ther.* **14**, 789–802 (2003).
46. Russell, S. J., Hawkins, R. E. & Winter, G. Retroviral vectors displaying functional antibody fragments. *Nucleic Acids Res.* **21**, 1081–1085 (1993).
The first demonstration of genetic incorporation of a single-chain antibody into an enveloped virus, conferring novel binding specificity to the vector.
47. Yang, Q. *et al.* Development of novel cell surface CD34-targeted recombinant adenoassociated virus vectors for gene therapy. *Hum. Gene Ther.* **9**, 1929–1937 (1998).
48. Chowdhury, S., Chester, K. A., Bridgewater, J., Collins, M. K. & Martin, F. Efficient retroviral vector targeting of carcinoembryonic antigen-positive tumors. *Mol. Ther.* **9**, 85–92 (2004).
49. Nakamura, T. *et al.* Rescue and propagation of fully retargeted oncolytic measles viruses. *Nature Biotechnol.* **23**, 209–214 (2005).
This study uses one of the most potent oncolytic virus types that is currently studied: the measles virus. Ablation of native tropism is achieved in combination with targeting by genetically incorporated single-chain antibodies, generating vectors that reduce tumour size and enhance survival in animal models.
50. Menotti, L., Cerretani, A. & Campadelli-Fiume, G. A herpes simplex virus recombinant that exhibits a single-chain antibody to HER2/neu enters cells through the mammary tumor receptor, independently of the gD receptors. *J. Virol.* **80**, 5531–5539 (2006).
51. Larochelle, A., Peng, K. W. & Russell, S. J. Lentiviral vector targeting. *Curr. Top. Microbiol. Immunol.* **261**, 143–163 (2002).
52. Zhou, G. & Roizman, B. Characterization of a recombinant herpes simplex virus 1 designed to enter cells via the IL13Rα2 receptor of malignant glioma cells. *J. Virol.* **79**, 5272–5277 (2005).
53. Hatziioannou, T., Valsesia-Wittmann, S., Russell, S. J. & Cosset, F. L. Incorporation of fowl plague virus hemagglutinin into murine leukemia virus particles and analysis of the infectivity of the pseudotyped retroviruses. *J. Virol.* **72**, 5313–5317 (1998).
54. Verhoeyen, E. *et al.* Novel lentiviral vectors displaying 'early-acting cytokines' selectively promote survival and transduction of NOD/SCID repopulating human hematopoietic stem cells. *Blood* **106**, 3386–3395 (2005).
55. Dreja, H. & Piechaczyk, M. The effects of N-terminal insertion into VSV-G of an scFv peptide. *Virol. J.* **3**, 69 (2006).
56. Magnusson, M. K., Hong, S. S., Henning, P., Boulanger, P. & Lindholm, L. Genetic retargeting of adenovirus vectors: functionality of targeting ligands and their influence on virus viability. *J. Gene Med.* **4**, 356–370 (2002).
57. Shimizu, Y. & Hendershot, L. M. Organization of the functions and components of the endoplasmic reticulum. *Adv. Exp. Med. Biol.* **594**, 37–46 (2007).
58. Maggioni, C. & Braakman, I. Synthesis and quality control of viral membrane proteins. *Curr. Top. Microbiol. Immunol.* **285**, 175–198 (2005).
59. Fielding, A. K., Maurice, M., Morling, F. J., Cosset, F. L. & Russell, S. J. Inverse targeting of retroviral vectors: selective gene transfer in a mixed population of hematopoietic and nonhematopoietic cells. *Blood* **91**, 1802–1809 (1998).
60. Cosset, F. L. *et al.* Retroviral retargeting by envelopes expressing an N-terminal binding domain. *J. Virol.* **69**, 6314–6322 (1995).
61. Chadwick, M. P., Morling, F. J., Cosset, F. L. & Russell, S. J. Modification of retroviral tropism by display of IGF-I. *J. Mol. Biol.* **285**, 485–494 (1999).
62. Sandrin, V., Russell, S. J. & Cosset, F. L. Targeting retroviral and lentiviral vectors. *Curr. Top. Microbiol. Immunol.* **281**, 137–178 (2003).
63. Szecsi, J. *et al.* Targeted retroviral vectors displaying a cleavage site-engineered hemagglutinin (HA) through HA-protease interactions. *Mol. Ther.* **14**, 735–744 (2006).
64. Martin, F., Chowdhury, S., Neil, S., Phillipps, N. & Collins, M. K. Envelope-targeted retrovirus vectors transduce melanoma xenografts but not spleen or liver. *Mol. Ther.* **5**, 269–274 (2002).
65. Peng, K. W. *et al.* Organ distribution of gene expression after intravenous infusion of targeted and untargeted lentiviral vectors. *Gene Ther.* **8**, 1456–1463 (2001).
66. Denis, C. V. Molecular and cellular biology of von Willebrand factor. *Int. J. Hematol.* **75**, 3–8 (2002).
67. Morse, M. Technology evaluation: Rexin-G, Epeius Biotechnologies. *Curr. Opin. Mol. Ther.* **7**, 164–169 (2005).
68. Gordon, E. M. *et al.* Systemic administration of a matrix-targeted retroviral vector is efficacious for cancer gene therapy in mice. *Hum. Gene Ther.* **12**, 193–204 (2001).
69. Gordon, E. M. *et al.* Pathotropic nanoparticles for cancer gene therapy Rexin-G IV: three-year clinical experience. *Int. J. Oncol.* **29**, 1053–1064 (2006).
70. Stachler, M. D. & Bartlett, J. S. Mosaic vectors comprised of modified AAV1 capsid proteins for efficient vector purification and targeting to vascular endothelial cells. *Gene Ther.* **13**, 926–931 (2006).
71. Stoff-Khalili, M. A. *et al.* Gene transfer to carcinoma of the breast with fiber-modified adenoviral vectors in a tissue slice model system. *Cancer Biol. Ther.* **4**, 1203–1210 (2005).
72. Wu, H. *et al.* Preclinical evaluation of a class of infectivity-enhanced adenoviral vectors in ovarian cancer gene therapy. *Gene Ther.* **11**, 874–878 (2004).
73. Gollan, T. J. & Green, M. R. Redirecting retroviral tropism by insertion of short, nondisruptive peptide ligands into envelope. *J. Virol.* **76**, 3558–3563 (2002).
74. Fjeldstad, K. & Kolset, S. O. Decreasing the metastatic potential in cancers — targeting the heparan sulfate proteoglycans. *Curr. Drug Targets* **6**, 665–682 (2005).
75. Bouri, K. *et al.* Polylysine modification of adenoviral fiber protein enhances muscle cell transduction. *Hum. Gene Ther.* **10**, 1633–1640 (1999).
76. Mahasreshti, P. J. *et al.* Ovarian cancer targeted adenoviral-mediated mda-7/IL-24 gene therapy. *Gynecol. Oncol.* **100**, 521–532 (2006).
77. Bauerschmitz, G. J. *et al.* Treatment of ovarian cancer with a tropism modified oncolytic adenovirus. *Cancer Res.* **62**, 1266–1270 (2002).
78. Page, J. G. *et al.* Identifying the safety profile of a novel infectivity-enhanced conditionally replicative adenovirus, Ad5-δ24-RGD, in anticipation of a phase I trial for recurrent ovarian cancer. *Am. J. Obstet. Gynecol.* **196**, 389 e1–e9; discussion **389** e9–e10 (2007).

79. Maheshri, N., Koerber, J. T., Kaspar, B. K. & Schaffer, D. V. Directed evolution of adeno-associated virus yields enhanced gene delivery vectors. *Nature Biotechnol.* **24**, 198–204 (2006).
A rational vector design strategy for infecting previously resistant cell types and escaping neutralizing antibodies is suggested in this seminal study. Randomly mutating the capsid protein of AAV, followed by screening of the newly generated AAV library by affinity chromatography and incubation with anti-AAV serum, yields vectors with altered binding affinities and antibody-evasion properties.
80. Barry, M. A., Dower, W. J. & Johnston, S. A. Toward cell-targeting gene therapy vectors: selection of cell-binding peptides from random peptide-presenting phage libraries. *Nature Med.* **2**, 299–305 (1996).
81. Ghosh, D. & Barry, M. A. Selection of muscle-binding peptides from context-specific peptide-presenting phage libraries for adenoviral vector targeting. *J. Virol.* **79**, 13667–13672 (2005).
82. Bupp, K., Sarangi, A. & Roth, M. J. Selection of feline leukemia virus envelope proteins from a library by functional association with a murine leukemia virus envelope. *Virology* **351**, 340–348 (2006).
83. Bupp, K. & Roth, M. J. Altering retroviral tropism using a random-display envelope library. *Mol. Ther.* **5**, 329–335 (2002).
84. Bupp, K., Sarangi, A. & Roth, M. J. Probing sequence variation in the receptor-targeting domain of feline leukemia virus envelope proteins with peptide display libraries. *J. Virol.* **79**, 1463–1469 (2005).
85. Noureddini, S. C. *et al.* Generation and selection of targeted adenoviruses embodying optimized vector properties. *Virus Res.* **116**, 185–195 (2006).
86. Soong, N. W. *et al.* Molecular breeding of viruses. *Nature Genet.* **25**, 436–439 (2000).
87. White, S. J. *et al.* Targeted gene delivery to vascular tissue *in vivo* by tropism-modified adeno-associated virus vectors. *Circulation* **109**, 513–519 (2004).
88. Nicklin, S. A., Wu, E., Nemerow, G. R. & Baker, A. H. The influence of adenovirus fiber structure and function on vector development for gene therapy. *Mol. Ther.* **12**, 384–393 (2005).
89. Bomsel, M. Transcytosis of infectious human immunodeficiency virus across a tight human epithelial cell line barrier. *Nature Med.* **3**, 42–47 (1997).
90. Di Pasquale, G. & Chiorini, J. A. AAV transcytosis through barrier epithelia and endothelium. *Mol. Ther.* **13**, 506–516 (2006).
Vector extravasation from the circulation into the target organ is frequently hindered by barrier layers. This work shows that some AAV serotypes cross such barriers in a serotype- and cell-type-specific manner by transcytosis.
91. Zhu, Z. B. *et al.* Transport across a polarized monolayer of Caco-2 cells by transferrin receptor-mediated adenovirus transcytosis. *Virology* **325**, 116–128 (2004).
92. Tang, Y. *et al.* Directing adenovirus across the blood–brain barrier via melanotransferrin (P97) transcytosis pathway in an in vitro model. *Gene Ther.* **14**, 523–532 (2007).
93. Pereboeva, L., Komarova, S., Mahasreshti, P. J. & Curiel, D. T. Fiber-mosaic adenovirus as a novel approach to design genetically modified adenoviral vectors. *Virus Res.* **105**, 35–46 (2004).
94. Nakamura, T. & Russell, S. J. Oncolytic measles viruses for cancer therapy. *Expert Opin. Biol. Ther.* **4**, 1685–1692 (2004).
95. Hallak, L. K., Merchan, J. R., Storgard, C. M., Loftus, J. C. & Russell, S. J. Targeted measles virus vector displaying echistatin infects endothelial cells via $\alpha_v\beta_3$ and leads to tumor regression. *Cancer Res.* **65**, 5292–5300 (2005).
96. Peng, K. W. *et al.* Oncolytic measles viruses displaying a single-chain antibody against CD38, a myeloma cell marker. *Blood* **101**, 2557–2562 (2003).
97. Hasegawa, K. *et al.* The use of a tropism-modified measles virus in folate receptor-targeted virotherapy of ovarian cancer. *Clin. Cancer Res.* **12**, 6170–6178 (2006).
98. Allen, C. *et al.* Retargeted oncolytic measles strains entering via the EGFRvIII receptor maintain significant antitumor activity against gliomas with increased tumor specificity. *Cancer Res.* **66**, 11840–11850 (2006).
99. Breun, S., Salmons, B., Gunzburg, W. H. & Baumann, J. G. Protection of MLV vector particles from human complement. *Biochem. Biophys. Res. Commun.* **264**, 1–5 (1999).
100. Kiang, A. *et al.* Multiple innate inflammatory responses induced after systemic adenovirus vector delivery depend on a functional complement system. *Mol. Ther.* **14**, 588–598 (2006).
101. Moskalenko, M. *et al.* Epitope mapping of human anti-adeno-associated virus type 2 neutralizing antibodies: implications for gene therapy and virus structure. *J. Virol.* **74**, 1761–1766 (2000).
102. Zhi, Y. *et al.* Efficacy of severe acute respiratory syndrome vaccine based on a nonhuman primate adenovirus in the presence of immunity against human adenovirus. *Hum. Gene Ther.* **17**, 500–506 (2006).
103. Croyle, M. A. *et al.* PEGylated helper-dependent adenoviral vectors: highly efficient vectors with an enhanced safety profile. *Gene Ther.* **12**, 579–587 (2005).
104. Parker, A. L. *et al.* Multiple vitamin K-dependent coagulation zymogens promote adenovirus-mediated gene delivery to hepatocytes. *Blood* **108**, 2554–2561 (2006).
105. Shayakhmetov, D. M., Gaggar, A., Ni, S., Li, Z. Y. & Lieber, A. Adenovirus binding to blood factors results in liver cell infection and hepatotoxicity. *J. Virol.* **79**, 7478–7491 (2005).
Systemic application of adenoviral vectors is frequently limited by liver sequestration and subsequent toxicity. This study shows that blood factors bridge the adenoviral fibre knob to receptors on liver cells and that mutations in the knob can ablate the binding of blood factors and reduce liver toxicity.
106. Lyons, M. *et al.* Adenovirus type 5 interactions with human blood cells may compromise systemic delivery. *Mol. Ther.* **14**, 118–128 (2006).
107. Li, Q., Kay, M. A., Finegold, M., Stratford-Perricaudet, L. D. & Woo, S. L. Assessment of recombinant adenoviral vectors for hepatic gene therapy. *Hum. Gene Ther.* **4**, 403–409 (1993).
108. Parry, S., Zhang, J., Koi, H., Arechavaleta-Velasco, F. & Elovitz, M. A. Transcytosis of human immunodeficiency virus 1 across the placenta is enhanced by treatment with tumour necrosis factor alpha. *J. Gen. Virol.* **87**, 2269–2278 (2006).
109. Fechner, H. *et al.* Expression of coxsackie adenovirus receptor and α_v-integrin does not correlate with adenovector targeting *in vivo* indicating anatomical vector barriers. *Gene Ther.* **6**, 1520–1535 (1999).
110. Komarova, S., Kawakami, Y., Stoff-Khalili, M. A., Curiel, D. T. & Pereboeva, L. Mesenchymal progenitor cells as cellular vehicles for delivery of oncolytic adenoviruses. *Mol. Cancer Ther.* **5**, 755–766 (2006).
The use of cellular vehicles as carriers of a vector load is a promising method to overcome barriers that are presented by the vascular bed, an extracellular matrix or stromal cells. Mesenchymal progenitor cells carrying oncolytic vectors are shown to reduce tumour size and increase survival in mice, as compared with treatment with the vector alone.
111. Stoff-Khalili, M. A. *et al.* Mesenchymal stem cells as a vehicle for targeted delivery of CRAds to lung metastases of breast carcinoma. *Breast Cancer Res. Treat.* 13 Jan 2007 (doi:10.1007/s10549-006-9449-8).
112. Shayakhmetov, D. M., Li, Z. Y., Ni, S. & Lieber, A. Targeting of adenovirus vectors to tumor cells does not enable efficient transduction of breast cancer metastases. *Cancer Res.* **62**, 1063–1068 (2002).
113. Kuppen, P. J. *et al.* Tumor structure and extracellular matrix as a possible barrier for therapeutic approaches using immune cells or adenoviruses in colorectal cancer. *Histochem. Cell Biol.* **115**, 67–72 (2001).
114. Wang, L. *et al.* Prolonged and inducible transgene expression in the liver using gutless adenovirus: a potential therapy for liver cancer. *Gastroenterology* **126**, 278–289 (2004).
115. Rivera, A. A. *et al.* Combining high selectivity of replication with fiber chimerism for effective adenoviral oncolysis of CAR-negative melanoma cells. *Gene Ther.* **11**, 1694–1702 (2004).
116. Lam, J. T. *et al.* Inter-patient variation in efficacy of five oncolytic adenovirus candidates for ovarian cancer therapy. *J. Gene Med.* **6**, 1333–1342 (2004).
117. Kim, J. B. Three-dimensional tissue culture models in cancer biology. *Semin. Cancer Biol.* **15**, 365–377 (2005).
118. Korokhov, N. *et al.* A single-component CD40-targeted adenovirus vector displays highly efficient transduction and activation of dendritic cells in a human skin substrate system. *Mol. Pharm.* **2**, 218–223 (2005).
119. Marie, J. C. *et al.* Linking innate and acquired immunity: divergent role of CD46 cytoplasmic domains in T cell induced inflammation. *Nature Immunol.* **3**, 659–666 (2002).
120. DiPaolo, N. *et al.* Evaluation of adenovirus vectors containing serotype 35 fibers for vaccination. *Mol. Ther.* **13**, 756–765 (2006).
121. Everts, M. *et al.* Selective induction of tumor-associated antigens in murine pulmonary vasculature using double-targeted adenoviral vectors. *Gene Ther.* **12**, 1042–1048 (2005).
122. Izumi, M. *et al. In vivo* analysis of a genetically modified adenoviral vector targeted to human CD40 using a novel transient transgenic model. *J. Gene Med.* **7**, 1517–1525 (2005).
123. Tallone, T. *et al.* A mouse model for adenovirus gene delivery. *Proc. Natl Acad. Sci. USA* **98**, 7910–7915 (2001).
124. Nakayama, M. *et al.* An adenovirus serotype 5 vector with fibers derived from ovine atadenovirus demonstrates CAR-independent tropism and unique biodistribution in mice. *Virology* **350**, 103–115 (2006).
125. Pan, D. *et al.* Biodistribution and toxicity studies of VSVG-pseudotyped lentiviral vector after intravenous administration in mice with the observation of *in vivo* transduction of bone marrow. *Mol. Ther.* **6**, 19–29 (2002).
126. Makower, D. *et al.* Phase II clinical trial of intralesional administration of the oncolytic adenovirus ONYX-015 in patients with hepatobiliary tumors with correlative p53 studies. *Clin. Cancer Res.* **9**, 693–702 (2003).
127. Galanis, E. *et al.* Phase I-II trial of ONYX-015 in combination with MAP chemotherapy in patients with advanced sarcomas. *Gene Ther.* **12**, 437–445 (2005).
128. Luker, G. D. *et al.* Noninvasive imaging of protein–protein interactions in living animals. *Proc. Natl Acad. Sci. USA* **99**, 6961–6966 (2002).
129. Soling, A., Theiss, C., Jungmichel, S. & Rainov, N. G. A dual function fusion protein of Herpes simplex virus type 1 thymidine kinase and firefly luciferase for noninvasive *in vivo* imaging of gene therapy in malignant glioma. *Genet. Vaccines Ther.* **2**, 7 (2004).
130. Shah, K. & Weissleder, R. Molecular optical imaging: applications leading to the development of present day therapeutics. *NeuroRx* **2**, 215–225 (2005).
131. Le, L. P. *et al.* Fluorescently labeled adenovirus with pIX-EGFP for vector detection. *Mol. Imaging* **3**, 105–116 (2004).
132. Le, L. P. *et al.* Dynamic monitoring of oncolytic adenovirus *in vivo* by genetic capsid labeling. *J. Natl Cancer Inst.* **98**, 203–214 (2006).
Whereas most imaging reporter systems require active transgene expression, the new system described here exploits genetic labelling of the capsid with a fluorescent protein to follow the dynamic processes of the vector, independent of transgene expression.
133. Le, L. P., Li, J., Ternovoi, V. V., Siegal, G. P. & Curiel, D. T. Fluorescently tagged canine adenovirus via modification with protein IX-enhanced green fluorescent protein. *J. Gen. Virol.* **86**, 3201–3208 (2005).
134. Li, J., Le, L., Sibley, D. A., Mathis, J. M. & Curiel, D. T. Genetic incorporation of HSV-1 thymidine kinase into the adenovirus protein IX for functional display on the virion. *Virology* **338**, 247–258 (2005).
135. Matthews, Q. L. *et al.* Genetic incorporation of a herpes simplex virus type 1 thymidine kinase and firefly luciferase fusion into the adenovirus protein IX for functional display on the virion. *Mol. Imaging* **5**, 510–519 (2006).
136. Waehler, R. *et al.* Low-dose adenoviral immunotherapy of rat hepatocellular carcinoma using single-chain interleukin-12. *Hum. Gene Ther.* **16**, 307–317 (2005).
137. Raty, J. K. *et al.* Magnetic resonance imaging of viral particle biodistribution in vivo. *Gene Ther.* **13**, 1440–1446 (2006).
138. Berk, A. J. *Fields Virology* vol. 2 (eds Knipe, D. M. & Howley, M. P.) 2355–2436 (Lippincott Williams & Wilkins, Philadelphia, 2007).
139. Summerford, C. & Samulski, R. J. Membrane-associated heparan sulfate proteoglycan is a receptor for adeno-associated virus type 2 virions. *J. Virol.* **72**, 1438–1445 (1998).
140. Wu, Z., Asokan, A. & Samulski, R. J. Adeno-associated virus serotypes: vector toolkit for human gene therapy. *Mol. Ther.* **14**, 316–327 (2006).
141. Goff, S. P. in *Fields Virology* vol. 2 (eds Knipe, D. M. & Howley, M. P.) 2000–2069 (Lippincott Williams & Wilkins, Philadelphia, 2007).

142. Pizzato, M., Marlow, S. A., Blair, E. D. & Takeuchi, Y. Initial binding of murine leukemia virus particles to cells does not require specific Env-receptor interaction. *J. Virol.* **73**, 8599–8611 (1999).
143. Haynes, C., Erlwein, O. & Schnierle, B. S. Modified envelope glycoproteins to retarget retroviral vectors. *Curr. Gene Ther.* **3**, 405–410 (2003).
144. Harrison, S. C. Mechanism of membrane fusion by viral envelope proteins. *Adv. Virus Res.* **64**, 231–261 (2005).
145. Bartlett, J. S., Kleinschmidt, J., Boucher, R. C. & Samulski, R. J. Targeted adeno-associated virus vector transduction of nonpermissive cells mediated by a bispecific F(ab′γ)2 antibody. *Nature Biotechnol.* **17**, 181–186 (1999).
146. Harding, T. C. *et al.* Enhanced gene transfer efficiency in the murine striatum and an orthotopic glioblastoma tumor model, using AAV-7- and AAV-8-pseudotyped vectors. *Hum. Gene Ther.* **17**, 807–820 (2006).
147. Reynolds, P. N. *et al.* Combined transductional and transcriptional targeting improves the specificity of transgene expression *in vivo*. *Nature Biotechnol.* **19**, 838–842 (2001).
Transductional vector targeting by itself does not always provide satisfactory transgene expression in the target organ versus non-target organs. This study pioneered the combination of a bispecific antibody that targets the vector to the pulmonary endothelium with a promoter that is specific for the same tissue, allowing up to two orders of magnitude greater transgene expression in the target versus non-target tissues.
148. Wurdinger, T. *et al.* Targeting non-human coronaviruses to human cancer cells using a bispecific single-chain antibody. *Gene Ther.* **12**, 1394–1404 (2005).
149. Stone, D. *et al.* Development and assessment of human adenovirus type 11 as a gene transfer vector. *J. Virol.* **79**, 5090–5104 (2005).

Acknowledgements
This work was supported with a grant by the German Research Foundation (DFG) to R.W., with grants from the US National Institutes of Health (NIH) to S.J.R. and grants from the NIH and the US Department of Defense (DOD) to D.T.C. The authors wish to thank J. Roth, J. T. Douglas, S. J. Hedley, S. Ponnazhagan, Q. L. Matthews, M. Everts and J. N. Glasgow for their critical reading of the manuscript.

Competing interests statement
The authors declare no competing financial interests.

DATABASES

The following terms in this article are linked online to:
OMIM: http://www.ncbi.nlm.nih.gov/entrez/query.fcgi?db=OMIM
cystic fibrosis | Parkinson disease
UniProtKB: http://ca.expasy.org/sprot
CAR | CCR5 | CD4 | CD40 | CD40L | CD46 | CXCR4

FURTHER INFORMATION

American Society of Gene Therapy: http://www.asgt.org
European Society of Gene and Cell Therapy: http://www.esgct.org
Gene and Virus Therapy Program, Mayo Clinic: http://mayoresearch.mayo.edu/mayo/research/gene_virus_therapy_program/
Gene Therapy Clinical Trials Worldwide web site: http://www.wiley.co.uk/genetherapy/clinical
The Gene Therapy Center, University of Alabama at Birmingham: www.uab.edu/genetherapy
Access to this links box is available online.

IV. Submitted & In-Press Manuscripts (as of Dec 18, 2007)

4. Glasgow JN, Hemminki A, Curiel DT. Modified adenoviruses for gene therapy. In *Gene and Cell Therapy: Therepeutic Mechanisms and Strategies*, 3rd edition. NS Templeton (ed). Taylor & Francis, CRC Press. In press.
5. Li HJ, Everts M. Yamamoto Y, Curiel DT, Herschman HR. Combined transductional targeting and transcriptional restriction enhanced adenovirus gene delivery. Cancer Res. Submitted.
6. Li HJ, Everts M, Curiel DT, Herschman HR. Trimerization of a bi-specific transductional adapter improves tumor targeting of adenoviral vectors, in culture and in vivo. Nat Biotech. Submitted.

Gene and Cell Therapy. Therapeutic Mechanisms and Strategies, Third Edition
Nancy Smyth Templeton, Editor
Taylor & Francis, CRC Press

Chapter: Modified adenoviruses for gene therapy

Joel N. Glasgow[1,2 *], Akseli Hemminki[3] and David T. Curiel[2]

[1]Division Cardiovascular Disease, [2]Division of Human Gene Therapy, Departments of Medicine, Pathology, Surgery and the Gene Therapy Center, University of Alabama at Birmingham, Birmingham, AL 35294-3300, USA, [3]K. Albin Johansson Research Professor (Finnish Cancer Institute) Cancer Gene Therapy Group, Molecular Cancer Biology Program & Transplantation Laboratory & Department of Oncology, University of Helsinki & Helsinki University Central Hospital, P.O. Box 63, Biomedicum, 00014 University of Helsinki, Finland (street address: Haartmaninkatu 8, 00290 Helsinki)

*Corresponding Author
Mailing Address:
University of Alabama at Birmingham
901 19th Street South
BMR2-408
Birmingham AL, 35294-2172
Ph: 205-975-7531
FAX: 205-975-7949
Email: jng@uab.edu

OUTLINE.

NOTE: Figure legends follow references

I. INTRODUCTION

While still in its infancy, gene-based therapy has emerged as a potentially powerful therapeutic platform. The concept of gene therapy as a rational molecular intervention is simple; that is, to correct or eradicate defective tissues via delivery of nucleic acids. However, practical implementation of safe, highly effective gene-based interventions has been difficult due to the stringent and complex requirements of this paradigm. Indeed, the introduction of functional foreign nucleic acids into mammalian target cells without oncogenicity or significant toxicity or immune response represents a daunting task unique in biomedicine. This realization has

spawned the field of vector design, which has for twenty years sought to engineer gene delivery vector systems compatible with the stringent mandates of human clinical use.

Vectors based on human adenovirus (Ad) serotypes 2 and 5 continue to show utility as gene therapy vectors, particularly in the context of cancer gene therapy, due to several innate biological characteristics: Replication-deficient Ad vectors display *in vivo* stability and superior gene transfer efficiency to numerous dividing and non-dividing cell targets *in vivo* and rarely cause severe disease in humans. Further, production parameters for clinical grade Ad vectors are well established. In 2007, Ad vectors were employed in one-fourth of clinical trials worldwide (326 of 1,309) with two-thirds of all trials being for cancer (871 of 1,309).[1]

Nonetheless, clinical trial results of Ad vectors have clearly exposed the need to advance Ad vector technology. Relatively lackluster clinical performance of Ad-based agents to date has provided clear direction for vector modifications designed to improve efficacy and safety. In this regard, two distinct approaches have been employed, 1) transductional targeting, which approaches limit the entry of agents to target cells, and 2) transcriptional targeting, which restricts expression of transgenes (or Ad replication, in some cases) to target tissues by using tissue- or tumor-specific promoters (TSPs). The following is a discussion of Ad biology, barriers to transductional targeting and a review of the vector modifications applied toward transforming the human adenovirus into a clinically effective therapeutic agent.

II. ADENOVIRUS STRUCTURE

The family *Adenoviridae* contains over one hundred serotypes, including fifty-two human serotypes that are divided among seven species (A-G) based on genome homology and organization, oncogenicity and hemagglutination properties.[2-6] The human adenovirus is a non-enveloped icosahedral particle that encapsulates up to a 36-kilobase double-stranded DNA genome. The Ad capsid is comprised of several minor and three major capsid proteins: hexon is

the most abundant structural component with 720 copies per virion and constitutes the bulk of the protein shell; five penton monomers form the penton base platform at each of the twelve capsid vertices to which the twelve fiber homo-trimers attach (Fig. 1). The distal tip of each fiber is composed of a globular knob domain which serves as the major viral attachment site for cellular receptors. Hexon appears to play only a structural role as a coating protein, while the penton base and the fiber are responsible for distinct virion-cell interactions that constitute Ad tropism. Detailed structures of hexon[7-11], penton base[12] and fiber[13,14] have been determined by crystallography; the high-resolution structure of the entire virion has been determined by various methods.[15,16]

III. ADENOVIRUS TRANSDUCTION PATHWAY

Intense research efforts into Ad biology has revealed crucial steps involved in gene transfer. The tropism of Ad is determined by two distinct virus-cell interactions: attachment to a primary receptor molecule at the cell surface, followed by interaction with molecules responsible for virion internalization. Initial high-affinity binding of the virion occurs via direct binding of the fiber knob domain to its cognate primary cellular receptor, which is the 346 amino acid coxsackie and adenovirus receptor (CAR) glycoprotein for most serotypes including Ad2 and Ad5, which are widely used in gene therapy approaches.[17,18] Other receptors have been described for Ad5, although the nature of their interaction(s) with the Ad5 virion is unclear and their roles appear limited. These receptors include heparin sulfate glycosaminoglycans,[19,20] class I major histocompatability complex,[21] and vascular cell adhesion molecule-1.[22] Receptor binding is followed by receptor-mediated endocytosis of the virion via interaction of penton base Arg-Gly-Asp (RGD) motifs with cellular integrins including $\alpha v\beta 3$ and $\alpha v\beta 5$[23], $\alpha v\beta 1$[24], $\alpha_3\beta 1$ and $\alpha_5\beta 1$.[25] Virus enters the cell in clathrin-coated vesicles[26] and is transported to endosomes. Acidification of the endosome results in stepwise virion disassembly and subsequent release of the virus core

into the cytosol, where it docks at the nuclear membrane. Further capsid disassembly and subsequent nuclear import of the Ad genome is then achieved via interaction of genome-associated Ad core proteins with transportin and importin components of the nuclear pore complex. [27-29]

IV. TRANSDUCTIONAL TARGETING OF ADENOVIRUS

Targeted gene delivery is ultimately predicated on the ability of the vector to discriminate between target and non-target cells via interaction with unique cell- or disease-specific surface markers. However, the CAR-dependence of Ad5 transduction results in a scenario wherein non-target but high-CAR cells can be infected, whereas target tissues, if low in CAR, remain poorly infected. This may be of particular relevance in Ad-based cancer gene therapy, as increased CAR expression appears to have a growth inhibitory effect on some cancer cell lines, while loss of CAR expression correlates with tumor progression and advanced disease. Indeed, a lack or down-regulation of CAR has been reported for various tumor types, such as ovarian, prostate, lung, breast and colorectal cancer, melanoma, glioma and rhabdomyosarcoma [30-39] (reviewed in [40,41]). Further, this may be a general phenomenon associated with the carcinogenesis of various tumor types, as inverse correlation with tumor grade has been suggested [37,38]. CAR is a 346 amino acid glycoprotein containing a single membrane-spanning domain and is localized to tight junctions[42] where it mediates homotypic cell adhesion.[43,44] The functions of CAR are not fully understood, but it plays role in cell adhesion and perhaps cell cycle regulation, as it has a role in suppression of tumor growth [38]. Interestingly, a preliminary report has suggested inverse correlation between activity of the tumor-associated Raf-MEK-ERK pathway and CAR expression.[45] For treatment of cancer with Ad-based vectors, these associations are problematic since CAR-dependant approaches may not be useful against advanced disease if CAR is variably expressed in these tumors. Thus, targeting of Ad to tumor cells should be useful for increasing

the clinical efficacy and safety of approaches. Further, considering the widespread expression of CAR, targeting approaches may be advantageous for increasing the specificity of any clinical Ad gene therapy application.

The biodistribution of Ad-based vectors *in vivo*, however, is not determined solely by receptor biodistribution.[46] Intravenous administration of Ad results in accumulation in the liver, spleen, heart, lung, and kidneys of mice, although these tissues may not necessarily be the highest in CAR expression.[47,48] Instead, the degree of blood flow and the structure of the vasculature in each organ probably contribute to the biodistribution. This is true with regard to the liver in particular, which retains the majority of systemically administered Ad particles via hepatic macrophage (Kupffer cell) uptake[49,50] and hepatocyte transduction,[51] leading to Ad-mediated inflammation and liver toxicity.[52-55] Thus, the nature of adenovirus-host interactions that determine the fate of systemically applied Ad has come under considerable scrutiny.

To this end, initial attempts to "de-target" the liver were based on the supposition that CAR- and integrin-based interactions were required for liver transduction *in vivo*. Strategies to inhibit hepatocyte and/or liver Kupffer cell uptake by ablating CAR- or integrin-binding motifs in the Ad capsid have been largely unsuccessful, however, indicating that native Ad tropism determinants contribute little to vector hepatotropism *in vivo*.[56-60] These data notwithstanding, work by several groups has implicated the fiber protein as a major structural determinant of liver tropism *in vivo* (reviewed by Nicklin, et al.[61]). For example, shortening of the native fiber shaft domain of the Ad 5 fiber,[62] or replacement of the Ad5 shaft with the short Ad3 shaft domain[63] was shown to attenuate liver uptake *in vivo* following intravenous delivery. In related work, Smith and co-workers examined the role of a putative heparan sulfate proteoglycan (HSPG)-binding motif, KKTK, in the third repeat of the native fiber shaft.[64] Replacement of this motif

with an irrelevant peptide sequence reduced reporter gene expression in the liver by 90 percent. This was also the first suggestion of the importance of HSPG as Ad receptors *in vivo*.

Critical work by Shayakhmetov and colleagues shed light on these apparently contradictory lines of evidence by uncovering a major role for coagulation factor IX (fIX) and complement component C4-binding protein (C4BP) in hepatocyte and Kupffer cell uptake of intravenous Ad.[65] A key finding was that these blood factors mediated *in vivo* tropism by cross-linking Ad particles to hepatocellular HSGP and the LDL-receptor related protein (reviewed in [66]). Kupffer cell sequestration of Ad particles was likewise heavily dependent on Ad association with fIX and C4BP. Importantly, Ad5 vectors containing fibers genetically modified to ablate fIX and C4BP binding provided 50-fold lower liver transduction with reduced inflammation and hepatotoxicity. Extending this work, this group also showed that Ad5 virions bind to circulating platelets *in vivo*, resulting in their aggregation, entrapment in liver sinusoids and eventual clearance by Kupffer cells.[49] Further, Ad sequestration in organs was reduced by platelet depletion prior to systemic vector injection.

These efforts serve to highlight the complexity of vector/host interplay, and have identified genetic modifications that have important practical implications for designing safer and more effective Ad-based vectors for clinical applications. In the absence of a clinically defined upper limit for ectopic liver transduction in humans, it is clear that the concepts of “de-targeting” and “re-targeting” must be simultaneously employed to allow for maximum Ad vector efficacy at the lowest possible dose. Two distinct approaches have been employed to transductionally target Ad-based therapeutic vectors: 1) adapter molecule-based targeting, and 2) genetic targeting via structural manipulation of the Ad capsid.

A. Adapter-based adenovirus targeting

The formation of a “molecular bridge” between the Ad vector and a cell surface receptor constitutes the adapter-based concept of Ad targeting (Fig. 2). Adapter function is performed by so called “bi-specific” molecules that cross-link the Ad vector to alternative cell surface receptors, bypassing the native CAR-based tropism. This approach is predicated by the aforementioned two-step entry mechanism of the Ad virion wherein attachment is distinct from internalization. In this way, alternative means of cellular attachment do not impede Ad cell entry. The majority of current adapter-based Ad targeting approaches incorporate the two mandates of delivery targeting, that of ablation of native CAR-dependent Ad tropism and formation of a novel tropism to previously identified cellular receptors. Bi-specific adapter molecules include, but are not limited to: bi-specific antibodies, chemical conjugates between antibody fragments (Fab) and cell-selective ligands such as folate, Fab-antibody conjugates using antibodies against target cell receptors, Fab-peptide ligand conjugates and multi-domain recombinant fusion proteins comprised of soluble CAR and peptide ligands or recombinant antibody fragments.

The first *in vitro* demonstration of Ad targeting via the adapter method resulted in CAR-independent, folate receptor-mediated cellular uptake of the virion by cancer cells overexpressing this receptor.[67] This was accomplished using a bi-specific conjugate consisting of an anti-knob neutralizing Fab chemically linked to folate. A similar targeting adapter comprised of the same anti-knob Fab as above fused to basic fibroblast growth factor (FGF2) was utilized to target Ad vectors to FGF receptor-positive Kaposi’s sarcoma and ovarian cancer substrates.[68,69] Upon intraperitoneal injection of Ad-Fab-FGF2 coding for Herpes simplex virus type I thymidine kinase (HSV-TK) into mice bearing human ovarian cancer, survival was prolonged.[70] Importantly, this targeting system also reduced hepatic toxicity and resulted in increased survival in melanoma[71] and ovarian cancer[72] xenograft mouse models. Other Fab-ligand conjugates

targeted against Ep-CAM, Tag-72, EGF receptor, CD40, and other cell markers have been employed in a similar manner with promising results.[31,34,73-77]

Dmitriev and colleagues developed a more elegant alternative to chemical conjugates by creating a single recombinant fusion molecule formed by a truncated, soluble form of CAR (sCAR) fused to either CD40[78] or epidermal growth factor (EGF).[79] Using the latter, a 9-fold increase in reporter gene expression was achieved in several EGFR-overexpressing cancer cell lines compared to untargeted Ad or EGFR-negative cells *in vitro*. EGF-directed targeting to EGFR-positive cells was shown to be dependent on cell surface EGFR density, an additional confirmation of Ad targeting specificity. Addressed also was the issue of virion/adapter complex stability, a critical issue if targeting adapters are to be employed *in vivo*. In this regard, pre-formed Ad/sCAR-EGF complexes subjected to gel filtration purification showed the same targeting profile as those not purified, indicating adequate Ad/adapter complex stability. To further increase Ad/sCAR-ligand complex stability, Kashentseva and colleagues developed a trimeric sCAR-anti-c-*erb*B2 single chain antibody adapter molecule. The trimeric sCAR-c-*erb*B2 adapter displayed increased affinity for the Ad fiber knob while augmenting gene transfer up to 17-fold in six c-*erb*B2-positive breast and ovarian cancer cell lines *in vitro*.[80] In similar work, Itoh and colleagues demonstrated improved efficiency of sCAR-based fusion molecule adapters.[81] Kim *et al*. showed that adapter trimerization yielded a 100-fold increase in infection of CAR-deficient human diploid fibroblasts compared to the monomeric sCAR adapter.[82] Importantly, *in vivo* employment of a non-targeted trimeric sCAR adapter attenuated liver transduction in mice following intravenous administration, indicating excellent *in vivo* stability of this Ad/trimeric adapter complex.

The above proof-of-principle studies and others have rationalized the further testing of targeting adapters *in vivo*. In this regard, Reynolds *et al*. employed a novel bi-specific adapter

composed of an anti-knob Fab chemically conjugated to a monoclonal antibody (9B9) raised against angiotensin converting enzyme (ACE), a surface molecule expressed preferentially on pulmonary capillary endothelium and upregulated in various disease states of the lung.[75] Following peripheral intravenous injection of the Ad/Fab-9B9 complex, reporter transgene expression and viral DNA in the lung was increased 20-fold over untargeted Ad and reporter gene expression in the liver, a non-target, high-CAR organ, was reduced by 83 percent. Further, ACE-targeted gene delivery of bone morphogenetic protein receptor type 2 (BMPR2) to the pulmonary vascular endothelium of rats reduced hypoxia-induced pulmonary hypertension, as reflected by reductions in pulmonary artery and right ventricular pressures, right ventricular hypertrophy, and muscularization of distal pulmonary arterioles.[83]

In another adapter-based *in vivo* targeting model, Everts and co-workers used a bi-functional adapter molecule comprised of sCAR fused to a single-chain antibody (MFE-23) directed against carcinoembryonic antigen (CEA).[84] Systemic administration of the Ad/sCAR-MFE-23 adapter complex increased gene expression in CEA-positive murine lung by 10-fold and reduced liver transduction, resulting in an improved lung-to-liver ratio of gene expression compared with untargeted Ad. In another study, the sCAR-MFE adapter was used to target Ad vectors to CEA-expressing cells *in vitro*, CEA-positive subcutaneous tumor grafts and hepatic tumor grafts following systemic administration of the Ad/sCAR-MFE complex[85]. Of note, Ad/sCAR-MFE liver transduction by was reduced by over 95% and CEA-negative tumors *in vivo* were not transduced, suggesting remarkable safety and specificity profiles for this approach.

Overall, adapter-based Ad targeting studies provide compelling evidence that Ad tropism modification can be achieved by targeting alternate cellular receptors and that this modality augments gene delivery to CAR-deficient target cells *in vitro*. Adapter targeted vectors have also performed well *in vivo*, although data so far is limited. While single-component systems have

been favored for employment in human gene therapy trials, rigorous analysis of the pharmoco-dynamics and -kinetics, and systemic stability of vector/adapter complexes may provide the rationale for clinical translation.

B. Adenovirus targeting via genetic modification: Fiber

Genetic manipulation of capsid proteins has yielded increasingly promising data in terms of Ad targeting. Direct capsid Ad modification may be advantageous over adapter molecules in that all virions harbor an identical modification and lack of stability is less likely. Redirection of Ad tropism via genetic capsid modification is conceptually elegant, but genetic targeting efforts must work within narrow structural constraints. The success of this approach depends upon modulation of the complex protein structure/function relationships that result in Ad tropism modification, without disrupting the innate molecular interactions required for proper biological function. Specifically, genetic modification can affect fiber trimerization, production, stability and ultimately packaging of infectious virions. Based on a clear understanding of Ad infection biology, development of genetically targeted vectors has rationally focused on the fiber, the primary capsid determinant of Ad tropism. In general, there have been three basic strategies for genetic tropism modification via structural modification of the Ad fiber: 1) so-called "fiber pseudotyping" 2) ligand incorporation into the fiber knob domain, and 3) "de-knobbing" of the fiber coupled with ligand addition (Fig. 3).

1. Fiber pseudotyping

As previously mentioned, clinically relevant tissues are often refractory to Ad5 infection, including several cancer cell types, due to negligible CAR levels. Ad fiber pseudotyping, the genetic replacement of either the entire fiber or knob domain with its structural counterpart from another human Ad serotype that recognizes a cellular receptor other than CAR, was first accomplished by Krasnykh *et al* to circumvent CAR deficiency.[86] This vector expresses a

chimeric fiber contains the Ad serotype 3 knob domain (Ad5/3) and demonstrates the same CAR-independent cell recognition as does Ad3. The use of another Ad5/3 vector selectively targeted low-CAR lymphoid cell lines *in vitro*, whereas these cells were refractory to Ad5 infection[87]. Ad5/3 has been useful for retargeting Ad5 to low-CAR primary ovarian carcinoma cells and cell lines[88,89] and primary glioma[90-92] *in vitro* and *in vivo*. Other fiber pseudotyped Ad vectors display CAR-independent tropism by virtue of the natural diversity in receptor recognition found in human species B and D fibers.[93] In this regard, primary receptors for species B Ads have been recently identified, including the complement regulatory protein CD46,[94-97] CD80 and CD86,[98] although an additional unknown receptor is postulated.[95] Species D adenovirus receptors include CD46 and α(2-3)-linked sialic acid, a common element of glycolipids.[99-101] Fiber pseudotyping has identified chimeric vectors with superior infectivity to Ad5 in several clinically relevant cell types including primary ovarian carcinoma cells,[88,89,102] vascular endothelial cells,[103] dendritic cells,[104] B-cells,[87] CD34+ hematopoietic cells,[105] synovial tissue,[106] human cardiovascular tissue[107] and others.[108,109] Interestingly, this strategy has been extended to exploit fiber elements from non-human Ads[110,111] and the fiber-like σ1 reovirus attachment protein, which targets cells expressing junctional adhesion molecule.[112,113]

2. Genetic ligand incorporation

To circumvent variable expression of CAR, targeting ligands have been incorporated into the Ad knob domain without ablating native CAR-binding. This has resulted in Ad vectors with expanded, rather than restricted, cell recognition. These efforts are based on rigorous structural analysis of the knob domain and have exploited two separate locations within the knob that tolerate genetic manipulation without loss of fiber function, the C-terminus and the HI-loop. Since the C-terminus of the Ad knob is solvent exposed, extension of the knob peptide to include a targeting peptide moiety is conceptually simple. Ads with C-terminal integrin-binding

arginine-glycine-aspartate (RGD) motifs and poly-lysine ligands have yielded some promising results *in vitro* and *in vivo,* but other peptide ligands were rendered ineffective in the C-terminus structural context,[114] presumably due to steric or other inhibition. On this basis, Krasnykh, *et al*. inserted a FLAG peptide sequence into an exposed loop structure that connects beta-sheets H and I (HI-loop) within the Ad5 knob, showing that this locale is structurally permissive to modification.[115] Indeed, the Ad5 HI-loop tolerates peptide insertions up to 100 amino acids with minimal negative effects on virion integrity, thus suggesting considerable potential for ligand incorporation at this site.[116] On this basis, Magnusson and colleagues developed a targeting approach via incorporation of complex ligands in the HI-loop. This group genetically inserted tandem HER2/neu reactive Affibody molecules in the HI-loop of a CAR binding-ablated fiber, resulting in CAR-independent, HER2-mediated cell infection *in vitro*.[117] Dmitriev and co-workers introduced an integrin-binding RGD peptide sequence into the HI-loop. The resulting vector, Ad5lucRGD, used the RGD/cellular integrin interaction to enhance gene delivery to ovarian cancer cell lines and primary tumors versus unmodified Ad5.[33,118,119] The expanded tropism of this vector has been useful in several other cancer contexts including carcinomas of the ovary, pancreas, colon cancer, and head and neck carcinomas, all of which frequently display highly variable CAR levels (reviewed in [120]). Wu *et al*. demonstrated that Ad vectors with a double fiber modification consisting of a C-terminal poly-lysine stretch, which interacts with heparan sulfates, and the HI-loop RGD provided increased infectivity in several CAR-deficient cell lines,[121] as well as human pancreatic islet cells,[122] ovarian carcinoma,[123] and cervical cancer cells *in vivo.*[124] Other targeting peptides have functioned in the HI-loop locale, including a vascular endothelial cell-binding motif SIGYLPLP.[125] This fiber modification also provided cancer cell selective infection.[126]

Korokhov, *et al*., Volpers *et al*. and others[127] have developed similar targeting approaches that embody elements of both genetic fiber modification and adapter based targeting by incorporating the immunoglobulin (Ig)-binding domain of *Staphylococcus aureus* protein A in to the fiber C-terminus or HI-loop.[128,129] As a result, these fiber-modified vectors form stable complexes with a wide variety of targeting molecules containing the Fc region of Ig. This provides the opportunity to screen numerous targeting molecules directed against a host of cell-surface elements. This approach was used to target and activate dendritic cells via an Fc-single chain antibody directed against CD40.[130] This system was also used to target ovarian cancer cells via an antibody directed against mesothelin,[131] as well as the pulmonary endothelium in a rat model in vivo.[132]

3. Knob-deleted fibers with complex ligands

The structural conflicts emerging from knob modifications and the observation that fiber-deleted Ad vectors could be produced[133,134] provided the conceptual basis for replacing the native fiber with knobless fibers. Virions containing a knobless fiber would be ablated for CAR binding, a hallmark of targeted Ad vectors. Simultaneous addition of a targeting ligand to the knobless fiber would result in a more specifically targeted Ad. The technical barrier to this approach is the innate trimerization function of the fiber knob domain, required for proper fiber function and capsid assembly. As solution was devised by addition of a foreign trimerization motif to replace the native fiber and/or knob.[135] Krasnykh *et al*. replaced the fiber and knob domains with bacteriophage T4 fibritin containing a C-terminal 6-His motif.[136] This novel Ad variant lacks the ability to interact with CAR and demonstrated up to a 100-fold increase in reporter gene expression to cells presenting an artificial 6-His binding receptor. A similar “de-knobbing” strategy was employed by Magnussen and colleagues, wherein an integrin-binding RGD motif was utilized, resulting in selective infection of integrin-expressing cell lines *in vitro*,[137] as well as human glandular cells.[138] Based on the feasibility of knob replacement with

foreign trimerization motifs, an elegant system was devised wherein the trimeric CD40 ligand was fused to the C-terminus of a knobless fiber.[139] Notably, this vector provided CD40-specific gene delivery *in vivo* following systemic delivery.[140] Further, this vector accomplished CD40-mediated infection of human monocyte derived dendritic cells, suggesting possible utility for cancer vaccine "antigen loading" approaches. In addition, Ad vectors simultaneously incorporating multiple fiber types with distinct receptor specificities has been proposed.[141,142]

Modification of Ad tropism via antibody-based adapter molecules has demonstrated considerable target specificity, as discussed above. On this basis, the development of single-component Ad vectors with genetically incorporated recombinant antibodies, antibody-derived moieties or other multi-domain ligands has been a long-standing field milestone. However, genetic incorporation of any moiety into the Ad capsid requires that the peptide be compatible with the non-reducing environment within the cytosol and nucleus, wherein Ad capsid proteins are translated and assembled. Capsid incorporation of several classes of complex targeting ligands, including single-chain antibodies (scFv) and growth factors, has been severely hampered by the innate biosynthetic incompatibilities between the ligand and Ad capsid proteins, resulting in unstable or insoluble ligands and/or reduced Ad replication.[143] On this basis, rational development of complex ligands with cytoplasmic solubility and stability will be required for their application to Ad vectors. Exemplifying this concept, Hedley and colleagues developed a single-component antibody targeted Ad vector by incorporating a cytoplasmically stable scFv into a de-knobbed fiber.[144] This vector targeted its cognate epitope expressed at the cell surface, suggesting that cytoplasmic stability of the targeting molecule, *per se*, allows retention of antigen recognition in the context of genetic capsid incorporation. In another field first, Ulasov *et al*. created an Ad vector targeted to a glioma-associated receptor, the α2 chain of the interleukin-13 receptor (IL-13Rα2), by fusing the full length human IL-13 cytokine was fused to the C-terminus

of a de-knobbed fiber containing the T4 fibritin trimerization motif.[145] This targeted vector provided IL-13Rα2-specific gene delivery to passaged and primary human glioma cells *in vitro* and in a xenograft model *in vivo.*

C. Adenovirus targeting via genetic modification: Other capsid locales

The field-wide appreciation of the difficulty of incorporating complex ligands into the Ad fiber has prompted the identification of other capsid proteins amenable to genetic ligand incorporation. These approaches have the potential, through increased capsid valency and unique capsid microenvironments, to incorporate an increased number of ligands per virion. To date, the hexon capsid protein as well as minor capsid protein pIX have been used as platforms for incorporation of heterologous peptides.

1. Hexon

Hexon is the largest (952 amino acids) and most abundant capsid protein, and as such is an attractive locale for peptide ligand incorporation due to both its surface exposure and high valency (240 hexon homotrimers per virion). The primary sequence of the hexon monomer is highly conserved among human serotypes with exception of nine non-conserved hypervariable regions (HVRs) of unknown function found mainly within solvent-exposed loops at the surface.[8,146,147] In this regard, Vigne and co-workers exploited hexon hypervariable region 5 (HVR5), a loop structure in hexon, as a site for incorporation of an integrin-binding RGD motif. Notably, virion stability was unaffected by the addition of the foreign peptide, while providing enhanced, fiber-independent transduction to low-CAR vascular smooth muscle cells.[148] Extending this work, Wu, *et al*. identified HVRs 2,3 and 5-7 as hexon sites tolerating 6-histidine (6-His) motifs without adverse affects to virion formation or stability[149]. 6-His motifs in HVRs 2 and 5 mediated virion binding to anti-6-His antibodies; however, 6-His mediated viral infection of cells was not observed, in contrast to Vigne *et al*. above, highlighting the importance of the

nature and the length of the incorporated peptides. While not related to Ad vector targeting *per se,* it bears mentioning that genetic alterations of hexon HVRs has been used as a method for evading host neutralizing antibodies (Nabs)[150], as most NAbs are directed against hexon.[151]

2. Protein IX

Polypeptide IX (pIX) has emerged as a versatile capsid locale well suited for display of ligands with utility for both targeting and imaging modalities (reviewed in [152]). The 14.3 kDa pIX is the smallest of the minor capsid proteins, a subset of capsid proteins that generally function to stabilize the capsid shell. In the mature Ad virion, eighty pIX homotrimers[153] stabilize hexon-hexon interactions during capsid assembly, and it is therefore termed a "cement" protein. Indeed, virions deleted for pIX have decreased thermostability and a DNA capacity that is approximately 2 kb less than the normal length.[154-156] Interest in employing pIX as a capsid site for incorporation of peptide ligands stemmed from the observation that the C-terminus of pIX is located at the capsid surface,[157,158] which prompted several groups to explore the fusion of several polypeptides to this terminus.

Dmitriev and colleagues first reported the incorporation of functional targeting peptides at the pIX C-terminus by inserting poly-lysine or FLAG motifs, resulting in augmented, CAR-independent gene transfer via binding to cellular heparan sulfate moieties.[159] Similarly, Vellinga and colleagues fused an integrin-binding RGD peptide to pIX, and used α-helical spacers (up to 7.5 nm in length and 113 amino acids) to extend the RGD motif away from the virion surface.[160] Increased gene transfer to CAR-deficient endothelioma cells was observed with increased spacer length, giving support to the notion that the pIX C-terminus may reside in a cavity formed by surrounding hexons. In a proof-of-principle study, this same group fused a hyper-stable scFv directed against beta-galactosidase onto a 7.5nm pIX C-terminal extension.[161] Of note, the scFv

was functional in this pIX structural context, as evidenced by binding of Ad particles to beta-galactosidase protein *in vitro*.

In order to evaluate the utility of multiple ligand types at the pIX capsid locale, Campos and coworkers fused to the pIX-C-terminus a 71-amino acid fragment of the *Propionibacterium shermanii* 1.3S transcarboxylase protein, which functions a biotin acceptor peptide (BAP).[162] During virus propagation the BAP is metabolically biotinylated, rendering this virus compatible with a host of avidin-tagged ligands including peptides, antibodies and carbohydrates. Importantly, it was noted in this study that coupling transferrin to virions via pIX-BAP resulted in specific transferrin receptor-mediated infection of C2C12 cells, but the use of an antibody directed against the transferrin receptor (CD71) did not. This dichotomy was not observed when these two ligands successfully redirected Ad tropism when incorporated into fiber. The authors speculate the difference was not due to a lack of receptor recognition by the pIX-anti-CD71 complex, but rather a difference between the dissociation of targeted fiber and pIX from the Ad particle in endosomes, resulting in trapping of the pIX-anti-CD71 variant, but not the fiber-anti-CD71 in the endosome. If this notion is fully validated, it will represent a key finding showing that the nature of pIX-incorporated ligands may influence successful redirection of Ad infection.

pIX has also been use for the display of relatively large imaging molecules as C-terminal fusions. While Ad vector imaging is beyond the scope of this chapter, the successful incorporation of the 240 amino acid enhanced green fluorescent protein (eGFP) into pIX bears mentioning due to the size and complexity of this fusion. Of note, the presence of the pIX-eGPF fusion in purified Ad virions did not appreciably decrease virus viability or capsid stability, and has allowed monitoring of Ad localization *in vitro* and *in vivo*.[163,164] Other Ad vectors have been reported that harbor complex imaging polypeptides at the pIX C-terminus, such as herpes simplex virus type 1 thymidine kinase[165], a firefly luciferase-thymidine kinase fusion[166] or

monomeric red fluorescent protein.[167] As a whole, these studies have established pIX as a highly relevant capsid locale marked by the highest structural compatibility with diverse targeting and imaging ligands observed to date. Based on its surface capsid position, pIIIa has been proposed as a platform for ligand display for modification of Ad tropism.[168,169] The minor capsid protein pIIIa is a 67 kDa monomer that is cleaved at the C-terminus during maturation of the virion, giving rise to the final 63.5 kDa form. Initial high resolution imaging studies originally indicated that pIIIa is an elongated protein penetrating the capsid and is located along the icosahedral edges of the virion.[15] However, later structural studies performed at higher resolution place pIIIa below the outer surface of the virion, likely precluding its utility for foreign peptide display.[170]

In the aggregate, these results highlight that genetic manipulation of a variety of Ad capsid proteins is currently feasible, and has brought to fruition several novel targeting and imaging paradigms. These successes confirm a level of capsid flexibility that was largely unexpected. There remains, however, an ongoing struggle to identify true targeting ligands that are structurally and/or biosynthetically compatible with Ad capsid formation and stability.

V. TRANSCRIPTIONAL TARGETING: USE OF TISSUE-SPECIFIC PROMOTERS

Transductional targeting approaches attempt to restrict Ad vector entry into target cells. In contrast, transcriptional targeting does not change vector tropism but instead restricts gene expression to target tissue by placing virally encoded transgenes under the control of cellular promoters that are specifically active or overactive in the target tissue. The ideal TSP element would exhibit the widest differential between “target on/liver off” expression profiles, key to ablation of liver toxicity from any ectopically localized vector. One of the first tissue-specific promoters (TSPs) explored for cancer was the carcinoembryonic antigen (CEA) promoter, expressed in most gastric, pancreatic, and lung cancers [171]. For hepatomas, the promoter of the alpha-fetoprotein (AFP) has been investigated [172,173], while the L-plastin promoter (LP-P) was

used in ovarian and breast cancer cell lines.[174,175] Other promoters tested for ovarian cancer include DF3[176], Cox2 and midkine[177], mesothelin[131] the secretory leukoprotease inhibitor (SLPI) promoter[178,179] as well as the ovarian-specific promoter-1[180]. The Cox-2 promoter has also been explored in the context of gastric carcinomas.[181] The CXCR4 promoter was shown to have general transcriptional selectivity for cancer cells,[182] breast cancer cell lines and primary cells[183] as well as renal cancer cell lines.[184] The survivin promoter has emerged as a potentially powerful element for transcriptional control in glioma and melanoma, and exhibits a "liver-off" activity profile.[185,186]

Osteocalcin (OC) is a bone protein expressed in osteotropic tumors and differentiated osteoblasts, as well as numerous solid tumors, including osteosarcoma and prostate cancer[187,188]. An Ad utilizing the OC promoter to drive *HSV-TK* expression in prostate cancer cells resulted in destruction of tumor cells *in vitro* and in subcutaneous or bone tumor xenografts. Interestingly, tissue-specific toxicity was seen to bone metastases. OC is expressed in osteoblastic lesions, thus offering the possibility for co-targeting of regenerating bone and tumor. Further, many types of cancers metastatic to the bone could be amenable to treatment.

The SLPI gene is expressed in several different carcinomas, including ovarian cancer. Its expression in normal organs, such as the liver, is low. Therefore, the SLPI promoter was utilized to drive transgene expression in ovarian cancer cell lines and primary tumor cells isolated from patient samples.[178] The promoter was activated in both cell lines and primary tumor cells in an Ad context *in vitro*. A murine orthotopic model of peritoneally disseminated ovarian cancer was used to demonstrate high tumor gene expression versus low liver expression with the SLPI promoter, and that Ad-delivered *HSV-TK* under the control of the SLPI promoter was able to increase survival.

A. Vasculature Specific Promoters

The vascular endothelium is an attractive therapeutic target for cancer, vascular and cardio-pulmonary diseases, and is easily accessible to intravascular vector administration. The vascular endothelial growth factor receptor type-1 (flt-1) promoter has been used to restrict transgene expression to the endothelium in rodents while reducing liver gene expression.[83,84,189] E-selectin expression is minimal in normal blood vessels but high in the capillaries of tumors and the promoter was used for driving gene expression in an Ad. Upon infection, endothelial cell (EC) cell lines expressed high levels of reporter gene expression, while non-EC cell lines showed low expression. The addition of TNF-alpha, an inducer of the promoter, further increased the E-selectin's activity.[190] The murine preproendothelin-1 (PPE-1) promoter was also used as a TSP for adenoviral-mediated delivery to EC cells. Systemic administration to lung tumor-bearing mice resulted in gene expression in the new vasculature of primary tumors.[191] The Roundabout-4 receptor (Robo4) is a transmembrane receptor with endothelial-specific expression in embryonic vasculature as well as in the adult.[192 193] On this basis, the Robo4 promoter has been employed for transcriptional targeting of Ad gene expression to the endothelium.[194]

B. Treatment Responsive Promoters

Another strategy for cancer gene therapy involves regulating gene expression with another form of treatment, such as radiation (reviewed in [195]). For example, the early growth response gene-1 (EGR-1) promoter, which is radiation inducible, has been used as a TSP for the specific expression of *lacZ* and *HSV-TK* in glioma and hepatocellular carcinoma cells. Radiation-induced transcription of EGR-1 in these cells was accomplished with relatively low doses.[196] Another approach for dynamically controlling promoter expression involves chemically inducible promoters. For example, a tetracycline activated promoter can be used to regulate gene expression and subsequent protein production by giving oral tetracycline.[197] Withdrawal of the

drug rapidly abrogates gene expression. Similarly, a mifepristone (RU486) and tamoxifen-inducible systems for controlled transgene expression have been developed.[198,199]

VI. DOUBLE-TARGETED ADENOVIRUS VECTORS

Transductional and transcriptional targeting can be combined to create double targeted viruses. Conceivably, this approach could be synergistic with regard to safety and efficacy. Initial proof-of-concept was achieved by using the vasculature specific flt-1 promoter and a lung endothelium targeted adaptor strategy [189]. Impressively, the tumor-to-liver ratio of gene expression was increased 300,000-fold when both targeting modalities were utilized. Also, double targeting for ovarian cancer has been achieved *in vitro* and *in vivo*[179]. Transductional targeting with a sCAR-fibritin-antiErbB2-sFv adapter was able to increase gene transfer to target cells while reducing transduction of non-target cells. When combined with transcriptional targeting with the SLPI promoter, an increase in selectivity was seen. Also, the transductional targeting increased the level of SLPI-mediated transgene expression in target cells, thereby compensating for the lower gene expression typically seen with TSPs.

VII. TRANSCIPTIONAL AND TRANSDUCTIONAL TARGETING OF CONDITIONALLY REPLICATING ADENOVIRUS

Although non-replicating first generation Ad vectors have provided high *in vitro* and *in vivo* transduction rates and good safety data, clinical cancer trials have suggested that the single agent antitumor effect may not be sufficient for all treatment approaches.[40] As early as the 1950's, the use of viruses that replicate and spread specifically inside the tumor have been suggested as a way to improve tumor penetration with an additional benefit of local amplification of effect.[200] To this end, conditionally replicative adenovirus (CRAd) agents have been explored. These viruses are genetically modified to take advantage of tumor-specific changes that allow preferential replication of the virus in target cells.[41,201,202] The adenovirus replication cycle

causes oncolysis of the cell, resulting in the release of newly generated virions and subsequent infection of neighboring cells. Thus, the anti-tumor effect is not delivered with a transgene but by replication of the virus *per se*. In theory, the oncolytic process continues as long as target cells for the virus persist. There are two main ways to control viral replication. One method is the control of replication regulators, such as the viral early genes, with tumor-specific promoter elements. The other method involves introduction of deletions in the viral genome that require specific cellular factors to compensate the effects of these deletions. Further, both approaches can be combined with the potential for increased specificity.

Numerous tumor-associated promoters have been used to control viral replication (reviewed in [120,203]). Typically, the promoter element is placed to control expression of *E1A*, the crucial regulator of Ad replication, sometimes combined with other genes such as *E1B* or *E4.* An interesting concept is targeting CRAds to tumor vasculature.[204] However, this strategy is more challenging to study preclinically, as animal models are unavailable – endothelial cells derive from the host in xenograft systems and murine cells do not support replication of human Ads. To further increase the oncolytic effect, transgenes for cytokines or prodrug-activating enzymes have been included in CRAds [205,206]. This approach may also allow non-invasive imaging and abrogation of virus replication in case of toxicity.

Heretofore, two approaches have been utilized for creation of deletion type CRAds. The first was ONYX-015 (initially reported as *dl*1520), which has two mutations in the gene coding for the E1B 55-kd protein.[207,208] The purpose of this protein is binding and inactivation of p53 in infected cells, for induction of S-phase, which is required for virus replication. Thus, this virus should only replicate in cells with an aberrant p53-p14ARF pathway, a common feature in human tumors. [209] While this is still subject of debate, initial studies suggested that this agent replicates more effectively in tumor than in normal cells [210-213]. Unfortunately, the function of

E1B55kD is not limited to p53 binding, which causes inefficient replication compared to wild type adenovirus.[207,208,214]

The second group of deletion mutant CRAds have a 24 bp deletion in the constant region (CR) 2 of *E1A*.[215,216] This domain of the E1A protein is responsible for binding the retinoblastoma tumor suppressor/cell cycle regulator protein (Rb), thereby allowing Ad to induce S-phase entry. Therefore, viruses with this type of deletion have reduced ability to overcome the G1-S checkpoint and replicate efficiently only in cells where this interaction is not necessary, *e.g.* tumor cells defective in the *Rb-p16* pathway. Appropriately, this pathway seems to be inactive in most all human tumors.[217] It has been shown that replication of CR2-deleted viruses is attenuated in non-proliferating normal cells.[215,216] Importantly, abrogation of replication was also demonstrated when Rb was re-introduced into otherwise permissive cells.[215] Ads with mutations in both CR1 and 2 of *E1A* have also been found to replicate selectively in tumor cells although increased in comparison to just CR2-deleted CRAds has not yet been demonstrated.[218-221]

As Ad5-based vectors, CRAds have native CAR-dependent tropism. As CAR expression is low or variable in many types of clinical cancers.[30-32,37-39,91] Nevertheless, even CRAds with wild type tropism have shown evidence of clinical utility.[222-224] These initial successes suggested that if efficiency of infection and specificity of replication of these agents could be enhanced, significant improvements in clinical efficacy could be gained. This was corroborated by a clear demonstration of the relationship between infectivity and oncolytic potency.[225-227] Consequently, genetic capsid modifications that allow CAR-independent and/or enhanced infectivity in non-replicative Ads have been applied to CRAds, resulting in impressive gains in preclinical efficacy. For example, Ad5-Δ24RGD features the integrin-binding RGD-4C peptide displayed from the HI-loop of the Ad5 fiber [228], and displays similar oncolytic potency to wild type virus in ovarian cancer cells. Further, this virus is able to replicate in ovarian cancer primary cell spheroids and

results in significantly prolonged survival in an orthotopic models of ovarian [229] and lung cancer.[230] In addition, Ad5-Δ24RGD has also been evaluated against osteosarcoma substrates. [231,232]

Based on the superior infectivity of Ad vectors containing human serotype 3 fiber knob domains in ovarian substrates[89,233], a Δ24-based CRAd featuring the serotype 3 knob (Ad5/3-Δ24) was created.[234] This agent demonstrated dramatic anti-tumor efficacy in ovarian cancer cells lines, primary tumor specimens and in orthotopic animal models of ovarian cancer. The first tumor associated promoter-controlled infectivity enhanced CRAd has been constructed and evaluated on ovarian, pancreatic and gastric cancer substrates. [235-237]

A major problem in assessing preclinical CRAd efficacy and safety is a severely limited number of appropriate animal models. Human adenoviruses (including CRAds) do not replicate productively in commonly used animal models. Therefore, meaningful safety data is difficult to obtain, and efficacy data is likely skewed due to deficient immune responses in xenograft models. Further, evaluation of host-virus interactions and their modulation has not been possible. To address this field-wide deficiency, Hemminki and colleagues have proposed the development of syngeneic CRAds for use in animal models of cancer.[238] To allow the evaluation of Ad5-based CRAds, the cotton rat has been put forth as a model.[239,240] Since this rodent is semi-permissive for human Ad replication, this immunocompetent tumor model allows investigation of host immune system effects on the CRAd-tumor interaction as well as the effects on normal host cells *in vivo*. Another promising model system for CRAd evaluation is the Syrian hamster. Human Ads replicate well in Syrian hamster cell lines *in vitro*, and demonstrate significant anti-tumor efficacy following injection into Syrian hamster tumors *in vivo*.[241]

VIII. CLINICAL TRIALS WITH MODIFIED ADENOVIRUS

No clinical trials have yet been completed with targeted adenoviruses. Nevertheless, some trials are in progress. For example, the first transductionally targeted CRAd trial with Ad5-Δ24RGD has received National Cancer Institute Rapid Access to Intervention Development (RAID) funding for vector production costs and has undergone full preclinical toxicological analysis in cotton rats.[242] As of this writing, a Phase I clinical trial is underway at the University of Alabama at Birmingham for recurrent epithelial ovarian cancer (Ronald D. Alvarez, M.D., personal communication).

IX. FUTURE DIRECTIONS

Despite the advances in Ad-based gene therapy vectors described in this chapter, several obstacles remain. The vascular endothelial wall is a significant physical barrier prohibiting access of systemically administered vectors to tumors and other target tissues. To overcome this obstacle, strategies need to be developed to route Ad vectors via transcytosis pathways through the endothelium. As an example, Zhu *et al.* redirected Ad vectors to the transcytosing transferrin receptor pathway, using the bifunctional adapter molecule.[243] The transcytosed Ad virions retained the ability to infect cells, establishing the feasibility of this approach. However, efficiency of Ad trafficking via this pathway is poor, and current efforts are directed towards exploring other transcytosing pathways such as the melanotransferrin pathway,[244] the poly immunoglobulin A receptor pathway,[245] or caveolae mediated transcytosis pathways.[246] One can envision the development of mosaic Ad vectors incorporating both targeting ligands directed to such transcytosis pathways as well as ligands mediating subsequent targeting and infection of target cells present beyond the vascular wall.

X. CONCLUSIONS

Ad-based vectors are the most widely used platform for gene delivery due to their efficacy in gene expression in dividing and non-dividing cells. They are of particular utility for cancer gene therapy applications, where temporary gene expression is acceptable or even beneficial. The history of Ad-based gene therapy studies clearly illustrates and confirms the critical linkage between improved vector design and improvement in therapeutic potential. Indeed, clinical breakthroughs have been dependent on advances in vector development. With regard to Ad-mediated cancer treatment, high-level tumor transduction remains a key developmental hurdle. To this end, both Ad and CRAd vectors possessing infectivity enhancement and targeting capabilities should be evaluated in the most stringent model systems possible. Advanced Ad-based vectors with imaging, targeting and therapeutic capabilities have yet to be fully employed; however, the feasibilities leading to this accomplishment are now being established.

ACKNOWLEDGEMENTS

This work was supported by a research grant from Actelion Pharmaceuticals (J.N.G.); by EU FP6 THERADPOX and APOTHERAPY, HUCH Research Funds (EVO), Sigrid Juselius Foundation, Academy of Finland, Emil Aaltonen Foundation and the Finnish Cancer Society (A.H.; A.H. is K. Albin Johansson Research Professor of the Finnish Cancer Institute); by the U.S. National Institutes of Health, 5P01 CA104177 and grant W81XWH-05-1-0035 from the US Department of Defense (D.T.C.).

REFERENCES

1. Clinicals Trials Database. The Journal of Gene Medicine Clinical Trials Database. *http://www.wiley.co.uk/genmed/clinical* 2007.

2. Benkö M, Harrach B, Both G *et al.* Family *Adenoviridae*. In: C Fauquet; MA Mayo; J Maniloff; U Desselberger; L Ball, editors. Virus Taxonomy. VIIIth Report of the International Committee on Taxonomy of Viruses. New York: Elsevier; 2005; p. 213-28.

3. Davison AJ, Benko M, Harrach B. Genetic content and evolution of adenoviruses. *J Gen Virol* 2003; 84: 2895-908.

4. Mei YF, Wadell G. Epitopes and hemagglutination binding domain on subgenus B:2 adenovirus fibers. *J Virol* 1996; 70: 3688-97.

5. Shenk T. Adenoviridae: and their replication. In: B Fields; P Howley; D Knipe, editors. Virology. New York: Raven Press; 1996; p. 2111-48.

6. Jones MS, 2nd, Harrach B, Ganac RD *et al.* New adenovirus species found in a patient presenting with gastroenteritis. *J Virol* 2007; 81: 5978-84.

7. Stewart PL, Burnett RM. Adenovirus structure by X-ray crystallography and electron microscopy. *Curr Top Microbiol Immunol* 1995; 199 (Pt 1): 25-38.

8. Rux JJ, Kuser PR, Burnett RM. Structural and phylogenetic analysis of adenovirus hexons by use of high-resolution x-ray crystallographic, molecular modeling, and sequence-based methods. *J Virol* 2003; 77: 9553-66.

9. Roberts MM, White JL, Grutter MG *et al.* Three-dimensional structure of the adenovirus major coat protein hexon. *Science* 1986; 232: 1148-51.

10. Pichla-Gollon SL, Drinker M, Zhou X *et al.* Structure-based identification of a major neutralizing site in an adenovirus hexon. *J Virol* 2007; 81: 1680-9.

11. Rux JJ, Burnett RM. Large-scale purification and crystallization of adenovirus hexon. *Methods Mol Med* 2007; 131: 231-50.

12. Zubieta C, Schoehn G, Chroboczek J *et al.* The structure of the human adenovirus 2 penton. *Mol Cell* 2005; 17: 121-35.

13. van Raaij MJ, Louis N, Chroboczek J *et al.* Structure of the human adenovirus serotype 2 fiber head domain at 1.5 A resolution. *Virology* 1999; 262: 333-43.

14. van Raaij MJ, Mitraki A, Lavigne G *et al.* A triple beta-spiral in the adenovirus fibre shaft reveals a new structural motif for a fibrous protein. *Nature* 1999; 401: 935-8.

15. Stewart PL, Fuller SD, Burnett RM. Difference imaging of adenovirus: bridging the resolution gap between X-ray crystallography and electron microscopy. *Embo J* 1993; 12: 2589-99.

16. Fabry CM, Rosa-Calatrava M, Conway JF *et al.* A quasi-atomic model of human adenovirus type 5 capsid. *Embo J* 2005; 24: 1645-54.

17. Tomko RP, Xu R, Philipson L. HCAR and MCAR: the human and mouse cellular receptors for subgroup C adenoviruses and group B coxsackieviruses. *Proc Natl Acad Sci U S A* 1997; 94: 3352-6.

18. Bergelson JM, Cunningham JA, Droguett G *et al.* Isolation of a common receptor for Coxsackie B viruses and adenoviruses 2 and 5. *Science* 1997; 275: 1320-3.

19. Dechecchi MC, Melotti P, Bonizzato A *et al.* Heparan sulfate glycosaminoglycans are receptors sufficient to mediate the initial binding of adenovirus types 2 and 5. *J Virol* 2001; 75: 8772-80.

20. Dechecchi MC, Tamanini A, Bonizzato A *et al.* Heparan sulfate glycosaminoglycans are involved in adenovirus type 5 and 2-host cell interactions. *Virology* 2000; 268: 382-90.

21. Hong SS, Karayan L, Tournier J *et al.* Adenovirus type 5 fiber knob binds to MHC class I alpha2 domain at the surface of human epithelial and B lymphoblastoid cells. *Embo J* 1997; 16: 2294-306.

22. Chu Y, Heistad D, Cybulsky MI *et al.* Vascular cell adhesion molecule-1 augments adenovirus-mediated gene transfer. *Arterioscler Thromb Vasc Biol* 2001; 21: 238-42.

23. Wickham TJ, Mathias P, Cheresh DA *et al.* Integrins alpha v beta 3 and alpha v beta 5 promote adenovirus internalization but not virus attachment. *Cell* 1993; 73: 309-19.

24. Li E, Brown SL, Stupack DG *et al.* Integrin alpha(v)beta1 is an adenovirus coreceptor. *J Virol* 2001; 75: 5405-9.

25. Davison E, Diaz RM, Hart IR *et al.* Integrin alpha5beta1-mediated adenovirus infection is enhanced by the integrin-activating antibody TS2/16. *J Virol* 1997; 71: 6204-7.

26. Meier O, Boucke K, Hammer SV *et al.* Adenovirus triggers macropinocytosis and endosomal leakage together with its clathrin-mediated uptake. *J Cell Biol* 2002; 158: 1119-31.

27. Trotman LC, Mosberger N, Fornerod M *et al.* Import of adenovirus DNA involves the nuclear pore complex receptor CAN/Nup214 and histone H1. *Nat Cell Biol* 2001; 3: 1092-100.

28. Saphire AC, Guan T, Schirmer EC *et al.* Nuclear import of adenovirus DNA in vitro involves the nuclear protein import pathway and hsc70. *J Biol Chem* 2000; 275: 4298-304.

29. Hindley CE, Lawrence FJ, Matthews DA. A role for transportin in the nuclear import of adenovirus core proteins and DNA. *Traffic* 2007; 8: 1313-22.

30. Li Y, Pong RC, Bergelson JM *et al.* Loss of adenoviral receptor expression in human bladder cancer cells: a potential impact on the efficacy of gene therapy. *Cancer Res* 1999; 59: 325-30.

31. Miller CR, Buchsbaum DJ, Reynolds PN *et al.* Differential susceptibility of primary and established human glioma cells to adenovirus infection: targeting via the epidermal growth factor receptor achieves fiber receptor-independent gene transfer. *Cancer Res* 1998; 58: 5738-48.

32. Cripe TP, Dunphy EJ, Holub AD *et al.* Fiber knob modifications overcome low, heterogeneous expression of the coxsackievirus-adenovirus receptor that limits adenovirus gene transfer and oncolysis for human rhabdomyosarcoma cells. *Cancer Res* 2001; 61: 2953-60.

33. Dmitriev I, Krasnykh V, Miller CR *et al.* An adenovirus vector with genetically modified fibers demonstrates expanded tropism via utilization of a coxsackievirus and adenovirus receptor-independent cell entry mechanism. *J Virol* 1998; 72: 9706-13.

34. Kelly FJ, Miller CR, Buchsbaum DJ *et al.* Selectivity of TAG-72-targeted adenovirus gene transfer to primary ovarian carcinoma cells versus autologous mesothelial cells in vitro. *Clin Cancer Res* 2000; 6: 4323-33.

35. Vanderkwaak TJ, Wang M, Gomez-Navarro J *et al.* An advanced generation of adenoviral vectors selectively enhances gene transfer for ovarian cancer gene therapy approaches. *Gynecol Oncol* 1999; 74: 227-34.

36. Kasono K, Blackwell JL, Douglas JT *et al.* Selective gene delivery to head and neck cancer cells via an integrin targeted adenoviral vector. *Clin Cancer Res* 1999; 5: 2571-9.

37. Okegawa T, Li Y, Pong RC *et al.* The dual impact of coxsackie and adenovirus receptor expression on human prostate cancer gene therapy. *Cancer Res* 2000; 60: 5031-6.

38. Okegawa T, Pong RC, Li Y *et al.* The mechanism of the growth-inhibitory effect of coxsackie and adenovirus receptor (CAR) on human bladder cancer: a functional analysis of car protein structure. *Cancer Res* 2001; 61: 6592-600.

39. Shayakhmetov DM, Li ZY, Ni S *et al.* Targeting of adenovirus vectors to tumor cells does not enable efficient transduction of breast cancer metastases. *Cancer Res* 2002; 62: 1063-8.

40. Hemminki A, Alvarez RD. Adenoviruses in oncology: a viable option? *BioDrugs* 2002; 16: 77-87.

41. Kanerva A, Hemminki A. Adenoviruses for treatment of cancer. *Ann Med* 2005; 37: 33-43.

42. Cohen CJ, Shieh JT, Pickles RJ *et al.* The coxsackievirus and adenovirus receptor is a transmembrane component of the tight junction. *Proc Natl Acad Sci U S A* 2001; 98: 15191-6.

43. Walters RW, Freimuth P, Moninger TO *et al.* Adenovirus fiber disrupts CAR-mediated intercellular adhesion allowing virus escape. *Cell* 2002; 110: 789-99.

44. Honda T, Saitoh H, Masuko M *et al.* The coxsackievirus-adenovirus receptor protein as a cell adhesion molecule in the developing mouse brain. *Brain Res Mol Brain Res* 2000; 77: 19-28.

45. Anders M, Christian C, McMahon M *et al.* Inhibition of the Raf/MEK/ERK pathway up-regulates expression of the coxsackievirus and adenovirus receptor in cancer cells. *Cancer Res* 2003; 63: 2088-95.

46. Fechner H, Haack A, Wang H *et al.* Expression of coxsackie adenovirus receptor and alphav-integrin does not correlate with adenovector targeting in vivo indicating anatomical vector barriers. *Gene Ther* 1999; 6: 1520-35.

47. Wood M, Perrotte P, Onishi E *et al.* Biodistribution of an adenoviral vector carrying the luciferase reporter gene following intravesical or intravenous administration to a mouse. *Cancer Gene Ther* 1999; 6: 367-72.

48. Reynolds P, Dmitriev I, Curiel D. Insertion of an RGD motif into the HI loop of adenovirus fiber protein alters the distribution of transgene expression of the systemically administered vector. *Gene Ther* 1999; 6: 1336-9.

49. Stone D, Liu Y, Shayakhmetov D *et al.* Adenovirus-platelet interaction in blood causes virus sequestration to the reticuloendothelial system of the liver. *J Virol* 2007; 81: 4866-71.

50. Tao N, Gao GP, Parr M *et al.* Sequestration of adenoviral vector by Kupffer cells leads to a nonlinear dose response of transduction in liver. *Mol Ther* 2001; 3: 28-35.

51. Connelly S. Adenoviral vectors for liver-directed gene therapy. *Curr Opin Mol Ther* 1999; 1: 565-72.

52. Lieber A, He CY, Meuse L *et al.* The role of Kupffer cell activation and viral gene expression in early liver toxicity after infusion of recombinant adenovirus vectors. *J Virol* 1997; 71: 8798-807.

53. Peeters MJ, Patijn GA, Lieber A *et al.* Adenovirus-mediated hepatic gene transfer in mice: comparison of intravascular and biliary administration. *Hum Gene Ther* 1996; 7: 1693-9.

54. Alemany R, Suzuki K, Curiel DT. Blood clearance rates of adenovirus type 5 in mice. *J Gen Virol* 2000a; 81: 2605-9.

55. Worgall S, Wolff G, Falck-Pedersen E *et al.* Innate immune mechanisms dominate elimination of adenoviral vectors following in vivo administration. *Hum Gene Ther* 1997; 8: 37-44.

56. Alemany R, Curiel DT. CAR-binding ablation does not change biodistribution and toxicity of adenoviral vectors. *Gene Ther* 2001; 8: 1347-53.

57. Smith TA, Idamakanti N, Marshall-Neff J *et al.* Receptor interactions involved in adenoviral-mediated gene delivery after systemic administration in non-human primates. *Hum Gene Ther* 2003; 14: 1595-604.

58. Smith T, Idamakanti N, Kylefjord H *et al.* In vivo hepatic adenoviral gene delivery occurs independently of the coxsackievirus-adenovirus receptor. *Mol Ther* 2002; 5: 770-9.

59. Martin K, Brie A, Saulnier P *et al.* Simultaneous CAR- and alpha V integrin-binding ablation fails to reduce Ad5 liver tropism. *Mol Ther* 2003; 8: 485-94.

60. Mizuguchi H, Koizumi N, Hosono T *et al.* CAR- or alphav integrin-binding ablated adenovirus vectors, but not fiber-modified vectors containing RGD peptide, do not change the systemic gene transfer properties in mice. *Gene Ther* 2002; 9: 769-76.

61. Nicklin SA, Wu E, Nemerow GR *et al.* The influence of adenovirus fiber structure and function on vector development for gene therapy. *Mol Ther* 2005; 12: 384-93.

62. Vigne E, Dedieu JF, Brie A *et al.* Genetic manipulations of adenovirus type 5 fiber resulting in liver tropism attenuation. *Gene Ther* 2003; 10: 153-62.

63. Breidenbach M, Rein DT, Wang M *et al.* Genetic replacement of the adenovirus shaft fiber reduces liver tropism in ovarian cancer gene therapy. *Hum Gene Ther* 2004; 15: 509-18.

64. Smith TA, Idamakanti N, Rollence ML *et al.* Adenovirus serotype 5 fiber shaft influences in vivo gene transfer in mice. *Hum Gene Ther* 2003; 14: 777-87.

65. Shayakhmetov DM, Li ZY, Ni S *et al.* Analysis of adenovirus sequestration in the liver, transduction of hepatic cells, and innate toxicity after injection of fiber-modified vectors. *J Virol* 2004; 78: 5368-81.

66. Baker AH, McVey JH, Waddington SN *et al.* The influence of blood on in vivo adenovirus bio-distribution and transduction. *Mol Ther* 2007; 15: 1410-6.

67. Douglas JT, Rogers BE, Rosenfeld ME *et al.* Targeted gene delivery by tropism-modified adenoviral vectors. *Nat Biotechnol* 1996; 14: 1574-8.

68. Goldman CK, Rogers BE, Douglas JT *et al.* Targeted gene delivery to Kaposi's sarcoma cells via the fibroblast growth factor receptor. *Cancer Res* 1997; 57: 1447-51.

69. Rogers BE, Douglas JT, Ahlem C *et al.* Use of a novel cross-linking method to modify adenovirus tropism. *Gene Ther* 1997; 4: 1387-92.

70. Rancourt C, Rogers BE, Sosnowski BA *et al.* Basic fibroblast growth factor enhancement of adenovirus-mediated delivery of the herpes simplex virus thymidine kinase gene results in

augmented therapeutic benefit in a murine model of ovarian cancer. *Clin Cancer Res* 1998; 4: 2455-61.

71. Gu DL, Gonzalez AM, Printz MA *et al.* Fibroblast growth factor 2 retargeted adenovirus has redirected cellular tropism: evidence for reduced toxicity and enhanced antitumor activity in mice. *Cancer Res* 1999; 59: 2608-14.

72. Printz MA, Gonzalez AM, Cunningham M *et al.* Fibroblast growth factor 2-retargeted adenoviral vectors exhibit a modified biolocalization pattern and display reduced toxicity relative to native adenoviral vectors. *Hum Gene Ther* 2000; 11: 191-204.

73. Haisma HJ, Pinedo HM, Rijswijk A *et al.* Tumor-specific gene transfer via an adenoviral vector targeted to the pan-carcinoma antigen EpCAM. *Gene Ther* 1999; 6: 1469-74.

74. Heideman DA, Snijders PJ, Craanen ME *et al.* Selective gene delivery toward gastric and esophageal adenocarcinoma cells via EpCAM-targeted adenoviral vectors. *Cancer Gene Ther* 2001; 8: 342-51.

75. Reynolds PN, Zinn KR, Gavrilyuk VD *et al.* A targetable, injectable adenoviral vector for selective gene delivery to pulmonary endothelium in vivo. *Mol Ther* 2000; 2: 562-78.

76. Tillman BW, de Gruijl TD, Luykx-de Bakker SA *et al.* Maturation of dendritic cells accompanies high-efficiency gene transfer by a CD40-targeted adenoviral vector. *J Immunol* 1999; 162: 6378-83.

77. Hakkarainen T, Hemminki A, Pereboev AV *et al.* CD40 is expressed on ovarian cancer cells and can be utilized for targeting adenoviruses. *Clin Cancer Res* 2003; 9: 619-24.

78. Pereboev AV, Asiedu CK, Kawakami Y *et al.* Coxsackievirus-adenovirus receptor genetically fused to anti-human CD40 scFv enhances adenoviral transduction of dendritic cells. *Gene Ther* 2002; 9: 1189-93.

79. Dmitriev I, Kashentseva E, Rogers BE *et al.* Ectodomain of coxsackievirus and adenovirus receptor genetically fused to epidermal growth factor mediates adenovirus targeting to epidermal growth factor receptor-positive cells. *J Virol* 2000; 74: 6875-84.

80. Kashentseva EA, Seki T, Curiel DT *et al.* Adenovirus targeting to c-erbB-2 oncoprotein by single-chain antibody fused to trimeric form of adenovirus receptor ectodomain. *Cancer Res* 2002; 62: 609-16.

81. Itoh A, Okada T, Mizuguchi H *et al.* A soluble CAR-SCF fusion protein improves adenoviral vector-mediated gene transfer to c-Kit-positive hematopoietic cells. *J Gene Med* 2003; 5: 929-40.

82. Kim J, Smith T, Idamakanti N *et al.* Targeting adenoviral vectors by using the extracellular domain of the coxsackie-adenovirus receptor: improved potency via trimerization. *J Virol* 2002; 76: 1892-903.

83. Reynolds AM, Xia W, Holmes MD *et al.* Bone morphogenetic protein type 2 receptor gene therapy attenuates hypoxic pulmonary hypertension. *Am J Physiol Lung Cell Mol Physiol* 2007; 292: L1182-92.

84. Everts M, Kim-Park SA, Preuss MA *et al.* Selective induction of tumor-associated antigens in murine pulmonary vasculature using double-targeted adenoviral vectors. *Gene Ther* 2005; 12: 1042-48.

85. Li HJ, Everts M, Pereboeva L *et al.* Adenovirus tumor targeting and hepatic untargeting by a coxsackie/adenovirus receptor ectodomain anti-carcinoembryonic antigen bispecific adapter. *Cancer Res* 2007; 67: 5354-61.

86. Krasnykh VN, Mikheeva GV, Douglas JT *et al.* Generation of recombinant adenovirus vectors with modified fibers for altering viral tropism. *J Virol* 1996; 70: 6839-46.

87. Von Seggern DJ, Huang S, Fleck SK *et al.* Adenovirus vector pseudotyping in fiber-expressing cell lines: improved transduction of Epstein-Barr virus-transformed B cells. *J Virol* 2000; 74: 354-62.

88. Kanerva A, Wang M, Bauerschmitz GJ *et al.* Gene transfer to ovarian cancer versus normal tissues with fiber-modified adenoviruses. *Mol Ther* 2002b; 5: 695-704.

89. Kanerva A, Mikheeva GV, Krasnykh V *et al.* Targeting adenovirus to the serotype 3 receptor increases gene transfer efficiency to ovarian cancer cells. *Clin Cancer Res* 2002; 8: 275-80.

90. Zheng S, Ulasov IV, Han Y *et al.* Fiber-knob modifications enhance adenoviral tropism and gene transfer in malignant glioma. *J Gene Med* 2007; 9: 151-60.

91. Ulasov IV, Tyler MA, Zheng S *et al.* CD46 represents a target for adenoviral gene therapy of malignant glioma. *Hum Gene Ther* 2006; 17: 556-64.

92. Ulasov IV, Rivera AA, Han Y *et al.* Targeting adenovirus to CD80 and CD86 receptors increases gene transfer efficiency to malignant glioma cells. *J Neurosurg* 2007; 107: 617-27.

93. Havenga MJ, Lemckert AA, Ophorst OJ *et al.* Exploiting the natural diversity in adenovirus tropism for therapy and prevention of disease. *J Virol* 2002; 76: 4612-20.

94. Gaggar A, Shayakhmetov DM, Lieber A. CD46 is a cellular receptor for group B adenoviruses. *Nat Med* 2003; 9: 1408-12.

95. Segerman A, Arnberg N, Erikson A *et al.* There are two different species B adenovirus receptors: sBAR, common to species B1 and B2 adenoviruses, and sB2AR, exclusively used by species B2 adenoviruses. *J Virol* 2003; 77: 1157-62.

96. Segerman A, Atkinson JP, Marttila M *et al.* Adenovirus type 11 uses CD46 as a cellular receptor. *J Virol* 2003; 77: 9183-91.

97. Sirena D, Lilienfeld B, Eisenhut M *et al.* The human membrane cofactor CD46 is a receptor for species B adenovirus serotype 3. *J Virol* 2004; 78: 4454-62.

98. Short JJ, Pereboev AV, Kawakami Y *et al.* Adenovirus serotype 3 utilizes CD80 (B7.1) and CD86 (B7.2) as cellular attachment receptors. *Virology* 2004; 322: 349-59.

99. Arnberg N, Edlund K, Kidd AH *et al.* Adenovirus type 37 uses sialic acid as a cellular receptor. *J Virol* 2000; 74: 42-8.

100. Arnberg N, Kidd AH, Edlund K *et al.* Adenovirus type 37 binds to cell surface sialic acid through a charge-dependent interaction. *Virology* 2002; 302: 33-43.

101. Wu E, Trauger SA, Pache L *et al.* Membrane cofactor protein is a receptor for adenoviruses associated with epidemic keratoconjunctivitis. *J Virol* 2004; 78: 3897-905.

102. Kanerva A, Zinn KR, Chaudhuri TR *et al.* Enhanced therapeutic efficacy for ovarian cancer with a serotype 3 receptor targeted oncolytic virus. *Mol. Ther.* 2003; 8: 449-58.

103. Zabner J, Chillon M, Grunst T *et al.* A chimeric type 2 adenovirus vector with a type 17 fiber enhances gene transfer to human airway epithelia. *J Virol* 1999; 73: 8689-95.

104. Rea D, Havenga MJ, van Den Assem M *et al.* Highly efficient transduction of human monocyte-derived dendritic cells with subgroup B fiber-modified adenovirus vectors enhances transgene-encoded antigen presentation to cytotoxic T cells. *J Immunol* 2001; 166: 5236-44.

105. Shayakhmetov DM, Papayannopoulou T, Stamatoyannopoulos G *et al.* Efficient gene transfer into human CD34(+) cells by a retargeted adenovirus vector. *J Virol* 2000; 74: 2567-83.

106. Goossens PH, Havenga MJ, Pieterman E *et al.* Infection efficiency of type 5 adenoviral vectors in synovial tissue can be enhanced with a type 16 fiber. *Arthritis Rheum* 2001; 44: 570-7.

107. Havenga MJ, Lemckert AA, Grimbergen JM *et al.* Improved adenovirus vectors for infection of cardiovascular tissues. *J Virol* 2001; 75: 3335-42.

108. Gall J, Kass-Eisler A, Leinwand L *et al.* Adenovirus type 5 and 7 capsid chimera: fiber replacement alters receptor tropism without affecting primary immune neutralization epitopes. *J Virol* 1996; 70: 2116-23.

109. Chillon M, Bosch A, Zabner J *et al.* Group D adenoviruses infect primary central nervous system cells more efficiently than those from group C. *J Virol* 1999; 73: 2537-40.

110. Stoff-Khalili MA, Rivera AA, Glasgow JN *et al.* A human adenoviral vector with a chimeric fiber from canine adenovirus type 1 results in novel expanded tropism for cancer gene therapy. *Gene Ther* 2005; 12: 1696-706.

111. Glasgow JN, Kremer EJ, Hemminki A *et al.* An adenovirus vector with a chimeric fiber derived from canine adenovirus type 2 displays novel tropism. *Virology* 2004; 324: 103-16.

112. Tsuruta Y, Pereboeva L, Glasgow JN *et al.* Reovirus sigma1 fiber incorporated into adenovirus serotype 5 enhances infectivity via a CAR-independent pathway. *Biochem Biophys Res Commun* 2005; 335: 205-14.

113. Mercier GT, Campbell JA, Chappell JD *et al.* A chimeric adenovirus vector encoding reovirus attachment protein sigma1 targets cells expressing junctional adhesion molecule 1. *Proc Natl Acad Sci U S A* 2004; 101: 6188-93.

114. Wickham TJ, Tzeng E, Shears LL, 2nd *et al.* Increased in vitro and in vivo gene transfer by adenovirus vectors containing chimeric fiber proteins. *J Virol* 1997; 71: 8221-9.

115. Krasnykh V, Dmitriev I, Mikheeva G *et al.* Characterization of an adenovirus vector containing a heterologous peptide epitope in the HI loop of the fiber knob. *J Virol* 1998; 72: 1844-52.

116. Belousova N, Krendelchtchikova V, Curiel DT *et al.* Modulation of adenovirus vector tropism via incorporation of polypeptide ligands into the fiber protein. *J Virol* 2002; 76: 8621-31.

117. Magnusson MK, Henning P, Myhre S *et al.* Adenovirus 5 vector genetically re-targeted by an Affibody molecule with specificity for tumor antigen HER2/neu. *Cancer Gene Ther* 2007; 14: 468-79.

118. Hemminki A, Wang M, Desmond RA *et al.* Serum and ascites neutralizing antibodies in ovarian cancer patients treated with intraperitoneal adenoviral gene therapy. *Hum Gene Ther* 2002; 13: 1505-14.

119. Hemminki A, Belousova N, Zinn KR *et al.* An adenovirus with enhanced infectivity mediates molecular chemotherapy of ovarian cancer cells and allows imaging of gene expression. *Mol Ther* 2001; 4: 223-31.

120. Bauerschmitz GJ, Barker SD, Hemminki A. Adenoviral gene therapy for cancer: From vectors to targeted and replication competent agents (Review). *Int J Oncol* 2002; 21: 1161-74.

121. Wu H, Seki T, Dmitriev I *et al.* Double modification of adenovirus fiber with RGD and polylysine motifs improves coxsackievirus-adenovirus receptor-independent gene transfer efficiency. *Hum Gene Ther* 2002; 13: 1647-53.

122. Contreras JL, Wu H, Smyth CA *et al.* Double genetic modification of adenovirus fiber with RGD polylysine motifs significantly enhances gene transfer to isolated human pancreatic islets. *Transplantation* 2003; 76: 252-61.

123. Wu H, Han T, Lam JT *et al.* Preclinical evaluation of a class of infectivity-enhanced adenoviral vectors in ovarian cancer gene therapy. *Gene Ther* 2004; 11: 874-8.

124. Rein DT, Breidenbach M, Wu H *et al.* Gene transfer to cervical cancer with fiber-modified adenoviruses. *Int J Cancer* 2004; 111: 698-704.

125. Nicklin SA, White SJ, Watkins SJ *et al.* Selective targeting of gene transfer to vascular endothelial cells by use of peptides isolated by phage display. *Circulation* 2000; 102: 231-7.

126. Nicklin SA, Dishart KL, Buening H *et al.* Transductional and transcriptional targeting of cancer cells using genetically engineered viral vectors. *Cancer Lett* 2003; 201: 165-73.

127. Henning P, Andersson KM, Frykholm K *et al.* Tumor cell targeted gene delivery by adenovirus 5 vectors carrying knobless fibers with antibody-binding domains. *Gene Ther* 2005; 12: 211-24.

128. Volpers C, Thirion C, Biermann V *et al.* Antibody-mediated targeting of an adenovirus vector modified to contain a synthetic immunoglobulin g-binding domain in the capsid. *J Virol* 2003; 77: 2093-104.

129. Korokhov N, Mikheeva G, Krendelshchikov A *et al.* Targeting of adenovirus via genetic modification of the viral capsid combined with a protein bridge. *J Virol* 2003; 77: 12931-40.

130. Korokhov N, de Gruijl TD, Aldrich WA *et al.* High Efficiency Transduction of Dendritic Cells by Adenoviral Vectors Targeted To DC-SIGN. *Cancer Biol Ther* 2005; 4: 289-94.

131. Breidenbach M, Rein DT, Everts M *et al.* Mesothelin-mediated targeting of adenoviral vectors for ovarian cancer gene therapy. *Gene Ther* 2005; 12: 187-93.

132. Balyasnikova IV, Metzger R, Visintine DJ *et al.* Selective rat lung endothelial targeting with a new set of monoclonal antibodies to angiotensin I-converting enzyme. *Pulm Pharmacol Ther* 2005; 18: 251-67.

133. Von Seggern DJ, Chiu CY, Fleck SK *et al.* A helper-independent adenovirus vector with E1, E3, and fiber deleted: structure and infectivity of fiberless particles. *J Virol* 1999; 73: 1601-8.

134. Falgout B, Ketner G. Characterization of adenovirus particles made by deletion mutants lacking the fiber gene. *J Virol* 1988; 62: 622-5.

135. Papanikolopoulou K, Forge V, Goeltz P *et al.* Formation of highly stable chimeric trimers by fusion of an adenovirus fiber shaft fragment with the foldon domain of bacteriophage t4 fibritin. *J Biol Chem* 2004; 279: 8991-8.

136. Krasnykh V, Belousova N, Korokhov N *et al.* Genetic targeting of an adenovirus vector via replacement of the fiber protein with the phage T4 fibritin. *J Virol* 2001; 75: 4176-83.

137. Magnusson MK, Hong SS, Boulanger P *et al.* Genetic retargeting of adenovirus: novel strategy employing "deknobbing" of the fiber. *J Virol* 2001; 75: 7280-9.

138. Gaden F, Franqueville L, Magnusson MK *et al.* Gene transduction and cell entry pathway of fiber-modified adenovirus type 5 vectors carrying novel endocytic peptide ligands selected on human tracheal glandular cells. *J Virol* 2004; 78: 7227-47.

139. Belousova N, Korokhov N, Krendelshchikova V *et al.* Genetically targeted adenovirus vector directed to CD40-expressing cells. *J Virol* 2003; 77: 11367-77.

140. Izumi M, Kawakami Y, Glasgow JN *et al.* In vivo analysis of a genetically modified adenoviral vector targeted to human CD40 using a novel transient transgenic model. *J Gene Med* 2005; 7: 1517-25.

141. Pereboeva L, Komarova S, Mahasreshti PJ *et al.* Fiber-mosaic adenovirus as a novel approach to design genetically modified adenoviral vectors. *Virus Res* 2004; 105: 35-46.

142. Takayama K, Reynolds PN, Short JJ *et al.* A mosaic adenovirus possessing serotype Ad5 and serotype Ad3 knobs exhibits expanded tropism. *Virology* 2003; 309: 282-93.

143. Magnusson MK, Hong SS, Henning P *et al.* Genetic retargeting of adenovirus vectors: functionality of targeting ligands and their influence on virus viability. *J Gene Med* 2002; 4: 356-70.

144. Hedley SJ, Auf der Maur A, Hohn S *et al.* An adenovirus vector with a chimeric fiber incorporating stabilized single chain antibody achieves targeted gene delivery. *Gene Ther* 2006; 13: 88-94.

145. Ulasov IV, Tyler MA, Han Y *et al.* Novel Recombinant Adenoviral Vector That Targets The Interleukin-13 Receptor alpha2 Chain Permits Effective Gene Transfer to Malignant Glioma. *Hum Gene Ther* 2007; 18: 118-29.

146. Athappilly FK, Murali R, Rux JJ *et al.* The refined crystal structure of hexon, the major coat protein of adenovirus type 2, at 2.9 A resolution. *J Mol Biol* 1994; 242: 430-55.

147. Crawford-Miksza L, Schnurr DP. Analysis of 15 adenovirus hexon proteins reveals the location and structure of seven hypervariable regions containing serotype-specific residues. *J Virol* 1996; 70: 1836-44.

148. Vigne E, Mahfouz I, Dedieu JF *et al.* RGD inclusion in the hexon monomer provides adenovirus type 5-based vectors with a fiber knob-independent pathway for infection. *J Virol* 1999; 73: 5156-61.

149. Wu H, Han T, Belousova N *et al.* Identification of sites in adenovirus hexon for foreign peptide incorporation. *J Virol* 2005; 79: 3382-90.

150. Roberts DM, Nanda A, Havenga MJ *et al.* Hexon-chimaeric adenovirus serotype 5 vectors circumvent pre-existing anti-vector immunity. *Nature* 2006; 441: 239-43.

151. Sumida SM, Truitt DM, Lemckert AA *et al.* Neutralizing antibodies to adenovirus serotype 5 vaccine vectors are directed primarily against the adenovirus hexon protein. *J Immunol* 2005; 174: 7179-85.

152. Parks RJ. Adenovirus protein IX: a new look at an old protein. *Mol Ther* 2005; 11: 19-25.

153. Vellinga J, van den Wollenberg DJ, van der Heijdt S *et al.* The coiled-coil domain of the adenovirus type 5 protein IX is dispensable for capsid incorporation and thermostability. *J Virol* 2005; 79: 3206-10.

154. Ghosh-Choudhury G, Haj-Ahmad Y, Graham FL. Protein IX, a minor component of the human adenovirus capsid, is essential for the packaging of full length genomes. *Embo J* 1987; 6: 1733-9.

155. Colby WW, Shenk T. Adenovirus type 5 virions can be assembled in vivo in the absence of detectable polypeptide IX. *J Virol* 1981; 39: 977-80.

156. Boulanger P, Lemay P, Blair GE *et al.* Characterization of adenovirus protein IX. *J Gen Virol* 1979; 44: 783-800.

157. Akalu A, Liebermann H, Bauer U *et al.* The subgenus-specific C-terminal region of protein IX is located on the surface of the adenovirus capsid. *J Virol* 1999; 73: 6182-7.

158. Rosa-Calatrava M, Grave L, Puvion-Dutilleul F *et al.* Functional analysis of adenovirus protein IX identifies domains involved in capsid stability, transcriptional activity, and nuclear reorganization. *J Virol* 2001; 75: 7131-41.

159. Dmitriev IP, Kashentseva EA, Curiel DT. Engineering of adenovirus vectors containing heterologous peptide sequences in the C terminus of capsid protein IX. *J Virol* 2002; 76: 6893-9.

160. Vellinga J, Rabelink MJ, Cramer SJ *et al.* Spacers increase the accessibility of peptide ligands linked to the carboxyl terminus of adenovirus minor capsid protein IX. *J Virol* 2004; 78: 3470-9.

161. Vellinga J, de Vrij J, Myhre S *et al.* Efficient incorporation of a functional hyper-stable single-chain antibody fragment protein-IX fusion in the adenovirus capsid. *Gene Ther* 2007; 14: 664-70.

162. Campos SK, Parrott MB, Barry MA. Avidin-based targeting and purification of a protein IX-modified, metabolically biotinylated adenoviral vector. *Mol Ther* 2004; 9: 942-54.

163. Meulenbroek RA, Sargent KL, Lunde J *et al.* Use of adenovirus protein IX (pIX) to display large polypeptides on the virion--generation of fluorescent virus through the incorporation of pIX-GFP. *Mol Ther* 2004; 9: 617-24.

164. Le LP, Everts M, Dmitriev IP *et al.* Fluorescently labeled adenovirus with pIX-EGFP for vector detection. *Mol Imaging* 2004; 3: 105-16.

165. Li J, Le LP, Sibley DA *et al.* Genetic Incorporation of HSV-1 Thymidine Kinase into the Adenovirus Protein IX for Functioal Display on the Virion. *Virology* 2005; 338: 247-58.

166. Matthews QL, Sibley DA, Wu H *et al.* Genetic incorporation of a herpes simplex virus type 1 thymidine kinase and firefly luciferase fusion into the adenovirus protein IX for functional display on the virion. *Mol Imaging* 2006; 5: 510-9.

167. Le LP, Le HN, Dmitriev IP *et al.* Dynamic monitoring of oncolytic adenovirus in vivo by genetic capsid labeling. *J Natl Cancer Inst* 2006; 98: 203-14.

168. Vellinga J, Van der Heijdt S, Hoeben RC. The adenovirus capsid: major progress in minor proteins. *J Gen Virol* 2005; 86: 1581-8.

169. Dmitriev I, Kashentseva EA, Seki T *et al.* Utilization of Minor Capsid polypeptides IX and IIIa for Adenovirus Targeting. *Mol Ther* 2001; 3: S167.

170. Saban SD, Silvestry M, Nemerow GR *et al.* Visualization of alpha-helices in a 6-angstrom resolution cryoelectron microscopy structure of adenovirus allows refinement of capsid protein assignments. *J Virol* 2006; 80: 12049-59.

171. Tanaka T, Kanai F, Lan KH *et al.* Adenovirus-mediated gene therapy of gastric carcinoma using cancer-specific gene expression in vivo. *Biochem Biophys Res Commun* 1997; 231: 775-9.

172. Kaneko S, Hallenbeck P, Kotani T *et al.* Adenovirus-mediated gene therapy of hepatocellular carcinoma using cancer-specific gene expression. *Cancer Res* 1995; 55: 5283-7.

173. Arbuthnot PB, Bralet MP, Le Jossic C *et al.* In vitro and in vivo hepatoma cell-specific expression of a gene transferred with an adenoviral vector. *Hum Gene Ther* 1996; 7: 1503-14.

174. Chung I, Schwartz PE, Crystal RG *et al.* Use of L-plastin promoter to develop an adenoviral system that confers transgene expression in ovarian cancer cells but not in normal mesothelial cells. *Cancer Gene Ther* 1999; 6: 99-106.

175. Peng XY, Won JH, Rutherford T *et al.* The use of the L-plastin promoter for adenoviral-mediated, tumor-specific gene expression in ovarian and bladder cancer cell lines. *Cancer Res* 2001; 61: 4405-13.

176. Tai YT, Strobel T, Kufe D *et al.* In vivo cytotoxicity of ovarian cancer cells through tumor-selective expression of the BAX gene. *Cancer Res* 1999; 59: 2121-6.

177. Casado E, Gomez-Navarro J, Yamamoto M *et al.* Strategies to accomplish targeted expression of transgenes in ovarian cancer for molecular therapeutic applications. *Clin Cancer Res* 2001; 7: 2496-504.

178. Barker SD, Coolidge CJ, Kanerva A *et al.* The secretory leukoprotease inhibitor (SLPI) promoter for ovarian cancer gene therapy. *J Gene Med* 2003; 5: 300-10.

179. Barker SD, Dmitriev IP, Nettelbeck DM *et al.* Combined transcriptional and transductional targeting improves the specificity and efficacy of adenoviral gene delivery to ovarian carcinoma. *Gene Ther* 2003; 10: 1198-204.

180. Bao R, Selvakumaran M, Hamilton TC. Targeted gene therapy of ovarian cancer using an ovarian-specific promoter. *Gynecol Oncol* 2002; 84: 228-34.

181. Yamamoto M, Alemany R, Adachi Y *et al.* Characterization of the cyclooxygenase-2 promoter in an adenoviral vector and its application for the mitigation of toxicity in suicide gene therapy of gastrointestinal cancers. *Mol Ther* 2001; 3: 385-94.

182. Zhu ZB, Makhija SK, Lu B *et al.* Transcriptional targeting of adenoviral vector through the CXCR4 tumor-specific promoter. *Gene Ther* 2004; 11: 645-8.

183. Stoff-Khalili MA, Stoff A, Rivera AA *et al.* Preclinical evaluation of transcriptional targeting strategies for carcinoma of the breast in a tissue slice model system. *Breast Cancer Res* 2005; 7: R1141-52.

184. Haviv YS, van Houdt WJ, Lu B *et al.* Transcriptional targeting in renal cancer cell lines via the human CXCR4 promoter. *Mol Cancer Ther* 2004; 3: 687-91.

185. Lu B, Makhija SK, Nettelbeck DM *et al.* Evaluation of tumor-specific promoter activities in melanoma. *Gene Ther* 2005; 12: 330-8.

186. Zhu ZB, Makhija SK, Lu B *et al.* Transcriptional targeting of tumors with a novel tumor-specific survivin promoter. *Cancer Gene Ther* 2004; 11: 256-62.

187. Ko SC, Cheon J, Kao C *et al.* Osteocalcin promoter-based toxic gene therapy for the treatment of osteosarcoma in experimental models. *Cancer Res* 1996; 56: 4614-9.

188. Koeneman KS, Kao C, Ko SC *et al.* Osteocalcin-directed gene therapy for prostate-cancer bone metastasis. *World J Urol* 2000; 18: 102-10.

189. Reynolds PN, Nicklin SA, Kaliberova L *et al.* Combined transductional and transcriptional targeting improves the specificity of transgene expression in vivo. *Nat Biotechnol* 2001; 19: 838-42.

190. Walton T, Wang JL, Ribas A *et al.* Endothelium-specific expression of an E-selectin promoter recombinant adenoviral vector. *Anticancer Res* 1998; 18: 1357-60.

191. Varda-Bloom N, Shaish A, Gonen A *et al.* Tissue-specific gene therapy directed to tumor angiogenesis. *Gene Ther* 2001; 8: 819-27.

192. Park KW, Morrison CM, Sorensen LK *et al.* Robo4 is a vascular-specific receptor that inhibits endothelial migration. *Dev Biol* 2003; 261: 251-67.

193. Huminiecki L, Gorn M, Suchting S *et al.* Magic roundabout is a new member of the roundabout receptor family that is endothelial specific and expressed at sites of active angiogenesis. *Genomics* 2002; 79: 547-52.

194. Preuss MP, Barnes JA, Glasgow JN *et al.* Transciptional Targeting of Gene Expression to the Endothelium using the Roundabout-4 Receptor Promoter. *Mol Ther* 2007; 15: S49.

195. Han Z, Wang H, Hallahan DE. Radiation-guided gene therapy of cancer. *Technol Cancer Res Treat* 2006; 5: 437-44.

196. Manome Y, Kunieda T, Wen PY *et al.* Transgene expression in malignant glioma using a replication-defective adenoviral vector containing the Egr-1 promoter: activation by ionizing radiation or uptake of radioactive iododeoxyuridine. *Hum Gene Ther* 1998; 9: 1409-17.

197. Pitzer C, Schindowski K, Pomer S *et al.* In vivo manipulation of interleukin-2 expression by a retroviral tetracycline (tet)-regulated system. *Cancer Gene Ther* 1999; 6: 139-46.

198. Wang L, Hernandez-Alcoceba R, Shankar V *et al.* Prolonged and inducible transgene expression in the liver using gutless adenovirus: a potential therapy for liver cancer. *Gastroenterology* 2004; 126: 278-89.

199. Zerby D, Sakhuja K, Reddy PS *et al.* In vivo ligand-inducible regulation of gene expression in a gutless adenoviral vector system. *Hum Gene Ther* 2003; 14: 749-61.

200. Southam CM, Noyes WF, Mellors R. Virus in human cancer cells in vivo. *Virology* 1958; 5: 395.

201. Oosterhoff D, van Beusechem VW. Conditionally replicating adenoviruses as anticancer agents and ways to improve their efficacy. *J Exp Ther Oncol* 2004; 4: 37-57.

202. Nettelbeck DM. Virotherapeutics: conditionally replicative adenoviruses for viral oncolysis. *Anticancer Drugs* 2003; 14: 577-84.

203. Everts B, van der Poel HG. Replication-selective oncolytic viruses in the treatment of cancer. *Cancer Gene Ther* 2005; 12: 141-61.

204. Savontaus MJ, Sauter BV, Huang TG *et al.* Transcriptional targeting of conditionally replicating adenovirus to dividing endothelial cells. *Gene Ther* 2002; 9: 972-9.

205. Freytag SO, Rogulski KR, Paielli DL *et al.* A novel three-pronged approach to kill cancer cells selectively: concomitant viral, double suicide gene, and radiotherapy. *Hum Gene Ther* 1998; 9: 1323-33.

206. Wildner O, Blaese RM, Morris JC. Therapy of colon cancer with oncolytic adenovirus is enhanced by the addition of herpes simplex virus-thymidine kinase. *Cancer Res* 1999; 59: 410-3.

207. Barker DD, Berk AJ. Adenovirus proteins from both E1B reading frames are required for transformation of rodent cells by viral infection and DNA transfection. *Virology* 1987; 156: 107-21.

208. Bischoff JR, Kirn DH, Williams A *et al.* An adenovirus mutant that replicates selectively in p53-deficient human tumor cells. *Science* 1996; 274: 373-6.

209. Ries SJ, Brandts CH, Chung AS *et al.* Loss of p14ARF in tumor cells facilitates replication of the adenovirus mutant dl1520 (ONYX-015). *Nat Med* 2000; 6: 1128-33.

210. Hay JG, Shapiro N, Sauthoff H *et al.* Targeting the replication of adenoviral gene therapy vectors to lung cancer cells: the importance of the adenoviral E1b-55kD gene. *Hum Gene Ther* 1999; 10: 579-90.

211. Heise C, Ganly I, Kim YT *et al.* Efficacy of a replication-selective adenovirus against ovarian carcinomatosis is dependent on tumor burden, viral replication and p53 status. *Gene Ther* 2000; 7: 1925-9.

212. Heise C, Sampson-Johannes A, Williams A *et al.* ONYX-015, an E1B gene-attenuated adenovirus, causes tumor-specific cytolysis and antitumoral efficacy that can be augmented by standard chemotherapeutic agents. *Nat Med* 1997; 3: 639-45.

213. Rothmann T, Hengstermann A, Whitaker NJ *et al.* Replication of ONYX-015, a potential anticancer adenovirus, is independent of p53 status in tumor cells. *J Virol* 1998; 72: 9470-8.

214. Dix BR, Edwards SJ, Braithwaite AW. Does the antitumor adenovirus ONYX-015/dl1520 selectively target cells defective in the p53 pathway? *J Virol* 2001; 75: 5443-7.

215. Fueyo J, Gomez-Manzano C, Alemany R *et al.* A mutant oncolytic adenovirus targeting the Rb pathway produces anti-glioma effect in vivo. *Oncogene* 2000; 19: 2-12.

216. Heise C, Hermiston T, Johnson L *et al.* An adenovirus E1A mutant that demonstrates potent and selective systemic anti-tumoral efficacy. *Nat Med* 2000; 6: 1134-9.

217. Sherr CJ. Cancer cell cycles. *Science* 1996; 274: 1672-7.

218. Doronin K, Toth K, Kuppuswamy M *et al.* Tumor-specific, replication-competent adenovirus vectors overexpressing the adenovirus death protein. *J Virol* 2000; 74: 6147-55.

219. Doronin K, Kuppuswamy M, Toth K *et al.* Tissue-specific, tumor-selective, replication-competent adenovirus vector for cancer gene therapy. *J Virol* 2001; 75: 3314-24.

220. Balague C, Noya F, Alemany R *et al.* Human papillomavirus E6E7-mediated adenovirus cell killing: selectivity of mutant adenovirus replication in organotypic cultures of human keratinocytes. *J Virol* 2001; 75: 7602-11.

221. Nettelbeck DM, Rivera AA, Balague C *et al.* Novel oncolytic adenoviruses targeted to melanoma: specific viral replication and cytolysis by expression of E1A mutants from the tyrosinase enhancer/promoter. *Cancer Res* 2002; 62: 4663-70.

222. Yu W, Fang H. Clinical trials with oncolytic adenovirus in China. *Curr Cancer Drug Targets* 2007; 7: 141-8.

223. Nemunaitis J, Ganly I, Khuri F *et al.* Selective replication and oncolysis in p53 mutant tumors with ONYX-015, an E1B-55kD gene-deleted adenovirus, in patients with advanced head and neck cancer: a phase II trial. *Cancer Res* 2000; 60: 6359-66.

224. Khuri FR, Nemunaitis J, Ganly I *et al.* a controlled trial of intratumoral ONYX-015, a selectively-replicating adenovirus, in combination with cisplatin and 5-fluorouracil in patients with recurrent head and neck cancer. *Nat Med* 2000; 6: 879-85.

225. Shinoura N, Yoshida Y, Tsunoda R *et al.* Highly augmented cytopathic effect of a fiber-mutant E1B-defective adenovirus for gene therapy of gliomas. *Cancer Res* 1999; 59: 3411-6.

226. Douglas JT, Kim M, Sumerel LA *et al.* Efficient oncolysis by a replicating adenovirus (ad) in vivo is critically dependent on tumor expression of primary ad receptors. *Cancer Res* 2001; 61: 813-7.

227. Hemminki A, Dmitriev I, Liu B *et al.* Targeting oncolytic adenoviral agents to the epidermal growth factor pathway with a secretory fusion molecule. *Cancer Res* 2001; 61: 6377-81.

228. Suzuki K, Fueyo J, Krasnykh V *et al.* A conditionally replicative adenovirus with enhanced infectivity shows improved oncolytic potency. *Clin Cancer Res* 2001; 7: 120-6.

229. Bauerschmitz GJ, Lam JT, Kanerva A *et al.* Treatment of ovarian cancer with a tropism modified oncolytic adenovirus. *Cancer Res* 2002; 62: 1266-70.

230. Sarkioja M, Kanerva A, Salo J *et al.* Noninvasive imaging for evaluation of the systemic delivery of capsid-modified adenoviruses in an orthotopic model of advanced lung cancer. *Cancer* 2006; 107: 1578-88.

231. Witlox AM, Van Beusechem VW, Molenaar B *et al.* Conditionally replicative adenovirus with tropism expanded towards integrins inhibits osteosarcoma tumor growth in vitro and in vivo. *Clin Cancer Res* 2004; 10: 61-7.

232. Graat HC, Witlox MA, Schagen FH *et al.* Different susceptibility of osteosarcoma cell lines and primary cells to treatment with oncolytic adenovirus and doxorubicin or cisplatin. *Br J Cancer* 2006; 94: 1837-44.

233. Kanerva A, Wang M, Bauerschmitz GJ *et al.* Gene transfer to ovarian cancer versus normal tissues with fiber-modified adenoviruses. *Mol Ther* 2002; 5: 695-704.

234. Kanerva A, Zinn KR, Chaudhuri TR *et al.* Enhanced therapeutic efficacy for ovarian cancer with a serotype 3 receptor-targeted oncolytic adenovirus. *Mol Ther* 2003; 8: 449-58.

235. Kanerva A, Lam J, Yamamoto M *et al.* A cyclooxygenase-2 promoter based conditionally replicating adenovirus with enhanced infectivity for treatment of ovarian carcinoma. *Mol Ther* 2002; 5: S414.

236. Ono HA, Davydova JG, Adachi Y *et al.* Promoter-controlled infectivity-enhanced conditionally replicative adenoviral vectors for the treatment of gastric cancer. *J Gastroenterol* 2005; 40: 31-42.

237. Yamamoto M, Davydova J, Wang M *et al.* Infectivity enhanced, cyclooxygenase-2 promoter-based conditionally replicative adenovirus for pancreatic cancer. *Gastroenterology* 2003; 125: 1203-18.

238. Hemminki A, Kanerva A, Kremer EJ *et al.* A canine conditionally replicating adenovirus for evaluating oncolytic virotherapy in a syngeneic animal model. *Mol. Ther.* 2003; 7: 163-73.

239. Toth K, Spencer JF, Tollefson AE *et al.* Cotton rat tumor model for the evaluation of oncolytic adenoviruses. *Hum Gene Ther* 2005; 16: 139-46.

240. Toth K, Spencer JF, Wold WS. Immunocompetent, semi-permissive cotton rat tumor model for the evaluation of oncolytic adenoviruses. *Methods Mol Med* 2007; 130: 157-68.

241. Thomas MA, Spencer JF, Wold WS. Use of the Syrian hamster as an animal model for oncolytic adenovirus vectors. *Methods Mol Med* 2007; 130: 169-83.

242. Page JG, Tian B, Schweikart K *et al.* Identifying the safety profile of a novel infectivity-enhanced conditionally replicative adenovirus, Ad5-delta24-RGD, in anticipation of a phase I trial for recurrent ovarian cancer. *Am J Obstet Gynecol* 2007; 196: 389 e1-9; discussion e9-10.

243. Zhu ZB, Makhija SK, Lu B *et al.* Transport across a polarized monolayer of Caco-2 cells by transferrin receptor-mediated adenovirus transcytosis. *Virology* 2004; 325: 116-28.

244. Moroo I, Ujiie M, Walker BL *et al.* Identification of a novel route of iron transcytosis across the mammalian blood-brain barrier. *Microcirculation* 2003; 10: 457-62.

245. Mostov KE. Transepithelial transport of immunoglobulins. *Annu Rev Immunol* 1994; 12: 63-84.

246. McIntosh DP, Tan XY, Oh P *et al.* Targeting endothelium and its dynamic caveolae for tissue-specific transcytosis in vivo: a pathway to overcome cell barriers to drug and gene delivery. *Proc Natl Acad Sci U S A* 2002; 99: 1996-2001.

FIGURE LEGENDS

Figure 1. A generalized adenovirus structure depicting major structural components of a wild type adenovirus capsid. Hexon is depicted as a hexagon with 12 homotrimers per capsid face (only 12 of 240 trimers are shown). The penton base, comprised of five subunits at each vertex, and trimeric fiber and pIX structures are shown. Adenovirus serotype 2 and 5 capsids contain a 36-kilobase double-stranded DNA genome (not shown).

Figure 2. Adapter molecules for receptor-specific adenovirus targeting. A generalized adapter molecule ablates native CAR-based tropism and targets adenovirus to an alternate cellular receptor molecule. The dual specificity of the adapter molecule for both the adenovirus and the alternative receptor provides novel, CAR-independent cell binding.

Figure 3. Genetically modified fibers for adenovirus targeting. (See text for specific examples of each genetic targeting approach and targeting moiety used.) (A) Trimeric wild type adenovirus fiber; tail, shaft and knob regions are shown. (B) Ad5 fiber knob with a constrained targeting peptide in the flexible H-I loop. (C) Ad5 fiber knob containing a C-terminal targeting ligand. (D) Pseudotyped chimeric fiber bearing an alternate human or animal serotype knob domain. (E) “de-knobbed” fiber containing a heterologous trimerization sequence and a C-terminal targeting moiety.

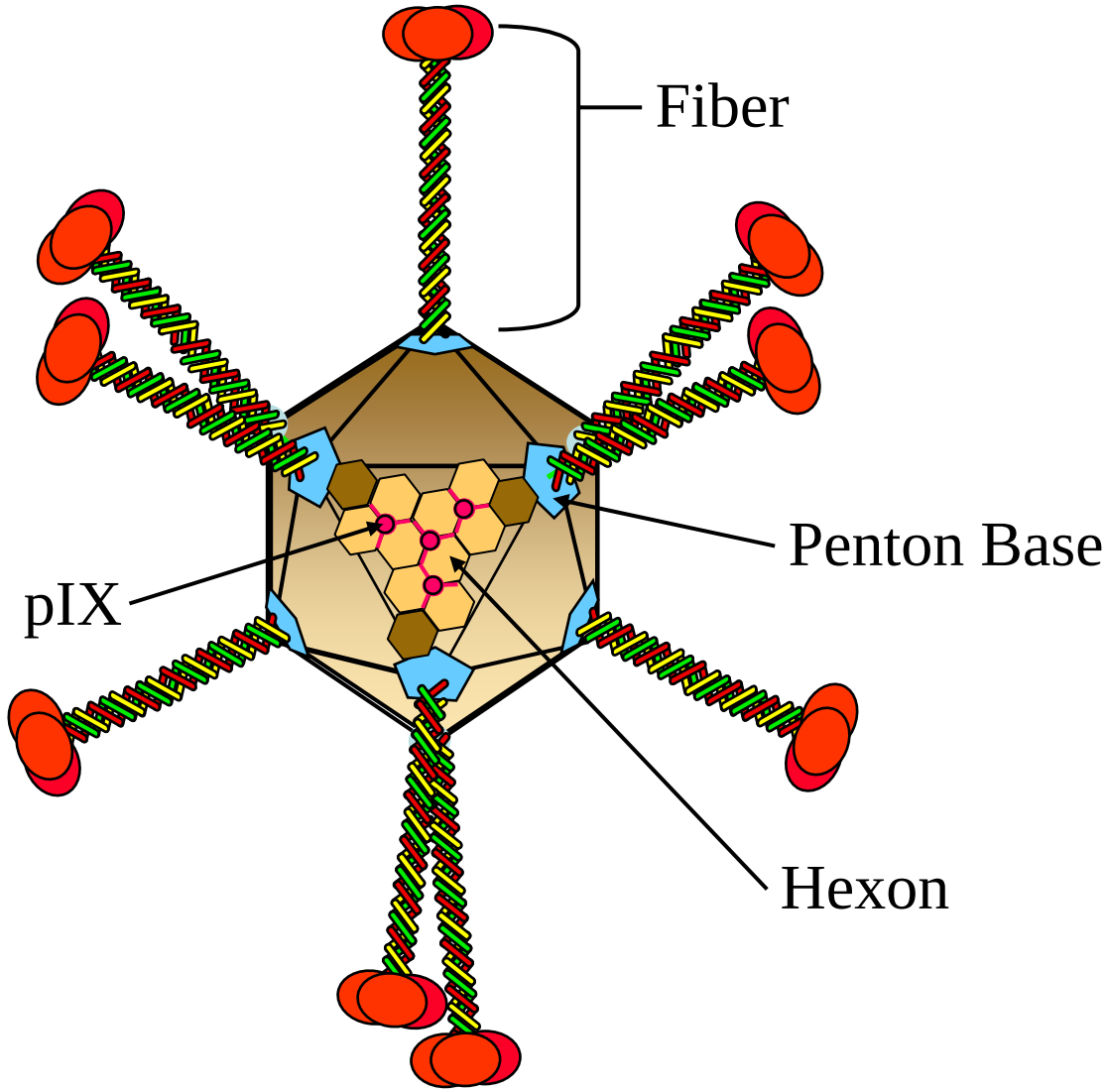
Fiber
Penton Base
pIX
Hexon

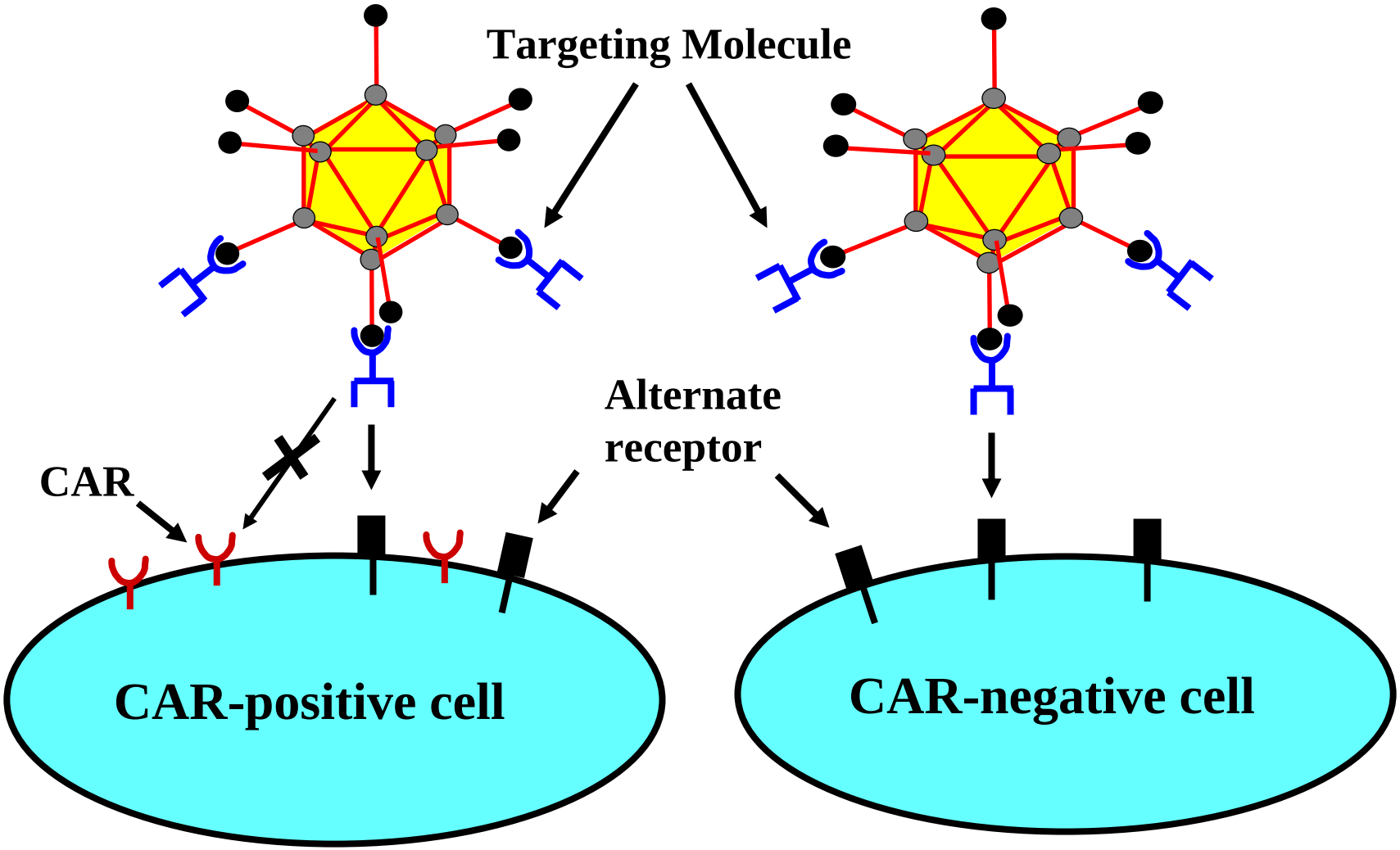
Targeting Molecule
Alternate
receptor
CAR
CAR-positive cell
CAR-negative cell

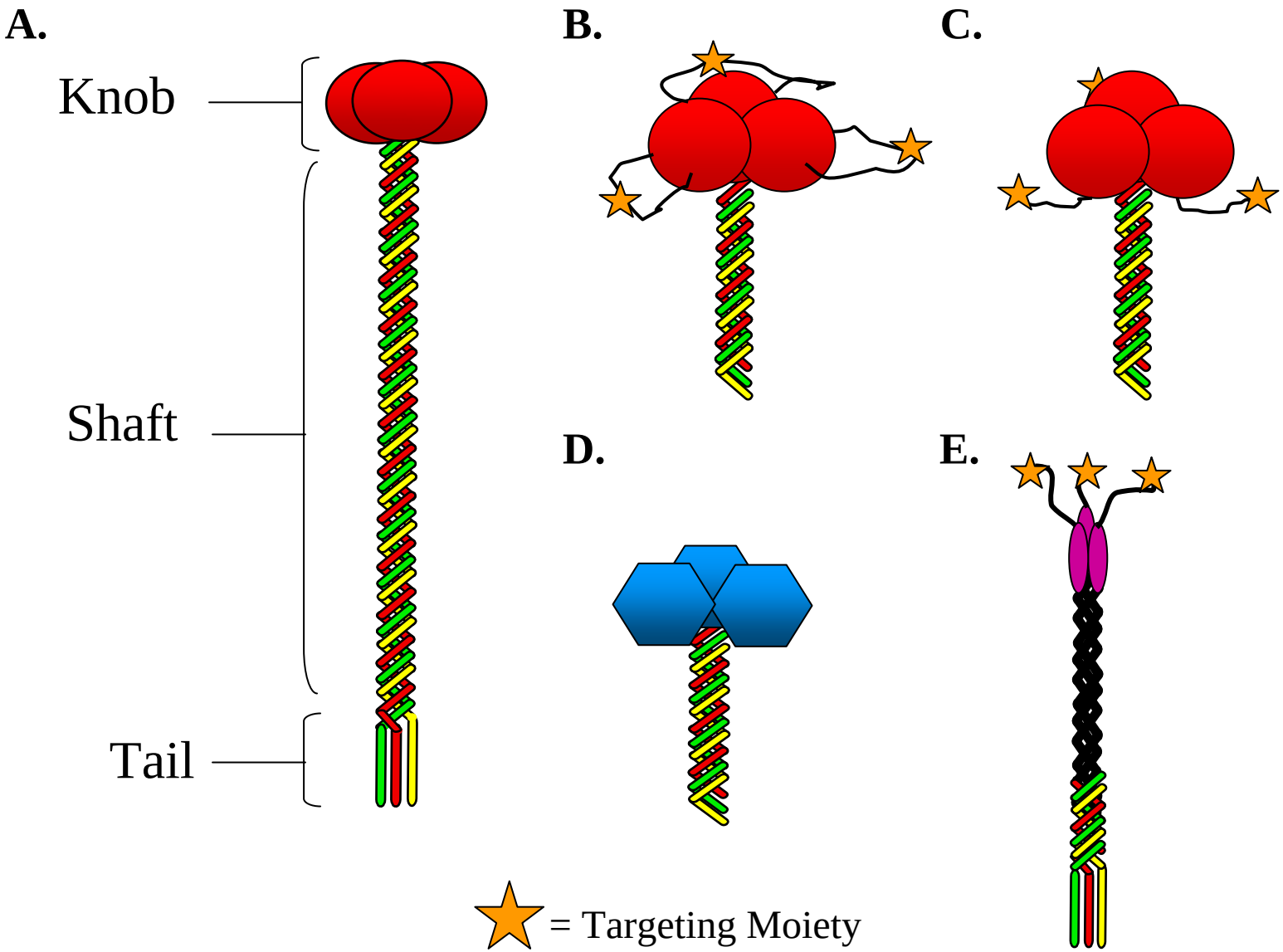
A.
Knob
Shaft
Tail
B.
C.
D.
E.
= Targeting Moiety

Title: Combined transductional targeting and transcriptional restriction enhance adenovirus gene delivery

Authors: Hua-Jung Li[1], Maaike Everts[2], Masato Yamamoto[2], David T. Curiel[2], and Harvey R. Herschman[1]

Affiliations: [1]Departments of Biological Chemistry and Pharmacology, and Molecular Biology Institute, UCLA, Los Angeles, CA 90095

[2]Division of Human Gene therapy, Departments of Medicine, Obstetrics and Gynecology, Pathology and Surgery and the Gene Therapy Center, University of Alabama at Birmingham, Birmingham, AL 35294.

Financial support: These studies were supported by National Cancer Institute grants R01 CA84572 and P50 CA86306 (H.R. Herschman) and NIH and Department of Defense grants 5R01 CA111569 and W812XWH-05-1-0035 (D.T. Curiel)

Corresponding Author: Harvey R. Herschman, 341 Boyer Hall, UCLA. 611 Charles E. Young Drive East, Los Angeles CA 90095, USA. Tel: 310 825 8735; Fax: 310 825 1447; e-mail, hherschman@mednet.ucla.edu

Running Title: Improved adenovirus tumor targeting in vivo

Key words: adenoviral vector, targeting, imaging, Cyclooxygenase-2, carcinoembryonic antigen

Footnotes: The current address for Masato Yamamoto is Division of Basic and Translational Research, Department of Surgery, University of Minnesota, Minneapolis, MN 55455

Abstract

Unresectable hepatic colorectal cancer (CRC) metastases are a leading cause of cancer mortality. Adenovirus gene-delivery vectors provide substantial promise as therapeutic agents, and have proven effective where local delivery is feasible. However, because adenovirus (Ad) vectors preferentially infect liver cells *in vivo* and lack tumor tropism, they cannot be utilized for systemic therapy of hepatic metastases. To overcome this problem, sCAR-MFE, a bi-functional adapter in which the coxsackie/adenovirus receptor (sCAR) ectodomain is fused to a single-chain CEA antibody (MFE-23), was used to "transductionally untarget" intravenously administered Ad from liver cells and to "retarget" the virus to CEA-expressing hepatic tumor xenografts.

Cyclooxygenase-2 (COX-2) is not expressed in liver, but is expressed constitutively in many epithelial tumors. Combining sCAR-MFE mediated hepatic transductional tumor retargeting with COX-2 transcriptional restriction substantially increased tumor:liver transgene expression ratios for hepatic tumor xenografts following systemic administration of adenoviral vectors. Combined transductional liver Ad untargeting, to reduce complications of hepatic viral infection, transductional tumor retargeting to increase efficacy and specificity of transgene delivery to hepatic tumors, and transcriptional restriction to enhance tumor-specific transgene expression suggests a means to engineer practical, effective therapeutic agents for hepatic CRC metastases in particular, as well as hepatic metastases of other epithelial cancers.

Introduction

Liver is the most common site of colorectal cancer (CRC) metastasis, as well as a site of metastasis for lung, breast and other epithelial cancers. Greater than 50% of patients with CRC will develop liver metastases; moreover, the liver can often be the only site of metastases (1, 2). Unfortunately, the 5-year survival rate for patients with CRC liver metastases is less than 5% (3-5). Surgical resection is a standard therapy for CRC liver metastases; however, only 10-20% of hepatic CRC metastases are resectable (6). As a result, it is of paramount importance to develop new approaches to treat hepatic CRC metastases to augment standard surgical, radiation and chemotherapies.

Gene therapy presents an approach distinct from conventional therapies for the treatment of cancer; an approach in which corrective or toxic genes, and imaging genes used to track the location, magnitude and duration of expression of the therapeutic genes, are delivered to tumor cells. Both viral and non-viral vectors have been investigated for the delivery of therapeutic and imaging genes to tumors. Among the viral vectors (retroviruses, Herpes Simplex viruses, measles viruses, etc), adenovirus (Ad) vectors have several properties that make them attractive; they provide high levels of transgene expression, they can accommodate substantial amounts of foreign DNA, they are quite stable *in vivo*, and their genomes are easily manipulated. Consequently, Ad vectors have been used extensively in animal models to investigate delivery of imaging and therapeutic genes (7-9)**.** However, systemically administered Ad preferentially infects the liver (10-12), in part because of the blood filtration properties of the liver and the high coxsackie/Ad receptor (CAR) levels present on hepatocytes. Thus, while current adenoviral vectors have some effectiveness as therapeutic agents for cancer following intratumoral or intraperitoneal delivery (13-17), their utility for transgene delivery to tumors cells following intravenous administration is quite limited (9, 18, 19)

Ad binds initially to cells via an interaction between the “knob” of the virus fiber protein and cellular CAR receptors (20). Selective targeting of Ad vectors to targeted cells can be

achieved by ‘transductional untargeting and retargeting’ with bi-specific adapter molecules; the virus particle is prevented from binding to CAR on cells and is redirected to receptors, antigens or other targets expressed specifically on the surfaces of retargeted cells (21-25).

Many epithelial tumors, including CRC cells, non-small cell lung cancers (NSCLC) and breast cancers produce ectopic carcinoembryonic antigen (CEA) (26). We have demonstrated that sCAR-MFE, a bi-specific adapter in which the ectodomain of the CAR protein (sCAR) is linked to a single chain antibody (MFE-23) directed against CEA, can ‘untarget” liver infection by greater than 90% following intravenous Ad administration (27). sCAR-MFE can also retarget Ad infection to CEA-positive human tumor cells in culture and can preferentially enhance infection of CEA-positive subcutaneous CRC grafts in mice following intratumoral injection of Ad vectors expressing the luciferase reporter (27).

Transcriptional restriction by “tumor-restricted” (e.g., carcinoembryonic antigen, cyclooxygenase-2) promoters has also been used both to optimize Ad vector transgene expression in tumor cells and – perhaps more importantly – to reduce transgene expression from Ad vectors in normal tissues (28-33). Like CEA, elevated cyclooxygenase-2 (COX-2) expression is associated with invasive colorectal cancers, and with tumors with higher metastatic potential (34, 35). Like CEA, COX-2 is not expressed significantly in normal liver (36). The *COX-2* promoter can restrict transgene expression from Ad vectors to subcutaneous COX-2 expressing tumor xenografts following intratumoral injection and can prevent transgene expression in the liver following intravenous injection (32). Therefore, following systemic administration, Ad vectors in which transgenes are under the control of the *COX-2* promoter should drive transgene expression in COX-2 positive hepatic metastases and restrict transgene expression in liver and in nearly all other normal tissues.

Combining transductional hepatic CAR untargeting and tumor cell-specific retargeting using sCAR-MFE with tumor-associated transcriptional restriction of transgene expression by the *Cox2* promoter should optimize targeted transgene expression in CEA-positive, COX-2-

positive hepatic tumors following systemic Ad vector administration. We previously combined transductional Ad vector retargeting to angiotensin converting enzyme (ACE) with transcriptional restriction utilizing the endothelial cell flt-1 promoter, achieving synergistic gains in the selectivity of transgene expression in the pulmonary vasculature (37). Although these results utilize an in vivo model in which the endothelial cell target is easily accessible to systemic vascular administration of virus, they provide a rationale for development of targeting strategies to disseminated cancers that combine transductional untargeting of CAR-expressing normal tissue, transductional retargeting to metastatic lesions, and transcriptional restriction of therapeutic and/or reporter genes to targeted tumor cells.

In this report we demonstrate, for the first time, that combined sCAR-MFE hepatic untargeting, sCAR-MFE CEA-mediated tumor retargeting and *COX-2* promoter-restricted expression substantially enhance transgene gene expression in COX-2 positive, CEA-positive CRC and NSCLC tumors in hepatic metastasis models, following systemic Ad administration. This combination of transductional untargeting, transductional tumor retargeting and tumor-associated transcriptional restriction provides the technological means to achieve selective transgene expression in metastatic cells while sparing normal tissue, furthering the potential for Ad-based cancer gene therapy as a viable therapeutic approach for disseminated disease.

Materials and Methods

Cell lines, cell culture, virus production, and sCAR-MFE preparation.

A549, HT29, Caco-2 and LS174T were grown in Dulbecco modified Eagle medium (Gibco, Rockville, MD) containing 10% fetal bovine serum (Cellegro, Washington, DC) with penicillin-streptomycin (Gibco), 0.1 mM non-essential amino acids (Gibco) and 1.0 mM sodium pyruvate (Gibco). H2122 was grown in RPMI1640 (Gibco) containing 10% fetal bovine serum with penicillin-streptomycin. sCAR-MFE was prepared as described previously (27, 76).

Ad vectors

Ad.CMVfLuc, encoding firefly luciferase (fLuc) under control of the cytomegalovirus (CMV) promoter, and Ad.cox2fLuc, encoding fLuc under the control of the human cyclooxygenase-2 promoter, were described previously (32), and prepared according to Li et al (27). Viruses were propagated in 293 cells and purified by double CsCl density gradient centrifugation, followed by dialysis against phosphate-buffered saline with 10% glycerol. The vectors were titrated by plaque assay and Adeno-X Rapid Titer Kit (BD Clontech, Mountain View, CA) and stored at -80°C.

Stable transfection

To establish stable cell lines that over express *Renilla* luciferase (rLuc), LS174T cells were transfected with a pcDNA3.1 expression vector in which the CMV promoter was replaced by the *Renilla* luciferase coding unit rLuc gene driven by an SV40 promoter, using Lipofectamine 2000 (Invitrogen, Carlsbad, CA). Neomycin-resistant cells were selected using medium containing G418 (1 mg/ml). Extracts of G418 resistant cells were screened for rLuc expression with the Luciferase assay system (Promega, Madison, WI).

Immunoblot Analysis

Cells were washed twice with phosphate-buffered saline (PBS) and incubated on ice for 10 min in lysis buffer containing 50 mM Tris-HCl, pH 7.4, 1% NP-40, 1% triton, 1% sodium deoxycholate, 150 mM NaCl, 1 mM EDTA and protease inhibitors (Complete Tablet; Roche,

Indianapolis, IN). After 10,000 x *g* centrifugation for 10 minutes, supernatant protein concentrations were measured with the Bio-Rad Protein Assay (Bio-Rad). The protein extracts were denatured in denaturing buffer. Equal amounts of protein (100 µg cell lysate) were loaded on SDS-polyacrylamide gels (8% for CEA and 12% for all others) for electrophoresis. Proteins were subsequently transferred to nitrocellulose membranes. The membranes were probed with anti-CEA antibody, cT84.66 (1:10,000 dilution; (77)), anti-human COX-2 monoclonal antibody (1:300 dilution; Cayman Chemical), or anti-14-3-3θ antibody (1:3,000 dilution; Santa Cruz Biotechnology, Santa Cruz, CA) overnight at 4 °C, followed by incubation at room temperature for 60 min with horseradish peroxidase (HRP)-conjugated secondary antibody. Immunoreactivity was determined by enhanced chemiluminescence (ECL; Amersham, Piscataway, NJ).

Analysis of *COX-2* promoter activity in cell culture

Tumor cell lines were infected with Ad.cox2fLuc or Ad.CMVfLuc (MOI=100). The adenovirus were diluted to 150 µl with medium containing 2% FBS, then added to cell monolayers in 24-well plates (2×10^5 cells/well). Virus-treated cells were incubated at 37 °C for 90 minutes. 1 mL medium containing 10% FBS was added after the 90 minutes incubation. After a 40-hour incubation at 37 °C in medium containing 10% FBS, cells were lysed and luciferase activity was measured. The relative activities of the *COX-2* promoters are presented as Relative Luciferase Units (RLU) of the Ad.cox2fLuc infected cells divided by the RLU of Ad.CMVfLuc infected cells.

Preparation of liver xenografts

Eight week-old (*nu/nu*) nude mice (Charles River Laboratories, Wilmington, MA) were anesthetized with ketamine/xylazine (100/10 mg/kg). A transverse incision was made across the xyphoid process and extended approximately two cm. LS174TrLuc or H2122 cells (1×10^6)/mouse in 15 µl were injected into the front of the left upper liver lobe, using a 27-gauge needle. The lobe was returned to the abdomen and the incision was closed with sutures and

wound clips. Buprenorphine was administered every 12 h for 48 h. Wound clips were removed after seven days. Experiments were performed 10-15 days after surgery.

Systemic Ad administration and measurement of *Renilla* and firefly luciferase activities

For transcriptional targeting, Ad.CMVfLuc or Ad.cox2fLuc (1×10^9 ifu/mouse) in 100 µl were administered by tail-vein injection. For transductional untargeting and retargeting, 5×10^8 ifu/mouse of AdCMVfLuc, AdCox2-fLuc, [Ad.CMVfLuc][sCAR-MFE], or [Ad.cox2fLuc][sCAR-MFE] were administered by tail-vein injection. Before injection, viruses were incubated for 1 h either with 10 µg sCAR-MFE/mouse or with PBS. Injection volumes were 100 µl.

On the fourth day after virus injection, coelenterazine (100 µl; ~0.7 mg/kg) was injected via tail-vein and mice were scanned for three min using the Xenogen IVIS Optical Imaging System to monitor tumor-directed rLuc activity. On the fifth day after virus injection, mice were injected intraperitoneally with D-luciferin (250 µl; ~125 mg/kg) and scanned to image Ad-directed fLuc activity. Immediately after imaging, mice were sacrificed. Livers were removed and imaged for fLuc (Ad-dependent) bioluminescence. The livers were then immersed in a solution containing coelenterazine (0.2 mg/ml) and imaged again, using one-minute scans to monitor tumor-derived rLuc activity. After optical imaging, tumor and liver extracts were prepared and firefly luciferase activity of the cell extracts was measured with the Luciferase assay system (Promega, Madison, WI). Protein concentrations were determined with the Bio-Rad Protein Assay (Bio-Rad, Hercules, CA).

Bioluminescent images were analyzed using Living Image software version 2.20 (Xenogen). Regions of interest (ROI) were drawn over tumor and liver areas and total photons were calculated. The ROI sizes in all images for a single experiment were maintained as a consistent area (27).

Statistical analysis

All experiments were performed at least in triplicate. Data are means +/- SEM and are compared by Student's *t* test.

Results

COX-2 and CEA levels are elevated in many epithelial cancer cell lines

To evaluate the retargeting efficacy of our strategy, which involves both CEA-dependent Ad retargeting and *COX-2* promoter restricted transgene expression, we utilized human tumor cells with high levels of COX-2 and CEA expression. Expression of COX-2 and CEA protein were determined by immunoblotting for a number of CRC and lung tumor cell lines, since colorectal and lung tumors are known to express COX-2 and CEA, and to metastasize to the liver. COX-2 protein is detectable in most of these tumor cell lines, including A549, H2122, HT29, Caco-2 and LS174T (Fig. 1A). CEA is detectable by Western blotting in H2122, HT29, and LS174T cells, but not in A549 and Caco-2 cells. Thus human H2122, HT29 and LS174T cells express both COX-2 and CEA proteins. In addition, because CEA is found on the surface of these three cell lines (27), they are excellent candidates for anti-CEA based Ad re-targeting and *COX-2* promoter restricted Ad transgene expression. These three cell lines also efficiently form hepatic tumors in nude mice (data not shown).

Although COX-2 protein is present in many of these tumor cells, for transcriptional targeting we require target cells with high promoter activity of the targeted gene, rather than high levels of protein expression. Activity of the *COX-2* promoter was measured by Ad.cox2fLuc infection of these tumor cell lines in culture. The *COX-2* promoter used for Ad.cox2fLuc includes the sequence from -1432 to +59 of the human *COX-2* gene. Ad.cox2fLuc or Ad.CMVfLuc, Ad vectors in which the firefly luciferase gene is expressed from the *COX-2* promoter or the CMV promoter respectively, were used to infect the different tumor cell lines (Fig. 1B). The relative promoter activity is reflected by the ratios of fLuc activity of Ad.cox2fLuc-infected cells divided by the fLuc activity of Ad.CMV-fLuc infected cells, to normalize for Ad infectivity. (We used this procedure for normalization because we find that various cell lines express different ratios of firefly and *Renilla* luciferase activities when co-transfected with plasmids that utilize the same promoter, demonstrating that normalization to a co-transfected *Renilla* luciferase – while valid

for comparisons within a cell line – cannot be used to normalize transfections across cell lines.) All cell lines tested have easily detectable levels of *COX-2* promoter-driven luciferase activity.

The *COX-2* promoter transcriptionally restricts expression from adenoviral vectors to hepatic CRC metastases

COX-2 is over expressed in most hepatic CRC metastases, and is not expressed in liver. Ad.cox2fLuc is a replication-defective Ad vector in which the *COX-2* promoter regulates firefly luciferase expression (31). Expression of the luciferase reporter gene from the *COX-2* promoter restricts reporter gene expression in the liver following systemic Ad.cox2fLuc administration to mice (32). To determine whether Ad.cox2fLuc can effectively deliver transgenes to COX-2 positive hepatic tumors and direct luciferase in these tumors, while remaining unable to express the transgene in the surrounding liver tissue, Ad.CMVfLuc and Ad.cox2fLuc were administrated intravenously to nude mice bearing hepatic LS174T(rLuc) CRC xenografts.

To noninvasively monitor tumor cell burden, the LS174T CRC tumor cells carry a stably transfected *Renilla* luciferase reporter gene. Coelenterazine-dependent bioluminescence from *Renilla* luciferase identifies the location of tumor xenografts (Fig. 2A, panels a-c, f, h-j and m). Luciferin-dependent bioluminescence from firefly luciferase indicates the location and degree of Ad-mediated transgene expression (Fig. 2A, panels d,g,k and n).

In Ad.CMVfLuc-injected mice, bioluminescence encoded from the Ad vector is not co-localized with LS174T(rLuc) tumor bioluminescence (compare panels c and d of Fig 2A for *in vivo* co-localization and panels f and g of Fig. 2A for tumor and liver co-localization in isolated organs). In contrast, in Ad.cox2fLuc injected mice the vector-encoded bioluminescence co-localizes with tumor-encoded bioluminescence (compare panels j and k of Fig 2A for *in vivo* co-localization and panels m and n of Fig. 2A for tumor and liver co-localization in isolated organs). These imaging data demonstrate that fLuc expression from the CMV promoter is extensive in

liver following Ad.CMVfLuc infection, but relatively weak in the LS174T hepatic xenograft; in contrast, virally-directed fLuc expression following systemic Ad.cox2fLuc administration is highly restricted in normal liver tissue, but is strong in the COX-2 expressing LS174T hepatic xenografts.

After imaging coelenterazine-dependent (tumor cell) rLuc activity and luciferin-dependent (virus encoded) fLuc activity from the isolated livers (Fig. 1A), the liver and tumor tissues were dissected. To quantitate *COX-2* promoter transcriptional restriction to LS174T CRC tumors, fLuc activities in tumor and liver extracts were analyzed with a conventional in vitro firefly luciferase assay (Fig. 2B). Following systemic Ad.CMVfLuc infection, the hepatic tumor:liver luciferase ratio is 1.6:1. In contrast, the tumor:liver ratio for Ad.cox2fLuc-driven luciferase activity is 37.6:1 (Fig. 2C). Transcriptional restriction increased the tumor:liver ratio of transgene expression nearly 25-fold in this setting. The bulk of the increase in tumor:liver ratio is due to reduced expression in the liver tissue from the *COX-2* promoter relative to the CMV promoter; expression from the CMV promoter and the *COX-2* promoter in the LS174T tumor tissue is essentially the same (Fig. 2B).

We used the subcapsular liver model for hepatic metasasis, rather than using spleen injection (38, 39) to create liver CRC metastatic model systems, to minimize tumor contamination in the normal hepatic tissues. Histologic analyses of tumor-bearing liver tissues like those used in these studies had no detectable human tumor cells (data not shown). If tumor cells were present in the “liver” samples, the apparent transductional efficiency would be reduced (as result of firefly luciferase activity generated from infected tumor cells); thus our estimates of “tumor to liver ratio” are minimal values.

sCAR-MFE hepatic untargeting, sCAR-MFE CEA-mediated tumor retargeting, and *COX-2* promoter transcriptional restriction combine to enhance Ad transgene expression in hepatic CEA-positive, COX-2-positive CRC tumor xenografts

To achieve maximal transgene targeting to hepatic tumors following systemic Ad administration, we combined sCAR-MFE hepatic untargeting (27), sCAR-MFE tumor retargeting (27), and *COX-2* promoter-restricted expression to CEA-expressing, COX-2-expressing liver metastases. Ad.CMVfLuc, Ad.cox2fLuc, [Ad.CMVfLuc][sCAR-MFE] and [Ad.cox2fLuc][sCAR-MFE] were injected intravenously into mice bearing LS174T CRC liver xenografts. fLuc bioluminescence, observed in living animals after intraperitoneal D-luciferin injection, indicates successful Ad infection and transgene expression (Fig. 3A). Viral transgene expression in the tumors versus the livers can be observed in the bioluminescence images of livers removed from these tumor-bearing mice (Fig. 3A). Virus-directed firefly luciferase transgene activity in extracts of tumors and of the livers from these mice were subsequently quantitated (Fig. 3B).

The sCAR-MFE adapter reduces liver Ad infection by greater than 90% (27). Thus, tumor-bearing mice infected with [Ad.CMVfLuc][sCAR-MFE] have reduced hepatic luciferase activity relative to tumor-bearing mice infected with Ad.CMVfLuc (Fig. 3A, panels d-f versus panels a-c). The tumor:liver bioluminescence ratio for Ad.CMVfLuc infection is increased from 0.75:1 to 2.5:1 by sCAR-MFE transductional hepatic untargeting and tumor retargeting (Fig. 3B). Mice infected with Ad.cox2fLuc exhibit substantially reduced hepatic bioluminescence (Fig. 3A, panels g-i); the tumor:liver bioluminescence ratio resulting from *COX-2* promoter transcriptional restriction is 33.5:1 (Fig. 3B). By combining sCAR-MFE transductional hepatic untargeting, sCAR-MFE transductional tumor retargeting and *COX-2* promoter-dependent transcriptional restriction, mice infected with [Ad.cox2fLuc][sCAR-MFE] demonstrate both low hepatic bioluminescence and strong tumor bioluminescence (Fig. 3A, panels j-l). Combining sCAR-MFE transductional hepatic untargeting, sCAR-MFE transductional tumor retargeting and *COX-2* promoter transcriptional restriction brings the tumor:liver luciferase expression ratio following systemic Ad infection from 0.75:1 to 116:1 (Fig. 3B) in LS174T CRC hepatic tumor xenografts; a 150 fold increase in tumor-restricted transgene expression.

sCAR-MFE hepatic untargeting, sCAR-MFE CEA-mediated tumor retargeting, and *COX-2* promoter transcriptional restriction combine to enhance Ad transgene expression in hepatic CEA-positive, COX-2-positive NSCLC tumor xenografts

A number of other epithelial tumors (breast, lung), in addition to CRC tumors, often express CEA. The combined efficacy of sCAR-MFE transductional hepatic untargeting, sCAR-MFE transductional tumor retargeting, and *COX-2* promoter transcriptional restriction was also evaluated in a CEA-positive, COX-2-positive NSCLC liver metastasis model. Ad.CMVfLuc, Ad.cox2fLuc and [Ad.cox2fLuc][sCAR-MFE] were injected intravenously into mice carrying H2122 human CEA-positive, COX-2-positive NSCLC hepatic tumors. Once again, mice infected with Ad.CMVfLuc (Fig. 4A, panels a-c) have much greater hepatic bioluminescence levels than do mice infected with Ad.cox2fLuc (Fig. 4A, panels d-f). The tumor:liver luciferase activity ratio in extracts is increased from 0.4:1 to 2.2:1 by *COX-2* promoter transcriptional restriction (Fig. 4B). Mice infected with [Ad.Cox2-fLuc][sCAR-MFE] have even lower hepatic bioluminescence and increased tumor bioluminescence (Fig. 4A, panels g-i). The tumor:liver luciferase ratio is increased from 2.2:1 for Ad.cox2fLuc to 11.1:1 when Ad.cox2fLuc virus is untargeted from liver and retargeted to CEA-positive H2122 xenografts by sCAR-MFE (Fig. 4B). Combining sCAR-MFE transductional hepatic untargeting, sCAR-MFE transductional tumor retargeting and *COX-2* promoter restricted transgene expression enhances the tumor:liver luciferase ratio from 0.4:1 to 11.1:1, an increase in tumor-restricted transgene expression of 28 fold for this NSCLC hepatic xenograft model (Fig. 4B)

Discussion

Circulating epithelial tumor cells frequently form hepatic metastases; tumor cells lodge in the liver during the process of blood filtration. The liver is the most common site for CRC metastases. Although surgical resection for hepatic CRC metastases is standard therapy, only a small percentage of these metastases are resectable; consequently additional therapeutic approaches are needed to increase survival rates for patients with hepatic CRC metastases.

Because of a reduced endothelial barrier, systemically administered adenoviruses have increased access to cells in the liver relative to other tissues. Consequently, hepatic metastases should – in principle – be more susceptible to systemic Ad-mediated therapies than would be metastases in other tissues. However, although Ad vectors have achieved some clinical success for intratumoral (16, 40) and intraperitoneal (41) tumor therapy, they are not currently used for systemic treatment of metastatic disease; extensive hepatocyte infection following systemic virus administration is potentially a major cause for adverse responses to Ad vector mediated therapy, as a result both of hepatic viral transgene expression and of Ad-induced host inflammatory responses. Our demonstration of enhanced delivery of transgenes by the combined use of transductional hepatic untargeting/transductional tumor retargeting, coupled with transcriptionally restricted gene expression in hepatic epithelial tumor xenografts, should make clinical application of Ad gene therapy for hepatic metastases more promising.

In principle, it might appear more efficient to “re-target” adenoviral vectors by modifying the virus structure, both to prevent CAR recognition on normal cells and to enhance recognition of tumor-associated cell-surface epitopes on cancer cells. While a number of genetically modified viruses that target cells via CAR-independent interactions have been reported (42-48), some of which have also used transcriptionally restricted transgene expression (49, 50) genetic modification to both enhance Ad tumor targeting and restrict normal cell infection has several drawbacks. For each tumor-targeting vector, genetic modifications that accomplish appropriate

untargeting/retargeting, but still permit proper virus assembly, must be found. Because these viruses are unable to propagate through CAR-mediated infection, cells that permit viral replication must be identified or created (51-55). Moreover, viral infection is not solely dependent on the initial interaction between the viral knob and cellular CAR; other interactions that involve integrins (56, 57) and other viral/target cell components (58-60) are utilized following knob:CAR recognition for proper viral binding, internalization and uncoating (61). Viruses genetically modified to evade knob/CAR-dependent virus binding and substitute alternative initial recognition schema must either remain competent for these secondary events and/or substitute alternatives following a redirected initial binding event, in order to complete viral infection successfully. Ad untargeting by bi-specific adapters and retargeting to tumor cells is – if not in principle, than in practice – often simpler and more scalable than is genetic modification to retarget adenoviral vectors to alternative tumor cell epitopes. Transductional targeting also offers a non-genetic means to direct Ad infection to tumor cells that express little or no CAR (e.g., H2122 cells (27)).

Although transductional untargeting is effective in reducing liver infection by Ad, complementary approaches to reduce transgene expression in normal cells and increase selective transgene expression in targeted tumor cells are necessary. A number of studies have demonstrated that transgene expression from Ad gene delivery vectors can also be regulated by transcriptional restriction, using targeted, cell-specific promoters (28, 62, 63). Even if Ad vectors infect hepatocytes, virally-delivered transgenes cannot be expressed in the liver cells if the transgenes are under the control of a promoter that is not expressed in the liver.

The *COX-2* gene is ectopically activated in many epithelial cancers (34, 64, 65). Moreover, COX-2 is not expressed in hepatocytes, even under conditions of substantial stress (66). The frequency of COX-2 overexpression in epithelial tumors, combined with the inability of normal liver cells to express COX-2, provides a fortuitous combination of circumstances that can hopefully be exploited to enhance tumor expression in hepatic metastases while reducing

complications resulting from the extensive liver infection that occurs following systemic viral administration.

Few studies exist that demonstrate effective and selective Ad infection in targeted cells as a result of combining transductional untargeting of normal cells, transductional retargeting to a selected cell population and transcriptional restriction to targeted cells following systemic vector administration. Reynolds et al (67) demonstrated transductional untargeting of normal cells and retargeting to rat pulmonary vasculature cells, along with transgene expression controlled by a promoter that exhibits enhanced endothelial cell expression. However, pulmonary endothelium is directly accessible from the circulation, thus facilitating target cell recognition by the transductionally targeted virus. In contrast, both liver toxicity (18) and low efficiency of Ad infection (68) prevent systemic (intravenous) Ad therapy of hepatic tumors; prior studies of Ad untargeting/retargeting have generally used either intratumoral or intraperitoneal administration to subcutaneous or peritoneal tumor models respectively (69-73). However, as demonstrated here, circulatory Ad access to hepatic tumors facilitates the efficacy of combined transductional Ad retargeting and transcriptional restriction to target tumor nodules within the liver following systemic Ad administration. To our knowledge, the combined use of transductional liver untargeting/tumor retargeting, coupled with tumor-enhanced transcriptional restriction, has not previously been described for the delivery of transgenes to hepatic tumors following systemic adenovirus administration.

Bi-specific adapters increase Ad vector size approximately 2-fold, to 300 nm in diameter (71). The size increase may further impede, but not fully prevent the Ad complex from penetrating endothelium to reach cells (71, 74). The bioavailability of adapter-coated Ad could, therefore, be affected by particle size. Our data suggest that the increased access of liver metastases to viral particles, relative to metastases in other tissues, minimizes this potential problem for hepatic tumors; hepatic metastasis models may more accurately reflect the clinical context than do subcutaneous xenograft animal models (75).

Combined transductional untargeting/retargeting and tumor-restricted transcriptional expression offer substantial flexibility. Recombinant proteins can be created that use alternative untargeting components (e.g. sCAR, anti-knob Fab) and a variety of tumor-directed retargeting agents (e.g., receptor recognition peptides, antibodies, lectins). Promoters for tumor-restricted expression can be chosen that utilize either tissue/cell specificity or tumor cell specificity. Tumor cell differences in the efficacy of adapter untargeting:retargeting and promoter-restricted transgene expression can be seen in the two examples presented here. Although sCAR-MFE retargeting and *COX-2* promoter restricted expression are successful for both LS174T CRC and H2122 NSCLC hepatic xenografts, *COX-2* promoter transcriptional restriction is 5-6 fold for H2122 cells, but is 45 fold for LS174T cells. In contrast, sCAR-MFE retargeting efficacy is 5-6 fold for H2122 cells and 3 fold for LS174T cells. By varying tumor retargeting moieties and transcriptionally restricted promoters one can "tailor" untargeting/retargeting and transcriptional restriction combinations for specific tumors. However, it will be important to validate assumptions about modular components; although the *CEA* promoter was a substantially more powerful promoter than the *COX-2* promoter when Ad vectors were used to infect CRC cells in culture, in studies in which these same tumor cells were grown in mouse liver, the *COX-2* promoter was more effective than the *CEA* promoter at restricting transcriptional expression to the tumor cells (data not shown).

By utilizing alternative transgenes, difference purposes can be achieved; cargo genes whose products can be imaged by bioluminescent, fluorescent, magnetic resonance imaging, positron emission tomography, single photon emission tomography, etc can be targeted to tumor cells. Alternatively, therapeutic genes that target tumor cells, tumor neovasculature, inflammatory cells and other cells that participate in tumor progression can be incorporated into these vectors.

Ad vectors for systemic cancer therapy continue to be an attractive goal, with important potential clinical consequences. Although substantial barriers (e.g, Ad immunity, cytokine

release in response to Ad recognition) still need to be overcome to perfect targeted Ad vectors for systemic cancer therapy, significant improvements have been achieved through the targeting approaches described here. In addition, by combining transductional untargeting, transductional retargeting, transcriptional restriction and the choice of proper reporter genes and imaging techniques, new methods that utilize Ad vectors to detect occult tumors (7) and to monitor both tumor burden and response to therapy are on the horizon.

Acknowledgements

These studies were supported by National Cancer Institute grants R01 CA84572 and P50 CA86306 (H.R. Herschman) and NIH and Department of Defense grants 5R01 CA111569 and W812XWH-05-1-0035 (D.T. Curiel). We thank Arthur Catapang for technical assistance, and the support staff of the UCLA Small Animal Imaging Shared Resource for assistance with optical imaging.

References

1. Wagner JS, Adson MA, Van Heerden JA, Adson MH, Ilstrup DM. The natural history of hepatic metastases from colorectal cancer. A comparison with resective treatment. Ann Surg 1984;199(5):502-8.

2. Gilbert HA, Kagan AR. Metastases: incidence, detection, and evaluation without histologic confirmation. Fundamental Aspects of Metastasis: North Holland Publishing Co; 1976. p. 385-405.

3. Macdonald JS. Adjuvant therapy of colon cancer. CA Cancer J Clin 1999;49(4):202-19.

4. Fong Y, Cohen AM, Fortner JG*, et al.* Liver resection for colorectal metastases. J Clin Oncol 1997;15(3):938-46.

5. Tuttle TM, Curley SA, Roh MS. Repeat hepatic resection as effective treatment of recurrent colorectal liver metastases. Ann Surg Oncol 1997;4(2):125-30.

6. Feliberti EC, Wagman LD. Radiofrequency ablation of liver metastases from colorectal carcinoma. Cancer Control 2006;13(1):48-51.

7. Adams JY, Johnson M, Sato M*, et al.* Visualization of advanced human prostate cancer lesions in living mice by a targeted gene transfer vector and optical imaging. Nat Med 2002;8(8):891-7.

8. Yamamoto M, Curiel DT. Nonreplicating DNA viral vectors for suicide gene therapy: the adenoviral vectors. Methods in molecular medicine 2004;90:61-70.

9. Nasu Y, Kusaka N, Saika T, Tsushima T, Kumon H. Suicide gene therapy for urogenital cancer: current outcome and prospects. Molecular urology 2000;4(2):67-71.

10. Zinn KR, Douglas JT, Smyth CA*, et al.* Imaging and tissue biodistribution of 99mTc-labeled adenovirus knob (serotype 5). Gene Ther 1998;5(6):798-808.

11. Tomko RP, Xu R, Philipson L. HCAR and MCAR: the human and mouse cellular receptors for subgroup C adenoviruses and group B coxsackieviruses. Proc Natl Acad Sci U S A 1997;94(7):3352-6.

12. Einfeld DA, Schroeder R, Roelvink PW*, et al.* Reducing the native tropism of adenovirus vectors requires removal of both CAR and integrin interactions. J Virol 2001;75(23):11284-91.

13. Harrison D, Sauthoff H, Heitner S, Jagirdar J, Rom WN, Hay JG. Wild-type adenovirus decreases tumor xenograft growth, but despite viral persistence complete tumor responses are rarely achieved--deletion of the viral E1b-19-kD gene increases the viral oncolytic effect. Hum Gene Ther 2001;12(10):1323-32.

14. Kuriyama N, Kuriyama H, Julin CM, Lamborn KR, Israel MA. Protease pretreatment increases the efficacy of adenovirus-mediated gene therapy for the treatment of an experimental glioblastoma model. Cancer Res 2001;61(5):1805-9.

15. Sung MW, Yeh HC, Thung SN*, et al.* Intratumoral adenovirus-mediated suicide gene transfer for hepatic metastases from colorectal adenocarcinoma: results of a phase I clinical trial. Mol Ther 2001;4(3):182-91.

16. Galanis E, Okuno SH, Nascimento AG*, et al.* Phase I-II trial of ONYX-015 in combination with MAP chemotherapy in patients with advanced sarcomas. Gene Ther 2005;12(5):437-45.

17. Kubo H, Gardner TA, Wada Y*, et al.* Phase I dose escalation clinical trial of adenovirus vector carrying osteocalcin promoter-driven herpes simplex virus thymidine kinase in localized and metastatic hormone-refractory prostate cancer. Hum Gene Ther 2003;14(3):227-41.

18. Mahasreshti PJ, Kataram M, Wang MH*, et al.* Intravenous delivery of adenovirus-mediated soluble FLT-1 results in liver toxicity. Clin Cancer Res 2003;9(7):2701-10.

19. Kirn D. Clinical research results with dl1520 (Onyx-015), a replication-selective adenovirus for the treatment of cancer: what have we learned? Gene Ther 2001;8(2):89-98.

20. Louis N, Fender P, Barge A, Kitts P, Chroboczek J. Cell-binding domain of adenovirus serotype 2 fiber. J Virol 1994;68(6):4104-6.

21. Wickham TJ, Segal DM, Roelvink PW*, et al.* Targeted adenovirus gene transfer to endothelial and smooth muscle cells by using bispecific antibodies. J Virol 1996;70(10):6831-8.

22. Watkins SJ, Mesyanzhinov VV, Kurochkina LP, Hawkins RE. The 'adenobody' approach to viral targeting: specific and enhanced adenoviral gene delivery. Gene Ther 1997;4(10):1004-12.

23. Trepel M, Grifman M, Weitzman MD, Pasqualini R. Molecular adaptors for vascular-targeted adenoviral gene delivery. Hum Gene Ther 2000;11(14):1971-81.

24. Glasgow JN, Everts M, Curiel DT. Transductional targeting of adenovirus vectors for gene therapy. Cancer Gene Ther 2006.

25. Kashentseva EA, Seki T, Curiel DT, Dmitriev IP. Adenovirus targeting to c-erbB-2 oncoprotein by single-chain antibody fused to trimeric form of adenovirus receptor ectodomain. Cancer Res 2002;62(2):609-16.

26. Goldstein MJ, Mitchell EP. Carcinoembryonic antigen in the staging and follow-up of patients with colorectal cancer. Cancer investigation 2005;23(4):338-51.

27. Li HJ, Everts M, Pereboeva L*, et al.* Adenovirus Tumor Targeting and Hepatic Untargeting by a Coxsackie/Adenovirus Receptor Ectodomain Anti-Carcinoembryonic Antigen Bispecific Adapter. Cancer Res 2007;67(11):5354-61.

28. Glasgow JN, Bauerschmitz GJ, Curiel DT, Hemminki A. Transductional and transcriptional targeting of adenovirus for clinical applications. Curr Gene Ther 2004;4(1):1-14.

29. Mathis JM, Stoff-Khalili MA, Curiel DT. Oncolytic adenoviruses - selective retargeting to tumor cells. Oncogene 2005;24(52):7775-91.

30. Stoff-Khalili MA, Stoff A, Rivera AA*, et al.* Preclinical evaluation of transcriptional targeting strategies for carcinoma of the breast in a tissue slice model system. Breast Cancer Res 2005;7(6):R1141-52.

31. Yamamoto M, Alemany R, Adachi Y, Grizzle WE, Curiel DT. Characterization of the cyclooxygenase-2 promoter in an adenoviral vector and its application for the mitigation of toxicity in suicide gene therapy of gastrointestinal cancers. Mol Ther 2001;3(3):385-94.

32. Liang Q, Yamamoto M, Curiel DT, Herschman HR. Noninvasive imaging of transcriptionally restricted transgene expression following intratumoral injection of an adenovirus in which the COX-2 promoter drives a reporter gene. Mol Imaging Biol 2004;6(6):395-404.

33. Terazaki Y, Yano S, Yuge K*, et al.* An optimal therapeutic expression level is crucial for suicide gene therapy for hepatic metastatic cancer in mice. Hepatology 2003;37(1):155-63.

34. Eberhart CE, Coffey RJ, Radhika A, Giardiello FM, Ferrenbach S, DuBois RN. Up-regulation of cyclooxygenase 2 gene expression in human colorectal adenomas and adenocarcinomas. Gastroenterology 1994;107(4):1183-8.

35. Chen WS, Wei SJ, Liu JM, Hsiao M, Kou-Lin J, Yang WK. Tumor invasiveness and liver metastasis of colon cancer cells correlated with cyclooxygenase-2 (COX-2) expression and inhibited by a COX-2-selective inhibitor, etodolac. Int J Cancer 2001;91(6):894-9.

36. DuBois RN. Cyclooxygenase-2 and colorectal cancer. Prog Exp Tumor Res 2003;37:124-37.

37. Reynolds PN, Zinn KR, Gavrilyuk VD*, et al.* A targetable, injectable adenoviral vector for selective gene delivery to pulmonary endothelium in vivo. Mol Ther 2000;2(6):562-78.

38. Tada H, Maron DJ, Choi EA*, et al.* Systemic IFN-beta gene therapy results in long-term survival in mice with established colorectal liver metastases. The Journal of clinical investigation 2001;108(1):83-95.

39. Morikawa K, Walker SM, Nakajima M, Pathak S, Jessup JM, Fidler IJ. Influence of organ environment on the growth, selection, and metastasis of human colon carcinoma cells in nude mice. Cancer Res 1988;48(23):6863-71.

40. Hecht JR, Bedford R, Abbruzzese JL*, et al.* A phase I/II trial of intratumoral endoscopic ultrasound injection of ONYX-015 with intravenous gemcitabine in unresectable pancreatic carcinoma. Clin Cancer Res 2003;9(2):555-61.

41. Alvarez RD, Gomez-Navarro J, Wang M*, et al.* Adenoviral-mediated suicide gene therapy for ovarian cancer. Mol Ther 2000;2(5):524-30.

42. Work LM, Nicklin SA, Brain NJ*, et al.* Development of efficient viral vectors selective for vascular smooth muscle cells. Mol Ther 2004;9(2):198-208.

43. Nicklin SA, Dishart KL, Buening H*, et al.* Transductional and transcriptional targeting of cancer cells using genetically engineered viral vectors. Cancer letters 2003;201(2):165-73.

44. Kanerva A, Mikheeva GV, Krasnykh V*, et al.* Targeting adenovirus to the serotype 3 receptor increases gene transfer efficiency to ovarian cancer cells. Clin Cancer Res 2002;8(1):275-80.

45. Nicklin SA, White SJ, Watkins SJ, Hawkins RE, Baker AH. Selective targeting of gene transfer to vascular endothelial cells by use of peptides isolated by phage display. Circulation 2000;102(2):231-7.

46. Rea D, Havenga MJ, van Den Assem M*, et al.* Highly efficient transduction of human monocyte-derived dendritic cells with subgroup B fiber-modified adenovirus vectors enhances transgene-encoded antigen presentation to cytotoxic T cells. J Immunol 2001;166(8):5236-44.

47. Von Seggern DJ, Huang S, Fleck SK, Stevenson SC, Nemerow GR. Adenovirus vector pseudotyping in fiber-expressing cell lines: improved transduction of Epstein-Barr virus-transformed B cells. J Virol 2000;74(1):354-62.

48. Xia H, Anderson B, Mao Q, Davidson BL. Recombinant human adenovirus: targeting to the human transferrin receptor improves gene transfer to brain microcapillary endothelium. J Virol 2000;74(23):11359-66.

49. Stoff-Khalili MA, Rivera AA, Stoff A*, et al.* Combining high selectivity of replication via CXCR4 promoter with fiber chimerism for effective adenoviral oncolysis in breast cancer. Int J Cancer 2007;120(4):935-41.

50. Zhu ZB, Makhija SK, Lu B*, et al.* Targeting mesothelioma using an infectivity enhanced survivin-conditionally replicative adenoviruses. J Thorac Oncol 2006;1(7):701-11.

51. Von Seggern DJ, Kehler J, Endo RI, Nemerow GR. Complementation of a fibre mutant adenovirus by packaging cell lines stably expressing the adenovirus type 5 fibre protein. The Journal of general virology 1998;79 (Pt 6):1461-8.

52. Douglas JT, Miller CR, Kim M*, et al.* A system for the propagation of adenoviral vectors with genetically modified receptor specificities. Nat Biotechnol 1999;17(5):470-5.

53. Roelvink PW, Mi Lee G, Einfeld DA, Kovesdi I, Wickham TJ. Identification of a conserved receptor-binding site on the fiber proteins of CAR-recognizing adenoviridae. Science 1999;286(5444):1568-71.

54. Legrand V, Spehner D, Schlesinger Y, Settelen N, Pavirani A, Mehtali M. Fiberless recombinant adenoviruses: virus maturation and infectivity in the absence of fiber. J Virol 1999;73(2):907-19.

55. Koizumi N, Mizuguchi H, Sakurai F, Yamaguchi T, Watanabe Y, Hayakawa T. Reduction of natural adenovirus tropism to mouse liver by fiber-shaft exchange in combination with both CAR- and alphav integrin-binding ablation. J Virol 2003;77(24):13062-72.

56. Wickham TJ, Mathias P, Cheresh DA, Nemerow GR. Integrins alpha v beta 3 and alpha v beta 5 promote adenovirus internalization but not virus attachment. Cell 1993;73(2):309-19.

57. Li E, Brown SL, Stupack DG, Puente XS, Cheresh DA, Nemerow GR. Integrin alpha(v)beta1 is an adenovirus coreceptor. J Virol 2001;75(11):5405-9.

58. Dechecchi MC, Melotti P, Bonizzato A, Santacatterina M, Chilosi M, Cabrini G. Heparan sulfate glycosaminoglycans are receptors sufficient to mediate the initial binding of adenovirus types 2 and 5. J Virol 2001;75(18):8772-80.

59. Hong SS, Karayan L, Tournier J, Curiel DT, Boulanger PA. Adenovirus type 5 fiber knob binds to MHC class I alpha2 domain at the surface of human epithelial and B lymphoblastoid cells. The EMBO journal 1997;16(9):2294-306.

60. Chu Y, Heistad D, Cybulsky MI, Davidson BL. Vascular cell adhesion molecule-1 augments adenovirus-mediated gene transfer. Arteriosclerosis, thrombosis, and vascular biology 2001;21(2):238-42.

61. Meier O, Boucke K, Hammer SV*, et al.* Adenovirus triggers macropinocytosis and endosomal leakage together with its clathrin-mediated uptake. The Journal of cell biology 2002;158(6):1119-31.

62. Saukkonen K, Hemminki A. Tissue-specific promoters for cancer gene therapy. Expert Opin Biol Ther 2004;4(5):683-96.

63. Robson T, Hirst DG. Transcriptional Targeting in Cancer Gene Therapy. J Biomed Biotechnol 2003;2003(2):110-37.

64. DuBois RN, Smalley WE. Cyclooxygenase, NSAIDs, and colorectal cancer. J Gastroenterol 1996;31(6):898-906.

65. Fujita T, Matsui M, Takaku K*, et al.* Size- and invasion-dependent increase in cyclooxygenase 2 levels in human colorectal carcinomas. Cancer Res 1998;58(21):4823-6.

66. Ishikawa TO, Jain NK, Taketo MM, Herschman HR. Imaging cyclooxygenase-2 (Cox-2) gene expression in living animals with a luciferase knock-in reporter gene. Mol Imaging Biol 2006;8(3):171-87.

67. Reynolds PN, Nicklin SA, Kaliberova L*, et al.* Combined transductional and transcriptional targeting improves the specificity of transgene expression in vivo. Nat Biotechnol 2001;19(9):838-42.

68. Tang DC, Johnston SA, Carbone DP. Butyrate-inducible and tumor-restricted gene expression by adenovirus vectors. Cancer Gene Ther 1994;1(1):15-20.

69. Rancourt C, Rogers BE, Sosnowski BA*, et al.* Basic fibroblast growth factor enhancement of adenovirus-mediated delivery of the herpes simplex virus thymidine kinase gene results in augmented therapeutic benefit in a murine model of ovarian cancer. Clin Cancer Res 1998;4(10):2455-61.

70. Gu DL, Gonzalez AM, Printz MA*, et al.* Fibroblast growth factor 2 retargeted adenovirus has redirected cellular tropism: evidence for reduced toxicity and enhanced antitumor activity in mice. Cancer Res 1999;59(11):2608-14.

71. Printz MA, Gonzalez AM, Cunningham M*, et al.* Fibroblast growth factor 2-retargeted adenoviral vectors exhibit a modified biolocalization pattern and display reduced toxicity relative to native adenoviral vectors. Hum Gene Ther 2000;11(1):191-204.

72. Khuri FR, Nemunaitis J, Ganly I*, et al.* a controlled trial of intratumoral ONYX-015, a selectively-replicating adenovirus, in combination with cisplatin and 5-fluorouracil in patients with recurrent head and neck cancer. Nat Med 2000;6(8):879-85.

73. Heise CC, Williams A, Olesch J, Kirn DH. Efficacy of a replication-competent adenovirus (ONYX-015) following intratumoral injection: intratumoral spread and distribution effects. Cancer Gene Ther 1999;6(6):499-504.

74. Kim J, Smith T, Idamakanti N*, et al.* Targeting adenoviral vectors by using the extracellular domain of the coxsackie-adenovirus receptor: improved potency via trimerization. J Virol 2002;76(4):1892-903.

75. Fukumura D, Yuan F, Monsky WL, Chen Y, Jain RK. Effect of host microenvironment on the microcirculation of human colon adenocarcinoma. The American journal of pathology 1997;151(3):679-88.

76. Everts M, Kim-Park SA, Preuss MA*, et al.* Selective induction of tumor-associated antigens in murine pulmonary vasculature using double-targeted adenoviral vectors. Gene Ther 2005;12(13):1042-8.

77. Neumaier M, Shively L, Chen FS*, et al.* Cloning of the genes for T84.66, an antibody that has a high specificity and affinity for carcinoembryonic antigen, and expression of chimeric human/mouse T84.66 genes in myeloma and Chinese hamster ovary cells. Cancer Res 1990;50(7):2128-34.

Figure Legends

Figure 1. COX-2 and CEA expression in human lung and colon cancer cell lines. (A) COX-2 and CEA protein expression was analyzed by Western Blotting in the cell lines shown. 14-3-3 was used as a loading control. (B) *COX-2* promoter activity in CRC and lung tumor cell lines. Cells were infected with Ad.cox2fLuc or Ad.CMVfLuc (MOI=100). After 40 hours, cell extracts were assayed for firefly luciferase activity. The activities of *COX-2* promoters are presented by relative light units (RLU) for Ad.cox2fLuc infected cells divided by the RLU values for Ad.CMVfLuc infected cells. Data are averages ± SEM (n=3)

Figure 2. Transcriptional restriction of adenoviral transgene expression by the *COX-2* promoter in liver CRC xenografts. (A) LS174T(rLuc) tumor burden was monitored by coelenterazine-dependent rLuc bioluminescence (RL) in living animals (panels a-c and h-j) at 8, 15 and 22 days after hepatic tumor cell surgical implantation into nude mice. Ad.CMVfLuc or Ad.cox2fLuc (1×10^9 ifu/mouse) were injected intravenously, at 18 days after surgery, into the mice containing these hepatic LS174T(rLuc) CRC xenografts. Ad-directed transgene expression was monitored by luciferin-dependent fLuc bioluminescence (FL) in the same mice five days after virus administration, i.e. one day after the final *in vivo* rLuc image (panels d and k). Following FL imaging, the mice were sacrificed and the tissues were removed and imaged for tumor-derived rLuc activity (panels f and m) and for Ad-directed fLuc transgene expression (panels g and n). Photographs of the tissues are shown in panels e and i. (B) and (C) Quantitation of Ad-directed fLuc transgene expression in liver and in tumor. After bioluminescent imaging of the livers, extracts were prepared from the dissected tumors and from tumor-free liver regions. Firefly luciferase activity, reflecting virally directed gene expression from the *COX-2* promoter, and tumor:liver fLuc activity ratios were quantitated with conventional luciferase and protein assays. Data are averages ± SEM (n = 3; *$p < 0.05$, **$p < 0.01$).

Figure 3. Combined sCAR-MFE transductional hepatic untargeting, sCAR-MFE transductional tumor retargeting and *COX-2* promoter transcriptional restriction of Ad transgene expression in hepatic CEA-positive CRC tumor xenografts. (A) Ad.CMVfLuc (5×10^8 ifu/mouse), [Ad.CMVfLuc][sCAR-MFE (10 μg/mouse)], Ad.cox2fLuc and [Ad.cox2fLuc][sCAR-MFE] were injected intravenously into nude mice bearing LS174T(rLuc) CRC liver xenografts. fLuc-derived bioluminescence was monitored in living mice and from isolated livers five days after virus administration. Photographs of the livers show the locations of tumors; bioluminescent overlays identify liver and tumor tissues where viral fLuc transgene expression occurs. (B) Quantitation of Ad-directed fLuc transgene expression. After bioluminescent imaging, extracts were prepared from the isolated tumors and from tumor free liver regions. Tumor:liver fLuc activity ratios, quantitated with conventional luciferase and protein assays, are shown. Data are averages ± SEM ($n = 3$; $^*p < 0.05$, compared to mice injected with Ad.CMVfLuc only).

Figure 4. Combined sCAR-MFE transductional hepatic untargeting, sCAR-MFE transductional tumor retargeting and *COX-2* promoter transcriptional restriction of Ad infection in hepatic CEA-positive NSCLC tumor xenografts. (A) Ad.CMVfLuc (5×10^8 ifu/mouse), Ad.cox2fLuc and [Ad.cox2fLuc][sCAR-MFE (10 μg/mouse)] were injected intravenously into nude mice bearing H2122 NSCLC liver xenografts. fLuc-derived bioluminescence was monitored in living mice and from isolated livers five days after virus administration. (B) Quantitation of Ad-directed fLuc transgene expression. After bioluminescent imaging, extracts were prepared from the isolated tumors and from tumor-free liver regions. Tumor:liver fLuc activity ratios, quantitated with conventional luciferase and protein assays, are shown. Data are averages ± SEM ($n = 3$; $^*p < 0.05$, $^{**}p < 0.01$ compared to mice injected with Ad.CMVfLuc only).

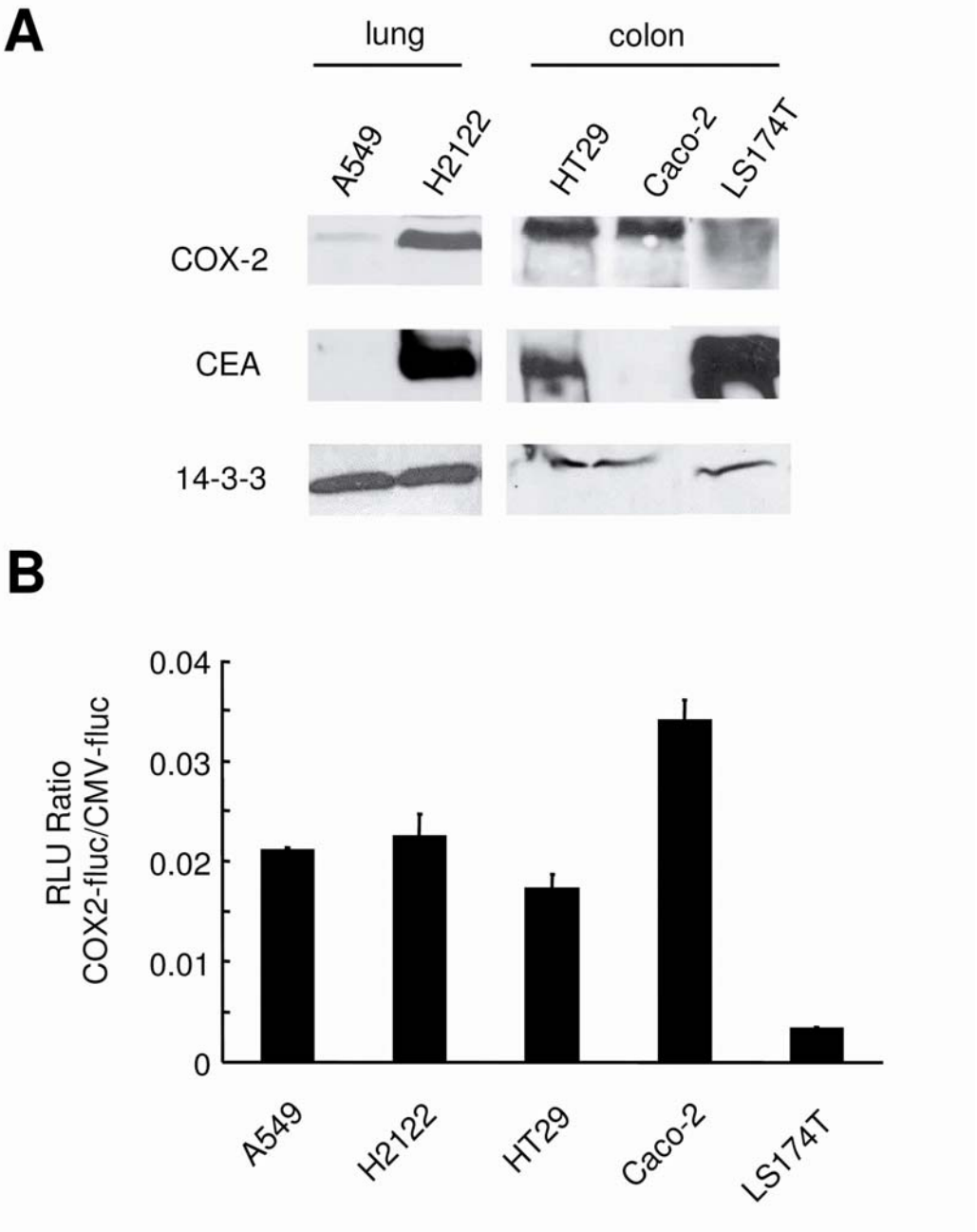

Figure 1 Li, H-J

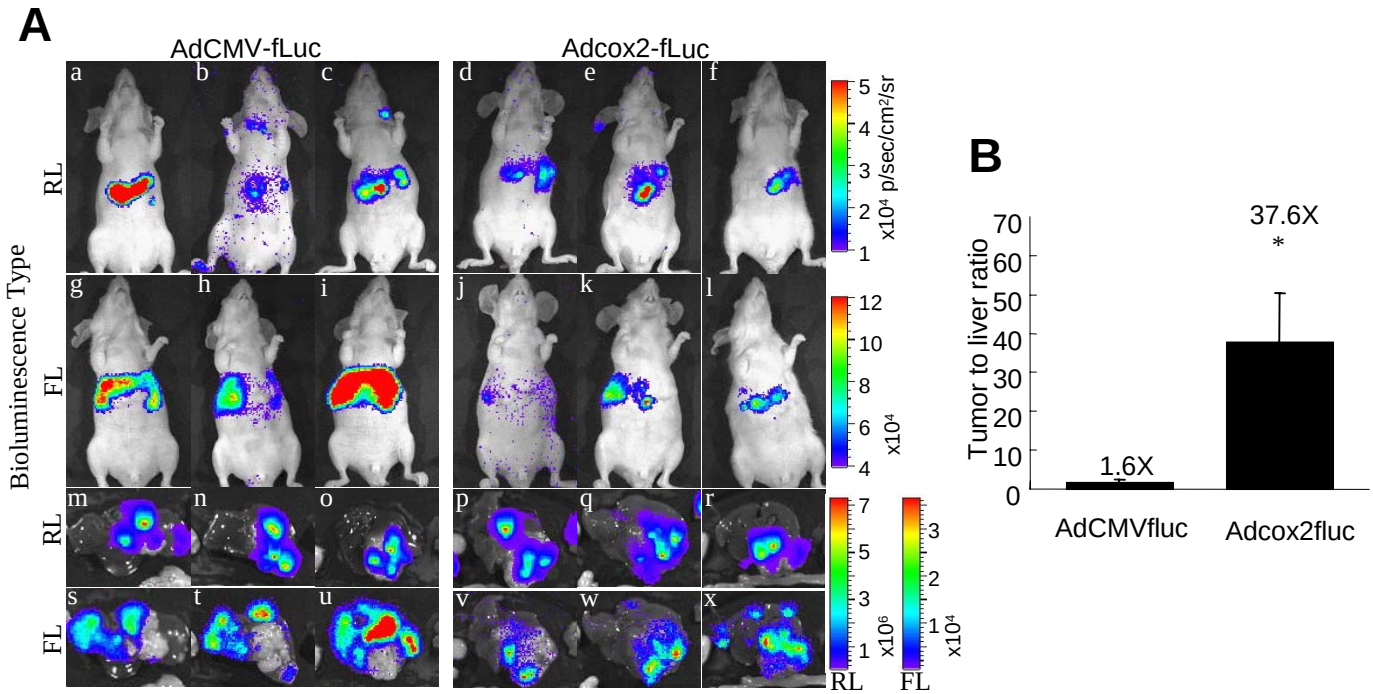
A
AdCMV-fLuc
Adcox2-fLuc
Bioluminescence Type
RL
FL
RL
FL
a
b
c
d
e
f
g
h
i
j
k
l
m
n
o
p
q
r
s
t
u
v
w
x
5
4
3
2
1
x10⁴ p/sec/cm²/sr
12
10
8
6
4
x10⁴
7
5
3
1
x10⁶
RL
3
2
1
x10⁴
FL
B
Tumor to liver ratio
70
60
50
40
30
20
10
0
37.6X
*
1.6X
AdCMVfluc
Adcox2fluc

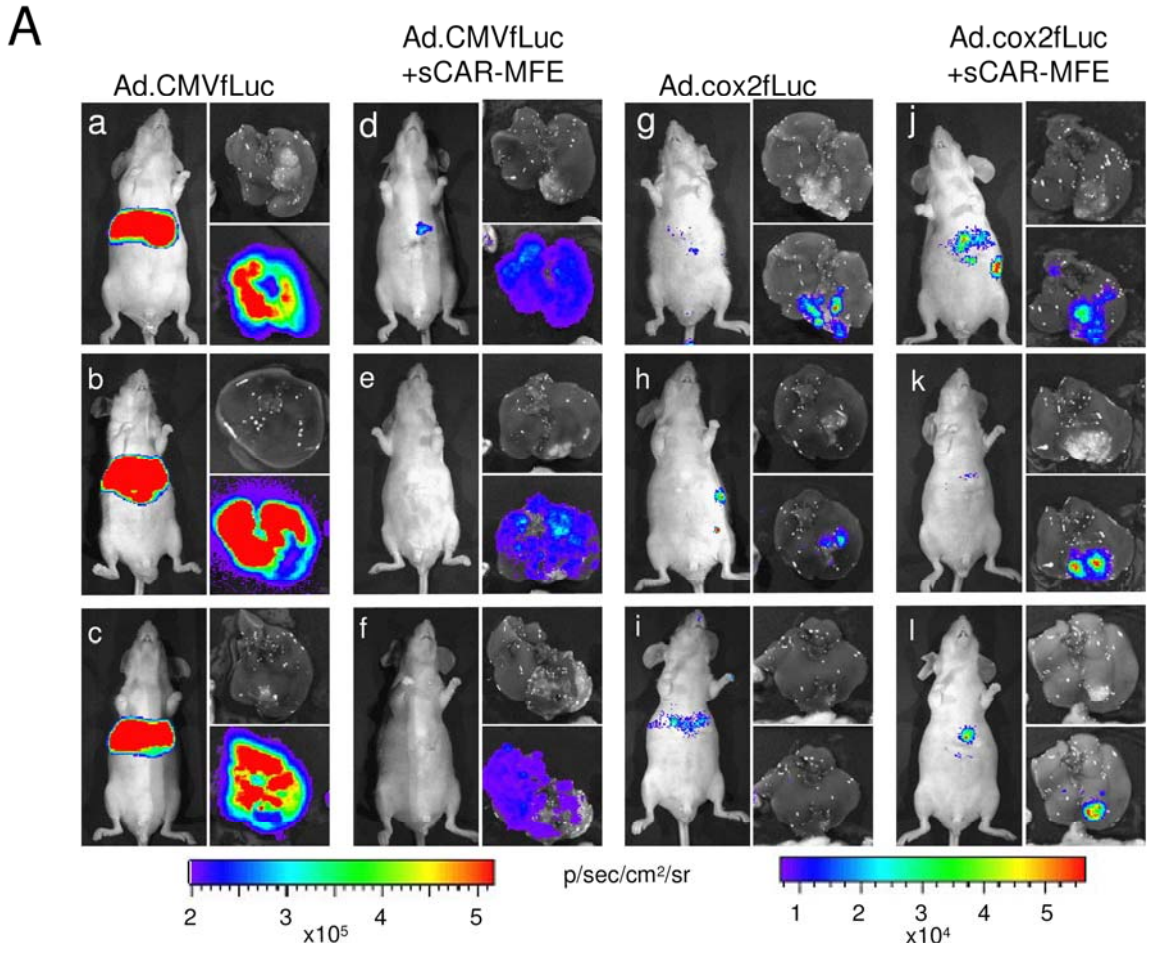

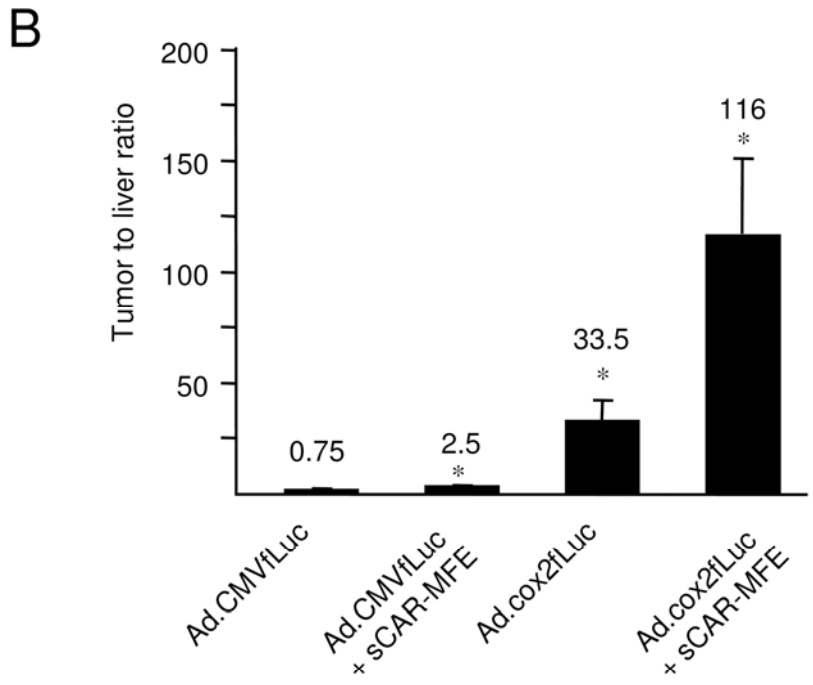

Figure 3 Li, H-J

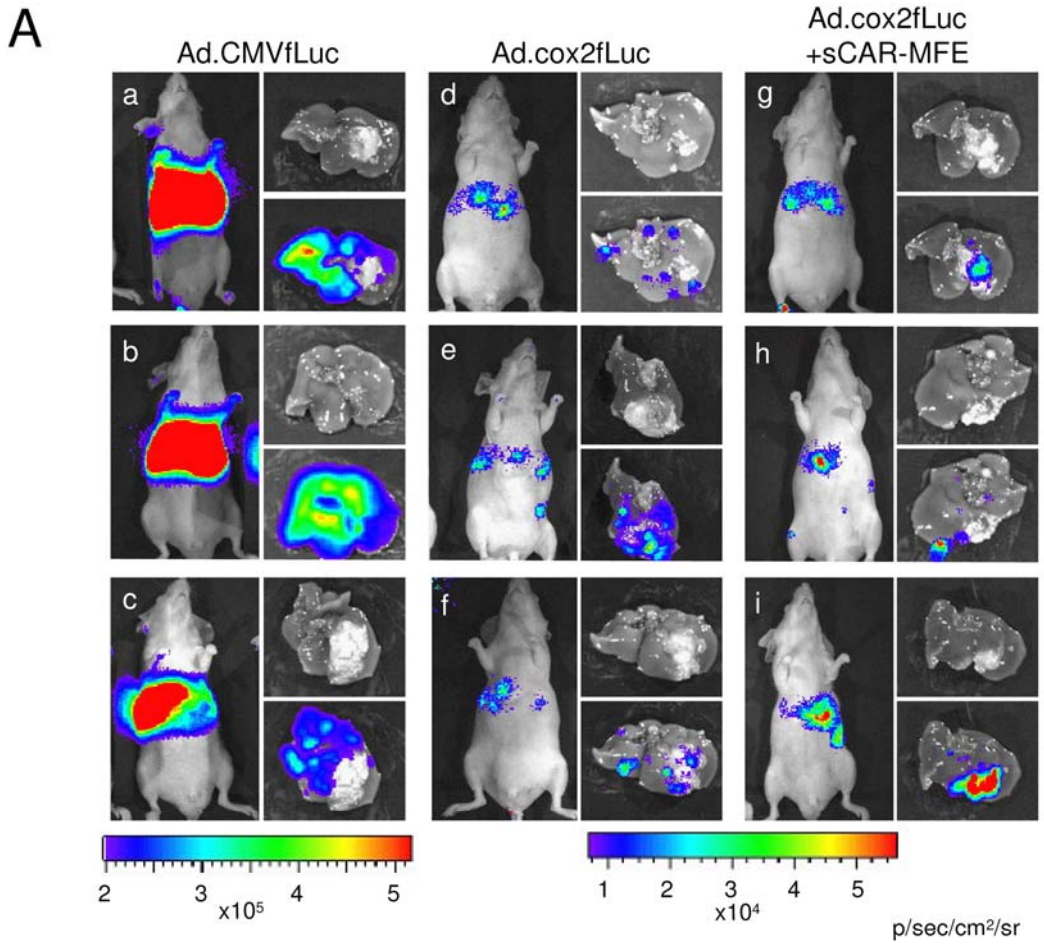

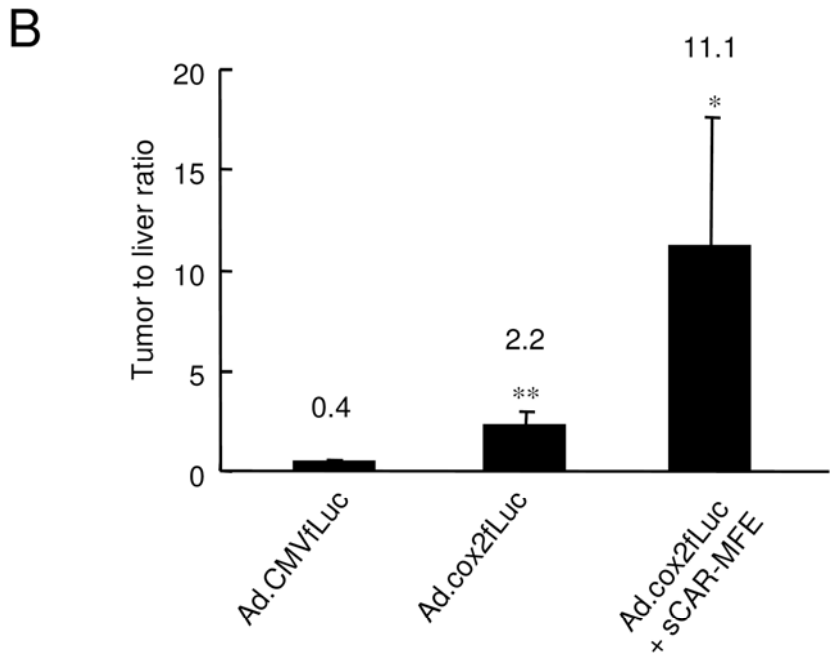

Figure 4 Li, H-J

Title: **Trimerization of a bi-specific transductional adapter improves tumor targeting of adenoviral vectors, in culture and *in vivo*.**

Authors: **Hua-Jung Li[1], Maaike Everts[2], David T. Curiel[2], and Harvey R. Herschman[1]**

Affiliations: **[1]Departments of Biological Chemistry and Pharmacology, and Molecular Biology Institute, UCLA, Los Angeles, CA 90095**

[2]Division of Human Gene therapy, Departments of Medicine, Pathology, Obstetrics and Gynecology, Surgery and the Gene Therapy Center, University of Alabama at Birmingham, Birmingham, AL 35294.

Contact/Corresponding Author: **Harvey R. Herschman**

hherschman@mednet.ucla.edu

Tel. 310-825-8735

FAX. 310-825-1447

Adenoviruses (Ad) attach to cells by interaction of the virus fiber/knob with coxsackie-adenovirus receptors (CAR)[1-3]. For systemic gene delivery, Ad must be "untargeted" from normal cells and re-targeted to tumor cells. Ad can be untargeted from CAR-expressing cells and retargeted to carcinoembryonic antigen (CEA)-positive tumor cells with a bi-specific adapter, sCARhMFE[4]. sCAR is the CAR ectodomain; MFE is a single-chain antiCEA antibody (Fig. 1). Ad fiber-knob is a trimer, suggesting adapter trimerization may augment tumor retargeting[5-7]. Trimeric sCARfMFE substantially increases adenovirus-adapter interaction, enhances CAR-dependent untargeting and enhances CEA-dependent tumor cell infection in culture. Although soluble CEA (sCEA) blocks monomer sCARhMFE-directed CEA-dependent infection, trimer sCARfMFE-mediated infection is resistant to sCEA competition. Trimer is also substantially more effective for untargeting adenovirus liver infection following systemic administration and for retargeting virus to hepatic CEA-positive colorectal cancer (CRC) xenografts. sCARfMFE trimer provides a major advance in adenovirus transgene gene delivery to hepatic CRC metastases.

Structure determinations and stoichiometric analyses[8] indicated that the Ad fiber-knob protein is trimeric. The CAR binding sites of the trimeric knob are located on lateral surfaces formed by interfaces of two adjacent knob monomers[9, 10], suggesting that three CARs bind to one knob trimer. Trivalent binding results in the high affinity observed between knob and CAR[11]. Therefore, to increase adapter efficacy, several groups trimerized bi-specific adapters. As proposed, adapter trimerization increased adenovirus targeting to cells in culture[5-7]. However, to date no enhancement of adenovirus tumor retargeting by trimerized adapter *in vivo* has been reported.

We previously demonstrated transductional untargeting of CAR-dependent Ad infection of normal cells and transductional retargeting of Ad to CEA-positive tumor cells by the monomeric bi-specific adapter sCARhMFE, both in cell culture and *in vivo*[4]. We first demonstrate that trimeric sCARfMFE is more effective in cell culture for both transductional

untargeting of CAR-dependent infection and for transductional retargeting to CEA expressing cells. Targeting efficacies of monomeric sCARhMFE and trimeric sCARfMFE were evaluated using cell lines with differing levels of CEA and CAR expression (Fig. 2a). LS174T cells, a human CRC line, express an endogenous 180 kDa CEA protein; MC38-cea-2 cells, a murine CRC cell line, express a stably transfected 70 kDa truncated human CEA isoform[12]. CEA is not detectable in 293A cells. CAR is easily detectable in 293A and LS174T cells; in contrast, only trace levels are detectable in MC38-cea-2 cells. Monomer sCARhMFE and trimer sCARfMFE were characterized by Western Blotting (Fig. 2b). Monomer and trimer concentrations used for cell culture and for *in vivo* untargeting and retargeting experiments are similar.

CEA-mediated sCARhMFE and sCARfMFE retargeting efficacies were compared on LS174T cells, which express high CEA levels. Cells were infected with Ad.CMVfLuc, an adenovirus expressing firefly luciferase under transcriptional control of the CMV promoter. Ad.CMVfLuc was pre-incubated with (1) buffer, (2) increasing monomer sCARhMFE concentrations, or (3) increasing trimer sCARfMFE concentrations. After incubation, washing and forty hours in culture medium, cell extracts were assayed for luciferase activity (Fig. 2c). Trimeric sCARfMFE increases Ad.CMVfLuc infectivity to 50% of maximum retargeting at a concentration of ~11 ng/3 × 10^8 vp. In comparison, to reach the same retargeting level, ~1100 ng of monomer sCARfMFE/3 × 10^8 vp is required; trimeric sCARfMFE targeting efficacy for CEA positive cells is ~100-fold higher than is targeting efficacy for monomeric sCARhMFE.

One critical problem facing practical use of adapter-Ad complexes *in vivo*, in the clinical context of systemic delivery to tumors, is dilution by the blood following injection. We suggest that the greater sCARfMFE targeting efficacy (Fig. 2c) results in part from increased binding between the trimeric Ad knob and the trimeric adapter, which should reduce the loss of adapter-mediated infection by dilution. To test this hypothesis, the effect of dilution on targeting efficacy of the monomer and trimer complexes was analyzed. Ad.CMVfLuc (3 × 10^8 vp/well) was pre-incubated with increasing concentrations of sCARhMFE monomer or sCARfMFE trimer. CEA-positive MC38-cea-2 cells were subsequently incubated with the virus:adapter complexes for 90

min in either a “small” (0.2 ml) or a “large” (1.0 ml) volume. Washed cells were incubated 40 hours before lysates were assayed for luciferase activity. The targeting efficacy of monomer adapter-Ad complex is reduced much more extensively by dilution than is the targeting efficacy of the trimer adapter-Ad complex (Fig. 2d), suggesting dilution *in vivo* following intravenous administration of monomer adapter:Ad complexes may result in substantial amelioration of Ad retargeting. In contrast, the retargeting efficacy of trimer adapter-Ad complexes is likely to be less effected by blood dilution.

To determine whether sCARfMFE trimer binds more effectively than does sCARhMFE monomer to the trimeric viral knob, we examined their ability to block binding to CAR-positive, CEA-negative cells. “Untargeting” of CEA-negative cells should be entirely dependent on the sCAR:knob interaction. CAR^+/CEA^- 293A cells (Fig. 2a), were infected with AdCMVfLuc, AdCMVfLuc pre-incubated with increasing amounts of sCARhMFE monomer ([Ad.CMVfLuc][sCARhMFE]), or with AdCMVfLuc pre-incubated with increasing amounts of sCARfMFE trimer ([Ad.CMVfLuc][sCARfMFE]). fLuc activity of [Ad.CMVfLuc (3×10^8 vp)][sCARhMFE] infected 293A cells is reduced to 40% at ~60 ng of sCARhMFE, and could not be further reduced (Fig. 2e). In contrast, sCARfMFE trimer reduces infection by 40% at only ~6 ng and – at higher concentrations – can block ~80% of infection, suggesting sCARfMFE trimer binds to the viral knob much more effectively than does sCARhMFE monomer.

To determine whether sCARfMFE trimer binds more effectively to cellular CEA, we examined the ability of soluble CEA (sCEA) to block adapter-mediated, CEA-dependent infection. CEA^+MC38-cea-2 cells, which express low CAR levels (Fig. 2a), were infected with [Ad.CMVfLuc][sCARhMFE] or [Ad.CMVfLuc][sCARfMFE] in the presence of increasing amounts of sCEA. Monomer sCARhMFE-mediated Ad retargeting of MCA-cea-2 cells is essentially completely blocked by soluble CEA (Fig. 2f). In contrast, nearly half the sCARfMFE trimer Ad retargeting cannot be competed by sCEA (Fig. 2f), suggesting that trimer binds to cell-surface CEA much more avidly than does monomer sCARhMFE. Trimerization apparently allows the MFE-containing adapter to utilize multiple CEA-binding interactions, each with a relatively high

possibility of dissociation, to achieve an overall low dissociation rate. Multimeric MFE:CEA binding on the cell membrane is likely to be facilitated by “capping” of membrane-anchored, mobile CEA molecules, resulting in a multivalent interaction (Fig. 1b). Since viruses contain multiple fiber-knob structures that can simultaneously contact cell surface receptors, the advantage of MFE-CEA trimerization interaction is further enhanced by multiple trimer sCARfMFE:$(CEA)_3$ interactions. It is likely that this increased binding to cellular CEA facilitates subsequent infection events. It is of interest to note that the MFE-23 affinity for CEA (K_d = 2.5 nM)[13, 14] is greater than that of Ad knob for CAR (K_d = 24 nM)[11]; trimeric sCARfMFE CEA-retargeted interactions of Ad with cells may rival or exceed interactions of the naked virus with CAR receptors.

The extraordinary trimer sCARfMFE-mediated Ad binding to CEA-positive cells may have a profound practical value in clinical application, both for adenovirus-mediated CRC therapy and for therapy for other CEA-positive hepatic metastases. CEA is often “shed” by tumors, resulting in substantial circulating CEA serum levels. Indeed, elevated serum CEA levels are often the first indication of CRC hepatic metastases[15, 16]. Circulating CEA may act as a competitor for MFE-based adapter-mediated retargeting of adenovirus vectors to CEA positive tumors; it is clear that a high enough concentration of soluble CEA can completely prevent monomer sCARhMFE-mediated Ad retargeting (Fig. 2f). In contrast, sCEA only modestly reduces trimer sCARfMFE adapter-mediated Ad binding and infection of CEA-positive target cells, even at extraordinarily high concentrations (Fig. 2f). In addition to increasing Adenovirus vector tumor retargeting and hepatic untargeting *in vivo*, trimerization of the retargeting agent should substantially reduce competition by antigen shedding in clinical applications of bi-specific adapter-mediated Ad therapies.

To examine the efficacy of transductional liver untargeting by monomeric versus trimeric adapters, mice were injected via tail vein with Ad.CMVfLuc, [Ad.CMVfLuc][sCARhMFE] or [Ad.CMVfLuc][sCARfMFE]. Three days later mice were injected with D-luciferin and imaged (Fig. 3a). Mice were then sacrificed, and livers were imaged (Fig. 3a, insets). Liver extracts were

subsequently assayed by conventional luciferase assays (Fig. 3b). Bioluminescence was quantified from the CCD images (Fig. 3b, panel A) and from luciferase assays (Fig. 3b, panel B). Liver Ad.CMVfLuc infection is decreased ~68-70% by 0.1 μg/mouse of trimeric sCARfMFE and ~74-77% by 1 μg/mouse of sCARfMFE. In contrast, no liver untargeting by monomer occurs at these concentrations; indeed, a slight increase in liver infection was observed at these low concentrations. Only at 3 μg sCARhMFE/mouse was liver infection reduced. Liver untargeting by trimer is at least ten-fold more effective than is liver untargeting by monomer.

We next examined the retargeting efficacy of trimer and monomer to CEA positive CRC hepatic tumors. Mice bearing LS174T(rLuc) hepatic tumors were injected intravenously with Ad.CMVfLuc, [Ad.CMVfLuc][sCARhMFE] or [Ad.CMVfLuc][sCARfMFE]. Five days later, following fLuc (FL) imaging of mice to monitor adenovirus infection (Fig, 4a, panels A, D and G), the mice were sacrificed and livers were imaged for tumor-derived rLuc activity (Fig. 4a, panels B, E and H) and for adenovirus-directed fLuc expression (Fig. 4a, panels C, F and I). After imaging the livers, tumors were dissected, and tumor extracts were assayed for fLuc activity (Fig. 4b). Preincubation with 1 μg of trimer produces a 3.6-fold retargeting increase in Ad.CMVfLuc infection of LS174T tumors. In contrast, a similar level of monomer does not enhance tumor infection *in vivo* (Fig. 4b).

In conclusion, we demonstrate here that trimerization of the sCAR-MFE bi-specific adapter results in (1) higher adapter affinity for the viral knob, (2) facilitated adenovirus binding to and infection of CEA positive cells, (3) increased efficacy of untargeting of CAR-mediated infection both in cultured cells and, following systemic administration, *in vivo*, and (4) increased efficacy of retargeted infection of CEA positive cells, both in cell culture and *in vivo*. These data support and enhance the potential of trimerized adaptors that untarget adenovirus infection of liver cells and retarget the virus to hepatic tumors as a promising strategy for gene therapy of disseminated disease.

Because trimerization of bi-specific adapters should be generalizable, the advantages described here should be applicable to a wide range of Ad-based transductional therapeutic

applications. Because many of the targets of other bi-specific adapters are also mobile membrane components (receptors, antigens), the advantages observed for trimerization of sCAR-MFE retargeting should also be true for other sCAR containing bi-fuctional adapters. In addition to the Ad knob-CAR interaction, many receptor-ligand binding reactions involve a trimeric partner(s). For example, the interaction between TNF family receptors TRAIL-R1 and TRAIL-R2 and their trimeric ligands (e.g. TRAIL)[17] is similar to the interaction between the Ad knob and CAR[9]. Because activation of TNF family receptors induces apoptosis, they have become targets for potential cancer therapies. Many recombinant ligands (e.g., Apo2L/TRAIL, TRAIL-His-LE and TRAIL-His) or antibodies (ex. HGS-ETR1 and HGS-ETR2) that bind to TRAIL-R1 or TRAIL-R2 are currently in Phase I or Phase II clinical trials. However, several of these reagents (e.g. sTRAIL, HGS-ETR1, HGS-ETR2) require a cross-linking step before application to maximize cell killing[18-24]. We suggest that trimerization of these reagents with fibritin M may enhance the efficacy of these ligands and antibodies targeted to the TRAIL receptor.

Methods

Cell Culture

MC38-cea-2 cells[12] were provided by Dr. Jeffrey Schlom, National Institutes of Health, and LS174T cells by Dr. Anna Wu, UCLA. 293A cells were purchased from Invitrogen. LS174T, 293A and MC38-cea-2 were grown in Dulbecco modified Eagle medium (Gibco, Rockville, MD) containing 10% fetal bovine serum (Cellegro, Washington, DC) with penicillin-streptomycin (Gibco), 0.1 mM non-essential amino acids (Gibco) and 1.0 mM sodium pyruvate (Gibco).

Stable transfection

To establish stable LS174T cells that over express *Renilla* luciferase (rLuc), cells were transfected with pcDNA3 expression vectors encoding rLuc and a neomycin selectable marker, using Lipofectamine 2000 (Invitrogen, Carlsbad, CA). Neomycin-resistant cells were selected using medium containing G418 (1 mg/ml) and screened for rLuc expression with the Luciferase assay system (Promega, Madison, WI)

Virus construction and production

The adenovirus vector encoding firefly luciferase (fLuc) under transcriptional control of the constitutively active cytomegalovirus (CMV) promoter is described in Liang *et al*[25]. Virus was prepared in 293 cells by double cesium chloride (CsCl) gradient centrifugation. Cells were infected in medium containing 2% fetal bovine serum. After overnight incubation, cells were shifted to medium containing 10% serum and incubated until a total cytopathic effect was observed. Cells were harvested, frozen and thawed three times, and virus was purified using standard CsCl purification methods. Viral particle number was determined by measuring absorbance at 260 nm, using a conversion factor of 1.1×10^{12} viral particles per absorbance unit. Viral titers were determined with the Adeno-X Rapid Titer Kit (BD Clontech, Mountain View, CA). “vp” (for viral particles) is used to indicate virus particles when considering virus mass interactions with bi-specific adapter; “ifu” (for plaque forming units) is used when viral infectivity is described.

Monomer sCARhMFE and trimer sCARfMFE construction and purification

sCARhMFE was prepared described previously[26]. To construct the plasmid encoding sCARfMFE, we used the pcDNA/CAR/F/m40L plasmid [7] and replaced the CD40L cDNA with the cDNA for anti-CEA scFv MFE-23. MFE-23 was amplified from a plasmid obtained from Dr. Kerry Chester. NotI and XhoI restriction sites were added at the 5' and 3' ends, along with a TAA stop codon. The pcDNA/CAR/F/m40L plasmid and the MFE-23 PCR product were digested with NotI and XhoI and gel purified. The MFE fragment was ligated into the vector, to create cDNA/CAR/F/MFE. HEK293 cells were transfected with the pcDNA/CAR/F/MFE plasmid linearized with PvuI restriction enzyme, using Superfect reagent (Qiagen, Valencia, CA), according to manufacturer's instructions. The day after transfection, cells were distributed in a 96-well plate and grown in medium supplemented with 500 µg/ml G418, until about 2/3 of the well surface was covered with cells. Supernatants of individual wells were tested for plasmid-directed production, using a dot-blot assay with a polyclonal rabbit antibody against CAR, produced in our laboratory. High producing clones were expanded for further protein production. The medium from stable sCARfMFE expressing 293 cells was collected and proteins were precipitated using ammonium sulphate. Precipitate was collected by centrifugation,redissolved in PBS and then dialyzed against PBS. Recombinant protein was purified using Ni-NTA Superflow resin (Qiagen), according to manufacturer's instructions, again followed by dialysis against PBS.

Dotblot assays were performed using either polyclonal rabbit anti-CAR or anti-fibritin antibodies, to confirm presence of these domains of the fusion proteins. Ten microliters of protein solution was dotted on pre-wetted a PVDF membrane, and allowed to dry. Membranes were re-wetted, rinsed with TBS, and blocked using 5% milk in TBS/Tween. After incubation with the primary antibody dissolved in blocking buffer, membranes were washed in TBS/T/Triton and incubated with HRP-conjugated secondary goat anti-rabbit antibody, dissolved in blocking

buffer. After washing, signal was detected using the Western Lightning Chemiluminescence Reagent Plus (PerkinElmer, Boston, MA) on Kodak Biomax MR film (Kodak, Rochester, NY).

Immunoblot Analysis to compare sCARhMFE and sCARfMFE concentrations

100, 250 and 500 ng of the two preparations were denatured in loading buffer, subjected to electrophoresis on 12% SDS-polyacrylamide gels, and transferred to nitrocellulose membranes. The membranes were probed with anti-CAR antibody (RmcB; 1:3,000 dilution, the antibody was produced using a hybridoma purchased from the ATCC and was kindly provided by J.T. Douglas, University of Alabama at Birmingham) or with anti-fibritin antibody (1:3,000 dilution). The rabbit serum against T4 fibritin protein was kindly provided by V. Mesyanzhinov from the Shemykin and Ovchinnicov Institute of Bioorganic Chemistry, Moscow, Russia). Blots were incubated overnight at 4 °C, followed by incubation at room temperature for 60 min with horseradish peroxidase (HRP)-conjugated secondary antibody. Immunoreactivity was determined by enhanced chemiluminescence (ECL; Amersham, Piscataway, NJ).

Immunoblot analysis for cellular CEA and CAR expression

Cells were washed twice with phosphate-buffered saline (PBS) and incubated on ice for 10 min in lysis buffer containing 50 mM Tris-HCl, pH 7.4, 1% NP-40, 1% triton, 1% sodium deoxycholate, 150 mM NaCl, 1 mM EDTA and protease inhibitors (Complete Tablet; Roche, Indianapolis, IN). After 10,000 x *g* centrifugation for 10 minutes, supernatant protein concentrations were measured with the Bio-Rad Protein Assay (Bio-Rad). The protein extracts were denatured in loading buffer prior to loading. Equal amounts of protein (30 µg) were loaded on 8% SDS-polyacrylamide gel for electrophoresis. Proteins were subsequently transferred to nitrocellulose membranes. The membranes were probed with anti-CEA antibody, cT84.66 (1:10,000 dilution[27]), anti-CAR antibody (RmcB) or anti-GAPDH antibody (1:1,000 dilution; Santa Cruz Biotechnology, Santa Cruz, CA) overnight at 4 °C, followed by incubation at room temperature for 60 min with horseradish peroxidase (HRP)-conjugated secondary antibody.

Immunoreactivity was determined by enhanced chemiluminescence (ECL; Amersham, Piscataway, NJ).

Comparing retargeting and untargeting efficacy of sCARfMFE and sCARhMFE in cell culture

Ad.CMVfLuc (3×10^8 vp) was incubated with sCARfMFE or sCARhMFE, in concentrations described for specific experiments, in 10 µl and incubated for 60 minutes at room temperature. The sCAR-MFE:adenovirus complexes were diluted to 200 µl or 1000 µl with medium containing 2% FBS, then added to monolayers of LS174T, 293A, or MC38-cea-2 cells in 24-well plates (2×10^5 cells/well). Virus-treated cells were incubated at 37 °C for 90 minutes. The virus-containing medium was then aspirated and cells were washed with PBS. After a 40-hour incubation at 37 °C in medium containing 10% FBS, cells were lysed and luciferase activity was measured.

CEA competition of virus infection

Ad.CMVfLuc (3×10^8 vp) was mixed with 63 ng of sCARfMFE or with 63 ng of sCAR6hMFE in 10 µl and incubated for 60 minutes at room temperature. The sCAR-MFE:adenovirus complexes were diluted to 200 µl with medium containing 2% FBS and increasing amounts of sCEA (0, 50, 150, 500, 1500, 3000 and 5000 ng sCEA; soluble CEA, Protein Sciences Corporation, Meriden, CT), then added to MC38-cea-2 cell monolayers in 24-well plates (2×10^5 cells/well). Virus-treated cells were incubated at 37 °C for 90 minutes. Medium was aspirated and cells were washed with PBS. After a 40-hour incubation at 37 °C in medium containing 10% FBS, cells were lysed and luciferase activity was measured.

Comparison of hepatic untargeting efficacy for sCARfMFE and sCARhMFE

4.5×10^{10} vp/mouse of Ad.CMVfLuc, [Ad.CMVfLuc][sCARfMFE] or [Ad.CMV.fluc][sCARhMFE] were administered by tail-vein injection into eight week-old (*nu/nu*) nude mice (Charles River Laboratories, Wilmington, MA). Before the injection, viruses were incubated for one hr either with sCARfMFE, sCARhMFE or PBS in a volume of 250 µl. Injection

volumes were 250 µl in all cases. On the third day after virus administration, the mice were injected intraperitoneally with D-luciferin (250 µl; ~125 mg/kg body weight) and scanned to image Ad-directed fLuc activity. Immediately after imaging, mice were sacrificed and the livers were removed and imaged for fLuc (Ad-dependent) bioluminescence. After optical imaging, liver extracts were prepared and assayed for fLuc activity.

Preparation of liver xenografts and virus administration.

Eight week-old (*nu/nu*) nude mice were anesthetized with ketamine/xylazine (100/10 mg/kg). Under aseptic conditions, a transverse incision was made across the xyphoid process and extended approximately two cm. The left upper liver lobe was held with a PVA Surgical Spear (Allegiance, IL) and LS174TrLuc cells (1×10^6/mouse) in 15 µl were injected into the front of the lobe liver, using a 27-gauge needle. The liver lobe was returned to the abdomen and the incision was closed with sutures and wound clips. Buprenorphine was administered every 12 hr for 48 hr. The wound clip was removed seven days after surgery. Virus was administered intravenously ten days after surgery. For transductional retargeting, ~ 3×10^{10} vp /mouse AdCMVfLuc, [Ad.CMVfLuc][sCARhMFE] or [Ad.CMVfLuc][sCARfMFE] were administered by tail-vein injection. Before the injection, viruses were incubated for one hr with 0, 0.5 or 1 µg sCAR-MFE/mouse in 100 µl PBS. Injection volumes were 250 µl in all cases.

Measurement of *Renilla* and firefly luciferase activities

Mice were injected intraperitoneally with D-luciferin (250 µl; ~125 mg/kg body weight) and scanned to image Ad-directed fLuc activity. Immediately after imaging, mice were sacrificed and the livers were removed and imaged for fLuc (Ad-dependent) bioluminescence. For tumor bearing mice, the livers were then immersed in a solution containing coelenterazine (0.2 mg/ml) and imaged again in the IVIS instrument, using one-minute scans to monitor tumor-derived rLuc activity. After optical imaging, extracts of the liver and tumor tissues were prepared and assayed for fLuc activity and for protein concentration.

Bioluminescence quantitation

Bioluminescence images were analyzed with Living Image software version 2.20 (Xenogen). Regions of interest (ROI) were drawn over the tumor or liver area and total photons the ROI were calculated. ROI in all images of an experiment were kept with a consistent area[25].

Statistical analysis

All experiments were performed at least in triplicate. Data are presented as means +/- SEM. The statistical significance (P values) in mean values of two-sample comparison (Fig. 3b and 4b) was determined with Student's t-test. The statistical significance in the comparison of multiple sample was examined with Bonferroni's post-hoc test (Fig. 2) after two-way ANOVA.

Acknowledgements

These studies were supported by National Cancer Institute grants R01 CA84572 and P50 CA86306 (H.R. Herschman) and NIH and Department of Defense grants 5R01 CA111569 and W812XWH-05-1-0035 (D.T. Curiel). We thank Arthur Catapang for technical assistance, and the support staff of the UCLA Small Animal Imaging Shared Resource for assistance with optical imaging. We thank Ryan Beam, Jill Warren, Svetlana Komarova and Larissa Pereboeva for assistance in adapter protein production and purification, and Jonathan Braun for helpful discussions.

Author Contributions

H-J.L., M.E., D.T.C and H.R.H. designed research protocols; M.E. constructed and prepared adapter proteins, H-J.L performed all western blot, cell culture, and animal experiments; H-J.L,, M.E., D.T.C. and H.R.H. contributed to manuscript preparation.

Competing financial interests statement

H-J.L., M.E., D.T.C. and H.R.H. have no competing financial interests.

References

1. Bergelson, J.M. et al. Isolation of a common receptor for Coxsackie B viruses and adenoviruses 2 and 5. *Science* **275**, 1320-1323 (1997).
2. Tomko, R.P., Xu, R. & Philipson, L. HCAR and MCAR: the human and mouse cellular receptors for subgroup C adenoviruses and group B coxsackieviruses. *Proc Natl Acad Sci U S A* **94**, 3352-3356 (1997).
3. Roelvink, P.W. et al. The coxsackievirus-adenovirus receptor protein can function as a cellular attachment protein for adenovirus serotypes from subgroups A, C, D, E, and F. *J Virol* **72**, 7909-7915 (1998).
4. Li, H.J. et al. Adenovirus Tumor Targeting and Hepatic Untargeting by a Coxsackie/Adenovirus Receptor Ectodomain Anti-Carcinoembryonic Antigen Bispecific Adapter. *Cancer Res* **67**, 5354-5361 (2007).
5. Kim, J. et al. Targeting adenoviral vectors by using the extracellular domain of the coxsackie-adenovirus receptor: improved potency via trimerization. *J Virol* **76**, 1892-1903 (2002).
6. Kashentseva, E.A., Seki, T., Curiel, D.T. & Dmitriev, I.P. Adenovirus targeting to c-erbB-2 oncoprotein by single-chain antibody fused to trimeric form of adenovirus receptor ectodomain. *Cancer Res* **62**, 609-616 (2002).
7. Pereboev, A.V. et al. Enhanced gene transfer to mouse dendritic cells using adenoviral vectors coated with a novel adapter molecule. *Mol Ther* **9**, 712-720 (2004).
8. van Oostrum, J. & Burnett, R.M. Molecular composition of the adenovirus type 2 virion. *J Virol* **56**, 439-448 (1985).
9. Bewley, M.C., Springer, K., Zhang, Y.B., Freimuth, P. & Flanagan, J.M. Structural analysis of the mechanism of adenovirus binding to its human cellular receptor, CAR. *Science* **286**, 1579-1583 (1999).
10. Roelvink, P.W., Mi Lee, G., Einfeld, D.A., Kovesdi, I. & Wickham, T.J. Identification of a conserved receptor-binding site on the fiber proteins of CAR-recognizing adenoviridae. *Science* **286**, 1568-1571 (1999).
11. Lortat-Jacob, H., Chouin, E., Cusack, S. & van Raaij, M.J. Kinetic analysis of adenovirus fiber binding to its receptor reveals an avidity mechanism for trimeric receptor-ligand interactions. *The Journal of biological chemistry* **276**, 9009-9015 (2001).
12. Robbins, P.F. et al. Transduction and expression of the human carcinoembryonic antigen gene in a murine colon carcinoma cell line. *Cancer Res* **51**, 3657-3662 (1991).
13. Chester, K.A. et al. Production and tumour-binding characterization of a chimeric anti-CEA Fab expressed in Escherichia coli. *Int J Cancer* **57**, 67-72 (1994).
14. Casey, J.L. et al. Purification of bacterially expressed single chain Fv antibodies for clinical applications using metal chelate chromatography. *Journal of immunological methods* **179**, 105-116 (1995).
15. Gold, P. & Freedman, S.O. Demonstration of Tumor-Specific Antigens in Human Colonic Carcinomata by Immunological Tolerance and Absorption Techniques. *The Journal of experimental medicine* **121**, 439-462 (1965).
16. Bakalakos, E.A., Burak, W.E., Jr., Young, D.C. & Martin, E.W., Jr. Is carcino-embryonic antigen useful in the follow-up management of patients with colorectal liver metastases? *American journal of surgery* **177**, 2-6 (1999).
17. Hymowitz, S.G. et al. Triggering cell death: the crystal structure of Apo2L/TRAIL in a complex with death receptor 5. *Molecular cell* **4**, 563-571 (1999).

18. Bremer, E. et al. Exceptionally potent anti-tumor bystander activity of an scFv:sTRAIL fusion protein with specificity for EGP2 toward target antigen-negative tumor cells. *Neoplasia (New York, N.Y* **6**, 636-645 (2004).
19. Schneider, P. et al. Conversion of membrane-bound Fas(CD95) ligand to its soluble form is associated with downregulation of its proapoptotic activity and loss of liver toxicity. *The Journal of experimental medicine* **187**, 1205-1213 (1998).
20. Meurette, O. et al. TRAIL (TNF-related apoptosis-inducing ligand) induces necrosis-like cell death in tumor cells at acidic extracellular pH. *Annals of the New York Academy of Sciences* **1056**, 379-387 (2005).
21. Muhlenbeck, F. et al. The tumor necrosis factor-related apoptosis-inducing ligand receptors TRAIL-R1 and TRAIL-R2 have distinct cross-linking requirements for initiation of apoptosis and are non-redundant in JNK activation. *The Journal of biological chemistry* **275**, 32208-32213 (2000).
22. Wajant, H. et al. Differential activation of TRAIL-R1 and -2 by soluble and membrane TRAIL allows selective surface antigen-directed activation of TRAIL-R2 by a soluble TRAIL derivative. *Oncogene* **20**, 4101-4106 (2001).
23. Wajant, H., Pfizenmaier, K. & Scheurich, P. TNF-related apoptosis inducing ligand (TRAIL) and its receptors in tumor surveillance and cancer therapy. *Apoptosis* **7**, 449-459 (2002).
24. Mita, M. & Tolcher, A.W. Novel apoptosis inducing agents in cancer therapy. *Current problems in cancer* **29**, 8-32 (2005).
25. Liang, Q., Yamamoto, M., Curiel, D.T. & Herschman, H.R. Noninvasive imaging of transcriptionally restricted transgene expression following intratumoral injection of an adenovirus in which the COX-2 promoter drives a reporter gene. *Mol Imaging Biol* **6**, 395-404 (2004).
26. Everts, M. et al. Selective induction of tumor-associated antigens in murine pulmonary vasculature using double-targeted adenoviral vectors. *Gene Ther* **12**, 1042-1048 (2005).
27. Neumaier, M. et al. Cloning of the genes for T84.66, an antibody that has a high specificity and affinity for carcinoembryonic antigen, and expression of chimeric human/mouse T84.66 genes in myeloma and Chinese hamster ovary cells. *Cancer Res* **50**, 2128-2134 (1990).

Figure Legends

Figure 1. Structure and targeting of monomeric sCARhMFE and trimeric sCARfMFE bi-specific adapters. (a) sCARhMFE, the monomeric adapter, consists of the CAR ectodomain (sCAR), a six-histidine tag (His_6) for purification and the anti-CEA single chain antibody svFc MFE23. sCARfMFE, the trimeric adapter, consists of sCAR, the His_6 tag, a fibritin trimeric motif, and MFE23. Fibritin is a homotrimer, with 12 consecutive α-helical coiled-coil segments flanked by small globular domains at both ends, produced by bacteriophage T4. A 27-amino-acid trimeric motif from T4 bacteriophage fibritin was utilized to trimerize trimeric sCARfMFE. (b) Proposed targeting of the adapters. Monomeric sCARhMFE can block CAR-dependent Ad infection and retarget the adenovirus in a CEA-dependent manner (left panel). The transductional targeting efficacy is determined by (i) the strength of binding between individual Ad knob domains and the sCAR domain of sCARhMFE and (ii) the strength of binding between cell-surface CEA and the MFE domain of sCARhMFE. We suggest that the strength of binding of sCARfMFE both to the virus and to cell-surface CEA can be increased by an enhanced avidity resulting from multimeric binding of the trimeric bi-specific adapter to the trimeric Ad knob complex and to multimeric trimer binding to membrane-associated CEA (right panel). By virtue of multimeric binding to the knob, sCARfMFE trimer should be more effective at untargeting Ad than sCARhMFE monomer. Similarly, by virtue of multimeric binding to cell-membrane CEA, sCARfMFE should be more effective than sCARhMFE at retargeting Ad to CEA positive cells.

Figure 2. Efficacy of transductional untargeting and retargeting of monomer sCARhFME and trimer sCARfMFE in culture. (a) CEA and CAR protein expression in cultured cell lines. CEA and CAR protein levels expressed in LS174T, MC38-cea-2 and 293A cells were analyzed by Western Blotting. GAPDH was used as a loading control. (open arrow head, full length CEA; closed arrowhead, truncated CEA; arrow, CAR). (b) Western blot quantitation of sCARhMFE and sCARfMFE. Dilutions of purified sCARhMFE monomer and sCARfMFE trimer were subjected to electrophoresis on denaturing SDS-PAGE gels. Blots were probed with anti-CAR

antibody (upper panel) or with anti-fibritin (lower panel) antibody. Equivalent amounts of sCARhMFE and sCARfMFE, based on these data, were used in all subsequent experiments. (c) Targeting efficacy of monomeric sCARhMFE and trimeric sCARfMFE on CEA-positive cells. Ad.CMVfLuc (3×10^8 vp/well) was pre-incubated with increasing amounts of sCARhMFE or sCARfMFE. LS174T cells were then infected with the viral preparations. After 40 hours, cell extracts were prepared and assayed for luciferase activity and protein concentration. Data are averages ± SEM (n = 3; ***p < 0.001, compared to cells infected with

[Ad.CMVfLuc][sCARhMFE]) (d) Effect of volume on the targeting efficacy of monomeric sCARhMFE and trimeric sCARfMFE. Ad.CMVfLuc (3×10^8 vp/well) was pre-incubated with increasing amounts of sCARhMFE or sCARfMFE. MC38-cea-2 cells were then infected with the viral preparations in two different volumes, 0.2 ml/well or 1.0 ml/well. After 40 hours, cell extracts were prepared and assayed for luciferase activity and protein concentration. Data are averages ± SEM of three cultures at each time point, and are plotted relative to the luciferase activity observed in extracts from cells infected with [trimeric sCARfMFE (100ng)][Ad.CMVfLuc] in 0.2 ml (left panel) and in 1.0 ml (right panel). Data are averages ± SEM (n = 3; **p < 0.01,

compared to cells infected with [Ad.CMVfLuc][sCARhMFE]) (e) Trimeric sCARfMFE is more effective than monomeric sCARhMFE at blocking Ad infection of CAR-positive/CEA-negative cells. Ad.CMVfLuc (3×10^8 vp/well) was pre-incubated with increasing amounts of sCARhMFE or sCARfMFE. 293A cells were then infected with the viral preparations. After 40 hours, cell extracts were prepared and assayed for luciferase activity and protein concentration. Data are averages ± SEM (n = 3; **p < 0.01, ***p < 0.001 compared to cells infected with

[Ad.CMVfLuc][sCARfMFE]). (f) Soluble CEA competes monomeric sCARhMFE retargeting of Ad to CEA-positive cells more effectively than it competes trimeric sCARfMFE retargeting of Ad to CEA-positive cells. Two samples of Ad.CMVfLuc (3×10^8 vp/well) were pre-incubated with

equal amounts of sCARhMFE or sCARfMFE (63 ng/well). MC38-cea-2 cells were then infected with the viral preparations in medium containing increasing amounts of sCEA. After 40 hours, cell extracts were prepared and assayed for luciferase activity and protein concentration. The Y axis indicates the percent of luciferase activity relative to the activity of cells infected in the absence of any sCEA competitor. Data are averages ± SEM (n = 3; **p < 0.01, compared to cells infected with [Ad.CMVfLuc][sCARhMFE]).

Figure 3. Trimeric sCARfMFE is more effective than monomeric sCARhMFE at untargeting adenovirus liver infection *in vivo*. (a) Ad.CMVfLuc (4.5×10^{10} vp/mouse), (panel A) [Ad.CMVfLuc][sCARhMFE], (panels B-D) and [Ad.CMVfLuc][sCARfMFE], (panels E and F) were injected by tail vein into groups of three mice. The living mice and their isolated livers were imaged by bioluminescence three days after virus injection. Intensity scales for all mice are the same and intensity scales for all livers are the same. (b) Quantitation of luciferase activity. After imaging, liver extracts were prepared. Luciferase activity from the intact livers was quantified by ROI analysis of Luciferin-dependent bioluminescence (graph A). Luciferase activity in liver extracts was quantified by conventional luciferase assays (graph B). Data are averages ± SEM (n = 3; *p < 0.05, compared to mice injected with Ad.CMVfLuc).

Figure 4. Trimeric sCARfMFE is more effective than monomeric sCARhMFE at retargeting adenovirus infection to CEA-positive hepatic tumor xenografts. (a) Mice bearing LS174T(rLuc) hepatic tumors were injected intravenously with [Ad.CMVfLuc (3×10^{10} vp/mouse)][sCARhMFE] or with [Ad.CMVfLuc][sCARfMFE]. Adenovirus-directed transgene expression was monitored in the living mice by luciferin-dependent fLuc bioluminescence (FL) five days after virus administration (Panels A, D and G). Following FL imaging, the mice were sacrificed. The livers were removed and imaged for tumor-derived rLuc activity (panels B, E AND H) and for adenovirus directed fLuc transgene expression (panels C, F and I). FL intensity scales indicate luciferin-dependent firefly luciferase activity, the RL intensity scale indicates

coelenterazine dependent *Renilla* luciferase activity. (b) Quantitation of adenovirus-directed fLuc transgene expression in LS174T(rLuc) tumors. After bioluminescent imaging, extracts were prepared from the dissected tumors. Firefly luciferase activity, reflecting virally directed gene expression, was assayed with conventional luciferase and protein assays. Data are averages ± SEM ($n = 3$; $^*p < 0.05$, comparing mice injected with [Ad.CMVfLuc][sCARhMFE] vs. [Ad.CMVfLuc][sCARfMFE]).

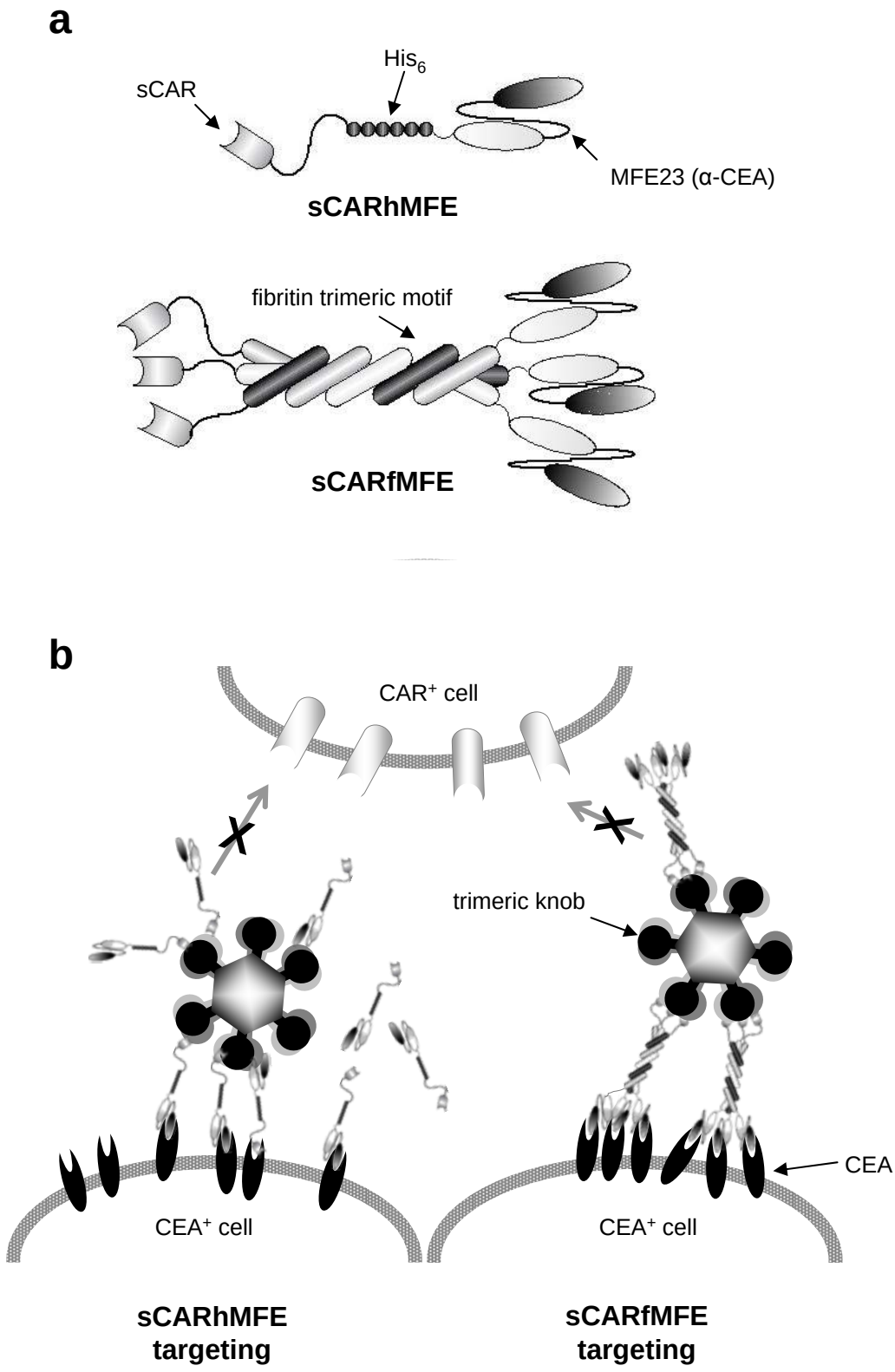

Figure.1 Li, H-J

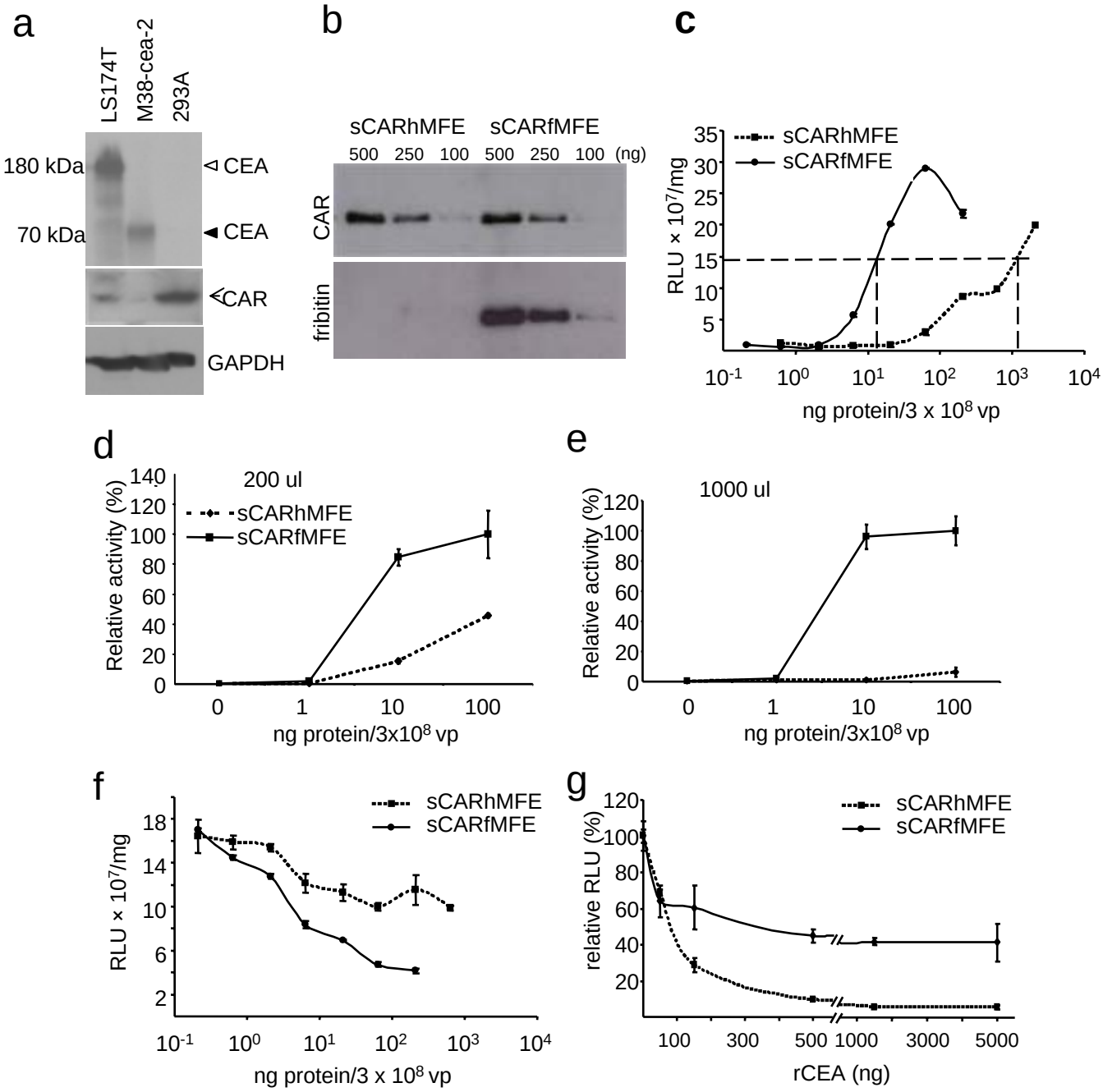

Figure.2 Li, H-J

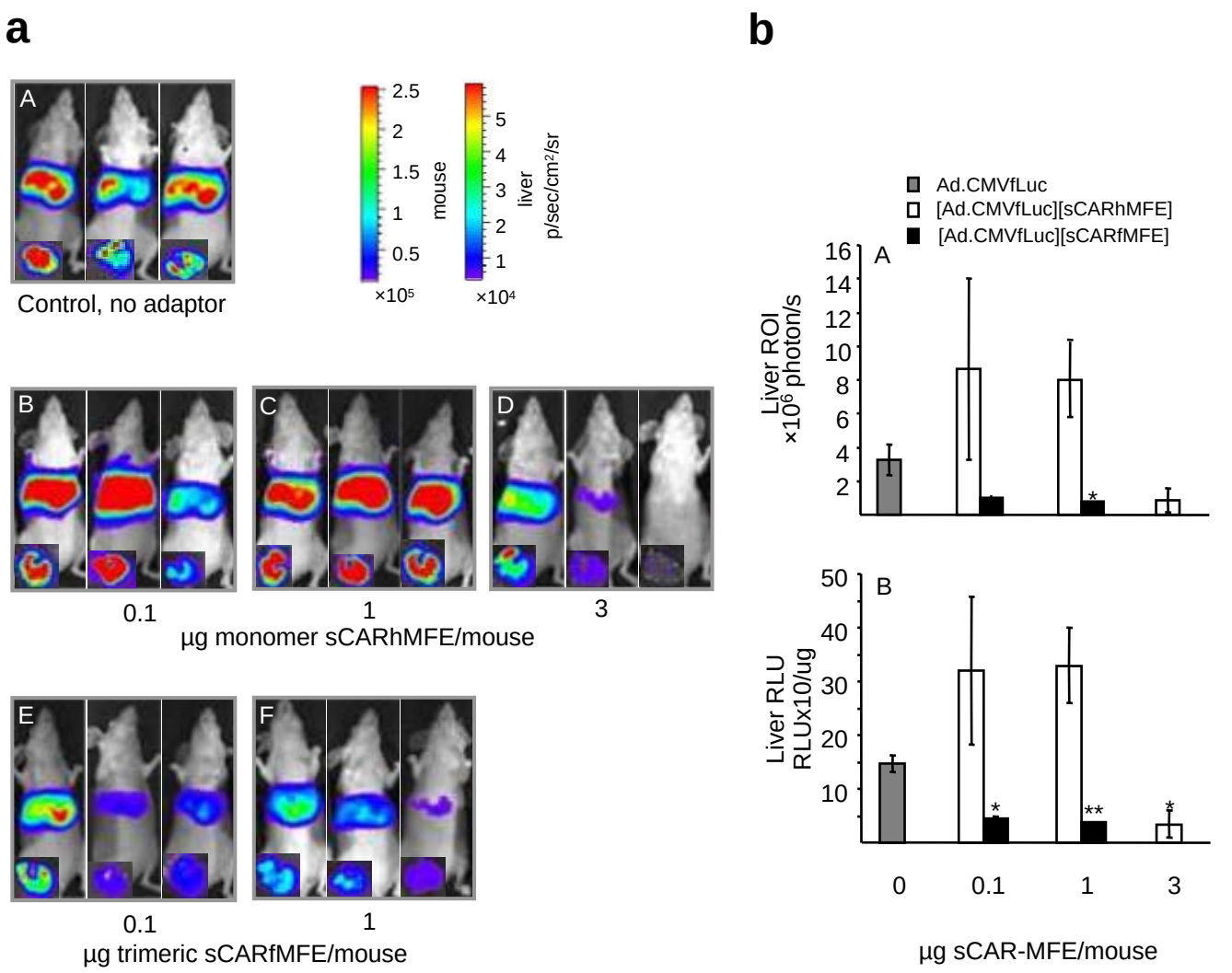

Figure.3 Li, H-J

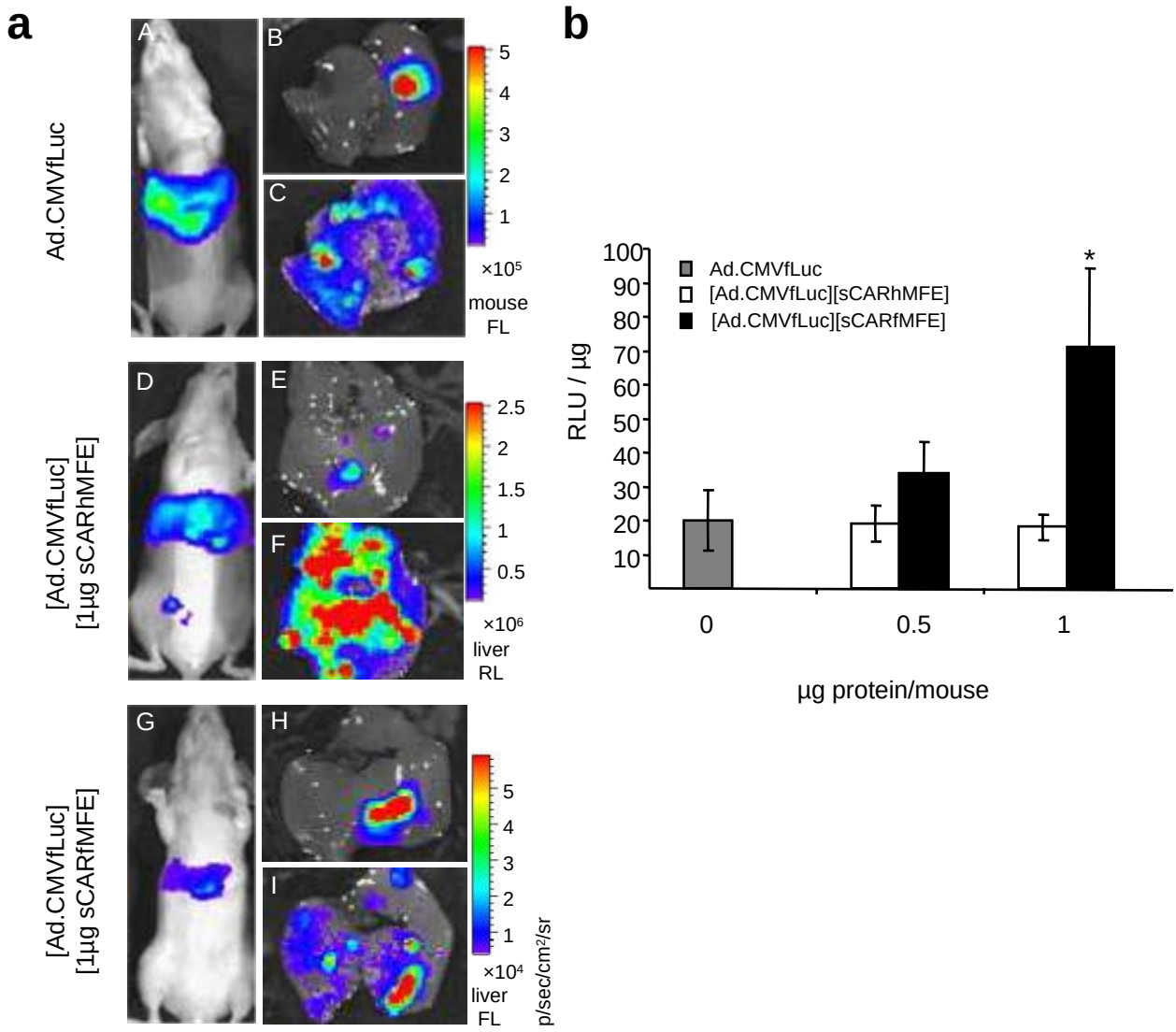

Figure.4 Li, H-J